

REPORT S2-R19B-RW-1

# Bridges for Service Life Beyond 100 Years: Service Limit State Design

S H R P 2 R E N E W A L R E S E A R C H

 **SHRP 2**  
STRATEGIC HIGHWAY RESEARCH PROGRAM  
*Accelerating solutions for highway safety, renewal, reliability, and capacity*

TRANSPORTATION RESEARCH BOARD  
OF THE NATIONAL ACADEMIES

## TRANSPORTATION RESEARCH BOARD 2015 EXECUTIVE COMMITTEE\*

### OFFICERS

CHAIR: **Daniel Sperling**, *Professor of Civil Engineering and Environmental Science and Policy; Director, Institute of Transportation Studies, University of California, Davis*

VICE CHAIR: **James M. Crites**, *Executive Vice President of Operations, Dallas–Fort Worth International Airport, Texas*

EXECUTIVE DIRECTOR: **Neil J. Pedersen**, *Transportation Research Board*

### MEMBERS

**Victoria A. Arroyo**, *Executive Director, Georgetown Climate Center; Assistant Dean, Centers and Institutes; and Professor and Director, Environmental Law Program, Georgetown University Law Center, Washington, D.C.*

**Scott E. Bennett**, *Director, Arkansas State Highway and Transportation Department, Little Rock*

**Deborah H. Butler**, *Executive Vice President, Planning, and CIO, Norfolk Southern Corporation, Norfolk, Virginia (Past Chair, 2013)*

**Malcolm Dougherty**, *Director, California Department of Transportation, Sacramento*

**A. Stewart Fotheringham**, *Professor, School of Geographical Sciences and Urban Planning, University of Arizona, Tempe*

**John S. Halikowski**, *Director, Arizona Department of Transportation, Phoenix*

**Michael W. Hancock**, *Secretary, Kentucky Transportation Cabinet, Frankfort*

**Susan Hanson**, *Distinguished University Professor Emerita, School of Geography, Clark University, Worcester, Massachusetts*

**Steve Heminger**, *Executive Director, Metropolitan Transportation Commission, Oakland, California*

**Chris T. Hendrickson**, *Professor, Carnegie Mellon University, Pittsburgh, Pennsylvania*

**Jeffrey D. Holt**, *Managing Director, Bank of Montreal Capital Markets, and Chairman, Utah Transportation Commission, Huntsville, Utah*

**Geraldine Knatz**, *Professor, Sol Price School of Public Policy, Viterbi School of Engineering, University of Southern California, Los Angeles*

**Michael P. Lewis**, *Director, Rhode Island Department of Transportation, Providence*

**Joan McDonald**, *Commissioner, New York State Department of Transportation, Albany*

**Abbas Mohaddes**, *President and CEO, Iteris, Inc., Santa Ana, California*

**Donald A. Osterberg**, *Senior Vice President, Safety and Security, Schneider National, Inc., Green Bay, Wisconsin*

**Sandra Rosenbloom**, *Professor, University of Texas, Austin (Past Chair, 2012)*

**Henry G. (Gerry) Schwartz, Jr.**, *Chairman (retired), Jacobs/Sverdrup Civil, Inc., St. Louis, Missouri*

**Kumares C. Sinha**, *Olson Distinguished Professor of Civil Engineering, Purdue University, West Lafayette, Indiana*

**Kirk T. Steudle**, *Director, Michigan Department of Transportation, Lansing (Past Chair, 2014)*

**Gary C. Thomas**, *President and Executive Director, Dallas Area Rapid Transit, Dallas, Texas*

**Paul Trombino III**, *Director, Iowa Department of Transportation, Ames*

**Phillip A. Washington**, *General Manager, Denver Regional Council of Governments, Denver, Colorado*

### EX OFFICIO MEMBERS

**Thomas P. Bostick** (*Lt. General, U.S. Army*), *Chief of Engineers and Commanding General, U.S. Army Corps of Engineers, Washington, D.C.*

**Timothy P. Butters**, *Acting Administrator, Pipeline and Hazardous Materials Safety Administration, U.S. Department of Transportation*

**Alison Jane Conway**, *Assistant Professor, Department of Civil Engineering, City College of New York, New York, and Chair, TRB Young Members Council*

**T. F. Scott Darling III**, *Acting Administrator and Chief Counsel, Federal Motor Carrier Safety Administration, U.S. Department of Transportation*

**Sarah Feinberg**, *Acting Administrator, Federal Railroad Administration, U.S. Department of Transportation*

**David J. Friedman**, *Acting Administrator, National Highway Traffic Safety Administration, U.S. Department of Transportation*

**LeRoy Gishi**, *Chief, Division of Transportation, Bureau of Indian Affairs, U.S. Department of the Interior, Washington, D.C.*

**John T. Gray II**, *Senior Vice President, Policy and Economics, Association of American Railroads, Washington, D.C.*

**Michael P. Huerta**, *Administrator, Federal Aviation Administration, U.S. Department of Transportation*

**Paul N. Jaenichen, Sr.**, *Administrator, Maritime Administration, U.S. Department of Transportation*

**Therese W. McMillan**, *Acting Administrator, Federal Transit Administration, U.S. Department of Transportation*

**Michael P. Melaniphy**, *President and CEO, American Public Transportation Association, Washington, D.C.*

**Gregory G. Nadeau**, *Acting Administrator, Federal Highway Administration, U.S. Department of Transportation*

**Peter M. Rogoff**, *Acting Under Secretary for Transportation Policy, Office of the Secretary, U.S. Department of Transportation*

**Mark R. Rosekind**, *Administrator, National Highway Traffic Safety Administration, U.S. Department of Transportation*

**Craig A. Rutland**, *U.S. Air Force Pavement Engineer, Air Force Civil Engineer Center, Tyndall Air Force Base, Florida*

**Barry R. Wallerstein**, *Executive Officer, South Coast Air Quality Management District, Diamond Bar, California*

**Gregory D. Winfree**, *Assistant Secretary for Research and Technology, Office of the Secretary, U.S. Department of Transportation*

**Frederick G. (Bud) Wright**, *Executive Director, American Association of State Highway and Transportation Officials, Washington, D.C.*

**Paul F. Zukunft**, *Adm., U.S. Coast Guard, Commandant, U.S. Coast Guard, U.S. Department of Homeland Security*

\*Membership as of February 2015.



SHRP 2 REPORT S2-R19B-RW-1

# Bridges for Service Life Beyond 100 Years: Service Limit State Design

MODJESKI AND MASTERS, INC.

with

UNIVERSITY OF NEBRASKA, LINCOLN

UNIVERSITY OF DELAWARE

NCS CONSULTANTS, LLC

---

**TRANSPORTATION RESEARCH BOARD**

WASHINGTON, D.C.

2015

[www.TRB.org](http://www.TRB.org)

## **Subject Areas**

Bridges and Other Structures

Highways

Maintenance and Preservation Materials

### **Figure 2.1 Credit**

With the permission of the Canadian Standards Association (operating as CSA Group), material is reproduced from CSA Group standard CAN/CSA S6-06, "Canadian Highway Bridge Design Code," which is copyrighted by CSA Group, 5060 Spectrum Way, Suite 100, Mississauga ON, L4W 5N6. This material is not the complete and official position of CSA Group on the referenced subject, which is represented solely by the standard in its entirety. While use of the material has been authorized, CSA is not responsible for the manner in which the data is presented, nor for any interpretations thereof. For more information or to purchase standards from CSA Group, please visit <http://shop.csa.ca/> or call 1-800-463-6727.



## The Second Strategic Highway Research Program

America's highway system is critical to meeting the mobility and economic needs of local communities, regions, and the nation. Developments in research and technology—such as advanced materials, communications technology, new data collection technologies, and human factors science—offer a new opportunity to improve the safety and reliability of this important national resource. Breakthrough resolution of significant transportation problems, however, requires concentrated resources over a short time frame. Reflecting this need, the second Strategic Highway Research Program (SHRP 2) has an intense, large-scale focus, integrates multiple fields of research and technology, and is fundamentally different from the broad, mission-oriented, discipline-based research programs that have been the mainstay of the highway research industry for half a century.

The need for SHRP 2 was identified in *TRB Special Report 260: Strategic Highway Research: Saving Lives, Reducing Congestion, Improving Quality of Life*, published in 2001 and based on a study sponsored by Congress through the Transportation Equity Act for the 21st Century (TEA-21). SHRP 2, modeled after the first Strategic Highway Research Program, is a focused, time-constrained, management-driven program designed to complement existing highway research programs. SHRP 2 focuses on applied research in four areas: Safety, to prevent or reduce the severity of highway crashes by understanding driver behavior; Renewal, to address the aging infrastructure through rapid design and construction methods that cause minimal disruptions and produce lasting facilities; Reliability, to reduce congestion through incident reduction, management, response, and mitigation; and Capacity, to integrate mobility, economic, environmental, and community needs in the planning and designing of new transportation capacity.

SHRP 2 was authorized in August 2005 as part of the Safe, Accountable, Flexible, Efficient Transportation Equity Act: A Legacy for Users (SAFETEA-LU). The program is managed by the Transportation Research Board (TRB) on behalf of the National Research Council (NRC). SHRP 2 is conducted under a memorandum of understanding among the American Association of State Highway and Transportation Officials (AASHTO), the Federal Highway Administration (FHWA), and the National Academy of Sciences, parent organization of TRB and NRC. The program provides for competitive, merit-based selection of research contractors; independent research project oversight; and dissemination of research results.

SHRP 2 Report S2-R19B-RW-1

ISBN: 978-0-309-27375-6

© 2015 National Academy of Sciences. All rights reserved.

### Copyright Information

Authors herein are responsible for the authenticity of their materials and for obtaining written permissions from publishers or persons who own the copyright to any previously published or copyrighted material used herein.

The second Strategic Highway Research Program grants permission to reproduce material in this publication for classroom and not-for-profit purposes. Permission is given with the understanding that none of the material will be used to imply TRB, AASHTO, or FHWA endorsement of a particular product, method, or practice. It is expected that those reproducing material in this document for educational and not-for-profit purposes will give appropriate acknowledgment of the source of any reprinted or reproduced material. For other uses of the material, request permission from SHRP 2.

*Note:* SHRP 2 report numbers convey the program, focus area, project number, and publication format. Report numbers ending in “w” are published as web documents only.

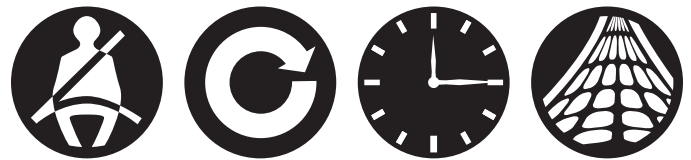
### Notice

The project that is the subject of this report was a part of the second Strategic Highway Research Program, conducted by the Transportation Research Board with the approval of the Governing Board of the National Research Council.

The members of the technical committee selected to monitor this project and to review this report were chosen for their special competencies and with regard for appropriate balance. The report was reviewed by the technical committee and accepted for publication according to procedures established and overseen by the Transportation Research Board and approved by the Governing Board of the National Research Council.

The opinions and conclusions expressed or implied in this report are those of the researchers who performed the research and are not necessarily those of the Transportation Research Board, the National Research Council, or the program sponsors.

The Transportation Research Board of the National Academies, the National Research Council, and the sponsors of the second Strategic Highway Research Program do not endorse products or manufacturers. Trade or manufacturers' names appear herein solely because they are considered essential to the object of the report.



### SHRP 2 Reports

Available by subscription and through the TRB online bookstore:  
[www.mytrb.org/store](http://www.mytrb.org/store)

Contact the TRB Business Office:  
202-334-3213

More information about SHRP 2:  
[www.TRB.org/SHRP2](http://www.TRB.org/SHRP2)

# THE NATIONAL ACADEMIES

## *Advisers to the Nation on Science, Engineering, and Medicine*

The **National Academy of Sciences** is a private, nonprofit, self-perpetuating society of distinguished scholars engaged in scientific and engineering research, dedicated to the furtherance of science and technology and to their use for the general welfare. On the authority of the charter granted to it by Congress in 1863, the Academy has a mandate that requires it to advise the federal government on scientific and technical matters. Dr. Ralph J. Cicerone is president of the National Academy of Sciences.

The **National Academy of Engineering** was established in 1964, under the charter of the National Academy of Sciences, as a parallel organization of outstanding engineers. It is autonomous in its administration and in the selection of its members, sharing with the National Academy of Sciences the responsibility for advising the federal government. The National Academy of Engineering also sponsors engineering programs aimed at meeting national needs, encourages education and research, and recognizes the superior achievements of engineers. Dr. C. D. (Dan) Mote, Jr., is president of the National Academy of Engineering.

The **Institute of Medicine** was established in 1970 by the National Academy of Sciences to secure the services of eminent members of appropriate professions in the examination of policy matters pertaining to the health of the public. The Institute acts under the responsibility given to the National Academy of Sciences by its congressional charter to be an adviser to the federal government and, on its own initiative, to identify issues of medical care, research, and education. Dr. Victor J. Dzau is president of the Institute of Medicine.

The **National Research Council** was organized by the National Academy of Sciences in 1916 to associate the broad community of science and technology with the Academy's purposes of furthering knowledge and advising the federal government. Functioning in accordance with general policies determined by the Academy, the Council has become the principal operating agency of both the National Academy of Sciences and the National Academy of Engineering in providing services to the government, the public, and the scientific and engineering communities. The Council is administered jointly by both Academies and the Institute of Medicine. Dr. Ralph J. Cicerone and Dr. C. D. (Dan) Mote, Jr., are chair and vice chair, respectively, of the National Research Council.

The **Transportation Research Board** is one of six major divisions of the National Research Council. The mission of the Transportation Research Board is to provide leadership in transportation innovation and progress through research and information exchange, conducted within a setting that is objective, interdisciplinary, and multimodal. The Board's varied activities annually engage about 7,000 engineers, scientists, and other transportation researchers and practitioners from the public and private sectors and academia, all of whom contribute their expertise in the public interest. The program is supported by state transportation departments, federal agencies including the component administrations of the U.S. Department of Transportation, and other organizations and individuals interested in the development of transportation. [www.TRB.org](http://www.TRB.org)

[www.national-academies.org](http://www.national-academies.org)

## SHRP 2 STAFF

**Ann M. Brach**, *Director*  
**Stephen J. Andrie**, *Deputy Director*  
**Cynthia Allen**, *Editor*  
**Kenneth Campbell**, *Chief Program Officer, Safety*  
**Jared Cazel**, *Editorial Assistant*  
**JoAnn Coleman**, *Senior Program Assistant, Capacity and Reliability*  
**Eduardo Cusicanqui**, *Financial Officer*  
**Richard Deering**, *Special Consultant, Safety Data Phase 1 Planning*  
**Shantia Douglas**, *Senior Financial Assistant*  
**Charles Fay**, *Senior Program Officer, Safety*  
**Carol Ford**, *Senior Program Assistant, Renewal and Safety*  
**James Hedlund**, *Special Consultant, Safety Coordination*  
**Alyssa Hernandez**, *Reports Coordinator*  
**Ralph Hessian**, *Special Consultant, Capacity and Reliability*  
**Andy Horosko**, *Special Consultant, Safety Field Data Collection*  
**William Hyman**, *Senior Program Officer, Reliability*  
**Linda Mason**, *Communications Officer*  
**David Plazak**, *Senior Program Officer, Capacity and Reliability*  
**Rachel Taylor**, *Senior Editorial Assistant*  
**Dean Trackman**, *Managing Editor*  
**Connie Woldu**, *Administrative Coordinator*

## ACKNOWLEDGMENTS

This work was sponsored by the Federal Highway Administration in cooperation with the American Association of State Highway and Transportation Officials. It was conducted in the second Strategic Highway Research Program (SHRP 2), which is administered by the Transportation Research Board of the National Academies. At various times the project was managed by Monica Starnes, Mark Bush, and Jerry DiMaggio. Because of the close relationship between this project and NCHRP Project 12-83, information and report sections were freely exchanged between the two projects. NCHRP 12-83 is being managed by Waseem Dekelbab, and the principal investigator is Wagdy G. Wassef of Modjeski and Masters, Inc.

The research described in this report was performed by Modjeski and Masters, Inc., supported by the University of Nebraska, Lincoln; the University of Delaware; and NCS Consultants, LLC. John M. Kulicki of Modjeski and Masters, Inc., was the principal investigator. Other authors are Wagdy G. Wassef of Modjeski and Masters, Inc.; Andrzej S. Nowak of the University of Nebraska, Lincoln; Dennis R. Mertz of the University of Delaware; Naresh C. Samtani of NCS Consultants; and through his participation in NCHRP Project 12-83, Hani Nassif of Rutgers University. The following graduate students contributed to this project at different times: Marek Kozikowski, Przemyslaw Rakoczy, Krzysztof Waszczuk, and Anna Maria Rakoczy of the University of Nebraska; Dustin M. Schopen and Benjamin Berwick of the University of Delaware; and Dan Su of Rutgers University.

## FOREWORD

Jerry A. DiMaggio, D.GE, PE, *SHRP 2 Senior Program Officer, Renewal*

This report, *Bridges for Service Life Beyond 100 Years: Service Limit State Design*, describes research, outcomes, and products on the basis of the R19B project objectives. The objectives were to develop design and detailing guidance and calibrated service limit states (SLSs) to provide 100-year bridge life and to develop a framework for further development of calibrated SLSs. The products of this study are expected to be directly usable by the American Association of State Highway and Transportation Officials (AASHTO) and departments of transportation (DOTs) and include

- Provisions needed to implement SLSs and the associated load and resistance factors necessary to produce calibrated bridge components and systems expected to have a predictable service life.
- Detailed design and detailing provisions required to design and construct the calibrated component or system.
- Databases used in the calibration, as well as instructions for a calibration spreadsheet, for use by DOTs to track and adjust service-based reliability with time.

Consideration of SLSs requires different input data from the previously calibrated Strength Limit State I (also known as “ultimate or strength limit states,” or ULSs). In ULSs, the limit state function is defined by resistance, which is considered constant in time, and loads. For SLSs, a different approach is needed because

- Exceeding a service limit state does not lead to a clear, immediate loss of functionality.
- Acceptable performance can be subjective (full life-cycle analysis is required).
- Resistance and load effects can be and often are correlated.
- Load must be considered to be a function of time, described by magnitude and frequency of occurrence.
- Resistance may be strongly affected by quality of workmanship, operation procedures, and maintenance.
- Resistance is subject to changes in time, mostly but not only by deterioration.
- Resistance can depend on geographical location (e.g., climate, exposure to industrial pollution, or deicing agents).

---

The topic of limit state design, also known as load resistance factor design (LRFD), within the United States has been under development and implementation for more than 25 years. The benefits of this design platform are now well understood by the bridge and structures community as well as by transportation decision makers. Generally, it has been assumed that maintenance activities will be sufficient to prevent significant loss of the strength and stiffness that would result in unsatisfactory service level performance. It has been recognized that advancements and further maturity of the LRFD platform need to focus on quantification and calibrations of the SLSs. Although previous work has been published in this area, the R19B study serves as a foundational reference to partially fill knowledge gaps and, perhaps more importantly, for direct application and reference for future study in this emerging technical area of design.

# CONTENTS

1	Executive Summary
4	<b>CHAPTER 1 Purpose of Report and Relation to Scope</b>
4	1.1 Objectives of Project R19B
5	1.2 Scope
6	1.3 Research Team
7	1.4 Relationship of Project R19B to Project R19A
7	1.5 Relationship of Project R19B to NCHRP Project 12-83
7	1.6 Special Challenges Related to SLSs
9	1.7 Serviceability Versus Deterioration
9	1.8 Durability
12	1.9 Initial Coordination with FHWA Long-Term Bridge Performance Program
13	1.10 Dialogue with AASHTO HSCOBs and Others
14	<b>CHAPTER 2 Current State of the Art</b>
14	2.1 Approach
14	2.2 Summary of Literature Survey
18	2.3 Serviceability Requirements in Several Modern Bridge Design Specifications
44	2.4 Surveys of Current Practice
47	2.5 SLSs to Be Considered in This Report
48	<b>CHAPTER 3 Overview of Calibration Process</b>
48	3.1 Introduction
49	3.2 Calibration by Determination of Reliability Indices
54	3.3 “Deemed to Satisfy”
55	3.4 Customizing the Process
56	<b>CHAPTER 4 Deterioration</b>
56	4.1 Introduction
56	4.2 Bolukbasi et al. (2004)
60	4.3 Jiang and Sinha (1989)
62	4.4 Hatami and Morcous (2011)
62	4.5 Comparison of Equations from Bolukbasi et al. (2004), Jiang and Sinha (1989), and Hatami and Morcous (2011)
69	4.6 Agrawal and Kawaguchi (2009)
78	4.7 Stukhart et al. (1991)
88	4.8 Massachusetts DOT
94	<b>CHAPTER 5 Live Load for Calibration</b>
94	5.1 Development of Live Load Models for Service Limit States
99	5.2 Initial Data Analysis
111	5.3 Statistical Parameters for Service Limit States Other than Fatigue

121	5.4 Development of Statistical Parameters of Fatigue Load
143	5.5 Development of Overload (Service II) Parameters
<b>145</b>	<b>CHAPTER 6 Calibration Results</b>
145	6.1 Foundation Deformations, Service I: Lifetime
171	6.2 Cracking of Reinforced Concrete Components, Service I Limit State: Annual Probability
176	6.3 Live Load Deflections, Service I: Annual Probability
180	6.4 Overload, Service II: Annual Probability
188	6.5 Tension in Prestressed Concrete Beams, Service III Limit State: Annual Probability
208	6.6 Fatigue Limit States: Lifetime
<b>217</b>	<b>CHAPTER 7 Proposed Changes to AASHTO LRFD</b>
218	7.1 Foundation Deformations—Service I
233	7.2 Live Load Response
238	7.3 Premature Yielding and Slip of Bolts—Service II
240	7.4 Cracking of Prestressed Concrete—Currently Service III
243	7.5 Fatigue
<b>260</b>	<b>CHAPTER 8 Purpose and Contents of Appendix F</b>
<b>261</b>	<b>CHAPTER 9 Summary and Recommendations</b>
261	9.1 Summary
262	9.2 Recommendations
262	9.3 Implementation
<b>263</b>	<b>References</b>
<b>269</b>	<b>Appendix A. SLS Requirements in the Eurocode</b>
<b>292</b>	<b>Appendix B. SHRP 2 R19B Survey of Bridge Owners</b>
<b>304</b>	<b>Appendix C. Comparison of Crack Width Prediction Equations for Prestressed Concrete Members</b>
<b>310</b>	<b>Appendix D. Derivation of the Resistance Prediction Equation of Prestressed Concrete Bridge Girders</b>
<b>313</b>	<b>Appendix E. Normal Probability Plots of Fatigue Data for the Various Detail Categories</b>
<b>322</b>	<b>Appendix F. Data Used for Calibration</b>

# Executive Summary

The objectives of SHRP 2 Project R19B were to develop design and detailing guidance and calibrated service limit states (SLSs) to provide 100-year bridge life and to develop a framework for further development of calibrated SLSs. Generally, it has been assumed that maintenance activities will be sufficient to prevent significant loss of the strength and stiffness that would result in unsatisfactory service-level performance.

Consideration of SLSs requires different input data from the previously calibrated Strength Limit State I (or “ultimate or strength limit states,” ULSs). In ULSs, the limit state function is defined with two variables: resistance, which was considered constant in time, and loads. For SLSs, a different approach is needed because of the following factors:

- Exceeding SLSs does not lead to a clear, immediate loss of functionality, so defining the resistance is very subjective.
- Acceptable performance can be subjective (full life-cycle analysis is required).
- Resistance and load effects can be and often are correlated.
- Load must be considered to be a function of time, described by magnitude and frequency of occurrence.
- Resistance may be strongly affected by quality of workmanship, operation procedures, and maintenance.
- Resistance is subject to changes in time, mostly but not only deterioration, with difficulty predicting initiation time and time-varying rates of deterioration (e.g., corrosion, accumulation of debris, cracking).
- Resistance can depend on geographical location (e.g., climate, exposure to industrial pollution, exposure to deicing agents, proximity to the ocean).

On the basis of a survey of owners and a literature review that included other national and international bridge design specifications, a set of possible SLSs was developed. Those SLSs were reviewed to determine which could be calibrated using reliability theory. Calibrated, reliability-based load factors or resistance factors, or both, were developed for

- Foundation deformations;
- Cracking of reinforced concrete components;
- Live load deflections;
- Permanent deformations;
- Cracking of prestressed concrete components; and
- Fatigue of steel and reinforced concrete components.

The calibration process produced target reliability levels much different from those used for the strength calibration. This outcome was expected because, in general, the consequences of



exceeding SLSs are an order, or even several orders, of magnitude smaller than those associated with ULSs. Thus, an acceptable probability of exceeding an SLS is much higher than for a ULS. Although the strength calibration was based on a target reliability index of about 3.5 for a 75-year life, with some exceptions, most of the SLS calibration was generally done with a target reliability index around 1.0 to 1.5 on the basis of an annual probability. Once the target reliabilities were determined, changes to load factors, resistance factors, or other design parameters were developed.

Extensive use was made of WIM (weigh in motion) collected at 32 sites around the country. The raw data consisted of 65 million vehicle records consisting of axle weights, axle spacing, speed, and vehicle classification. After filtering, about 35 million records formed the database from which live load biases and coefficients of variation (CVs) were computed for a variety of span lengths, average daily truck traffic, and time periods. To acknowledge the assumption that the 32 sites were representative of the whole country, project live load biases were set at the mean plus 1.5 standard deviations.

WIM data processing for fatigue consisted of passing the complete string of vehicles over influence lines for simple spans and two-span continuous units of various spans. The resulting histories of live load moments were processed using rainflow counting and cumulative damage methodologies to provide damage-equivalent moments and axle loads and cycles per design truck passage. Fatigue test results for the American Association of State Highway and Transportation Officials (AASHTO) fatigue categories were reassessed using a new damage accumulation model combined with fitted distributions to calculate biases and CVs for each category. Reliability indices for current designs were also evaluated. All this information was used in calibrating new load factors and new constants for some of the categories.

A general procedure has been developed for calibration of SLSs based on an evaluation of the effect of vertical or horizontal foundation deformations on bridge structures. The procedure is demonstrated by using measured field data for immediate settlements of spread footings on soils. The prediction accuracy for several methods of calculating immediate vertical movement of spread footings on soils was developed from the measured field data. This prediction accuracy is expressed in terms of the probability of exceeding a deformation criterion (performance criterion) chosen by the bridge designer. Using the correlation between probability of exceedance and the reliability index, the prediction accuracy of calculation methods can be expressed in terms of the reliability index. The target reliability index for the current calculation method by Hough (1959) recommended in the *AASHTO LRFD Bridge Design Specifications* was determined for comparison with several other calculation methods. The conservatism of Hough's method is demonstrated, and use of the method by Schmertmann et al. (1978) is recommended.

Given the regional nature of geotechnical engineering, a step-by-step process is included to enable the process to be repeated with local data. This step-by-step process can be applied to both vertical and horizontal deformations of all structural foundation types such as footings, drilled shafts, and driven piles. Also recommended for consideration by the AASHTO Highway Subcommittee on Bridges and Structures (HSCOBs) is adoption of the construction point and  $\delta$ -0 concepts for calculating vertical deformations, which take into account the angular distortions within bridge spans in the context of construction stages.

The criteria used by the Canadian Highway Bridge Design Code, which is based on deflection, frequency, and perception, were evaluated and calibrated as a possible alternative to the current deflection criteria. In this case, the reason for change was not found to be quite as compelling as some of the other SLSs, but the rationale has been presented. Several other SLSs were either found unsuitable for calibration, or the difference in application did not justify a change in the *AASHTO LRFD*. In these cases, the rationale is also presented.

On the basis of the reported research and calibrations, draft agenda items required to implement the findings of this project through changes to the *AASHTO LRFD Bridge Design Specifications* are presented for consideration by the AASHTO HSCOBs. Most of these items are evolutionary, but several would require changes to the typical American bridge design process if they are adopted. These required changes are detailed in the report.



Owners who make exceptions to some of the *AASHTO LRFD* requirements will have to evaluate the findings of this research and decide their jurisdiction-specific requirements. The effect of the proposed specifications revisions on specific types of components will be debated by AASHTO's technical committees and HSCOBs when the revisions are considered.

The products of this research, which are expected to be directly usable by AASHTO and departments of transportation, include the following:

- Provisions needed to implement SLSs and the associated load and resistance factors necessary to produce calibrated bridge components and systems expected to have a predictable service life. When practical, the provisions are based on a 100-year life; if a component or system cannot reasonably be expected to last 100 years, the expected life is given.
- Some detailed design and detailing provisions required to design and build the calibrated component or system.
- Appendix F, containing the databases used in the calibration, as well as instructions for a calibration spreadsheet for use by departments of transportation to track and adjust service-based reliability with time. It is expected that implementing owners will track deterioration and changes to load regimes with time and adjust built-in models and assumptions over time.

The lack of quality information regarding the change in serviceability over time for bridges in different environments and traffic conditions was a continual challenge during this project. There is a national database summarizing the results of the National Bridge Inspection system that could provide a wealth of information. However, no well-accepted direct link between the National Bridge Inventory (NBI) condition data and the types of unsatisfactory performance related to the SLSs calibrated in this study has been found. Several locally developed predictors of changes in the NBI condition number over time have been presented to provide guidance to owners on possible changes to the resistance side of the limit states used in this report within the context of the caveat above. This lack of correspondence between the NBI condition numbers and quantifiable changes in behavior or resistance as they relate to service response and, ultimately, to the strength limit states, limits the use of this information to both owners and researchers. One of the recommendations coming out of this project is to initiate work to close this gap.

Finally, there is much interest nationally and internationally on the improved implementation of SLSs that should be considered in any continued development of the *AASHTO LRFD*.

## CHAPTER 1

# Purpose of Report and Relation to Scope

### 1.1 Objectives of Project R19B

The request for proposal for SHRP 2 Project R19B stated the following objectives:

- Develop new design codes that incorporate a rational approach based on service limit states (SLSs) for durability and performance of bridge systems, subsystems, components, and details that are critical to reaching the expected service life and assuring an actual life beyond 100 years. Special focus should be given to problematic systems, subsystems, components, and details. The proposed SLSs will include data sets related to durability, fatigue, fracture, and redundancy as integral issues of service life as reported in SHRP 2 Project R19A.
- Develop performance measures incorporating predefined component classifications that will use full probability-based service life design criteria to maximize the actual life of the system. Consider material performance (including durability); structural performance of systems, subsystems, and components (optimum joints and bearings); and design practices leading to longer and more predictable service life.
- Develop comprehensive design procedures, proposed specification changes, and implementation tools that include durability design in addition to structural design. The development should also consider structural and material redundancy, and system, subsystem, and component performance measures that will use service life design criteria to maximize the actual life of the system. The adjustments to SLSs should not adversely affect ultimate or strength limit states (ULSs) and extreme event limit states.

To best accomplish the project objectives, the project team first developed a list of the applicable SLSs for various components. A framework for calibration that accommodates aging and deterioration models, applicable loads, and other design parameters for the components was developed. Calibration

was defined as the process of determining values of load and resistance factors so that the designed components will satisfy the selected reliability-based criterion (i.e., the reliability of the structure is close to the target value). Calibration involved the development of statistical models for load and resistance, selection of the target reliability index, and reliability analysis.

The products of this research, expected to be directly usable by the American Association of State Highway and Transportation Officials (AASHTO) and departments of transportation (DOTs), include the following:

- Provisions needed to implement SLSs and the associated load and resistance factors necessary to produce calibrated bridge components and systems expected to have a predictable service life. When practical, the provisions are based on a 100-year life; if a component or system cannot reasonably be expected to last 100 years, the expected life is given.
- Some detailed design and detailing provisions required to design and build the calibrated component or system.
- Appendix F, which contains the databases used in the calibration, as well as instructions for a calibration spreadsheet for use by DOTs to track and adjust service-based reliability with time. It is expected that implementing owners will track deterioration and changes to load regimes with time and adjust built-in models and assumptions over time.

It is assumed that the *AASHTO LRFD Bridge Design Specifications (AASHTO LRFD)* requirements are a package that has to be considered together. Owners who make exceptions to some *AASHTO LRFD* requirements will have to evaluate the findings of this research and decide their jurisdiction-specific requirements. The effect of the proposed specifications revisions on specific types of components will be debated by AASHTO's technical committees and Highway Subcommittee of Bridges and Structures (HSCOBs) when the revisions are considered.

## 1.2 Scope

### 1.2.1 Original Scope

As originally scoped, the project was broken into two phases containing the tasks described below.

#### Phase 1

##### TASK 1

Conduct a review of the literature to review and identify current practices of using SLS principles for determining structural service life approaches.

##### TASK 2

Supplement the interim report provided by Project R19A at the beginning of this contract with a follow-up survey to identify successful systems, subsystems, components, and details that have lasted 100-plus years. Systems, subsystems, components, and details that have proven to or have the potential to solve common bridge durability and structural performance problems were of special interest for this task. In addition, identify problematic components and the nature and cause of failures that resulted in reduced service life, and document any available maintenance and rehabilitative costs. Compile any existing data regarding loadings and accelerated environmental testing results as documented by others for evaluating the performance of developed systems, subsystems, components, and details. The research team was not aware of significant relevant information, so this type of data was not incorporated into the SLS calibration approach. Owner-supplied information can be used to supplement the calibration.

##### TASK 3

Develop an SLS approach that can be used to calibrate 100-plus-year service life. A benchmark in the calibration will evaluate the suitability of the existing 75-year load and resistance factor design (LRFD) approach presented in the current specifications.

##### TASK 4

Prepare an interim report documenting Tasks 1 through 3 and a detailed work plan for executing the SLS calibration.

The research team proposed and the sponsor approved moving Task 5 into Phase 1. The work of an independent committee takes place in later tasks still left in Phase 2. Task 5 deals with identifying the members of the committee.

##### TASK 5

The research team proposed, for SHRP 2 approval, an independent national committee (INC) of experts to review and critique the suitability of the data set and the SLS approach.

The INC included appropriate experts from AASHTO, the Federal Highway Administration (FHWA), state DOTs, industry, and academia (a minimum of seven volunteers is expected for this committee).

#### Phase 2

##### TASK 6

Conduct analytical trial runs as appropriate for evaluating the performance of systems, subsystems, components, and details developed under Project R19A, as well as existing systems, subsystems, components, and details that are critical to reaching the expected service life beyond 100 years. Submit an interim report to SHRP 2 and to the approved INC.

##### TASK 7

Plan a working session with the INC to review and gather feedback on the interim report. Submit to SHRP 2 an updated interim report based on the input from the INC.

##### TASK 8

Incorporate the framework for the long-term bridge performance program (LTBPP), and use the LTBPP framework to validate performance expectations. Ensure that the ULs and extreme event limit states are not compromised. The approach from the research team was to include recommendations for future bridge practitioners on how to adjust the SLSs to include semiprobabilistic assumptions developed under this project.

##### TASK 9

Develop a data set format that will be adaptable for future maintenance by the AASHTO Technical Committee on Loads and Loads Distribution (T-5).

##### TASK 10

Work with the Project R19A team and industry to develop recommendations for AASHTO-formatted LRFD design and load rating specifications and analysis methods, including detailed examples for bridge systems, subsystems, components, and details that incorporate results from Project R19A.

##### TASK 11

Develop an implementation plan suitable for adoption and maintenance by AASHTO that is based on the findings of this work.

##### TASK 12

Prepare a final report, including recommendations for future research.

The first five tasks were developed in the Phase 1 report previously submitted and reviewed by the project expert technical group.

## 1.2.2 Revised Scope for Tasks 5 and 6

Task 5 was completed. Members of the INC were selected and approved. However, as the project unfolded, the expert technical group was augmented with additional experts in the areas of calibration and deterioration, and the value of the INC decreased accordingly. Copies of the Phase 1 report were provided to members of the INC in August 2011, but little response was received. Written comments received from one reviewer were very supportive of the approach outlined in the Phase 1 report, and those comments were submitted to the SHRP 2 staff.

Task 6 of the research plan for Project R19B, as modified and submitted in November 2011, initially required the submission of an interim report documenting a proof-of-concept demonstration of the proposed calibration of SLSs. After consulting with SHRP 2 staff, the research team decided that the interim report served little purpose and that, due to the unforeseen difficulty in finding suitable data for calibration and other analytical work, the resources originally programmed for the trial calibration runs, the interim report, and the working sessions with the INC (i.e., Tasks 6 and 7) could be better used to advance the other tasks. The specific requirements for a revised Task 6 are described below.

### *Revised Task 6*

Conduct analytical trial runs as appropriate for evaluating the performance of systems, subsystems, components, and details developed under Project R19A, as well as existing systems, subsystems, components, and details that are critical to reaching the expected service life beyond 100 years. Submit an interim report to SHRP 2 and to the approved INC.

The research team developed serviceability provisions based on the findings and calibration approach outlined in Chapters 3 and 6. These provisions include improvements to the existing service and fatigue limit states as shown below:

- Load-induced fatigue of steel and concrete details and components;
- Live load deflection;
- Permanent deformation of compact steel components;
- Cracking of reinforced-concrete components;
- Tension in prestressed concrete components;
- Settlement of foundations;
- Horizontal movements of abutments; and
- Slip of slip-critical bolted connections.

Initially, the calibration was to proceed in two stages: a proof-of-concept stage involving a subset of the SLSs and a subset of parameters (random variables), followed by a production calibration involving all SLSs and a wider range of

parameters. At the completion of a proof-of-concept partial calibration, the research team developed an interim report on findings. Once the calibration procedures were coded into spreadsheets, the value of trial runs or partial calibrations became insignificant. That report has been folded into the present report.

A database of bridges was useful during the calibration process to assess current reliability versus the reliability resulting from proposed changes in design equations and methodologies, as well as selecting load and resistance factors. For this project, the database compiled under National Cooperative Highway Research Program (NCHRP) Project 12-78 (Mlynarski et al. 2011) was selected as the source of sample bridges. The database contains information on over 18,000 bridges suitable for analysis using AASHTOWare's Bridge Rating analytical software.

The NCHRP 12-78 database was sorted to select relatively modern bridges, potential candidate bridges were identified, and a partial list of candidate bridges was submitted to SHRP 2.

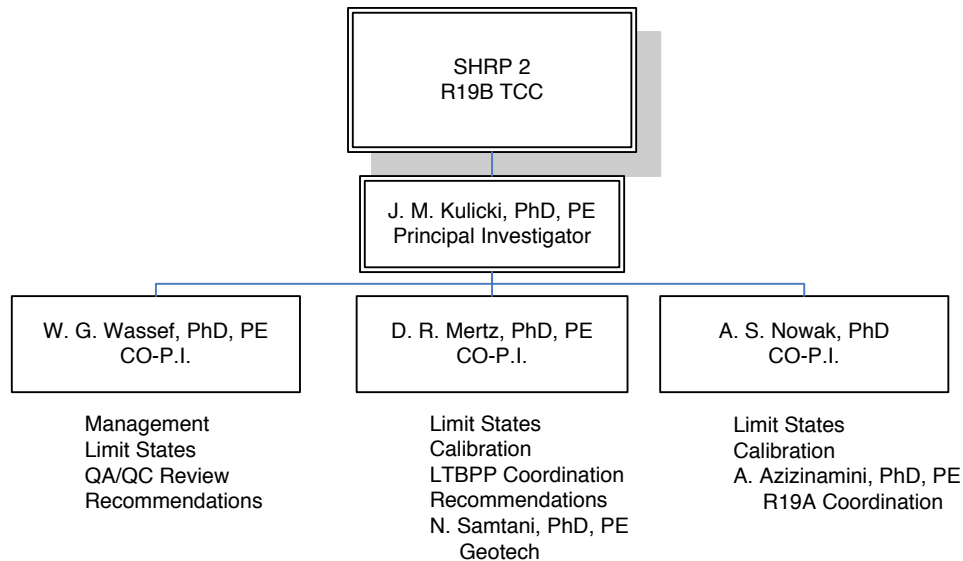
As the calibration procedures were more fully developed and it was determined that insufficient data were available to fully calibrate some of the SLSs, the sample bridge population was used with three SLSs: cracking of prestressed concrete beams, settlement, and deflections. The sample bridge population was also used to investigate the ramifications of potential changes to two SLSs: cracking of prestressed concrete beams and overload of steel bridges. Subsets of the candidate bridge database used for these purposes are included in Appendix F.

## 1.3 Research Team

The organization and relationship of the primary team members are shown in the organizational chart in Figure 1.1.

The functional lead responsibilities for leading individual tasks were as follows:

- Task 1. The two universities.
- Task 2. University of Nebraska–Lincoln (UNL) (Atorod Azizinamini took the lead).
- Task 3. All components of the team participated in the work, but it was Modjeski and Masters' role to see that the group reached a conclusion and a product.
- Task 4. Modjeski and Masters, with help from the other team members.
- Task 5. As with Task 3, this task was done by the entire group with Modjeski and Masters seeing that a successful outcome occurred.
- Task 6. UNL took the lead.
- Task 7. Modjeski and Masters took the lead.
- Task 8. University of Delaware took the lead.
- Task 9. University of Delaware took the lead, with assistance from UNL.



**Figure 1.1. Project R19B organizational chart.**

- Task 10. Modjeski and Masters took the lead, working primarily with the University of Delaware.
- Task 11. Modjeski and Masters took the lead.
- Task 12. Modjeski and Masters took the lead.

#### 1.4 Relationship of Project R19B to Project R19A

Projects R19A and R19B combined should have resulted in the development of AASHTO-formatted provisions for design of bridges capable of providing more than 100 years of service life. The provisions should address both existing and new bridges. The procedures have to be quantifiable for both existing and new bridges.

One of the major tasks within R19A was identifying promising systems, subsystems, components, details, and retrofit concepts capable of prolonging the service life of bridges at optimal total costs. R19A was to have developed details and subsystems requiring calibration or development (or both) of new limit state design provisions. The R19B work depended on R19A's developing these details or subsystems. For selected ideas, R19A was also to have developed deterioration models. Incorporating these deterioration models into a general SLS design provision framework was to be a major undertaking within R19B. The choice of a general SLS design framework was an important issue that affected the research directions of both the R19B and R19A projects.

As of this writing, no new details and subsystems have been recommended to R19B. One existing system, integral and semi-integral abutments, has been identified by R19A for calibration, but no limit states have been suggested or databases identified.

#### 1.5 Relationship of Project R19B to NCHRP Project 12-83

Several members of the research team were also involved with NCHRP Project 12-83, Calibration of LRFD Concrete Bridge Design Specifications for Serviceability. The goal of the NCHRP 12-83 project was to calibrate the concrete-related SLSs currently in the *AASHTO LRFD* (2012) and, as needed, to develop new calibrated concrete-related limit states for incorporation into the AASHTO LRFD. Significant overlap exists between the SHRP 2 R19B and NCHRP 12-83 projects in the area of concrete structures. All aspects of the work under NCHRP 12-83 are fully applicable to SHRP 2 R19B. Most of the concrete-related aspects of this report were originally developed in NCHRP 12-83 and are incorporated here.

#### 1.6 Special Challenges Related to SLSs

The ULSs of the *AASHTO LRFD* are calibrated through structural-reliability theory to achieve a certain level of safety. They are intended to achieve similar component proportions to those of the *Standard Specifications for Highway Bridges*. These ULSs do not consider the integration of the daily, seasonal, and long-term service stresses that directly affect long-term bridge performance and subsequent service life.

The current SLSs of the AASHTO LRFD are intended to ensure a serviceable bridge for the specified 75-year design life. These limit states are based on the traditional serviceability provisions of the *Standard Specifications for Highway Bridges*. The SLSs are not calibrated using reliability theory to truly



achieve a determined life with a specific level of certainty because the tools and data to accomplish this calibration were not available to the AASHTO LRFD code writers.

The current AASHTO LRFD SLSs include limits on the following:

- Live load deflection of structures;
- Cracking of reinforced-concrete components;
- Tensile stresses in prestressed concrete components;
- Compressive stresses in prestressed concrete components;
- Permanent deformations of compact steel components;
- Slip of slip-critical friction bolted connections; and
- Settlement of shallow and deep foundations, among others.

The background of the current *AASHTO LRFD* (2012) SLSs is presented in Chapter 2. Some of these SLSs may relate to a specified design life; others do not. Many are presently deterministic, such as limiting the tensile stresses in prestressed concrete components to a level thought to result in a crack-free component. This SLS could be calibrated to achieve a certain probability of a crack-free component, but the calibration would include a service life only in determining the live load the component must resist (e.g., a 75-year live load).

To achieve the objective of developing the appropriate tools, candidate SLSs were evaluated against a set of criteria. This evaluation applied both to the retention of some of the existing SLSs in the AASHTO LRFD and any new limit states developed as part of this project and Project R19A. The criteria include the following:

- **Is the limit state quantitatively and qualitatively meaningful?** Does it tell us something that we can use to maintain a structure in service and continue or extend its service life?
- **Can the limit state be calibrated?** Can we develop limit state functions, such as indicated in Task 3, and develop a means either through the resources of Project R19B or by leveraging the results of Project R19A or the LTBP to determine the data necessary to do a calibration? (When no such data existed, expert elicitation [Delphi process] was used to determine the range of data and the relative importance of certain characteristics in the data, including uncertainty, so that some calibration could proceed.)
- **Does a limit state really relate to the service life rather than to some other characteristic?** For example, the Model Code for Service Life Design specifically states that it excludes fatigue as part of the SLSs (Fédération Internationale du Béton 2006). This exclusion may be in part because this document was developed primarily for concrete structures. The current *AASHTO LRFD* contains fatigue requirements under a separate limit state, the fatigue-and-fracture limit state. The assessment of fatigue life is very much related to

the service life of steel structures. Should this limit state now be transferred to the SLSs? In many ways, fatigue is one of the more quantifiable and calibratable of the SLSs compared with those that may be developed dealing with deterioration of joints, bearings, coatings, and similar structural features.

- **Does it provide a method to evaluate the significance of interventions in extending the service life of the structure component?** Can the proposed limit states distinguish between interventions that slow deterioration and those that effectively halt deterioration for some period of time before it starts again? Can they respond to repairs that restate or increase load-carrying capacity?

Consideration of SLSs requires different input data than ULSs require. In ULSs, the limit state function is defined with two variables: resistance (which is considered constant in time) and loads. For SLSs, a different approach is needed for the following reasons:

- The definition of resistance is very difficult.
- Acceptable performance can be subjective (full life-cycle analysis is required).
- Resistance and load effects can be and often are correlated.
- Load is considered as a function of time, described by magnitude and frequency of occurrence.
- Resistance is strongly affected by quality of workmanship, operation procedures, and maintenance.
- Resistance is subject to changes (mostly but not only deterioration) in time, with difficulty predicting initiation time and time-varying rates of deterioration (e.g., corrosion, accumulation of debris, cracking).
- Resistance can depend on geographical location (climate, exposure to industrial pollution, exposure to salt as a deicing agent, or proximity to the ocean).

In general, the consequences of exceeding SLSs are an order, or even several orders, of magnitude smaller than those associated with ULSs. Thus, an acceptable probability of exceeding an SLS is much higher than for a ULS. If the target reliability index ( $\beta_T$ ) for ULS is  $\beta_T = 3.5$  to  $4.0$ , then for SLS,  $\beta_T = 0.0$  to  $1.0$  might be quite acceptable.

The current *AASHTO LRFD* (2012) considers foundation settlement as an SLS. Foundation SLSs were probably the most difficult issue dealt with in R19B because of the wide range of physical parameters, numerous analytical solutions, and the regional nature of the practice of geotechnical engineering. Bridge foundations and other appurtenant structures such as approach embankments should be designed so that their deformations will not damage the bridge superstructure or other structural elements or ancillary elements such as utilities, which are often attached to bridge structures.

Various aspects of deformations that should be considered in the design of bridges include

- The effect of uneven settlement between various support elements;
- The rotation and horizontal movements of the foundation system affecting movements at the bridge-seat level; and
- Serviceability problems near a bridge abutment, in particular the ubiquitous “bump at the end of the bridge” that affects joint serviceability and abutment performance.

The cumulative effect of these deformations may generate uneven deformations and stresses across a bridge system and its subsystems. In the case of an irregular pattern of settlement, a reversal of stresses may occur in a bridge deck, resulting in the deck cracking at various locations. Cracking allows moisture ingress, initiation of corrosion, and degradation of various bridge elements, resulting in reduced structural integrity. Thus, foundation deformations affect not only the quality of ride and the safety of the traveling public, but also the structural integrity of the bridge and its various components. In addition, such deformations often lead to costly maintenance and repair measures. The service life of a bridge structure, its components, or ancillary elements such as utilities attached to the bridge can be significantly affected by the deformation characteristics of the foundation system.

In addition, it may be found that changes to material or construction specifications are a more effective way to deal with apparent serviceability issues than codified SLSs. This could be the case, for example, with deck cracking, for which changes to mix proportions or the use of curing practices designed to reduce shrinkage may be as effective as limit states based on strain calculations.

The conservative nature of bridge engineering practice leads to one final special challenge for the development and calibration of SLSs. This challenge is that the concern for public safety and the stewardship of public funds often results in a long institutional memory of past unsatisfactory experience. It is often a slow process to recognize when advances in technology or codification have addressed a past problem. In the case of SLSs in particular, which are often subjective, it is difficult to ascertain whether changes to design provisions have resulted in the desired improvement. It is analogous to the axiom that one cannot prove a negative. For example, several years ago major changes were made to the provisions for the design of modular expansion joints, particularly in regard to fatigue. Have these changes solved the problem so that the service life of these joints has been increased to the point that they need not be considered in this project? Has enough experience been gained to know? How much good experience is needed to alter any lingering perceptions based on earlier designs? To the research team, these issues imply that when the results of R19B lead to

a reduced design requirement rather than a new or more stringent requirement, there is an enhanced need to thoroughly and prudently evaluate the design implications.

## 1.7 Serviceability Versus Deterioration

Various researchers have considered deterioration of highway bridges and tried to track change over time for various types of bridge and service conditions (i.e., type of roadway) by using National Bridge Inventory (NBI) condition numbers or a similar state-specific index. Others have tried to relate deterioration to bridge type as the primary variable. Although the general deterioration of the bridge inventory is important from an administrative point of view, the specific impact on load-carrying capacity that might reduce the service life is a microlevel consideration. The various deterioration models are of limited value in that context. Nevertheless, they are part of the current state of the art and can inform an owner’s effort to account for the effects on resistance over time. With that in mind, several deterioration models found in the literature that use information currently available to owners are reviewed in Chapter 4 of this report.

As discussed in Chapter 2, a survey of bridge owners was conducted to identify which bridge components required sufficient periodic maintenance to be a significant factor in their maintenance budgets. The number of times 23 components were cited is shown in Chapter 2, Figure 2.6.

## 1.8 Durability

*Design Guide for Bridges for Service Life* (Azizinamini et al. 2013), a product of SHRP 2 Project R19A, contains guidance for selecting system, subsystems, and components of bridges believed to promote long life. That information is not repeated here.

Producing more durable bridges is best achieved through a holistic approach starting with type and location decisions through the entire bridge life to decommissioning. A study for the Alabama DOT that addressed virtually every aspect of the bridge delivery and maintenance system identified 57 factors needed to provide more durable bridges (Ramey and Wright 1994). The DuraCrete report (2000) describes how the ability to quantify the durability and service life of a bridge changes during the design phase, construction phase ending with transfer (handing over), subsequent inspection and assessment phase, and possible repurposing phase. It is pointed out that the designer has the least accurate information about environmental loads, material properties, and quality of the constructed facility than at any other time in the service life of the facility.

Rostam (2005) describes two overarching strategies for addressing durability:

- Strategy A, avoidance (such as use of corrosion-resistant rebar); and
- Strategy B, selection of materials and details to resist deterioration for a given time.

Reliability modeling of deterioration is relevant only for Strategy B, and European researchers have developed some deterioration models and reliability applications for concrete components (DuraCrete 2000). In particular, models have been proposed for corrosion of rebar from salt intrusion and carbonation. Some of the necessary data have been accumulated in Europe.

Freyermuth (2009) lists the following options for achieving extended service life of concrete bridges, although the extension is not quantified:

- Use of high-performance concrete to decrease permeability;
- Use of prestressing to reduce or control cracking;
- Use of jointless bridges, or bridge segments, and integral bridges;
- Use of integral deck overlays on precast concrete segmental bridges in aggressive environments; and
- Selective use of stainless steel reinforcing.

These important strategies may be regarded as high-level decisions that should be made before the detailed numerical design proceeds. Use of noncorrosive deicing and fixed anti-icing spray technology was also noted as an in-service strategy for enhancing concrete deck life, in particular.

It is of interest to consider the number of railroad bridges that have served for over 100 years with minimal maintenance. Although corrosion is often evident in railroad bridges, the severe attack of structural steel and reinforcing steel from deicing salt, in particular, is a major distinction in the deterioration of highway bridges, as is the pounding from truck traffic.

Structures intended to provide at least a 100-year service life must have the following four attributes, which are discussed in detail below:

- Be conceived, sited, and designed to provide an acceptable level of reliability with respect to the natural environment and human-made loads.
- Be properly constructed with suitable materials and details.
- Be provided with adequate control of deck drainage, especially in areas where deicing or environmental salt is applied.
- Be treated with timely preventative maintenance of protective coatings, drainage systems, joints, and bearings.

1. *Acceptable level of reliability with respect to the natural environment and human-made loads.* The particular modification to the AASHTO LRFD proposed in Chapter 7 of this report relates to cracking of reinforced concrete, control of stresses in prestressed concrete, control of fatigue cracking in steel and concrete construction, and settlement. This recommended modification, as well as the endorsement of current practice for limiting stresses due to overloads, will contribute to reduced damage and hence extended service life.

2. *Properly constructed with suitable materials.* The benefits of quality construction are self-evident. Every DOT has construction and material specifications, as well as field and plant inspections, intended to ascertain that those requirements are achieved in the completed project. It is outside the scope of this project to critique those processes. Generally, concrete structures are adversely affected by ingress of salt, which leads to corrosion of embedded steel; chemical attack, such as alkali-silica reactivity and sulfate attack; and scaling, such as that associated with freeze-thaw cycles. Langley (1999) details some of the steps taken to address these issues on the Confederation Bridge. Mirza (2007) summarizes the concrete durability provisions of various Canadian Standards Association specifications.

Some well-accepted durability-enhancing materials and processes are described below. The cost of these enhancements and the benefit achieved vary from state to state and even within a state. Environmental regulations and maintenance and protection of traffic can add tremendously to the total cost of maintenance operations, and these associated costs also vary widely. Therefore, no attempt has been made to quantify cost-benefit characteristics.

- Salt intrusion is slowed by drainage control; providing suitable cover; use of dense, low-permeability concrete (such as high-performance concrete (HPC) and ultra-high-performance concrete); and control of cracking.
- The effects of salt intrusion and depassivation due to carbonation can be mitigated by using corrosion inhibitors, coated reinforcing, bimetallic reinforcement, stainless steel reinforcing, or nonmetallic reinforcement such as fiber-reinforced plastic composites. Without citing cost-benefit specifics, it will generally be found that cost increases with each step in the reinforcing path above.
- Aggregate reactivity issues such as alkali-silica reactivity are usually handled by prescreening possible sources by using laboratory tests to identify susceptibility. Most states have approved sources that largely eliminate aggregate reactivity. Use of low-alkali cement can also reduce susceptibility of a concrete mix.
- Sulfate attack is a result of the growth of minerals caused by reaction of chemicals in the cement with



sulfates in the mix; usually these sulfates are in the water, but they may be in the aggregate. Sulfate attack debonds the aggregate and creates expansive pressure leading to crack or delimitation. The causes and effects are similar to alkali–silica reactivity. Use of Type II, Type V, or blended cement is often indicated as well as use of approved material sources. Factors that reduce permeability are also usually helpful. Detwiler (2008) states that “Maximum limits on the water-cementitious materials ratio, combined with good concreting practices—especially good curing—are even more important to sulfate resistance than the right cement.” ACI 201.2R-08 (ACI Committee 201 2008) provides recommended mix practices for various sulfate concentrations.

- Freeze–thaw cycles can lead to scaling of the concrete surface due to pressure caused by the expansion of water in the concrete. Use of air-entraining, high-strength mixes and low permeability are effective countermeasures, although air entrainment can result in reduced strength and may not be compatible with HPC or high-strength concrete. Use of fly ash can be counterproductive if delayed strength gain exposes the concrete to freezing before sufficient strength has been developed.
- Prestressing contributes to control of salt intrusion by reducing in-service cracking. Although some cracking may result from overloads, thermal gradients, and shrinkage, the cracks will generally close when the causative effect is reduced or eliminated. Beam ends exposed to salt-laden deck drainage have been found to be susceptible to corrosion damage resulting from water entering the beam via the strand ends. Tabatabai et al. (2004) documented the benefit of coating the end 2 ft with sealing materials and concluded that of four tested materials, a polymer resin coating was most effective and easiest to apply.

Modern bridge steels are produced to tight tolerances of strength and element sizes. Toughness varies somewhat more than other properties, but it usually exceeds the minimum specified values, sometimes substantially. Corrosion can have a significant effect on service life if not addressed. From a material point of view there are five general ranges of corrosion susceptibility provided by conventional steel, weathering steel, high-performance steel, 1035 steel (sometimes referred to as semistainless steel), and stainless steel. Improved corrosion resistance and cost increase with each step along the product line. Stainless steel has received little use in bridge construction primarily due to cost. However, it has seen more use in recent years.

Fatigue is an in-service design issue that is virtually unaffected by material choice and seems to be well addressed from the resistance side by current design criteria.

*Properly constructed*, the key descriptor in the second attribute contributing to 100-year bridge service life, carries with it the requirement to provide sufficient field monitoring of construction to ensure that the work is executed within tolerances that are consistent with those assumed in the design. For example, the concrete cover is one of the major factors related to the rate of chloride intrusion and carbonation, yet it is difficult to control in the field unless suitable spacers are provided and the rebar cage, tendon ducts, and so forth are sufficiently tied to maintain their position during concrete placement. Proper consolidation, curing, and water control are critical, especially in regard to cracking and permeability. This requires vigilance by laborers, supervisors, and inspectors.

3. *Providing adequate control of deck drainage*. Damage caused by deck drainage, particularly salt-laden drainage, has been a major cause of deterioration in both steel and concrete bridges. The reduction in the number of deck joints through the use of continuous construction, combined with the widespread use of coated reinforcing, has reduced the impact of this problem. Although fully integral bridges have eliminated all deck joints, many bridges are still designed with some joints. In addition, most existing bridges contain joints, and they will be in use for a long time.
4. *Timely preventative maintenance of protective coatings, drainage systems, joints, and bearings*. Preservation of coating systems is probably the most important step in the preservation of painted steel bridges and contributes to reduced permeability of concrete surfaces. Weathering steel bridges often have the area under and adjacent to deck joints coated, in which case preservation of that coating is as important as maintaining the coating system on painted steel bridges.

Maintenance of joints, troughs, and drainage hardware helps to control the flow of deck drainage to reduce deterioration of bearings, girders pier caps, and abutments. The use of continuity and integral and semi-integral abutments has been found to be effective in drainage control.

Washing of bridges is usually thought to be a cost-effective means of bridge maintenance. However, Klaiber et al. (2004) found that for bridges on secondary roads, after 10 years deck washing did not produce significant improvement in deck durability.

The effects of degradation were not included in the reported calibrations. It is assumed that maintenance will take place before deterioration significantly affects service load response. Further, the deterioration that might affect service response (other than appearance issues, which

could be considered an SLS for some bridges) could be quite different from that which affects deflection, vibrations, concrete cracking, and so forth. The condition of the bridge can be included as a change to resistance at a given point in time, and reliability indices can be recalculated on that basis.

Although details, materials, and techniques that are anticipated to increase service life can be identified, the quantification of that increased life, or the change in reliability, is not generally possible at this time. An exception may be the rates of chloride ingress and carbonization for uncracked concrete under conditions similar to those in laboratory testing. For example, Fick's Second Law of Diffusion has been used to estimate the time until chlorides reach a threshold value at reinforcement in the Confederation Bridge given cover, a diffusion constant, and a chloride content.

Rostam (2005) lists the following parameters required to determine mix design qualities to provide a target service life:

- The design surface chloride concentration;
- The background chloride concentration foreseen in the concrete mix;
- The chloride diffusivity;
- The critical chloride concentration triggering corrosion of the reinforcement (the threshold value); and
- The aging factor, represented by a decreasing diffusion coefficient with increasing age.

Procedures are available (DuraCrete 2000) to develop a distribution of time to reach the threshold for a given cover from which the criteria exceedances, and hence a reliability index, can be found.

To date this approach has not been widely used. Development of various parameters for regional or local material sources and concrete mixes would probably be needed for wide application.

## 1.9 Initial Coordination with FHWA Long-Term Bridge Performance Program

As indicated above, very little usable data have been found for use in developing and calibrating SLSs. FHWA recently initiated the long-term bridge performance program (LTBPP), which is intended to measure response factors for in-service bridges for as long as 20 years. This project could collect data needed for future development and improved calibration of SLSs, possibly even a full probabilistic approach. Task 8 in Phase 2 of this project requires that the R19B research team establish a dialogue with the LTBPP research team. SHRP 2 staff asked that this dialogue be started earlier, and a joint

project coordination meeting was held in the autumn of 2009. Both teams recognized the benefit that could result from an open sharing of information and data needs. An initial list of worthwhile types of data that the LTBPP team might consider measuring in the bridges they will be instrumenting was presented to the LTBPP team for their consideration:

- Put survey targets on substructures (piers and abutments), preferably starting with a bridge under construction, using some sort of laser monitoring to determine displacements and rotations with time. Possible foundation monitoring points were discussed with the LTBPP team.
- Try to measure the relative and absolute movement between substructure and superstructure.
- Collect data on the rate of aging of joints and bearings, including debris collection and initiation of leaking.
- Collect data on vehicular damage to joints.
- Try to collect data on traffic patterns, including convoying and lane usage.
- Measure relative movements at and across joints, similar to what bridge inspection teams sometimes measure (sometimes hard to relate to temperature).
- Try to monitor longitudinal forces in structures. This could apply to the design of joints and bearings, as well as columns and foundations.
- Try to determine if there is any in-service way to monitor change in friction with age and wear of expansion joints and bearings.
- Try to monitor pavement growth and effectiveness of cycle control joints.
- Assess corrosion loss or other elements of resistance change.
- Monitor coating deterioration.
- Try to measure something on jointless bridges involving the potential for pier damage or movements of integral and semi-integral abutments, pressure behind abutments, and movements and stresses in the piles of integral and semi-integral abutments.
- Start to assemble data on the variability of prestress camber.
- Monitor possible development of cracks in prestressed concrete beams and relate to overloads and environmental factors.
- Monitor regional thermal gradients in superstructures, as well as large exposed box members such as tie girders and ribs. Verify Imbsen's NCHRP study and extend to steel.
- Monitor salt ingress regionally and relate to application rate and structural parameters.

In order to remain in active contact with the LTBPP team, the R19B principal investigator accepted a position on the Transportation Research Board's Long-Term Bridge

Performance Committee. In addition, one of the coprincipal investigators has been associated with LTBPP virtually throughout the project and is now technical director of the project.

### **1.10 Dialogue with AASHTO HSCOBS and Others**

Numerous presentations were made to keep the bridge community apprised of issues related to Project R19B, to seek information for the project, and to gauge reactions of owners to potential new design requirements.

Venues included the following:

- The AASHTO Technical Committees: T-5 (Loads and Load Distribution) in 2011 and 2012; T-10 (Concrete Design) in 2012 and 2013; T-14 (Steel Design) in 2010, 2011, 2012, and 2013; and T-15 (Foundations) in 2012, as well as the full HSCOBS meeting in 2009, 2010, 2011, and 2012
- The 2012 Annual Meeting of the National Transportation Board in Washington, D.C.
- The 2010 Annual Meeting of the Prestressed Concrete Institute in Philadelphia, Pennsylvania
- The International Association for Bridge Maintenance and Safety meeting, 2012
- The U.S.–China Seminar on Highway Technology in Beijing, 2012
- The SHRP 2–Forum of European National Highway Research Laboratories Joint Symposium in Brussels, Belgium, 2010
- The poster session at the 2009 Annual Meeting of the National Transportation Board in Washington, D.C.

## CHAPTER 2

# Current State of the Art

### 2.1 Approach

As part of Phase 1, an assessment of the current state of the art related to service limit states (SLSs) was conducted as follows:

- A review of technical literature was conducted and is summarized in Section 2.2.
- A survey was made of the requirements for SLSs in several modern bridge design specifications, including the American Association of State Highway and Transportation Officials' (AASHTO) *AASHTO LRFD Bridge Design Specifications*. This survey included reconstructing the background of the existing SLS requirements. Much of the detail on concrete requirements was developed under NCHRP Project 12-83 after initial identification was made in SHRP Project R19B. This approach is consistent with the relationship between these projects as introduced in Chapter 1. The requirements of the *Eurocode* and the *Canadian Highway Bridge Design Code (CHBDC)* (2006) were also reviewed, and significant clauses are summarized here.
- A survey of owners and some industry groups was conducted by the R19B research team. Surveys were also conducted by the R19A and NCHRP 12-83 teams. The survey results obtained by the R19B team are discussed in detail in Section 2.4.1, and the results obtained during NCHRP 12-83 and those obtained during R19A that relate to R19B are summarized in Sections 2.4.2 and 2.4.3, respectively.

### 2.2 Summary of Literature Survey

Results of the literature survey as they relate to the current requirements in various design specifications are summarized in Section 2.3.

#### 2.2.1 Serviceability, SLS, Deterioration, and Maintenance in the Technical Literature

A limited survey was made of sources readily available at Modjeski and Masters and on the Internet to investigate the range of issues and phenomena various organizations associate with the terms *serviceability*, *SLS*, *deterioration*, and *maintenance*. The results are listed in the following subsections.

##### Serviceability

- Merriam-Webster (2010)—Fit for use, of adequate quality (comes from definition for serviceable).
- Wikipedia (2010)—Conditions under which a structure is still considered useful.
- *Manual for Bridge Evaluation* (2008)—A term that denotes restrictions on stress, deformation, and crack opening under regular service conditions.
- *Steel Construction Manual* (2011)—A state in which the function of a building, its appearance, maintainability, durability, and comfort of its occupants are preserved under normal usage.
- *ASCE/SEI 7-10: Minimum Design Loads for Buildings and Other Structures* (2010)—Structural systems, and members thereof, shall be designed to have adequate stiffness to limit deflections, lateral drift, vibration, or any other deformations that adversely affect the intended use and performance of buildings and other structures.
- *2006 Seattle Building Code* (International Code Council 2007)—Structural systems and members thereof shall be designed to have adequate stiffness to limit deflections and lateral drift as set by code writing bodies such as the American Concrete Institute (ACI), the American Institute of Steel Construction (AISC), and the International Building Code (IBC).

- *Eurocode (EN 1992-2 2005)*—Perform adequately under all expected actions.
- *ISO 2394 (1998)*—Ability of a structure or structural element to perform adequately for normal use under all expected actions.

### Service Limit State

- Wikipedia (2010)—Fails to meet technical requirements for use while remaining strong enough to stand (serviceability limit).
- *Manual for Bridge Evaluation (2008)*—Limit state relating to stress, deformation, and cracking.
- *AASHTO LRFD (2012)*
  - Service I—Deflection control, crack-width control in R/C members, slope stability;
  - Service II—Control yielding of steel structures, slip of slip-critical connections;
  - Service III—Crack control in prestressed concrete members;
  - Service IV—Relating to tension in prestressed concrete columns with the objective of crack control;
  - Deformations—Article 2.5.2.6;
  - Concrete—Cracking, deformation, and concrete stresses specified by Articles 5.7.3.4, 5.7.3.6, and 5.9.4;
  - Steel—Permanent deformations due to localized yielding that would impair rideability under severe traffic loadings as specified by Articles 6.10.4.2 and 6.11.4; and
  - Decks—Deck deformation (9.5.2).
- *AISC Steel Design Guide 3 (2003)*—Define the functional performance of the structure (should be met), involve response of people and objects to the behavior of the structure under load.
- *AISC Steel Construction Manual (2011)*—Limiting condition affecting the ability of a structure to preserve its appearance, maintainability, durability or the comfort of its occupants or function of machinery, under normal usage.
- *ASCE/SEI 7-10: Minimum Design Loads for Buildings and Other Structures (2010)*—Conditions in which the functions of a building or other structure are impaired because of local minor damage or deterioration of building components or because of occupant discomfort or annoyance.
- *2006 Seattle Building Code (International Code Council 2007)*—A condition beyond which a structure or member becomes unfit for service and is judged to be no longer useful for its intended function.
- *Eurocode (EN 1992-2 2005)*—Associated with conditions of normal use, concerned with the performance of structure or part of structure, comfort of people, and appearance of structure.
- *CHBDC (2006)*—See Section 2.3.3.
- *ISO 2394 (1998)*—A state that corresponds to conditions beyond which specified service requirements for a structure or structural element are no longer met.
  - Local damage (includes cracking) that may reduce the working life of the structure or affect the efficiency or appearance of structural or nonstructural elements;
  - Unacceptable deformations that affect the efficient use or appearance of structural or nonstructural elements or functioning of equipment; and
  - Excessive vibrations that cause discomfort to people or affect nonstructural elements or functioning of equipment.
- *International Federation for Structural Concrete (fib) Bulletin 34 (Fédération Internationale du Béton 2006)*—States that correspond to conditions beyond which specified service requirements for a structure or structural member are no longer met.
- Louisiana Department of Transportation and Development *LRFD Bridge Design Manual (2006)*—Stress, deformation, and crack width are limited under service conditions.
  - Pile foundations—settlement and horizontal movement.
- West Virginia Department of Transportation (DOT), Division of Highways, *Bridge Design Manual (2006)*—Covers cracking, deformations, deflections and concrete stresses.

### Deterioration

- Merriam-Webster (2010)—Action or process of deteriorating (*deteriorating* defined as “to make inferior in quality or value”).
- Wikipedia (2010)—To make worse.
- *CHBDC (2006)*—Includes corrosion.
- U.S. Army Corps of Engineers *Coastal Engineering Manual (2002)*—Gradual aging of the structure and or its components over time.
- *Bridge Inspector’s Reference Manual (2002)*—Definition: decline in quality over a period of time due to chemical or physical degradation.
- *Bridge Inspector’s Reference Manual (2002)*—Types of deterioration for different materials.
  - Timber.
    - Natural defects—checks, splits, shakes, fungi, and insects;
    - Chemical—acids, bases or alkalis; and
    - Other types—delamination, loose connections, surface depressions, fire, impact or collisions, abrasion or mechanical wear, overstress, weathering or warping, protective coating failure.
  - Concrete.
    - Reinforced concrete—cracking, scaling, delamination, spalling, chloride contamination, efflorescence, ettringite formation, honeycombs, pop-outs, wear, collision damage, abrasion, overload damage;



- Prestressed concrete—structural cracks, exposed prestressing tendons, corrosion of tendons in bond zone, loss of camber due to creep or prestress losses;
- Reinforcement—corrosion; and
- Causes—temperature fluctuation, chemical attack, moisture absorption, differential foundation movement, design and construction deficiencies, fire.
- Steel—corrosion, fatigue cracking, overloads, collision, heat, paint failures;
- Concrete decks—cracking, scaling, delamination, spalling, efflorescence, honeycombs, pop-outs, wear, collision damage, abrasion, overload damage, reinforcement corrosion, prestressed concrete deterioration; and
- Steel decks—bent, damaged, or missing members; corrosion, fatigue cracks, other stress-related cracks.

### Maintenance

- Merriam-Webster (2010)—The upkeep of property or equipment.
- Wiktionary (2010)—Actions performed to keep a system or machine functioning or in service.
- Eurocode (EN 1992-2 2005)—Under “Use and Maintenance”: Monitoring performance, inspection for deterioration or distress, investigation of problems, and certification of work.
- Ontario Traffic Manual: Book 5: Regulatory Signs (2000)—The upkeep of highways, traffic control devices, other transportation facilities, property, and/or equipment.
- CHBDC (2006)—Under “Inspection and Maintenance” of commentary: Without routine inspection, maintenance, repair or rehabilitation it is unlikely that any structure will achieve its design life.
- U.S. Army Corps of Engineers’ Coastal Engineering Manual (2002)—Recognize potential problems and take appropriate action to assure project continues to function at acceptable level.
- Bridge Inspector’s Reference Manual (2002)—Basic repairs performed on a facility to keep it at an adequate level of service.
- ISO 2394 (1998)—Total set of activities performed during the design working life of a structure to enable it to fulfill the requirements for reliability.
- fib Bulletin 34 (Fédération Internationale du Béton 2006)—Set of activities that [is] planned to take place during the service life of the structure in order to fulfill the requirements of reliability.
- Maryland Manual on Uniform Traffic Control Devices for Streets and Highways (2006)—Activities performed to retain the legibility and visibility of the device, and to retain proper functioning of the device.
- Ohio DOT Bridge Design Manual (2007)—Keeping all portions in good condition with regard to strength, safety, and rideability.

There is broad similarity in the use of the terms investigated, especially for *maintenance* and *deterioration*, with the *Bridge Inspector’s Reference Manual* providing much more detail, as would be expected. The term *serviceability* generally relates to high-level statements on structural behavior. SLS ranges from generalities to very specific quantitative requirements, although most of the surveyed sources deal with vibrations, deflections including foundation settlement, user comfort, and cracking.

There is little mention of appearance-related issues such as rusting of steel or cracking or discoloration of concrete in relation to serviceability.

Generally, the SLSs currently specified in AASHTO LRFD consider most of the behaviors found in this part of the literature survey. This does not preclude the improvement of functionality through calibration, nor the possibility that new limit states might be identified through other aspects of the literature search reported in this section; more extensive evaluation of the state of the art summarized in Sections 2.2 and 2.3; the results of surveys reported in Section 2.4; or the experience of the research team.

### 2.2.2 Search for SLSs not yet Implemented

Several reports were reviewed to determine whether any additional SLSs should be considered when designing bridges. The additional information was meant to supplement the literature review performed as part of SHRP 2 Project R19A. Reports were gathered from sources such as the National Cooperative Highway Research Program, the Federal Highway Administration, the *ACI Structural Journal*, American Concrete Institute (ACI) committee documents, and conference proceedings of the Structures Congress and the American Society of Civil Engineers (ASCE).

The investigated reports pertained to establishing foundation limit states, concrete cracking of beams and bridge decks, concrete shrinkage, fatigue of prestressed concrete members, and methods of controlling vibration. Each report was reviewed to determine the usefulness of the information. Any methods that could potentially be used in creating new SLSs were noted and investigated further.

Many sources provided information that was too general to be useful, with many of the discussed methods for reducing serviceability issues relating to nonstructural aspects of the design process, which would not be useful in calibrating limit states. Some of the sources, however, provided useful methods of anticipating and determining the effects of serviceability issues such as crack width, crack spacing, and prestressed concrete fatigue.

Bridge-related research problem statements are reviewed annually by Technical Committee 11 of the Highway Subcommittee on Bridges and Structures. It was thought that a review

of these documents could show a need for additional SLSs that were not approved for funding but may still be worthwhile in the context of this project. However, there is apparently no archive of old research problem statements.

### 2.2.3 Joints and Bearings

The design lives of bearings and expansion joints are important with regard to the serviceability of bridges. With the exception of deck deterioration, poor performance of these components probably results in most of the deterioration and maintenance activities on typical bridges. Even a cursory investigation into the design life of these components showed widely varying results.

Several codes and design guides included expected lives of bearings:

- *fib Bulletin 34*—10 to 25 years (Fédération Internationale du Béton 2006).
- Queensland Government *Main Roads Specification MRS81: Bridge Bearings* (2012), Section 6.3—100 years for Exposure Classification B1, design life for bearings in Second Gateway Bridge (Outokumpu 2013). The steps involved to achieve a specified service life include
  - Definition of the characteristics of the environment;
  - Identification of the potential deterioration mechanisms in that environment;
  - Determination of the likely rate of deterioration;
  - Assessment of the material life;
  - Definition of the required material performance;
  - Consideration of a probabilistic approach to the variability of the relevant parameters; and
  - Assessment and definition of the need for further protection.
- *Steel Bridge Bearing Selection and Design Guide* (1996)—Shorter than that of other bridge elements.
- Japan (Itoh and Kitagawa 2001)—25 to 35 years with an average replacement at 30 years (these values are estimated to determine life-cycle cost).
- Indian Railways Institute of Civil Engineering (*Bridge Bearings* 2006)—Attempt to specify a bearing with an expected life similar to that of the bridge.

Project R19A completed a survey of state DOTs with regard to their experiences with bearings. The results from their interim report are summarized below:

- Elastomeric—15 to 50 years experienced, 50 to 75 expected.
- Polytetrafluoroethylene—20 to 50 years experienced, 20 to 75 expected.
- Cotton duck—35 to 50 years experienced, 75 expected.

- High-load multirotational—For pots, 10+ years experienced; for other high-load multirotational, 15 to 40 years experienced, 30 to 75 expected.
- Fabricated steel—15 to 100 years experienced, 50 to 75 expected.

In addition to the suggested or expected design service life of bearings proposed by various design manuals or industry publications, bearing manufacturers also provided expected life for their products. The expected life of the bearing depends on the manufacturer and the quality of installation, but is typically within the range of 20 to 80 years. Maurer Söhne (2011) suggests that their MSM sliding bearings provide a service life of up to 80 years. Agom International, srl. (2013) and D.S. Brown (Kaczinski 2008) suggest a service life of more than 50 years for their pot bearings and steel-reinforced elastomeric bearings, respectively. Technoslide (2013) provides documentation on plain bearings manufactured by Bearing Technologies that suggests a service life of 20 to 40 years for elastomeric bearings; stainless steel, polytetrafluoroethylene, and CSB-10 bearings have a life that is assumed to match the life of the bridge. CSB-10 is a proprietary material manufactured by CSB Bearings Co.

The service life for expansion joints has been examined by at least two agencies within the United States. Reports summarizing estimated service life along with a minimum and maximum estimate were developed. The results are shown in Table 2.1 (Indiana sent out two surveys; the results of both surveys are included in the table).

Several other organizations and projects have also looked into the service life of expansion joints. The Bridge Joint Association (2010) suggests that the service life of the expansion joint should equal the service life of adjacent surfaces. The same life-cycle cost analysis completed in Japan (Itoh and Kitagawa 2001) for bearings also suggested the service life of expansion joints as 15 to 25 years, with the average being 20 years. NCHRP Synthesis 319 (Purvis 2003) noted that in Florida elastomers used in joint seals must provide a service life warranty for a minimum of 5 years. Research completed as part of Project R19A (AASHTO 2013) shows the following for estimates of service lives:

- Field molded joints—1 to 3 years.
- Strip seal joints—3 to 30 years.
- Compression seal joints—3 to 30 years (also listed as 2 to 20 years).
- Finger plate joints—10 to 50 years.
- Modular expansion joints—10 to 50 years.

As joints and bearings typically have service lives much less than the 100-year criterion for this project, these elements were not calibrated, but instead should be designed to be

**Table 2.1. Service Life of Expansion Joints**

Joint Type	Arizona			Indiana		
	Mean	Min	Max	Mean	Min	Max
Pourable seals	11.5	4	30	5.2, 5.6	1, 0	15, 20
Compression seals	12.7	5	25	11.7, 10.3	0, 2	20, 20
Strip seals	18.0	8	30	11.9, 10.9	0, 1.5	20, 25
Finger or slide plate joints	28.1	10	75	—	—	—
Modular joints	19.2	10	25	—	—	—
Integral abutments	50.9	15	100	8.7, 7.3–9.8	0, 1.5	20, 15–20
Polymer-modified asphalt	—	—	—	3.5, 5.7–5.8	1, 0–1.5	10, 10–20

Note: — = not available.

Sources: For Arizona, *Evaluation of Various Types of Bridge Deck Joints* 2006; for Indiana, Chang and Lee 2001.

replaceable. Expansion joint manufacturers also provided estimates of service life for their products. One modular expansion joint manufactured by Maurer provides an estimated service life of 40 years and 20 years for replaceable components. D.S. Brown (Kaczinski 2008) notes that soft joints (silicone–urethane and asphaltic plug joints) have a life expectancy of less than 5 years. Miska (2013) noted that their neoprene compression seal has over 30 years of proven durability.

## 2.3 Serviceability Requirements in Several Modern Bridge Design Specifications

### 2.3.1 AASHTO LRFD

The current *AASHTO LRFD* (2012) SLSs include limits on

- Live load deflection of structures.
- Fatigue of steel and concrete details.
- Cracking of reinforced-concrete components.
- Tensile stresses in prestressed concrete components.
- Compressive stresses in prestressed concrete components.
- Settlement of shallow and deep foundations.
- Permanent deformations of compact steel components.
- Slip of slip-critical friction bolted connections.

Design provisions are specified either in the resistance sections or Section 3 of *AASHTO LRFD*. The design load combinations in *AASHTO LRFD* are presented in Table 3.4.1-1. As stated in Chapter 1, these SLSs and the associated load and resistance factors are based on apparent successful past practice and have not been subject to a reliability-based calibration. There are no consistent performance levels associated with these limit states, although some are associated with differences in environmental or traffic exposure.

As decisions were made as to the retention or modification of the current *AASHTO LRFD* provisions, background information for the current SLSs is provided below.

### Settlement of Shallow and Deep Foundations

Serviceability aspects of foundations and walls are related to the deformation characteristics of geomaterials and structural elements. In the current *AASHTO LRFD* (2012), Section 10 (Foundations) and Section 11 (Abutments, Piers, and Walls) present a variety of formulations for estimating deformation of foundations and walls. These formulations are not consistent in the sense that they range from theoretical, semiempirical formulations to charts based on measured deformations. For example, the vertical settlement of spread footings is based on Hough's (1959) method, which is largely a theoretical method, but the settlement of pile groups is based on a choice of one of four idealized cases that use Hough's method. In contrast, the lateral deformations of retaining walls are based on semiempirical methods and charts. Such approaches are adopted for all types of foundations and walls in Sections 10 and 11 of *AASHTO LRFD*. Although this wide range of approaches is understandable given that foundation design is more an art based on observations than a science, it created a challenge in the context of SLS calibration using a consistent basis. The calibration processes proposed for geotechnical features in Chapter 6 could be considered to establish a consistent framework for foundations and walls. An example of this approach is demonstrated for vertical settlement of spread footings.

#### TOLERABLE VERTICAL DEFORMATION CRITERIA

From the viewpoint of serviceability of a bridge structure, the geotechnical limit states relate to foundation deformations. Uneven displacements of bridge abutments and pier



foundations can affect the ride quality, functioning of deck drainage, and the safety of the traveling public, as well as the structural integrity and aesthetics of the bridge. Such movements often lead to costly maintenance and repair measures. However, overly conservative criteria can be wasteful. Determination of deformation criteria should be a collaboration between the geotechnical engineer and the structural engineer to find the optimum solution. Within the context of foundation deformation, the geotechnical limit states can be broadly categorized into vertical and horizontal deformations for any foundation type (e.g., spread footings, driven piles, drilled shafts, or micropiles).

Agencies often limit the deformation to values of 1 in. or less without any rational basis. The literature survey revealed that the only definitive rational guidance related to the effect of foundation deformations on bridge structures is based on a report by Moulton et al. (1985). From an evaluation of 314 bridges nationwide, the report offered the following conclusions:

The results of this study have shown that, depending on type of spans, length and stiffness of spans, and the type of construction material, many highway bridges can tolerate significant magnitudes of total and differential vertical settlement without becoming seriously overstressed, sustaining serious structural damage, or suffering impaired riding quality. In particular, it was found that a longitudinal angular distortion (differential settlement/span length) of 0.004 would most likely be tolerable for continuous bridges of both steel and concrete, while a value of angular distortion of 0.005 would be a more suitable limit for simply supported bridges (Moulton et al. 1985).

Another study states the following:

In summary, it is very clear that the tolerable settlement criteria currently used by most transportation agencies are extremely conservative and are needlessly restricting the use of spread footings for bridge foundations on many soils. Angular distortions of 1/250 of the span length and differential vertical movements

of 2 to 4 in. (50 to 100 mm), depending on span length, appear to be acceptable, assuming that approach slabs or other provisions are made to minimize the effects of any differential movements between abutments and approach embankments. Finally, horizontal movements in excess of 2 in. (50 mm) appear likely to cause structural distress. The potential for horizontal movements of abutments and piers should be considered more carefully than is done in current practice. (Wahls 1983)

AASHTO *LRFD* used data from Moulton et al. (1985) and Wahls (1983) to produce the guidance summarized in Table 2.2 for the evaluation of tolerable vertical movements in terms of angular distortions.

The criteria in Table 2.2 suggest that for a 100-ft span, a differential settlement of 4.8 in. is acceptable for a continuous span, and 6 in. is acceptable for a simple span. These relatively large values of differential settlement create concern for structural designers, who often arbitrarily limit tolerable movements to one-half to one-quarter of the values listed in Table 2.2 or develop guidance such as that shown in Table 2.3.

Another example of the use of more stringent criteria is from Chapter 10 of the *Arizona Department of Transportation (ADOT) Bridge Design Guidelines* (2009), which states the following:

The bridge designer should limit the total settlement of a foundation per 100 ft span to 0.5 in. Linear interpolation should be used for other span lengths. Higher total settlement

**Table 2.2. Tolerable Movement Criteria for Highway Bridges (AASHTO LRFD 2012)**

Limiting Angular Distortion, $\delta/L$ (radians)	Type of Bridge
0.004	Multiple-span (continuous-span) bridges
0.008	Simple-span bridges

**Table 2.3. Tolerable Movement Criteria for Highway Bridges (Geotechnical Design Manual 2012)**

Total Settlement at Pier or Abutment	Differential Settlement over 100 ft Within Pier or Abutments and Differential Settlement Between Piers (Implied Limiting Angular Distortion, radians)	Action
$\delta \leq 1$ in.	$\delta_{100\text{ft}} \leq 0.75$ in. (0.000625)	Design and construct
1 in. < $\delta \leq 4$ in.	0.75 in. < $\delta_{100\text{ft}} \leq 3$ in. (0.000625–0.0025)	Ensure structure can tolerate settlement
$\delta > 4$ in.	$\delta_{100\text{ft}} > 3$ in. (>0.0025)	Need departmental approval

limits may be used when the superstructure is adequately designed for such settlements. The designer shall also check other factors such as rideability and aesthetics. Any total settlement that is higher than 2.5 in, per 100 ft span, must be approved by the ADOT Bridge Group.

Although from the viewpoint of structural integrity there are no technical reasons for structural designers to set arbitrary additional limits to the criteria listed in Table 2.2, there are often practical reasons based on the tolerable limits of deformation of other structures associated with a bridge, such as approach slabs, wingwalls, pavement structures, drainage grades, utilities on the bridge, and deformations that adversely affect ride quality. Thus, the relatively large differential settlements based on Table 2.2 should be considered in conjunction with functional or performance criteria not only for the bridge structure but also for all associated facilities. Samtani and Nowatzki (2006) suggest the following steps in this regard:

1. *Identify all possible facilities associated with the bridge structure and the tolerance of those facilities to movement.* An example of a facility on a bridge is a utility (e.g., gas, power, or water). The owners of the facility can identify the tolerance of their facility to movements. Alternatively, the facility owners should design their facilities for the movements anticipated for the bridge structure.
2. *Due to the inherent uncertainty associated with estimated values of settlement, determine the differential settlement by using conservative assumptions for geomaterial properties and prediction methods.* It is important that the estimation of angular distortion be based on a realistic evaluation of the construction sequence and the magnitude of loads at each stage of the construction sequence.
3. *Compare the angular distortion from Step 2 with the various tolerances identified in Step 1 and in Table 2.2.* Using this comparison, identify the critical component of the facility. Review this critical component to check if it can be relocated or if it can be redesigned to more relaxed tolerances. Repeat this process as necessary for other facilities. In some cases, a simple resequencing of the construction of the facility based on the construction sequence of the bridge structure may help mitigate the issues associated with intolerable movements.

This three-step approach can be used to develop project-specific limiting angular distortion criteria that may differ from the general guidelines listed in Table 2.2. For example, if a compressed-gas line is fixed to a simple-span bridge deck and the gas line can tolerate an angular distortion of only 0.002, then the utility will limit the angular distortion value for the bridge structure, not the criterion listed in Table 2.2. However, this problem is typically avoided by providing

flexible joints along the utility such that it does not control the bridge design.

#### *TOLERABLE HORIZONTAL DEFORMATION CRITERIA*

Horizontal deformations cause more severe and widespread problems for highway bridge structures than do equal magnitudes of vertical movement. Tolerance of the superstructure to horizontal (lateral) movement will depend on bridge seat or joint widths, bearing type(s), structure type, and load distribution effects. Moulton et al. (1985) found that horizontal movements less than 1 in. were almost always reported as being tolerable, while horizontal movements greater than 2 in. were typically considered to be intolerable. On the basis of this observation, Moulton et al. (1985) recommended that horizontal movements be limited to 1.5 in. The data presented by Moulton et al. (1985) show that horizontal movements resulted in more damage when accompanied by settlement than when occurring alone.

#### **Limitations on the Live Load Deflection of Structures**

The current requirements for live load deflection limits in the AASHTO LRFD have their roots in the corresponding provisions of the *Standard Specifications for Highway Bridges*, 17th ed. (2002). These provisions have been reviewed repeatedly. Summaries by Wright and Walker (1972), Roeder et al. (2002), and Barker and Barth (2007) are often referenced.

The ASCE Committee on Deflection Limitations of Bridges of the Structural Division (1958) reported on their examination of the live load deflection limits and depth-to-span ratios in the 1953 American Association of State Highway Officials (AASHTO) *Standard Specifications for Highway Bridges*. The earliest deflection limits were adopted in 1871 by the Phoenix Bridge Company, which limited deflection to 1/1,200 of the span length for a train moving 30 mph. The American Railway Engineering Association (AREA) adopted depth-to-span ratios in the early 1900s, although the limits were without basis. Depth-to-span ratios for highway bridges were initially set forth in 1913 and adopted by AASHTO in 1924. Vibrations became an issue in the 1930s, and the Bureau of Public Roads attempted to provide a correlation between the bridges with vibration problems and bridge properties. The result was limiting deflections to L/800 for simple and continuous spans without pedestrians, L/1,000 for simple and continuous spans with pedestrians, and L/300 for cantilevered spans. The ASCE Committee surveyed state highway departments to obtain data on the behavior of bridges and the views of experienced bridge designers. The conclusions of the survey included the following: maximum oscillations occur with passage of medium-weight vehicles, not heavy vehicles; reports of objectionable vibrations came from continuous-span bridges more often

than simple-span bridges; and there is no defined level of vibration that constitutes being undesirable. The vibration of the bridge is affected by the following quantities:

- Bridge flexibility and associated natural frequency.
- Flexibility of vehicle suspension and associated natural frequency.
- Relative weight of vehicles and bridge.
- Vehicle speed.
- Profile of approach roadway and bridge deck.
- Frequency of load application.
- Motion caused by loads in adjacent spans of continuous-span structures.
- Damping characteristics of bridge and vehicle.

The use of depth-to-span ratios began in the early 1900s with the American Railway Engineering and Maintenance of Way Association (AREMA) (at that time AREA) specification that pony trusses and plate girders should have a depth not less than 1/10 of the span length. These ratios have changed little over the years. The current depth-to-span limits are 1/10 for trusses and 1/12 for rolled shapes and plate girders.

The early specifications for highway bridges adopted with some modification the depth-to-span ratios from AREMA. The changes in depth-to-span ratios for highway bridges are shown in Table 2.4 for selected time periods.

Both AREMA and AASHTO specifications included statements that required flanges to be strengthened if section depths smaller than those required by the limiting depth-to-span ratio were used.

The use of depth-to-span ratios was primarily to limit deflections, but it was also driven by economics. The limiting values of depth-to-span ratios have decreased with time, while allowable stresses have increased. This would result in shallower sections being used, which would result in larger deflections. This result confused the ASCE Committee on Deflection Limitations of Bridges of the Structural Division, which was tasked with investigating the origins of the deflection and depth-to-span limits. The committee quoted the 1905 AREA Committee's explanation of their depth-to-span ratios: "We established the rule because we could not agree on

any. Some of us in designing a girder that is very shallow in proportion to its length decrease the unit stress or increase the section according to some rule which we guess at. We put that in there so that a man would have a warrant for using whatever he pleased."

The report concluded that the reasons for the two criteria, deflection limit and depth-to-span ratio, are of different origin. The deflection limit is to limit undesired vibration, but the depth-to-span ratio is a result of economics. In addition, the report writers could not provide recommendations as to what constitutes undesirable deflection or vibration or how best to limit deflections or vibrations. The ASCE Committee had minor modifications, but due to the empirical nature of the current limits, they believed that they could not suggest the revisions. They also believed that the then-current limits were sufficient until further test data became available, but that girders with composite action should be limited to smaller deflections.

In U.S. practice, the deflection of bridges supporting vehicular traffic is generally limited to the span length divided by 800 for simple spans and continuous spans and divided by 300 for cantilever arms. The specifications have placed further limits on bridges also intended to carry pedestrian and bicycle traffic. There is little technical support for the efficacy of the current deflection provisions. They are simple to use, but they do not directly relate to the actual issue of concern, namely, the vibration response under live load. Although the quasistatic deflection and dynamic response both involve the stiffness of the bridge, the dynamic response also involves the mass, damping, and the characteristics of the forcing function, which is in turn related to the surface roughness, suspension characteristics of the vehicle, and other parameters.

Wright and Walker (1972) developed a summary of the experience with the deflection limitation provisions in the era during which the bulk of the steel structures were of non-composite construction. Roeder et al. (2002) revisited the subject decades later and suggested that

- the current AASHTO limits are insufficient for control of vibrations and should ultimately be removed;
- the current limit of L/800 for bridges without pedestrians is not always sufficient to control vibrations, but should not be removed as there is insufficient documentation to warrant removing it from the design specifications; and
- the applied loading and use of load factors and distribution factors should be clarified.

Roeder et al. (2002) also suggested immediately removing the L/1,000 deflection limit for bridges with pedestrian access. As alternatives to the deflection limits (L/800 and L/1,000) and until a method for controlling vibration frequency and amplitude is approved by AASHTO, they suggest using the

**Table 2.4. Historic Depth-to-Span Ratios for Highway Bridges**

Year	Trusses	Plate Girders	Rolled Shapes
1913, 1924	1/10	1/12	1/20
1931	1/10	1/15	1/20
1935, 1941, 1949, 1953	1/10	1/25	1/25
2012	1/10	1/25	1/25

equations developed by Wright and Walker (1972) or the criteria provided in the *CHBDC* (2006) for simple-span bridges. Barker and Barth (2007) have compared the procedure in *AASHTO LRFD*, which was intended to provide some uniformity in application, to the specific procedures used in several states. They found wide variations in load, load distribution, and deflection limits. In some states, the individual interpretation is severe enough to frequently control the design, particularly of steel bridges, by a significant margin. A sample of the reported variation follows:

- Bridges without pedestrian access
  - L/1,600 (one state);
  - L/1,100 (one state);
  - L/1,000 (five states); and
  - L/800 (40 states).
- Bridges with pedestrian access
  - L/1,600 (one state);
  - L/1,200 (two states);
  - L/1,100 (one state);
  - L/1,000 (39 states); and
  - L/800 (three states).
- Loads used based on AASHTO load factor design (LFD) requirements
  - HS20 truck only (one state);
  - HS20 truck plus impact (16 states);
  - HS20 lane load plus impact (one state);
  - HS20 truck plus lane load without impact (one state);
  - Larger of HS20 truck plus impact or HS20 lane load plus impact (seven states);
  - HS20 truck plus lane plus impact (17 states);
  - Military or permit vehicles (four states); and
  - HS25 truck (eight states).

Live load deflection is sometimes postulated to be a contributor to the cracking of concrete decks. A sample of the conflicting literature on this issue follows:

- Fountain and Thunman (1987) conducted a study in which they examined the live load deflection criteria for steel girder bridges with concrete decks and how the deflection criteria are associated with cracking of the concrete deck. Cracking can be caused by numerous factors, including plastic shrinkage, deck restraint, drying shrinkage, long-term flexure due to service loads, and repetitive vibrations. The results indicated that the live load deflection criteria did not meet the desired goals, which were strength, durability, and safety of steel bridges. Fountain and Thunman questioned the applicability of the live load deflection criteria as a majority of steel girder bridges are built with composite decks, and composite decks lead to small tensile stresses in the deck. In addition, as bridge stiffness increases,

the stresses in the deck may also increase due to interaction between the deck and girder. The increased stresses may lead to additional cracking or deterioration of the bridge deck. Dynamic response of the bridge is affected minimally by increases in flexibility; the increased flexibility leads to more lateral distribution of the load to adjacent girders.

- Krauss and Rogalla (1996) examined available literature; surveyed 52 transportation agencies in the United States and Canada; and performed research using analytical methods, as well as field and laboratory measurements. The survey was used to develop an understanding of how often transverse cracks are noted in new bridge decks, as well as how they are believed to form. More than 18,000 bridges were analyzed to examine the stresses in the concrete deck. Laboratory testing indicated that concrete mix, environmental conditions during concrete placement, and construction practices significantly affected the formation of transverse cracks. It was also determined that bridge characteristics such as deck geometry and girder type, spacing, and size significantly affect the formation of transverse cracks. It was determined that continuous multigirder steel spans are more susceptible to transverse cracks due to restraint of the deck. Krauss and Rogalla also noted that longer spans are more susceptible to cracking than shorter spans.
- Goodpasture and Goodwin (1971) evaluated whether any relationship existed between deck deterioration and live load deflection. They examined 27 bridges to determine which bridge type had the most cracking. Bridge types included plate girders, rolled shapes, concrete girders, prestressed girders, and trusses. Ten continuous steel girder bridges were evaluated to determine if the stiffness of the bridge influenced transverse cracking. The results indicated no correlation between girder flexibility and amount of transverse cracking.
- Walker and Wright's (1971) analysis indicated that spalling, scaling, and longitudinal cracking are not associated with girder flexibility. Transverse deck moments result in tension along the top surface of the deck, possibly resulting in deck cracking. Increased girder flexibility results in larger positive transverse moments and smaller negative moments resulting in reduced likelihood of deck cracking.
- Nevels and Hixon (1973) examined 195 girder bridges consisting of simple- and continuous-span steel plate and rolled girders and prestressed concrete girders. Span lengths ranged from 40 to 115 ft. They concluded that there was no relationship between flexibility and deck deterioration. Similarly, the Portland Cement Association (1970) presented results of a study in which substantial evidence was collected that indicated flexible bridges, typically steel girder bridges, do not have a greater tendency to exhibit deck cracking damage than other bridge types.



- Barker et al. (2008) examined deflection limits and deflection loadings from various states for a suite of 10 bridges for both LFD and load and resistance factor design methods. The results indicate that states using larger loads and more restrictive deflection limits end up with designs controlled by deflection. To meet the more restrictive deflection limits, a significantly stiffer bridge would be needed. Furthermore, it was noted that the 10 bridges were performing well and had not demonstrated any detrimental effects, either user comfort or structural damage, due to excessive deflections. The suite of 10 bridges would not satisfy the deflection criteria in several states and would require additional steel be added; the additional steel would not be required for strength but rather to meet the deflection criteria.

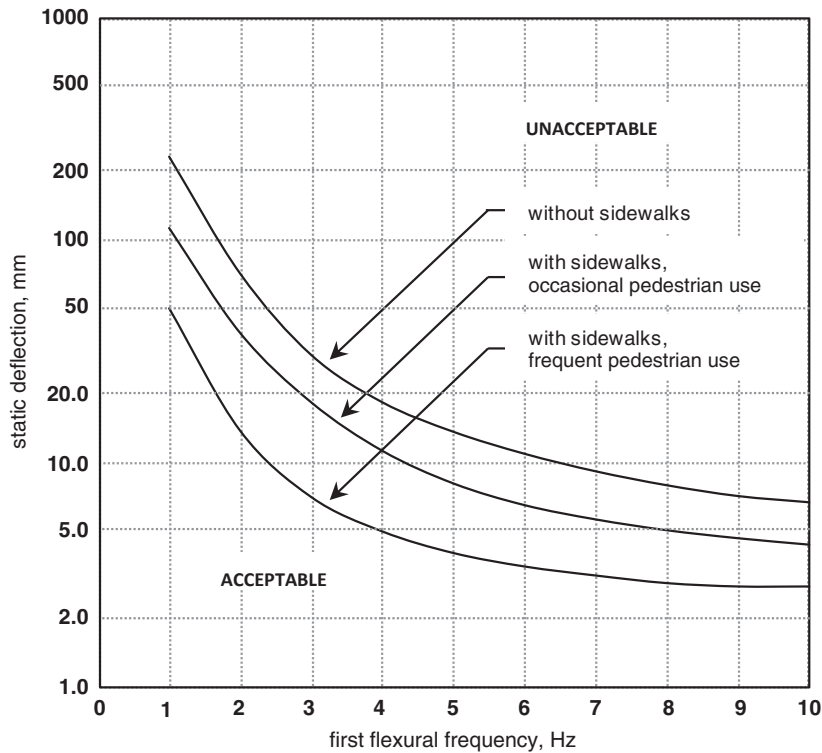
The literature reviewed above indicates that transverse deck cracking can be affected by many factors. In addition, there is disagreement on whether limiting static live load deflections (girder flexibility) is a satisfactory method to prevent deck cracking. Of the articles reviewed, the conclusions are equally divided between those that concluded that girder flexibility affects deck cracking and those that concluded that girder flexibility does not affect deck cracking. As indicated by some of the studies presented above, concrete material factors may be more important to reduce the formation of early age deck cracks.

Some modern specifications, such as the *Ontario Highway Bridge Design Code* (1979) and its successor the *CHBDC*, use a combination of frequency, perception levels, and deflection limits to distinguish between acceptable and unacceptable response. Figure 2.1, taken from *CHBDC* (2006), illustrates this approach, which has the benefit of directly addressing the design issue of vibration control. This is similar to the procedure for building design developed by Murray et al. (2003).

In the *Eurocode*, live loads include a vibration factor to account for stresses caused by vibration; no checks for frequency or displacement are required (*EN 1990* 2002). In New Zealand, vertical velocity is limited to 0.055 m/s (2.2 in./s) under two 120 kN (27 kip axles) of one HN unit if a bridge carries significant pedestrian traffic or where cars are likely to be stationary. Previous versions included span-to-depth ratios and deflection limits, but these have been removed.

Several proposed dynamics-based approaches in the literature are summarized below:

- Wright and Walker (1972) recommended limits based on vertical acceleration to control vibration; this includes composite action.
  - $\delta_s$  = static deflection caused by live load with a wheel line distribution factor of 0.7 on one stringer acting with its share of deck



Source: Canadian Standards Association.

Figure 2.1. Deflection provisions in CHBDC (2006).

- Natural frequency for simple or equal spans:

$$f_b = \frac{\pi}{2L^2} \sqrt{\frac{E_b I_b g}{w}}$$

- Speed parameter:  $\alpha = \frac{v}{2f_b L}$

- Impact factor:  $DI = \alpha + 0.15$

- Dynamic component of acceleration =  $a = DI \times \delta_s (2\pi f_b)^2$  must be less than 100 in./s<sup>2</sup>

- Barth and Wu (2007) provide equations to estimate the natural frequency of continuous-span steel I-girder bridges

- $f = \lambda^2 f_{sb}$  for continuous spans

- $f_{sb} = \frac{\pi}{2L^2} \sqrt{\frac{E_b I_b g}{w}}$  for simple spans

- $\lambda^2 = a \frac{I^c}{L_{max}^b}$

where

$L$  = span length;

$E_b I_b$  = flexural rigidity of composite steel girder;

$g$  = acceleration due to gravity;

$w$  = weight per unit length of composite steel girder;

$L_{max}^b$  = maximum span length; and

$I^c$  = average moment of inertia of composite girder section.

- For two-span bridges

- $a = 0.95$  (1.44 for metric units)
- $b = 0.046$
- $c = 0.032$

- For three- or more span bridges

- $a = 0.88$  (1.49 for metric units)
- $b = -0.033$
- $c = 0.033$

Presently, specifications based on determining the frequency have not received wide acceptance in U.S. practice. There has been a perceived difficulty in determining the first fundamental frequency of the bridge. Equations for simple-span structures have been available for decades [e.g., Biggs (1964)]. Similarly, formulas for frequency have been developed for continuous structures of regular geometry. Historically, frequencies could be calculated using the Rayleigh method typically implemented through Newmark’s numerical integration. Roeder et al. (2002) summarized empirical equations that are based not only on theoretical structural dynamics but also have adjustments for apparent behavior in the field. Modern refined computational methods make the determination of frequencies and mode shapes relatively straightforward. Thus, there does not seem to be any impediment to adopting an approach similar to that specified in the CHBDC.

### Fatigue-and-Fracture Limit States

#### GENERAL

The fatigue-and-fracture limit state is divided into two load combinations: Fatigue I for infinite-life fatigue resistance and Fatigue II for finite-life fatigue resistance. These relatively new provisions appeared in the 2009 interim changes to load provisions in Section 3 of the AASHTO LRFD published in early 2009. The fatigue resistance provisions for concrete and steel bridges in Sections 5 and 6 of the AASHTO LRFD, respectively, were modified accordingly.

#### LOADS

The fatigue load of AASHTO LRFD Article 3.6.1.4 and the fatigue live load load factors of AASHTO LRFD Table 3.4.1-1 are based on extensive research of structural steel highway bridges. The fatigue load is the AASHTO LRFD design truck (HS20-44 truck of the *Standard Specifications for Highway Bridges*) but with a fixed rear-axle spacing of 30 ft. The live load load factors for the fatigue limit state load combinations are summarized in Table 2.5.

#### Infinite-Life Fatigue

The Fatigue I load factor of 1.50, used to design highway bridges with higher traffic volumes for infinite fatigue life, is based on a 1-in-10,000 rate of exceedance (Dexter and Fisher 2000). The infinite-life fatigue or constant amplitude fatigue threshold stress range is the stress range below which the inherent flaws in steel do not propagate significantly during the design life of the bridge. If all the stress ranges experienced by a detail are below this value, the detail is assumed to have infinite life. Thus, this stress range represents a maximum limit to achieve infinite life. This stress range is revisited in Section 6.6 through simulation using weigh-in-motion data.

#### Finite-Life Fatigue

NCHRP Report 267 (Fisher et al. 1983) established that the root mean cube of the stress ranges experienced by a steel-bridge detail characterizes accumulated fatigue damage well when portions of the stress range distribution exceed the constant amplitude fatigue threshold more often than the 1-in-10,000 rate cited above, no matter how small these portions exceeding the threshold are. Thus, the effective stress

**Table 2.5. Fatigue Live Load Load Factors**

Fatigue Limit State Load Combination	Live Load Load Factor
Fatigue I	1.50
Fatigue II	0.75

range for estimating accumulated fatigue damage may be taken as shown by Equation 2.1:

$$(\Delta\sigma)_{\text{effective}} = \sqrt[3]{\sum_i (\Delta\sigma_i)^3} \quad (2.1)$$

The Fatigue II load factor produces a force effect that replicates the fatigue damage due to the entire spectrum of stress ranges experienced by the bridge detail. In other words, the fatigue damage due to passage of the effective truck over the bridge for a total number of cycles, equal to the average daily truck traffic averaged over the 75-year life span, is assumed equal to the fatigue damage due to the actual truck traffic crossing the bridge in 75 years.

### Recommendations

The stress ranges represented by both load factors (the root mean cube and the exceedance of 1 in 10,000) are based on observations of steel highway bridges and structural steel laboratory specimens. Extending these stress ranges to steel reinforcement, both nonprestressed and prestressed, is quite appropriate as the stress ranges represent fatigue damage accumulation in steel. It is assumed that these fatigue damage accumulation models apply to concrete in compression, as well as steel reinforcement. This approach is proposed for this study. A validation of these principles for concrete highway bridges is far beyond the scope and funding of this study.

### FATIGUE RESISTANCE OF CONCRETE STRUCTURES

The fatigue resistance values of concrete, nonprestressed reinforcement and prestressing tendons in the *AASHTO LRFD* are based on ACI 215R-74(92), *Considerations for Design of Concrete Structures Subjected to Fatigue Loading* (ACI Committee 215 1974). This reference includes an extensive bibliography on fatigue resistance of concrete and its reinforcement.

### Concrete

The compressive stress limit of  $0.40f'_c$  for fully prestressed components in other than segmentally constructed bridges in Article 5.5.3.1 of *AASHTO LRFD* applies to a combination of the Fatigue I limit state load combination (which includes only live load) plus one-half the sum of the effective prestress and permanent loads after losses (a load combination derived from a modified Goodman diagram). This suggests that compressive stress limit represents an infinite-life check, as the Fatigue I limit state load combination corresponds with infinite fatigue life.

ACI 215R-74(92) indicates that the fatigue resistance of concrete in the form of an *S-N* curve (stress range versus number of cycles) is approximately linear between 100 and 10 million cycles. It does not exhibit a constant amplitude

fatigue threshold (indicated by a horizontal *S-N* curve) up to that point. Further, it suggests that the compression stress limit of  $0.40f'_c$  is based on a target fatigue life of 10 million cycles. For highway bridges, a target fatigue life of 10 million cycles is significantly less than the design life. A highway bridge with average daily truck traffic of 2,000 trucks per day would experience over 50 million cycles during its 75-year design life.

For this study, the research by Ople and Hulsbos (1966) used to define these *S-N* curves was reevaluated to estimate the fatigue resistance to about  $10^8$  (100 million) cycles, a practical upper bound for highway bridges. The uncertainty of the fatigue resistance is quantified in terms of bias, mean, and coefficient of variation.

### Nonprestressed Reinforcement

As used here, *nonprestressed reinforcement* includes straight reinforcing bars and welded-wire reinforcement. *AASHTO LRFD* (Article 5.5.3.2) specifies the fatigue resistance of these types of reinforcement.

The fatigue resistance of straight reinforcing bars and welded-wire reinforcement without a cross weld in the high-stress region (defined as one-third of the span on each side of the section of maximum moment) is specified by Equation 2.2:

$$(\Delta F)_{\text{TH}} = 24 - 0.33f_{\text{min}} \quad (2.2)$$

where  $f_{\text{min}}$  is the minimum stress; TH is threshold.

For welded-wire reinforcement with a cross weld in the high-stress region, the fatigue resistance is specified by Equation 2.3:

$$(\Delta F)_{\text{TH}} = 16 - 0.33f_{\text{min}} \quad (2.3)$$

Equations 2.2 and 2.3 implicitly assume a ratio of radius to height (i.e.,  $r/h$ ) of the rolled-in transverse bar deformations of 0.3.

These fatigue resistances are defined as constant amplitude fatigue thresholds in *AASHTO LRFD*. ACI Committee report ACI 215R-74(92) and the supporting literature indicate that nonprestressed reinforcement exhibits a constant amplitude fatigue threshold, yet it is unclear that these equations are in fact the threshold values. ACI 215R-74(92) suggests that the resistances are “a conservative lower bound of all available test results.” In other words, a horizontal constant amplitude fatigue threshold has been drawn beneath all the curves.

The studies used to define the fatigue resistance of nonprestressed reinforcement (Fisher and Viest 1961; Pfister and Hognestad 1964; Burton and Hognestad 1967; Hanson et al. 1968; Helgason et al. 1976; Lash 1969; MacGregor et al. 1971; Amorn et al. 2007) were reanalyzed to estimate constant amplitude fatigue thresholds for each case (analogous to the various detail categories defined for steel details) that could be

identified in the research and to determine their uncertainty in terms of bias, mean, and coefficient of variation. The various thresholds were grouped together to make design practical and more rational than the single threshold currently defined.

The *AASHTO Road Test* (1962) demonstrated that a bridge does not necessarily collapse due to fracture following fatigue of nonprestressed reinforcement. Such nonprestressed reinforcement fracture results in distress such as excessive deflection and wide cracks, which facilitate detection and subsequent repair. This consequence suggests that a target reliability index ( $\beta_T$ ) less than that for ultimate limit states (ULSs) is acceptable (in other words,  $\beta_T < 3.5$ ).

#### *Prestressing Tendons*

Fully prestressed components satisfying the tensile stress limits specified in *AASHTO LRFD* Table 5.9.4.2.2-1 at the Service III limit state load combination are exempt from fatigue considerations. (The Service III limit state load combination and its calibration are discussed in Chapter 6.) This exemption acknowledges that tendons in uncracked prestressed beams do not experience stress ranges resulting in fatigue cracking. Most prestressed concrete bridge members are covered by this exemption.

For segmentally constructed bridges, *AASHTO LRFD* Article 5.5.3.3 specifies the fatigue resistance of prestressing tendons as given in Table 2.6. Reductions in constant amplitude fatigue threshold limits for fretting fatigue are not included in the tabulated values.

In-service fatigue cracking of prestressing tendons has not been observed, thus justifying the exemption. The majority of research on fatigue cracking of prestressing strands is based on testing of tendons in air. Application of the resultant fatigue resistance to concrete members with prestressing tendons is questionable (Hanson et al. 1970; Tachau 1971; Warner and Hulsbos 1966). Thus, the uncertainty of the fatigue resistance of prestressing tendons in concrete members is not well documented. In addition, the determination of stress ranges in cracked prestressed concrete members is complicated and beyond the normal prestressed concrete member design procedure (Abeles et al. 1969, 1974; Abeles and Brown 1971). The uncertainty of this determination is also not well defined. In

response to these various uncertainties, it is proposed that this fatigue limit state not be calibrated.

#### *Welded and Mechanical Splices of Reinforcement*

In *AASHTO LRFD* Article 5.5.3.4, constant amplitude fatigue thresholds are given in Table 5.5.3.4-1. These values are used in the general fatigue limit state equation (*AASHTO LRFD* Equation 5.5.3.1-1) for the design of welded or mechanical splices of reinforcement for infinite fatigue life.

Review of the available test data in NCHRP Research Results Digest 197 (1994) suggests that any splice capable of developing 125% of the yield strength of the bar will sustain 1 million cycles of a 4-ksi constant amplitude stress range. This fatigue limit is a close lower bound for the splice fatigue data contained in NCHRP Research Results Digest 197 (1994).

NCHRP Research Results Digest 197 (1994) found that there is substantial uncertainty in the fatigue performance of different types of welds and connectors, much as in structural steel details. However, all types of splices appeared to exhibit a constant amplitude fatigue limit for repetitive loading exceeding about 1 million cycles. The stress ranges for over 1 million cycles of loading given in *AASHTO LRFD* Table 5.5.3.4-1 are based on statistical tolerance limits to constant amplitude staircase test data, such that there is a 95% level of confidence that 95% of the data would exceed the given values for 5 million cycles of loading. These values may, therefore, be regarded as a fatigue limit below which fatigue damage is unlikely to occur during the design lifetime of the structure. This is the same basis used to establish the fatigue design provisions for unspliced reinforcing bars in *AASHTO LRFD* Article 5.5.3.2, which is based on fatigue tests reported in NCHRP Report 164 (Helgason et al. 1976).

#### STEEL STRUCTURES

##### *Finite-Life Fatigue*

The statistical bias and coefficient of variation of finite-life steel fatigue resistances are relatively well defined. NCHRP Report 286 (Keating and Fisher 1986) summarizes the mean finite-life fatigue resistance curves for the *AASHTO* detail categories A through E' and their standard deviations. The *AASHTO* nominal finite-life fatigue resistance curves, defined in log-log space, are illustrated in Figure 2.2 (Figure C6.6.1.2.5-1 of *AASHTO LRFD*). The finite-life fatigue resistances are represented by the sloping portions of the curves. The nominal fatigue resistance curves are determined by subtracting two standard deviations from the mean curves.

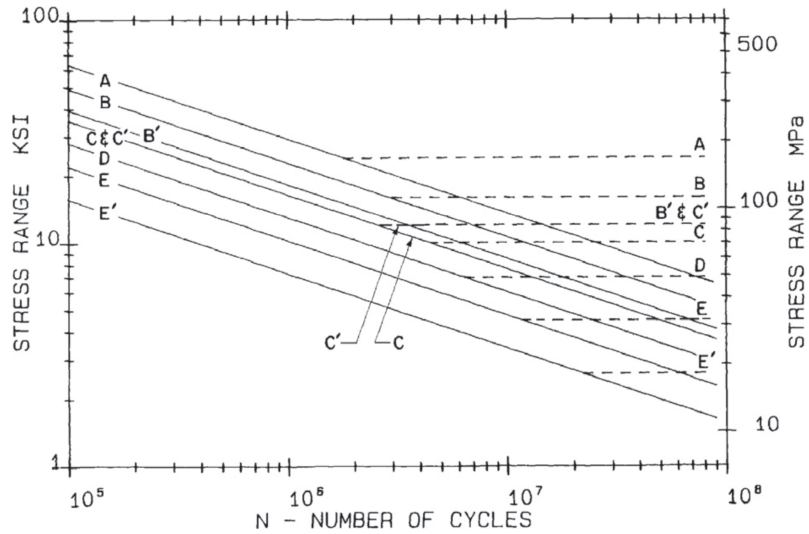
The finite-life fatigue resistance (i.e., the allowable stress range to reach a certain number of cycles) is defined by Equation 2.4:

$$\Delta\sigma = \left(\frac{A}{N}\right)^{\frac{1}{3}} \quad (2.4)$$

**Table 2.6. Prestressing Tendon Fatigue Resistance**

Radius of Curvature (ft)	Constant Amplitude Fatigue Threshold (ksi)
>30	18
≤30 and >12	Linear interpolation between 18 and 10
≤12	10





Source: American Association of State Highway and Transportation Officials.

**Figure 2.2. Nominal fatigue resistances in AASHTO LRFD.**

where  $A$  is a constant defined for each detail category, and  $N$  is the number of cycles to failure.

The current constant,  $A$ , is tabulated for each detail category in Table 2.7 for the mean finite-life fatigue resistance.

The current estimates of uncertainty for finite-life fatigue resistances are tabulated in Table 2.8.

*Infinite-Life Fatigue*

The uncertainty of statistical parameters for infinite-life fatigue resistances is not well defined. The infinite-life fatigue resistance is defined by a constant amplitude fatigue threshold for each detail category. These thresholds, used for design, are tabulated in Table 2.9 (Table 6.6.1.2.5-3 of the *AASHTO LRFD*).

These threshold values were not determined as rigorously as the finite-life curves discussed above because experimental

**Table 2.8. Statistical Parameters for Finite-Life Fatigue Resistance**

Detail Category	Bias	Coefficient of Variation
A	2.8	0.59
B	2.0	0.71
B'	2.4	0.67
C	1.3	0.83
C'	1.3	0.83
D	1.6	0.77
E	1.6	0.77
E'	2.5	0.63

**Table 2.7. Constant A for Mean Fatigue Resistance**

Detail Category	A ( $\times 10^6$ )
A	700
B	240
B'	146
C	57
C'	57
D	35
E	18
E'	10

**Table 2.9. Nominal Constant Amplitude Fatigue Thresholds**

Detail Category	Nominal Constant Amplitude Fatigue Threshold (ksi)
A	24
B	16
B'	12
C	10
C'	12
D	7
E	4.5
E'	2.6

testing near the threshold is time consuming and costly. Conservative thresholds were estimated graphically by using limited experimental test observations. Thus, the uncertainty of these threshold values is not defined.

A Delphi process was employed to investigate the uncertainty of the infinite-life fatigue resistances represented by the constant fatigue thresholds. At the winter 2010 meeting of the Bridge Task Force, in conjunction with the winter 2010 meeting of AASHTO Technical Committee T-14, the topic of the uncertainty of the thresholds was discussed. As the same characteristics that influence the uncertainty of the finite-life fatigue resistance of welded details influence the uncertainty of the infinite-life fatigue resistance, the Bridge Task Force concluded that the statistical parameters associated with the well-defined finite-life fatigue resistance (i.e., the bias and coefficient of variation) would be assumed appropriate for the infinite-life fatigue resistance, as well.

With this assumption, the mean values of infinite-life fatigue resistance are tabulated in Table 2.10 below.

The statistical parameters for infinite-life fatigue resistance are those tabulated in Table 2.8 for finite-life fatigue resistance.

### Cracking in Concrete Structures

Cracking in concrete structures is controversial but must be controlled for aesthetic purposes, durability, and corrosion resistance. Cracking is primarily caused by flexural and tensile stresses, but also from temperature, shrinkage, shear, and torsion. Although researchers do not agree on any single crack-width spacing, the most significant parameters to control cracking are widely agreed on. The most sensitive factor is the reinforcing steel stress, followed by concrete cover, bar spacing, and the area of concrete surrounding each bar. It has

been agreed that the bar diameter is not a major variable. For engineering practice, equations in the ACI 318-08 Code (ACI Committee 318 2008) and AASHTO LRFD (2012) are used to control cracking. The corresponding provisions are discussed below.

#### CRACK CONTROL REINFORCEMENT

This section reviews previous research studies on control of cracking and predicting crack width in concrete members. A significant amount of research has been conducted to investigate crack control in concrete members. The research resulted in the development of numerous equations to predict the crack width on the tension surface and the side faces at the level of reinforcement. Equations available to predict crack width were developed for concrete members with cover less than 2.5 in. and are not applicable for beams with larger concrete cover. Different equations have been adopted by different codes. However, for calibration purposes, these equations were evaluated with regard to accuracy and applicability. The results from various equations were compared and validated using data collected from available literature.

One of the early studies by Clark (1956) included testing 58 specimens and collecting over 105 crack-width readings. Clark concluded that the average crack width is closely related to the following parameters: (1) the diameter of the reinforcing bar, (2) the total reinforcement ratio, (3) the area of the beam section, and (4) the distance from the bottom reinforcement to the beam bottom surface. Clark stated that the average width was also proportional to the stresses in the reinforcing bars beyond the cracking stress. He suggested that the width of the cracks can be reduced by using a large number of small-diameter bars and by increasing the amount of the steel reinforcement. On the basis of these results, Equation 2.5 was developed to predict the average crack width of the concrete beams. The maximum crack width was estimated by multiplying the average crack width by 1.64 (Clark 1956).

$$w_{ave} = C_1 \frac{D}{p} \left[ f_s - C_2 \left( \frac{1}{p} + n \right) \right] \quad (2.5)$$

where

$w_{ave}$  = average width of cracks (in.);

$C_1, C_2$  = coefficients that depend on distribution of bond stress, bond strength, and tensile strength of concrete; for Clark's study,  $C_1 = 2.27 \times 10^{-8} (h - d)/d$ ,  $C_2 = 56.6$ ;

$D$  = diameter of reinforcing bar (in.);

$p = A_s/A_c$  = cross-sectional area of reinforcement/cross-sectional area of concrete;

$A_c = bd$  (in.<sup>2</sup>);

$b$  = width of component (in.);

$f_s$  = computed stress in reinforcement (psi);

**Table 2.10. Mean Infinite-Life Fatigue Resistance**

Detail Category	Constant Amplitude Fatigue Threshold (ksi)
A	67
B	32
B'	29
C	13
C'	16
D	11
E	7
E'	6

$n$  = ratio of modulus of elasticity of steel to concrete (assumed to be 8 in Clark's study);  
 $h$  = overall depth of beam/slab (in.); and  
 $d$  = distance from compressive face of beam/slab to centroid of longitudinal tensile reinforcement.

Kaar and Mattock (1963) also developed a well-known crack-width equation for bottom face cracking, as given by Equation 2.6:

$$w_b = 0.115\beta f_s \sqrt[4]{A} \quad (2.6)$$

where

$w_b$  = maximum crack width (taken as 0.001 in.);  
 $\beta$  = ratio of distances to neutral axis from extreme tension fiber and from centroid of reinforcement;  
 $f_s$  = steel stress calculated by elastic cracked-section theory (ksi); and  
 $A$  = average effective concrete area around reinforcing bar, having same centroid as reinforcement (in.<sup>2</sup>).

Broms (1965) conducted tests on 37 tension and 10 flexural members to analyze crack width and crack spacing. Broms observed that crack spacing decreased rapidly with increasing load, and a number of primary tensile cracks formed on the surface of flexural and tension members. Secondary tensile cracks were confined to the surrounding area of reinforcement. The study concluded that the absolute minimum visible crack spacing is the same as the distance from the surface to the center of the reinforcing bar located nearest to the surface of the member. Thus, the theoretical minimum crack spacing is equal to the thickness of the concrete cover (Broms 1965).

Gergely and Lutz (1968) developed an equation to predict the crack width based on a detailed statistical assessment of experimental data available in the literature at the time. Gergely and Lutz identified various parameters, such as reinforcing bar locations, stresses in the reinforcement, concrete cover depth, and spacing of the reinforcement, as the controlling factors affecting the crack width. The Gergely and Lutz equation is presented as shown in Equation 2.7:

$$w_b = 0.076\beta f_s \sqrt[3]{Ad_c} \quad (2.7)$$

where

$w_b$  = maximum crack width (taken as 0.001 in.);  
 $\beta$  = ratio of distances to neutral axis from extreme tension fiber and from centroid of reinforcement;  
 $f_s$  = steel stress calculated by elastic cracked-section theory (ksi);  
 $d_c$  = bottom cover measured from center of lowest bar (in.); and  
 $A$  = average effective concrete area around reinforcing bar, having same centroid as reinforcement (in.<sup>2</sup>).

The maximum concrete cover tested in this study was 3.31 in.; however, only three test specimens over 2.5-in. cover were tested.

In the study by Frosch (1999), crack widths were determined from an equation developed from a physical model. Results were compared with the test data used in Kaar and Mattock (1963) and Gergely and Lutz (1968). The crack-width model developed in this study showed that the crack spacing and width are functions of the distance between the reinforcing steel bars. Crack control can be achieved by limiting the spacing of these reinforcing bars. On the basis of these research findings, Frosch (1999) suggested that limiting the maximum bar spacing would prevent large cracks in concrete beams.

The equation to calculate the maximum crack width for uncoated reinforcement was developed on the basis of the physical model as shown by Equation 2.8 (Frosch 1999):

$$w_c = \frac{2f_s}{E_s} \beta \sqrt{\left(d_c^2 + \left(\frac{s}{2}\right)^2\right)} \quad (2.8)$$

where

$s$  = maximum permissible bar spacing (in.);  
 $w_c$  = limiting crack width (in.) [0.016 in., based on ACI 318-95 (ACI Committee 318 1995)];  
 $E_s$  = elastic modulus of steel reinforcement (can be taken as 29,000 ksi);  
 $\beta$  =  $1.0 + 0.08d_c$ ;  
 $d_c$  = bottom cover measured from center of lowest bar (in.); and  
 $f_s$  = stress in steel reinforcement.

Frosch (1999) suggested that for epoxy-coated reinforcement, Equation 2.8 (for uncoated reinforcement) should be multiplied by a factor of 2. Equation 2.8 has been rearranged to solve for the allowable uncoated bar spacing, as shown in Equation 2.9:

$$s = 2\sqrt{\left(\left(\frac{w_c E_s}{2f_s \beta}\right)^2 - d_c^2\right)} \quad (2.9)$$

The following design recommendation, which was based on the physical model and addresses the use of both uncoated and coated reinforcement, was presented. The equation to calculate the maximum spacing of reinforcement was given as shown by Equation 2.10 (Frosch 1999):

$$s = 12\alpha_s \left[2 - \frac{d_c}{3\alpha_s}\right] \leq 12\alpha_s \quad (2.10)$$

where

$$\alpha_s = \frac{36}{f_s} \gamma_c$$

$d_c$  = thickness of concrete cover measured from extreme tension fiber to center of bar or wire located closest thereto, in.;

$s$  = maximum spacing of reinforcement (in.);

$\alpha_s$  = reinforcement factor;

$\gamma_c$  = reinforcement coating factor: 1.0 for uncoated reinforcement, 0.5 for epoxy-coated reinforcement, unless test data can justify a higher value; and

$f_s$  = calculated stress in reinforcement at service load (ksi).

The calculated stress in reinforcement at service load ( $f_s$ ) should be computed as the moment divided by the product of steel area and internal moment arm;  $f_s$  should not exceed 60% of the specified yield strength  $f_y$ .

Frosch (2001) summarized the physical model for cracking and illustrated the development and limitations of the proposed design method. He recommended formulas for calculating the maximum crack width for uncoated and epoxy-coated reinforcement, as well as the design recommendation for their use, similar to those in Frosch (1999).

In general, the largest crack widths are expected at the extreme tensile face of the beam. However, Beeby (1979) conducted studies that showed the largest crack widths in the web along the beam side face occurred at about midheight. Frosch (2002) conducted research on the modeling and control of cracking on the side face of concrete beams. The study showed that to provide adequate crack control, the maximum skin reinforcement spacing is a function of the side cover. It was also shown that a maximum bar spacing of 12 in. provides reasonable crack control for up to 3 in. of concrete cover. The crack model developed by Frosch (2002) allows for the calculation of the crack width at any location along the cross section. A profile of the crack width through the depth of the section is more easily created and allows for information regarding optimum locations for placing skin reinforcement for the purpose of controlling side face cracks.

Frosch (2002) showed that the crack spacing and crack width along the side face are functions of the distance from the reinforcement, so the crack can be controlled by adding skin reinforcement and limiting the reinforcement spacing. As the maximum crack width was observed halfway between the reinforcement and neutral axis, Equation 2.11 can be used to solve for crack width  $w_c$  at  $x = (d - c)/2$ :

$$w_c = \epsilon_s \sqrt{d_s^2 + \left(\frac{1}{2}(d - c)\right)^2} \quad (2.11)$$

where

$\epsilon_s$  = strain in steel reinforcement =  $f_s/E_s$ ;

$d_s$  = concrete cover for skin reinforcement (in.);

$d$  = effective depth (in.); and

$c$  = depth of neutral axis from compression face (in.).

The study of the physical model showed that sections with an effective depth of 36 in. and covers up to 3 in. can be designed without skin reinforcement. For thicker covers, the maximum effective depth not requiring skin reinforcement should be decreased. Maximum effective depth decreases for covers thicker than 3 in. for Grade 60 reinforcement, resulting in the maximum depth ( $d = 36$  in.).

To prevent excessive cracks throughout the depth of the section, maximum spacing of the reinforcement should be determined. According to Frosch (2002), the placement of the first bar is the most critical for the spacing of the skin reinforcement. The maximum crack width ( $w_s$ ) was calculated halfway between the primary reinforcement and the first skin reinforcement bar at a distance  $x = s/2$ , yielding Equation 2.12:

$$w_s = 2 \frac{f_s}{E_s} \sqrt{d_s^2 + \left(\frac{s}{2}\right)^2} \quad (2.12)$$

For sections with skin reinforcement, it is necessary to determine the location in the section at which the reinforcement can be discontinued. As crack widths are controlled by skin reinforcement below its end point, it is necessary to calculate the maximum distance where the skin reinforcement can be eliminated. The maximum crack width will occur approximately halfway between the neutral axis and the location of the first layer of skin reinforcement at a distance  $x = s_{na}/2$  from the neutral axis (Frosch 2002). The maximum crack width can be calculated with Equation 2.13 based on the physical model developed by Frosch (2002):

$$w_s = s_{na} \left(\frac{\epsilon_s}{d - c}\right) \sqrt{d_s^2 + \left(\frac{s_{na}}{2}\right)^2} \quad (2.13)$$

where  $s_{na}$  is the maximum distance where the skin reinforcement can be eliminated.

Frosch (2002) recommended that the design formula should be based on a physical model to address the control of cracking in reinforced-concrete structures and to unify the design criteria for controlling cracking in side and tension faces. Frosch (2002) recommended the maximum spacing of flexural tension reinforcement as given by Equation 2.14:

$$s = 12\alpha_s \left[ 2 - \frac{d_c}{3\alpha_s} \right] \leq 12\alpha_s \quad (2.14)$$

where

$$\alpha_s = \frac{36}{f_s}$$

$d_c$  = thickness of concrete cover (in.) (for bottom face reinforcement, measured from extreme tension fiber to center of bar, and for skin reinforcement, measured from side face to center of bar);  
 $s$  = maximum spacing of reinforcement (in.);  
 $\alpha_s$  = reinforcement factor; and  
 $f_s$  = calculated stress in reinforcement at service load (ksi).

The  $f_s$  value should be computed as the moment divided by the product of steel area and internal moment arm;  $f_s$  should not be more than 60% of the specified yield strength  $f_y$ .

Skin reinforcement is required along both side faces of a member for a distance  $d/2$  from the nearest flexural tension reinforcement if the effective depth exceeds the depth calculated by Equation 2.15:

$$d = 42\alpha_s - 2d_c \leq 36\alpha_s \quad (2.15)$$

Epoxy-coated reinforcement is widely used to increase the durability of structures. The epoxy coating has been shown to decrease bond strength, which can decrease crack spacing and increase crack widths when compared with uncoated reinforcement (Blackman and Frosch 2005). Blackman and Frosch investigated crack widths in concrete beams by using epoxy-coated reinforcement. The primary variables used in the study included epoxy coating thickness and reinforcing bar spacing. Blackman and Frosch designed 10 slab specimens to examine the effect of epoxy coating on cracks and concluded that the epoxy coating thickness did not significantly affect the concrete cracking behavior. Frosch (1999, 2001, 2002) and Blackman and Frosch (2005) presented an equation, given here as Equation 2.16, to compare the average measured crack spacing for the uncoated and epoxy-coated bars with the calculated values:

$$S_c = \Psi_s d^* \quad (2.16)$$

where

$S_c$  = crack spacing (in.);  
 $d^*$  = controlling cover distance (in.); and  
 $\Psi_s$  = crack spacing factor (1.0 for minimum crack spacing, 1.5 for average crack spacing, and 2.0 for maximum crack spacing).

Cracking of structures is rather common and is not always damaging to the structure. However, when considering a bridge deck, moderately sized cracks can be detrimental to the longevity of the structure due to the harsh environmental exposure. Recently, increased concrete cover coupled with high-performance concrete has become increasingly popular because of its durability. However, this practice results in unrealistically small bar spacing and prevents the use of contemporary crack control practices that are based on statistical studies. Thus, it is desirable to develop methods to predict

average and maximum crack widths of reinforced-concrete members with thicker concrete covers at various locations.

Choi and Oh (2009) studied crack widths in transversely posttensioned concrete deck slabs in box girder bridges. They tested four full-scale concrete box girder segments and derived the maximum-crack-width equation from the testing data, as given by Equations 2.17 and 2.18:

$$w_{\max} = 3 \times 10^{-6} (f_s - f_0) \Phi_s \left( \frac{A_{t,\text{eff}}}{A_{st} + \xi A_{pt}} \right)^{0.75} \frac{h - x}{d - x} \quad (2.17)$$

$$\xi = \sqrt{\frac{\tau_{ap} \pi + (n - 1) \Phi_s}{\tau_{as} n \pi \Phi_p}} \quad (2.18)$$

where

$A_{st}$  = total area of reinforcing bars ( $\text{mm}^2$ );  
 $A_{pt}$  = total area of prestressing tendons ( $\text{mm}^2$ );  
 $A_{t,\text{eff}}$  = effective tensile concrete area ( $\text{mm}^2$ );  
 $d$  = effective depth (mm);  
 $f_s$  = increment of reinforcing bar stress after decompression (MPa);  
 $f_0$  = steel stress at initial occurrence of crack (MPa);  
 $h$  = height of cross section (mm);  
 $n$  = number of strands in a flat duct;  
 $x$  = depth of neutral axis (mm);  
 $w_{\max}$  = predicted maximum crack width (mm);  
 $\Phi_s$  = diameter of reinforcing bar (mm);  
 $\Phi_p$  = diameter of prestressing tendons (mm); and  
 $\frac{\tau_{ap}}{\tau_{as}} = 0.465$  for grouted posttensioned tendons.

#### CONTROL OF CRACKS IN CURRENT CODE PROVISIONS

The current code provisions specifying the distribution of reinforcement are reviewed in this section.

ACI requirements for flexural crack control in beams and thick one-way slabs are based on the statistical analysis of maximum-crack-width data from several sources (Gergely and Lutz 1968). ACI maintains that crack control is particularly important when reinforcement with yield strength over 40,000 psi is used. Good detailing practices such as concrete cover and spacing of reinforcement should lead to adequate crack control even when reinforcement with a yield strength of 60,000 psi is used. ACI 318-08 Article 10.6 (ACI Committee 318 2008) does not distinguish between interior and exterior exposure because corrosion is not clearly correlated with surface crack widths in the range normally found at service-load levels. ACI 318-08 only requires that the spacing of reinforcement closest to the tension face ( $s$ ) does not exceed that given by Equation 2.19

$$s = 15 \left( \frac{40,000}{f_s} \right) - 2.5c_c \quad (2.19)$$



but not greater than  $12\left(\frac{40,000}{f_s}\right)$ , where  $c_c$  is the least distance from the surface of reinforcement or prestressing steel to the tension face. If there is only one bar or wire nearest to the extreme tension face,  $s$  in Equation 2.19 is the width of the extreme tension face. These provisions are not sufficient for structures subject to very aggressive exposure or designed to be watertight.

Special investigation is required for structures subject to very aggressive exposure or designed to be watertight. ACI 318-99/318R-99 (ACI Committee 318 1999) limited the maximum spacing to 12 in., but this limitation was removed in ACI 318-08 (ACI Committee 318 2008). ACI 318-08 also recommends the use of several bars at moderate spacing rather than fewer bars at larger spacing to control cracking. These provisions were updated recently to reflect the higher service stresses that occur in flexural reinforcement with the use of the load combinations introduced in ACI 318-02/318R-02 (ACI Committee 318 2002). The maximum bar spacing to directly control cracking is specified. Similar recommendations have been stated for deep beams with the requirement of skin reinforcement.

AASHTO LRFD (2012) also provides provisions of reinforcement spacing to control flexural cracking. Like ACI, AASHTO emphasizes the importance of reinforcement detailing and that smaller bars at moderate spacing tend to be more effective than an equivalent area of larger bars. AASHTO LRFD also agrees with ACI 318-08 on the most important parameters affecting crack width and specifies a formula for the distribution of reinforcement to control cracking. The equation in AASHTO LRFD (2008) is based on the physical crack model of Frosch (2001) rather than the statistically based model used in previous editions. The equation (given here as Equation 2.20) limits bar spacing rather than crack width:

$$s \leq \frac{700\gamma_e}{\beta_s f_{ss}} - 2d_c \quad (2.20)$$

where

$\beta_s = 1 + \frac{d_c}{0.7(h - d_c)}$  (the geometric relationship between crack width at tension face versus crack width at reinforcement level);

$\gamma_e$  = exposure factor (1.00 for Class 1 exposure, 0.75 for Class 2 exposure);

$d_c$  = thickness of concrete cover measured from extreme tension fiber to center of the flexural reinforcement located closest thereto, in.;

$f_{ss}$  = tensile stress in steel reinforcement at the SLS (ksi); and

$h$  = overall thickness of depth of the component (in.).

Unlike ACI, AASHTO specifies exposure conditions to meet the needs of the authority having jurisdiction. The Class 1 exposure condition is based on a maximum crack width of 0.017 in. and applies when cracks can be tolerated due to reduced concerns of appearance or corrosion. This exposure class can be thought of as an upper bound in regard to crack width for appearance and corrosion. The Class 2 exposure condition generally applies to decks and substructures exposed to water and any other components exposed to corrosive environments. AASHTO LRFD (2008) also specifies requirements for skin reinforcement based on ACI 318-11 (ACI Committee 318 2011). AASHTO Equation 5.7.3.4-1 (given here as Equation 2.20) applies to both reinforced and prestressed concrete, with specifications on the steel stresses used. In general, if the AASHTO Class 2 exposure condition is used, AASHTO spacings are less than those derived by the ACI equation. However, if the Class 1 exposure condition is used, ACI spacing becomes more conservative.

#### PRINCIPAL STRESSES IN WEBS OF SEGMENTAL CONCRETE BRIDGES

Okeil (2006) studied the allowable tensile stress for webs of prestressed segmental concrete bridges by using a reliability-based approach. In this study, six prestressed segmental concrete bridge designs were analyzed. Okeil stated that by complying with the allowable tensile stresses, flexural cracking at the top and bottom fibers is controlled. However, for the webs, cracks might develop due to a biaxial stress state resulting from a combination of shear and normal stresses. To control shear cracking, the principal stress must be limited to an allowable tensile stress ( $f_{t,all}$ ). This issue was addressed by the Florida DOT (*Structures Manual* 2013) and resulted in a recommendation for the allowable tensile stresses to be used in checking web tensile principal stress ( $\sigma_1$ ). However, the recommendation ignored the accompanying compressive principal stress ( $\sigma_2$ ), which has a significant effect on the tensile strength of concrete. The objective of Okeil's study was to develop an allowable stress limit under which cracking in webs of prestressed segmental bridges under service-load conditions can be controlled.

Three equations were considered: ACI (ACI Committee 318 2005), Kupfer and Gerstle (1973), and Oluokun (1991), as shown in Equations 2.21 to 2.23, respectively:

$$f_{tu} = 6.7(f'_c)^{0.5} \quad (2.21)$$

$$f_{tu} = 1.59(f'_c)^{0.67} \quad (2.22)$$

$$f_{tu} = 1.38(f'_c)^{0.69} \quad (2.23)$$

where  $f_{tu}$  is uniaxial tensile strength of concrete (psi), and  $f'_c$  is concrete compressive strength (psi).



Okeil (2006) concluded that Equation 2.23 provides a better estimate of the tensile strength over a wider range of concrete compressive strengths. Using a biaxial state of stress and regression analysis, Okeil developed a relationship between the tensile strength and the corresponding compressive strength, as shown in Equation 2.24:

$$\frac{\sigma_{tu}}{f_{tu}} = 1 + 0.85 \frac{\sigma_{cu}}{f'_c} \quad (2.24)$$

where  $\sigma_{cu}$  and  $\sigma_{tu}$  are the ultimate strengths of concrete under a compression–tension biaxial state of stress (psi).

By combining Equations 2.23 and 2.24, Equation 2.25 is obtained:

$$\sigma_{tu} = 1.38(f'_c)^{0.69} \left( 1 + 0.85 \frac{\sigma_{cu}}{f'_c} \right) \quad (2.25)$$

After a detailed parametric study and reliability analysis, Okeil (2006) recommended an expression, given in Equation 2.26, for estimating the allowable tensile stress in the webs of posttensioned segmental bridges under biaxial stresses:

$$f_{ct} = 0.60(f'_c)^{0.7} \left( 1 + 0.85 \frac{\sigma_2}{f'_c} \right) \quad (2.26)$$

where  $\sigma_2$  is the principal stress in the centroidal stress block in the web of a posttensioned segmental bridge.

The findings of this study are limited to the range of concrete compressive strengths between 5 and 8 ksi.

#### STRESS LIMITATIONS FOR PRESTRESSING TENDONS

AASHTO LRFD (2012) provides stress limits for prestressing tendons at various service conditions. These stress limits are listed in Table 2.11.

ACI 318-08 provides similar limits on the tensile stress in prestressing tendons and rebars (ACI Committee 318 2008). Major revisions to the limits were made in the 1983 version of ACI 318 to incorporate the higher yield strength of low-relaxation wire and strand (ACI Committee 318 1983). The ACI 318-08 stress limits for prestressing steel are listed as follows (ACI Committee 318 2008):

Due to prestressing steel jacking force:  $0.94f_{py}$  but not greater than the lesser of  $0.80f_{pu}$  and the maximum value recommended by the manufacturer of prestressing steel or anchorage devices.

Immediately after prestress transfer:  $0.82f_{py}$  but not greater than  $0.74f_{pu}$ . Post-tensioning tendons, at anchorage devices and couplers, immediately after force transfer:  $0.70f_{pu}$ .

EN 1992-2 (Eurocode 2): Design of Concrete Structures (EN 1992-2 2005) restricts inelastic deformation of the steel in concrete structures at the SLS to prevent large, permanently open cracks. In EN1992-2, at the SLSs, the stress limit for prestressing steel is  $0.75f_{pk}$  after allowance for losses, where  $f_{pk}$  is the characteristic tensile strength of prestressing steel. The exact meaning of *characteristic* tensile strength is not defined in EN1992-2 and is interpreted here as the specified strength. This limit of  $0.75f_{pk}$  is listed in EN1992-2 Section 7.

#### CONCRETE TENSION STRESSES

The early discussion of cracking control is diverse. At the First United States Conference on Prestressed Concrete in 1951,

**Table 2.11. Stress Limits for Prestressing Tendons (AASHTO LRFD 2012)**

Condition	Tendon Type		
	Stress-Relieved Strand and Plain High-Strength Bars	Low-Relaxation Strand	Deformed High-Strength Bars
<b>Pretensioning</b>			
Immediately before transfer ( $f_{pbt}$ )	$0.70f_{pu}$	$0.75f_{pu}$	—
At SLS after all losses ( $f_{pe}$ )	$0.80f_{py}$	$0.80f_{py}$	$0.80f_{py}$
<b>Posttensioning</b>			
Before seating, short-term $f_{pbt}$ may be allowed	$0.90f_{py}$	$0.90f_{py}$	$0.90f_{py}$
At anchorages and couplers immediately after anchor set	$0.70f_{pu}$	$0.70f_{pu}$	$0.70f_{pu}$
Elsewhere along length of member away from anchorages and couplers immediately after anchor set	$0.70f_{pu}$	$0.74f_{pu}$	$0.70f_{pu}$
At SLS after losses ( $f_{pe}$ )	$0.80f_{py}$	$0.80f_{py}$	$0.80f_{py}$

Note: — = not applicable.

some experts opined that a completely crackless concrete member is only better for the specific purpose, but others thought that cracking of prestressed concrete beams is as important as yielding. In 1958, the Tentative Recommendations for Prestressed Concrete proposed by ACI-ASCE Joint Committee 323 suggested that prestressed concrete, before losses due to creep and shrinkage, should meet the following limits (note units in the following provisions are in pounds per square inch for the allowable tensile stress):

$3\sqrt{f'_c}$  for members without nonprestressed reinforcement;

$6\sqrt{f'_c}$  for members with nonprestressed reinforcement provided to resist the tensile force in concrete; computed on the basis of an uncracked section.

The 1963 *Building Code Requirements for Reinforced Concrete* (ACI Committee 318 1963) included the recommendation for the tensile stress limits proposed by ACI-ASCE Joint Committee 323 (1958), with some modifications:

$3\sqrt{f'_c}$  for members without auxiliary reinforcement in the tension zone;

[w]hen the calculated tension stress exceeds  $3\sqrt{f'_c}$ , reinforcement shall be provided to resist the total tension force in the concrete computed on the assumption of uncracked section.

The 1977 *Building Code Requirements for Reinforced Concrete* modified the allowable tensile stress limit as follows (ACI Committee 318 1977):

$6\sqrt{f'_c}$  for the extreme fiber stress in tension at ends of simply supported members;

$3\sqrt{f'_c}$  for the extreme fiber stress in tension at other locations.

In the current ACI 318-11, Section 18.4.1 specifies the allowable tensile stress in concrete immediately after prestress transfer (before time-dependent prestress losses) as follows (ACI Committee 318 2011):

Where computed concrete tensile stresses,  $f_t$ , exceeds  $6\sqrt{f'_c}$  at ends of simply supported members, or  $3\sqrt{f'_c}$  at other locations, additional bonded reinforcement shall be provided in the tensile zone to resist the total tensile force in concrete computed with the assumption of an uncracked section.

The AASHTO *Standard Specifications for Highway Bridges* (1992) specified the allowable tensile stresses, before losses due to creep and shrinkage, as follows:

200 psi or  $3\sqrt{f'_c}$  for members in tension areas with no bonded reinforcement;

[w]here the calculated tensile stress exceeds this value, reinforcement shall be provided to resist the total tension force in the concrete computed on the assumption of uncracked section. The maximum tensile stress shall not exceed  $7.5\sqrt{f'_c}$ .

Table 2.12 shows the tensile stress limits and provisions of AASHTO LRFD (2008).

*EXISTING LIMIT STATES THAT ARE DETERMINISTIC OR REPRESENT DETAILING REQUIREMENTS*

The following limit states exist in AASHTO LRFD. Reviewing the background of these limit states revealed that they are either deterministic or represent detailing requirements that cannot be calibrated. No calibration is anticipated for these limit states.

**Table 2.12. Tensile Stress Limits in Prestressed Concrete at SLS After Losses, Fully Prestressed Components (AASHTO LRFD Table 5.9.4.2.2-1 [2008])**

Bridge Type	Location	Stress Limit
Other Than Segmentally Constructed Bridges	Tension in the precompressed Tensile Zone Bridges, Assuming Uncracked Sections	
	For components with bonded prestressing tendons or reinforcement that are subjected to not worse than moderate corrosion condition.	$0.19\sqrt{f'_c}$ (ksi)
	For components with bonded prestressing tendons or reinforcement that are subjected to severe corrosive conditions	$0.0948\sqrt{f'_c}$ (ksi)
	For components with unbonded prestressing tendons	No tension
Segmentally Constructed Bridges	Longitudinal Stresses Through Joints in the Precompressed Tensile Zone	
	Joints with minimum bonded auxiliary reinforcement through the joints sufficient to carry the calculated longitudinal tensile force at a stress of 0.5 fy; internal tendons or external tendons	$0.0948\sqrt{f'_c}$ (ksi)
	Joints without the minimum bonded auxiliary reinforcement through joints	No tension
	Transverse Stress Through Joints	
	Tension in the transverse direction in precompressed tensile zone	$0.0948\sqrt{f'_c}$ (ksi)
	Principal Tensile Stress at Neutral Axis in Web	
	All types of segmental concrete bridges with internal and/or external tendons, unless the Owner imposes other criteria for critical structures.	$0.110\sqrt{f'_c}$ (ksi)

### *Fatigue in Concrete Deck Slabs and Culvert Top Slabs*

(AASHTO LRFD Article 5.5.3.1)

Stresses measured in concrete deck slabs of bridges and top slabs of box culverts in service are far below infinite fatigue life, most probably due to internal arching action.

AASHTO *Standard Specifications for Highway Bridges* (1975) includes the background that led to waiving fatigue requirements for these components.

### *Fatigue of Reinforcement of Fully Prestressed Components*

(AASHTO LRFD Article 5.5.3.1)

For fully prestressed components designed to have extreme fiber tensile stress due to a Service III limit state within the tensile stress limit specified in AASHTO LRFD Table 5.9.4.2.2-1, the fatigue limit state load factors, the girder distribution factors, and dynamic load allowance cause fatigue limit state stress to be considerably less than the corresponding value determined from Service III. For fully prestressed components, the net concrete stress is usually significantly less than the concrete tensile stress limit specified in AASHTO LRFD Table 5.9.4.2.2-1. As a result, the calculated flexural stresses are significantly reduced. For this situation, the calculated steel stress range, which is equal to the modular ratio times the concrete stress range, is almost always less than the steel fatigue stress range limit specified in AASHTO LRFD Article 5.5.3.3.

### *Fatigue of Prestressing Tendons* (AASHTO LRFD Article 5.5.3.3)

With fatigue in fully prestressed components waived (see above), these provisions are only applicable to segmental bridges. Little data are available on the randomness of load and resistance of segmental bridges. There is no evidence of fatigue damage on these structures, so no changes are recommended, and calibration will not be made.

### *Crack Control Reinforcement for Components Designed Using Strut and Tie Model* (AASHTO LRFD Article 5.6.3.6)

Birrcher et al. (2009) proposed new provisions regarding crack control reinforcement as follows: “The spacing of the bars in these grids shall not exceed the smaller of  $d/4$  and 12.0 in.” Moreover, they continued, “The reinforcement in the vertical and horizontal direction shall satisfy the following [shown here as Equation 2.27]”:

$$\frac{A_v}{b_w s_v} \geq 0.003, \frac{A_h}{b_w s_h} \geq 0.003 \quad (2.27)$$

where

$A_v, A_h$  = total area of vertical and horizontal crack control reinforcement within spacing  $s_v$  and  $s_h$ , respectively;

$b_w$  = width of member web (in.); and

$s_v, s_h$  = spacing of vertical and horizontal crack control reinforcement, respectively.

Birrcher et al. (2009) concluded that “[c]rack control reinforcement shall be distributed evenly near the side faces of the strut. Where necessary, interior layers of crack control reinforcement may be used.”

### **Control of Permanent Deformation**

Steel structures are subject to requirements intended to prevent changes in riding quality and appearance resulting from permanent deflections in service. Starting with specifications for LFD in the early 1970s, steel structures have been subject to two limitations to guard against these undesirable behaviors. There is a requirement that the service-load stress under an overload be less than 95% of yield in a composite girder or 80% of yield in a noncomposite girder and that slip-critical connections be designed for the same overload requirement. In LFD, the overload requirement was dead load plus 5/3 of the HS20 loading. Due to the increased demand of the HL-93 live load, the corresponding provisions in the AASHTO LRFD are investigated at the Service II limit state, which involves a load factor on live load of 1.30.

The response of girder structures to excessive overloads was one of several issues explored during the AASHTO *Road Test* of the late 1950s and early 1960s and documented in a series of reports issued by the Highway Research Board (AASHTO *Road Test* 1962), the predecessor of the Transportation Research Board. The structures of the AASHTO *Road Test* were designed to undergo many repetitions to relatively high stresses.

Table 2.13 shows a summary of the initial stresses in steel bridges of composite and noncomposite construction. The nominal yield stress for the material in these bridges was 33 ksi, so it can be seen that in many cases these bridges were subjected to loads beyond the yield stress.

Table 2.13 also indicates the number of live load passages to which these structures were subjected. After the repetitions of actual truck loading, some of the structures were subjected to further cycles of load to investigate fatigue through the use of eccentric mass dampers.

In American Iron and Steel Institute Bulletin 15, Vincent (1969) summarizes the basis for LFD of steel structures. Bulletin 15 contains the following statement: “There is, however, a definite need for a control on the possibility of permanent deformations under infrequent overloads which may impair the riding quality of the bridges.” The establishment of the 80% and 95% criteria is demonstrated in Figure 2.3, taken from Bulletin 15, which shows the permanent set at midspan of several of the bridges from the AASHTO *Road Test* and the corresponding ratio between test stress and the actual measured yield point of the steel in the bridges. The two criteria for composite and noncomposite structures are seen to produce an accumulated displacement of

Table 2.13. Data from AASHTO Road Test (1962)

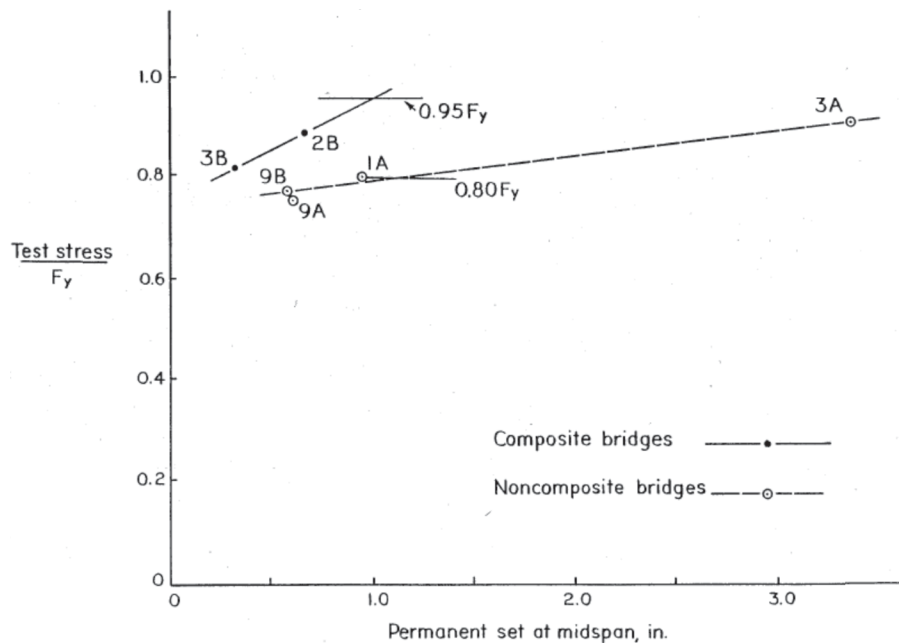
Summary of Initial Stresses in Steel Bridges						No. of Vehicle Passages	
Design Stress (ksi)			Actual Stress (ksi)				
Bridge	Center Beam	Exterior Beam	Interior Beam	Center Beam	Exterior Beam	To First Cracking	Total
<b>Noncomposite Bridges</b>							
1A	27.0	—	25.3	27.7	30.1	536,000	557,400
1B	34.8	—	32.5	35.4	40.5	—	235
2A	35.0	—	35.0	39.4	41.1	—	26
3A	27.3	—	28.6	30.9	35.4	—	392,400
4A	34.7	—	35.9	38.9	41.1	—	106
4B	34.7	—	39.1	42.1	42.3	—	106
9A	—	27.0	22.9	24.7	25.5	477,900	477,900
9B	—	27.0	24.0	24.6	26.0	477,900	477,900
<b>Composite Bridges</b>							
2B	35.0	—	30.2	33.8	35.8	531,500	558,400
3B	26.9	—	26.0	28.8	31.0	535,500	557,800

Note: — = not available.

approximately 1 in. at the midspan of bridges of an approximately 50-ft span. Deflection measurements at various times during the road test indicate that most structures accumulated most of the eventual permanent set in the very early repetitions of loading.

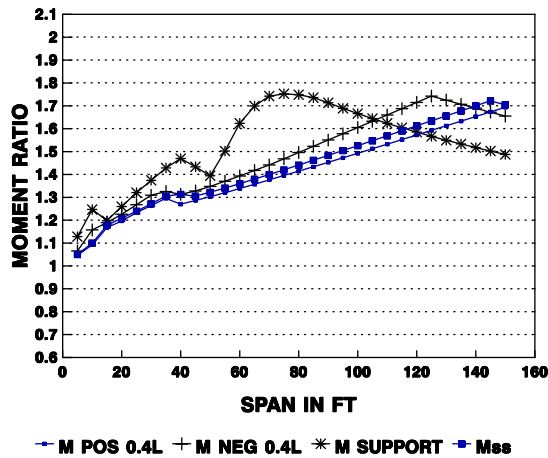
The provisions for control of permanent deformations in steel structures were incorporated into *AASHTO LRFD* with an adjustment for the increased live load with the intent of

providing generally the same, or even higher, level of overload performance as was provided by LFD in most cases. Consider Figure 2.4, which shows the ratio of the HL-93 loading to the HS20 loading in the Standard Specifications. The load factor in the Standard Specifications for this case was 1.67; the current load factor for the *AASHTO LRFD* Service II load combination is 1.3. That means that whenever the moment ratio in Figure 2.4 is greater than 1.28, then the



Source: Vincent (1969). Reproduced with permission from the American Iron & Steel Institute.

Figure 2.3. Development of service stress limits.



Source: American Association of State Highway and Transportation Officials.

**Figure 2.4. Ratio of HL-93 moment to HS20 moment.**

current demand is higher than that required by the Standard Specifications.

Several issues arose regarding retention of, or revisions to, the provisions related to control of permanent deformations; these are discussed in Section 6.4.

### 2.3.2 Eurocode

The *Eurocode* contains the following sections, to which reference is made in subsequent sections of this report:

- EN 1990 (*Eurocode 0*): *Basis of Structural Design*
- EN 1991 (*Eurocode 1*): *Actions on Structures*
- EN 1992 (*Eurocode 2*): *Design of Concrete Structures*
- EN 1993 (*Eurocode 3*): *Design of Steel Structure*
- EN 1994 (*Eurocode 4*): *Design of Composite Steel and Concrete Structures*
- EN 1995 (*Eurocode 5*): *Design of Timber Structures*
- EN 1996 (*Eurocode 6*): *Design of Masonry Structure*
- EN 1997 (*Eurocode 7*): *Geotechnical Design*
- EN 1998 (*Eurocode 8*): *Design of Structures for Earthquake Resistance*
- EN 1999 (*Eurocode 9*): *Design of Aluminum Structures*

These *Eurocode* sections allow the user countries to incorporate country-specific requirements through the incorporation of a national annex.

The *Eurocode* replaced most previous country specifications, such as the German Institute for Standardization and the British BS5400, and it is expected to eventually replace all other European Union member country specifications. It is assumed that the requirements of the *Eurocode* encompass those of the previous specifications and, thus, no other European specifications were reviewed.

### Definition of SLS

The *Eurocode* (EN 1990 2002) defines SLSs as those concerning

- The functioning of the structure or structural members under normal use;
- The comfort of users; and
- The appearance of the construction works.

The *Eurocode* (EN 1990 2002) includes requirements calling for

- The serviceability requirements to be agreed on for each individual project;
- A distinction to be made between reversible and irreversible serviceability limit states; and
- The verification of SLS based on criteria concerning the following aspects:
  - a. Deformations that affect
    - The appearance,
    - The comfort of users,
    - The functioning of the structure (including the functioning of machines or services), or
    - That cause damage to finishes of nonstructural members.
  - b. Vibrations
    - That cause discomfort to people, or
    - That limit the functional effectiveness of the structure.
  - c. Damage that is likely to adversely affect
    - The appearance,
    - The durability, or
    - The functioning of the structure.

In the context of serviceability, the *Eurocode* considers the term *appearance* to be concerned with such criteria as high deflection and extensive cracking, rather than aesthetics (EN 1990 2002).

### Background on the Eurocode's Reliability Basis

The *Eurocode* specifies that structures be designed for a particular design working life (EN 1990 2002). The design working life is defined as the period for which a structure is assumed to be usable for its intended purpose with anticipated maintenance but without major repair being necessary. Examples of design working life are given in Table 2.14.

The levels of reliability relating to ULS and SLS can be achieved by suitable combinations of protective measures (e.g., protection against fire or corrosion), measures relating to design calculations (e.g., choice of partial factors), measures relating to quality management, measures aimed to reduce errors in design (e.g., project supervision), and



**Table 2.14. Design Working Lives**

Design Working Life Category	Design Working Life (years)	Examples
1	10	Temporary structures
2	10–25	Replaceable structural parts (e.g., gantry girders, bearings)
3	15–30	Agricultural and similar structures
4	50	Building structures and other common structures
5	100	Monumental building structures, bridges, and other civil engineering structures

Source: Adapted from Table 2.1 of EN 1990 (EN 1990 2002).

execution (construction) of the structure (e.g., inspection during execution) and other kinds of measures.

The *Eurocode* defines three levels of consequences classes (CC1, CC2, and CC3), as defined in Table 2.15. Three reliability classes (RC1, RC2, and RC3) may be associated with the three consequence classes.

The vast majority of bridges are designed to CC2, with CC3 a possibility only for those bridges with very high consequences of failure, such as a signature bridge.

The provisions of the *Eurocode*, specifically EN 1990 (EN 1990 2002) with the partial factors given in Annex A1 and EN 1991 to EN 1999, yield designs consistent with reliability class RC2. The *Eurocode* uses the multiplication factors ( $K_{F1}$ ) given in Table 2.16 applied to load factors to differentiate the three reliability classes. Other measures (e.g., differing levels of quality control) in lieu of modifying the load factors are sometimes preferred.

**Table 2.15. Eurocode Consequence Classes**

Consequence Class	Description Related to Consequences	Reliability Class
CC1	Low consequence for loss of human life; economic, social, or environmental consequences small or negligible	RC1
CC2	Moderate consequence for loss of human life; economic, social, or environmental consequences considerable	RC2
CC3	Serious consequences for loss of human life or for economic, social, or environmental concerns	RC3

Source: Adapted from Table B1 of EN 1990 (EN 1990 2002).

**Table 2.16. Multiplication Factor ( $K_{F1}$ ) for Reliability Differentiation**

Reliability Class	$K_{F1}$
RC1	0.9
RC2	1.0
RC3	1.1

Table 2.17 summarizes the probabilities of failure ( $P_f$ ) inherent to the *Eurocode* and the *AASHTO LRFD* for ULSs, along with the corresponding reliability indices ( $\beta$ ) below them in italics. The defining probabilities of failure in the case of the *Eurocode* and the defining reliability indices for the *AASHTO LRFD* are shown in boldface.

#### SLS RELIABILITY

The SLSs of the *Eurocode* are categorized as reversible and irreversible. Reversible SLSs are those for which no consequences remain once a load is removed from a structure. For example, a crack-width limit state with a sufficiently small size is a reversible limit state, but one defined by a high width (e.g., 0.5 mm) is irreversible because, if the crack width is high enough, once the live load is removed the crack does not close completely.

The irreversible SLSs, which do not concern the safety of the traveling public, are calibrated to a higher probability of failure and corresponding reliability index than the strength limit states, as shown in Table 2.18.

#### SLS LOAD COMBINATIONS

EN 1990 (2002) includes three types of load combinations for the SLSs: characteristic combination, frequent combination, and quasipermanent combination. Table 2.19 summarizes the *Eurocode* SLS load combinations.

### Serviceability Design Basic Approach

#### BASIC EQUATION

The basic equation in the *Eurocode* (EN 1990 2002) for verifying that an SLS is satisfied is

$$E_d \leq C_d$$

where

$C_d$  = is the limiting design value of the relevant serviceability criterion and

$E_d$  = is the design value of the effects of actions specified in the serviceability criterion, determined on the basis of the relevant combination.



**Table 2.17. Target Probabilities of Failure ( $P_f$ ) and Target Reliability Indices ( $\beta_T$ )**

Code		Reference Period (years)				
		1	50	75	100	120
Eurocode	CC2 ( $K_{F1} = 1.0$ )	<b>1.00E-06</b>	5.00E-05	7.50E-05	1.00E-04	1.20E-04
		4.75	3.89	3.79	3.72	3.67
	CC3 ( $K_{F1} = 1.1$ )	<b>1.00E-07</b>	5.00E-06	7.50E-06	1.00E-05	1.20E-05
		5.20	4.42	4.33	4.26	4.22
AASHTO LRFD	Typical bridges ( $\eta_I = 1.0$ )	2.67E-06	1.33E-04	2.00E-04	2.67E-04	3.20E-04
		4.55	3.65	<b>3.50</b>	3.46	3.41
	Important bridges ( $\eta_I = 1.05$ )	9.60E-07	4.80E-05	7.20E-05	9.60E-05	1.15E-04
		4.76	3.90	<b>3.80</b>	3.73	3.68

**Table 2.18. Irreversible SLS Target Probabilities of Failure and Corresponding Reliability Indices**

Reliability Class	Reference Period (years)	
	1	50
RC2	1.00E-03	1.00E-01
	2.9	1.5

Source: Adapted from Table C2 of EN 1990 (Eurocode 0) (EN 1990 2002).

#### SERVICEABILITY CRITERIA

Specific serviceability criteria such as crack width, stress or strain limitation, and slip resistance exist in separate sections of the Eurocode (EN 1991 to EN 1999). In addition to these requirements, project-specific deformations to be considered in relation to serviceability requirements are required to be as detailed in relevant code annexes in accordance with the type

of construction works or agreed with the client or the national authority.

#### COMBINATION OF ACTIONS (LOAD COMBINATIONS)

The combinations of actions (load combinations) for serviceability limit states in the Eurocode are defined symbolically by Equation 2.28, which is the characteristic (rare) combination; Equation 2.29, which is the infrequent combination; Equation 2.30, which is the frequent combination; and Equation 2.31, which is the quasipermanent combination. The characteristic combination (Equation 2.28) is normally used for irreversible limit states; the frequent combination (Equation 2.30) is normally used for reversible limit states.

$$E_d = E \left\{ \sum_{j \geq 1} G_{k,j} + P_k + Q_{k,1} + \sum_{i > 1} \psi_{0,i} \cdot Q_{k,i} \right\} \quad (2.28)$$

$$E_d = E \left\{ \sum_{j \geq 1} G_{k,j} + P_k + \psi'_{1,1} \cdot Q_{k,1} + \sum_{i > 1} \psi_{1,i} \cdot Q_{k,i} \right\} \quad (2.29)$$

**Table 2.19. SLS Combinations**

SLS		Load Combination		
Type	Description	Type	Acceptance of Infringement	Example
Reversible	Limit states that will not be exceeded when the actions that caused the infringement are removed	Frequent	Specified duration and frequency of infringements are accepted	Crack-width limit state of a prestressed concrete beam with bonded tendons characterized by a 0.2-mm crack width
		Quasipermanent	Specified long-term infringement is accepted	Crack-width limit state for a reinforced-concrete or prestressed-concrete beam with unbonded tendons characterized by a 0.3-mm crack width
Irreversible	Limit states that remain permanently exceeded after the actions that caused the infringement are removed	Characteristic (5% probability of exceedance)	No infringement accepted	Crack-width limit state characterized by a 0.5-mm crack width, because such a wide crack cannot completely close once the loads that caused it are removed

$$E_d = E \left\{ \sum_{j \geq 1} G_{k,j} + P_k + \psi_{1,1} \cdot Q_{k,1} + \sum_{i > 1} \psi_{1,i} \cdot Q_{k,i} \right\} \quad (2.30)$$

$$E_d = E \left\{ \sum_{j \geq 1} G_{k,j} + P_k + \sum_{i > 1} \psi_{2,i} \cdot Q_{k,i} \right\} \quad (2.31)$$

where

$G_{k,j}$  = characteristic (extreme) value of permanent action  $j$ ;

$G_{k,j,\text{sup}}/G_{k,j,\text{inf}}$  = upper/lower value of permanent action  $j$ ;

$P$  = relevant prestressing value of prestressing action;

$Q_{k,1}$  = characteristic value of the leading (dominant) Variable Action 1;

$Q_{k,i}$  = characteristic value of the accompanying Variable Action 1;

$\psi_0$  = factor for characteristic value of a variable action;

$\psi_1$  = factor for frequent value of a variable action; and

$\psi_2$  = factor for quasipermanent value of a variable action.

The terms in Equations 2.28 through 2.31 are further defined as follows:

- **effect of action (E):** Effect of actions (or action effect) on structural members (e.g., internal force, moment, stress, strain) or on the whole structure (e.g., deflection, rotation).
- **permanent action (G):** Action that is likely to act throughout a given reference period and for which the variation in magnitude with time is negligible, or for which the variation is always in the same direction (monotonic) until the action attains a certain limiting value.
- **variable action (Q):** Action for which the variation in magnitude with time is neither negligible nor monotonic.
- **characteristic value of a variable action ( $\psi_0 Q_k$ ):** Value chosen (insofar as it can be fixed on statistical bases) so that the probability that the effects caused by the combination will be exceeded is approximately the same as by the characteristic value of an individual action. It may be expressed as a determined part of the characteristic value by using a factor ( $\psi_0 \leq 1.0$ ).
- **frequent value of a variable action ( $\psi_1 Q_k$ ):** Value determined (insofar as it can be fixed on statistical bases) so that either the total time within the reference period during which it is exceeded is only a small given part of the reference period, or the frequency of its being exceeded is limited to a given value. It may be expressed as a determined part of the characteristic value by using a factor ( $\psi_1 \leq 1.0$ ).
- **quasipermanent value of a variable action ( $\psi_2 Q_k$ ):** Value determined so that the total period of time for which it will

be exceeded is a large fraction of the reference period. It may be expressed as a determined part of the characteristic value by using a factor ( $\psi_2 \leq 1.0$ ).

The *Eurocode* allows some of the above expressions to be modified and gives detailed rules in relevant sections of the code (parts of *EN 1991* to *EN 1999*). Each *Eurocode* country has its own national annex in which country-specific requirements are placed; thus, the *Eurocode* allows each country to specify its own serviceability criteria in its national annex. Recommended values of the  $\psi$  factors for different types of structures (e.g., buildings, highway bridges, or railway bridges) are tabulated in the *Eurocode*. Table 2.20 shows the recommended values for highway bridges.

Note 1: The  $\psi$  values may be set by the National Annex. Recommended values of  $\psi$  factors for the groups of traffic loads and other more common actions are given in

- Table A2.1 for road bridges;
- Table A2.2 for foot bridges; and
- Table A2.3 for railway bridges.

Note 2: When the National Annex refers to the infrequent combination of actions for some serviceability limit states of concrete bridges, the National Annex may define the values of  $\psi_{\text{infq}}$ . The recommended values of  $\psi_{\text{infq}}$  are

- 0,80 for gr1a (LM1), gr1b (LM2), gr3 (pedestrian loads), gr4 (LM4, crowd loading), and  $T$  (thermal actions);
- 0,60 for  $F_w$  in persistent design situations; and
- 1,00 in other cases (i.e., the characteristic value is substituted for the infrequent value).

Note 3: The characteristic values of wind actions and snow loads during execution are defined in *EN 1991-1-6* (2005). When relevant, representative values of water forces ( $F_{wa}$ ) may be defined for the individual project.

### Existing Limit State

A summary of the SLS requirements in the *Eurocode* is in Appendix A.

## 2.3.3 Canadian Highway Bridge Design Code

### Background

The *CHBDC* (2006) and earlier *Ontario Highway Bridge Design Code* (1991) cover ULS and SLS. The serviceability limit states in the *CHBDC* include fatigue, deflection, cracking, and compressive stress in concrete. The SLS acceptability criterion was

**Table 2.20. Eurocode Recommended Values of  $\psi$  Factors for Highway Bridges**

Action	Symbol	$\Psi_0$	$\Psi_1$	$\Psi_2$	
Traffic loads ( <i>EN 1991-2</i> Table 4.4 [ <i>EN 1991-2 2003</i> ])	gr1a (LM1 + pedestrian or cycle-track loads) <sup>a</sup>	TS	0,75	0,75	0
		UDL	0,40	0,40	0
		Pedestrian + cycle-track loads <sup>b</sup>	0,40	0,40	0
	gr1b (single axle)	0	0,75	0	
	gr2 (horizontal forces)	0	0	0	
	gr3 (pedestrian loads)	0	0	0	
	gr4 (LM4—crowd loading)	0	0,75	0	
gr5 (LM3—special vehicles)	0	0	0		
Wind forces	$F_{wk}$ Persistent design situations Execution	0,6	0,2	0	
		0,8	—	0	
	$F_W^*$	1,0	—	—	
Thermal actions	$T_k$	0,6 <sup>c</sup>	0,6	0,5	
Snow loads	$Q_{snk}$ (during execution)	0,8	—	—	
Construction loads	$Q_c$	1,0	—	1,0	

<sup>a</sup>The recommended values of  $\psi_0$ ,  $\psi_1$ , and  $\psi_2$  for gr1a and gr1b are given for roads with traffic corresponding to adjusting  $\alpha_{cl}$ ,  $\alpha_{ej}$ ,  $\alpha_{gr}$ , and  $\beta_0$  equal to 1. Those relating to unified distribution load (UDL) correspond to the most common traffic scenarios, in which an accumulation of lorries can occur, but not frequently. Other values may be envisaged for other classes of routes, or of expected traffic, related to the choice of the corresponding  $\alpha$  factors. For example, a value of  $\psi_2$  other than zero may be envisaged for the UDL system of LM1 only, for bridges supporting a severe continuous traffic. See also *EN 1998-2* (2005).

<sup>b</sup>The combination value of the pedestrian and cycle-track load, which is mentioned in Table 4.4a of *EN 1991-2* (2003), is a “reduced” value.  $\psi_0$  and  $\psi_1$  factors are applicable to this value.

<sup>c</sup>The recommended  $\psi_0$  value for thermal actions may in most cases be reduced to zero for ULSs EQU, STR, and GEO. See also the design *Eurocodes*.

Source: Adapted from Table A2.1 of *EN 1990* (*EN 1990 2002*).

determined by reference to past practice. As an example of this process, special consideration was given to the tensile stress limit state in prestressed concrete girders. The acceptability criterion was formulated in terms of the minimum return period for exceeding the decompression moment. It was assumed that the girders will crack due to shrinkage before installation or under exceptionally heavy trucks and that the crack will reopen each time the decompression moment is exceeded. An open crack, even for a fraction of a second, is assumed to allow water with salt or other pollutants to penetrate and eventually reach the rebar and prestressing steel, resulting in corrosion, delamination, spalling of concrete, and girder failure. The minimum acceptable return period for exceeding the decompression moment was then determined by a group of experts invited by the Code Control Committee using a process of expert elicitation (Delphi process). The group was asked to provide their expert opinion. They deliberated and came to a conclusion that a return

period of 3 weeks is acceptable. However, the group did not feel strongly about it, so they agreed that the target probability of exceeding this limit state is 50%, which corresponds to the target reliability index ( $\beta_T = 0$ ).

### Existing Limit States

In general, the SLSs in the *CHBDC* are very similar to the SLSs currently specified in *AASHTO LRFD*. There are some differences in application, but the general phenomena being treated are basically the same. No new limit states that do not exist in *AASHTO LRFD* were found in the 2006 *CHBDC*.

*CHBDC* Clause 3.5.1 and Table 3.1, in particular, contain the requirements for load factors and load combinations. Table 3.6.1(a) lists only two load combinations for serviceability limit states. Service-load combinations use a load factor of 0.9 for the live load that is based on the CL-W-625 truck (140.5 kips, 59 ft long) or lane loading. The CL-W-625 truck

is considerably larger than the HL-93 truck alone (i.e., without the uniform distributed load). Load Combination 2 applies to superstructure vibration only. The *CHBDC* also specifies a lane load that consists of 80% of the axles of the CL-W truck superimposed on a UDL of 9 kN/m, which is similar to the UDL used with the HL-93 loading.

*CHBDC* Clause 6.4.1.3 deals with serviceability limit states and foundations. Three criteria are noted:

- Foundation deformations that cause SLS limits to be exceeded;
- Deformations that cause the riding surface or transitions between the approaches and the bridge to become unacceptable; and
- Deformations that cause unacceptable structural misalignment, distortion, or tilting.

Clause 7.6.5.2 deals with construction requirements for pipe arches and limits to downward deflection. The commentary reinforces that this is a construction requirement rather than a design control.

Clause 7.7.5.2 speaks to upward or downward crown deflection during construction of metal box structures and provides a 1% requirement. Little additional information is provided in the commentary, which notes that AASHTO Article 12.8.5.3 has limits for live load deflection.

Clause 8.5.1 states that cracking, deformation, stress, and vibration SLSs should be considered.

Clause 8.5.2 specifies serviceability limit states for concrete structures and indicates that these are cracking, deformations, stress, and vibration.

Clause 8.5.2.2 deals with a cross reference to Clause 8.12 with some limits on earth cover.

Clause 8.5.2.3 deals with deformation provisions and indicates that short-term and long-term deformations may affect the function of the structure.

Clause 8.5.2.4 deals with stresses in the component not exceeding certain values of Clauses 8.7.1, 8.8.4.6, and 8.23.7.

Clause 8.5.2.5 deals with vibrations and refers back to clauses in Section 3 on loads.

The commentary for Clause 8.5.2.1 speaks to the fact that, in general, nonprestressed and partially prestressed components are expected to crack under the service loads. The commentary indicates that it is generally a good practice to provide sufficient prestress so that under permanent loads, any cracks previously caused due to the application of live load are closed under permanent loads to enhance durability.

Clause 8.12 deals with control of cracking by specifying distribution requirements and a tensile strain limit.

Clause 8.12.3.1 specifies limits on crack width for nonprestressed and prestressed components for several types of exposure.

Clause 8.12.3.2 provides guidance on calculating the crack width and spacing based on parameters that include the average strain in the reinforcing. A distinction is made for epoxy-coated reinforcement, for which the calculated crack width is increased 20%.

Clause 10.5.3.1 specifies serviceability limit states for steel structures; these include deflection, yielding, slipping of bolted joints, and vibrations.

Clause 10.5.3.2 for deflections is a cross reference for Clause 10.16.4, which applies to orthotropic decks only.

Clause 10.5.3.3 deals with the prevention of general yielding at the SLSs, which appears to pertain to Clause 10.11.4 (permanent deflections for composite sections). The latter is similar to the AASHTO overload requirements, except that the *CHBDC* load factor for live load is 0.9 as opposed to the AASHTO load factor of 1.3. As discussed in Chapter 6, the net result is probably similar because of the heavier *CHBDC* live load. This is not a new limit state, although the numerical values might differ somewhat from AASHTO.

Clause 10.11.3 is an SLS for differential shrinkage between restrained and free shrinkage of concrete and steel composite members.

### 2.3.4 Japanese Geotechnical Society Foundation Design Guideline

The Japanese Geotechnical Society (JGS) prepared a draft foundation design guideline in 2002. This document attempts to phrase the structural and geotechnical design principles following the general requirements of ISO 2394. Three limit states are defined on the basis of the following functional statements:

- With respect to the various magnitudes and frequencies of loading during the expected service life, the structures shall satisfy structural performance as characterized by structural strength, stability, deformability, and durability, including serviceability, repairability, and safety with appropriate levels of reliability.
- The structures shall be designed to be sufficiently safe so as to prevent serious injury to occupants and surrounding personnel during all possible design situations through the design working life. This functional statement is related to the topic of safety.
- The structures may be designed, by judgment of the owner based on the importance of the structure, such that normal functions are preserved (serviceability) or damage is limited within a certain tolerable level (repairability) against specified loading conditions during the design working life with appropriate reliability.
- It is not prohibited for owners of the structures to specify additional functional statements other than those stated above based on their own judgment.

The above functional statements are in the context of design working life. The JGS document indicates that the design working life may be determined by considering various factors including life-cycle cost, durability, deterioration, and the functional life of the structure. The document notes that care should be taken to ensure that the safety margin (i.e., reliability) introduced to each limit state is strongly related to the design working life of the structure. The structural performance requirements of the structure are specified by several limit states according to the load levels classified according to their frequencies, as follows:

- High-frequency variable actions are those expected to occur once or a few times with significantly high probability during the design working life of the structure.
- Low-frequency variable actions are those that may or may not occur during the design working life of the structure (i.e., a low-frequency variable action is an event with a very low occurrence probability).

Using the preceding concepts, the JGS presents three major limit states in the following qualitative manner:

- *ULS*—The structures may sustain considerable damages but not to the extent of collapse that would result in serious injury or loss of life. This limit state corresponds to the functional statement of safety as noted above.
- *Repairable limit state*—Damage to the structure, although it may influence durability, is limited to a level that can be

repaired at a reasonable cost and in a relatively short period of time. This limit state, therefore, can be interpreted as a state in which the majority of the value of the structure is preserved. Furthermore, this limit state sometimes implies a state in which marginal use of the structure is possible for rescue operations right after an extraordinary event such as a large earthquake. This limit state corresponds to the reparability defined in the functional statement above.

- *SLS*—Damage to the structure is limited to a level at which all common functions of the structure are preserved and do not influence structural durability. This limit state corresponds to the serviceability defined in the functional statement above.

The JGS document indicates that additional performance requirements and limit states other than those defined above may be defined as deemed necessary. With respect to the three limit states identified above, the JGS document provides a conceptual view of a performance matrix for describing the performance requirements of a structure. In the performance matrix, design situations and limit states are taken as the axes of the coordinate system, and performance requirements are coordinated according to the importance of the structure. The example performance matrix presented in Figure 2.5 consists of three levels of design situations and limit states. It reflects a seismic design situation, which for most structures in Japan is the critical design situation.

The performance requirements defined above are required to be verified by two approaches: Approach A and Approach B.

	SLS	Repairable Limit State	ULS
High frequency, low impact	Important, ordinary and easily repairable structures	—	—
Medium frequency, medium impact	Important and ordinary structures	Easily repairable structures	—
Low frequency, high impact	—	Important structures	Ordinary and easily repairable structures

**Figure 2.5. Conceptual view of a performance matrix. Note: — = performance requirement not specified by Japanese Geotechnical Society.**



Approach A does not require any specified method for performance verification of the structure. It requires, however, that the designer prove the structure satisfies the specified performance requirements with an appropriate level of reliability. A designer who uses Approach A is required to submit the necessary design report and documentation for examination to the administrative organization or local government responsible for controlling the safety of the structure. In contrast, in Approach B the verification of performance requirements is based on specific design codes specified by the owner. The JGS document recommends use of the partial-factors format for design.

### 2.3.5 Overarching Characteristics of Other Specifications to Be Considered

#### *Reversible Versus Irreversible Limit States*

SLSs may be categorized as reversible and irreversible. Reversible SLSs are those for which no consequences remain once a load is removed from a structure. Irreversible SLSs are those for which consequences remain.

Due to their reduced safety implications, irreversible SLSs, which do not concern the safety of the traveling public, are calibrated to a higher probability of failure and a corresponding lower reliability index than the strength limit states. Reversible SLSs are calibrated to an even lower reliability index.

#### *Load-Driven Versus Non-Load-Driven Limit States*

The difference between load-driven and non-load-driven limit states is basically in the degree of involvement of externally applied load components in the formulation of the limit state function. In the load-driven limit states, the damage occurs due to accumulated applications of external loads, usually live load (trucks). Examples of load-driven limit states include decompression and cracking of prestressed concrete and vibrations or deflection. The damage caused by exceeding SLSs may be reversible or irreversible and, therefore, the cost of repair may vary significantly. However, in non-load-driven SLSs, the damage occurs due to deterioration or degradation as a function of time and aggressive environment or as inherent behavior due to certain material properties. Examples of non-load-driven SLSs include penetration of chlorides leading to corrosion of reinforcement, leaking joints leading to corrosion under the joints, and shrinkage cracking of concrete components. In these examples, the external load occurrence plays a secondary role.

### 2.3.6 Lessons Learned from Review of Existing Design Specifications

Review of existing design specifications revealed that the SLSs covered by different specifications are somewhat similar. It

was concluded that other specifications do not include “new” SLSs that need to be added to *AASHTO LRFD*. However, the review resulted in some concepts that were of interest. These concepts include

- The target reliability index for SLSs may have different values for different limit states. Furthermore, the target reliability for a certain limit state may vary depending on the consequences of exceeding that limit state.
- To differentiate between different limit states according to the consequences of exceeding the limit state, the following factors were considered:
  - Whether the limit state is reversible or irreversible: Irreversible limit states may have higher target reliability than reversible limit states.
  - Relative cost of repairs: Limit states that have the potential to cause damage that is costly to repair may have higher target reliability than limit states that have the potential of causing only minor damage.

## 2.4 Surveys of Current Practice

### 2.4.1 Summary of R19B Survey

A focused survey was sent to 31 bridge owners, four industry representatives, and one university. A copy of the survey questionnaire and a summary of responses are included in Appendix B. The state bridge engineers who received the survey specifically included the chairs of the AASHTO Technical Committees for joints and bearings, culverts, steel design, concrete design, loads, and foundations. Sixteen responses were received. The survey consisted of two parts: one was superstructure oriented, and the other was substructure and foundation movement oriented.

Although there were only 16 responses, some consistency was apparent in the most significant items in structural maintenance budgets, as seen in Figure 2.6.

The most-cited responses confirmed that serviceability issues relating to expansion joints and deck cracking are widespread. Responses highlighted the following: deterioration and section loss of beam ends, painting of steel members, problems with bearings, corrosion of reinforcement, and deck overlays. Although there were many serviceability issues, many responses indicated that the SLSs are adequate in their current form or would be adequate with some additional limit states, such as

- Foundation settlement;
- Guidance on stress checks based on corrosion-reduced section properties;
- Better crack control reinforcement provisions and stress limits for concrete flexural members; and

Responses to SHRP 2 R19B Survey Question 1

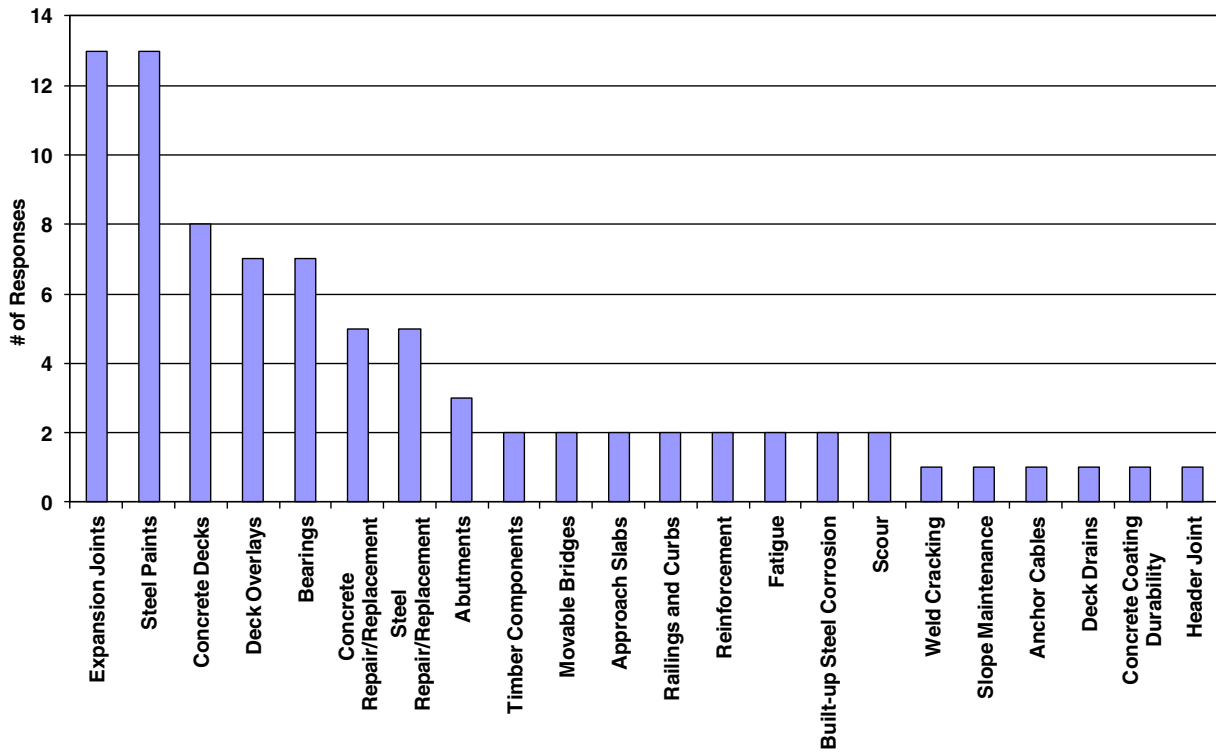


Figure 2.6. Survey responses indicating the most significant structural maintenance budget items.

- Additional limit states for connections, expansion joints, and bearings.

Despite suggestions for additional limit states, there was a common theme that additional limit states would not have affected or prevented the observed reduced serviceability.

Approximately half the responses indicated that the respondents did not use deterioration models other than Pontis, while the other half used engineering judgment, had developed their own models, or were collecting data to develop their own model. In addition, approximately one-half of the responses indicated that no additional assessments were completed beyond those that are a part of Pontis, and one-quarter indicated that they complete additional qualitative assessments but no additional quantitative assessments. The other one-quarter of the responses indicated that they complete additional qualitative and quantitative assessments, including condition surveys, chloride penetration depth measurements, ultrasonic testing, and condition scales for each component combined with figures and notes that show the overall condition and deficiencies. The qualitative assessments have indicated a correlation between deterioration and reduced serviceability, but the reduction in serviceability was not quantified.

There were few responses to the second questionnaire about bridge movement and observed distress. The responses

that were received focused on structures typically built within the last two decades. All the structures mentioned in the responses were continuous spans with integral or stub abutments. In addition, the approach fill was either a mechanically stabilized earth wall or fill with side slope. The responses regarding tolerable movements were split almost evenly between acceptable and not acceptable. The responses appeared to be specific to the structures described in the section about bridge movement and observed distress rather than a generalized response indicative of a population of bridges. The final questions dealt with the allowable movement of new structures, with a majority of agencies noting that they are not following the guidance on tolerable movements found in *AASHTO LRFD* Article C10.5.5.2. Agencies differed in what their criteria for allowable movements were, with some determining criteria on a case-by-case basis, and others using general-purpose quantitative requirements.

#### 2.4.2 Summary of NCHRP Project 12-83 Survey Related to Concrete Design

A survey of current practices related to the SLs of concrete structures was developed in NCHRP Project 12-83. The survey was sent to major bridge owners across North America, including all 50 state DOTs, the Ministry of Transport in all

Canadian provinces, the District of Columbia, and many turnpike authorities, bridge authorities, and commissions.

The survey included 20 questions covering the following topics:

- Modifications to the specification loading (HL-93 loading) for SLSs;
- Checking SLSs under the effects of legal loads as part of the normal design procedure;
- Revisions to the SLS stress limits for prestressed concrete components;
- Revisions to existing SLSs for concrete structures;
- Method used for designing for control of cracking by distribution of reinforcement;
- Checking concrete superstructure and substructures for any additional service-load combinations beyond those in *AASHTO LRFD*;
- Checking concrete structures for SLSs under overloads;
- Cracking of pretensioned concrete beams immediately after prestressing force release;
- Observations of cracking of prestressed concrete beams in service;
- Damage to ends of prestressed beams under expansion joints;
- Use of the deck empirical design method and the performance of these decks in service;
- Observations of deck cracking;
- Type of reinforcement bars used in newer decks (e.g., black bars, epoxy-coated, galvanized, stainless steel);
- Average life span of concrete decks and the main reasons decks are replaced;
- Types of concrete superstructures in use;
- Problems with bearings in concrete structures;
- Cracking of abutments and piers;
- Average service life span of the concrete substructures;
- Fatigue problems in concrete superstructures; and
- Use of coatings in concrete substructures.

Responses from 27 state DOTs and the Ontario Ministry of Transportation were received. The responses to the questionnaire indicated that most bridge owners apply the SLSs included in *AASHTO LRFD* with few or no revisions. The additional limit states used by bridge owners appear to be related either to owner-specified vehicles or to address a specific issue that does not seem to be shared by other bridge owners, as evident by the lack of use of these additional limit states by other owners. It is expected that some of the other agencies that did not respond to the questionnaire also use permit vehicles in checking some aspects of the design under service loads. The use of permit vehicles to check some service conditions and the desire expressed by some bridge designers to have guidance on applying permit vehicles to

service conditions suggest a need exists for a service-load combination akin to the Strength II limit state that applies to permit (overload) vehicles. The load factors for live load for such a load combination can be determined using the same principles used for calibrating other SLSs. However, the statistical parameters to be used for permit vehicles differ from those for random traffic.

One important modification to the existing limit state is the load factor for live load in the Service III limit state in *AASHTO LRFD*. One state, Louisiana, uses a load factor of 1.0 for live load to check tension in prestressed concrete under the Service III limit state instead of the 0.8 specified in *AASHTO LRFD*. The higher load factor addresses an issue that has gained importance with AASHTO's adoption of newer prestress loss equations in 2005. Some engineers are of the opinion that the lower load factor compensated for the conservatism in the older prestressing loss equations and, thus, guarded against excessive conservatism in the design. The use of the new equations, which are believed to provide a more accurate estimate of the prestressing losses, may have eliminated the need for the 0.8 load factor.

### 2.4.3 Summary of the R19As Survey as it Relates to R19B

One of the main objectives in Phase 1 of Project R19A was the identification and ranking of the problematic areas preventing bridges from providing long service life. The research team considered two alternatives for ranking of the performance:

- Ranking based on quantitative performance data that are obtained from experimental investigations or field observations of bridges that are currently in service; and
- Ranking based on qualitative opinion data (an expert elicitation or Delphi process).

The R19A research team concluded that despite the availability of some experimental data, it is very difficult to quantify the performance of actual in-service components. The majority of the reported tests were performed using accelerated testing methods, which are not easily correlated with field conditions. They often focused only on the effect of one degradation process, while experience shows that reality is more complex, and often several degradation processes interact with the environmental loads. The combined effects and complexity of deterioration processes and the uncertain nature of environmental loads complicate the prediction of the service life for both new and existing structures.

The other source of quantitative data is from long-term monitoring of bridges in service, but such data are not available at this time. In summary, the research team concluded that there are no available data for quantitative evaluation

**Table 2.21. SLSs Identified for Development**

LRFD Article	Reversible	No. of Lanes	MPF
2.5.2.6.2 Criteria for Deflection	Yes	Single	—
3.4.1 Load Factors and Load Combinations for Fatigue	No	Single	—
5.5.3.1 General—Compressive Stress Limit for Concrete— A Fatigue Criterion	No	Single	No
5.5.3.2 Fatigue of Reinforcing Bars	No	Single	—
5.5.3.4 Fatigue of Welded or Mechanical Splices of Reinforcement	No	Single	—
5.6.3.6 Crack Control Reinforcement—To be revised but not calibrated—Deemed to satisfy	No	—	—
5.7.3.4 Control of Cracking by Distribution of Reinforcement— Not calibratable—Deemed to satisfy	No	na	—
5.9.3 Stress Limitations for Prestressing Tendons	No	Multiple	Yes
5.9.4.2.2 Tension Stresses	Yes	Single	No
6.10.4.2 Permanent Deformations of Steel Structures	No	Single	No
6.13.2.8 Slip Resistance of Bolts	No	Single	No
10.6.2.4 Settlement Analysis of Shallow Foundations	No for footing, possible for superstructure	Multiple for sands, none for clays	—
10.8.2.2 Settlement (related to drilled shaft groups)	No	Multiple	Yes
10.8.2.4 Horizontal Movement of Shaft and Shaft Groups	No	—	—

Note: MPF = multiple presence factor; — = current criteria do not specify whether or not the MPF is applicable; na = not applicable.

and ranking of existing or promising strategies to quantify the reduction in service life due to deterioration.

As there are no quantitative data for ranking and selection of the problematic areas, the R19A research team prioritized the research topics based on the qualitative opinion of experts. Obtained information was organized and presented in technology, strategy, and research tables that provide the information on the potential service life issues and available solutions. The tables also provide information on the advantages and disadvantages of different design concepts, along with other relevant data necessary to evaluate different strategies addressing durability. Four major problem research areas were identified: decks, joints, bearings, and durability.

The major product from the R19A research effort is *Design Guide for Bridges for Service Life* (Azizinamini et al. 2013), which is intended to complement AASHTO LRFD specifications and incorporate the design for durability and enhanced service life. The document provides a basis for the selection, design, fabrication, construction, inspection, management, and maintenance of bridge systems.

In summary, the R19A research team stated that due to the lack of quantitative data with respect to almost all bridge elements, it was difficult to propose or develop new design methodologies that are based on deterioration models.

## 2.5 SLSs to Be Considered in This Report

Potential limit states and possible calibration approaches for general requirements, concrete structures, steel structures, geotechnical issues, joints, and bearings have been reviewed. Some of the potential limit states have since been determined to be uncalibratable. For example, some are deterministic or are based on judgment and experience. The SLSs believed to be calibratable are listed in Table 2.21 along with whether the phenomena being addressed are reversible or irreversible and whether the live load involves single-lane or multiple-lane loading.

Note that SLS references to partial prestressing have been removed. AASHTO no longer accepts partial prestressing as a design strategy.

## CHAPTER 3

# Overview of Calibration Process

### 3.1 Introduction

The new generation of bridge design codes is based on probabilistic methods. Load and resistance (load-carrying capacity) parameters are treated as random variables, and structural performance is quantified in terms of the reliability index (Nowak and Collins 2013). This approach allows for a rational comparison of different materials and load combinations. An increased degree of uncertainty causes a reduction in reliability, and strict control of structural parameters results in a safer structure. The probabilistic analysis requires statistical models of load and resistance parameters. The load models for bridges can be based on truck surveys and other field tests. Resistance models for structural components (e.g., bridge girders) can be derived from material tests, lab tests, and analytical simulations.

With the advent of limit states design methodology in North American design specifications, there has been an increasing demand to obtain statistical data to assess the reliability of designs. Reliability depends on load and resistance factors that are determined through calibration procedures using available statistical data. Methodologies that can be used to determine load and resistance factors, including the basic reliability concepts and detailed procedures that can be used to characterize data to develop the statistics and functions needed for reliability analysis, are described in NCHRP Report 368 (Nowak 1999) and TRB Circular E-C079 (Allen et al. 2005).

The code calibration procedure can include closed-form solutions for estimating load and resistance factors that can be used for simple cases, as well as more rigorous probabilistic analysis methods such as the Monte Carlo method, which is described in Section 3.2.3. There are three levels of probabilistic design: Levels I, II, and III (Nowak and Collins 2013). The Level I method is the least accurate, and Level III is the only fully probabilistic method. However, Level III requires complex statistical data beyond what are generally available in engineering practice. Level I and Level II probabilistic

methods are more viable approaches for structural design. In Level I design methods, safety is measured in terms of a safety factor, or the ratio of nominal (design) resistance to nominal (design) load. In Level II, safety is expressed in terms of a reliability index ( $\beta$ ). The Level II approach generally requires iterative techniques best performed using computer algorithms. For simpler cases, closed-form solutions to estimate  $\beta$  are available. Closed-form analytical procedures to estimate load and resistance factors should be considered approximate, with the exception of very simple cases for which an exact closed-form solution exists. Alternatively, spreadsheet programs can be used to estimate load and resistance factors using the more rigorous and adaptable Monte Carlo simulation technique, which in turn can be used to accomplish a Level II probabilistic analysis.

The goal of Level I or II analyses is to develop factors that increase the nominal load or decrease the nominal resistance to give a design with an acceptable and consistent reliability. To accomplish this, an equation that incorporates and relates all the variables that affect the potential for failure of the structure or structural component must be developed for each limit state.

For load and resistance factor design (LRFD) calibration purposes, statistical characterization should focus on the prediction of load or resistance relative to what is actually measured in a structure. Thus, this statistical characterization is typically applied to the bias, the ratio of the measured to predicted value. The predicted (nominal) value is calculated using the design model being investigated. The degree of variation is measured in terms of the coefficient of variation (CV), which is the ratio of the standard deviation to the mean value.

Regardless of the level of probabilistic design used to perform LRFD calibration, the steps needed to conduct a calibration are as follows:

- Develop the limit state equation to be evaluated so that the correct random variables are considered. Each limit



state equation must be developed on the basis of a prescribed failure mechanism. The limit state equation should include all the parameters that describe the failure mechanism and that would normally be used to carry out a deterministic design of the structure or structural component.

- Statistically characterize the data on which the calibration is based (i.e., the data that statistically represent each random variable in the limit state equation being calibrated). Key parameters include the mean, standard deviation, and CV, as well as the type of distribution that best fits the data (often normal or lognormal).
- Select a target reliability value based on the margin of safety implied in current designs, considering the need for consistency with reliability values used in the development of other *AASHTO LRFD* specifications, the consequence of exceeding the limit state, cost, and the levels of reliability for design as reported in the literature for similar structures. If the performance of existing structures that were designed using the current code provisions is acceptable, then there is no need to increase the safety margin in the newly developed code. Furthermore, the acceptable safety level can be taken as corresponding to the lower tail of distribution of betas.
- Determine load and resistance factors by using reliability theory consistent with the selected target reliability.

The accuracy of the results of a reliability theory analysis is directly dependent on the adequacy, in terms of quantity and quality, of the input data used. The final decision made regarding the magnitude of the load and resistance factors selected for a given limit state must consider the adequacy of the data. If the adequacy of the input data is questionable, the final load and resistance factor combination selected should be weighted toward a level of safety that is consistent with past successful design practice, using the reliability theory results to gain insight as to whether past practice is conservative or unconservative.

The calibration procedure can be different depending on the type of limit state. In the case of serviceability limit states, it is much more complex, mostly due to difficulties in formulation of the limit state equation. The parameters of load and resistance are determined not only by magnitude, as is the case with strength limit states, but also by frequency of occurrence (e.g., crack opening) and as a function of time (e.g., corrosion rate, chloride penetration rate). Acceptability criteria are not well defined as they are subjective (e.g., deflection limit, allowable tensile stress), and the code-specified limit state function does not necessarily have a physical meaning (e.g., allowable compression stress in concrete).

## 3.2 Calibration by Determination of Reliability Indices

### 3.2.1 Basic Framework

Expanding on the four basic steps outlined above, the framework for calibration of service limit state (SLS) using reliability indices is summarized as follows:

1. *Formulate the limit state function and identify basic variables.* Identify the load and resistance parameters and formulate the limit state function. For each considered limit state, the acceptability criteria were established. In most cases, it was not possible to select a deterministic boundary between what is acceptable and unacceptable. Some of the code-specified limit state functions do not have a physical meaning (e.g., allowable compression stress in concrete).
2. *Identify and select representative structural types and design cases.* Select the representative components and structures to be considered in the development of code provisions for the SLSs.
3. *Determine load and resistance parameters for the selected design cases.* Identify the design parameters on the basis of typical structural types, loads, and locations (climate, exposure to harsh environment). For each considered element and structure, the values of typical load components must be determined.
4. *Develop statistical models for load and resistance.* Gather statistical information about the performance of the considered types and models in selected representative locations and traffic. Gather statistical information about quality of workmanship. Ideally, for a given location and traffic, the required data include general assessment of performance, assumed time to initiation of deterioration, assumed deterioration rate as a function of time, maintenance, and repair (frequency and extent). Develop statistical load and resistance models (as a minimum, determine the bias factors and CVs). The parameters of load and resistance are determined not only by magnitude, as is the case with strength limit states, but also by frequency of occurrence (e.g., crack opening) and as a function of time (e.g., corrosion rate, chloride penetration rate). The available statistical parameters were used, but the database is limited, and for some serviceability limit states there is a need to assess, develop, or derive the statistical parameters. The parameters of time-varying loads were determined for various time periods. The analyses were performed for various traffic parameters (average daily truck traffic, legal loads, multiple presence, traffic patterns). The load frequencies served as a basis for determination of acceptability criteria.

5. *Develop the reliability analysis procedure.* Reliability can be calculated using either a closed-form formula or the Monte Carlo method. The reliability index for each case can be calculated using closed formulas available for particular types of probability distribution functions in the literature or the Monte Carlo method. In this study, all the reliability calculations were based on Monte Carlo analysis. The Monte Carlo method is a stochastic technique that is based on the use of random numbers and probability statistics to simulate a large number of computer-based experiments. The outcome of the simulation is a large number of solutions that takes into account all the random variables in the resistance equation.
6. *Calculate the reliability indices for current design code and current practice.* Calculate the reliability indices for selected representative bridge components corresponding to current design and practice.
7. *Review the results and select the target reliability index.* Use the calculated reliability indices to select the target reliability index ( $\beta_T$ ). Select the acceptability criteria (i.e., performance parameters) that are acceptable and the performance parameters that are not acceptable.
8. *Select potential load and resistance factors.* Prepare a recommended set of load and resistance factors. The objective is that the design parameters (load and resistance factors) have to meet the acceptability criteria for the considered design situations (location and traffic). The design parameters should provide reliability that is consistent, uniform, and conceivably close to the target level.
9. *Calculate reliability indices.* Calculate the reliability indices corresponding to the recommended set of load and resistance factors for verification. If the design parameters do not provide consistent safety levels, modify the parameters and repeat Step 8.

Figure 3.1 presents the flowchart for the basic calibration framework described in the nine steps above.

Step 4 requires the analysis of data describing load and resistance. Normal probability paper is a special scale that facilitates the statistical interpretation of data. The horizontal axis represents the variable (e.g., gross vehicle weight, mid-span moment, or shear) for which the cumulative distribution function (CDF) is plotted. The vertical axis represents the number of standard deviations from the mean value, which is often referred to as the standard normal variable, or the  $Z$ -score. The vertical axis can also be interpreted as the probability of being exceeded; for example, one standard deviation corresponds to 0.159 probability of being exceeded. The most important property of normal probability paper is that the CDF of a normal random variable is represented by a straight line. The straighter the plot of data, the more

accurately it can be represented as a normal distribution. In addition, the curve representing the CDF of any other type of random variable can be evaluated, and its shape can provide an indication about the statistical parameters, such as the maximum value and type of distribution for the whole CDF or, if needed, only for the upper or lower tail of the CDF. Furthermore, the intersection of the CDF with the horizontal axis (zero on the vertical scale) corresponds to the mean. The slope of the CDF determines the standard deviation, or  $\sigma_x$  as shown in Figure 3.2. A steeper CDF on probability paper indicates a smaller standard deviation. Further information about the construction and use of probability paper can be found in textbooks (e.g., Nowak and Collins 2013).

### 3.2.2 Closed-Form Solutions

The reliability index ( $\beta$ ) is defined as shown by Equation 3.1:

$$\beta = \Phi^{-1}(P_f) \quad (3.1)$$

where  $\Phi^{-1}$  is the inverse of the standard normal distribution, and  $P_f$  is the probability of failure.

If the limit state function ( $g$ ) can be expressed in terms of two random variables,  $R$  representing resistance and  $Q$  representing the load effect, then  $g$  is given by Equation 3.2:

$$g = R - Q \quad (3.2)$$

and the probability of failure is expressed by Equation 3.3:

$$P_f = \text{Prob}(g < 0) \quad (3.3)$$

$\beta$  can then be calculated using a closed-form formula in two cases: when both  $R$  and  $Q$  are normal random variables or when both  $R$  and  $Q$  are lognormal random variables. In all other cases, the available procedures produce approximate results.

If both  $R$  and  $Q$  are normal random variables,  $\beta$  can be calculated using Equation 3.4:

$$\beta = \frac{\bar{R} - \bar{Q}}{\sqrt{\sigma_R^2 + \sigma_Q^2}} \quad (3.4)$$

where

$\bar{R}$  = mean or expected value of the distribution of resistance;

$\bar{Q}$  = mean or expected value of the distribution of load;

$\sigma_R$  = standard deviation of the distribution of resistance; and

$\sigma_Q$  = standard deviation of the distribution of load.

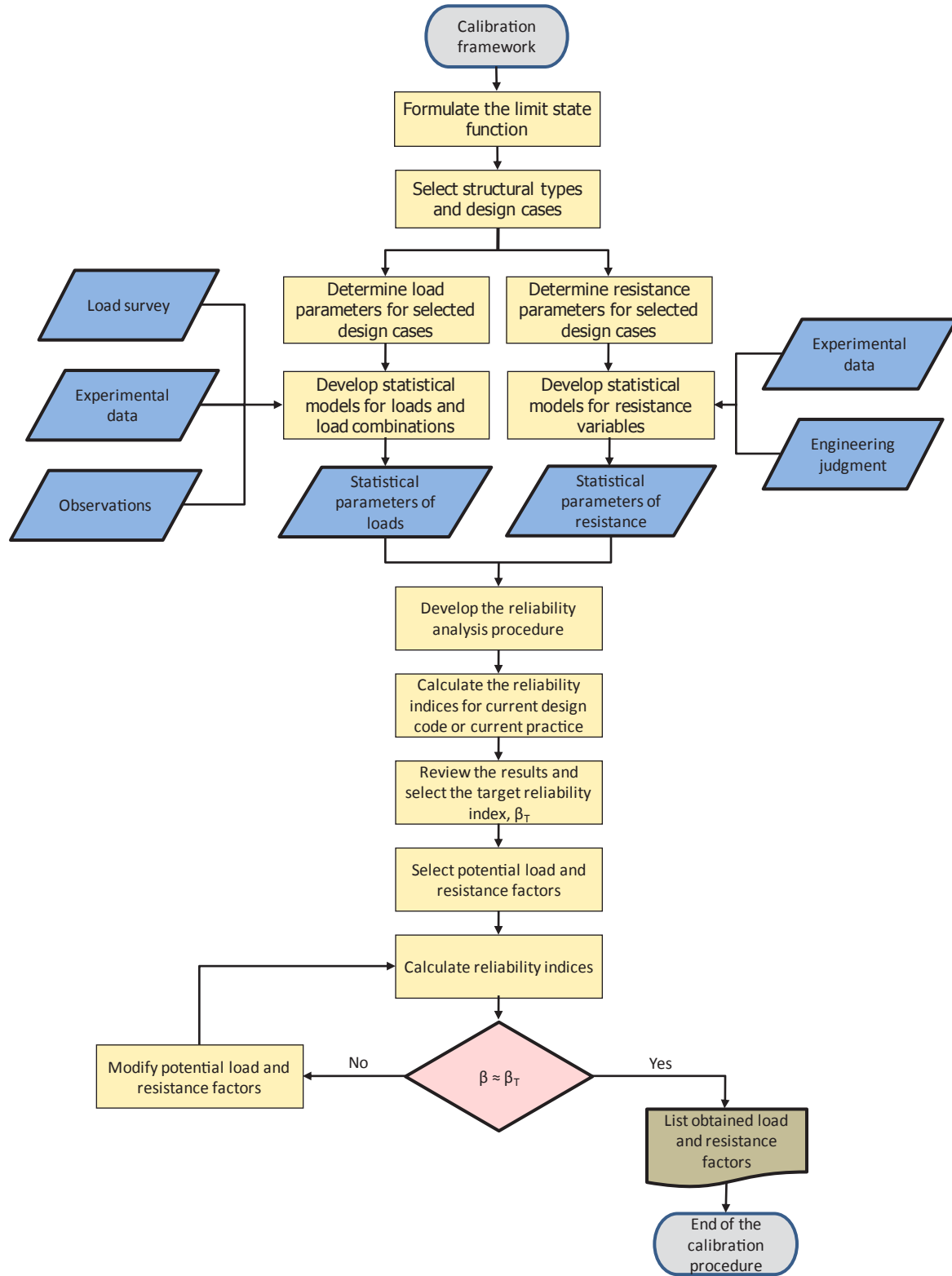


Figure 3.1. Flowchart of basic calibration framework.

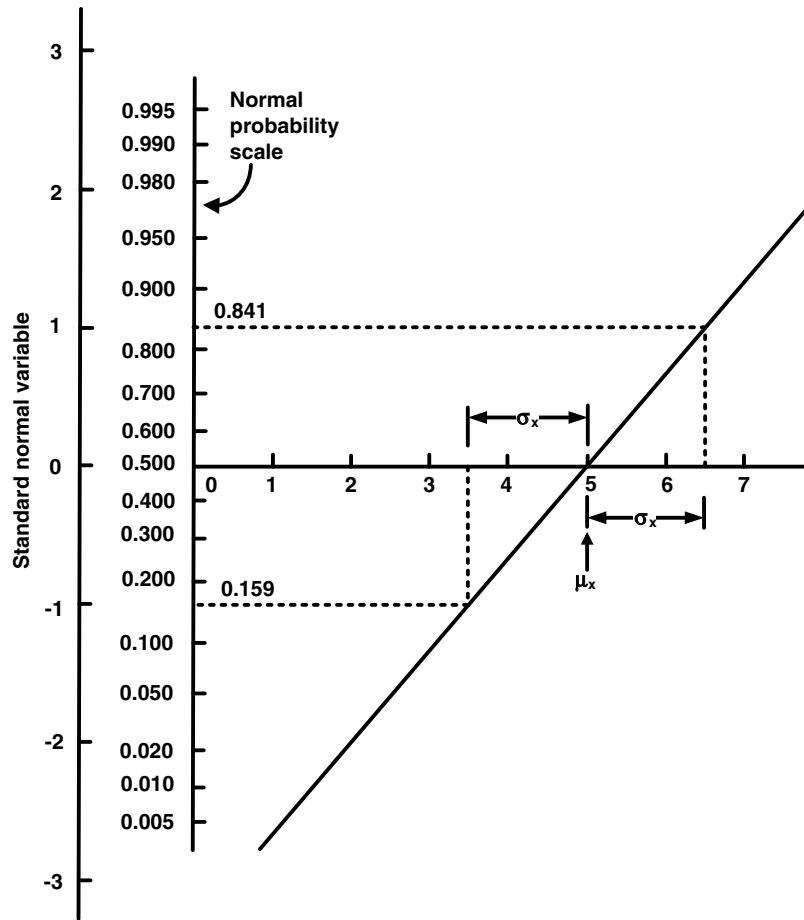


Figure 3.2. Use of normal probability paper.

Sometimes,  $R - Q$  is termed  $M$ , the margin of safety. Using this terminology,  $\beta$  is given by Equation 3.5:

$$\beta = \frac{\bar{M}}{\sigma_M} \tag{3.5}$$

For the case in which both distributions are lognormally distributed, a more complete derivation of the closed-form solutions and how they can be applied to LRFD calibration is shown by Allen et al. (2005). Although closed-form solutions are useful for illustrative purposes, in practice either load or resistance or both are not normally distributed, which limits the use of closed-form solutions in code calibration.

### 3.2.3 Using Monte Carlo Simulation in the Calibration Process

The typical application of Monte Carlo simulation, referenced in Step 5 for bridge structural reliability and as reported in the literature (Allen et al. 2005; Nowak and Collins 2013),

is well known. Application of Monte Carlo simulation follows these steps:

- It is assumed that dead load is normally distributed and live load CDF is as shown on the probability paper [directly from WIM (weigh in motion) data]. The statistical parameters of live load depend on the time period. For longer time periods, the statistical parameters are obtained by extrapolation of the available WIM data. The total load is a sum of dead load and live load and, therefore, in practice it can be treated as a normal variable. This assumption is partly justified by the central limit theorem, and it is acceptable if the load components are of similar magnitude (Nowak and Collins 2013).
- Resistance is assumed to be lognormally distributed. The resistance side of the LRFD equation is a product of terms.
- The minimum statistical parameters needed for each random variable are the CV ( $V$ ) and the bias ( $\lambda$ ). Using the reported statistics of load and resistance along with computer-generated random numbers, the distributions of load and resistance are developed, and values are chosen

randomly from these distributions. For example, for the simple load combination of dead load plus live load, random values of dead load and live load are chosen from the normal distributions fitted in the region of interest. A random value of resistance is chosen from the lognormal distribution of resistance.

- The simulation is run by selecting random values from both the load and resistance distributions. The limit state function  $[R_i - (D_i + L_i)]$  is calculated for each set of random variables. If the value is equal to or greater than zero, the function is satisfied, and the individual case is safe. If the value is negative, the criterion is not satisfied, and the case represents a failure.
- After a large number of iterations, the failures are counted, and the failure rate is determined. For the sampling to be significant at least 10 failures should be observed; otherwise, more iteration is necessary. If the expected probability of failure is very low, then the number of iterations can be prohibitively large. An alternative way to determine the reliability index is to generate a smaller number of limit state function values, plot the results on normal probability paper, and extrapolate the obtained lower tail of the distribution function. The extrapolated lower tail will allow for assessment of the reliability index and probability of failure (or failure rate).
- By using the failure rate, the reliability index is determined as the inverse of the standard normal cumulative distribution.

A step-by-step procedure for implementing the Monte Carlo method by using statistical functions commonly available in spreadsheet programs is presented in Appendix F.

### 3.2.4 Statistical Parameters for Resistance and Other Loads

The discussion in this section is excerpted from Kulicki et al. (2007).

#### Resistance Models

Resistance was considered as a product of a nominal resistance ( $R_n$ ) and three factors:  $M$ , or material factor (strength of material, modulus of elasticity);  $F$ , or fabrication factor (geometry, dimensions); and  $P$ , or professional factor (use of approximate resistance models; e.g., the Whitney stress block, idealized stress and strain distribution model). Resistance ( $R$ ) is given by Equation 3.6:

$$R = R_n \cdot M \cdot F \cdot P \quad (3.6)$$

The mean value of resistance ( $\mu_R$ ) and the CV of resistance ( $V_R$ ) may be approximated by Equations 3.7 and 3.8,

respectively, which are accepted equations for the range of values that were considered:

$$\mu_R = R_n \cdot \mu_M \cdot \mu_F \cdot \mu_P \quad (3.7)$$

$$V_R = \sqrt{V_M^2 + V_F^2 + V_P^2} \quad (3.8)$$

The statistical parameters of resistance were determined using the test results available before 1990, special simulations, and engineering judgment. They were developed for noncomposite and composite steel girders, reinforced concrete T-beams, and prestressed concrete AASHTO-type girders. Bias factors and CVs were determined for material factor  $M$ , fabrication factor  $F$ , and analysis factor  $P$ . Factors  $M$  and  $F$  were combined.

For structural steel, the statistical parameters are found in papers by Ravindra and Galambos (1978), Yura et al. (1978), Cooper et al. (1978), and Hansell et al. (1978), which are summarized in Ellingwood et al. (1980). The information included the mean values and CV for the yield strength of steel, tensile strength of steel, and modulus of elasticity for hot-rolled beams and plates. In addition, they provided the statistical parameters (mean value and CV) for the fabrication factor and the professional factor. In the very last phase of calibration for AASHTO LRFD, the American Iron and Steel Institute provided the upgraded bias factors and CVs for yield strength of structural steel. These values were then used in Monte Carlo simulations to determine the parameters of resistance for noncomposite and composite girders for the moment-carrying capacity and shear. [More recent data gathered after the Northridge earthquake by Dexter et al. (2000) and Dexter and Melendrez (2000), and data reported by Bartlett et al. (2003), show improved statistics, although Bartlett et al. recommend no resistance factor changes until more is known. In the case of the steel SLSs calibrated in this study, the newer data could affect only the overload limit state, making the reliability analysis somewhat conservative. Given the paucity of resistance data on which this limit state is based, the analysis was not updated for the more recent data.]

For concrete components, the material parameters were taken from Ellingwood et al. (1980). As in the case of structural steel, the statistical parameters were obtained, but no raw test data. The basis for these parameters was research by Mirza and MacGregor (1979a, 1979b). The data included mean value and CV for the compressive strength of concrete, yield strength of reinforcing bars, and prestressing strands. In addition, the data included the statistical parameters of fabrication factor and professional factor.

The material data, combined with the statistical parameters of the fabrication factor and professional factor, were used in Monte Carlo simulations that resulted in the statistical parameters of resistance for steel girders (noncomposite



**Table 3.1. Statistical Parameters of Component Resistance**

Type of Structure	Material and Fabrication Factors (M and F)		Professional Factor (P)		Resistance (R)	
	$\lambda$	V	$\lambda$	V	$\lambda$	V
<b>Noncomposite steel girders</b>						
Moment (compact)	1.095	0.075	1.02	0.06	1.12	0.10
Moment (noncompact)	1.085	0.075	1.03	0.06	1.12	0.10
Shear	1.12	0.08	1.02	0.07	1.14	0.105
<b>Composite steel girders</b>						
Moment	1.07	0.08	1.05	0.06	1.12	0.10
Shear	1.12	0.08	1.02	0.07	1.14	0.105
<b>Reinforced concrete</b>						
Moment	1.12	0.12	1.02	0.06	1.14	0.13
Shear with steel	1.13	0.12	1.075	0.10	1.20	0.155
Shear without steel	1.165	0.135	1.20	0.10	1.40	0.17
<b>Prestressed concrete</b>						
Moment	1.04	0.045	1.01	0.06	1.05	0.075
Shear with steel	1.07	0.10	1.075	0.10	1.15	0.14

Source: Nowak (1999).

and composite), reinforced concrete T-beams, and prestressed concrete girders, for moment and shear, as shown in Table 3.1 (Nowak 1999). The statistical parameters include three factors representing uncertainty in materials, dimensions and geometry, and analytical model.

It was assumed that resistance is a lognormal random variable.

### Statistics of Loads Other Than Live Load

The data presented below were developed in support of strength calibrations, but they are equally applicable to load calculations related to SLS calibration (see Table 3.2).

The bias factors for  $DL_1$  and  $DL_2$  were provided by the Ontario Ministry of Transportation and were based on surveys of actual bridges in conjunction with calibration of the *Ontario Highway Bridge Design Code* (OHBDC 1979; Lind and Nowak 1978). The CVs provided by the Ministry of Transportation for dead load were 0.04 and 0.08 for  $DL_1$  and

**Table 3.2. Statistical Parameters of Dead Load**

Dead Load Component	Bias Factor	CV
Factory-made members, $DL_1$	1.03	0.08
Cast-in-place, $DL_2$	1.05	0.10
Wearing surface, $DL_3$	3 in. (mean thickness)	0.25
Miscellaneous, $DL_4$	1.03 ~ 1.05	0.08 ~ 0.10

$DL_2$ , respectively (Lind and Nowak 1978). However, there is no report available to support these data. The CVs used in calibration were taken from the National Bureau of Standards Special Publication 577 (Ellingwood et al. 1980) and include other uncertainties (also human error).

The parameters of  $DL_3$  were calculated using the survey data provided by the Ontario Ministry of Transportation in conjunction with calibration of the OHBDC (1979).

### 3.3 “Deemed to Satisfy”

When you can measure what you are speaking about, and express it in numbers, you know something about it, when you cannot express it in numbers, your knowledge is of a meager and unsatisfactory kind; it may be the beginning of knowledge, but you have scarcely, in your thoughts advanced to the stage of science.—William Thomson, Lord Kelvin

The least rigorous process for establishing design requirements, and load and resistance factors in particular, is referred to as “deemed to satisfy.” In this process, experience and empirical observation are used to define the boundary between satisfactory performance and unsatisfactory performance. It provides no quantifiable way of assessing the provided margin of adequacy, such as safety or reliability. As there is no way to quantify the performance margin, there is no way to assess the benefit of a change in requirement other than a general knowledge that changing this or that should move in the direction of higher performance. The obvious corollary is that cost–benefit cannot be quantified. An example of “deemed to satisfy” is the specification of concrete cover requirements in U.S. practice, which is based only on experience and has no consistent mathematical basis.

Nonetheless, “deemed to satisfy” has a place in the pantheon of engineering tools. It is often the basis of detailing requirements and may serve as the beginning of design specification development, as in “experience shows that if we do (or do not do) this or that the results are generally acceptable.” Expert elicitation (Delphi process) or an experimental program may provide insight into the adequacy of “deemed to satisfy.”

### 3.4 Customizing the Process

The data used in the calibration described in this report are provided in Appendix F. The key to providing the ability for owners to adjust the calibration of the SLSs for their own experience is to either adjust the data in Appendix F or supply state-specific information of the same type.

The following attributes were identified as necessary to allow bridge owners to customize the calibration process and to develop spreadsheets for their particular needs.

The ability of the process to address these issues is provided as follows:

- *Ability of the Monte Carlo procedure to produce a probability of criteria exceedance and the associated reliability index.* This ability is at the core of applying the Monte Carlo procedure. If 100,000 trial calculations of a given limit state function are produced using randomly generated loads and resistances that are consistent with the mean values and CVs for that limit state function, and the function is not satisfied 100 times, then the failure rate is 0.001 and the success rate is 0.999. The corresponding reliability index from a handbook of probability functions or inverse standard normal CDF available in many computer applications is 3.09.
  - *Ability to accept a user-supplied deterioration of load-carrying capacity.* A possible approach to downgrading the resistance with time is discussed in Chapter 4 by using condition number as a surrogate for deterioration. For example, assume that
- it is expected that at some point in time corrosion will have resulted in a 10% reduction in resistance of a class of bridges. Referring to the box marked Statistical Parameters of Resistance in Figure 3.1, the resistance would be adjusted (lowered) by 10%. If it is determined that not only is it expected that the average resistance will be lowered, but that the values of resistance are becoming more diverse (random), then the bias and CV of resistance can also be adjusted based on that experience, as they are simply input variables. Rerunning the calculations for the affected population of the originally provided bridges, or an owner-supplied set, will allow the owner to track the change in reliability indices. If one wanted to estimate the effect on reliability-based ratings or postings, one could keep or modify the target reliability index and repeat the lower iteration loop by using revised trial load factors until sufficient convergence of the reliability indices was found. This would essentially be a recalibration.
- *Ability to react to user intervention as reflected in an improved resistance (also user supplied).* This is basically the opposite of the process of downgrading resistance discussed above.
  - *Ability to accept either a user-supplied database from which the product will determine a new bias and CV or a user-supplied bias and CV from an external calculation.* As discussed above, the bias and CV are input variables that a bridge owner is able to adjust.
  - *Ability to accommodate a user-supplied resistance model.* This is especially important for the geotechnical community due to the regional nature of practice in that discipline.

## CHAPTER 4

# Deterioration

### 4.1 Introduction

Deterioration and a degradation of serviceability indicated by a reduction in usable capacity (either by a change in rating or a change in reliability index) are not interchangeable terms, although they may be related for some elements or systems. For example, a steel girder, especially a rolled beam, may have visible corrosion suggesting that the element is deteriorating and in need of maintenance, but it may have little or no perceptible change in deformations, stresses, or rider comfort. Sometimes a corrosion hole may exist in a place that does not control an evaluation. Similar observations can be made about the early stages of damage to prestressed beams resulting from poor drainage control at expansion joints. The resulting spalling and possible rusting of rebar and strands may be unsightly but have relatively little structural effect until the damage is well advanced. For these types of elements or systems, deterioration models or databases geared to predicting maintenance budget needs are not especially useful to the calibration process needed for Project R19B. Degradation first leads to loss of service, and if left untreated, can lead to loss of load-carrying capacity resulting in failure.

However, for some elements and subsystems, a high correlation may exist between loss of serviceability and deterioration as indicated by a change in National Bridge Inspection Standards (NBIS) sufficiency ratings or the results of a deterioration model. Such might be the case for decks and bearings, for which a deteriorated state could be considered in the calibration by owner adjustment of nominal resistance based on bridge-specific knowledge or deterioration modeling.

Several researchers have proposed algorithms predicting the change in condition number, either the National Bridge Inventory (NBI) condition number or a variation, over time for bridge details or complete structures. Five of these proposals are reviewed in this chapter. Bridge owners could use one or more of these proposals, or others that may be found to more accurately reflect local conditions, as a basis for

including an estimate of deterioration in recalibrating the service limit states by using the framework described in Chapter 3 of this report. One simple way to do this would be to accept the premise that until more usable data on the change of resistance with time are available, it is reasonable to treat the percentage change in condition number as a surrogate for change in resistance and adjust the resistance in the calibration spreadsheets accordingly. In some cases, the use of the equations included in this chapter may be beyond the range for which they were developed.

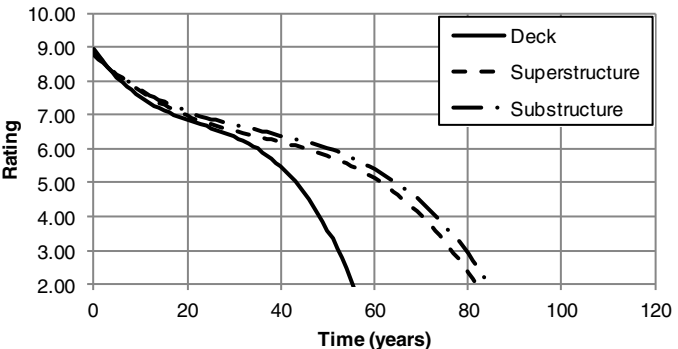
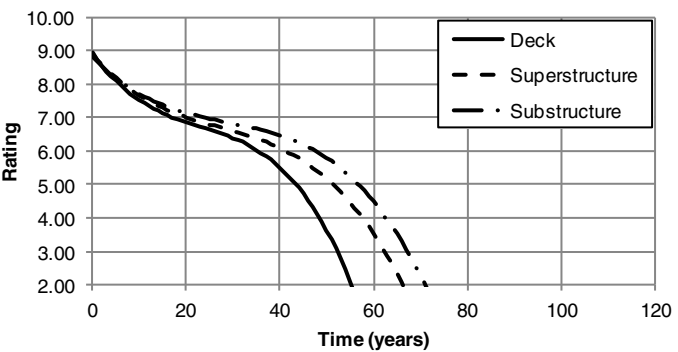
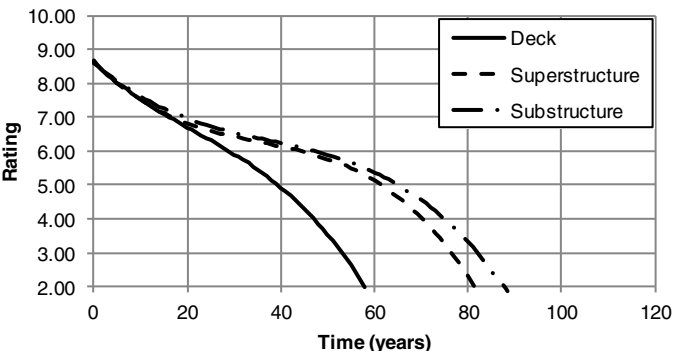
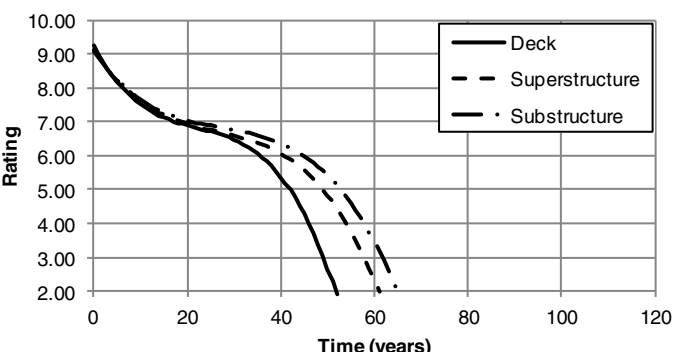
### 4.2 Bolukbasi et al. (2004)

Bolukbasi et al. (2004) used historic NBI rating data for 2,601 bridges from Illinois to determine regression equations relating the bridge age to the condition rating of the deck, superstructure, and substructure. No distinction between cast-in-place (CIP) decks and precast panels was indicated in the reference. The data were adjusted such that bridges with a sudden rating increase are excluded from the study (a sudden increase in rating indicates performance of maintenance). The resulting equations suggest the rating and a corresponding service life if no maintenance occurs. Equations are provided for the following categories: all bridges; steel bridges; reinforced-concrete (RC) bridges; prestressed concrete bridges; Interstate bridges; non-Interstate bridges; bridges with annual average daily traffic (AADT) <5,000; bridges with 5,000 < AADT < 10,000; and bridges with AADT >10,000. Within each bridge category, equations are provided to estimate the rating for the deck, superstructure, and substructure.

Table 4.1 shows the rating prediction equations for the nine categories, as well as a graph showing the condition rating versus time. The end of service life is typically defined as when a rating of 3 is achieved, and maintenance would be required to continue using the structure.

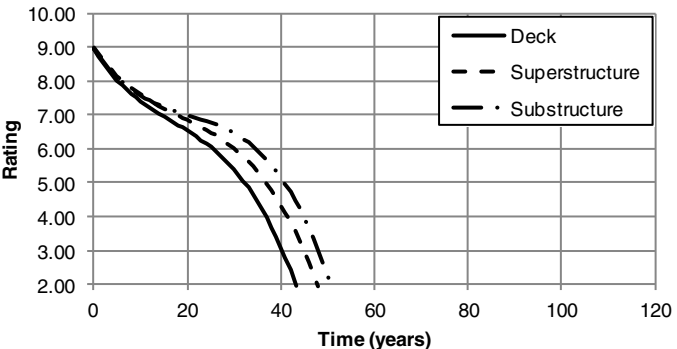
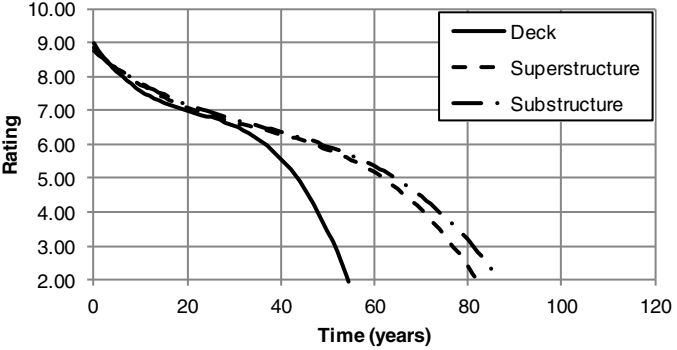
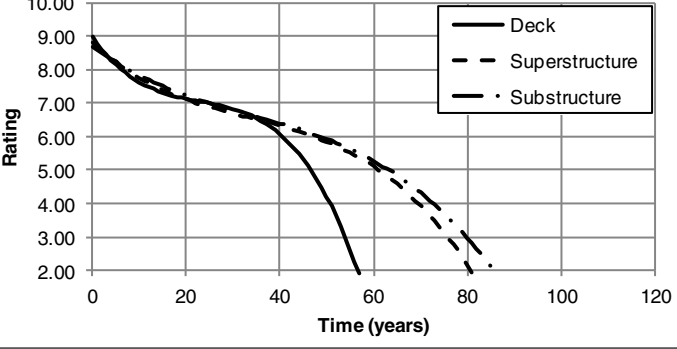
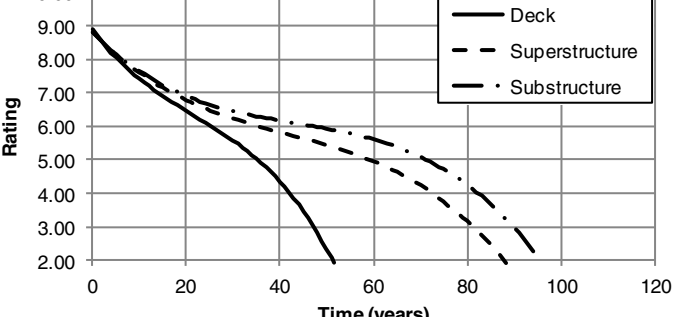
The equations were also plotted by component (deck, superstructure, substructure), allowing an investigation into

**Table 4.1. Rating Prediction Equations and Graphs for Nine Categories of Bridges**

<p style="text-align: center;"><b>All Bridges</b></p>  <p>The graph for 'All Bridges' plots Rating (y-axis, 2.00 to 10.00) against Time in years (x-axis, 0 to 120). Three data series are shown: Deck (solid line), Superstructure (dashed line), and Substructure (dash-dot line). All three series start at a rating of approximately 9.0 at time 0 and decrease over time. The Deck rating drops most sharply, reaching a rating of 2.0 around 55 years. The Superstructure and Substructure ratings decrease more gradually, with the Superstructure reaching a rating of 2.0 around 85 years and the Substructure around 90 years.</p>	<p>Deck: <math>R = 8.960814 - 0.20144T + 0.0067197T^2 - 9.67 \times 10^{-5}T^3</math></p> <p>Superstructure: <math>R = 8.854089461 - 0.144890772T + 0.0031227167T^2 - 2.91 \times 10^{-5}T^3</math></p> <p>Substructure: <math>R = 8.767383274 - 0.127816817T + 0.002736488T^2 - 2.57 \times 10^{-5}T^3</math></p>
<p style="text-align: center;"><b>Steel Bridges</b></p>  <p>The graph for 'Steel Bridges' plots Rating (y-axis, 2.00 to 10.00) against Time in years (x-axis, 0 to 120). Three data series are shown: Deck (solid line), Superstructure (dashed line), and Substructure (dash-dot line). All three series start at a rating of approximately 9.0 at time 0 and decrease over time. The Deck rating drops most sharply, reaching a rating of 2.0 around 55 years. The Superstructure and Substructure ratings decrease more gradually, with the Superstructure reaching a rating of 2.0 around 85 years and the Substructure around 90 years.</p>	<p>Deck: <math>R = 8.922947 - 0.19861T + 0.0067357T^2 - 9.77 \times 10^{-5}T^3</math></p> <p>Superstructure: <math>R = 8.895666888 - 0.160854616T + 0.004406448T^2 - 5.36 \times 10^{-5}T^3</math></p> <p>Substructure: <math>R = 8.822326892 - 0.148338077T + 0.004166181T^2 - 4.83 \times 10^{-5}T^3</math></p>
<p style="text-align: center;"><b>Reinforced Concrete Bridges</b></p>  <p>The graph for 'Reinforced Concrete Bridges' plots Rating (y-axis, 2.00 to 10.00) against Time in years (x-axis, 0 to 120). Three data series are shown: Deck (solid line), Superstructure (dashed line), and Substructure (dash-dot line). All three series start at a rating of approximately 9.0 at time 0 and decrease over time. The Deck rating drops most sharply, reaching a rating of 2.0 around 55 years. The Superstructure and Substructure ratings decrease more gradually, with the Superstructure reaching a rating of 2.0 around 85 years and the Substructure around 90 years.</p>	<p>Deck: <math>R = 8.605268604 - 0.1277358696T + 0.0023501188T^2 - 3.643 \times 10^{-5}T^3</math></p> <p>Superstructure: <math>R = 8.662249581 - 0.145660594T + 0.003299188T^2 - 3.09 \times 10^{-5}T^3</math></p> <p>Substructure: <math>R = 8.624414481 - 0.123890228T + 0.002486843T^2 - 2.21 \times 10^{-5}T^3</math></p>
<p style="text-align: center;"><b>Prestressed Concrete Bridges</b></p>  <p>The graph for 'Prestressed Concrete Bridges' plots Rating (y-axis, 2.00 to 10.00) against Time in years (x-axis, 0 to 120). Three data series are shown: Deck (solid line), Superstructure (dashed line), and Substructure (dash-dot line). All three series start at a rating of approximately 9.0 at time 0 and decrease over time. The Deck rating drops most sharply, reaching a rating of 2.0 around 55 years. The Superstructure and Substructure ratings decrease more gradually, with the Superstructure reaching a rating of 2.0 around 85 years and the Substructure around 90 years.</p>	<p>Deck: <math>R = 9.243165 - 0.25857T + 0.01004T^2 - 1.5 \times 10^{-4}T^3</math></p> <p>Superstructure: <math>R = 9.134415141 - 0.213185033T + 0.006920265T^2 - 8.77 \times 10^{-5}T^3</math></p> <p>Substructure: <math>R = 9.075226897 - 0.19604399T + 0.006203563T^2 - 7.49 \times 10^{-5}T^3</math></p>

(continued on next page)

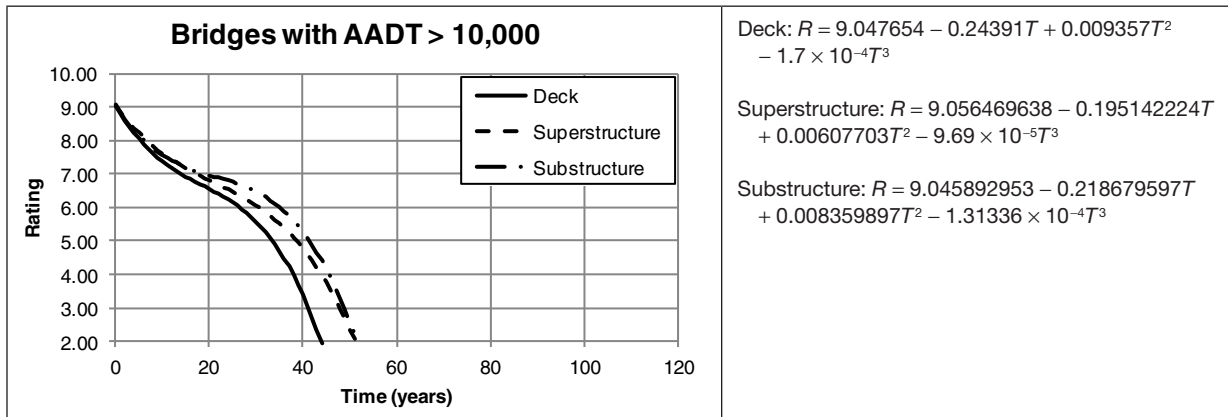
**Table 4.1. Rating Prediction Equations and Graphs for Nine Categories of Bridges (continued)**

<p style="text-align: center;"><b>Interstate Bridges</b></p> 	<p>Deck: <math>R = 8.920346 - 0.21323T + 0.007687T^2 - 1.5 \times 10^{-4}T^3</math></p> <p>Superstructure: <math>R = 8.974079168 - 0.193652056T + 0.006771473T^2 - 1.2065 \times 10^{-4}T^3</math></p> <p>Substructure: <math>R = 8.956002854 - 0.205796117T + 0.008041095T^2 - 1.31981 \times 10^{-4}T^3</math></p>
<p style="text-align: center;"><b>Non-Interstate Bridges</b></p> 	<p>Deck: <math>R = 8.981204 - 0.20173T + 0.007319T^2 - 1.1 \times 10^{-4}T^3</math></p> <p>Superstructure: <math>R = 8.823963724 - 0.134551029T + 0.002855493T^2 - 2.73 \times 10^{-5}T^3</math></p> <p>Substructure: <math>R = 8.745705917 - 0.113435369T + 0.002153535T^2 - 2.01 \times 10^{-5}T^3</math></p>
<p style="text-align: center;"><b>Bridges with AADT &lt; 5,000</b></p> 	<p>Deck: <math>R = 8.974903 - 0.20009T + 0.007589T^2 - 1.1 \times 10^{-4}T^3</math></p> <p>Superstructure: <math>R = 8.793293844 - 0.128307613T + 0.002753594T^2 - 2.73 \times 10^{-5}T^3</math></p> <p>Substructure: <math>R = 8.688714213 - 0.10308987T + 0.001890448T^2 - 1.87 \times 10^{-5}T^3</math></p>
<p style="text-align: center;"><b>Bridges with 5,000 &lt; AADT &lt; 10,000</b></p> 	<p>Deck: <math>R = 8.887719688 - 0.1873850501T + 0.0047333447T^2 - 7.2279 \times 10^{-5}T^3</math></p> <p>Superstructure: <math>R = 8.812137936 - 0.144747111T + 0.002574894T^2 - 2.06 \times 10^{-5}T^3</math></p> <p>Substructure: <math>R = 8.791762968 - 0.139058986T + 0.0026443T^2 - 2.02 \times 10^{-5}T^3</math></p>

(continued on next page)



**Table 4.1. Rating Prediction Equations and Graphs for Nine Categories of Bridges (continued)**



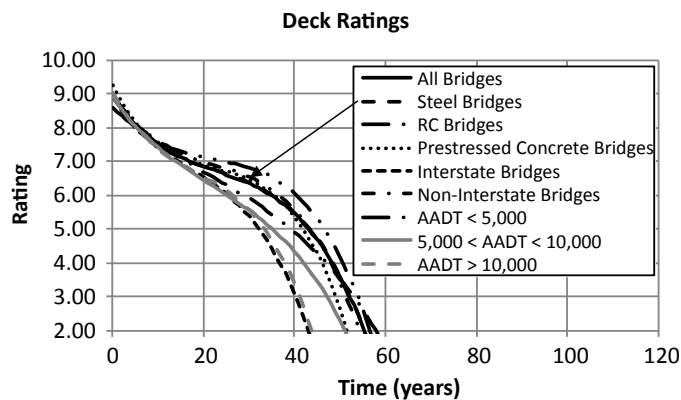
Source: Bolukbasi et al. (2004).

how other criteria affect the service life of the bridge. Figure 4.1, Figure 4.2, and Figure 4.3 show the predicted deck, superstructure, and substructure condition rating, respectively, versus time. The graphs in Table 4.1 show that the service life of the deck is typically shorter than the service life of either the superstructure or the substructure. All categories have a deck service life less than 55 years. For Interstate bridges and high-traffic-volume bridges, Figure 4.1 shows the deck service life is much closer to 40 years. High-traffic-volume bridges have an estimated service life of 41 years, medium-traffic-volume bridges have an estimated service life of 47 years, and low-traffic-volume bridges have an estimated service life of 54 years. The medium- and high-traffic bridge deck condition ratings decrease at a faster rate than the low-volume bridges. For the first 30 years, the medium and high traffic have nearly identical deck condition ratings. After the first 30 years they split, with the high-traffic bridges decreasing faster.

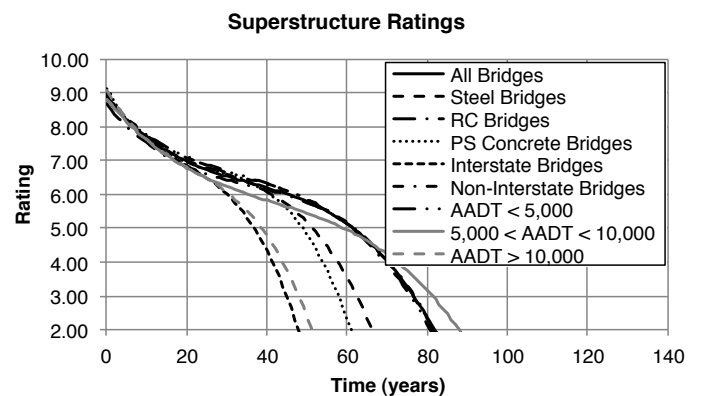
Figure 4.2 shows the superstructure rating versus time for the nine bridge categories. Similar to the deck condition rating, Interstate bridges and bridges with AADT >10,000 have the

shortest service life (45 to 50 years). Steel and prestressed concrete bridges also have shorter service lives (55 to 65 years), but this is likely due to the fact that many of these are located on the Interstate and are subject to high traffic counts. The basis for this difference, 55 years and 65 years, could not be found in the reference. Non-Interstate, RC, and low-traffic bridges have an estimated service life of approximately 75 years. Bridges with AADT between 5,000 and 10,000 are shown to have the longest service life, greater than 80 years. The AADT between 5,000 and 10,000 category may have a longer estimated life due to less traffic than the Interstate and AADT >10,000 categories, combined with routine maintenance and repair, resulting in a longer service life.

Figure 4.3 shows the substructure condition rating versus time for the nine bridge categories. As with the other condition ratings, bridges falling into the high-traffic and Interstate categories have the shortest service life (an estimated 50 years). The substructures of prestressed concrete bridges and steel girder bridges have estimated service lives of approximately 62 and 67 years, respectively. The basis of this difference could



**Figure 4.1. Deck condition rating versus time.**



**Figure 4.2. Superstructure condition rating versus time.**

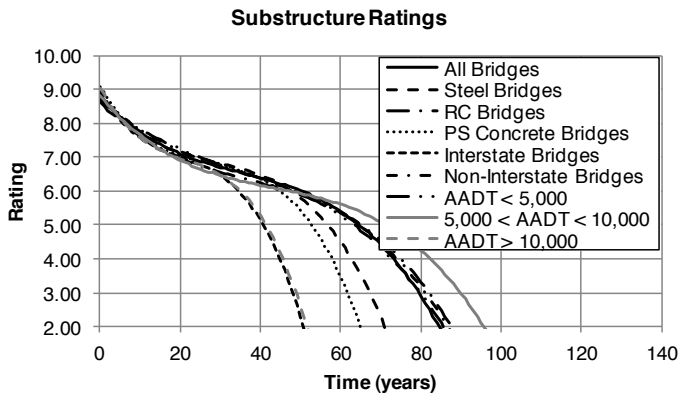


Figure 4.3. Substructure condition rating versus time.

not be found in the reference. Non-Interstate, RC, and low-traffic bridges all have an estimated service life of approximately 80 years, and bridges in the medium-traffic category have the longest estimated service life (approximately 90 years). Similar to the superstructure ratings, the substructure service life for the medium-traffic category is the longest and may be due to better maintenance.

### 4.3 Jiang and Sinha (1989)

In their 1989 report on bridge performance and optimization, Jiang and Sinha discussed the results of regression analysis and Markov chain analysis to estimate the average rating of a group of bridges. They considered Interstate and non-Interstate bridges, as well as steel and concrete bridges; no distinction was made between reinforced or prestressed concrete construction. Geographic location and traffic volume were initially considered, but because they did not appear to influence the regression analysis, they were not considered as separate categories. A relatively small sample (several hundred bridges) was used in the regression analysis, and at the time of the analysis, biennial NBI inspections had only been occurring for approximately 10 years. Thus, the results may have been influenced by the limited amount of data available and used.

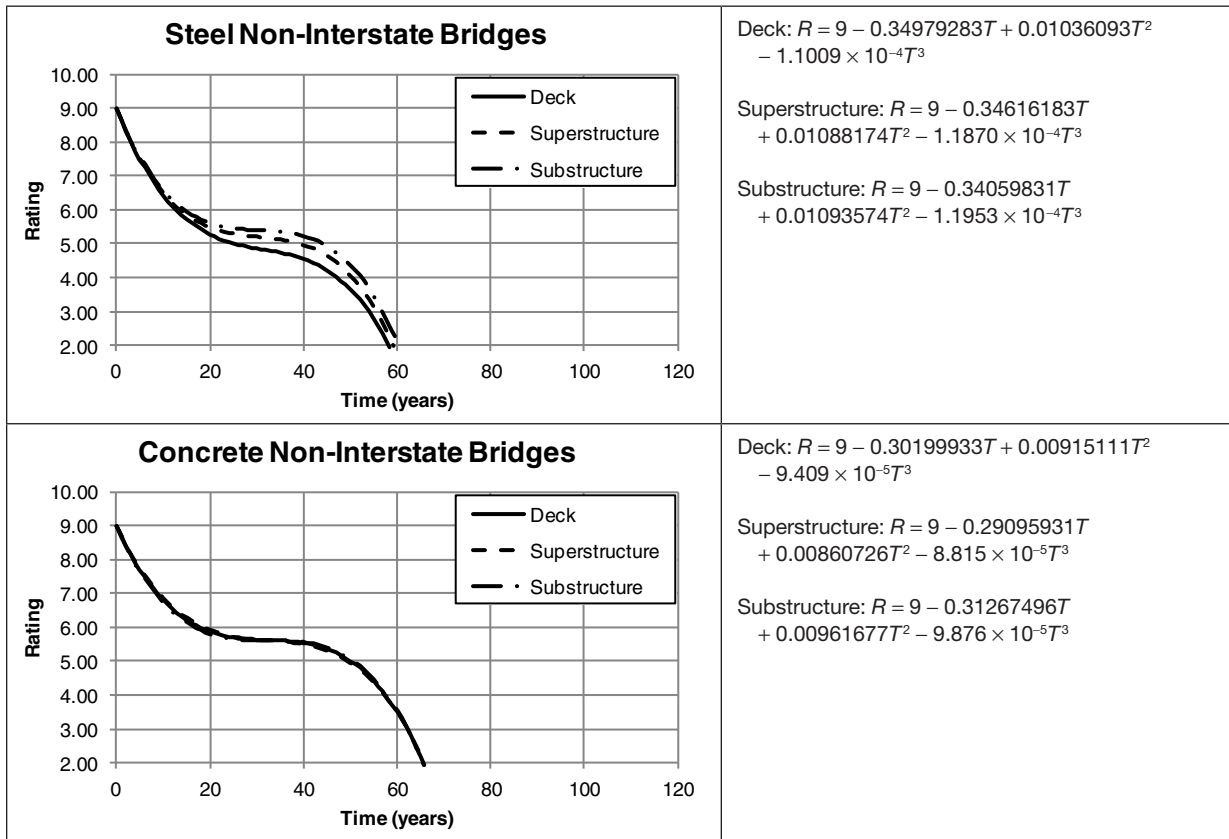
The results of the regression analysis were coefficients for a third-order polynomial describing the NBI condition rating as a function of bridge age. Coefficients were determined for the different bridge types and for the deck, superstructure, and substructure. The equations and a graph of the equations showing the NBI condition rating as a function of time are shown in Table 4.2. Unlike the equations by Bolukbasi et al.

Table 4.2. Rating Prediction Equations and Graphs for Four Categories of Bridges

<p style="text-align: center;"><b>Steel Interstate Bridges</b></p>	<p>Deck: <math>R = 9 - 0.411417907T + 0.021165637T^2 - 4.0387 \times 10^{-4}T^3</math></p> <p>Superstructure: <math>R = 9 - 0.455722067T + 0.023999587T^2 - 4.4201 \times 10^{-4}T^3</math></p> <p>Substructure: <math>R = 9 - 0.448181057T + 0.025559007T^2 - 4.9875 \times 10^{-4}T^3</math></p>
<p style="text-align: center;"><b>Concrete Interstate Bridges</b></p>	<p>Deck: <math>R = 9 - 0.366226177T + 0.016595207T^2 - 2.7162 \times 10^{-4}T^3</math></p> <p>Superstructure: <math>R = 9 - 0.347047917T + 0.015989667T^2 - 2.7160 \times 10^{-4}T^3</math></p> <p>Substructure: <math>R = 9 - 0.345084557T + 0.015758577T^2 - 2.6681 \times 10^{-4}T^3</math></p>

(continued on next page)

**Table 4.2. Rating Prediction Equations and Graphs for Four Categories of Bridges (continued)**

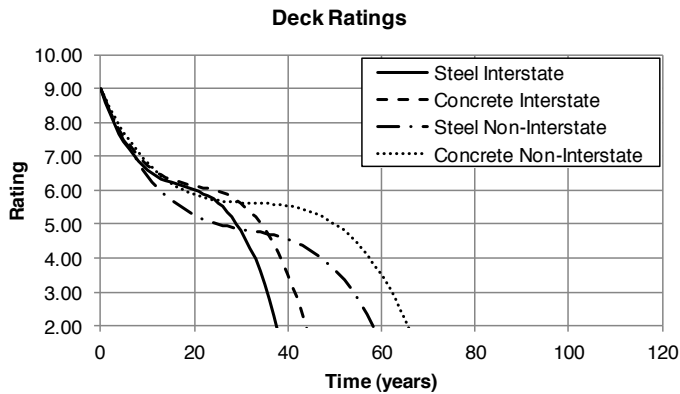


Source: Jiang and Sinha (1989).

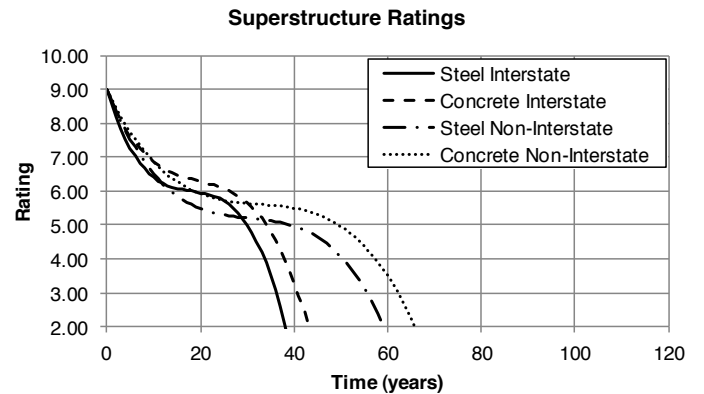
(2004), the constant term in the prediction equation is always 9; this assumes that the bridge component was in perfect condition when new.

The equations were also plotted by component (deck, superstructure, substructure), allowing an investigation into how other criteria affect the service life of the bridge. Decks are believed to be CIP concrete decks. Figure 4.4, Figure 4.5,

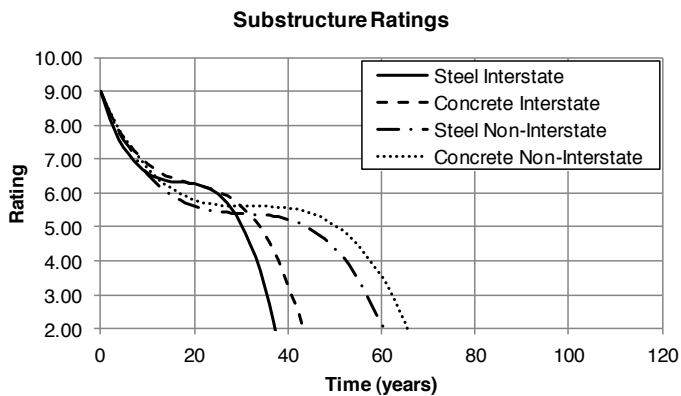
and Figure 4.6 show the predicted deck, superstructure, and substructure condition ratings, respectively, versus time. It is typically assumed that the end of service life occurs when the condition rating reaches a value of 3. Figure 4.4 shows that the Interstate bridges typically have a shorter deck service life than the non-Interstate bridges. All bridge types have a similar deterioration rate until approximately 10 years.



**Figure 4.4. Deck predicted condition ratings for different bridge types.**



**Figure 4.5. Superstructure predicted condition ratings for different bridge types.**



**Figure 4.6. Substructure predicted condition ratings for different bridge types.**

Non-Interstate bridges have a longer period during which the rating does not change significantly; the concrete bridge rating is higher than the steel bridge rating during this plateau period and throughout most of the service life. Concrete bridges are shown to have longer deck service lives than steel bridges. The predicted service life for Interstate bridge decks is approximately 36 years for steel bridges and 42 years for concrete bridges. For non-Interstate bridges, the service life increases to approximately 59 years for steel bridges and 62 years for concrete bridges. The reference did not provide any information as to why the deck service life varies between steel and concrete bridges for both Interstate and non-Interstate conditions.

Figure 4.5 is very similar to Figure 4.4 with regard to material and highway type. Concrete superstructures have longer service lives than steel bridges subjected to the same volume of traffic. Interstate bridges have a shorter service life than non-Interstate bridges. The superstructure service lives predicted are very similar to those predicted for the deck. The difference in service life between concrete and steel bridges is not discussed in the reference.

Figure 4.6 shows the predicted substructure condition ratings versus times. This figure is similar to the two previous figures for deck and superstructure service lives. The predicted substructure service lives are very similar to those predicted for the deck and also for the superstructure. This is a surprising result as it is typically expected that the substructure will last longer than either the deck or the superstructure. The report did not indicate any specific reasons for the substructure having predicted service lives similar to the deck and superstructure.

#### 4.4 Hatami and Morcouc (2011)

A 2011 report by Hatami and Morcouc, *Developing Deterioration Models for Nebraska Bridges*, presented the results of a project performed for the Nebraska Department of Roads in

which deterioration models were developed specifically for Nebraska bridges. The deterioration models were based on NBI condition ratings for bridge decks, superstructures, and substructures by using data from 1998 to 2010. Factors such as structure type, deck type, wearing surface, deck protection, average daily traffic (ADT), average daily truck traffic (ADTT), and location were considered in the development of the deterioration models, which were determined using deterministic and stochastic methods.

NBI data were obtained for all bridges in Nebraska from 1998 to 2010; only data for state bridges were used in the analysis as the authors believed that inspections performed by state inspectors have stricter requirements. The deterministic deterioration models developed for state bridges in Nebraska are shown in Table 4.3. In the second figure in the table, in which deterioration is related to ADTT, decks subjected to more truck traffic appear to have a longer expected life than those subjected to fewer trucks, which is contrary to what would be expected. In the third figure, the rating starts to increase in District 2 after approximately 60 years, which is likely a sign that more data were needed to more accurately develop the deterioration model. The last figure shown in Table 4.3 indicates that the service life of the deck exceeds that of either the superstructure or substructure, which is also contrary to what would be expected.

### 4.5 Comparison of Equations from Bolukbasi et al. (2004), Jiang and Sinha (1989), and Hatami and Morcouc (2011)

#### 4.5.1 Introduction

The results from Bolukbasi et al. (2004), Jiang and Sinha (1989), and Hatami and Morcouc (2011) are generally similar. The equations are plotted together to provide a comparison between resulting equations. Various comparisons are provided below. Comparisons are based on material type, as well as highway type and ADTT. Typically the Bolukbasi et al. equations have a slower deterioration rate over the service life of the structure. This may be due to a larger number of structures being considered and the availability of more inspection data. The equations from the Nebraska study are only included in the superstructure ratings for steel bridges; the results for other bridge and component types were not specific enough to include elsewhere.

#### 4.5.2 Concrete Superstructure Bridges

Plots of the prediction equations for deck, superstructure, and substructure condition ratings for concrete bridges are

Table 4.3. Nebraska Deterioration Models

<p style="text-align: center;"><b>Deck and Overlay Ratings</b></p>	<p>Original Deck: <math>R = 10.2915 - 0.2531T + 0.0093T^2 - 0.0001T^3</math></p> <p>Replacement Deck: <math>R = 8.48681 + 0.34139T - 0.05392T^2 + 0.00222T^3 - 0.00003T^4</math></p> <p>Overlay: <math>R = 9.6499 - 0.0829T + 0.0009T^2 - 0.0002T^3</math></p> <p>Low Slump Concrete Overlay: <math>R = 10.094 - 0.1902T + 0.0087T^2 - 0.0004T^3</math></p>
<p style="text-align: center;"><b>Deck Ratings based on ADTT</b></p>	<p>ADTT &lt; 100: <math>R = 10.189 - 0.233T + 0.0092T^2 - 0.0002T^3</math></p> <p>100 &lt; ADTT &lt; 500: <math>R = 10.754 - 0.342T + 0.0127T^2 - 0.0002T^3</math></p> <p>ADTT &gt; 500: <math>R = 10.372 - 0.2311T + 0.0039T^2 - 0.00004T^3</math></p>
<p style="text-align: center;"><b>Deck Ratings based on Location</b></p>	<p>Districts 1, 3, and 4: <math>R = 9.9984 - 0.1948T + 0.0052T^2 - 0.00008T^3</math></p> <p>District 2: <math>R = 9.9374 - 0.1267T - 0.0015T^2 + 0.00003T^3</math></p> <p>Districts 5-8: <math>R = 10.252 - 0.2214T + 0.0067T^2 - 0.0001T^3</math></p>
<p style="text-align: center;"><b>Deck and Overlay Ratings</b></p>	<p>Original Deck: <math>R = 10.2915 - 0.2531T + 0.0093T^2 - 0.0001T^3</math></p> <p>Steel Superstructure: <math>R = 10.2731 - 0.1727T + 0.0046T^2 - 0.0001T^3</math></p> <p>Substructure: <math>R = 9.6098 - 0.0657T - 0.0017T^2 + 0.00001T^3</math></p>

Source: Hatami and Morcous (2011).



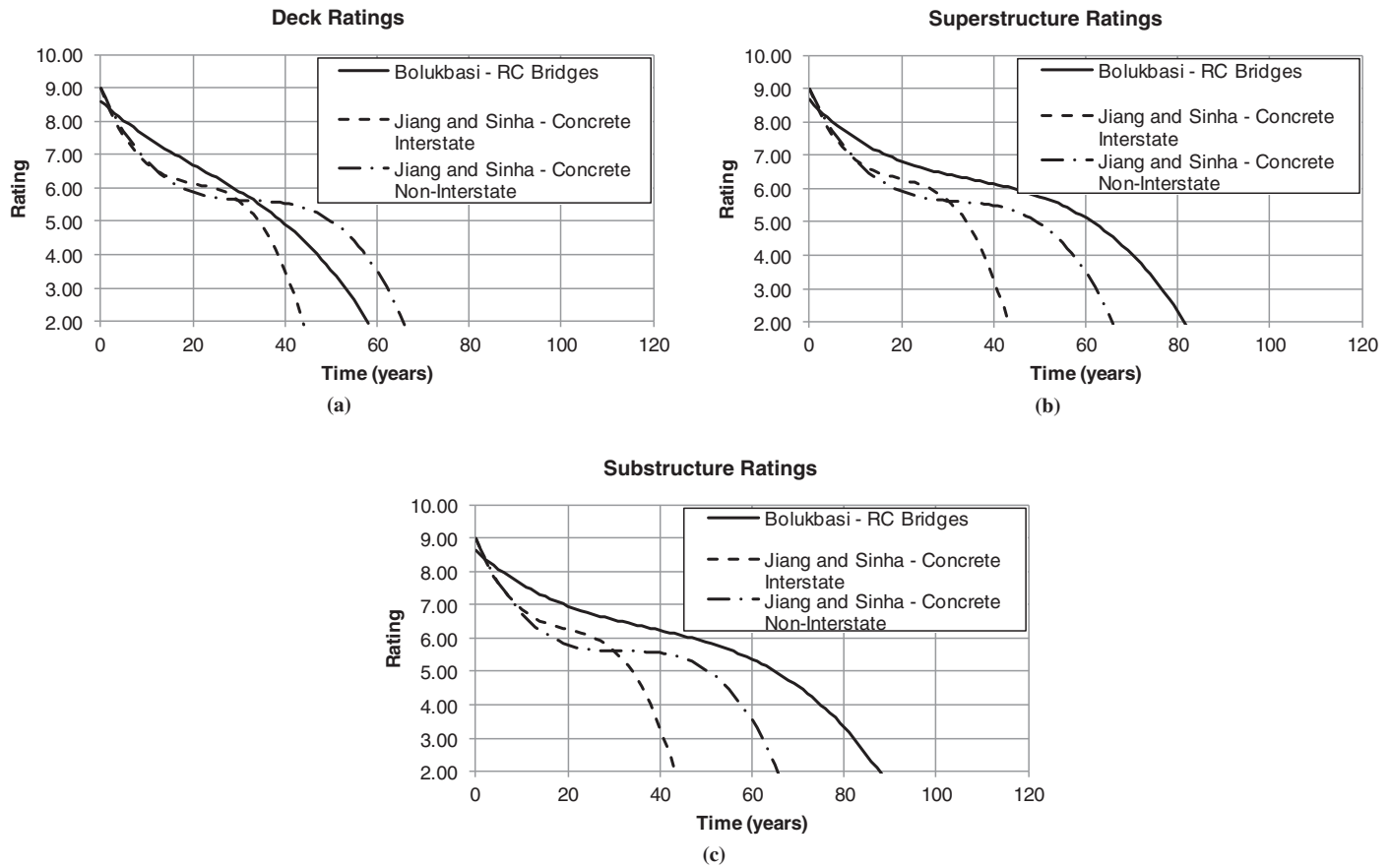


Figure 4.7. Comparisons of concrete bridge predicted condition ratings for (a) decks, (b) superstructures, and (c) substructures.

shown in Figure 4.7. For the deck condition ratings, the Bolukbasi et al. (2004) equation indicates the highest condition rating until an age of approximately 35 years, after which the non-Interstate equation for concrete bridges proposed by Jiang and Sinha (1989) indicates the highest condition rating. For the superstructure and substructure, the Bolukbasi et al. equations always indicate the highest condition rating. The prediction equations provide an estimated service life for the deck, superstructure, and substructure. The estimated service lives, or the predicted times until a condition rating of 3 is achieved, are provided in Table 4.4. The Jiang and Sinha equations generally predict a similar service life for all major components of a bridge. The Bolukbasi et al. equation suggests that the deck has the shortest service life. The superstructure and substructure service lives are significantly longer.

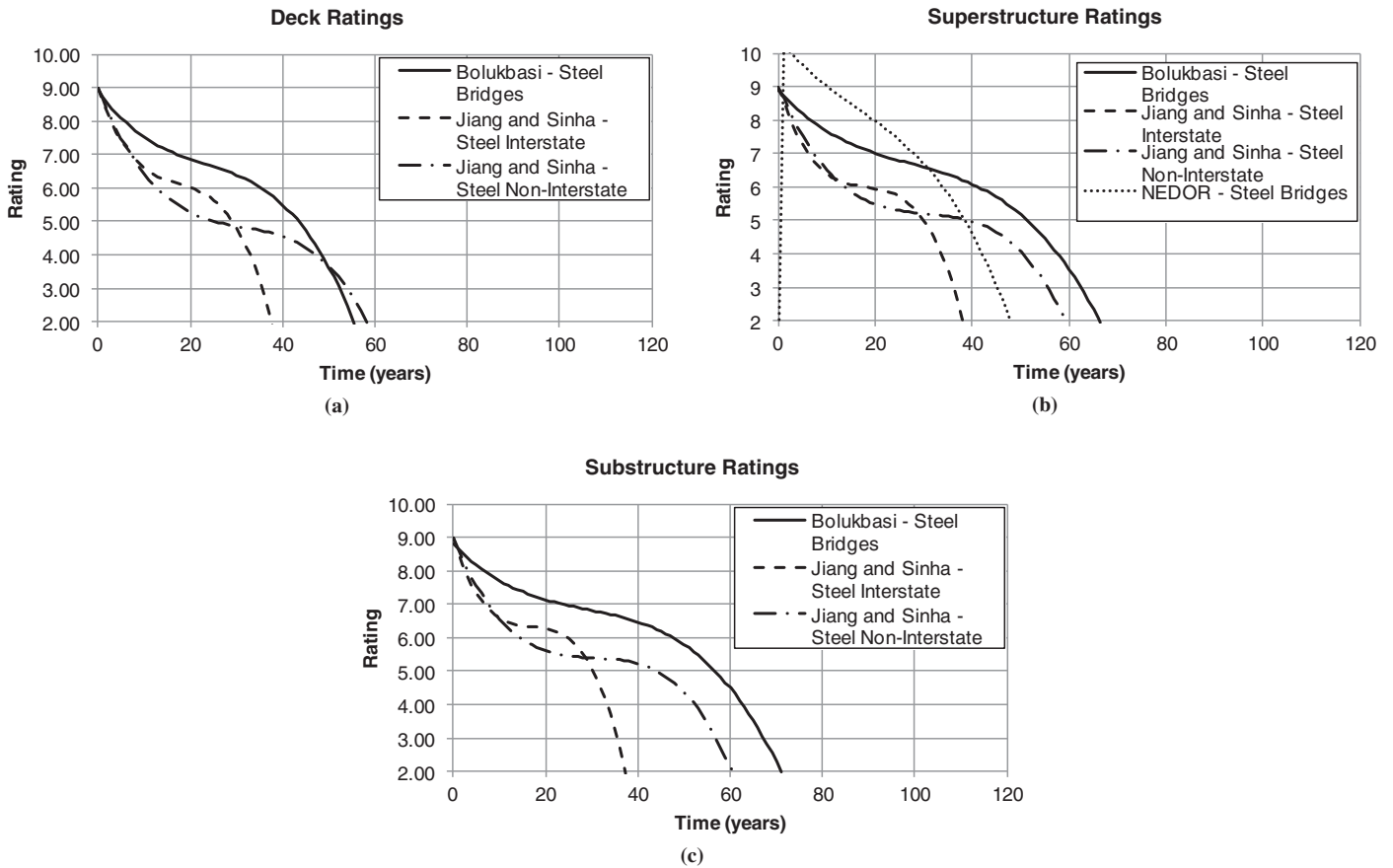
**4.5.3 Steel Superstructure Bridges**

Plots of the prediction equations for deck, superstructure, and substructure condition ratings for steel bridges are shown in

Figure 4.8. For the deck condition ratings, the Bolukbasi et al. (2004) equation indicates a higher condition rating until an age of approximately 50 years, after which the non-Interstate equation for steel bridges proposed by Jiang and Sinha (1989) indicates a higher condition rating. The superstructure and substructure condition ratings are always higher when using the Bolukbasi et al. equations versus either Jiang and Sinha equation. The Hatami and Morcouc (2011) equation

**Table 4.4. Service Life Comparison: Reinforced Concrete (RC) Bridges**

Equation	Service Life (years)		
	Deck	Superstructure	Substructure
Bolukbasi et al., RC	54	77	82
Jiang and Sinha, RC Interstate	42	41	41
Jiang and Sinha, RC non-Interstate	63	63	63



**Figure 4.8. Comparisons of steel bridge predicted condition ratings for (a) decks, (b) superstructures, and (c) substructures.**

[identified as NEDOR (Nebraska Department of Roads) in Figure 4.8] predicts higher condition ratings than both Bolukbasi et al. and Jiang and Sinha until approximately 30 years. Unlike the other equations, the Hatami and Morcoux equation does not indicate a period of time when the condition rating plateaus. The prediction equations provide an estimated service life for the deck, superstructure, and substructure. The estimated service lives, or the predicted times until a condition rating of 3 is achieved, are provided in Table 4.5. The Jiang and Sinha equations generally predict a similar service life for the major components of a bridge. The Bolukbasi et al. equation suggests that the deck has the shortest service life. The superstructure and substructure service lives are somewhat longer.

**4.5.4 Interstate Bridges**

Plots of the prediction equations for deck, superstructure, and substructure condition ratings for Interstate bridges are shown in Figure 4.9. For the deck condition ratings, the Bolukbasi et al. (2004) equation indicates a higher condition

rating until an age of approximately 25 years. After 25 years, the Bolukbasi et al. equation and the Jiang and Sinha (1989) concrete equations are very similar. The superstructure and substructure condition ratings are always higher when using the Bolukbasi et al. equations versus either Jiang and Sinha equation, but overall the three indicate similar estimated

**Table 4.5. Service Life Comparison: Steel Bridges**

Equation	Service Life (years)		
	Deck	Superstructure	Substructure
Bolukbasi et al., steel	53	63	68
Jiang and Sinha, steel Interstate	36	37	36
Jiang and Sinha, steel non-Interstate	54	56	57
Hatami and Morcoux, steel	NA	47	NA

Note: NA = not available.

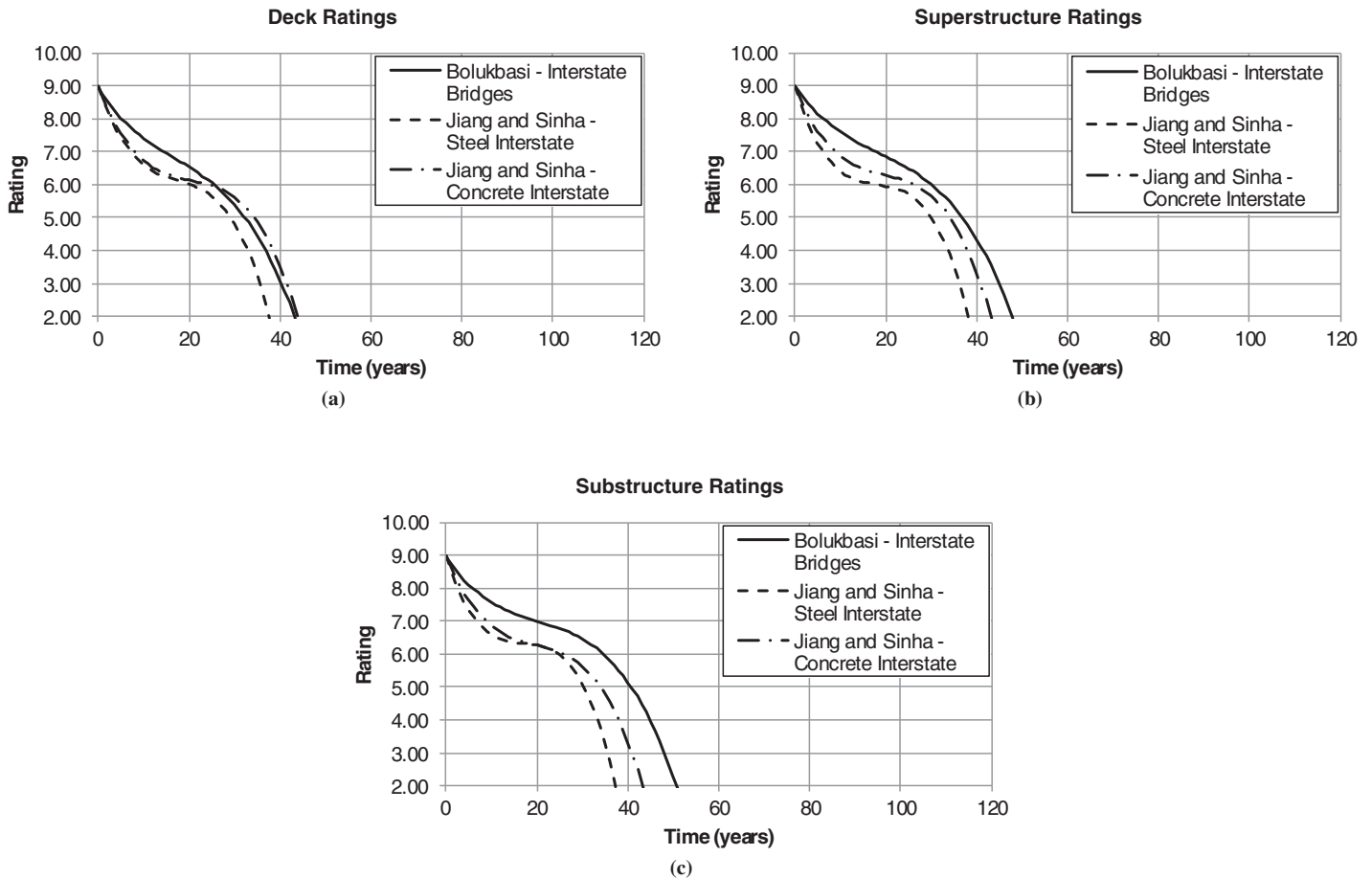


Figure 4.9. Comparisons of Interstate bridge predicted condition ratings for (a) decks, (b) superstructures, and (c) substructures.

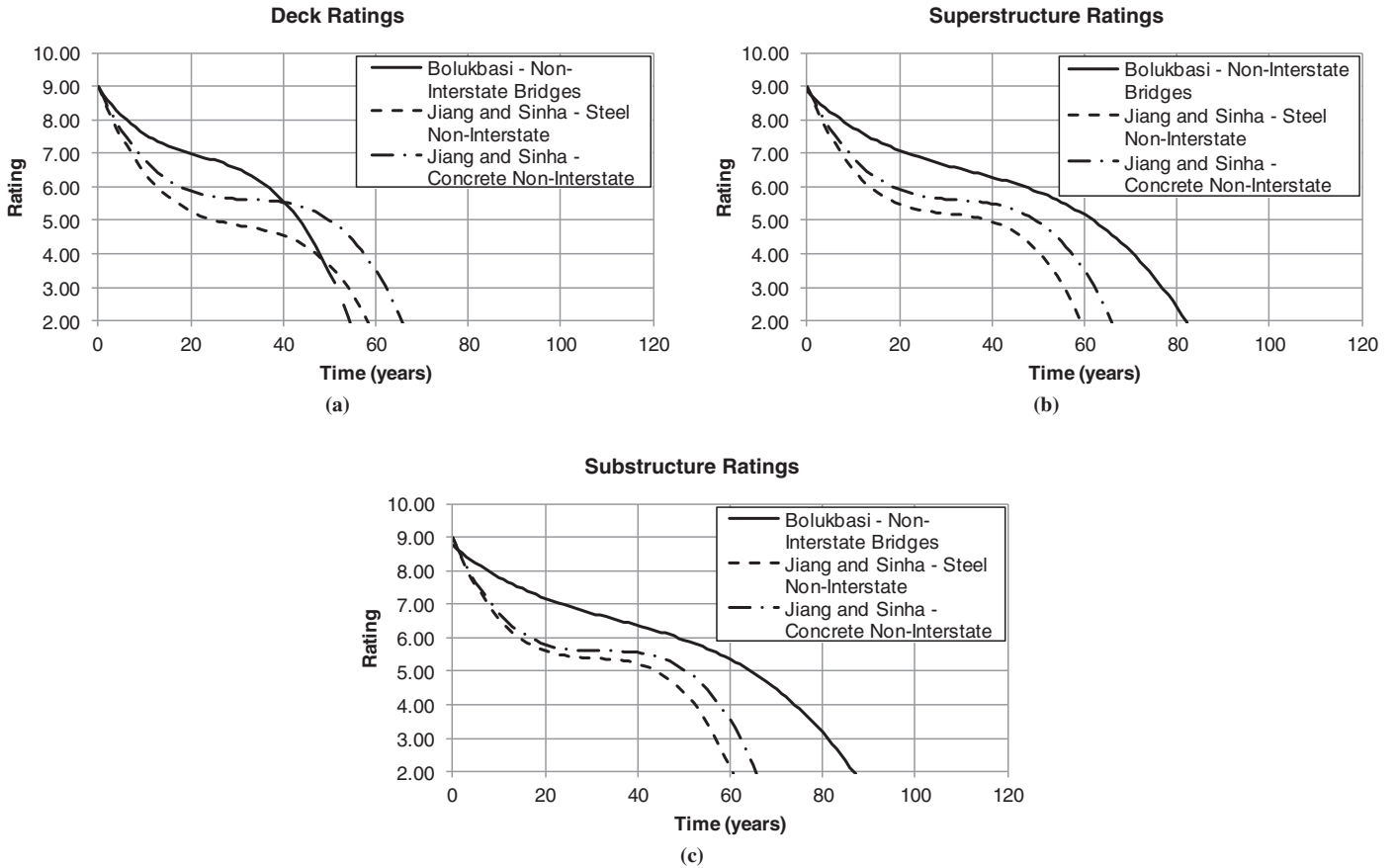
service lives. The prediction equations provide an estimated service life for the deck, superstructure, and substructure. The estimated service lives, or the predicted times until a condition rating of 3 is achieved, are provided in Table 4.6. The estimated service lives are similar for all components and equations.

Table 4.6. Service Life Comparison: Interstate Bridges

Equation	Service Life (years)		
	Deck	Superstructure	Substructure
Bolukbasi et al., Interstate	41	45	48
Jiang and Sinha, steel Interstate	36	37	36
Jiang and Sinha, concrete Interstate	42	41	41

#### 4.5.5 Non-Interstate Bridges

The prediction equations for deck, superstructure, and substructure condition ratings for non-Interstate bridges are shown in Figure 4.10. For the deck condition ratings, the Bolukbasi et al. (2004) equation indicates a higher rating until an age of approximately 40 years. After 40 years, the Jiang and Sinha (1989) concrete equation indicates the highest condition rating, and after approximately 45 years, the Jiang and Sinha steel equation provides an estimated service life greater than the Bolukbasi et al. equation. The superstructure and substructure condition ratings are always higher when using the Bolukbasi et al. equations versus either Jiang and Sinha equation. The Bolukbasi et al. equations indicate an overall slower deterioration rate. The prediction equations provide an estimated service life for the deck, superstructure, and substructure. The estimated service lives, or the predicted times until a condition rating of 3 is achieved, are provided in Table 4.7. The table shows that the Bolukbasi et al.



**Figure 4.10. Comparisons of non-Interstate bridge predicted condition ratings for (a) decks, (b) superstructures, and (c) substructures.**

equations predict the shortest deck service life, but they also predict the longest superstructure and substructure service lives.

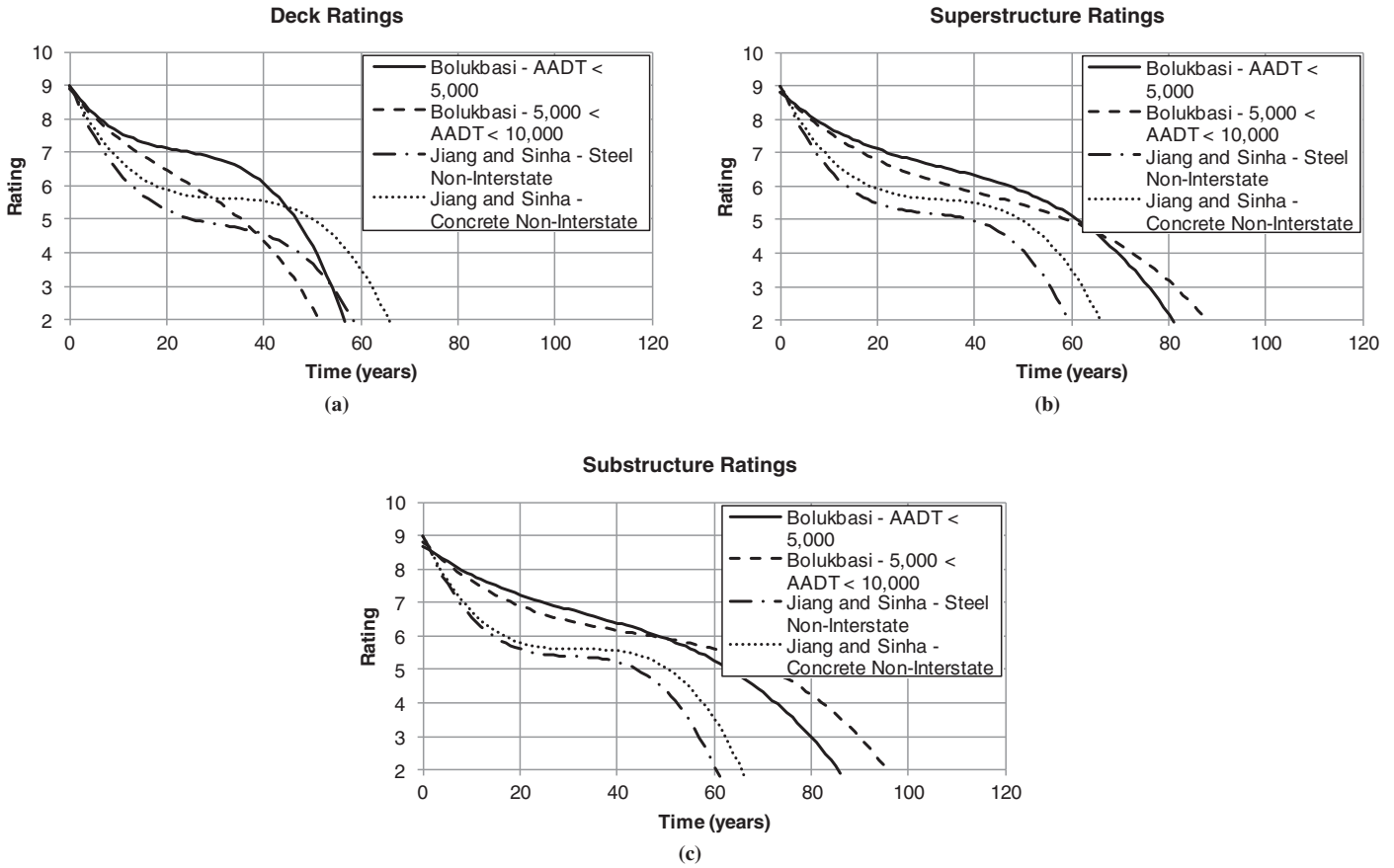
**4.5.6 Low- and Medium-AADT Bridges**

The prediction equations for deck, superstructure, and substructure condition ratings for bridges with AADT

<10,000 for Bolukbasi et al. (2004) and for non-Interstate bridges for Jiang and Sinha (1989) are shown in Figure 4.11. For the deck condition ratings, the Bolukbasi et al. equation for AADT <5,000 indicates the highest condition rating until an age of approximately 42 years. After this time, the Jiang and Sinha concrete non-Interstate equation indicates the highest condition rating, and after approximately 50 years, the Jiang and Sinha steel non-Interstate equation provides an estimated service life similar to the Bolukbasi et al. equation for AADT <5,000. The Bolukbasi et al. equation for AADT between 5,000 and 10,000 is greater than the Jiang and Sinha equations until approximately 27 years. The superstructure and substructure condition ratings are always higher when using the Bolukbasi et al. equations versus the Jiang and Sinha equations. The Bolukbasi et al. equations indicate an overall slower deterioration rate. The equation for AADT <5,000 is greater until approximately 63 years for the superstructure and approximately 50 years for the substructure. The prediction equations provide an estimated service life for the deck, superstructure, and

**Table 4.7. Service Life Comparison: Non-Interstate Bridges**

Equation	Service Life (years)		
	Deck	Superstructure	Substructure
Bolukbasi et al., non-Interstate	52	77	81
Jiang and Sinha, steel non-Interstate	54	56	57
Jiang and Sinha, concrete non-Interstate	62	62	63



**Figure 4.11. Comparisons of low- to medium-AADT bridge predicted condition ratings for (a) decks, (b) superstructures, and (c) substructures.**

substructure. The estimated service lives, or the predicted times until a condition rating of 3 is achieved, are provided in Table 4.8. The table shows that the Bolukbasi et al. equations predict the shortest deck service life, but they also predict the longest superstructure and substructure service lives.

**Table 4.8. Service Life Comparison: Low- to Medium-AADT Bridges**

Equation	Service Life (years)		
	Deck	Superstructure	Substructure
Bolukbasi et al., AADT <5,000	54	76	80
Bolukbasi et al., 5,000 < AADT < 10,000	47	81	90
Jiang and Sinha, steel non-Interstate	54	56	57
Jiang and Sinha, concrete non-Interstate	62	62	63

#### 4.5.7 High-AADT Bridges

The prediction equations for deck, superstructure, and substructure condition ratings for bridges with AADT >10,000 for Bolukbasi et al. (2004) and for Interstate bridges for Jiang and Sinha (1989) are shown in Figure 4.12. The Bolukbasi et al. deck condition rating equation is greater for approximately 30 years, after which it is very similar to the Jiang and Sinha concrete Interstate prediction equation. The superstructure and substructure condition ratings are always higher when using the Bolukbasi et al. equation versus the Jiang and Sinha equations. The Bolukbasi et al. equations indicate an overall slower deterioration rate. The prediction equations provide an estimated service life for the deck, superstructure, and substructure. The estimated service lives, or the predicted times until a condition rating of 3 is achieved, are provided in Table 4.9. The table shows that the Bolukbasi et al. equations predict a deck service life approximately equal to the service life predicted by the Jiang and Sinha concrete Interstate bridge equation, and they also predict the longest superstructure and substructure service lives.



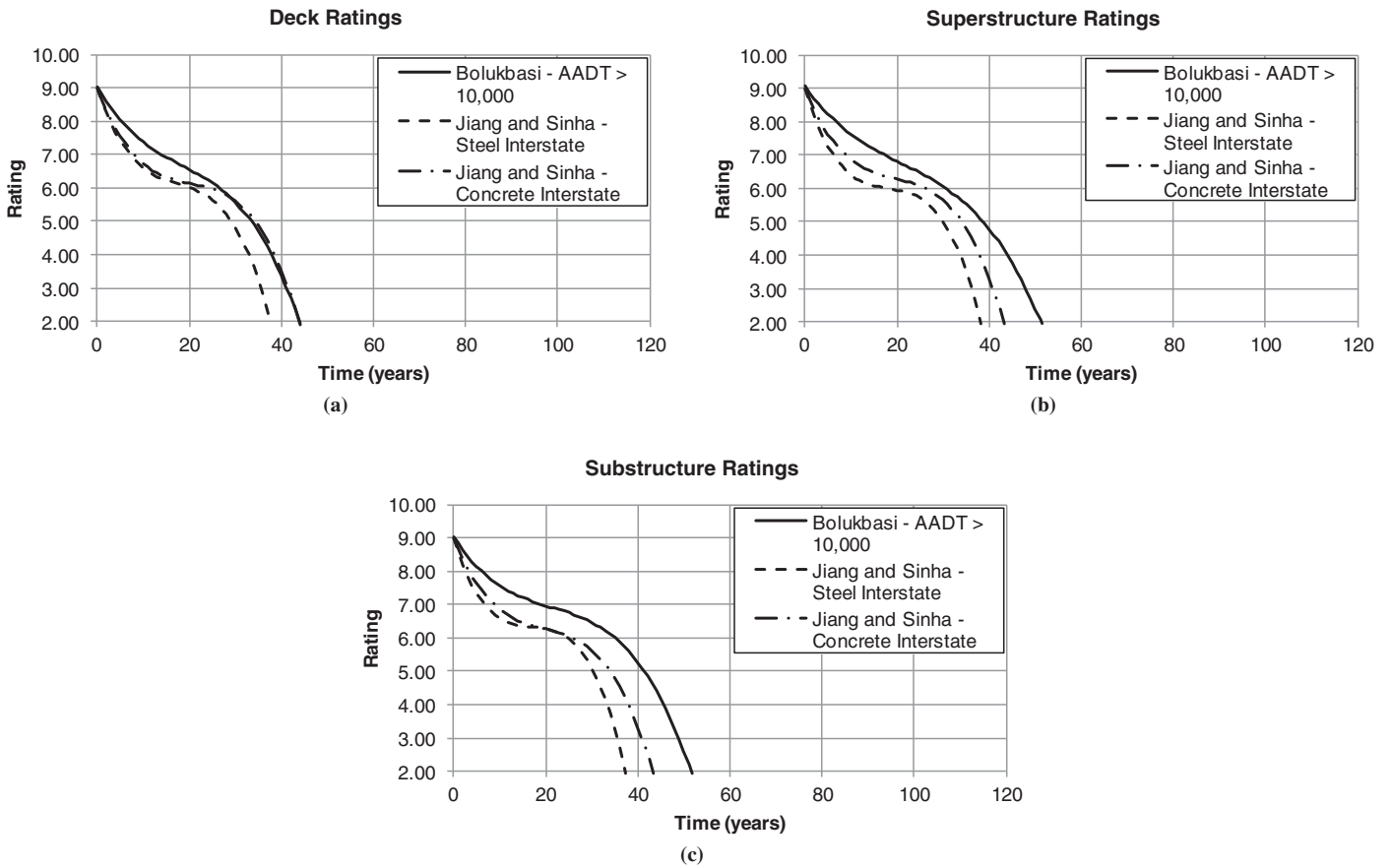


Figure 4.12. Comparisons of high-AADT bridge predicted condition ratings for (a) decks, (b) superstructures, and (c) substructures.

### 4.6 Agrawal and Kawaguchi (2009)

A 2009 report by Agrawal and Kawaguchi provides regression equations relating condition rating (CR) to age for common bridge components in New York State. The following list indicates the number of options and examples of each component:

- Abutment backwall (all grouped together);
- Abutment stem (all grouped together);

- Abutment wingwall (four options: none, other, wingwall exists, and reinforced earth wingwall);
- Abutment bearing (six options: none, steel, polytetrafluoroethylene [PTFE], multirotational, elastomeric, and others);
- Abutment pedestal (all grouped together);
- Abutment joint (12 options: none, open, finger, sliding plate, filled elastic material, preformed elastomeric seals, strip seal, sawed and filled, compression, modular, armored, and other or unknown);
- Pier bearing (six options: none, steel, PTFE, multirotational, elastomeric, and other or unknown);
- Pier pedestal (five options: none, concrete, masonry, steel, and timber);
- Pier cap top (five options: none, concrete, masonry, steel, and timber);
- Pier cap (five options: none, concrete, masonry, steel, and timber);
- Pier stem (all grouped together);
- Pier column (five options: none, concrete, masonry, steel, and timber);
- Pier footing (all grouped together);

Table 4.9. Service Life Comparison: High-AADT Bridges

Equation	Service Life (years)		
	Deck	Superstructure	Substructure
Bolukbasi et al., AADT >10,000	41	48	49
Jiang and Sinha, steel Interstate	36	37	36
Jiang and Sinha, concrete Interstate	42	41	41

- Pier recommendation (five options: none, concrete, masonry, steel, and timber);
- Pier joint (12 options: none, open, finger, sliding plate, filled elastic material, preformed elastomeric seals, strip seal, sawed and filled, compression, modular, armored, and other or unknown); and
- Primary member design type (19 options, such as rolled beam, truss, and deck arch).

The work by Agrawal and Kawaguchi resulted in a computer program based on synthesized Pontis data that calculates the deterioration rates of bridge components using Pontis data. The program contains a cascading algorithm to classify bridges based on several factors. These factors are

- *Element design type*—For bearings, for example, the type can be one of six choices (none, steel, PTFE, multirotational, elastomeric, and others);
- *New York State Department of Transportation (NYSDOT) Region*—There are 11 regions in New York State;
- *Bridge ownership*—Various organizations own bridges within New York State, including NYSDOT, park authorities or commissions, nonpark authorities or commissions, and the New York State Thruway Authority. Bridges are also owned locally, privately, by railroads, and by other entities;
- *Superstructure design type*—These include girder and floorbeam system, truss, and suspension;
- *Superstructure material type*—These include weathering steel, timber, and prestressed concrete;
- *AADT*—AADT is divided into five groups ranging from no trucks to >5,000 trucks per day;
- *Salt usage*—Salt usage is divided into four categories: low (between 6,893 and 13,492 tons), medium (between

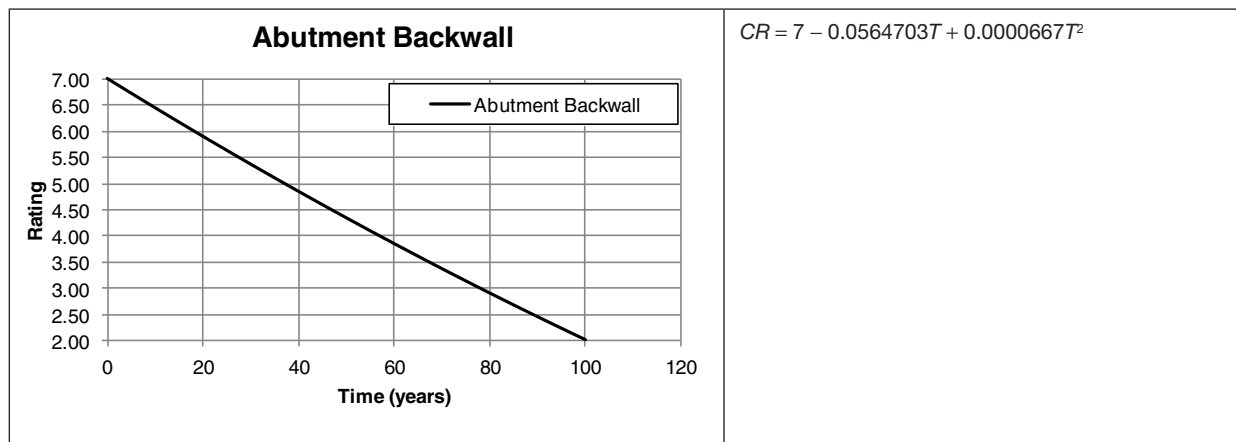
- 10,175 and 25,457 tons), high (between 16,969 and 40,195 tons), and very high (between 46,375 and 94,739 tons);
- *Snow accumulation*—There are three snow accumulation categories: low (<171 in.), medium (between 171 and 278 in.), and high (between 278 and 458 in.);
- *Climate groups*—The 10 groups are based on climate data provided by the National Oceanic and Atmospheric Administration;
- *Functional class*—There are five functional classes ranging from Interstate to none; and
- *Feature under*—This factor has three categories: Interstate under, highway under, and water under.

The factors listed above were used to create a class of bridges that have similar characteristics. The number of characteristics selected allows the deterioration rate to be calculated for a very narrow or a very broad group of bridges.

Within a specific component, multiple equations may be provided for different materials or types of components. As an example, for abutment bearings, four equations (one each for steel bearings, elastomeric bearings, multirotational bearings, and PTFE sliding bearings) were provided. The equations and graphs are shown in Table 4.10. The ratings in New York vary from 1 to 7, with 7 indicating perfect condition; 5 indicating minor deterioration but still functioning as designed; 3 indicating serious deterioration or not functioning as designed; and 1 indicating a failed condition. Even-numbered ratings (2, 4, and 6) are used to provide a middle ground between the odd numbered, defined ratings (1, 3, 5, and 7).

If *failure* is defined as a condition rating of 3 and the component no longer functioning as intended, then the  
(text continues on page 78)

**Table 4.10. Regression Equations and Graphs Based on New York State Bridge Data**



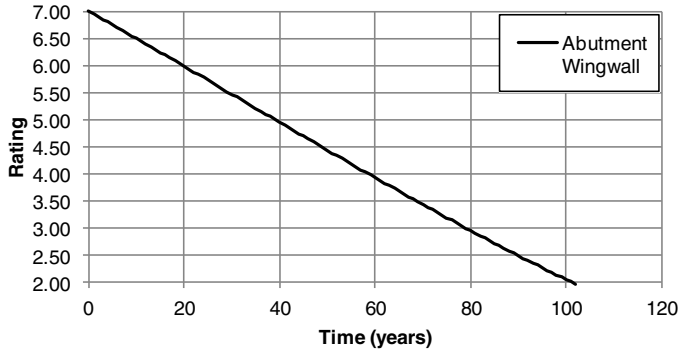
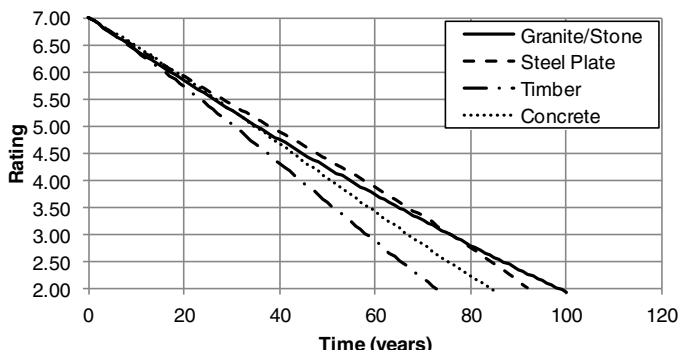
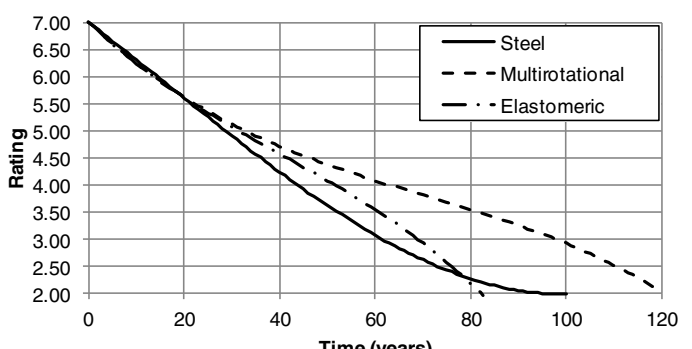
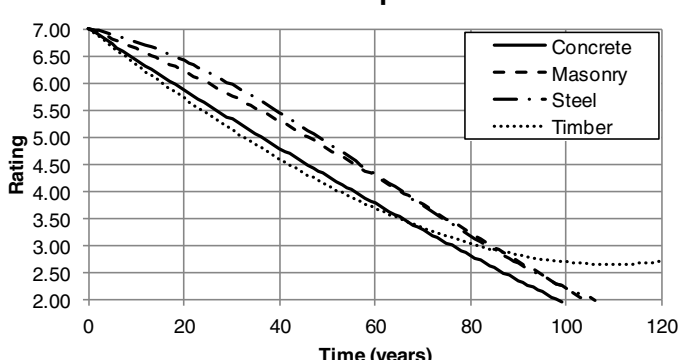
(continued on next page)

Table 4.10. Regression Equations and Graphs Based on New York State Bridge Data (continued)

<p style="text-align: center;"><b>Abutment Bearings</b></p>	<p>Steel: <math>CR = 7 - 0.0773187T + 0.0002408T^2</math></p> <p>PTFE: <math>CR = 7 - 0.1369652T + 0.0023073T^2 - 2.25 \times 10^{-5}T^3</math></p> <p>Multirotational: <math>CR = 7 - 0.1276043T + 0.0020318T^2 - 1.8 \times 10^{-5}T^3</math></p> <p>Elastomeric: <math>CR = 7 - 0.0633160T + 0.0002109T^2 - 1 \times 10^{-7}T^3</math></p>
<p style="text-align: center;"><b>Abutment Joints</b></p>	<p>Open: <math>CR = 7 - 0.1544542T + 0.0019093T^2 - 1.01 \times 10^{-5}T^3</math></p> <p>Compression: <math>CR = 7 - 0.1546255T + 0.0019008T^2 - 9.3 \times 10^{-6}T^3</math></p> <p>Modular: <math>CR = 7 - 0.1944402T + 0.0054188T^2 - 7.4 \times 10^{-5}T^3</math></p> <p>Armor: <math>CR = 7 - 0.1667466T + 0.0022536T^2 - 1.29 \times 10^{-5}T^3</math></p> <p>Sliding Plate: <math>CR = 7 - 0.1955859T + 0.0043095T^2 - 3.42 \times 10^{-5}T^3</math></p> <p>Filled Elastic: <math>CR = 7 - 0.1416458T + 0.0016176T^2 - 6.3 \times 10^{-6}T^3</math></p> <p>Preformed: <math>CR = 7 - 0.1563427T + 0.0014834T^2 - 5.0 \times 10^{-6}T^3</math></p>
<p style="text-align: center;"><b>Abutment Pedestal</b></p>	<p><math>CR = 7 - 0.0484691T - 0.0000925T^2</math></p>
<p style="text-align: center;"><b>Abutment Stem</b></p>	<p><math>CR = 7 - 0.0562065T - 0.0000832T^2</math></p>

(continued on next page)

Table 4.10. Regression Equations and Graphs Based on New York State Bridge Data (continued)

<p style="text-align: center;"><b>Abutment Wingwall</b></p> 	$CR = 7 - 0.0500728T - 0.0000546T^2 - 6.0 \times 10^{-7}T^3$
<p style="text-align: center;"><b>Deck Curb</b></p> 	<p>Granite/Stone: <math>CR = 7 - 0.0605424T + 0.0001089T^2 - 1.0 \times 10^{-7}T^3</math></p> <p>Steel Plate: <math>CR = 7 - 0.0577393T - 0.0001956T^2 - 1.7 \times 10^{-6}T^3</math></p> <p>Timber: <math>CR = 7 - 0.0584921T - 0.0003144T^2 - 2.4 \times 10^{-6}T^3</math></p> <p>Concrete: <math>CR = 7 - 0.0507576T - 0.0002625T^2 - 1.9 \times 10^{-6}T^3</math></p>
<p style="text-align: center;"><b>Pier Bearings</b></p> 	<p>Steel: <math>CR = 7 - 0.0681319T - 0.0001597T^2 + 3.4 \times 10^{-6}T^3</math></p> <p>Multirotational: <math>CR = 7 - 0.0833154T + 0.0008055T^2 - 3.8 \times 10^{-6}T^3</math></p> <p>Elastomeric: <math>CR = 7 - 0.0845871T + 0.0008876T^2 - 7.3 \times 10^{-6}T^3</math></p>
<p style="text-align: center;"><b>Pier Cap</b></p> 	<p>Concrete: <math>CR = 7 - 0.0575767T + 0.0000583T^2 + 1.0 \times 10^{-7}T^3</math></p> <p>Masonry: <math>CR = 7 - 0.0347071T - 0.0002426T^2 + 1.1 \times 10^{-6}T^3</math></p> <p>Steel: <math>CR = 7 - 0.0172139T - 0.0008876T^2 + 3.8 \times 10^{-6}T^3</math></p> <p>Timber: <math>CR = 7 - 0.0674187T + 0.0001438T^2 + 1.0 \times 10^{-6}T^3</math></p>

(continued on next page)

Table 4.10. Regression Equations and Graphs Based on New York State Bridge Data (continued)

<p style="text-align: center;"><b>Pier Cap Top</b></p>	<p>Concrete: <math>CR = 7 - 0.0475800T - 0.0001091T^2 + 1.2 \times 10^{-6}T^3</math></p> <p>Masonry: <math>CR = 7 - 0.0094394T - 0.0007153T^2 + 3.8 \times 10^{-6}T^3</math></p> <p>Steel: <math>CR = 7 - 0.0131302T - 0.0007820T^2 + 4.9 \times 10^{-6}T^3</math></p> <p>Timber: <math>CR = 7 - 0.0467232T + 0.0001051T^2 - 1.3 \times 10^{-6}T^3</math></p>
<p style="text-align: center;"><b>Pier Column</b></p>	<p>Concrete: <math>CR = 7 - 0.0486218T - 0.0001326T^2 + 1.2 \times 10^{-6}T^3</math></p> <p>Masonry: <math>CR = 7 - 0.1461181T + 0.0028522T^2 - 2.66 \times 10^{-5}T^3</math></p> <p>Steel: <math>CR = 7 - 0.0594952T + 0.0002300T^2 - 4.0 \times 10^{-7}T^3</math></p> <p>Timber: <math>CR = 7 - 0.1077933T + 0.0012051T^2 - 7.9 \times 10^{-6}T^3</math></p>
<p style="text-align: center;"><b>Pier Footing</b></p>	<p><math>CR = 7 - 0.0361181T - 0.0001836T^2</math></p>
<p style="text-align: center;"><b>Pier Joint</b></p>	<p>Open: <math>CR = 7 - 0.1746867T + 0.0029733T^2 - 2.24 \times 10^{-5}T^3</math></p> <p>Strip Seal: <math>CR = 7 - 0.2222855T + 0.0043429T^2 - 3.68 \times 10^{-5}T^3</math></p> <p>Compression: <math>CR = 7 - 0.2047452T + 0.0034777T^2 - 2.09 \times 10^{-5}T^3</math></p> <p>Modular: <math>CR = 7 - 0.1178004T + 0.0000691T^2 + 1.37 \times 10^{-5}T^3</math></p> <p>Armor: <math>CR = 7 - 0.1623125T + 0.0012891T^2 - 1.0 \times 10^{-7}T^3</math></p> <p>Sliding Plate: <math>CR = 7 - 0.1581306T + 0.0016926T^2 - 8.9 \times 10^{-6}T^3</math></p> <p>Filled Elastic: <math>CR = 7 - 0.1937046T + 0.0028916T^2 - 1.3 \times 10^{-5}T^3</math></p> <p>Preformed: <math>CR = 7 - 0.1725949T + 0.0020362T^2 - 9.6 \times 10^{-6}T^3</math></p>

(continued on next page)

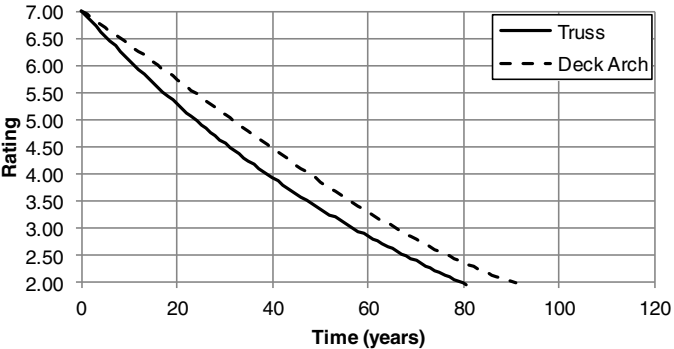
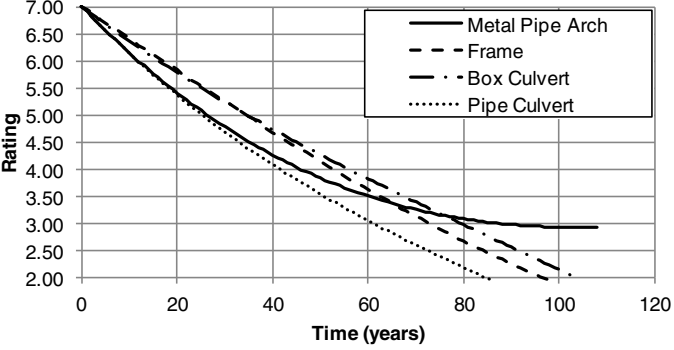
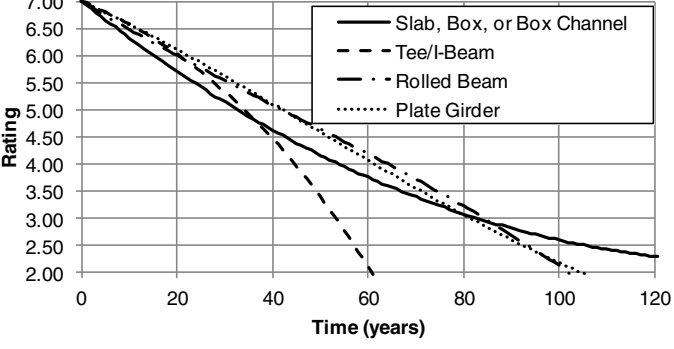
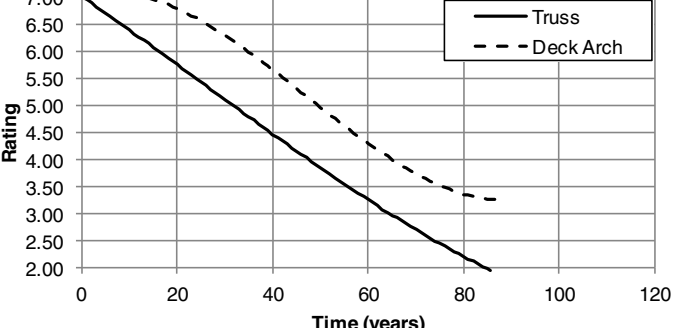


**Table 4.10. Regression Equations and Graphs Based on New York State Bridge Data (continued)**

<p style="text-align: center;"><b>Pier Pedestal</b></p>	<p>Concrete: <math>CR = 7 - 0.0427029T - 0.0003432T^2 + 2.8 \times 10^{-6}T^3</math></p> <p>Masonry: <math>CR = 7 - 0.0214166T - 0.0007708T^2 + 5.0 \times 10^{-6}T^3</math></p> <p>Steel: <math>CR = 7 - 0.0294246T - 0.0002940T^2 + 1.5 \times 10^{-6}T^3</math></p>
<p style="text-align: center;"><b>Pier Design</b></p>	<p>Concrete: <math>CR = 7 - 0.0616063T + 0.0001235T^2 - 1.0 \times 10^{-7}T^3</math></p> <p>Masonry: <math>CR = 7 + 0.0189981T - 0.0013498T^2 + 7.5 \times 10^{-6}T^3</math></p> <p>Steel: <math>CR = 7 - 0.0335030T - 0.0004089T^2 + 2.4 \times 10^{-6}T^3</math></p> <p>Timber: <math>CR = 7 - 0.1156794T + 0.0014818T^2 - 9.8 \times 10^{-6}T^3</math></p>
<p style="text-align: center;"><b>Pier Stem</b></p>	<p><math>CR = 7 - 0.0445180T - 0.0001482T^2 + 1.1 \times 10^{-6}T^3</math></p>
<p style="text-align: center;"><b>Primary Members</b></p>	<p>Slab, Box, Box Channel: <math>CR = 7 - 0.0724412T + 0.0002255T^2 - 4.0 \times 10^{-7}T^3</math></p> <p>Tee or I-Beam: <math>CR = 7 - 0.0509168T - 0.0001729T^2 + 2.1 \times 10^{-6}T^3</math></p> <p>Rolled Beam: <math>CR = 7 - 0.0573849T + 0.0000603T^2 + 1.0 \times 10^{-7}T^3</math></p> <p>Plate Girder: <math>CR = 7 - 0.0533815T + 0.0000618T^2</math></p>

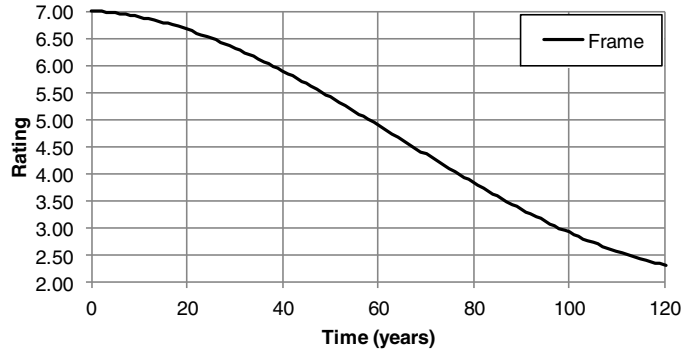
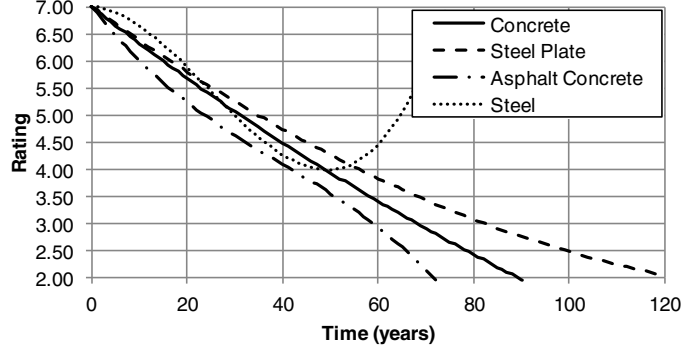
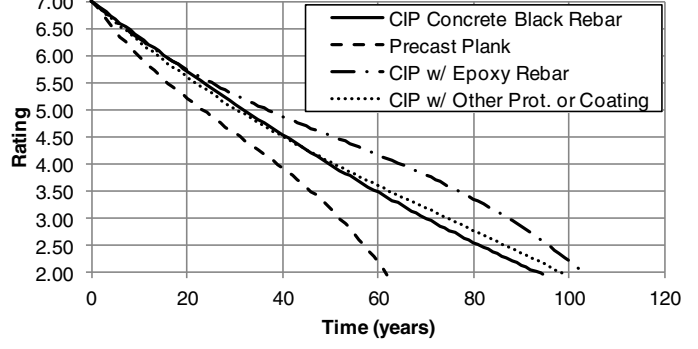
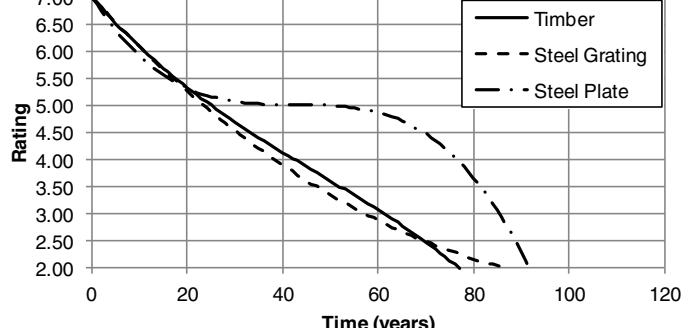
(continued on next page)

**Table 4.10. Regression Equations and Graphs Based on New York State Bridge Data (continued)**

<p style="text-align: center;"><b>Primary Members</b></p> 	<p>Truss: <math>CR = 7 - 0.0962120T + 0.0005460T^2 - 1.6 \times 10^{-6}T^3</math></p> <p>Deck Arch: <math>CR = 7 - 0.0608540T - 0.0001644T^2 + 2.5 \times 10^{-6}T^3</math></p>
<p style="text-align: center;"><b>Primary Members</b></p> 	<p>Metal Pipe Arch: <math>CR = 7 - 0.0917752T + 0.0006315T^2 - 1.2 \times 10^{-6}T^3</math></p> <p>Frame: <math>CR = 7 - 0.0586090T - 0.0000153T^2 + 9.0 \times 10^{-7}T^3</math></p> <p>Box Culvert: <math>CR = 7 - 0.0662312T + 0.0002877T^2 - 1.1 \times 10^{-6}T^3</math></p> <p>Pipe Culvert: <math>CR = 7 - 0.0918358T + 0.0005486T^2 - 1.9 \times 10^{-6}T^3</math></p>
<p style="text-align: center;"><b>Secondary Members</b></p> 	<p>Slab, Box, or Box Channel: <math>CR = 7 - 0.0705115T + 0.0002846T^2 - 2.0 \times 10^{-7}T^3</math></p> <p>Tee or I-Beam: <math>CR = 7 - 0.0371296T - 0.0004970T^2 - 4.1 \times 10^{-6}T^3</math></p> <p>Rolled Beam: <math>CR = 7 - 0.0536963T + 0.0002090T^2 - 1.6 \times 10^{-6}T^3</math></p> <p>Plate Girder: <math>CR = 7 - 0.0403950T - 0.0002383T^2 + 1.6 \times 10^{-6}T^3</math></p>
<p style="text-align: center;"><b>Secondary Members</b></p> 	<p>Truss: <math>CR = 7 - 0.0600905T - 0.0001653T^2 + 2.1 \times 10^{-6}T^3</math></p> <p>Deck Arch: <math>CR = 7 + 0.0225284T - 0.0019546T^2 + 1.38 \times 10^{-5}T^3</math></p>

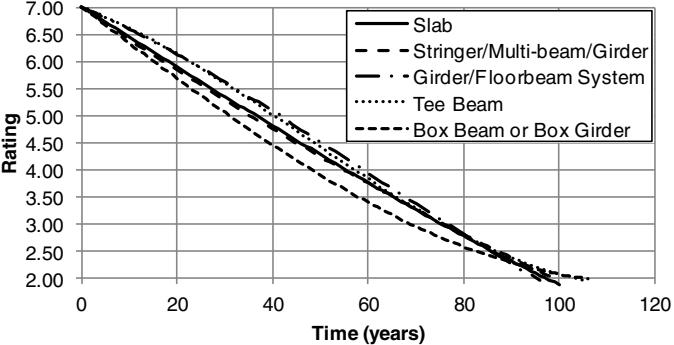
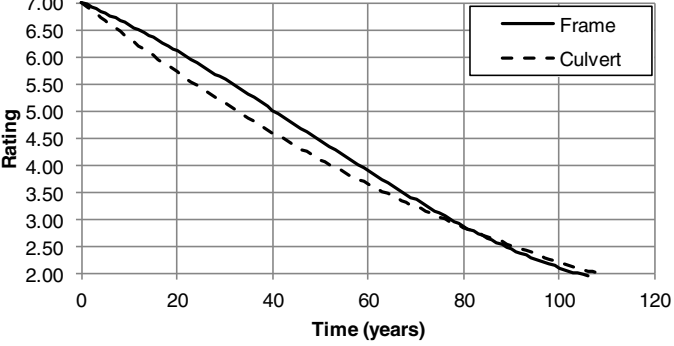
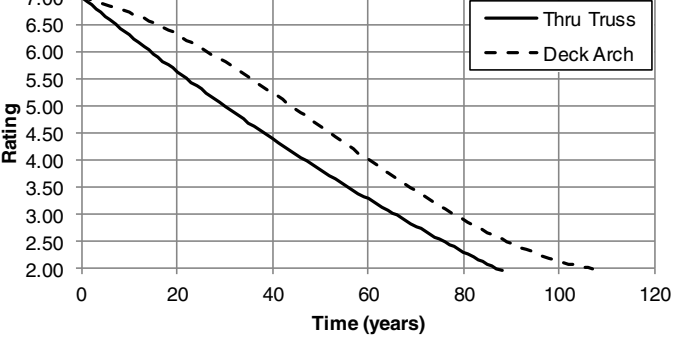
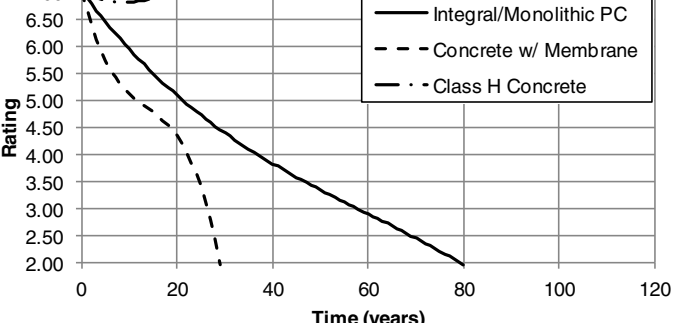
(continued on next page)

Table 4.10. Regression Equations and Graphs Based on New York State Bridge Data (continued)

<p style="text-align: center;"><b>Secondary Members</b></p> 	<p>Frame: <math>CR = 7 - 0.0031620T - 0.0007666T^2 + 3.9 \times 10^{-6}T^3</math></p>
<p style="text-align: center;"><b>Sidewalk/Fascia</b></p> 	<p>Concrete: <math>CR = 7 - 0.0697598T + 0.0001899T^2 - 4.0 \times 10^{-7}T^3</math></p> <p>Steel Plate: <math>CR = 7 - 0.0636279T + 0.0001742T^2 + 1.0 \times 10^{-7}T^3</math></p> <p>Asphalt Concrete: <math>CR = 7 - 0.1145251T + 0.0015822T^2 - 1.34 \times 10^{-5}T^3</math></p> <p>Steel<sup>2</sup>: <math>CR = 7 - 0.0055077T - 0.0034812T^2 + 4.78 \times 10^{-5}T^3</math></p>
<p style="text-align: center;"><b>Structural Deck</b></p> 	<p>CIP Concrete Black Rebar: <math>CR = 7 - 0.0675608T + 0.0001411T^2 + 1.0 \times 10^{-7}T^3</math></p> <p>Precast Plank: <math>CR = 7 - 0.1188157T + 0.0018646T^2 - 2.04 \times 10^{-5}T^3</math></p> <p>CIP with Epoxy Rebar: <math>CR = 7 - 0.0767927T + 0.0007988T^2 - 5.1 \times 10^{-6}T^3</math></p> <p>CIP with Other Protection or Coating: <math>CR = 7 - 0.0793700T + 0.0005157T^2 - 2.3 \times 10^{-6}T^3</math></p>
<p style="text-align: center;"><b>Structural Deck</b></p> 	<p>Timber: <math>CR = 7 - 0.1015141T + 0.0010366T^2 - 7.3 \times 10^{-6}T^3</math></p> <p>Steel Grating: <math>CR = 7 - 0.0971087T + 0.0005147T^2 - 7 \times 10^{-7}T^3</math></p> <p>Steel Plate: <math>CR = 7 - 0.1387853T + 0.0032377T^2 - 2.53 \times 10^{-5}T^3</math></p>

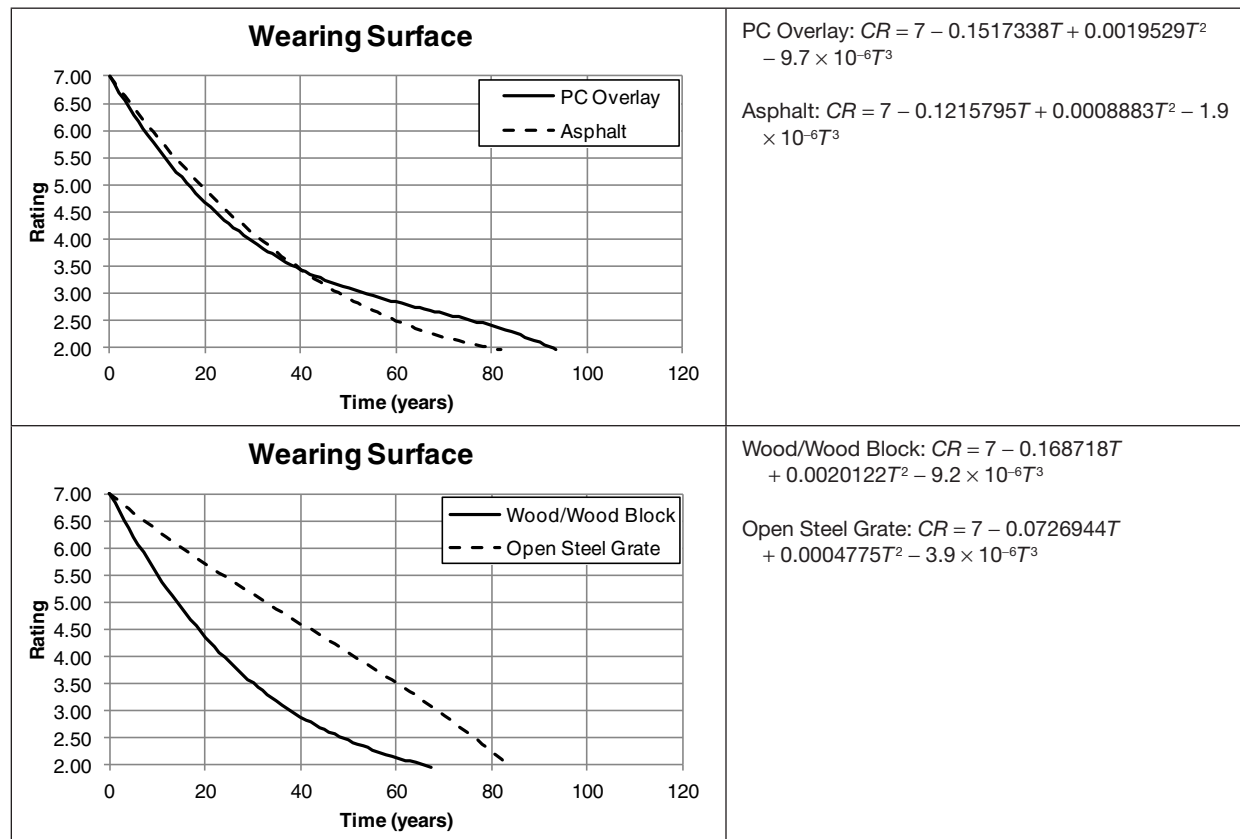
(continued on next page)

Table 4.10. Regression Equations and Graphs Based on New York State Bridge Data (continued)

<p style="text-align: center;"><b>Superstructure Type</b></p> 	<p>Slab: <math>CR = 7 - 0.0550966T - 0.0000107T^2 + 5.0 \times 10^{-7}T^3</math></p> <p>Stringer/Multi-beam/Girder: <math>CR = 7 - 0.0608104T + 0.0001228T^2 - 2 \times 10^{-7}T^3</math></p> <p>Girder/Floorbeam System: <math>CR = 7 - 0.0375553T - 0.0003374T^2 + 1.9 \times 10^{-6}T^3</math></p> <p>Tee Beam: <math>CR = 7 - 0.0334694T - 0.0005675T^2 + 4.1 \times 10^{-6}T^3</math></p> <p>Box Beam or Box Girder: <math>CR = 7 - 0.0671339T + 0.0000287T^2 + 1.5 \times 10^{-6}T^3</math></p>
<p style="text-align: center;"><b>Superstructure Type</b></p> 	<p>Frame: <math>CR = 7 - 0.0374148T - 0.0004245T^2 + 3.1 \times 10^{-6}T^3</math></p> <p>Culvert: <math>CR = 7 - 0.0683836T + 0.0002159T^2 - 1.0 \times 10^{-7}T^3</math></p>
<p style="text-align: center;"><b>Superstructure Type</b></p> 	<p>Thru Truss: <math>CR = 7 - 0.0719036T + 0.0001651T^2</math></p> <p>Deck Arch: <math>CR = 7 - 0.0209106T + 0.0007879T^2 + 5.1 \times 10^{-6}T^3</math></p>
<p style="text-align: center;"><b>Wearing Surface</b></p> 	<p>Integral/Monolithic Portland Cement (PC): <math>CR = 7 - 0.1178904T + 0.0012462T^2 + 7.0 \times 10^{-6}T^3</math></p> <p>Concrete with Membrane: <math>CR = 7 - 0.3488945T + 0.021168T^2 - 5.196 \times 10^{-4}T^3</math></p> <p>Class H Concrete<sup>a</sup>: <math>CR = 7 - 0.0417046T + 0.0022971T^2</math></p>

(continued on next page)

**Table 4.10. Regression Equations and Graphs Based on New York State Bridge Data (continued)**



Note: CR = condition rating.

<sup>a</sup> Indicates equations that, when plotted, do not appear correct based on graphs provided in the report.

Source: Agrawal and Kawaguchi (2009).

(continued from page 70)

service life of each component can be estimated. The estimated service lives are shown in Table 4.11 to Table 4.13. The reported service lives were determined by extending the graph until a condition rating of 3 was reached. Doing so may have resulted in some equations being used outside their intended range of applicability. In addition, the bridges used in this analysis were combined into one large group. This grouping may result in service lives for one material being greater than that for another material that might be expected to last longer. As an example, in Table 4.12 timber pier caps are predicted to last longer than concrete pier caps. Performing the analysis on a smaller group of bridges may result in the concrete service life being greater than that of the timber.

#### 4.7 Stukhart et al. (1991)

In a report to the Texas Department of Transportation (DOT), Stukhart et al. (1991) presented numerous equations predicting the condition rating for bridge decks,

superstructures, and substructures. No distinction between CIP decks and precast panels was noted in the reference. Several of the equations are from work completed by others, but most of the equations either use NBI data for Texas bridges or the expert opinion of Texas bridge engineers. The equations are shown and plotted in Table 4.14. The first set of equations was determined using regression analysis by the Transportation Systems Center and is a function of both age and ADT.

NBI data for Texas bridges were used to determine additional equations relating age and ADT to condition ratings. Linear, piecewise linear, and nonlinear equations were proposed; in addition, through a survey, equations based on expert opinion were determined considering the worst-case scenario, the most likely scenario, and the best-case scenario. Table 4.15 shows the prediction equations for coastal bridge substructures for different functional classifications, and Table 4.16 shows the prediction equations for substructures in all regions not considering functional classification. The graphs in Table 4.16 and Table 4.17 show that the linear equations suggest service lives (time to reach



**Table 4.11. Abutment Component Estimated Service Lives**

Component	Service Life (years)
<b>Abutment Backwall</b>	78.0
<b>Abutment Bearings</b>	
Steel	65.0
PTFE	51.4
Multitrotational	57.0
Elastomeric	88.0
<b>Abutment Joints</b>	
Open	45.0
Compression	46.0
Modular	41.3
Armor	42.4
Sliding plate	66.4
Filled elastic	58.0
Preformed	37.0
<b>Abutment Pedestal</b>	72.5
<b>Abutment Stem</b>	81.0
<b>Abutment Wingwall</b>	79.0

a condition rating of 3) significantly longer than 100 years, which is possible, but unlikely. The nonlinear equations are terminated at the minimum value; beyond this point the condition rating would appear to increase, which is not possible without maintenance. As only bridges without maintenance, repair, or rehabilitation were used in the analysis, the rating should not increase with increasing age. A new structure would have a condition rating of 9; all the prediction equations indicate the condition rating to be near 8 when new.

Piecewise linear equations were determined for different functional classifications for the deck, superstructure, and substructure condition ratings. The coefficients  $B_0$ ,  $B_1$ ,  $B_2$ , and  $B_3$  used in the piecewise linear equations are presented in Table 4.17. The condition rating is described by three linear equations that are applicable during certain times of the bridge life; these equations are shown as Equation 4.1. In the study by Stukhart et al.,  $t_1$  and  $t_2$  are defined as 25 and 45 years, respectively. Several of the graphs are terminated at 45 years as the results of the regression analysis indicate that the condition rating would increase, which cannot be true without maintenance being performed.

**Table 4.12. Pier Component Estimated Service Lives**

Component	Service Life (years)
<b>Pier Bearings</b>	
Steel	61.4
Multitrotational	98.0
Elastomeric	69.0
<b>Pier Cap</b>	
Concrete	76.0
Masonry	84.5
Steel	83.4
Timber	81.6
<b>Pier Cap Top</b>	
Concrete	82.6
Masonry	93.0
Steel	91.7
Timber	84.8
<b>Pier Column</b>	
Concrete	77.4
Masonry	57.1
Steel	98.0
Timber	63.3
<b>Pier Footing</b>	79.0
<b>Pier Joints</b>	
Open	47.7
Strip seal	34.3
Compression	41.5
Modular	49.0
Armor	33.7
Sliding plate	37.2
Filled elastic	42.0
Preformed	35.6
<b>Pier Pedestal</b>	
Concrete	76.0
Masonry	78.3
Steel	91.4
<b>Overall Pier</b>	
Concrete	75.7
Masonry	96.6
Steel	78.7
Timber	66.0
<b>Pier Stem</b>	81.0

Table 4.13. Superstructure and Deck Estimated Service Lives

Component	Service Life (years)	Component	Service Life (years)
<b>Deck Curb</b>		Rolled beam	84.3
Granite or stone	75.6	Plate girder	81.3
Steel plate	75.9	Truss	64.5
Timber	58.3	Deck arch	NA
Concrete	66.9	Frame	98.0
<b>Primary Member</b>		<b>Structural Deck</b>	
Slab, box, or box channel	67.8	CIP with black rebar	69.9
Tee or I-beam	77.3	Precast plank	51.9
Rolled beam	76.7	CIP with epoxy rebar	87.0
Plate girder	82.9	CIP with other coating	74.5
Truss	56.9	Timber	61.0
Deck arch	65.7	Steel grating	57.0
Metal pipe arch	87.0	Steel plate	85.4
Frame	72.8	<b>Wearing Surface</b>	
Box culvert	79.5	Integral or monolithic	
Pipe culvert	61.0	Portland cement	57.7
<b>Overall Superstructure</b>		Concrete with membrane	26.3
Slab	75.4	Class H concrete	NA
Multistringer or beam	76.0	Portland cement overlay	53.0
Girder or floorbeam	76.6	Asphalt	48.0
Tee beam	75.6	Wood or wood block	37.8
Box beam or girder	68.9	Open steel grate	68.6
Frame	77.4	<b>Sidewalk or Fascia</b>	
Culvert	76.0	Concrete	68.0
Through truss	65.5	Steel plate	82.0
Deck arch	77.9	Asphalt concrete	59.0
<b>Secondary Member</b>		Steel	NA
Slab, box, or box channel	82.8		
Tee or I-beam	53.2		

Note: NA = not available.

CR =

$$\left\{ \begin{array}{l} B_0 + B_1 t \text{ if } t \leq t_1 \\ B_0 + B_1 t_1 + B_2 (t - t_1) \text{ if } t_1 < t \leq t_2 \\ B_0 + B_1 t_1 + B_2 (t_2 - t_1) + \beta_3 (t - t_2) \text{ if } t > t_2 \end{array} \right. \quad (4.1)$$

A nonlinear regression analysis was performed to determine the parameters for the best-fit exponential decay curve. Parameters were determined for bridge decks and superstructures based on functional classification using the multiyear data set. The best-fit parameters and equations were used to estimate the service life of bridge decks and

superstructures; for most cases, the estimated service lives were in excess of 150 years. Although this would seem like a good thing, it is known that most bridge decks and superstructures will not have a service life of this length. In fact, it is more likely that the service life of a bridge deck is closer to 40 or 50 years than 150 years. Although the estimated service lives seem extreme, the results are shown to indicate the available data. The basic equation used to estimate the service life is shown as Equation 4.2; the graphs and parameters are shown in Table 4.18. The estimated service life is approximately equal to the absolute value of  $\beta_2$  for this set of data. Looking at the values of  $\beta_2$ , the only reasonable values are for

*(text continues on page 86)*

**Table 4.14. Transportation Systems Center Prediction Equations**

<p style="text-align: center;"><b>Deck Ratings</b></p>	$CR = 9 - 0.119t - 2.158 \times 10^{-6} (ADTAGE)$ $ADTAGE = \frac{(ADT)(AGE)}{10}$
<p style="text-align: center;"><b>Substructure Ratings</b></p>	$CR = 9 - 0.105t - 2.105 \times 10^{-6} ADT$
<p style="text-align: center;"><b>Superstructure Ratings</b></p>	$CR = 9 - 0.103t - 1.982 \times 10^{-6} ADT$

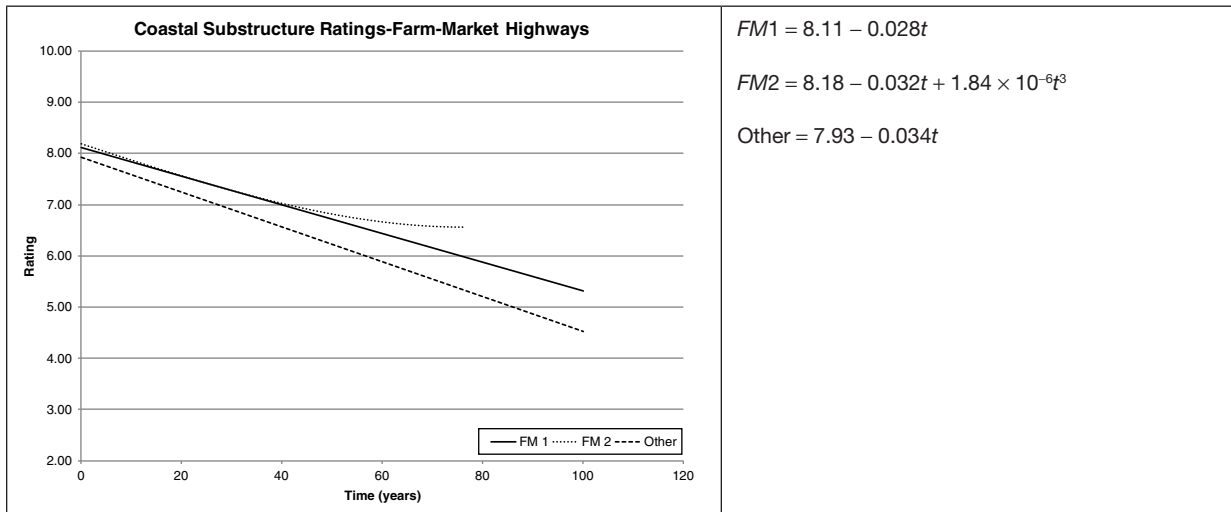
Source: Stukhart et al. (1991).

**Table 4.15. Coastal Substructure Condition Rating Prediction Equations**

<p style="text-align: center;"><b>Coastal Substructure Rating-Interstate Highways</b></p>	<p><math>IH1 = 7.80 - 0.022t</math></p> <p><math>IH2 = 7.98 - 0.036t + 3.89 \times 10^{-4}t^2 - 8.00 \times 10^{-8} \times t \times ADT</math></p> <p>ADT assumed as 25,000 vehicles</p>
<p style="text-align: center;"><b>Coastal Substructure Ratings-US Highways</b></p>	<p><math>US1 = 7.81 - 0.017t</math></p> <p><math>US2 = 7.94 - 0.028t + 2.02 \times 10^{-4}t^2 - 6.00 \times 10^{-8} \times t \times ADT</math></p> <p>ADT assumed as 15,000 vehicles</p>
<p style="text-align: center;"><b>Coastal Substructure Ratings-State Highways</b></p>	<p><math>SH1 = 8.12 - 0.025t</math></p> <p><math>SH2 = 8.47 - 0.064t + 7.45 \times 10^{-4}t^2 - 2.20 \times 10^{-7} \times t \times ADT</math></p> <p>ADT assumed as 10,000 vehicles</p>

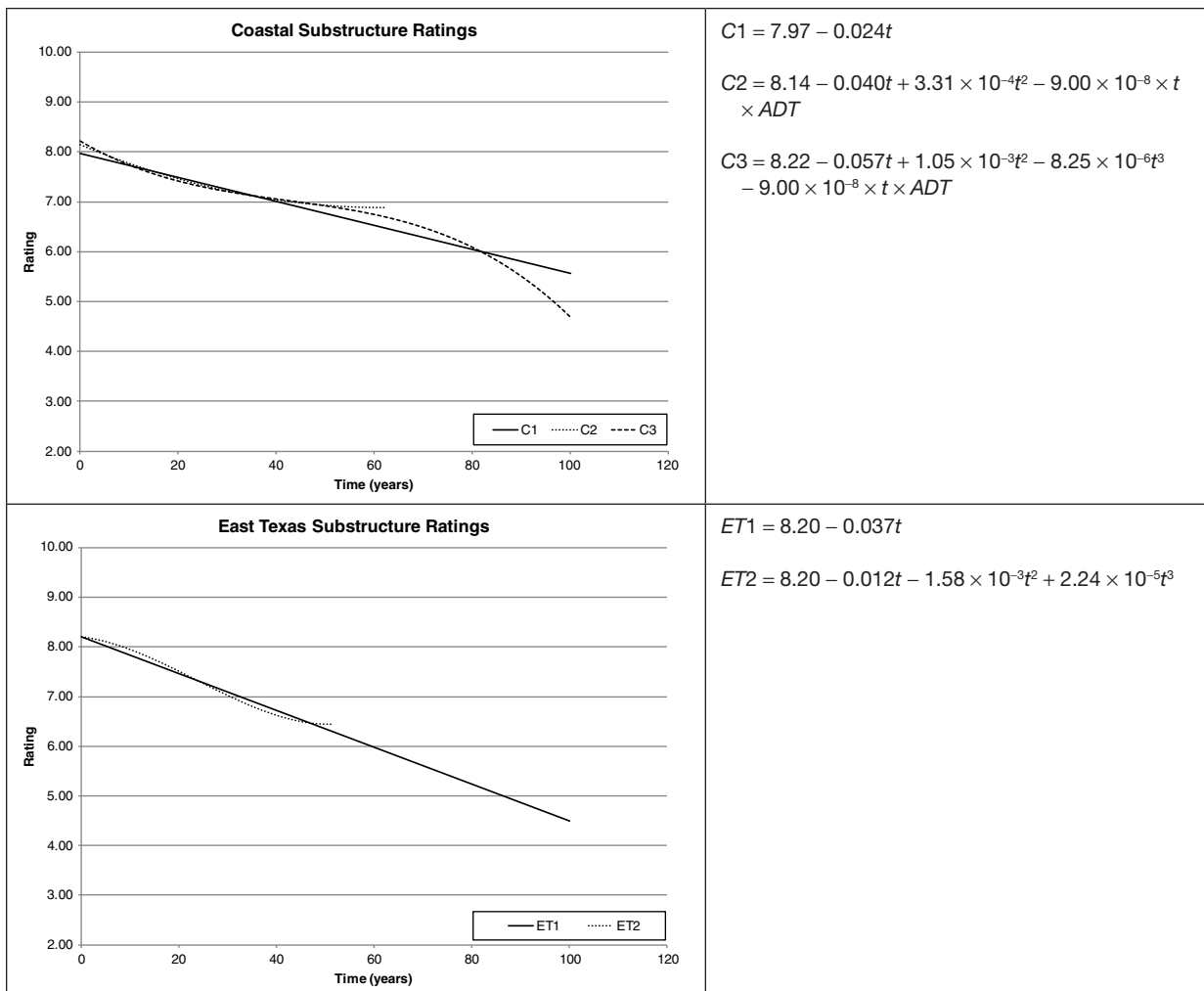
(continued on next page)

**Table 4.15. Coastal Substructure Condition Rating Prediction Equations (continued)**



Note: IH = Interstate highways or principal arterials; US = U.S. highways (non-Interstate) or minor arterials; SH = state highways or minor arterials; FM = farm-to-market roads or collectors.  
 Source: Stukhart et al. (1991).

**Table 4.16. Substructure Condition Rating Prediction Equations by Region (continued)**



(continued on next page)

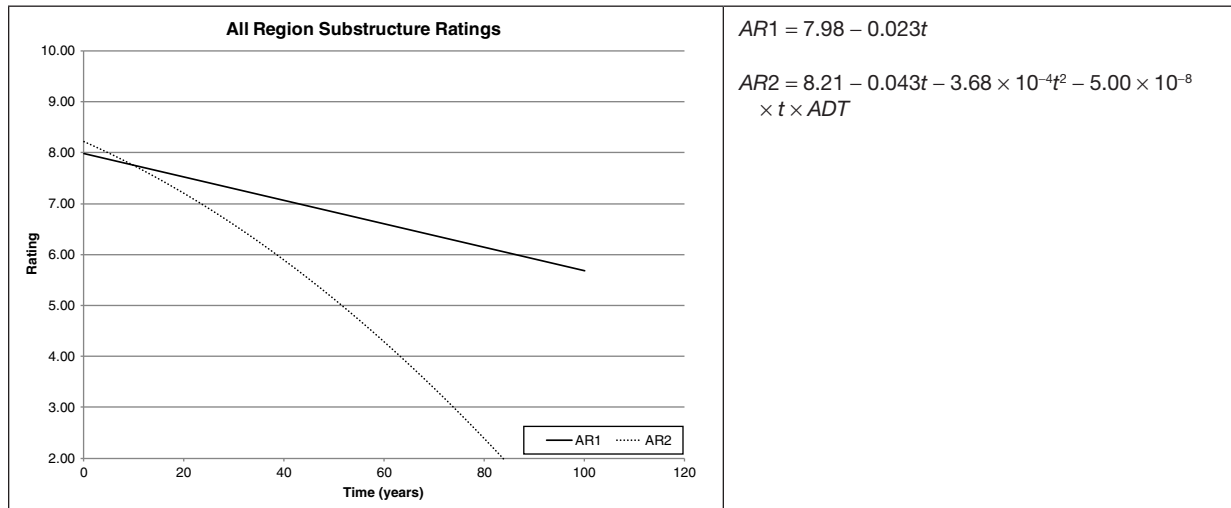


**Table 4.16. Substructure Condition Rating Prediction Equations by Region (continued)**

<p style="text-align: center;"><b>Inland Texas Substructure Ratings</b></p> <p style="text-align: center;">Time (years)</p>	$IT1 = 7.93 - 0.015t$ $IT2 = 8.05 - 0.028t - 4.40 \times 10^{-4}t^2 + 3.76 \times 10^{-6}t^3 - 6.00 \times 10^{-8} \times t \times ADT$
<p style="text-align: center;"><b>West Texas Substructure Ratings</b></p> <p style="text-align: center;">Time (years)</p>	$WT1 = 7.85 - 0.015t$ $WT2 = 8.27 - 0.059t - 1.22 \times 10^{-3}t^2 + 9.00 \times 10^{-6}t^3 - 4.40 \times 10^{-7} \times t \times ADT$
<p style="text-align: center;"><b>Panhandle Region Substructure Ratings</b></p> <p style="text-align: center;">Time (years)</p>	$PH1 = 7.72 - 0.015t$ $PH2 = 8.56 - 0.109t - 2.52 \times 10^{-3}t^2 + 1.62 \times 10^{-5}t^3 - 3.60 \times 10^{-7} \times t \times ADT$

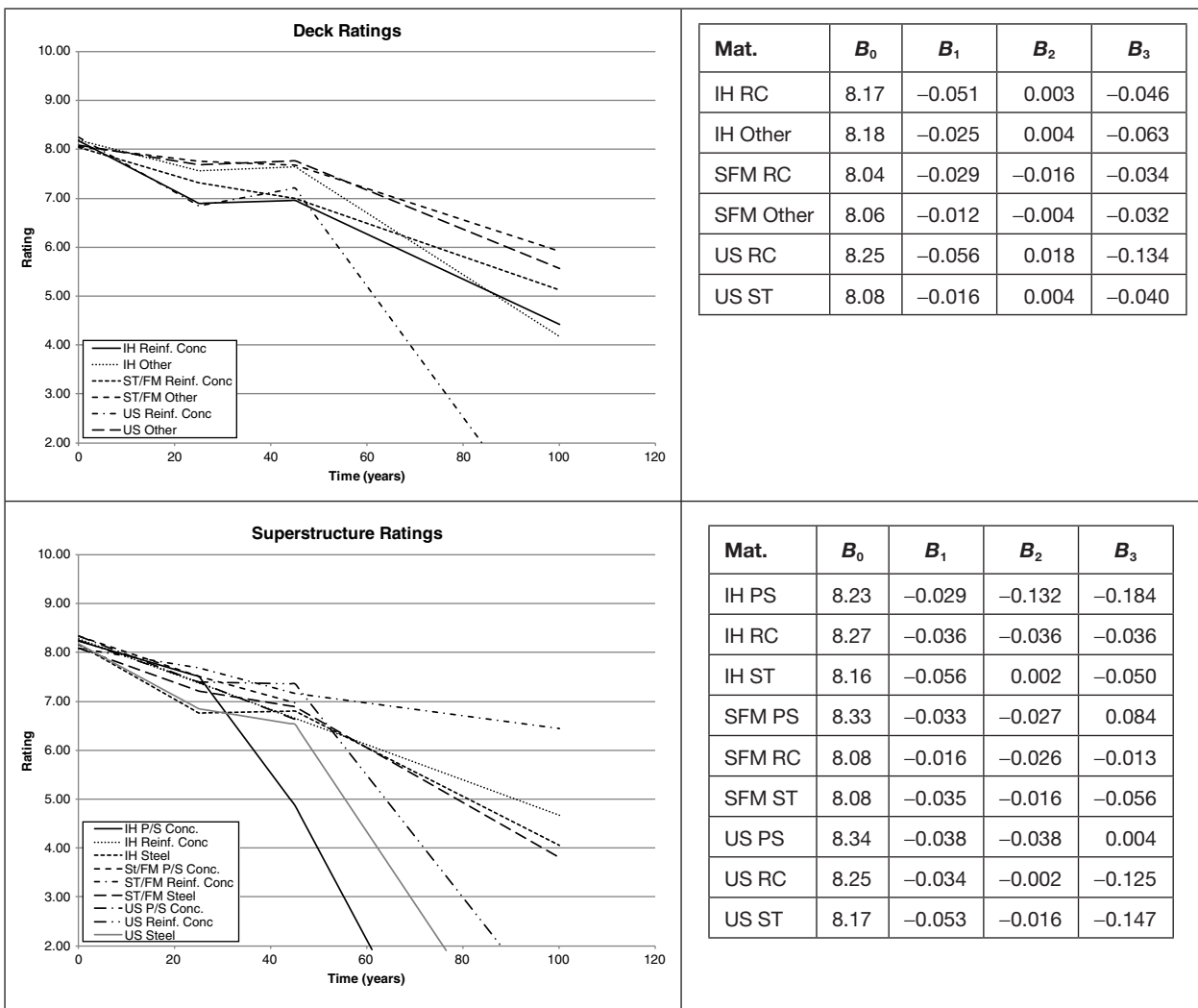
(continued on next page)

**Table 4.16. Substructure Condition Rating Prediction Equations by Region (continued)**

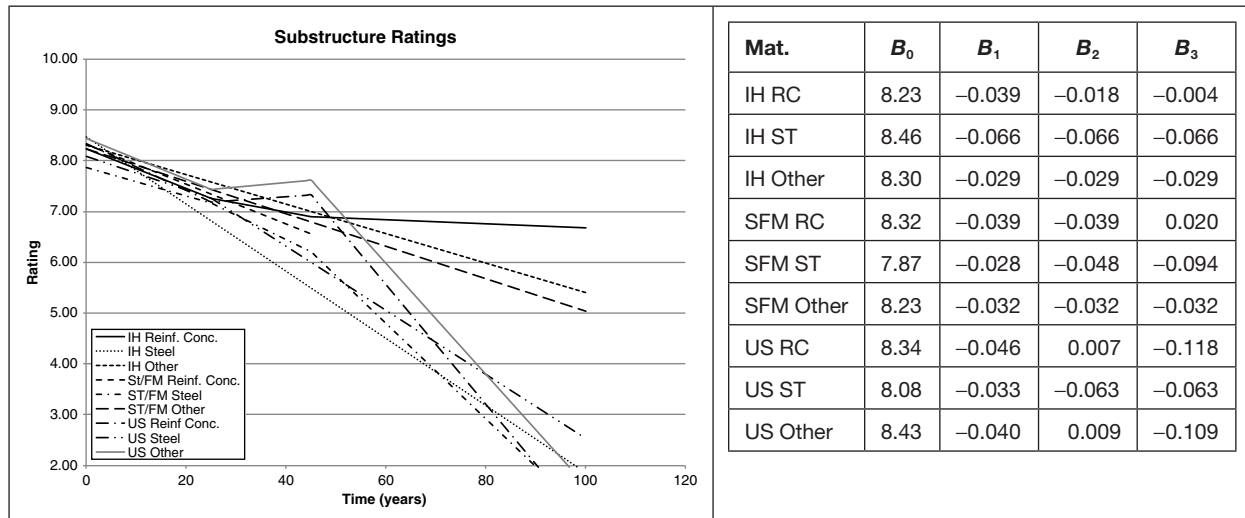


Note: Equations are named according to region (C for coastline, ET for east Texas, and so forth) and are numbered in the order in which they are presented in Stukhart et al. (1991).  
 Source: Stukhart et al. (1991).

**Table 4.17. Piecewise Linear Condition Rating Equations and Coefficients**



**Table 4.17. Piecewise Linear Condition Rating Equations and Coefficients (continued)**



Note: IH = Interstate highways or principal arterials; RC = reinforced concrete; SFM = state farm-to-market road; US = U.S. highways (non-Interstate) or minor arterials; ST = state highways; PS = prestressed; SH = state highways or minor arterials; FM = farm-to-market roads or collectors; ST/FM = state highways and farm-to-market combined.  
Source: Stukhart et al. (1991).

(continued from page 80)

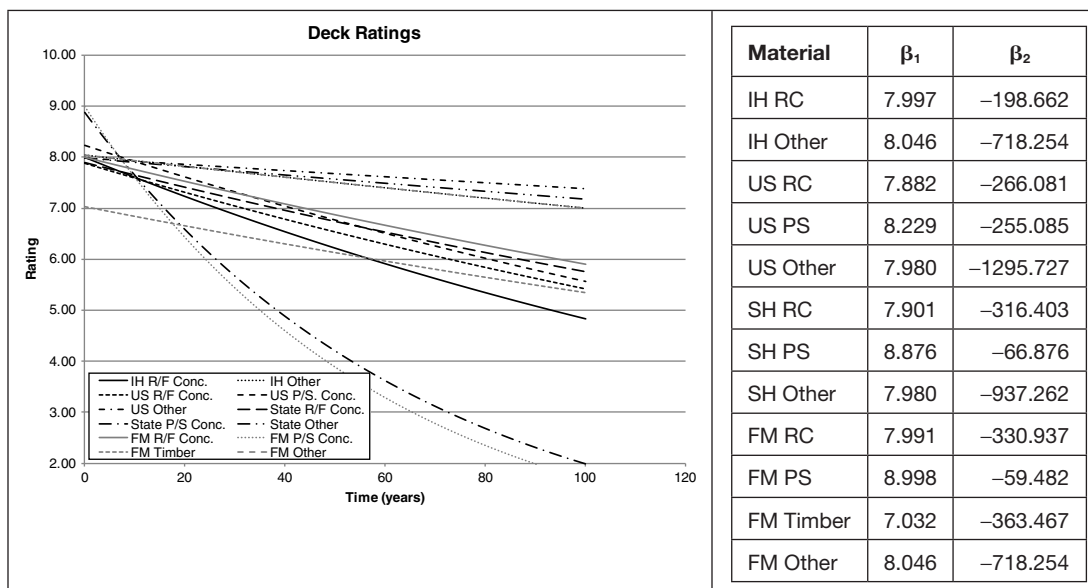
decks of prestressed concrete bridge on the state and farm-to-market highway systems.

$$CR = \beta_1 e^{\frac{t}{\beta_2}} \quad (4.2)$$

The final method used to develop equations to predict condition ratings for the deck, superstructure, and substructure was a survey of Texas bridge engineers, who were asked to provide estimates of the worst-case, the most likely, and the

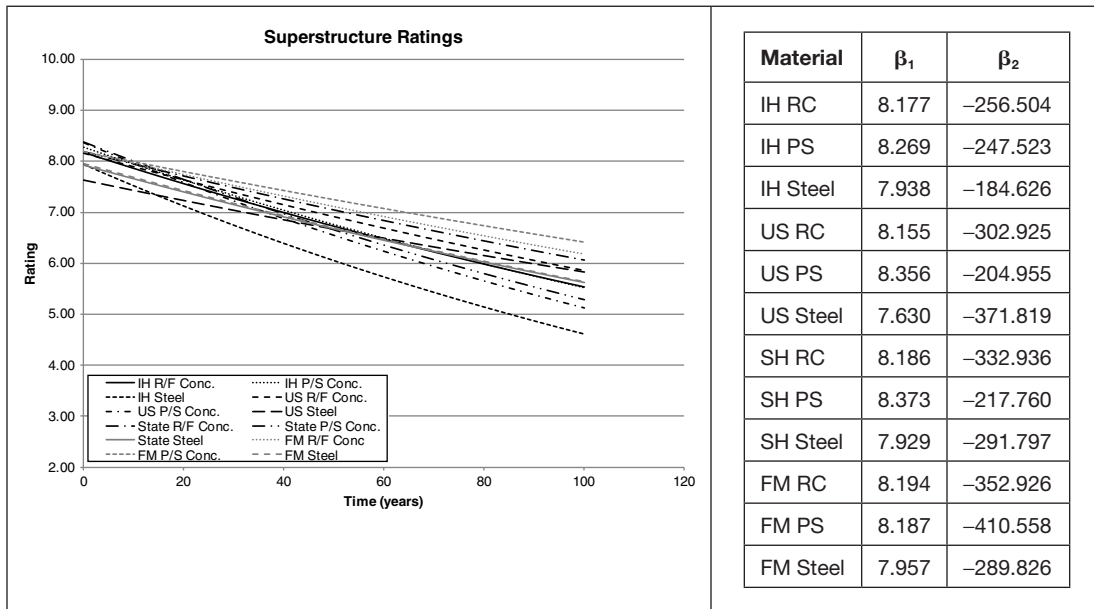
best-case expected remaining service life based on expert opinion. The expected remaining service life was based on a given condition rating: new (9), good (7), fair (5), and poor (3). From these responses, an estimated condition rating deterioration rate was determined. As would be expected with any opinion-based survey, there was significant variation in the responses; in several cases, the standard deviation was greater than the mean. The equations and graphs are shown in Table 4.19 for the deck, superstructure, and substructure condition ratings.

**Table 4.18. Exponential Best-Fit Graphs and Parameters**



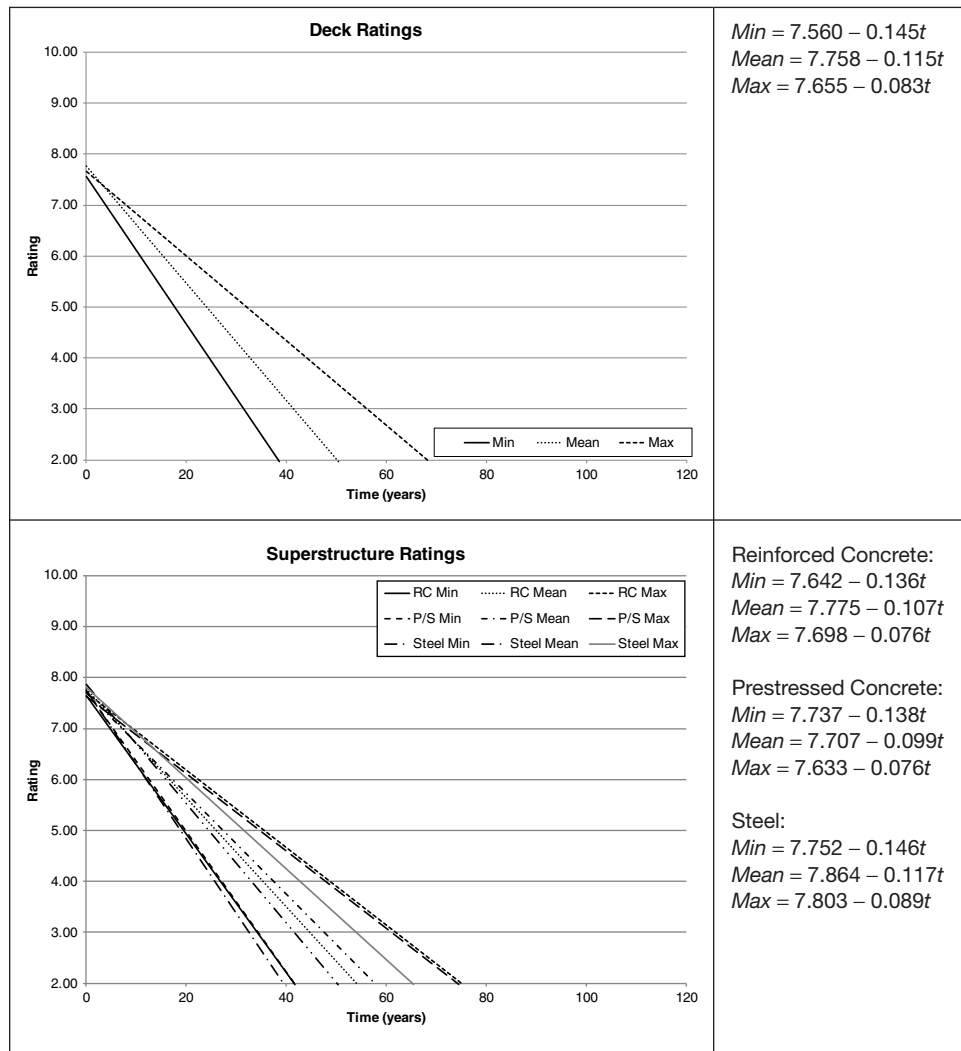
(continued on next page)

**Table 4.18. Exponential Best-Fit Graphs and Parameters (continued)**



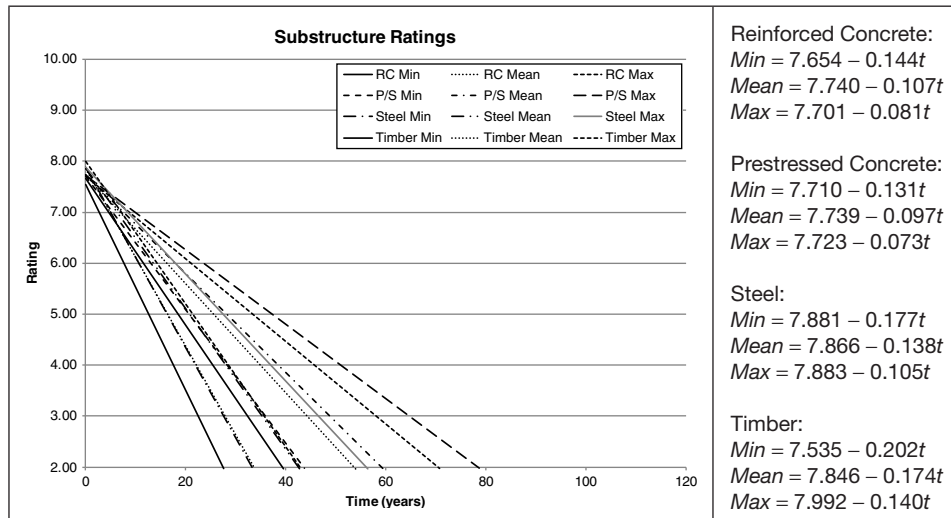
Source: Stukhart et al. (1991).

**Table 4.19. Expert Opinion Condition Rating Prediction Equations**



(continued on next page)

**Table 4.19. Expert Opinion Condition Rating Prediction Equations (continued)**



Source: Stukhart et al. (1991).

### 4.8 Massachusetts DOT

The Massachusetts DOT conducted a study of its bridges to gain a better understanding of the dynamics of how bridges age and deteriorate. This knowledge is intended to be used to plan strategies for bridge work and to determine required levels of funding.

The main aspects of this study were to determine the following:

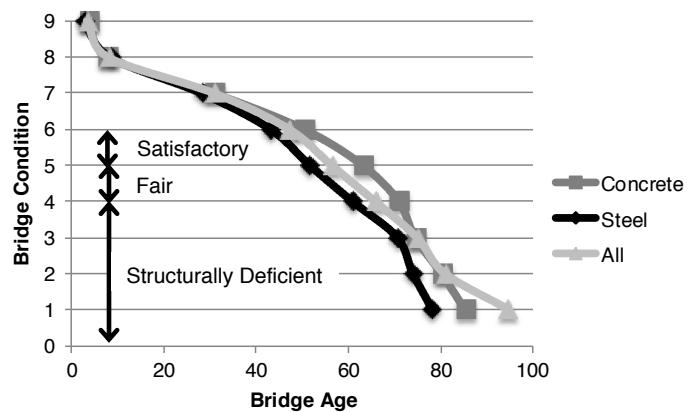
- The makeup of the bridge population by age and material of construction;
- The average age of bridges for a given average condition rating by material;
- The probability that a bridge in a given average condition rating will transition to a structurally deficient condition in the following year based on the age and current condition of the bridge;
- The percentage of bridges in each age group that are in one of the following categories: structurally deficient, fair, or satisfactory; and
- Equations to predict the growth of bridges in the fair or satisfactory condition categories.

In undertaking this analysis, the Massachusetts DOT defined the bridge condition categories as described here. A *structurally deficient* bridge was defined as a bridge with any one of the NBI Items 58, 59, or 60 (deck, superstructure, or substructure, respectively) condition ratings less than or equal to 4. A *fair* bridge was defined as a bridge with an average condition rating of Items 58, 59, and 60 greater than 4 but less than or equal to 5, but with none of the individual condition ratings being 4 or lower. Similarly, a *satisfactory* bridge

was defined as a bridge with an average condition rating of Items 58, 59, and 60 greater than 5 but less than or equal to 6, but with none of the individual condition ratings being 4 or lower. Bridges with a condition rating average greater than 6 were considered *excellent*.

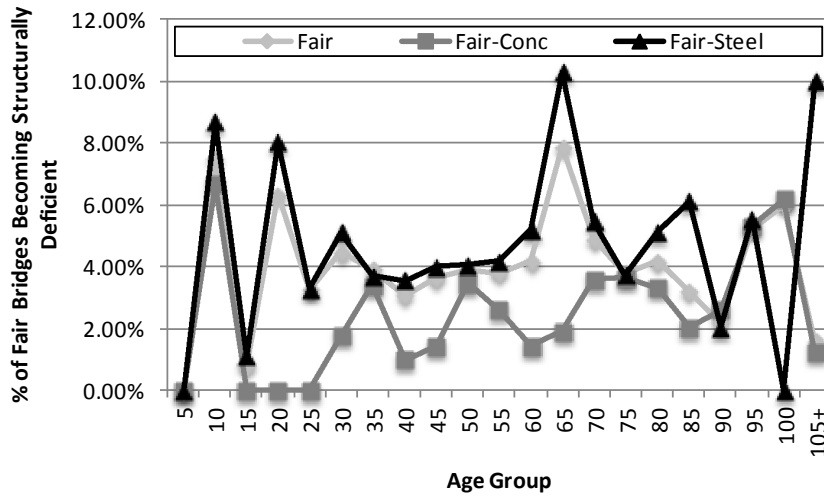
Figure 4.13 shows the average age of a Massachusetts bridge in a given average condition rating. The average age for all bridges to reach an average condition rating of 1.0 is greater than that for either steel or concrete and can be attributed to the age effect from old masonry bridges, the oldest of which in Massachusetts is 250 years old.

By knowing the time it takes a bridge to deteriorate into the next lower average condition rating, the additional service life that could be obtained by increasing the average condition rating can be estimated for a given preservation strategy. A regression analysis could be used to develop equations relating age to condition rating, as done in the previously



**Figure 4.13. Massachusetts bridge conditions by age.**





**Figure 4.14. Probability of all bridges in fair condition becoming structurally deficient in the following year.**

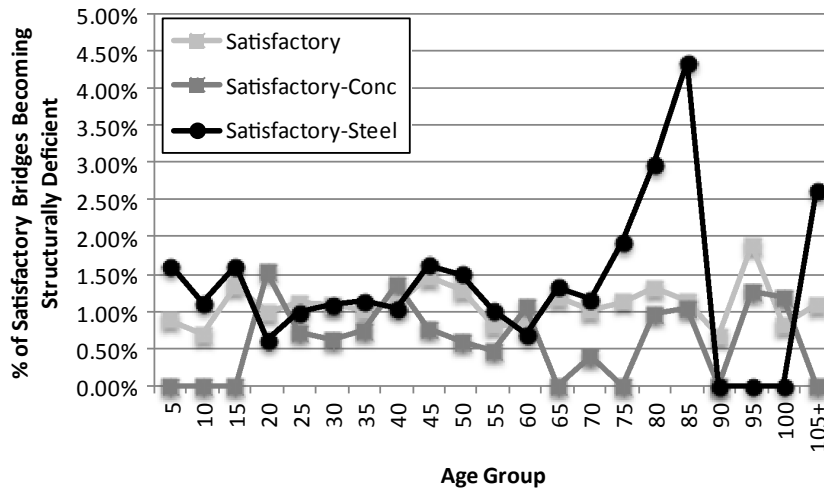
presented studies. The same process could be used to develop additional equations based on ADTT, location, or owner if the required data were available. The average condition rating versus age for Massachusetts bridges is similar to those presented above for other states.

However, the purpose of the Massachusetts DOT study was not to develop equations to predict the condition rating as a function of time (or age) as the studies presented previously, though if desired, equations could be developed using the available data. Instead, using the data acquired for the third and fifth bullet points above, the number of bridges that become structurally deficient in any given year can be estimated from the number of bridges predicted to be in a given condition (i.e., satisfactory or fair).

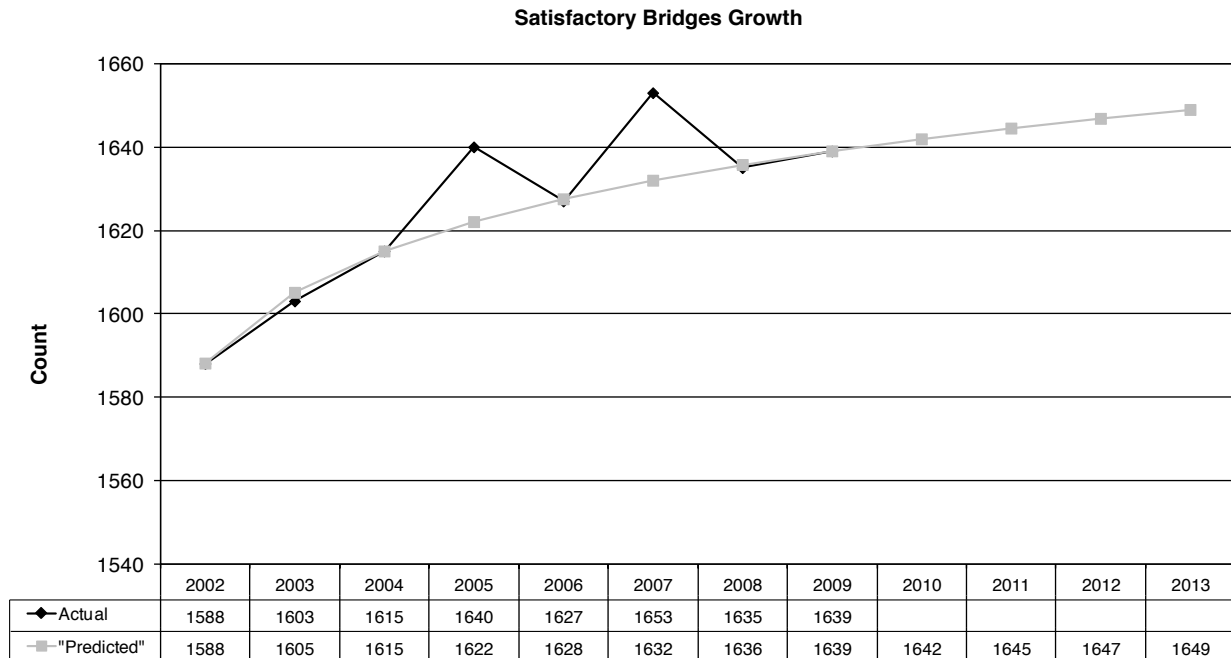
The analysis results indicated that, for the bridge population as a whole, approximately 4.25% of bridges in fair condition

transition to structurally deficient the following year (see Figure 4.14). Similarly, Figure 4.15 indicates that approximately 1.11% of bridges in satisfactory condition transition to structurally deficient the following year. Figure 4.14 and Figure 4.15 also show the transition probabilities for steel bridges and concrete bridges; these probabilities could be used if the analyst wished to look only at steel or concrete bridges. The graphing of these transition probabilities indicates that, except for concrete bridges in the fair category, which show some age-related influence, age is not as much of a factor as the current condition category of the bridge in determining the transition probability. Similar transition probabilities could be developed for different geographic regions or different levels of ADT or ADTT.

To predict the growth of bridges in the fair and satisfactory categories, best-fit equations were developed from a regression



**Figure 4.15. Probability of all bridges in satisfactory condition becoming structurally deficient in the following year.**



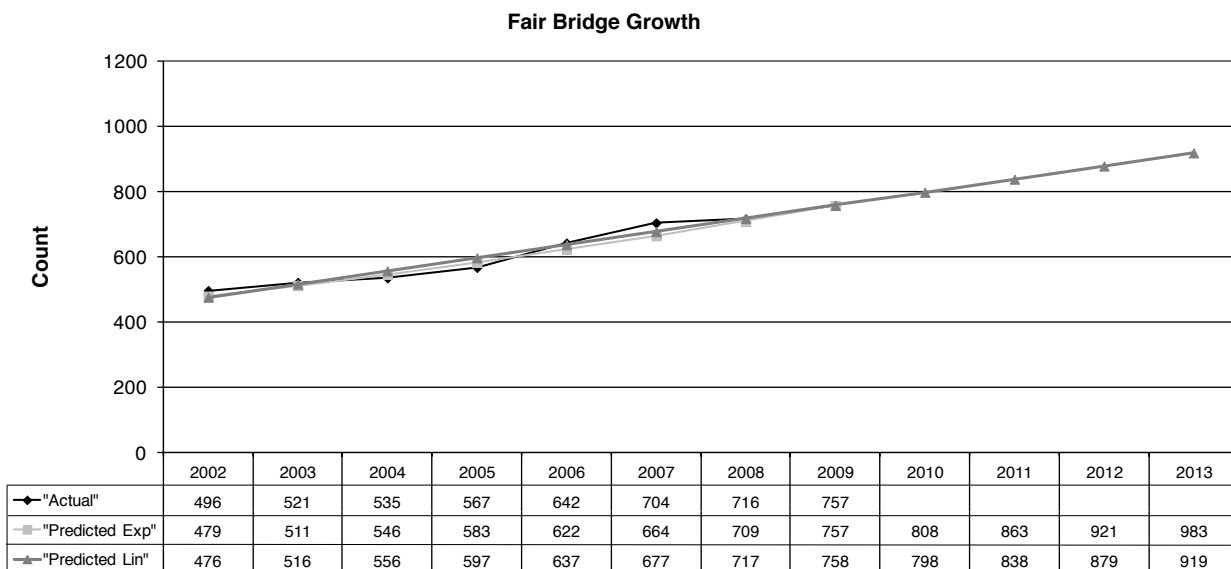
**Figure 4.16. Growth of bridges in satisfactory category.**

analysis of the number of bridges that were in those two categories for each year from 2002 through 2009. These equations were used to predict the number of fair and satisfactory bridges in future years. These equations are graphed in Figure 4.16 and Figure 4.17 and show the predicted numbers compared with the actual numbers from 2002 to 2009.

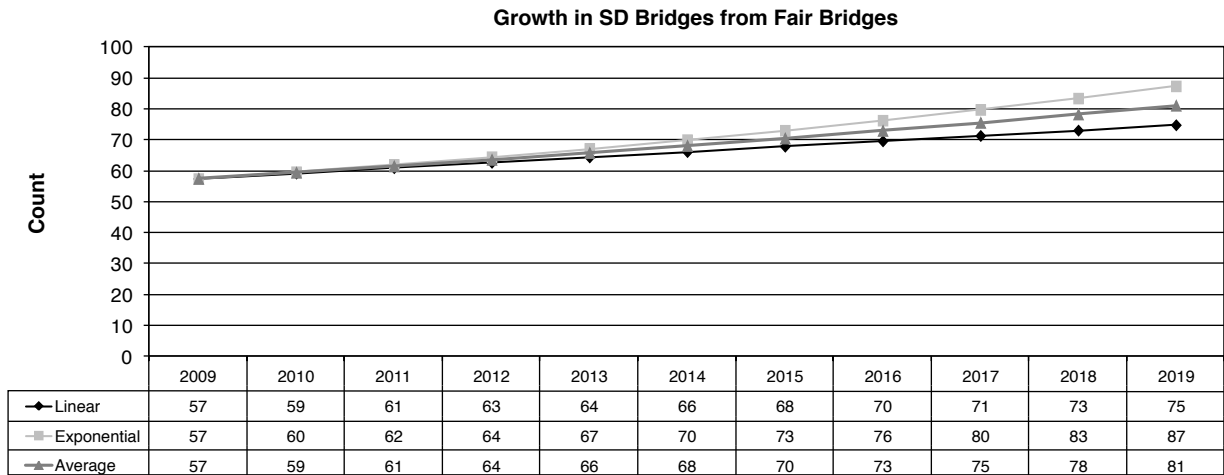
Due to concerns that the regressed exponential equation for the growth of fair bridges was too aggressive, the Massachusetts DOT decided to use the number of fair bridges that would be obtained by averaging the number of fair bridges

predicted by the best-fit exponential equation and the best-fit straight line equation for further analysis. After applying the transition probability for fair bridges, the growth in structurally deficient bridges from this category is shown in Figure 4.18 for each of the regression equations, as well as from the average.

A final needs analysis spreadsheet was developed that combined the structurally deficient growth predictions and the predictions of the number of projects that could be undertaken for a given amount of funding. The number of



**Figure 4.17. Growth of bridges in fair category.**



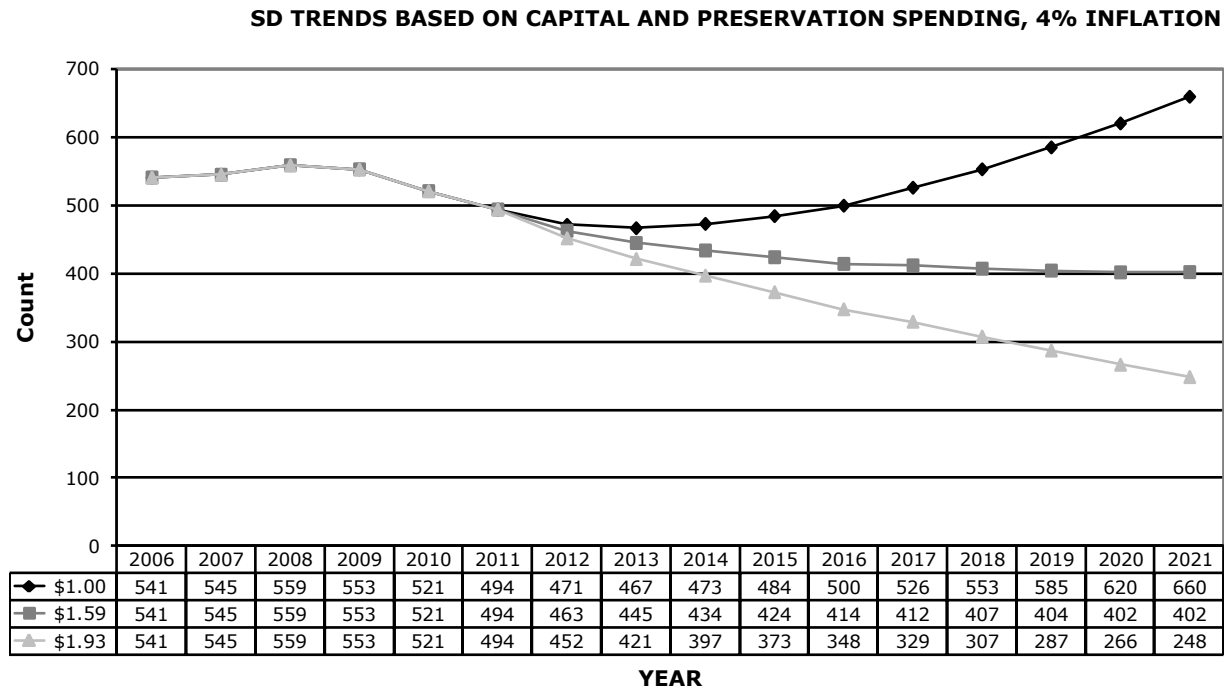
**Figure 4.18. Number of fair bridges becoming structurally deficient (SD).**

structurally deficient bridges for a given year was estimated by multiplying the transitional probability by the predicted number of fair or satisfactory bridges for that year.

The cost model was calibrated with actual project costs and considered the costs for a full replacement versus a preservation project. Replacement projects assumed the replacement of an already structurally deficient bridge and hence resulted in a reduction in the number of structurally deficient bridges estimated for the following year. It was assumed that preservation projects were to be performed on fair bridges and that only a percentage of bridges, based on the transitional probability times the number of preservation projects undertaken,

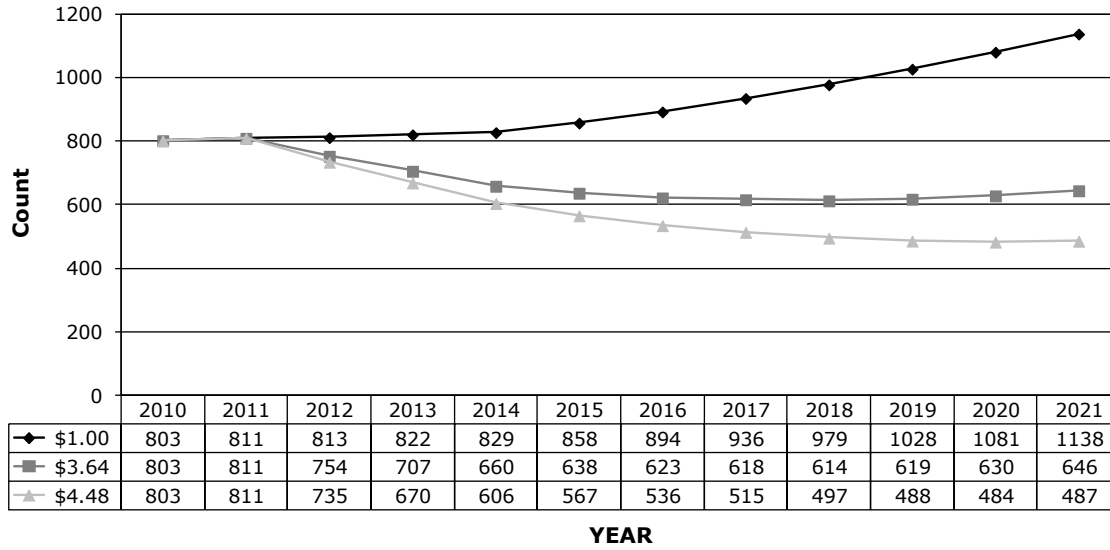
would be prevented from becoming structurally deficient in the following year. However, the total number of bridges that had preservation work done were removed from the fair condition rating population in calculating structurally deficient bridges for subsequent years.

Figure 4.19 and Figure 4.20, respectively, show the effect of different funding levels on the number of bridges that will be structurally deficient or in fair condition. The funding levels, shown in the far-left column of Figure 4.19 and Figure 4.20, are normalized to the lowest funding level shown in the top row. Figure 4.19 shows the overall bridge program funding level and includes both replacement and preservation projects.



**Figure 4.19. Number of structurally deficient bridges based on various spending levels.**

**FAIR BRIDGE GROWTH TRENDS BY PRESERVATION SPENDING, 4% INFLATION**



**Figure 4.20. Number of fair bridges based on various spending levels.**

The second and third rows of Figure 4.19 assume that 1.59 and 1.93 times as much money is available for structurally deficient bridges. The 1.53 funding level will trend to a steady state number of structurally deficient bridges. The 1.93 funding level will reduce the number of structurally deficient bridges at a rate that will result in zero structurally deficient bridges in 20 years. In Figure 4.20, the spending levels correlate to the preservation spending for each of the total funding levels in Figure 4.19.

As expected, spending more money leads to fewer bridges that are structurally deficient or in fair condition and spending less money leads to more bridges that are either structurally deficient or in fair condition. This graph also indicates the level of funding that would be needed to achieve a given desired outcome. For example, to achieve a net annual reduction in the number of structurally deficient bridges for the long term, program funding above the 1.59 level is needed.

In addition to the preceding analysis, the Massachusetts DOT also developed a utility to rank all the bridges in the state to prioritize which bridges should be worked on first. This ranking methodology is being used to develop the bridge State Transportation Improvement Program lists. The ranking is a function of three values: the condition loss value, the change in health index, and the highway evaluation factor. Condition loss is simply the difference between a perfect condition rating (9.0) and the current average condition rating divided by nine and multiplied by 100 to achieve a percentage value. Health index is the change in the bridge’s health index that AASHTOWare Bridge Management (formerly Pontis) predicts will occur over 15 years, expressed as a percentage value. The health index is calculated using the current CoRe

Element condition state for an existing bridge versus that of a new bridge, as given in Equation 4.3 (Thompson and Shepard 2000). Current element value is calculated using Equation 4.4, and total element value is calculated using Equation 4.5. The CoRe elements and associated condition states can be found in the *AASHTO Guide Manual for Bridge Element Inspection* (2011).

$$\text{Health Index (HI)} = \frac{\sum \text{CEV}}{\sum \text{TEV}} \times 100 \tag{4.3}$$

where CEV is current element value and TEV is total element value.

$$\text{CEV} = \left( \sum [\text{Quantity in Condition State } i \times \text{WF}(i)] \right) \times \text{FC} \tag{4.4}$$

where  $\text{WF}(i)$  is the condition state weighting factor given in Table 4.20 and FC is the failure cost of the element.

$$\text{TEV} = \text{Total Element Quantity} \times \text{FC} \tag{4.5}$$

**Table 4.20. Condition State Weighting Factors**

Number of Condition States	State 1	State 2	State 3	State 4	State 5
3	1.00	0.50	0.00		
4	1.00	0.67	0.33	0.00	
5	1.00	0.75	0.50	0.25	0.00

The highway evaluation factor is a measure of the functionality of the bridge and considers the ADT, detour length, functional classification, load-carrying restrictions, and deck geometry deficiencies. The categories within each variable are given a value between 1 and 5; the average value for the five variables is determined and then divided by five and multiplied by 100 to achieve a percentage value. The values for condition loss (CL), health index (HI), and highway evaluation factor (HEF) are then combined using Equation 4.6 to determine the final ranking factor for each bridge:

$$\text{Ranking Factor} = 0.3\text{CL} + 0.4\text{HI} + 0.3\text{HEF} \quad (4.6)$$

The ranking factor is then used to sort the bridges to determine each bridge's overall rank within the Massachusetts bridge population and, hence, its priority for work; bridges with the highest ranking factor values are those that require repair or maintenance in the future. The ranking is not a set order (Bridge 2 can go before Bridge 1) but, in general, higher-ranked bridges should be improved before lower-ranked bridges. The ranking factor, if calculated over a number of years, may lead to a reasonable estimate of the amount of deterioration and possible loss of serviceability for a bridge.

## CHAPTER 5

# Live Load for Calibration

## 5.1 Development of Live Load Models for Service Limit States

### 5.1.1 Introduction

The consideration of limit states, both ultimate (strength) and serviceability, requires the knowledge of loads. The objective of this task is to determine the statistical parameters of live load for the limit states considered in *AASHTO LRFD* (2012). For strength limit states, the live load statistics were determined in NCHRP Project 12-33 and documented in NCHRP Report 368 (Nowak 1999). The emphasis was placed on prediction of the extreme expected live load effects in the 75-year lifetime of a bridge. The database at that time was a truck survey carried out by the Ontario Ministry of Transportation in Canada. The basic statistical parameters of the maximum 75-year live load effect (moment and shear force) were determined by extrapolating the truck survey data. It was assumed that the survey represented 2 weeks of heavy traffic. The procedure is described in NCHRP Report 368 (Nowak 1999).

The serviceability limit states require additional statistical parameters, not only the maximum values, but also load spectra (i.e., frequency of occurrence of loads). The maximum values are needed for shorter time periods, such as a day, week, month, or year. At present, a considerable amount of WIM (weigh in motion) truck data is available and the research team had access to two sources: NCHRP Project 12-76 data (Sivakumar et al. 2011) and Federal Highway Administration (FHWA) files. This chapter provides documentation on the development of the statistical parameters of live load for service limit states (SLSs) and fatigue.

The analysis includes consideration of the WIM database from NCHRP Project 12-76 and FHWA. The obtained data included over 65 million vehicles. Of that number, about 10 million were deleted or filtered because of obvious errors, leaving about 55 million. Data from New York (about 7.8 million records) and Indiana other than site SPS-6 (about

13 million records) were also removed. The New York data were not considered because they included a considerable number of extremely heavy vehicles. It was decided that these data would have a strong effect on the statistical parameters, which would cause the remaining states to be unnecessarily penalized. Indiana data could not be considered because the format was not compatible with the other states. The considered database included about 35 million vehicles.

The obtained WIM data include the following information for each location and each recorded vehicle: number of axles, spacing between axles, axle loads, gross vehicle weight (GVW), vehicle speed, and exact time of measurement. Statistical parameters are determined for the GVW and moment caused by the vehicles, including a cumulative distribution function (CDF); a bias factor ( $\lambda$ ) that is equal to the mean-to-nominal ratio (i.e., the ratio of the mean value and the nominal, or design, value); and the coefficient of variation (CV),  $V$ , which is equal to the ratio of the standard deviation ( $\sigma$ ) to the mean ( $\mu$ ).

The CDFs for the WIM data for each site were plotted on normal probability paper, which is described in Chapter 3, Section 3.2.1.

### 5.1.2 WIM Database

The truck survey includes WIM truck measurements from 52 sites obtained from NCHRP Project 12-76 and FHWA.

The data obtained from FHWA, which are summarized below, included trucks recorded from special pavement studies (SPSs); each SPS is followed by a number that identifies the study's location (e.g., SPS-1 is Special Pavement Study, Location 1):

- Arizona (SPS-1)—Data recorded continuously from January 2008 until December 2008;
- Arizona (SPS-2)—Data recorded continuously from January 2008 until December 2008;



- Arkansas (SPS-2)—Data recorded continuously from January 2008 until December 2008;
- Colorado (SPS-2)—Data recorded continuously from January 2008 until December 2008;
- Delaware (SPS-1)—Data recorded continuously from January 2008 until December 2008;
- Illinois (SPS-6)—Data recorded continuously from January 2008 until December 2008;
- Indiana (SPS-6)—Data recorded continuously from July 2008 until December 2008;
- Kansas (SPS-2)—Data recorded continuously from January 2008 until December 2008;
- Louisiana (SPS-1)—Data recorded continuously from January 2008 until December 2008;
- Maine (SPS-5)—Data recorded continuously from January 2008 until December 2008;
- Maryland (SPS-5)—Data recorded continuously from January 2008 until December 2008;
- Minnesota (SPS-5)—Data recorded continuously from January 2008 until December 2008;
- New Mexico (SPS-1)—Data recorded continuously from May 2008 until December 2008;
- New Mexico (SPS-5)—Data recorded continuously from May 2008 until December 2008;
- Pennsylvania (SPS-6)—Data recorded continuously from January 2008 until December 2008;
- Tennessee (SPS-6)—Data recorded continuously from January 2008 until December 2008;
- Virginia (SPS-1)—Data recorded continuously from January 2008 until December 2008; and
- Wisconsin (SPS-1)—Data recorded continuously from January 2008 until December 2008.

Data obtained from NCHRP projects are also summarized here, and include trucks recorded from

### **California**

- Lodi (Site 003)—Data recorded continuously from June 2006 until March 2007;
- Antelope Eastbound (Site 003)—Data recorded almost continuously from April 2006 until March 2007 (107 days missing);
- Antelope Westbound (Site 003)—Data recorded almost continuously from April 2006 until March 2007 (109 days missing);
- LA 710 Southbound (Site 059)—Data recorded continuously from April 2006 until March 2007;
- LA 710 Northbound (Site 060)—Data recorded almost continuously from April 2006 until March 2007 (32 days missing); and
- Bowman (Site 072)—Data recorded almost continuously from April 2006 until February 2007 (139 days missing).

### **Florida**

- US-29 (Site 9916)—Data recorded continuously from January 2005 until December 2005 (11 days missing);
- I-95 (Site 9919)—Data recorded continuously from January 2005 until December 2005 (16 days missing);
- I-75 (Site 9926)—Data recorded almost continuously from January 2005 until December 2005 (100 days missing);
- I-10 (Site 9936)—Data recorded almost continuously from January 2005 until December 2005 (100 days missing); and
- State Route (Site 9927)—Data recorded almost continuously from January 2004 until December 2004 (5 days missing).

### **Indiana**

- Site 9511—Data recorded continuously from January 2006 until December 2006;
- Site 9512—Data recorded continuously from January 2006 until December 2006;
- Site 9532—Data recorded continuously from January 2006 until December 2006;
- Site 9534—Data recorded continuously from January 2006 until December 2006; and
- Site 9552—Data recorded continuously from January 2006 until December 2006.

### **Mississippi**

- I-10 (Site 3015)—Data recorded almost continuously from January 2006 until December 2006 (28 days missing);
- I-55 (Site 2606)—Data recorded almost continuously from January 2006 until December 2006 (16 days missing);
- I-55 (Site 4506)—Data recorded almost continuously from March 2006 until December 2006 (39 days missing);
- US-49 (Site 6104)—Data recorded almost continuously from January 2006 until December 2006 (5 days missing); and
- US-61 (Site 7900)—Data recorded almost continuously from January 2006 until December 2006 (49 days missing).

### **New York**

- I-95 Northbound (Site 0199)—Data recorded continuously from March 2006 until December 2006;
- I-95 Southbound (Site 0199)—Data recorded continuously from July 2006 until November 2006;
- I-495 Westbound (Site 0580)—Data recorded continuously from January 2006 until December 2006;
- I-495 Eastbound (Site 0580)—Data recorded continuously from January 2006 until December 2006;
- Highway 12 (Site 2680)—Data recorded continuously from January 2005 until December 2005;
- I-84 Eastbound and Westbound (Site 8280)—Data recorded continuously from January 2006 until December 2006;
- I-84 Eastbound and Westbound (Site 8382)—Data recorded continuously from January 2005 until December 2005;

- I-81 Northbound and Southbound (Site 9121)—Data recorded continuously from January 2005 until December 2005; and
- Highway 17 Eastbound and Westbound (Site 9631)—Data recorded continuously from February 2006 until December 2006.

**5.1.3 WIM Data Filtering**

The WIM data both from NCHRP Project 12-76 and FHWA include vehicle records that appear to be incorrect. There are various reasons for questioning the data (e.g., GVW is too low, unrealistic geometry). The data were filtered to eliminate questionable vehicles by using the following criteria:

- Weight per axle less than 2 kips or greater than 70 kips, based on NCHRP 12-76;
- Record in which the first axle spacing was less than 5 ft, based on NCHRP 12-76;
- Record in which any axle spacing was less than 3.4 ft, based on NCHRP 12-76;
- Record in which GVW varied from the sum of the axle weights by more than 10%, based on NCHRP 12-76;

- Record in which the length of the truck varied from the sum of the axle spacings by more than 1 ft, based on NCHRP 12-76;
- Record that had a GVW less than a threshold; at various times the threshold was 10 or 12 kips;
- Record in which the steering axle was less than 6 kips, based on NCHRP 12-76;
- Record in which the sum of the axle spacing lengths was less than 7 ft, based on Pelphrey et al. (2008);
- Class of the vehicle according to FHWA, from Class 3 to 14, to filter out cars, motorcycles, and so on; and
- Speed ranges from 10 to 100 mph, based on NCHRP 12-76.

The filtering process is illustrated in the flowchart in Figure 5.1. Because a heavy vehicle meeting all the conditional filters involving GVW would pass the filters, the research team reviewed exceptionally heavy vehicles to check if their configuration resembled permit vehicles, such as cranes and garbage trucks. The data were divided into two sets. The first set contained regular truck traffic. These data were used for the live load model for SLSs. The remaining set of data included permit vehicles and illegally overloaded vehicles, which occurred relatively infrequently. The latter data were used along with the

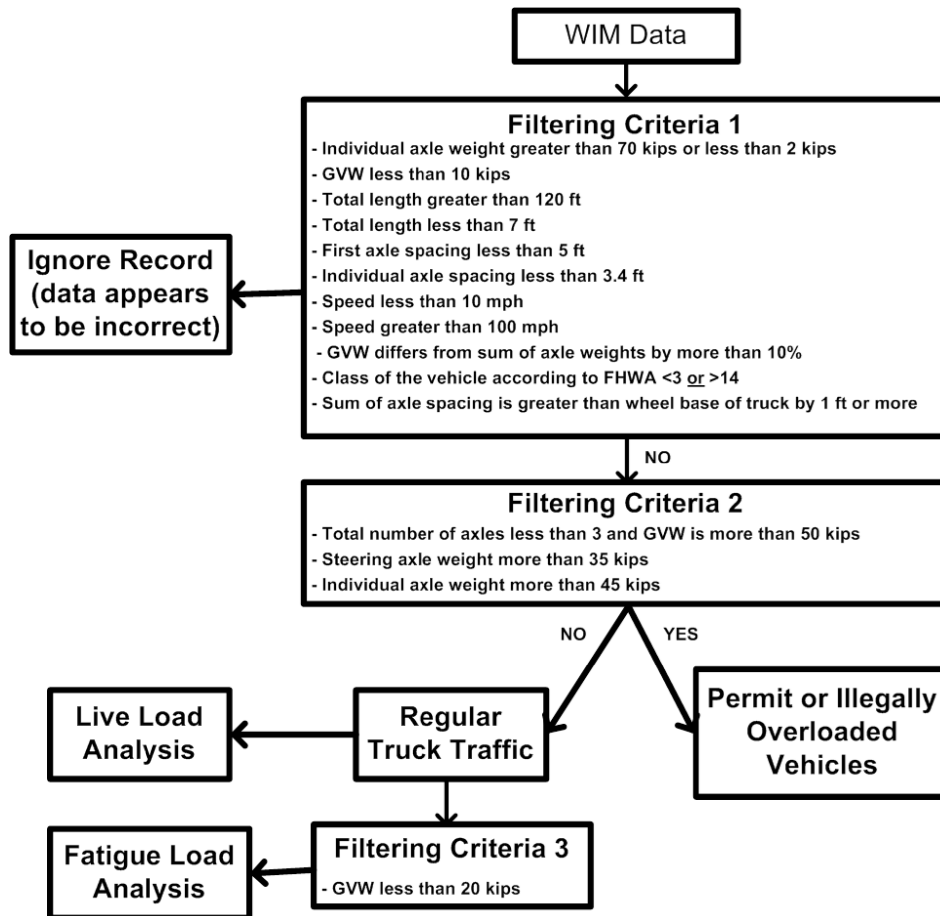


Figure 5.1. Flowchart of the filtering process.

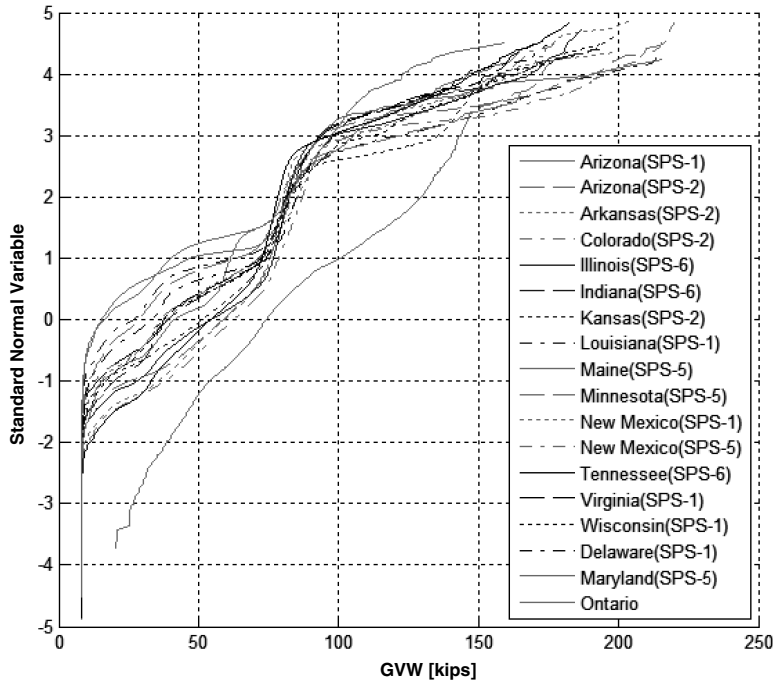


Figure 5.2. CDF of GWW FHWA and Ontario data.

regular truck traffic for live load for SLS II. The GWW criteria of 20 kips in Step 3 is a traditional, albeit arbitrary, cutoff used in virtually all previous fatigue studies to reduce the calculation effort by not considering light traffic, which does not contribute significantly to cumulative damage.

The CDFs of GWWs were plotted on probability paper; examples are shown in Figure 5.2 to Figure 5.5. The live load model based on the Ontario truck survey data that were used in calibration for strength limit states is also shown. The relative position of the Ontario curve is a result of the intentional selection of seemingly heavy vehicles, albeit based solely on the appearance of the vehicles.

Figure 5.2 represents the CDF of the GWW of trucks from FHWA sites plotted on probability paper. Data collected from 14 sites represent 1 year of traffic, data from the Indiana site represent 6 months of traffic, and data from the New Mexico sites represent 8 months of traffic. The maximum truck GWW was 220 kips. Mean values ranged from 20 to 65 kips.

Figure 5.3 to Figure 5.5 represent CDFs of the GWWs for Ontario and the following states: Oregon and Florida (Figure 5.3), Indiana and Mississippi (Figure 5.4), and California and New York (Figure 5.5) (i.e., the NCHRP 12-76 data). The corresponding traffic data from these figures are given in Table 5.1.

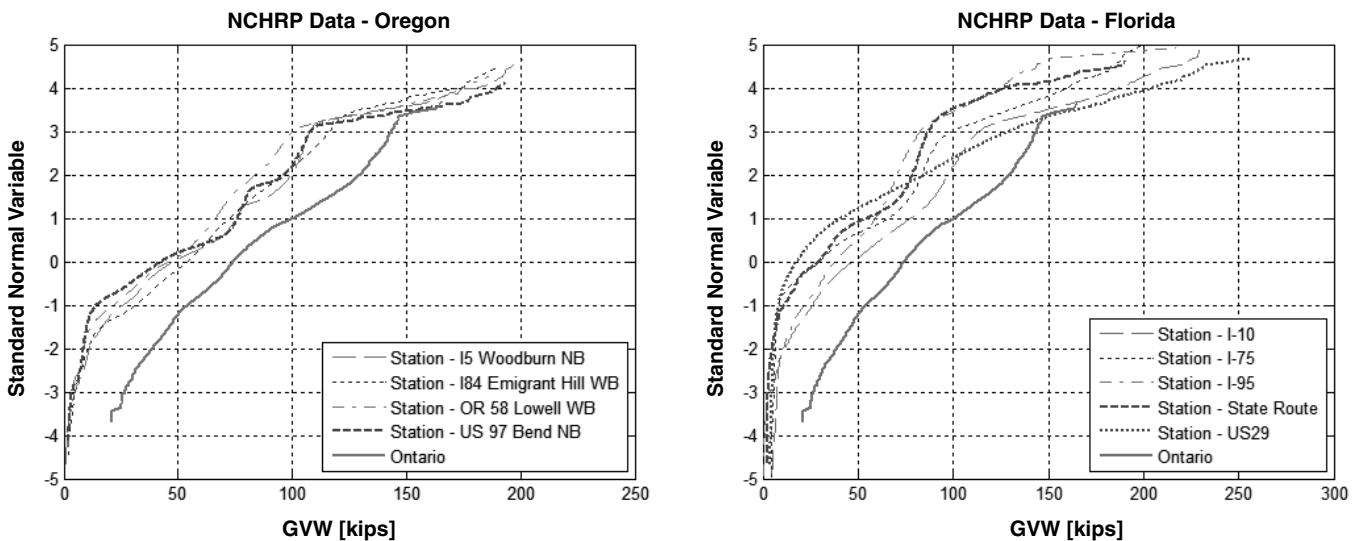


Figure 5.3. CDFs of GWW for Oregon, Florida, and Ontario.

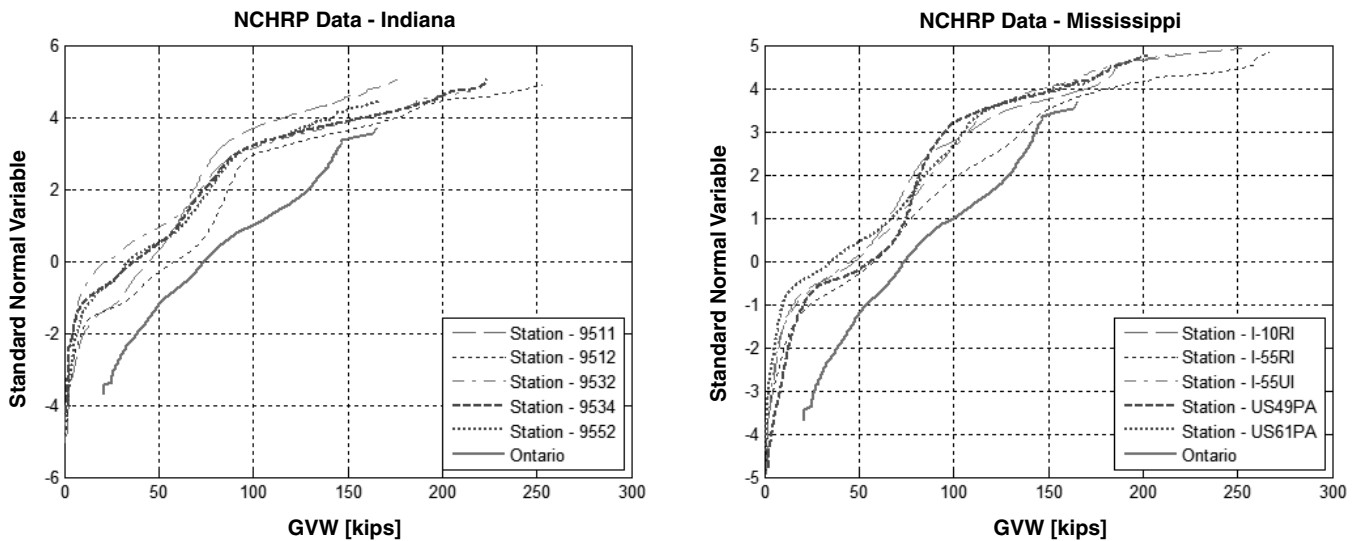


Figure 5.4. CDFs of GVW for Indiana, Mississippi, and Ontario.

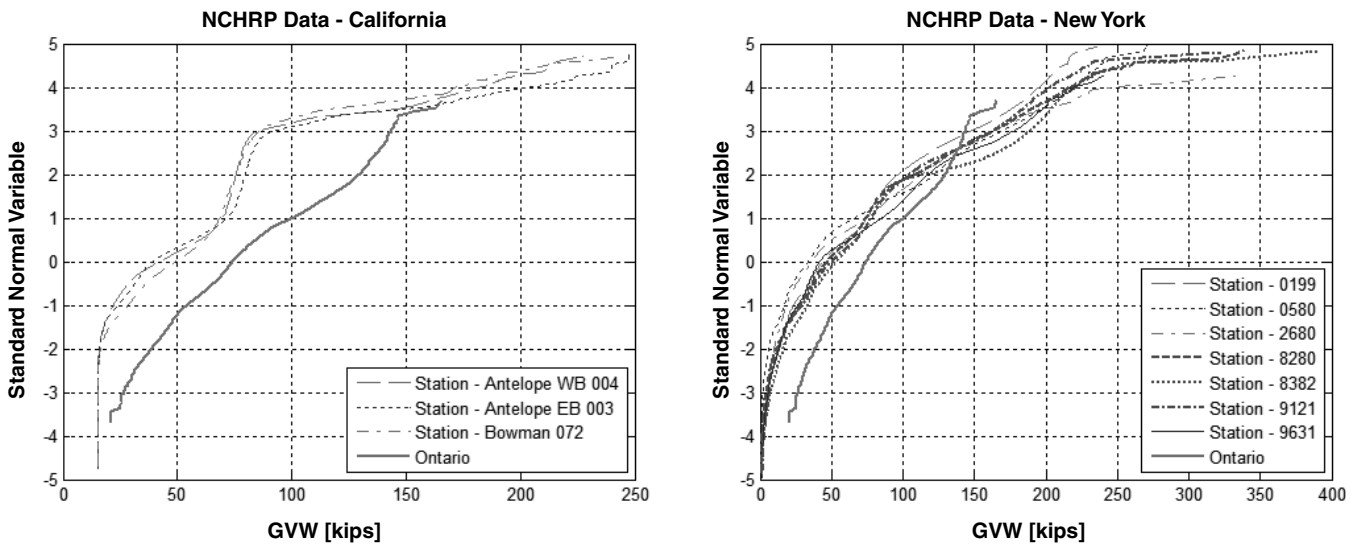


Figure 5.5. CDFs of GVW for California, New York, and Ontario.

Table 5.1. Summary of State Sites and Their Traffic Data for Figures 5.3 to 5.5

Figure	State	No. of Sites	No. of Months of Data	Maximum GVW (kips)	Mean Value Range (kips)
Figure 5.3	Oregon	4	4	200	43–52
	Florida	5	12	250	20–50
Figure 5.4	Indiana	5	12	250	25–57
	Mississippi	5	12	260	38–57
Figure 5.5	California	2	8.7	250	40–50
		1	7		
	New York	7	12	380	35–50

As an initial observation, the data shown in Figure 5.2 to Figure 5.5 are generally consistent for the majority of the sites (*consistent* refers to the similarity of the general shape of the curves, i.e., the CDFs). Exceptions are the following heavily loaded sites from New York:

- Site 9121 on I-81 by Whitney Point;
- Site 8382 on I-84 by Port Jervis;
- Site 8280 on I-84 by Fishkill; and
- Site 0580 on I-495 in Queens in New York City.

Because these sites were so exceptional, it was decided not to include the New York WIM data in developing a national, notional SLS live load. In addition, several sites for which the recording format differed or had considerably less than one tier of data were eliminated from consideration. A summary of the remaining 32 sites and filtered data, including the WIM locations, number of records, and average daily truck traffic (ADTT), is shown in Table 5.2. Approximately 35 million records are represented by these sites.

A copy of the raw WIM data and of the filtered WIM data is available at <http://www.trb.org/Main/Blurbs/170201.aspx>. A sample of the filtered WIM data is included in Appendix F.

The CDFs of GVWs and moment are plotted as separate curves for each location. The legend for all CDFs is shown in Figure 5.6.

## 5.2 Initial Data Analysis

### 5.2.1 Gross Vehicle Weight

The CDFs for the GVWs from the remaining FHWA and NCHRP sites are plotted on probability paper in Figure 5.7. Each of the 32 curves represents a different location. The resulting curves indicate that the distribution of GVW is not normal. Irregularity of the CDFs is a result of different types of vehicles (such as long and short, fully loaded and empty, or loaded by volume only) in the WIM data. For the considered locations, the mean GVWs are between 25 and 65 kips. The upper tails of the CDF curves show a similar trend, but there is a considerable spread of the maximum values, from 150 to over 250 kips.

### 5.2.2 Moments from WIM Data

The distribution of simple-span moments due to WIM trucks was obtained by calculating the maximum bending moment for each vehicle in the database. Each vehicle was run over influence lines to determine the maximum moment by using a specially developed computer program. The calculations were carried out for spans from 30 to 200 ft. For easier interpretation and comparison of results, the calculated WIM data moments were then divided by the corresponding HL-93 moment. Normalizing the data to a common reference makes

**Table 5.2. WIM Locations and Number of Recorded Vehicles**

Site	No. of Days in Data	Total No. of Truck Records	Lane ADTT
Arizona (SPS-1)	365	35,572	97
Arizona (SPS-2)	365	1,430,461	3,919
Arkansas (SPS-2)	365	1,675,349	4,590
Colorado (SPS-2)	365	343,603	941
Delaware (SPS-1)	365	201,677	553
Illinois (SPS-6)	365	854,075	2,340
Indiana (SPS-6)	214	185,267	508
Kansas (SPS-2)	365	477,922	1,309
Louisiana (SPS-1)	365	85,702	235
Maine (SPS-5)	365	183,576	503
Maryland (SPS-5)	365	164,389	450
Minnesota (SPS-5)	365	55,572	152
New Mexico (SPS-1)	245	117,102	321
New Mexico (SPS-5)	245	608,280	1,667
Pennsylvania (SPS-6)	365	1,495,741	4,098
Tennessee (SPS-6)	365	1,622,320	4,445
Virginia (SPS-1)	365	259,190	710
Wisconsin (SPS-1)	365	226,943	622
California Antelope EB	258	837,667	2,192 <sup>a</sup>
California Antelope WB	256	943,147	2,258 <sup>a</sup>
California Bowman	134	651,090	2,018 <sup>a</sup>
California LA-710 NB	333	4,092,484	6,380 <sup>a</sup>
California LA-710 SB	365	4,661,287	8,366 <sup>a</sup>
California Lodi	304	3,298,499	5,186 <sup>a</sup>
Florida I-10	354	1,641,480	2,207 <sup>a</sup>
Florida I-95	349	2,112,518	2,558 <sup>a</sup>
Florida US-29	354	389,164	606 <sup>a</sup>
Mississippi I-10	337	1,965,022	2,967 <sup>a</sup>
Mississippi I-55UI	268	1,232,223	2,054 <sup>a</sup>
Mississippi I-55R	349	1,333,268	1,790 <sup>a</sup>
Mississippi US-49	359	1,225,138	1,475 <sup>a</sup>
Mississippi US-61	319	159,299	254 <sup>a</sup>
<b>Total</b>		<b>35,856,898</b>	

Note: EB = eastbound; WB = westbound; NB = northbound; SB = southbound.

<sup>a</sup> NCHRP data are for multilane cases; the lane with maximum ADTT is listed.



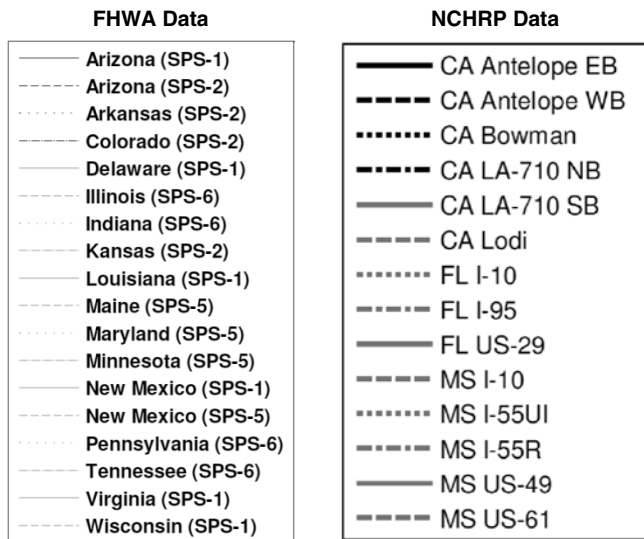


Figure 5.6. Legend for all graphs.

the data easier to interpret. HL-93 was a convenient reference and ties this work to the original strength limit state calibration and associated published information.

The CDFs for the ratio of the WIM truck moment and HL-93 moment are plotted on normal probability paper in Figure 5.8 to Figure 5.12; the shape of the CDF curves is similar to that of GVW. The mean WIM moments were between 0.2 and 0.4 of the HL-93 moments for all span lengths considered. The probability of a WIM moment exceeding 0.4 to 0.5 of the HL-93 moment was about 0.15. The maximum values of the WIM moment were between 1.0 and 1.4 of HL-93 moment in most cases.

The obtained results served as the basis for determining the statistical parameters of live load needed for the reliability analysis of the serviceability limit states.

### 5.2.3 Filtering of Presumed Illegal Overloads and Special Permit Loads

The goal of this analysis was to observe the change in the very top tail of the distribution after removing the heaviest vehicles from the database. These extremely heavy vehicles seemed to be either permit vehicles that should be included in the design process (as some states do) or vehicles reviewed for permit issuance by using the Strength II limit state load combination; otherwise, they are illegal overloads. An example of the heaviest truck in the WIM data is presented in Figure 5.13. This truck was recorded at Site 8382 near Port Jervis, New York. The total length of the truck was 100.6 ft. The GVW was 391.4 kips. The position of the 12 axles, their weight, and the vehicle's length suggest that it should be categorized as a permit vehicle. WIM equipment captures each vehicle, including permit vehicles, as a string of axles, and an FHWA designation is given based on the best FHWA

category that fits the detected configuration. Heavy vehicles are assumed to be permit vehicles or illegally loaded vehicles.

The initial study indicated that the removal of a very small number of the heaviest vehicles drastically changed the upper tail of the CDF of moments and shears. It was decided to explore this by investigating the number of vehicles that exceeded an upper value of 1.35 times HL-93, which corresponds to the maximum bias ratio obtained from the Ontario measurements.

The results of the analysis for sites from New York and Mississippi were plotted on probability paper and are shown in Figures 5.14 to 5.16. It can be observed that, as expected, the very upper tail of the distribution changed drastically by removing only a very small percentage of vehicles.

For example, for 90-ft spans at New York Site 8382 (Figure 5.15), the bias changes from about 2.35 to about 1.65—but only when considering the six largest moment ratios (corresponding to the six heaviest trucks, including the 391-kip vehicle shown in Figure 5.13) out of the 1.55 million data records remaining after application of the additional filter to remove moments less than 15% of the corresponding HL-93 moment. Even for the WIM sites that demonstrated very extreme tails, these extreme trucks constituted only the upper 0.01% to 0.22% of the truck population. For most of the locations reviewed, the percentage was lower (see Table 5.3). The heaviest loads may have an important impact on calibration of the ultimate or strength limit states; however, in the case of SLSs, the upper tail of the CDF of the live load is not important, as it is the main body of the CDF that affects SLS performance. Therefore, for SLS calibration, it was decided to ignore the upper tip of the CDF of live load.

### 5.2.4 Multiple Presence Analysis

Multiple presence was investigated by a correlation analysis of the WIM data sets. The objective of the correlation analysis was to select two trucks that were simultaneously positioned on the bridge as shown in Figure 5.17 and that satisfied the following requirements:

- Both trucks had the same number of axles.
- GVWs of the trucks were within  $\pm 5\%$ .
- All corresponding spacings between axles were within  $\pm 10\%$ .

The maximum load effect is often caused by the simultaneous presence of two or more trucks on a bridge. The statistical parameters of these effects are influenced by the degree of correlation. In calibration for the strength limit states, certain probabilities of occurrence of correlated trucks were assumed on the basis of engineering judgment applied to limited observations of the presence of multiple trucks of unknown weight. The available WIM data allowed for verification of these assumptions.

(text continues on page 108)



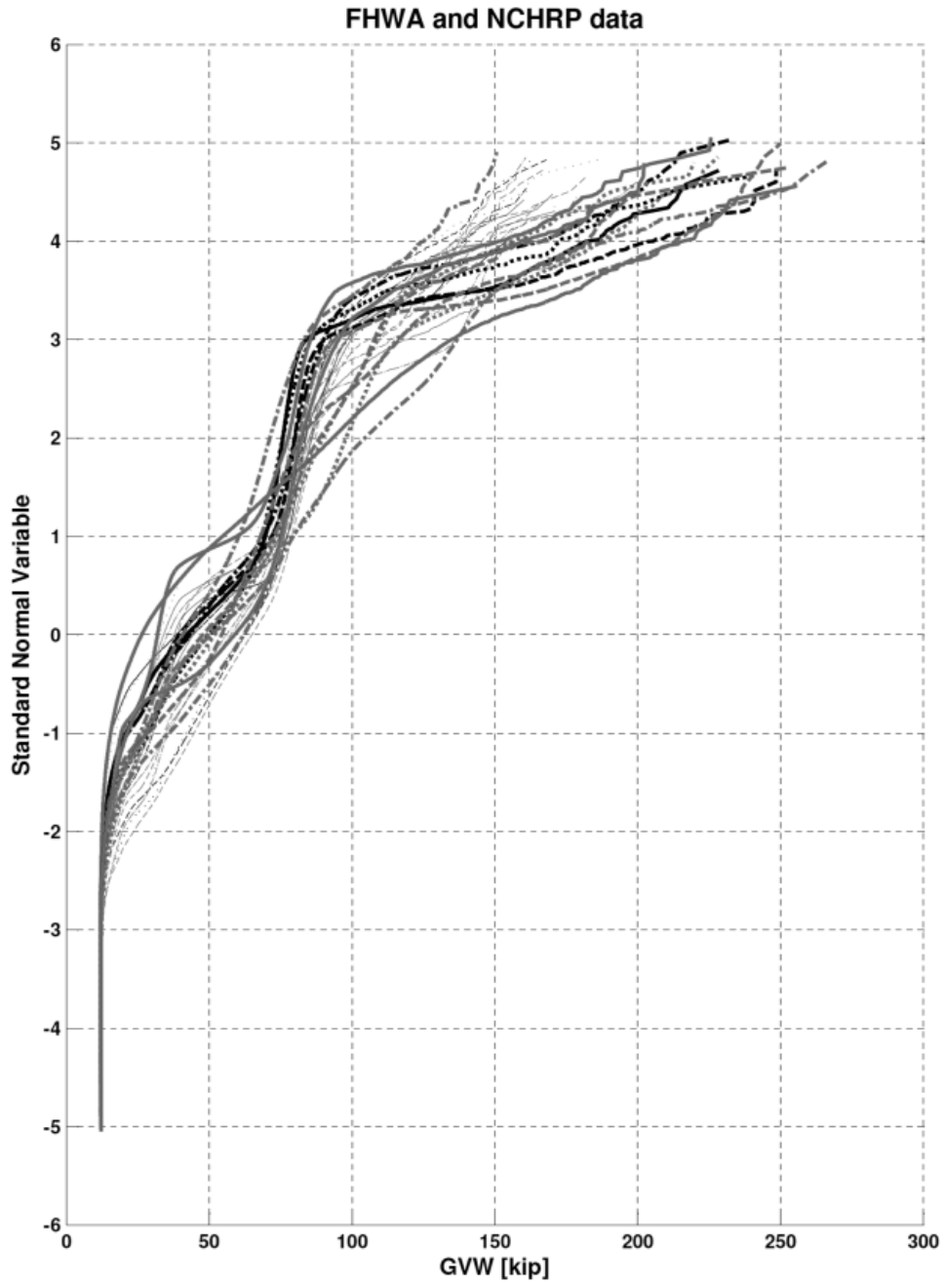
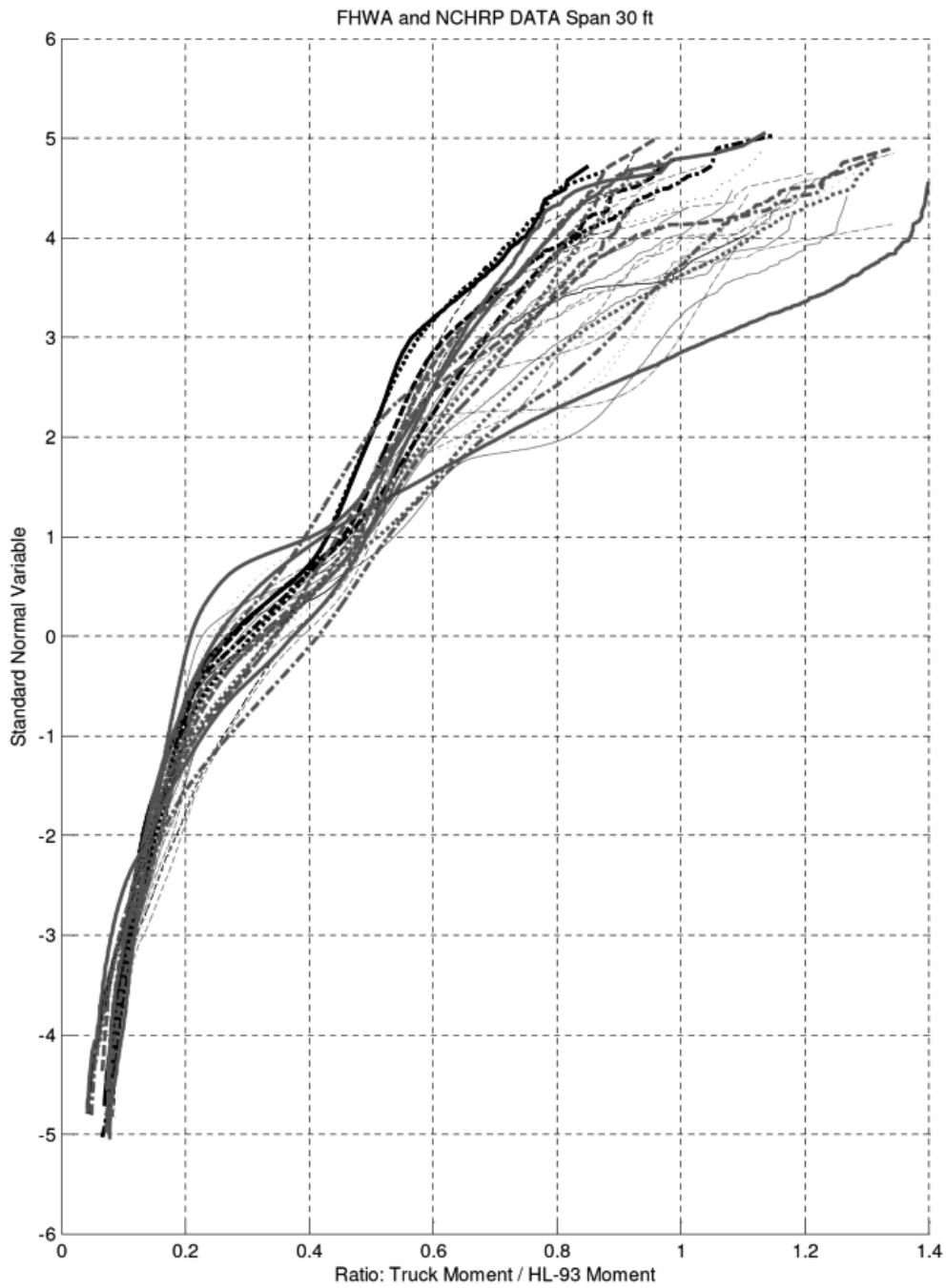


Figure 5.7. CDFs of GVWs.



**Figure 5.8.** CDFs of WIM moment and HL-93 moment ratio, span = 30 ft.

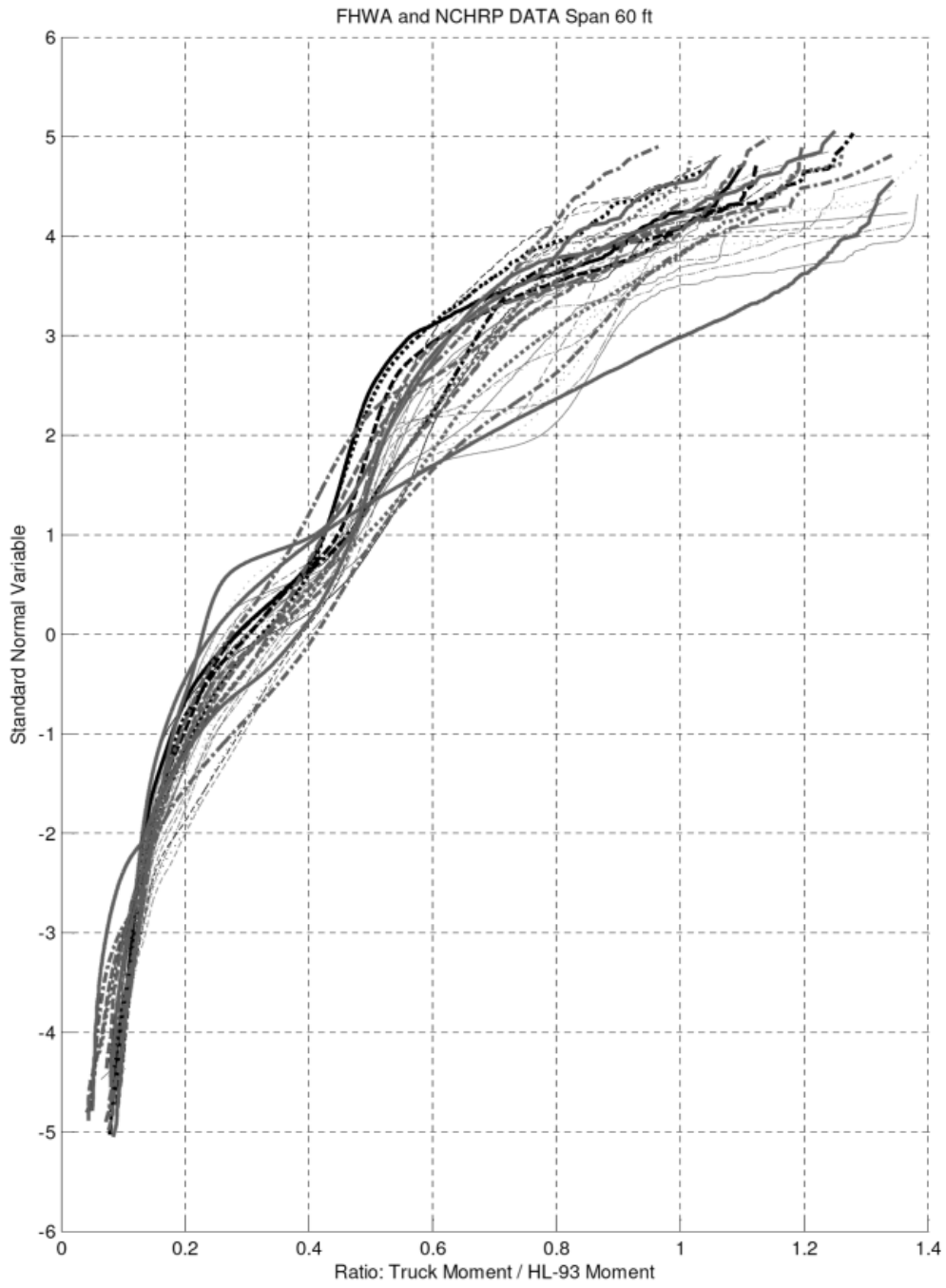
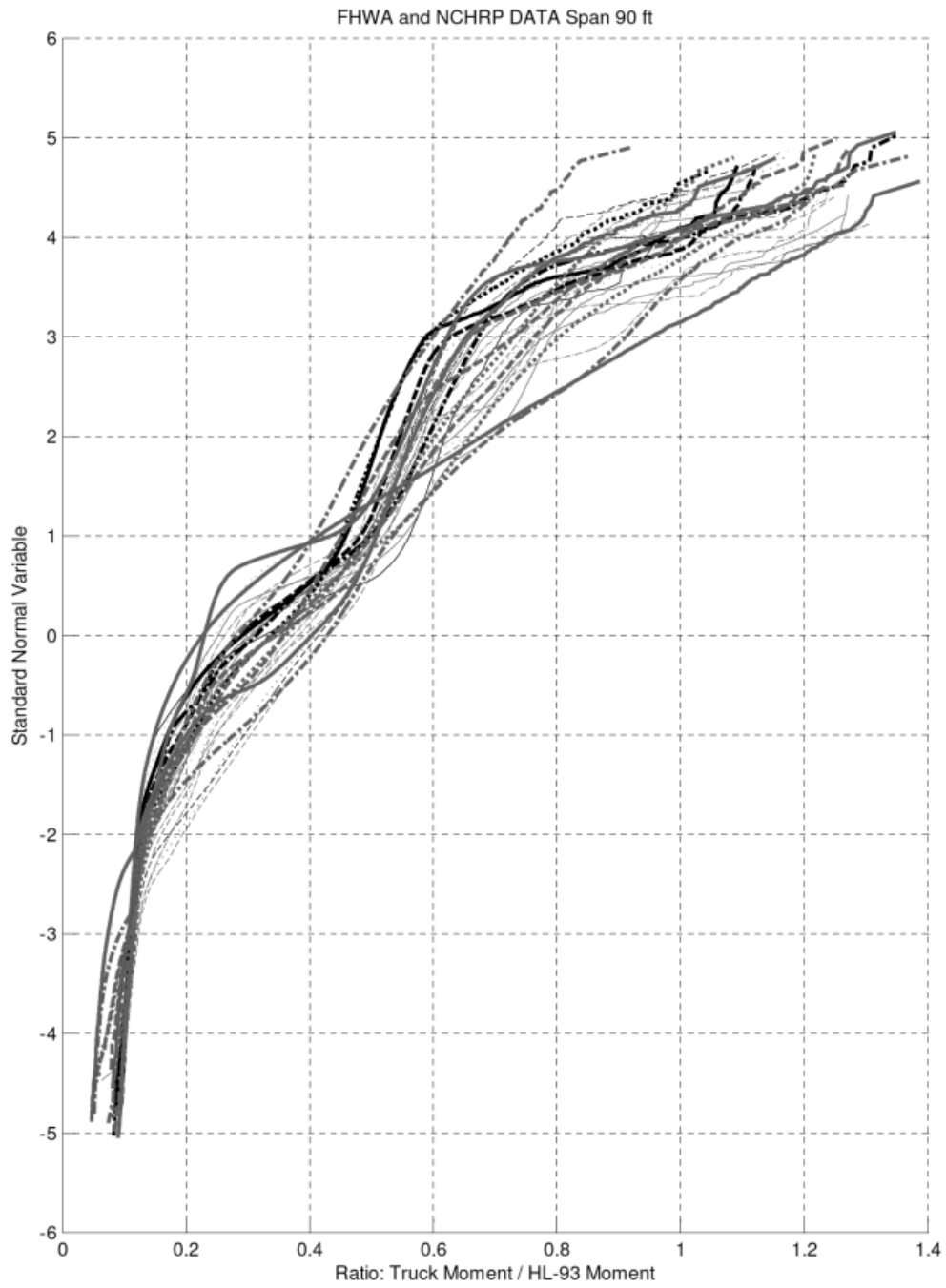


Figure 5.9. CDFs of WIM moment and HL-93 moment ratio, span = 60 ft.



**Figure 5.10.** CDFs of WIM moment and HL-93 moment ratio, span = 90 ft.

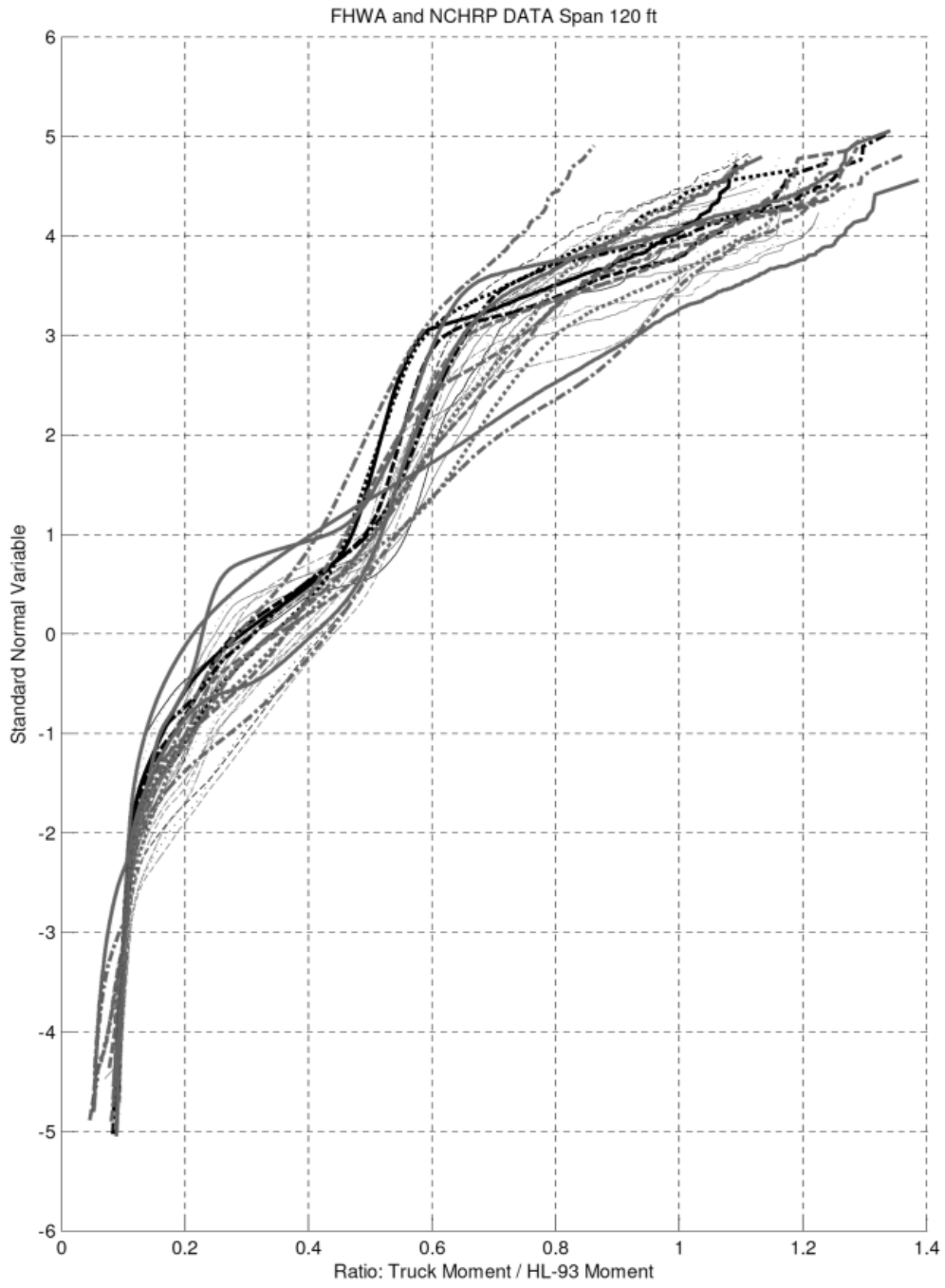
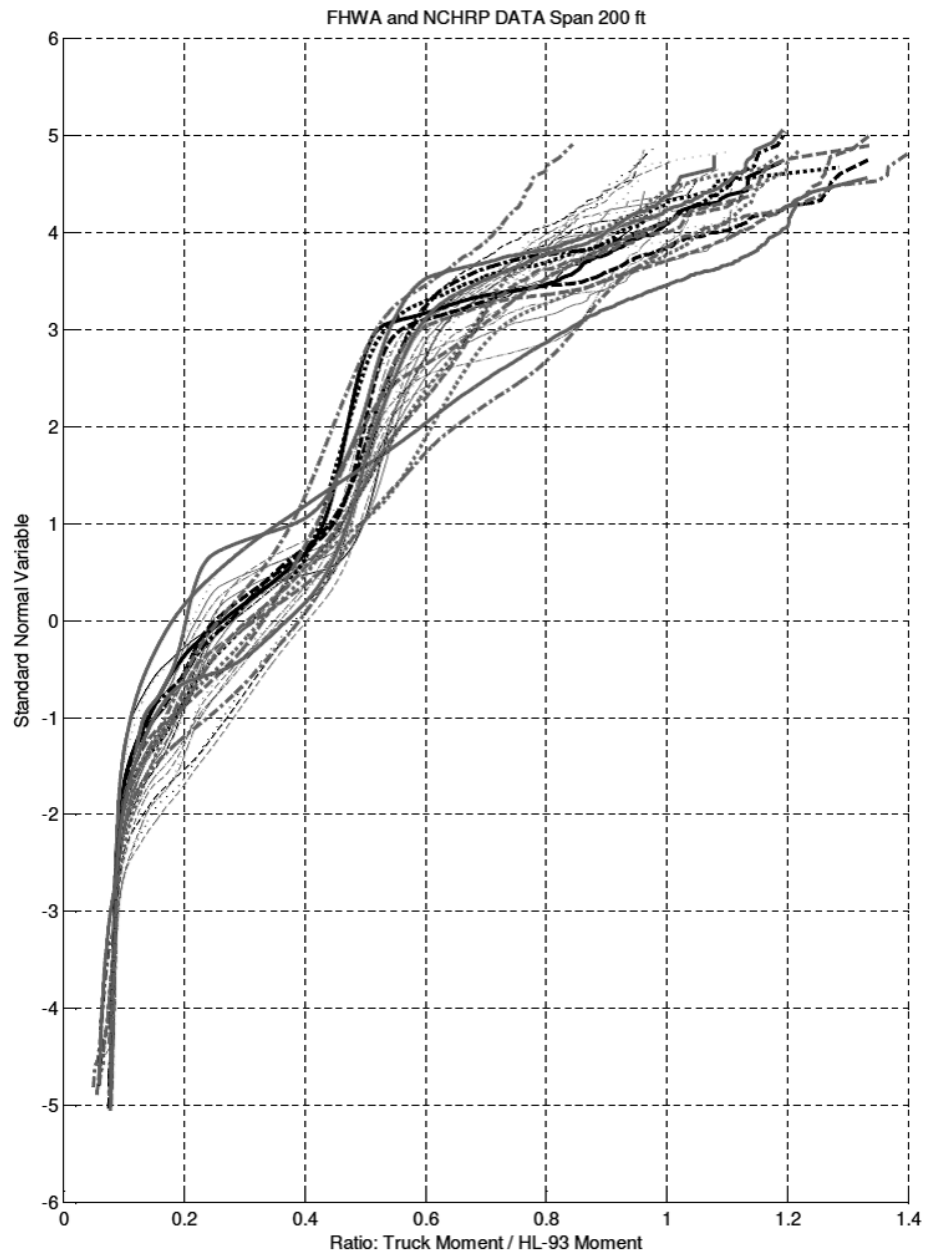


Figure 5.11. CDFs of WIM moment and HL-93 moment ratio, span = 120 ft.



**Figure 5.12. CDFs of WIM moment and HL-93 moment ratio, span = 200 ft.**



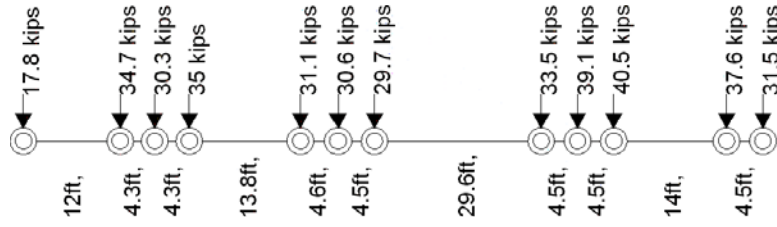


Figure 5.13. Configuration of extremely loaded truck.

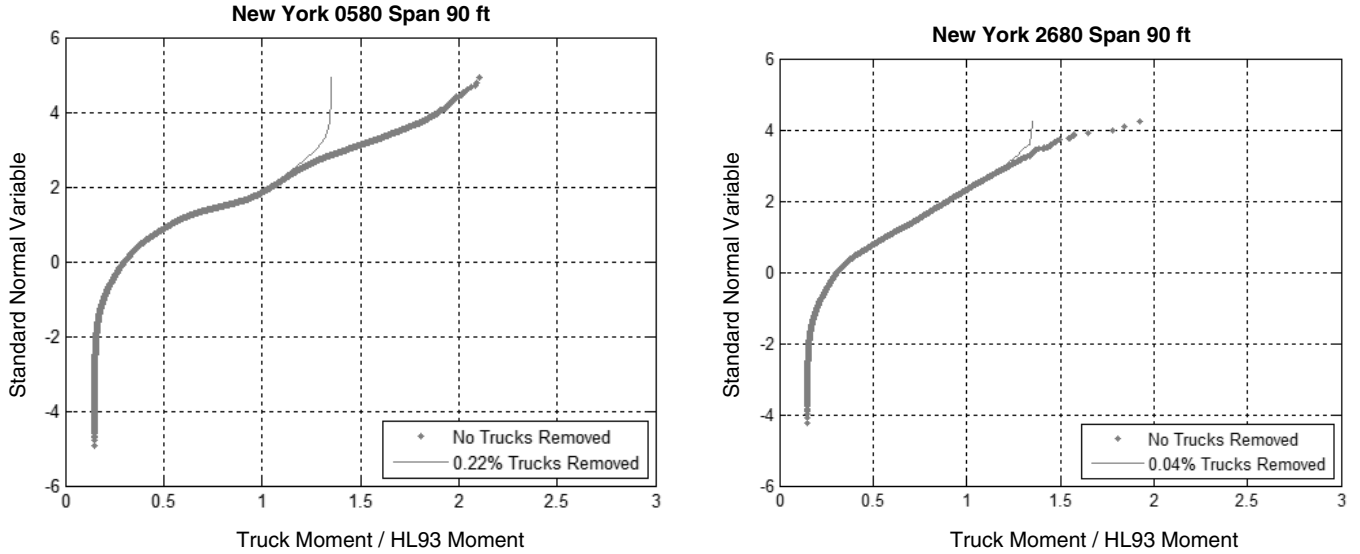


Figure 5.14. Data removal from New York Sites 0580 and 2680.

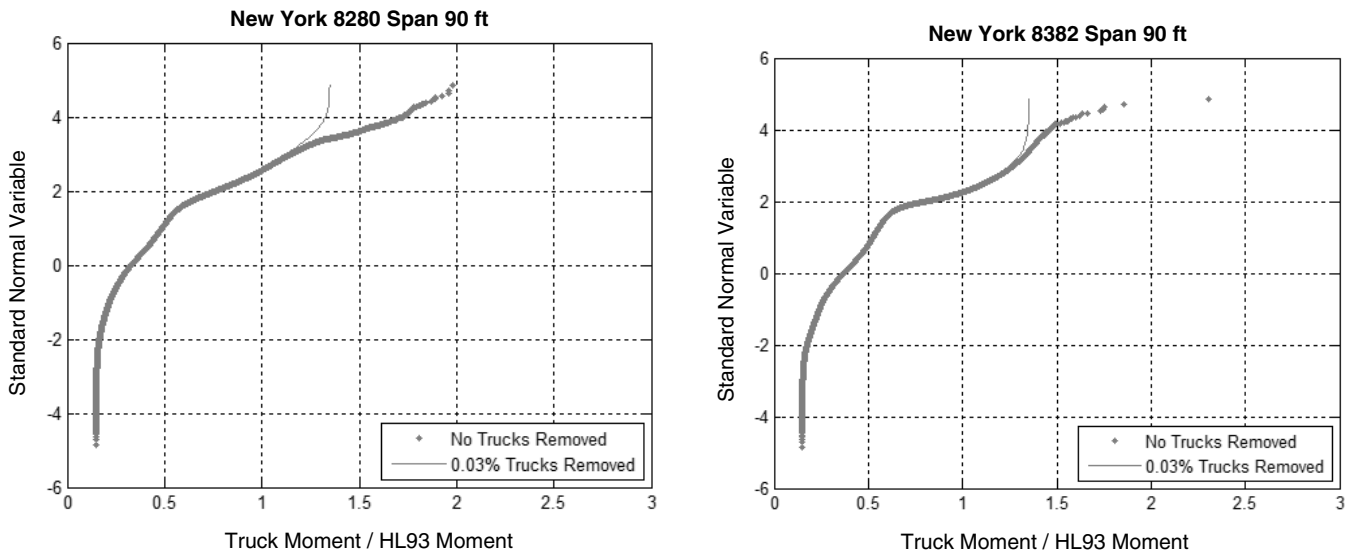


Figure 5.15. Data removal from New York Sites 8280 and 8382.

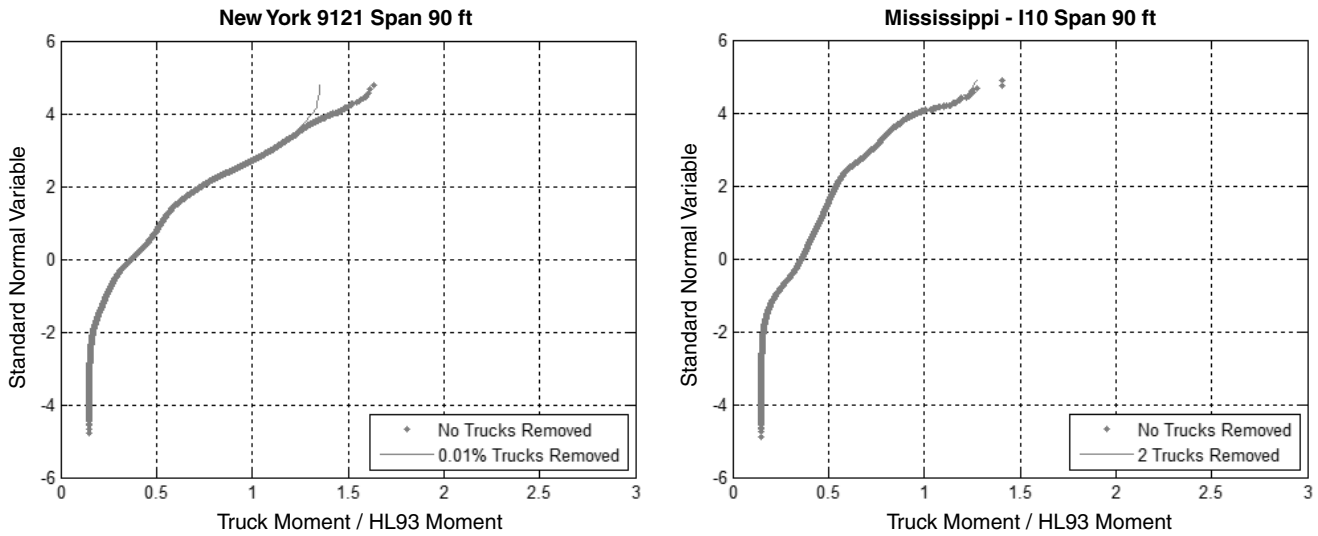


Figure 5.16. Data removal from New York Site 9121 and Mississippi I-10 locations.

(continued from page 100)

A special program was developed to filter the data by using the time of a record and the speed of the truck to find instances when either of the events shown in Figure 5.17 occurred involving similar trucks. The filter resulted in selecting the observed cases of two trucks with a headway distance less than 200 ft in either the same lane or two adjacent lanes.

**Two Trucks: Side by Side**

The analysis of the degree of correlation was performed for Site 9936 in Florida along I-10 and Site 8382 in New York with 1,654,004 and 1,594,674 site-specific total records, respectively. Filtering the data resulted in the selection of 2,518 fully correlated trucks in adjacent lanes in Florida and 3,748 fully correlated trucks in adjacent lanes in New York. Histograms of the GVWs of these fully correlated side-by-side trucks are shown in Figure 5.18.

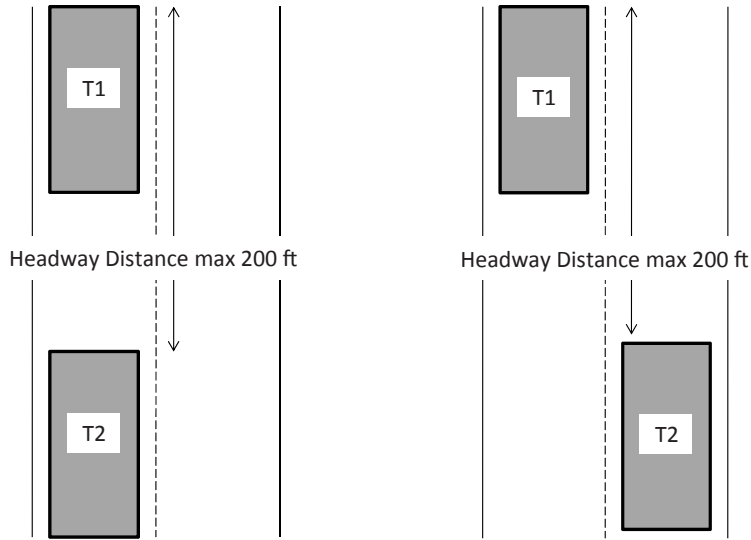
The selected trucks were plotted on probability paper and compared with all recorded vehicles. The GVW of both correlated trucks were added together and divided by two to obtain the average GVW. (Note that the correlation criteria ensure that the average is similar to the two selected trucks in each pair.) The comparison of the mean correlated GVW of the trucks recorded in adjacent lanes with the GVW of the whole population from Florida and New York is shown in Figure 5.19.

**TWO TRUCKS: ONE AFTER THE OTHER**

Filtering the data resulted in the selection of 8,380 fully correlated trucks in one lane in Florida and 9,868 fully correlated trucks in one lane in New York. Histograms of these trucks are shown in Figure 5.20. The comparison of the mean correlated GVW of the trucks recorded in one lane with the GVW of the whole data set from Florida and New York is shown in Figure 5.21.

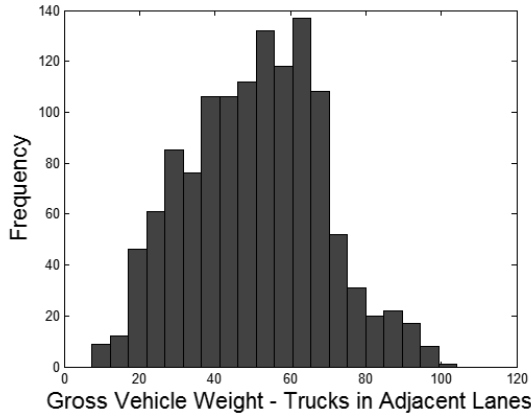
Table 5.3. Removal of Heaviest Vehicles (90-ft Span)

Figure	State	Site	No. of Trucks Before Filtering	No. of Trucks After Filtering	No. of Removed Trucks	Removed Trucks (%)
Figure 5.14	New York	0580	2,474,407	2,468,952	5,455	0.22
Figure 5.14	New York	2680	89,286	89,250	36	0.04
Figure 5.15	New York	8280	1,717,972	1,717,428	544	0.03
Figure 5.15	New York	8382	1,551,454	1,550,914	540	0.03
Figure 5.16	New York	9121	1,235,963	1,235,886	77	0.01
Figure 5.16	Mississippi	I-10	2,103,302	2,103,300	2	0.00



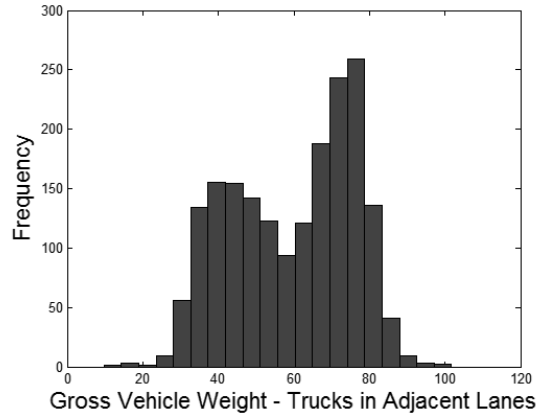
**Figure 5.17. Two cases of the simultaneous presence of two trucks with headway distance less than 200 ft.**

Florida I-10



(a)

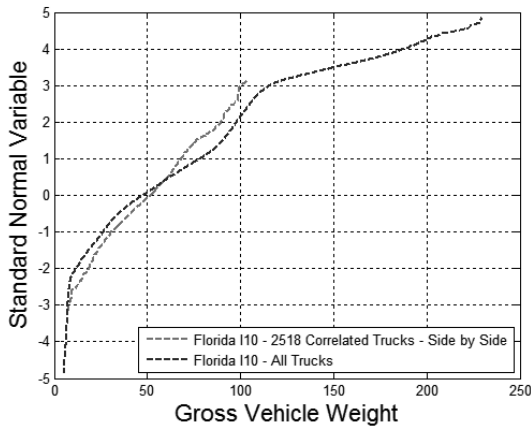
New York Site 8382



(b)

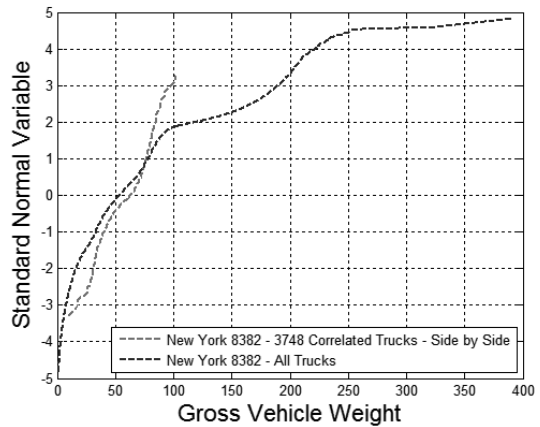
**Figure 5.18. Histograms of trucks side by side (a) on Florida I-10 and (b) at New York Site 8382.**

Florida I-10



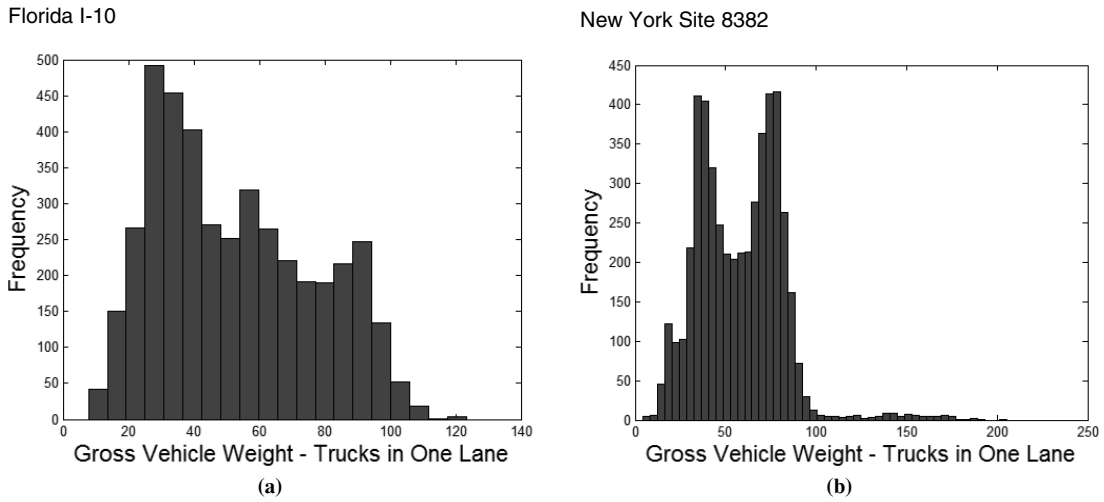
(a)

New York Site 8382



(b)

**Figure 5.19. Comparison of mean GWV and GWV of the whole population for (a) Florida and (b) New York.**



**Figure 5.20. Histogram of trucks one after another (a) on Florida I-10 and (b) at New York Site 8382.**

*IMPLICATIONS FOR SPECIFICATION DEVELOPMENT*

The study of multiple presence based on WIM data indicated that, for SLSs, the vehicles representing the extreme tails of the CDF need not be considered as being simultaneously present in multiple lanes. The implication is that only a single-lane live load model needs to be considered on the load side (*Q*) of limit state functions. The resistance side (*R*) of limit state functions should represent the requirements of the applicable design requirement, even if that is a multiple-lane loading situation.

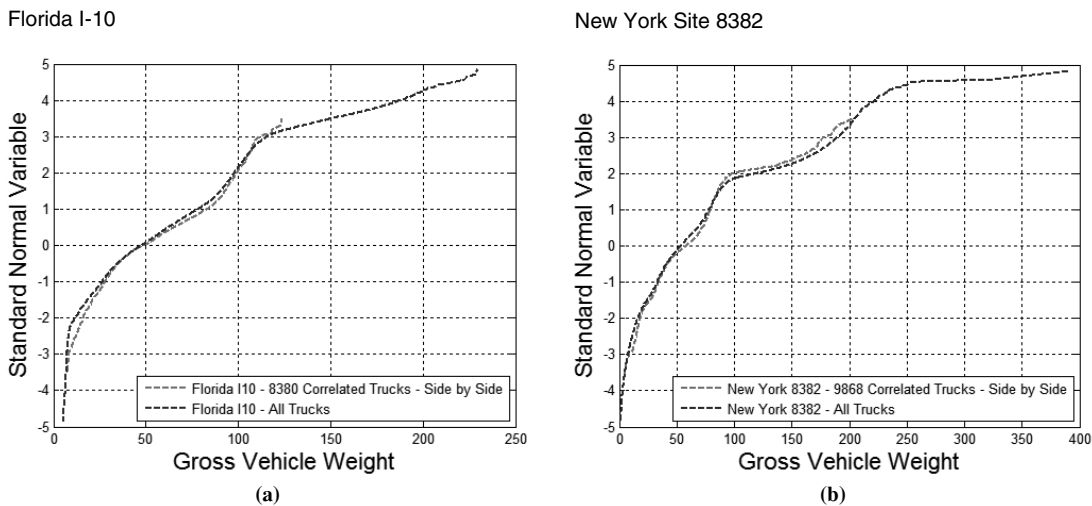
The issue of multiple load lanes was considered in the development of HL-93 for *AASHTO LRFD* strength limit states, and the conclusion was that extreme truck load does not occur simultaneously with another fully correlated extreme truck, but was considered to occur simultaneously with a truck about 15% to 20% lighter. This two-lane loading was

correlated to the design loading of two lanes of HL-93 with a load factor of 1.75 and a multiple presence factor of 1.0. (The multiple presence factor for a single-lane loading is 1.20 to account for the occasional truck that creates more force effect than the family of configurations used to develop the HL-93 load configuration.)

**5.2.5 Project Guidelines Regarding Live load**

The following guidelines are based on live load bias factors and CVs determined from the preliminary analysis of WIM measurements and previous work by the research team (Nowak 1999):

- The use of dynamic load as 10% of live load, with CV = 80%, is recommended.



**Figure 5.21. Comparison of mean GWW and GWW of the whole population for (a) Florida and (b) New York.**

- Generally use a single loaded lane (no multiple loaded lanes).
- The national load (i.e., notional load) should not try to encompass all WIM records. Some of the extremely heavy vehicles are permit loads and some are illegal overloads. A relatively small number of loads were excluded for most of the SLS studies, but they were included for the overload limit state.
- It is likely that different probabilities of exceedance will be used for various limit states based on consequences.
- Some jurisdictions may need exceptions based on their legal loads and extent of enforcement.
- The basic HL-93 load model, scaled by calibrated load factors, is appropriate for SLS.

With these recommendations, the evaluation of numerical live load models continued. The processes used and results obtained are summarized here. Further details and extensive graphical presentations are contained in Rakoczy (2011).

### 5.3 Statistical Parameters for Service Limit States Other than Fatigue

#### 5.3.1 Maximum Moments for Different Time Periods

The maximum moment is a random variable. It depends on the period of time, ADTT, and distribution of traffic (e.g., CDF of WIM moments). For a given CDF of WIM moments  $[F(x)]$ , period of time ( $T$ ), and ADTT, the mean value of the maximum moment can be determined as follows. The total number of vehicles ( $N$ ) expected during the considered time period  $T$  (in days) is  $T \times \text{ADTT}$ . The expected or mean value of the maximum moment for time  $T$   $[M_{\max}(T)]$  is equal to the moment corresponding to probability  $\{1 - F[1/N(T)]\}$ , where  $F(x)$  is the CDF of WIM moments, which is  $F^{-1}[1 - 1/N(T)]$ , where  $F^{-1}$  is the inverse of CDF.

The objective is to determine the mean maximum moment for different time periods (i.e., 1 day, 2 weeks, 1 month, 2 months, 6 months, 1 year, 5 years, 50 years, 75 years, and 100 years). The number of recorded vehicles for each location is given in Table 5.2. The data were collected over different time periods, in most cases about 1 year, but the number of vehicles varies because ADTT varies. Each CDF in Figure 5.8 to Figure 5.12 includes the number of data points equal to the corresponding number of vehicles ( $N$ ). For each CDF, the vertical coordinate of the maximum moment ( $Z_{\max}$ ) is given by Equation 5.1:

$$z_{\max} = -\Phi^{-1}(1/N) \quad (5.1)$$

where  $-\Phi^{-1}$  is the inverse standard normal distribution function. For example, if  $N = 1,000,000$ , then  $Z_{\max} = 4.75$ .

In further analysis, five ADTTs were considered: 250, 1,000, 2,500, 5,000, and 10,000. The calculations were performed separately for each ADTT. To determine the mean maximum moments corresponding to the considered time periods, the vertical coordinates were found first.

Starting with ADTT = 250, the vertical coordinate of the mean maximum 1-day moment  $z$  is given by Equation 5.2:

$$z = -\Phi^{-1}(1/250) = 2.65 \quad (5.2)$$

because the number of trucks per 1 day is 250.

The mean maximum 2-week moment  $z$  is given by Equation 5.3:

$$z = -\Phi^{-1}(1/3500) = 3.44 \quad (5.3)$$

because the number of trucks per 2 weeks is (250 trucks) (14 days) = 3,500 trucks.

Finally, the mean maximum 100-year moment  $z$  is given by Equation 5.4:

$$z = -\Phi^{-1}(1/9,125,000) = 5.18 \quad (5.4)$$

because the number of trucks per 100 years is (250 trucks) (365 days)(100 years) = 9,125,000 trucks.

Similarly, for ADTT = 1,000, the vertical coordinate of the mean maximum 1-day moment  $z$  is given by Equation 5.5:

$$z = -\Phi^{-1}(1/1000) = 3.09 \quad (5.5)$$

because the number of trucks per 1 day is 1,000.

The mean maximum 2-week moment  $z$  is given by Equation 5.6:

$$z = -\Phi^{-1}(1/14,000) = 3.8 \quad (5.6)$$

because the number of trucks per 2 weeks is (1,000 trucks) (14 days) = 14,000 trucks.

Finally, the mean maximum 100-year moment  $z$  is given by Equation 5.7:

$$z = -\Phi^{-1}(1/36,500,000) = 5.67 \quad (5.7)$$

because the number of trucks per 100 years is (1,000 trucks) (365 days)(100 years) = 36,500,000 trucks.

Values of  $z$  for the considered ADTTs and time periods from 1 day to 100 years are summarized in Table 5.4.

For example, for the WIM moments in Figure 5.11 (span = 120 ft), the vertical coordinates corresponding to different time periods are shown in Figure 5.22 for ADTT = 1,000.

There were 32 WIM locations and, therefore, 32 curves representing CDFs of WIM moments in each of Figures 5.8 to 5.12. The mean maximum moment can be obtained directly

**Table 5.4. Vertical Coordinates for the Mean Maximum Moment**

Time Period	ADTT				
	250	1,000	2,500	5,000	10,000
1 Day	2.65	3.09	3.35	3.54	3.72
2 Weeks	3.44	3.08	4.02	4.18	4.33
1 Month	3.65	4.00	4.20	4.35	4.50
2 Months	3.82	4.15	4.35	4.50	4.65
6 Months	4.09	4.39	4.59	4.73	4.87
1 Year	4.24	4.55	4.73	4.87	5.01
5 Years	4.59	4.87	5.05	5.18	5.31
50 Years	5.05	5.31	5.47	5.60	5.72
75 Years	5.13	5.38	5.55	5.67	5.78
100 Years	5.18	5.44	5.60	5.72	5.83

from the graph by reading the moment ratio (horizontal axis) corresponding to the vertical coordinate representing the considered time period. For example, from Figure 5.22, the mean maximum 1-day moment ratio for Florida US-29 is 0.95, and the mean maximum 1-year moment ratio is 1.39. Values for longer time periods were projected or interpolated as appropriate.

For each ADTT and span length, there are 32 values of the mean maximum 1-day moment, 32 values of the mean maximum 2-week moment, and so on. For an easier review and comparison, CDFs of these 32 values obtained from Figure 5.22 were plotted on normal probability paper and are shown in Figure 5.23. There is one CDF for 1-day values, one for 2 weeks, and so on. These are CDFs of extreme variables, as each of the 32 values is the maximum moment for a WIM location. The obtained CDFs are almost parallel; in particular, this applies to the upper part. Because of regularity, it is easier to determine the statistical parameters. Each data point represents the mean of the maximum value for one of 32 WIM locations, which means that the CDFs in Figure 5.23 are extreme value distributions rather than hypothetical curves.

### 5.3.2 Statistical Parameters of Live Load

It was assumed that the 32 WIM locations considered are representative for the truck traffic in the United States. The statistical parameters (the mean maximum and CV of the maximum live load) were determined for each WIM location. The CDFs of the mean maximum values were plotted on probability paper. This is an extreme value distribution. The mean of these mean maximum values can be considered as the mean maximum national live load. The standard deviation of the mean maximum values can be determined from the graphs (slope of the CDF). However, the WIM locations were not selected

randomly; rather, the selection was based on the availability of WIM stations with truck data and the credibility of the measured data (truck records). If the considered WIM locations are biased (i.e., nonrepresentative), then the processed database can underestimate or overestimate the statistical parameters of the national live load. Therefore, for the purpose of further reliability analysis, it is conservatively assumed that the calculated mean maximum live load is increased by 1.5 standard deviations. The probability of exceeding this value (mean plus 1.5 standard deviations) is about 5%, so that it will be exceeded by 5% of 32 WIM locations (i.e., in one or two WIM locations).

As the upper parts of the CDFs are almost straight lines, the fitting by normal distributions is justified. The mean values can be read directly from the graph as the intersection of CDFs (represented by straight lines) and the horizontal axis at zero on the vertical scale. This process is depicted in Figure 5.24. The visual comparison of how the actual CDF fits a straight line is much better than any curve-fitting formula because the research team was mostly interested in only some parts of the CDF. Different curves can have different slopes, which are reflected in the standard deviations.

Calculations were carried out for all considered cases of ADTT and span length. The results, which were extrapolated to 100 years and span length of 300 ft, are summarized in Table 5.5 to Table 5.9. Statistical parameters were calculated for a variety of ADTTs (500, 1,000, 2,500, 5,000, and 10,000); however, the *AASHTO LRFD* is based on 5,000 (consistent with strength limit states). Live load data for values of ADTT other than 5,000 were tabulated so owners can repeat the calibration process with other data. For a given bridge, use of a lower ADTT should lead to a higher reliability index.

Bias factors vary depending on ADTT for shorter time periods; however, for longer time periods, the bias factor is about 1.4.

### 5.3.3 Reactions

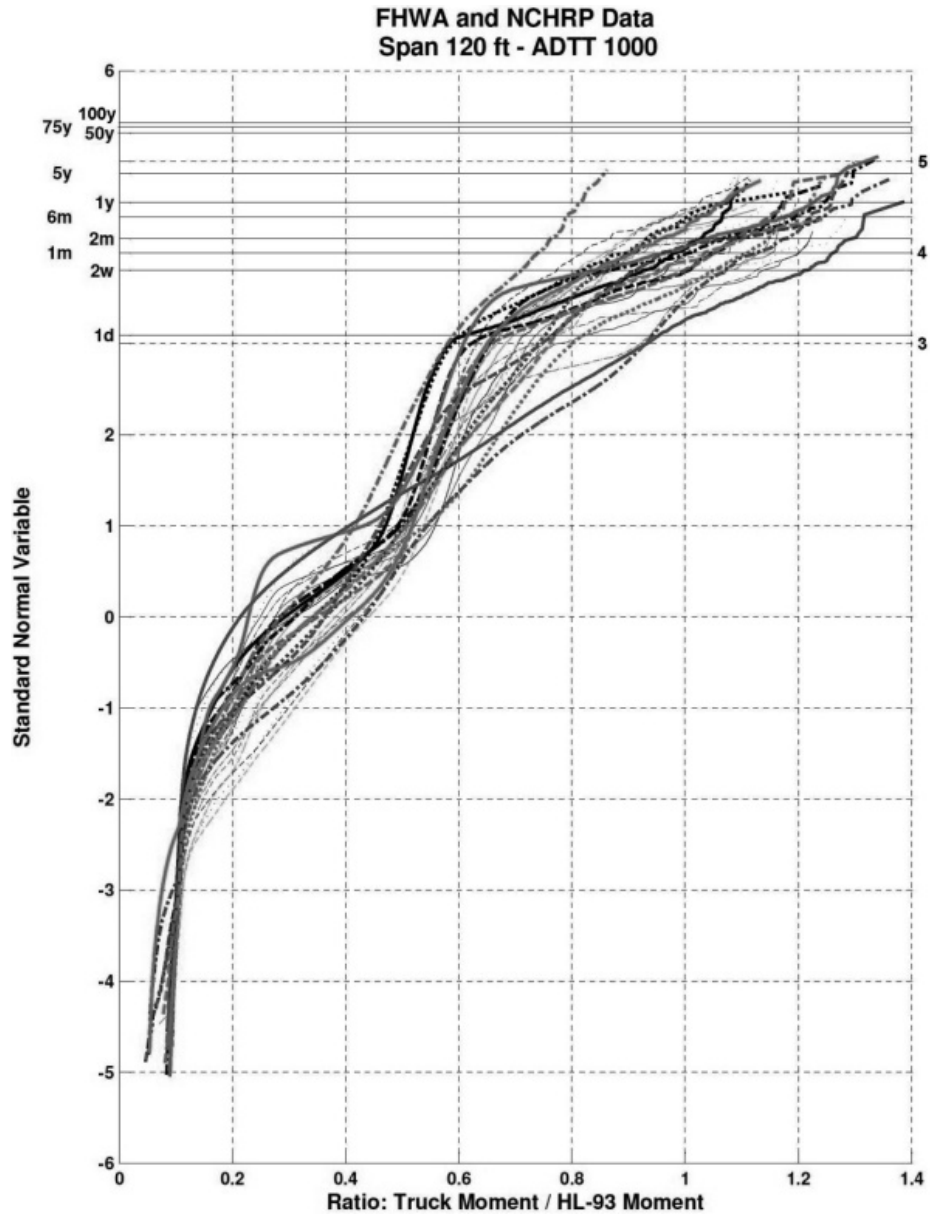
Tables of statistics for reactions of simply supported spans were developed for the same spans, time periods, and ADTTs as presented for bending moments by using a methodology analogous to the one presented in Section 5.3.2. The results are shown in Table 5.10 to Table 5.14. Graphical representations are presented in Rakoczy (2011).

### 5.3.4 Axle Loads

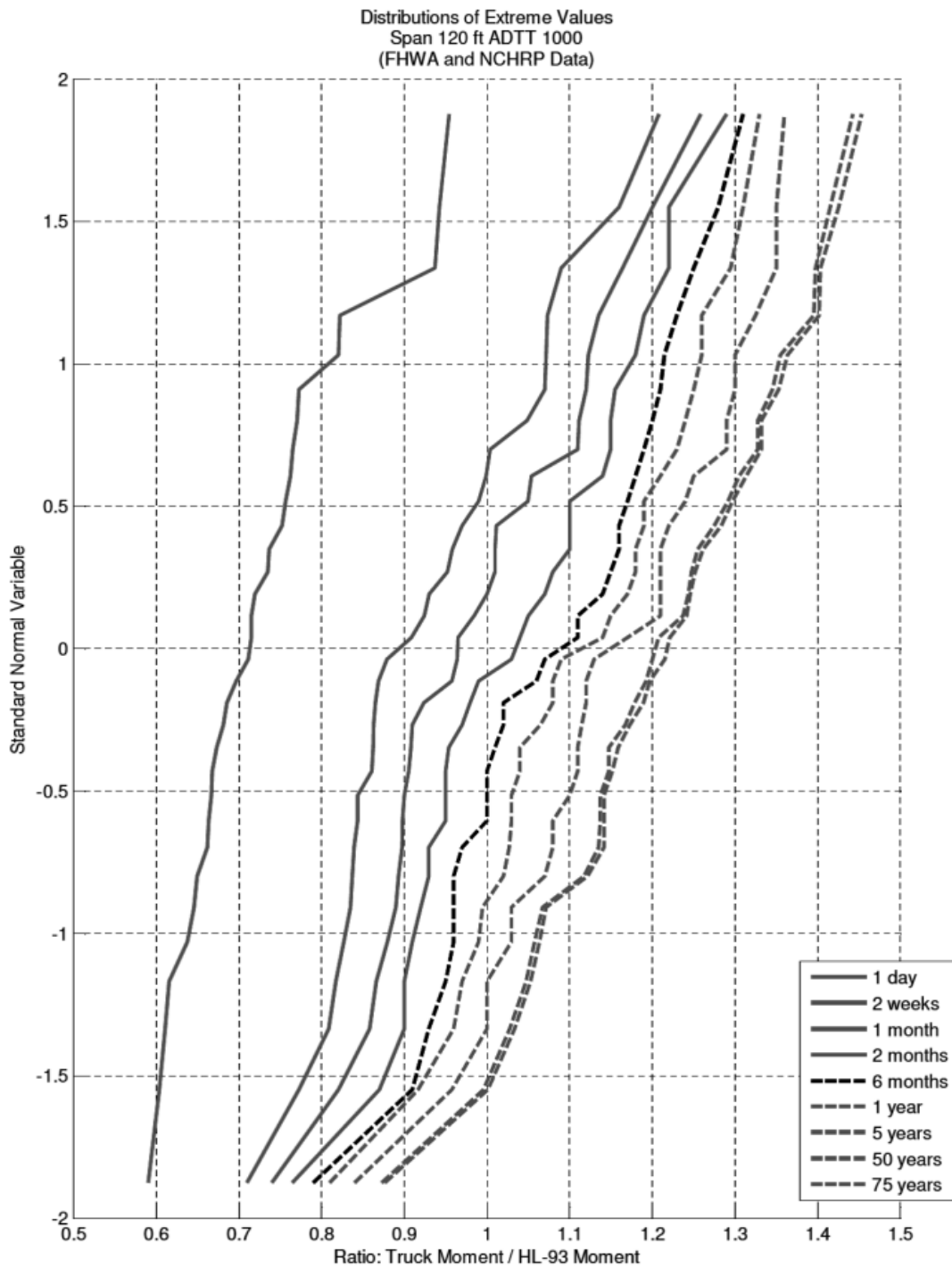
Statistical parameters for various time periods and ADTTs are developed using a methodology analogous to that presented in Section 5.3.2 applied to axle loads instead of moments. The results are presented in Table 5.15.

(text continues on page 121)





*Figure 5.22. Vertical coordinates for different time periods for ADTT = 1,000 and span = 120 ft.*



**Figure 5.23.** CDFs of mean maximum moment ratios for ADTT = 1,000 and span length = 120 ft.

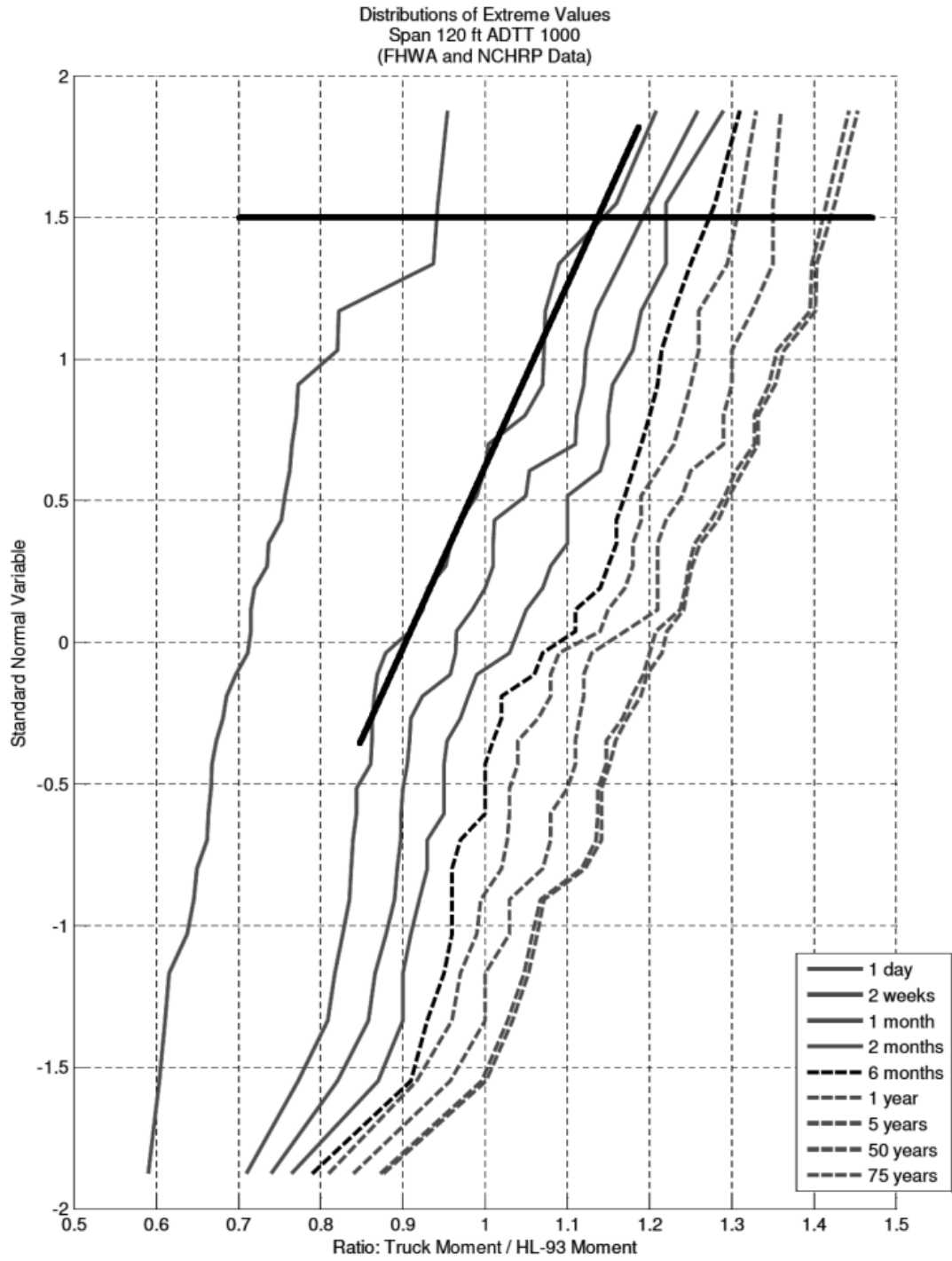


Figure 5.24. Determination of mean values at  $1.5 \sigma$ .

**Table 5.5. Statistical Parameters of Live Load Moments for ADTT 250,  $\lambda = \mu + 1.5\sigma$**

Time Period	Span																	
	30 ft			60 ft			90 ft			120 ft			200 ft			300 ft		
	$\lambda$	$\mu$	CV	$\lambda$	$\mu$	CV	$\lambda$	$\mu$	CV	$\lambda$	$\mu$	CV	$\lambda$	$\mu$	CV	$\lambda$	$\mu$	CV
1 Day	0.92	0.65	0.28	0.82	0.64	0.23	0.80	0.66	0.17	0.79	0.65	0.15	0.71	0.56	0.18	0.61	0.48	0.18
2 Weeks	1.06	0.80	0.21	1.05	0.80	0.16	1.01	0.80	0.18	1.02	0.80	0.16	0.93	0.73	0.16	0.84	0.67	0.16
1 Month	1.12	0.85	0.21	1.09	0.85	0.19	1.08	0.85	0.18	1.08	0.85	0.17	1.01	0.78	0.19	0.90	0.73	0.16
2 Months	1.14	0.90	0.18	1.15	0.91	0.17	1.14	0.90	0.18	1.14	0.90	0.17	1.05	0.85	0.15	0.95	0.77	0.15
6 Months	1.19	0.95	0.17	1.23	0.96	0.19	1.20	0.97	0.15	1.19	0.98	0.14	1.12	0.91	0.15	1.04	0.85	0.15
1 Year	1.23	1.00	0.15	1.27	0.98	0.19	1.24	1.00	0.16	1.22	1.04	0.12	1.15	0.94	0.15	1.08	0.88	0.15
5 Years	1.31	1.07	0.15	1.35	1.09	0.16	1.31	1.13	0.11	1.31	1.14	0.10	1.25	1.02	0.15	1.18	0.97	0.15
50 Years	1.37	1.17	0.11	1.39	1.16	0.13	1.39	1.25	0.07	1.37	1.19	0.10	1.32	1.06	0.16	1.25	1.02	0.15
75 Years	1.38	1.20	0.10	1.40	1.19	0.12	1.41	1.27	0.07	1.39	1.21	0.10	1.34	1.08	0.16	1.27	1.04	0.15
100 Years	1.39	1.22	0.09	1.43	1.21	0.12	1.42	1.28	0.07	1.41	1.22	0.10	1.35	1.09	0.16	1.29	1.05	0.15

**Table 5.6. Statistical Parameters of Live Load Moments for ADTT 1,000,  $\lambda = \mu + 1.5\sigma$**

Time Period	Span																	
	30 ft			60 ft			90 ft			120 ft			200 ft			300 ft		
	$\lambda$	$\mu$	CV	$\lambda$	$\mu$	CV	$\lambda$	$\mu$	CV	$\lambda$	$\mu$	CV	$\lambda$	$\mu$	CV	$\lambda$	$\mu$	CV
1 Day	0.99	0.72	0.28	0.89	0.71	0.20	0.90	0.72	0.17	0.89	0.71	0.17	0.81	0.63	0.19	0.71	0.55	0.19
2 Weeks	1.14	0.87	0.21	1.13	0.90	0.16	1.13	0.89	0.18	1.14	0.91	0.16	1.06	0.85	0.16	0.97	0.77	0.16
1 Month	1.18	0.95	0.16	1.19	0.95	0.16	1.19	0.95	0.17	1.19	0.96	0.16	1.11	0.91	0.14	1.01	0.83	0.14
2 Months	1.23	0.99	0.16	1.26	0.99	0.18	1.26	1.00	0.17	1.23	1.03	0.13	1.16	0.96	0.14	1.07	0.89	0.14
6 Months	1.27	1.04	0.14	1.31	1.05	0.16	1.30	1.10	0.12	1.27	1.09	0.11	1.22	0.99	0.15	1.15	0.93	0.15
1 Year	1.33	1.07	0.16	1.34	1.08	0.16	1.32	1.15	0.10	1.31	1.14	0.10	1.25	1.01	0.16	1.18	0.95	0.16
5 Years	1.37	1.11	0.15	1.37	1.14	0.13	1.36	1.21	0.08	1.35	1.17	0.10	1.30	1.06	0.15	1.24	1.01	0.15
50 Years	1.38	1.24	0.07	1.42	1.21	0.12	1.41	1.26	0.08	1.41	1.21	0.11	1.35	1.11	0.14	1.28	1.05	0.14
75 Years	1.40	1.26	0.07	1.42	1.23	0.11	1.42	1.28	0.07	1.41	1.23	0.10	1.36	1.13	0.13	1.29	1.07	0.13
100 Years	1.40	1.27	0.07	1.44	1.24	0.11	1.43	1.29	0.07	1.43	1.24	0.10	1.37	1.14	0.13	1.30	1.09	0.13

**Table 5.7. Statistical Parameters of Live Load Moments for ADTT 2,500,  $\lambda = \mu + 1.5\sigma$**

Time Period	Span																	
	30 ft			60 ft			90 ft			120 ft			200 ft			300 ft		
	$\lambda$	$\mu$	CV	$\lambda$	$\mu$	CV	$\lambda$	$\mu$	CV	$\lambda$	$\mu$	CV	$\lambda$	$\mu$	CV	$\lambda$	$\mu$	CV
1 Day	1.03	0.80	0.19	0.97	0.79	0.18	0.97	0.77	0.17	0.98	0.78	0.17	0.90	0.70	0.19	0.80	0.62	0.19
2 Weeks	1.20	0.93	0.19	1.20	0.96	0.17	1.20	0.96	0.17	1.20	0.97	0.15	1.12	0.92	0.14	1.02	0.84	0.14
1 Month	1.23	0.99	0.16	1.25	0.99	0.17	1.26	1.00	0.17	1.22	1.04	0.12	1.16	0.95	0.15	1.09	0.89	0.15
2 Months	1.28	1.04	0.15	1.31	1.04	0.17	1.29	1.11	0.11	1.27	1.12	0.09	1.21	0.98	0.15	1.12	0.91	0.15
6 Months	1.31	1.07	0.15	1.34	1.07	0.17	1.32	1.15	0.10	1.31	1.14	0.10	1.25	1.01	0.16	1.18	0.95	0.16
1 Year	1.34	1.11	0.14	1.35	1.11	0.14	1.36	1.19	0.09	1.34	1.17	0.09	1.28	1.04	0.15	1.21	0.98	0.15
5 Years	1.36	1.15	0.12	1.39	1.18	0.12	1.39	1.24	0.08	1.38	1.20	0.10	1.33	1.07	0.16	1.26	1.01	0.16
50 Years	1.40	1.25	0.08	1.42	1.22	0.11	1.43	1.29	0.07	1.43	1.23	0.11	1.37	1.11	0.15	1.29	1.05	0.15
75 Years	1.40	1.26	0.07	1.43	1.24	0.10	1.43	1.30	0.07	1.44	1.24	0.10	1.37	1.13	0.14	1.29	1.06	0.14
100 Years	1.40	1.27	0.07	1.44	1.25	0.10	1.44	1.31	0.07	1.44	1.25	0.10	1.39	1.14	0.14	1.32	1.09	0.14

**Table 5.8. Statistical Parameters of Live Load Moments for ADTT 5,000,  $\lambda = \mu + 1.5\sigma$**

Time Period	Span																	
	30 ft			60 ft			90 ft			120 ft			200 ft			300 ft		
	$\lambda$	$\mu$	CV	$\lambda$	$\mu$	CV	$\lambda$	$\mu$	CV	$\lambda$	$\mu$	CV	$\lambda$	$\mu$	CV	$\lambda$	$\mu$	CV
1 Day	1.08	0.85	0.18	1.02	0.82	0.17	1.03	0.82	0.17	1.03	0.82	0.17	0.95	0.75	0.17	0.84	0.67	0.17
2 Weeks	1.24	0.98	0.17	1.26	1.00	0.17	1.24	1.00	0.16	1.24	1.04	0.13	1.16	0.96	0.14	1.06	0.88	0.14
1 Month	1.28	1.04	0.15	1.32	1.03	0.18	1.30	1.12	0.11	1.26	1.11	0.09	1.20	0.99	0.14	1.13	0.93	0.14
2 Months	1.31	1.07	0.15	1.34	1.07	0.17	1.32	1.15	0.10	1.31	1.14	0.10	1.23	1.02	0.14	1.16	0.96	0.14
6 Months	1.34	1.11	0.14	1.35	1.11	0.14	1.34	1.19	0.08	1.32	1.17	0.09	1.28	1.04	0.15	1.23	1.00	0.15
1 Year	1.35	1.14	0.12	1.38	1.14	0.14	1.38	1.21	0.09	1.36	1.19	0.09	1.31	1.07	0.15	1.25	1.02	0.15
5 Years	1.39	1.16	0.13	1.40	1.19	0.12	1.40	1.25	0.08	1.41	1.21	0.11	1.34	1.10	0.15	1.28	1.05	0.15
50 Years	1.41	1.21	0.11	1.44	1.24	0.10	1.44	1.27	0.09	1.46	1.23	0.12	1.39	1.13	0.15	1.30	1.06	0.15
75 Years	1.42	1.22	0.11	1.45	1.25	0.10	1.45	1.29	0.08	1.46	1.25	0.11	1.40	1.14	0.15	1.31	1.07	0.15
100 Years	1.42	1.23	0.11	1.45	1.26	0.10	1.47	1.30	0.08	1.47	1.26	0.11	1.40	1.15	0.15	1.33	1.08	0.15

**Table 5.9. Statistical Parameters of Live Load Moments for ADTT 10,000,  $\lambda = \mu + 1.5\sigma$**

Time Period	Span																	
	30 ft			60 ft			90 ft			120 ft			200 ft			300 ft		
	$\lambda$	$\mu$	CV	$\lambda$	$\mu$	CV	$\lambda$	$\mu$	CV	$\lambda$	$\mu$	CV	$\lambda$	$\mu$	CV	$\lambda$	$\mu$	CV
<b>1 Day</b>	1.17	0.88	0.22	1.09	0.89	0.16	1.11	0.87	0.18	1.13	0.87	0.20	1.02	0.81	0.17	0.91	0.75	0.17
<b>2 Weeks</b>	1.29	1.02	0.18	1.31	1.04	0.17	1.29	1.11	0.11	1.27	1.12	0.09	1.22	0.98	0.16	1.16	0.93	0.16
<b>1 Month</b>	1.32	1.06	0.16	1.34	1.08	0.16	1.32	1.15	0.10	1.29	1.14	0.09	1.25	1.01	0.16	1.20	0.97	0.16
<b>2 Months</b>	1.35	1.09	0.16	1.35	1.11	0.14	1.35	1.18	0.09	1.32	1.17	0.09	1.28	1.04	0.15	1.23	1.00	0.15
<b>6 Months</b>	1.35	1.12	0.13	1.37	1.14	0.13	1.37	1.20	0.09	1.34	1.19	0.08	1.30	1.06	0.15	1.25	1.02	0.15
<b>1 Year</b>	1.37	1.17	0.11	1.39	1.16	0.13	1.39	1.24	0.08	1.38	1.20	0.10	1.32	1.08	0.15	1.27	1.04	0.15
<b>5 Years</b>	1.39	1.24	0.08	1.41	1.21	0.11	1.42	1.27	0.08	1.42	1.22	0.11	1.37	1.11	0.15	1.30	1.06	0.15
<b>50 Years</b>	1.40	1.28	0.06	1.45	1.24	0.11	1.45	1.30	0.08	1.46	1.25	0.11	1.40	1.14	0.15	1.31	1.07	0.15
<b>75 Years</b>	1.41	1.29	0.06	1.46	1.26	0.10	1.47	1.32	0.08	1.47	1.26	0.11	1.40	1.16	0.14	1.32	1.09	0.14
<b>100 Years</b>	1.42	1.30	0.06	1.47	1.27	0.10	1.49	1.33	0.08	1.48	1.27	0.11	1.42	1.17	0.14	1.33	1.10	0.14

**Table 5.10. Statistical Parameters of Live Load Reactions for ADTT 250,  $\lambda = \mu + 1.5\sigma$**

Time Period	Span																	
	30 ft			60 ft			90 ft			120 ft			200 ft			300 ft		
	$\mu + 1.5\sigma$	$\mu$	CV	$\mu + 1.5\sigma$	$\mu$	CV	$\mu + 1.5\sigma$	$\mu$	CV	$\mu + 1.5\sigma$	$\mu$	CV	$\mu + 1.5\sigma$	$\mu$	CV	$\mu + 1.5\sigma$	$\mu$	CV
<b>1 Day</b>	1.02	0.85	0.13	0.88	0.74	0.12	0.88	0.74	0.12	0.86	0.72	0.13	0.73	0.61	0.13	0.57	0.48	0.13
<b>2 Weeks</b>	1.22	1.02	0.13	1.08	0.91	0.12	1.11	0.94	0.12	1.08	0.90	0.13	0.97	0.80	0.14	0.82	0.68	0.14
<b>1 Month</b>	1.28	1.07	0.13	1.14	0.96	0.13	1.17	0.99	0.12	1.15	0.97	0.12	1.06	0.88	0.14	0.93	0.77	0.14
<b>2 Months</b>	1.32	1.11	0.13	1.19	1.01	0.12	1.22	1.04	0.12	1.20	1.02	0.12	1.12	0.92	0.14	0.98	0.81	0.14
<b>6 Months</b>	1.37	1.16	0.12	1.27	1.07	0.12	1.32	1.11	0.13	1.30	1.10	0.12	1.18	0.97	0.14	1.08	0.89	0.14
<b>1 Year</b>	1.41	1.20	0.12	1.31	1.10	0.13	1.37	1.14	0.13	1.35	1.12	0.13	1.22	1.01	0.14	1.12	0.93	0.14
<b>5 Years</b>	1.49	1.26	0.12	1.38	1.15	0.13	1.46	1.22	0.13	1.44	1.20	0.13	1.35	1.11	0.14	1.24	1.02	0.14
<b>50 Years</b>	1.54	1.30	0.12	1.49	1.23	0.14	1.52	1.28	0.13	1.52	1.28	0.13	1.45	1.18	0.15	1.36	1.11	0.15
<b>75 Years</b>	1.55	1.31	0.12	1.50	1.24	0.14	1.55	1.29	0.13	1.55	1.29	0.13	1.46	1.19	0.15	1.37	1.12	0.15
<b>100 Years</b>	1.56	1.32	0.12	1.50	1.25	0.14	1.55	1.30	0.13	1.55	1.30	0.13	1.47	1.20	0.15	1.38	1.12	0.15



**Table 5.11. Statistical Parameters of Live Load Reactions for ADTT 1,000,  $\lambda = \mu + 1.5\sigma$**

Time Period	Span																	
	30 ft			60 ft			90 ft			120 ft			200 ft			300 ft		
	$\mu + 1.5\sigma$	$\mu$	CV	$\mu + 1.5\sigma$	$\mu$	CV	$\mu + 1.5\sigma$	$\mu$	CV	$\mu + 1.5\sigma$	$\mu$	CV	$\mu + 1.5\sigma$	$\mu$	CV	$\mu + 1.5\sigma$	$\mu$	CV
1 Day	1.14	0.94	0.14	0.95	0.80	0.13	0.94	0.80	0.11	0.91	0.79	0.10	0.84	0.70	0.13	0.74	0.62	0.13
2 Weeks	1.31	1.10	0.13	1.17	0.99	0.12	1.19	1.02	0.11	1.19	1.02	0.11	1.09	0.91	0.13	0.97	0.81	0.13
1 Month	1.35	1.15	0.12	1.23	1.03	0.13	1.26	1.08	0.11	1.25	1.07	0.11	1.17	0.97	0.13	1.06	0.88	0.13
2 Months	1.38	1.18	0.11	1.26	1.08	0.11	1.31	1.11	0.12	1.31	1.11	0.12	1.22	1.01	0.14	1.11	0.92	0.14
6 Months	1.42	1.22	0.11	1.29	1.11	0.11	1.38	1.15	0.13	1.37	1.16	0.12	1.28	1.05	0.14	1.18	0.97	0.14
1 Year	1.45	1.25	0.11	1.32	1.14	0.11	1.40	1.19	0.12	1.40	1.19	0.12	1.32	1.09	0.14	1.21	1.00	0.14
5 Years	1.50	1.29	0.11	1.40	1.20	0.11	1.49	1.26	0.12	1.50	1.26	0.13	1.38	1.14	0.14	1.28	1.06	0.14
50 Years	1.56	1.33	0.11	1.46	1.25	0.11	1.56	1.30	0.13	1.57	1.30	0.14	1.47	1.20	0.15	1.35	1.10	0.15
75 Years	1.57	1.34	0.11	1.47	1.26	0.11	1.57	1.31	0.13	1.58	1.31	0.14	1.48	1.21	0.15	1.36	1.11	0.15
100 Years	1.57	1.35	0.11	1.48	1.27	0.11	1.57	1.32	0.13	1.59	1.32	0.14	1.49	1.22	0.15	1.36	1.12	0.15

**Table 5.12. Statistical Parameters of Live Load Reactions for ADTT 2,500,  $\lambda = \mu + 1.5\sigma$**

Time Period	Span																	
	30 ft			60 ft			90 ft			120 ft			200 ft			300 ft		
	$\mu + 1.5\sigma$	$\mu$	CV	$\mu + 1.5\sigma$	$\mu$	CV	$\mu + 1.5\sigma$	$\mu$	CV	$\mu + 1.5\sigma$	$\mu$	CV	$\mu + 1.5\sigma$	$\mu$	CV	$\mu + 1.5\sigma$	$\mu$	CV
1 Day	1.18	1.00	0.12	1.02	0.88	0.10	1.07	0.90	0.12	1.04	0.89	0.11	0.93	0.78	0.13	0.79	0.66	0.13
2 Weeks	1.35	1.14	0.12	1.23	1.05	0.11	1.29	1.09	0.12	1.29	1.09	0.12	1.19	0.99	0.13	1.06	0.89	0.13
1 Month	1.38	1.17	0.12	1.26	1.08	0.11	1.35	1.14	0.12	1.34	1.13	0.12	1.23	1.02	0.14	1.12	0.93	0.14
2 Months	1.41	1.20	0.12	1.29	1.11	0.11	1.40	1.17	0.13	1.38	1.17	0.12	1.29	1.06	0.14	1.17	0.96	0.14
6 Months	1.47	1.24	0.12	1.34	1.14	0.11	1.44	1.20	0.13	1.44	1.20	0.13	1.33	1.09	0.15	1.22	1.00	0.15
1 Year	1.49	1.25	0.13	1.36	1.16	0.11	1.47	1.23	0.13	1.48	1.24	0.13	1.38	1.12	0.15	1.25	1.02	0.15
5 Years	1.55	1.29	0.13	1.44	1.21	0.12	1.55	1.29	0.13	1.54	1.28	0.13	1.43	1.17	0.15	1.31	1.08	0.15
50 Years	1.59	1.33	0.13	1.53	1.27	0.13	1.58	1.32	0.13	1.59	1.32	0.14	1.50	1.21	0.16	1.38	1.11	0.16
75 Years	1.60	1.34	0.13	1.54	1.28	0.13	1.59	1.33	0.13	1.60	1.33	0.14	1.51	1.22	0.16	1.39	1.12	0.16
100 Years	1.60	1.35	0.13	1.54	1.29	0.13	1.59	1.34	0.13	1.61	1.34	0.14	1.51	1.23	0.16	1.40	1.13	0.16

Table 5.13. Statistical Parameters of Live Load Reactions for ADTT 5,000,  $\lambda = \mu + 1.5\sigma$ 

Time Period	Span																	
	30 ft			60 ft			90 ft			120 ft			200 ft			300 ft		
	$\mu + 1.5\sigma$	$\mu$	CV	$\mu + 1.5\sigma$	$\mu$	CV	$\mu + 1.5\sigma$	$\mu$	CV	$\mu + 1.5\sigma$	$\mu$	CV	$\mu + 1.5\sigma$	$\mu$	CV	$\mu + 1.5\sigma$	$\mu$	CV
1 Day	1.25	1.05	0.12	1.09	0.94	0.11	1.14	0.96	0.13	1.12	0.94	0.13	1.02	0.84	0.14	0.90	0.74	0.14
2 Weeks	1.42	1.19	0.13	1.30	1.10	0.12	1.36	1.13	0.13	1.36	1.13	0.13	1.26	1.03	0.15	1.13	0.93	0.15
1 Month	1.46	1.22	0.13	1.34	1.13	0.12	1.39	1.16	0.13	1.40	1.17	0.13	1.30	1.06	0.15	1.18	0.96	0.15
2 Months	1.48	1.24	0.13	1.36	1.15	0.12	1.43	1.20	0.13	1.44	1.20	0.13	1.33	1.09	0.15	1.21	0.99	0.15
6 Months	1.51	1.27	0.13	1.39	1.18	0.12	1.47	1.23	0.13	1.48	1.24	0.13	1.39	1.13	0.15	1.27	1.03	0.15
1 Year	1.54	1.28	0.13	1.41	1.20	0.12	1.50	1.26	0.13	1.51	1.27	0.13	1.41	1.15	0.15	1.29	1.06	0.15
5 Years	1.58	1.32	0.13	1.48	1.25	0.12	1.54	1.30	0.12	1.56	1.30	0.13	1.46	1.19	0.15	1.34	1.09	0.15
50 Years	1.62	1.36	0.13	1.53	1.29	0.12	1.59	1.35	0.12	1.61	1.35	0.13	1.52	1.23	0.15	1.40	1.14	0.15
75 Years	1.63	1.37	0.12	1.54	1.30	0.12	1.60	1.36	0.12	1.62	1.36	0.13	1.53	1.24	0.15	1.41	1.15	0.15
100 Years	1.63	1.38	0.12	1.55	1.31	0.12	1.61	1.37	0.12	1.62	1.37	0.13	1.53	1.25	0.15	1.42	1.15	0.15

Table 5.14. Statistical Parameters of Live Load Reactions for ADTT 10,000,  $\lambda = \mu + 1.5\sigma$ 

Time Period	Span																	
	30 ft			60 ft			90 ft			120 ft			200 ft			300 ft		
	$\mu + 1.5\sigma$	$\mu$	CV	$\mu + 1.5\sigma$	$\mu$	CV	$\mu + 1.5\sigma$	$\mu$	CV	$\mu + 1.5\sigma$	$\mu$	CV	$\mu + 1.5\sigma$	$\mu$	CV	$\mu + 1.5\sigma$	$\mu$	CV
1 Day	1.31	1.10	0.13	1.20	1.00	0.13	1.23	1.03	0.13	1.21	1.01	0.13	1.11	0.91	0.14	0.98	0.81	0.14
2 Weeks	1.45	1.21	0.13	1.35	1.12	0.13	1.40	1.17	0.13	1.41	1.18	0.13	1.31	1.07	0.15	1.19	0.97	0.15
1 Month	1.48	1.24	0.13	1.39	1.16	0.13	1.43	1.20	0.13	1.45	1.21	0.13	1.36	1.10	0.15	1.24	1.00	0.15
2 Months	1.50	1.26	0.13	1.42	1.19	0.13	1.46	1.23	0.12	1.48	1.24	0.13	1.39	1.13	0.15	1.27	1.03	0.15
6 Months	1.52	1.28	0.13	1.45	1.21	0.13	1.48	1.25	0.12	1.52	1.26	0.13	1.41	1.15	0.15	1.31	1.07	0.15
1 Year	1.55	1.29	0.13	1.46	1.22	0.13	1.51	1.28	0.12	1.54	1.28	0.13	1.44	1.17	0.15	1.33	1.08	0.15
5 Years	1.60	1.34	0.13	1.50	1.26	0.13	1.55	1.31	0.12	1.59	1.33	0.13	1.49	1.22	0.15	1.37	1.12	0.15
50 Years	1.64	1.37	0.13	1.56	1.30	0.13	1.62	1.36	0.13	1.62	1.35	0.13	1.54	1.25	0.15	1.43	1.16	0.15
75 Years	1.65	1.38	0.13	1.57	1.31	0.13	1.63	1.37	0.12	1.63	1.36	0.13	1.55	1.26	0.15	1.44	1.17	0.15
100 Years	1.66	1.39	0.13	1.57	1.32	0.13	1.63	1.38	0.12	1.64	1.37	0.13	1.55	1.27	0.15	1.45	1.18	0.15

**Table 5.15. Statistical Parameters for Axle Loads,  $\lambda = \mu + 1.5\sigma$**

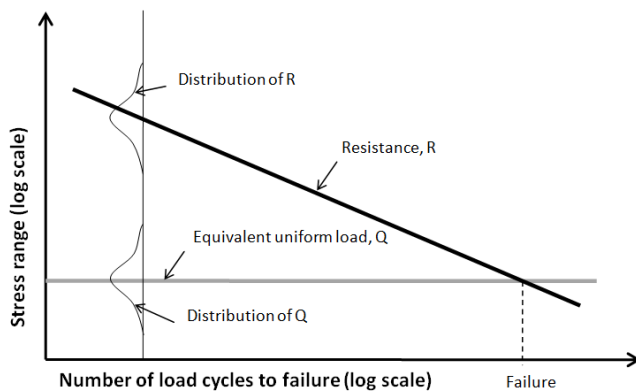
Time Period	ADTT									
	250		1,000		2,500		5,000		10,000	
	$\lambda$	CV (%)	$\lambda$	CV (%)	$\lambda$	CV (%)	$\lambda$	CV (%)	$\lambda$	CV (%)
1 Day	0.91	0.17	1.00	0.17	1.07	0.16	1.11	0.16	1.15	0.16
2 Weeks	1.09	0.16	1.17	0.16	1.24	0.15	1.29	0.15	1.32	0.15
1 Month	1.14	0.16	1.23	0.15	1.28	0.15	1.32	0.14	1.36	0.14
2 Months	1.18	0.15	1.27	0.15	1.32	0.14	1.36	0.14	1.38	0.14
6 Months	1.24	0.15	1.32	0.14	1.37	0.14	1.40	0.14	1.42	0.13
1 Year	1.30	0.14	1.37	0.14	1.41	0.13	1.42	0.13	1.45	0.13
5 Years	1.38	0.14	1.43	0.13	1.46	0.13	1.47	0.13	1.49	0.13
50 Years	1.45	0.13	1.48	0.13	1.50	0.13	1.51	0.13	1.53	0.12
75 Years	1.45	0.13	1.48	0.12	1.50	0.12	1.51	0.12	1.53	0.12
100 Years	1.46	0.13	1.49	0.12	1.51	0.12	1.52	0.12	1.53	0.12

(continued from page 112)

## 5.4 Development of Statistical Parameters of Fatigue Load

### 5.4.1 Objective

Fatigue is one of the major causes of distress in steel highway bridges. Cracking or rupture of components and connections calls for costly repairs or replacements. The durability of affected structures can be enhanced by applying reliability theory to this limit state. The limit state of fatigue is reached when accumulated load spectra exceed the fatigue resistance of material. A rational approach to the evaluation of existing bridges and design for new bridges requires knowledge of the load-carrying capacity and accumulated loads, as shown on Figure 5.25. A considerable effort was directed toward tests of materials under cyclic loading to establish the so-called *S-N* curves, where *S* is the applied stress, and *N* is the number of load applications to



**Figure 5.25. Fatigue failure on S-N curve.**

failure. However, knowledge about the real fatigue stress caused by current truck traffic, which was based on research done in the 1980s, was limited and outdated.

The current *AASHTO LRFD* (2012) has two fatigue limit states. Fatigue Limit State I is related to infinite load-induced fatigue life. The fatigue load in this limit state reflects the load levels found to be representative of the maximum stress range of the truck population for infinite fatigue life design. Fatigue Limit State II is related to finite load-induced fatigue life. The fatigue load in this limit state is intended to reflect a load level found to be representative of the effective stress range of the truck population with respect to the induced number of load cycles and their cumulative damage effects on the bridge components. Only Fatigue I applies to fatigue of concrete and the considered types of reinforcement.

The focus of this section is to develop statistical models of fatigue load based on the WIM truck survey data. The fatigue load is intended to be used in calibration of the design provisions in the *AASHTO LRFD* (2012). The WIM measurements provide an unbiased data set. The 15 WIM sites provided by FHWA are considered as representative for the United States for this analysis. Only sites with one full year of constant reading were used for fatigue analysis.

Three cases are considered: midspan moment for a simply supported bridge, moment at the interior support of a two-span continuous bridge, and moment at 0.4 of the span length of a continuous bridge. The surveyed vehicles were run over influence lines as traffic streams to determine the number and magnitude of moment cycles for a wide range of span lengths for each case. The fatigue load time history was then developed for the bending moment. The Fatigue II (finite life) load

was calculated as an equivalent moment by using the linear damage rule first proposed by Palmgren (1924) and later popularized by Miner (1945) as the Palmgren–Miner rule. The Fatigue I (infinite life) load for each location was determined by finding the highest 0.01% of the load cycles and using the smallest of them as the fatigue load for the considered location. The obtained results combined with fatigue resistance models served as the basis for the development of calibrated criteria for SLS in the *AASHTO LRFD*.

#### 5.4.2 WIM Data Used for Fatigue Calculation

To be consistent with research done by Fisher (1977), in addition to the two filters used for live load, a third filter was used to remove light trucks with GVW under 20 kips because light vehicles cause relatively low fatigue damage. A summary of the data used for fatigue analysis, including WIM locations, number of records, and ADTT, is shown in Table 5.16.

#### 5.4.3 Truck Traffic Simulation and Calculation of Bending Moment Time History

Live load on bridges is caused mainly by moving trucks. Longer bridges often experience more than one vehicle in one span at the same time. Multiple vehicles in one span produce a larger load effect than a single truck. For fatigue load calculations, it

**Table 5.16. WIM Locations and Number of Vehicles Used for Fatigue Analysis**

Site	No. of Days in Data	Total No. of Truck Records	Single-Lane ADTT
Arizona (SPS-1)	365	26,501	97
Arizona (SPS-2)	365	1,391,098	3,919
Arkansas (SPS-2)	365	1,642,334	4,590
Colorado (SPS-2)	365	326,017	941
Delaware (SPS-1)	365	175,889	553
Illinois (SPS-6)	365	821,809	2,340
Kansas (SPS-2)	365	456,881	1,309
Louisiana (SPS-1)	365	70,831	235
Maine (SPS-5)	365	172,333	503
Maryland (SPS-5)	365	124,474	450
Minnesota (SPS-5)	365	47,794	152
Pennsylvania (SPS-6)	365	1,458,818	4,098
Tennessee (SPS-6)	365	1,583,151	4,445
Virginia (SPS-1)	365	237,804	710
Wisconsin (SPS-1)	365	209,239	622

is very important to find the largest load cycles, because they cause the major fatigue damage. Experimental studies showed that there is a linear relationship between the magnitude of load cycle and fatigue damage. *S-N* curves for fatigue load tests show a log-log relationship between the cycle amplitude and the number of cycles to failure. This relationship is reflected in the Palmgren–Miner formula for equivalent load, shown as Equations 5.13 and 5.14.

Recent WIM data provide much more complex and more accurate information about measured trucks. The WIM data include not only axle loads and spacing between axles, but also truck speed and time of measurement with an accuracy of 1 s. Using these data, the team simulated truck traffic on a bridge for a 1-year period, and the time history of the bending moment was recorded. This allowed calculation of the load effect due to the presence of multiple trucks. Calculations were carried out for span lengths from 30 to 200 ft. The considered continuous bridges had two equal-length spans. Examples of moment time histories for a single truck passage are shown in Figure 5.26, Figure 5.27, and Figure 5.28.

#### 5.4.4 Rainflow Cycle-Counting Method

The development of fatigue load models requires a collection of the actual load time histories. The collected time histories must be processed to obtain a usable form. In general, load histories may be considered as either narrow-band or wide-band processes, as shown in Figure 5.29. Narrow-band time histories are characterized by an approximately constant period. Wide-band time histories are characterized by a variable frequency and random amplitude. For fatigue calculations, the stress range is determined (i.e., the difference between peak and valley).

Bending moment histories due to truck passages are wide band. The cycles are irregular with variable frequencies and amplitudes. Wide-band histories do not allow for simple cycle counting. The Palmgren–Miner rule is applicable only when the individual events are isolated, (i.e., narrow-band time histories). Different counting procedures have been proposed and used, all of which were studied and compared to select the most efficient approach for this study. Only two counting algorithms seemed to provide accurate results: rainflow and range pair (Dowling 1972). Rainflow counting was used in this study.

A rainflow cycle-counting procedure was proposed for the first time by Matsuishi and Endo in 1968. This method counts the number of full reversal cycles, as well as partial cycles, and their range amplitude for a given load time history. A full reversal cycle occurs when the cycle range goes up to its peak and back to the starting position. A partial cycle goes in only one direction, from the valley to the peak or from the peak to the valley.

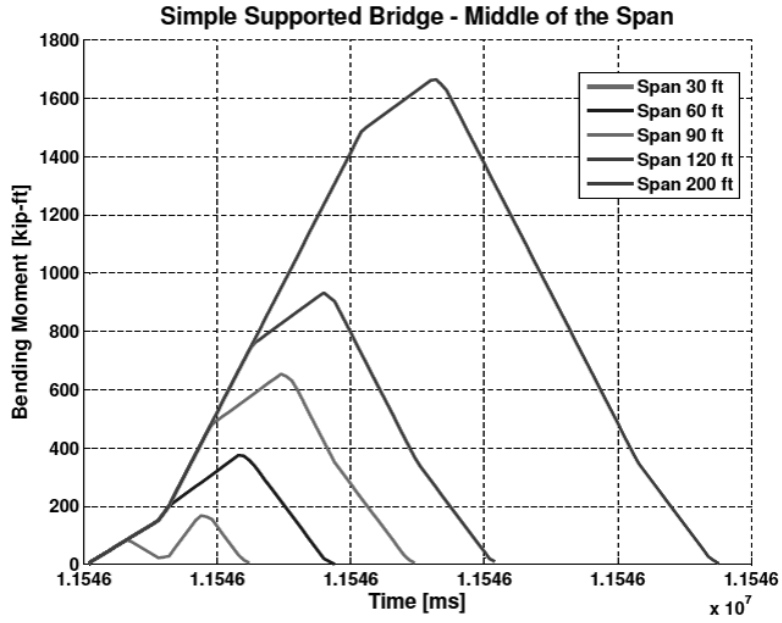


Figure 5.26. Bending moment time history for a single truck passage on simple-supported bridges at middle of the span.

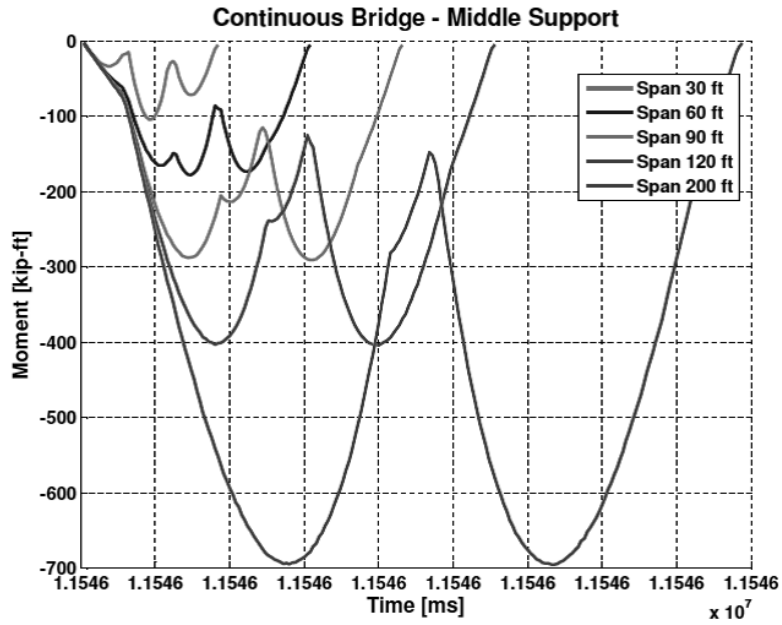
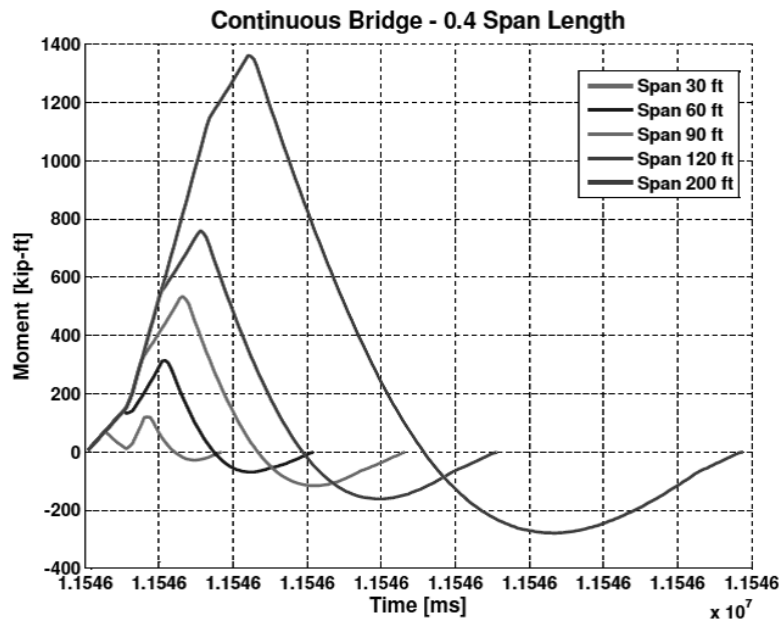


Figure 5.27. Bending moment time history for a single truck passage on continuous bridges at middle support.



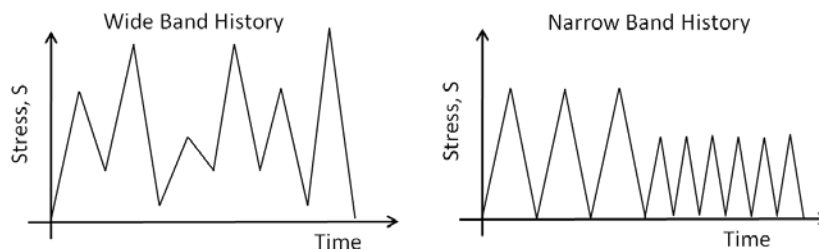
**Figure 5.28. Bending moment time history for a single truck passage on continuous bridges at 0.4 of the span length.**

The summary of the steps in rainflow cycle counting are as follows:

1. Reduce the time history to a sequence of (tensile) peaks and (compressive) troughs.
2. Imagine that the time history is a template for a rigid sheet (pagoda roof).
3. Turn the sheet clockwise  $90^\circ$  (earliest time to the top).
4. Each tensile peak is imagined as a source of water that “drips” down the pagoda.
5. Count the number of half-cycles by looking for terminations in the flow occurring when
  - It reaches the end of the time history (Figure 5.30, Path 3-4-end or Path 4-5-7-9-11-end);
  - It merges with a flow that started at an earlier tensile peak; or
  - It flows opposite a tensile peak of greater magnitude (Figure 5.30, Path 5-6, 6-6', 8-8', or 10-10').
6. Repeat Step 5 for compressive troughs.

7. Assign a magnitude to each half-cycle equal to the stress difference between its start and termination (Table 5.17).
8. Pair up half-cycles of identical magnitude to count the number of complete cycles (Table 5.18). Typically, there are some residual half-cycles (Downing and Socie 1982).

The moment time histories obtained from the truck traffic simulation for each WIM site, span length, and case were processed using the rainflow counting method. Total number of cycles was divided by number of trucks in the database to get an average number of load cycles per truck passage. The results for the simple-span case are summarized in Table 5.19, for the negative moment over the support in continuous spans in Table 5.20, and for positive moment at 0.4 of the span length in continuous bridges in Table 5.21. For simply supported bridges, the number of cycles at the midspan was 2 to 2.5 cycles per truck passage for short spans; this value dropped linearly to 1 cycle for a span length of about 100 ft. Similarly, for continuous bridges at 0.4 of the span length, the



**Figure 5.29. Wide-band versus narrow-band history.**



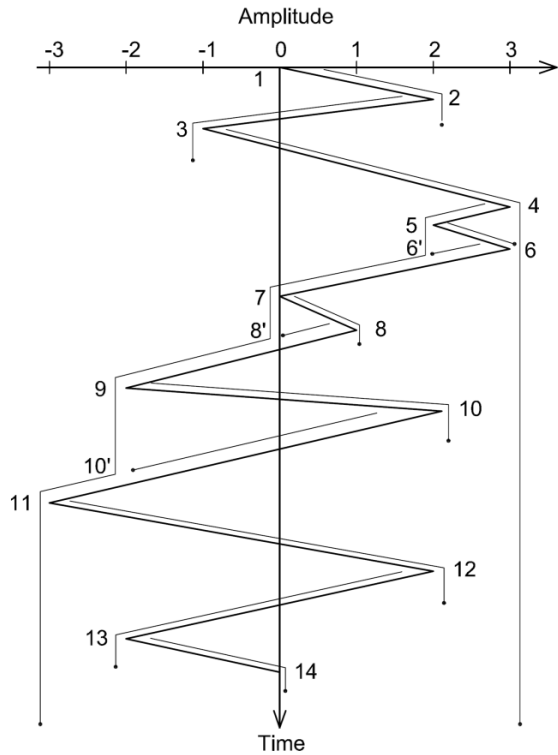


Figure 5.30. Rainflow counting diagram.

Table 5.17. Half-Cycles After Rainflow Counting

Positive Direction		Negative Direction	
Range	Amplitude	Range	Amplitude
1-2	2	2-3	3
3-4-end	4	4-5-7-9-11-end	6
5-6	1	6-6'	1
7-8	1	8-8'	1
9-10	4	10-10'	4
11-12	5	12-13	4
13-14	2	-	-

Note: For range values, see Figure 5.30; - = no further negative direction values.

Table 5.18. Load Cycles After Rainflow Counting

Amplitude	No. of Cycles
1	2
2	1
3	0.5
4	2
5	0.5
6	0.5

Table 5.19. Total Number of Load Cycles and Average Number of Load Cycles per Truck Passage for Simply Supported Bridges at the Midspan

Site	No. of Vehicles	No. of Cycles					No. of Cycles per Truck				
		30 ft	60 ft	90 ft	120 ft	200 ft	30 ft	60 ft	90 ft	120 ft	200 ft
Arizona (SPS-1)	26,501	59,427.5	36,397	27,321	26,505	26,501	2.24	1.37	1.03	1.00	1.00
Arizona (SPS-2)	1,391,098	3,667,719.5	2,632,482.5	1,650,818.0	1,407,468.0	1,397,629.5	2.64	1.89	1.19	1.01	1.00
Arkansas (SPS-2)	1,642,334	4,216,668.5	3,108,866.5	1,983,249.5	1,667,856.0	1,640,182.5	2.57	1.89	1.21	1.02	1.00
Colorado (SPS-2)	326,017	824,366.5	591,565.5	377,138.0	328,271.0	327,680.5	2.53	1.81	1.16	1.01	1.01
Delaware (SPS-1)	175,889	391,173.0	272,989.0	184,061.0	176,696.5	175,664.5	2.22	1.55	1.05	1.00	1.00
Illinois (SPS-6)	821,809	2,104,493.5	1,552,007.5	990,256.0	831,086.0	823,435.0	2.56	1.89	1.20	1.01	1.00
Kansas (SPS-2)	456,881	1,182,596.0	839,726.0	542,967.5	460,973.5	459,671.5	2.59	1.84	1.19	1.01	1.01
Louisiana (SPS-1)	70,831	162,679.5	113,121.5	74,619.5	70,947.0	70,838.0	2.30	1.60	1.05	1.00	1.00
Maine (SPS-5)	172,333	417,837.5	294,010.5	185,121.0	173,174.0	172,727.0	2.42	1.71	1.07	1.00	1.00

(continued on next page)

**Table 5.19. Total Number of Load Cycles and Average Number of Load Cycles per Truck Passage for Simply Supported Bridges at the Midspan (continued)**

Site	No. of Vehicles	No. of Cycles					No. of Cycles per Truck				
		30 ft	60 ft	90 ft	120 ft	200 ft	30 ft	60 ft	90 ft	120 ft	200 ft
Maryland (SPS-5)	124,474	271,233.5	186,120.0	129,968.0	124,930.5	124,482.0	2.18	1.50	1.04	1.00	1.00
Minnesota (SPS-5)	47,794	96,065.0	68,750.0	48,829.0	47,798.0	47,752.0	2.01	1.44	1.02	1.00	1.00
Pennsylvania (SPS-6)	1,458,818	3,669,978.0	2,667,443.0	1,676,101.0	1,477,196.0	1,459,284.0	2.52	1.83	1.15	1.01	1.00
Tennessee (SPS-6)	1,583,151	3,492,829.0	2,816,652.0	1,673,936.0	1,600,563.0	1,583,300.0	2.21	1.78	1.06	1.01	1.00
Virginia (SPS-1)	237,804	563,467.5	416,252.5	260,806.0	239,251.0	238,315.0	2.37	1.75	1.10	1.01	1.00
Wisconsin (SPS-1)	209,239	483,546.0	366,955.0	225,109.0	210,644.0	210,164.5	2.31	1.75	1.08	1.01	1.00

**Table 5.20. Total Number of Load Cycles and Average Number of Load Cycles per Truck Passage for Continuous Bridges at the Middle Support**

Site	No. of Vehicles	No. of Cycles					No. of Cycles per Truck				
		30 ft	60 ft	90 ft	120 ft	200 ft	30 ft	60 ft	90 ft	120 ft	200 ft
Arizona (SPS-1)	26,501	65,563.5	64,115.5	69,703.5	65,402	58,905	2.47	2.42	2.63	2.47	2.22
Arizona (SPS-2)	1,391,098	4,584,915.0	4,804,207.0	4,971,600.0	4,220,277.5	3,423,766.0	3.30	3.45	3.57	3.03	2.46
Arkansas (SPS-2)	1,642,334	5,437,711.0	5,654,802.0	5,774,335.5	4,949,930.5	3,902,161.0	3.31	3.44	3.52	3.01	2.38
Colorado (SPS-2)	326,017	1,020,374.5	989,200.0	1,100,728.5	983,802.0	767,937.0	3.13	3.03	3.38	3.02	2.36
Delaware (SPS-1)	175,889	543,754.5	502,112.5	527,143.0	484,787.5	419,294.5	3.09	2.85	3.00	2.76	2.38
Illinois (SPS-6)	821,809	2,716,902.0	2,768,327.0	2,836,337.0	2,489,643.5	1,987,891.5	3.31	3.37	3.45	3.03	2.42
Kansas (SPS-2)	456,881	1,505,890.5	1,507,880.5	1,608,769.0	1,387,383.0	1,116,965.5	3.30	3.30	3.52	3.04	2.44
Louisiana (SPS-1)	70,831	217,990.0	199,088.0	215,738.0	200,995.5	166,450.5	3.08	2.81	3.05	2.84	2.35
Maine (SPS-5)	172,333	518,377.5	502,246.5	558,181.0	508,993.0	383,351.5	3.01	2.91	3.24	2.95	2.22
Maryland (SPS-5)	124,474	397,197.5	346,614.5	376,056.5	342,106.5	290,348.0	3.19	2.78	3.02	2.75	2.33
Minnesota (SPS-5)	47,794	135,741.0	131,289.0	139,940.0	123,124.0	107,837.0	2.84	2.75	2.93	2.58	2.26
Pennsylvania (SPS-6)	1,458,818	3,896,713.0	3,604,125.0	4,019,137.0	3,955,368.0	3,174,582.0	2.67	2.47	2.76	2.71	2.18
Tennessee (SPS-6)	1,583,151	4,298,789.0	3,889,255.0	4,468,069.0	4,346,233.0	3,427,878.0	2.72	2.46	2.82	2.75	2.17
Virginia (SPS-1)	237,804	743,162.0	716,559.5	770,125.5	700,670.5	561,742.5	3.13	3.01	3.24	2.95	2.36
Wisconsin (SPS-1)	209,239	646,250.5	633,403.0	657,828.5	608,381.0	492,283.5	3.09	3.03	3.14	2.91	2.35

**Table 5.21. Total Number of Load Cycles and Average Number of Load Cycles per Truck Passage for Continuous Bridges at 0.4 of the Span Length**

Site	No. of Vehicles	No. of Cycles					No. of Cycles per Truck				
		30 ft	60 ft	90 ft	120 ft	200 ft	30 ft	60 ft	90 ft	120 ft	200 ft
Arizona (SPS-1)	26,501	68,688.0	39,328.0	29,363.0	27,695.0	26,509.0	2.59	1.48	1.11	1.05	1.00
Arizona (SPS-2)	1,391,098	4,032,130.0	2,699,800.5	2,281,797.0	2,017,321.5	1,767,920.0	2.90	1.94	1.64	1.45	1.27
Arkansas (SPS-2)	1,642,334	5,610,372.0	4,069,843.0	3,532,308.0	3,132,234.0	2,872,888.0	3.42	2.48	2.15	1.91	1.75
Colorado (SPS-2)	326,017	885,651.0	617,440.5	458,136.5	410,761.5	385,205.5	2.72	1.89	1.41	1.26	1.18
Delaware (SPS-1)	175,889	410,830.0	293,946.0	223,028.5	210,104.0	199,350.0	2.34	1.67	1.27	1.19	1.13
Illinois (SPS-6)	821,809	2,304,196.0	1,579,655.0	1,313,036.5	1,118,188.0	1,037,709.5	2.80	1.92	1.60	1.36	1.26
Kansas (SPS-2)	456,881	1,292,694.0	872,400.0	702,959.5	616,645.0	554,203.0	2.83	1.91	1.54	1.35	1.21
Louisiana (SPS-1)	70,831	171,703.5	120,584.5	91,168.0	85,553.5	80,458.0	2.42	1.70	1.29	1.21	1.14
Maine (SPS-5)	172,333	433,793.5	313,517.0	231,617.0	204,775.5	190,443.0	2.52	1.82	1.34	1.19	1.11
Maryland (SPS-5)	124,474	279,856.5	200,955.5	155,882.5	143,168.0	138,347.5	2.25	1.61	1.25	1.15	1.11
Minnesota (SPS-5)	47,794	123,298.0	70,383.5	59,891.5	52,727.5	48,541.5	2.58	1.47	1.25	1.10	1.02
Pennsylvania (SPS-6)	1,458,818	3,992,907.0	2,784,565.0	2,243,835.5	1,943,551.0	1,756,756.0	2.74	1.91	1.54	1.33	1.20
Tennessee (SPS-6)	1,583,151	4,590,126.0	2,929,061.5	2,273,958.5	1,888,805.5	1,651,117.5	2.90	1.85	1.44	1.19	1.04
Virginia (SPS-1)	237,804	599,977.0	434,778.0	338,100.0	299,309.0	278,883.5	2.52	1.83	1.42	1.26	1.17
Wisconsin (SPS-1)	209,239	516,843.0	376,098.5	298,936.5	267,981.0	246,176.0	2.47	1.80	1.43	1.28	1.18

number of cycles per truck was 2.3 to 3.5 for short spans, which dropped to 1 to 1.5 cycles for a span length of about 100 ft. The results for negative moment over the support in continuous bridges were 2.5 to 3.5 for short spans and about 2.5 for longer spans. More load cycles for short spans is caused by groups of axles rather than whole trucks due to relatively short spans compared with the vehicle length.

#### 5.4.5 Fatigue Damage Accumulation and Equivalent Fatigue Load

Because bridge structures are subjected to loads of different magnitude and frequency occurring at different times, the load can be considered as a randomly varying amplitude load. The effect of such a loading can be accounted for by

applying a cumulative damage rule. Many rules have been proposed. According to the Palmgren–Miner rule, which seems to provide a reasonable means of accounting for random variable loading, fatigue damage due to variable amplitude loading is expressed by Equation 5.8:

$$\frac{n_1}{N_1} + \frac{n_2}{N_2} + \frac{n_3}{N_3} + \dots + \frac{n_n}{N_n} = \sum \frac{n_i}{N_i} = 1 \quad (5.8)$$

where  $n_i/N_i$  is the incremental damage that results from the stress range cycles with magnitude  $S_i$  that occurs  $n_i$  times (Figure 5.31), and  $N_i$  is the number of cycles to failure with a constant amplitude equal to  $S_i$  (Figure 5.32). Failure occurs when the sum of the incremental damage equals or exceeds 1. The tests of welded details (Fisher et al. 1983; Schilling et al.

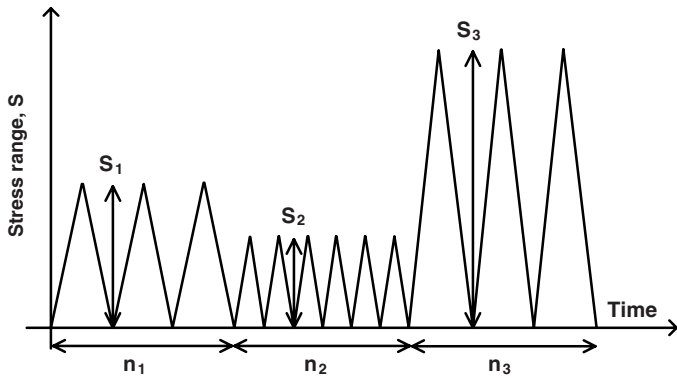


Figure 5.31. Number of cycles  $n_i$  for stress range  $S_i$ .

1977) and Barsom's crack growth studies (Rolfe and Barsom 1977) showed a good correlation with the Palmgren–Miner rule assumptions.

Schilling et al. (1977) showed that the Palmgren–Miner rule can be used to develop an equivalent constant amplitude cyclic loading that produces the same fatigue damage as a variable amplitude load for the same number of load cycles. This theory is based on the exponential model of the stress range–life relationship as given by Equation 5.9 (Fisher 1977):

$$N = AS^{-n} \quad (5.9)$$

where

- $N$  = number of cycles to failure;
- $S$  = nominal stress range;
- $A$  = a constant for a given detail; and
- $n$  = slope constant.

The concept of fatigue design based on stress range alone was adopted by AASHTO in 1974 (Fisher et al. 1970, 1974). Equation 5.10 is obtained by substituting Equation 5.9 into Equation 5.8:

$$\sum \frac{n_i}{AS_i^{-n}} = 1 \quad (5.10)$$

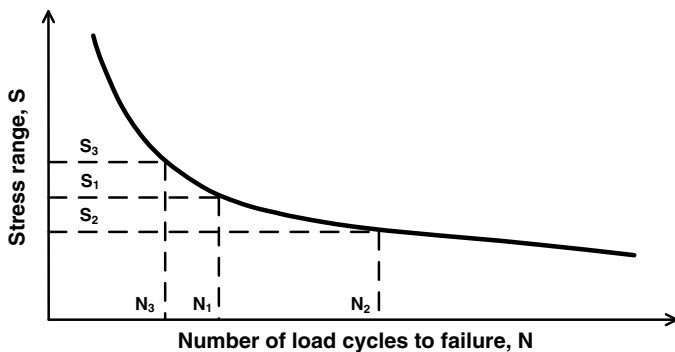


Figure 5.32. Number of load cycles to failure  $N_i$  for stress range  $S_i$ .

Substituting Equation 5.11 into Equation 5.10 yields

$$n_i = p_i N_T \quad (5.11)$$

$$\sum \frac{p_i N_T}{AS_i^{-n}} = \sum \frac{p_i S_e^{-n}}{AS_i^{-n}} = 1 \quad (5.12)$$

$$\text{or } S_e^n = \sum p_i S_i^n$$

$$S_e = \sqrt[n]{\sum p_i S_i^n} \quad (5.13)$$

The exponent  $n$  for most structural metal details is about 3. Equation 5.13 is often referred to as a root mean cube of the stress distribution. The equivalent stress is a convenient concept to be used for comparison of stress histograms obtained using the rainflow counting method.

Because fatigue crack nucleation and further propagation occur mostly at tensile stress conditions that are related to bending moment, it is convenient to use the bending moment formulation instead of the stress formulation for an equivalent load. The bending moment formulation of Equation 5.13 is given by Equation 5.14:

$$M_{eq} = \sqrt[n]{\sum p_i M_i^n} \quad (5.14)$$

where

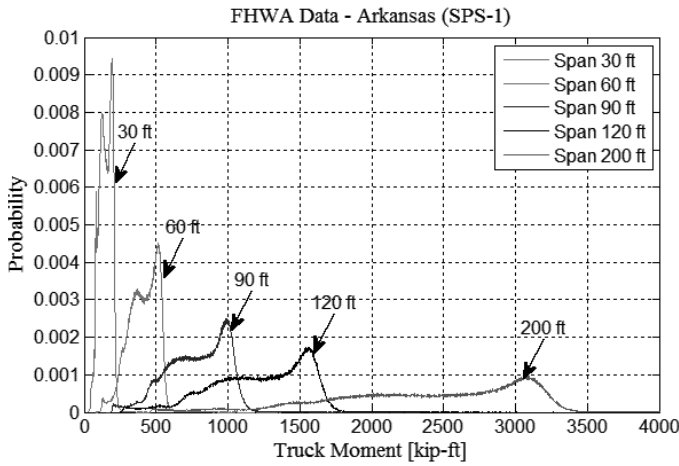
- $M_{eq}$  = equivalent moment cycle load;
- $M_i$  = incremental moment cycle; and
- $p_i$  = probability of occurrence of  $M_i$ .

Calculation of the equivalent moment requires the probability of occurrence for each incremental moment  $M_i$ . The corresponding probability distribution functions (PDFs) of the moment cycles for each site were calculated for spans from 30 to 200 ft. As an example, the PDFs for moments corresponding to the FHWA WIM data from Arkansas (SPS-1) are shown in Figure 5.33. The area under the curve representing the PDF for each span length is equal to 1.

The equivalent moment was calculated from moment cycles obtained using rainflow counting. The equivalent load was calculated for all considered WIM sites, a wide range of span lengths between 30 and 200 ft, and three bridge configurations. Next, the calculated equivalent moments were divided by moment due to the AASHTO LRFD fatigue truck. Results are summarized in Table 5.22 to Table 5.24. The results show that the moment ratio is smaller for short spans.

#### 5.4.6 Fatigue Limit State II: Fatigue Damage Ratio

Finite fatigue life depends on the number of load cycles during the service life and their magnitude. According to the AASHTO LRFD (2012) provisions, the number of load cycles



**Figure 5.33. PDFs of WIM moments for data from Arkansas (SPS-1).**

during bridge service life ( $N$ ) is calculated using Equation 6.6.1.2.5-3, shown here as Equation 5.15:

$$N = (365)(75)n(ADTT)_{SL} \tag{5.15}$$

where  $(ADTT)_{SL}$  is a single lane of ADTT, and  $n$  is the number of load cycles per truck taken from Table 5.25 [AASHTO LRFD (2012, Table 6.6.1.2.5-2)].

The magnitude of load cycles is calculated as a stress due to the HL-93 fatigue truck with the second axle spacing equal to

30 ft. To compare fatigue damage due to design fatigue load and actual fatigue load, it is convenient to remove the resistance part from limit state Equations 5.16, 5.17, and 5.18 [AASHTO LRFD (2012, Equations 6.6.1.2.5-1 and 6.6.1.2.5-2)]:

$$\gamma(\Delta f) \leq (\Delta F)_n \tag{5.16}$$

$$(\Delta F)_n = \sqrt[3]{\frac{A}{N}} \tag{5.17}$$

$$\gamma(\Delta f) \leq \sqrt[3]{\frac{A}{N}} \tag{5.18}$$

where

$\gamma$  = load factor;

$\Delta f$  = force effect (i.e., live load stress range due to the passage of a fatigue truck);

$A$  = resistance constant that depends on the class of the structural detail; and

$N$  = number of load cycles during the service life calculated according to Equation 5.15.

Stress due to truck passage is calculated according to Equation 5.19:

$$\Delta f = M/S \tag{5.19}$$

where  $S$  is section modulus and  $M$  is moment due to truck passage.

**Table 5.22. Equivalent Moments for Simply Supported Bridges at the Midspan**

Site	No. of Vehicles	Equivalent Moment (kip-ft)					Equivalent Moment/HL-93 Fatigue Moment				
		30 ft	60 ft	90 ft	120 ft	200 ft	30 ft	60 ft	90 ft	120 ft	200 ft
Arizona (SPS-1)	26,501	151.63	426.18	889.67	1,362.17	2,593.90	0.62	0.78	0.82	0.84	0.85
Arizona (SPS-2)	1,391,098	145.82	357.81	790.59	1,316.93	2,601.01	0.60	0.66	0.73	0.81	0.85
Arkansas (SPS-2)	1,642,334	146.25	354.83	770.41	1,290.54	2,554.63	0.60	0.65	0.71	0.79	0.83
Colorado (SPS-2)	326,017	132.61	325.49	713.45	1,173.08	2,311.31	0.54	0.60	0.66	0.72	0.75
Delaware (SPS-1)	175,889	155.16	400.92	831.01	1,270.55	2,424.36	0.64	0.74	0.77	0.78	0.79
Illinois (SPS-6)	821,809	146.48	354.91	762.76	1,279.33	2,532.79	0.60	0.65	0.70	0.79	0.83
Kansas (SPS-2)	456,881	141.00	355.18	767.58	1,277.57	2,524.67	0.58	0.65	0.71	0.79	0.82
Louisiana (SPS-1)	70,831	142.42	363.30	775.00	1,202.37	2,318.98	0.58	0.67	0.72	0.74	0.76
Maine (SPS-5)	172,333	129.72	328.38	707.39	1,126.24	2,206.36	0.53	0.60	0.65	0.69	0.72
Maryland (SPS-5)	124,474	132.44	335.88	675.87	1,033.81	1,982.63	0.54	0.62	0.62	0.64	0.65
Minnesota (SPS-5)	47,794	142.39	353.48	731.81	1,138.96	2,219.99	0.58	0.65	0.68	0.70	0.72
Pennsylvania (SPS-6)	1,458,818	151.46	363.23	777.74	1,259.78	2,468.70	0.62	0.67	0.72	0.78	0.81
Tennessee (SPS-6)	1,583,151	153.14	351.05	772.72	1,227.46	2,417.64	0.63	0.65	0.71	0.76	0.79
Virginia (SPS-1)	237,804	140.35	344.56	749.93	1,202.76	2,356.27	0.58	0.63	0.69	0.74	0.77
Wisconsin (SPS-1)	209,239	142.47	360.19	772.69	1,213.03	2,349.64	0.58	0.66	0.71	0.75	0.77

**Table 5.23. Equivalent Moments for Continuous Bridges at the Middle Support**

Site	No. of Vehicles	Equivalent Moment (kip-ft)					Equivalent Moment/HL-93 Fatigue Moment				
		30 ft	60 ft	90 ft	120 ft	200 ft	30 ft	60 ft	90 ft	120 ft	200 ft
Arizona (SPS-1)	26,501	-96.91	-212.79	-314.01	-483.56	-960.50	0.53	0.59	0.59	0.63	0.72
Arizona (SPS-2)	1,391,098	-89.91	-221.06	-296.65	-454.32	-975.62	0.49	0.61	0.56	0.60	0.73
Arkansas (SPS-2)	1,642,334	-87.98	-219.14	-294.68	-450.44	-998.99	0.48	0.61	0.56	0.59	0.74
Colorado (SPS-2)	326,017	-82.94	-203.52	-268.50	-407.76	-844.78	0.45	0.56	0.51	0.54	0.63
Delaware (SPS-1)	175,889	-90.38	-214.99	-299.91	-451.62	-896.29	0.49	0.60	0.57	0.59	0.67
Illinois (SPS-6)	821,809	-87.55	-219.79	-295.45	-444.61	-964.62	0.48	0.61	0.56	0.58	0.72
Kansas (SPS-2)	456,881	-85.97	-216.73	-290.84	-439.49	-916.36	0.47	0.60	0.55	0.58	0.68
Louisiana (SPS-1)	70,831	-86.45	-205.76	-280.85	-423.51	-858.73	0.47	0.57	0.53	0.56	0.64
Maine (SPS-5)	172,333	-79.39	-198.30	-262.39	-393.39	-825.92	0.43	0.55	0.50	0.52	0.62
Maryland (SPS-5)	124,474	-79.35	-192.49	-263.24	-403.19	-814.86	0.43	0.53	0.50	0.53	0.61
Minnesota (SPS-5)	47,794	-79.86	-201.32	-270.79	-405.61	-814.03	0.43	0.56	0.51	0.53	0.61
Pennsylvania (SPS-6)	1,458,818	-90.89	-235.11	-310.77	-449.53	-974.43	0.49	0.65	0.59	0.59	0.73
Tennessee (SPS-6)	1,583,151	-87.39	-231.37	-300.99	-436.22	-961.13	0.48	0.64	0.57	0.57	0.72
Virginia (SPS-1)	237,804	-84.56	-208.61	-278.84	-418.94	-868.36	0.46	0.58	0.53	0.55	0.65
Wisconsin (SPS-1)	209,239	-83.68	-206.92	-285.18	-422.87	-860.95	0.45	0.57	0.54	0.56	0.64

**Table 5.24. Equivalent Moments for Continuous Bridges at 0.4 of the Span Length**

Site	No. of Vehicles	Equivalent Moment (kip-ft)					Equivalent Moment/HL-93 Fatigue Moment				
		30 ft	60 ft	90 ft	120 ft	200 ft	30 ft	60 ft	90 ft	120 ft	200 ft
Arizona (SPS-1)	26,501	134.25	413.51	838.11	1,291.21	2,503.65	0.55	0.71	0.76	0.80	0.83
Arizona (SPS-2)	1,391,098	133.46	349.66	663.89	1,096.11	2,282.14	0.54	0.60	0.60	0.68	0.75
Arkansas (SPS-2)	1,642,334	122.64	272.45	540.68	899.92	1,881.91	0.50	0.47	0.49	0.55	0.62
Colorado (SPS-2)	326,017	121.69	317.11	634.34	1,032.34	2,101.21	0.49	0.54	0.58	0.64	0.69
Delaware (SPS-1)	175,889	144.84	386.50	743.25	1,143.10	2,230.39	0.59	0.66	0.68	0.70	0.74
Illinois (SPS-6)	821,809	135.47	345.78	657.19	1,091.43	2,222.58	0.55	0.59	0.60	0.67	0.73
Kansas (SPS-2)	456,881	129.86	342.26	665.25	1,095.22	2,272.29	0.53	0.58	0.61	0.68	0.75
Louisiana (SPS-1)	70,831	131.42	353.55	691.10	1,076.33	2,130.97	0.53	0.60	0.63	0.66	0.70
Maine (SPS-5)	172,333	121.26	312.87	618.65	1,008.24	2,050.51	0.49	0.53	0.56	0.62	0.68
Maryland (SPS-5)	124,474	126.68	339.42	654.83	1,023.41	1,994.36	0.52	0.58	0.60	0.63	0.66
Minnesota (SPS-5)	47,794	120.71	344.34	655.63	1,054.97	2,132.90	0.49	0.59	0.60	0.65	0.70
Pennsylvania (SPS-6)	1,458,818	135.74	352.48	668.88	1,087.55	2,204.49	0.55	0.60	0.61	0.67	0.73
Tennessee (SPS-6)	1,583,151	128.44	339.17	665.81	1,104.94	2,275.40	0.52	0.58	0.61	0.68	0.75
Virginia (SPS-1)	237,804	130.01	334.69	649.10	1,055.60	2,142.89	0.53	0.57	0.59	0.65	0.71
Wisconsin (SPS-1)	209,239	133.10	349.47	666.43	1,061.17	2,138.88	0.54	0.60	0.61	0.65	0.71



**Table 5.25. Number of Cycles per Truck Passage (n) for AASHTO Fatigue Design**

Longitudinal Members	n	
	Span Length >40 ft	Span Length ≤40 ft
Simple-span girders	1.0	2.0
Continuous girders	Near interior support	1.5
	Elsewhere	1.0

To calculate the ratio of fatigue damage caused by the actual fatigue load and design fatigue load, the load factor has to be removed from Equation 5.18. From Equations 5.18 and 5.19, it is possible to calculate the ratio of fatigue damage due to the actual load and fatigue damage due to design load by using Equation 5.20:

#### Boundary of Actual Fatigue Damage

$$S \frac{M_{eq}}{S} = \sqrt[3]{\frac{A}{N_R}}$$

where

$M_{eq}$  = equivalent moment from Miner's Rule;

A = resistance constant; and

$N_R$  = actual number of cycles.

$$1 = \sqrt[3]{\frac{A}{N_R}} * \frac{S}{M_{eq}}$$

#### Boundary of Code Fatigue Damage

$$S \frac{M}{S} = \sqrt[3]{\frac{A}{N}}$$

where

M = moment due to fatigue design truck;

A = resistance constant; and

N = number of cycles (from Equation 5.15).

$$1 = \sqrt[3]{\frac{A}{N}} * \frac{S}{M}$$

$$\sqrt[3]{\frac{A}{N_R}} * \frac{S}{M_{eq}} = \sqrt[3]{\frac{A}{N}} * \frac{S}{M}$$

$$\lambda = \sqrt[3]{\frac{A}{N} * \frac{N_R}{A}} * \frac{SM_{eq}}{SM}$$

$$\lambda = \sqrt[3]{\frac{N_R}{N}} * \frac{M_{eq}}{M} \quad (5.20)$$

$\lambda$  is the ratio of the fatigue damage due to the *actual* fatigue load to the fatigue damage due to the *design* fatigue load. Because resistance was removed from Equation 5.20, the fatigue damage ratio is the same regardless of the bridge component or detail class.

The fatigue damage ratio was calculated according to the current AASHTO LRFD provisions for each WIM site, span length, and case. Results are summarized in Table 5.27 to Table 5.29 in the column labeled Fatigue Damage Ratio (current). The fatigue damage ratio is smaller for shorter spans. The difference between short and longer spans is due to different code provisions for short spans with a given number of load cycles per truck passage (see Table 5.25). For short spans, a truck causes more load cycles than for longer spans. However, it is balanced by a smaller moment ratio (equivalent moment/HL-93 fatigue truck moment) for short spans. If the number of load cycles due to a truck passage were equal for all spans, as shown in Table 5.26, then the resulting fatigue damage ratio would be more uniform.

The fatigue damage ratio for the proposed fatigue design was calculated for each WIM site, span length, and case. The results are summarized in Table 5.27 to Table 5.29 in the column labeled Fatigue Damage Ratio (proposed). For simply supported bridges at midspan and continuous bridges at 0.4 of the span length, the results are very uniform for all span lengths. At the middle support of continuous bridges, the difference between short and longer spans is reduced by about 10%.

Because fatigue resistance depends on structural detail and material characteristics but not on span length, the variation in fatigue load due to span length produces a variation in reliability indices. The design parameters proposed in Section 5.4.9 eliminate this problem.

#### 5.4.7 Fatigue Limit State I: Maximum Moment Range Ratio

Fatigue Limit State I is related to an infinite load-induced fatigue life. The fatigue load in this limit state reflects the load levels found to be representative of the maximum stress range of the truck population for an infinite fatigue life design (AASHTO LRFD 2012). In other words, if the majority of stress cycles are below a threshold magnitude  $[(\Delta F)_{TH}]$ , then failure will require so many load cycles that the considered detail will have an infinite fatigue life.  $(\Delta F)_{TH}$  is a boundary between the finite and infinite fatigue life, as shown in Figure 5.34.

**Table 5.26. Number of Cycles per Truck Passage (n) for Proposed Fatigue Design**

Longitudinal Members	n	
Simple-span girders	1.0	
Continuous girders	Near interior support	1.5
	Elsewhere	1.0

**Table 5.27. Fatigue Damage Ratios for Simply Supported Bridges at the Midspan**

Site	No. of Vehicles	Fatigue Damage Ratio (current)					Fatigue Damage Ratio (proposed)				
		30 ft	60 ft	90 ft	120 ft	200 ft	30 ft	60 ft	90 ft	120 ft	200 ft
Arizona (SPS-1)	26,501	0.65	0.87	0.83	0.84	0.85	0.81	0.87	0.83	0.84	0.85
Arizona (SPS-2)	1,391,098	0.66	0.81	0.77	0.81	0.85	0.83	0.81	0.77	0.81	0.85
Arkansas (SPS-2)	1,642,334	0.65	0.81	0.76	0.80	0.83	0.82	0.81	0.76	0.80	0.83
Colorado (SPS-2)	326,017	0.59	0.73	0.69	0.72	0.76	0.74	0.73	0.69	0.72	0.76
Delaware (SPS-1)	175,889	0.66	0.85	0.78	0.78	0.79	0.83	0.85	0.78	0.78	0.79
Illinois (SPS-6)	821,809	0.65	0.81	0.75	0.79	0.83	0.82	0.81	0.75	0.79	0.83
Kansas (SPS-2)	456,881	0.63	0.80	0.75	0.79	0.83	0.79	0.80	0.75	0.79	0.83
Louisiana (SPS-1)	70,831	0.61	0.78	0.73	0.74	0.76	0.77	0.78	0.73	0.74	0.76
Maine (SPS-5)	172,333	0.57	0.72	0.67	0.69	0.72	0.71	0.72	0.67	0.69	0.72
Maryland (SPS-5)	124,474	0.56	0.71	0.63	0.64	0.65	0.70	0.71	0.63	0.64	0.65
Minnesota (SPS-5)	47,794	0.58	0.73	0.68	0.70	0.72	0.74	0.73	0.68	0.70	0.72
Pennsylvania (SPS-6)	1,458,818	0.67	0.82	0.75	0.78	0.81	0.84	0.82	0.75	0.78	0.81
Tennessee (SPS-6)	1,583,151	0.65	0.78	0.73	0.76	0.79	0.82	0.78	0.73	0.76	0.79
Virginia (SPS-1)	237,804	0.61	0.76	0.71	0.74	0.77	0.77	0.76	0.71	0.74	0.77
Wisconsin (SPS-1)	209,239	0.61	0.80	0.73	0.75	0.77	0.77	0.80	0.73	0.75	0.77

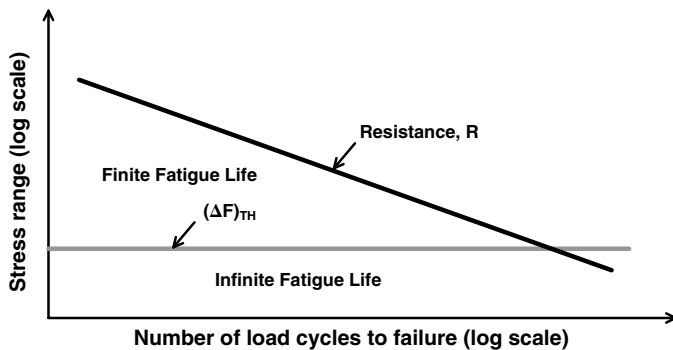
**Table 5.28. Fatigue Damage Ratios for Continuous Bridges at the Middle Support**

Site	No. of Vehicles	Fatigue Damage Ratio (current)					Fatigue Damage Ratio (proposed)				
		30 ft	60 ft	90 ft	120 ft	200 ft	30 ft	60 ft	90 ft	120 ft	200 ft
Arizona (SPS-1)	26,501	0.57	0.69	0.71	0.75	0.82	0.62	0.69	0.71	0.75	0.82
Arizona (SPS-2)	1,391,098	0.58	0.81	0.75	0.75	0.86	0.64	0.81	0.75	0.75	0.86
Arkansas (SPS-2)	1,642,334	0.57	0.80	0.74	0.75	0.87	0.62	0.80	0.74	0.75	0.87
Colorado (SPS-2)	326,017	0.52	0.71	0.66	0.68	0.73	0.58	0.71	0.66	0.68	0.73
Delaware (SPS-1)	175,889	0.57	0.74	0.71	0.73	0.78	0.63	0.74	0.71	0.73	0.78
Illinois (SPS-6)	821,809	0.56	0.80	0.74	0.74	0.84	0.62	0.80	0.74	0.74	0.84
Kansas (SPS-2)	456,881	0.55	0.78	0.73	0.73	0.80	0.61	0.78	0.73	0.73	0.80
Louisiana (SPS-1)	70,831	0.54	0.70	0.67	0.69	0.74	0.60	0.70	0.67	0.69	0.74
Maine (SPS-5)	172,333	0.49	0.69	0.64	0.65	0.70	0.54	0.69	0.64	0.65	0.70
Maryland (SPS-5)	124,474	0.50	0.66	0.63	0.65	0.70	0.55	0.66	0.63	0.65	0.70
Minnesota (SPS-5)	47,794	0.49	0.68	0.64	0.64	0.70	0.54	0.68	0.64	0.64	0.70
Pennsylvania (SPS-6)	1,458,818	0.54	0.77	0.72	0.72	0.82	0.60	0.77	0.72	0.72	0.82
Tennessee (SPS-6)	1,583,151	0.53	0.76	0.70	0.70	0.81	0.58	0.76	0.70	0.70	0.81
Virginia (SPS-1)	237,804	0.53	0.73	0.68	0.69	0.75	0.59	0.73	0.68	0.69	0.75
Wisconsin (SPS-1)	209,239	0.53	0.73	0.69	0.69	0.75	0.58	0.73	0.69	0.69	0.75

**Table 5.29. Fatigue Damage Ratios for Continuous Bridges at 0.4 of the Span Length**

Site	No. of Vehicles	Fatigue Damage Ratio (current)					Fatigue Damage Ratio (proposed)				
		30 ft	60 ft	90 ft	120 ft	200 ft	30 ft	60 ft	90 ft	120 ft	200 ft
Arizona (SPS-1)	26,501	0.60	0.81	0.79	0.81	0.83	0.75	0.81	0.79	0.81	0.83
Arizona (SPS-2)	1,391,098	0.61	0.75	0.71	0.76	0.82	0.77	0.75	0.71	0.76	0.82
Arkansas (SPS-2)	1,642,334	0.60	0.63	0.64	0.69	0.75	0.75	0.63	0.64	0.69	0.75
Colorado (SPS-2)	326,017	0.55	0.67	0.65	0.69	0.73	0.69	0.67	0.65	0.69	0.73
Delaware (SPS-1)	175,889	0.62	0.78	0.73	0.75	0.77	0.78	0.78	0.73	0.75	0.77
Illinois (SPS-6)	821,809	0.62	0.73	0.70	0.75	0.79	0.78	0.73	0.70	0.75	0.79
Kansas (SPS-2)	456,881	0.59	0.73	0.70	0.75	0.80	0.75	0.73	0.70	0.75	0.80
Louisiana (SPS-1)	70,831	0.57	0.72	0.68	0.71	0.73	0.72	0.72	0.68	0.71	0.73
Maine (SPS-5)	172,333	0.53	0.65	0.62	0.66	0.70	0.67	0.65	0.62	0.66	0.70
Maryland (SPS-5)	124,474	0.54	0.68	0.64	0.66	0.68	0.67	0.68	0.64	0.66	0.68
Minnesota (SPS-5)	47,794	0.53	0.67	0.64	0.67	0.71	0.67	0.67	0.64	0.67	0.71
Pennsylvania (SPS-6)	1,458,818	0.61	0.75	0.70	0.74	0.77	0.77	0.75	0.70	0.74	0.77
Tennessee (SPS-6)	1,583,151	0.59	0.71	0.68	0.72	0.76	0.74	0.71	0.68	0.72	0.76
Virginia (SPS-1)	237,804	0.57	0.70	0.66	0.70	0.75	0.72	0.70	0.66	0.70	0.75
Wisconsin (SPS-1)	209,239	0.58	0.73	0.68	0.71	0.75	0.73	0.73	0.68	0.71	0.75

Fatigue Limit State I refers to the stress value that has 1/10,000 probability of being exceeded. It is assumed that the distribution of stress has the same CDF shape as that of the corresponding moments. Thus, the fatigue load analysis is performed using the developed CDFs for moments for various considered sites, cases, and spans from 30 to 200 ft. The moment corresponding to the upper 0.01% is determined as a percentile corresponding to the probability of 0.9999, or 3.8 on the vertical axis in Figure 5.35. This moment represents the maximum stress range corresponding to an unlimited fatigue life. For example, for the WIM data from Arkansas (SPS-1), the moment for span of 120 ft corresponding to the upper 0.01% is 2,505.5 kip-ft (Figure 5.35).



**Figure 5.34. The threshold stress  $(\Delta F)_{TH}$  on an S-N curve.**

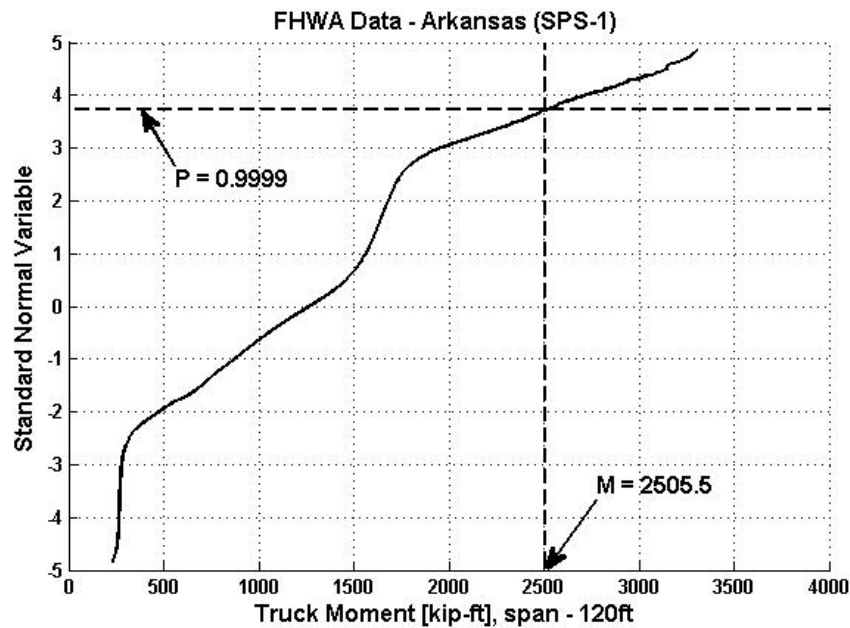
The calculations were performed for the considered locations, cases, and span lengths. The obtained values of moment were divided by the corresponding AASHTO fatigue truck moment. The results are summarized in Table 5.30 to Table 5.32.

**5.4.8 Statistical Parameters of Fatigue Live Load**

The objective was to determine the statistical parameters of fatigue load that can be considered as representative for the national load. The statistical parameters will be different for the maximum and equivalent fatigue load specified for Fatigue Limit States I and II, respectively. The ratios of the 1/10,000 moment to the HL-93 fatigue moment were plotted on normal probability paper and are shown in Figure 5.36 to Figure 5.38, and the proposed fatigue damage ratios are shown in Figure 5.39 to Figure 5.41. Each point on the graphs represents one of 15 sites considered.

To determine the statistical parameters from the graphs, a straight line was fitted for each distribution. A straight line corresponds to a normal distribution on the normal probability paper. The intersection of the straight line with the horizontal axis is at the mean value. The standard deviation is determined from the slope of the straight line. The statistical parameters of fatigue load (i.e., mean,  $\mu$ , and CV), based on data from 15 considered sites, were calculated as the ratio of standard deviation ( $\sigma$ ) and the mean and are listed in Table 5.33 and Table 5.34.

*(text continues on page 142)*



**Figure 5.35. Moment corresponding to the upper 0.01%, span = 120 ft.**

**Table 5.30. Maximum Moment Range for Simply Supported Bridges at the Midspan**

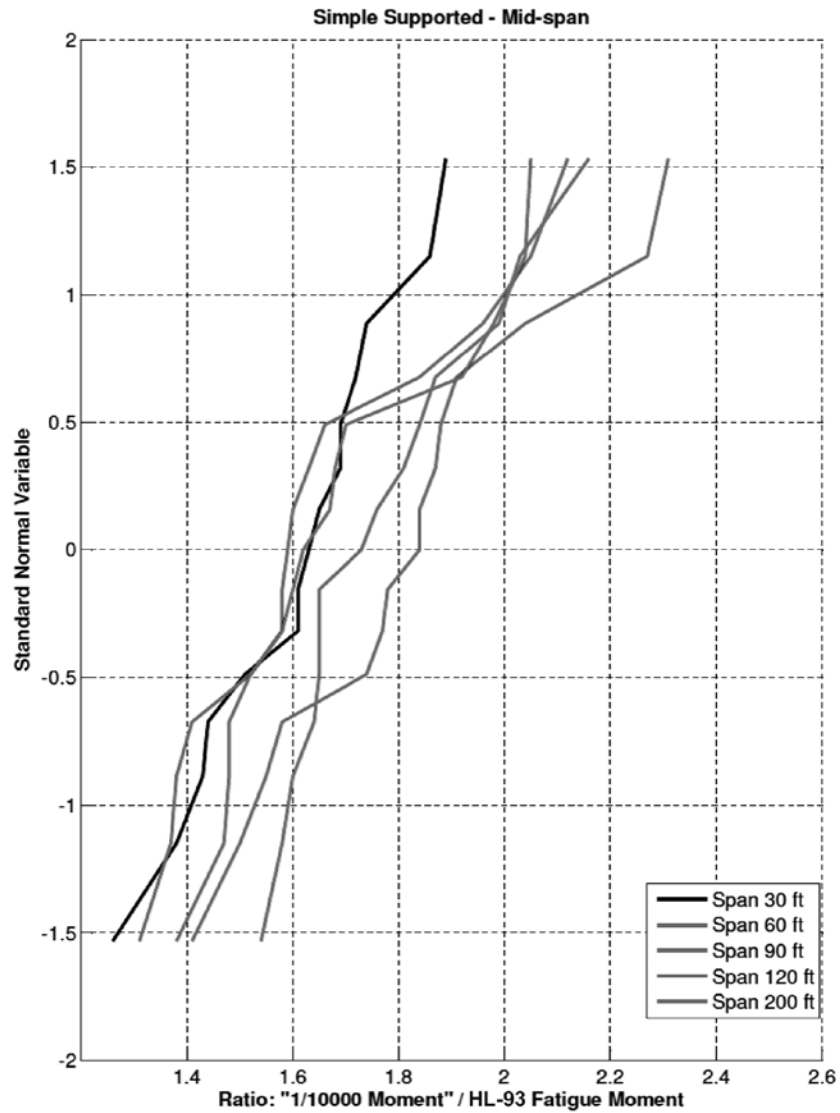
Site	No. of Vehicles	1/10,000 Moment Cycle					1/10,000 Moment/HL-93 Fatigue Moment				
		30 ft	60 ft	90 ft	120 ft	200 ft	30 ft	60 ft	90 ft	120 ft	200 ft
Arizona (SPS-1)	26,501	424	1,003	1,761	2,754	5,640	1.74	1.84	1.63	1.70	1.84
Arizona (SPS-2)	1,391,098	308	765	1,416	2,246	4,711	1.26	1.41	1.31	1.38	1.54
Arkansas (SPS-2)	1,642,334	352	860	1,526	2,460	5,066	1.44	1.58	1.41	1.52	1.65
Colorado (SPS-2)	326,017	336	814	1,497	2,409	4,854	1.38	1.50	1.38	1.48	1.58
Delaware (SPS-1)	175,889	454	1,257	2,302	3,212	5,735	1.86	2.31	2.12	1.98	1.87
Illinois (SPS-6)	821,809	350	844	1,480	2,408	5,033	1.43	1.55	1.37	1.48	1.64
Kansas (SPS-2)	456,881	411	1,018	1,989	3,112	6,083	1.69	1.87	1.84	1.92	1.99
Louisiana (SPS-1)	70,831	460	1,237	2,126	3,332	6,616	1.89	2.27	1.96	2.05	2.16
Maine (SPS-5)	172,333	397	964	1,722	2,726	5,549	1.63	1.77	1.59	1.68	1.81
Maryland (SPS-5)	124,474	412	1,038	1,802	2,599	5,061	1.69	1.91	1.66	1.60	1.65
Minnesota (SPS-5)	47,794	392	1,111	2,220	3,316	6,225	1.61	2.04	2.05	2.04	2.03
Pennsylvania (SPS-6)	1,458,818	402	1,003	1,730	2,623	5,291	1.65	1.84	1.60	1.62	1.73
Tennessee (SPS-6)	1,583,151	419	1,020	1,652	2,387	4,906	1.72	1.88	1.52	1.47	1.60
Virginia (SPS-1)	237,804	369	946	1,709	2,562	5,055	1.51	1.74	1.58	1.58	1.65
Wisconsin (SPS-1)	209,239	393	968	1,712	2,717	5,396	1.61	1.78	1.58	1.67	1.76

**Table 5.31. Maximum Moment Range for Continuous Bridges at the Middle Support**

Site	No. of Vehicles	1/10,000 Moment Cycle					1/10,000 Moment/HL-93 Fatigue Moment				
		30 ft	60 ft	90 ft	120 ft	200 ft	30 ft	60 ft	90 ft	120 ft	200 ft
Arizona (SPS-1)	26,501	-266	-701	-1,026	-1,608	-3,089	1.45	1.95	1.94	2.11	2.30
Arizona (SPS-2)	1,391,098	-211	-549	-968	-1,526	-3,019	1.15	1.52	1.83	2.00	2.25
Arkansas (SPS-2)	1,642,334	-213	-643	-995	-1,522	-3,187	1.16	1.78	1.88	2.00	2.38
Colorado (SPS-2)	326,017	-231	-579	-877	-1,312	-2,813	1.25	1.61	1.66	1.72	2.10
Delaware (SPS-1)	175,889	-248	-650	-1,173	-1,643	-3,303	1.35	1.80	2.21	2.16	2.46
Illinois (SPS-6)	821,809	-207	-640	-1,005	-1,506	-3,093	1.13	1.78	1.90	1.98	2.31
Kansas (SPS-2)	456,881	-294	-755	-1,015	-1,469	-2,937	1.60	2.10	1.92	1.93	2.19
Louisiana (SPS-1)	70,831	-278	-815	-1,128	-1,539	-3,255	1.51	2.26	2.13	2.02	2.43
Maine (SPS-5)	172,333	-251	-694	-970	-1,418	-2,967	1.37	1.93	1.83	1.86	2.21
Maryland (SPS-5)	124,474	-240	-592	-1,049	-1,564	-3,281	1.31	1.64	1.98	2.05	2.45
Minnesota (SPS-5)	47,794	-292	-695	-1,034	-1,487	-2,753	1.59	1.93	1.95	1.95	2.05
Pennsylvania (SPS-6)	1,458,818	-245	-638	-1,067	-1,588	-3,131	1.33	1.77	2.01	2.09	2.33
Tennessee (SPS-6)	1,583,151	-222	-628	-1,025	-1,559	-2,977	1.21	1.74	1.93	2.05	2.22
Virginia (SPS-1)	237,804	-223	-603	-973	-1,477	-3,010	1.21	1.67	1.84	1.94	2.24
Wisconsin (SPS-1)	209,239	-250	-671	-953	-1,394	-2,892	1.36	1.86	1.80	1.83	2.16

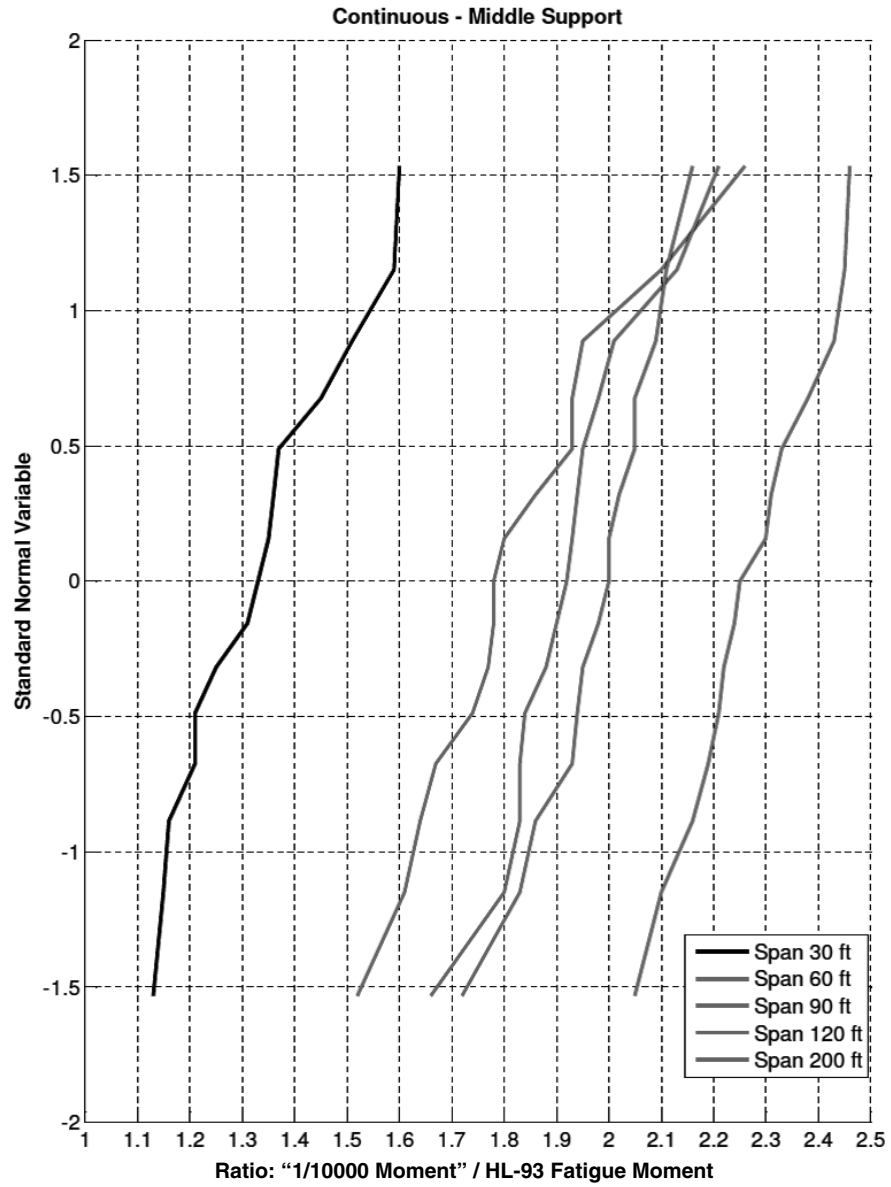
**Table 5.32. Maximum Moment Range for Continuous Bridges at 0.4 of the Span Length**

Site	No. of Vehicles	1/10,000 Moment Cycle					1/10,000 Moment/HL-93 Fatigue Moment				
		30 ft	60 ft	90 ft	120 ft	200 ft	30 ft	60 ft	90 ft	120 ft	200 ft
Arizona (SPS-1)	26,501	399	976	1,764	2,769	5,542	1.62	1.67	1.61	1.71	1.83
Arizona (SPS-2)	1,391,098	293	761	1,431	2,228	4,636	1.19	1.30	1.30	1.37	1.53
Arkansas (SPS-2)	1,642,334	338	849	1,527	2,416	4,914	1.37	1.45	1.39	1.49	1.62
Colorado (SPS-2)	326,017	319	805	1,528	2,428	4,857	1.30	1.38	1.39	1.50	1.60
Delaware (SPS-1)	175,889	439	1,279	2,243	3,141	5,635	1.78	2.19	2.04	1.94	1.86
Illinois (SPS-6)	821,809	334	814	1,508	2,399	4,893	1.36	1.39	1.37	1.48	1.61
Kansas (SPS-2)	456,881	394	1,049	1,983	3,088	5,988	1.60	1.79	1.81	1.90	1.98
Louisiana (SPS-1)	70,831	458	1,126	2,174	3,349	6,486	1.86	1.92	1.98	2.06	2.14
Maine (SPS-5)	172,333	377	937	1,811	2,768	5,525	1.53	1.60	1.65	1.71	1.82
Maryland (SPS-5)	124,474	406	1,036	1,817	2,618	4,941	1.65	1.77	1.65	1.61	1.63
Minnesota (SPS-5)	47,794	382	1,142	2,134	3,223	6,065	1.55	1.95	1.94	1.99	2.00
Pennsylvania (SPS-6)	1,458,818	395	1,020	1,726	2,608	5,243	1.61	1.74	1.57	1.61	1.73
Tennessee (SPS-6)	1,583,151	416	1,012	1,636	2,379	4,868	1.69	1.73	1.49	1.47	1.61
Virginia (SPS-1)	237,804	356	955	1,704	2,509	4,947	1.45	1.63	1.55	1.55	1.63
Wisconsin (SPS-1)	209,239	375	958	1,705	2,662	5,326	1.53	1.64	1.55	1.64	1.76

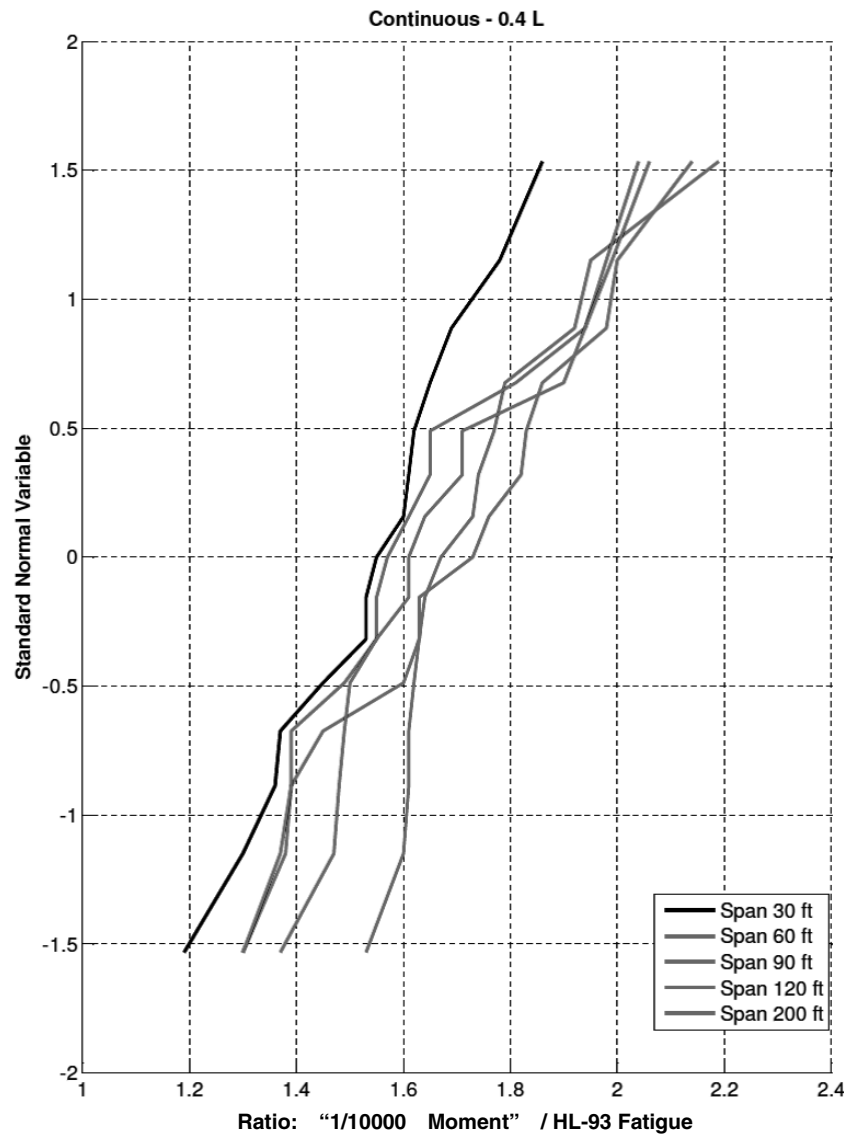


**Figure 5.36. Maximum moment range ratio (Fatigue Limit State I) for simple-supported bridges at the midspan.**





**Figure 5.37. Maximum moment range ratio (Fatigue Limit State I) for continuous bridges at the middle support.**



**Figure 5.38. Maximum moment range ratio (Fatigue Limit State I) for continuous bridges at 0.4 of the span length.**

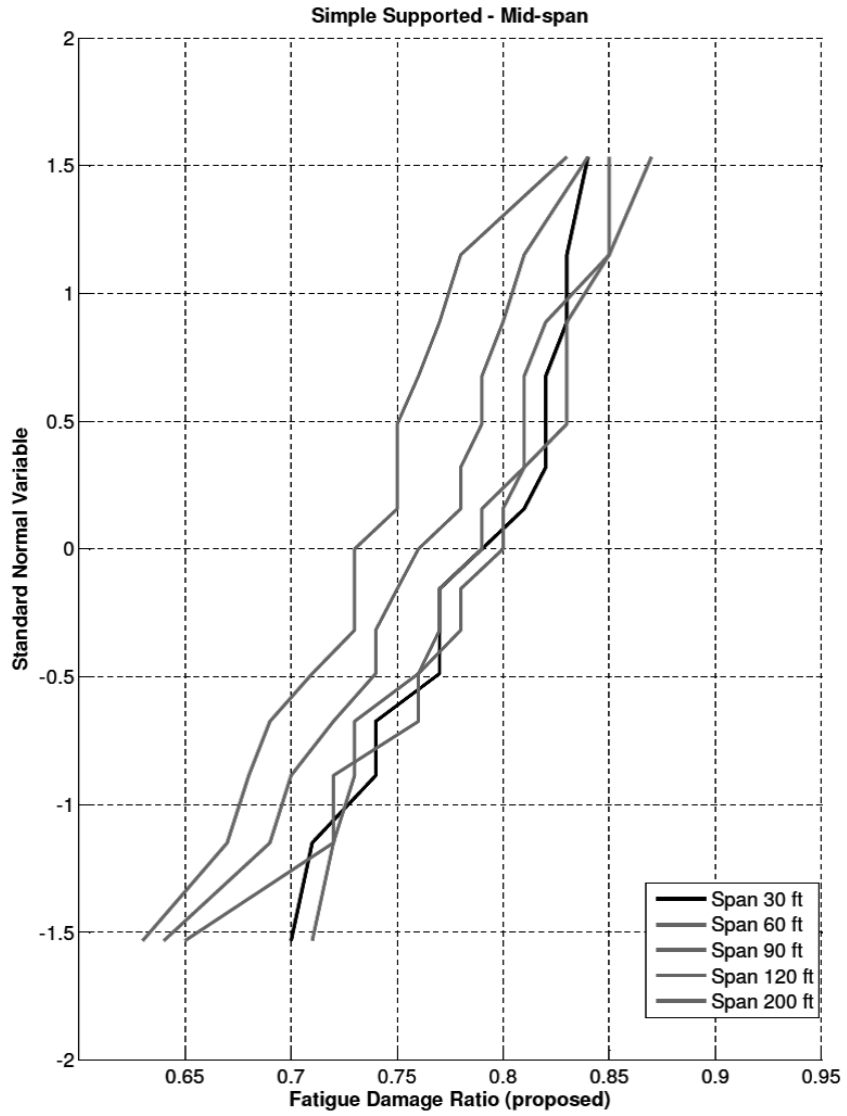
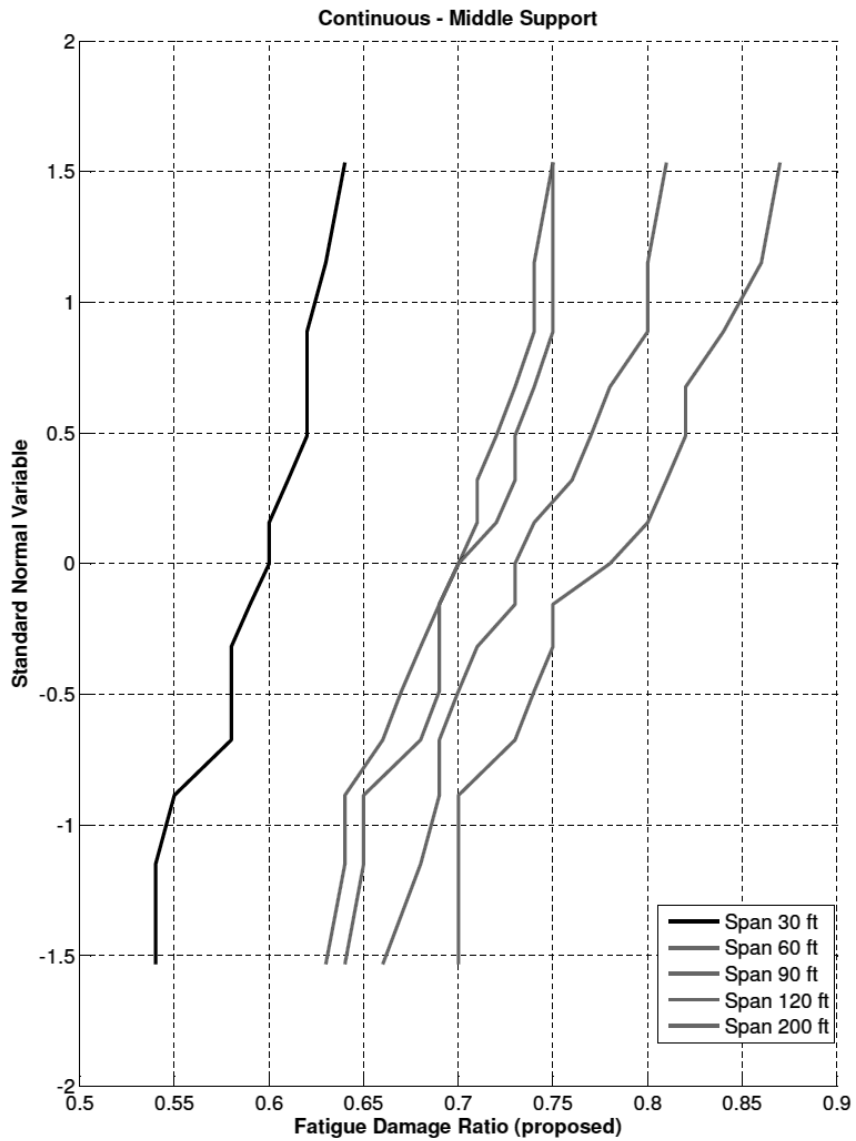


Figure 5.39. Fatigue damage ratio for proposed change (Fatigue Limit State II) for simple-supported bridges at the midspan.



**Figure 5.40. Fatigue damage ratio for proposed change (Fatigue Limit State II) for continuous bridges at the middle support.**

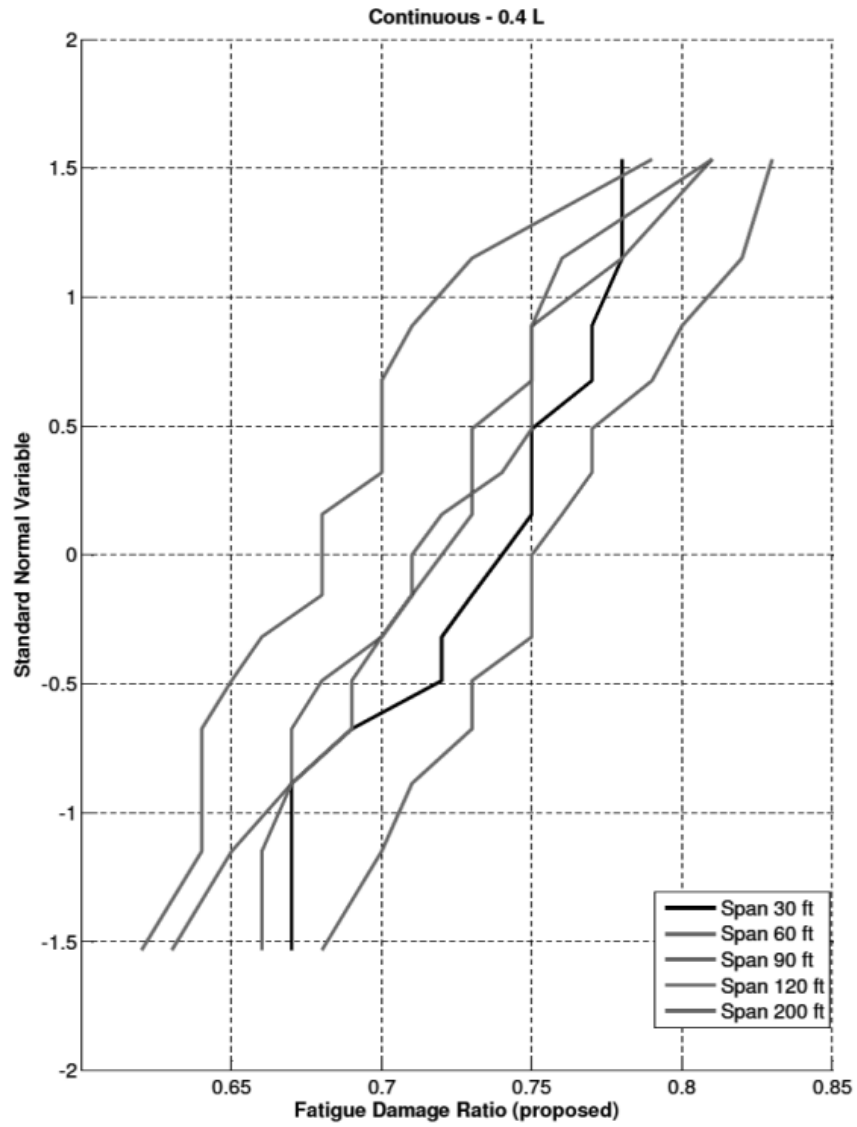


Figure 5.41. Fatigue damage ratio for proposed change (Fatigue Limit State II) for continuous bridges at 0.4 of the span length.

**Table 5.33. Maximum Moment Range Ratio for Fatigue Limit State I**

Bridge Type	Span (ft)	Mean	Mean + 1.5σ	CV
Simple-supported midspan	30	1.60	1.90	0.13
	60	1.83	2.24	0.15
	90	1.60	1.96	0.15
	120	1.64	1.88	0.10
	200	1.70	2.15	0.18
Continuous middle support	30	1.35	1.61	0.13
	60	1.81	2.13	0.12
	90	1.92	2.18	0.09
	120	1.97	2.17	0.07
	200	2.27	2.47	0.06
Continuous 0.4 of the span length	30	1.54	1.86	0.14
	60	1.67	2.06	0.16
	90	1.60	1.92	0.13
	120	1.65	1.97	0.13
	200	1.72	2.11	0.15

**Table 5.34. Proposed Fatigue Damage Ratio for Fatigue Limit State II**

Bridge Type	Span (ft)	Mean	Mean + 1.5σ	CV
Simple-supported midspan	30	0.79	0.87	0.07
	60	0.78	0.86	0.06
	90	0.73	0.81	0.07
	120	0.76	0.84	0.07
	200	0.78	0.86	0.07
Continuous middle support	30	0.59	0.65	0.07
	60	0.74	0.82	0.07
	90	0.69	0.77	0.07
	120	0.71	0.78	0.06
	200	0.79	0.87	0.07
Continuous 0.4 of the span length	30	0.73	0.81	0.07
	60	0.72	0.80	0.07
	90	0.68	0.75	0.07
	120	0.72	0.79	0.06
	200	0.76	0.84	0.07

(continued from page 133)

It is assumed that the considered 15 WIM locations are representative of the truck traffic in the United States. For the purpose of further reliability analysis, it is recommended to assume that the mean fatigue load is equal to the mean for the 15 WIM locations plus 1.5 standard deviations (1.5 σ). The probability of exceeding this value is about 5%, and as Figure 5.42 shows, 95% of sites in the United States are below this value. The moment ratios corresponding to the mean plus 1.5 standard deviations are also listed in Table 5.33 and Table 5.34.

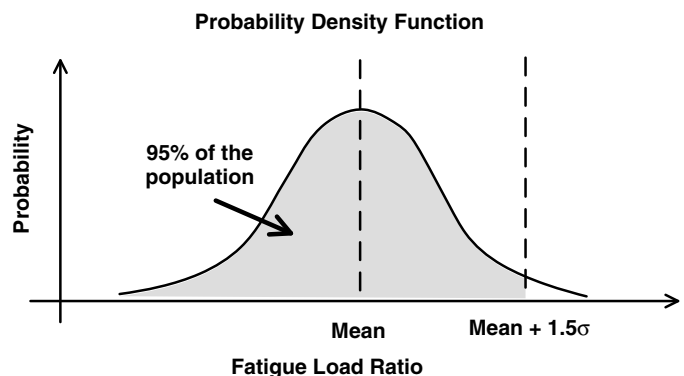
The statistical parameters were calculated for all considered cases and span length.

**5.4.9 Recommendations**

Use of the proposed number of cycles of stress range per truck shown in Table 5.26 resulted in the relatively tightly clustered moment range ratios shown in Table 5.33 and Table 5.34 for the Fatigue II and Fatigue I limit states, respectively. As with other live load recommendations in this report, the values to be considered for calibration are the moment ratios at the “mean plus 1.5 standard deviations” and the CVs. For simplicity, the recommended values for the calibration of the fatigue limit states are further simplified into single values independent of span length as follows:

- For Fatigue I, use stress ranges (loads) based on 2.0 HL-93 and a CV = 0.12.
- For Fatigue II, use stress ranges (loads) based on 0.80 HL-93 and a CV = 0.07.

The corresponding load factors are determined from Monte Carlo simulation using the statistics of resistance based on past laboratory testing, as summarized in Keating and Fisher (1986). The development of the load factors for steel and concrete components and details is explained in Chapter 6.



**Figure 5.42. Probability density function of the national fatigue load.**



### 5.5 Development of Overload (Service II) Parameters

WIM data also forms the basis for estimating how often a given design moment (or shear) is exceeded. Table 5.35 shows the number of times the live load moment exceeded 100%, 110%, 120%, and 130% of HL-93 for the 32 WIM sites. One of the sites, Florida Route 29, clearly has a unique traffic pattern. The Florida Department of Transportation explained that truck traffic from several other highways was being

directed onto this road, which undoubtedly accounted for the relatively large number of times the HL-93 was exceeded for the various percentages indicated. The total number of times the various ratios of HL-93 were exceeded, excluding Florida Route 29, is shown in the Table 5.35, as well as the average number per site. Most of the data were collected for a year, so that the lowest row in the table indicates the average number of times each of the criteria was exceeded on an average site during a year. This information was used to assess the significance of the Service II limit states in Chapter 6.

**Table 5.35. Number of Times WIM Moments Exceeded Factored HL-93 Loadings**

Site	Moment														
	Ratio Truck/HL-93 ≥1.1					Ratio Truck/HL-93 ≥1.2					Ratio Truck/HL-93 ≥1.3				
	30 ft	60 ft	90 ft	120 ft	200 ft	30 ft	60 ft	90 ft	120 ft	200 ft	30 ft	60 ft	90 ft	120 ft	200 ft
Arizona (SPS-1)	1	0	0	0	0	0	0	0	0	0	0	0	0	0	0
Arizona (SPS-2)	0	0	1	1	0	0	0	0	0	0	0	0	0	0	0
Arkansas (SPS-2)	2	7	3	0	0	0	3	0	0	0	0	0	0	0	0
Colorado (SPS-2)	0	2	5	4	0	0	0	2	0	0	0	0	0	0	0
Delaware (SPS-1)	36	33	22	11	0	10	22	10	1	0	1	11	1	0	0
Illinois (SPS-6)	0	0	1	0	0	0	0	0	0	0	0	0	0	0	0
Indiana (SPS-6)	3	11	11	10	2	2	4	5	4	0	0	0	1	0	0
Kansas (SPS-2)	16	33	35	31	2	7	16	17	7	0	6	7	6	0	0
Louisiana (SPS-1)	44	6	12	14	7	26	6	7	7	0	6	6	5	4	0
Maine (SPS-5)	4	4	5	2	0	0	4	2	0	0	0	2	0	0	0
Maryland (SPS-5)	5	6	2	2	0	0	1	1	0	0	0	1	0	0	0
Minnesota (SPS-5)	7	5	6	5	0	4	2	2	1	0	2	1	1	0	0
New Mexico (SPS-1)	0	1	1	1	0	0	0	0	0	0	0	0	0	0	0
New Mexico (SPS-5)	3	1	1	2	0	2	0	0	0	0	0	0	0	0	0
Pennsylvania (SPS-6)	32	22	17	14	1	13	17	13	1	0	3	13	2	0	0
Tennessee (SPS-6)	53	4	4	0	0	5	1	0	0	0	1	0	0	0	0

(continued on next page)

Table 5.35. Number of Times WIM Moments Exceeded Factored HL-93 Loadings (continued)

Site	Moment														
	Ratio Truck/HL-93 $\geq 1.1$					Ratio Truck/HL-93 $\geq 1.2$					Ratio Truck/HL-93 $\geq 1.3$				
	30 ft	60 ft	90 ft	120 ft	200 ft	30 ft	60 ft	90 ft	120 ft	200 ft	30 ft	60 ft	90 ft	120 ft	200 ft
Virginia (SPS-1)	0	0	1	1	0	0	0	0	0	0	0	0	0	0	0
Wisconsin (SPS-1)	1	0	3	3	1	0	0	1	1	0	0	0	0	0	0
California Antelope EB	0	1	0	0	5	0	0	0	0	0	0	0	0	0	0
California Antelope WB	0	5	4	13	28	0	0	0	1	9	0	0	0	0	1
California Bowman	0	0	0	1	1	0	0	0	0	1	0	0	0	0	0
California LA-710 NB	1	31	50	51	15	0	6	24	19	0	0	0	4	1	0
California LA-710 SB	1	17	45	48	14	0	3	18	19	0	0	0	1	1	0
California Lodi	0	4	16	46	140	0	0	1	2	32	0	0	0	0	2
Florida I-10	79	40	46	75	37	22	16	14	17	5	10	5	4	5	2
Florida I-95	0	0	0	0	0	0	0	0	0	0	0	0	0	0	0
Florida US-29	653	495	322	245	106	360	266	174	119	51	177	160	82	59	21
Mississippi I-10	24	22	31	33	22	7	2	10	19	2	2	2	2	2	1
Mississippi I-55UI	0	0	0	1	2	0	0	0	0	0	0	0	0	0	0
Mississippi I-55R	19	30	48	58	32	7	8	16	21	19	2	3	5	8	9
Mississippi US-49	0	0	2	1	0	0	0	0	0	0	0	0	0	0	0
Mississippi US-61	0	0	1	2	1	0	0	1	1	0	0	0	0	0	0
<b>Total (without Florida US-29)</b>	331	285	373	430	310	105	111	144	121	68	33	51	32	21	15
<b>Average per site per year</b>	10.7	9.2	12.0	13.9	10.0	3.4	3.6	4.6	3.9	2.2	1.1	1.6	1.0	0.7	0.5

## CHAPTER 6

# Calibration Results

### 6.1 Foundation Deformations, Service I: Lifetime

The geotechnical limit states for serviceability of a bridge structure relate to foundation deformations. Within the context of foundation deformation, the geotechnical limit states can be broadly categorized into vertical and horizontal deformations for any foundation type (e.g., spread footings, driven piles, drilled shafts, micropiles). Table 6.1 summarizes the various relevant articles in *AASHTO LRFD* (2012) that address vertical (settlement) and horizontal deformations for various types of structural foundations.

This section describes procedures that can be used for calibrating service limit states (SLSs) to evaluate the effect of vertical or horizontal deformations of all structural foundation types such as footings, drilled shafts, and driven piles. The procedure is demonstrated by using the case of immediate settlements of spread footings, and the effect of foundation deformations on bridge superstructures is discussed in the context of construction stages.

#### 6.1.1 Target Reliability Index

For strength limit states, reliability index values in the range of 3.09 to 3.54 are used. Strength (or ultimate) limit states pertain to structural safety and the loss of load-carrying capacity. In contrast, SLSs are user-defined limiting conditions that affect the function of the structure under expected service conditions. Violation of SLSs occurs at loads much smaller than those for strength limit states. As there is no danger of collapse if an SLS is violated, a smaller value of target reliability index may be used for SLSs. In the case of foundation deformation, such as settlement, the structural load effect is manifested in terms of increased moments and potential cracking. The load effect due to settlement relative to the load effect due to dead and live loads would generally be small because in the Service I limit state the load factor  $\gamma_{SE}$ , which represents the uncertainty in

estimated settlement, is only one of many load factors. Furthermore, the primary moments due to the dead and live loads are much larger than the additional (secondary) moments due to settlement. Because of these considerations and based on a consideration of the reversible and irreversible SLSs for bridge superstructures described earlier in this report, a target reliability index ( $\beta_T$ ) in the range of 0.50 to 1.00 for the calibration of load factor  $\gamma_{SE}$  for foundation deformation in the Service I limit state is used.

#### 6.1.2 Calculation Models

Evaluation of an SLS involves consideration of the deformation aspects of the structure or members of the structure. The load deformation characteristics of the structure or its member are important to understand because resistance must now be quantified as a function of the deformation. This section first discusses the extension of the *AASHTO LRFD* framework to incorporate the load deformation behavior, after which a calibration framework for SLSs for foundation deformations is presented. The proposed step-by-step procedure for calibration is described in Section 6.1.2.5, which leads to a load factor for deformations based on the target reliability index that was discussed in Section 6.1.1. The proposed procedure is demonstrated by an example for immediate settlements of spread footings by using various analytical methods in Section 6.1.3.

##### 6.1.2.1 Incorporation of Load Effect Deformation ( $Q$ - $\delta$ ) Characteristics in the *AASHTO LRFD* Framework

The basic *AASHTO LRFD* framework in terms of distributions of load effects and resistances is shown in Figure 6.1, where

$$Q = \text{load};$$
$$Q_{\text{mean}} = \text{mean load};$$

**Table 6.1. Summary of AASHTO LRFD (2012) Articles for Estimation of Vertical and Horizontal Deformation of Structural Foundations**

AASHTO LRFD Article	Comment
10.6.2.4 Settlement Analyses for Spread Footings	Article 10.6.2.4 presents methods to estimate the settlement of spread footings. Settlement analysis is based on the elastic and semiempirical Hough (1959) method for immediate settlement and the one-dimensional consolidation method for long-term settlement.
10.7.2.3 Settlement (related to driven pile groups) 10.8.2.2 Settlement (related to drilled shaft groups) 10.9.2.3 Settlement (related to micropile groups)	The procedures in these articles (10.7.2.3, 10.8.2.2, and 10.9.2.3) refer to settlement analysis for an equivalent spread footing; see AASHTO LRFD (2012, Figure 10.7.2.3.1-1).
10.7.2.4 Horizontal Pile Foundation Movement 10.8.2.4 Horizontal Movement of Shaft and Shaft Groups 10.9.2.4 Horizontal Micropile Foundation Movement	Lateral analysis based on the $p$ - $y$ method and strain wedge method is included in AASHTO LRFD (2012) for estimating horizontal (lateral) deformations of deep foundations.

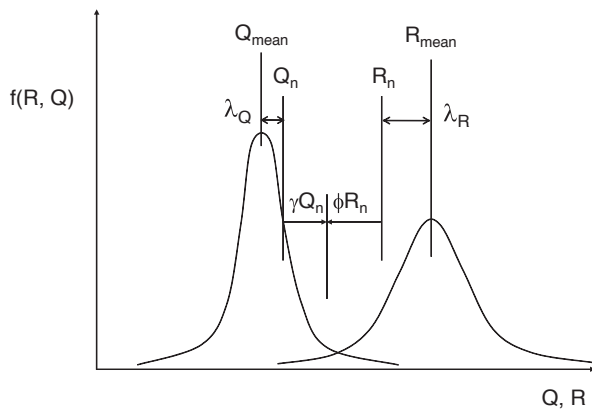
Note: Section 11 (Abutments, Piers and Walls) Article 11.6.2 refers to the various articles noted in the left column of this table. Thus, the articles noted in this table also apply to fill retaining walls and their foundations.

- $\gamma$  = load factor;
- $R$  = resistance;
- $R_{mean}$  = mean resistance;
- $\phi$  = resistance factor;
- $Q_n$  = nominal load;
- $\lambda_Q$  = bias factor for load;
- $f$  = frequency;
- $R_n$  = nominal resistance; and
- $\lambda_R$  = bias factor for resistance.

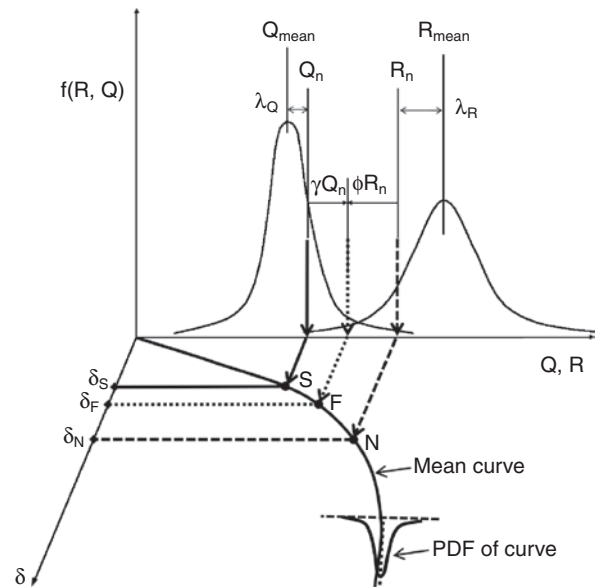
Details of the AASHTO LRFD framework can be found in Nowak and Collins (2013). Strength limit states were evaluated by using this framework. Because determination of deformation is a necessary part of the evaluation of serviceability, for

the evaluation of SLS, the basic AASHTO LRFD framework shown in Figure 6.1 needs to be modified to include load effect deformation, or  $Q$ - $\delta$  behavior. The  $Q$ - $\delta$  behavior can be considered as another dimension of the basic AASHTO LRFD framework, as shown in Figure 6.2, where

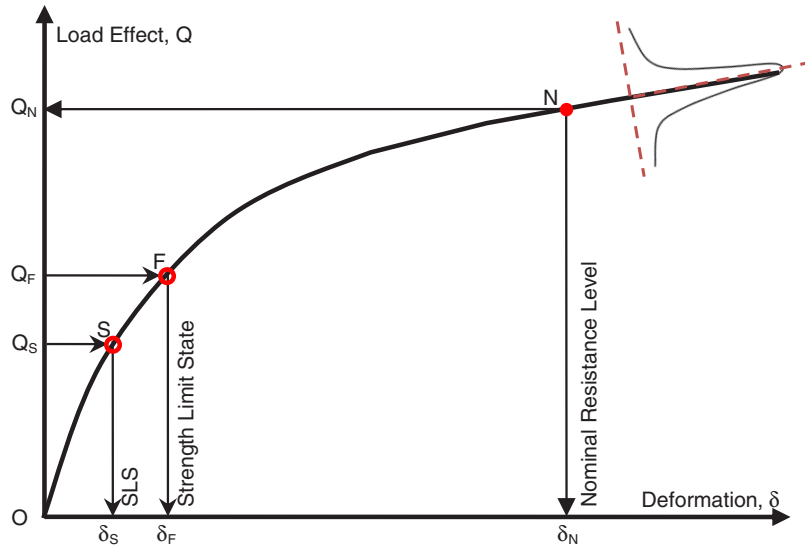
- $\delta$  = deformation;
- $\delta_s$  = deformation at nominal load effect ( $Q_n$ );



**Figure 6.1. Basic AASHTO LRFD framework for load effects and resistances.**



**Figure 6.2. Incorporation of  $Q$ - $\delta$  mechanism into the basic AASHTO LRFD framework.**



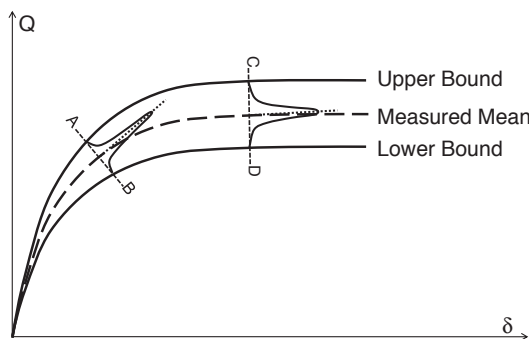
**Figure 6.3. Significant points of interest on the mean  $Q-\delta$  curve.**

$\delta_F$  = deformation at factored load effect [ $Q_F = \gamma(Q_n)$ ]; and  $\delta_N$  = deformation at load corresponding to nominal resistance ( $R_n$ ).

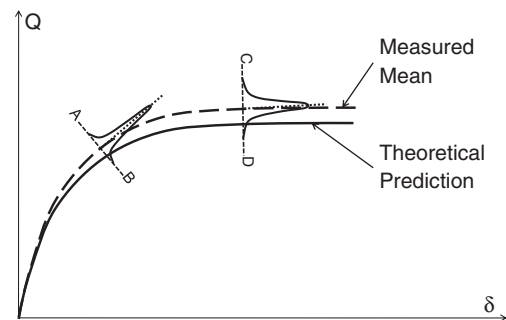
Although  $Q-\delta$  curves can have many shapes, for illustration purposes, a strain-hardening curve is shown in Figure 6.2. For discussion purposes, the mean  $Q-\delta$  curve is shown, and the spread of the  $Q-\delta$  data about the mean curve is represented schematically by a probability distribution function (PDF) that is discussed later in this chapter. The various relevant load effect and deformation quantities shown in the  $Q-\delta$  space in Figure 6.2 are shown in the regular first quadrant of the two-dimensional plot in Figure 6.3. Note that the nominal resistance is equated to a load effect that would correspond to this resistance.

Figure 6.2 combines different aspects of material behavior that cover both load effects and resistances. It is important to understand the interrelationships among the various parameters displayed on the curves. To that end the following points are made:

- The load effect deformation ( $Q-\delta$ ) curves shown in Figure 6.2 and Figure 6.3 represent the measured mean curves based on field measurements.
- Field measurements have upper and lower bounds with respect to the mean of the measured data. These bounds are shown schematically in Figure 6.4 and also in Figure 6.2 and Figure 6.3 through a PDF. Although PDFs for normal distributions are shown, the spread of the data about the mean may be represented by normal or nonnormal distributions, as appropriate. In general, the spread of the data around the mean curve increases with increasing deformations.
- Many theoretical methods are available to predict load effect deformation behavior. The theoretical models may predict a stiffer or softer material response compared with the actual response. For the purpose of discussion, a softer material behavior is shown in Figure 6.5. Because the bias factor is defined as the ratio of measured mean to predicted values,



**Figure 6.4. Significant points of interest on the  $Q-\delta$  curve.**



**Figure 6.5. Relationship of measured mean with theoretical prediction.**

the bias factor for deformations ( $\lambda_\delta$ ) will vary over the full range of the  $Q$ - $\delta$  curve.

### 6.1.2.2 Consideration of Bias Factor in Calibration of SLS

A varying bias factor along the  $Q$ - $\delta$  curve, although a reality, can be cumbersome to handle in the calibration process. However, the problem is made easier by realizing that for calibration of SLS the load effects between Points O and S, as shown in Figure 6.3, are of primary interest. Point S represents the service load effects, and the deformation corresponding to this point is of primary interest. As the bias factor will generally increase with increasing deformations, the value of the bias factor at Point S will be the maximum between Points O and S. Thus, use of the bias factor at Point S will be conservative. In this context, the bias factor at Point S is most relevant and, at a minimum, field data under full service loads are of importance in geotechnical SLS calibrations. The data most particularly needed for SLS evaluations are the full range of incremental loads and deformations measured on in-service structures from the beginning of construction of the first element (e.g., the foundation) to the completion of the roadway and beyond. Such data will help in the evaluation of the variability in predicted deformations for structural, as well as geotechnical, features. At present, these types of data are not routinely available; however, programs such as the Federal Highway Administration's (FHWA) Long-Term Bridge Performance Program may offer a good avenue to collect such data.

### 6.1.2.3 Application of $Q$ - $\delta$ Curves in the LRFD Framework

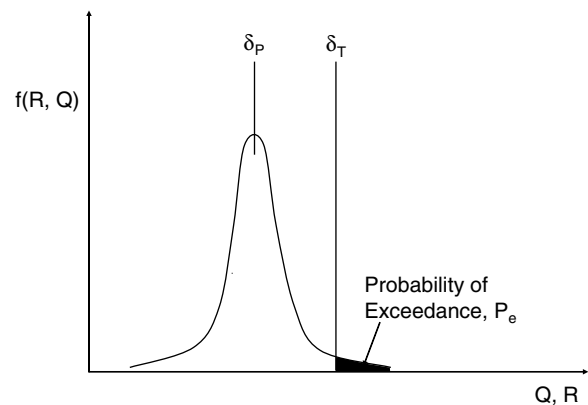
The AASHTO LRFD calibration of the strength limit state was performed by using the general concepts in Figure 6.1. This approach presumes that statistical data are available to quantify the spread of the load effects and resistances. In the context of deformations, tolerable deformations ( $\delta_T$ ) can be considered as resistances, and predicted deformations ( $\delta_p$ ) can be considered as loads. Thus, a limit state function ( $g$ ) can be written as shown by Equation 6.1:

$$g = \delta_T - \delta_p \quad (6.1)$$

Once the deformations are expressed in the form of a limit state, probabilistic calibration processes similar to those used for the strength limit state can be used. For strength limit states, Monte Carlo analysis is often used for calibrations. One of the assumptions of the Monte Carlo procedure is that PDFs for both the load ( $Q$ ) and resistance ( $R$ ) are available. However, for geotechnical SLS calibration, there are practical limitations to this approach. Although the statistical data for

modeling the uncertainty in predicted deformations ( $\delta_p$ ) are available, the same is not true for tolerable deformations ( $\delta_T$ ). Some attempts have been made (e.g., Zhang and Ng 2005) to evaluate the distribution of tolerable deformations, but from a geotechnical viewpoint, it may not be possible to obtain a PDF for tolerable deformation that is applicable to the various structural SLSs discussed in other sections of this report. This is largely because it is virtually impossible to identify a consistent tolerable deformation across all elements of a structure. Many variables can affect the value of tolerable deformation for a given element. To bypass these difficulties, a single deterministic value of  $\delta_T$  is often used for comparison against the potential spread of data for  $\delta_p$ . In practical terms, a bridge engineer often assumes a deterministic tolerable deformation that would limit deformations according to the type of bridge structure being designed. In this case, the conventional calibration processes, such as the Monte Carlo procedure, would not be necessary as there would be a PDF for load ( $Q$ ), but a deterministic value for resistance ( $R$ ). To use Monte Carlo in this situation an arbitrarily small value of standard deviation or coefficient of variation (CV) would have to be used. Although theoretically possible, this process could lead to spurious results. Thus, an alternative approach to calibration of SLSs for geotechnical features is necessary.

When a deterministic value for  $\delta_T$  is used, then by using Figure 6.1 as the basis, the resistance PDF is reduced to a single value while the load effect PDF can be used to represent the predicted deformations. This modified treatment for deformations is shown in Figure 6.6. In this approach, the probability of exceedance ( $P_e$ ) for the predicted deformations to exceed the tolerable deformation is given by the area of the overlap of the two curves (the shaded zone shown in Figure 6.6). As the goal is to prevent serviceability-related problems,  $P_e$  can



**Figure 6.6. Relationship of deterministic value of tolerable deformation ( $\delta_T$ ) and a PDF for predicted deformation ( $\delta_p$ ).  $Q$  = load effect;  $R$  = resistance;  $\delta_p$  = predicted deformations (load effect); and  $\delta_T$  = deterministic value of tolerable deformation (resistance).**



be selected on the basis of the acceptable value of the target reliability index ( $\beta_T$ ). The ratio  $\delta_T/\delta_p$  can be thought of as a load factor for deformations for a given  $P_e$  corresponding to  $\beta_T$ .

The PDF for the predicted deformations shown in Figure 6.6 is obtained from the data at Point S shown in Figure 6.2 and Figure 6.3. This is where the concept of the  $Q$ - $\delta$  curve fits into the framework to calibrate the SLS on the basis of on deformations. Thus, any model that can predict a  $Q$ - $\delta$  curve can be used in the conventional *AASHTO LRFD* framework as long as the data at Point S corresponding to SLS load effects are available through field measurements. The effect of material brittleness (or ductility) can now be introduced in the *AASHTO LRFD* framework through the use of an appropriate  $Q$ - $\delta$  model. Examples of  $Q$ - $\delta$  models are stress–strain curves, vertical load–settlement curves for foundations,  $p$ - $y$  (lateral load–lateral displacement) curves for laterally loaded piles, shear force–shear strain curves, moment–curvature curves, and so forth. The proposed framework can incorporate any  $Q$ - $\delta$  model and is therefore a general framework that is applicable to structural or geotechnical aspects.

#### 6.1.2.4 Deterioration of Foundation and Wall Elements

Most, if not all, foundation elements are buried in geomaterials. This is also true for most earth-retaining structures. Thus, the long-term performance of the foundation and wall elements can be affected by the corrosion or degradation potential of the geomaterials. The term *corrosion* applies to metal components, and *degradation* applies to nonmetal components such as polymeric soil reinforcements in mechanically stabilized earth (MSE) walls.

If the geomaterials have significant corrosion or degradation potential, then the sectional properties of the foundation and wall elements will deteriorate by reduction in the section or loss of strength, or both. The *AASHTO LRFD Specifications* clearly recognizes this mode of deterioration and provides definitive guidelines. For example, Articles 10.7.5 and 10.9.5 of Section 10 (Foundations) provide guidelines for evaluation of corrosion and deterioration of driven piles and micropiles, respectively. Similarly, Section 11 (Abutments, Piers, and Walls) provides guidance in Article 11.8.7 for nongravity cantilevered walls, Article 11.9.7 for anchored walls, and Articles 11.10.2.3.3 and 11.10.6.4 for MSE walls. Supplementary guidance can be found in Elias et al. (2009) and Fishman and Withiam (2011). The AASHTO, Elias et al., and Fishman and Withiam documents cross reference various publications that discuss the corrosion or degradation potential of geomaterials.

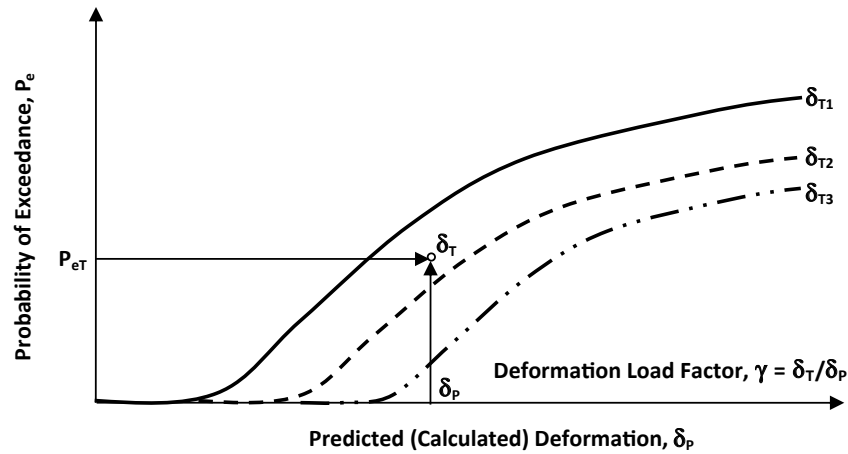
In general, the AASHTO articles and other documents cited above provide guidance for testing frequencies and protocols to evaluate the corrosion or degradation potential of various geomaterials. It is assumed that the foundation and wall

designer will perform the necessary tests and, as appropriate, implement the necessary mitigation measures to minimize the inevitable effects of corrosion or degradation on the foundation and wall elements and the structures these elements support. The most common approach is to estimate the rate of corrosion or degradation over the design life of the structure and provide additional sectional or strength properties (or both) that will permit the structure to perform within its strength and serviceability requirements. For example, metal elements are often provided additional section based on the anticipated loss of metal over the design life of the structure. Concrete deterioration due to sulfate attack is often mitigated by use of an appropriate type of cement.

#### 6.1.2.5 Determination of Load Factor for Deformations

The concept presented in Figure 6.6 assumes that the designer has unique (fixed) values of tolerable deformation ( $\delta_T$ ) and predicted deformation ( $\delta_p$ ). However, these values are functions of many parameters for a given element and the mode of deformation being evaluated. Thus, it is more practical to express the load factor for deformation as a function of the value of  $\delta_p$ . The load factor is more conveniently determined by using an alternative form of the concept, as shown in Figure 6.7, in which the cumulative distribution function (CDF) is used instead of the PDF. In this concept it is more convenient to use the data based on the inverse of the bias factor because the predicted (calculated) deformation is plotted on the  $x$ -axis. The format shown in Figure 6.7 is used as follows:

1. Obtain data for predicted ( $\delta_p$ ) and measured ( $\delta_M$ ) deformations for the deformation mode of interest (e.g., immediate settlement of spread footings). Recognize that the value of  $\delta_M$  can be considered as resistance and equivalent to the tolerable settlement ( $\delta_T$ ).
2. Modify the data to be expressed in terms of the ratio  $\delta_p/\delta_T$ . In geotechnical literature (e.g., Tan and Duncan 1991) this ratio is often referred to as *accuracy*. Label this ratio as  $X$ .  $X$  is a random variable that can now be modeled by an appropriate PDF. Develop the appropriate statistics, and select a suitable distribution function. Express the data in terms of a CDF.
3. As shown in Figure 6.7, plot a family of CDF curves for a range of values of tolerable deformation (e.g.,  $\delta_{T1} > \delta_{T2} > \delta_{T3}$ ) that permits the determination of values of the probability of exceedance ( $P_e$ ) for a range of  $\delta_p$ . The CDFs are generated by multiplying the CDF for accuracy (i.e.,  $X = \delta_p/\delta_T$ ) or by selected values of tolerable deformations ( $\delta_{T1}$ ,  $\delta_{T2}$ ,  $\delta_{T3}$ ). The plot shown in Figure 6.7 is referred to as a probability exceedance chart (PEC).



**Figure 6.7. PEC for evaluation of load factor for a target probability of exceedance ( $P_{eT}$ ) at the applicable SLS combination.**

4. Select the design value of probability of exceedance ( $P_{eT}$ ) corresponding to the target reliability index ( $\beta_{eT}$ ), and determine the value of  $\delta_T$  for a given value of  $\delta_p$ , as shown in Figure 6.7.
5. Compute the value of the deformation load factor ( $\gamma = \delta_T/\delta_p$ ), as shown in Figure 6.7.

The benefit of this approach is that once the designer computes (predicts) a deformation for any given deformation mechanism, then the designer simply multiplies the computed value by the deformation load factor corresponding to that value of deformation and uses the factored value for evaluation at the applicable SLS load combination. This concept is valid whether structural or geotechnical deformation mechanisms are evaluated. This concept is demonstrated in the next section, in which immediate settlements for spread footings are evaluated.

### 6.1.3 Calibration Results

The proposed procedure for calibration described in Section 6.1.2.5 is demonstrated by an example for immediate settlement of spread footings. The calibration results are presented in a step-by-step format that is generally consistent with other similar results presented in this report.

#### 6.1.3.1 Step 1: Formulate the Limit State Function and Identify Basic Variables

In the context of deformations, tolerable deformations ( $\delta_T$ ) can be considered as resistances, and predicted deformations ( $\delta_p$ ) can be considered as loads. Thus, a limit state function ( $g$ ) can be given by Equation 6.2 (first introduced as Equation 6.1):

$$g = \delta_T - \delta_p \quad (6.2)$$

For SLS calibration for foundation deformation, the limit state  $g$  expressed as a ratio is more appropriate, as given by Equation 6.3:

$$g = \delta_p / \delta_T \quad (6.3)$$

#### 6.1.3.2 Step 2: Identify and Select Representative Structural Types and Design Cases

In general, the vertical and lateral deformations for all structural foundation types (e.g., footings, drilled shafts, and driven piles) can be calibrated using the process described in this example. For the purpose of demonstration of the calibration process, immediate vertical settlement of spread footings is used as a design case.

#### 6.1.3.3 Step 3: Determine Load and Resistance Parameters for the Selected Design Cases

The load and resistance parameters for the selected design case of immediate vertical settlement of spread footings are as follows. *Load* is predicted (or calculated) immediate vertical settlement ( $\delta_p$ ) and *resistance* is tolerable (or limiting or measured) immediate vertical settlement ( $\delta_T$ ).

#### 6.1.3.4 Step 4: Develop Statistical Models for Load and Resistance

Table 6.2 shows a data set for spread footings based on vertical settlements of footings measured at 20 footings for 10 instrumented bridges in the northeastern United States (Gifford et al. 1987). The bridges included five simple-span and five continuous-beam structures. Each of the footing designations in Table 6.2 represents a footing supporting a single sub-structure unit (abutment or pier). Four of the instrumented

**Table 6.2. Data for Measured Settlement ( $\delta_M$ ) and Calculated Settlement ( $\delta_P$ ) Shown in Figure 6.8**

Site	Measured Settlement (in.)	Calculated Settlement (in.)				
		Schmertmann et al. (1978)	Hough (1959)	D'Appolonia et al. (1968)	Peck and Bazaraa (1969)	Burland and Burbridge (1984)
S1	0.35	0.79	0.75	0.65	0.29	0.30
S2	0.67	1.85	0.94	0.39	0.16	0.12
S3	0.94	0.86	1.21	0.30	0.19	0.13
S4	0.76	0.46	1.46	0.58	0.36	0.39
S5	0.61	0.30	0.98	0.38	0.42	0.57
S6	0.42	0.52	0.61	0.50	0.17	0.34
S7	0.61	0.18	0.40	0.19	0.30	0.19
S8	0.28	0.30	0.60	0.26	0.16	0.14
S9	0.26	0.18	0.53	0.20	0.16	0.11
S10	0.29	0.29	0.40	0.23	0.16	0.09
S11	0.25	0.36	0.47	0.29	0.16	0.06
S14	0.46	0.41	1.27	0.57	0.50	0.40
S15	0.34	1.57	1.46	0.74	1.36	1.61
S16	0.23	0.26	0.74	0.39	0.17	0.17
S17	0.44	0.40	0.82	0.46	0.28	0.23
S20	0.64	1.21	0.33	0.10	0.07	0.65
S21	0.46	0.29	1.05	0.49	0.21	0.54
S22	0.66	0.54	0.84	0.56	0.52	0.31
S23	0.61	1.02	1.39	0.61	0.34	0.64
S24	0.28	0.64	0.99	0.59	0.33	0.44

Note: Gifford et al. (1987), the source for the table, note that data for Footings S12, S13, and S18 were not included because construction problems at these sites resulted in disturbance of the subgrade soils, and short-term settlement was increased. Data for Footing S19 appear to be anomalous and have been excluded in this table and Figure 6.8.

bridges were single-span structures. Two two-span and three four-span bridges were also monitored, in addition to a single five-span structure. Nine of the structures were designed to carry highway traffic, and one four-span bridge carried railroad traffic across an Interstate highway. Additional information on the instrumentation and data collection at the 10 bridges can be found in Gifford et al. (1987). Similar and more extensive databases are available for spread footings (e.g., Sargand et al. 1999; Sargand and Masada 2006; Akbas and Kulhawy 2009; Samtani et al. 2010) and other foundation types, such as driven piles and drilled shafts. Similar databases are also available for lateral load behavior. However, for this report, the calibration concepts for SLS evaluations are demonstrated by use of the limited data set for spread footings shown in Table 6.2. Although spread footings are used as an example, all the concepts discussed here are applicable to other foundation types and deformation patterns.

Figure 6.8 shows a plot of the data in Table 6.2 and the spread of the data about the 1:1 diagonal line, which defines the case for which the predicted and measured values are equal. Such a plot provides a visual frame of reference to judge the accuracy of the prediction method. If the data points align closely with the 1:1 diagonal line, then the predictions based on the analytical method being evaluated are close to the measured values and are more accurate than the case for which the data points do not align closely with the 1:1 diagonal line. In the geotechnical literature (e.g., Tan and Duncan 1991), *accuracy* is defined as the mean value of the ratio of the predicted (calculated) to the measured settlements. Table 6.3 shows the values of accuracy (denoted by  $X$ , where  $X = \delta_P/\delta_M$ ) for each footing based on the data in Table 6.2.

As noted in Step 3 of the calibration process, the value of  $\delta_M$  can be considered as the resistance and equivalent to the tolerable settlement ( $\delta_T$ ). The accuracy (i.e.,  $X = \delta_P/\delta_M$

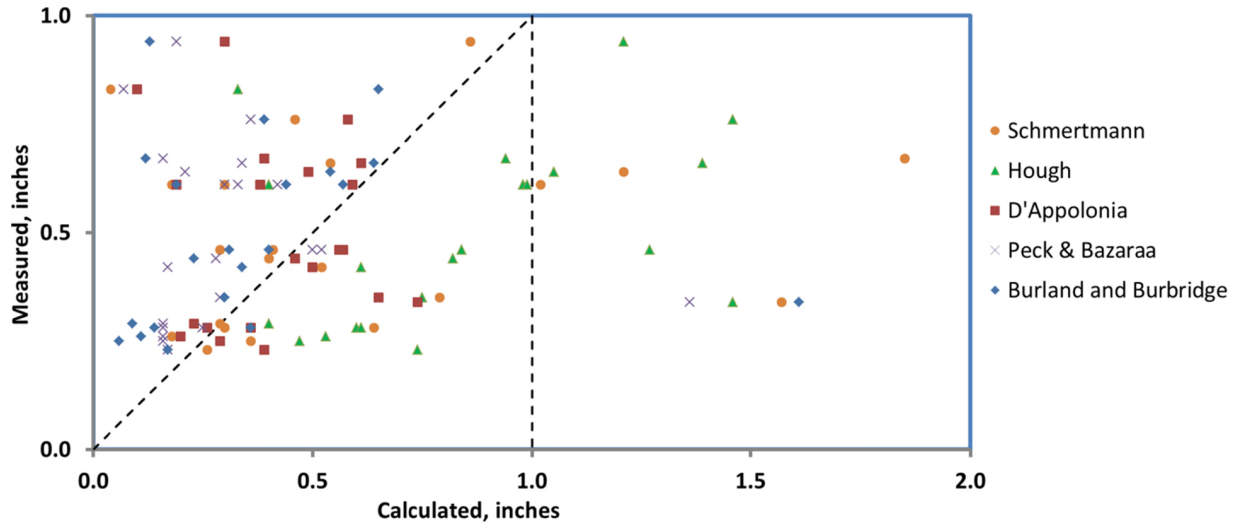


Figure 6.8. Comparison of measured and calculated (predicted) settlements based on service load data in Table 6.2.

Table 6.3. Accuracy ( $X = \delta_P/\delta_M$ ) Values Based on Data Shown in Table 6.2

Site	Schmertmann et al. (1978)	Hough (1959)	D'Appolonia et al. (1968)	Peck and Bazaraa (1969)	Burland and Burbridge (1984)
S1	2.257	2.143	1.857	0.829	0.857
S2	2.761	1.403	0.582	0.239	0.179
S3	0.915	1.287	0.319	0.202	0.138
S4	0.605	1.921	0.763	0.474	0.513
S5	0.492	1.607	0.623	0.689	0.934
S6	1.238	1.452	1.190	0.405	0.810
S7	0.295	0.656	0.311	0.492	0.311
S8	1.071	2.143	0.929	0.571	0.500
S9	0.692	2.038	0.769	0.615	0.423
S10	1.000	1.379	0.793	0.552	0.310
S11	1.440	1.880	1.160	0.640	0.240
S14	0.891	2.761	1.239	1.087	0.870
S15	4.618	4.294	2.176	4.000	4.735
S16	1.130	3.217	1.696	0.739	0.739
S17	0.909	1.864	1.045	0.636	0.523
S20	1.891	1.641	0.766	0.328	0.844
S21	0.630	1.826	1.217	1.130	0.674
S22	0.818	2.106	0.924	0.515	0.970
S23	1.672	1.623	0.967	0.541	0.721
S24	2.286	2.179	1.286	0.893	1.286

[or  $\delta_p/\delta_T$ ] is a random variable that can now be modeled by an appropriate PDF. To develop an appropriate PDF, an evaluation of the data spread around the mean value is needed. This evaluation involves statistical analysis and the development of histograms.

Table 6.4 presents the arithmetic mean ( $\mu$ ) and standard deviation ( $\sigma$ ) values for various methods. *AASHTO LRFD* recommends the use of Hough's (1959) method, which has the smallest CV, for calculating immediate settlement. However, the Hough method is conservative by a factor of approximately two (see mean value in Table 6.4), which leads to an unnecessary use of deep foundations instead of spread footings. FHWA (Samtani and Nowatzki 2006; Samtani et al. 2010) recommends the use of the method proposed by Schmertmann et al. (1978) because it is a rational method that considers not only the applied stress and its associated strain influence distribution with depth for various footing shapes, but also the elastic properties of the foundation soils, even if they are layered.

Even though FHWA and AASHTO recommend the Schmertmann et al. (1978) and Hough (1959) methods, respectively, all the methods noted in Table 6.2 to Table 6.4 were evaluated as part of the calibration process because some agencies may use one of the remaining three methods as a result of past successful local practice.

As noted earlier, accuracy ( $X = \delta_p/\delta_M$ ) is a random variable that can be modeled by an appropriate PDF. The data for  $X$  in Table 6.3 were used to develop histograms.

The histograms of the data for  $X$  taken from Columns 2 to 6 of Table 6.3 are shown in Figure 6.9a to Figure 6.13a, respectively. None of the histograms resembles a classic bell shape characteristic of normally distributed data. Thus, nonnormal distributions would be more appropriate in these cases. To evaluate the deviation of the data from a classic normal PDF, the data for the value of  $X$  in Table 6.3 were plotted against the standard normal variable ( $z$ ) to generate CDFs, as shown in Figure 6.9b to Figure 6.13b. See Allen et al. (2005, Chapter 5) for a definition of  $z$  and procedures to develop the lower graphs (b) in Figures 6.9–6.13. The beneficial attributes of this probability plot are

discussed above. As Figure 6.9b to Figure 6.13b show, the data points based on Table 6.3 do not plot on the straight line, which confirms the observation of nonnormal distributions made on the basis of the histograms in Figure 6.9a to Figure 6.13a.

By using procedures described in Allen et al. (2005), a lognormal distribution was used to evaluate the nonnormal data. As seen in Figure 6.9b to Figure 6.13b, the lognormal distribution fits the data better than the normal distribution. The lognormal distribution, which is valid between values of 0 and  $+\infty$ , is used in these figures because (1) immediate settlement cannot have negative values, and (2) lognormal PDFs have been used in the past for nonnormal distributions during calibration of the strength limit state for geotechnical, as well as structural, features in the *AASHTO LRFD* framework. For SLS, a PDF with an upper bound and lower bound (e.g., beta distribution) instead of open tail(s) (e.g., normal or lognormal distribution) may be more appropriate because the conditions represented by an open-tail PDF are not physically possible when one considers foundation deformations. As noted, the lognormal PDF is used here to be consistent with the PDFs that have been used in LRFD calibration processes to date. Guidance for the selection of an appropriate PDF and development of the distribution parameters shown in Table 6.5 is provided in Nowak and Collins (2013) or other similar books that deal with probabilistic methods.

Values of the lognormal mean and lognormal standard deviation are needed to use the lognormal PDF. These values can be obtained by using correlations with the mean and standard deviation values for normal distribution or calculated directly from the natural logarithm ( $\ln$ ) of the values of the data points. Table 6.5 presents the values for correlated mean ( $\mu_{LNC}$ ) and correlated standard deviation ( $\sigma_{LNC}$ ). Table 6.6 shows the lognormal of accuracy values of data in Table 6.3, and Table 6.7 presents the values for arithmetic mean ( $\mu_{LNA}$ ) and arithmetic standard deviation ( $\sigma_{LNA}$ ) based on the  $\ln(X)$  values in Table 6.6.

The correlated and arithmetic values of the mean ( $\mu_{LNC}$  and  $\mu_{LNA}$ , respectively) and standard deviation ( $\sigma_{LNC}$  and  $\sigma_{LNA}$ , respectively) are presented in Table 6.8. (text continues on page 160)

**Table 6.4. Statistics of Accuracy ( $X$ ) Values Based on Data Shown in Table 6.3**

Statistic	Schmertmann et al. (1978)	Hough (1959)	D'Appolonia et al. (1968)	Peck and Bazaraa (1969)	Burland and Burbridge (1984)
Count	20	20	20	20	20
Minimum	0.295	0.656	0.311	0.202	0.138
Maximum	4.618	4.294	2.176	4.000	4.735
$\mu$	1.381	1.971	1.031	0.779	0.829
$\sigma$	1.006	0.769	0.476	0.796	0.968
CV	0.729	0.390	0.462	1.022	1.168

Note: CV =  $\sigma/\mu$ .

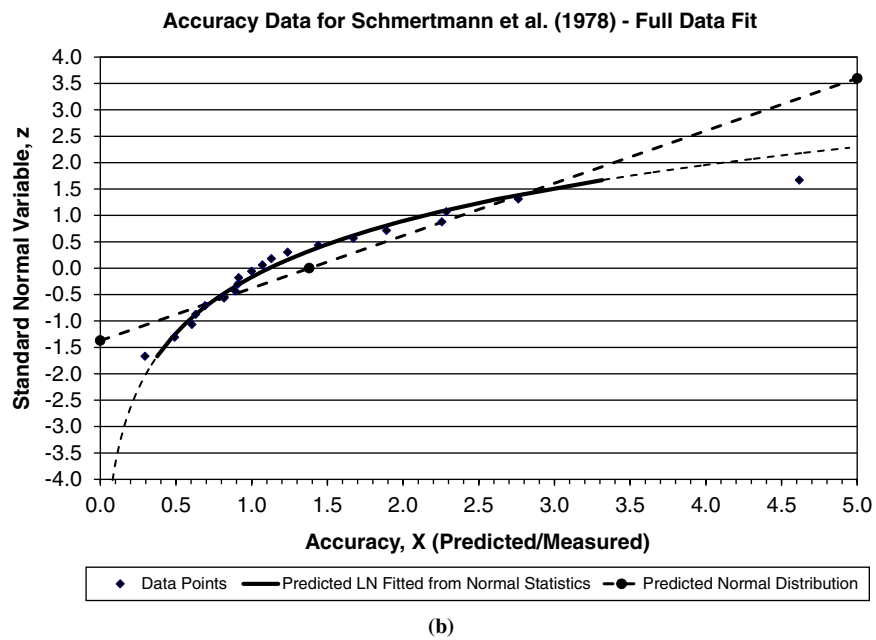
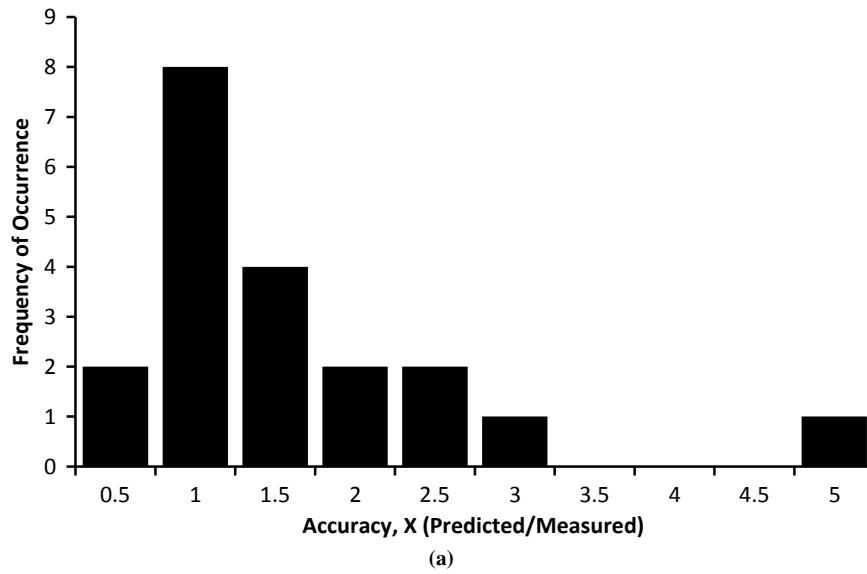


Figure 6.9. Schmertmann et al. (1978) method: (a) histograms for accuracy ( $X$ ) and (b) plot of standard normal variable ( $z$ ) as a function of  $X$ .



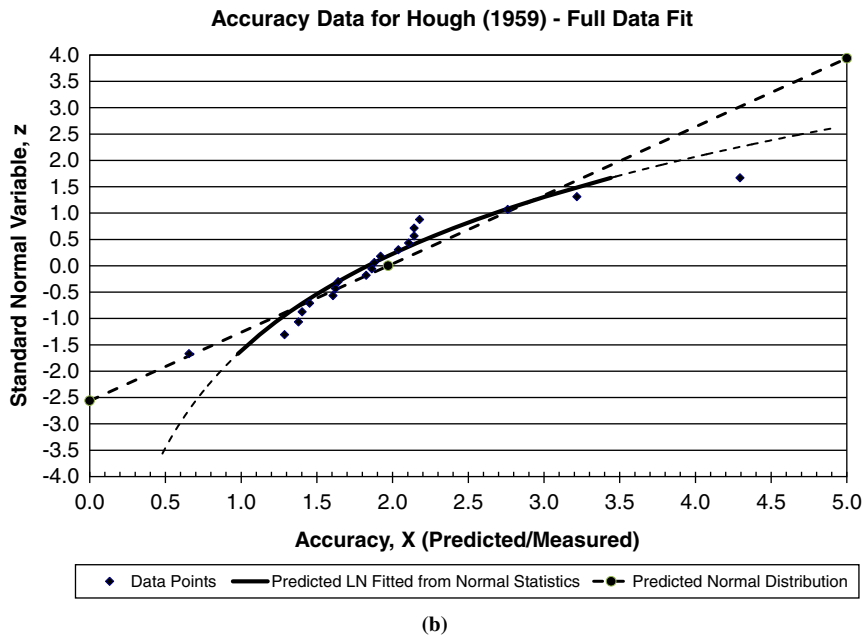
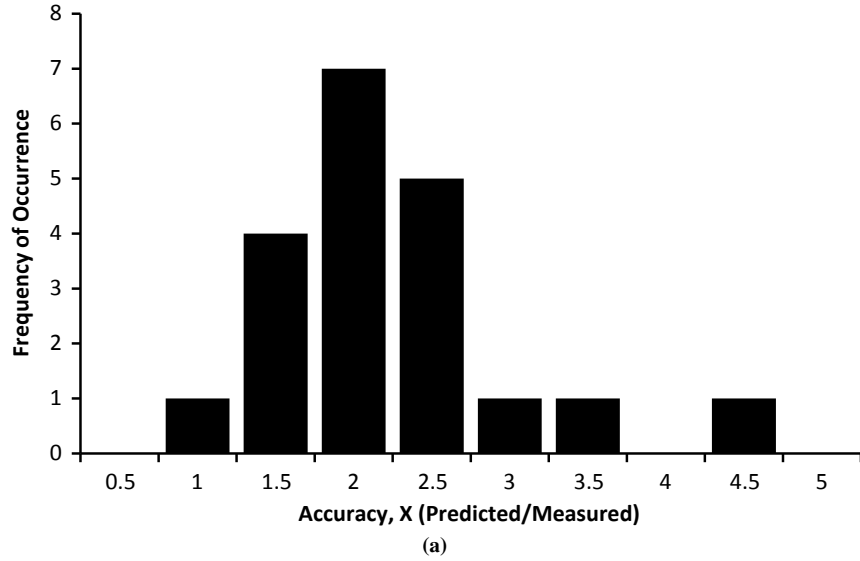
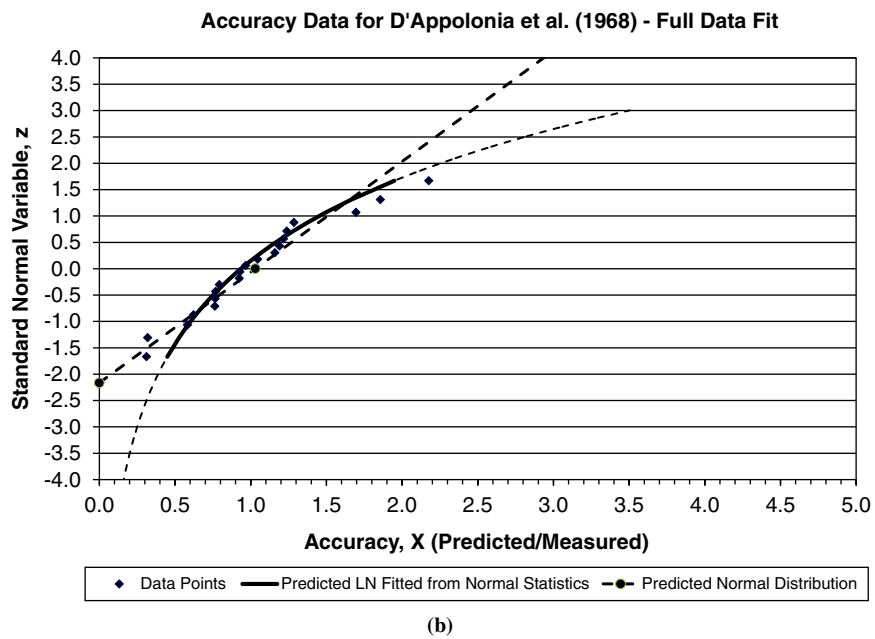
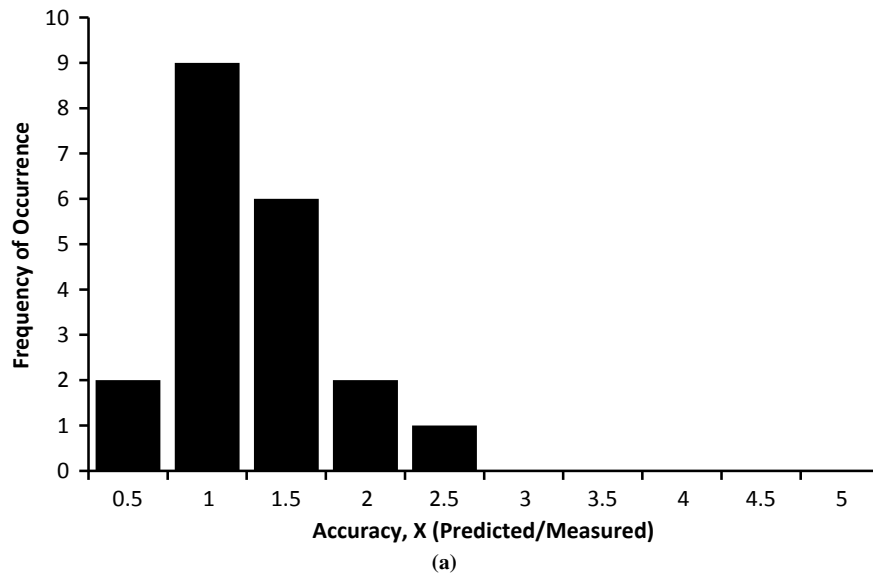


Figure 6.10. Hough (1959) method: (a) histograms for accuracy (X) and (b) plot of standard normal variable (z) as a function of X.



**Figure 6.11.** *D'Appolonia et al. (1968) method: (a) histograms for accuracy (X) and (b) plot of standard normal variable (z) as a function of X.*

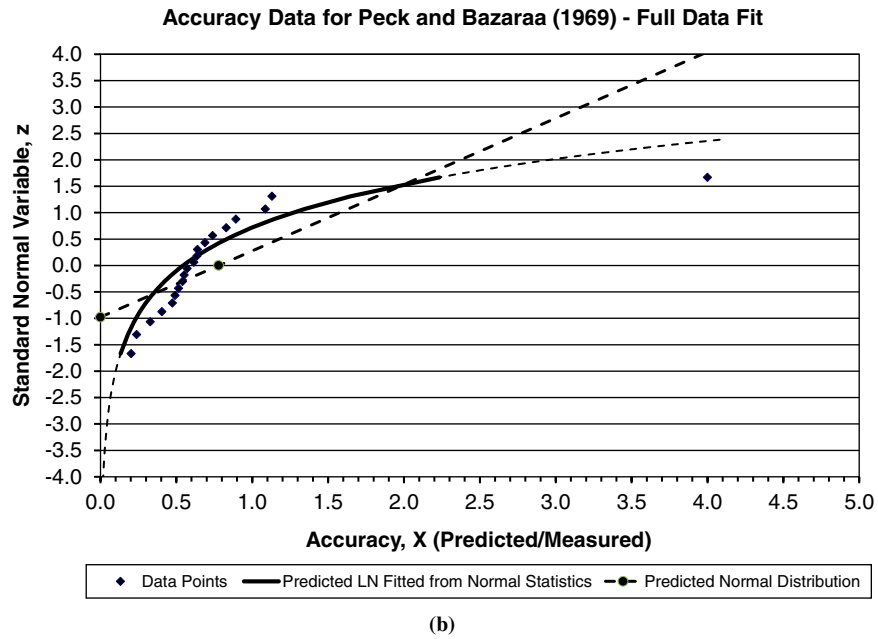
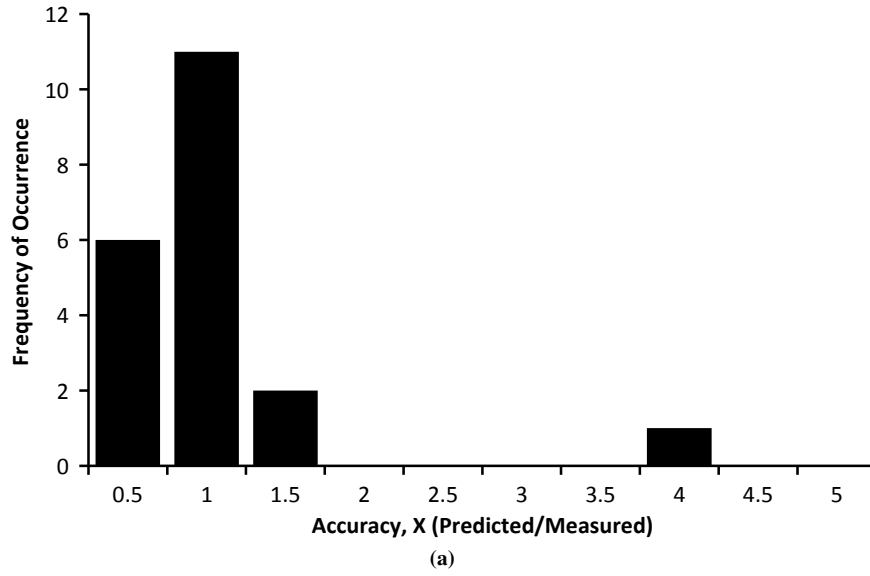
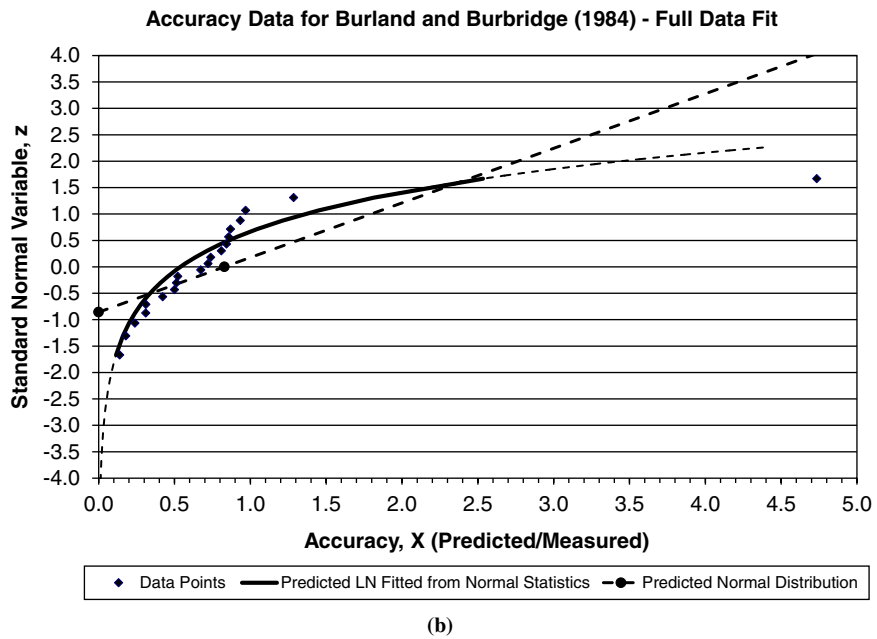
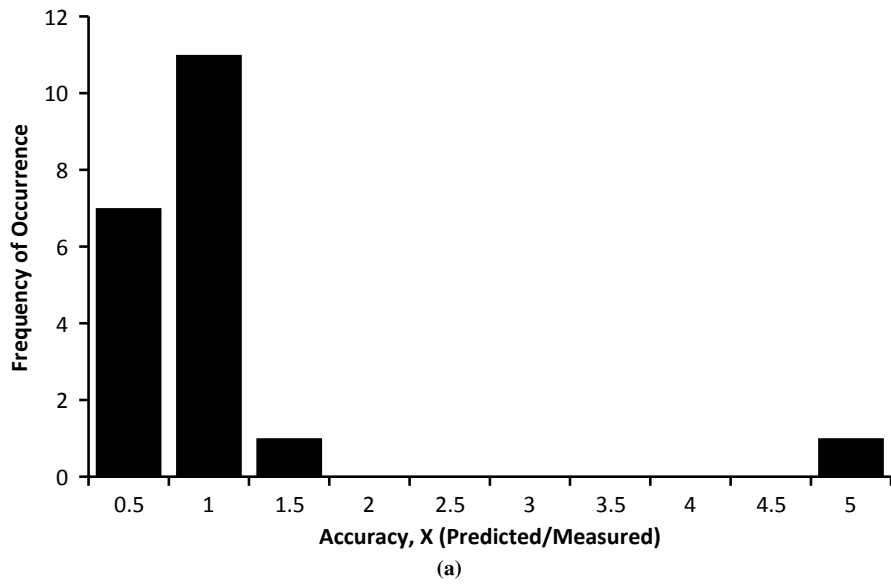


Figure 6.12. Peck and Bazaraa (1969) method: (a) histograms for accuracy (X) and (b) plot of standard normal variable (z) as a function of X.



**Figure 6.13. Burland and Burbridge (1984) method: (a) histograms for accuracy (X) and (b) plot of standard normal variable (z) as a function of X.**

**Table 6.5. Correlated Statistics of Accuracy (X) for Lognormal PDFs**

Statistic	Schmertmann et al. (1978)	Hough (1959)	D'Appolonia et al. (1968)	Peck and Bazaraa (1969)	Burland and Burbridge (1984)
$\mu_{LNC}$	0.1095	0.6076	-0.0665	-0.6078	-0.6177
$\sigma_{LNC}$	0.6528	0.3766	0.4398	0.8459	0.9274

Note: The  $\mu_{LNC}$  and  $\sigma_{LNC}$  values for lognormal distribution were calculated from the normal (arithmetic) mean and standard deviation values in Table 6.4, respectively, by using the following equations based on idealized normal and lognormal PDFs:  $\mu_{LNC} = \ln(\mu) - 0.50(\sigma_{LNC})^2$ ; and  $\sigma_{LNC} = [\ln\{(\sigma/\mu)^2 + 1\}]^{0.5}$ .

**Table 6.6. Lognormal of Accuracy Values [ln(X)] Based on Data Shown in Table 6.3**

Site	Schmertmann et al. (1978)	Hough (1959)	D'Appolonia et al. (1968)	Peck and Bazaraa (1969)	Burland and Burbridge (1984)
S1	0.8141	0.7621	0.6190	-0.1881	-0.1542
S2	1.0157	0.3386	-0.5411	-1.4321	-1.7198
S3	-0.0889	0.2525	-1.1421	-1.5989	-1.9783
S4	-0.5021	0.6529	-0.2703	-0.7472	-0.6672
S5	-0.7097	0.4741	-0.4733	-0.3732	-0.0678
S6	0.2136	0.3732	0.1744	-0.9045	-0.2113
S7	-1.2205	-0.4220	-1.1664	-0.7097	-1.1664
S8	0.0690	0.7621	-0.0741	-0.5596	-0.6931
S9	-0.3677	0.7122	-0.2624	-0.4855	-0.8602
S10	0.0000	0.3216	-0.2318	-0.5947	-1.1701
S11	0.3646	0.6313	0.1484	-0.4463	-1.4271
S14	-0.1151	1.0155	0.2144	0.0834	-0.1398
S15	1.5299	1.4572	0.7777	1.3863	1.5550
S16	0.1226	1.1686	0.5281	-0.3023	-0.3023
S17	-0.0953	0.6225	0.0445	-0.4520	-0.6487
S20	0.6369	0.4951	-0.2671	-1.1144	-0.1699
S21	-0.4613	0.6022	0.1967	0.1226	-0.3947
S22	-0.2007	0.7448	-0.0788	-0.6633	-0.0308
S23	0.5141	0.4842	-0.0333	-0.6144	-0.3267
S24	0.8267	0.7787	0.2513	-0.1133	0.2513

**Table 6.7. Statistics of ln(X) Values Based on Data Shown in Table 6.6**

Statistic	Schmertmann et al. (1978)	Hough (1959)	D'Appolonia et al. (1968)	Peck and Bazaraa (1969)	Burland and Burbridge (1984)
Count	20	20	20	20	20
Minimum	-1.2205	-0.4220	-1.1664	-1.5989	-1.9783
Maximum	1.5299	1.4572	0.7777	1.3863	1.5550
$\mu_{LNA}$	0.1173	0.6114	-0.0793	-0.4854	-0.5161
$\sigma_{LNA}$	0.6479	0.3807	0.5029	0.6226	0.7731

Note:  $\mu_{LNA}$  = arithmetic mean of ln(X) values;  $\sigma_{LNA}$  = arithmetic standard deviation of ln(X) values.

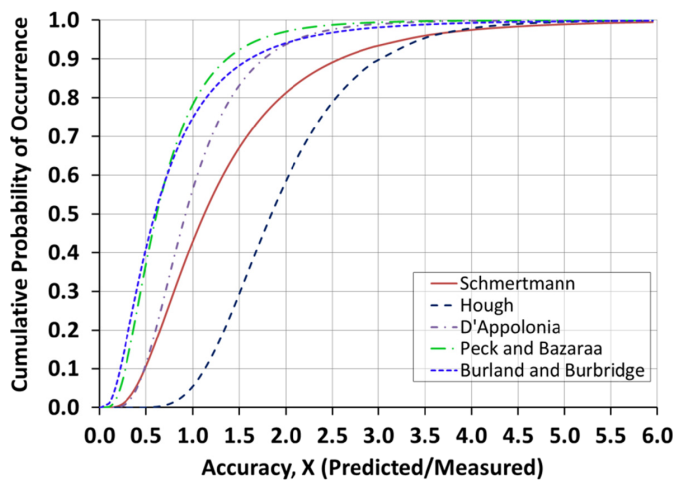
(continued from page 153)

respectively) for lognormal distributions are not equal. This is because the correlated values were based on derivations for an idealized lognormal distribution and not a sample distribution from actual data, which may not necessarily fit an idealized lognormal distribution. In contrast, the arithmetic values were obtained by taking the arithmetic mean and standard deviation directly from the  $\ln(X)$  value of each data point noted in Columns 2 to 6 of Table 6.3.

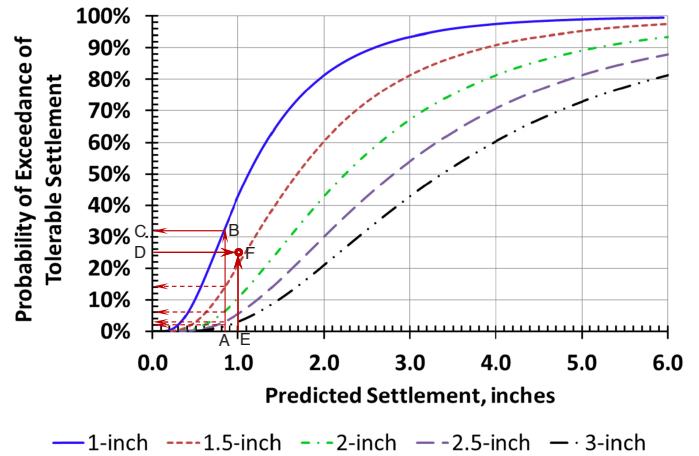
It is important to use the appropriate values of mean and standard deviation based on the syntax for a lognormal distribution function used by a particular computational program. For example, if one is using the @RISK program by Palisade Corporation, then the RISKLOGNORM function in that program is based on arithmetic values ( $\mu$  and  $\sigma$ ) of the normal distribution. In contrast, the Microsoft Excel LOGNORMDIST (or LOGNORM.DIST) function uses the arithmetic mean ( $\mu_{LNA}$ ) and standard deviation ( $\sigma_{LNA}$ ) values of  $\ln(X)$ . Use of improper values of mean and standard deviation can lead to drastically different results. This issue is of critical importance because calibration in this report, as mentioned earlier, is based on Microsoft Excel.

Figure 6.14 shows the CDFs for accuracy ( $X$ ) for various analytical methods based on the LOGNORM.DIST function in the 2010 version of Microsoft Excel using the  $\mu_{LNA}$  and  $\sigma_{LNA}$  values noted in Table 6.7. These CDFs can now be used to develop the PEC discussed in Section 6.1.2 for various analytical methods.

Figure 6.15 shows the PEC for the method by Schmertmann et al. (1978). The probability of exceedance corresponding to a given predicted settlement can now be readily determined. For example, assume that the geotechnical engineer has predicted a settlement of 0.85 in. The probability of exceedance of 1 in. in this case is approximately 32%. This can be found



**Figure 6.14. CDFs for various analytical methods for estimation of immediate settlement of spread footings.**



**Figure 6.15. PEC for the Schmertmann et al. (1978) method.**

by drawing line AB, finding the intersection of the line with the curve for 1 in., drawing line BC, and reading the value from the ordinate of the PEC in Figure 6.15. Four additional curves for settlements of 1.5, 2, 2.5, and 3 in. are shown in Figure 6.15. Using the procedure demonstrated for the example above (see dashed arrows in Figure 6.15), if the predicted (calculated) value is 0.85 in., then the probability of the measured value being greater than 1.5, 2, 2.5, and 3 in. is approximately 14%, 6%, 3%, and 2%, respectively.

A load factor for settlement ( $\gamma_{SE}$ ) can be determined using the procedure in Section 6.1.2.5. For example, assume the predicted settlement is 1 in. To determine the value of  $\gamma_{SE}$  for a 25% target probability of exceedance ( $P_{eT}$ ), draw a horizontal line from Point D on the ordinate corresponding to a value of 25%. Next, draw a vertical line from Point E on the abscissa corresponding to a value of 1 in. Locate the point of intersection, F, which lies between the curves for 1 in. and 1.5 in. Interpolating between the two curves leads to a value of approximately 1.35 in. Based on the definition of  $\gamma_{SE}$  noted above, the value of  $\gamma_{SE}$  is equal to 1.35 in./1.0 in., or 1.35.

PECs for other analytical methods noted in Figure 6.14 are given in Figure 6.16 to Figure 6.19. Those PECs can be used in a similar manner as demonstrated for the PEC for the Schmertmann et al. (1978) method.

A PEC chart is essentially a representation of the CDF of accuracy, or  $X$ . Similar charts are referred to as probabilistic design charts by Das and Sivakugan (2007) and Sivakugan and Johnson (2002, 2004) and artificial neural network charts by Shahin et al. (2002) and Musso and Provenzano (2003). Although not specifically in chart format, similar concepts are presented in Tan and Duncan (1991) and Duncan (2000). The specific format of PEC that is developed and used here is amenable to correlation to the AASHTO LRFD-based concept of target reliability index, as explained in Step 5.



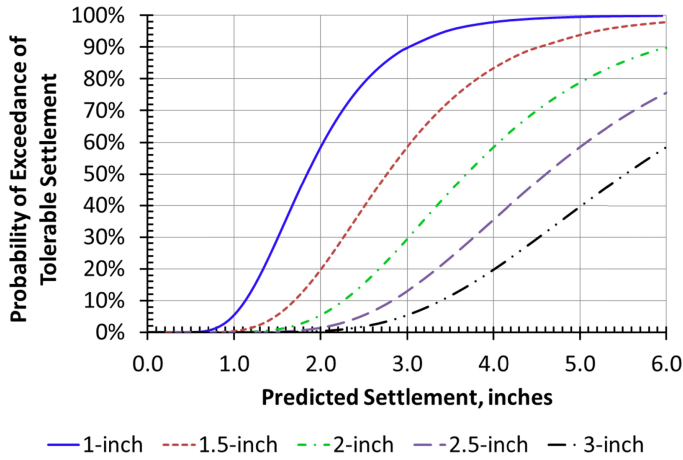


Figure 6.16. PEC for the Hough (1959) method.

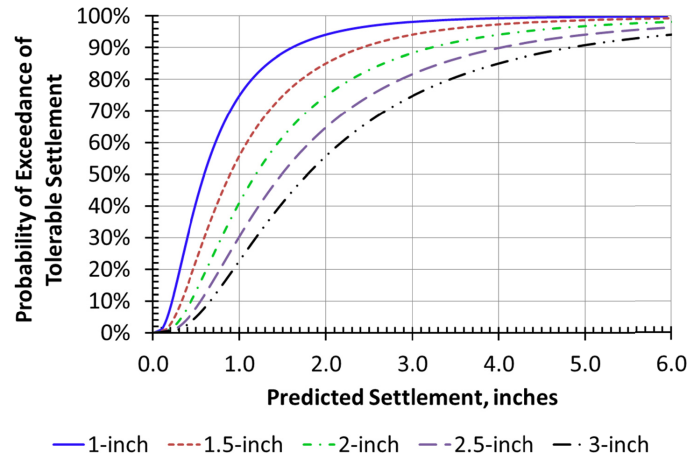


Figure 6.19. PEC for the Burland and Burbridge (1984) method.

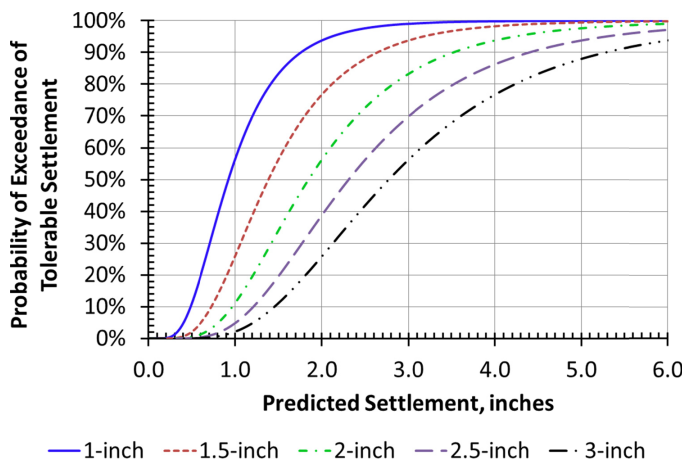


Figure 6.17. PEC for the D'Appolonia et al. (1968) method.

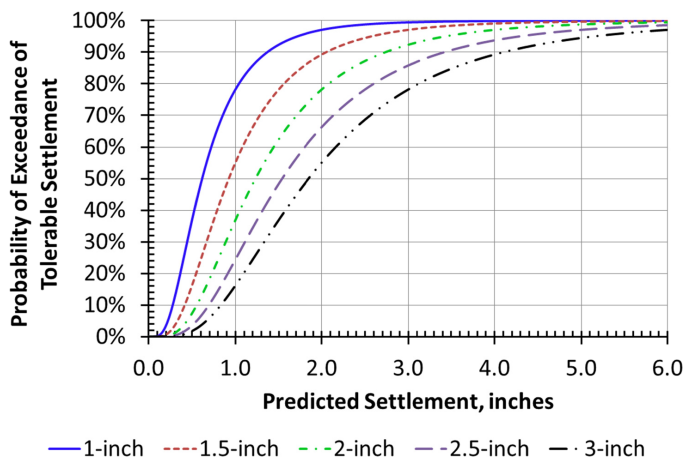


Figure 6.18. PEC for the Peck and Bazaraa (1969) method.

### 6.1.3.5 Step 5: Develop Reliability Analysis Procedure

The estimation of load factor for settlement ( $\gamma_{SE}$ ) in terms of probability of exceedance ( $P_e$ ) was demonstrated in the previous step. In the AASHTO LRFD framework, calibrations are expressed in terms of a reliability index ( $\beta$ ).  $\beta$  can be expressed in terms of  $P_e$  of a predicted value by using Equation 6.4, which applies to normally distributed data. As observed from Step 4, lognormal distributions have been used. Furthermore, the CV values noted in Table 6.4 are rather large. For a normal random variable, the relationship between  $\beta$  and  $P_e$  depends only on CV (i.e., one parameter), but for a lognormal distribution, it depends on the mean and standard deviation or the mean and CV (i.e., two parameters). Therefore, strictly speaking,  $\beta$  should be based on a lognormal function. However, for  $\beta < 2.0$  there is not a significant practical difference in the  $P_e$  values for data that are normally or lognormally distributed for the wide range of CVs noted in Table 6.4. An assumption of a normal distribution is generally conservative in the sense that for a given  $\beta$  it gives a larger  $P_e$  compared with a lognormal distribution. Furthermore, conventionally the normal distribution has been assumed for strength limit states in AASHTO LRFD (as well as other international codes), which has  $\beta$  values larger than 2.0. The key consideration is that the type of distribution is not as important as being consistent and not mixing different distributions while comparing  $\beta$  values. When these various issues are taken into account, the Microsoft Excel formula that assumes normally distributed data is considered to be acceptable for SLS calibrations.

Table 6.8 and Figure 6.20 were generated by using Equation 6.4:

$$\beta = \text{NORMSINV}(1 - P_e) \tag{6.4}$$

**Table 6.8. Values of  $\beta$  and Corresponding  $P_e$  Based on Normally Distributed Data**

$\beta$	$P_e$ (%)	$\beta$	$P_e$ (%)	$\beta$	$P_e$ (%)	$\beta$	$P_e$ (%)
2.00	2.28	1.50	6.68	1.00	15.87	0.50	30.85
1.95	2.56	1.45	7.35	0.95	17.11	0.45	32.64
1.90	2.87	1.40	8.08	0.90	18.41	0.40	34.46
1.85	3.22	1.35	8.85	0.85	19.77	0.35	36.32
1.80	3.59	1.30	9.68	0.80	21.19	0.30	38.21
1.75	4.01	1.25	10.56	0.75	22.66	0.25	40.13
1.70	4.46	1.20	11.51	0.70	24.20	0.20	42.07
1.65	4.95	1.15	12.51	0.65	25.78	0.15	44.04
1.60	5.48	1.10	13.57	0.60	27.43	0.10	46.02
1.55	6.06	1.05	14.69	0.55	29.12	0.05	48.01
						0.00	50.00

Note: Linear interpolation may be used as an approximation for intermediate values.

The correlation between  $\beta$  and  $P_e$  can now be used to rephrase the earlier discussion with respect to Figure 6.15. In that discussion, as an example, it was assumed that the geotechnical engineer has predicted a settlement of 0.85 in. From Figure 6.15, it was determined that the probability of exceedance of 1, 1.5, 2, 2.5, and 3 in. was approximately 32%, 14%, 6%, 3%, and 2%, respectively. Using Table 6.8 (or Figure 6.20 or Equation 6.3), the results can now be expressed in terms of reliability index values. Thus, it can be stated that if the predicted settlement is 0.85 in., then the assumption of tolerable settlement values of 1, 1.5, 2, 2.5, and 3 in. means a reliability index of approximately 0.45, 1.10, 1.55, 1.90, and >2.00, respectively.

In the example, the geotechnical engineer has predicted settlement  $\delta_p = 0.85$  in. by using the Schmertmann et al. (1978) method. The owner has specified that the SLS design for the



**Figure 6.20. Relationship between  $\beta$  and  $P_e$  for the case of a single load and single resistance.**

bridge should be performed using a reliability index of 0.50. What is the value of  $\gamma_{SE}$  and the tolerable settlement that the bridge designer should use?

The load factor ( $\gamma_{SE}$ ) is a function of the probability of exceedance ( $P_e$ ) of the foundation deformation under consideration, which in this example is the immediate settlement of spread footings calculated by using the analytical method of Schmertmann et al. (1978). By using either Equation 6.4 or Table 6.8, a value of  $P_e \approx 0.3085$  (or 30.85%) is obtained for  $\beta = 0.50$ .

Equation 6.5 is the formula used in Microsoft Excel to determine a value of accuracy ( $X$ ) in terms of  $P_e$ , the mean value ( $\mu_{LNA}$ ), and the standard deviation ( $\sigma_{LNA}$ ) of the lognormal distribution function as computed in Step 4. The value of  $X$  represents the probability of the accuracy value ( $\delta_p/\delta_T$ ) being less than a specified value.

$$P_e = \text{LOGNORMDIST}(X, \mu_{LNA}, \sigma_{LNA}) \tag{6.5}$$

From Table 6.7, for the Schmertmann et al. (1978) method,  $\mu_{LNA} = 0.1173$  and  $\sigma_{LNA} = 0.6479$ . The goal is to determine the value of  $X$  that gives  $P_e = 0.3085$ . Thus, for this example, the expression for  $P_e$  can be written as shown by Equation 6.6:

$$P_e = \text{LOGNORMDIST}(X, 0.1173, 0.6479) = 0.3085 \text{ or } 30.85\% \tag{6.6}$$

Using Goal Seek in Microsoft Excel,  $X$  (i.e.,  $\delta_p/\delta_T$ )  $\approx 0.813$ . Note that in the 2010 version of Microsoft Excel, another function, LOGNORM.DIST, can also be used. In this case, the same result ( $X \approx 0.813$ ) is obtained by using the following syntax and using the Goal Seek function to determine  $X$  (TRUE indicates the use of a CDF):

$$P_e = \text{LOGNORM.DIST}(X, 0.1173, 0.6479, \text{TRUE}) = 0.3085.$$

In the context of the AASHTO LRFD framework, the load factor ( $\gamma_{SE}$ ) is the reciprocal of  $X$ . Thus, for immediate settlement of spread footings based on the method of Schmertmann et al. (1978),  $\gamma_{SE} = 1/0.813 \approx 1.23$ .

As per the AASHTO LRFD framework, the load factor is rounded up to the nearest 0.05, and thus  $\gamma_{SE} = 1.25$  should be used.

Therefore, in the bridge design example, the bridge designer should use a settlement value of  $(\gamma_{SE})(\delta_p) = (1.25)(0.85 \text{ in.}) = 1.06$  in. to assess the effect of settlement on the structure. This value can also be obtained using the graphic technique explained earlier with respect to Figure 6.15. The example demonstrated with respect to Figure 6.15 also assumed a tolerable settlement of 0.85 in., and it was found that a settlement of 1 in. would imply a 32% probability of exceedance. These

**Table 6.9. Computed Values of  $\gamma_{SE}$  for Various Methods to Estimate Immediate Settlement of Spread Footings on Cohesionless Soils**

Reliability Index ( $\beta$ )	Schmertmann et al. (1978)	Hough (1959)	D'Appolonia et al. (1968)	Peck and Bazaraa (1969)	Burland and Burbridge (1984)
0.00	0.89	0.54	1.08	1.62	1.68
0.50	1.23	0.66	1.39	2.22	2.47
1.00	1.70	0.79	1.79	3.03	3.63
1.50	2.35	0.96	2.30	4.13	5.34
2.00	3.25	1.16	2.96	5.64	7.86
2.50	4.49	1.41	3.81	7.71	11.58
3.00	6.21	1.70	4.89	10.52	17.04
3.50	8.59	2.06	6.29	14.36	25.08

values are close to the value of 1.06 in. for a 30.85% probability of exceedance obtained here. Given that the load factor is rounded to the nearest 0.05, the result from the graphic technique is sufficiently accurate.

The procedure demonstrated in the above example can be used to develop values of  $\gamma_{SE}$  for any desired  $\beta$  by using the lognormal distribution of  $X$  for the method of Schmertmann et al. (1978). A similar approach can be used for other analytical methods and distributions.

Table 6.9 presents the values of  $\gamma_{SE}$  results for the various analytical methods shown in Figure 6.8 and Table 6.2. Obviously,  $\gamma_{SE}$  values less than 1.0 should not be allowed to prevent the risk of bridges being underdesigned. Furthermore, the values of  $\gamma_{SE}$  should be rounded to the nearest 0.05, because not doing so implies a level of confidence that is not justified by the available data. Table 6.10 presents values of  $\gamma_{SE}$  that are bounded by 1.0 and rounded to the nearest 0.05.

### 6.1.3.6 Step 6: Review Results and Selection of Load Factor for Settlement

Figure 6.21 shows a plot of  $\gamma_{SE}$  versus  $\beta$  based on the data shown in Table 6.10. The current practice based on *AASHTO LRFD* (2012) is as follows:

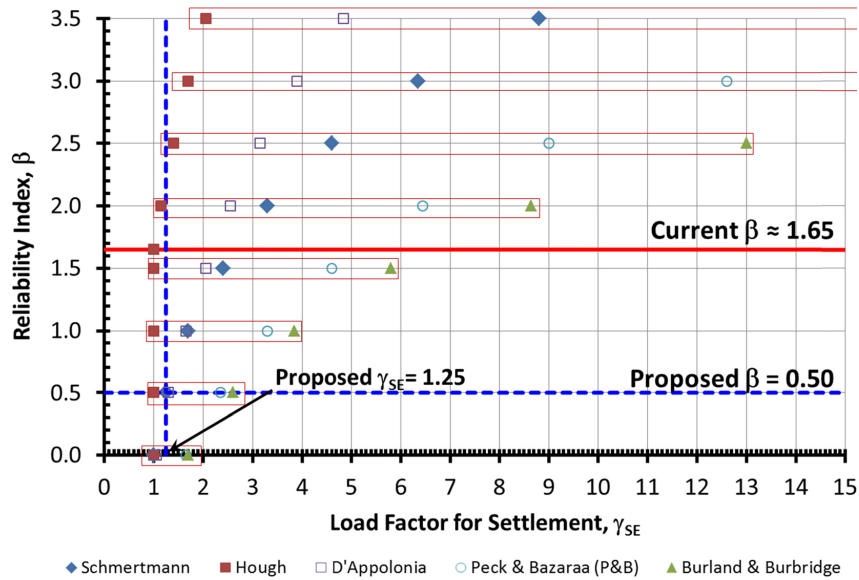
1. Use the Hough (1959) method to estimate immediate settlements.
2. Use  $\gamma_{SE} = 1.0$ .

The data in Table 6.10 and the graph in Figure 6.21 imply that  $\beta \approx 1.65$  corresponds to the current practice noted above.  $\beta \approx 1.65$  is based on the data set in Table 6.2. If additional data were included, or if a different regional data set were to be used, then the value of  $\beta$  may be different. However, based on a review of state practices performed as part of Samtani and

**Table 6.10. Proposed Values of  $\gamma_{SE}$  for Various Methods to Estimate Immediate Settlement of Spread Footings on Cohesionless Soils**

Reliability Index ( $\beta$ )	Schmertmann et al. (1978)	Hough (1959)	D'Appolonia et al. (1968)	Peck and Bazaraa (1969)	Burland and Burbridge (1984)
0.00	1.00	1.00	1.10	1.60	1.70
0.50	1.25	1.00	1.40	2.20	2.45
1.00	1.70	1.00	1.80	3.05	3.65
1.50	2.35	1.00	2.30	4.15	5.35
2.00	3.25	1.15	2.95	5.65	7.85
2.50	4.50	1.40	3.80	7.70	11.60
3.00	6.20	1.70	4.90	10.50	17.05
3.50	8.60	2.05	6.30	14.35	25.10

Note: The values of  $\gamma_{SE}$  have been rounded to the nearest 0.05 and limited to 1.00 or larger.



**Figure 6.21. Evaluation of  $\gamma_{SE}$  based on current and target reliability indices.**

Nowatzki (2006) and Samtani et al. (2010), it is anticipated that, based on its inherent conservatism, the value of  $\beta$  is anticipated to be large and greater than 1.0 for the Hough (1959) method and  $\gamma_{SE} = 1.0$ . The majority of the data points for the Hough method plot below  $\gamma_{SE} = 1.0$ , which suggests a significant conservatism in the Hough method. This is consistent with the earlier observation that the Hough method is conservative (overpredicts) by a factor of approximately two (see Table 6.4), which leads to an unnecessary use of deep foundations instead of spread footings. Based on a consideration of reversible and irreversible SLSs for bridge superstructures, as shown earlier, a target reliability index ( $\beta_T$ ) in the range of 0.50 to 1.00 for calibration of load factor  $\gamma_{SE}$  for foundation deformation in the Service I limit state is acceptable. Settlement is clearly an irreversible limit state with respect to the foundation elements, but it may be reversible through intervention with respect to the superstructure. This type of logic would lead to consideration of 0.50 as the  $\beta_T$  for calibration of immediate settlements under spread footings on cohesionless soils.

In Figure 6.21, the horizontal bold dashed line corresponds to  $\beta = 0.50$  for SLS evaluation. The boxes around the markers for various methods represent the spread of predicted values for the five methods evaluated here. For  $\beta = 0.50$ , if  $\gamma_{SE} = 1.25$  is adopted, then it would encompass three of the five methods. The value of  $\gamma_{SE} = 1.25$  includes the Schmertmann et al. (1978) method, which is currently recommended by Samtani and Nowatzki (2006) and Samtani et al. (2010) and is commonly used in U.S. practice. Based on these observations,  $\gamma_{SE} = 1.25$  is recommended.

### 6.1.3.7 Step 7: Select $\gamma_{SE}$ for Service I Limit State

As demonstrated in Steps 5 and 6, the  $\gamma_{SE}$  value can be determined for any reliability index ( $\beta$ ) for various analytical methods. Use of the format shown in Figure 6.21 will lead to better regional practices in the sense that owners desiring to calibrate their local practices can readily see the implication of a certain method on the selection and cost of a foundation system. This is because the chart in Figure 6.21 shows the reliability of various methods and permits selection of an appropriate method that would lead to selection of a proper foundation system for a given set of  $\beta$  and  $\gamma_{SE}$  values (i.e., not using a deep foundation system when a spread foundation would be feasible). The agency that calibrates a value of  $\gamma_{SE}$  based on a locally accepted analytical method must ensure that the chosen value of  $\gamma_{SE}$  is consistent with the serviceability of the substructure and superstructure design, as discussed in Step 6.

### 6.1.4 Meaning and Use of $\gamma_{SE}$

The meaning and use of  $\gamma_{SE}$  must be understood in the specific context of structural implications within the *AASHTO LRFD* framework. In particular, the value of  $\gamma_{SE}$  is used to assess structural implications, such as the generation of additional (secondary) moments within a given span because of settlement of one of the support elements and effect on the riding surface, and conceivably even appearance and roadway damage issues. If taken literally, the value of  $\gamma_{SE} = 1.25$  in the example could be interpreted to mean that the settlement predicted ( $\delta_p$ )



by the analytical method of Schmertmann et al. (1978) needs to be increased by 25% to limit the probability of exceedance ( $P_e$ ) of the tolerable settlement ( $\delta_T$ ) to less than 30.85%, corresponding to a target reliability index ( $\beta_T$ ) of 0.50. However, this literal interpretation is not entirely correct because the value of  $\gamma_{SE}$  (1.25 in this case) is just one of many load factors in the Service I limit state load combinations within the overall *AASHTO LRFD* framework.

In addition to the SLS, settlements need to be considered at applicable strength limit states, because although settlements can cause serviceability problems, they can also have a significant effect on moments in continuous superstructures that can result in increased member sizes. Settlement is handled more explicitly in *AASHTO LRFD* (in which it is listed among the loads in Table 3.4.1-1, Load Combinations and Load Factors) than it was in the *Standard Specifications for Highway Bridges*. It appears in four of the five strength load combinations and three of the four service load combinations. This emphasis may appear to be a departure from past practice, as exemplified by *AASHTO's Standard Specifications for Highway Bridges*, in that settlement does not appear in those load combinations. But settlement is mentioned in Article 3.3.2.1 of *Standard Specifications* (2002), which states "If differential settlement is anticipated in a structure, consideration should be given to stresses resulting from this settlement." The parent article (3.3, Dead Load) implies that settlement effects should be considered wherever dead load appears in the allowable stress design or load factor design (LFD) load combinations.

The additional moments due to the effect of settlement are very dependent on the stiffness of the bridge, as well as the angular rotation (i.e., differential settlement normalized with respect to span length, as discussed in Chapter 2 in the section on tolerable vertical deformation criteria). A limited study (Schopen 2010) of several two- and three-span steel and prestressed concrete continuous bridges selected from the NCHRP Project 12-78 database showed that allowing the full angular distortion suggested in Table 2.2 could result in an increase in the factored Strength I moments on the general order of as little as 10% for the more flexible units considered to more than double the moment from only the factored dead and live load moments for the stiffer units. These order of magnitude estimates are based on elastic analysis without consideration of creep, which could significantly reduce the moments, especially for relatively stiff concrete bridges. For example, a  $W 36 \times 194$  rolled beam with a  $10 \times 1\frac{7}{8}$ -in. bottom cover plate composite with a  $96 \times 7\frac{3}{4}$ -in. deck is presented in Brockenbrough and Merritt (2011). The computed moments of inertia for the basic beam and short-term composite and long-term composite sections were in the approximate ratio 1:2:3. This indicates that consideration of construction sequence, an appropriate choice of section properties, and possibly even a time-dependent

calculation of creep effects could be beneficial in some cases. Use of the construction point concept (see next section) would also mitigate the settlement moments. Nevertheless, Schopen's results suggest that the use of permissible angular distortions approaching those currently allowed by *AASHTO LRFD* requires careful consideration of the particular bridge and its design objectives.

As the predicted (estimated or calculated) settlement ( $\delta_p$ ) is based on the Service I load combination and the load factor ( $\gamma_{SE}$ ) is used to modify the Service I load combination, the use of  $\gamma_{SE}$  can potentially lead to a circular reference in the bridge design process that may require significant iterations. The following procedure is recommended to avoid a circular reference:

1. Assume zero settlement and determine the service load by using the Service I load combination. When settlement is assumed to be zero, the value of  $\gamma_{SE}$  is irrelevant.
2. Determine  $\delta_p$  based on the method that has been calibrated using the procedure described here.
3. Multiply  $\delta_p$  by  $\gamma_{SE} = 1.25$  to determine the tolerable (limiting) settlement ( $\delta_T$ ) that should be incorporated into bridge design through use of the  $\delta$ -0 angular distortion and construction point concept described below. The use of the  $\delta$ -0 angular distortion and construction point concept incorporates the span lengths, differential settlements between support elements, and the various stages of construction into the bridge design process.

### 6.1.5 Effect of Foundation Deformations on Bridge Superstructures

Uneven displacements of bridge abutments and pier foundations often lead to costly maintenance and repair measures associated with the structural distress that the bridge superstructure and substructure might experience. The bridge superstructure and substructure displacements can be due to a variety of reasons, including foundation deformations. The foundation deformations need to be evaluated in the context of span lengths and various construction steps to understand their effect on the bridge superstructures. These aspects and the concepts of angular distortion and construction points are discussed in this section. The application of load factors due to deformation (e.g.,  $\gamma_{SE}$ ) is also presented.

For all bridges, stiffness should be appropriate to the considered limit state. Similarly, the effects of continuity with the substructure should be considered. In assessing the structural implications of foundation deformations of concrete bridges, the determination of the stiffness of the bridge components should consider the effects of cracking, creep, and other inelastic responses.

**6.1.5.1  $\delta$ -0 Concept for Vertical Deformations (Settlements)**

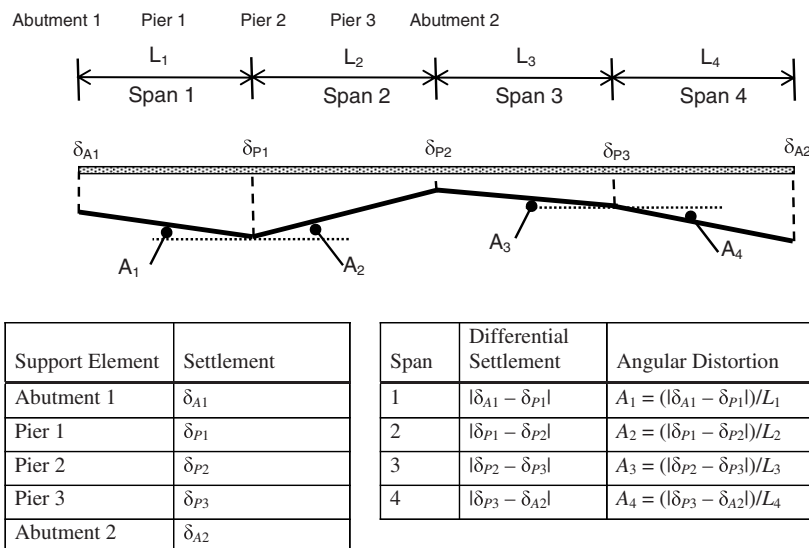
Because of the inherent variability of geomaterials, the vertical deformations at the support elements of a given bridge (i.e., piers and abutments) will generally be different. This is true regardless of whether deep foundations or spread footings are used. Figure 6.22 shows the hypothetical case of a four-span bridge structure with five support elements (two abutments and three piers) for which the calculated settlement ( $\delta$ ) at each support is different (the figure assumes rigid substructure units between the foundations and bridge superstructure). Differential settlements induce bending moments and shear in the bridge superstructure when spans are continuous over supports and potentially cause structural damage. To a lesser extent, they can also cause damage to a simple-span bridge. However, the major concern with simple-span bridges is the quality of the riding surface and aesthetics. Due to a lack of continuity over the supports, the changes in slope of the riding surface near the supports of a simple-span bridge induced by differential settlements may be more severe than those in a continuous-span bridge.

Depending on factors such as the type of superstructure, the connections between the superstructure and substructure units, and the span lengths and widths, the magnitudes of differential settlement that can cause damage to the bridge structure can vary significantly. For example, the damage to the bridge structure due to a differential settlement of 2 in. over a 50-ft span is likely to be more severe than the same amount of differential settlement over a 150-ft span. Various studies, including Grant et al. (1974) and Skempton and MacDonald (1956), have determined that the severity of

differential settlement on structures is roughly proportional to the angular distortion ( $A$ ), which is a normalized measure of differential settlement that includes the distance over which the differential settlement occurs. Angular distortion is defined as the difference in settlement between two points ( $\Delta\delta$ ) divided by the distance between the two points ( $L$ ), as shown in Figure 6.22. Angular distortion is a dimensionless quantity that is expressed as an angle in radians. Theoretically, the ratio  $\Delta\delta/L$  represents the tangent of the angle of distortion, but for small values of the tangent, the angles are also very small. Thus, the tangents (i.e.,  $A$ ) are shown as angles in Figure 6.22. For bridge structures, the two points used to evaluate the differential settlement are commonly selected as the distance between adjacent support elements (see Figure 6.22).

Although all analytical methods for estimating settlements have a certain degree of uncertainty, the uncertainty of the calculated differential settlement is larger than the uncertainty of the calculated total settlement at each of the two support elements used to calculate the differential settlement (e.g., between an abutment and a pier or between two adjacent piers). For example, if one support element settles less than the amount calculated, and the other support element settles the amount calculated, the actual differential settlement will be larger than the difference between the two values of calculated settlement at the support elements. On the basis of these considerations and guidance in Samtani and Nowatzki (2006) and Barker et al. (1991), the following limit state criteria are suggested to estimate a realistic value of differential settlement and angular distortion:

- The actual settlement of any support element could be as large as the value calculated by using a given method.



**Figure 6.22. Concept of settlement and angular distortion in bridges.**



**Table 6.11. Estimation of Design Differential Settlements and Design Angular Distortions for Hypothetical Case Shown in Figure 6.22**

Span	Design Differential Settlement	Design Angular Distortion
1	$\delta_{P1} = \delta_{P1}$ (assume $\delta_{A1} = 0$ )	$A_1 = \delta_{P1}/L_1$
2	$\delta_{P1} = \delta_{P1}$ (assume $\delta_{P2} = 0$ )	$A_2 = \delta_{P1}/L_2$
3	$\delta_{P3} = \delta_{P3}$ (assume $\delta_{P2} = 0$ )	$A_3 = \delta_{P3}/L_3$
4	$\delta_{A2} = \delta_{A2}$ (assume $\delta_{P3} = 0$ )	$A_4 = \delta_{A2}/L_4$

- At the same time, the actual settlement of the adjacent support element could be zero instead of the value calculated by using the same given method.

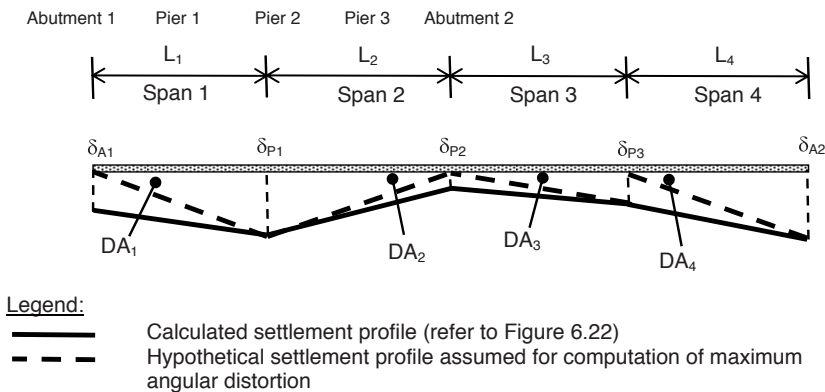
The concept outlined above is referred to as the  $\delta$ -0 concept, with a value of  $\delta$  representing full calculated settlement at one support of a span and a value of 0 representing zero settlement at an adjacent support. Use of the  $\delta$ -0 approach would result in an estimated maximum possible differential settlement between two adjacent supports equal to the larger of the two total settlements calculated at either end of any span. Thus, with respect to Figure 6.22, where  $\delta_{A1} < \delta_{P1} > \delta_{P2} < \delta_{P3} < \delta_{A2}$  represents the relative magnitudes of the total settlement at each support point, the differential settlements and angular distortion for design are evaluated as shown in Table 6.11. The values in Table 6.11 represent the maximum values for each span according to the criteria above and should be used for design. The hypothetical settlement profile assumed for computation of the design angular distortion for each span is represented by the dashed lines in Figure 6.23. It should not be confused with the calculated total settlement profile, which is represented by the solid lines. From the viewpoint of the

damage to the bridge superstructure, the concept shown in Figure 6.23 is more important for continuous-span structures than single-span structures because of the ability of the latter to permit larger movements at support elements.

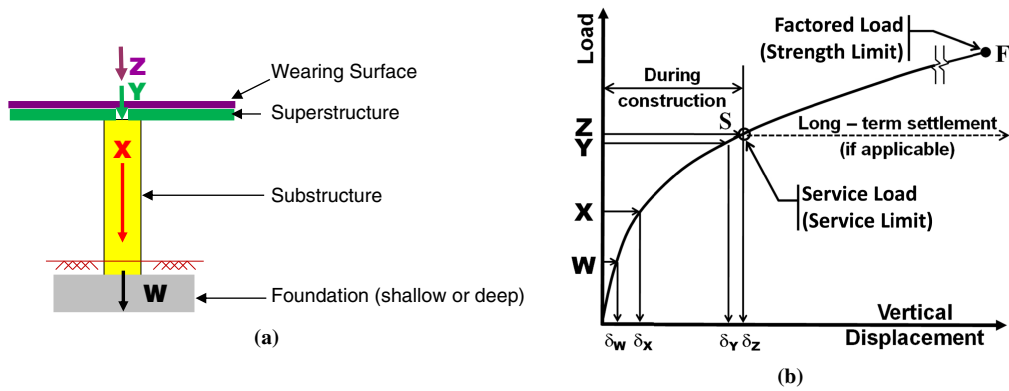
**6.1.5.2 Construction Point Concept**

Most designers analyze foundation deformations as if a weightless bridge structure is instantaneously set in place and all the loads are applied at the same time. In reality, loads are applied gradually as construction proceeds. Consequently, settlements also occur gradually as construction proceeds. Several critical construction points or stages during construction should be evaluated separately by the designer. Figure 6.3 shows the critical construction stages and their associated load-displacement behavior. The baseline format of Figure 6.24 is the same as that of Figure 6.3 except that the figure considers vertical load and vertical displacement (i.e., settlement). Formulation of settlements in the manner shown in Figure 6.24 would permit an assessment of settlements up to that point that can affect the bridge superstructure. For example, the settlements that occur before placement of the superstructure may not be relevant to the design of the superstructure. Thus, the settlements between application of loads X and Z are the most relevant.

The percentage of settlement between the placement of beams and the end of construction is generally in the range of 25% to 75%, depending on the type of superstructure and the construction sequence. With respect to the example of the four-span bridge and the angular distortions in Table 6.11, the use of the construction point concept would result in smaller angular distortions to be considered in the structural design. This will be true of any bridge evaluation. Using Figure 6.22 as a reference, Figure 6.25 compares the profiles of the calculated settlements (solid lines), hypothetical maximum angular distortions (dashed lines), and the range of actual angular



**Figure 6.23. Estimation of maximum angular distortion in bridges.**



Legend:

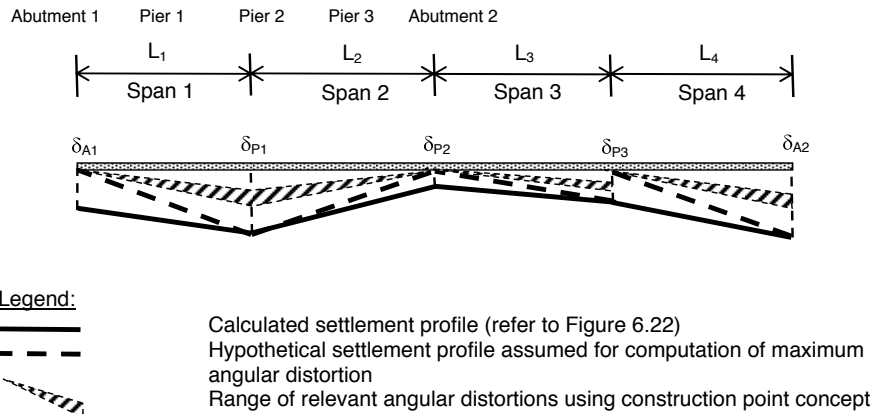
W	load after foundation construction	$\delta_w$	displacement under load W
X	load after pier column and wall construction	$\delta_x$	displacement under load X
Y	load after superstructure construction	$\delta_y$	displacement under load Y
Z	load after wearing surface construction	$\delta_z$	displacement under load Z
S	service load (or limit) state (SLS)		
F	factored load (strength limit state)		

**Figure 6.24. Construction point concept for a bridge pier: (a) identification of critical construction points and (b) conceptual load-displacement pattern for a given foundation.**

distortions (hatched-pattern zones) based on the construction point concept. The angular distortions shown in Figure 6.25 should be compared with the limit state criteria for angular distortions provided in Article 10.5.2.2 of *AASHTO LRFD* (2012) and Table 6.2 here.

On the basis of the discussions above, it is recommended that the limit state of vertical deformations (i.e., settlements)

should be evaluated in terms of angular distortions using the construction point concept. While using the construction point concept, it is important to recognize that the various quantities are being measured at discrete construction stages, and the associated settlements are considered to be immediate. However, the evaluation of total settlement and the maximum (design) angular distortion must also account for long-term



Legend:

- Calculated settlement profile (refer to Figure 6.22)
- Hypothetical settlement profile assumed for computation of maximum angular distortion
- Range of relevant angular distortions using construction point concept

**Figure 6.25. Angular distortion in bridges based on construction point concept.**

settlements. For example, significant long-term settlements may occur if foundations are founded on saturated clay deposits or if a layer of saturated clay falls within the zone of stress influence below the foundation, even though the foundation itself is founded on competent soil. In such cases, long-term settlements will continue under the total construction load ( $Z$ ), as shown by the dashed line in Figure 6.24. Continued settlements during the service life of the structure will tend to reduce the vertical clearance under the bridge, which may cause problems when large vehicles pass below the bridge superstructure. As a result, the geotechnical specialist must estimate and report to the structural specialist the magnitude of the long-term settlement that will occur during the design life of the bridge. A key point in evaluating settlements at critical construction points is the close coordination required between the structural and geotechnical specialists.

### 6.1.5.3 Foundations Proportioned for Equal Settlement

Often geotechnical and structural specialists will try to proportion foundations for equal settlement. In this case, the argument is made that there will be no differential settlement. Although this concept may work for a building structure because the footprint is localized, it is a fallacy to assume zero differential settlement for a long linear highway structure such as a bridge or a wall due to the inevitable variation of the properties of geomaterials along the length of the structure. Furthermore, as noted earlier, the prediction of settlements from any given method is uncertain in itself. Thus for highway structures, even when the foundations are proportioned for equal settlement, it is advisable to evaluate differential settlement assuming that the settlement of any support element could be as large as the value calculated by using a given method, while at the same time, the settlement of the adjacent support element could be zero.

### 6.1.5.4 Horizontal Deformations

Horizontal deformations generally occur due to sliding or rotation (or both) of the foundation. Horizontal deformations cause more severe and widespread problems than do equal magnitudes of vertical movement (Moulton et al. 1985). The most common location of horizontal deformations is at the abutments, which are subject to lateral earth pressure. Horizontal movements can also occur at the piers as a result of lateral loads and moments at the top of the substructure unit. The estimation of the magnitudes of horizontal movements should take into account the movements associated with lateral squeeze, as discussed in Samtani and Nowatzki (2006) and Samtani et al. (2010). Lateral movements due to lateral squeeze can be estimated by geotechnical specialists,

and lateral movements due to sliding or lateral deformations of deep foundations can be estimated by structural specialists using input from geotechnical specialists. The limiting horizontal movements are strongly dependent on the type of superstructure and the connection with substructure and are therefore project specific.

## 6.1.6 Practical AASHTO LRFD Application of the Load Factor for Deformation Using the Construction Point Concept

Article 10.5.2.2 of *AASHTO LRFD* (2012) addresses the topic of tolerable movements and movement criteria. This section is intended to provide additional guidance to incorporate the concept of the load factor for deformation and the construction point concept into *LRFD* Article 10.5.2.2. The following steps should be followed to estimate a practical value of angular distortion of the superstructure on the basis of foundation settlement; a similar approach can be applied and is recommended for evaluation of horizontal movement and rotation of foundations.

### 6.1.6.1 Vertical Deformations (Settlement)

1. Compute total foundation settlement at each support element by using an owner-approved method for the assumed foundation type (e.g., spread footings, driven piles, drilled shafts) as follows:
  - a. Determine  $\delta_{ta}$ , the total foundation settlement using all applicable loads in the Service I load combination.
  - b. Determine  $\delta_{tp}$ , the total foundation settlement before construction of bridge superstructure. This settlement would generally be as a result of all applicable substructure loads computed in accordance with a Service I load combination.
  - c. Determine  $\delta_{tr}$ , relevant total settlement:  $\delta_{tr} = \delta_{ta} - \delta_{tp}$ .
2. At a given support element assume that the actual relevant settlement could be as large as the value calculated by the chosen method. At the same time, assume that the settlement of the adjacent support element could be zero instead of the relevant settlement value calculated by the same chosen method. Thus, differential settlement ( $\delta_d$ ) within a given bridge span is equal to the larger of the relevant settlement at each of two supports of a bridge span. Compute angular distortion ( $A_d$ ) as the ratio of  $\delta_d$  to span length ( $L_s$ ), where  $A_d$  is measured in radians.

The discussion with respect to Table 6.11 and Figure 6.23 in Section 6.1.5 is applicable to this step.

3. Compute modified angular distortion ( $A_{dm}$ ) by multiplying  $A_d$  from Step 2 with the  $\gamma_{SE}$  values for settlement using the approach discussed in Section 6.1.4 based on the analytical method used for computing the total settlement value.

4. Compare the  $A_{dm}$  value with owner-specified angular distortion criteria. If owner-specified criteria are not available, then use 0.008 radians for the case of simple spans and 0.004 radians for the case of continuous spans as the limiting angular distortions. This was discussed in Chapter 2 in the section on tolerable vertical deformation criteria. Other angular distortion limits may be appropriate after consideration of
  - Cost of mitigation through larger foundations, realignment, or surcharge;
  - Rideability;
  - Vertical clearance;
  - Tolerable limits of deformation of other structures associated with the bridge (e.g., approach slabs, wing-walls, pavement structures, drainage grades, utilities on the bridge);
  - Roadway drainage;
  - Aesthetics; and
  - Safety.
5. Evaluate the structural ramifications of the computed angular distortions that are within acceptable limits as per Step 4. Modify foundation design as appropriate based on structural ramifications.
6. The above procedure should also be used for cases in which the foundations of various support elements are proportioned for equal total settlement, because the prediction of settlements from any given method is in itself uncertain.

#### 6.1.6.2 Lateral Deformations

Using procedures similar to settlement evaluation specified for vertical deformation in the previous subsection, lateral (horizontal) movement at the foundation level can also be evaluated. Horizontal movement criteria should be established at the top of the foundation based on the tolerance of the structure to lateral movement, with consideration of the column length and stiffness.

The above guidance should take into account the following guidance from Article C10.5.2.2 of *AASHTO LRFD* (2012):

Rotation movements should be evaluated at the top of the substructure unit in plan location and at the deck elevation.

Tolerance of the superstructure to lateral movement will depend on bridge seat or joint widths, bearing type(s), structure type, and load distribution effects.

#### 6.1.6.3 Walls

The procedure for computing angular distortions can also be applied for evaluating angular distortions along and transverse to retaining walls, as well as the junction of the approach

walls to abutment walls. The angular distortion values along a retaining wall can be used to select an appropriate wall type (e.g., MSE walls can tolerate larger angular distortions than cast-in-place walls).

#### 6.1.6.4 General Comments

The following guidance from *AASHTO LRFD* Article 10.5.2.2 should be followed while implementing the recommendations made in previous sections:

Foundation movement criteria shall be consistent with the function and type of structure, anticipated service life, and consequences of unacceptable movements on structure performance. Foundation movement shall include vertical, horizontal, and rotational movements. The tolerable movement criteria shall be established by either empirical procedures or structural analyses, or by consideration of both.

Foundation settlement shall be investigated using all applicable loads in the Service I load combination specified in Table 3.4.1-1. Transient loads may be omitted from settlement analyses for foundations bearing on or in cohesive soil deposits that are subject to time-dependent consolidation settlements.

All applicable service limit state load combinations in Table 3.4.1-1 shall be used for evaluating horizontal movement and rotation of foundations.

Additional guidance is provided below:

- All foundation deformation evaluations should be based on the geomaterial information obtained in accordance with Article 10.4 of *AASHTO LRFD* (2012).
- The bridge engineer should add deformations from the substructure (elements between foundation and superstructure) as appropriate in evaluation of angular distortions at the deck elevation.
- Although the angular distortion is generally applied in the longitudinal direction of a bridge, similar analyses should be performed in the transverse direction based on consideration of bridge width and stiffness.

#### 6.1.7 Proposed *AASHTO LRFD* Provisions

In *AASHTO LRFD* (2012), Article 10.5.2 (Service Limit States) in Section 10 (Foundations) is the primary article that provides guidance for SLS design for bridge foundations in terms of tolerable movements. Article 10.5.2 is referenced in other articles, as indicated in Table 6.12.

The changes based on geotechnical considerations are primarily needed in Article 10.5.2. As Article 10.5.2 references Article 3.4, changes are also needed in that article. These changes are provided in Chapter 7.

**Table 6.12. Summary of Relevant Articles in AASHTO LRFD for Foundation Deformations**

Article	Title	Relates to
10.6.2.2	Tolerable Movements	Spread footings
10.6.2.5	Overall Stability	Spread footings
10.7.2.2	Tolerable Movements	Driven piles
10.7.2.4	Horizontal Pile Foundation Movement	Driven piles
C10.7.2.5	Commentary to Settlement Due to Downdrag	Driven piles
10.8.2.1	Service Limit State	Drilled shafts
10.8.2.2.1	General	Drilled shafts
10.8.2.3	Horizontal Movements of Shafts and Shaft Groups	Drilled shafts
10.9.2.2	Tolerable Movements	Micropiles
10.9.2.4	Horizontal Micropile Foundation Movement	Micropiles
C11.10.11	Commentary to MSE Abutments	MSE walls
14.5.2.1	Number of Joints	Joints and bearings

Note: Article 10.5.2 and its subarticles are frequently referenced in the articles noted in the left-hand column and their corresponding commentary portion. In this table, the article number is based on the first occurrence of the reference to Article 10.5.2.

## 6.2 Cracking of Reinforced Concrete Components, Service I Limit State: Annual Probability

Traditionally, reinforced concrete components are designed to satisfy the requirements of the strength limit state, after which they are checked for the Service I limit state load combination to ensure that the crack width under service conditions does not exceed a certain value. However, the specifications provisions are written in a form emphasizing reinforcement details (i.e., limiting bar spacing rather than crack width). Satisfying the Service I limit state for crack control through the distribution of reinforcement may require a reduction in the reinforcement spacing. This may require the use of smaller bar diameters or, if the smallest allowed bar diameters are already being used, an increase in the number of reinforcement bars leading to an increase in the reinforcement area.

Two exposure classifications exist in *AASHTO LRFD*: Class 1 exposure condition and Class 2 exposure condition. Class 1 relates to an estimated maximum crack width of 0.017 in., and Class 2 relates to an estimated maximum crack width of 0.01275 in. Class 2 is typically used for situations in which the concrete is subjected to severe corrosion conditions, such as

bridge decks exposed to deicing salts and substructures exposed to water. Class 1 is used for less corrosive conditions and could be thought of as an upper bound in regard to crack width for appearance and corrosion. Previous research indicates that there appears to be little or no correlation between crack width and corrosion. However, the different classes of exposure conditions have been so defined in the design specifications in order to provide flexibility in the application of these provisions to meet the needs of the bridge owner.

The load factors for dead load (DL) and live load (LL) specified for the Service I load combination are as follows: DL load factor = 1.0 and LL load factor = 1.0.

When designing reinforced concrete bridge decks using the conventional design method, most designers follow a similar approach in selecting the deck thickness and reinforcement. The thickness is typically selected as the minimum acceptable thickness, often based on the owner's standards. The choice of main reinforcement bar diameter is typically limited to No. 5 and No. 6 bars, and the designer does not switch to No. 6 bars unless No. 5 bars result in bar spacing less than the minimum spacing allowed. This practice limits the number of possible variations and allows the development of a deck database that can be used in the calibration.

For decks designed using the empirical method, not determined on the basis of a calculated design load, the reinforcement does not change with the change in girder spacing, which results in varying crack resistance. As the statistical parameters for both the load effect and the resistance are required to perform the calibration, a meaningful calibration of decks designed using the empirical design method could not be performed.

For other components, including prestressed decks, designers may select different member dimensions, resulting in different reinforcement areas. Even for the same reinforcement area, the designer may use bars or strands of different diameters and spacing and, consequently, obtain different crack resistance and a different reliability index for each possible variation. The variation in the cracking behavior of the same component with the change in the selected reinforcement prohibits the performance of a meaningful calibration for such components.

Due to the reasons indicated above, the calibration for the Service I limit state for crack control through the distribution of reinforcement was limited to reinforced concrete decks designed using the conventional design method. The decks are assumed to be supported on parallel longitudinal girders.

### 6.2.1 Live Load Model

Reinforced concrete decks designed using the conventional method have been designed for the heavy axles of the design



truck. This practice required developing the statistical parameters of the axle loads of the trucks in the weigh-in-motion (WIM) data. The statistical parameters for the axle loads are presented in Chapter 5. Statistical parameters corresponding to a 1-year return period were assumed in the reliability analysis. Average daily truck traffic (ADTT) of 1,000, 2,500, 5,000, and 10,000 were considered; however, an ADTT of 5,000 was used as the basis for the calibration.

## 6.2.2 Target Reliability Index

### 6.2.2.1 Limit State Function

For the control of cracking of reinforced concrete through the distribution of reinforcement, the limiting criteria are the calculated crack widths, assumed to be 0.017 and 0.01275 in. for Class 1 and Class 2, respectively. Due to the lack of clear consequences for violating the limiting crack width, there was no basis to change the nature or the limiting values of the limit state function (i.e., the crack width criteria). The work was based on maintaining the current crack width values and calibrating the limit state to produce a uniform reliability index similar to the average reliability index produced by the current designs.

### 6.2.2.2 Statistical Parameters of Variables Included in the Design

Several variables affect the resistance of prestressed components. Table 6.13 shows a list of variables that were considered to be random variables during the performance of the reliability analyses. These variables represent a summary of the information based on research studies by Siriakson and Naaman (1980) and Nowak et al. (2008).

### 6.2.2.3 Database of Reinforced Concrete Decks

A database consisting of 15 reinforced concrete decks designed using the conventional method of deck design was developed. As typical in deck design, No. 5 bars were used unless they resulted in bar spacing less than 5 in., the minimum spacing many jurisdictions allow in deck design. If No. 5 bars resulted in a bar spacing less than 5 in., No. 6 bars were used. No maximum bar spacing was considered in the design to ensure that all decks produced a calculated crack width equal to the maximum allowed crack width allowed by the specifications. The designs were not checked for other limit states because the purpose was to calibrate the Service I limit state. The design of the 15 decks was repeated twice, once assuming Class 1

**Table 6.13. Summary of Statistical Information for Variables Used in the Calibration of Service I Limit State for Crack Control**

Variable	Distribution	Mean	CV	Source
$A_s$	Normal	$0.9A_s$	0.015	Siriakson and Naaman (1980)
$b$	Normal	$b_n$	0.04	Siriakson and Naaman (1980)
$C_{E_c}$	Normal	33.6	0.1217	Siriakson and Naaman (1980)
$d$	Normal	$0.99d_n$	0.04	Nowak et al. (2008)
$d_c$	Normal	$d_{cn}$	0.04	Nowak et al. (2008)
$E_s$	Normal	$E_{sn}$	0.024	Siriakson and Naaman (1980)
$f'_c$	Lognormal $E_c = C_{E_c}$ $\gamma_c^{1.5} \sqrt{f'_c}$	3,000 psi:1.31 $f'_{cn}$ 3,500 psi:1.27 $f'_{cn}$ 4,000 psi:1.24 $f'_{cn}$ 4,500 psi:1.21 $f'_{cn}$ 5,000 psi:1.19 $f'_{cn}$	3,000:0.17 3,500:0.16 4,000:0.15 4,500:0.14 5,000:0.135	Siriakson and Naaman (1980)
$f_y$	Lognormal	$1.13f_{yn}$	0.03	Nowak et al. (2008)
$h$	Normal	$h_n$	$1/(6.4\mu)$	Siriakson and Naaman (1980)
$\gamma_c$	Normal	150	0.03	Siriakson and Naaman (1980)

$A_s$  = area of steel rebar (in.<sup>2</sup>);

$b$  = width of equivalent transverse strip of concrete deck (in.);

$C_{E_c}$  = constant parameter for concrete elasticity modulus;

$d$  = effective depth of concrete section (in.);

$d_c$  = bottom cover measured from center of lowest bar (in.);

$E_s$  = modulus of elasticity of steel reinforcement (psi);

$f'_c$  = specified compressive strength of concrete (psi);

$f_y$  = yield strength of steel reinforcement (psi);

$h$  = deck thickness (in.); and

$\gamma_c$  = unit weight of concrete (lb/ft<sup>3</sup>).



**Table 6.14. Summary Information of 15 Bridge Decks Designed Using AASHTO LRFD Conventional Deck Design Method**

Deck Group No.	Girder Spacing (ft)	Deck Thickness (in.)
1	6	7
		7.5
		8
2	8	7.5
		8
		8.5
3	10	8
		8.5
		9
		9.5
4	12	8
		8.5
		9
		9.5
		10

exposure conditions and a second time assuming Class 2 exposure conditions.

Table 6.14 presents the summary information of the 15 designed bridge decks.

#### 6.2.2.4 Selection of Target Reliability Index

Monte Carlo simulation was used to obtain the statistical parameters of resistance (or capacity) and dead load, and

the statistical parameters for live load were taken from Section 5.3.4. The reliability indices for various ADTTs and exposure conditions for the 15 decks are summarized in Table 6.15. Due to the difference in positive and negative moment (bottom and top) reinforcement of the deck, the reliability index was calculated separately for the positive and negative moment reinforcement.

Even though the design for Class 2 resulted in more reinforcement than for Class 1 exposure conditions, the reliability index for Class 2 is lower than that for Class 1 due to the more stringent limiting criteria (narrower crack width).

Current practices rarely result in the deck positive moment reinforcement being controlled by the Service I limit state due to the small bottom concrete cover. When Strength I limit state is considered, more positive moment reinforcement is typically required than by Service I. The additional reinforcement results in reliability indices for the positive moment region higher than those shown in Table 6.15.

For the negative moment region, the design is often controlled by the Service I limit state. Thus, the reliability indices shown for the negative moment region in Table 6.15 are considered representative of the reliability indices that would be calculated when all limit states, including Strength I, are considered in the design.

Therefore, it is recommended that the target reliability index be based on the reliability index for the negative moment region. Because the Class 2 case is the more common case for decks, the reliability index for Class 2 was used as the basis for selecting the target reliability index. The reliability index for Class 1 was assumed to represent a relaxation of the base requirements. The case of ADTT = 5,000 was also considered as the base case on which the reliability analysis was performed. Table 6.16 shows the inherent reliability indices for the negative

**Table 6.15. Summary of Reliability Indices for Concrete Decks Designed According to AASHTO LRFD (2012)**

ADTT	Positive Moment Region		Negative Moment Region	
	Reliability Index (Class 1)	Reliability Index (Class 2)	Reliability Index (Class 1)	Reliability Index (Class 2)
1,000	2.44	1.54	2.37	1.77
2,500	1.95	1.07	1.79	1.27
5,000	1.66	0.85	1.61	1.05
10,000	1.39	0.33	1.02	0.5
Average	1.86	0.95	1.70	1.15
Maximum	2.44	1.54	2.37	1.77
Minimum	1.39	0.33	1.02	0.50
Standard deviation	0.45	0.50	0.56	0.53
CV	24%	53%	33%	46%

**Table 6.16. Reliability Indices of Existing Bridges Based on 1-Year Return Period**

ADTT	Current Practice (Class 1, Negative)	Current Practice (Class 2, Negative)
1,000	2.37	1.77
2,500	1.79	1.27
5,000	1.61	1.05
10,000	1.02	0.50

moment region of decks designed for the current *AASHTO LRFD*. The selected target reliability indices are 1.6 and 1.0 for Class 1 and Class 2, respectively, based on ADTT = 5,000.

### 6.2.3 Calibration Result

The basic steps of the calibration process are shown below as they relate to the Service I calibration.

#### 6.2.3.1 Step 1: Formulate Limit State Function and Identify Basic Variables

The limit state function considered was the limit on the estimated crack width. In the absence of information suggesting that the current criteria (based on a crack width of 0.017 and 0.01275 in. for Class 1 and Class 2, respectively) are not adequate, the current crack widths were maintained as the limiting criteria. A discussion of crack width equations in the literature is included in Appendix C.

#### 6.2.3.2 Step 2: Identify and Select Representative Structural Types and Design Cases

The database of decks used in this study is described in Section 6.2.2.3.

#### 6.2.3.3 Step 3: Determine Load and Resistance Parameters for Selected Design Cases

The variables include the dimension of the cross section and the material properties. The statistical information includes the probability distribution and statistical parameters such as mean ( $\mu$ ) and standard deviation ( $\sigma$ ).

#### 6.2.3.4 Step 4: Develop Statistical Models for Load and Resistance

The variables affecting the load and resistance were identified. These include live load; resistance, including the dimensions of the cross section; and the material properties. The statistical

information includes the probability distribution and statistical parameters for axle loads presented in Section 5.3.4 in Chapter 5 and for other variables affecting the resistance presented in Section 6.2.2.2.

#### 6.2.3.5 Step 5: Develop Reliability Analysis Procedure

The statistical information of all the required variables was used to determine the statistical parameters of the resistance by using Monte Carlo simulation.

For each deck, Monte Carlo simulation was performed for each random variable associated with the calculation of the resistance and dead load. One thousand simulations were performed. For each random variable 1,000 values were generated independently on the basis of the statistics and distribution of that random variable. For each simulation, the dead load and the resistance were calculated using one of the 1,000 sets of values of the random variable (i.e., the  $n$ th simulation used the  $n$ th value of each random variable, where  $n$  varied from 1 to 1,000). This process resulted in 1,000 values of the dead load and the resistance. The mean and standard deviation of the dead load and the resistance were then calculated based on the 1,000 simulations.

#### 6.2.3.6 Step 6: Calculate Reliability Indices for Current Design Code and Current Practice

Using the statistics of the dead load and the resistance, calculated from the Monte Carlo simulation as described above, and the statistics of the live load as derived from the WIM data, as described in Chapter 5, the reliability index ( $\beta$ ) was calculated for each deck by using Equation 6.7:

$$\beta = \frac{\mu_R - \mu_Q}{\sqrt{\sigma_R^2 + \sigma_Q^2}} \quad (6.7)$$

where

$\mu_R$  = mean value of the resistance;

$\mu_Q$  = mean value of the applied loads;

$\sigma_R$  = standard deviation of the resistance; and

$\sigma_Q$  = standard deviation of the applied loads.

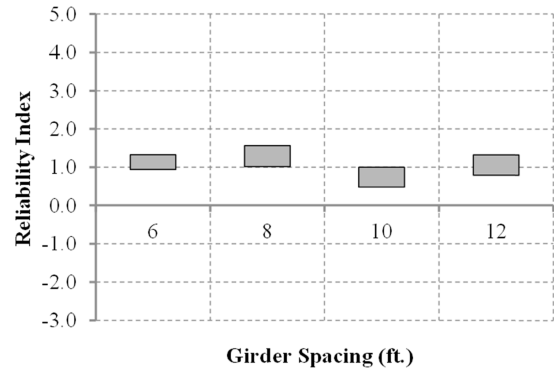
The calculated reliability indices of the decks in the database are shown in Table 6.15 for both positive and negative moment reinforcement and for Class 1 and Class 2 exposure conditions.

#### 6.2.3.7 Step 7: Review Results and Select Target Reliability Index

The initial target reliability index ( $\beta_T$ ) was determined as shown in Table 6.16.



**Figure 6.26. Reliability indices of various bridge decks designed using a 1.0 live load factor over a 1-year return period (ADTT = 5,000) for positive moment region, Class 1 exposure.**



**Figure 6.28. Reliability indices of various bridge decks designed using a 1.0 live load factor over a 1-year return period (ADTT = 5,000) for positive moment region, Class 2 exposure.**

**6.2.3.8 Step 8: Select Potential Load and Resistance Factors for Service I, Crack Control Through the Distribution of Reinforcement**

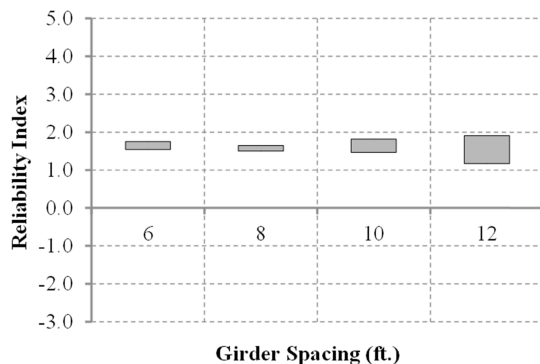
The load factors for dead loads and live loads for the Service I limit state in the *AASHTO LRFD* (2012) are 1.0. The existing specifications do not explicitly include a resistance factor for the distribution of the control of cracking through the distribution of reinforcement. This omission results in an implied resistance factor of 1.0. The load and resistance factors were maintained for the initial reliability index calculations.

For a Class 1 exposure condition (maximum crack width of 0.017 in.), Figure 6.26 and Figure 6.27 present the reliability indices for the bridge decks in the database designed using a live load factor of 1.0 over a 1-year return period for an ADTT of 5,000. As indicated in Table 6.15, the average values of the

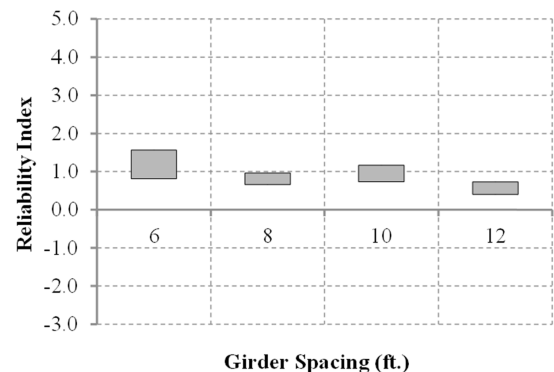
reliability index are 1.66 and 1.61 for positive and negative moment regions, respectively.

For a Class 2 exposure condition (maximum crack width of 0.01275 in.), Figure 6.28 and Figure 6.29 present the reliability indices for the bridge decks in the database designed using a live load factor of 1.0 over a 1-year return period for an ADTT of 5,000. As indicated in Table 6.15, the average values of the reliability index are 0.85 and 1.05 for positive and negative moment regions, respectively.

As discussed above, for positive moment (bottom) reinforcement, Strength I limit state requirements typically result in more reinforcement than needed to satisfy Service I requirements, and the reliability index for cracking at the bottom will be higher than shown in Figure 6.26 and Figure 6.28. This difference in required reinforcement resulted in the recommendation that the reliability index should be based on the negative moment (top) reinforcement.



**Figure 6.27. Reliability indices of various bridge decks designed using a 1.0 live load factor over a 1-year return period (ADTT = 5,000) for negative moment region, Class 1 exposure.**



**Figure 6.29. Reliability indices of various bridge decks designed using a 1.0 live load factor over a 1-year return period (ADTT = 5,000) for negative moment region, Class 2 exposure.**

6.2.3.9 Step 9: Calculate Reliability Indices

As shown in Figure 6.27 and Figure 6.29, the reliability index associated with cracking at the top of the deck appears to be very uniform across the range of girder spacings considered. It was concluded that there was no need to redesign the decks for different load or resistance factors to improve the uniformity of the results. With this conclusion, the reliability indices are the same as shown in Table 6.15 and Table 6.16 and in Figure 6.27 and Figure 6.29.

6.2.3.10 Summary and Recommendations for Service I Limit State, Crack Control Through the Distribution of Reinforcement

The following conclusions are based on the reported reliability analyses:

- Assessment of current practice led to recommended target reliability indices of 1.6 for the base case (Class 1 exposure) and 1.0 for the enhanced requirements (i.e., smaller maximum crack width) for Class 2 exposure conditions. These values correspond to an ADTT of 5,000.
- The current requirements in the specifications produce uniform reliability across the range of girder spacings considered, so there is no need to change the load or the resistance factors.

6.2.4 Proposed AASHTO LRFD Revisions

As indicated above, no revisions to applicable AASHTO LRFD provisions related to control of cracking by distributed reinforcement in reinforced concrete components are warranted by the results of this research.

6.3 Live Load Deflections, Service I: Annual Probability

6.3.1 Proposed Resistance Criteria

The background and state of the art of SLS for live load deflection was reviewed in Chapter 2. There is considerable disagreement in the literature as to whether live load deflection alone is an effective measure of dynamic response or a principal contributor to deck deterioration. Human beings are more sensitive to acceleration than displacement per se, especially when stationary on a bridge. The combined frequency–displacement criteria in the *Canadian Highway Bridge Design Code (CHBDC)* (2006), based on a comparison of computed values to Figure 2.1, appear to have more aspects of response accounted for than merely comparing a computed live load deflection to span length divided by a constant (L/N criterion), which is the case in *AASHTO LRFD*.

A direct comparison to Canadian practice (*CHBDC* 2006) requires consideration of the magnitude of the design live load, dynamic load allowance, load factors, and analysis assumptions. For consideration of vibrations, the *CHBDC* uses 90% of one CL-625 truck loading without a dynamic load allowance. The CL-625 truck has six axles totaling about 140 kips and a wheel base of about 58 ft. *AASHTO LRFD* uses the larger of the design truck without the uniform load or 25% of the design truck with the uniform load. The dynamic load allowance is included for this purpose; the current load factor is 1.0. A comparison of one lane of *CHBDC* and *AASHTO LRFD* loadings for this limit state is shown in Figure 6.30. Note that the current provisions of *AASHTO LRFD* consider live load in each design lane.

To determine whether the L/N criterion captures the dynamic response criteria in Figure 2.1 sufficiently to be “deemed to

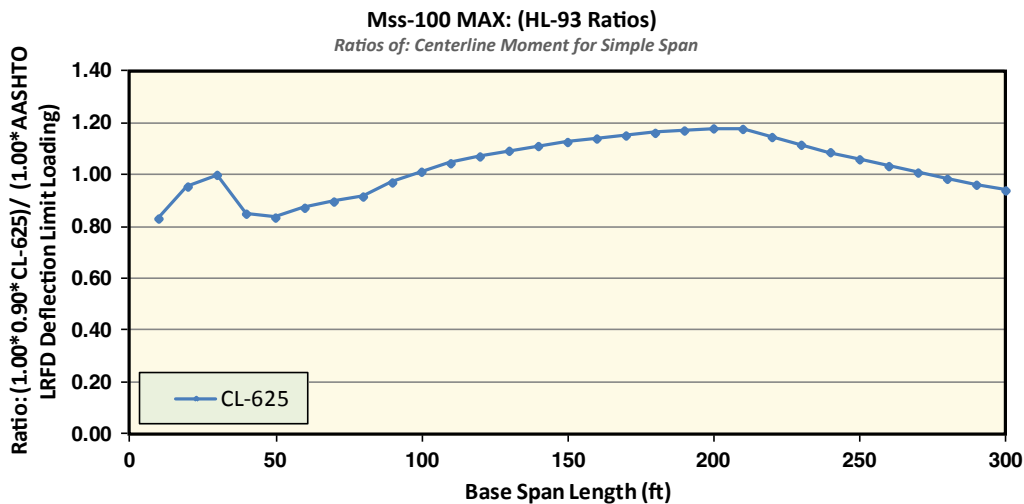


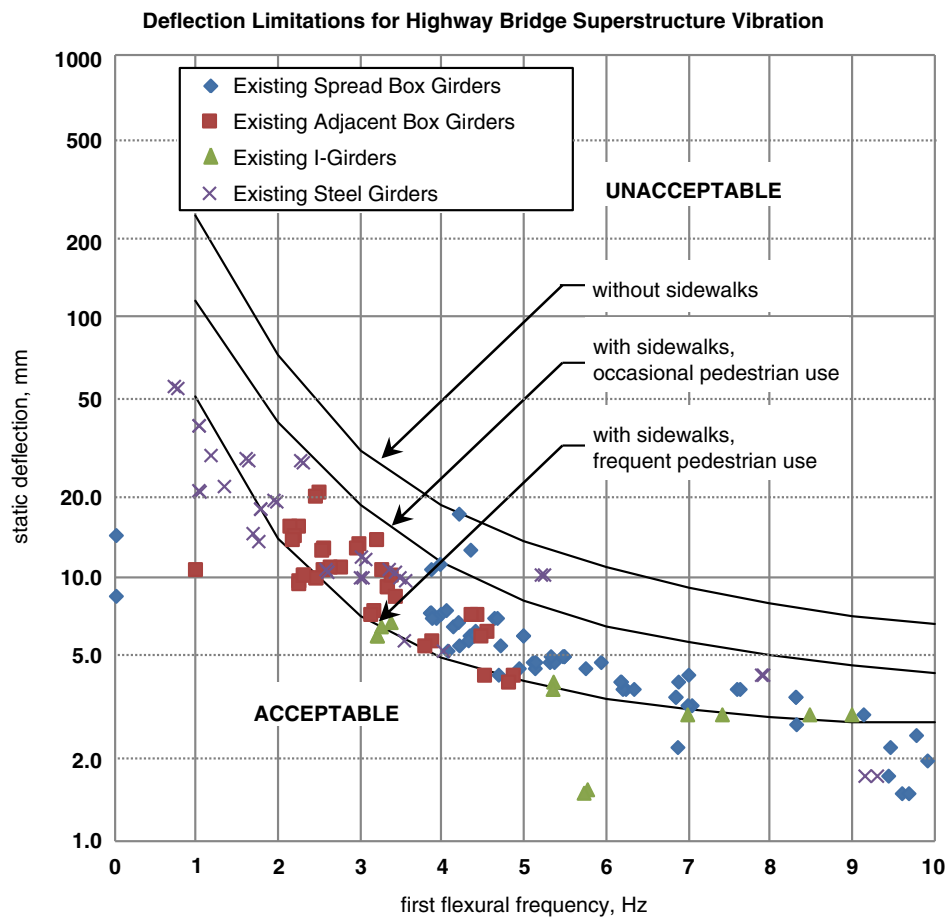
Figure 6.30. Comparison of CHBDC and AASHTO LRFD service load moments.

satisfy” a need for minimum global stiffness, the live load deflection for 41 bridges chosen from the NCHRP Project 12-78 database (Mlynarski et al. 2011) was calculated using VIRTIS and plotted against frequency, as shown in Figure 6.31. The frequency was calculated using the method of Barth and Wu (2007) presented in Section 2.3.1.2 in Chapter 2, with  $\lambda = 1.0$ . The 41 bridges contained simple-span and continuous bridges and steel and prestressed concrete bridges, which satisfy all applicable requirements, not just live load deflection. The general trend of results was similar to the criteria curves in the figure and fell mostly between the curves for bridges with sidewalks and frequent pedestrian use and bridges with sidewalks and occasional pedestrian usage. It is reasonable to assume that most, if not all, of the 41 sample bridges were essentially highway bridges without sidewalks. As shown in Figure 6.31, concrete bridges tend to be stiffer than steel bridges, but some of the concrete sample bridges exhibited responses relatively close to the *CHBDC* acceptance curves.

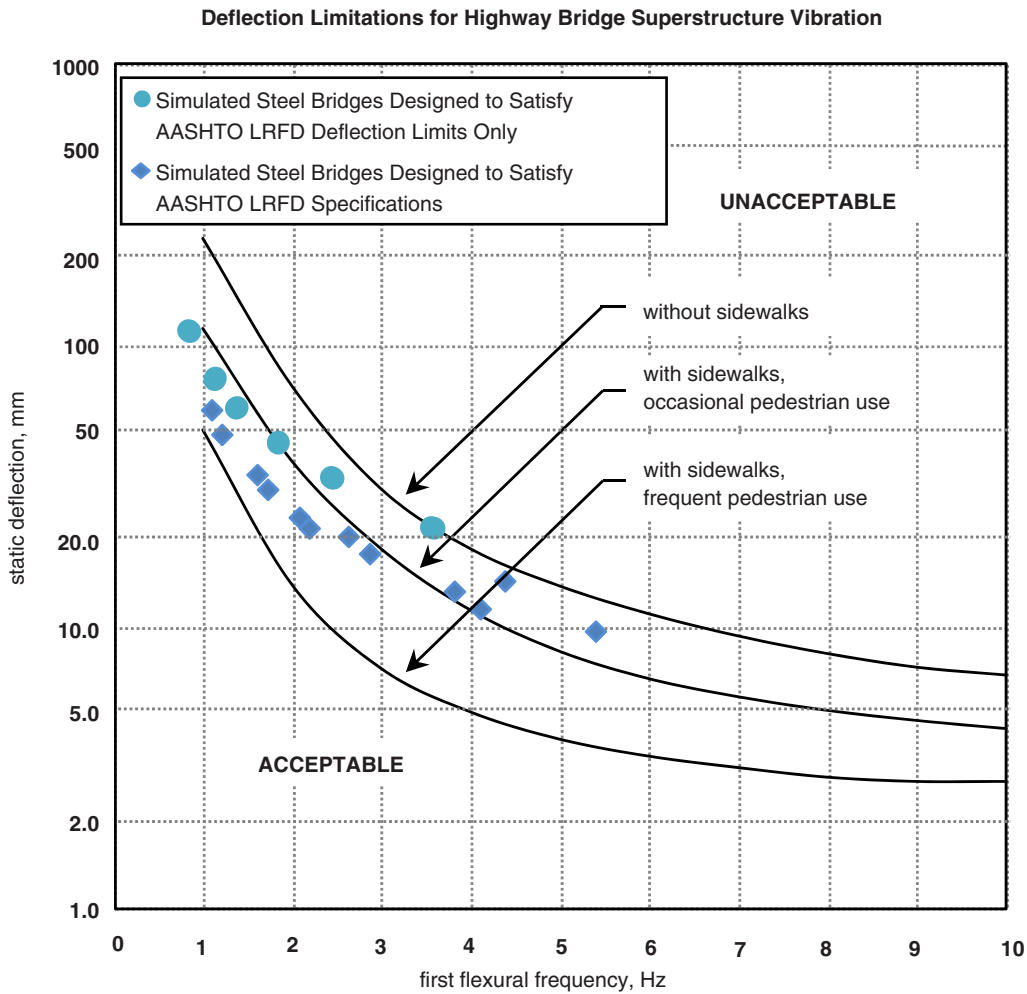
For this purpose, the comparisons were made between the provisions of *AASHTO LRFD* and acceptable *CHBDC* response as indicated by the criteria curves. As the 41 bridges satisfied

all applicable requirements, it is reasonable to suspect they are overdesigned with respect to just the live load deflection requirement. For calibration purposes, the considered database should satisfy the limit state under investigation but not necessarily other limit states. To accomplish this, a set of simply supported bridges was designed to satisfy all applicable limit states by using the load and resistance factor design of the Pennsylvania Department of Transportation’s girder design program and then forced to satisfy only the *AASHTO LRFD* L/800 criteria. If the designs forced to satisfy L/800 satisfied any other criteria, that outcome was unintentional. The considered span lengths were 60, 90, 120, 160, 200, and 300 ft, and girder spacings were 9 and 12 ft. Deflections and frequencies were calculated, plotted, and compared with the *CHBDC* criteria. The results are shown in Figure 6.32. When the girders were forced to meet the L/800 criteria, the frequencies for each pair of spacings for a given span were so similar that the solid circles in the figure cannot be distinguished.

For calibration purposes, the *CHBDC* curves were treated as deterministic (i.e., the bias was assumed to be 1.0, and the CV was assumed to be 0.0). This is analogous to the geotechnical



**Figure 6.31. Comparison of *CHBDC* requirements and various bridges satisfying all *AASHTO LRFD* design requirements.**



**Figure 6.32. Comparison of CHBDC requirements and various steel bridges satisfying all AASHTO LRFD design requirements and similar bridges satisfying only L/800 criteria.**

calibration using a deterministic value of tolerable deformation, as presented in Section 6.1.2.3 and illustrated in Figure 6.6.

### 6.3.2 Calibration Results

#### 6.3.2.1 Formulate Limit State Function

The live load deflection limit state function is merely the sum of the factored loads and must be less than or equal to the factored resistance, as shown by Equation 6.8:

$$\sum_i \gamma_i Q_i \leq \phi R \tag{6.8}$$

The basic load effect for live load deflection is obviously the deflection due to live load. The resistance was taken as the appropriate deflection limit from Figure 2.1, as discussed in Chapter 2.

Substituting these variables into the general limit state function yields Equation 6.9:

$$\gamma_{LL} \Delta_{LL} \leq \Delta_{limit} \tag{6.9}$$

#### 6.3.2.2 Select Structural Types and Design Cases

All structural types and materials were considered for this limit state.

#### 6.3.2.3 Determine Load and Resistance Parameters for Selected Design Cases

As discussed above, the load currently used for deflection calculations in AASHTO LRFD was maintained with a bias of 1.35 and a CV of 0.12 per Section 5.5.2, which is representative of the 1-year live load results for ADTT = 5,000 shown in



Table 5.8. The resistance was taken from the *CHBDC* curves, which were treated as deterministic (i.e., the bias was assumed to be 1.0, and the CV was assumed to be 0.0).

#### 6.3.2.4 Develop Statistical Models for Loads, Load Combinations, and Resistance Variables

##### UNCERTAINTIES OF LOAD

From Tables 5.6 to 5.9, the uncertainties of live load moment were taken as approximately 0.12 for the CV and 1.35 for the bias. It was assumed that the uncertainty of deflections is the same as the uncertainty of moments.

##### UNCERTAINTIES OF RESISTANCE

The live load deflection limits in Figure 2.1 were taken as invariant with a bias of unity and a CV of zero. Thus resistance was set equal to the curves shown in Figure 2.1 for the purpose of calibration.

#### 6.3.2.5 Develop Reliability Analysis Procedure

As discussed in Chapter 3, Monte Carlo simulation using MS Excel formed the basis of the reliability analysis procedure for the live load deflection limit state.

#### 6.3.2.6 Calculate Reliability Indices for Current Design Code or Current Practice

Using the current *AASHTO LRFD* Service I limit state with load factors equal to unity, the probability of failure is almost 100%. Thus, load and resistance factors other than unity must be considered to achieve reliability indices comparable to the other SLSs considered.

#### 6.3.2.7 Review Results and Select Target Reliability Index

Using the SLS reliability indices developed above and a reliability analysis that showed current practice for most fatigue limit states yields a reliability index of 1.0, a target reliability index ( $\beta_T$ ) of about 1.0 was chosen for the calibration of the live load deflection limit state to be consistent with other reversible SLSs. Thus, the proposed specifications maintain the historic level of reliability.

#### 6.3.2.8 Select Potential Load and Resistance Factors

Through trial-and-error testing, the live load load factor for the deflection limit state was selected as 1.50, along with a resistance factor of unity.

#### 6.3.2.9 Calculate Reliability Indices

A Monte Carlo simulation was again performed for the live load deflection limit state. With the live load deflection limit considered invariant, all cases yield a reliability index of about 1.0 using a live load load factor of 1.5 and a resistance factor of 1.0.

### 6.3.3 Potential LRFD Revisions

#### 6.3.3.1 Theoretical Conclusions

The live load deflection limit state provisions could be modified from those of the *AASHTO LRFD* to satisfy frequency, perception, and deflection by adopting the *CHBDC* provisions. A recommendation to use user comfort was made by Roeder et al. (2002). The provisions of Article 2.5.2.6 could be revised to include Figure 2.1 and remove the L/N criterion for steel, aluminum, and concrete vehicular bridges. If this were done, the live load deflection limit state should be as defined in *AASHTO LRFD* Table 3.4.1-1 as Service V, with the load factor for live load given as 1.50. Dead load would also be needed in the load combination for use in calculating frequency. Descriptive text and commentary would be needed in Article 3.4.1.

#### 6.3.3.2 Practical Assessment of Results

The use of the *CHBDC* criteria appears to be a more realistic approach in that it incorporates both deflection and frequency and compares them with a set of human factors response curves. The current (and historic) *AASHTO* requirement includes only stiffness and compares the result to a criterion, L/N, whose background is reviewed in Article 2.3.1.2. The survey of owners (Barker and Barth 2007) indicated that the range of applications of the current criteria could produce results that differ more than mere consideration of the variability of loads would indicate.

Despite the obvious limitations of the current *AASHTO LRFD* criteria, Figure 6.31 and Figure 6.32 indicate that the two criteria are somewhat similar. A review of the 12 steel bridge designs that satisfied all the relevant *AASHTO LRFD* requirements showed that they would not be changed if the deflection criteria were based on a load factor of 1.40, which resulted from the calibration described above. Stated more simply, other criteria still controlled those 12 bridges.

#### 6.3.3.3 Recommendations

Based on this research, there does not appear to be a compelling need to change the current *AASHTO LRFD* provision for live load response (i.e., load deflection) in Article 2.5.6.2. Such an approach is basically “deemed to satisfy.” However,

if AASHTO chooses to adopt the more complete approach of combining frequency, displacement, and perception, a possible set of revisions to accomplish that change are proposed in Chapter 7. Other considerations could include basing the determination of deflection on the fatigue truck of Article 3.6.1.4.1, as its longer wheel base is more representative of actual traffic. The fatigue truck for orthotropic decks could also be used, but the substitution of tandem axles for the 32K single axle is not apt to be significant except for very short spans.

## 6.4 Overload, Service II: Annual Probability

### 6.4.1 Basis of Limit State

The basis for this limit state was presented in Section 2.3.1.5. Several questions regarding the criteria for control of permanent deformations arose:

1. Was the LFD requirement a good target?
2. What is the current level of experience with these provisions? That is, has there been a significant issue with permanent set in girder bridges that affect appearance or rideability?
3. What reliability index is provided in current designs for which the overload provision controlled?
4. How often can these criteria be exceeded without creating a significant permanent deflection of the structure?
5. Is another choice of load factor, other than the 1.30 used in the current Service II load combination, equally valid?
6. Should this requirement be applied to multilane loading?
7. If it is used as a single-lane criterion, should the multiple presence factor (MPF) of 1.2 currently used for single-lane loading in the *AASHTO LRFD* be applicable to this condition?

The LFD criteria resulted from an assessment of experience at the *AASHTO Road Test* (1962); these criteria are summarized in Figure 2.3. The six data points shown, three for composite structures and three for noncomposite structures, comprise the full data set known to the research team. Most of the permanent set occurred during the early repetitions of load, as would be expected. Because the weight of the test trucks did not vary during most of the circuits of the test track, the permanent set accumulated slowly after the period of initial load cycles. This behavior was expected.

Two of the questions to be explored in regard to the control of permanent deformations noted above were Question 1, “Was the LFD requirement a good target?” and Question 2, “What is the current level of experience with these provisions? That is, has there been a significant issue with permanent deformations in girder bridges that affect appearance or

rideability?” This subject was discussed with the AASHTO Subcommittee on Bridges and Structures Steel Structures Technical Committee. Several states are represented on that committee, but the meeting was open to researchers and practitioners. No one present offered any evidence, either documented or anecdotal, that there has been any significant issue with permanent deformations. The research team is aware of some anecdotal discussion of permanent set in stringers in the floor systems of some long-span bridges, but that has not been documented. In summary, the current provisions appear to be serving well but just how well has not been quantified statistically.

Question 3, “What reliability index is provided in current designs for which the overload provision controlled?” is discussed in Section 6.4.3. As detailed below, it is possible to provide some insight into how often the factored live load is exceeded, which bears on Question 4, “How often can this criteria be exceeded without creating a significant permanent deflection of the structure?”

### 6.4.2 Load Model

The application of WIM data to the development of load models for the SLSs was discussed in Chapter 5. The location of WIM sites, the number of days of measurements, and the number of trucks after filtering are shown in Figure 5.1. The indicated number of filtered truck records includes the trucks thought to be permit trucks, as discussed in Section 5.2.3. Thus the trucks used in this study include the permit trucks, which were filtered for consideration of other limit states.

Table 6.17 shows the number of times bending moments from the trucks in the database exceeded 1.0, 1.1, 1.2, and 1.3 times the HL-93 moment for simple spans of 30, 60, 90, 120, and 200 ft for each WIM site scaled to 1 year of data. Note that results for the WIM site on Florida US-29 look much different from the other sites. It was determined that trucks from other parallel routes were being diverted to Route 29, creating an unusual situation. This site was excluded from the discussion below.

Figure 6.33 shows the average exceedance for the 31 remaining WIM sites by HL-93 ratio for each span length considered. Figure 6.34 shows the same information by span length for each HL-93 ratio considered. The reduction in the rate of exceedance with increasing HL-93 ratio is clearly evident. These data do not show how much a given HL-93 ratio was exceeded in terms of stress, but this limit state has historically been based on infrequently exceeding the criteria. The rate of exceedance of 1.3 HL-93, the current criteria, is seen to be quite small.

A more meaningful assessment of the exceedance rate is presented in Table 6.18, Figure 6.35, and Figure 6.36. In this case, the exceedance data have been scaled to an assumed ADTT of 2,500 at each site assuming that the distribution of trucks

*(text continues on page 186)*

**Table 6.17. Bending Moment Exceedances per Year**

Site	Ratio Truck/HL-93 $\geq 1.0$					Ratio Truck/HL-93 $\geq 1.1$					Ratio Truck/HL-93 $\geq 1.2$					Ratio Truck/HL-93 $\geq 1.3$				
	30 ft	60 ft	90 ft	120 ft	200 ft	30 ft	60 ft	90 ft	120 ft	200 ft	30 ft	60 ft	90 ft	120 ft	200 ft	30 ft	60 ft	90 ft	120 ft	200 ft
Arizona (SPS-1)	4	0	0	1	0	1	0	0	0	0	0	0	0	0	0	0	0	0	0	0
Arizona (SPS-2)	0	2	6	5	0	0	0	1	1	0	0	0	0	0	0	0	0	0	0	0
Arkansas (SPS-2)	14	10	17	10	0	2	7	3	0	0	0	3	0	0	0	0	0	0	0	0
Colorado (SPS-2)	0	5	6	6	2	0	2	5	4	0	0	0	2	0	0	0	0	0	0	0
Delaware (SPS-1)	140	48	33	27	1	36	33	22	11	0	10	22	10	1	0	1	11	1	0	0
Illinois (SPS-6)	1	3	4	4	1	0	0	1	0	0	0	0	0	0	0	0	0	0	0	0
Indiana (SPS-6)	27	32	24	19	14	5	19	19	17	3	3	7	9	7	0	0	0	2	0	0
Kansas (SPS-2)	42	47	80	96	10	16	33	35	31	2	7	16	17	7	0	6	7	6	0	0
Louisiana (SPS-1)	76	16	25	30	13	44	6	12	14	7	26	6	7	7	0	6	6	5	4	0
Maine (SPS-5)	6	7	8	7	1	4	4	5	2	0	0	4	2	0	0	0	2	0	0	0
Maryland (SPS-5)	25	8	8	2	1	5	6	2	2	0	0	1	1	0	0	0	1	0	0	0
Minnesota (SPS-5)	9	8	18	19	2	7	5	6	5	0	4	2	2	1	0	2	1	1	0	0
New Mexico (SPS-1)	1	1	1	3	0	0	1	1	1	0	0	0	0	0	0	0	0	0	0	0
New Mexico (SPS-5)	12	7	7	9	4	4	1	1	3	0	3	0	0	0	0	0	0	0	0	0
Pennsylvania (SPS-6)	155	45	22	21	1	32	22	17	14	1	13	17	13	1	0	3	13	2	0	0
Tennessee (SPS-6)	2,085	29	8	7	0	53	4	4	0	0	5	1	0	0	0	1	0	0	0	0
Virginia (SPS-1)	7	10	1	2	1	0	0	1	1	0	0	0	0	0	0	0	0	0	0	0

(continued on next page)

Table 6.17. Bending Moment Exceedances per Year (continued)

Site	Ratio Truck/HL-93 $\geq 1.0$					Ratio Truck/HL-93 $\geq 1.1$					Ratio Truck/HL-93 $\geq 1.2$					Ratio Truck/HL-93 $\geq 1.3$				
	30 ft	60 ft	90 ft	120 ft	200 ft	30 ft	60 ft	90 ft	120 ft	200 ft	30 ft	60 ft	90 ft	120 ft	200 ft	30 ft	60 ft	90 ft	120 ft	200 ft
Wisconsin (SPS-1)	6	3	5	4	2	1	0	3	3	1	0	0	1	1	0	0	0	0	0	0
California Antelope EB	0	13	25	31	25	0	1	0	0	7	0	0	0	0	0	0	0	0	0	0
California Antelope WB	0	30	71	100	84	0	7	6	19	40	0	0	0	1	13	0	0	0	0	1
California Bowman	0	3	3	8	16	0	0	0	3	3	0	0	0	0	3	0	0	0	0	0
California LA-710 NB	10	99	150	153	85	1	34	55	56	16	0	7	26	21	0	0	0	4	1	0
California LA-710 SB	3	62	105	111	54	1	17	45	48	14	0	3	18	19	0	0	0	1	1	0
California Lodi	0	110	137	281	417	0	5	19	55	168	0	0	1	2	38	0	0	0	0	2
Florida I-10	279	141	159	264	152	81	41	47	77	38	23	16	14	18	5	10	5	4	5	2
Florida I-95	0	0	0	0	0	0	0	0	0	0	0	0	0	0	0	0	0	0	0	0
Mississippi I-10	41	48	53	53	44	26	24	34	36	24	8	2	11	21	2	2	2	2	2	1
Mississippi I-55UI	0	4	5	11	8	0	0	0	1	3	0	0	0	0	0	0	0	0	0	0
Mississippi I-55R	142	100	255	349	89	20	31	50	61	33	7	8	17	22	20	2	3	5	8	9
Mississippi US-49	0	3	11	13	7	0	0	2	1	0	0	0	0	0	0	0	0	0	0	0
Mississippi US-61	0	1	5	8	6	0	0	1	2	1	0	0	1	1	0	0	0	0	0	0
Florida US-29	1,291	995	651	496	204	673	510	332	253	109	371	274	179	123	53	183	165	85	61	22
Annual Average	99.6	28.9	40.4	53.4	33.6	11.0	9.8	12.8	15.1	11.7	3.5	3.7	4.9	4.2	2.6	1.1	1.7	1.1	0.7	0.5

Note: EB = eastbound; WB = westbound; NB = northbound; SB = southbound.

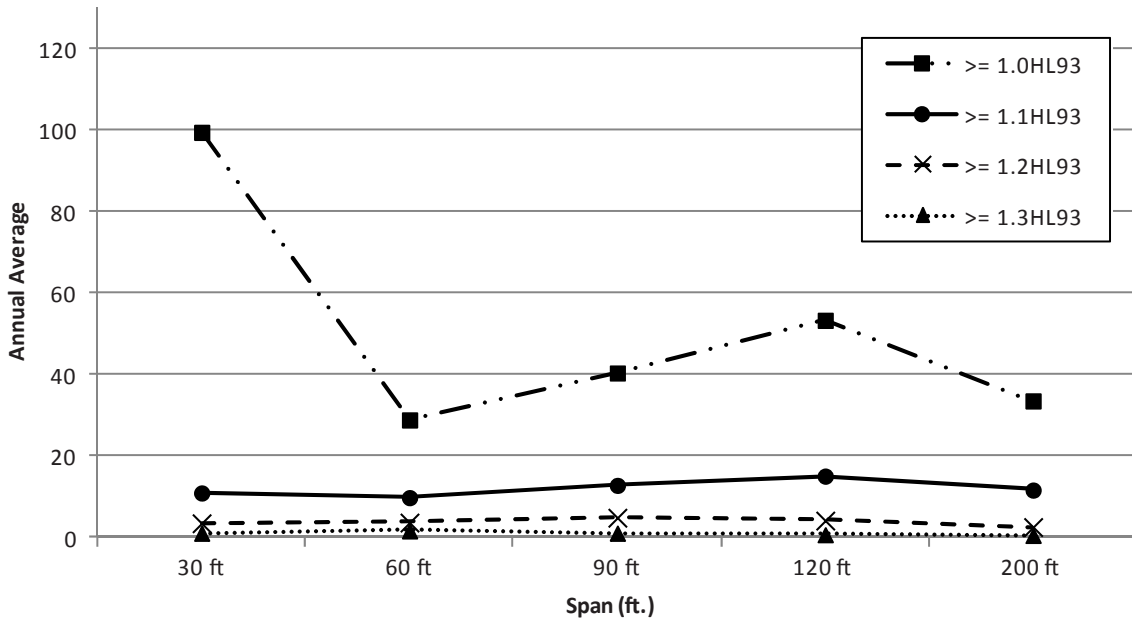


Figure 6.33. Annual average exceedances versus span.

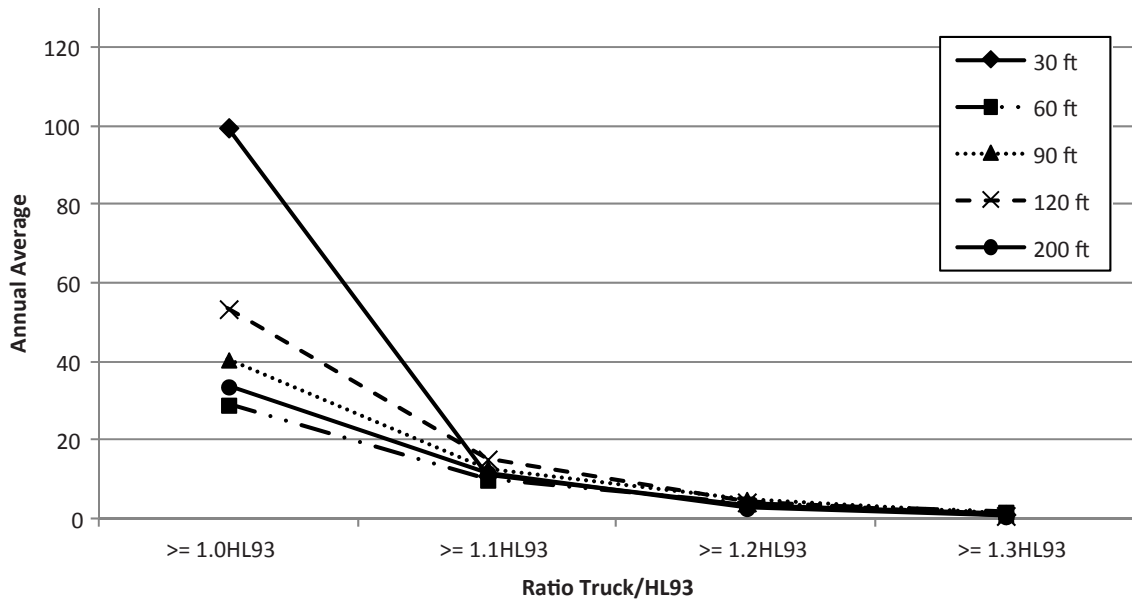


Figure 6.34. Annual average exceedances versus ratio truck/HL-93.

Table 6.18. Events per Year Scaled to ADTT = 2,500

Site	Ratio Truck/HL-93 $\geq 1.0$					Ratio Truck/HL-93 $\geq 1.1$					Ratio Truck/HL-93 $\geq 1.2$					Ratio Truck/HL-93 $\geq 1.3$				
	30 ft	60 ft	90 ft	120 ft	200 ft	30 ft	60 ft	90 ft	120 ft	200 ft	30 ft	60 ft	90 ft	120 ft	200 ft	30 ft	60 ft	90 ft	120 ft	200 ft
Arizona (SPS-1)	103	0	0	26	0	0	0	0	0	0	0	0	0	0	0	0	0	0	0	0
Arizona (SPS-2)	0	1	4	3	0	0	0	1	1	0	0	0	0	0	0	0	0	0	0	0
Arkansas (SPS-2)	8	5	9	5	0	1	4	2	0	0	0	2	0	0	0	0	0	0	0	0
Colorado (SPS-2)	0	13	16	16	5	0	5	13	11	0	0	0	5	0	0	0	0	0	0	0
Delaware (SPS-1)	633	217	149	122	5	163	149	100	50	0	45	100	45	5	0	5	50	5	0	0
Illinois (SPS-6)	1	3	4	4	1	0	0	1	0	0	0	0	0	0	0	0	0	0	0	0
Indiana (SPS-6)	79	94	69	54	39	15	54	54	49	10	10	20	25	20	0	0	0	5	0	0
Kansas (SPS-2)	80	90	153	183	19	31	63	67	59	4	13	31	32	13	0	11	13	11	0	0
Louisiana (SPS-1)	808	170	266	319	138	468	64	128	149	74	277	64	74	74	0	64	64	53	43	0
Maine (SPS-5)	30	35	40	35	5	20	20	25	10	0	0	20	10	0	0	0	10	0	0	0
Maryland (SPS-5)	139	44	44	11	6	28	33	11	11	0	0	6	6	0	0	0	6	0	0	0
Minnesota (SPS-5)	148	131	296	312	33	115	82	99	82	0	66	33	33	16	0	33	16	16	0	0
New Mexico (SPS-1)	8	8	8	16	0	0	8	8	8	0	0	0	0	0	0	0	0	0	0	0
New Mexico (SPS-5)	12	8	8	9	5	5	2	2	3	0	3	0	0	0	0	0	0	0	0	0
Pennsylvania (SPS-6)	95	27	13	13	1	20	13	10	9	1	8	10	8	1	0	2	8	1	0	0
Tennessee (SPS-6)	1,173	16	4	4	0	30	2	2	0	0	3	1	0	0	0	1	0	0	0	0
Virginia (SPS-1)	25	35	4	7	4	0	0	4	4	0	0	0	0	0	0	0	0	0	0	0

(continued on next page)



**Table 6.18. Events per Year Scaled to ADTT = 2,500 (continued)**

Site	Ratio Truck/HL-93 ≥1.0					Ratio Truck/HL-93 ≥1.1					Ratio Truck/HL-93 ≥1.2					Ratio Truck/HL-93 ≥1.3				
	30 ft	60 ft	90 ft	120 ft	200 ft	30 ft	60 ft	90 ft	120 ft	200 ft	30 ft	60 ft	90 ft	120 ft	200 ft	30 ft	60 ft	90 ft	120 ft	200 ft
Wisconsin (SPS-1)	24	12	20	16	8	4	0	12	12	4	0	0	4	4	0	0	0	0	0	0
California Antelope EB	0	10	20	24	20	0	1	0	0	5	0	0	0	0	0	0	0	0	0	0
California Antelope WB	0	20	48	68	57	0	5	4	13	27	0	0	0	1	9	0	0	0	0	1
California Bowman	0	1	1	4	8	0	0	0	1	1	0	0	0	0	1	0	0	0	0	0
California LA-710 NB	2	20	31	31	17	0	7	11	11	3	0	1	5	4	0	0	0	1	0	0
California LA-710 SB	1	12	21	22	11	0	3	9	9	3	0	1	4	4	0	0	0	0	0	0
California Lodi	0	25	32	65	96	0	1	4	13	39	0	0	0	1	9	0	0	0	0	1
Florida I-10	151	76	86	142	82	44	22	26	42	21	12	9	8	9	3	6	3	2	3	1
Florida I-95	0	0	0	0	0	0	0	0	0	0	0	0	0	0	0	0	0	0	0	0
Mississippi I-10	0	2	3	6	4	0	0	0	1	1	0	0	0	0	0	0	0	0	0	0
Mississippi I-55UI	0	2	3	6	4	0	0	0	1	1	0	0	0	0	0	0	0	0	0	0
Mississippi I-55R	93	66	167	229	58	13	21	33	40	22	5	5	11	14	13	1	2	3	5	6
Mississippi US-49	0	2	8	10	5	0	0	1	1	0	0	0	0	0	0	0	0	0	0	0
Mississippi US-61	0	6	23	40	29	0	0	6	11	6	0	0	6	6	0	0	0	0	0	0
Florida US-29	2,922	2,252	1,473	1,122	462	1,524	1,155	751	572	247	840	621	406	278	119	413	373	191	138	49
Annual Average	117.0	37.8	50.6	58.7	21.7	32.0	18.4	20.8	19.8	7.5	14.3	9.7	9.1	5.8	1.2	4.0	5.6	3.2	1.7	0.3

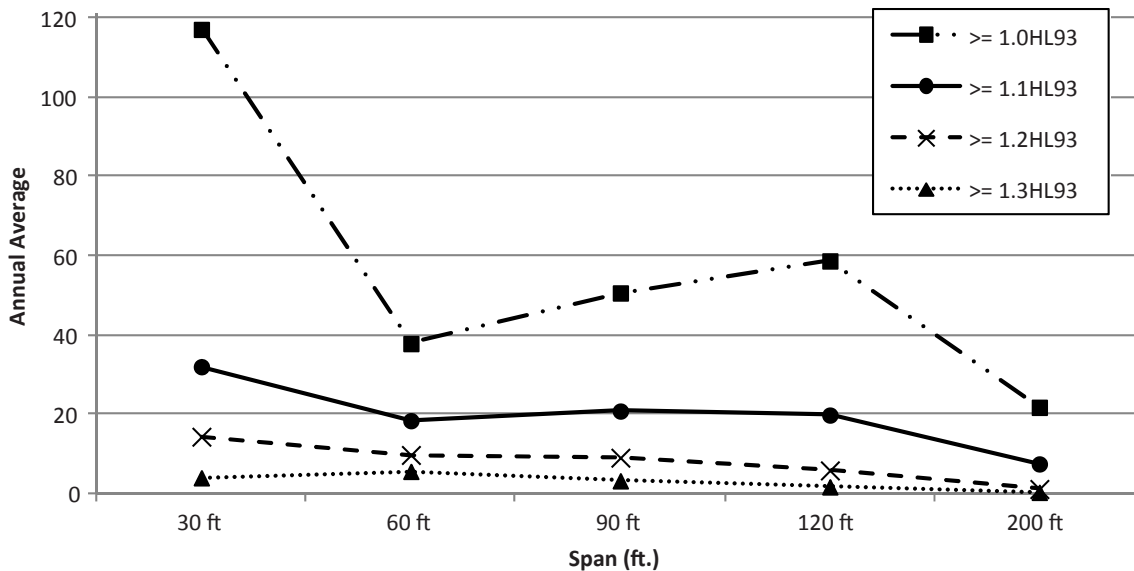


Figure 6.35. Annual average events scaled to ADTT = 2,500 versus span.

(continued from page 180)

is the same (i.e., the data are scalable). The average rate of exceedance in Table 6.18 is higher than in Table 6.17 because many of the WIM sites were on roads with ADTTs less than 2,500. Nevertheless, the rate at which 1.3 HL-93 was exceeded remains quite low. The values in Table 6.18 can be scaled for locations with an ADTT other than 2,500 with the same assumption of scalability.

Question 5 asked, “Is another choice of load factor, other than the 1.30 used in the current Service II load combination, equally valid?” Given the relatively low number of exceedances in Table 6.18, it is difficult to rationalize the need for a national

load factor higher than the current value of 1.30 except possibly for locations with extraordinary levels of truck traffic. For example, for a location with an ADTT of 7,500, over a 100-year service life the average exceedance would be on the order of 1,000 events, although one of the sites shown in Table 6.18 could see about 10 times that number. However, slightly over half the sites recorded no events when the moments for the spans indicated in Table 6.17 exceeded 1.3 HL-93 during the recording period. Given the lack of field evidence of a significant number of bridges with a permanent deformation due to overloads, it was not possible to establish an ADTT criterion at which the load factor should be increased.

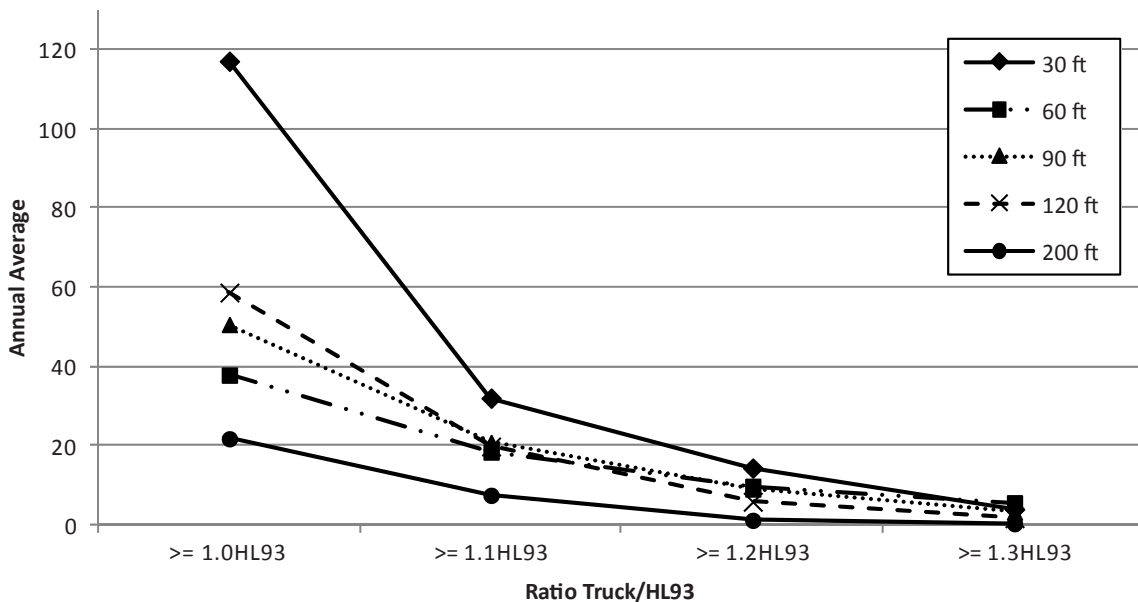


Figure 6.36. Annual average events scaled to ADTT = 2,500 versus ratio truck/HL-93.

Judgment and experience are still necessary. This issue is also clouded by the issues in Questions 6 and 7, “Should this requirement be applied to multilane loading?” and “If it is used as a single-lane criterion, should the MPF of 1.2 currently used for single-lane loading in the *AASHTO LRFD* be applicable to this condition?”

The issue of number of loaded lanes is discussed in Section 5.2.4. For the WIM sites where data were recorded in two lanes, and given the definition of correlated events in that discussion, it was shown that the number of events of multiple lanes loaded with correlated trucks was quite small, and the histograms of gross vehicle weight showed that the number of events of two heavy trucks was even smaller. It was concluded that multiple lanes of heavy trucks need not be considered for the SLs. Thus, it was concluded that in most cases, design for control of permanent distortions need not be based on multiple lanes of overload (i.e., 1.3 HL-93). In the calibration process described in Section 6.4.3, a single-lane loading with no MPF was used on the load side of the limit state function.

To summarize, based on a review of the WIM data

- There is little basis for lowering the current Service II load factor.
- Site-specific consideration of sites with unusually high volumes of heavy trucks is warranted.
- Design for a single-lane loading is justified by this study.
- Elimination of the single-lane MPF of 1.20 for Service II is justified by this study.

### 6.4.3 Calibration Procedure and Results

#### 6.4.3.1 Formulate Limit State Function

The Service II limit state function requires that the sum of the factored loads must be less than or equal to the factored resistance, as shown by Equation 6.10:

$$\sum_i \gamma_i Q_i \leq \phi R \quad (6.10)$$

The two basic loads for Service II are dead load (DC + DW) and live load (LL); DC is the load factor for structural components and attachments, and DW is the load factor for wearing surfaces and utilities. Currently, the resistance is taken as  $0.95 F_y$  for composite sections and  $0.80 F_y$  for noncomposite sections with resistance factors of unity for both. The limited basis for these criteria was presented in Section 2.3.1.5. Substituting these variables and the current Service II load factors of *AASHTO LRFD* Table 3.4.1-1 yields Equation 6.11 and Equation 6.12:

$$1.3 LL + 1.0 (DC + DW) \leq 0.95 F_y \text{ for composite sections} \quad (6.11)$$

$$1.3 LL + 1.0 (DC + DW) \leq 0.80 F_y \text{ for noncomposite sections} \quad (6.12)$$

These are the current Service II limit state functions for investigation.

#### 6.4.3.2 Select Structural Types and Design Cases

The Service II limit state is currently intended only for steel superstructures and governs only for composite and compact sections in the positive moment region. For these regions of composite and compact sections, the Service II limit state often governs the design over the Strength I limit state. Non-composite sections are not typically compact.

Thus, the structure types being considered are positive moment regions of steel girder superstructures that were modeled as simple spans, and the design case is a composite girder, which is the governing case.

#### 6.4.3.3 Determine Load and Resistance Parameters for Selected Design Cases

As discussed in the previous subsection, the Service II limit state can be investigated by concentrating on simple spans of composite steel girders. A set of 41 simple-span composite steel girder bridges was extracted from Mlynarski et al. (2011). The flexural resistances of the interior girders of these bridges were used to study the Service II limit states. The documentation of the 41 bridges is given in Appendix F.

It was established in Chapter 5 that although the Service II limit state is evaluated assuming multiple lanes loaded, the WIM study suggests that the Service II live load does not occur often enough to warrant design for multiple lanes.

#### 6.4.3.4 Develop Statistical Models for Loads, Load Combinations, and Resistance Variables

##### UNCERTAINTIES OF LOAD

The uncertainties of the various components of dead load were investigated previously with the results documented in Kulicki et al. (2007) and reproduced in Table 3.2.

From Table 5.5 to Table 5.9, the uncertainties of live load are taken as approximately 0.12 for the CV and 1.35 for the bias.

##### UNCERTAINTIES OF RESISTANCE

The uncertainties of the flexural resistance of composite steel girders have also been investigated and similarly documented in Kulicki et al. (2007) and reproduced in Table 3.1.

#### 6.4.3.5 Develop Reliability Analysis Procedure

Monte Carlo simulation using Microsoft Excel formed the basis of the reliability analysis procedure for the Service II

limit states. Use of the Monte Carlo analysis is presented in Section 3.2.3.

#### 6.4.3.6 Calculate Reliability Indices for Current Design Code or Current Practice

The Service II limit state was first introduced with LFD in the *AASHTO Standard Specifications for Highway Bridges* (2002) as “overload” provisions. In the development of the *AASHTO LRFD*, a simple calibration was made in an attempt to yield similar member proportions as with the *Standard Specifications*; this attempt is discussed in Section 2.3.1.5.

The calculation of the inherent reliability indices for current design practice was based on LFD overload provisions. Monte Carlo simulations were performed for the 41 bridges by using a single lane of AASHTO LFD live load times the overload load factor of 5/3 compared with the flexural resistance consistent with multiple lanes of the LFD live load. This is the requirement for which most of today’s in-service bridges were designed. The results are summarized in Table 6.19. In addition, similar simulations were made assuming that the load was multiple lanes of *AASHTO LRFD* live load, as the original conceivers of the limit state assumed traffic to be.

These results suggest that the current inherent reliability index associated with the Service II limit state is on average about 2.0. The originally assumed multiple lanes of loading suggest lower reliability but, as discussed, this loading is not very probable.

#### 6.4.3.7 Review Results and Select Target Reliability Index

Using the values in Table 6.19, a target reliability index ( $\beta_T$ ) of about 2.0 was chosen for the calibration of the Service II limit state.

#### 6.4.3.8 Select Potential Load and Resistance Factors

As an initial trial, the Service II load factors of the *AASHTO LRFD* (1.3 for live load and 1.0 for dead load) were selected, along with resistance factors of unity.

**Table 6.19. Inherent Reliability Indices**

Live Load	$\beta$	CV
Single lane (reality)	1.8	0.32
Multiple lane (assumed)	1.6	0.92

#### 6.4.3.9 Calibrate Reliability Indices

Monte Carlo simulations were again performed for the 41 bridges by using a single lane of *AASHTO LRFD* live load (which represents the load today as suggested by the WIM studies) and dead load times the *AASHTO LRFD* load factors compared with the flexural resistance consistent with multiple lanes of the *AASHTO LRFD* live load, as most of today’s new bridges will be designed. This assumes that design for multiple lanes of live load will continue.

An average reliability index of 1.8 with a CV of 0.09 resulted from using the current *AASHTO LRFD* load and resistance factors. Thus, the reliability is comparable to the inherent reliability of current practice, but with much more uniformity and with a low CV compared with the original overload provisions.

#### 6.4.4 Proposed AASHTO LRFD Revisions

The Service II limit state provisions do not require any modification from those of the *AASHTO LRFD*. Thus, the Service II limit state will continue as defined in *AASHTO LRFD* Table 3.4.1-1.

Given the limited background on this limit state, the possibility of reducing the demand was discussed informally with three of the AASHTO Technical Committees: T-5, T-10, and T-14, although in the case of T-14 fewer than half the members were present. Most of the members of these three committees expressed reservations about decreasing the current design requirement, citing the increasing numbers of trucks on the roads and the continual pressure to increase legal loads. At the time of this work, an increase of about 20% in legal gross vehicle weight is under discussion.

### 6.5 Tension in Prestressed Concrete Beams, Service III Limit State: Annual Probability

Traditionally, prestressed concrete beams are proportioned for the SLS such that the concrete tensile and compressive stresses immediately after transfer and at the final stage are within certain stress limits defined in the specifications. Under the current *AASHTO LRFD* (2012), two SLS load combinations are used to calculate the stresses in prestressed concrete components: the Service I and Service III load combinations. The two service load combinations are described as follows:

- *Service I*—Load combination relating to the normal operational use of the bridge with a 55 mph wind and all loads taken at their nominal values. Service I is also related to

deflection control in buried metal structures, tunnel liner plate, and thermoplastic pipe; to control crack width in reinforced concrete structures; and for transverse analysis relating to tension in concrete segmental girders. This load combination should also be used for the investigation of slope stability.

- *Service III*—Load combination for longitudinal analysis relating to tension in prestressed concrete superstructures with the objective of crack control and to the principal tension in the webs of segmental concrete girders.

The load factors for DL and LL specified for the two load combinations are as follows.

- Service I: DL load factor = 1.0, and LL load factor = 1.0.
- Service III: DL load factor = 1.0, and LL load factor = 0.8.

On the basis of the definition of the two limit states, the Service I limit state is used for calculating all service stresses in the superstructure and substructure components at all stages, with the exception that the Service III limit state is used to calculate the tensile stresses in the superstructure components under full service loads and the principal tension in webs of segmental concrete.

Stresses immediately after transfer are independent of the live loads. At the final stage, typically the design is controlled by the tensile stress in the concrete and not by the compressive stresses on the opposite side of the girders. Thus, the calibration for prestressed concrete superstructures was performed for the Service III limit state, and no calibration was performed for the Service I limit state.

In addition to being designed for the SLS, all prestressed concrete components are checked for the strength limit state. For typical precast prestressed superstructure beams (e.g., I-shapes, bulb-T shapes, and adjacent and spread box beams), the controlling case of the design is usually the SLS.

The SLS stresses are calculated assuming an uncracked section. The concrete is assumed to be subjected to tensile stresses. However, due to the relatively low load factors used for the SLSs, it is highly probable that the structure is subjected to heavy trucks that produce live load effects higher than those produced by the design-factored service loads. When a heavy truck causes the tensile stress in the concrete to exceed the modulus of rupture, the concrete is expected to crack. Once the load passes, the prestressing force will cause the crack to close, and it will remain closed as long as the concrete at the crack location remains under compression. However, if a truck heavy enough to cause the concrete stress calculated on the basis of the uncracked section to be tensile, the crack will reopen.

Successful past performance of prestressed concrete components suggests that past design requirements result in a

frequency of the crack opening being sufficiently small that adverse strand fatigue problems at crack locations are not produced.

## 6.5.1 History of Major Relevant Design Provisions and Revisions to AASHTO LRFD

### 6.5.1.1 Load Factor for Live Load in Service III Load Combination

During the early stages of the development of *AASHTO LRFD* in the early 1990s, only the Service I load combination was considered for calculating all stresses in prestressed concrete components. The load factor for live load was 1.0, which is the same load factor used for service loads under the *AASHTO Standard Specifications for Highway Bridges*, the predecessor to *AASHTO LRFD*.

The design live load specified in *AASHTO LRFD* produces higher unfactored, undistributed load effects than that specified in the *AASHTO Standard Specifications*. The girder distribution factors, particularly for interior girders, for many typical girder systems in *AASHTO LRFD* are lower than those in *Standard Specifications*, thus reducing the difference between the unfactored distributed load effects in the two specifications. Even with the smaller distribution factor, the unfactored distributed load effects from *AASHTO LRFD* were higher for most girder systems. Using the same load factor for SLS (1.0) resulted in higher design-factored load effects for the *AASHTO LRFD* designs than for those designed to the *AASHTO Standard Specifications* requirements. The results from the trial designs conducted during the development of *AASHTO LRFD* indicated a larger number of strands than required by *AASHTO Standard Specifications*. This finding would suggest that designs performed under *AASHTO Standard Specifications* resulted in underdesigned components that should have shown signs of cracking. In the absence of widespread cracking, the load factor for live load was decreased to 0.8, and the Service III load combination was created and was specified for tension in prestressed concrete components. This resulted in a similar number of strands for the designs conducted using both *AASHTO Standard Specifications* and *AASHTO LRFD*.

### 6.5.1.2 Method of Calculating Prestressing Losses

*AASHTO LRFD* (2012) includes three methods for determining the time-dependent prestressing losses. These three methods are as follows:

1. *Approximate method*—This method is termed approximate estimate of time-dependent losses and is the least detailed method. It requires limited calculations to estimate



the time-dependent losses. Before 2005, the specifications included a simpler approximate method termed approximate lump-sum estimate of time-dependent losses. The lump-sum method allowed selecting a value for the time-dependent losses from a table. The value varied according to the type of girders and the type and grade of prestressing steel. Some concrete compressive strength requirements were allowed to use this method.

2. *Refined estimates of time-dependent losses*—This method is more detailed than the approximate method. More details on this method are presented below.
3. *Time-step method*—This method is highly detailed and is based on tracking the changes in the material properties with time. The loss calculations are based on the time of the application of loads and the material properties at the time of the load application. This method is required to be used in the design of posttensioned segmental bridges. It may also be used for other types of bridges; however, due to the level of effort required, it is typically limited to segmental bridges.

Throughout the remainder of this section, unless explicitly indicated otherwise, time-dependent losses are calculated using the techniques outlined in Refined Estimates of Time-Dependent Losses in *AASHTO LRFD*.

Originally, the method of calculating prestressing force losses in *AASHTO LRFD* (the “pre-2005” method) was the same method used in *AASHTO Standard Specifications*. A new method of loss calculations (the “post-2005” method) first appeared in the 2005 Interim to the third edition of *AASHTO LRFD*. The post-2005 method is thought to produce a more accurate estimate of the losses. The post-2005 method has new equations for calculating the time-dependent prestressing losses, and it also introduced the concept of “elastic gain.” After the initial prestressing loss at transfer, when load components that produce tensile stresses in the concrete at the strand locations are applied to the girder, the strands are subjected to an additional tensile strain equal to the strain in the surrounding concrete due to the application of the loads. This results in an increase in the force in the strands. The increase in the force in the strands was termed “elastic gain,” and the post-2005 prestressing loss method allows including elastic gain to be used to offset some of the losses.

When the elastic gain was considered, the post-2005 prestress loss method produced lower prestressing force losses than the earlier method. The reduction in prestressing losses resulted in fewer strands than what was required under *AASHTO Standard Specifications* and under earlier editions of *AASHTO LRFD*. This change raised some concern as some practitioners and researchers thought that the higher prestressing losses calculated using the pre-2005 loss method compensated for the lower live load effects caused by the lower design live load used in *AASHTO Standard Specifications* or

the lower load factor used for the Service III load combination of *AASHTO LRFD*. Some of the work presented in the following subsections was intended to investigate the effect of different loss methods and different design specifications on the reliability index for the Service III load combination.

### 6.5.2 Live Load Model

Traditionally, prestressed concrete components have been designed for the number of traffic lanes, including MPFs, which produced the highest load effects. This was assumed to continue in the future, and all sections designed as part of this study used this approach.

However, as indicated in Section 5.2.4, the presence of heavy loads in adjacent traffic lanes simultaneously is not likely. Thus, the load side of the limit state function in the reliability analysis was calculated assuming the live load existed in only one lane, and no MPF was included. The design truck, tandem, and uniform lane load specified in *AASHTO LRFD* were used unless otherwise noted. The live load distribution factors specified in *AASHTO LRFD* were used in distributing the design loads. The dynamic load allowance (10%) used in the original calibration of the strength limit state in *AASHTO LRFD* was applied to the load side.

The return period considered in the calibration of the Service III limit state was 1 year. This return period was selected because the live load statistics were developed based on 1 year of reliable WIM data from various WIM sites. Furthermore, as only three of the 32 WIM sites had an ADTT larger than 5,000, and only one of the 32 WIM sites had an ADTT larger than 8,000, an ADTT of 5,000 was used for the bulk of the calibration. The bias and CV of live load were taken as shown in Table 5.5 to Table 5.9.

### 6.5.3 Methods of Analysis for Study Bridges

Unless explicitly indicated otherwise, the methods of analysis used in designing and analyzing the study bridges throughout Section 6.5.4 and Section 6.5.5 are listed below.

For bridges designed or analyzed using the post-2005 prestressing loss method,

- The time-dependent prestressing loss method used is the method designated in *AASHTO LRFD* (2012) as the Refined Estimates of Time-Dependent Losses.
- The section properties used in the analysis were based on the gross section of the concrete.
- The calculations of prestressing losses considered the effects of elastic gain as allowed by the current design provisions.

Regardless of the method of design used in designing a girder, the stresses in the girder used as part of the reliability



index calculations were determined by analyzing the girder using the above assumptions.

For bridges designed using the pre-2005 prestressing loss method,

- The time-dependent prestressing loss method used is the method designated in the pre-2005 *AASHTO LRFD* editions as the Refined Estimates of Time-Dependent Losses.
- The section properties used in the analysis were based on the gross section of the concrete.
- The calculations neglected the effects of elastic gain.

### 6.5.4 Target Reliability Index

In the development of *AASHTO LRFD*, the target reliability index for the strength limit states was 3.5. The limit state was assumed to be violated when the applied load effects exceeded the resistance, which was in turn assumed to be equal to the design-factored load. Failure under the strength limit state is well defined as it relates to a certain criterion related to the properties of the materials used (such as steel yield stress or concrete compressive strength) or to a behavior criterion that, if violated, may lead to instability of the component (such as local or global buckling). Due to the lack of clear consequences for violating the limiting stress specified for the concrete in a prestressed concrete component, selecting the limit state function required investigating different alternatives.

#### 6.5.4.1 Limit State Functions Investigated

The following three limit state functions were investigated:

- *Decompression limit state*—This limit state assumes that failure occurs when the stress in the concrete on the tension face calculated on the basis of the uncracked section under the combined effect of factored dead load and live load ceases to be in compression.
- *Stress limit state*—This limit state assumes that failure occurs when the tensile stress in the concrete on the tension face calculated on the basis of the uncracked section under the combined effect of factored dead load and live load exceeds a certain tensile stress limit calculated on the basis of the uncracked section properties regardless of whether the section has previously been cracked. Stress limits of  $f_t = 0.0948\sqrt{f'_c}$ ,  $f_t = 0.19\sqrt{f'_c}$ , and  $f_t = 0.25\sqrt{f'_c}$  were initially considered in the reliability analysis;  $f_t = 0.19\sqrt{f'_c}$  was used for the final calibration.
- *Crack width limit state*—This limit state assumes that failure occurs when a previously formed crack in the concrete opens, and the crack width reaches a certain prespecified crack width. Crack widths of 0.008, 0.012, and 0.016 in. were initially considered in the reliability analysis, but none

produced uniform reliability. The bulk of the calibration was performed using a crack width of 0.016 in. The differentiation between different environments was accounted for through the use of different reliability indices in association with the same crack width.

For each girder, the design was performed according to certain stress limits, as is conventionally done, and the girder section and number of strands were determined. The reliability index was determined for each of the three limit state functions described above by using the same girder design (i.e., the same girder section and same number of strands).

Each of the limit state functions requires a different level of loading before the criteria are violated. The frequency at which any of the three limit states will be violated and the corresponding reliability index depend on the level of loading required to cause the limit state to be violated. For a specific cross section with a specific prestressing area and force, reaching the decompression limit state requires less applied load than reaching a specified tensile stress, which in turn requires less load than that required to reach a specific crack width. Requiring a higher load to violate a specific limit state means that the section resistance is higher, which would cause the curve representing the resistance in Figure 6.1 to be shifted to the right. This results in a higher reliability index. Table 6.20 shows the required load and the corresponding reliability index for the three limit states relative to each other.

With the target reliability index dependent on the definition of the limit state, selecting the target reliability index required investigating all three criteria and selecting the one that provided more uniform reliability across a wide range of bridge geometrical characteristics.

#### 6.5.4.2 Statistical Parameters of Variables Included in the Design

Several variables affect the resistance of prestressed components. Table 6.21 shows a list of variables considered to be

**Table 6.20. Relation Between Limiting Criteria and Reliability Index for a Given Girder**

Limiting Criterion	Live Load Required to Violate the Limiting Criterion	Frequency of Exceeding the Limiting Criterion	Reliability Index
Decompression	Lowest	Highest	Lowest
Maximum allowable tensile stress limit	Middle	Middle	Middle
Maximum allowable crack width limit state	Highest	Lowest	Highest

**Table 6.21. Random Variables and the Value of Their Statistical Parameters**

Variable	Distribution	Mean ( $\mu$ )	CV ( $\Omega$ )	Remarks
$A_s$	Normal	$0.9A_{sn}$	0.015	Siriakson and Naaman (1980)
$A_{ps}$	Normal	$1.01176A_{psn}$	0.0125	Siriakson and Naaman (1980)
$b, b_0, b_1, b_w$	Normal	$b_n$	0.04	Siriakson and Naaman (1980)
$C_{Ec}$	Normal	33.6	0.1217	Siriakson and Naaman (1980); nominal = 33 $C_{Ec} = E_c/(\gamma_c^{1.5} \cdot \sqrt{f'_c})$
$C_{fci}$	Normal	0.6445	0.073	nominal = 0.8; $C_{fci} = f_{ci}/f'_c$
$d_p, d_s$	Normal	$d_{pn}, d_{sn}$	0.04	Siriakson and Naaman (1980)
$e_1$	Normal	$e_{0n}$	0.04	Siriakson and Naaman (1980)
$E_{ps}$	Normal	$1.011E_{psn}$	0.01	Siriakson and Naaman (1980); $E_{psn} = 29,000$ ksi
$E_s$	Normal	$E_{sn}$	0.024	Siriakson and Naaman (1980)
$f'_c$	Lognormal	$1.11f'_{cn}$	0.11	Nowak et al. (2008)
$f_{pu}$	Lognormal	$1.03f_{pun}$	0.015	Nowak et al. (2008); $f_{pun} = 270$ ksi
$f_{si}$	Normal	$0.97f_{sin}$	0.08	Developed from Gross and Burns (2000)
$f_y$	Lognormal	$1.13f_{yn}$	0.03	Nowak et al. (2008)
$h, h_t, h_{t1}, h_{t2}$	Normal	$h_n, h_{tn}, h_{t1n}, h_{t2n}$	0.025	Siriakson and Naaman (1980)
$l$	Normal	$l_n$	$11/(32\mu)$	Siriakson and Naaman (1980)
$\gamma_c$	Normal	$\gamma_{cn} = 150$	0.03	Siriakson and Naaman (1980)
$\Delta f_s$	Normal	$1.05\Delta f_{sn}$	0.10	Developed from Gross and Burns (2000) and Tadros et al. (2003)
$\Sigma 0$	Normal	$\Sigma 0_n$	0.03	Siriakson and Naaman (1980)

Note: Subscript  $n$  refers to nominal values.

Notations:

$A_s$  = area of nonprestressing steel (in.<sup>2</sup>);

$A_{ps}$  = area of prestressing steel in tension zone (in.<sup>2</sup>);

$b$  = prestressed beam top flange width (in.);

$b_0$  = deck width transformed to beam material (in.);

$b_1$  = prestressed beam bottom flange width (in.);

$b_w$  = web thickness (in.);

$c$  = depth of neutral axis from extreme compression fiber (in.);

$C_{fci} = f_{ci}/f'_c$ ;

$d_p$  = distance from extreme compression fiber to centroid of prestressing steel (in.);

$d_s$  = distance from extreme compression fiber to centroid of nonprestressing steel (in.);

$e_1$  = eccentricity of prestressing force with respect to centroid of the section at midspan (in.);

$E_{ps}$  = modulus of elasticity of prestressing steel (psi);

$E_s$  = modulus of elasticity of nonprestressing steel (psi);

$f'_c$  = specified compressive strength of concrete (psi);

$f_{pu}$  = specified tensile strength of prestressing steel (psi);

$f_{si}$  = initial stress in prestressing steel (psi);

$f_y$  = yield strength of nonprestressing steel (psi);

$h$  = girder depth (in.);

$h_t$  = deck thickness (in.);

$h_{t1}$  = top flange thickness (in.);

$h_{t2}$  = bottom flange thickness (in.);

$l$  = clear span length of beam members (ft);

$\gamma_c$  = unit weight of concrete (lb/ft<sup>3</sup>);

$\Delta f_s$  = prestress losses (psi); and

$\Sigma 0$  = sum of reinforcing element circumferences (in.).

random during the performance of the reliability analyses. These variables represent a summary of the information from research studies by Siriakorn and Naaman (1980) and Nowak et al. (2008).

#### 6.5.4.3 Database of Existing Bridges

A database of existing prestressed concrete girder bridges was extracted from the database of bridges used in the NCHRP 12-78 project (Mlynarski et al. 2011). The database used in this study included 30 I- and bulb-T girder bridges, 31 adjacent box girder bridges, and 36 spread box girder bridges. The geometric characteristics of the bridges are included in Appendix F.

Depending on the environmental exposure conditions, both AASHTO *Standard Specifications* and AASHTO *LRFD* allow designing conventional prestressed components for a maximum concrete tensile stress of  $f_i = 0.0948\sqrt{f'_c}$  or  $f_i = 0.19\sqrt{f'_c}$  for severe corrosion conditions or no worse than moderate corrosion conditions, respectively. When either specification is applied without owner's exceptions, most bridges are designed for  $f_i = 0.19\sqrt{f'_c}$ , with a small number of bridges in coastal areas designed for  $f_i = 0.0948\sqrt{f'_c}$ . The stress limit for which each bridge in the database was designed was unknown. As the percentage of bridges designed for severe corrosive conditions is small, it was assumed that most bridges in the database were likely to have been designed for the higher limit.

The construction dates of the bridges considered suggest that they were all designed using the prestressing loss provisions method that existed in both the AASHTO *Standard Specifications* and the pre-2005 AASHTO *LRFD*.

The database of existing bridges was used to estimate the reliability index inherent in the existing bridge system and used this as the starting point for the calibration.

#### 6.5.4.4 Estimated Reliability Index of Existing Bridges

Table 6.22 summarizes the average reliability indices for the existing I- and bulb-T girder bridges database. For example, the average reliability indices at decompression level, maximum allowable tensile stress limit under service loads of  $f_i = 0.19\sqrt{f'_c}$ , and maximum allowable crack width limit of 0.016 in. are 0.74, 1.05, and 2.69, respectively, for an ADTT of 5,000 and a return period of 1 year.

#### 6.5.4.5 Database of Simulated Bridges

A database of simulated simple-span bridges was designed using AASHTO I-girder sections for four cases. The simulated bridges have span lengths of 30, 60, 80, 100, and 140 ft and

**Table 6.22. Summary of Reliability Indices for Existing I- and Bulb-T Girder Bridges with One Lane Loaded and Return Period of 1 Year**

Performance Level		ADTT			
		1,000	2,500	5,000	10,000
Decompression		0.95	0.85	0.74	0.61
Maximum tensile stress limit	$f_i = 0.0948\sqrt{f'_c}$	1.15	1.01	0.94	0.82
	$f_i = 0.19\sqrt{f'_c}$	1.24	1.14	1.05	0.95
	$f_i = 0.25\sqrt{f'_c}$	1.40	1.27	1.19	1.07
Maximum crack width (in.)	0.008	2.29	2.21	1.99	1.85
	0.012	2.65	2.60	2.37	2.22
	0.016	3.06	2.89	2.69	2.56

girder spacing of 6, 8, 10, and 12 ft. This database was analyzed to determine the effect of the change in the method of estimating prestressing losses (pre-2005 and post-2005 methods) and the design environment (severe corrosive conditions and normal or not worse than moderate corrosion conditions). The two environmental conditions were signified by the maximum concrete tensile stress limit ( $f_i = 0.0948\sqrt{f'_c}$  or  $f_i = 0.19\sqrt{f'_c}$ ) used in the design. The four cases of design considered were as follows:

- Case 1: AASHTO *LRFD* with maximum concrete tensile stress of  $f_i = 0.0948\sqrt{f'_c}$  and pre-2005 prestress loss method;
- Case 2: AASHTO *LRFD* with maximum concrete tensile stress of  $f_i = 0.0948\sqrt{f'_c}$  and post-2005 prestress loss method;
- Case 3: AASHTO *LRFD* with maximum concrete tensile stress of  $f_i = 0.19\sqrt{f'_c}$  and pre-2005 prestress loss method; and
- Case 4: AASHTO *LRFD* with maximum concrete tensile stress of  $f_i = 0.19\sqrt{f'_c}$  and post-2005 prestress loss method.

Table 6.23 and Table 6.24, respectively, show the span length and girder spacing along with the calculated reliability indices for I-girder bridges designed for maximum concrete tensile stress  $f_i = 0.0948\sqrt{f'_c}$  (Case 1 and Case 2) and  $f_i = 0.19\sqrt{f'_c}$  (Case 3 and Case 4) for ADTT = 5,000.

In performing the design, the cases using the post-2005 prestress loss method (Case 2 and Case 4) were designed using the smallest possible AASHTO girder size. To facilitate the comparisons, when possible, Case 1 and Case 3 were then designed using the same AASHTO section used for Case 2 and Case 4, respectively. For the cases for which the section used for Case 2 or Case 4 was too small to be used for the corresponding Case 1 or Case 3, no design is shown in Table 6.23 for Case 1 or in Table 6.24 for Case 3. For the 140-ft span bridges with 12-ft girder spacing, no AASHTO I-girder section was sufficient.

**Table 6.23. Summary of Reliability Indices of Simulated Bridges Designed Using AASHTO Girders with  $ADTT = 5,000$  and  $f_t = 0.0948\sqrt{f'_c}$**

Case	Section Type	Span Length (ft)	Spacing (ft)	Case 1			Case 2		
				Designed Using Pre-2005 Loss Method			Designed Using Post-2005 Loss Method		
				Decompression	Maximum Tensile	Maximum Crack	Decompression	Maximum Tensile	Maximum Crack
1	AASHTO I	30	6	1.05	1.49	2.92	1.03	1.51	2.55
2	AASHTO I	30	8	0.90	0.94	2.41	0.93	1.00	2.32
3	AASHTO I	30	10	1.16	1.68	2.87	1.28	1.67	2.82
4	AASHTO I	30	12	1.28	1.67	2.91	0.63	0.97	2.29
<b>Average for 30-ft span</b>				<b>1.10</b>	<b>1.45</b>	<b>2.78</b>	<b>0.97</b>	<b>1.29</b>	<b>2.50</b>
5	AASHTO II	60	6	0.66	1.01	3.35	0.23	0.61	2.47
6	AASHTO II	60	8	—	—	—	0.73	1.04	2.42
7	AASHTO III	60	10	1.22	1.62	3.01	0.43	0.76	1.97
8	AASHTO III	60	12	1.57	1.96	3.68	0.73	0.99	2.51
<b>Average for 60-ft span</b>				<b>1.15</b>	<b>1.53</b>	<b>3.35</b>	<b>0.53</b>	<b>0.85</b>	<b>2.34</b>
9	AASHTO III	80	6	1.35	1.66	4.1	0.61	0.92	3.07
10	AASHTO III	80	8	1.8	2.14	5.23	0.82	1.13	3.64
11	AASHTO III	80	10	—	—	—	0.90	1.19	2.93
12	AASHTO IV	80	12	2.2	2.49	5.11	0.83	1.17	3.32
<b>Average for 80-ft span</b>				<b>1.78</b>	<b>2.10</b>	<b>4.81</b>	<b>0.79</b>	<b>1.10</b>	<b>3.24</b>
13	AASHTO III	100	6	—	—	—	1.45	1.85	3.51
14	AASHTO IV	100	8	1.86	2.00	3.86	1.33	1.43	3.44
15	AASHTO IV	100	10	—	—	—	1.33	1.65	3.37
16	AASHTO V	100	12	1.68	1.99	4.08	0.93	1.24	3.33
<b>Average for 100-ft span</b>				<b>1.77</b>	<b>2.00</b>	<b>3.97</b>	<b>1.26</b>	<b>1.54</b>	<b>3.41</b>
17	AASHTO IV	120	6	—	—	—	1.32	1.76	3.81
18	AASHTO V	120	8	1.54	2.05	3.65	0.92	1.4	3.14
19	AASHTO V	120	10	—	—	—	0.95	1.46	3.02
20	AASHTO VI	120	12	1.82	2.26	3.88	0.9	1.35	3.38
<b>Average for 120-ft span</b>				<b>1.68</b>	<b>2.16</b>	<b>3.77</b>	<b>1.02</b>	<b>1.49</b>	<b>3.34</b>
21	AASHTO VI	140	6	1.48	1.99	3.91	0.86	1.36	2.32
22	AASHTO VI	140	8	—	—	—	0.99	1.47	2.79
23	AASHTO VI	140	10	—	—	—	1.05	1.53	3.22
24	na	140	12	—	—	—	—	—	—
<b>Average for 140-ft span</b>				<b>1.48</b>	<b>1.99</b>	<b>3.91</b>	<b>0.97</b>	<b>1.45</b>	<b>2.78</b>
<b>Average for all spans</b>				<b>1.44</b>	<b>1.80</b>	<b>3.66</b>	<b>0.92</b>	<b>1.28</b>	<b>2.94</b>

Note: — = there is no design; na = not applicable because no AASHTO I-girder was sufficient.

**Table 6.24. Summary of Reliability Indices of Simulated Bridges Designed Using AASHTO Girders with  $ADTT = 5,000$  and  $f_t = 0.19\sqrt{f'_c}$**

Case	Section Type	Span Length (ft)	Spacing (ft)	Case 3			Case 4		
				Designed Using Pre-2005 Loss Method			Designed Using Post-2005 Loss Method		
				Decompression	Maximum Tensile	Maximum Crack	Decompression	Maximum Tensile	Maximum Crack
1	AASHTO I	30	6	1.00	1.55	2.39	0.97	1.55	2.46
2	AASHTO I	30	8	0.94	0.92	2.35	0.91	1.00	2.16
3	AASHTO I	30	10	1.29	1.66	2.91	1.18	1.66	2.79
4	AASHTO I	30	12	1.30	1.72	3.02	1.26	1.70	2.91
<b>Average for 30-ft span</b>				<b>1.13</b>	<b>1.46</b>	<b>2.67</b>	<b>1.08</b>	<b>1.48</b>	<b>2.58</b>
5	AASHTO II	60	6	0.74	1.13	3.11	0.18	0.58	2.41
6	AASHTO II	60	8	1.04	1.39	2.82	0.28	0.66	1.91
7	AASHTO III	60	10	0.42	0.79	2.05	0.42	0.78	2.07
8	AASHTO III	60	12	0.66	1.00	2.5	0.68	0.96	2.53
<b>Average for 60-ft span</b>				<b>0.72</b>	<b>1.08</b>	<b>2.62</b>	<b>0.39</b>	<b>0.75</b>	<b>2.23</b>
9	AASHTO III	80	6	0.56	0.97	3.13	0.13	0.51	2.53
10	AASHTO III	80	8	1.06	1.46	3.43	0.42	0.78	3.2
11	AASHTO III	80	10	1.58	1.84	3.65	0.37	0.65	2.72
12	AASHTO IV	80	12	0.83	1.15	3.72	0.51	0.87	3.11
<b>Average for 80-ft span</b>				<b>1.01</b>	<b>1.36</b>	<b>3.48</b>	<b>0.36</b>	<b>0.70</b>	<b>2.89</b>
13	AASHTO III	100	6	—	—	—	0.82	1.23	3.44
14	AASHTO IV	100	8	1.31	1.42	3.60	0.69	0.76	2.76
15	AASHTO IV	100	10	1.80	1.98	3.67	0.75	1.04	3.12
16	AASHTO V	100	12	1.08	1.37	3.43	0.40	0.72	2.55
<b>Average for 100-ft span</b>				<b>1.40</b>	<b>1.59</b>	<b>3.57</b>	<b>0.67</b>	<b>0.94</b>	<b>2.97</b>
17	AASHTO IV	120	6	1.53	1.98	3.71	0.70	1.28	3.10
18	AASHTO V	120	8	0.90	1.30	3.31	0.46	0.85	2.55
19	AASHTO V	120	10	1.25	1.65	3.35	0.26	0.78	2.68
20	AASHTO VI	120	12	1.19	1.66	3.37	0.47	0.91	2.69
<b>Average for 120-ft span</b>				<b>1.22</b>	<b>1.65</b>	<b>3.44</b>	<b>0.47</b>	<b>0.96</b>	<b>2.76</b>
21	AASHTO VI	140	6	0.84	1.41	3.23	0.28	0.82	2.41
22	AASHTO VI	140	8	1.22	1.68	3.30	0.53	0.98	3.04
23	AASHTO VI	140	10	—	—	—	0.62	1.08	2.46
24	na	140	12	—	—	—	—	—	—
<b>Average for 140-ft span</b>				<b>1.03</b>	<b>1.55</b>	<b>3.27</b>	<b>0.48</b>	<b>0.96</b>	<b>2.64</b>
<b>Average for all spans</b>				<b>1.07</b>	<b>1.43</b>	<b>3.15</b>	<b>0.58</b>	<b>0.96</b>	<b>2.68</b>

Note: — = there is no design; na = not applicable because no AASHTO I-girder was sufficient.

Bridges designed for Case 1 and Case 3 are also thought to be similar to those designed using AASHTO *Standard Specifications* for the two environmental conditions. The reliability indices calculated for Case 1 and Case 3 represent the inherent reliability of bridges currently on the system, as most of them were designed before 2005. Case 2 and Case 4 generally represent the inherent reliability of newer bridges designed using the 2005 and later versions of AASHTO *LRFD* for severe and normal environmental conditions, respectively.

Comparing Case 1 with Case 2 and Case 3 with Case 4 shows the effect of changing the prestressing loss method.

Using the post-2005 prestress loss method resulted in a smaller number of strands than the pre-2005 loss method. As shown in Table 6.23 and Table 6.24, the lower number of strands resulted in lower reliability indices for bridges designed using the post-2005 prestress loss method.

As shown in Table 6.23 and Table 6.24, regardless of the loss method and/or the limit state used, the reliability indices for each case varied significantly. This variation in values suggested the need to calibrate the limit state to develop a combination of load and resistance factors to produce a more uniform reliability index across the range of different span lengths and girder spacings.

#### 6.5.4.6 Selection of Target Reliability Index

The target reliability indices were selected on the basis of the calculated average values of the reliability levels of existing bridges and previous practice, with some consideration given to experiences from other codes (*Eurocode* and ISO 2394 document). A return period of 1 year and an ADTT equal to 5,000 were used.

Table 6.25 shows the target reliability indices selected in this study, as well as the reliability indices for the existing and simulated bridge databases. Note that the environmental condition for existing bridges was not known and that the

two columns showing the reliability indices of the simulated bridges are for cases for which the pre-2005 prestressing loss method was used, as these are thought to better represent the bridges currently on the system.

For example, the reliability index at the decompression performance level for existing bridges, simulated bridges designed for severe environments, and simulated bridges designed for normal environments was around 0.74, 1.44, and 1.07, respectively (see Table 6.22 to Table 6.25). Consequently, a target reliability index of 1.2 and 1.0 was selected for the decompression performance level for bridges designed for severe environments and bridges designed for normal environments, respectively. A reliability index of 1.0 means that 15 of 100 bridges will probably have the bottom of the girder decompress in any given year.

### 6.5.5 Calibration Result

The basic steps of the calibration process are shown below as they relate to the Service III calibration.

#### 6.5.5.1 Step 1: Formulate Limit State Function and Identify Basic Variables

The three limit state functions that were investigated are listed in Section 6.5.4.1. The limit state function is formulated by deriving an expression for the resistance prediction equation. For the decompression and tensile stress limits, the stress in the concrete is calculated as it is usually done for the design of prestressed concrete components. For the crack width limit state, Appendix D presents a detailed derivation of the resistance prediction equation for a typical prestressed concrete bridge girder. The derived equation considers uncracked and cracked section behavior in a general format by including the crack width equation. In lieu of setting the stress to zero, the resistance for the decompression limit state can also be

**Table 6.25. Reliability Indices ( $\beta$ ) for Existing and Simulated Bridges with Return Period of 1 Year and ADTT = 5,000**

Performance Level	Average $\beta$ for			Proposed Target $\beta$ for	
	Existing Bridges in NCHRP 12-78	Simulated Bridges Designed for $f_t = 0.0948 \sqrt{f'_c}$ and Pre-2005 Loss Method	Simulated Bridges Designed for $f_t = 0.19 \sqrt{f'_c}$ and Pre-2005 Loss Method	Bridges in Severe Environment	
				Bridges in Severe Environment	Bridges in Normal Environment
Decompression	0.74	1.44	1.07	1.20	1.00
Maximum allowable tensile stress of $f_t = 0.19 \sqrt{f'_c}$	1.05	1.80	1.43	1.50	1.25
Maximum allowable crack width of 0.016 in.	2.69	3.68	3.15	3.30	3.10



derived by setting the crack width to zero in the general equation for crack width.

The majority of the equations for the prediction of the maximum crack width are given in terms of the stress in the steel. Various maximum crack width prediction equations were evaluated using test data available in the literature. Appendix C presents a comparison and evaluation of maximum crack width prediction equations for prestressed concrete members.

#### 6.5.5.2 Step 2: Identify and Select Representative Structural Types and Design Cases

Various design cases for span lengths ranging from 30 to 140 ft were designed, as shown in Section 6.5.4.5. For a maximum crack width limit state, a crack width of 0.016 in. was considered. For the maximum allowable stress limit state, the stress considered is as stated in the discussion included in the following sections.

#### 6.5.5.3 Step 3: Determine Load and Resistance Parameters for Selected Design Cases

The variables included the dimension of the cross section and the material properties. The statistical information included the probability distribution and statistical parameters, such as mean ( $\mu$ ) and standard deviation ( $\sigma$ ).

#### 6.5.5.4 Step 4: Develop Statistical Models for Load and Resistance

The variables affecting the load and resistance were identified. These variables included live load; those affecting resistance, such as the dimensions of the cross section; and the material properties. The statistical information included the probability distribution and statistical parameters for live load presented in Section 5.3.2 and for other variables affecting the resistance presented in Section 6.5.4.2.

#### 6.5.5.5 Step 5: Develop Reliability Analysis Procedure

The statistical information of all the required variables was used to determine the statistical parameters of the resistance by using Monte Carlo simulation. Monte Carlo simulation is useful in generating a large number of random cases that are used in defining the mean and standard deviation of the resistance.

For each girder, Monte Carlo simulation was performed for each random variable associated with calculation of the resistance and dead load. One thousand simulations were performed. For each random variable, 1,000 values were

generated independently on the basis of the statistics and distribution of that random variable. For each simulation, the dead load and the resistance were calculated using one of the 1,000 sets of values of each random variable, resulting in 1,000 values of the dead load and the resistance. The mean and standard deviation of the dead load and the resistance were then calculated on the basis of the 1,000 simulations.

#### 6.5.5.6 Step 6: Calculate Reliability Indices for Current Design Code and Current Practice

Using the statistics of the dead load and the resistance calculated from Monte Carlo simulation (as described above) and the statistics of the live load as derived from the WIM data (as described in Section 5), the reliability index was calculated for each girder.

The reliability index ( $\beta$ ) was calculated using Equation 6.13:

$$\beta = \frac{\mu_R - \mu_Q}{\sqrt{\sigma_R^2 + \sigma_Q^2}} \quad (6.13)$$

where

$\mu_R$  = mean value of resistance;

$\mu_Q$  = mean value of applied loads;

$\sigma_R$  = standard deviation of resistance; and

$\sigma_Q$  = standard deviation of applied loads.

The calculated reliability indices of existing and simulated bridges are shown in Table 6.22 to Table 6.24.

#### 6.5.5.7 Step 7: Review Results and Select Target Reliability Index

The initial target reliability index ( $\beta_T$ ) was determined as shown in Table 6.25.

#### 6.5.5.8 Step 8: Select Potential Load and Resistance Factors for Service III

For all steps, the resistance factor was assumed to be the same as in the current *AASHTO LRFD* (2012) (i.e., equal to 1.0).

The Service III limit state resistance is affected by the tensile stress limit used in the design. Therefore, in addition to trying different load factors, different stress limits for the design were also investigated. Maximum concrete design tensile stresses of  $f_t = 0.0948\sqrt{f'_c}$ ,  $f_t = 0.19\sqrt{f'_c}$ , and  $f_t = 0.25\sqrt{f'_c}$  were considered. In addition, the simulated bridge database used in determining the target resistance factor was expanded to allow longer spans.

Because there were three concrete tensile stress limits, Step 8 is divided into three repetitions designated 8a, 8b, and 8c. For this step, the range of span lengths was increased to 220 ft.

**STEP 8A: SELECT POTENTIAL LOAD AND RESISTANCE FACTORS FOR SERVICE III: BRIDGES DESIGNED FOR MAXIMUM CONCRETE TENSILE STRESS OF  $f_t = 0.0948\sqrt{f'_c}$**

The calibration for a selected bridge database (shown in Table 6.26) was performed assuming an ADTT of 5,000 and a maximum concrete design tensile stress of  $f_t = 0.0948\sqrt{f'_c}$ .

1. Calculate the reliability level of designs according to *AASHTO LRFD* (2012) (Figure 6.37 to Figure 6.39).

Figures 6.37 to 6.39 show the reliability indices for the bridges designed using AASHTO type girders according to *AASHTO LRFD* (2012), including a load factor of 0.8 for the Service III limit state, and assuming a maximum concrete tensile stress of  $f_t = 0.0948\sqrt{f'_c}$ . The geometric characteristics

of the bridges are shown in Table 6.26. The average reliability index for the decompression limit state, maximum allowable tensile stress limit state, and maximum allowable crack width limit state were 0.97, 1.31, and 3.06, respectively. As the reliability indices were lower than the target reliability indices and were not uniform across different spans, modifications to the load factor were applied in the next step in an attempt to achieve higher, and more uniform, reliability indices.

2. Redesign the bridges with a live load factor of 1.0.

In this step, the bridges were redesigned using a live load factor of 1.0, and the dead load and resistance factors were kept the same. Table 6.27 shows the design geometric characteristics of the redesigned bridges.

**Table 6.26. Summary Information of Bridges Designed with  $\gamma_{LL} = 0.8$  and  $f_t = 0.0948\sqrt{f'_c}$**

Case	Section Type	Span Length (ft)	Girder Spacing (ft)	$A_{ps}$ (in. <sup>2</sup> )	No. of Strands
1	AASHTO I	30	6	1.224	8
2	AASHTO I	30	8	1.530	10
3	AASHTO I	30	10	1.836	12
4	AASHTO I	30	12	2.142	14
5	AASHTO II	60	6	2.448	16
6	AASHTO II	60	8	3.366	22
7	AASHTO III	60	10	3.060	20
8	AASHTO III	60	12	3.672	24
9	AASHTO III	80	6	3.672	24
10	AASHTO III	80	8	4.590	30
11	AASHTO III	80	10	5.508	36
12	AASHTO IV	80	12	5.202	34
13	AASHTO III	100	6	6.120	40
14	AASHTO IV	100	8	6.426	42
15	AASHTO IV	100	10	7.344	48
16	AASHTO V	100	12	7.038	46
17	AASHTO IV	120	6	7.956	52
18	AASHTO V	120	8	7.956	52
19	AASHTO V	120	10	9.180	60
20	AASHTO VI	120	12	8.874	58
21	AASHTO VI	140	6	8.262	54
22	AASHTO VI	140	8	9.792	64
23	AASHTO VI	140	10	11.322	74
24	AASHTO VI	140	12	—	—
25	FIB-96	160	6	5.508	36

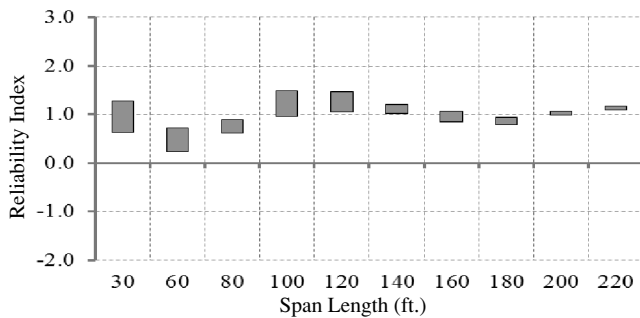
(continued on next page)

**Table 6.26. Summary Information of Bridges Designed with  $\gamma_{LL} = 0.8$  and  $f_t = 0.0948 \sqrt{f'_c}$  (continued)**

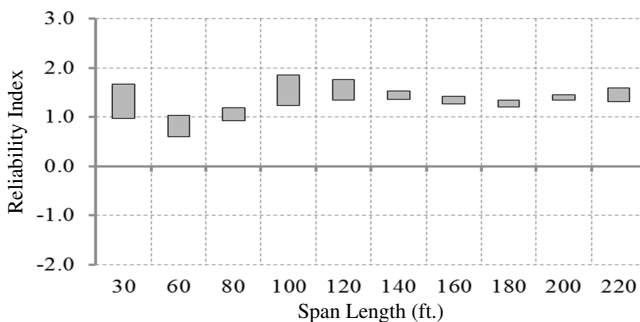
Case	Section Type	Span Length (ft)	Girder Spacing (ft)	$A_{ps}$ (in. <sup>2</sup> )	No. of Strands
26	FIB-96	160	8	6.426	42
27	FIB-96	160	10	7.344	48
28	FIB-96	160	12	—	—
29	FIB-96	180	6	7.344	48
30	Mod. BT-72	180	9	16.218	106
31	Mod. AASHTO VI	180	9	15.912	104
32	Mod. AASHTO VI	200	9	20.502	134
33	Mod. NEBT-2200	200	9	16.830	110
34	Mod. W95PTMG	200	9	16.830	110
35	Mod. NEBT-2200	220	9	20.808	136

Note: — = a practical solution was not found.

Figure 6.40 to Figure 6.42 show the reliability indices for the redesigned bridges using a live load factor of 1.0. The average reliability indices for the decompression limit state, the maximum allowable tensile stress limit state, and the maximum allowable crack width limit state were 1.33, 1.70, and 3.32, respectively. The reliability level of bridges became



**Figure 6.37. Reliability indices for bridges at decompression limit state (ADTT = 5,000,  $\gamma_{LL} = 0.8$ , and  $f_t = 0.0948 \sqrt{f'_c}$ ).**



**Figure 6.38. Reliability indices for bridges at maximum allowable tensile stress limit state (ADTT = 5,000,  $\gamma_{LL} = 0.8$ , and  $f_t = 0.0948 \sqrt{f'_c}$ ).**

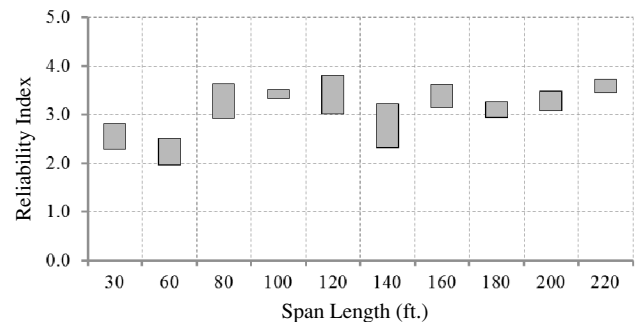
more uniform than for the case of using a live load factor of 0.8, particularly for the decompression and maximum tensile stress limit states. Consequently, a live load factor of 1.0 was proposed if the tensile stress was limited to  $f_t = 0.0948 \sqrt{f'_c}$ .

**STEP 8B: SELECT POTENTIAL LOAD AND RESISTANCE FACTORS FOR SERVICE III: BRIDGES DESIGNED FOR MAXIMUM CONCRETE TENSILE STRESS OF  $f_t = 0.19 \sqrt{f'_c}$**

The work described under Step 8a was repeated, except the girders were redesigned assuming a maximum concrete tensile stress of  $f_t = 0.19 \sqrt{f'_c}$ .

1. Calculate the reliability level of designs according to AASHTO LRFD (2012) with a maximum concrete tensile stress for design of  $f_t = 0.19 \sqrt{f'_c}$  (Figure 6.43 to Figure 6.45).
2. Redesign the bridges with a live load factor of 1.0.

Figure 6.46 to Figure 6.48 show the reliability indices for the redesigned bridges using a live load factor of 1.0 and  $f_t = 0.19$

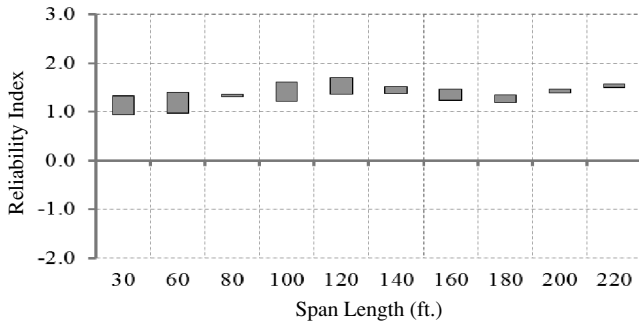


**Figure 6.39. Reliability indices for bridges at maximum allowable crack width limit state (ADTT = 5,000,  $\gamma_{LL} = 0.8$ , and  $f_t = 0.0948 \sqrt{f'_c}$ ).**

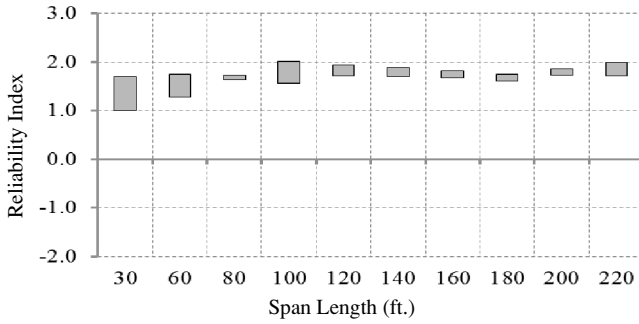
**Table 6.27. Summary Information of Bridges Designed with  $\gamma_{LL} = 1.0$  and  $f_t = 0.0948\sqrt{f'_c}$**

Case	Section Type	Span Length (ft)	Girder Spacing (ft)	$A_{ps}$ (in. <sup>2</sup> )	No. of Strands
1	AASHTO I	30	6	1.224	8
2	AASHTO I	30	8	1.530	10
3	AASHTO I	30	10	1.836	12
4	AASHTO I	30	12	2.142	14
5	AASHTO II	60	6	3.06	20
6	AASHTO II	60	8	3.978	26
7	AASHTO III	60	10	3.366	22
8	AASHTO III	60	12	4.284	28
9	AASHTO III	80	6	4.284	28
10	AASHTO III	80	8	5.202	34
11	AASHTO III	80	10	6.120	40
12	AASHTO IV	80	12	5.814	38
13	AASHTO III	100	6	7.038	46
14	AASHTO IV	100	8	7.038	46
15	AASHTO IV	100	10	8.262	54
16	AASHTO V	100	12	7.650	50
17	AASHTO IV	120	6	8.874	58
18	AASHTO V	120	8	8.874	58
19	AASHTO V	120	10	10.404	68
20	AASHTO VI	120	12	9.792	64
21	AASHTO VI	140	6	8.874	58
22	AASHTO VI	140	8	10.710	70
23	AASHTO VI	140	10	—	—
24	AASHTO VI	140	12	—	—
25	FIB-96	160	6	5.814	38
26	FIB-96	160	8	7.344	48
27	FIB-96	160	10	7.956	52
28	FIB-96	160	12	—	—
29	FIB-96	180	6	7.956	52
30	Mod. BT-72	180	9	17.442	114
31	Mod. AASHTO VI	180	9	17.442	114
32	Mod. AASHTO VI	200	9	22.032	144
33	Mod. NEBT-2200	200	9	18.360	120
34	Mod. W95PTMG	200	9	18.360	120
35	Mod. NEBT-2200	220	9	22.338	146

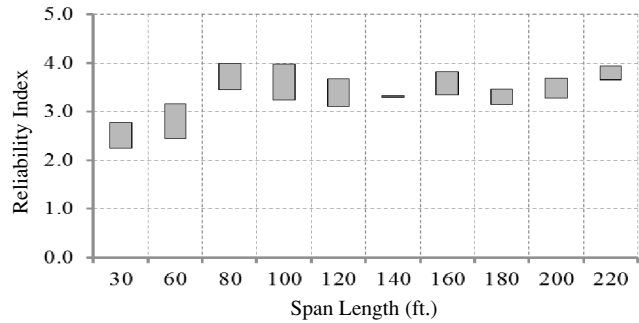
Note: — = a practical solution was not found.



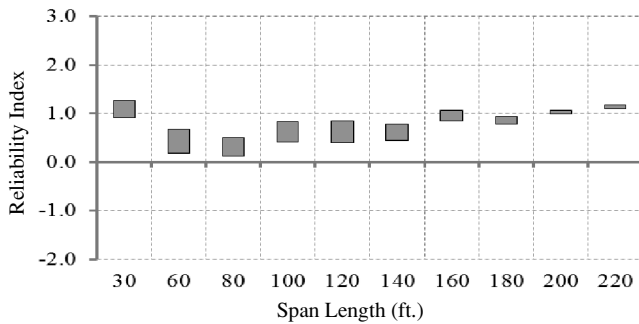
**Figure 6.40. Reliability indices for bridges at decomposition limit state (ADTT = 5,000,  $\gamma_{LL} = 1.0$ , and  $f_t = 0.0948\sqrt{f'_c}$ ).**



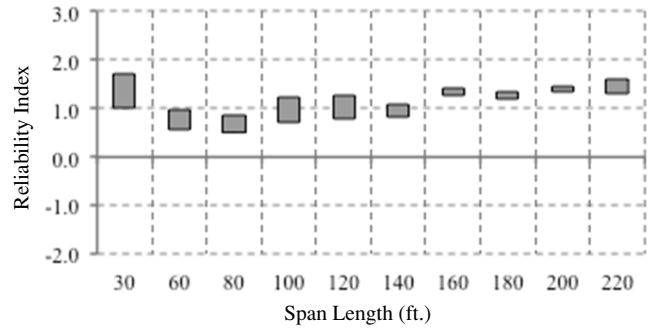
**Figure 6.41. Reliability indices for bridges at maximum allowable tensile stress limit state (ADTT = 5,000,  $\gamma_{LL} = 1.0$ , and  $f_t = 0.0948\sqrt{f'_c}$ ).**



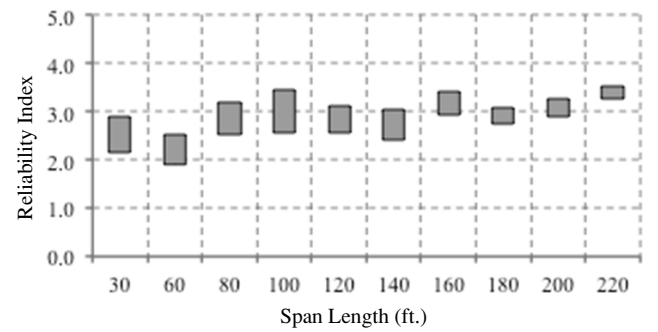
**Figure 6.42. Reliability indices for bridges at maximum allowable crack width limit state (ADTT = 5,000,  $\gamma_{LL} = 1.0$ , and  $f_t = 0.0948\sqrt{f'_c}$ ).**



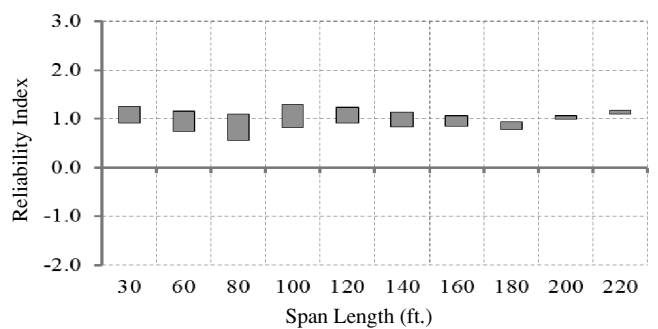
**Figure 6.43. Reliability indices for bridges at decomposition limit state (ADTT = 5,000,  $\gamma_{LL} = 0.8$ , and  $f_t = 0.19\sqrt{f'_c}$ ).**



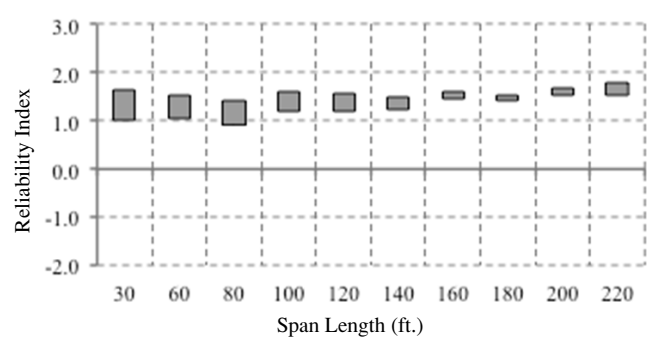
**Figure 6.44. Reliability indices for bridges at maximum allowable tensile stress limit state (ADTT = 5,000,  $\gamma_{LL} = 0.8$ , and  $f_t = 0.19\sqrt{f'_c}$ ).**



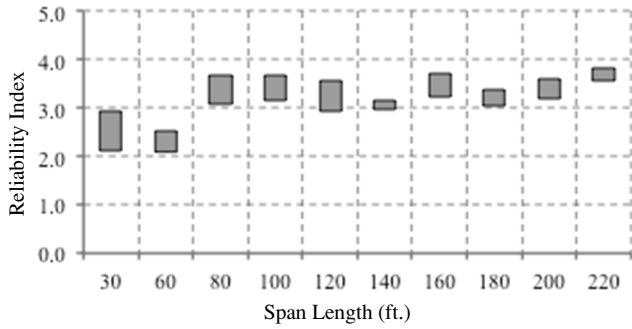
**Figure 6.45. Reliability indices for bridges at maximum allowable crack width limit state (ADTT = 5,000,  $\gamma_{LL} = 0.8$ , and  $f_t = 0.19\sqrt{f'_c}$ ).**



**Figure 6.46. Reliability indices for bridges at decomposition limit state (ADTT = 5,000,  $\gamma_{LL} = 1.0$ , and  $f_t = 0.19\sqrt{f'_c}$ ).**



**Figure 6.47. Reliability indices for bridges at maximum tensile stress limit state (ADTT = 5,000,  $\gamma_{LL} = 1.0$ , and  $f_t = 0.19\sqrt{f'_c}$ ).**



**Figure 6.48. Reliability indices for bridges at maximum crack width limit state (ADTT = 5,000,  $\gamma_{LL} = 1.0$ , and  $f_t = 0.19\sqrt{f'_c}$ ).**

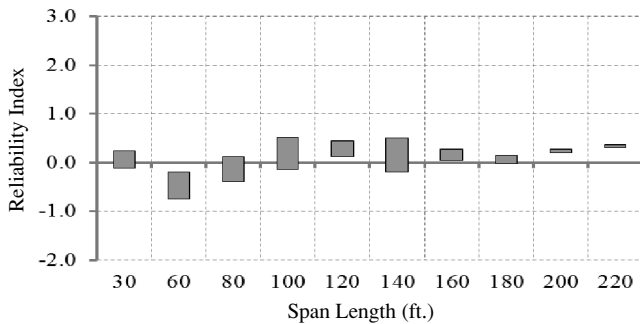
$\sqrt{f'_c}$ . Similar to the case of bridges designed for a maximum concrete tensile stress of  $f_t = 0.0948\sqrt{f'_c}$ , the reliability level of bridges became more uniform than the case of using a live load factor of 0.8, particularly for the decompression and maximum tensile stress limit states. Consequently, a live load factor of 1.0 was proposed if the maximum tensile stress was limited to  $0.19\sqrt{f'_c}$ .

**STEP 8C: SELECT POTENTIAL LOAD AND RESISTANCE FACTORS FOR SERVICE III: BRIDGES DESIGNED FOR MAXIMUM CONCRETE TENSILE STRESS OF  $f_t = 0.25\sqrt{f'_c}$**

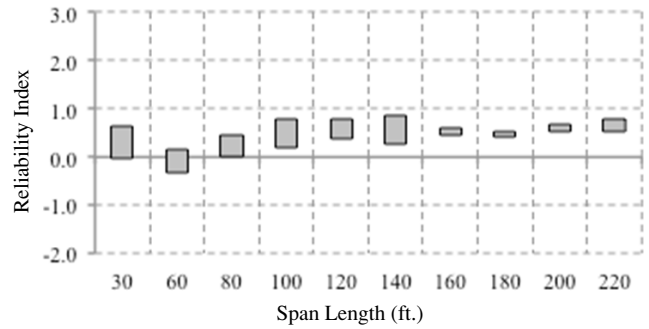
The work described under Step 8a and Step 8b was repeated, except the girders were redesigned assuming a maximum concrete tensile stress of  $f_t = 0.25\sqrt{f'_c}$ .

1. Calculate the reliability level of designs according to AASHTO LRFD (2010) with a maximum concrete tensile stress for design of  $f_t = 0.25\sqrt{f'_c}$  (Figure 6.49 to Figure 6.51).
2. Redesign the bridges with a live load factor of 1.0.

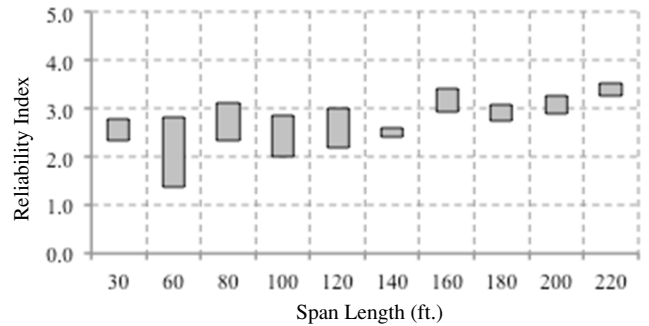
Figure 6.52 to Figure 6.54 show the reliability indices for the redesigned bridges using a live load factor of 1.0 and  $f_t = 0.25\sqrt{f'_c}$ . Similar to the case of bridges designed for maximum concrete tensile stresses of  $f_t = 0.0948\sqrt{f'_c}$  and



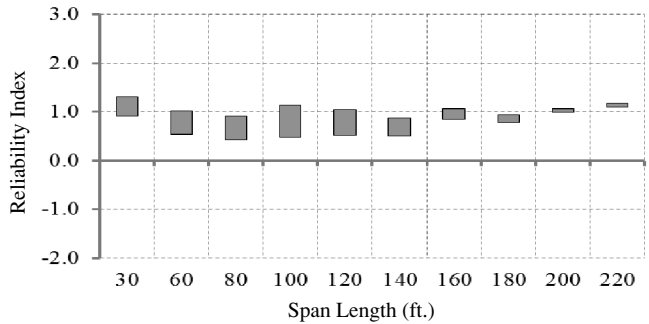
**Figure 6.49. Reliability indices for bridges at decompression limit state (ADTT = 5,000,  $\gamma_{LL} = 0.8$ , and  $f_t = 0.25\sqrt{f'_c}$ ).**



**Figure 6.50. Reliability indices for bridges at maximum allowable tensile stress limit state (ADTT = 5,000,  $\gamma_{LL} = 0.8$ , and  $f_t = 0.25\sqrt{f'_c}$ ).**



**Figure 6.51. Reliability indices for bridges at maximum allowable crack width limit state (ADTT = 5,000,  $\gamma_{LL} = 0.8$ , and  $f_t = 0.25\sqrt{f'_c}$ ).**



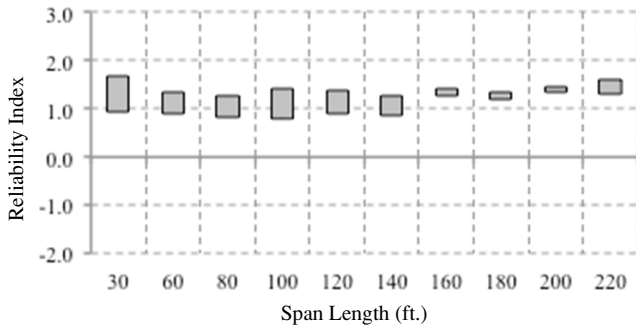
**Figure 6.52. Reliability indices for bridges at decompression limit state (ADTT = 5,000,  $\gamma_{LL} = 1.0$ , and  $f_t = 0.25\sqrt{f'_c}$ ).**

$f_t = 0.16\sqrt{f'_c}$ , the reliability level of bridges became more uniform than the case of using a live load factor of 0.8, particularly for the decompression and maximum tensile stress limit states. Consequently, a live load factor of 1.0 was proposed if the maximum tensile stress was limited to  $f_t = 0.25\sqrt{f'_c}$ .

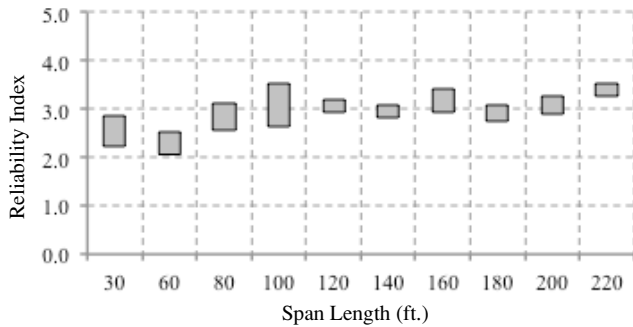
**6.5.5.9 Step 9: Calculate Reliability Indices**

The reliability indices were calculated for three cases, as shown in Step 8. In Step 9, the calculated values were reviewed to determine whether they were close to the target reliability





**Figure 6.53. Reliability indices for bridges at maximum tensile stress limit state (ADTT = 5,000,  $\gamma_{LL} = 1.0$ , and  $f_t = 0.25\sqrt{f'_c}$ ).**



**Figure 6.54. Reliability indices for bridges at maximum crack width limit state (ADTT = 5,000,  $\gamma_{LL} = 1.0$ , and  $f_t = 0.25\sqrt{f'_c}$ ).**

index and whether they were uniform across the range of spans considered. If they were not, the load factors, resistance factors, and/or the concrete tensile stress limit used for design were changed, and Step 8 was repeated. The limit state function to be used as the basis for the calibration was also determined in Step 9.

**6.5.5.10 Summary of Target Reliability Indices for Different Design and Performance Levels**

Summaries of the average reliability indices calculated for the different cases are given in Table 6.28 to Table 6.30. Regardless of the maximum tensile stress limits used in the design, the limiting criterion for the maximum tensile stress when determining the reliability index was taken as  $f_t = 0.19\sqrt{f'_c}$ .

As indicated earlier, the calibration of the specifications were based on an ADTT of 5,000. For this ADTT, the reliability indices obtained assuming the bridges were designed for maximum stress limits of  $f_t = 0.0948\sqrt{f'_c}$  and  $f_t = 0.19\sqrt{f'_c}$  (see the bold outlined cells below in Table 6.28 and Table 6.29, respectively) are very close to the target reliability indices shown in Table 6.25.

**6.5.5.11 Effect of Proposed Changes on Design**

To investigate the effect of the proposed change in the load factor, the number of strands required for different design cases

**Table 6.28. Summary of Reliability Indices for Simulated Bridges Designed for  $f_t = 0.0948\sqrt{f'_c}$**

ADTT	Live Load Factor = 0.8			Live Load Factor = 1.0		
	Decompression	Maximum Tensile Stress Limit	Crack Width (in.)	Decompression	Maximum Tensile Stress Limit	Crack Width (in.)
1,000	1.05	1.41	3.16	1.42	1.79	3.36
2,500	1.01	1.35	3.11	1.38	1.75	3.33
5,000	0.97	1.31	3.06	1.33	1.70	3.32
10,000	0.94	1.30	3.00	1.32	1.66	3.28

**Table 6.29. Summary of Reliability Indices for Simulated Bridges Designed for  $f_t = 0.19\sqrt{f'_c}$**

ADTT	Live Load Factor = 0.8			Live Load Factor = 1.0		
	Decompression	Maximum Tensile Stress Limit	Crack Width (in.)	Decompression	Maximum Tensile Stress Limit	Crack Width (in.)
1,000	0.84	1.27	2.92	1.11	1.53	3.25
2,500	0.70	1.15	2.87	1.04	1.46	3.17
5,000	0.68	1.10	2.82	1.00	1.41	3.14
10,000	0.64	1.07	2.78	0.98	1.34	3.11

**Table 6.30. Summary of Reliability Indices for Simulated Bridges Designed for  $f_t = 0.25\sqrt{f'_c}$** 

ADTT	Live Load Factor = 0.8			Live Load Factor = 1.0		
	Decompression	Maximum Tensile Stress Limit	Crack Width (in.)	Decompression	Maximum Tensile Stress Limit	Crack Width (in.)
1,000	0.20	0.55	2.83	0.93	1.29	3.03
2,500	0.08	0.49	2.77	0.89	1.27	2.95
5,000	0.06	0.44	2.72	0.85	1.23	2.92
10,000	0.02	0.41	2.66	0.82	1.20	2.88

was compared (see Table 6.31). The comparison indicated that when a live load factor of 0.8 was used in both cases, the post-2005 prestress loss method resulted in a smaller number of strands than when the pre-2005 prestress loss method was used. It also indicated that when the post-2005 loss method was used with a load factor of 1.0, the required number of strands was similar to that required when a load factor of 0.8 was used in conjunction with the pre-2005 prestress loss method (i.e., the designs were similar between the pre-2005 and post-2005 methods).

#### 6.5.5.12 Summary and Recommendations for Service III Limit State

For typical I-girders designed using the post-2005 prestress loss method and the assumptions listed in Section 6.5.3, and comparing the target reliability indices shown in Table 6.25 and the calculated reliability indices for different design criteria, load factors, and design live load as shown in Table 6.28 to Table 6.30 and Figure 6.37 to Figure 6.54, the following conclusions were drawn and summarized:

- For a specific girder of known cross section and specific number and arrangement of prestressing strands, the reliability index varies on the basis of the following:
  - The design maximum concrete tensile stress [maximum tensile stresses of  $f_t = 0.0948\sqrt{f'_c}$  and  $f_t = 0.19\sqrt{f'_c}$  are currently shown in *AASHTO LRFD* (2012) and are proposed to remain the same];
  - The limit state function [i.e., decompression, tensile stress of a certain value (assumed to be  $f_t = 0.19\sqrt{f'_c}$  in the work shown above), or a crack width of a certain value (assumed to be 0.016 in.)]; and
  - ADTT.

The effect of different factors can be deduced from Table 6.28 to Table 6.30.
- The target reliability index can be achieved uniformly across various span lengths by using the load factor developed by following the proposed calibration procedure. The level of uniformity varies with the limiting criteria.

The decompression limit state showed the highest level of uniformity and is recommended to be used as the basis for the reliability analysis (i.e., the determination of the load and resistance factors and associated design criteria).

- It is recommended that the reliability indices corresponding to an ADTT of 5,000 be used as the basis for the calibration. The reliability index is not highly sensitive to changes in the ADTT, so there is no need to use different load factors for ADTTs up to 10,000.
- With satisfactory past performance of prestressed beams, the target reliability index is selected to be similar to the average inherent reliability index of the bridges on the system. There is no scientific reason to support targeting a different (either higher or lower) reliability index.
- The recommended target reliability index for the decompression limit state is 1.0 for bridges designed for no worse than moderate corrosion conditions and 1.2 for bridges designed for severe corrosion conditions. The reliability index, which was based on the study of the WIM data, is determined assuming live load exists in a single lane and without applying the MPF. This would appear on the “load side” of the limit state function.
- Based on the reliability indices calculated for different design and load scenarios, to achieve the target reliability index, it is recommended that the following parameters be used for designing for the Service III limit state:
  - Live load factor of 1.0;
  - Maximum concrete tensile stress of  $f_t = 0.0948\sqrt{f'_c}$  and  $f_t = 0.19\sqrt{f'_c}$  for bridges in severe corrosion conditions and for bridges in no worse than moderate corrosion conditions, respectively; and
  - Girders to be designed following conventional design methods and assuming that live loads exist in single lane or multiple lanes, whichever produces higher load effects. The appropriate MPF applies.

These design parameters would appear on the resistance side of the limit state function during calibration.
- The results of the calibration demonstrated that girders designed using the conventional design methods and the controlling number of loaded traffic lanes produce uniform

**Table 6.31. Comparison of Number of Strands Required for Different Design Assumptions**

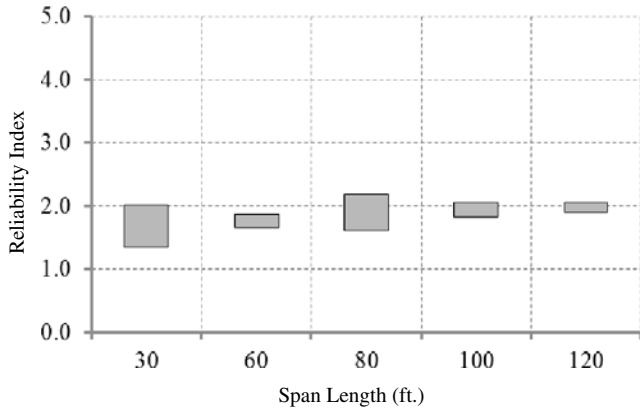
Case	Section Type	Span Length (ft)	Girder Spacing (ft)	$f_t = 0.0948 \sqrt{f'_c}$ , $\gamma_{LL} = 0.8$ , Pre-2005 Losses	$f_t = 0.0948 \sqrt{f'_c}$ , $\gamma_{LL} = 0.8$ , Post-2005 Losses	$f_t = 0.0948 \sqrt{f'_c}$ , $\gamma_{LL} = 1.0$ , Post-2005 Losses	$f_t = 0.19 \sqrt{f'_c}$ , $\gamma_{LL} = 0.8$ , Pre-2005 Losses	$f_t = 0.19 \sqrt{f'_c}$ , $\gamma_{LL} = 0.8$ , Post-2005 Losses	$f_t = 0.19 \sqrt{f'_c}$ , $\gamma_{LL} = 1.0$ , Post-2005 Losses
1	AASHTO I	30	6	8	8	8	8	8	8
2	AASHTO I	30	8	10	10	10	10	10	10
3	AASHTO I	30	10	12	12	12	12	12	12
4	AASHTO I	30	12	14	14	14	14	14	14
5	AASHTO II	60	6	20	16	20	18	16	16
6	AASHTO II	60	8	—	22	26	24	20	22
7	AASHTO III	60	10	22	20	22	20	20	20
8	AASHTO III	60	12	28	24	28	24	24	24
9	AASHTO III	80	6	28	24	28	24	22	24
10	AASHTO III	80	8	38	30	34	32	28	30
11	AASHTO III	80	10	—	36	40	42	32	38
12	AASHTO IV	80	12	40	34	38	34	32	34
13	AASHTO III	100	6	—	40	46	—	38	42
14	AASHTO IV	100	8	50	42	46	44	38	42
15	AASHTO IV	100	10	—	48	54	56	44	50
16	AASHTO V	100	12	56	46	50	48	42	46
17	AASHTO IV	120	6	—	52	58	58	48	52
18	AASHTO V	120	8	62	52	58	54	48	52
19	AASHTO V	120	10	—	60	68	68	54	60
20	AASHTO VI	120	12	74	58	64	64	54	58
21	AASHTO VI	140	6	62	54	58	54	48	52
22	AASHTO VI	140	8	—	64	70	68	58	64
23	AASHTO VI	140	10	—	74	—	—	68	74
24	na	140	12	—	—	—	—	—	—

Note: — = a practical solution was not found; na = not applicable.

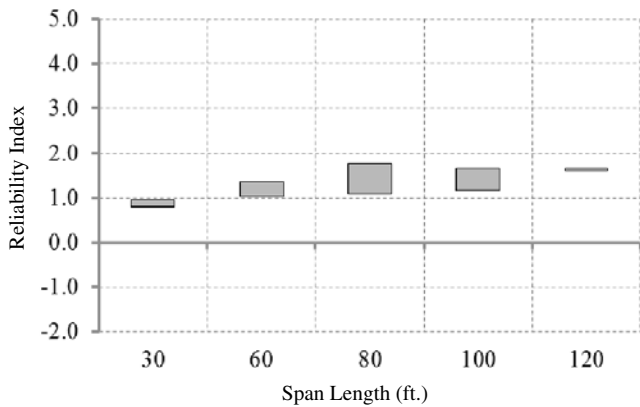
reliability approximately equal to the target reliability index provided that the load factor is based on a reliability index calculated using the decompression criteria and assuming one lane of traffic.

**6.5.6 Results for Adjacent Box Beams, Spread Box Beams, and American Segmental Box Institute Box Beams**

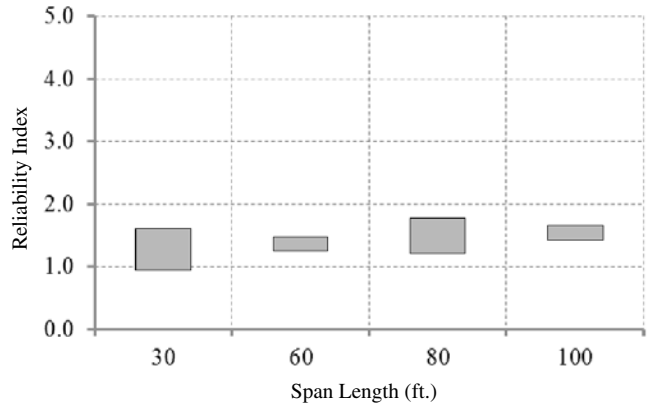
Work similar to that described above for I-beams was performed for adjacent box beams, spread box beams, and American Segmental Box Institute (ASBI) box beams. The details of the work are shown in Appendix D. The final results assuming the decompression limit state, ADTT of 5,000, return period of 1 year, and a load factor of 1.0 for live load are shown in Figure 6.55 to Figure 6.60. Table 6.32 shows the average reliability indices represented graphically in Figure 6.55 to Figure 6.60.



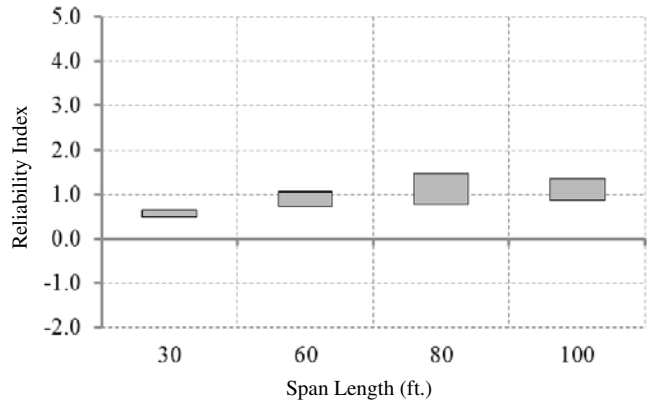
**Figure 6.55. Adjacent box beams, reliability indices for bridges at decompression limit state (ADTT = 5,000,  $\gamma_{LL} = 1.0$ , and  $f_t = 0.0948\sqrt{f'_c}$ ).**



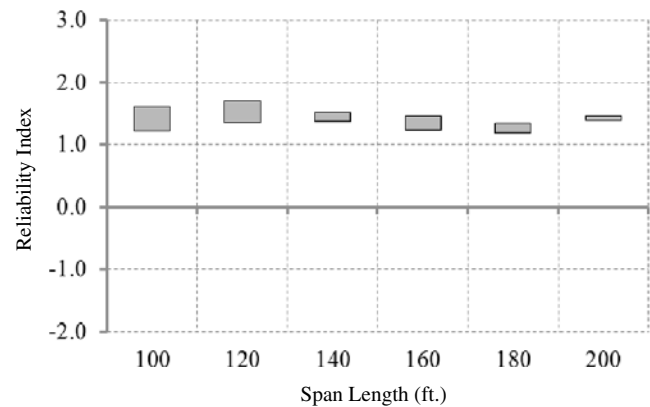
**Figure 6.56. Adjacent box beams, reliability indices for bridges at decompression limit state (ADTT = 5,000,  $\gamma_{LL} = 1.0$ , and  $f_t = 0.19\sqrt{f'_c}$ ).**



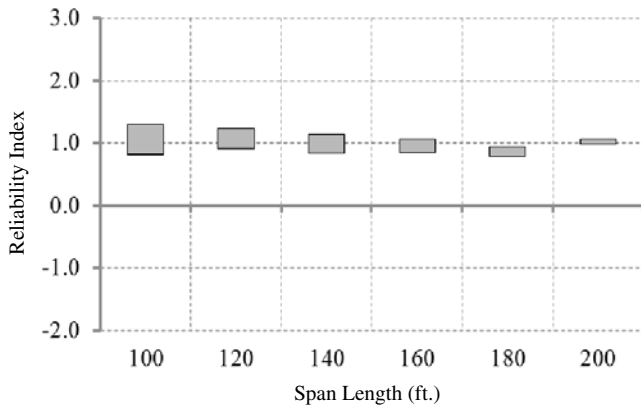
**Figure 6.57. Spread box beams, reliability indices for bridges at decompression limit state (ADTT = 5,000,  $\gamma_{LL} = 1.0$ , and  $f_t = 0.0948\sqrt{f'_c}$ ).**



**Figure 6.58. Spread box beams, reliability indices for bridges at decompression limit state (ADTT = 5,000,  $\gamma_{LL} = 1.0$ , and  $f_t = 0.19\sqrt{f'_c}$ ).**



**Figure 6.59. ASBI box beams, reliability indices for bridges at decompression limit state (ADTT = 5,000,  $\gamma_{LL} = 1.0$ , and  $f_t = 0.0948\sqrt{f'_c}$ ).**



**Figure 6.60. ASBI box beams, reliability indices for bridges at decompression limit state (ADTT = 5,000,  $\gamma_{LL} = 1.0$ , and  $f_t = 0.19\sqrt{f'_c}$ ).**

The results shown in Figure 6.55 to Figure 6.60 indicate that the reliability indices for each type of girder are reasonably uniform across the range of spans considered. With the exception of the adjacent box beams, the average reliability indices for other section types were very close to each other and to the target reliability index. For adjacent box beams, the average reliability index was slightly higher. However, the difference did not warrant incorporating measures to reduce the resistance of the beams, such as revising the distribution factor equations or using lower load factors for adjacent box beams.

**6.5.7 Sections Designed Using Other Methods of Determining Prestressing Time-Dependent Losses or Section Properties**

As indicated in Section 6.5.3, the calibration of Service III limit states assumed that the sections were designed using the *AASHTO LRFD* Refined Estimates of Time-Dependent

Losses. *AASHTO LRFD* requires the time-dependent losses for segmental bridges to be determined using detailed time-step methods. The 2005 revisions to Refined Estimates of Time-Dependent Losses did not affect the time-dependent prestressing loss calculations for segmental bridges. Historically, segmental bridges have been designed using gross section properties, not transformed section properties, and the effects of elastic gain have been neglected. If approved by the owner, the time-step method may also be used to design prestressed concrete components other than segmental bridges. However, the level of effort required to perform time-step analysis typically precludes this method for nonsegmental construction.

The proposed increase in the load factor for live load for the Service III limit state from 0.8 to 1.0 is based on comparing sections designed using the *AASHTO LRFD* pre-2005 provisions and the post-2005 provisions without making any exceptions to the specifications requirements and assuming that the Refined Estimates of Time-Dependent Losses method in the *AASHTO LRFD* was used for calculating the time-dependent losses.

The development of the method termed Approximate Estimate of Time-Dependent Losses in *AASHTO LRFD* was based on producing prestress losses similar to those produced by the Refined Estimates of Time-Dependent Losses method. Thus, the change in the load factor should also be applied to the former method.

Because the changes in the prestress loss methods in 2005 did not affect the time-step method, the increase in the load factor should not be applied to sections designed using the time-step method. These sections have to satisfy the following conditions to continue using the 0.8 load factor for live load:

- Time-dependent losses are determined using the time-step method.
- Gross sections properties are used for the calculations.
- The calculations of the force in the prestressing steel neglects the effects of the elastic gain.

**6.5.8 Proposed AASHTO LRFD Revisions**

*AASHTO LRFD* (2012) Article 5.9.4.2.2 (Tension Stresses, which discusses stresses in fully prestressed components at SLS after losses) contains the design stress limits that are affected by the calibration of the Service III limit state. Due to the lack of changes to the design stress limits, no revisions to this section are required.

With respect to the calibration of the limit state for tension in prestressed concrete presented above, the only required revisions to the specifications are those in Article 3.4.1, which should specify the load factor for live load as 0.8 or 1.0 depending on the design procedure used.

**Table 6.32. Average Reliability Indices for Different Types of Girders**

Type of Section	Maximum Tensile Stress Used in Design (ksi)	
	$f_t = 0.0948 \sqrt{f'_c}$	$f_t = 0.19 \sqrt{f'_c}$
I- and bulb-T girders	1.33	1.00
Adjacent box beams	1.85	1.31
Spread box beams	1.45	1.01
ASBI box beams	1.41	1.00

## 6.6 Fatigue Limit States: Lifetime

### 6.6.1 Steel Members

#### 6.6.1.1 Formulate Limit State Function

Two limit states for load-induced fatigue of steel details are defined in *AASHTO LRFD* Article 3.4.1: Fatigue I, related to infinite load-induced fatigue life; and Fatigue II, related to finite load-induced fatigue life.

For load-induced fatigue considerations, according to *AASHTO LRFD* Article 6.6.1.2.2, each steel detail should satisfy Equation 6.14:

$$\gamma(\Delta f) \leq (\Delta F)_n \tag{6.14}$$

where

$\gamma$  = load factor;

$\Delta f$  = force effect (live load stress range due to the passage of the fatigue load); and

$(\Delta F)_n$  = nominal fatigue resistance.

This general limit state function is used for the calibration of the fatigue limit states.

The fatigue load of *AASHTO LRFD* Article 3.7.1.4 and the fatigue live load load factors of *AASHTO LRFD* Table 3.4.1-1 are based on extensive research of structural steel highway bridges. The fatigue load is the *AASHTO LRFD* design truck [the HS20-44 truck of *AASHTO Standard Specifications* (2002)], but with a fixed rear-axle spacing of 30 ft. The live load load factors for the fatigue limit state load combinations are summarized in Table 6.33.

The load factor for the Fatigue I load combination reflects load levels found to be representative of the maximum stress

**Table 6.33. Current Fatigue Load Factors**

Fatigue Limit State	Live Load Load Factor
Fatigue I	1.5
Fatigue II	0.75

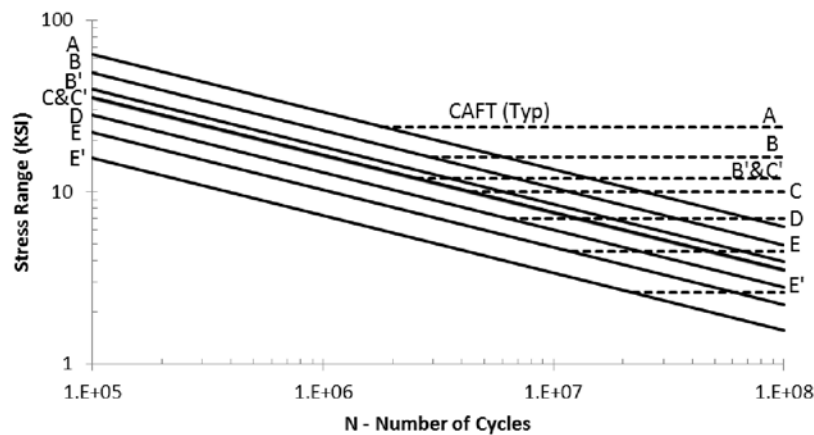
range of the truck population for infinite fatigue life design. The factor was chosen on the assumption that the maximum stress range in the random variable spectrum is twice the effective stress range caused by the Fatigue II load combination.

The load factor for the Fatigue II load combination reflects load levels found to be representative of the effective stress range of the truck population with respect to a small number of stress range cycles and to their cumulative effects in steel elements, components, and connections for finite fatigue life design.

The resistance factors for the fatigue limit states ( $\phi$ ) are inherently taken as unity and hence do not appear in Equation 6.14.

#### 6.6.1.2 Select Structural Types and Design Cases

Components and details susceptible to load-induced fatigue cracking have been grouped into eight groups, called detail categories, by fatigue resistance. *AASHTO LRFD* Table 6.6.1.2.3-1 illustrates many common details found in steel bridge construction and identifies potential crack sites for each detail. Figure 6.61 shows the current *AASHTO LRFD* fatigue design curves with the eight detail categories ranging from A to E'.



Source: *AASHTO LRFD* (2012).

**Figure 6.61. AASHTO fatigue design curves: stress range versus number of cycles. Used with permission of the American Association of State Highway and Transportation Officials.**



### 6.6.1.3 Determine Load and Resistance Parameters for Selected Design Cases

A comprehensive database containing constant and variable amplitude fatigue test results for various welded steel bridge detail types was developed by Keating and Fisher (1986). This database includes the test data from various NCHRP test programs and other available data. These data are presented in Appendix F.

The fatigue data include the detail type of each specimen, the minimum and maximum stress values, and the number of cycles observed until fatigue failure was evident. From these data, the stress range was taken as the only significant parameter in the determination of the fatigue life, and a relationship between the stress range and number of cycles to failure was developed for the combined fatigue data (Keating and Fisher 1986). The regression analysis performed on the stress range versus cycle relation showed that this relation was log-log in nature. The curves of the data plotted in log form are characterized by Equation 6.15:

$$\log N = \log A - B \log S_r \quad (6.15)$$

or in exponential form as shown in Equation 6.16

$$N = AS_r^{-B} \quad (6.16)$$

where

$N$  = number of cycles to failure;

$S_r$  = constant amplitude stress range (ksi);

$\log A$  = log- $N$ -axis intercept of  $S$ - $N$  curve (a constant taken from *AASHTO LRFD* Table 6.6.1.2.5-1 for the various detail categories); and

$B$  = slope of the curve.

The combined fatigue data for each detail type were placed in the eight detail categories on the basis of the fatigue performance of the details as specified by *AASHTO LRFD* Article 6.6.1.2.3. Fatigue design curves were then determined for each of the fatigue categories. The design curves represent allowable stress range values that are based on a 98% confidence limit or lower bound of fatigue resistance. Thus, for a particular detail type, most of the fatigue data fall above the design curve, and the test data should not deviate significantly from the curve. The slopes of all the design curves were determined to be very close to a constant value of  $-3.0$ , as shown through the use of regression analysis (Keating and Fisher 1986). Thus, a constant slope of  $-3.0$  was imposed on the equations in the regression analysis. Figure 6.61 showed the current *AASHTO LRFD* fatigue design curves with the eight detail categories.

### 6.6.1.4 Develop Statistical Models for Loads and Resistances

#### LOAD UNCERTAINTIES

On the basis of the analysis of WIM data discussed in Chapter 5, it is suggested that the current load factor of 1.5 for the Fatigue I limit state be increased to 2.0 to account for current and projected truck loads. Similarly, it is proposed that the load factor of 0.75 for the Fatigue II limit state be increased to 0.80. The mean values and CVs from Chapter 5 are shown in Table 6.34.

#### RESISTANCE UNCERTAINTIES

##### Fatigue Damage Parameter

To properly calibrate the fatigue limit states of the *AASHTO LRFD*, it was necessary to determine the statistical parameters of the fatigue test data used in the bridge fatigue resistance model. These parameters include the bias and the CV of the fatigue test data. As previously described, the fatigue data are commonly presented in terms of the stress range and number of cycles to failure, or  $S$ - $N$  curves in log-log space. The use of this relationship with the given constant amplitude fatigue test data, however, causes difficulty in accurately determining the statistical parameters. The available data were not sufficiently distributed along the  $S$ - $N$  curves in log-log space for a regression analysis; the data were often gathered over a small increment of stress ranges and were limited in number. Any number of regression lines could have been used to describe this relationship between the stress range and fatigue life. To better analyze the fatigue data, a different relationship between the number of cycles and stress range was developed.

The test data were arranged to couple the number of cycles and stress range in the form of an effective stress range for each test specimen. The effective stress range as presented in Article 6.6.2.2 of *AASHTO LRFD* (2010) was taken as the cube root of the sum of the cubes of the measured stress ranges, as seen in Equation 6.17. The effective stress range is an accepted means to compare variable amplitude fatigue data with constant amplitude fatigue test data.

$$(S_r)_{\text{eff}} = (\sum \gamma_i S_{ri}^3)^{1/3} \quad (6.17)$$

**Table 6.34. Load Uncertainties**

Limit State	Mean	CV
Fatigue I	2.0	0.12
Fatigue II	0.8	0.07

where

- $(S_r)_{\text{eff}}$  = effective constant amplitude stress range;
- $\gamma_i$  = percentage of cycles at a particular stress range; and
- $S_{ri}$  = constant amplitude stress range for a group of cycles (ksi).

The formula describing the parameter used for the test data follows the form of Equation 6.17; however, this equation is applied to each of the test specimens. Thus, the percentage term is equated to a value of one and is subsequently multiplied by the number of cycles ( $N$ ) to yield Equation 6.18:

$$S_{fi} = (N * S_{ri}^3)^{1/3} \quad (6.18)$$

where  $S_{fi}$  is a fatigue damage parameter.

The fatigue damage parameter is taken as a normally distributed random variable in order to determine the bias and CV of the fatigue resistance for each of the detail categories. The data were fitted to many of the typical distributions commonly used, and it was determined that the normal distribution best characterized the nature of the fatigue data. The bias is a ratio of the mean value of the test data to the nominal value described in the specifications. The calculation of the nominal, mean, and CV values are described in the following subsections.

#### *Probability Paper to Determine Statistical Parameters*

The collection of the fatigue data in terms of the new fatigue parameter for each detail category was statistically analyzed using normal probability paper, as the data best fit the normal distribution. The use of normal probability paper is explained in Chapter 3.

The fatigue data for each detail category were filtered to include the data that most accurately reflected the fatigue behavior of each category. In other words, the data were truncated based on the nature of the curve within each normal probability plot to include the pertinent fatigue data. In

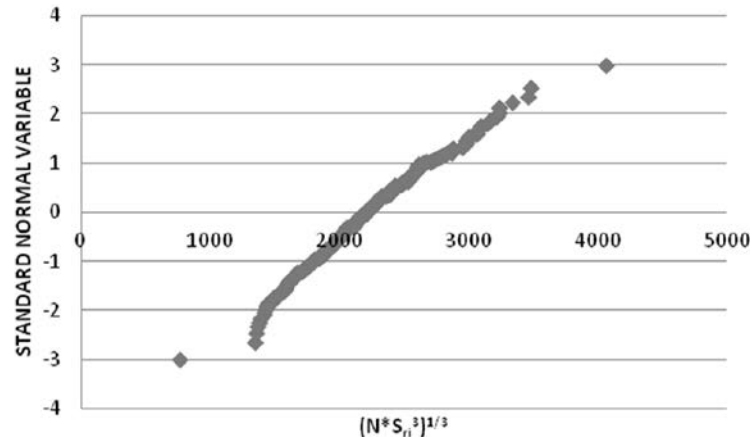
general, the majority of the lower portion of each curve was selected for each detail category. The lower tail of the data was selected because it was the portion of the curve that fit the normal distribution (i.e., it was the straight portion of the normal probability plot). Moreover, the lower portion of the fatigue data represented the range of values within which fatigue cracking was expected to occur when analyzed for the fatigue limit state load combinations using the Monte Carlo simulation approach, which is discussed in more detail below. Failure occurs when load exceeds resistance; thus, the higher portions of the fatigue data sets represented fatigue resistance data that were very unlikely to be exceeded by the fatigue loads used within this study and were therefore considered insignificant.

Different approaches for selecting the cutoff values for each category were investigated to determine the sensitivity of the resulting reliability indices. It was determined that the relative differences of the results determined from the different techniques were negligible. Other techniques used to determine the cutoff values included the use of constant cutoff values for all the detail categories and having different analysts manually insert best-fit lines. Table 6.35 shows the resulting cutoff values for the standard normal variable. Figure 6.62 and Figure 6.63 show the normal probability plots of the full fatigue data set and the truncated data for categories C and C', respectively.

Determining the statistical parameters of the data was relatively straightforward once the data for each detail category were filtered and fitted with a line of best fit by using Microsoft Excel software. The mean value of the stress parameter is simply the intersection of the best-fit line with the horizontal axis. The standard deviation of the data is taken as the inverse of the slope of the best-fit line. More simply stated, the standard deviation is the change in the horizontal coordinates divided by the change in the vertical coordinates. CV is the ratio of the standard deviation to the mean of the data. The resulting statistical parameters are given in Table 6.35. The probability plots of the fatigue data and corresponding truncated data for all detail categories can be seen in Appendix E.

**Table 6.35. Resistance Uncertainties**

Category	Standard Deviation	CV	Bias	$S_{f, \text{Mean}}$	$S_{f, \text{AASHTO}}$	Cutoff Standard Normal Variable
A	1,000.0	0.24	1.43	4,167.40	2,924	1
B	666.7	0.22	1.34	3,077.47	2,289	1
B'	250.0	0.11	1.28	2,336.10	1,827	1
C and C'	454.6	0.21	1.35	2,210.77	1,638	1
D	185.2	0.10	1.36	1,773.69	1,300	1
E	140.9	0.12	1.17	1,207.41	1,032	1
E'	232.6	0.20	1.56	1,140.28	730	1



**Figure 6.62. Normal probability plot of detail categories C and C' fatigue data.**

*Determination of Nominal Fatigue Parameter and Bias Values*

CV and the mean of the fatigue resistance data were determined as described in the previous subsection. These values, along with the nominal fatigue resistance, were needed to determine the bias of the data. The nominal value of the chosen fatigue parameter was calculated using *AASHTO LRFD* Equation 6.6.1.2.5-2 and rearranged to achieve the relationship in terms of the desired fatigue damage parameter, as seen in Equation 6.19. The resulting nominal resistance values can be seen in Table 6.35.

$$S_{f\_AASHTO} = (N * S_r^3)^{1/3} = A^{1/3} \tag{6.19}$$

where  $S_{f\_AASHTO}$  is the nominal value of the fatigue parameter using *AASHTO LRFD* specifications for each detail category, and  $A$  is a constant taken from *AASHTO LRFD* Table 6.6.1.2.5-1 for the various detail categories.

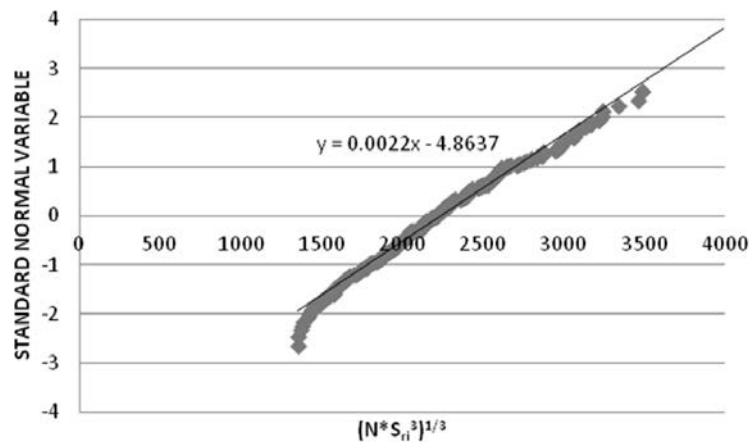
The bias value for each category was determined by taking the ratio of the mean value to the nominal value of the fatigue parameter, as seen in Equation 6.20; the results are shown in Table 6.35.

$$\text{Bias} = S_{f\_Mean} / S_{f\_AASHTO} \tag{6.20}$$

where  $S_{f\_Mean}$  is the mean value of the fatigue parameter using the fatigue data for each detail category.

**6.6.1.5 Develop Reliability Analysis Procedure**

In code calibration, it is necessary to develop a process by which to express the structural reliability or the probability of the loads on the member being greater than its resistance; in other words, failure of the criteria. The reliability analysis performed within this project was an iterative process that consisted of Monte Carlo simulations to select load and



**Figure 6.63. Normal probability plot of detail categories C and C' truncated fatigue data with best-fit line.**

resistance factors that would achieve reliability close to the target reliability index. The Monte Carlo technique samples load and resistance parameters from selected statistical distributions, such as a normal distribution. Reliability is measured in terms of  $\beta$ , the reliability index or safety index.  $\beta$  is defined as a function of the probability of failure by using Equation 6.21. Thus  $\beta$  is the number of standard deviations that the mean safety margin falls on the safe side. The higher the  $\beta$  value, the higher the reliability.

$$\beta = -\Phi^{-1}(P_f) \quad (6.21)$$

where  $\Phi^{-1}$  is the inverse standard normal distribution function, and  $P_f$  is the probability of failure.

#### MONTE CARLO SIMULATION

The Monte Carlo analysis is described more fully in Chapter 3. A step-by-step outline of the Monte Carlo simulation using Microsoft Excel is included in Appendix F.

The distribution of loads was assumed to be normally distributed as the loads are a summation of force effects. The fatigue resistance was also assumed to follow normal distributions. These distributions for load and resistance were developed using determined statistical parameters from the available data.

#### 6.6.1.6 Calculate Reliability Indices for Current Design Code or Current Practice

The current reliability indices inherent for the various fatigue detail categories were determined using the Monte Carlo simulation technique with the provisions for the Fatigue I and II limit states as specified in *AASHTO LRFD*. The Fatigue I limit state uses a load factor of 1.5, which is common to all the detail types. The CV for the Fatigue I limit state was determined to be 0.12 through the work discussed in Chapter 5. The resistance parameters for the Monte Carlo simulation were determined by equating the nominal load and resistance values and then applying the statistical parameters for each of the detail categories (see Table 6.35). Insufficient fatigue data exist to determine the constant amplitude fatigue threshold portions of the fatigue design curves for finite fatigue design life (Fatigue II limit state). In consultation with AASHTO Technical Committee T-14 and the American Iron and Steel Institute Bridge Task Force, the research team deemed it acceptable to use the statistical parameters for the sloping portions of these curves for the constant amplitude fatigue thresholds of the different bridge detail categories. In *AASHTO LRFD*, the Fatigue II limit state currently has a load factor of 0.75 for all the detail categories and a CV of 0.07. The nominal resistance values were determined using Equation 6.22, which resulted from setting the *AASHTO LRFD* fatigue resistance Equation 6.6.1.2.5-2

equal to the design fatigue load, which was normalized to a stress range equal to 1 ksi.

$$R = A/0.75^3 \quad (6.22)$$

where  $R$  is resistance, and  $A$  is a constant taken from *AASHTO LRFD* Table 6.6.1.2.5-1 for the various detail categories.

The simulations for both limit states were completed using a total of 10,000 replicates to achieve a sufficient number of failures. The resulting reliability indices for each of the eight detail categories are reported in Table 6.36.

#### 6.6.1.7 Select Target Reliability Index

Target reliability indices ( $\beta_T$ ) were based on the inherent reliability of the current specifications (see Table 6.36). The fatigue limit states were harmonized by selecting a single, common target reliability index for both steel and concrete members equal to 1.0. This proposed target was selected to best reflect the inherent reliability of the Fatigue I and II limit states for structural steel members and the Fatigue I limit state for reinforcement and concrete.

#### 6.6.1.8 Select Potential Load and Resistance Factors

When the proposed load factors of 2.0 and 0.8 for the Fatigue I and Fatigue II limit states, respectively, and the inherent resistance factor of 1.0 were applied along with the statistical data, the reliability indices for each detail category remained essentially unchanged from those reported in Table 6.36. Accepting a range of  $\pm 0.2$  on the reliability index, three Fatigue I limit state reliability indices appear to be too large: detail Category B' at  $\beta = 1.5$ , detail Category D at  $\beta = 2.0$ , and detail Category E'

**Table 6.36. Current Reliability Indices ( $\beta$ ) Using AASHTO LRFD Fatigue I and Fatigue II Limit States**

Category	Fatigue I	Fatigue II
A	1.2	1.0
B	1.1	0.9
B'	1.5	1.0
C	1.2	0.9
C'	1.2	0.9
D	2.0	1.3
E	0.9	0.7
E'	1.7	1.4

**Table 6.37. Proposed Fatigue I Limit State Resistance Factors**

Detail Category	Proposed Resistance Factor ( $\phi$ )	Reliability Index ( $\beta$ )
A	1.0	1.2
B	1.0	1.1
B'	<b>1.10</b>	0.9
C	1.0	1.2
C'	1.0	1.2
D	<b>1.15</b>	1.1
E	1.0	0.9
E'	<b>1.20</b>	1.0

at  $\beta = 1.7$ . Similarly, two Fatigue II limit state reliability indices appear to be too large (detail Category D at  $\beta = 1.3$  and detail Category E' at  $\beta = 1.4$ ) and one appears to be too small (detail Category E at  $\beta = 0.7$ ).

Proposed resistance factors for the Fatigue I limit state and the Fatigue II limit state are given in Table 6.37 and Table 6.38, respectively. Resistance factors other than the current values of unity are shown in boldface. Reliability index values using the proposed resistance factors are shown in the right-hand column.

#### 6.6.1.9 Calculate Reliability Indices

With the proposed resistance factors, the reliability indices were all within  $\pm 0.2$  of the target reliability index of 1.0.

The reliability indices shown in Tables 6.37 and 6.38 can also be achieved by revising the *AASHTO LRFD* fatigue resistance equations for steel members. This may be a better solution than including resistance factors for only a few of the detail

**Table 6.38. Proposed Fatigue II Limit State Resistance Factors**

Detail Category	Proposed Resistance Factor ( $\phi$ )	Reliability Index ( $\beta$ )
A	1.0	1.0
B	1.0	0.9
B'	1.0	1.0
C	1.0	0.9
C'	1.0	0.9
D	<b>0.95</b>	1.0
E	<b>1.10</b>	1.0
E'	<b>0.90</b>	1.0

**Table 6.39. Proposed Revisions to AASHTO LRFD Table 6.6.1.2.5-1**

Detail Category	Current Constant A $\times 10^8$	Proposed Constant A $\times 10^8$
A	250	250
B	120	120
B'	61	<b>61</b>
C	44	44
C'	44	44
D	22	<b>21</b>
E	11	12
E'	3.9	<b>3.5</b>

categories and in some cases greater than unity. The required revisions to the *AASHTO LRFD* tables are given in Table 6.39 and Table 6.40 with changes shown in boldface.

## 6.6.2 Concrete Members

This section deals with concrete and reinforcing steel. Prestressing strand is not covered as there are currently no design checks required for fully prestressed components, as explained in Chapter 2.

### 6.6.2.1 Formulate Limit State Function

Two limit states for load-induced fatigue are defined in *AASHTO LRFD* Article 3.4.1; however, only Fatigue I, related to infinite load-induced fatigue life, is valid for concrete members as they are always designed for infinite life.

For load-induced fatigue considerations, according to *AASHTO LRFD* Article 5.5.3.1, concrete members shall satisfy

**Table 6.40. Proposed Revisions to AASHTO LRFD Table 6.6.1.2.5-3**

Detail Category	Current Constant Amplitude Fatigue Threshold (ksi)	Proposed Constant Amplitude Fatigue Threshold (ksi)
A	24	24
B	16	16
B'	12	13
C	10	10
C'	12	12
D	7	<b>8.0</b>
E	4.5	<b>4.5</b>
E'	2.6	<b>3.1</b>



Equation 6.23, which is seen as a variation of Equation 6.14 applicable only to infinite life:

$$\gamma(\Delta f) \leq (\Delta F)_{TH} \quad (6.23)$$

where

$\gamma$  = load factor;

$\Delta f$  = force effect (live load stress range due to the passage of the fatigue load); and

$(\Delta F)_{TH}$  = constant amplitude fatigue threshold.

The general limit state function given by Equation 6.23 will be used for the calibration of the fatigue limit states for concrete members.

As discussed in Section 6.6.1.1, the Fatigue I limit state load factor is currently 1.5, and all resistance factors are inherently unity for the fatigue limit states.

### 6.6.2.2 Select Structural Types and Design Cases

Two fatigue limit states for concrete members can be rationally calibrated on the basis of current practice and the available data: steel reinforcement in tension (*AASHTO LRFD* Article 5.5.3.2) and concrete in compression (*AASHTO LRFD* Article 5.5.3.1).

### 6.6.2.3 Determine Load and Resistance Parameters for Selected Design Cases

#### STEEL REINFORCEMENT IN TENSION

Steel reinforcement as it is considered here includes straight reinforcing bars and welded-wire reinforcement. *AASHTO LRFD* Article 5.5.3.2 specifies the fatigue resistance of these types of reinforcement.

The fatigue resistance of straight reinforcing bars and welded-wire reinforcement without a cross weld in the high-stress region (defined as one-third of the span on each side of the section of maximum moment) is specified by Equation 6.24:

$$(\Delta F)_{TH} = 24 - 20f_{\min}/f_y \quad (6.24)$$

where  $f_{\min}$  is the minimum stress.

For welded-wire reinforcement with a cross weld in the high-stress region, the fatigue resistance is specified by Equation 6.25:

$$(\Delta F)_{TH} = 16 - 0.33f_{\min} \quad (6.25)$$

Equations 6.24 and 6.25 implicitly assume a ratio of radius to height (in other words,  $r/h$ ) of the rolled-in transverse bar deformations of 0.3.

These fatigue resistances are defined as constant amplitude fatigue thresholds in *AASHTO LRFD*. ACI Committee Report

ACI 215R-74 and the supporting literature indicate that steel reinforcement exhibits a constant amplitude fatigue threshold. ACI 215R-74 suggests that the resistances are “a conservative lower bound of all available test results.” In other words, a horizontal constant amplitude threshold has been drawn beneath all the curves.

The studies used to define the fatigue resistance of steel reinforcement (Fisher and Viest 1961; Pfister and Hognestad 1964; Burton and Hognestad 1967; Hanson et al. 1968; Helgason et al. 1976; Lash 1969; MacGregor et al. 1971; Amorn et al. 2007) were reanalyzed to estimate constant amplitude fatigue thresholds for every case that could be identified in the research to determine their uncertainty in terms of bias, mean, and CV. The various thresholds were grouped together to make design practical.

#### CONCRETE IN COMPRESSION

The compressive stress limit of  $0.40 f'_c$  for fully prestressed components in other than segmentally constructed bridges of *AASHTO LRFD* Article 5.5.3.1 applies to a combination of the live load specified in the Fatigue I limit state load combination plus one-half the sum of the effective prestress and permanent loads after losses (i.e., a load combination derived from a modified Goodman diagram). This suggests that the compressive stress limit represents an infinite life check, as the Fatigue I limit state load combination corresponds with infinite fatigue life.

For this study, the research used to define these  $S-N$  curves (Hilsdorf and Kesler 1966) was reevaluated to estimate the constant amplitude fatigue threshold, which is the infinite life fatigue resistance. The uncertainty of the fatigue resistance was quantified in terms of bias, mean, and CV.

### 6.6.2.4 Develop Statistical Models for Loads and Resistances

#### LOAD UNCERTAINTIES

The distribution of fatigue loads was determined on the basis of studies conducted on the WIM data, as described in Chapter 5. The fatigue load uncertainties in terms of the mean values and CVs are tabulated in Table 6.34.

#### RESISTANCE UNCERTAINTIES

As discussed in Section 6.6.1.4.2b, the lower tail of the fatigue resistance data plots was used to characterize the uncertainties, biases, and CVs. Figure 6.64 and Figure 6.65, respectively, show the normal probability plots of the full fatigue data set and the truncated data for fatigue resistance of steel reinforcement in tension. The resulting statistical parameters, along with the cutoff scores, are given in Table 6.41. The probability plots of the fatigue data and corresponding truncated data for both steel reinforcement in tension and concrete in compression can be seen in Appendix E.



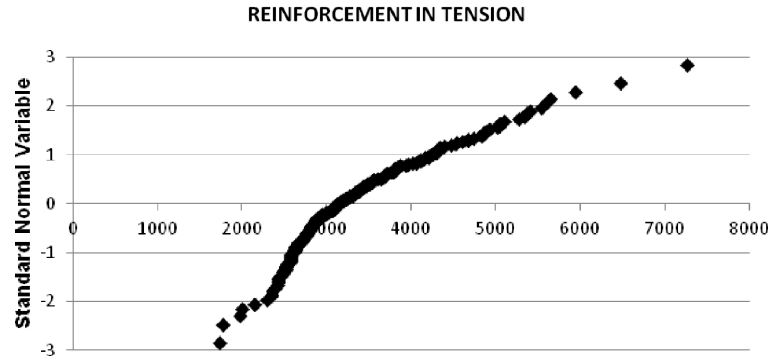


Figure 6.64. Normal probability plot of fatigue resistance data for steel reinforcement in tension.

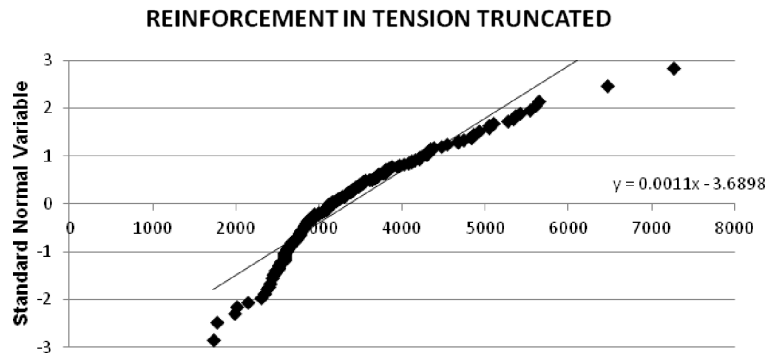


Figure 6.65. Normal probability plot of truncated fatigue resistance data with best-fit line for steel reinforcement in tension.

6.6.2.5 Develop Reliability Analysis Procedure

As discussed in Section 6.6.1.5, Monte Carlo simulation using Microsoft Excel formed the basis of the reliability analysis procedure for fatigue of concrete members.

6.6.2.6 Calculate Reliability Indices for Current Design Code or Current Practice

Monte Carlo simulation was used to estimate the current inherent reliability indices by comparing the distribution of fatigue load with the distribution of fatigue resistance on the basis of the uncertainties of load and resistance.

For steel reinforcement in reinforced concrete members, the current inherent  $\beta$  is approximately 2.0, and the current

inherent  $\beta$  for compression of concrete members is approximately 1.0. Both fatigue limit states are based on the Fatigue I limit state and design for infinite life. The calculated inherent values of  $\beta$  are given in Table 6.42.

6.6.2.7 Select Target Reliability Index

Theoretically, the target reliability index ( $\beta_T$ ) should be identical for all members and all fatigue limit states. Thus, the work on reinforcement and concrete fatigue was performed concurrently with, and was compared with, the work on structural steel fatigue.

It is proposed to use a constant  $\beta_T$  of 1.0 for steel reinforcement in tension, concrete in compression, and structural steel members. This proposed target reflects the inherent reliability

Table 6.41. Resistance Uncertainties

Resistance	Standard Deviation	CV	Bias	Mean	Nominal	Cutoff Standard Normal Variable
Steel reinforcement in tension	769.23	0.24	1.94	3,261.54	1,681.21	2
Concrete in compression	117.65	0.45	1.74	260.35	149.66	2

**Table 6.42. Current Reliability Indices for AASHTO LRFD Fatigue I Limit States**

Resistance	$\beta$
Steel reinforcement in tension	1.9
Concrete in compression	0.9

of the current Fatigue I limit state for concrete in compression and the Fatigue I and II limit states for structural steel members. This proposed target reduces the reliability of steel reinforcement in tension to levels consistent with the three other calibrated fatigue limit states.

#### 6.6.2.8 Select Potential Load and Resistance Factors

Proposed resistance factors for the Fatigue I limit state are given in Table 6.43. Resistance factors other than the current values of unity are shown in boldface.

#### 6.6.2.9 Calculate Reliability Indices

With the proposed resistance factors, the reliability indices were all within  $\pm 0.1$  of the target reliability index of 1.0.

The reliability indices shown in Table 6.43 can also be achieved by revising the *AASHTO LRFD* constant amplitude fatigue thresholds for steel reinforcement in tension. This may be a better solution than including a resistance factor other than unity for only one of the concrete member fatigue limit states. The required revisions to the *AASHTO LRFD* equations for the thresholds are given below.

The revised fatigue resistance of straight reinforcing bars and welded-wire reinforcement without a cross weld in the high-stress region would be specified by Equation 6.26:

$$(\Delta F)_{TH} = 30 - 25f_{min}/f_y \quad (6.26)$$

where  $f_{min}$  is the minimum stress.

For welded-wire reinforcement with a cross weld in the high-stress region, the fatigue resistance would be specified by Equation 6.27:

$$(\Delta F)_{TH} = 20 - 0.41f_{min} \quad (6.27)$$

#### 6.6.3 Proposed AASHTO LRFD Revisions

In *AASHTO LRFD* (2012), the fatigue limit state is addressed in Sections 3, 5, and 6. The articles that require modification to implement the revisions recommended here are indicated in Table 6.44.

**Table 6.43. Proposed Fatigue I Limit State Resistance Factors**

Resistance	Proposed Resistance Factor ( $\Phi$ )	Reliability Index ( $\beta$ )
Steel reinforcement in tension	<b>1.25</b>	1.1
Concrete in compression	1.0	0.9

**Table 6.44. Summary of Relevant Articles in AASHTO LRFD for Foundation Fatigue Deformations**

Article	Title	Relates to
3.4.1, Table 3.4.1-1	Load Factors and Load Combinations	Fatigue I and II
5.5.3.2	Reinforcing Bars	Fatigue threshold
5.5.3.3	Prestressing Tendons	Fatigue threshold
6.6.1.2.3	Detail Categories, Table 6.6.1.2.3-1	Constant A
6.6.1.2.5	Fatigue Resistance, Table 6.6.1.2.5-1	Constant A
6.6.1.2.5	Fatigue Resistance, Table 6.6.1.2.5-2	Cycle parameter ( $n$ )
6.6.1.2.5	Fatigue Resistance, Table 6.6.1.2.5-3	Constant amplitude fatigue threshold

Note: The proposed article revisions are detailed in Chapter 7.

## CHAPTER 7

# Proposed Changes to *AASHTO LRFD*

In Chapter 6, various articles of *AASHTO LRFD* were identified that would need to be modified to implement the calibrated SLS resulting from this research. This chapter contains the suggested modifications formatted in a form suitable for consideration by the affected technical committees that could be potential AASHTO Highway Subcommittee on Bridges and Structures agenda items. Excerpted material is used by

permission of the American Association of State Highway and Transportation Officials. Since the various SLS revisions are independent of each other and could be implemented individually, the suggested provisions are presented in separate subsections for each SLS. The article numbering system used in *AASHTO LRFD* has been preserved. The proposed revisions are underlined and deletions are shown as strikethrough.

## 7.1 Foundation Deformations – Service I

### 7.1.1 Proposed Revisions to Section 3

#### 3.4—LOAD FACTORS AND COMBINATIONS

##### 3.4.1—Load Factors and Load Combinations

- 
- 
- 
- 

- Service I—Load combination relating to the normal operational use of the bridge with a 55 mph wind and all loads taken at their nominal values. Also related to deflection control in buried metal structures, tunnel liner plate, and thermoplastic pipe, to control crack width in reinforced concrete structures, and for transverse analysis relating to tension in concrete segmental girders. This load combination should also be used for the investigation of slope stability, and settlement of foundations.
- Service II—Load combination intended to control yielding of steel structures and slip of slip-critical connections due to vehicular live load.
- Service III—Load combination for longitudinal analysis relating to tension in prestressed concrete superstructures with the objective of crack control and to principal tension in the webs of segmental concrete girders.
- Service IV—Load combination relating only to tension in prestressed concrete columns with the objective of crack control.

##### C3.4.1

Compression in prestressed concrete components and tension in prestressed bent caps are investigated using this load combination. Service III is used to investigate tensile stresses in prestressed concrete components.

This load combination corresponds to the overload provision for steel structures in past editions of the AASHTO Specifications, and it is applicable only to steel structures. From the point of view of load level, this combination is approximately halfway between that used for Service I and Strength I Limit States.

The live load specified in these specifications reflects, among other things, current exclusion weight limits mandated by various jurisdictions. Vehicles permitted under these limits have been in service for many years prior to 1993. For longitudinal loading, there is no nationwide physical evidence that these vehicles have caused cracking in existing prestressed concrete components. The statistical significance of the 0.80 factor on live load is that the event is expected to occur about once a year for bridges with two traffic lanes, less often for bridges with more than two traffic lanes, and about once a day for bridges with a single traffic lane. Service I should be used for checking tension related to transverse analysis of concrete segmental girders.

The principal tensile stress check is introduced in order to verify the adequacy of webs of segmental concrete girder bridges for longitudinal shear and torsion.

The 0.70 factor on wind represents an 84 mph wind. This should result in zero tension in prestressed concrete columns for ten-year mean reoccurrence winds. The prestressed concrete columns must still meet strength requirements as set forth in Load Combination Strength III in Article 3.4.1.

It is not recommended that thermal gradient be combined with high wind forces. Superstructure

- 
- 
- 
- 

The evaluation of overall stability of retained fills, as well as earth slopes with or without a shallow or deep foundation unit should be investigated at the service limit state based on the Service I Load Combination and an appropriate resistance factor as specified in Article 11.5.6 and Article 11.6.2.3.

The investigation of foundation settlement shall proceed using the provisions of Article 10.6.2.4 using the load factor,  $\gamma_{SE}$ , specified in Table 3.4.1-4.

For structural plate box structures complying with the provisions of Article 12.9, the live load factor for the vehicular live loads *LL* and *IM* shall be taken as 2.0.

The load factor for temperature gradient,  $\gamma_{TG}$ , should be considered on a project-specific basis. In lieu of project-specific information to the contrary,  $\gamma_{TG}$  may be taken as:

- 0.0 at the strength and extreme event limit states,
- 1.0 at the service limit state when live load is not considered, and
- 0.50 at the service limit state when live load is considered.

expansion forces are included.

Applying these criteria for the evaluation of the sliding resistance of walls:

- The vertical earth load on the rear of a cantilevered retaining wall would be multiplied by  $\gamma_{pmin}$  (1.00) and the weight of the structure would be multiplied by  $\gamma_{pmin}$  (0.90) because these forces result in an increase in the contact stress (and shear strength) at the base of the wall and foundation.
- The horizontal earth load on a cantilevered retaining wall would be multiplied by  $\gamma_{pmax}$  (1.50) for an active earth pressure distribution because the force results in a more critical sliding force at the base of the wall.

Similarly, the values of  $\gamma_{pmax}$  for structure weight (1.25), vertical earth load (1.35) and horizontal active earth pressure (1.50) would represent the critical load combination for an evaluation of foundation bearing resistance.

Water load and friction are included in all strength load combinations at their respective nominal values. For creep and shrinkage, the specified nominal values should be used. For friction, settlement, and water loads, both minimum and maximum values need to be investigated to produce extreme load combinations.

The load factor for temperature gradient should be determined on the basis of the:

- Type of structure, and
- Limit state being investigated.

Open girder construction and multiple steel box girders have traditionally, but perhaps not necessarily correctly, been designed without consideration of temperature gradient, i.e.,  $\gamma_{TG} = 0.0$ .

The effects of the foundation deformation on the bridge superstructure, retaining walls, or other load bearing structures shall be evaluated at applicable strength and service limit states using the provisions of Article 10.5.2.2 and the settlement load factor ( $\gamma_{SE}$ ) specified in Table 3.4.1-4.

~~The load factor for settlement,  $\gamma_{SE}$ , should be considered on a project specific basis. In lieu of project specific information to the contrary,  $\gamma_{SE}$  may be taken as 1.0. Load combinations which include settlement shall also be applied without settlement.~~

For segmentally constructed bridges, the following combination shall be investigated at the service limit state:

$$DC + DW + EH + EV + ES + WA + CR + SH + TG + EL + PS \quad (3.4.1-2)$$

Methods for estimation of settlement based on local geologic conditions and calibration may be used subject to approval from the Owner. Calibration of local methods should be based on processes as described in SHRP 2 R19B program report (Kulicki et al., 2013).

The value of  $\gamma_{SE}=1.25$  for soil-structure interaction methods in Table 3.4.1-4 for estimation of lateral deformations has been established based on judgment at this time.

Table 3.4.1-1—Load Combinations and Load Factors

Load Combination Limit State	DC DD DW EH EV ES EL PS CR SH	LL IM CE BR PL LS	WA	WS	WL	FR	TU	TG	SE	Use One of These at a Time				
										EQ	BL	IC	CT	CV
Strength I (unless noted)	$\gamma_p$	1.75	1.00	—	—	1.00	0.50/1.20	$\gamma_{TG}$	$\gamma_{SE}$	—	—	—	—	—
Strength II	$\gamma_p$	1.35	1.00	—	—	1.00	0.50/1.20	$\gamma_{TG}$	$\gamma_{SE}$	—	—	—	—	—
Strength III	$\gamma_p$	—	1.00	1.40	—	1.00	0.50/1.20	$\gamma_{TG}$	$\gamma_{SE}$	—	—	—	—	—
Strength IV	$\gamma_p$	—	1.00	—	—	1.00	0.50/1.20	—	—	—	—	—	—	—
Strength V	$\gamma_p$	1.35	1.00	0.40	1.0	1.00	0.50/1.20	$\gamma_{TG}$	$\gamma_{SE}$	—	—	—	—	—
Extreme Event I	$\gamma_p$	$\gamma_{EQ}$	1.00	—	—	1.00	—	—	—	1.00	—	—	—	—
Extreme Event II	$\gamma_p$	0.50	1.00	—	—	1.00	—	—	—	—	1.00	1.00	1.00	1.00
Service I	1.00	1.00	1.00	0.30	1.0	1.00	1.00/1.20	$\gamma_{TG}$	$\gamma_{SE}$	—	—	—	—	—
Service II	1.00	1.30	1.00	—	—	1.00	1.00/1.20	—	—	—	—	—	—	—
Service III	1.00	0.80	1.00	—	—	1.00	1.00/1.20	$\gamma_{TG}$	$\gamma_{SE}$	—	—	—	—	—
Service IV	1.00	—	1.00	0.70	—	1.00	1.00/1.20	—	1.0	—	—	—	—	—
Fatigue I— LL, IM & CE only	—	1.50	—	—	—	—	—	—	—	—	—	—	—	—
Fatigue II— LL, IM & CE only	—	0.75	—	—	—	—	—	—	—	—	—	—	—	—

- 
- 
- 
-



**Table 3.4.1-4—Load Factors for Permanent Loads Due to Foundation Deformations,  $\gamma_{SE}$**

<u>Foundation Deformation and Deformation Estimation Method</u>	<u>SE</u>
<u>Immediate Settlement</u>	
• <u>Hough method</u>	<u>1.00</u>
• <u>Schmertmann method</u>	<u>1.25</u>
• <u>Local method</u>	<u>*</u>
<u>Consolidation settlement</u>	<u>1.00</u>
<u>Lateral Deformation</u>	
• <u>Soil-structure interaction method (P-y or Strain Wedge)</u>	<u>1.25</u>
• <u>Local method</u>	<u>*</u>
<u>*To be determined by the owner based on local geologic conditions and calibration using a target reliability index of 0.50 for Service I limit state.</u>	

- 
- 
- 
- 

**3.4.2—Load Factors for Construction Loads**

**3.4.2.2—Evaluation of Deflection at the Service Limit State**

Refer to Article 3.4.1 for evaluation of foundation deformations due to construction loads.

In the absence of special provisions to the contrary, where evaluation of construction deflections are required by the contract documents, Load Combination Service I shall apply. Construction dead loads shall be considered as part of the permanent load and construction transient loads considered part of the live load. The associated permitted deflections shall be included in the contract documents.

## 7.1.2 Proposed Revisions to Section 10

### 10.3—NOTATION

$A_d$	=	angular distortion (10.5.2)
$A_{dm}$	=	modified angular distortion (10.5.2)
$C_1$	=	correction factor to incorporate the effect of strain relief due to embedment (10.6.2.4.2b)
$C_2$	=	correction factor to incorporate time-dependent (creep) increase in settlement for t (years) after construction (10.6.2.4.2b)
$E$	=	modulus of elasticity of pile material (ksi) (10.7.3.8.2); elastic modulus of layer i based on guidance provided in Table C10.4.6.3-1
$I_s$	=	strain influence factor from Figure 10.6.2.4.2c-1a
$L_s$	=	bridge span length over which $A_d$ and $A_{dm}$ are computed (10.5.2)
$S_d$	=	differential settlement between two bridge support elements spaced at a distance of $L_s$ (ft) (10.5.2.2)
$S_{ta}$	=	total foundation settlement using all applicable loads in the Service I load combination (ft) (10.5.2)
$S_{tp}$	=	total foundation settlement using all applicable loads prior to construction of bridge superstructure in the Service I load combination (ft) (10.5.2.2)
$S_{tr}$	=	relevant total settlement defined as $S_{ta} - S_{tp}$ (10.5.2.2)
$X$	=	width or smallest dimension of pile group (ft) (10.7.3.9); a factor used to determine the value of elastic modulus (10.6.2.4.2b)
	=	load factor for settlement (10.5.2.2)
$\Delta p$	=	net uniform applied stress (load intensity) at the foundation depth (Figure 10.6.2.4.2c-1b)

### 10.5—LIMIT STATES AND RESISTANCE FACTORS

#### 10.5.1—General

The limit states shall be as specified in Article 1.3.2; foundation-specific provisions are contained in this Section.

Foundations shall be proportioned so that the factored resistance is not less than the effects of the factored loads specified in Section 3.

#### 10.5.2—Service Limit States

##### 10.5.2.1—General

Foundation design at the service limit state shall include:

- Settlements,
- Horizontal movements,
- Overall stability, and
- Scour at the design flood.

Consideration of foundation movements shall be based upon structure tolerance to total and differential movements, rideability and economy. Foundation movements shall include all movement from settlement, horizontal movement, and rotation.

Bearing resistance estimated using the presumptive allowable bearing pressure for spread footings, if used, shall be applied only to address the service limit state.

##### C10.5.2.1

In bridges where the superstructure and substructure are not integrated, settlement corrections can be made by jacking and shimming bearings. Article 2.5.2.3 requires jacking provisions for these bridges.

The cost of limiting foundation movements should be compared with the cost of designing the superstructure so that it can tolerate larger movements or of correcting the consequences of movements through maintenance to determine minimum lifetime cost. The Owner may establish more stringent criteria.

The foundation movements should be translated to the deck elevation to evaluate the effect of such movements on the superstructure. In this process, deformations of the substructure, i.e., elements between foundation and superstructure, should be added to foundation deformations as appropriate.

The foundations for retaining walls and other load bearing structures such as tunnels may also be evaluated using the provisions of this Article.

The design flood for scour is defined in Article 2.6.4.4.2, and is specified in Article 3.7.5 as applicable at the service limit state.

Presumptive bearing pressures were developed for use with working stress design. These values may be used for preliminary sizing of foundations, but should generally not be used for final design. If used for final design, presumptive values are only applicable at service limit states.

## 10.5.2.2—Tolerable Movements and Movement Criteria

### 10.5.2.2.1—General

Foundation movement criteria shall be consistent with the function and type of structure, anticipated service life, and consequences of unacceptable movements on structure performance. Foundation movement shall include vertical, horizontal, and rotational movements. The tolerable movement criteria shall be established by either empirical procedures or structural analyses, or by consideration of both.

Foundation settlement shall be investigated using all applicable loads in the Service I Load Combination specified in Table 3.4.1-1. Transient loads may be omitted from settlement analyses for foundations bearing on or in cohesive soil deposits that are subject to time-dependent consolidation settlements.

All applicable service limit state load combinations in Table 3.4.1-1 shall be used for evaluating horizontal movement and rotation of foundations.

All foundation deformation evaluations shall be based on the geomaterial information obtained in accordance with Article 10.4.

The following steps shall be followed to estimate a practical value of angular distortion of the superstructure based on foundation settlement; a similar approach can be applied and is recommended for evaluation of horizontal movement and rotation of foundations:

1. Compute total foundation settlement at each support element using an Owner approved method for the assumed foundation type (e.g., spread footings, driven piles, drilled shafts, etc.) as follows:
  - a. Determine the total foundation settlement,  $S_{ta}$ , using all applicable loads in the Service I load combination.
  - b. Determine the total foundation settlement,  $S_{tp}$ , prior to construction of bridge superstructure. This settlement would generally be as a result of all applicable substructure loads computed in accordance with Service I load combination.
  - c. Determine relevant total settlement,  $S_{tr}$ , as  $S_{tr} = S_{ta} - S_{tp}$ .

### C10.5.2.2.1

Experience has shown that bridges can and often do accommodate more movement and/or rotation than traditionally allowed or anticipated in design. Creep, relaxation, and redistribution of force effects accommodate these movements. Some studies have been made to synthesize apparent response. These studies indicate that angular distortions between adjacent foundations greater than 0.008 radians in simple spans and 0.004 radians in continuous spans should not be permitted in settlement criteria (Moulton et al., 1985; DiMillio, 1982; Barker et al., 1991; Samtani et al. 2010). Other angular distortion limits may be appropriate after consideration of:

- cost of mitigation through larger foundations, realignment or surcharge,
- rideability,
- vertical clearance
- tolerable limits of deformation of other structures associated with a bridge, e.g., approach slabs, wingwalls, pavement structures, drainage grades, utilities on the bridge, etc.
- roadway drainage
- aesthetics, and
- safety.

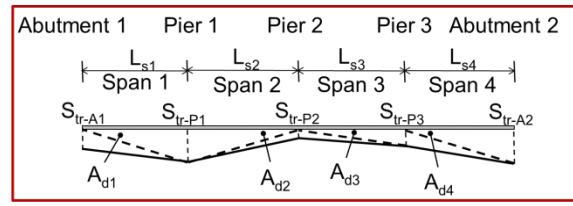
The bridge engineer shall add deformations from the substructure (elements between foundation and superstructure) as appropriate in evaluation of angular distortions at the deck elevation.

While the angular distortion is generally applied in the longitudinal direction of a bridge, similar analyses should be performed in transverse direction based on consideration of bridge width and stiffness. For all bridges, stiffness should be appropriate to the considered limit state. Similarly, the effects of continuity with the substructure should be considered. In assessing the structural implications of foundation deformations of concrete bridges, the determination of the stiffness of

the bridge components should consider the effects of cracking, creep, and other inelastic responses

Example: In Figure C10.5.2.2-1, a hypothetical 4-span bridge structure with span lengths,  $L_{s1}$ ,  $L_{s2}$ ,  $L_{s3}$  and  $L_{s4}$ . The relevant total settlement,  $S_{tr}$ , is computed at each support element and the profile of  $S_{tr}$  along the bridge is shown by the solid line. In this example,  $S_{tr-A1} < S_{tr-P1} > S_{tr-P2} < S_{tr-P3} < S_{tr-A2}$ . The  $S_{tr}$  profile assumed for computation of the angular distortion,  $A_d$ , for each span is represented by the dashed lines.

2. At a given support element assume that the actual relevant settlement could be as large as the value calculated by the chosen method. At the same time, assume that the settlement of an adjacent support element could be zero instead of the relevant settlement value calculated by the same chosen method. Thus, differential settlement,  $S_{ds}$ , within a given bridge span is equal to the larger of the relevant settlement at each of two supports of a bridge span. Compute angular distortion,  $A_d$ , as the ratio of the differential settlement,  $S_{ds}$ , to the span length,  $L_{s}$ . Express  $A_d$  value in radians.
3. Compute modified angular distortion,  $A_{dm}$ , by multiplying the angular distortion value from Step 2 with the  $\gamma_{SE}$  values for settlement in Table 3.4.1-4 based on the method used for computing the total settlement value.
4. Compare the  $A_{dm}$  value with owner specified angular distortion criteria. If owner specified criteria is not available then use 0.008 radians for the case of simple spans and 0.004 radians for the case of continuous spans as the limiting angular distortions.
5. Evaluate the structural ramifications of the computed angular distortions that are within acceptable limits as per Step 4. Modify foundation design as appropriate based on structural ramifications.



**Figure C10.5.2.2-1—Example for Computing Angular Distortion,  $A_d$ , Based on Relevant Total Settlement,  $S_{tr}$ , along a hypothetical 4-span Bridge (Modified after Samtani, et al., 2010)**

The angular distortion,  $A_d$ , within each span is as follows:  $A_{d1} = S_{tr-P1}/L_{s1}$ ;  $A_{d2} = S_{tr-P1}/L_{s2}$ ;  $A_{d3} = S_{tr-P3}/L_{s3}$ ; and  $A_{d4} = S_{tr-A2}/L_{s4}$ . Express  $A_d$  value in radians. Multiply the  $A_d$  values with appropriate  $\gamma_{SE}$  as per Step 3.

The above procedure shall also be used for the cases where foundations of various support elements are proportioned for equal total settlement because the prediction of settlements from any given method is uncertain by itself.

10.5.2.2.2—Lateral Deformations

Using a procedure similar to settlement evaluation specified in Article 10.5.2.2.1, lateral (horizontal) movement at foundation level shall also be evaluated. Horizontal movement criteria should be established at the top of the foundation based on the tolerance of the structure to lateral movement, with consideration of the column length and stiffness. Table 3.4.1-4 provides

C10.5.2.2.2

Rotation movements should be evaluated at the top of the substructure unit in plan location and at the deck elevation.

Tolerance of the superstructure to lateral movement will depend on bridge seat or joint widths, bearing type(s), structure type, and load distribution effects.

values of  $\gamma_{SE}$  for lateral deformations.

#### 10.5.2.2.3—Walls

The procedure for computing angular distortions shall also be applied for evaluating angular distortions along and transverse to retaining walls as well as the junction of the approach walls to abutment walls. The angular distortion values along a retaining wall can be used to select an appropriate wall type, e.g., MSE walls can tolerate larger angular distortions compared to cast-in-place walls

#### **10.5.2.3—Overall Stability**

The evaluation of overall stability of earth slopes with or without a foundation unit shall be investigated at the service limit state as specified in Article 11.6.2.3.

#### **10.5.2.4—Abutment Transitions**

Vertical and horizontal movements caused by embankment loads behind bridge abutments shall be investigated.

#### **C10.5.2.4**

Settlement of foundation soils induced by embankment loads can result in excessive movements of substructure elements. Both short and long term settlement potential should be considered.

Settlement of improperly placed or compacted backfill behind abutments can cause poor rideability and a possibly dangerous bump at the end of the bridge. Guidance for proper detailing and material requirements for abutment backfill is provided in Cheney and Chassie Samtani and Nowatzki (2006).

Lateral earth pressure behind and/or lateral squeeze below abutments can also contribute to lateral movement of abutments and should be investigated, if applicable.

### **10.6.2—Service Limit State Design**

#### **10.6.2.1—General**

- 
- 
- 
- 

#### **C10.6.2.1**

#### **10.6.2.4—Settlement Analyses**

##### *10.6.2.4.1—General*

Foundation settlements should be estimated using computational methods based on the results of laboratory or insitu testing, or both. The soil parameters used in the computations should be chosen to reflect the loading history of the ground, the construction sequence, and the effects of soil layering.

Both total and differential settlements, including time dependant effects, shall be considered.

Total settlement, including elastic, consolidation,

##### *C10.6.2.4.1*

Elastic, or immediate, settlement is the instantaneous deformation of the soil mass that occurs as the soil is loaded. The magnitude of elastic settlement is estimated as a function of the applied stress beneath a footing or embankment. Elastic settlement is usually small and neglected in design, but where settlement is critical, it is the most important deformation consideration in cohesionless soil deposits and for footings bearing on rock. For footings located on over-

and secondary components may be taken as:

$$S_t = S_e + S_c + S_s \quad (10.6.2.4.1-1)$$

where:

$S_e$  = elastic settlement (ft)

$S_c$  = primary consolidation settlement (ft)

$S_s$  = secondary settlement (ft)

The effects of the zone of stress influence, or vertical stress distribution, beneath a footing shall be considered in estimating the settlement of the footing.

Spread footings bearing on a layered profile consisting of a combination of cohesive soil, cohesionless soil and/or rock shall be evaluated using an appropriate settlement estimation procedure for each layer within the zone of influence of induced stress beneath the footing.

The distribution of vertical stress increase below circular or square and long rectangular footings, i.e., where  $L > 5B$ , may be estimated using Figure 10.6.2.4.1-1.

consolidated clays, the magnitude of elastic settlement is not necessarily small and should be checked.

In a nearly saturated or saturated cohesive soil, the pore water pressure initially carries the applied stress. As pore water is forced from the voids in the soil by the applied load, the load is transferred to the soil skeleton. Consolidation settlement is the gradual compression of the soil skeleton as the pore water is forced from the voids in the soil. Consolidation settlement is the most important deformation consideration in cohesive soil deposits that possess sufficient strength to safely support a spread footing. While consolidation settlement can occur in saturated cohesionless soils, the consolidation occurs quickly and is normally not distinguishable from the elastic settlement.

Secondary settlement, or creep, occurs as a result of the plastic deformation of the soil skeleton under a constant effective stress. Secondary settlement is of principal concern in highly plastic or organic soil deposits. Such deposits are normally so obviously weak and soft as to preclude consideration of bearing a spread footing on such materials.

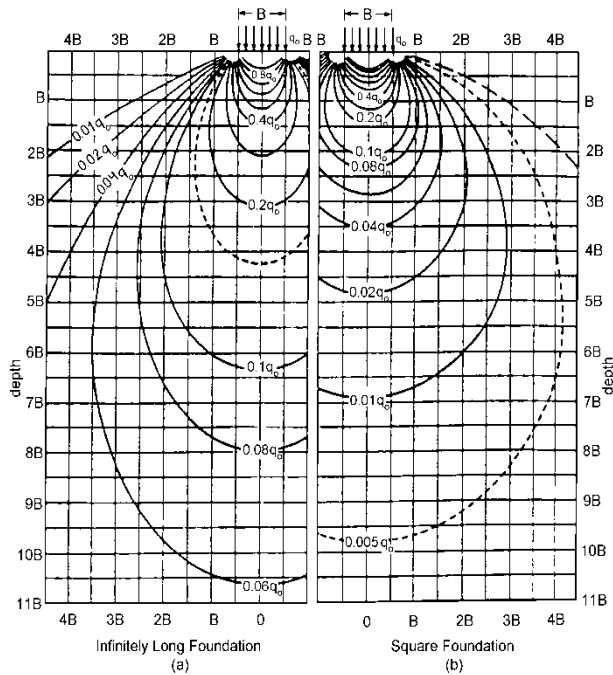
The principal deformation component for footings on rock is elastic settlement, unless the rock or included discontinuities exhibit noticeable time-dependent behavior.

To avoid overestimation, relevant settlements should be evaluated using the construction point concept noted in Samtani et al. (2010). The effect of settlement on superstructure shall be evaluated based on Article 10.5.2.2.

For guidance on vertical stress distribution for complex footing geometries, see Poulos and Davis (1974) or Lambe and Whitman (1969).

Some methods used for estimating settlement of footings on sand include an integral method to account for the effects of vertical stress increase variations. For guidance regarding application of these procedures, see Gifford et al. (1987).





**Figure 10.6.2.4.1-1—Boussinesq Vertical Stress Contours for Continuous and Square Footings Modified after Sowers (1979)**

#### 10.6.2.4.2—Settlement of Footings on Cohesionless Soils

##### 10.6.2.4.2a—General

The settlement of spread footings bearing on cohesionless soil deposits shall be estimated as a function of effective footing width and shall consider the effects of footing geometry and soil and rock layering with depth.

Settlements of footings on cohesionless soils shall be estimated using elastic theory or empirical procedures.

##### C10.6.2.4.2a

Although methods are recommended for the determination of settlement of cohesionless soils, experience has indicated that settlements can vary considerably in a construction site, and this variation may not be predicted by conventional calculations.

Settlements of cohesionless soils occur rapidly, essentially as soon as the foundation is loaded. Therefore, the total settlement under the service loads may not be as important as the incremental settlement between intermediate load stages. For example, the total and differential settlement due to loads applied by columns and cross beams is generally less important than the total and differential settlements due to girder placement and casting of continuous concrete decks.

Generally conservative settlement estimates may be obtained using the elastic half-space procedure or the empirical method by Hough. Additional information regarding the accuracy of the methods described herein is provided in Gifford et al. (1987), and Kimmerling (2002) and Samtani and Notwazki (2006). This information, in combination with local experience and engineering judgment, should be used when determining the estimated settlement for a structure foundation, as there may be cases, such as attempting to build a structure grade high to account for the estimated settlement, when overestimating the settlement magnitude could be problematic.

Details of other procedures can be found in

textbooks and engineering manuals, including:

- Terzaghi and Peck (1967)
- Sowers (1979)
- U.S. Department of the Navy (1982)
- D'Appolonia (Gifford et al., 1987)—This method includes consideration for over-consolidated sands.
- Tomlinson (1986)
- Gifford et al. (1987)

#### 10.6.2.4.2b—Elastic Half-space Method

The elastic half-space method assumes the footing is flexible and is supported on a homogeneous soil of infinite depth. The elastic settlement of spread footings, in feet, by the elastic half-space method shall be estimated as:

$$S_e = \frac{\left[ q_o (1 - \nu^2) \sqrt{A'} \right]}{144 E_s \beta_z} \quad (10.6.2.4.2b-1)$$

where:

$q_o$  = applied vertical stress (ksf)

$A'$  = effective area of footing (ft<sup>2</sup>)

$E_s$  = Young's modulus of soil taken as specified in Article 10.4.6.3 if direct measurements of  $E_s$  are not available from the results of in situ or laboratory tests (ksi)

$\beta_z$  = shape factor taken as specified in Table 10.6.2.4.2b-1 (dim)

$\nu$  = Poisson's Ratio, taken as specified in Article 10.4.6.3 if direct measurements of  $\nu$  are not available from the results of in situ or laboratory tests (dim)

Unless  $E_s$  varies significantly with depth,  $E_s$  should be determined at a depth of about 1/2 to 2/3 of  $B$  below the footing, where  $B$  is the footing width. If the soil modulus varies significantly with depth, a weighted average value of  $E_s$  should be used.

#### C10.6.2.4.2b

For general guidance regarding the estimation of elastic settlement of footings on sand, see Gifford et al. (1987), and Kimmerling (2002), and Samtani and Notwazki (2006).

The stress distributions used to calculate elastic settlement assume the footing is flexible and supported on a homogeneous soil of infinite depth. The settlement below a flexible footing varies from a maximum near the center to a minimum at the edge equal to about 50 percent and 64 percent of the maximum for rectangular and circular footings, respectively. The settlement profile for rigid footings is assumed to be uniform across the width of the footing.

Spread footings of the dimensions normally used for bridges are generally assumed to be rigid, although the actual performance will be somewhere between perfectly rigid and perfectly flexible, even for relatively thick concrete footings, due to stress redistribution and concrete creep.

The accuracy of settlement estimates using elastic theory are strongly affected by the selection of soil modulus and the inherent assumptions of infinite elastic half space. Accurate estimates of soil moduli are difficult to obtain because the analyses are based on only a single value of soil modulus, and Young's modulus varies with depth as a function of overburden stress. Therefore, in selecting an appropriate value for soil modulus, consideration should be given to the influence of soil layering, bedrock at a shallow depth, and adjacent footings.

For footings with eccentric loads, the area,  $A'$ , should be computed based on reduced footing dimensions as specified in Article 10.6.1.3.

**Table 10.6.2.4.2b-1—Elastic Shape and Rigidity Factors, EPRI (1983)**

$L/B$	Flexible, $\beta_z$ (average)	$\beta_z$ Rigid
Circular	1.04	1.13
1	1.06	1.08
2	1.09	1.10
3	1.13	1.15
5	1.22	1.24
10	1.41	1.41

10.6.2.4.2c—Hough Method

Estimation of spread footing settlement on cohesionless soils by the empirical Hough method shall be determined using Eqs. 10.6.2.4.2c-2 and 10.6.2.4.2c-3. *SPT* blow counts shall be corrected as specified in Article 10.4.6.2.4 for depth, i.e. overburden stress, before correlating the *SPT* blow counts to the bearing capacity index,  $C'$ .

$$S_e = \sum_{i=1}^n \Delta H_i \quad (10.6.2.4.2c-1)$$

in which:

$$\Delta H_i = H_c \frac{1}{C'} \log \left( \frac{\sigma'_o + \Delta \sigma_v}{\sigma'_o} \right) \quad (10.6.2.4.2c-2)$$

where:

$n$  = number of soil layers within zone of stress influence of the footing

$\Delta H_i$  = elastic settlement of layer  $i$  (ft)

$H_c$  = initial height of layer  $i$  (ft)

$C'$  = bearing capacity index from Figure 10.6.2.4.2c-1 (dim)

In Figure 10.6.2.4.2c-1,  $N1$  shall be taken as  $N1_{60}$ , Standard Penetration Resistance,  $N$  (blows/ft), corrected for overburden pressure as specified in Article 10.4.6.2.4.

$\sigma'_o$  = initial vertical effective stress at the midpoint of layer  $i$  (ksf)

$\Delta \sigma_v$  = increase in vertical stress at the midpoint of layer  $i$  (ksf)

10.6.2.4.2c

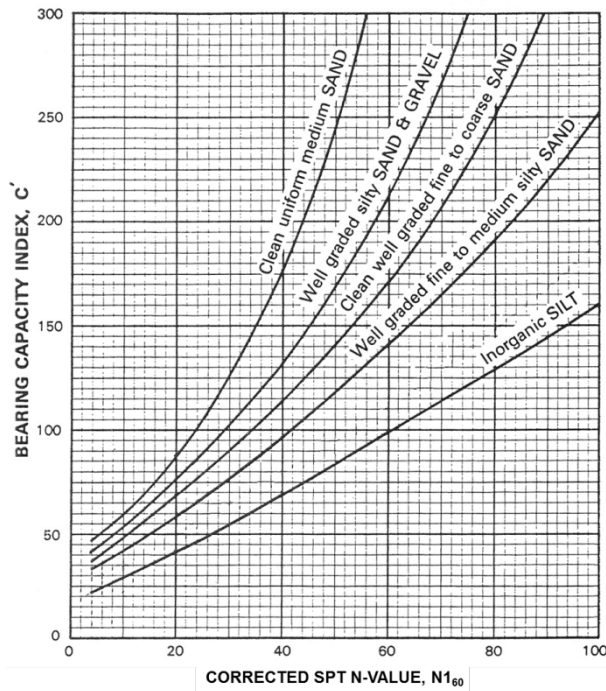
The Hough method was developed for normally consolidated cohesionless soils.

The Hough method has several advantages over other methods used to estimate settlement in cohesionless soil deposits, including express consideration of soil layering and the zone of stress influence beneath a footing of finite size.

The subsurface soil profile should be subdivided into layers based on stratigraphy to a depth of about three times the footing width. The maximum layer thickness should be about 10 ft.

While ~~Cheney and Chassie (2000)~~, and Hough (1959), did not specifically state that the *SPT*  $N$  values should be corrected for hammer energy in addition to overburden pressure, due to the vintage of the original work, hammers that typically have an efficiency of approximately 60 percent were in general used to develop the empirical correlations contained in the method. If using *SPT* hammers with efficiencies that differ significantly from this 60 percent value, the  $N$  values should also be corrected for hammer energy, in effect requiring that  $N1_{60}$  be used (Samtani and Nowatzki, 2006).

Studies conducted by Gifford et al. (1987) and Samtani and Nowatzki (2006) indicate that Hough's procedure is conservative and over-predicts settlement by a factor of 2 or more. Such conservatism may be acceptable for the evaluation of the settlement of embankments. However, in the case of shallow foundations such conservatism may lead to unnecessary use of costlier deep foundations in cases where shallow foundations may be viable.



**Figure 10.6.2.4.2c-1—Bearing Capacity Index versus Corrected SPT (Samtani and Nowatzki, 2006, after Hough, 1959)**

10.6.2.4.2d—Schmertmann Method

An estimate of the immediate settlement,  $S_i$ , of spread footings may be made by using Eq. 10.6.2.4.2d-1 as proposed by Schmertmann, et al. (1978).

$$S_i = C_1 C_2 D_p \sum_{i=1}^n \frac{\Delta H_i}{E} \quad (10.6.2.4.2d-1)$$

in which:

$$\Delta H_i = H_c \left( \frac{I_z}{XE} \right) \quad (10.6.2.4.2d-2)$$

$$C_1 = 1 - 0.5 \left( \frac{p_0}{\Delta p} \right) \geq 0.5 \quad (10.6.2.4.2d-3)$$

$$C_2 = 1 + 0.2 \log_{10} \left( \frac{t(\text{years})}{0.1} \right) \quad (10.6.2.4.2d-4)$$

where:

$I_z$  = strain influence factor from Figure 10.6.2.4.2d-1a. The dimension  $B_f$  represents the least lateral dimension of the footing after correction for eccentricities, i.e. use least lateral effective footing dimension. The strain influence factor is a function of depth and is obtained from the strain influence diagram. The strain influence diagram is easily constructed for the

The Hough method is applicable to cohesionless soil deposits. The “Inorganic Silt” curve should generally not be applied to soils that exhibit plasticity because N-values in such soils are unreliable. The settlement characteristics of cohesive soils that exhibit plasticity should be investigated using undisturbed samples and laboratory consolidation tests as prescribed in Article 10.6.2.4.3.

C10.6.2.4.2d

To overcome the conservatism of the Hough method, use of a more rigorous procedure such as Schmertmann’s method (1978) may be used for shallow foundations.

- **Effect of lateral strain:** Schmertmann method is based on the results of displacement measurements within sand masses loaded by model footings, as well as finite element analyses of deformations of materials with nonlinear stress-strain behavior that expressly incorporated Poisson’s ratio. Therefore, the effect of the lateral strain on the vertical strain is included in the strain influence factor diagrams.
- **Effect of preloading:** The equations used in Schmertmann’s method are applicable to normally loaded sands. If the sand was pre-strained by previous loading, then the actual settlements will be overpredicted. Schmertmann, et al. (1970) and Holtz (1991) recommend a reduction in settlement after preloading or other means of compaction of half the predicted settlement. Alternatively, in case of preloaded soil deposits, the settlement can be computed by using the method proposed by D’Appolonia (1968, 1970), which includes explicit consideration of preloading.
- **C<sub>2</sub> correction factor and applicability of the method:** The time duration, t, in Eq. 10.6.2.4.2d-4 is set to 0.1 years to evaluate the settlement immediately after construction, i.e., C<sub>2</sub> = 1. If long-

axisymmetric case ( $L_f/B_f = 1$ ) and the plane strain case ( $L_f/B_f \geq 10$ ) as shown in Figure 10.6.2.4.2d-1a. The strain influence diagram for intermediate conditions can be determined by simple linear interpolation.

$n$  = number of soil layers within the zone of strain influence (strain influence diagram).

$\Delta p$  = net uniform applied stress (load intensity) at the foundation depth (see Figure 10.6.2.4.2d-1b).

$E$  = elastic modulus of layer  $i$  based on guidance provided in Table C10.4.6.3-1.

$X$  = a factor used to determine the value of elastic modulus. If the value of elastic modulus is based on correlations with  $N_{160}$ -values or  $q_c$  from Table C10.4.6.3-1, then use  $X$  as follows.

$X = 1.25$  for axisymmetric case ( $L_f/B_f = 1$ )  
 $X = 1.75$  for plane strain case ( $L_f/B_f \geq 10$ )

Use interpolation for footings with  $1 < L_f/B_f < 10$

If the value of elastic modulus is estimated based on the range of elastic moduli in Table C10.4.6.3-1 or other sources use  $X = 1.0$ .

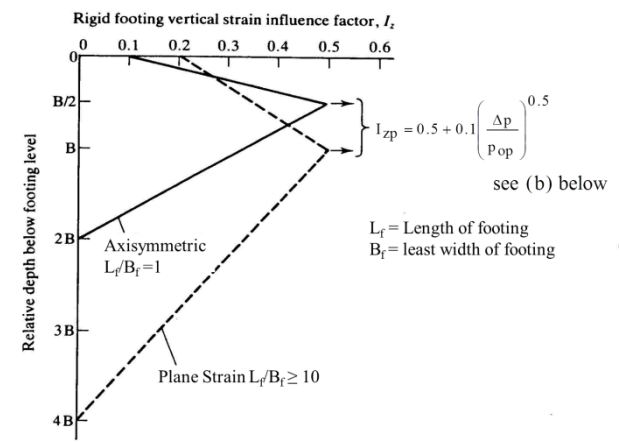
$C_1$  = correction factor to incorporate the effect of strain relief due to embedment

$p_o$  = effective in-situ overburden stress at the foundation depth and  $\Delta p$  is the net foundation pressure as shown in Figure 10.6.2.4.2d-1b

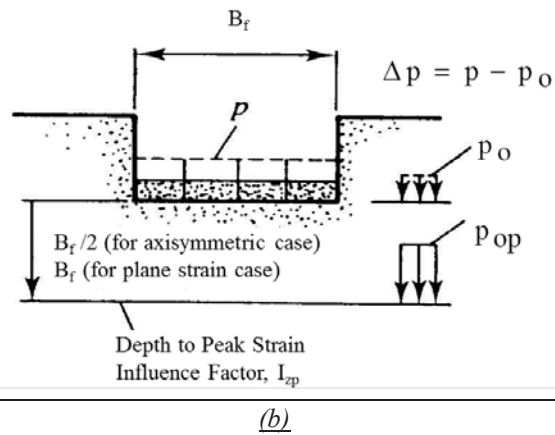
$C_2$  = correction factor to incorporate time-dependent (creep) increase in settlement for  $t$  (years) after construction where:

term creep deformation of the soil is suspected then an appropriate time duration,  $t$ , can be used in the computation of  $C_2$ . Creep deformation is not the same as consolidation settlement. This factor can have an important influence on the reported settlement since it is included in Eq. 10.6.2.4.2d-1 as a multiplier. For example, the  $C_2$  factor for time durations of 0.1 yrs, 1 yr, 10 yrs and 50 yrs are 1.0, 1.2, 1.4 and 1.54, respectively. In cohesionless soils and unsaturated fine-grained cohesive soils with low plasticity, time durations of 0.1 yr and 1 yr, respectively, are generally appropriate and sufficient for cases of static loads.

The  $C_2$  parameter shall not be used to estimate time-dependent consolidation settlements. Where consolidation settlement can occur within the depth of the strain distribution diagram, the magnitude of the consolidation settlement shall be estimated as per Article 10.6.2.4.3 and added to the immediate settlement of other layers within the strain distribution diagram where consolidation settlement may not occur.



(a)



**Figure 10.6.2.4.2d-1—(a) Simplified vertical strain influence factor distributions, (b) Explanation of pressure terms in equation for  $I_{zp}$  (after Schmertmann, et al., 1978, Samtani and Notatzki, 2006).**

#### 10.6.2.4.2e—Local Method

Methods based on local geologic conditions and calibration may be used subject to approval from the Owner.

#### C10.6.2.4.2e

Calibration of local methods should be based on processes as described in SHRP 2 R19B program report (Kulicki et al., 2013).

## **10.10—REFERENCES**

- D'Appolonia, D. J., D'Appolonia, E. E., and Brissette, R. F. (1968). "Settlement of Spread Footings on Sand." American Society of Civil Engineers, *Journal of the Soil Mechanics and Foundations Division*, 94 (SM3), 735-760.
- D'Appolonia, D. J., D'Appolonia, E. E., and Brissette, R. F. (1970). Closure to discussions on "Settlement of Spread Footings on Sand." American Society of Civil Engineers, *Journal of the Soil Mechanics and Foundations Division*, 96 (SM2), 754-761.
- Holtz, R. D. 1991. "Stress Distribution and Settlement of Shallow Foundations." In *Foundation Engineering Handbook*, 2<sup>nd</sup> Edition, H. Y. Fang, editor. Van Nostrand Reinhold Co., New York, NY, Chapter 5, pp. 166–185.
- Samtani, N. C., and Nowatzki, E. A. 2006. *Soils and Foundations*, FHWA NHI-06-088 and FHWA NHI 06-089, Federal Highway Administration, U.S. Department of Transportation, Washington, DC.
- Samtani, N. C., Nowatzki, E. A., and Mertz, D.R. 2010. *Selection of Spread Footings on Soils to Support Highway Bridge Structures*, FHWA-RC/TD-10-001, Federal Highway Administration, Resource Center, Matteson, IL.
- Schmertmann, J. H. 1970. "Static Cone to Compute Static Settlement Over Sand." American Society of Civil Engineers, *Journal of the Soil Mechanics and Foundations Division*, 96(SM3), 1011-1043.
- Schmertmann, J. H., Hartman, J. P., and Brown, P. R. 1978. "Improved Strain Influence Factor Diagrams." American Society of Civil Engineers, *Journal of the Geotechnical Engineering Division*, 104 (No. GT8), 1131-1135.



## 7.2 Live Load Response

### 7.2.1 Proposed Revisions to Section 2

#### 2.5.2.6—Deformations

##### 2.5.2.6.1—General

- 
- 
- 
- 

##### 2.5.2.6.2—Criteria for ~~Deflection~~ Live Load Response

The criteria in this Section shall be considered optional, except for the following:

- The provisions for orthotropic decks shall be considered mandatory.
- The provisions in Article 12.14.5.9 for precast reinforced concrete three-sided structures shall be considered mandatory.
- Metal grid decks and other lightweight metal and concrete bridge decks shall be subject to the serviceability provisions of Article 9.5.2.

In applying these criteria, the vehicular load shall include the dynamic load allowance.

If an Owner chooses to invoke deflection control, the following principles may be applied:

- When investigating the maximum absolute deflection for straight girder systems, all design lanes should be loaded, and all supporting components should be assumed to deflect equally;
- For curved steel box and I-girder systems, the deflection of each girder should be determined individually based on its response as part of a system;
- For composite design, the stiffness of the design cross-section used for the determination of deflection and frequency should include the entire width of the roadway and the structurally continuous portions of the railings, sidewalks, and median barriers;
- For straight girder systems, the composite bending stiffness of an individual girder may be taken as the

##### C2.5.2.6.1

- 
- 
- 
- 

##### C2.5.2.6.2

These provisions permit, but do not encourage, the use of past practice for deflection control. Designers were permitted to exceed these limits at their discretion in the past. Calculated deflections of structures have often been found to be difficult to verify in the field due to numerous sources of stiffness not accounted for in calculations. Despite this, many Owners and designers have found comfort in the past requirements to limit the overall stiffness of bridges. The desire for continued availability of some guidance in this area, often stated during the development of these Specifications, has resulted in the retention of optional criteria, except for orthotropic decks, for which the criteria are required. Deflection criteria are also mandatory for lightweight decks comprised of metal and concrete, such as filled and partially filled grid decks, and unfilled grid decks composite with reinforced concrete slabs, as provided in Article 9.5.2.

Additional guidance regarding deflection of steel bridges can be found in Wright and Walker (1971).

Additional considerations and recommendations for deflection in timber bridge components are discussed in more detail in Chapters 7, 8, and 9 in Ritter (1990).

For a straight multibeam bridge, this is equivalent to saying that the distribution factor for deflection is equal to the number of lanes divided by the number of beams.

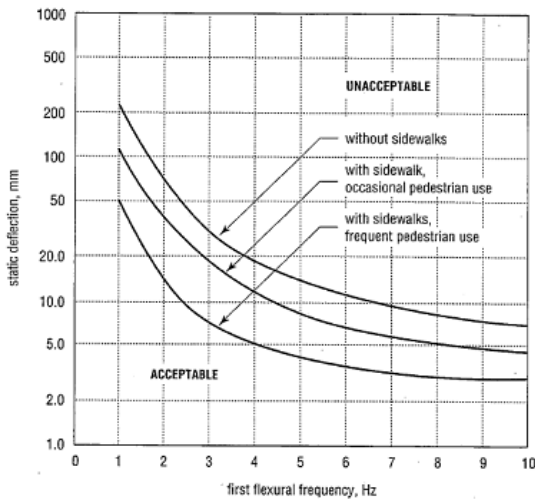
For curved steel girder systems, the deflection limit is applied to each individual girder because the curvature causes each girder to deflect differently than the adjacent girder so that an average deflection has little meaning. For curved steel girder systems, the span used to compute the deflection limit should be taken as the arc girder length between bearings.

stiffness determined as specified above, divided by the number of girders;

- When investigating maximum relative displacements, the number and position of loaded lanes should be selected to provide the worst differential effect;
- The live load portion of Load Combination Service I of Table 3.4.1-1 should be used, including the dynamic load allowance, IM;
- The live load shall be taken from Article 3.6.1.3.2;
- The provisions of Article 3.6.1.1.2 should apply; and
- For skewed bridges, a right cross-section may be used, and for curved and curved skewed bridges, a radial cross-section may be used.

In the absence of other criteria, ~~the following deflection limits may be considered for steel, aluminum, and/or concrete vehicular bridges: should meet the criteria shown in Figure 2.5.2.6.1-1 for the anticipated level of pedestrian usage. Unless otherwise specified herein, the deflection and frequency may be calculated on a system or component basis using any recognized method of analysis.~~

Frequency may be determined by refined analysis methods or by equations available in the literature if they apply to the girder or structure being analyzed.



**Figure 2.5.2.6.1-1—Criteria for Live Load Response (Used with permission of the Canadian Standards Association)**

- Vehicular load, general ..... Span/800;
- Vehicular and pedestrian loads ..... Span/1000;
- Vehicular load on cantilever arms .....  
Span/300, and
- Vehicular and pedestrian loads on cantilever arms...  
Span/375.

For steel I-shaped beams and girders, and for steel box

and tub girders, the provisions of Articles 6.10.4.2 and 6.11.4, respectively, regarding the control of permanent deflections through flange stress controls, shall apply. For pedestrian bridges, i.e., bridges whose primary function is to carry pedestrians, bicyclists, equestrians, and light maintenance vehicles, the provisions of Section 5 of AASHTO’s *LRFD Guide Specifications for the Design of Pedestrian Bridges* shall apply.

In the absence of other criteria, the following deflection limits may be considered for wood construction:

- Vehicular and pedestrian loads .....Span/425, and
- Vehicular load on wood planks and panels (extreme relative deflection between adjacent edges) ..... 0.10 in.

The following provisions shall apply to orthotropic plate decks:

- Vehicular load on deck plate ..... Span/300,
- Vehicular load on ribs of orthotropic metal decks Span/1000, and
- Vehicular load on ribs of orthotropic metal decks (extreme relative deflection between adjacent ribs) 0.10 in.

7.2.2 Proposed Revisions to Section 3

3.4—LOAD FACTORS AND COMBINATIONS

3.4.1—Load Factors and Load Combinations

- 
- 
- 
- 
- Service I—Load combination relating to the normal operational use of the bridge with a 55 mph wind and all loads taken at their nominal values. Also related to dynamic response of superstructures, deflection control in buried metal structures, tunnel liner plate, and thermoplastic pipe, to control crack width in reinforced concrete structures, and for transverse analysis relating to tension in concrete segmental girders. This load combination should also be used for the investigation of slope stability.
- Service II—Load combination intended to control yielding of steel structures and slip of slip-critical connections due to vehicular live load.
- Service III—Load combination for longitudinal

From a structural viewpoint, large deflections in wood components cause fasteners to loosen and brittle materials, such as asphalt pavement, to crack and break. In addition, members that sag below a level plane present a poor appearance and can give the public a perception of structural inadequacy. Deflections from moving vehicle loads also produce vertical movement and vibrations that annoy motorists and alarm pedestrians (Ritter, 1990).

Excessive deformation can cause premature deterioration of the wearing surface and affect the performance of fasteners, but limits on the latter have not yet been established.

The intent of the relative deflection criterion is to protect the wearing surface from debonding and fracturing due to excessive flexing of the deck.

The 0.10-in. relative deflection limitation is tentative.

C3.4.1

- 
- 
- 
- 
- Compression in prestressed concrete components and tension in prestressed bent caps are investigated using this load combination. Service III is used to investigate tensile stresses in prestressed concrete components.

This load combination corresponds to the overload provision for steel structures in past editions of the AASHTO Specifications, and it is applicable only to steel structures. From the point of view of load level, this combination is approximately halfway between that used for Service I and Strength I Limit States.

The live load specified in these specifications

analysis relating to tension in prestressed concrete superstructures with the objective of crack control and to principal tension in the webs of segmental concrete girders.

- Service IV—Load combination relating only to tension in prestressed concrete columns with the objective of crack control.
  
- Service V—Load combination to be used to investigate deflection and vibration response under traffic in accordance with Article 2.5.2.6.2.
  
- 
- 
- 
- 

reflects, among other things, current exclusion weight limits mandated by various jurisdictions. Vehicles permitted under these limits have been in service for many years prior to 1993. For longitudinal loading, there is no nationwide physical evidence that these vehicles have caused cracking in existing prestressed concrete components. The statistical significance of the 0.80 factor on live load is that the event is expected to occur about once a year for bridges with two traffic lanes, less often for bridges with more than two traffic lanes, and about once a day for bridges with a single traffic lane. Service I should be used for checking tension related to transverse analysis of concrete segmental girders.

The principal tensile stress check is introduced in order to verify the adequacy of webs of segmental concrete girder bridges for longitudinal shear and torsion.

The 0.70 factor on wind represents an 84 mph wind. This should result in zero tension in prestressed concrete columns for ten-year mean reoccurrence winds. The prestressed concrete columns must still meet strength requirements as set forth in Load Combination Strength III in Article 3.4.1.

It is not recommended that thermal gradient be combined with high wind forces. Superstructure expansion forces are included.

Dead load is included in this load combination because mass is part of the required calculation of frequency.



## 7.3 Premature Yielding and Slip of Bolts – Service II

### 7.3.1 Proposed Revisions to Section 3

#### 3.4—LOAD FACTORS AND COMBINATIONS

- 
- 
- 
- 

- Service I—Load combination relating to the normal operational use of the bridge with a 55 mph wind and all loads taken at their nominal values. Also related to deflection control in buried metal structures, tunnel liner plate, and thermoplastic pipe, to control crack width in reinforced concrete structures, and for transverse analysis relating to tension in concrete segmental girders. Relevant elements of this load combination should also be used for the investigation of slope stability.
- Service II—Load combination intended to control yielding of steel structures and slip of slip-critical connections due to vehicular live load.
- Service III—Load combination for longitudinal analysis relating to tension in prestressed concrete superstructures with the objective of crack control and to principal tension in the webs of segmental concrete girders.

Compression in prestressed concrete components and tension in prestressed bent caps are investigated using this load combination. Service III is used to investigate tensile stresses in prestressed concrete components.

This load combination corresponds to the overload provision for steel structures in past editions of the AASHTO Specifications, and it is applicable only to steel structures. From the point of view of load level, this combination is approximately halfway between that used for Service I and Strength I Limit States. A recent evaluation of WIM data from 31 sites around the country indicated that the load level specified in Table 3.4.1-1 for this limit state could reasonably be expected to be exceeded less than once every six months on average. For structures with unique truck loading conditions, such as access roads to ports or industrial sites which might lead to a disproportionate number of permit loads, a site-specific increase in the load factor or number of loaded lanes should be considered.

The live load specified in these specifications reflects, among other things, current exclusion weight limits mandated by various jurisdictions. Vehicles permitted under these limits have been in service for many years prior to 1993. For longitudinal loading, there is no nationwide physical evidence that these vehicles have caused cracking in existing prestressed concrete components. The statistical significance of the 0.80 factor on live load is that the event is expected to occur about once a year for bridges with two traffic lanes, less often for bridges with more than two traffic lanes, and about once a day for bridges with a single traffic lane. Service I should be used for checking tension related to transverse analysis of concrete segmental girders.

The principal tensile stress check is introduced in order to verify the adequacy of webs of segmental concrete girder bridges for longitudinal shear and torsion.



- Service IV—Load combination relating only to tension in prestressed concrete columns with the objective of crack control.

The 0.70 factor on wind represents an 84 mph wind. This should result in zero tension in prestressed concrete columns for ten-year mean reoccurrence winds. The prestressed concrete columns must still meet strength requirements as set forth in Load Combination Strength III in Article 3.4.1.

It is not recommended that thermal gradient be combined with high wind forces. Superstructure expansion forces are included.

- 
- 
- 
-

## 7.4 Cracking of Prestressed Concrete – Currently Service III

### 7.4.1 Proposed Revisions to Section 3

#### 3.4—LOAD FACTORS AND COMBINATIONS

##### 3.4.1—Load Factors and Load Combinations

The total factored force effect shall .....  
 .  
 ---.

Service I—Load combination relating to the normal operational use of the bridge with a 55 mph wind and all loads taken at their nominal values. Also related to deflection control in buried metal structures, tunnel liner plate, and thermoplastic pipe, to control crack width in reinforced concrete structures, and for transverse analysis relating to tension in concrete segmental girders. This load combination should also be used for the investigation of slope stability.

Service II—Load combination intended to control yielding of steel structures and slip of slip-critical connections due to vehicular live load.

Service III—Load combination for longitudinal analysis relating to tension in prestressed concrete superstructures with the objective of crack control and to principal tension in the webs of segmental concrete girders.

##### C3.4.1

The background for the load factors .....  
 .  
 .

Compression in prestressed concrete components and tension in prestressed bent caps are investigated using this load combination. Service III is used to investigate tensile stresses in prestressed concrete components.

This load combination corresponds to the overload provision for steel structures in past editions of the AASHTO Specifications, and it is applicable only to steel structures. From the point of view of load level, this combination is approximately halfway between that used for Service I and Strength I Limit States.

Prior to 2014, the longitudinal analysis relating to tension in prestressed concrete superstructures was investigated using a load factor for live load of 0.8. The live load specified in these specifications This load factor reflected, among other things, current exclusion weight limits mandated by various jurisdictions at the time of the development of the specifications in 1993. Vehicles permitted under these limits have been in service for many years prior to 1993. It was concluded at that time that, for longitudinal loading, there is no nationwide physical evidence that these vehicles have caused cracking in existing prestressed concrete components. The 0.8 load factor was applied regardless of the method used for determining the loss of prestressing. The statistical significance of the 0.80 factor on live load is that the event is expected to occur about once a year for bridges with two traffic lanes, less often for bridges with more than two traffic lanes, and about once a day for bridges with a single traffic lane.

The calibration of the service limit states for concrete components (Wassef et. al. 2014) concluded that typical components designed using the Refined Estimates of Time-Dependent Losses method incorporated in the specifications in 2005 have a lower reliability index against flexural cracking in prestressed components than components designed using the prestress loss calculation method specified prior to 2005. For components designed using the currently-specified methods for instantaneous prestressing losses and the



**Table 3.4.1-4—Load Factors for Live Load for Service III Load Combination,  $\gamma_{LL}$** 

<u>Component</u>	<u><math>\gamma_{LL}</math></u>
<u>Prestressed concrete components designed using a refined time step method to determine the time-dependant prestressing losses in conjunction with the gross section properties and without taking advantage of the elastic gain</u>	<u>0.8</u>
<u>All other prestressed concrete components</u>	<u>1.0</u>

## 7.5 Fatigue

### 7.5.1 Proposed Revisions to Section 3

#### 3.4—LOAD FACTORS AND COMBINATIONS

- 
- 
- 
- 

Table 3.4.1-1—Load Combinations and Load Factors

Load Combination Limit State	DC DD DW EH EV ES EL PS CR SH	LL IM CE BR PL LS	WA	WS	WL	FR	TU	TG	SE	Use One of These at a Time				
										EQ	BL	IC	CT	CV
Strength I (unless noted)	$\gamma_p$	1.75	1.00	—	—	1.00	0.50/1.20	$\gamma_{TG}$	$\gamma_{SE}$	—	—	—	—	—
Strength II	$\gamma_p$	1.35	1.00	—	—	1.00	0.50/1.20	$\gamma_{TG}$	$\gamma_{SE}$	—	—	—	—	—
Strength III	$\gamma_p$	—	1.00	1.40	—	1.00	0.50/1.20	$\gamma_{TG}$	$\gamma_{SE}$	—	—	—	—	—
Strength IV	$\gamma_p$	—	1.00	—	—	1.00	0.50/1.20	—	—	—	—	—	—	—
Strength V	$\gamma_p$	1.35	1.00	0.40	1.0	1.00	0.50/1.20	$\gamma_{TG}$	$\gamma_{SE}$	—	—	—	—	—
Extreme Event I	$\gamma_p$	$\gamma_{EQ}$	1.00	—	—	1.00	—	—	—	1.00	—	—	—	—
Extreme Event II	$\gamma_p$	0.50	1.00	—	—	1.00	—	—	—	—	1.00	1.00	1.00	1.00
Service I	1.00	1.00	1.00	0.30	1.0	1.00	1.00/1.20	$\gamma_{TG}$	$\gamma_{SE}$	—	—	—	—	—
Service II	1.00	1.30	1.00	—	—	1.00	1.00/1.20	—	—	—	—	—	—	—
Service III	1.00	0.80	1.00	—	—	1.00	1.00/1.20	$\gamma_{TG}$	$\gamma_{SE}$	—	—	—	—	—
Service IV	1.00	—	1.00	0.70	—	1.00	1.00/1.20	—	1.0	—	—	—	—	—
Fatigue I— LL, IM & CE only	—	<del>1.50</del> 2.0	—	—	—	—	—	—	—	—	—	—	—	—
Fatigue II— LL, IM & CE only	—	<del>0.75</del> 0.80	—	—	—	—	—	—	—	—	—	—	—	—

### 7.5.2 Proposed Revisions to Section 5

#### 5.5.3 Fatigue Limit State

- 
- 
- 
-

### 5.5.3.2—Reinforcing Bars

The constant-amplitude fatigue threshold,  $(\Delta F)_{TH}$ , for straight reinforcement and welded wire reinforcement without a cross weld in the high-stress region shall be taken as:

$$\frac{(\Delta F)_{TH}}{f_y} = 24 - 20 f_{min} / f_y \quad (5.5.3.2-1)$$

$$\frac{(\Delta F)_{TH}}{f_y} = 30 - 25 f_{min} / f_y \quad (5.5.3.2-1)$$

The constant-amplitude fatigue threshold,  $(\Delta F)_{TH}$ , for straight welded wire reinforcement with a cross weld in the high-stress region shall be taken as:

$$\frac{(\Delta F)_{TH}}{f_y} = 16 - 0.33 f_{min} \quad (5.5.3.2-2)$$

$$\frac{(\Delta F)_{TH}}{f_y} = 20 - 0.41 f_{min} \quad (5.5.3.2-2)$$

where:

$f_{min}$  = minimum live load stress resulting from the Fatigue I load combination, combined with the more severe stress from either the permanent loads or the permanent loads, shrinkage, and creep-induced external loads; positive if tension, negative if compression (ksi)

The definition of the high-stress region for application of Eqs. 5.5.3.2-1 and 5.5.3.2-2 for flexural reinforcement shall be taken as one-third of the span on each side of the section of maximum moment.

## 7.5.3 Proposed Revisions to Section 6

### 6.6.1—Fatigue

#### 6.6.1.1—General

- 
- 
- 
- 

### C5.5.3.2

Bends in primary reinforcement should be avoided in regions of high stress range.

Structural welded wire reinforcement has been increasingly used in bridge applications in recent years, especially as auxiliary reinforcement in bridge I- and box beams and as primary reinforcement in slabs. Design for shear has traditionally not included a fatigue check of the reinforcement as the member is expected to be uncracked under service conditions and the stress range in steel bars has existed in previous editions. It is based on Hansen et al. (1976). The simplified form in this edition replaces the  $(r/h)$  parameter with the default value 0.3 recommended by Hansen et al. Inclusion of limits for WWR is based on recent studies by Hawkins et al. (1971, 1987) and Tadros et al. (2004). Coefficients in Eqs. 5.5.3.2-1 and 5.5.3.2-2 have been updated based on calibration reported in Kulicki et al. (2013).

Since the fatigue provisions were developed based primarily on ASTM A615 steel reinforcement, their applicability to other types of reinforcement is largely unknown. Consequently, a cautionary note is added to the Commentary.

#### C6.6.1.1



### 6.6.1.2.3—Detail Categories

Components and details shall be designed to satisfy the requirements of their respective detail categories summarized in Table 6.6.1.2.3-1. Where bolt holes are depicted in Table 6.6.1.2.3-1, their fabrication shall conform to the provisions of Article 11.4.8.5 of the *AASHTO LRFD Bridge Construction Specifications*. Where permitted for use, unless specific information is available to the contrary, bolt holes in cross-frame, diaphragm, and lateral bracing members and their connection plates shall be assumed for design to be punched full size.

Except as specified herein for fracture critical members, where the projected 75-year single lane Average Daily Truck Traffic ( $ADTT$ )<sub>SL</sub> is less than or equal to that specified in Table 6.6.1.2.3-2 for the component or detail under consideration, that component or detail should be designed for finite life using the Fatigue II load combination specified in Table 3.4.1-1. Otherwise, the component or detail shall be designed for infinite life using the Fatigue I load combination. The single-lane Average Daily Truck Traffic ( $ADTT$ )<sub>SL</sub> shall be computed as specified in Article 3.6.1.4.2.

For components and details on fracture-critical members, the Fatigue I load combination specified in Table 3.4.1-1 should be used in combination with the nominal fatigue resistance for infinite life specified in Article 6.6.1.2.5.

Orthotropic deck components and details shall be designed to satisfy the requirements of their respective detail categories summarized in Table 6.6.1.2.3-1 for the chosen design level shown in the table and as specified in Article 9.8.3.4.

**The constant in the denominator of the equation to the right has been changed from 2 to 2.5.**

### C6.6.1.2.3

Components and details susceptible to load-induced fatigue cracking have been grouped into eight categories, called detail categories, by fatigue resistance.

Experience indicates that in the design process the fatigue considerations for Detail Categories A through B' rarely, if ever, govern. Nevertheless, Detail Categories A through B' have been included in Table 6.6.1.2.3-1 for completeness. Investigation of components and details with a fatigue resistance based on Detail Categories A through B' may be appropriate in unusual design cases.

Table 6.6.1.2.3-1 illustrates many common details found in bridge construction and identifies potential crack initiation points for each detail. In Table 6.6.1.2.3-1, "Longitudinal" signifies that the direction of applied stress is parallel to the longitudinal axis of the detail. "Transverse" signifies that the direction of applied stress is perpendicular to the longitudinal axis of the detail.

Category F for allowable shear stress range on the throat of a fillet weld has been eliminated from Table 6.6.1.2.3-1. When fillet welds are properly sized for strength considerations, Category F should not govern. Fatigue will be governed by cracking in the base metal at the weld toe and not by shear on the throat of the weld. Research on end-bolted cover plates is discussed in Wattar et al. (1985).

Where the design stress range calculated using the Fatigue I load combination is less than  $(\Delta F)_{TH}$ , the detail will theoretically provide infinite life. Except for Categories E and E', for higher traffic volumes, the design will most often be governed by the infinite life check. Table 6.6.1.2.3-2 shows for each detail category the values of ( $ADTT$ )<sub>SL</sub> above which the infinite life check governs, assuming a 75-yr design life and one stress range cycle per truck.

The values in the second column of Table 6.6.1.2.3-2 were computed as follows:

$$75\_Year(ADTT)_{SL} = \frac{A}{\left[\frac{(\Delta F)_{TH}}{2.5}\right]^3 (365)(75)(n)} \quad (C6.6.1.2.3-1)$$

using the values for  $A$  and  $(\Delta F)_{TH}$  specified in Tables 6.6.1.2.5-1 and 6.6.1.2.5-3, respectively, a fatigue design life of 75 yr and a number of stress range cycles per truck passage,  $n$ , equal to one. These values were rounded up to the nearest five trucks per day. That is, the indicated values were determined by equating infinite life and finite life resistances with due regard to the difference in load factors used with the Fatigue I and Fatigue II load combinations. For other values of  $n$ , the values in Table 6.6.1.2.3-2 should be modified by dividing by the appropriate value of  $n$  taken from Table 6.6.1.2.5-2. For other values of the fatigue design life, the values in Table 6.6.1.2.3-2 should be modified by multiplying the values by the ratio of 75 divided by the fatigue life sought in years. Some of the values of the parameter  $A$  and the threshold  $(\Delta F)_{TH}$  have been revised based on a calibration reported in Kulicki et al. (2013).

The procedures for load-induced fatigue are followed for orthotropic deck design. Although the local structural stress range for certain fatigue details can be caused by distortion of the deck plate, ribs, and floorbeams, research has demonstrated that load-induced fatigue analysis produces a reliable assessment of fatigue performance.

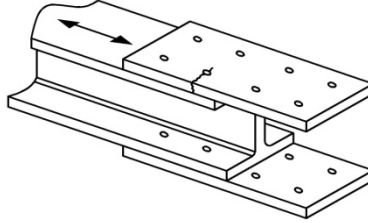
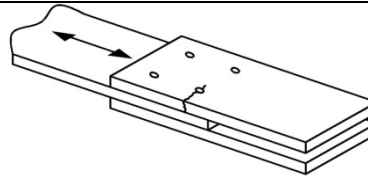
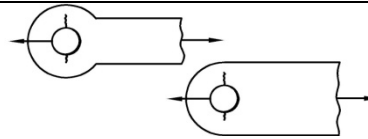
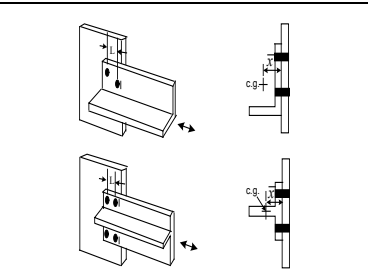
Considering the increased  $\gamma_{LL}$  and cycles per truck passage ( $n$ ) in orthotropic decks, the 75-yr  $ADTT_{SL}$  equivalent to infinite life (trucks per day) results in 870 for deck plate details and 4350 for all other details, based on Category C. Thus, finite life design may produce more economical designs on lower-volume roadways.

**Table 6.6.1.2.3-1—Detail Categories for Load-Induced Fatigue**

Description	Category	Constant $A$ (ksi <sup>3</sup> )	Threshold $(\Delta F)_{TH}$ ksi	Potential Crack Initiation Point	Illustrative Examples
<b>Section 1—Plain Material away from Any Welding</b>					
1.1 Base metal, except noncoated weathering steel, with rolled or cleaned surfaces. Flame-cut edges with surface roughness value of 1,000 μ-in. or less, but without re-entrant corners.	A	$250 \times 10^8$	24	Away from all welds or structural connections	
1.2 Noncoated weathering steel base metal with rolled or cleaned surfaces designed and detailed in accordance with FHWA (1989). Flame-cut edges with surface roughness value of 1,000 μ-in. or less, but without re-entrant corners.	B	$120 \times 10^8$	16	Away from all welds or structural connections	
1.3 Member with re-entrant corners at copes, cuts, block-outs or other geometrical discontinuities made to the requirements of AASHTO/AWS D1.5, except weld access holes.	C	$44 \times 10^8$	10	At any external edge	
1.4 Rolled cross sections with weld access holes made to the requirements of AASHTO/AWS D1.5, Article 3.2.4.	C	$44 \times 10^8$	10	In the base metal at the re-entrant corner of the weld access hole	
1.5 Open holes in members (Brown et al., 2007).	D	$22 \times 10^8$ $21 \times 10^8$	7 8	In the net section originating at the side of the hole	
<b>Section 2—Connected Material in Mechanically Fastened Joints</b>					
2.1 Base metal at the gross section of high-strength bolted joints designed as slip-critical connections with pretensioned high-strength bolts installed in holes drilled full size or subpunched and reamed to size—e.g., bolted flange and web splices and bolted stiffeners. (Note: see Condition 2.3 for bolt holes punched full size; see Condition 2.5 for bolted angle or tee section member connections to gusset or connection plates.)	B	$120 \times 10^8$	16	Through the gross section near the hole	

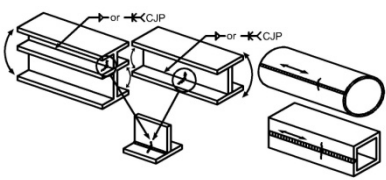
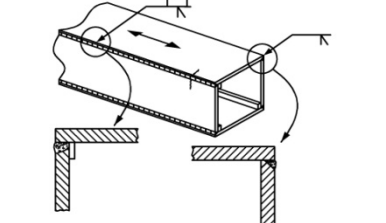
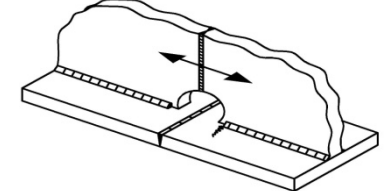
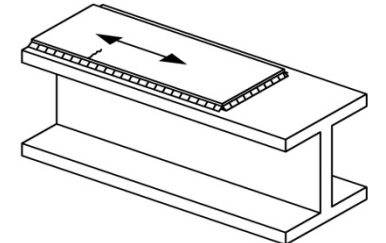
(continued on next page)

Table 6.6.1.2.3-1 (continued)—Detail Categories for Load-Induced Fatigue

Description	Category	Constant $A$ (ksi <sup>3</sup> )	Threshold $(\Delta F)_{TH}$ ksi	Potential Crack Initiation Point	Illustrative Examples
Section 2—Connected Material in Mechanically Fastened Joints (continued)					
<p>2.2 Base metal at the net section of high-strength bolted joints designed as bearing-type connections but fabricated and installed to all requirements for slip-critical connections with pretensioned high-strength bolts installed in holes drilled full size or subpunched and reamed to size. (Note: see Condition 2.3 for bolt holes punched full size; see Condition 2.5 for bolted angle or tee section member connections to gusset or connection plates.)</p>	B	$120 \times 10^8$	16	In the net section originating at the side of the hole	
<p>2.3 Base metal at the net section of all bolted connections in hot dipped galvanized members (Huhn and Valtinat, 2004); base metal at the appropriate section defined in Condition 2.1 or 2.2, as applicable, of high-strength bolted joints with pretensioned bolts installed in holes punched full size (Brown et al., 2007); and base metal at the net section of other mechanically fastened joints, except for eyebars and pin plates, e.g., joints using ASTM A307 bolts or non-pretensioned high-strength bolts. (Note: see Condition 2.5 for bolted angle or tee section member connections to gusset or connection plates).</p>	D	$\frac{22 \times 10^8}{21 \times 10^8}$	$\frac{7}{8}$	In the net section originating at the side of the hole or through the gross section near the hole, as applicable	
<p>2.4 Base metal at the net section of eyebar heads or pin plates (Note: for base metal in the shank of eyebars or through the gross section of pin plates, see Condition 1.1 or 1.2, as applicable.)</p>	E	$\frac{11 \times 10^8}{12 \times 10^8}$	4.5	In the net section originating at the side of the hole	
<p>2.5 Base metal in angle or tee section members connected to a gusset or connection plate with high-strength bolted slip-critical connections. The fatigue stress range shall be calculated on the effective net area of the member, <math>A_e = UA_g</math>, in which <math>U = (1 - \bar{x}/L)</math> and where <math>A_g</math> is the gross area of the member. <math>\bar{x}</math> is the distance from the centroid of the member to the surface of the gusset or connection plate and <math>L</math> is the out-to-out distance between the bolts in the connection parallel to the line of force. The effect of the moment due to the eccentricities in the connection shall be ignored in computing the stress range (McDonald and Frank, 2009).</p>	<i>See applicable Category above</i>	<i>See applicable Constant above</i>	<i>See applicable Threshold above</i>	Through the gross section near the hole, or in the net section originating at the side of the hole, as applicable	

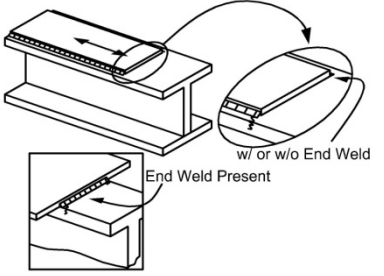
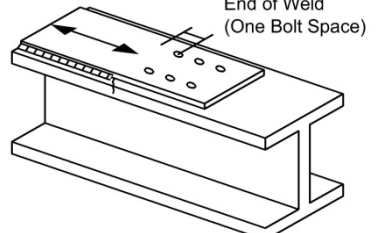
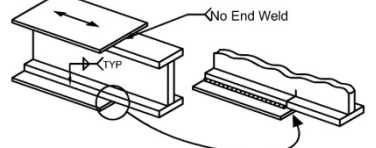
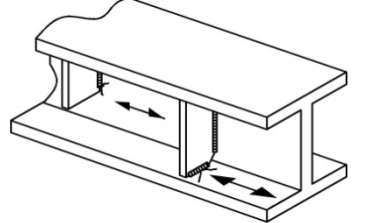
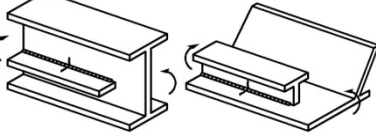
(continued on next page)

Table 6.6.1.2.3-1 (continued)—Detail Categories for Load-Induced Fatigue

Description	Category	Constant $A$ (ksi <sup>3</sup> )	Threshold $(\Delta F)_{TH}$ ksi	Potential Crack Initiation Point	Illustrative Examples
<p>2.5 (continued) The fatigue category shall be taken as that specified for Condition 2.1. For all other types of bolted connections, replace <math>A_g</math> with the net area of the member, <math>A_n</math>, in computing the effective net area according to the preceding equation and use the appropriate fatigue category for that connection type specified for Condition 2.2 or 2.3, as applicable.</p>					
Section 3—Welded Joints Joining Components of Built-Up Members					
<p>3.1 Base metal and weld metal in members without attachments built up of plates or shapes connected by continuous longitudinal complete joint penetration groove welds back-gouged and welded from the second side, or by continuous fillet welds parallel to the direction of applied stress.</p>	B	$120 \times 10^8$	16	From surface or internal discontinuities in the weld away from the end of the weld	
<p>3.2 Base metal and weld metal in members without attachments built up of plates or shapes connected by continuous longitudinal complete joint penetration groove welds with backing bars not removed, or by continuous partial joint penetration groove welds parallel to the direction of applied stress.</p>	B'	$61 \times 10^8$	<u>12</u> <u>13</u>	From surface or internal discontinuities in the weld, including weld attaching backing bars	
<p>3.3 Base metal and weld metal at the termination of longitudinal welds at weld access holes made to the requirements of AASHTO/AWS D1.5, Article 3.2.4 in built-up members. (Note: does not include the flange butt splice).</p>	D	<u><math>22 \times 10^8</math></u> <u><math>21 \times 10^8</math></u>	7 8	From the weld termination into the web or flange	
<p>3.4 Base metal and weld metal in partial length welded cover plates connected by continuous fillet welds parallel to the direction of applied stress.</p>	B	$120 \times 10^8$	16	From surface or internal discontinuities in the weld away from the end of the weld	

(continued on next page)

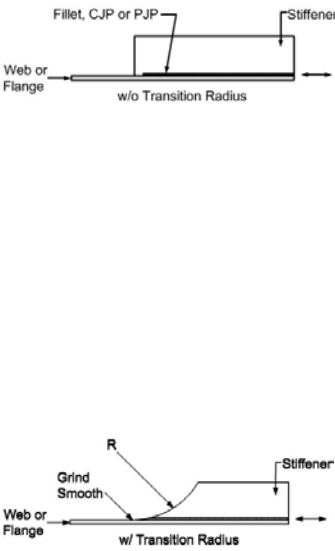
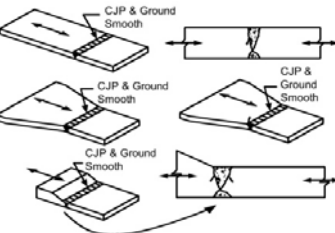
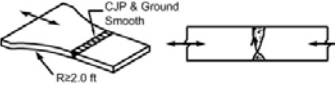
**Table 6.6.1.2.3-1 (continued)—Detail Categories for Load-Induced Fatigue**

Description	Category	Constant $A$ (ksi <sup>3</sup> )	Threshold $(\Delta f)_{TH}$ ksi	Potential Crack Initiation Point	Illustrative Examples
<b>Section 3—Welded Joints Joining Components of Built-Up Members (continued)</b>					
<p>3.5 Base metal at the termination of partial length welded cover plates having square or tapered ends that are narrower than the flange, with or without welds across the ends, or cover plates that are wider than the flange with welds across the ends:</p> <p style="text-align: center;">Flange thickness <math>\leq 0.8</math> in.</p> <p style="text-align: center;">Flange thickness <math>&gt; 0.8</math> in.</p>	<p style="text-align: center;">E</p> <p style="text-align: center;">E'</p>	<p style="text-align: center;"><math>41 \times 10^8</math></p> <p style="text-align: center;"><math>12 \times 10^8</math></p> <p style="text-align: center;"><math>3.9 \times 10^8</math></p> <p style="text-align: center;"><math>3.5 \times 10^8</math></p>	<p style="text-align: center;">4.5</p> <p style="text-align: center;">2.6</p> <p style="text-align: center;"><u>3.1</u></p>	<p>In the flange at the toe of the end weld or in the flange at the termination of the longitudinal weld or in the edge of the flange with wide cover plates</p>	
<p>3.6 Base metal at the termination of partial length welded cover plates with slip-critical bolted end connections satisfying the requirements of Article 6.10.12.2.3.</p>	<p style="text-align: center;">B</p>	<p style="text-align: center;"><math>120 \times 10^8</math></p>	<p style="text-align: center;">16</p>	<p>In the flange at the termination of the longitudinal weld</p>	
<p>3.7 Base metal at the termination of partial length welded cover plates that are wider than the flange and without welds across the ends.</p>	<p style="text-align: center;">E'</p>	<p style="text-align: center;"><math>3.9 \times 10^8</math></p> <p style="text-align: center;"><u><math>3.5 \times 10^8</math></u></p>	<p style="text-align: center;">2.6</p> <p style="text-align: center;"><u>3.1</u></p>	<p>In the edge of the flange at the end of the cover plate weld</p>	
<b>Section 4—Welded Stiffener Connections</b>					
<p>4.1 Base metal at the toe of transverse stiffener-to-flange fillet welds and transverse stiffener-to-web fillet welds. (Note: includes similar welds on bearing stiffeners and connection plates).</p>	<p style="text-align: center;">C'</p>	<p style="text-align: center;"><math>44 \times 10^8</math></p>	<p style="text-align: center;">12</p>	<p>Initiating from the geometrical discontinuity at the toe of the fillet weld extending into the base metal</p>	
<p>4.2 Base metal and weld metal in longitudinal web or longitudinal box-flange stiffeners connected by continuous fillet welds parallel to the direction of applied stress.</p>	<p style="text-align: center;">B</p>	<p style="text-align: center;"><math>120 \times 10^8</math></p>	<p style="text-align: center;">16</p>	<p>From the surface or internal discontinuities in the weld away from the end of the weld</p>	

(continued on next page)

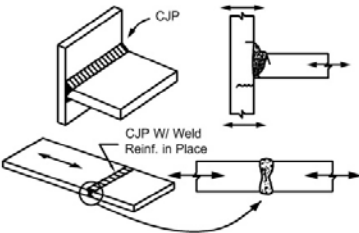
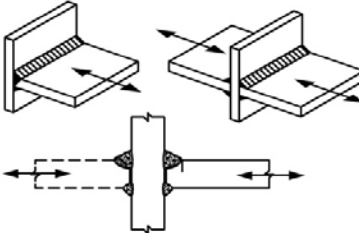
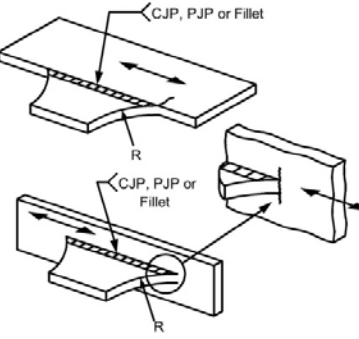


Table 6.6.1.2.3-1 (continued)—Detail Categories for Load-Induced Fatigue

Description	Category	Constant $A$ (ksi <sup>3</sup> )	Threshold $(\Delta f)_{TH}$ ksi	Potential Crack Initiation Point	Illustrative Examples
Section 4—Welded Stiffener Connections (continued)					
<p>4.3 Base metal at the termination of longitudinal stiffener-to-web or longitudinal stiffener-to-box flange welds:</p> <p>With the stiffener attached by fillet welds and with no transition radius provided at the termination:</p> <p>Stiffener thickness &lt; 1.0 in.</p> <p>Stiffener thickness ≥ 1.0 in.</p> <p>With the stiffener attached by welds and with a transition radius <math>R</math> provided at the termination with the weld termination ground smooth:</p> <p><math>R \geq 24</math> in.</p> <p>24 in. &gt; <math>R \geq 6</math> in.</p> <p>6 in. &gt; <math>R \geq 2</math> in.</p> <p>2 in. &gt; <math>R</math></p>	<p>E</p> <p>E'</p> <p>B</p> <p>C</p> <p>D</p> <p><u>E</u></p>	<p><math>11 \times 10^8</math></p> <p><math>12 \times 10^8</math></p> <p><math>3.9 \times 10^8</math></p> <p><math>3.5 \times 10^8</math></p> <p><math>120 \times 10^8</math></p> <p><math>44 \times 10^8</math></p> <p><math>22 \times 10^8</math></p> <p><math>21 \times 10^8</math></p> <p><math>11 \times 10^8</math></p> <p><math>12 \times 10^8</math></p>	<p>4.5</p> <p>2.6</p> <p><u>3.1</u></p> <p>16</p> <p>10</p> <p>7</p> <p><u>8</u></p> <p>4.5</p>	<p>In the primary member at the end of the weld at the weld toe</p> <p>In the primary member near the point of tangency of the radius</p>	
Section 5—Welded Joints Transverse to the Direction of Primary Stress					
<p>5.1 Base metal and weld metal in or adjacent to complete joint penetration groove welded butt splices, with weld soundness established by NDT and with welds ground smooth and flush parallel to the direction of stress. Transitions in thickness or width shall be made on a slope no greater than 1:2.5 (see also Figure 6.13.6.2-1).</p> <p><math>F_y &lt; 100</math> ksi</p> <p><math>F_y \geq 100</math> ksi</p>	<p>B</p> <p>B'</p>	<p><math>120 \times 10^8</math></p> <p><math>61 \times 10^8</math></p>	<p>16</p> <p><u>12</u></p> <p><u>13</u></p>	<p>From internal discontinuities in the filler metal or along the fusion boundary or at the start of the transition</p>	
<p>5.2 Base metal and weld metal in or adjacent to complete joint penetration groove welded butt splices, with weld soundness established by NDT and with welds ground parallel to the direction of stress at transitions in width made on a radius of not less than 2 ft with the point of tangency at the end of the groove weld (see also Figure 6.13.6.2-1).</p>	<p>B</p>	<p><math>120 \times 10^8</math></p>	<p>16</p>	<p>From internal discontinuities in the filler metal or discontinuities along the fusion boundary</p>	

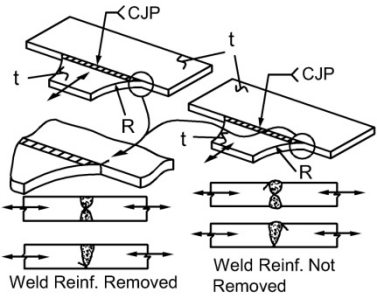
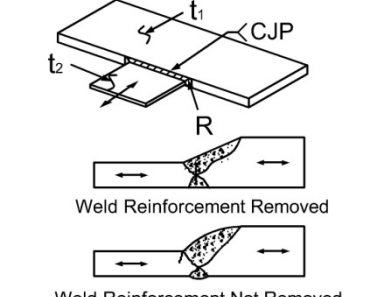
(continued on next page)

Table 6.6.1.2.3-1 (continued)—Detail Categories for Load-Induced Fatigue

Description	Category	Constant $A$ (ksi <sup>3</sup> )	Threshold $(\Delta f)_{TH}$ ksi	Potential Crack Initiation Point	Illustrative Examples
5.3 Base metal and weld metal in or adjacent to the toe of complete joint penetration groove welded T or corner joints, or in complete joint penetration groove welded butt splices, with or without transitions in thickness having slopes no greater than 1:2.5 when weld reinforcement is not removed. (Note: cracking in the flange of the "T" may occur due to out-of-plane bending stresses induced by the stem).	C	$44 \times 10^8$	10	From the surface discontinuity at the toe of the weld extending into the base metal or along the fusion boundary	
5.4 Base metal and weld metal at details where loaded discontinuous plate elements are connected with a pair of fillet welds or partial joint penetration groove welds on opposite sides of the plate normal to the direction of primary stress.	C as adjusted in Eq. 6.6.1.2.5-4	$44 \times 10^8$	10	Initiating from the geometrical discontinuity at the toe of the weld extending into the base metal or initiating at the weld root subject to tension extending up and then out through the weld	
<b>Section 6—Transversely Loaded Welded Attachments</b>					
6.1 Base metal in a longitudinally loaded component at a transversely loaded detail (e.g. a lateral connection plate) attached by a weld parallel to the direction of primary stress and incorporating a transition radius $R$ with the weld termination ground smooth.				Near point of tangency of the radius at the edge of the longitudinally loaded component or at the toe of the weld at the weld termination if not ground smooth	
$R \geq 24$ in.	B	$120 \times 10^8$	16		
$24$ in. $> R \geq 6$ in.	C	$44 \times 10^8$	10		
$6$ in. $> R \geq 2$ in.	D	$\frac{22 \times 10^8}{21 \times 10^8}$	7 8		
$2$ in. $> R$	E	$\frac{11 \times 10^8}{12 \times 10^8}$	4.5		
For any transition radius with the weld termination not ground smooth (Note: Condition 6.2, 6.3 or 6.4, as applicable, shall also be checked.)	E	$\frac{11 \times 10^8}{12 \times 10^8}$	4.5		

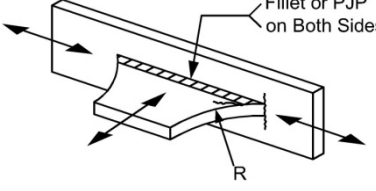
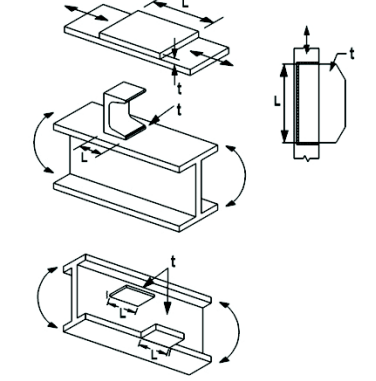
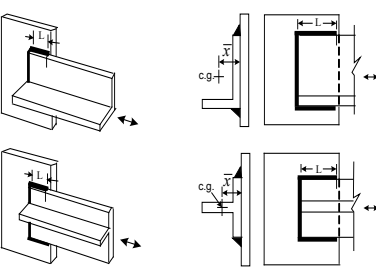
(continued on next page)

Table 6.6.1.2.3-1 (continued)—Detail Categories for Load-Induced Fatigue

Description	Category	Constant $A$ (ksi <sup>3</sup> )	Threshold $(\Delta f)_{TH}$ ksi	Potential Crack Initiation Point	Illustrative Examples
Section 6—Transversely Loaded Welded Attachments (continued)					
<p>6.2 Base metal in a transversely loaded detail (e.g. a lateral connection plate) attached to a longitudinally loaded component of equal thickness by a complete joint penetration groove weld parallel to the direction of primary stress and incorporating a transition radius <math>R</math>, with weld soundness established by NDT and with the weld termination ground smooth:</p> <p>With the weld reinforcement removed:</p> <p style="padding-left: 40px;"><math>R \geq 24</math> in.</p> <p style="padding-left: 40px;">24 in. <math>&gt; R \geq 6</math> in.</p> <p style="padding-left: 40px;">6 in. <math>&gt; R \geq 2</math> in.</p> <p style="padding-left: 40px;">2 in. <math>&gt; R</math></p> <p>With the weld reinforcement not removed:</p> <p style="padding-left: 40px;"><math>R \geq 24</math> in.</p> <p style="padding-left: 40px;">24 in. <math>&gt; R \geq 6</math> in.</p> <p style="padding-left: 40px;">6 in. <math>&gt; R \geq 2</math> in.</p> <p style="padding-left: 40px;">2 in. <math>&gt; R</math></p> <p>(Note: Condition 6.1 shall also be checked.)</p>		<p><math>120 \times 10^8</math></p> <p><math>44 \times 10^8</math></p> <p><math>22 \times 10^8</math> <u><math>21 \times 10^8</math></u></p> <p><math>11 \times 10^8</math> <math>12 \times 10^8</math></p>	<p>16</p> <p>10</p> <p>7 <u>8</u></p> <p>4.5</p> <p>10</p> <p>10</p> <p>7 <u>8</u></p> <p>4.5</p>	<p>Near points of tangency of the radius or in the weld or at the fusion boundary of the longitudinally loaded component or the transversely loaded attachment</p> <p>At the toe of the weld either along the edge of the longitudinally loaded component or the transversely loaded attachment</p>	
<p>6.3 Base metal in a transversely loaded detail (e.g. a lateral connection plate) attached to a longitudinally loaded component of unequal thickness by a complete joint penetration groove weld parallel to the direction of primary stress and incorporating a weld transition radius <math>R</math>, with weld soundness established by NDT and with the weld termination ground smooth:</p> <p>With the weld reinforcement removed:</p> <p style="padding-left: 40px;"><math>R \geq 2</math> in.</p> <p style="padding-left: 40px;"><math>R &lt; 2</math> in.</p> <p>For any weld transition radius with the weld reinforcement not removed (Note: Condition 6.1 shall also be checked.)</p>		<p><math>22 \times 10^8</math> <u><math>21 \times 10^8</math></u> <math>11 \times 10^8</math></p> <p><math>12 \times 10^8</math> <math>11 \times 10^8</math> <math>12 \times 10^8</math></p>	<p>7 <u>8</u></p> <p>4.5</p> <p>4.5</p>	<p>At the toe of the weld along the edge of the thinner plate</p> <p>In the weld termination of small radius weld transitions</p> <p>At the toe of the weld along the edge of the thinner plate</p>	

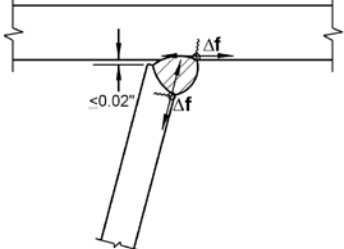
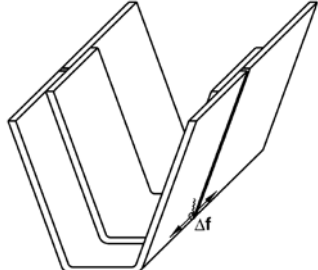
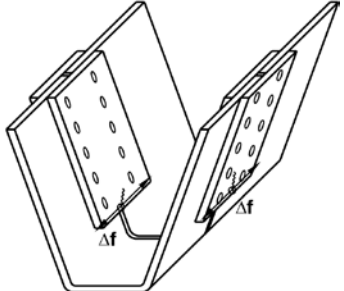
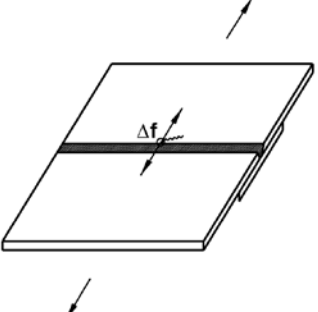
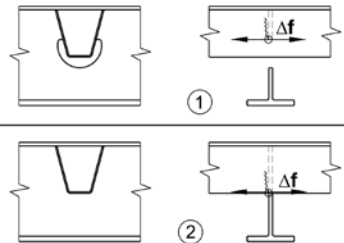
(continued on next page)

Table 6.6.1.2.3-1 (continued)—Detail Categories for Load-Induced Fatigue

Description	Category	Constant $A$ (ksi <sup>3</sup> )	Threshold $(\Delta f)_{TH}$ ksi	Potential Crack Initiation Point	Illustrative Examples
Section 6—Transversely Loaded Welded Attachments (continued)					
6.4 Base metal in a transversely loaded detail (e.g. a lateral connection plate) attached to a longitudinally loaded component by a fillet weld or a partial joint penetration groove weld, with the weld parallel to the direction of primary stress (Note: Condition 6.1 shall also be checked.)	See Condition 5.4				
Section 7—Longitudinally Loaded Welded Attachments					
7.1 Base metal in a longitudinally loaded component at a detail with a length $L$ in the direction of the primary stress and a thickness $t$ attached by groove or fillet welds parallel or transverse to the direction of primary stress where the detail incorporates no transition radius:  $L < 2$ in. $2$ in. $\leq L \leq 12t$ or 4 in.  $L > 12t$ or 4 in.  $t < 1.0$ in.  $t \geq 1.0$ in.  (Note: see Condition 7.2 for welded angle or tee section member connections to gusset or connection plates.)				In the primary member at the end of the weld at the weld toe	
7.2 Base metal in angle or tee section members connected to a gusset or connection plate by longitudinal fillet welds along both sides of the connected element of the member cross-section. The fatigue stress range shall be calculated on the effective net area of the member, $A_e = UA_g$ , in which $U = (1 - \bar{x}/L)$ and where $A_g$ is the gross area of the member. $\bar{x}$ is the distance from the centroid of the member to the surface of the gusset or connection plate and $L$ is the maximum length of the longitudinal welds. The effect of the moment due to the eccentricities in the connection shall be ignored in computing the stress range (McDonald and Frank, 2009).	E	$44 \times 10^8$ $12 \times 10^8$	4.5	Toe of fillet welds in connected element	

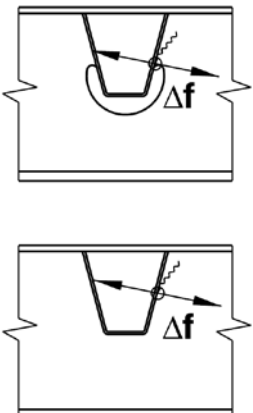
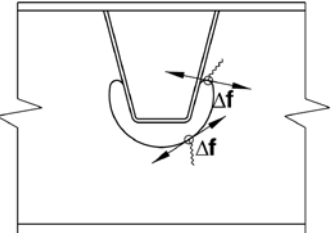
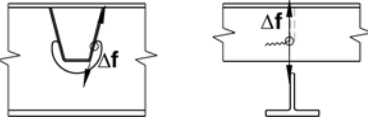
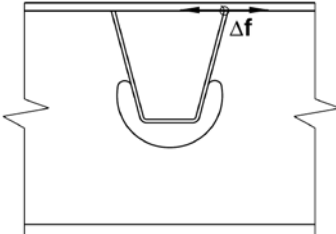
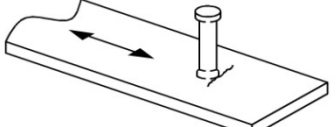
(continued on next page)

Table 6.6.1.2.3-1 (continued)—Detail Categories for Load-Induced Fatigue

Description	Category	Constant $A$ (ksi <sup>3</sup> )	Threshold $(\Delta f)_{TH}$ ksi	Potential Crack Initiation Point	Illustrative Examples
Section 8—Miscellaneous					
8.1 Rib to Deck Weld—One-sided 80% (70% min) penetration weld with root gap $\leq 0.02$ in. prior to welding  Allowable Design Level 1, 2, or 3	C	$44 \times 10^8$	10	See Figure	
8.2 Rib Splice (Welded)—Single groove butt weld with permanent backing bar left in place. Weld gap > rib wall thickness  Allowable Design Level 1, 2, or 3	D	$22 \times 10^8$ $21 \times 10^8$	7 8	See Figure	
8.3 Rib Splice (Bolted)—Base metal at gross section of high strength slip critical connection  Allowable Design Level 1, 2, or 3	B	$120 \times 10^8$	16	See Figure	
8.4 Deck Plate Splice (in Plane)—Transverse or Longitudinal single groove butt splice with permanent backing bar left in place  Allowable Design Level 1, 2, or 3	D	$22 \times 10^8$ $21 \times 10^8$	7 8	See Figure	
8.5 Rib to FB Weld (Rib)—Rib wall at rib to FB weld (fillet or CJP)  Allowable Design Level 1, 2, or 3	C	$44 \times 10^8$	10	See Figure	

(continued on next page)

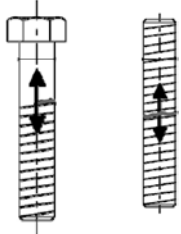
Table 6.6.1.2.3-1 (continued)—Detail Categories for Load-Induced Fatigue

Description	Category	Constant $A$ (ksi <sup>3</sup> )	Threshold $(\Delta f)_{TH}$ ksi	Potential Crack Initiation Point	Illustrative Examples
8.6 Rib to FB Weld (FB Web)—FB web at rib to FB weld (fillet, PJP, or CJP)  Allowable Design Level 1 or 3	C  (see Note 1)	$44 \times 10^8$	10	See Figure	
8.7 FB Cutout—Base metal at edge with “smooth” flame cut finish as per AWS D1.5  Allowable Design Level 1 or 3	A	$250 \times 10^8$	24	See Figure	
8.8 Rib Wall at Cutout—Rib wall at rib to FB weld (fillet, PJP, or CJP)  Allowable Design Level 1 or 3	C	$44 \times 10^8$	10	See Figure	
8.9 Rib to Deck Plate at FB  Allowable Design Level 1 or 3	C	$44 \times 10^8$	10	See Figure	
Note 1: Where stresses are dominated by in-plane component at fillet or PJP welds, Eq. 6.6.1.2.5-4 shall be considered. In this case, $\Delta f$ should be calculated at the mid-thickness and the extrapolation procedure as per Article 9.8.3.4.3 need not be applied.					
Section 9—Miscellaneous					
9.1 Base metal at stud-type shear connectors attached by fillet or automatic stud welding		$44 \times 10^8$	10	At the toe of the weld in the base metal	

(continued on next page)



**Table 6.6.1.2.3-1 (continued)—Detail Categories for Load-Induced Fatigue**

Description	Category	Constant $A$ (ksi <sup>3</sup> )	Threshold $(\Delta F)_{TH}$ ksi	Potential Crack Initiation Point	Illustrative Examples
Section 9—Miscellaneous (continued)					
9.2 Nonpretensioned high-strength bolts, common bolts, threaded anchor rods, and hanger rods with cut, ground, or rolled threads. Use the stress range acting on the tensile stress area due to live load plus prying action when applicable.				At the root of the threads extending into the tensile stress area	
(Fatigue II) Finite Life	E'	$3.9 \times 10^8$	N/A		
		$3.5 \times 10^8$			
(Fatigue I) Infinite Life	D	N/A	7 8		

**Table 6.6.1.2.3-2—75-yr  $(ADTT)_{SL}$  Equivalent to Infinite Life**

Detail Category	75-yrs $(ADTT)_{SL}$ Equivalent to Infinite Life (trucks per day)
A	1030
B	1670
B'	1585
C	2510
C'	1455
D	2340
E	7515
E'	6710

6.6.1.2.5—Fatigue Resistance

- 
- 
- 
- 

C6.6.1.2.5

Table 6.6.1.2.5-1—Detail Category Constant,  $A$ 

Detail Category	Constant, $A$ times $10^8$ (ksi <sup>3</sup> )
A	250.0
B	120.0
B'	61.0
C	44.0
C'	44.0
D	<del>22.0</del> 21.0
E	<del>12.0</del>
E'	<del>3.9</del> 3.5
M 164 (A325) Bolts in Axial Tension	17.1
M 253 (A490) Bolts in Axial Tension	31.5

Table 6.6.1.2.5-2—Cycles per Truck Passage,  $n$ 

Longitudinal Members	Span Length	
	>40.0 ft	≤40.0 ft
Simple Span Girders	1.0	<del>2.0</del>
Continuous Girders		
1) near interior support	1.5	<del>2.0</del>
2) elsewhere	1.0	<del>2.0</del>
Cantilever Girders	5.0	
Orthotropic Deck Plate Connections Subjected to Wheel Load Cycling	5.0	
Trusses	1.0	
Transverse Members	Spacing	
	> 20.0 ft	≤20.0 ft
	1.0	2.0

For the purpose of determining the stress range cycles per truck passage for continuous spans, a distance equal to one-tenth the span on each side of an interior support should be considered to be near the support. Values of  $n$  for longitudinal members have been revised based on the calibration reported in Kulicki et al., 2013.

The number of stress range cycles per passage is taken as 5.0 for cantilever girders because this type of bridge is susceptible to large vibrations, which cause additional cycles after the truck has left the bridge (*Moses et al., 1987; Schilling, 1990*).

Orthotropic deck details that are connected to the deck plate (e.g., the rib-to-deck weld) are subjected to cycling from direct individual wheel loads. Thus, the passage of one design truck results in five fatigue load cycles as each axle produces one load cycle. The force effect ( $\Delta f$ ) can be conservatively taken as the worst case from the five wheels or by application of Miner's Rule to determine the effective stress range from the group of wheels.

**Table 6.6.1.2.5-3—Constant-Amplitude Fatigue Thresholds**

Detail Category	Threshold (ksi)
A	24.0
B	16.0
B'	<del>12.0</del> 13.0
C	10.0
C'	12.0
D	<del>7.0</del> 8.0
E	4.5
E'	<del>2.6</del> 3.1
M 164 (A 325) Bolts in Axial Tension	31.0
M 253 (A 490) Bolts in Axial Tension	38.0

## CHAPTER 8

# Purpose and Contents of Appendix F

The purpose of Appendix F to the main report is to facilitate future enhancement of service limit state calibration, as well as to allow for customization by individual bridge owners. To accomplish this purpose, certain guidelines and databases have been included in Appendix F.

- *Section F.2*—A step-by-step description of the implementation of the Monte Carlo analysis introduced in Chapter 3.
- *Section F.3*—Excerpt from the database of WIM (weigh in motion) data used in the development of live load models presented in Chapter 5. These data are available at <http://www.trb.org/Main/Blurbs/170201.aspx>.
- *Section F.4*—A condensed version of the geotechnical calibration reported in Chapter 6. It is anticipated that the regional nature of geotechnical practice will result in

calibration of locally preferred methods of predicting settlement of shallow and deep foundations in lieu of the Hough (1959) and Schmertmann et al. (1978) methods used in this report.

- *Sections F.5 and F.6*—Descriptions of the concrete and steel bridges, respectively, selected from the NCHRP Project 12-78 database and used for various studies reported here (Mlynarski et al. 2011). Other bridges could be substituted.
- *Section F.7*—A database of fatigue tests on steel details (Keating and Fisher 1986; P.B. Keating, personal communication, 2012).
- *Section F.8*—A database of fatigue tests on plain concrete and reinforcement (Ople and Hulsbos 1966; Fisher and Viest 1961; Pfister and Hognestad 1964; Hanson et al. 1968; Lash 1969).

# Summary and Recommendations

## 9.1 Summary

From a survey of owners and a literature review that included other national and international bridge design specifications, a set of possible service limit states (SLSs) was developed. Those SLSs were reviewed to determine which could be calibrated using reliability theory. These are identified in Table 2.21 in Chapter 2. Calibrated, reliability-based load factors or resistance factors, or both, were developed for each of the following SLSs:

- Foundation deformations;
- Cracking of reinforced concrete components;
- Live load deflections;
- Permanent deformations;
- Tensile stresses in prestressed concrete components; and
- Fatigue of steel and reinforced concrete components.

Although the same general process was followed in calibrating each of the SLSs, customization was needed in most cases.

The calibration process produced target reliability levels that were much different from those used for the strength calibration. This was expected. Although the strength calibration, with some exceptions, was based on a target reliability index of about 3.5 for a 75-year life, most of the SLS calibration was done with a target reliability index of around 1.0 to 1.5 based on an annual probability. Once the target reliabilities were determined, changes to load factors, resistance factors, or other design parameters were developed. Proposed modifications to AASHTO LRFD design provisions were drafted for consideration by the appropriate AASHTO Highway Subcommittee on Bridges and Structures Technical Committees.

Several of the more important underlying changes needed to develop the proposed specification changes included the following:

- Use of WIM (weigh in motion) data to develop multipliers for the HL-93 live load model to be used in the calibration

processes for the various SLSs. These statistical parameters were tabulated for various average daily truck traffic values from 250 to 10,000, time periods ranging from 1 day to 100 years, and spans ranging from 30 to 200 ft.

- Analysis for fatigue that included treating the WIM data for each site as a continuous stream of traffic for rainflow counting and estimation of cumulative damage using the Palmgren–Miner model. This calibration also involved a reassessment of a comprehensive international database of fatigue tests.
- Verification of the Service II load factor for permanent deformations based on a WIM-based multiplier on HL-93 and a set of bridges from the NCHRP Project 12-78 database. This verification was further informed by considering the average number of times per year that bending moment for various spans exceeded various percentages of the HL-93 bending moment.
- A statistically calibrated load factor for live load for use in the Service III load combination for prestressed concrete in tension.
- A reliability-based comparison of pre- and post-2005 loss calculations for prestressed concrete components.
- A calibration process for foundation deformations, which was demonstrated by calibration of both the Schmertmann et al. (1978) and Hough (1959) methods of predicting settlement of footings on the basis of measured field data and the presentation of a methodology to allow for calibration of locally preferred settlement models. The same processes can be applied to horizontal movements, as well as other foundation types (e.g., deep foundations). The foundation deformation calibration processes are formulated to allow adaptation to different levels of reliability as expressed by different values of probability of exceedance (or reliability index).
- Use of frequency–deflection–perception–based criteria to calibrated bridge movement. These criteria have been used by Ontario and Canadian bridge codes for over two decades.

The objectives of this project were to provide calibrated SLSs to provide 100-year life and to develop a framework for further development of calibrated SLSs. Generally, it has been assumed that maintenance activities will be sufficient to prevent significant loss of the strength and stiffness that would result in unsatisfactory performance. No well-accepted direct link between the National Bridge Inventory (NBI) condition data and the types of unsatisfactory performance related to the SLSs calibrated in this study has been found. Several locally developed predictors of changes in the NBI condition number over time have been presented to provide guidance to owners on possible changes to the resistance side of the limit states used here within the context of the direct-link caveat above.

There are three sources of significant future improvements to the reported work:

- Improved limit state functions;
- Improved knowledge of structural behavior; and
- Improved knowledge of the change in strength and stiffness with time (i.e., response deterioration).

As discussed in Chapter 2, the limit state function related to permanent deformations is based on six data points from the *AASHTO Road Tests* (1962) and the anecdotal evidence that there appears to be virtually no record of permanent deformation in the superstructures of modern steel bridges that has been tied to premature yielding or bolt slip. It is reasonable to ask whether any systematic assessment of this type of response is being made.

The same question about systematic assessment applies to live load response, settlement, and cracking. Certainly very exceptional cases are probably noted by individual owners, but detailed investigations are few in number and not centrally archived. Fatigue cracking of steel components is probably the most identified and best recorded of the SLS responses, as well as being the most directly tied to truck traffic density and time in the design process.

The ongoing Long-Term Bridge Performance Program (LTBPP) is probably the best source of improved future data on loads, response, and deterioration (both response deterioration and routine maintenance needs as a function of time and environment). The initial focus, based on stake-holder input, is on bridge decks, but other aspects of bridge performance will also be considered. The project objective to capture research-quality performance data on a systematically selected national bridge set through visual inspection and nondestructive evaluation techniques should provide the information needed to advance calibrated SLSs further.

## 9.2 Recommendations

The following recommendations are made:

- Submit the specification proposals in Chapter 7 to the AASHTO Highway Subcommittee on Bridges and Structures for possible implementation.
- Evaluate the feasibility of establishing a clearinghouse for observed SLS issues, such as unsatisfactory user perception, permanent distortion, unanticipated cracking of concrete components, and settlement.
- Continue to interact with LTBPP to recommend SLS-oriented data collection, as well as to take advantage of evolving data and knowledge on behavior and deterioration to improve SLS calibration and design provisions.
- Assess the impact of any of the specification proposals that are adopted by working directly with the states involved or by engaging LTBPP to include data gathering in those projects. In either event, a set of expectations, associated metrics, and assessment protocols should be developed for consistent evaluation of impacts.
- Initiate a research project to identify possible ways to more directly link NBI data to changes in resistance, as they may affect both service and strength behavior.
- Initiate a research project to identify failure modes in decks, potentially differentiating among shear and bending failure modes, failure modes in composite and noncomposite systems, end diaphragm and flange width and fillet effects, and possible fatigue effects.

Finally, there is much interest nationally and internationally on the improved implementation of SLSs that should be considered in any continued development of *AASHTO LRFD*. Some late developments are described in Walraven and Bicaĵ (2011), Balázs et al. (2013), and Helland (2013), all of which address provisions in the 2010 *fib Model Code* (Fédération Internationale du Béton 2010).

## 9.3 Implementation

If the recommendations in Chapter 7 are accepted by the AASHTO Highway Subcommittee on Bridges and Structures, a webinar is probably the most effective way to explain changes in design to state engineers and consultants.

A separate webinar or short National Highway Institute course would be valuable to owners who want to modify the databases in Appendix F and rerun calibration calculations.



# References

- AASHTO Road Test: Report 4: Bridge Research. 1962. Special Report 61D. AASHTO, Highway Research Board, Washington, D.C.
- AASHTO. 2013. Bridges for Service Life Beyond 100 Years: Innovative Systems, Subsystems, and Components. SHRP 2 Project R19A. <http://onlinepubs.trb.org/onlinepubs/shrp2/SHRP2prepubR19Areport.pdf>. Accessed Nov. 25.
- AASHTO Guide Manual for Bridge Element Inspection. 2011. American Association of State Highway and Transportation Officials, Washington, D.C.
- AASHTO LRFD Bridge Design Specifications, 4th ed. 2008. Includes 2008 Interim. American Association of State Highway and Transportation Officials, Washington, D.C.
- AASHTO LRFD Bridge Design Specifications, 4th ed. 2009. Includes 2008 and 2009 Interims. American Association of State Highway and Transportation Officials, Washington, D.C.
- AASHTO LRFD Bridge Design Specifications, 5th ed. 2010. Includes 2010 Interim. American Association of State Highway and Transportation Officials, Washington, D.C.
- AASHTO LRFD Bridge Design Specifications, 6th ed. 2012. American Association of State Highway and Transportation Officials, Washington, D.C.
- Abeles, P., F. Barton, and E. Brown, II. 1969. Fatigue Behavior of Prestressed Concrete Bridge Beams. In *First International Symposium on Concrete Bridge Design*, SP-23, American Concrete Institute, Detroit, Mich., pp. 579–599.
- Abeles, P., and E. Brown, II. 1971. Expected Fatigue Life of Prestressed Concrete Highway Bridges As Related to the Expected Load Spectrum. In *Second International Symposium on Concrete Bridge Design*, SP-26, American Concrete Institute, Detroit, Mich., pp. 962–1010.
- Abeles, P., E. Brown, II, and C. Hu. 1974. Fatigue Resistance of Under-Reinforced Prestressed Beams Subjected to Different Stress Ranges; Miner's Hypothesis. In *Abeles Symposium: Fatigue of Concrete*, SP-41, American Concrete Institute, Detroit, Mich., pp. 279–300.
- ACI Committee 201. 2008. *Guide to Durable Concrete*. ACI 201.2R-08. American Concrete Institute, Farmington Hills, Mich.
- ACI Committee 215. 1974. *Considerations for Design of Concrete Structures Subjected to Fatigue Loading*. ACI 215R-74. American Concrete Institute, Detroit, Mich.
- ACI Committee 318. 1963. *Building Code Requirements for Reinforced Concrete*. ACI 318-63. American Concrete Institute, Detroit, Mich.
- ACI Committee 318. 1977. *Building Code Requirements for Reinforced Concrete*. ACI 318-77. American Concrete Institute, Detroit, Mich.
- ACI Committee 318. 1983. *Building Code Requirements for Reinforced Concrete*. ACI 318-83. American Concrete Institute, Detroit, Mich.
- ACI Committee 318. 1995. *Building Code Requirements for Structural Concrete and Commentary*. ACI 318-95/318R-95. American Concrete Institute, Farmington Hills, Mich.
- ACI Committee 318. 1999. *Building Code Requirements for Structural Concrete and Commentary*. ACI 318-99/318R-99. American Concrete Institute, Farmington Hills, Mich.
- ACI Committee 318. 2002. *Building Code Requirements for Structural Concrete and Commentary*. ACI 318-02/318R-02. American Concrete Institute, Farmington Hills, Mich.
- ACI Committee 318. 2005. *Building Code Requirements for Structural Concrete and Commentary*. ACI 318-05. American Concrete Institute, Farmington Hills, Mich.
- ACI Committee 318. 2008. *Building Code Requirements for Structural Concrete and Commentary*. ACI 318-08. American Concrete Institute, Farmington Hills, Mich.
- ACI Committee 318. 2011. *Building Code Requirements for Structural Concrete and Commentary*. ACI 318-11. American Concrete Institute, Farmington Hills, Mich.
- ACI-ASCE Joint Committee 323. 1958. Tentative Recommendations for Prestressed Concrete. *Journal, American Concrete Institute*, Vol. 54, No. 1, pp. 545–578.
- Agom International, srl. 2013. Catalog for V-MAX Pot Bearings. <http://www.agom.it/index.aspx?m=85&f=3&idf=212>. Accessed Nov. 25.
- Agrawal, A., and A. Kawaguchi. 2009. *Bridge Element Deterioration Rates*. Project Number C-01-51. City College of New York, Transportation Infrastructure Research Consortium, and New York State Department of Transportation, New York.
- Akbas, S., and F. Kulhawy. 2009. Axial Compression of Footings in Cohesionless Soils: I—Load-Settlement Behavior. *ASCE Journal of Geotechnical and Geoenvironmental Engineering*, Vol. 135, No. 11, pp. 1562–1574.
- Allen, T., A. Nowak, and R. Bathurst. 2005. *Transportation Research Circular E-C079: Calibration to Determine Load and Resistance Factors for Geotechnical and Structural Design*. Transportation Research Board of the National Academies, Washington, D.C. <http://onlinepubs.trb.org/onlinepubs/circulars/ec079.pdf>.
- Amorn, W., J. Bowers, A. Girgis, and M. Tadros. 2007. Fatigue of Deformed Welded-Wire Reinforcement. *Journal, Precast/Prestressed Concrete Institute*, Vol. 52, No. 1, pp. 106–120.
- Arizona Department of Transportation (ADOT) Bridge Design Guidelines. 2009. Arizona Department of Transportation, Phoenix.
- ASCE Committee on Deflections Limitations of Bridges of the Structural Division. 1958. Deflection limitations of bridges. *Journal of the Structural Division, Proc. ASCE*, 84(ST 3): 1633-1 to 1633-20.

- ASCE/SEI 7-10: *Minimum Design Loads for Buildings and Other Structures*. 2010. American Society of Civil Engineers, Reston, Va.
- Azzinamini, A., E. Power, G. Myers, and H. Ozyildirim. 2013. *Design Guide for Bridges for Service Life*. Prepublication draft. Transportation Research Board of the National Academies, Washington, D.C.
- Balázs, G., P. Bisch, A. Borosnyói, O. Burdet, C. Burns, F. Ceroni, V. Cervenka, M. Chiorino, P. Debernardi, L. Eckfeldt, M. El-Badry, E. Fehling, S. Foster, A. Ghali, V. Gribniak, M. Guiglia, G. Kaklauskas, R. Lark, P. Lenkei, M. Lorrain, A. Mari, J. Ozbolt, M. Pecce, A. Pérez Caldentey, M. Taliano, D. Tkalcic, J. Torrenti, L. Torres, F. Toutlemonde, T. Ueda, J. Vitek, and L. Vráblík. 2013. Design for SLS According to fib Model Code 2010. *Structural Concrete, Journal of the fib*, Vol. 14, No. 2, pp. 99–123.
- Barker, M., and K. Barth. 2007. Live Load Deflection Serviceability of HPS Composite Steel Girder Bridges. *2007 World Steel Bridge Symposium Papers*, New Orleans, La.
- Barker, M., L. Gandiaga, and J. Staebler. 2008. *Serviceability Limits and Economical Steel Bridge Design*. MPC-08-206. Mountain-Plains Consortium, Fargo, N.Dak.
- Barker, R., J. Duncan, K. Rojiani, P. Ooi, C. Tan, and S. Kim. 1991. *NCHRP Report 343: Manuals for the Design of Bridge Foundations: Shallow Foundations, Driven Piles, Retaining Walls and Abutments, Drilled Shafts, Estimating Tolerable Movements, Load Factor Design Specifications, and Commentary*. TRB, National Research Council, Washington, D.C.
- Barth, K., and H. Wu. 2007. Development of Improved Natural Frequency Equations for Continuous Span Steel I-Girder Bridges. *Engineering Structures*, Vol. 29, No. 12, pp. 3432–3442.
- Bartlett, F., R. Dexter, M. Graeser, J. Jelinek, B. Schmidt, and T. Galambos. 2003. Updating Standard Shape Material Properties Database for Design and Reliability. *Engineering Journal, American Institute of Steel Construction*, Vol. 40, No. 1, pp. 1–14.
- Beeby, A. 1979. The Prediction of Crack Widths in Hardened Concrete. *The Structural Engineer*, Vol. 57A, No. 1, p. 9.
- Biggs, J. 1964. *Introduction to Structural Dynamics*. McGraw-Hill, New York.
- Birrcer, D., R. Tuchscherer, M. Huizinga, O. Bayrak, S. Wood, and J. Jirsa. 2009. *Strength and Serviceability Design of Reinforced Concrete Deep Beams*. FHWA/TX-09/0-5253-1. Center for Transportation Research at the University of Texas at Austin and Texas Department of Transportation, Austin.
- Blackman, D., and R. Frosch. 2005. Epoxy-Coated Reinforcement and Crack Control. In *Serviceability of Concrete: A Symposium Honoring Dr. Edward G. Nawy*, SP-225, American Concrete Institute, Farmington Hills, Mich., pp. 163–178.
- Bolukbasi, M., J. Mohammadi, and D. Arditi. 2004. Estimating the Future Condition of Highway Bridge Components Using National Bridge Inventory Data. *ASCE Practice Periodical on Structural Design and Construction*, Vol. 9, No. 1, pp. 16–25.
- Bridge Bearings*. 2006. Indian Railways Institute of Civil Engineering, Pune, India.
- Bridge Design Manual*. 2006. Includes 2006 Interim and Errata. Engineering Division, Division of Highways, West Virginia Department of Transportation, Charleston.
- Bridge Design Manual*. 2007. Office of Structural Engineering, Ohio Department of Transportation, Columbus.
- Bridge Inspector's Reference Manual*. 2002. Federal Highway Administration, U.S. Department of Transportation.
- Bridge Joint Association. 2010. Current Practice Sheet. [www.bridgejoints.org.uk/Current%20Practice%20Sheet%20on%20Bridge%20Joints.pdf](http://www.bridgejoints.org.uk/Current%20Practice%20Sheet%20on%20Bridge%20Joints.pdf). Accessed April 13.
- Brockenbrough, R., and F. Merritt (eds.). 2011. *Structural Steel Designer's Handbook*, 5th ed. McGraw-Hill, New York.
- Broms, B. 1965. Crack Width and Crack Spacing in Reinforced Concrete Members. *Journal, American Concrete Institute*, Vol. 62, No. 10, p. 1237.
- Burland, J., and M. Burbridge. 1984. Settlement of Foundations on Sand and Gravel. *Proceedings, Part I, Institution of Civil Engineers*, Vol. 78, No. 6, pp. 1325–1381.
- Burton, K., and E. Hognestad. 1967. Fatigue Test of Reinforcing Bars-Tack Welding of Stirrups. *Journal, American Concrete Institute*, Vol. 64, No. 5, pp. 244–252.
- Canadian Highway Bridge Design Code*. 2006. Includes Supplement 1, Supplement 2, and Supplement 3. Canadian Standards Association International, Toronto, Ontario, Canada.
- Chang, L., and Y. Lee. 2001. *Evaluation and Policy for Bridge Deck Expansion Joints*. FHWA/IN/JTRP-2000/01. Joint Transportation Research Program, Indiana Department of Transportation, Indianapolis, and Purdue University, West Lafayette, Ind.
- Choi, Y., and B. Oh. 2009. Crack Width Formula for Transversely Post-Tensioned Concrete Deck Slabs on Box Girder Bridges. *Structural Journal, American Concrete Institute*, Vol. 106, No. 6, pp. 753–761.
- Clark, A. 1956. Cracking in Reinforced Concrete Flexural Members. *Journal Proceedings, American Concrete Institute*, Vol. 52, No. 4, p. 851.
- Coastal Engineering Manual*. 2002. Engineer Manual 1110-2-1100. U.S. Army Corps of Engineers, Washington, D.C.
- Committee on Deflection Limitations of Bridges of the Structural Division. 1958. Deflection Limitations. *ASCE Journal of the Structural Division*, Vol. 84, No. 3, pp. 1633.1–1633.20.
- Cooper, P., T. Galambos, and M. Ravindra. 1978. LRFD Criteria for Plate Girders. *ASCE Journal of the Structural Division*, Vol. 104, No. 9, pp. 1389–1407.
- D'Appolonia, D., E. D'Appolonia, and R. Brissette. 1968. Settlement of Spread Footings on Sand. *ASCE Journal of Soil Mechanics and Foundations Division*, Vol. 94, No. 3, pp. 735–762.
- Das, B., and B. Sivakugan. 2007. Settlements of Shallow Foundations on Granular Soil: An Overview. *International Journal of Geotechnical Engineering*, No. 1, pp. 19–29.
- Detwiler, R. 2008. Protecting concrete from sulfate attack. 2008. *Concrete News*, January. L&M Construction Chemicals, Inc. [http://www.lmcc.com/concrete\\_news/0801/protecting\\_concrete\\_from\\_sulfate\\_attack.asp](http://www.lmcc.com/concrete_news/0801/protecting_concrete_from_sulfate_attack.asp). Accessed Oct. 8, 2014.
- Dexter, R., and J. Fisher. 2000. Fatigue and Fracture. In *Bridge Engineering Handbook* (Chen and Duan, eds.), CRC Press, New York, pp. 53.1–53.23.
- Dexter, R., M. Graeser, W. Saari, C. Pascoe, C. Gardner, and T. Galambos. 2000. *Structural Shape Material Property Survey*. Final report. University of Minnesota, Minneapolis.
- Dexter, R., and M. Melendrez. 2000. Through-Thickness Properties of Column Flanges in Welded Moment Connections. *ASCE Journal of Structural Engineering*, Vol. 126, No. 1, pp. 24–31.
- Dowling, N. 1972. Fatigue Failure Predictions for Complicated Stress-Strain Histories. *Journal of Mechanics, JMLSA*, Vol. 7, No. 1, pp. 71–87.
- Downing, S., and D. Socie. 1982. Simple Rainflow Counting Algorithms. *International Journal of Fatigue*, Vol. 4, No. 1, pp. 31–40.
- Duncan, J. 2000. Factors of Safety and Reliability in Geotechnical Engineering. *ASCE Journal of Geotechnical and Geoenvironmental Engineering*, Vol. 126, No. 4, pp. 307–316.
- DuraCrete: Final Technical Report: General Guidelines for Durability Design and Redesign*. 2000. Project BE95-1347/R17. European Union, Brite EuRam III, CUR, Gouda, Netherlands.
- Elias, V., K. Fishman, B. Christopher, and R. Berg. 2009. *Corrosion/Degradation of Soil Reinforcements for Mechanically Stabilized Earth*

- Walls and Reinforced Soil Slopes*. FHWA-NHI-09-087. National Highway Institute, Federal Highway Administration, Washington, D.C.
- Ellingwood, B., J. Galambos, J. MacGregor, and C. Cornell. 1980. *Development of a Probability-Based Load Criterion for American National Standard A58*. NBS Special Publication 577. National Bureau of Standards, U.S. Department of Commerce.
- EN 1990 (*Eurocode 0*): *Basis of Structural Design*. 2002. European Committee for Standardization, Brussels, Belgium.
- EN 1991-1-6 (*Eurocode 1*): *Actions on Structures: Part 1-6: General Actions: Actions During Execution*. 2005. European Committee for Standardization, Brussels, Belgium.
- EN 1991-2 (*Eurocode 1*): *Actions on Structures: Part 2: Traffic Loads on Bridges*. 2003. European Committee for Standardization, Brussels, Belgium.
- EN 1992-2 (*Eurocode 2*): *Design of Concrete Structures: Part 2: Concrete Bridges: Design and Detailing Rules*. 2005. European Committee for Standardization, Brussels, Belgium.
- EN 1998-2 (*Eurocode 8*): *Design of Structures for Earthquake Resistance: Part 2: Bridges*. 2005. European Committee for Standardization, Brussels, Belgium.
- Evaluation of Various Types of Bridge Deck Joints*. 2006. FHWA-AZ-06-510. Baker Engineering and Energy; Arizona Department of Transportation, Phoenix; and Federal Highway Administration, U.S. Department of Transportation.
- Fédération Internationale du Béton. 2006. Model Code for Service Life Design. *fib Bulletin 34*, p. 47.
- Fédération Internationale du Béton. 2010. *fib Model Code for Concrete Structures*. Ernst and Sohn, Berlin.
- Fisher, J. 1977. *Bridge Fatigue Guide: Design and Details*. American Institute of Steel Construction, Chicago, Ill.
- Fisher, J., P. Albrecht, B. Yen, D. Klingerman, and B. McNamee. 1974. *NCHRP Report 147: Fatigue Strength of Steel Beams with Transverse Stiffeners and Attachments*. TRB, National Research Council, Washington, D.C.
- Fisher, J., K. Frank, M. Hirt, and B. McNamee. 1970. *NCHRP Report 102: Effect of Weldments on the Fatigue Strength of Steel Beams*. HRB, National Research Council, Washington, D.C.
- Fisher, J., D. Mertz, and A. Zhong. 1983. *NCHRP Report 267: Steel Bridge Members Under Variable-Amplitude Long-Life Fatigue Loading*. TRB, National Research Council, Washington, D.C.
- Fisher, J.W., and I.M. Viest. 1961. *Special Report 66: Fatigue Tests of Bridge Materials of the AASHO Road Test*. HRB, National Research Council, Washington, D.C.
- Fishman, K., and J. Withiam. 2011. *NCHRP Report 675: LRFD Metal Loss and Service-Life Strength Reduction Factors for Metal-Reinforced Systems*. TRB, National Research Council, Washington, D.C.
- Fountain, R., and C. Thunman. 1987. Deflection Criteria for Steel Highway Bridges. *Proc., AISC National Engineering Conference*, American Institute of Steel Construction, New Orleans, La., pp. 20-1–20-12.
- Freyermuth, C. 2009. Service Life and Sustainability of Concrete Bridges. *ASPIRE*, Fall 2009, pp. 12–15.
- Frosch, R. 1999. Another Look at Cracking and Crack Control in Reinforced Concrete. *Structural Journal, American Concrete Institute*, Vol. 96, No. 3, pp. 437–442.
- Frosch, R. 2001. Flexural Crack Control in Reinforced Concrete. In *Design and Construction Practices to Mitigate Cracking*, SP-204, American Concrete Institute, Farmington Hills, Mich., pp. 135–154.
- Frosch, R. 2002. Modeling and Control of Side Face Beam Cracking. *Structural Journal, American Concrete Institute*, Vol. 99, No. 3, pp. 376–385.
- Geotechnical Design Manual*. 2012. M 46-03.07. Washington State Department of Transportation, Olympia.
- Gergely, P., and L. Lutz. 1968. Maximum Crack Width in Reinforced Concrete Members. In *Causes, Mechanisms and Control of Cracking in Concrete*, SP-20, American Concrete Institute, Detroit, Mich., pp. 87–117.
- Gifford, D., S. Kraemer, J. Wheeler, and A. McKown. 1987. *Spread Footings for Highway Bridges*. FHWA/RD-86-185. Haley and Aldrich, Cambridge, Mass.
- Goodpasture, D., and W. Goodwin. 1971. *Final Report on the Evaluation of Bridge Vibration As Related to Bridge Deck Performance*. University of Tennessee, Knoxville; Tennessee Department of Transportation, Nashville; and Federal Highway Administration, Washington, D.C.
- Grant, R., J. Christian, and E. Vanmarcke. 1974. Differential Settlement of Buildings. *ASCE Journal of the Geotechnical Engineering Division*, Vol. 100, No. 9, pp. 973–991.
- Gross, S., and S. Burns. 2000. *Field Performance of Prestressed High Performance Concrete Bridges in Texas*. FHWA/TX-05/9-580/589-2. Center for Transportation Research at the University of Texas and Texas Department of Transportation, Austin.
- Hansell, W., T. Galambos, M. Ravindra, and I. Viest. 1978. Composite Beam Criteria in LRFD. *ASCE Journal of the Structural Division*, Vol. 104, No. 9, pp. 1409–1426.
- Hanson, J.M., K. T. Burton, and E. Hognestad. 1968. Fatigue Tests of Reinforcing Bars: Effect of Deformation Pattern. *Journal of the Portland Cement Association Research and Development Laboratories*, Vol. 10, No. 3, pp. 2–13.
- Hanson, J., C. Hulsbos, and D. VanHorn. 1970. Fatigue Tests of Prestressed Concrete I-Beams. *ASCE Journal of the Structural Division*, Vol. 96, No. 11, pp. 2443–2464.
- Hatami, A., and A. Morcous. 2011. *Developing Deterioration Models for Nebraska Bridges*. Project No. SPR-P1(11) M302. University of Nebraska, Lincoln, and Nebraska Department of Roads, Omaha.
- Helgason, T., J. Hanson, N. Somes, W. Corley, and E. Hognestad. 1976. *NCHRP Report 164: Fatigue Strength of High-Yield Reinforcing Bars*. TRB, National Research Council, Washington, D.C.
- Helland, S. 2013. Design for Service Life: Implementation of fib Model Code 2010, Rules in the Operational Code ISO 16204. *Structural Concrete, Journal of the fib*, Vol. 14, No. 1, pp. 10–18.
- Hilsdorf, H., and C. Kesler. 1966. Fatigue Strength of Concrete Under Varying Flexural Stresses. *Journal Proceedings, American Concrete Institute*, Vol. 63, No. 10, pp. 1059–1076.
- Hough, B. 1959. Compressibility as the Basis for Soil Bearing Value. *ASCE Journal of the Soil Mechanics and Foundations Division*, Vol. 85, No. 4, pp. 11–40.
- Imbsen, R.A., D.E. Vandershaf, R.A. Schamber, and R.V. Nutt. 1985. *NCHRP Report 276: Thermal Effects in Concrete Bridge Superstructures*. TRB, National Research Council, Washington, D.C.
- International Code Council. 2007. *2006 Seattle Building Code*. ICC, Washington, D.C.
- ISO 2394: *General Principles on Reliability for Structures*, 3rd ed. 1998. International Organization for Standardization, Geneva.
- Itoh, Y., and T. Kitagawa. 2001. Bridge Lifecycle Analysis and Durability Evaluation Using Accelerated Exposure Test. Presented at U.S.–Japan Seminar on Advanced Stability and Seismicity Concept for Performance-Based Design of Steel and Composite Structures, Kyoto, Japan.
- Jiang, Y., and K. Sinha. 1989. *The Development of Optimal Strategies for Maintenance, Rehabilitation, and Replacement of Highway Bridges: Volume 6: Performance Analysis and Optimization*. FHWA/IN/JHRP-89/13. Purdue University, West Lafayette, Ind., and Indiana Department of Transportation, Indianapolis.
- Kaar, P., and A. Mattock. 1963. High-Strength Bars As Concrete Reinforcement, Part 4: Control of Cracking. *Portland Cement Association Development Department Bulletin D59*, pp. 15–38.



- Kaczinski, M. 2008. New Developments in Expansion Joints, Bearings, Cable Corrosion Protection, and Grid Deck Systems. Presented at 2008 IBTTA Fall Maintenance Meeting, New Orleans, La.
- Keating, P.B., and J.W. Fisher. 1986. *NCHRP Report 286: Evaluation of Fatigue Tests and Design Criteria on Welded Details*. TRB, National Research Council, Washington, D.C.
- Klaiber, F., T. Wipf, and F. Russo. 2004. *NCHRP Synthesis 327: Cost-Effective Practices for Off-System and Local Interest Bridges*. TRB, National Research Council, Washington, D.C.
- Krauss, P., and E. Rogalla. 1996. *NCHRP Report 380: Transverse Cracking in Newly Constructed Bridge Decks*. TRB, National Research Council, Washington, D.C.
- Kulicki, J., Z. Prucz, C. Clancy, D. Mertz, and A. Nowak. 2007. *Updating the Calibration Report for AASHTO LRFD Code*. Report on NCHRP Project 20-7/186. Transportation Research Board of the National Academies, Washington, D.C.
- Kulicki, J., W. Wassef, D. Mertz, A. Nowak, N. Samtani, and H. Nassif. 2013. *Service Load Design for 100-Year Life*. SHRP 2 Project R19B. TRB, National Research Council, Washington, D.C. (Draft.)
- Kupfer, H., and K. Gerstle. 1973. Behavior of Concrete Under Biaxial Stress. *ASCE Journal of the Engineering Mechanics Division*, Vol. 99, No. 4, pp. 853–866.
- Langley, W. 1999. Concrete Mix Proportioning to Meet Durability Concerns for Confederation Bridge. In *High-Performance Concrete: Performance and Quality of Concrete Structures*, SP-186, American Concrete Institute, Detroit, Mich., pp. 129–148.
- Lash, S. 1969. Can High-Strength Reinforcement Be Used in Highway Bridges? In *First International Symposium on Concrete Bridge Design*, SP-23, American Concrete Institute, Detroit, Mich., pp. 283–300.
- Lind, N., and A. Nowak. 1978. *Calculation of Load and Performance Factors*. Ontario Ministry of Transportation and Communications, Toronto, Canada.
- LRFD Bridge Design Manual*. 2006. Louisiana Department of Transportation and Development, Baton Rouge.
- MacGregor, J., I. Jhamb, and N. Nuttall. 1971. Fatigue Strength of Hot-Rolled Deformed Reinforcing Bars. *Journal Proceedings, American Concrete Institute*, Vol. 68, No. 3, pp. 169–179.
- Main Roads Specification MRS81: Bridge Bearings*. 2012. MRS81. Queensland Government, Department of Main Roads, Queensland, Australia.
- Manual for Bridge Evaluation*. 2008. American Association of State Highway and Transportation Officials, Washington, D.C.
- Maryland Manual on Uniform Traffic Control Devices for Streets and Highways*. 2006. Includes Revision 1, July 2009. Maryland State Highway Administration, Baltimore.
- Matsuishi, M., and T. Endo. 1968. *Fatigue of Metals Subjected to Varying Stress*. Japan Society of Mechanical Engineers, Fukuoka, Japan.
- Maurer Söhne. 2011. Maurer MSM Sliding Bearings. [http://www.maurer.co.uk/doc/MSM\\_Prosppekt\\_1208\\_engl.pdf](http://www.maurer.co.uk/doc/MSM_Prosppekt_1208_engl.pdf). Accessed Nov. 25.
- Maurer Söhne. 2013. Head Made of Stainless Steel: Expansion Joints with Hybrid Profile. [http://www.maurer-soehne.com/files/bauwerk\\_schutzsysteme/pdf/de/news/MAU\\_PR\\_Hybrid\\_Profile\\_0707\\_engl.pdf](http://www.maurer-soehne.com/files/bauwerk_schutzsysteme/pdf/de/news/MAU_PR_Hybrid_Profile_0707_engl.pdf). Accessed Nov. 25.
- Merriam-Webster. 2010. Deterioration. <http://www.merriam-webster.com/dictionary/deterioration>. Accessed Nov. 25.
- Merriam-Webster. 2010. Maintenance. <http://www.merriam-webster.com/dictionary/maintenance>. Accessed Nov. 25.
- Merriam-Webster. 2010. Serviceable. <http://www.merriam-webster.com/dictionary/serviceable>. Accessed Nov. 25.
- Miner, M. 1945. Cumulative Damage in Fatigue. *Journal of Applied Mechanics, American Society of Mechanical Engineers*, Vol. 12, pp. A159–A164.
- Mirza, S. 2007. Design of Durable and Sustainable Concrete Bridges. *Proc., CBM-CI International Workshop*, NED University of Engineering and Technology, Karachi, Pakistan, pp. 333–344.
- Mirza, S., and J. MacGregor. 1979a. Variability of Mechanical Properties of Reinforcing Bars. *ASCE Journal of the Structural Division*, Vol. 105, No. 5, pp. 921–937.
- Mirza, S., and J. MacGregor. 1979b. Variations in Dimensions of Reinforced Concrete Members. *ASCE Journal of the Structural Division*, Vol. 105, No. 4, pp. 751–766.
- Miska. 2013. Compression Seals: Neoprene. [www.miska.com.au/ebm3-doc/130914/comsealdatasheet.pdf](http://www.miska.com.au/ebm3-doc/130914/comsealdatasheet.pdf). Accessed May 9.
- Mlynarski, M., W. Wassef, and A. Nowak. 2011. *NCHRP Report 700: A Comparison of AASHTO Bridge Load Rating Methods*. TRB, National Research Council, Washington, D.C.
- Moulton, L., H. Ganga Rao, and G. Halvorsen. 1985. *Tolerable Movement Criteria for Highway Bridges*. FHWA/RD-85-107. West Virginia University, Morgantown.
- Murray, T., D. Allen, and E. Ungar. 2003. *Design Guide 11: Floor Vibrations Due to Human Activity*. American Institute of Steel Construction, Chicago, Ill.
- Musso, A., and P. Provenzano. 2003. Discussion of Predicting Settlement of Shallow Foundations Using Neural Networks. *ASCE Journal of Geotechnical and Geoenvironmental Engineering*, Vol. 129, No. 12, pp. 1172–1175.
- Nawy, E., and P. Huang. 1977. Crack and Deflection Control of Prestensioned Prestressed Beams. *Journal, Precast/Prestressed Concrete Institute*, Vol. 23, No. 3, pp. 30–43.
- NCHRP Research Results Digest 197: Fatigue Behavior of Welded and Mechanical Splices in Reinforcing Steel*. 1994. TRB, National Research Council, Washington, D.C.
- Nevels, J., and D. Hixon. 1973. *A Study to Determine the Causes of Bridge Deck Deterioration*. Research and Development Division, Oklahoma Department of Highways, Oklahoma City.
- Nowak, A. 1999. *NCHRP Report 368: Calibration of LRFD Bridge Design Code*. TRB, National Research Council, Washington, D.C.
- Nowak, A., and K. Collins. 2013. *Reliability of Structures*. McGraw-Hill, New York.
- Nowak, A., E. Szeliga, and M. Szerszen. 2008. Reliability-Based Calibration for Structural Concrete, Phase 3. *Portland Cement Association Research and Development Serial No. 2849*, pp. 1–110.
- Okeil, A. 2006. Allowable Tensile Stress for Webs of Prestressed Segmental Concrete Bridges. *Structural Journal, American Concrete Institute*, Vol. 103, No. 4, pp. 488–495.
- Oluokun, F. 1991. Prediction of Concrete Tensile Strength from Its Compressive Strength: Evaluation of Existing Relations for Normal-Weight Concrete. *Materials Journal, American Concrete Institute*, Vol. 88, No. 3, pp. 302–309.
- Ontario Highway Bridge Design Code*. 1979. Ontario Ministry of Transportation, Toronto, Canada.
- Ontario Highway Bridge Design Code*. 1991. Ontario Ministry of Transportation, Toronto, Canada.
- Ontario Traffic Manual: Book 5: Regulatory Signs*. 2000. Ontario Ministry of Transportation, Toronto, Canada.
- Ople, F.S., and C.L. Hulsbos. 1966. Probable Fatigue Life of Plain Concrete with Stress Gradient. *Journal Proceedings, American Concrete Institute*, Vol. 63, No. 1, pp. 59–82.
- Outokumpu. 2013. Sustainable Bridges: 300 Year Design Life for Second Gateway Bridge. <http://www.outokumpu.com/SiteCollection>

- Documents/SiteCollectionDocumentsSustainable%20Bridges\_44664.pdf. Accessed Nov. 25.
- Palmgren, A. 1924. Die Lebensdauer von Kugellagern [Life Length of Roller Bearings (in German)]. *Zeitschrift des Vereines Deutscher Ingenieure (VDI Zeitschrift)*, Vol. 68, No. 14, pp. 339–341.
- Peck, R., and A. Bazaraa. 1969. Discussion of Settlement of Spread Footings on Sand. *ASCE Journal of the Soil Mechanics and Foundations Division*, Vol. 95, No. 3, pp. 900–916.
- Pelphrey, J., C. Higgins, B. Sivakumar, R. Groff, B. Hartman, J. Charbonneau, J. Rooper, and B. Johnson. 2008. State-Specific LRFR Live Load Factors Using Weigh-in-Motion Data. *Journal of Bridge Engineering*, July/August, pp. 339–350.
- Pfister, J. F., and E. Hognestad. 1964. High-Strength Bars As Concrete Reinforcement, Part 6: Fatigue Tests. *Journal of the Portland Cement Association Research and Development Laboratories*, Vol. 6, No. 1, pp. 65–84.
- Portland Cement Association. 1970. Durability of Concrete Bridge Decks: A Cooperative Study, Final Report. Portland Cement Association (PCA), Skokie, Ill.
- Purvis, R. 2003. *NCHRP Synthesis 319: Bridge Deck Joint Performance: A Synthesis of Highway Performance*. TRB, National Research Council, Washington, D.C.
- Rakoczy, P. 2011. *WIM-Based Load Models for Bridge Serviceability Limit States*. PhD dissertation. University of Nebraska, Lincoln.
- Ramey, G., and R. Wright. 1994. *Assessing and Enhancing the Durability/Longevity Performances of Highway Bridges*. Final report. HRC Research Project 2-13506. Highway Research Center, Auburn University, Auburn, Ala.
- Ravindra, M., and T. Galambos. 1978. Load and Resistance Factor Design for Steel. *ASCE Journal of the Structural Division*, Vol. 104, No. 9, pp. 1337–1353.
- Roeder, C., K. Barth, and A. Bergman. 2002. *NCHRP Web Document 46: Improved Live Load Deflection Criteria for Steel Bridges*. TRB, National Research Council, Washington, D.C.
- Rolfe, S., and J. Barsom. 1977. *Fracture and Fatigue Control in Structures: Applications of Fracture Mechanics*. Prentice-Hall, Englewood Cliffs, N.J.
- Rostam, S. 2005. *Design and Construction of Segmental Concrete Bridges for Service Life of 100 to 150 Years*. American Segmental Bridge Institute, Buda, Tex.
- Samtani, N., A. Nowatzki, and D. Mertz. 2010. *Selection of Spread Footings on Soils to Support Highway Bridge Structures*. FHWA RC/TD-10-001. Federal Highway Administration Resource Center, Matteson, Ill.
- Samtani, N., and E. Nowatzki. 2006. *Soils and Foundations: Volumes I and II*. FHWA-NHI-06-088 and FHWA-NHI-06-089. Federal Highway Administration, U.S. Department of Transportation.
- Sargand, S., and T. Masada. 2006. *Further Use of Spread Footing Foundations for Highway Bridges*. State Job No. 14747(0), FHWA-OH-2006/8. Ohio Research Institute for Transportation and the Environment, Athens; Ohio Department of Transportation, Columbus; and Office of Research and Development, Federal Highway Administration, U.S. Department of Transportation.
- Sargand, S., T. Masada, and R. Engle. 1999. Spread Footing Foundation for Highway Bridge Applications. *ASCE Journal of Geotechnical and Geoenvironmental Engineering*, Vol. 125, No. 5, pp. 373–382.
- Schilling, C., K. Klippstein, J. Barsom, and G. Blake. 1977. *NCHRP Report 188: Fatigue of Welded Steel Bridge Members Under Variable-Amplitude Loadings*. TRB, National Research Council, Washington, D.C.
- Schmertmann, J., P. Brown, and J. Hartman. 1978. Improved Strain Influence Factor Diagrams. *ASCE Journal of the Geotechnical Engineering Division*, Vol. 104, No. 8, pp. 1131–1135.
- Schopen, D. 2010. *Analyzing and Designing for Substructure Movement in Highway Bridges: An LRFD Approach*. Master's thesis. University of Delaware, Newark.
- Shahin, M., H. Maier, and M. Jaksa. 2002. Predicting Settlement of Shallow Foundations Using Neural Networks. *ASCE Journal of Geotechnical and Geoenvironmental Engineering*, Vol. 128, No. 9, pp. 785–793.
- Siriakorn, A., and A. Naaman. 1980. *Reliability of Partially Prestressed Beams at Serviceability Limit States*. University of Illinois at Chicago Circle, Chicago, Ill.
- Sivakugan, N., and K. Johnson. 2002. Probabilistic Design Chart for Settlements of Shallow Foundations in Granular Soils. *Australian Civil Engineering Transactions*, No. 43, pp. 19–24.
- Sivakugan, N., and K. Johnson. 2004. Settlement Predictions in Granular Soils: A Probabilistic Approach. *Geotechnique*, Vol. 54, No. 7, pp. 499–502.
- Sivakumar, B., M. Ghosn, and F. Moses. 2011. *NCHRP Report 683: Protocols for Collecting and Using Traffic Data in Bridge Design*. TRB, National Research Council, Washington, D.C.
- Skempton, A., and D. MacDonald. 1956. Allowable Settlement of Buildings. *Proceedings, Part III, Institution of Civil Engineers*, No. 5, pp. 727–768.
- Standard Specifications for Highway Bridges*, 6th ed. 1953. American Association of State Highway Officials, Washington, D.C.
- Standard Specifications for Highway Bridges*, 11th ed. 1975. Includes 1974 and 1975 Interims. American Association of State Highway Officials, Washington, D.C.
- Standard Specifications for Highway Bridges*, 15th ed. 1992. American Association of State Highway and Transportation Officials, Washington, D.C.
- Standard Specifications for Highway Bridges*, 17th ed. 2002. American Association of State Highway and Transportation Officials, Washington, D.C.
- Steel Bridge Bearing Selection and Design Guide. 1996. In *Highway Structures Design Handbook*. American Iron and Steel Institute, National Steel Bridge Alliance, Washington, D.C., p. A-3.
- Steel Construction Manual*, 14th ed. 2011. American Institute of Steel Construction, Chicago, Ill.
- Steel Design Guide 3: Serviceability Design Considerations for Steel Bridges*, 2nd ed. 2003. American Institute of Steel Construction, Chicago, Ill.
- Structures Manual*. 2013. Florida Department of Transportation, Tallahassee.
- Stukhart, G., R. James, A. Garcia-Diaz, R. Bligh, J. Sobanjo, and W. McFarland. 1991. *Study for a Comprehensive Bridge Management System for Texas*. FHWA/TX-90/1212-1F. Texas Transportation Institute, College Station, and Texas State Department of Highways and Public Transportation, Arlington.
- Tabatabai, H., A. Ghorbanpoor, and A. Turnquist-Nass. 2004. *Rehabilitation Techniques for Concrete Bridges*. Project No. 0092-01-06. University of Wisconsin, Milwaukee, and Wisconsin Department of Transportation, Madison.
- Tachau, H. 1971. Discussion of Fatigue Tests on Prestressed Concrete I-Beams. *ASCE Journal of the Structural Division*, Vol. 97, No. 9, pp. 2429–2431.
- Tadros, M., N. Al-Omaishi, S. Seguirant, and J. Gallt. 2003. *NCHRP Report 496: Prestress Losses in Pretensioned High-Strength Concrete Bridge Girders*. TRB, National Research Council, Washington, D.C.
- Tan, C., and J. Duncan. 1991. Settlement of Footings on Sands: Accuracy and Reliability. *Proc., Geotechnical Engineering Congress 1991, ASCE Geotechnical Special Publication No. 27*, Vol. 1, pp. 446–455.

- Technoslide. 2013. Bearings for Bridges and Structures. <http://www.technoslide.com/pdf/elastomeric/elastomeric-plain-sliding-bearings-for-bridges-structures-brochure.pdf>. Accessed Nov. 25.
- Thompson, P., and R. Shepard. 2000. *AASHTO Commonly Recognized Bridge Elements: Successful Applications and Lessons Learned*. National Workshop on Commonly Recognized Measures for Maintenance, American Association of State Highway and Transportation Officials, Washington, D.C.
- Vincent, G. 1969. Tentative Criteria for Load Factor Design of Steel Highway Bridges. *Bulletin for the American Iron and Steel Institute*, No. 15.
- Wahls, H. 1983. *NCHRP Synthesis of Highway Practice 107: Shallow Foundations for Highway Structures*. TRB, National Research Council, Washington, D.C.
- Walker, W., and R. Wright. 1971. Criteria for the Deflection of Steel Bridges. *Bulletin for the American Iron and Steel Institute*, No. 19, pp. 1–75.
- Walraven, J., and A. Bicaj. 2011. The 2010 fib Model Code for Concrete Structures: A New Approach to Structural Engineering. *Structural Concrete, Journal of the fib*, Vol. 12, No. 2, pp. 139–147.
- Warner, R., and C. Hulsbos. 1966. Probable Fatigue Life of Prestressed Concrete Beams. *Journal, Precast/Prestressed Concrete Institute*, Vol. 11, No. 2, pp. 16–39.
- Wikipedia. 2010. Deterioration. <http://en.wikipedia.org/wiki/Deterioration>. Accessed Nov. 25.
- Wikipedia. 2010. Serviceability (Structure). [http://en.wikipedia.org/wiki/Serviceability\\_\(structure\)](http://en.wikipedia.org/wiki/Serviceability_(structure)). Accessed Nov. 25.
- Wiktionary. 2010. Maintenance. <http://en.wiktionary.org/wiki/maintenance>. Accessed Nov. 25.
- Wright, R., and W. Walker. 1972. Vibration and Deflection of Steel Bridges. *Engineering Journal, American Institute of Steel Construction*, Vol. 9, No. 1, pp. 20–31.
- Yura, J., T. Galambos, and M. Ravindra. 1978. The Bending Resistance of Steel Beams. *ASCE Journal of the Structural Division*, Vol. 104, No. 9, pp. 1355–1370.
- Zhang, L., and A. Ng. 2005. Probabilistic Limiting Tolerable Displacements for Serviceability Limit State Design of Foundations. *Geotechnique*, Vol. 55, No. 2, pp. 151–161.



## APPENDIX A

# SLS Requirements in the Eurocode

## A.1 Introduction

### A.1.1 General Information

The Structural Eurocode program provides comprehensive information for the structural design and verification of buildings and civil engineering works (including geotechnical aspects). The program comprises the following standards, each one consisting of a number of parts. [Often only a limited number of parts of each standard may be relevant to bridge structures.]

- EN 1990 Eurocode 0: Basis of structural design
- EN 1991 Eurocode 1: Actions on structures
- EN 1992 Eurocode 2: Design of concrete structures
- EN 1993 Eurocode 3: Design of steel structures
- EN 1994 Eurocode 4: Design of composite steel and concrete structures
- EN 1995 Eurocode 5: Design of timber structures
- EN 1996 Eurocode 6: Design of masonry structures
- EN 1997 Eurocode 7: Geotechnical design
- EN 1998 Eurocode 8: Design of structures for earthquake resistance
- EN 1999 Eurocode 9: Design of aluminum structures

Following is a description of the serviceability limit state (SLS) requirements in sections relevant to bridges.

### A.1.2 Structural Eurocodes

The Structural Eurocode standards provide common structural design rules for everyday use for the design of whole structures and component products of both a traditional and an innovative nature. Unusual forms of construction or design conditions are not specifically covered and additional expert consideration is required by the designer in such cases.

The Eurocodes are being implemented by each member country of the European Union through National Standards

which comprise the full text of each Eurocode (including any annexes) and may be followed by a National Annex.

The National Annex only contains information on those parameters which are left open in the Eurocode for national choice, (known as Nationally Determined Parameters). They are to be used for the design of buildings and civil engineering works to be constructed in the country concerned and are usually one or more of the following:

- Values and/or classes where alternatives are given in the Eurocode;
- Values to be used where a symbol only is given in the Eurocode.
- Country specific data (geographical, climatic, etc.) e.g. snow map.
- The procedure to be used where alternative procedures are given in the Eurocode.

The National Annex may also contain the following:

- Decisions on the application of informative annexes, and
- References to non-contradictory complementary information to help the user apply the Eurocode.

This summary does not include any numeric values presented in any National Annex.

The following sections address some of the Structural Eurocodes in turn and summarize the relevant articles relating to the serviceability limit state used in bridge design.

## A.2 EN 1990 Eurocode 0: Basis of Structural Design

Eurocode 0 (Basis of structural design) is the lead document in the Eurocode suite. It describes the principles and requirements for safety, serviceability, and durability of structures. It is based on the limit state concept used in conjunction

with a partial factor method. It provides the basis and general principles for the structural design and verification of buildings and civil engineering works (including geotechnical aspects).

EN 1990:2002 should be used in conjunction with all the other Eurocodes (EN 1991 to EN 1999) for design.

NOTE: For the design of special construction works (e.g. nuclear installations, dams), other provisions than those in EN 1990 to EN 1999 might be necessary.

EN 1990 also gives guidelines for the aspects of structural reliability relating to safety, serviceability, and durability:

- For design cases not covered by EN 1991 to EN 1999 (other actions, structures not treated, other materials);
- To serve as a reference document for other European Committee for Standardization Technical Committees (CEN/TCs) concerning structural matters.

EN 1990 is also applicable as a guidance document for the design of structures where other materials or other actions outside the scope of EN 1991 to EN 1999 are involved.

EN 1990 is applicable for the structural appraisal of existing construction, in developing the design of repairs and alterations, or in assessing changes of use.

NOTE: Additional or amended provisions might be necessary where appropriate.

EN 1990 is intended for use by

- Committees drafting standards for structural design and related product, testing, and execution standards;
- Clients (e.g., for the formulation of their specific requirements on reliability levels and durability);
- Designers and constructors; and
- Relevant authorities.

The general assumptions of EN 1990 are as follows:

- The choice of the structural system and the design of the structure are made by appropriately qualified and experienced personnel.
- Execution is carried out by personnel having the appropriate skill and experience.
- Adequate supervision and quality control are provided during execution of the work (i.e. in design offices, factories, plants, and on site).
- The construction materials and products are used as specified in EN 1990 or in EN 1991 to EN 1999 or in the relevant execution standards, or reference material, or product specifications.
- The structure will be adequately maintained; and
- The structure will be used in accordance with the design assumptions.

NOTE: There may be cases when these assumptions need to be supplemented.

It should be noted that clauses are listed and enumerated within each article of the Eurocodes and that distinction is made between clauses that present principles and those that present Application Rules. This distinction is preserved in the summaries given in this report.

The Principles comprise

- General statements and definitions for which there is no alternative, as well as
- Requirements and analytical models for which no alternative is permitted unless specifically stated.

The Principles are identified by the letter P following the paragraph number. [e.g. (2)P]

The Application Rules [identified by a number in brackets, e.g. (2)] are generally recognized rules which comply with the principles and satisfy their requirements.

It is permissible to use alternative design rules different from the Application Rules given in EN 1990 for works, provided that it is shown that the alternative rules accord with the relevant principles and are at least equivalent with regard to the structural safety, serviceability, and durability which would be expected when using the Eurocodes.

The clauses relating to serviceability limit state design presented in Eurocode 0 are summarized in Table A.1.

### A.3 EN 1991 Eurocode 1: Actions on Structures

Eurocode 1 (Actions on structures) provides information on all actions that should normally be considered in the design of buildings and civil engineering works. It is in four main parts. The first part is divided into seven sub-parts which cover densities, self-weight, and imposed loads; actions due to fire; snow; wind; thermal actions; loads during execution; and accidental actions. The remaining three parts cover traffic loads on bridges, actions by cranes and machinery, and actions for silos and tanks.

The second part (EN 1991-2:2003) concerns the design of bridges. Sections from this standard relating to the serviceability limit state are summarized in Table A.2.

For the design of bridges, EN 1991-2 defines imposed loads (models and representative values) associated with road traffic, pedestrian actions, and rail traffic which include, when relevant, dynamic effects and centrifugal, braking, and acceleration actions and actions for accidental design situations. For the design of new bridges, EN 1991-2 is intended to be used, for direct application, together with Eurocodes EN 1990 to EN 1999. The bases for combinations of traffic loads with non-traffic loads are given in EN 1990, A2.

A summary of clauses relating to loads and actions in Eurocode EN 1991-2 is presented in Table A.2.

**Table A.1. Summary of Clauses Relating to Serviceability Limit State Design in Eurocode 0**

Eurocode Article	Basic Provision	Discussion
<p>Eurocode 0</p> <p><b>3.4 Serviceability limit states</b></p>	<p>(1)P The limit states that concern</p> <ul style="list-style-type: none"> <li>– the functioning of the structure or structural members under normal use;</li> <li>– the comfort of people;</li> <li>– the appearance of the construction works, shall be classified as serviceability limit states.</li> </ul> <p>NOTE 1: In the context of serviceability, the term “appearance” is concerned with such criteria as high deflection and extensive cracking, rather than aesthetics.</p> <p>NOTE 2: Usually the serviceability requirements are specific to each individual project.</p> <p>(2)P A distinction shall be made between reversible and irreversible serviceability limit states.</p> <p>NOTE: ‘Reversible’ = where no consequences of actions exceeding the specified service requirement will remain when the actions are removed.</p> <p>‘Irreversible’ = where some consequences of actions will remain when the actions are removed.</p> <p>(3) The verification of serviceability limit states should be based on criteria concerning the following aspects:</p> <ol style="list-style-type: none"> <li>a) deformations that affect <ul style="list-style-type: none"> <li>– the appearance,</li> <li>– the comfort of users, or</li> <li>– the functioning of the structure (including the functioning of machines or services), or that cause damage to finishes or non-structural members;</li> </ul> </li> <li>b) vibrations <ul style="list-style-type: none"> <li>– that cause discomfort to people, or</li> <li>– that limit the functional effectiveness of the structure;</li> </ul> </li> <li>c) damage that is likely to adversely affect <ul style="list-style-type: none"> <li>– the appearance,</li> <li>– the durability, or</li> <li>– the functioning of the structure.</li> </ul> </li> </ol> <p>NOTE: Additional provisions related to serviceability criteria are given in the relevant EN 1992 to EN 1999.</p>	
<p>Eurocode 0</p> <p><b>6.5.1 Verifications</b></p>	<p>(1)P It shall be verified that</p> $Ed \leq Cd \quad (6.13)$ <p>where:</p> <p>Cd is the limiting design value of the relevant serviceability criterion.</p> <p>Ed is the design value of the effects of actions specified in the serviceability criterion, determined on the basis of the relevant combination.</p>	
<p>Eurocode 0</p> <p><b>6.5.2 Serviceability criteria</b></p>	<p>(1) The deformations to be taken into account in relation to serviceability requirements should be as detailed in the relevant Annex A according to the type of construction works, or agreed with the client or the National authority.</p> <p>NOTE: For other specific serviceability criteria such as crack width, stress or strain limitation, slip resistance, see EN 1991 to EN 1999.</p>	
<p>Eurocode 0</p> <p><b>6.5.3 Combination of actions</b></p>	<p>(1) The combinations of actions to be taken into account in the relevant design situations should be appropriate for the serviceability requirements and performance criteria being verified.</p> <p>(2) The combinations of actions for serviceability limit states are defined symbolically (see also 6.5.4):</p> <p>NOTE: It is assumed, in these expressions, that all partial factors are equal to 1. See Annex A and EN 1991 to EN 1999.</p> <ol style="list-style-type: none"> <li>a) Characteristic combination: (equation given at 6.14a)</li> </ol> <p>NOTE: The characteristic combination is normally used for irreversible limit states.</p> <ol style="list-style-type: none"> <li>b) Frequent combination: (equation given at 6.15a)</li> </ol> <p>NOTE: The frequent combination is normally used for reversible limit states.</p> <ol style="list-style-type: none"> <li>c) Quasi-permanent combination: (equation given at 6.16a)</li> </ol> <p>NOTE: The quasi-permanent combination is normally used for long-term effects and the appearance of the structure.</p>	

(continued on next page)

**Table A.1. Summary of Clauses Relating to Serviceability Limit State Design in Eurocode 0 (continued)**

Eurocode Article	Basic Provision	Discussion
	<p>(3) For the representative value of the prestressing action (<i>i.e.</i> <math>P_k</math> or <math>P_m</math>), reference should be made to the relevant design Eurocode for the type of prestress under consideration.</p> <p>(4)P Effects of actions due to imposed deformations shall be considered where relevant.</p> <p>NOTE: In some cases expressions (6.14) to (6.16) require modification. Detailed rules are given in the relevant parts of EN 1991 to EN 1999.</p>	
Eurocode 0 <b>6.5.4 Partial factors for materials</b>	<p>(1) For serviceability limit states the partial factors <math>\gamma_M</math> for the properties of materials should be taken as 1.0 except if differently specified in EN 1992 to EN 1999.</p>	
Eurocode 0 Annex A2 <b>A2.1 Field of application</b>	<p>(1) This Annex A2 to EN 1990 gives rules and methods for establishing combinations of actions for serviceability and ultimate limit state verifications (except fatigue verifications) with the recommended design values of permanent, variable, and accidental actions and <math>\psi</math> factors (applied to actions) to be used in the design of road bridges, footbridges, and railway bridges. It also applies to actions during execution. Methods and rules for verifications relating to some material-independent serviceability limit states are also given.</p> <p>NOTE 1: Symbols, notations, Load Models, and groups of loads are those used or defined in the relevant section of EN 1991-2.</p> <p>NOTE 2: Symbols, notations, and models of construction loads are those defined in EN 1991-1-6.</p> <p>NOTE 3: Guidance may be given in the National Annex with regard to the use of Table 2.1 (design working life—for UK bridges this is normally 120 years).</p> <p>NOTE 4: Most of the combination rules defined in clauses A2.2.2 to A2.2.5 are simplifications intended to avoid needlessly complicated calculations. They may be changed in the National Annex or for the individual project as described in A2.2.1 to A2.2.5.</p> <p>NOTE 5: This Annex A2 to EN 1990 does not include rules for the determination of actions on structural bearings (forces and moments) and associated movements of bearings or give rules for the analysis of bridges involving ground-structure interaction that may depend on movements or deformations of structural bearings.</p> <p>(2) The rules given in this Annex A2 to EN 1990 may not be sufficient for</p> <ul style="list-style-type: none"> <li>– bridges that are not covered by EN 1991-2 (<i>e.g.</i> bridges under an airport runway, mechanically-moveable bridges, roofed bridges, bridges carrying water),</li> <li>– bridges carrying both road and rail traffic, and</li> <li>– other civil engineering structures carrying traffic loads (<i>e.g.</i> backfill behind a retaining wall).</li> </ul>	
Eurocode 0 Annex A2 <b>A2.2 Combination of actions</b> <b>A2.2.1 General</b>	<p>(1) Effects of actions that cannot occur simultaneously due to physical or functional reasons need not be considered together in combinations of actions.</p> <p>(2) Combinations involving actions which are outside the scope of EN 1991 (<i>e.g.</i> due to mining subsidence, particular wind effects, water, floating debris, flooding, mud slides, avalanches, fire, and ice pressure) should be defined in accordance with EN 1990, 1.1(3).</p> <p>NOTE 1: Combinations involving actions that are outside the scope of EN 1991 may be defined either in the National Annex or for the individual project.</p> <p>NOTE 2: For seismic actions, see EN 1998.</p> <p>NOTE 3: For water actions exerted by currents and debris effects, see also EN 1991-1-6.</p> <p>(4) The combinations of actions given in expressions 6.14a to 6.16b should be used when verifying serviceability limit states. Additional rules are given in A2.4 for verifications regarding deformations and vibrations.</p>	

(continued on next page)

**Table A.1. Summary of Clauses Relating to Serviceability Limit State Design in Eurocode 0 (continued)**

Eurocode Article	Basic Provision	Discussion
Eurocode 0 Annex A2  <b>A2.2 Combination of actions</b> <b>A2.2.2 Combination rules for road bridges</b>	(1) The infrequent values of variable actions may be used for certain serviceability limit states of concrete bridges.  NOTE: The National Annex may refer to the infrequent combination of actions.  (6) Wind actions and thermal actions need not be taken into account simultaneously unless otherwise specified for local climatic conditions.  NOTE: Depending upon the local climatic conditions, a different simultaneity rule for wind and thermal actions may be defined either in the National Annex or for the individual project.	
Eurocode 0 Annex A2  <b>A2.4 Serviceability and other specific limit states</b> <b>A2.4.1 General</b>	(2) The serviceability criteria should be defined in relation to the serviceability requirements in accordance with 3.4 and EN 1992 to EN 1999. Deformations should be calculated in accordance with EN 1991 to EN 1999 by using the appropriate combinations of actions according to expressions (6.14a) to (6.16b) (see Table A2.6), taking into account the serviceability requirements and the distinction between reversible and irreversible limit states.  NOTE: Serviceability requirements and criteria may be defined as appropriate in the National Annex or for the individual project.	
Eurocode 0 Annex A2  <b>A2.4.2 Serviceability criteria regarding deformation and vibration for road bridges</b>	(1) Where relevant, requirements and criteria should be defined for road bridges concerning – uplift of the bridge deck at supports, and – damage to structural bearings.  NOTE: Uplift at the end of a deck can jeopardize traffic safety and damage structural and non-structural elements. Uplift may be avoided by using a higher safety level than usually accepted for serviceability limit states.  (2) Serviceability limit states during execution should be defined in accordance with EN 1990 to EN 1999.  (3) Requirements and criteria should be defined for road bridges concerning deformations and vibrations, where relevant.  NOTE 1: The verification of serviceability limit states concerning deformation and vibration needs to be considered only in exceptional cases for road bridges. The frequent combination of actions is recommended for the assessment of deformation.  NOTE 2: Vibrations of road bridges may have various origins, in particular traffic actions and wind actions. For vibrations due to wind actions, see EN 1991-1-4. For vibrations due to traffic actions, comfort criteria may have to be considered. Fatigue may also have to be taken into account.	
Eurocode 0 Annex A2  <b>A2.4.3.2 Pedestrian comfort criteria (for serviceability)</b>	(1) The comfort criteria should be defined in terms of maximum acceptable acceleration of any part of the deck.  NOTE: The criteria may be defined as appropriate in the National Annex or for the individual project.  The following accelerations (m/s <sup>2</sup> ) are the recommended maximum values for any part of the deck: i) 0.7 for vertical vibrations, ii) 0.2 for horizontal vibrations due to normal use, and iii) 0.4 for exceptional crowd conditions.  (2) A verification of the comfort criteria should be performed if the fundamental frequency of the deck is less than – 5 Hz for vertical vibrations, or – 2.5 Hz for horizontal (lateral) and torsional vibrations.  NOTE: The data used in the calculations, and therefore the results, are subject to very high uncertainties. When the comfort criteria are not satisfied with a significant margin, it may be necessary to make provision in the design for the possible installation of dampers in the structure after its completion. In such cases the designer should consider and identify any requirements for commissioning tests.	

(continued on next page)

**Table A.1. Summary of Clauses Relating to Serviceability Limit State Design in Eurocode 0 (continued)**

Eurocode Article	Basic Provision	Discussion
Eurocode 0 Annex A2 <b>A2.4.4.3 Limiting values for the maximum vertical deflection for passenger comfort</b> <b>A2.4.4.3.1 Comfort criteria</b>	(1) Passenger comfort depends on the vertical acceleration $b_v$ inside the coach during travel on the approach to, passage over, and departure from the bridge. (2) The levels of comfort and associated limiting values for the vertical acceleration should be specified.  NOTE: These levels of comfort and associated limiting values may be defined for the individual project. Recommended levels of comfort are given in Table A2.9.	
Eurocode 0 Annex A2 <b>A2.4.4.3 Limiting values for the maximum vertical deflection for passenger comfort</b> <b>A2.4.4.3.3 Requirements for a dynamic vehicle/bridge interaction analysis for checking passenger comfort</b>	(1) Where a vehicle/bridge dynamic interaction analysis is required, the analysis should take account of the following behaviors: iv) a series of vehicle speeds up to the maximum speed specified, v) characteristic loading of the real trains specified for the individual project in accordance with EN 1991-2, 6.4.6.1.1, vi) dynamic mass interaction between vehicles in the real train and the structure, vii) the damping and stiffness characteristics of the vehicle suspension, viii) a sufficient number of vehicles to produce the maximum load effects in the longest span, ix) a sufficient number of spans in a structure with multiple spans to develop any resonance effects in the vehicle suspension.  NOTE: Any requirements for taking track roughness into account in the vehicle/bridge dynamic interaction analysis may be defined for the individual project.	

**Table A.2. Summary of Clauses Relating to Loads and Actions in Eurocode EN 1991-2**

Eurocode Article	Basic Provision	Discussion
Eurocode 1 <b>1.3 Distinction between Principles and Application Rules</b>	(5) It is permissible to use alternative design rules different from the Application Rules given in EN 1991-2 for works, provided that it is shown that the alternative rules accord with the relevant principles and are at least equivalent with regard to the structural safety, serviceability, and durability which would be expected when using the Eurocodes.	
Eurocode 1 <b>Section 2 Classification of actions</b> <b>2.2 Variable actions</b>	(1) For normal conditions of use ( <i>i.e.</i> excluding any accidental situation), the traffic and pedestrian loads (dynamic amplification included where relevant) should be considered as variable actions. (2) The various representative values are – characteristic values, which are either statistical ( <i>i.e.</i> corresponding to a limited probability of being exceeded on a bridge during its design working life) or nominal; see EN 1990, 4.1.2(7); – frequent values; and – quasi-permanent values. (3) For calculation of fatigue lives, separate models, associated values, and where relevant, specific requirements are given in 4.6 for road bridges, in 6.9 for railway bridges, and in the relevant annexes.	
Eurocode 1 <b>Section 4 Road traffic actions and other actions specifically for road bridges</b> <b>4.1 Field of application</b>	(1) Load models defined in this section should be used for the design of road bridges with loaded lengths less than 200 m.  NOTE 1: 200 m corresponds to the maximum length taken into account for the calibration of Load Model 1 (see 4.3.2). In general, the use of Load Model 1 is safe-sided for loaded lengths over 200 m.  NOTE 2: Load models for loaded lengths greater than 200 m may be defined in the National Annex or for the individual project. (2) The models and associated rules are intended to cover all normally foreseeable traffic situations ( <i>i.e.</i> traffic conditions in either direction on any lane due to the road traffic) to be taken into account for design [see however (3) and the notes in 4.2.1]. (3) The effects of loads on road construction sites ( <i>e.g.</i> due to scrapers, lorries carrying earth) or of loads specifically for inspection and tests are not intended to be covered by the load models and should be separately specified, where relevant.	

(continued on next page)



**Table A.2. Summary of Clauses Relating to Loads and Actions in Eurocode EN 1991-2 (continued)**

Eurocode Article	Basic Provision	Discussion
Eurocode 1 <b>4.2 Representation of actions</b> <b>4.2.1 Models of road traffic loads</b>	(1) Loads due to the road traffic, consisting of cars, lorries, and special vehicles (e.g. for industrial transport), give rise to vertical and horizontal, static and dynamic forces.  NOTE 1: The load models defined in this section do not describe actual loads. They have been selected and calibrated so that their effects (with dynamic amplification included where indicated).  NOTE 2: The National Annex may define complementary load models, with associated combination rules where traffic outside the scope of the load models specified in this section needs to be considered.  NOTE 3: The dynamic amplification included in the models (except for fatigue), although established for a medium pavement quality (see Annex B) and pneumatic vehicle suspension, depends on various parameters and on the action effect under consideration. Therefore, it cannot be represented by a unique factor. In some unfavorable cases, it may reach 1,7 (local effects), but still more unfavorable values can be reached for poorer pavement quality, or if there is a risk of resonance. These cases can be avoided by appropriate quality and design measures. Therefore, an additional dynamic amplification may have to be taken into account for particular calculations [see 4.6.1.(6)] or for the individual project.	
Eurocode 1 <b>4.3 Vertical loads—Characteristic values</b> <b>4.3.1 General and associated design situations</b>	(1) Characteristic loads are intended for the determination of road traffic effects associated with ultimate limit state verifications and with particular serviceability verifications (see EN 1990 to EN 1999).  NOTE: There are 4 load models described in detail to cover most of the effects of the traffic of lorries and cars, special vehicles, and pedestrian crowd loading. They are used for general and local verifications. One of these models is used to represent dynamic effects on short structural members.	
Eurocode 1 <b>4.6 Fatigue load models</b> <b>4.6.1 General</b>	(1) Traffic running on bridges produces a stress spectrum which may cause fatigue. The stress spectrum depends on the geometry of the vehicles, the axle loads, the vehicle spacing, the composition of the traffic, and its dynamic effects.  NOTE: There are 5 load models described in detail. The first two are intended to be used to check whether the fatigue life may be considered unlimited when a constant stress amplitude fatigue limit is given. Therefore, they are appropriate for steel constructions and may be inappropriate for other materials. The remaining 3 load models are intended to be used for fatigue life assessment. Each of these last three models is more accurate than its predecessor, culminating in the last model which is based on actual traffic data.	

## A.4 EN 1992 Eurocode 2: Design of Concrete Structures

Eurocode 2 (Design of concrete structures) is concerned with the requirements for resistance, serviceability, durability, and fire resistance of concrete structures. (Other requirements, e.g. concerning thermal or sound insulation, are not considered.) It applies to the design of buildings and civil engineering works in plain, reinforced, and prestressed concrete.

EN 1992 is presented in three main parts. The first part has two sub-parts covering buildings and structural fire design. The last two main parts cover concrete bridges and liquid retaining and containing structures, as in the following list. Those underlined have been reviewed in the compilation of this report.

EN 1992-1.1:2004 Design of concrete structures. General rules and rules for buildings

EN 1992-1.2:2004 Design of concrete structures. Fire design

EN 1992-2:2005 Design of concrete structures. Concrete bridges. Design and detailing rules

EN 1992-3:2006 Design of concrete structures. Liquid retaining and containing structures

Note also

PD 6687:2006 Background paper to the UK National Annexes to BS EN 1992-1

PD 6687-2:2008 Recommendations for the design of structures to BS EN 1992-2

The second part, EN 1992-2:2005 (*Design of concrete structures. Concrete bridges. Design and detailing rules*) is relevant for the design of concrete bridges. Sections from this standard relating to the serviceability limit state are summarized

in Table A.3. It should be noted that EN 1992-2 draws heavily from the general clauses presented in EN 1992-1.1 (*Design of concrete structures. General rules and rules for buildings*); where relevant, these clauses are also included in the summaries given in the table.

EN 1992-2 describes the principles and requirements for safety, serviceability, and durability of concrete structures,

together with specific provisions for bridges. For the design of new bridges, EN 1992-2 is intended to be used, for direct application, together with other parts of EN 1992 and Eurocodes EN 1990, 1991, 1997, and 1998.

A summary of clauses relating to the serviceability limit state design of concrete bridges Eurocode EN 1992-1 is presented in Table A.3.

**Table A.3. Summary of Clauses Relating to the Serviceability Limit State Design of Concrete Bridges in Eurocode EN 1992-1**

Eurocode Article	Basic Provision	Discussion
Eurocode 2 <b>Section 2 Basis of Design</b> <b>2.1 Requirements</b> <b>2.1.1 Basic requirements</b>	(3) The basic requirements of EN 1990, Section 2 are deemed to be satisfied for concrete structures when the following are applied together: – limit state design in conjunction with the partial factor method in accordance with EN 1990, – actions in accordance with EN 1991, – combination of actions in accordance with EN 1990, and – resistances, durability and serviceability in accordance with this standard.  NOTE: Requirements for fire resistance (see EN 1990 Section 5 and EN 1992-1.2) may dictate a greater size of member than that required for structural resistance at normal temperature.	
Eurocode 2 <b>2.3.1.2 Thermal effects</b>	(1) Thermal effects should be taken into account when checking serviceability limit states. (2) Thermal effects should be considered for ultimate limit states only where they are significant (e.g. fatigue conditions, in the verification of stability where second order effects are of importance). In other cases they need not be considered, provided that the ductility and rotation capacity of the elements are sufficient. (3) Where thermal effects are taken into account, they should be considered as variable actions and applied with a partial factor and $\psi$ factor.  NOTE: The $\psi$ factor is defined in the relevant annex of EN 1990 and EN 1991-1.5.	
Eurocode 2 <b>2.3.1.3 Differential settlements/movements</b>	(2) The effects of differential settlements should generally be taken into account for the verification of serviceability limit states.	
Eurocode 2 <b>2.3.2 Material and product properties</b> <b>2.3.2.1 General</b> <b>2.3.2.2 Shrinkage and creep</b>	(1) Shrinkage and creep are time-dependent properties of concrete. Their effects should generally be taken into account for the verification of serviceability limit states. (3) When creep is taken into account, its design effects should be evaluated under the quasi-permanent combination of actions irrespective of the design situation considered ( <i>i.e.</i> persistent, transient, or accidental).  NOTE: In most cases the effects of creep may be evaluated under permanent loads and the mean value of prestress.	
Eurocode 2 <b>2.4.2 Design values</b> <b>2.4.2.4 Partial factors for materials</b>	(2) The values for partial factors for materials for serviceability limit state verification should be taken as those given in the particular clauses of this Eurocode.  NOTE: The values of $\gamma_c$ and $\gamma_s$ in the serviceability limit state for use in a country may be found in its National Annex. The recommended value for situations not covered by particular clauses of this Eurocode is 1.0.	
Eurocode 2 <b>Section 3 Materials</b> <b>3.1 Concrete</b> <b>3.1.1 General</b>	(1)P The following clauses give principles and rules for normal and high-strength concrete. (2) Rules for lightweight aggregate concrete are given in Section 11.	
Eurocode 2 <b>3.3 Prestressing steel</b> <b>3.3.1 General</b>	(1)P This clause applies to wires, bars, and strands used as prestressing tendons in concrete structures. (2)P Prestressing tendons shall have an acceptably low level of susceptibility to stress corrosion. (3) The level of susceptibility to stress corrosion may be assumed to be acceptably low if the prestressing tendons comply with the criteria specified in EN 10138 or given in an appropriate European Technical Approval.	

(continued on next page)

**Table A.3. Summary of Clauses Relating to the Serviceability Limit State Design of Concrete Bridges in Eurocode EN 1992-1 (continued)**

Eurocode Article	Basic Provision	Discussion
Eurocode 2 <b>Section 4 Durability and cover to reinforcement</b> <b>4.1 General</b>	(1)P A durable structure shall meet the requirements of serviceability, strength, and stability throughout its design working life, without significant loss of utility or excessive unforeseen maintenance (for general requirements see also EN 1990). (2)P The required protection of the structure shall be established by considering its intended use, design working life (see EN 1990), maintenance program, and actions. (3)P The possible significance of direct and indirect actions, environmental conditions (4.2), and consequential effects shall be considered.  NOTE: Examples include deformations due to creep and shrinkage (see 2.3.2).	
Eurocode 2 <b>Section 5 Structural analysis</b> <b>5.2 Geometric imperfections</b>	(3) Imperfections need not be considered for serviceability limit states.	
Eurocode 2 <b>5.4 Linear elastic analysis</b>	(1) Linear analysis of elements based on the theory of elasticity may be used for both the serviceability and ultimate limit states. (3) For thermal deformation, settlement, and shrinkage effects at the ultimate limit state (ULS), a reduced stiffness corresponding to the cracked sections, neglecting tension stiffening but including the effects of creep, may be assumed. For the serviceability limit state (SLS), a gradual evolution of cracking should be considered.	
Eurocode 2 <b>5.6 Plastic analysis</b> <b>5.6.4 Analysis with strut-and-tie models</b>	(2) Verifications in SLS may be carried out using strut-and-tie models (e.g. verification of steel stresses and crack width control) if approximate compatibility for strut-and-tie models is ensured (in particular the position and direction of important struts should be oriented according to linear elasticity theory).	
Eurocode 2 <b>5.7 Non-linear analysis</b>	(1) Non-linear methods of analysis may be used for both ULS and SLS, provided that equilibrium and compatibility are satisfied and an adequate non-linear behavior for materials is assumed. The analysis may be first or second order. (105) Non-linear analysis may be used, provided that the model can appropriately cover all failure modes (e.g. bending, axial force, shear, compression failure affected by reduced effective concrete strength) and that the concrete tensile strength is not utilized as a primary load resisting mechanism. If one analysis is not sufficient to verify all the failure mechanisms, separate additional analyses should be carried out. The following design format should be used: – The resistance should be evaluated for different levels of appropriate actions which should be increased from their serviceability values by incremental steps, such that the value of $\gamma_c \cdot G_k$ and $\gamma_c \cdot Q_k$ are reached in the same step. The incrementing process should be continued until one region of the structure attains the ultimate strength, evaluated taking account of $\alpha_{cc}$ , or there is global failure of the structure. The corresponding load is referred to as $q_{ud}$ .  Further steps in the design format that should be used are given.	
Eurocode 2 <b>5.10 Prestressed members and structures</b> <b>5.10.9 Effects of prestressing at serviceability limit state and limit state of fatigue</b>	(1)P For serviceability and fatigue calculations, allowance shall be made for possible variations in prestress. Two characteristic values of the prestressing force at the serviceability limit state are estimated. These are based on the upper characteristic value and the lower characteristic value.	
Eurocode 2 <b>Section 7 Serviceability limit states (SLS)</b> <b>7.1 General</b>	(1)P This section covers the common serviceability limit states. These are – stress limitation (see 7.2), – crack control (see 7.3), and – deflection control (see 7.4). Other limit states (such as vibration) may be of importance in particular structures but are not covered in this standard.	

(continued on next page)

**Table A.3. Summary of Clauses Relating to the Serviceability Limit State Design of Concrete Bridges in Eurocode EN 1992-1 (continued)**

Eurocode Article	Basic Provision	Discussion
	<p>(2) In the calculation of stresses and deflections, cross sections should be assumed to be uncracked, provided that the flexural tensile stress does not exceed <math>f_{ct,eff}</math>. The value of <math>f_{ct,eff}</math> may be taken as <math>f_{ctm}</math> or <math>f_{ctm,n}</math>, provided that the calculation for minimum tension reinforcement is also based on the same value. For the purposes of calculating crack widths and tension stiffening, <math>f_{ctm}</math> should be used.</p>	
<p>Eurocode 2 <b>7.2 Stress limitation</b></p>	<p>(1)P The compressive stress in the concrete shall be limited to avoid longitudinal cracks, micro-cracks, or high levels of creep, where they could result in unacceptable effects on the function of the structure.</p> <p>(102) Longitudinal cracks may occur if the stress level under the characteristic combination of loads exceeds a critical value. Such cracking may lead to a reduction of durability. In the absence of other measures, such as an increase in the cover to reinforcement in the compressive zone or confinement by transverse reinforcement, it may be appropriate to limit the compressive stress to the value <math>k_1 f_{ck}</math> in areas exposed to environments of exposure classes XD, XF, and XS (see Table 4.1 of EN 1992-1-1).</p> <p>NOTE: The value of <math>k_1</math> for use in a country may be found in its National Annex. The recommended value is 0.6. The maximum increase in the stress limit above <math>k_1 f_{ck}</math> in the presence of confinement may also be found in a country's National Annex. The recommended maximum increase is 10%.</p> <p>NOTE: British National Document PD 6687:2006 (Background paper to the UK National Annexes to BS EN 1992-1) gives non-contradictory complimentary information for use with EN 1992-1. In particular, when considering stress limitation in serviceability it notes</p> <p>a) Stress checks in reinforced concrete members have not been required in the UK for the past 50 years or so, and there has been no known adverse effect. Provided that the design has been carried out properly for ultimate limit state, there will be no significant effect at serviceability in respect of longitudinal cracking.</p> <p>b) There has been no evidence either from research or practice that there is a correlation between high compressive stress and durability problems.</p> <p>(3) If the stress in the concrete under the quasi-permanent loads is less than <math>k_2 f_{ck}</math>, linear creep may be assumed. If the stress in concrete exceeds <math>k_2 f_{ck}</math>, non-linear creep should be considered (see 3.1.4).</p> <p>NOTE: The value of <math>k_2</math> for use in a country may be found in its National Annex. The recommended value is 0.45.</p> <p>(4)P Tensile stresses in the reinforcement shall be limited to avoid inelastic strain, unacceptable cracking, or deformation.</p> <p>(5) When structural appearance is considered, unacceptable cracking or deformation may be assumed to be avoided if, under the characteristic combination of loads, the tensile strength in the reinforcement does not exceed <math>k_3 f_{yk}</math>. Where the stress is caused by an imposed deformation, the tensile strength should not exceed <math>k_4 f_{yk}</math>. The mean value of the stress in pre-stressing tendons should not exceed <math>k_5 f_{yk}</math>.</p> <p>NOTE: The values of <math>k_3</math>, <math>k_4</math>, and <math>k_5</math> for use in a country may be found in its National Annex. The recommended values are 0.8, 1, and 0.75, respectively.</p>	
<p>Eurocode 2 <b>7.3 Crack control</b> <b>7.3.1 General considerations</b></p>	<p>(1)P Cracking shall be limited to an extent that will not impair the proper functioning or durability of the structure or cause its appearance to be unacceptable.</p> <p>(2) Cracking is normal in reinforced concrete structures subject to bending, shear, torsion, or tension resulting from either direct loading or restraint or imposed deformations.</p> <p>(3) Cracks may also arise from other causes such as plastic shrinkage or expansive chemical reactions within the hardened concrete. Such cracks may be unacceptably large, but their avoidance and control lie outside the scope of this section.</p> <p>(4) Cracks may be permitted to form without any attempt to control their width, provided they do not impair the functioning of the structure.</p>	

(continued on next page)

**Table A.3. Summary of Clauses Relating to the Serviceability Limit State Design of Concrete Bridges in Eurocode EN 1992-1 (continued)**

Eurocode Article	Basic Provision	Discussion
	<p>(105) A limiting calculated crack width <math>w_{max}</math>, taking account of the proposed function and nature of the structure and the costs of limiting cracking, should be established. Due to the random nature of the cracking phenomenon, actual crack widths cannot be predicted. However, if the crack widths calculated in accordance with the models given in this standard are limited to the values given in Table 7.101N, the performance of the structure is unlikely to be impaired.</p> <p>NOTE: The value of <math>w_{max}</math> and the definition of decompression and its application for use in a country may be found in its National Annex. The recommended value for <math>w_{max}</math> and the application of the decompression limit are given in Table 7.101N. The recommended definition of decompression is noted in the text under the table.</p> <p>NOTE: British National Document PD 6687-2:2008 (Recommendations for the design of structures to BS EN 1992-2:2005) gives non-contradictory complimentary information for use with EN 1992-2. In particular, it contains a Section 8, Serviceability limit states. Under 8.2.1 it makes recommendations for the values of <math>w_{max}</math> and notes a lack of clarity. Under 8.2.2 it offers a simplification in crack calculation methods. Under 8.2.3 it gives guidance on calculating crack widths due to early age restraint of imposed deformations, which can arise due to early thermal contraction and shrinkage. Such effects should be taken into account in design.</p> <p>(6) For members with only unbonded tendons, the requirements for reinforced concrete elements apply. For members with a combination of bonded and unbonded tendons, requirements for prestressed concrete members with bonded tendons apply.</p> <p>(7) Special measures may be necessary for members subjected to exposure class XD3. The choice of appropriate measures will depend upon the nature of the aggressive agent involved.</p> <p>(8) When using strut-and-tie models with the struts oriented according to the compressive stress trajectories in the uncracked state, it is possible to use the forces in the ties to obtain the corresponding steel stresses to estimate the crack width [see 5.6.4 (2)].</p> <p>(9) Crack widths may be calculated according to 7.3.4. A simplified alternative is to limit the bar size or spacing according to 7.3.3.</p> <p>(110) In some cases it may be necessary to check and control shear cracking in webs.</p> <p>NOTE: Further information may be found in Annex QQ.</p>	
<p>Eurocode 2</p> <p><b>7.3 Crack control</b></p> <p><b>7.3.2 Minimum reinforcement areas</b></p>	<p>(1)P If crack control is required, a minimum amount of bonded reinforcement is required to control cracking in areas where tension is expected. The amount may be estimated from equilibrium between the tensile force in concrete just before cracking and the tensile force in reinforcement at yielding or at a lower stress if necessary to limit the crack width.</p> <p>(102) Unless a more rigorous calculation shows lesser areas to be adequate, the required minimum areas of reinforcement may be calculated; a procedure is given.</p> <p>(3) Bonded tendons in the tension zone may be assumed to contribute to crack control within a distance 5 150 mm from the centre of the tendon.</p> <p>(4) In prestressed members, no minimum reinforcement is required in sections where, under the characteristic combination of loads and the characteristic value of prestress, the concrete is compressed or the absolute value of the tensile stress in the concrete is below a given value.</p>	
<p>Eurocode 2</p> <p><b>7.3 Crack control</b></p> <p><b>7.3.3 Control of cracking without direct calculation</b></p>	<p>(101) The control of cracking without direct calculation may be performed by means of simplified methods. A recommended method is given with several sub-clauses indicating where crack control is deemed to be adequate, provided relevant detailing rules have been followed.</p>	
<p>Eurocode 2</p> <p><b>7.3 Crack control</b></p> <p><b>7.3.4 Calculation of crack widths</b></p>	<p>(101) The evaluation of crack width may be performed using recognized methods.</p> <p>NOTE: Details of recognized methods for crack width control may be found in a country's National Annex. The recommended method is that in EN 1992-1-1, 7.3.4.</p>	

(continued on next page)

**Table A.3. Summary of Clauses Relating to the Serviceability Limit State Design of Concrete Bridges in Eurocode EN 1992-1 (continued)**

Eurocode Article	Basic Provision	Discussion
Eurocode 2 <b>7.4 Deflection control</b> <b>7.4.1 General considerations</b>	(1)P The deformation of a member or structure shall not be such that it adversely affects its proper functioning or appearance. (2) Appropriate limiting values of deflection taking into account the nature of the structure, of the finishes, partitions and fixings and upon the function of the structure should be established.	
Eurocode 2 <b>7.4 Deflection control</b> <b>7.4.3 Checking deflections by calculation</b>	(1)P Where a calculation is deemed necessary, the deformations shall be calculated under load conditions which are appropriate to the purpose of the check. (2) P The calculation method adopted shall represent the true behavior of the structure under relevant actions to an accuracy appropriate to the objectives of the calculation. (3) Members which are not expected to be loaded above the level which would cause the tensile strength of the concrete to be exceeded anywhere within the member should be considered to be uncracked. Members which are expected to crack, but may not be fully cracked, will behave in a manner intermediate between the uncracked and fully cracked conditions. And for members subjected mainly to flexure, an adequate prediction of behavior is given by Expression (7.18) presented in EN 1992-1.1. (4) Deformations due to loading may be assessed using the tensile strength and modulus of elasticity of the concrete [see (5)]. (5) For loads with a duration causing creep, the total deformation including creep may be calculated by using an effective modulus of elasticity for concrete according to Expression (7.20) presented in EN 1992-1.1. (6) Shrinkage curvatures may be assessed using Expression (7.21) presented in EN 1992-1.1. (7) The most rigorous method of assessing deflections using the method given in (3) above is to compute the curvatures at frequent sections along the member and then calculate the deflection by numerical integration. In most cases it will be acceptable to compute the deflection twice, assuming the whole member to be in the uncracked and fully cracked condition in turn, and then interpolate using Expression (7.18).	
Eurocode 2 <b>Section 8 Detailing of reinforcement and prestressing tendons— General</b>	No rules peculiar to the serviceability limit state are given.	
Eurocode 2 <b>Section 9 Detailing of members and particular rules</b> <b>9.1 General</b>	(103) Minimum areas of reinforcement are given to prevent a brittle failure and wide cracks and also to resist forces arising from restrained actions.  NOTE: Additional rules concerning the minimum thickness of structural elements and the minimum reinforcement for all surfaces of members in bridges, with minimum bar diameter and maximum bar spacing for use in a country may be found in its National Annex. No additional rules are recommended in this standard.	
Eurocode 2 <b>Section 10 Additional rules for precast concrete elements and structures</b> <b>10.3 Materials</b> <b>10.3.1 Concrete</b> <b>10.3.1.1 Strength</b>	(1) For precast products in continuous production, subjected to an appropriate quality control system according to the product standards, with the concrete tensile strength tested, a statistical analysis of test results may be used as a basis for the evaluation of the tensile strength that is used for serviceability limit states verifications, as an alternative to Table 3.1. (2) Intermediate strength classes within Table 3.1 may be used.	
Eurocode 2 <b>Section 11 Lightweight aggregate concrete structures</b> <b>11.7 Serviceability limit states</b>	(1)P The basic ratios of span/effective depth for reinforced concrete members without axial compression, given in 7.4.2, should be reduced by a factor when applied to LWAC [lightweight aggregate concrete].	

(continued on next page)



**Table A.3. Summary of Clauses Relating to the Serviceability Limit State Design of Concrete Bridges in Eurocode EN 1992-1 (continued)**

Eurocode Article	Basic Provision	Discussion
Eurocode 2 <b>Section 12 Plain and lightly reinforced concrete structures</b> <b>12.1 General</b>	(4) Members using plain concrete do not preclude the provision of steel reinforcement needed to satisfy serviceability and/or durability requirements, nor reinforcement in certain parts of the members. This reinforcement may be taken into account for the verification of local ultimate limit states as well as for the checks of the serviceability limit states.	
Eurocode 2 <b>12.5 Structural analysis: ultimate limit states</b>	(1) Since plain concrete members have limited ductility, linear analysis with redistribution or a plastic approach to analysis (e.g. methods without an explicit check of the deformation capacity) should not be used unless their application can be justified. (2) Structural analysis may be based on the non-linear or the linear elastic theory. In the case of a non-linear analysis (e.g. fracture mechanics) a check of the deformation capacity should be carried out.	
Eurocode 2 <b>12.7 Serviceability limit states</b>	(1) Stresses should be checked where structural restraint is expected to occur. (2) The following measures to ensure adequate serviceability should be considered: a) with regard to crack formation, – limitation of concrete tensile stresses to acceptable values, – provision of subsidiary structural reinforcement (surface reinforcement, tying system where necessary), – provision of joints, – choice of concrete technology (e.g. appropriate concrete composition, curing), and – choice of appropriate method of construction. b) with regard to limitation of deformations, – a minimum section size, and – limitation of slenderness in the case of compression members. (3) Any reinforcement provided in plain concrete members, although not taken into account for load bearing purposes, should comply with 4.4.1.	
Eurocode 2 <b>Section 113 Design for the execution stages</b> <b>113.3 Verification criteria</b> <b>113.3.2 Serviceability limit states</b>	(101) The verifications for the execution stage should be the same as those for the completed structure, with the following exceptions. (102) Serviceability criteria for the completed structure need not be applied to intermediate execution stages, provided that durability and final appearance of the completed structure are not affected (e.g. deformations). (103) Even for bridges or elements of bridges in which the limit state of decompression is checked under the quasi-permanent or frequent combination of actions on the completed structure, tensile stresses less than $k.f_{ctm}(t)$ under the quasi-permanent combination of actions during execution are permitted.  NOTE: The value of $k$ to be used in a country may be found in its National Annex. The recommended value of $k$ is 1.0. (104) For bridges or elements of bridges in which the limit-state of cracking is checked under frequent combination on the completed structure, the limit state of cracking should be verified under the quasi-permanent combination of actions during execution.	
Eurocode 2 <b>Annex B (informative)</b> <b>Creep and shrinkage strain</b> <b>B.100 General</b>	(101) This Annex may be used for calculating creep and shrinkage, including development with time. However, typical experimental values can exhibit a scatter of $\pm 30\%$ around the values of creep and shrinkage predicted in accordance with this Annex. Where greater accuracy is required due to the structural sensitivity to creep and/or shrinkage, an experimental assessment of these effects and of the development of delayed strains with time should be undertaken. Section B.104 includes guidelines for the experimental determination of creep and shrinkage coefficients.	

(continued on next page)

**Table A.3. Summary of Clauses Relating to the Serviceability Limit State Design of Concrete Bridges in Eurocode EN 1992-1 (continued)**

Eurocode Article	Basic Provision	Discussion
Eurocode 2 <b>Annex E (informative)</b> <b>Indicative strength classes for durability</b> <b>E.1 General</b>	(1) The choice of adequately durable concrete for corrosion protection of reinforcement and protection of concrete attack requires consideration of the composition of concrete. This may result in a higher compressive strength of the concrete than is required for structural design. The relationship between concrete strength classes and exposure classes (see Table 4.1) may be described by indicative strength classes.  (2) When the chosen strength is higher than that required for structural design, the value of $f_{ctm}$ should be associated with the higher strength in the calculation of minimum reinforcement according to 7.3.2 and 9.2.1.1 and crack width control according to 7.3.3 and 7.3.4.	
Eurocode 2 <b>Annex F (informative)</b> <b>Tension reinforcement expressions for in-plane stress conditions</b> <b>F.1 General</b>	To avoid unacceptable cracks for the serviceability limit state, and to ensure the required deformation capacity for the ultimate limit state, the reinforcement derived from Expressions (F.8) and (F.9) for each direction should not be more than twice and not less than half the reinforcement determined by Expressions (F.2) and (F.3) or (F.5) and (F.6).	
Eurocode 2 <b>Annex G (informative)</b> <b>Soil structure interaction</b> <b>G.1 Shallow foundations</b> <b>G.1.1 General</b>	(1) The interaction between the ground, the foundation, and the superstructure should be considered. The contact pressure distribution on the foundations and the column forces are both dependent on the relative settlements. More guidance is given in this annex.	
Eurocode 2 <b>G.1.2 Levels of analysis</b>	(1) For design purposes, various levels of analysis are permitted, depending on conditions at both the serviceability and the ultimate limit states. More guidance is given.	
Eurocode 2 <b>Annex KK (informative)</b> <b>Structural effects of time-dependent behavior of concrete</b> <b>KK.1 Introduction</b>	This Annex describes different methods of evaluating the time-dependent effects of concrete behavior.	
Eurocode 2 <b>KK.2 General considerations</b>	(101) Structural effects of time-dependent behavior of concrete, such as variation of deformation and/or of internal actions, shall be considered, in general, in serviceability conditions.  NOTE: In particular cases (e.g. structures or structural elements sensitive to second order effects or structures in which action effects cannot be redistributed), time-dependent effects may also have an influence at ULS.  (102) It is noted that for higher compressive stresses, non-linear creep effects should be considered. (104) Different types of analysis and their typical applications are shown in a table.  Brief outline details of some of the analysis methods are given in the sections that follow.	
Eurocode 2 <b>Annex QQ (informative)</b> <b>Control of shear cracks within webs</b>	At present, the prediction of shear cracking in webs is accompanied by large model uncertainty. Where it is considered necessary to check shear cracking, particularly for prestressed members, the reinforcement required for crack control can be determined. Some detailed guidance is given.	

## A.5 EN 1993 Eurocode 3: Design of Steel Structures

The scope of EN 1993 is wider than most of the other design Eurocodes due to the diversity of steel structures. This Eurocode covers both bolted and welded joints, and the possible slenderness of construction. The differences when compared with existing British standards are that the Eurocode brings new methods into the scope. For example, the design of semi-rigid joints in buildings is explained, and more advanced methods of design for cold-formed steelwork are included. The rules for shell structures and for the design of piles, sheet piling, and silos are new, and rules for stainless steel appear for the first time.

EN 1993 has 20 parts covering common rules for fire design, bridges, buildings, tanks, silos, pipelined piling, crane supported structures, chimneys, towers and masts, and so on, as in the following list. Those underlined have been reviewed in the compilation of this report.

<u>EN 1993-1.1:2005</u>	<u>Design of steel structures. General rules and rules for buildings</u>
EN 1993-1.2:2005	Design of steel structures. General rules. Structural fire design
EN 1993-1.3:2006	Design of steel structures. General rules. Supplementary rules for cold-formed members and sheeting
EN 1993-1.4:2006	Design of steel structures. General rules. Supplementary rules for stainless steels
<u>EN 1993-1.5:2006</u>	<u>Design of steel structures. Plated structural elements</u>
EN 1993-1.6:2007	Design of steel structures. General. Strength and stability of shell structures
<u>EN 1993-1.7:2007</u>	<u>Design of steel structures. General. Plated structures subject to out of plane loading</u>
<u>EN 1993-1.8:2005</u>	<u>Design of steel structures. Design of joints</u>
EN 1993-1.9:2005	Design of steel structures. Fatigue strength
EN 1993-1.10:2005	Design of steel structures. Material toughness and through-thickness properties
<u>EN 1993-1.11:2006</u>	<u>Design of steel structures. Design of structures with tension components</u>
EN 1993-1.12:2007	Design of steel structures. Additional rules for the extension of EN 1993 up to steel grades S 700
<u>EN 1993-2:2006</u>	<u>Design of steel structures. Steel bridges</u>
EN 1993-3.1:2007	Design of steel structures. Towers, masts, and chimneys. Towers and masts
EN 1993-3.2:2008	Design of steel structures. Towers, masts, and chimneys. Chimneys

EN 1993-4.1:2007	Design of steel structures. Silos, tanks, and pipelines. Silos
EN 1993-4.2:2007	Design of steel structures. Silos, tanks, and pipelines. Tanks
EN 1993-4.3:2007	Design of steel structures. Silos, tanks, and pipelines. Pipelines
EN 1993-5:2007	Design of steel structures. Piling
EN 1993-6:2007	Design of steel structures. Crane supporting structures

Note also

EN 1090-2:2008	Execution of steel structures and aluminum structures. Technical requirements for the execution of steel structures
PD 6695-1.9:2008	Recommendations for the design of structures to BS EN 1993-1.9
PD 6695-1.10:2009	Recommendations for the design of structures to BS EN 1993-1.10
<u>PD 6695-2:2008</u>	<u>Recommendations for the design of bridges to BS EN 1993</u>

EN 1993-2:2006 (*Design of steel structures. Steel bridges*) provides a general basis for the structural design of steel bridges and steel parts of composite bridges. EN 1993-2 gives design rules which are supplementary to the generic rules in EN 1993-1-1. EN 1993-2 is intended to be used with Eurocodes EN 1990 (*Basis of design*), EN 1991 (*Actions on structures*), and the Parts 2 of EN 1992 to EN 1998 when steel structures or steel components for bridges are referred to. Matters that are already covered in those documents are not repeated within EN 1993-2.

Sections from this standard (and, where noted, the other highlighted parts of EN 1993) relating to the serviceability limit state are summarized in Table A.4.

## A.6 EN 1994 Eurocode 4: Design of Composite Steel and Concrete Structures

Eurocode 4 applies to the design of composite structures and members for buildings and civil engineering works. It complies with the principles and requirements for the safety and serviceability of structures, the basis of their design, and verification that are given in EN 1990:2002 (*Basis of structural design*). Eurocode 4 is concerned only with requirements for resistance, serviceability, durability, and fire resistance of composite structures. Other requirements (*e.g.* concerning thermal or sound insulation) are not considered.

Eurocode 4 is intended to be used in conjunction with

EN 1990	Basis of structural design
EN 1991	Actions on structures

(text continues on page 289)

**Table A.4. Summary of Clauses Relating to the Serviceability Limit State Design of Steel Bridges in Eurocode EN 1993-1 and 1993-2**

Eurocode Article	Basic Provision	Discussion
Eurocode 3 <b>Section 2 Basis of design and modeling</b> <b>2.1 General</b>	<p><b>EN 1993-1.5 (Plated structural elements) stipulates</b>            (1)P The effects of shear lag and plate buckling shall be taken into account at the ultimate, serviceability, or fatigue limit states.</p> <p><b>EN 1993-1.11 (Tension components) stipulates</b>            2.2(1)P Due to the difficulties in modeling the excitation characteristics of tension elements, serviceability limit state checks should be carried out in addition to fatigue checks.            2.2(3) Any attachments to prefabricated tension components, such as saddles or clamps, should be designed for ultimate limit states and serviceability limit states using the breaking strength or proof strength of cables as actions; see Section 6. For fatigue see EN 1993-1-9.</p> <p>NOTE: Fatigue action on the ropes is governed by the radius in the saddle or anchorage area (see Figure 6.1 for minimum radius).</p>	
Eurocode 3 <b>2.3 Plate buckling effects on uniform members</b>	<p><b>EN 1993-1.5 (Plated structural elements) stipulates</b>            (2) For the calculation of stresses at the serviceability and fatigue limit state the effective area may be used if the condition in 3.1 is fulfilled. For ultimate limit states the effective area according to 3.3 should be used with <math>\beta</math> replaced by <math>\beta_{ult}</math>.</p>	
Eurocode 3 <b>Section 3 Shear lag in member design</b> <b>3.1 General</b>	<p><b>EN 1993-1.5 (Plated structural elements) stipulates</b>            (1) Shear lag in flanges may be neglected if <math>b_0 &lt; Le/50</math> where <math>b_0</math> is taken as the flange outstand or half the width of an internal element and <math>Le</math> is the length between points of zero bending moment; see 3.2.1(2).            (2) Where the above limit for <math>b_0</math> is exceeded, the effects due to shear lag in flanges should be considered at serviceability and fatigue limit state verifications by the use of an effective width according to 3.2.1 and a stress distribution according to 3.2.2. For the ultimate limit state verification an effective area according to 3.3 may be used.</p>	
Eurocode 3 <b>3.2 Effective width for elastic shear lag</b> <b>3.2.1 Effective width</b>	<p><b>EN 1993-1.5 (Plated structural elements) stipulates</b>            (1) The effective width <math>b_{eff}</math> for shear lag under elastic conditions should be determined from</p> $b_{eff} = \beta b_0 \quad (3.1)$ <p>where the effective factor <math>\beta</math> is given in Table 3.1.            This effective width may be relevant for serviceability and fatigue limit states.</p> <p><b>EN 1993-1.5 Annex E</b> gives alternative methods for determining effective cross sections. It gives a calculation for the serviceability limit slenderness to give effective area for stiffness. It also gives that</p> <p>(3) The effective second moment of area <math>I_{eff}</math> may be taken as variable along the span according to the most severe locations. Alternatively a uniform value may be used based on the maximum absolute sagging moment under serviceability loading.</p>	
Eurocode 3 <b>Section 4 Durability</b>	<p>(6) Components that cannot be designed with sufficient reliability to achieve the total design working life of the bridge should be replaceable. These may include</p> <ul style="list-style-type: none"> <li>– stays, cables, hangers;</li> <li>– bearings;</li> <li>– expansion joints;</li> <li>– drainage devices;</li> <li>– guardrails, parapets;</li> <li>– asphalt layer and other surface protection;</li> <li>– wind shields; and</li> <li>– noise barriers.</li> </ul> <p><b>EN 1993-1.11 (Tension components)</b> contains a section (4) devoted to durability of wires, ropes, and strands. This gives details of corrosion protection for the three classes of tension components defined at the beginning of this standard.</p> <p><b>EN 1993-1.11 (Tension components)</b> covers transport, storage, and handling of tension components in its Annex B (informative).</p>	

(continued on next page)

**Table A.4. Summary of Clauses Relating to the Serviceability Limit State Design of Steel Bridges in Eurocode EN 1993-1 and 1993-2 (continued)**

Eurocode Article	Basic Provision	Discussion
<p>Eurocode 3</p> <p><b>Section 7 Serviceability limit states</b></p> <p><b>7.1 General</b></p>	<p>(1) A steel structure should be designed and constructed such that all relevant serviceability criteria are satisfied.</p> <p>(2) The basic requirements for serviceability limit states are given in 3.4 of EN 1990.</p> <p>(3) Any serviceability limit state and the associated loading and analysis model should be specified for a project.</p> <p>(4) The following serviceability criteria should be met:</p> <ul style="list-style-type: none"> <li>a) Restriction to elastic behavior to limit <ul style="list-style-type: none"> <li>– excessive yielding, see 7.3(1);</li> <li>– deviations from the intended geometry by residual deflections, see 7.3(1); and</li> <li>– excessive deformations, see 7.3(4).</li> </ul> </li> <li>b) Limitation of deflections and curvature to prevent <ul style="list-style-type: none"> <li>– unwanted dynamic impacts due to traffic (combination of deflection and natural frequency limitations), see 7.7 and 7.8;</li> <li>– infringement of required clearances, see 7.5 or 7.6;</li> <li>– cracking of surfacing layers, see 7.8; and</li> <li>– damage of drainage, see 7.12.</li> </ul> </li> <li>c) Limitation of natural frequencies (see 7.8 and 7.9) to <ul style="list-style-type: none"> <li>– exclude vibrations due to traffic or wind which are unacceptable to pedestrians or passengers in cars using the bridge;</li> <li>– limit fatigue damages caused by resonance; and</li> <li>– limit excessive noise emission.</li> </ul> </li> <li>d) Restriction of plate slenderness (see 7.4) to limit <ul style="list-style-type: none"> <li>– excessive rippling of plates;</li> <li>– breathing of plates; and</li> <li>– reduction of stiffness due to plate buckling, resulting in an increase of deflection, see EN 1993-1-5.</li> </ul> </li> <li>e) Improved durability by appropriate detailing to reduce corrosion and excessive wear; see 7.11.</li> <li>f) Ease of maintenance and repair (see 7.11) to ensure <ul style="list-style-type: none"> <li>– accessibility of structural parts for maintenance and inspection, renewal of corrosion protection and asphaltic pavements; and</li> <li>– replacement of bearings, anchors, cables, expansion joints with minimum disruption to the use of the structure.</li> </ul> </li> </ul> <p>(5) In most situations serviceability aspects should be dealt with in the conceptual design of the bridge, or by suitable detailing. However, in appropriate cases, serviceability limit states may be verified by numerical assessment (e.g. for calculating deflections or Eigen frequencies).</p> <p>NOTE: The National Annex may give guidance on serviceability requirements for specific types of bridges.</p> <p><b>EN 1993-1.11 (Tension components) stipulates</b></p> <p>7.1(1) The following serviceability criteria should be considered:</p> <ol style="list-style-type: none"> <li>1. Deformations or vibrations, and</li> <li>2. Elastic service conditions.</li> </ol> <p>NOTE 1: Limits for deformations or vibrations may result in a stiffness requirement governed by the structural system, the dimensions and the preloading of high-strength tension components, and by the slipping resistance of attachments.</p> <p>NOTE 2: Limits to retain elastic behavior and durability are related to maximum and minimum values of stresses for serviceability load combinations.</p> <p>7.1(2) Bending stresses in the anchorage zone may be reduced by suitable measures (e.g. neoprene pads for transverse loading).</p>	
<p>Eurocode 3</p> <p><b>7.2 Calculation models</b></p>	<p>(1) Stresses at serviceability limit states should be determined from a linear elastic analysis, using the appropriate section properties; see EN 1993-1-5.</p> <p>(2) In modeling the structure, the non-uniform distribution of loads and stiffness resulting from the changes in plate thickness, stiffening, etc. should be taken into account.</p> <p>(3) Deflections should be determined by linear elastic analysis using the appropriate section properties; see EN 1993-1-5.</p> <p>NOTE: Simplified calculation models may be used for stress calculations, provided that the effects of the simplification are conservative.</p>	

(continued on next page)

**Table A.4. Summary of Clauses Relating to the Serviceability Limit State Design of Steel Bridges in Eurocode EN 1993-1 and 1993-2 (continued)**

Eurocode Article	Basic Provision	Discussion
<p>Eurocode 3</p> <p><b>7.3 Limitations for stress</b></p>	<p>(1) The nominal stresses <math>\sigma_{Ed,ser}</math> and <math>\tau_{Ed,ser}</math> resulting from the characteristic load combinations, calculated making due allowance for the effects of shear lag in flanges and the secondary effects caused by deflections (e.g. secondary moments in trusses), should be limited. The standard gives equations for maximum allowable stresses.</p> <p>NOTE 1: Where relevant, the above checks should include stresses <math>\sigma_z</math> from transverse loads; see EN 1993-1-5.</p> <p>NOTE 2: The National Annex may give the value for <math>\gamma_{Mser}</math>. <math>\gamma_{Mser} = 1,00</math> is recommended.</p> <p>NOTE 3: Plate buckling effects may be ignored as specified in EN 1993-1-5, 2.2(5).</p> <p>(2) The nominal stress range <math>\Delta\sigma_{fre}</math>, due to the frequent load combination, should be limited to <math>1.5 f_y/\gamma_{Mser}</math>; see EN 1993-1-9.</p> <p>(3) For non-preloaded bolted connections subject to shear, the bolt forces due to the characteristic load combination should be limited to</p> $F_{b,Rd,ser} \leq 0.7 F_{b,Rd} \quad (7.4)$ <p>where <math>F_{b,Rd}</math> is the bearing resistance for ultimate limit states verifications.</p> <p>(4) For slip-resistant preloaded bolted connections category B (slip-resistant at serviceability, see EN 1993-1-8), the assessment for serviceability should be carried out using the characteristic load combination.</p> <p><b>EN 1993-1.11 (Tension components) stipulates</b></p> <p>7.2(1) Limiting stress may be specified for the characteristic load combination for the following purposes:</p> <ul style="list-style-type: none"> <li>– to keep stresses in the elastic range for the relevant design situations during construction and in the service phase;</li> <li>– to limit strains such that corrosion control measures are not affected (i.e., cracking of sheaths, hard fillers, opening of joints) and also to cater for uncertainty in the fatigue design;</li> <li>– ULS verifications for linear and sub-linear structural response to actions.</li> </ul> <p>Numeric values of limiting stress in the serviceability limit state are given.</p>	
<p>Eurocode 3</p> <p><b>7.4 Limitation of web breathing</b></p>	<p>(1) The slenderness of web plates should be limited to avoid excessive breathing that might result in fatigue at or adjacent to the web-to-flange connections.</p> <p>NOTE: The National Annex may define cases where web breathing checks are not necessary.</p> <p>(2) Web breathing may be neglected for web panels without longitudinal stiffeners or for subpanels of stiffened webs, where certain criteria are met. (Criteria for road bridges and for rail bridges are given in the standard. If the criteria are not met, a method for checking web breathing is given.)</p> <p><b>NOTE also EN 1993-1.7 (Plated structures subject to out of plane loading)</b> gives a note (8.2) on the out of plane deflection limit as the condition in which the effective use of a plate segment is ended.</p>	
<p>Eurocode 3</p> <p><b>7.6 Limits for visual impression</b></p>	<p>(1) To achieve a satisfactory appearance of the bridge, consideration should be given to precambering.</p> <p>(2) In calculating camber, the effects of shear deformation and slip in riveted or bolted connections should be considered.</p> <p>(3) For connections with rivets or fitted bolts, a fastener slip of 0.2 mm should be assumed. For preloaded bolts, slip does not need to be considered.</p>	
<p>Eurocode 3</p> <p><b>7.8 Performance criteria for road bridges</b></p> <p><b>7.8.1 General</b></p>	<p>(1) Excessive deformation should be avoided where it could</p> <ul style="list-style-type: none"> <li>– endanger traffic by excessive transverse slope when the surface is iced;</li> <li>– affect the dynamic load on the bridge by impact from wheels;</li> <li>– affect the dynamic behavior causing discomfort to users;</li> <li>– lead to cracks in asphaltic surfacing;</li> <li>– adversely affect the drainage of water from the bridge deck.</li> </ul> <p>NOTE: For durability requirements, see Annex C.</p>	

(continued on next page)



**Table A.4. Summary of Clauses Relating to the Serviceability Limit State Design of Steel Bridges in Eurocode EN 1993-1 and 1993-2 (continued)**

Eurocode Article	Basic Provision	Discussion
	<p>(2) Deformations should be calculated using the frequent load combination.</p> <p>(3) The natural frequency of vibrations and deflections of the bridge should be limited to avoid discomfort to users.</p> <p><b>NOTE also EN 1993-1.7 (Plated structures subject to out of plane loading)</b> gives guidance on excessive vibration limits:</p> <p>8.3(1) Excessive vibrations should be defined as the limit condition in which either the failure of a plated structure occurs by fatigue caused by excessive vibrations of the plate or serviceability limits apply.</p> <p><b>EN 1993-1.11 (Tension components)</b> contains a section (8) devoted to vibration of cables. A general section is followed by a section on measures to limit vibration of cables and a section giving estimation of risks.</p>	
<p>Eurocode 3</p> <p><b>7.8.2 Deflection limits to avoid excessive impact from traffic</b></p>	<p>(1) The deck structure should be designed to ensure that its deflection along the length is uniform and that there is no abrupt change in cross section giving rise to impact. Sudden changes in the slope of the deck and changes of level at the expansion joints should be eliminated. Any transverse girders at the end of the bridge should be designed to ensure that the deflection does not exceed</p> <ul style="list-style-type: none"> <li>– the limit specified for the proper functioning of the expansion joint;</li> <li>– 5 mm under frequent loads unless other limits are specified for the particular type of expansion joint.</li> </ul> <p>NOTE: Guidance on the deflection limit of expansion joints is given in Annex B.</p> <p>(2) Where the deck structure is irregularly supported (e.g. by additional bracings at intermediate bridge piers), the deck area adjacent to these additional deck supports should be designed for the enhanced impact factors given in EN 1991-2 for the area close to the expansion joints.</p>	
<p>Eurocode 3</p> <p><b>7.8.3 Resonance effects</b></p>	<p>(1) Mechanical resonance should be taken into account when relevant. Where light bracing members, cable stays, or similar components have natural frequencies that are close to the frequency of any mechanical excitation due to regular passage of vehicles over deck joints, consideration should be given to either increasing the stiffness or providing artificial dampers (i.e. oscillation dampers).</p> <p>NOTE: Guidance on members supporting expansion joints is given in Annex B.</p>	
<p>Eurocode 3</p> <p><b>7.12 Drainage</b></p>	<p>(1) All decks should be waterproofed, and the surfaces of carriageways and footpaths should be sealed to prevent the ingress of water.</p> <p>(2) The layout of the drainage should take into account the slope of the bridge deck as well as the location, diameter, and slope of the pipes.</p> <p>(3) Free fall drains should carry water to a point clear of the underside of the structure to prevent water entering into the structure.</p> <p>(4) Drainage pipes should be designed so that they can be cleaned easily. The distance between centers of the cleaning openings should be shown on drawings.</p> <p>(5) Where drainage pipes are used inside box girder bridges, provisions should be made to prevent accumulation of water during leaks or breakage of pipes.</p> <p>(6) For road bridges, drains should be provided at expansion joints on both sides where [it] is appropriate.</p> <p>(7) Provision should be made for the drainage of all closed cross sections, unless these are fully sealed by welding.</p>	
<p>Eurocode 3</p> <p><b>Section 8 Fasteners, welds, connections, and joints</b></p> <p><b>8.1 Connections made of bolts, rivets, and pins</b></p> <p><b>8.1.1 Categories of bolted connections</b></p>	<p><b>EN 1993-1.8 (Design of joints) stipulates</b></p> <p><b>3.4 Categories of bolted connections</b></p> <p><b>3.4.1 Shear connections</b></p> <p>(1) Bolted connections loaded in shear should be designed as one of the following:</p> <p>a) <b>Category A: Bearing type</b></p> <p>In this category, bolts from Class 4.6 up to and including Class 10.9 should be used. No preloading and special provisions for contact surfaces are required. The design ultimate shear load should not exceed the design shear resistance, obtained from 3.6, nor the design bearing resistance, obtained from 3.6 and 3.7.</p>	

(continued on next page)

**Table A.4. Summary of Clauses Relating to the Serviceability Limit State Design of Steel Bridges in Eurocode EN 1993-1 and 1993-2 (continued)**

Eurocode Article	Basic Provision	Discussion
	<p>b) <b>Category B: Slip-resistant at serviceability limit state</b>            In this category, preloaded bolts in accordance with 3.1.2(1) should be used. Slip should not occur at the serviceability limit state. The design serviceability shear load should not exceed the design slip resistance, obtained from 3.9. The design ultimate shear load should not exceed the design shear resistance, obtained from 3.6, nor the design bearing resistance, obtained from 3.6 and 3.7.</p> <p>c) <b>Category C: Slip-resistant at ultimate limit state</b>            In this category, preloaded bolts in accordance with 3.1.2(1) should be used. Slip should not occur at the ultimate limit state. The design ultimate shear load should not exceed the design slip resistance, obtained from 3.9, nor the design bearing resistance, obtained from 3.6 and 3.7. In addition, for a connection in tension, the design plastic resistance of the net cross section at bolt holes <math>N_{net,Rd}</math>, (see 6.2 of EN 1993-1-1), should be checked, at the ultimate limit state.</p> <p><b>3.4.2 Tension connections</b></p> <p>(1) Bolted connection loaded in tension should be designed as one of the following:</p> <p>a) <b>Category D: Non-preloaded</b>            In this category, bolts from Class 4.6 up to and including Class 10.9 should be used. No preloading is required. This category should not be used where the connections are frequently subjected to variations of tensile loading. However, they may be used in connections designed to resist normal wind loads.</p> <p>b) <b>Category E: Preloaded</b>            In this category, preloaded 8.8 and 10.9 bolts with controlled tightening in conformity with 1.2.7 Reference Standards: Group 7 should be used.            The design checks for these connections are summarized in Table 3.2.</p>	
<p>Eurocode 3</p> <p><b>Section 9 Fatigue assessment</b></p> <p><b>9.1 General</b></p> <p><b>9.1.1 Requirements for fatigue assessment</b></p>	<p>(1) Fatigue assessments should be carried out for all critical areas in accordance with EN 1993-1.9.</p> <p>(2) Fatigue assessment is not applicable to</p> <ul style="list-style-type: none"> <li>– pedestrian bridges, bridges carrying canals, or other bridges that are predominantly statically loaded, unless such bridges or parts of them are likely to be excited by wind loads or pedestrians;</li> <li>– parts of railway or road bridges that are neither stressed by traffic loads nor likely to be excited by wind loads.</li> </ul> <p><b>NOTE that EN 1993-1.9 (Fatigue)</b> specifies that the actions applied for a fatigue limit state verification are different from those used for ultimate limit state or for serviceability state. However, the stresses should be calculated at the serviceability state [Clause 5(1)].</p> <p><b>NOTE that EN 1993-1.11 (Tension components)</b> comments [2.2(1)P] that, due to the difficulties in modeling the excitation characteristics of tension elements, serviceability limit state checks should be carried out in addition to fatigue checks.</p>	
<p>Eurocode 3</p> <p><b>9.1.2 Design of road bridges for fatigue</b></p>	<p>(1) Fatigue assessments should be carried out for all bridge components unless the structural detailing complies with standard requirements for durable structures established through testing.</p> <p>NOTE: The National Annex may give guidance on the conditions where no fatigue assessment is necessary.</p> <p>(2) Fatigue assessment should be carried out using the procedure given in this section and EN 1993-1-9.</p>	
<p>Eurocode 3</p> <p><b>Section 10 Design assisted by testing</b></p> <p><b>10.1 General</b></p>	<p>(1) Design can be assisted by testing. If so, it should be in accordance with EN 1990, supplemented by the additional provisions given in 10.2 and 10.3.</p>	

(continued from page 283)

European Standards (ENs), Harmonized European Standards (hENs), Guidelines for European Technical Approval (ETAGs), and European Technical Approvals (ETAs) for construction products relevant for composite structures

EN 1090	Execution of steel structures and aluminum structures
EN 13670	Execution of concrete structures
EN 1992	Design of concrete structures
EN 1993	Design of steel structures
EN 1997	Geotechnical design
EN 1998	Design of structures for earthquake resistance

EN 1994 has three parts covering common rules and rules for buildings, structural fire design, and bridges, as in the following list. Those underlined have been reviewed in the compilation of this report.

EN 1994-1.1:2004	Design of composite steel and concrete structures. General rules and rules for buildings
EN 1994-1.2:2005	Design of composite steel and concrete structures. General rules. Structural fire design

EN 1994-2:2005      Design of composite steel and concrete structures. General rules and rules for bridges

Note also

PD 6696-2:2007      Recommendations for the design of structures to BS EN 1994-2:2005

EN 1994-2 describes the principles and requirements for safety, serviceability, and durability of composite steel and concrete structures, together with specific provisions for bridges. It is based on the limit state concept used in conjunction with a partial factor method. It gives design rules for steel-concrete composite bridges or members of bridges, additional to the general rules in EN 1994-1-1. Cable stayed bridges are not fully covered by this part.

EN 1994-2 contains the general rules from EN 1994-1-1 as well as the specific rules for the design of composite steel and concrete bridges or composite members of bridges.

EN 1994-2 is intended to be used with EN 1990, the relevant parts of EN 1991, EN 1992 for the design of concrete structures, and EN 1993 for the design of steel structures.

Sections from this standard (and, where noted, the other highlighted recommendations) relating to the serviceability limit state are summarized in Table A.5.

**Table A.5. Summary of Clauses Relating to Serviceability Limit State Design of Composite Steel and Concrete Bridges in Eurocode EN 1994-2**

Eurocode Article	Basic Provision	Discussion
Eurocode 4 <b>Section 2 Basis of design</b> <b>2.1 Requirements</b>	(3) The basic requirements of EN 1990:2002, Section 2 are deemed to be satisfied for composite structures when the following are applied together: – limit state design in conjunction with the partial factor method in accordance with EN 1990:2002; – actions in accordance with EN 1991; – combination of actions in accordance with EN 1990:2002; and – resistances, durability, and serviceability in accordance with this standard.	
Eurocode 4 <b>2.3.3 Classification of actions</b>	(1)P The effects of shrinkage and creep of concrete and non-uniform changes of temperature result in internal forces in cross sections, and curvatures and longitudinal strains in members; the effects that occur in statically determinate structures, and in statically indeterminate structures when compatibility of the deformations is not considered, shall be classified as primary effects. (2)P In statically indeterminate structures the primary effects of shrinkage, creep, and temperature are associated with additional action effects, such that the total effects are compatible; these shall be classified as secondary effects and shall be considered as indirect actions.	
Eurocode 4 <b>4.2 Corrosion protection at the steel-concrete interface in bridges</b>	(1) The corrosion protection of the steel flange should extend into the steel-concrete interface at least 50 mm. For additional rules for bridges with precast deck slabs, see Section 8.	
Eurocode 4 <b>Section 7 Serviceability limit states</b> <b>7.2 Stresses</b> <b>7.2.1 General</b>	(1)P Calculation of stresses for beams at the serviceability limit state shall take into account the following effects, where relevant: – shear lag; – creep and shrinkage of concrete; – cracking of concrete and tension stiffening of concrete; – sequence of construction;	

(continued on next page)

**Table A.5. Summary of Clauses Relating to Serviceability Limit State Design of Composite Steel and Concrete Bridges in Eurocode EN 1994-2 (continued)**

Eurocode Article	Basic Provision	Discussion
	<ul style="list-style-type: none"> <li>– increased flexibility resulting from significant incomplete interaction due to slip of shear connection;</li> <li>– inelastic behavior of steel and reinforcement, if any;</li> <li>– torsional and distortional warping, if any.</li> </ul> <p>(2) Shear lag may be taken into account according to 5.4.1.2.</p> <p>(3) Unless a more accurate method is used, effects of creep and shrinkage may be taken into account by use of modular ratios according to 5.4.2.2.</p> <p>(4) In cracked sections, the primary effects of shrinkage may be neglected when verifying stresses.</p> <p>(5)P In section analysis, the tensile strength of concrete shall be neglected.</p> <p>(6) The influence of tension stiffening of concrete between cracks on stresses in reinforcement and prestressing steel should be taken into account. Unless more accurate methods are used, the stresses in reinforcement should be determined according to 7.4.3.</p> <p>(7) The influences of tension stiffening on stresses in structural steel may be neglected.</p> <p>(8) Stresses in the concrete slab and its reinforcement caused by simultaneous global and local actions should be added.</p>	
<p>Eurocode 4</p> <p><b>7.2 Stresses</b></p> <p><b>7.2.2 Stress limitation for bridges</b></p>	<p>(1)P Excessive creep and microcracking shall be avoided by limiting the compressive stress in concrete.</p> <p>(2) Stress limitation for concrete to the value <math>k_1 f_{ck}</math> should be in accordance with EN 1991-1-1:2002, 7.2, as modified by EN 1992-2.</p> <p>(3)P The stress in reinforcing steel and in prestressing tendons shall be such that inelastic strains in the steel are avoided.</p> <p>(4) Under the characteristic combination of actions, the stresses should be limited to <math>k_1 f_{sk}</math> in reinforcing steel and to <math>k_5 f_{pk}</math> in tendons, where the values <math>k_1</math> and <math>k_5</math> are given in EN 1992-1-1:2004, 7.2(5).</p> <p>(5) The stresses in structural steel should be in accordance with EN 1993-2, 7.3.</p> <p>(6) For serviceability limit states, the longitudinal shear force per connector should be limited according to 6.8.1 (3).</p>	
<p>Eurocode 4</p> <p><b>7.2.3 Web breathing</b></p>	<p>(1) The slenderness of unstiffened or stiffened web plates of composite girders should be limited according to 7.4 of EN 1993-2.</p>	
<p>Eurocode 4</p> <p><b>7.3 Deformations in bridges</b></p> <p><b>7.3.1 Deflections</b></p>	<p>(1) For the limit state of deformation, EN 1990:2002; A2.4 of Annex A2; and EN 1993-2, 7.5 to 7.8 and 7.12 apply where relevant.</p> <p>(2) Deflections should be calculated using elastic analysis in accordance with Section 5.</p> <p>(3) Deformations during construction should be controlled such that the concrete is not impaired during its placing and setting by uncontrolled displacements and the required long-term geometry is achieved.</p>	
<p>Eurocode 4</p> <p><b>7.3.2 Vibrations</b></p>	<p>(1) For the limit state of vibration, EN 1990:2002; A2.4 of Annex A2; EN 1991-2:2003, 5.7 and 6.4; and EN 1993-2, 7.7 to 7.10 apply where relevant.</p>	
<p>Eurocode 4</p> <p><b>7.4 Cracking of concrete</b></p> <p><b>7.4.1 General</b></p>	<p>(1) For the limitation of crack width in bridges, the general considerations of EN 1992-1-1:2004, 7.3.1 as modified in EN 1992-2 apply to composite structures. The limitation of crack width depends on the exposure classes according to EN 1992-2, 4.</p> <p>(2) An estimation of crack width can be obtained from EN 1992-1-1:2004, 7.3.4, where the stress <math>\sigma_s</math> should be calculated by taking into account the effects of tension stiffening. Unless a more precise method is used, <math>\sigma_s</math> may be determined according to 7.4.3(3).</p> <p>(3) As a simplified and conservative alternative, crack width limitation to acceptable width can be achieved by ensuring a minimum reinforcement defined in 7.4.2, and bar spacing or diameters not exceeding the limits defined in 7.4.3.</p> <p>(4) Application rules for the limitation of crack widths to <math>w_k</math> are given in 7.4.2 and 7.4.3.</p> <p>NOTE: The values of <math>w_k</math> and the combination of actions may be found in the National Annex. The recommended values for relevant exposure classes are as given (as <math>w_{max}</math>) in the note to EN 1992-2, 7.3.1(105).</p>	

(continued on next page)

**Table A.5. Summary of Clauses Relating to Serviceability Limit State Design of Composite Steel and Concrete Bridges in Eurocode EN 1994-2 (continued)**

Eurocode Article	Basic Provision	Discussion
	<p>(5) Where composite action becomes effective as concrete hardens, effects of heat of hydration of cement and corresponding thermal shrinkage should be taken into account only during the construction stage for the serviceability limit state to define areas where tension is expected.</p> <p>(6) Unless specific measures are taken to limit the effects of heat of hydration of cement, for simplification a constant temperature difference between the concrete section and the steel section (concrete cooler) should be assumed for the determination of the cracked regions according to 7.4.2 (5) and for limitation of crack width according to 7.4.2 and 7.4.3. For the determination of stresses in concrete, the short-term modulus should be used.</p> <p>NOTE: The National Annex may give specific measures and a temperature difference. The recommended value for the temperature difference is 20K.</p>	
<p>Eurocode 4 <b>7.4.2 Minimum reinforcement</b></p>	<p>(1) Unless a more accurate method is used in accordance with EN 1992-1-1:2004, 7.3.2(1), in all sections without prestressing by tendons and subjected to significant tension due to restraint of imposed deformations (e.g. primary and secondary effects of shrinkage), in combination or not with effects of direct loading, the required minimum reinforcement area <math>A_s</math> for the slabs of composite beams is given in this section together with rules on its placement.</p>	
<p>Eurocode 4 <b>7.4.3 Control of cracking due to direct loading</b></p>	<p>(1) Where at least the minimum reinforcement given by 7.4.2 is provided, the limitation of crack widths to acceptable values may generally be achieved by limiting bar spacing or bar diameters. Maximum bar diameter and maximum bar spacing depend on the stress <math>\sigma_s</math> in the reinforcement and the design crack width are given in tables.</p> <p>(2) The internal forces should be determined by elastic analysis in accordance with Section 5, taking into account the effects of cracking of concrete. The stresses in the reinforcement should be determined taking into account effects of tension stiffening of concrete between cracks. Unless a more precise method is used, the stresses may be calculated according to the method given in (3).</p>	
<p>Eurocode 4 <b>7.5 Filler beam decks</b> (a deck consisting of a reinforced concrete slab and partially concrete-encased rolled or welded steel beams, having their bottom flange on the level of the slab bottom) <b>7.5.1 General</b></p>	<p>(1) The action effects for the serviceability limit states should be determined according to paragraphs given earlier in the standard (5.4.2.9). Rules for cracking of concrete, minimum reinforcement, and control of cracking due to direct loading are also given for filler beam decks in this section. Guidance for transverse filler beams is given in <b>PD 6696-2:2007</b>. It indicates that for the determination of stresses in the concrete slab and steel beams, the concrete slab and steel beams should be considered to be</p> <ul style="list-style-type: none"> <li>• non-composite at ultimate limit state (ULS)</li> <li>• composite and to have equal deflections at serviceability limit state (SLS).</li> </ul>	
<p>Eurocode 4 <b>Section 9 Composite plates in bridges</b> <b>9.1 General</b> <b>9.4 Design of shear connectors</b></p>	<p>(1)P Resistance to fatigue and requirements for serviceability limit states shall be verified for the combined local and simultaneous global effect.</p>	

**APPENDIX B**

**SHRP 2 R19B Survey of Bridge Owners**



### Questionnaire #1 Summary of Experience with Service Issues

Your Name and Title:

Your Phone Number and Email Address:

Please address the following questions as they relate to summarizing your experience by material type, structure type and subsystem, component and element type. The following are possible examples of these various features:

- Material Type: steel, plain concrete, reinforced concrete, prestressed concrete, etc.
- Structure Type: I girder bridge, box girder bridge, segmental bridges, truss, cable stayed, etc.
- Subsystems: superstructure, substructure, foundations, drainage systems, etc.
- Component: bearing, expansion joint

Please make as many copies of the appropriate questions as needed for the structure types, materials, subsystems or components for which you are responding.

#### General Questions

1. What are the five or ten most costly maintenance/durability items in your structural maintenance budget?
2. Does your agency utilize deterioration models other than those in Pontis? If so, What and why?
3. The current LRFD service limit states include limits on:
  - live load deflection of bridges,
  - cracking of reinforced-concrete components,
  - tensile stresses of prestressed-concrete components,
  - compressive stresses of prestressed concrete components,
  - permanent deformations of compact steel components,
  - slip of slip-critical friction bolted connections, and
  - settlement of shallow and deep foundations.

In your experience, are these service limit states adequate for your needs or are further safeguards required? If more are required, what should they guard against for what types of members, systems or details?

#### Specific Questions for Structure Type, Material Subsystem or Component

Structure Type:

Material:

Subsystem or Component if Appropriate:

4. What have you seen as the important service and durability issues (not strength) and bridge age affects that impact the serviceability of bridge components?
5. Have you seen issues resulting in reduced serviceability (or a trend in that direction) that could have been avoided if the design specifications had additional service (not strength) design requirements? If so, what?
6. What type of foundation/wall settlement or other movements have resulted in maintenance issues or reduced serviceability?
7. Do you make Quantitative/Qualitative condition assessments beyond what is in Pontis? If so, has this data provided insight into serviceability requirements?
8. Have you seen a direct correlation between deterioration and reduced serviceability (not nuisance maintenance)? If so, in what types of structures/components? Have you been able to quantify the rate of reduced serviceability or service life?
9. Are there other questions we should have asked to gain more insight into your experience with service limit states? If so, what are they and what would your responses have been?

Questionnaire #2 Geotechnical Service Issues

FORM FOR BRIDGE MOVEMENTS AND OBSERVED DISTRESS

**1. Preparer Information** (fill one form per structure)

Prepared by/Title/Agency (Dept.)	
Phone/E-mail	

**2. Bridge Information**

State/County/Town		Route No./Structure No.	
Year built		Crossing (over/under)	
No. of spans		Type of spans (simple, continuous, cantilever, etc.)	
Type of superstructure (steel, concrete, girder, slab, box beam, etc.)		Type of abutments (integral, spill-through, full height, perched, stub, etc.)	
Pier foundation type (spread footings, driven piles, drilled shafts, etc.)		Approach fill or wall type (Fill with side slope, MSE wall, etc.)	
Approach height		As-built drawings available?	
Geotechnical report available?		Boring logs available?	
Were repairs performed?		Maintenance records available?	
Any instrumentation data available?		Any photos of bridge damage and/or repairs available?	

**3. Construction Sequence:** Fill in 1, 2 and 3 based on sequence of construction of following elements

Substructure \_\_\_\_\_ Superstructure \_\_\_\_\_ Approach fill/wall \_\_\_\_\_

**4. Geologic Information:** Describe generalized geologic strata including soil types, water table location, Standard Penetration Test (SPT) N-values, consolidation parameters, etc. If geotechnical report including boring logs is provided, refer to the report and no further information is necessary.

**5. Bridge Movements** (horizontal movements are movements in longitudinal direction of bridge)

Vertical Movements	Abutments	Piers	Horizontal Movements	Abutments	Piers
Estimated			Estimated		
Observed			Observed		

Note: If varied movement was observed at different support elements, provide additional information on a separate page as appropriate.

**6. Effect of Movements on Bridge Structure:** Indicate if distress types were tolerable or not based on the following definition:

*“Movement is NOT tolerable if damage requires costly maintenance and/or repairs AND a more expensive construction to avoid this would have been preferable.”*

(Use additional pages if necessary to provide detailed information on any distress type)

#	Distress Type	Tolerable? (Yes/No), Description
1	<u>Damage to abutments</u> : cracking and spalling of abutments, abutment footings, abutment pile caps, or abutment slope protection; also included in this category are the opening, closing or damage to abutment joints, the separation of the wingwall from abutment, and the rupturing or exposure of abutment foundations.	
2	<u>Damage to piers</u> : cracking and spalling of piers, pier footing, pier pile caps, or struts of diaphragms between pier columns.	
3	<u>Vertical displacement</u> : raising or lowering of the superstructure above or below planned grade or a sag or heave in the deck; structures requiring shimming or jacking as well as truss structures with increase camber are also included.	
4	<u>Horizontal displacement</u> : structures with a misalignment of bearings and superstructure, or beams jammed against abutments; bridges where superstructure extended beyond the abutment, where beams required cutting, or where there was horizontal movement of the floor system.	
5	<u>Distress in superstructure</u> : cracks or other evidence of excessive stress in beams, girders, struts, and diaphragms as well as cracking and spalling or the deck; shearing of anchor bolts; opening, closing or damage of deck joints and cases where the cutting or relief joints were required.	
6	<u>Damage to railings, curbs, sidewalks or parapets</u> : cracking, deformation, or misalignment of railing, curb, sidewalks, or parapets; jammed curbs and crushed concrete and open, closed or damaged portions of these elements.	
7	<u>Damage to bearings</u> : tilting or jamming or rockers as well as cases where rockers have pulled off bearing, or where movement results in an improper fit between bearing shoes and rockers requiring re-positioning; deformed neoprene/elastomeric bearing pads, sheared anchor bolts in the bearing shoes, damage to expansion devices, and cracking of concrete at the bearings.	
8	<u>Poor riding quality</u> : reported noticeable driver discomfort.	
9	<u>Not given or corrected during construction</u> : those cases where any mention of structural effects was omitted or where foundation movement was corrected prior to construction of the superstructure.	
10	<u>None</u> : no damage or repairs.	
11	<u>Other</u> : other observed distress types not included in above categories.	

**Agency's Tolerable Movement Criteria for New Bridge Structures**

1. Article C10.5.5.2 of AASHTO (2007) allows angular distortion of 0.004 for multiple (continuous) spans and 0.008 for single-span bridges. Does your agency follow these criteria? (Yes/No) \_\_\_\_\_.

[Note: Angular distortion is defined as  $DS/L$  where DS is the differential settlement between two support elements and L is the distance between support elements (i.e., span length). Example: limiting angular distortion of 0.004 permits a differential settlement of 4.8-inches over a 100-ft span length.]

If answer to above question is "No," please provide following information. If criteria vary by span length, number of spans and/or structure type (steel vs. concrete, girder vs. box beam, etc.) provide additional information as appropriate:

Permissible total vertical movement (settlement), S, at any given support element	
Permissible differential vertical movement (settlement), DS, within a given span	
Permissible angular distortion, DS/L (where L is span length)	
Permissible horizontal movement, H (in longitudinal direction of the bridge)	
<u>Additional Information:</u>	

2. Does the agency have criteria for permissible horizontal movement (in longitudinal direction of the bridge)? (Yes/No) \_\_\_\_\_.

If answer to above question is "Yes," please provide following information. If criteria vary by span length, number of spans and/or structure type (steel vs. concrete, girder vs. box beam, etc.) provide additional information as appropriate:

Permissible horizontal movement, H (in longitudinal direction of the bridge)	
<u>Additional Information:</u>	

## **Response to Questionnaire 1 on Superstructure Issues**

### **Question 1: What are the five or ten most costly maintenance/durability items in your structural maintenance budget?**

The most costly maintenance/durability items within the structural maintenance budget as reported in the survey responses are:

- Expansion joints and steel coating systems (13 each);
- Concrete decks (cracking, repair, and sealing for cracking) (8);
- Deck overlays and bearings (7 each);
- Concrete and steel repair or replacement (5 each);
- Abutment maintenance (3);
- Timber components, movable bridges, approach slabs, railings and curbs, reinforcement, fatigue, built-up steel corrosion, and scour (2 each); and
- Weld cracking, slope maintenance, anchor cables, deck drains, concrete coatings, header joints, and concrete spalling (1 each).

### **Question 2: Does your agency utilize deterioration models other than those in Pontis? If so, what and why?**

Fifteen survey responses were received and indicate that the following are used to estimate deterioration:

- Utilize Pontis only (8);
- Use a DOT created program (5); and
- Use experience or use no deterioration models (1 each).

The responses indicate that most agencies use models to estimate deterioration. Those that do not use either Pontis or a DOT specific program use engineering judgment or do not attempt to estimate deterioration. Some programs consist of computer software created using data combined with experience in estimating remaining service life. Other programs combine condition assessments completed for NBI inspections and curves developed based on the structure type. Several of the DOT programs use different elements in the deterioration models than are used in Pontis.

### **Question 3: In your experience, are the current SLS adequate for your needs or are further safeguard required? If more are required, what should they guard against for what types of members, systems or details?**

The responses to this question were as follows:

- Adequate but a need for additional requirements (9);
- Adequate (6); and
- Some of the current SLS are over conservative (2).

Most respondents felt that the current SLS are adequate as currently specified. Two responses felt that at least one limit state was over conservative, with one believing the L/800 limit for live load deflections is over conservative while the other related to whether AASHTO LRFD 5.7.3.4-Control of Cracking by Distribution of Reinforcement is over conservative. The responses suggested adding serviceability limit states with regards to:

- foundation settlement of approach pavement;
- relative movement between adjacent girders and determination the factored out-of-plane resistance for this condition;
- consider steel corrosion/section loss based on type of steel coating and a corrosion model and then rechecking stresses based on reduced section;
- consider local deflections or incompatible deformations at component interfaces;
- requirements for stress and cracking of reinforced concrete flexural members (current method of designing for strength and then checking crack control reinforcement is not adequate and members crack resulting in reduced service life, this agency no longer uses reinforced concrete bridge beams);
- serviceability of connections; and
- SLS for expansion joints and bearings.

### **Question 4: What have you seen as important service and durability issues (not strength) and bridge age affects that impact the serviceability of bridge components?**

The fourteen responses to the above question included:

- Deck cracking (6);
- Corrosion of steel, steel coating systems, and leaking expansion joints (5 each);
- Fatigue (4);
- Bearing failure, chloride penetration, and deterioration of beam ends (3 each);
- Preparation for steel painting, ADT combined with salt (2 each); and
- Slope failure, end bent movement, deck drainage, deck membrane durability, bond and splice lengths, deterioration of non-composite bridge decks, exodermic bridge decks, bent cracking, concrete mix design, foundation movement, concrete deterioration, deflections and vibrations, adequate detailing, and the requirements for appropriate cover versus the requirements for crack control steel (1 each).

The results are combined for all bridge types and components. The most common issue mentioned was deck cracking closely followed by corrosion of steel in reinforced concrete and steel superstructures and painting of steel. Often times both were mentioned as “proper painting of the steel girders will slow down the corrosion process.” In addition, leaking expansion

joints was a common response, which may be related to many of the other issues mentioned. As would be expected, the chloride penetration and “ADT and salt” categories were focused in the northern part of the country where winter weather conditions require the use of salt for traffic safety.

**Question 5: Have you seen issues resulting in reduced serviceability (or a trend in that direction) that could have been avoided if the design specification had additional service (not strength) design requirements? If so, what?**

The thirteen responses to the above question included:

- Reduced serviceability could not have been avoided with additional service requirements (7)
- Additional requirements that would have helped avoid reduced serviceability were as follows:
  - Crack control requirements for concrete decks and provisions to limit corrosion of deck reinforcement;
  - Requirements to check for expansion caused by thermal loading (this is already included in the design specification for ULS and SLS);
  - Provisions for use of proprietary deck systems;
  - Specifications for proper fill materials to prevent slope failures; and
  - Cracking of cantilevered portions of bents—for sections with shear span to depth ratios of approximately 1.5, limit service load stresses in longitudinal reinforcement are limited to 30 ksi at column face (up to 36 ksi at column center) for moderate exposures and up to 24 ksi and 30 ksi at the column face and center, respectively, for severe exposures.

Most respondents believe that no, new additional serviceability requirements are necessary. Those that believed reduced serviceability could have been avoided suggested new serviceability requirements for the bridge deck and foundation and substructure. Others were not sure whether issues resulting in reduced serviceability could have been avoided had there been additional service requirements.

**Question 6: What type of foundation/wall settlement or other movements have resulted in maintenance issues or reduced serviceability?**

Twelve respondents indicated different types of foundation or wall settlement and movement that have resulted in reduced serviceability or maintenance include:

- No foundation problems (3);
- Scour at spread footings and retaining structures, settlement or movement of approach slabs, MSE and retaining walls, and wingwalls (3 each);

- Poor soil, movement of piles, and movement of abutments (2 each); and
- Movement of end bents and rotation of spread footings (1 each).

Foundation problems varied greatly, with some responses indicating no foundation problems while others had many problems. One response said that they had no foundation problems but indicated that they had previously had some but these were eliminated using rules of thumb or by setting guidelines that require all foundations to be at the same level. They also said that the service issues with foundations were caused by construction issues. Those that noted movement of MSE or retaining walls as causing reduced serviceability noted that in one case the movement was caused by thermal loading and the other was a result of the bridge being supported by piling while the retaining walls were not.

**Question 7: Do you make Quantitative/Qualitative condition assessments beyond what is in Pontis? If so, has this data provided insight into serviceability requirements?**

Thirteen responses were received indicating whether additional assessments are completed and if they provide insight into serviceability requirements:

- No additional quantitative or qualitative assessments (7);
- No additional quantitative but do complete additional qualitative assessments (3); and
- Complete both additional quantitative and qualitative assessments (3).

The first agency that completes both additional assessments used various methods, such as, bridge deck condition surveys, measurement of chloride penetration depth, and ultrasonic testing to measure corrosion combined with engineering judgment to determine priority for replacement or rehabilitation. The second agency completing additional assessments uses a condition scale for each bridge component and provides relevant notes and figures that portray the overall condition and what deficiencies exist. This agency also noted that the use of additional inspections show the same conditions over and over in their bridge inventory but did not state what conditions these were, suggesting that there is a need for enhanced serviceability requirements. The third agency completing additional quantitative/qualitative assessments while providing insight into the deterioration of the structure have not been used with regard to additional serviceability requirements.

**Question 8: a. Have you seen a direct correlation between deterioration and reduced serviceability (not nuisance maintenance)? If so, in what types of structures or components?**



**b. Have you been able to quantify the rate of reduced serviceability or service life?**

Thirteen responses were received in regards to Question 8a. The responses included:

- Expansion joints and associated deterioration of beam ends and substructure units (11);
- Bridge decks (5);
- No correlation (2); and
- Joints and timber piles (1 each).

The results suggest that many of the responding agencies have determined that there is a correlation between deterioration in different bridge components and reduced serviceability. The most common response was corrosion or section loss of a steel girder/beam resulting in higher stresses under service loads. Additionally, correlations between deterioration and reduced serviceability were noted for all components of a bridge, from the foundation to the superstructure and deck. The results noted that there was a reduction in service life for bridge decks and load carrying capacity for girders.

The fourteen responses were received for Question 8b regarding the quantification of reduced serviceability are:

- No (12); and
- Yes (2).

The second part of question 8 was whether the different agencies had tried to quantify the rate of reduced serviceability. The overwhelming response was No, but two indicated that they had, or were trying to, quantify the reduction in serviceability. One agency used engineering judgment to quantify the reduction in serviceability and service life of bridge decks while the other was trying to determine a method to quantify the rate of deterioration for deck systems which incorporated a sealer and also to quantify the difference in deterioration between steel girders with and without a protective coating.

**Question 9: Are there other questions we should have asked to gain more insight into your experience with SLS? If so, what are they and what would your responses have been?**

Seven agencies answered Question 9 regarding other questions that should have been asked. Their responses are as follows:

- No (4) and
- Yes (3).

Approximately half of the agencies that provided a response to the question (i.e., 3 agencies) had additional questions that could have been asked or comments/suggestions. The following are their suggestions:

- Provide SLS for permit trucks similar to the Strength II limit state.
- Load test all bridge type/material combinations except for steel.

Additional questions regarding the following items could have been asked:

- What alternative design loads (alternatives to HL-93) are being used to check limit states by other agencies? (This was covered by NCHRP 12-83)
- What types of corrosion protection systems are required?
- What types of exposures and associated environmental distresses have you observed?
- How have locked in connection forces due to permanent deformations affected serviceability?
- What effects on bearings and joints have you seen due to creep, shrinkage, and uniform and gradient temperature changes? and
- How do live load deformations affect connections?

**Responses to Questionnaire #2 on Geotechnical Issues**

Only three respondents provided significant information in response to this part of the survey. All respondents framed their response in terms of experience with specific bridges. The relevant information is summarized in the following table. The first four bridges are from the same state. They indicated that they had observed distress in almost all cases where an integral abutment and an unisolated MSE mass were used and foundation movement occurred.

Four responses were obtained to Question 6 regarding effects of movement on the structure. Three of the four are from the agencies that provided responses to Questions 1 through 5 of this questionnaire.

A majority of responses believe that the different types of movement listed are not tolerable while some believe that movement is tolerable until it starts affecting other structural components. The effects of movement resulted in varying degrees of damage or distress to the structure.

The first response indicated that movement and damage caused by movement is not tolerable according to the definition provided. While movement and associated damage is not tolerated, they believe that poor riding quality is tolerable.

The second response provided repair methods for the different types of movement listed. These include repairing vertical settlement due to beam deterioration by jacking the beam and repairing the section loss. Poor riding quality was improved by mudjacking the approach slabs. Damage to bearings is repaired by either replacing bearings with elastomeric bearing pads or resetting rocker bearings.

The third response indicated that movement occurred causing a hinge to form over the pier resulting in the loss of bearing

**Table B.1. Bridge Characteristics, Geological Information, and Movements**

Question 1: Preparer	Assistant Geotechnical Engineer (State A)				DOT (State B)	DOT (State C)
<b>Question 2: Bridge Characteristics</b>						
Year built	1999	1998	2007	2002	1963	1999
No. of spans	5	5	5	3	3	6
Type of superstructure (steel, concrete, girder, slab, box beam, etc.)	Steel	Concrete	Steel	Concrete	CIP Concrete Slab Span	Prestressed concrete I-Beam
Pier foundation type (spread footings, driven piles, drilled shafts, etc.)	Driven Piles	Drilled Shafts	Drilled Shafts	Driven Piles	Spread footing	Pier footing on Piles
Approach height	23	27	23	23	20	
Geotechnical report available?	Yes	Yes	No	Yes	No	Yes
Were repairs performed?	Yes	Yes	Yes	Yes	Yes	No
Any instrumentation data available?	No	No	No	No	No	Yes
Route No./Structure No.	I-135	US 75	I-35	US 50	I-40 15725	6015
Crossing (over/under)	Broadway and 1st St.	Over 46th St.	Under 87th St.	Over Mary St.	SH-9A	Over Johnson Creek and Lower Arnot Rd.
Type of spans (simple, continuous, cantilever, etc.)	Continuous	Continuous	Continuous	Continuous	Continuous	Continuous
Type of abutments (integral, spill- through, full height, perched, stub, etc.)	Integral	Integral	Integral	Integral	Stub	Stub
Approach fill or wall type (Fill with side slope, MSE wall, etc.)	MSE Wall	MSE Wall	MSE Wall	MSE Wall	Fill w/ side slope	Fill w/ side slope
As-built drawings available?	No	No	No	No	No	Yes
Boring logs available?	Yes	Yes	No	Yes	Yes	Yes
Maintenance records available?	No	No	No	No	Yes	Yes
Any photos of bridge damage and/or repairs available?	Probably	???	No	No	Yes	Yes

*(continued on next page)*

**Table B.1. Bridge Characteristics, Geological Information, and Movements (continued)**

<b>Question 3: Construction Sequence</b>						
	Substructure, Approach Fill/Wall, Superstructure	Substructure, Approach Fill/Wall, Superstructure	Substructure, Approach Fill/Wall, Superstructure	Substructure, Approach Fill/Wall, Superstructure	Approach Fill/Wall, Substructure, Superstructure	
<b>Question 4: Geological Info</b>						
	Alluvial and residual clay overlying sand or shale bedrock	Glacial drift and alluvial soils over glacial till followed by Pennsylvanian bedrock	Residual clay soil over Pennsylvanian bedrock	Loessial soil and fill above alluvial sand	Stiff to hard sandy clay (Liquid Limit (LL) ~50, Plasticity Index (PI)~30, #200 75%)	Silt with gravel and cobbles overlying non-plastic silt and silty sand and gravel
<b>Question 5: Bridge Movements</b>						
Vertical Movement	NA	NA	NA	NA	12" at abutment	1-4" prior to construction
Horizontal Movement	NA	NA	NA	NA	NA	NA

Note: NA = not available.

**Table B.2. Effects of Movement on Structure**

<b>Question 6: Effects of Movement on Structure</b> Indicate if distress types were tolerable or not based on the following definition: <i>"Movement is NOT tolerable if damage requires costly maintenance and/or repairs AND a more expensive construction to avoid this would have been preferable."</i>	
State A	Damage to abutments: NO Damage to piers: NO Vertical Displacement: NO Horizontal Displacement: NO Distress in superstructure: NO Damage to railings, curbs, sidewalks or parapets: NO Damage to bearings: NO Poor riding quality: YES Not given or corrected: NA None: YES Other: YES
State A	Damage to abutments: Tolerable until it effects bearings or severe deterioration of rebar Damage to piers: same as abutments Vertical Displacement: not much of a problem, typically caused by deterioration of beam end, fixed by jacking beam and repairing section loss Horizontal Displacement: not much of a problem, let it go until it gets excessive Distress in superstructure: not tolerated if cracks in steel beam or shear cracks in concrete beam. Joint normally tolerated unless pushing bents or abutments and causing damage Damage to railings, curbs, sidewalks or parapets: tolerated Damage to bearings: not tolerated-repair by replacing bearings with elastomeric pads or resetting rocker bearings Poor riding quality: generally tolerated, mud-jack approach slabs if excessive Not given or corrected: NA None: NA Other: NA

(continued on next page)

**Table B.2. Effects of Movement on Structure (continued)**

State B	<p>Damage to abutments: NO, settlement resulted in end span cantilevered from pier, loss of bearing</p> <p>Damage to piers:</p> <p>Vertical Displacement: NO, shims added, caused crack to form over pier</p> <p>Horizontal Displacement:</p> <p>Distress in superstructure: NO, crack/hinge over pier</p> <p>Damage to railings, curbs, sidewalks or parapets: NO, cracks in parapet</p> <p>Damage to bearings: NO</p> <p>Poor riding quality: NO</p> <p>Not given or corrected: NA</p> <p>None: NA</p> <p>Other: After hinge/crack in slab span, end span acted as simply supported. End span was not designed or reinforced to act as a simple span</p>
State C	<p>Damage to abutments: Not tolerable, except for slope protection and minor separation of wing wall from the abutment</p> <p>Damage to Piers: Not tolerable, tolerable if crack widths are less than 0.025" based on Oregon DOT cracking guidelines</p> <p>Vertical Displacement: tolerable</p> <p>Horizontal Displacement: assumed tolerable</p> <p>Distress in superstructure: not tolerable, tolerable if crack width is less than 0.025" based on Oregon DOT crack guidelines</p> <p>Damage to railings, curbs, sidewalks, or parapets: tolerable</p> <p>Damage to bearings: tolerable</p> <p>Poor Riding quality: tolerable</p> <p>Not given or corrected during construction: potential settlement was addressed in construction</p> <p>None: NA</p> <p>Other: NA</p>

Note: NA = not available.

for the end span. This resulted in the end span becoming a simple span which was not considered in the design. The movement was a result of drilled shafts for the abutments being founded in fill instead of bedrock.

The fourth response indicated that damage to railings, curbs, sidewalks, parapets, and bearings are tolerable. Cracking of piers and superstructure components are tolerable up to a certain limit based upon guidelines used by the Oregon DOT.

Ten agencies responded to two questions about criteria for movements permitted on new bridges. Their responses are below.

**Question 1: Does your agency follow the criteria of Article C10.5.5.2 of AASHTO (2007)?**

Responses are:

- Yes, we use the criteria of Article C10.5.5.2 of the AASHTO LRFD Specification (2)
- No, we do not use the criteria of Article C10.5.5.2 of the AASHTO LRFD Specification (8)
- No response (6)

Those agencies that do not follow the criteria of Article C10.5.5.2 of the AASHTO LRFD Specification were asked to provide the deflection limits that they use. These limits are provided in Table B.3.

**Question 2: Does the agency have criteria for permissible horizontal movement (in longitudinal direction of the bridge)?**

The responses to the above question are:

- Yes (3)
- No (7)
- No response (6)

The allowable horizontal movement limits are shown in the table on the following page Agency D limits horizontal movement to that which can be accommodated by the bearings and joints within the structure while others provide a finite value.

Limits provided by various agencies which do not follow Article C10.5.5.2 of AASHTO are shown in Table B.3.

**Table B.3. Allowable Vertical and Horizontal Movements**

<b>Movement</b>	<b>Agency A</b>	<b>Agency B</b>	<b>Agency C</b>	<b>Agency D</b>	<b>Agency E</b>	<b>Agency F</b>	<b>Agency G</b>
Total Vertical Movement	Axial Elastic Only	1"	Assessed on a case by case basis, and if likely to continue steps are taken to stop settlement.	1"	1"	Follows local/ state requirements	1.5"
Differential Vertical Movement	0"	1"		Case by case	1"		Structure Specific
Angular Distortion	0"	0.1% of Span Length			0.0025 for simple span 0.0015 for continuous span		Structure Specific
Horizontal Movement	<2" due to thermal loading for integral abutments founded on a single row of piles	0"		Case by case, thermal, shrinkage, and live load movement must be less than that allowed by bearings and expansion joints	Not specified in design, is specified for construction		1"

## APPENDIX C

# Comparison of Crack Width Prediction Equations for Prestressed Concrete Members

This appendix presents a review and comparison of various prediction equations for the maximum crack width in prestressed concrete members. Test data from various sources were used in the comparisons. The equations are presented in chronological order.

### C.1 CEB-FIP (1970) Equation

The 1970 Euro-International Committee for Concrete and International Federation for Prestressing (CEB-FIP) recommended adopting the following equation (C.1) to predict the maximum crack width in partially prestressed beams:

$$w_{\max} = (Df_s - 4000) \times 10^{-6} \quad (\text{C.1})$$

For static loads, the equation is this (C.2):

$$w_{\max} = \Delta f_s \times 10^{-6} \quad (\text{C.2})$$

where  $Df_s$  is the stress change in steel after decompression of concrete at centroid of steel. Please note that the  $\Delta f_s$  in the CEB-FIP equation is in N/cm<sup>2</sup>.

### C.2 Nawy and Potyondy (1971) Equation

Nawy and Potyondy (1971) conducted a research program to study the flexural cracking behavior of pretensioned I- and T-beams. Table C.1 shows the geometric and mechanical properties of the prestressed beam specimens.  $A_s$  represents the area of tension reinforcement comprising both prestressing and normal steel reinforcement,  $A'_s$  represents the area of compression reinforcement,  $f'_c$  is the concrete cylinder compressive strength, and  $f'_t$  is the concrete tensile splitting strength.

Based on a regression analysis of the test data, the authors proposed Equation C.3:

$$w_{\max} = 1.13 \times 10^{-6} \left( \frac{A_t}{A_s} \right)^{1/4} a_c \sqrt{\Delta f_{s1}^3} \quad (\text{C.3})$$

where

$$\Delta f_{s1} = [f_s - f_d - 3.75] \text{ (ksi);}$$

$a_c$  = stabilized crack spacing (in.);

$A_t$  = area of concrete in tension (in.<sup>2</sup>);

$A_s$  = total area of reinforcement (in.<sup>2</sup>);

$E = 27.5 \times 10^3$  ksi was used;

$f_s$  = stress in prestressing steel after cracking (ksi); and

$f_d$  = stress in the prestressing steel when the modulus of rupture of concrete at the extreme tensile fibers is reached (ksi).

After further simplification of Equation C.3, Nawy and Potyondy (1971) recommended the following expression (Equation C.4):

$$w_{\max} = 1.44(\Delta f_s - 8.3) \quad (\text{C.4})$$

where  $\Delta f_s$  is the net stress in prestressing steel, or the magnitude of tensile stress in normal steel at any crack width level. Note the units for  $\Delta f_s$  in Equation C.4 are ksi, and the units for crack width are inches.

### C.3 Bennett and Veerasubramanian (1972) Equation

Bennett and Veerasubramanian (1972) investigated the behavior of nonrectangular beams with limited prestress after flexural cracking. They tested 34 prestressed concrete beams with the following cross sections:

- Rectangular: 12-in. deep  $\times$  6-in. wide;
- I-Beam: 12-in. deep with 6-in. wide top and bottom flanges;



**Table C.1. Geometrical Properties of Prestressed Beams**

Beam	Section	Width $b$ (in.)	Depth $d$ (in.) <sup>a</sup>	$A_s$ (in. <sup>2</sup> )	$\rho = \frac{A_s}{bd}$ (%)	$A'_s$ (in. <sup>2</sup> ) <sup>b</sup>	$\rho' = \frac{A'_s}{bd}$ (%)	$f'_c$ (psi)	$f'_t$ (psi)	Slump (in.)
B1	T	8	8.75	0.271	0.389	—	—	4865	400	3
B2	I	6	8.90	0.271	0.518	—	—	4865	400	3
B3	T	8	8.75	0.271	.0389	—	—	4330	430	4
B4	I	6	8.90	0.271	0.518	—	—	4290	430	4
B5	I	6	8.90	0.271	0.518	—	—	4340	430	4
B6	T	8	8.75	0.271	0.389	—	—	4375	430	4
B7	T	8	8.75	0.271	0.389	—	—	4290	390	6
B8	I	6	8.90	0.271	0.518	—	—	4260	390	6
B9	I	6	8.90	0.271	0.518	—	—	4190	390	6
B10	T	8	8.75	0.271	0.389	—	—	4280	390	6
B11	T	8	8.75	0.271	0.389	—	—	4150	370	8
B12	I	6	8.90	0.271	0.518	—	—	3920	370	8
B13	I	6	8.90	0.281	0.518	—	—	3890	370	8
B14	T	8	8.75	0.271	0.389	—	—	4110	370	8
B15	T	8	8.75	0.271	0.389	0.93	1.332	3490	340	5½
B16	I	6	8.90	0.271	0.518	0.33	0.631	3400	340	5½
B17	I	6	8.90	0.271	0.518	0.93	1.776	3390	340	5½
B18	T	8	8.75	0.271	0.389	0.33	0.473	3510	340	5½
B19 <sup>c</sup>	I	6	8.90	0.235	0.448	—	—	3610	385	6
B20 <sup>c</sup>	I	6	8.90	0.235	0.448	—	—	3495	385	6
B21 <sup>c</sup>	I	6	8.90	0.235	0.448	—	—	3430	355	6½
B22 <sup>c</sup>	I	6	8.90	0.235	0.448	—	—	3280	355	6½
B23	I	6	8.90	0.271	0.518	—	—	4060	380	5
B24	I	6	8.90	0.271	0.518	—	—	4095	380	5
B25	I	6	8.90	0.271	0.518	—	—	3950	380	5
B26	I	6	8.90	0.271	0.518	—	—	4000	380	5

Note: — = no compression steel in the specimen.

<sup>a</sup> Total depth  $h$  of all beams = 12 in.

<sup>b</sup>  $A_s$  includes two ¼-in.-diameter high-strength steel wire ( $f_y = 96,000$  psi) cage bars in addition to prestressing strands.

<sup>c</sup> Beams B19–B22 were continuous beams and were not included in the cracking analysis.

Source: Nawy and Potyondy (1971); used by permission of the American Concrete Institute.

- I-Beam: 12-in. deep with 12-in. wide top flange and 6-in. wide bottom flange; and
- I-Beam: 8-in. deep. A slab 24-in. wide was cast later to represent the deck.

All beams were simple spans with a span length of 10 ft. Two concentrated loads spaced 6 ft. apart and centered on the span were used for loading.

Bennett and Veerasubramanian recommended a prediction equation for the maximum crack width as follows in Equation C.5:

$$w_{\max} = \beta_1 + \beta_2 \epsilon_s d_c \quad (\text{C.5})$$

where

$\beta_1$  = a constant representing the residual crack width measured after the first cycle of loading. The value suggested for deformed bars is 0.02 mm.

$\beta_2$  = a constant depending on bond characteristics of the nonprestressed steel. The value recommended for deformed bars is 6.5.

$\epsilon_s$  = increase in strain in nonprestressed steel from stage of decompression of concrete at tensile face of beam ( $\mu\epsilon$ ).

$d_c$  = clear cover over the nearest reinforcing bar to the tensile face (mm).

Note that this equation uses the International System of Units (SI).

### C.4 Nawy and Huang (1977) Equation

Nawy and Huang (1977) studied crack and deflection control in pretensioned prestressed beams. They performed tests on 20 single-span and four continuous beams. Based on a detailed statistical analysis of the test data, they proposed the following equation (Equation C.6):

$$w_{\max} = 5.85 \times 10^{-5} \frac{A_t}{\beta \Sigma 0} (\Delta f_{ps}) \quad (\text{C.6})$$

where

$A_t$  = area of concrete in tension (in.<sup>2</sup>);

$\beta$  = ratio of distance from neutral axis of beam to concrete outside tension face to distance from neutral axis to steel reinforcement centroid;

$\Delta f_{ps}$  = increase in stress in the prestressing steel beyond decompression state (ksi); and

$\Sigma 0$  = sum of reinforcing element circumferences (in.).

Table C.2 presents a comparison of the crack widths measured from the beam tests performed by Nawy and Huang (1977) and the ones predicted using the equation developed by Nawy and Huang (1977). On average, Equation C.6 provides prediction results that are within 20% of the measured maximum crack width of prestressed concrete beams.

### C.5 Rao and Dilger (1992) Equation

Rao and Dilger (1992) developed a detailed crack control procedure for prestressed concrete members. The authors studied the prediction equation of maximum crack width

**Table C.2. Observed Versus Theoretical Maximum Crack Width at Tensile Face of Beam**

Net Steel Stress											
30 ksi			40 ksi			60 ksi			80 ksi		
$w_{\text{obs.}}$	$w_{\text{theory}}$	Error (%)	$w_{\text{obs.}}$	$w_{\text{theory}}$	Error (%)	$w_{\text{obs.}}$	$w_{\text{theory}}$	Error (%)	$w_{\text{obs.}}$	$w_{\text{theory}}$	Error (%)
0.0111	0.0131	-15.3	0.0151	0.0175	-13.7	0.0261	0.0262	-0.4	0.04	0.0349	14.6
0.0127	0.0118	7.6	0.0204	0.0157	29.9	0.0275	0.0236	16.5	0.0409	0.0313	30.7
0.0131	0.0128	2.3	0.0166	0.0172	-3.5	0.0304	0.0256	18.8	0.0382	0.0344	11.0
0.0097	0.013	-25.4	0.0158	0.0174	-9.2	0.0226	0.0259	-12.7	0.0304	0.0347	-12.4
0.0091	0.0147	-38.1	0.0117	0.0197	-40.6	0.0205	0.0294	-30.3	0.032	0.0393	-18.6
0.0124	0.0148	-16.2	0.0181	0.0199	-9.0	0.0213	0.0297	-28.3	0.0364	0.0397	-8.3
0.0052	0.0051	2.0	0.0068	0.0069	-1.4	0.0117	0.0103	13.6	0.0188	0.0137	37.2
0.0049	0.0051	-3.9	0.0061	0.0069	-11.6	0.0111	0.0103	7.8	0.0146	0.0137	6.6
0.0051	0.0045	13.3	0.0064	0.0061	4.9	0.0107	0.009	18.9	0.0165	0.0121	36.4
0.0058	0.0045	28.9	0.0082	0.0061	34.4	0.0134	0.009	48.9	0.0185	0.0121	52.9
0.0054	0.0059	-8.5	0.0069	0.0079	-12.7	0.0112	0.0119	-5.9	0.0172	0.0158	8.9
0.0048	0.0059	-18.6	0.0076	0.0079	-3.8	0.0134	0.0119	12.6	0.0192	0.0158	21.5
0.0043	0.0046	-6.5	0.0058	0.0062	-6.5	0.0105	0.0092	14.1	0.0138	0.0123	12.2
0.0052	0.0046	13.0	0.0059	0.0062	-4.8	0.0103	0.0092	12.0	0.0145	0.0123	17.9
0.0039	0.0057	-31.6	0.0061	0.0076	-19.7	0.0115	0.0114	0.9	0.0181	0.0153	18.3
0.0038	0.0057	-33.3	0.0057	0.0076	-25.0	0.0093	0.0114	-18.4	0.016	0.0153	4.6
0.0039	0.0056	-30.4	0.006	0.0074	-18.9	0.0098	0.0112	-12.5	0.0159	0.0148	7.4
0.003	0.0056	-46.4	0.0045	0.0074	-39.2	0.0086	0.0112	-23.2	0.0147	0.0148	-0.7
0.0057	0.0061	-6.6	0.0085	0.0081	4.9	0.0129	0.0121	6.6	0.0202	0.0163	23.9
0.0034	0.0045	-24.4	0.0045	0.0059	-23.7	0.0089	0.0089	0.0	0.0139	0.0119	16.8
Average		18.6	Average		15.9	Average		15.1	Average		18.0

Source: Adapted from Nawy and Huang (1977).

developed by various previous researchers and proposed a new equation (C.7) expressed as follows:

$$w_{\max} = k_1 f_s d_c (A_t / A_s)^{0.5} \quad (\text{C.7})$$

where

$k_1$  = the bond coefficient defined for each combination of prestressed and nonprestressed reinforcement;

$f_s$  = stress in steel after decompression (MPa);

$d_c$  = concrete cover measured from surface to the center of nearest reinforcement bar (mm);

$A_t$  = area of concrete in tension (mm<sup>2</sup>);

$A_s$  = total area of reinforcement (mm<sup>2</sup>).

## C.6 Eurocode 2 (2004) Provisions

Eurocode 2 (2004) provides the following provisions to calculate the crack widths (Equation C.8):

$$w_k = s_{r,\max} (\epsilon_{sm} - \epsilon_{cm}) \quad (\text{C.8})$$

where

$s_{r,\max}$  = maximum crack spacing.

$w_k$  = crack width.

$\epsilon_{sm}$  = mean strain in the reinforcement under the relevant combination of loads, including the effect of imposed deformations and taking into account the effects of tension stiffening. Only the additional tensile strain beyond the state of zero concrete strain at the same level is considered.

$\epsilon_{cm}$  = mean strain in the concrete between cracks.

In Equation C.8, the quantity  $(\epsilon_{sm} - \epsilon_{cm})$  can be calculated from the following expression (C.9):

$$(\epsilon_{sm} - \epsilon_{cm}) = \frac{\sigma_s - k_t \frac{f_{ct,\text{eff}}}{\rho_{p,\text{eff}}} (1 + \alpha_e \rho_{p,\text{eff}})}{E_s} \geq 0.6 \frac{\sigma_s}{E_s} \quad (\text{C.9})$$

where

$A'_p$  = area of pre- or posttensioned tendons within  $A_{c,\text{eff}}$ .

$A_{c,\text{eff}}$  = effective area of concrete in tension surrounding the reinforcement or prestressing tendons of depth,  $h_{c,\text{ef}}$ , where  $h_{c,\text{ef}}$  is the lesser of  $2.5(h - d)$ ,  $(h - x) / 3$  or  $h / 2$ , where  $h$  is the height of the beam,  $d$  is the effective depth of a cross section, and  $x$  is the neutral axis depth.

$k_t$  = factor dependent on the duration of the load.

$\alpha_e = E_s / E_{cm}$ , where  $E_{cm}$  is the secant modulus of elasticity of concrete and  $E_s$  is the design value of modulus of elasticity of reinforcing steel.

$\rho_{p,\text{eff}} = (A_s + \xi_1^2 A'_p) / A_{c,\text{eff}}$

$\sigma_s$  = stress in the tension reinforcement assuming a cracked section. For pretensioned members,  $\sigma_s$  may be replaced by  $\Delta\sigma_p$ , the stress variation in prestressing tendons from the state of zero strain of the concrete at the same level.

$\xi_1$  = adjusted ratio of bond strength, taking into account the different diameters of prestressing and reinforcing steel, calculated as  $\sqrt{\xi \cdot \frac{\phi_s}{\phi_p}}$ , where  $\xi$  is the ratio of bond strength of prestressing and reinforcing steel,  $\phi_s$  is the largest bar diameter of reinforcing steel, and  $\phi_p$  is equivalent diameter of tendon. Equation C.10 follows.

$$s_{r,\max} = k_3 c + k_1 k_2 k_4 \phi / \rho_{p,\text{eff}} \quad (\text{C.10})$$

where

$\phi$  = bar diameter;

$c$  = cover to the longitudinal reinforcement;

$k_1$  = coefficient that takes account of the bond properties of the bonded reinforcement;

$k_2$  = coefficient that takes account of the distribution of strain;

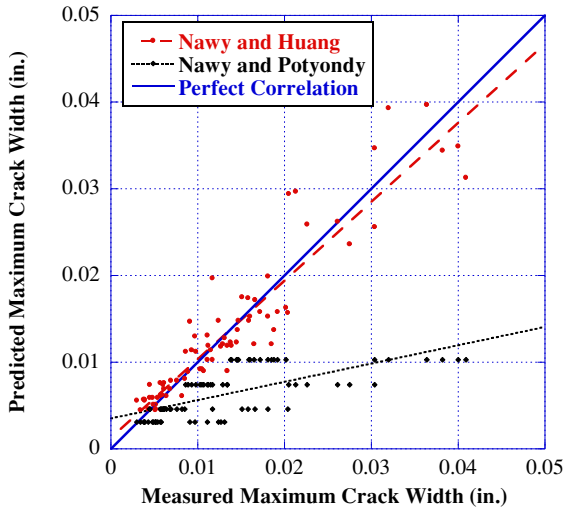
$k_3$  = coefficient that can be found in the National Annex according to different countries (recommended value is 3.4); and

$k_4$  = coefficient that can be found in the National Annex according to different countries (recommended value is 0.425).

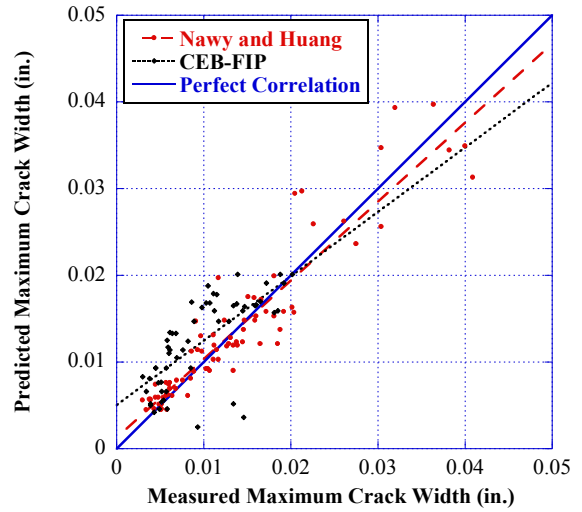
## C.7 Comparison Between Measured and Predicted Maximum Crack Width Using Various Equations

Figure C.1 through Figure C.4 present a comparison of the equation developed by Nawy and Huang (1977) and four other prediction equations. Any points that fall on the 45° line plotted on the figures indicate agreement between sources. The equations used in Eurocode were not compared with the testing data since there is not sufficient information to apply this equation. Figure C.1 indicates that the equation developed by Nawy and Potyondy (1971) did not provide good prediction results compared with the measured data since it relates the maximum crack width with the  $\Delta f_{ps}$  only. The equation developed by Nawy and Huang (1977) exhibited excellent correlation at low values of crack width. The predicted values are slightly different from the measured data when the loading increases, but the results are still close to the measured data.

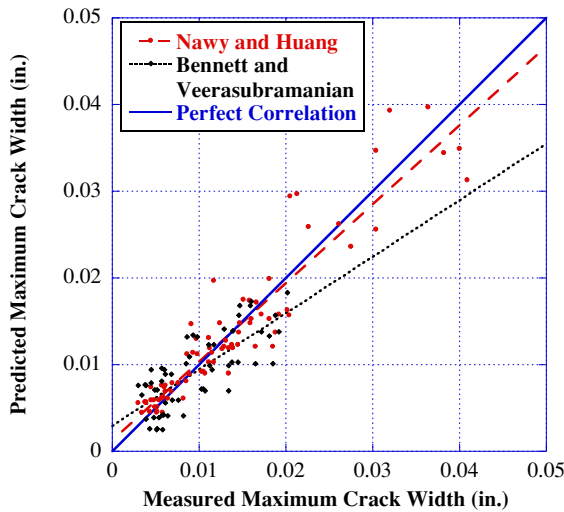
Figure C.2 indicates the equation developed by Bennett and Veerasubramanian (1972) does not exhibit good correlation with measured results when the maximum crack width increases.



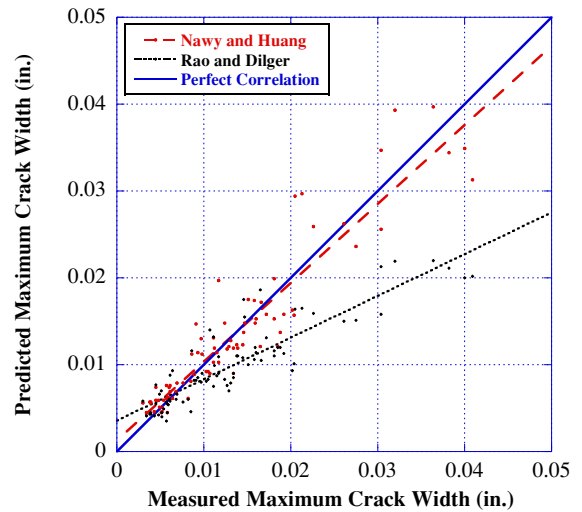
**Figure C.1.** Comparison of measured and predicted maximum crack widths using equations developed by Nawy and Huang (1977) and Nawy and Potyondy (1971).



**Figure C.3.** Comparison of measured and predicted maximum crack widths using equations developed by Nawy and Huang (1977) and CEB-FIP (1970).



**Figure C.2.** Comparison of measured and predicted maximum crack widths using equations developed by Nawy and Huang (1977) and Bennett and Veerasubramanian (1972).



**Figure C.4.** Comparison of measured and predicted maximum crack widths using equations developed by Nawy and Huang (1977) and Rao and Dilger (1992).

Figure C.3 indicates that the equation recommended by CEB-FIP (1970) overestimates the crack width prediction at small load. A number of beam specimens had fully prestressed tendons, and the measured data does not compare well with the predicted value.

Figure C.4 indicates that the equation recommended by Rao and Dilger (1992) underestimates the crack width prediction, especially under heavy load.

In summary, based on the comparisons, the equation developed by Nawy and Huang (1977) provides the best correlation with measured data. Furthermore, this equation takes the effect of bar size and steel stress into account and can be easily incorporated into the calibration procedure. The equation by Nawy and Hwang (1977) was used in the calibration of the tension in prestressed concrete when the crack width was considered.

## References

- Bennett, E., and N. Veerasubramanian. 1972. Behavior of Nonrectangular Beams with Limited Prestress after Flexural Cracking. *Journal Proceedings, American Concrete Institute*, Vol. 69, No. 9, pp. 533–542.
- CEB-FIP Joint Committee. 1970. *International Recommendations for the Design and Construction of Concrete Structures*. Cement and Concrete Association, London, England.
- EN 1992-2 (Eurocode 2): *Design of Concrete Structures—Part 2: Concrete Bridges—Design and Detailing Rules*. 2004. European Committee for Standardization, Brussels, Belgium.
- Nawy, E., and P. Huang. 1977. Crack and Deflection Control of Pretensioned Prestressed Beams. *Journal, Precast/Prestressed Concrete Institute*, Vol. 23, No. 3, pp. 30–43.
- Nawy, E., and J. Potyondy. 1971. Flexural Cracking Behavior of Pretensioned Prestressed Concrete I- and T-Beams. *Journal Proceedings, American Concrete Institute*, Vol. 68, No. 5, pp. 355–360.
- Rao, S., and W. Dilger. 1992. Control of Flexural Crack Width in Cracked Prestressed Concrete Members. *Structural Journal, American Concrete Institute*, Vol. 89, No. 2, pp. 127–138.

## APPENDIX D

# Derivation of the Resistance Prediction Equation of Prestressed Concrete Bridge Girders

The derivation of the resistance prediction equation for a prestressed concrete girder subjected to flexural loading is shown in this appendix. Figure D.1 displays the stress distribution diagram for a typical prestressed concrete bridge girder at various stages of loading. In this study, decompression is considered as the stress state producing a zero stress at the extreme bottom fibers of the prestressed girder.

Using axial force equilibrium, we have Equation D.1:

$$A_{ps}f_{ps} + A_s f_s = \frac{f_{ct}}{2} b_0 c - \frac{2}{c} (b_0 - b)(c - h_f) f_{ct} - \frac{c - h_f - h_{f1}}{2} (b - b_w)(c - h_f - h_{f1}) f_{ct} = \frac{f_{ct}}{2c} \left[ b_0 c^2 - (c - h_f)^2 (b_0 - b) - (c - h_f - h_{f1})^2 (b - b_w) \right] \quad (D.1)$$

where

- $A_s$  = area of nonprestressing steel;
- $A_{ps}$  = area of prestressing steel in tension zone;
- $b$  = prestressed beam top flange width;
- $b_0$  = effective deck width transformed to the beam material;
- $b_w$  = web thickness;
- $c$  = depth of neutral axis from the from extreme compression fiber;
- $f_{ct}$  = calculated stress in concrete at the top fiber;
- $f_{ps}$  = calculated stress in prestressing steel;
- $f_s$  = calculated stress in nonprestressing steel;
- $h_f$  = deck thickness; and
- $h_{f1}$  = top flange thickness.

The stress in the prestressing steel can be calculated as follows (Equation D.2):

$$f_{ps} = E_{ps} \epsilon_{ps} = E_{ps} (\epsilon_{se} + \epsilon_{ce}) + \frac{E_{ps}}{E_c} f_{ct} \left( \frac{d_p - c}{c} \right) \quad (D.2)$$

By rearranging Equation D.2, the stress in the concrete at the top fiber can be calculated as follows (Equation D.3):

$$f_{ct} = \frac{[f_{ps} - E_{ps} (\epsilon_{se} + \epsilon_{ce})] E_c c}{E_{ps} (d_p - c)} \quad (D.3)$$

From strain compatibility, we have Equation D.4,

$$f_s = E_s \epsilon_s = \frac{E_s}{E_c} f_{ct} \left( \frac{d_s - c}{c} \right) \quad (D.4)$$

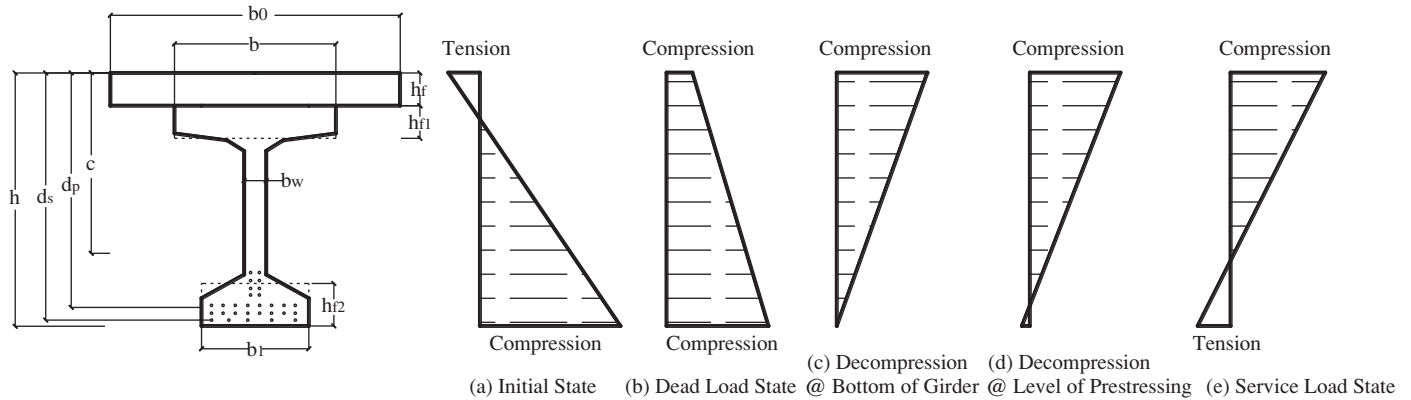
where

- $c$  = depth of neutral axis from the from extreme compression fiber;
- $d_p$  = distance from extreme compression fiber to centroid of prestressing steel;
- $d_s$  = distance from extreme compression fiber to centroid of nonprestressing steel;
- $E_c$  = modulus of elasticity of concrete;
- $E_{ps}$  = modulus of elasticity of prestressing steel;
- $E_s$  = modulus of elasticity of nonprestressing steel;
- $f_{ct}$  = stress in the concrete at the top of the beam after losses at service load;
- $\epsilon_{ce}$  = strain in concrete at the level of prestressing steel after losses at dead load state;
- $\epsilon_{ps}$  = strain in prestressing steel after losses at service load;
- $\epsilon_s$  = strain in nonprestressing steel after losses at service load; and
- $\epsilon_{se}$  = strain in prestressing steel after losses at dead load state.

Substitute Equation D.3 and Equation D.4 into Equation D.1 to obtain Equation D.5:

$$A_{ps} f_{ps} = \frac{[f_{ps} - E_{ps} (\epsilon_{se} + \epsilon_{ce})] E_c}{2 E_{ps} (d_p - c)} \cdot \left[ b_0 c^2 - (c - h_f)^2 (b_0 - b) - (c - h_f - h_{f1})^2 (b - b_w) - \frac{2 A_s E_s (d_s - c)}{E_c} \right] \quad (D.5)$$





**Figure D.1. Stress distribution diagrams for a typical prestressed concrete bridge girder at various stages of loading.**

Equation D.5 can be simplified and rewritten as a quadratic equation with unknown  $c$ , neutral axis depth, as follows in Equation D.6:

$$c^2 + \frac{2}{b_w} \left[ \frac{A_{ps} f_{ps} E_{ps}}{[f_{ps} - E_{ps} (\epsilon_{se} + \epsilon_{ce})] E_c} + b_0 h_f + b h_{f1} \right] \cdot c - \frac{2}{b_w} \left[ \frac{A_{ps} f_{ps} E_{ps}}{[f_{ps} - E_{ps} (\epsilon_{se} + \epsilon_{ce})] E_c} - \frac{1}{2} (b - b_0) h_f^2 + \frac{1}{2} (b - b_w) (h_f + h_{f1})^2 + \frac{A_s E_s d_s}{E_c} \right] = 0 \quad (D.6)$$

The moment resistance can be expressed as follows (Equation D.7):

$$M_n = A_{ps} f_{ps} d_p + A_s f_s d_s - \frac{1}{6} f_{ct} b_0 c^2 + \frac{(c - h_f)^2 (b_0 - b)}{2c} f_{ct} \left( \frac{c + 2h_f}{3} \right) + \frac{(c - h_f - h_{f1})^2 (b - b_w)}{2c} f_{ct} \left( \frac{c + 2h_f + 2h_{f1}}{3} \right) \quad (D.7)$$

where

$M_n$  = nominal moment resistance.

$f_s$  is calculated using Equation D.3, and  $f_{ct}$  is calculated using Equation D.4.

The depth of neutral axis from the compression face,  $c$ , can be computed from Equation D.6.

Also, assuming a linear elastic relationship in the behavior of the prestressing steel, we have Equation D.8,

$$\epsilon_{se} = \frac{f_{se}}{E_{ps}} \quad (D.8)$$

Then Equation D.9 follows,

$$\epsilon_{ce} = \frac{A_{ps} f_{se}}{E_c} \left( \frac{1}{A_c} + \frac{e_0^2}{I} \right) - \frac{M_D e_0}{E_c I} \quad (D.9)$$

where

$A_c$  = area of concrete at the cross section considered;  
 $e_0$  = eccentricity of the prestressing force with respect to the centroid of the section;

$E_c$  = modulus of elasticity of concrete;

$E_{ps}$  = modulus of elasticity of prestressing steel;

$f_{se}$  = effective stress in prestressing steel after losses;

$I$  = moment of inertia; and

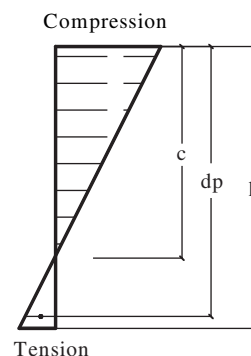
$M_D$  = dead load moment.

Considering an uncracked section under service loads and plane section remains plane, the linear strain distribution diagram is as follows in Figure D.2:

From Figure D.2, the relationship between top and bottom strain is as follows (Equations D.10 and D.11):

$$\frac{d_p - c}{h - c} \cdot \epsilon_c = \epsilon_{ps} \quad (D.10)$$

$$\frac{d_p - c}{h - c} \cdot f_{cb} \frac{E_{ps}}{E_c} = \Delta f_{pt} \quad (D.11)$$



**Figure D.2. Strain distribution at service loads.**

where

$\epsilon_c$  = strain in concrete at bottom fiber;

$E_c$  = elastic modulus of concrete;

$\Delta f_{pt}$  = change in prestressing tendons stress between decompression and the stress in concrete at the bottom of the girder reaching  $f_{ct}$  assuming uncracked section; and

$f_{cb}$  = concrete allowable tensile stress at the bottom of the girder.

According to the current *AASHTO LRFD Bridge Design Specifications* (2012),  $f_{cb} = 0.19\sqrt{f'_c}$  or  $f_{cb} = 0.0948\sqrt{f'_c}$ , depending on the exposure conditions.

Then  $f_{ps}$  for the uncracked section should be as follows (Equation D.12):

$$f_{ps} = \Delta f_{pt} + f_{ps(M_{Dec})} \quad (D.12)$$

For the cracked section, the  $f_{ps}$  can be calculated by Equation D.13:

$$f_{ps} = \Delta f_{ps} + f_{ps(M_{Dec})} \quad (D.13)$$

where

$f_{ps(M_{Dec})}$  = the stress in prestressing steel at decompression;

$\Delta f_{ps}$  = the increase in the prestressing steel stress beyond the decompression state for cracked members; and

$M_{Dec}$  = the decompression moment.

$\Delta f_{ps}$  in Equation D.13 can be calculated based on the equation of maximum crack width at the bottom of prestressed concrete girder. In this study, Equation D.14, developed by Nawy and Huang (1977), was used:

$$w_{max} = 5.85 \times 10^{-5} \frac{A_t}{\beta \Sigma 0} (\Delta f_{ps}) \quad (D.14)$$

where

$\Sigma 0$  = sum of reinforcing element circumferences;

$A_t$  = area of concrete in tension; and

$\beta$  = ratio of distance from neutral axis of beam to concrete outside tension face to distance from neutral axis to steel reinforcement centroid.

By rearranging Equation D.14,  $\Delta f_{ps}$  can be calculated using Equation D.15:

$$\Delta f_{ps} = \frac{w_{max} \cdot \beta \cdot \Sigma 0}{5.85 \times 10^{-5} \cdot A_t} \quad (D.15)$$

$\Delta f_{pt}$  varies according to the maximum allowable tensile stress at the bottom of the concrete girder.

Moreover,  $f_{ps(M_{Dec})}$  can be calculated using Equation D.16:

$$f_{ps(M_{Dec})} = f_{se} + \frac{E_{ps} [M_{Dec} - M_D]}{IE_c \left[ 1 + \frac{A_{ps} E_{ps}}{E_c} \left( \frac{1}{A_c} + \frac{e_0^2}{I} \right) \right]} \quad (D.16)$$

The decompression moment at the level of prestressing strands,  $M_{Decp}$ , can be calculated using Equation D.17:

$$M_{Decp} = \frac{\left[ f_{se} - \frac{M_D e_0 E_{ps}}{\left[ I + \frac{A_{ps} E_{ps}}{E_c} \left( \frac{1}{A_c} + \frac{e_0^2}{I} \right) \right] IE_c} \right]}{e_0 E_{ps}} \quad (D.17)$$

The decompression moment at the bottom fiber of the concrete girder,  $M_{Decb}$ , can be calculated using Equation D.18:

$$M_{Decb} = \frac{\left[ f_{se} - \frac{M_D e_0 E_{ps}}{\left[ I + \frac{A_{ps} E_{ps}}{E_c} \left( \frac{1}{A_c} + \frac{e_0^2}{I} \right) \right] IE_c} \right]}{\frac{y_b}{I \left[ \frac{1}{A_c} + \frac{e_0 y_b}{I} \right] A_{ps}} - \frac{e_0 E_{ps}}{\left[ 1 + \frac{A_{ps} E_{ps}}{E_c} \left( \frac{1}{A_c} + \frac{e_0^2}{I} \right) \right] IE_c}} \quad (D.18)$$

where

$A_c$  = area of concrete at the cross section considered;

$A_{ps}$  = area of prestressing steel in tension zone;

$e_0$  = eccentricity of the prestressing force with respect to the centroid of the section at supports;

$y_b$  = distance from centroidal axis to extreme bottom fiber;

$E_c$  = modulus of elasticity of concrete;

$E_{ps}$  = modulus of elasticity of prestressing steel;

$f_{se}$  = effective stress in prestressing steel after losses;

$I$  = moment of inertia;

$M_D$  = dead load moment;

$M_{Decb}$  = decompression moment at the bottom of the girder; and

$M_{Decp}$  = decompression moment at the level of the prestressing strands.

## References

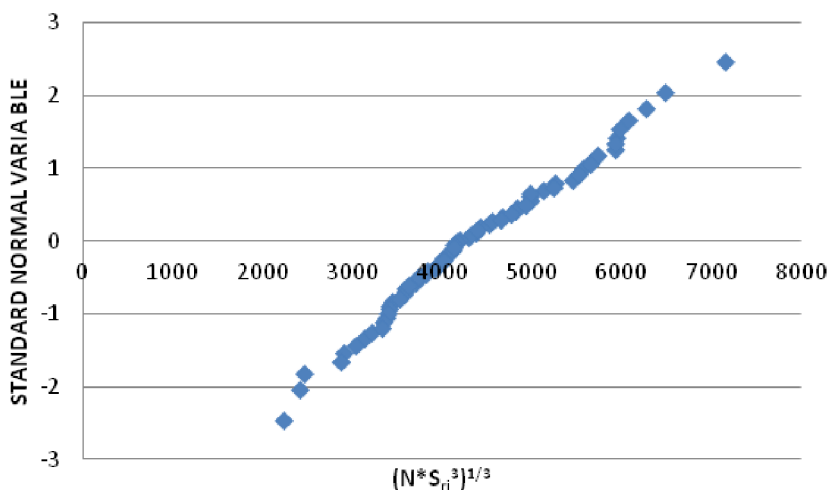
- AASHTO LRFD Bridge Design Specifications*, 6th ed. 2012. American Association of State Highway and Transportation Officials, Washington, D.C.
- Nawy, E., and P. Huang. 1977. Crack and Deflection Control of Prestressed Beams. *Journal, Precast/Prestressed Concrete Institute*, Vol. 23, No. 3, pp. 30–43.

## APPENDIX E

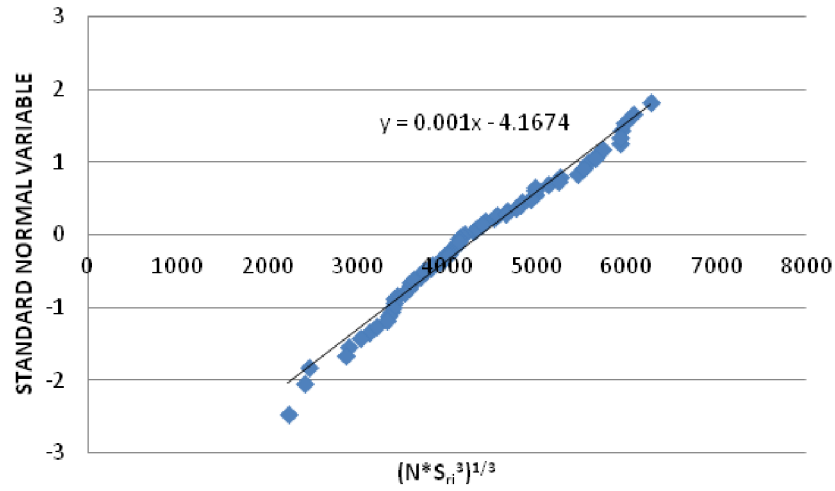
# Normal Probability Plots of Fatigue Data for the Various Detail Categories

The data in the various steel-category plots (A through E) are from Keating and Fisher 1986. The data on the plots for steel reinforcement in tension are from Fisher and Viest 1961; Pfister and Hognestad 1964; Burton and Hognestad

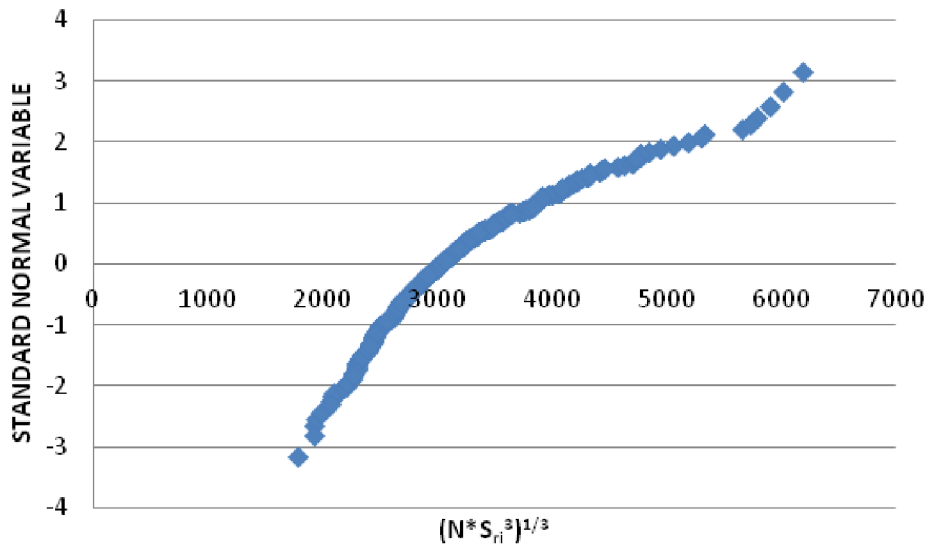
1967; Hanson et al. 1968; Helgason et al. 1976; Lash 1969; MacGregor et al. 1971; and Amorn et al. 2007. The data for the plots of concrete in compression are from Hilsdorf and Kesler 1966.



**Figure E.1.** Normal probability plot of Detail Category A fatigue data.



*Figure E.2. Normal probability plot of Detail Category A truncated fatigue data with best fit line.*



*Figure E.3. Normal probability plot of Detail Category B fatigue data.*

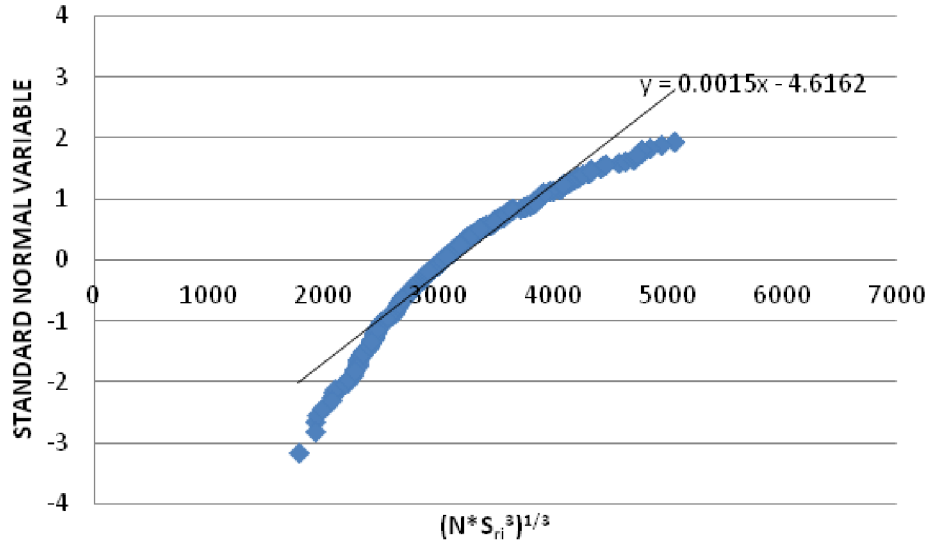


Figure E.4. Normal probability plot of Detail Category B truncated fatigue data with best fit line.

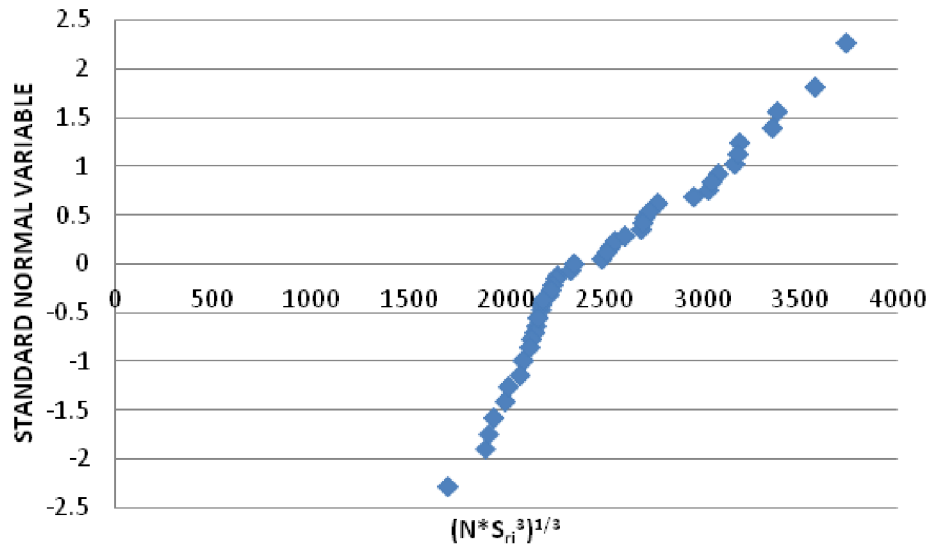


Figure E.5. Normal probability plot of Detail Category B' fatigue data.

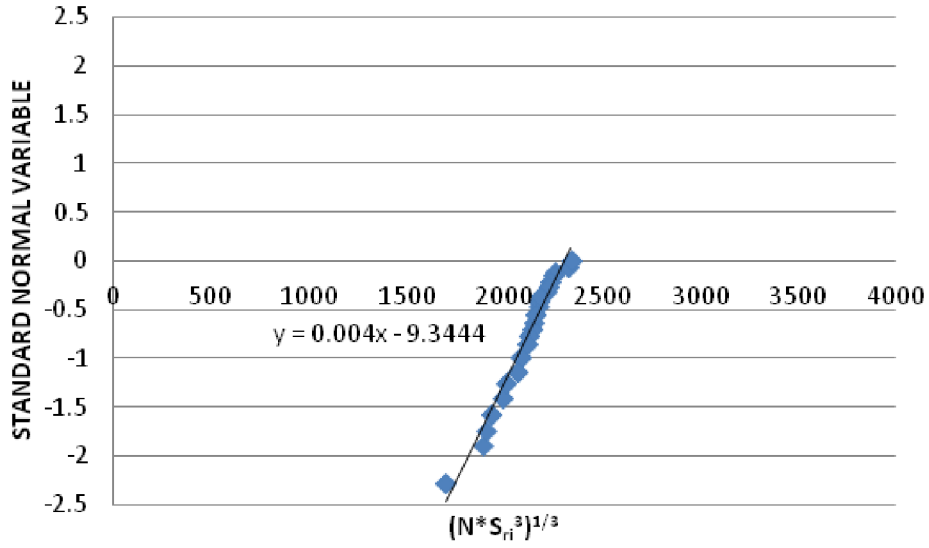


Figure E.6. Normal probability plot of Detail Category B' truncated fatigue data with best fit line.

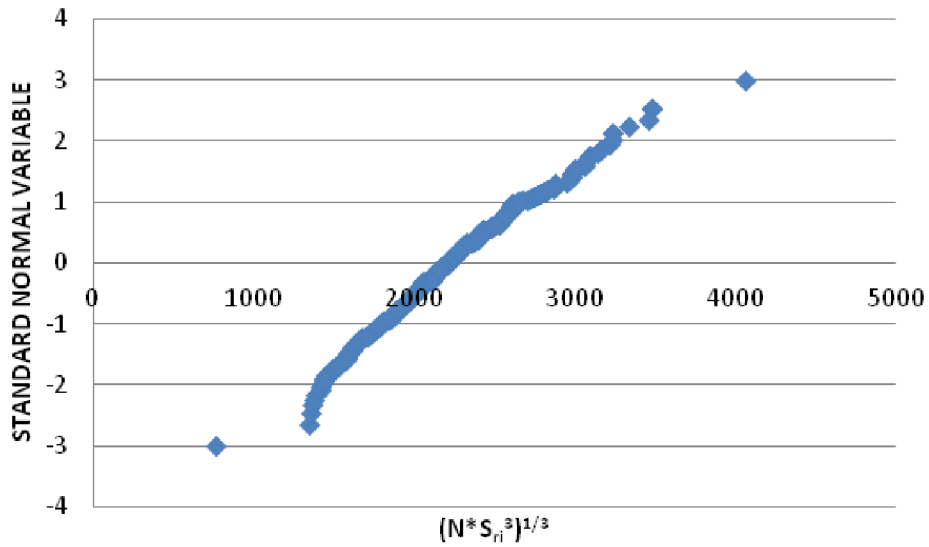
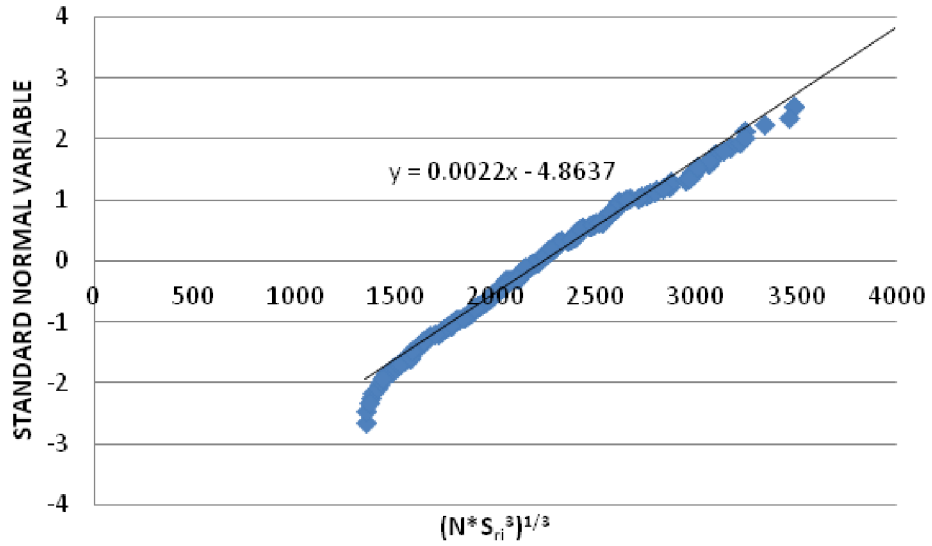
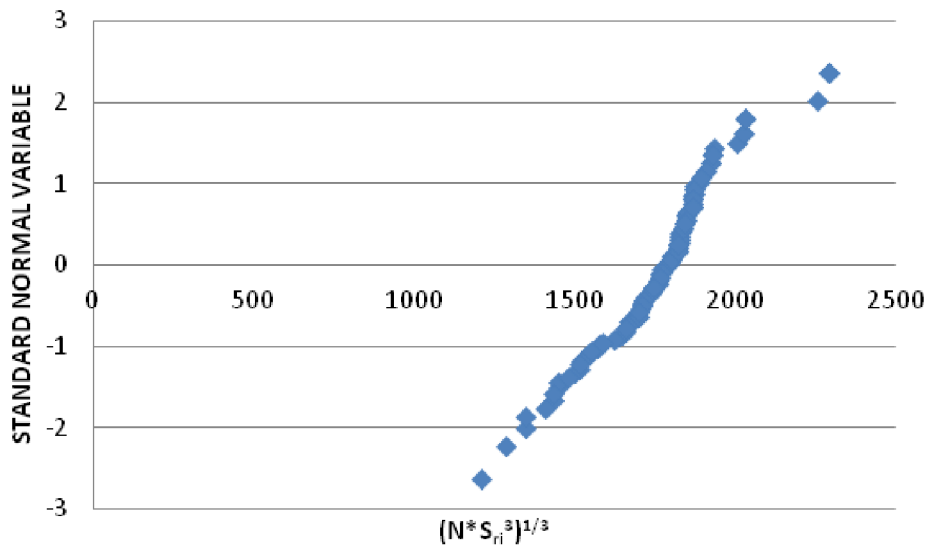


Figure E.7. Normal probability plot of Detail Categories C and C' fatigue data.





**Figure E.8.** Normal probability plot of Detail Categories C and C' truncated fatigue data with best fit line.



**Figure E.9.** Normal probability plot of Detail Category D fatigue data.

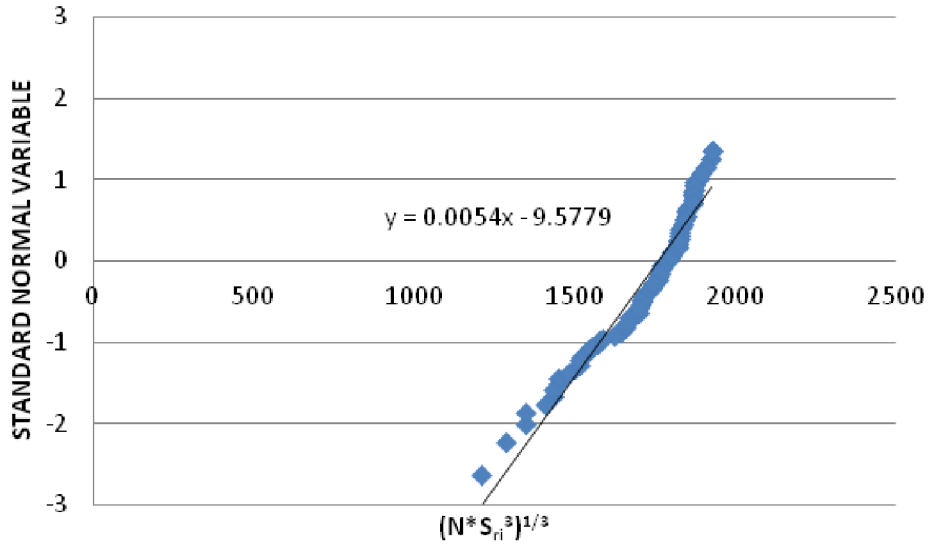


Figure E.10. Normal probability plot of Detail Category D truncated fatigue data with best fit line.

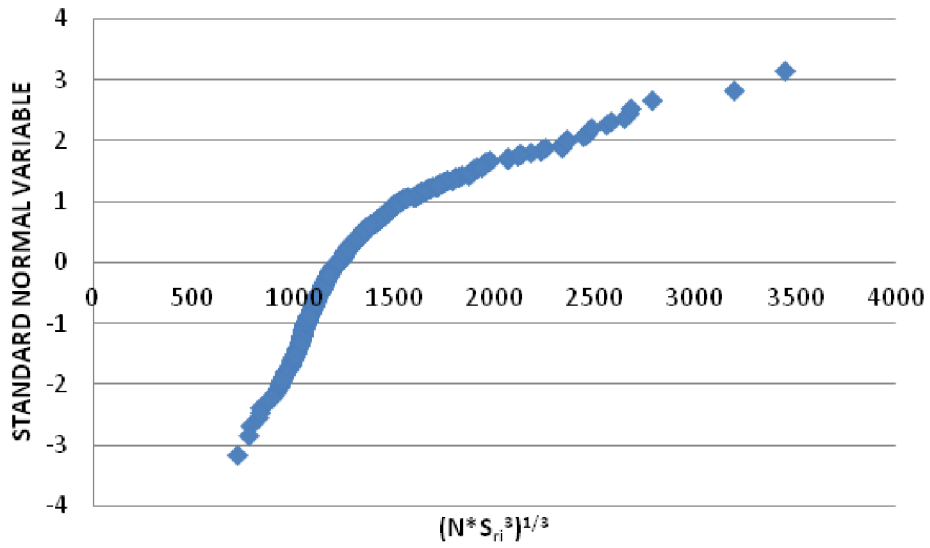
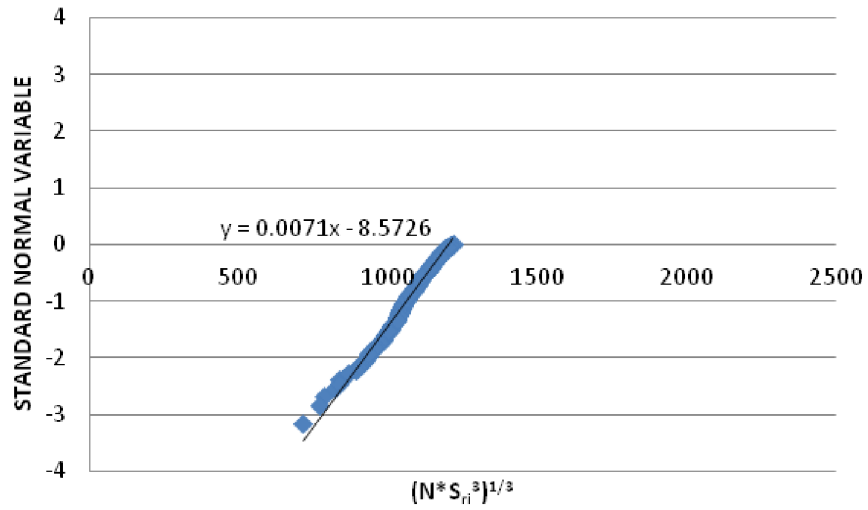
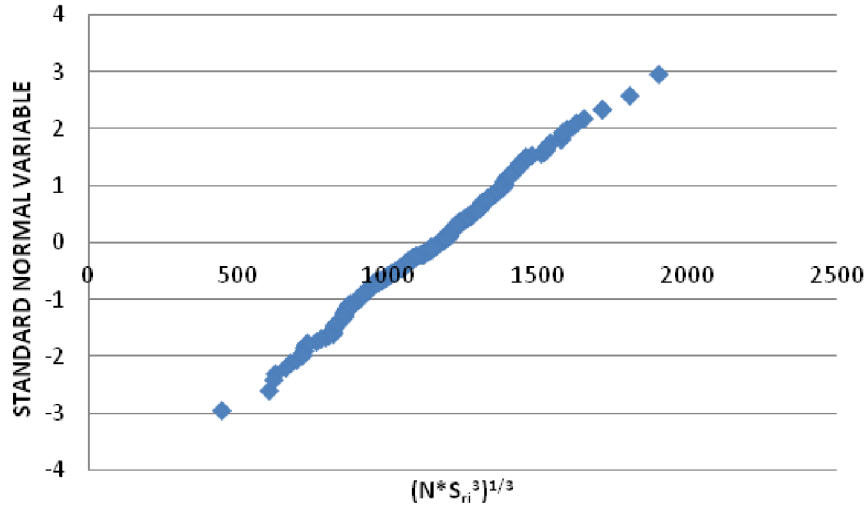


Figure E.11. Normal probability plot of Detail Category E fatigue data.



**Figure E.12. Normal probability plot of Detail Category E truncated fatigue data with best fit line.**



**Figure E.13. Normal probability plot of Detail Category E' fatigue data.**

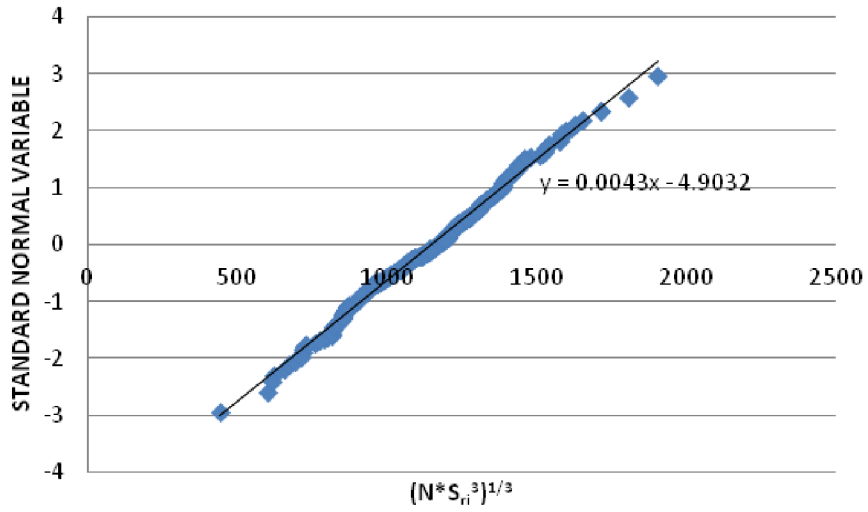


Figure E.14. Normal probability plot of Detail Category E' truncated fatigue data with best fit line.

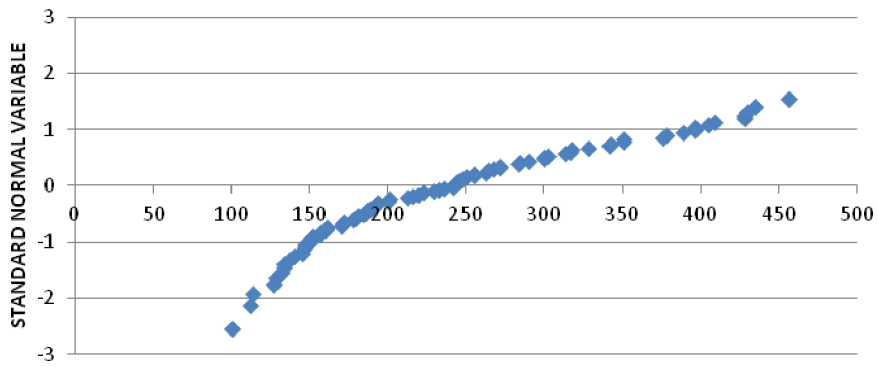


Figure E.15. Normal probability plot for concrete in compression.

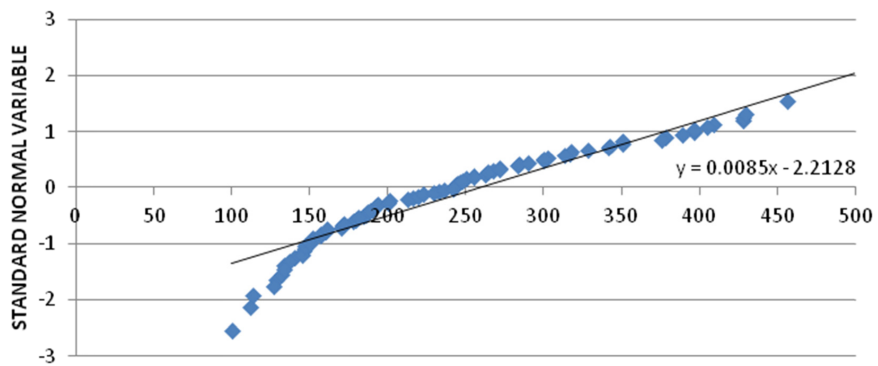


Figure E.16. Normal probability plot for concrete in compression truncated fatigue data with best fit line.

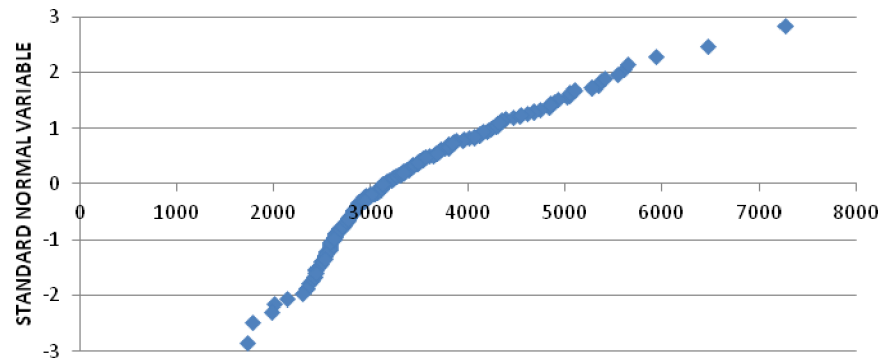


Figure E.17. Normal probability plot for steel reinforcement in tension.

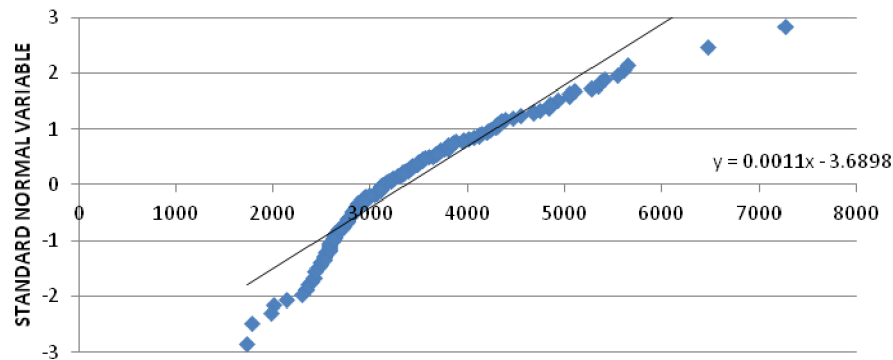


Figure E.18. Normal probability plot for steel reinforcement in tension truncated fatigue data with best fit line.

## References

- Amorn, W., J. Bowers, A. Girgis, and M. Tadros. 2007. Fatigue of Deformed Welded-Wire Reinforcement. *Journal, Precast/Prestressed Concrete Institute*, Vol. 52, No. 1, pp. 106–120.
- Burton, K., and E. Hognestad. 1967. Fatigue Test of Reinforcing Bars-Tack Welding of Stirrups. *Journal, American Concrete Institute*, Vol. 64, No. 5, pp. 244–252.
- Fisher, J., and I. Viest. 1961. *Special Report 66: Fatigue Tests of Bridge Materials of the AASHO Road Test*. HRB, National Research Council, Washington, D.C.
- Hanson, J., K. Burton, and E. Hognestad. 1968. Fatigue Tests of Reinforcing Bars: Effect of Deformation Pattern. *Journal of the Portland Cement Association Research and Development Laboratories*, Vol. 10, No. 3, pp. 2–13.
- Helgason, T., J. Hanson, N. Somes, W. Corley, and E. Hognestad. 1976. *NCHRP Report 164: Fatigue Strength of High-Yield Reinforcing Bars*. TRB, National Research Council, Washington, D.C.
- Hilsdorf, H., and C. Kesler. 1966. Fatigue Strength of Concrete Under Varying Flexural Stresses. *Journal Proceedings, American Concrete Institute*, Vol. 63, No. 10, pp. 1059–1076.
- Keating, P., and J. Fisher. 1986. *NCHRP Report 286: Evaluation of Fatigue Tests and Design Criteria on Welded Details*. TRB, National Research Council, Washington, D.C.
- Lash, S. 1969. Can High-Strength Reinforcement Be Used in Highway Bridges? In *First International Symposium on Concrete Bridge Design*, SP-23, American Concrete Institute, Detroit, Mich., pp. 283–300.
- MacGregor, J., I. Jhamb, and N. Nuttall. 1971. Fatigue Strength of Hot-Rolled Deformed Reinforcing Bars. *Journal Proceedings, American Concrete Institute*, Vol. 68, No. 3, pp. 169–179.
- Pfister, J., and E. Hognestad. 1964. High-Strength Bars As Concrete Reinforcement, Part 6: Fatigue Tests. *Journal of the Portland Cement Association Research and Development Laboratories*, Vol. 6, No. 1, pp. 65–84.

## APPENDIX F

# Data Used for Calibration

### F.1 Purpose and Contents of this Appendix

The purpose of this appendix is to facilitate future enhancement of service limit state (SLS) calibration as well as to allow for customization by individual bridge owners. To accomplish this purpose, certain guidelines and databases have been included. (Section F.1 references are included in the References, page 263.)

- Section F.2: a step-by-step description of the implementation of the Monte Carlo analysis introduced in Chapter 3.
- Section F.3: an excerpt from the database of WIM (weigh-in-motion) data used in the development of live load models presented in Chapter 5. These data are available at <http://www.trb.org/Main/Blurbs/170201.aspx>.
- Section F.4: a condensed version of the geotechnical calibration reported in Chapter 6 with additional information provided on the geotechnical properties of the test sites discussed in Chapter 6. It is anticipated that the regional nature of geotechnical practice will result in calibration of locally preferred methods of predicting settlement of shallow and deep foundations in lieu of the Hough (1959) and Schmertmann et al. (1978) methods used herein.
- Sections F.5 and F.6: descriptions of the concrete and steel bridges selected from the NCHRP Project 12-78 database and used for various studies reported here (Mlynarski et al. 2011). Other bridges could be substituted.
- Section F.7: a database of fatigue tests on steel details (Keating and Fisher 1986; P. B. Keating, personal communication, 2012).
- Section F.8: a database of fatigue tests on plain concrete and reinforcement (Ople and Hulsbos 1966; Fisher and Viest 1961; Pfister and Hognestad 1964; Hanson et al. 1968; Lash 1969).

### F.2 Monte Carlo Analysis Using Microsoft Excel

Determination of the failure rate and the associated reliability index,  $\beta$ , through Monte Carlo simulation using Microsoft (MS) Excel involves the following 15-step computational procedure adapted from Nowak and Collins (2013):

1. Determine the nominal dead load,  $D_n$ , the nominal live load plus impact,  $L_n$ , and the nominal resistance,  $R_n$ , for the subject bridge according to the *AASHTO LRFD Bridge Design Specifications* (2012).
2. Assume  $i = 1$ .
3. Generate a uniformly distributed random number  $0 \leq u_{D_i} \leq 1$  using the command RAND.
4. Calculate the corresponding value of  $D_i$  (a normal random variable). Equation F.2.1 follows:

$$D_i = \mu_D + \sigma_D \phi^{-1}(u_{D_i}) \quad (\text{F.2.1})$$

where  $\phi^{-1}$  is the inverse standard normal distribution function calculated using the command NORMSINV. Equations F.2.2 and F.2.3 follow as shown:

$$\mu_D = \lambda_D D_n \quad (\text{F.2.2})$$

$$\sigma_D = V_D \mu_D \quad (\text{F.2.3})$$

5. Generate a uniformly distributed random number  $0 \leq u_{L_i} \leq 1$  using the command RAND.
6. Calculate the corresponding value of  $L_i$  (a normal random variable). Equation F.2.4 follows:

$$L_i = \mu_L + \sigma_L \phi^{-1}(u_{L_i}) \quad (\text{F.2.4})$$

where  $\phi^{-1}$  is the inverse standard normal distribution function calculated using the command NORMSINV. Equations F.2.5 and F.2.6 follow as shown:

$$\mu_L = \lambda_L L_n \quad (\text{F.2.5})$$



$$\sigma_L = V_L \mu_L \quad (\text{F.2.6})$$

7. Generate a uniformly distributed random number  $0 \leq u_{Ri} \leq 1$  using the command RAND.
8. Calculate the corresponding value of  $R_i$  (a lognormal random variable). Equation F.2.7 follows.

$$R_i = \exp(\mu_{\ln R} + \sigma_{\ln R} \phi^{-1}(u_{Ri})) \quad (\text{F.2.7})$$

where  $\phi^{-1}$  is the inverse standard normal distribution function calculated using the command NORMSINV.

$$\mu_{\ln R} = \ln(\mu_R) - \frac{1}{2} \sigma_{\ln R}^2$$

$$\sigma_{\ln R} = (\ln(V_{R^2} + 1))^{1/2}.$$

9. Calculate the limit state function,  $Y_i = R_i - (D_i + L_i)$ , and save the value.
10. Assume  $i = i + 1$ ; go back to Step 3 and iterate until the desired number of simulations,  $N$ , is obtained.
11. Rearrange the values of  $Y_i$  in ascending order using the command RANK and reassign the values of  $i$  in ascending order also.
12. Calculate the probabilities. Equation F.2.8 follows.

$$p_i = i/(1 + N) \quad (\text{F.2.8})$$

13. Calculate the corresponding values of the inverse standard normal distribution function,  $\phi^{-1}(p_i)$  using the command NORMSINV.
14. Plot  $\phi^{-1}(p_i)$  versus  $Y_i$ ; the resulting curve is the cumulative distribution function of  $Y$ .
15. The reliability index,  $\beta$ , is equal to the negative value of the plotted cumulative distribution function for  $Y = 0$ .

**Table F.3.1. Filtered WIM Data Format**

Entry Number	Description	Entry Number	Description
1	Direction	23	11th spacing between axles [ft]
2	Lane	24	12th spacing between axles [ft]
3	Year	25	13th spacing between axles [ft]
4	Day	26	1st axle weight [kip]
5	Hour	27	2nd axle weight [kip]
6	Min	28	3rd axle weight [kip]
7	Sec	29	4th axle weight [kip]
8	Total weight	30	5th axle weight [kip]
9	Total length	31	6th axle weight [kip]
10	Speed	32	7th axle weight [kip]
11	Vehicle class	33	8th axle weight [kip]
12	Number of axles	34	9th axle weight [kip]
13	1st spacing between axles [ft]	35	10th axle weight [kip]
14	2nd spacing between axles [ft]	36	11th axle weight [kip]
15	3rd spacing between axles [ft]	37	12th axle weight [kip]
16	4th spacing between axles [ft]	38	13th axle weight [kip]
17	5th spacing between axles [ft]	39	14th axle weight [kip]
18	6th spacing between axles [ft]	40	Ratio of truck moment to HL93 moment for 30-ft span
19	7th spacing between axles [ft]	41	Ratio of truck moment to HL93 moment for 60-ft span
20	8th spacing between axles [ft]	42	Ratio of truck moment to HL93 moment for 90-ft span
21	9th spacing between axles [ft]	43	Ratio of truck moment to HL93 moment for 120-ft span
22	10th spacing between axles [ft]	44	Ratio of truck moment to HL93 moment for 200-ft span





complicating the process with esoteric probabilistic principles which in the end lead to the same result.

#### F.4.1 Step 1: Express the Service Limit State in Terms of Load and Resistance

In the context of deformations, tolerable deformations,  $\delta_T$ , are considered as resistances while the predicted deformations,  $\delta_p$ , are considered as loads. For service limit state calibration for foundation deformation, the limit state,  $g$ , is expressed as follows (Equation F.4.1):

$$g = \delta_p / \delta_T \quad (\text{F.4.1})$$

For the example of immediate settlements, the load and the resistance parameters are as follows:

- Load: Predicted (estimated or calculated) immediate vertical settlement,  $\delta_p$
- Resistance: Tolerable (limiting or measured) immediate vertical settlement,  $\delta_T$

#### F.4.2 Step 2: Develop Statistical Model for Load ( $\delta_p$ )

The usefulness of this appendix will be demonstrated by using the analytical method proposed by Schmertmann et al. (1978). Tables F.4.1 and F.4.2 show a data set for spread footings based on vertical settlements of footings measured at 20 footings for 10 instrumented bridges in the northeastern United States (Gifford et al. 1987). More detailed subsurface data are given in that report. Each of the footing designations in the tables represents a footing supporting a single substructure unit (abutment or pier). Four of the instrumented bridges were single-span structures. Two 2-span and three 4-span bridges were also monitored in addition to a single 5-span structure. Nine of the structures were designed to carry highway traffic, while the one instrumented bridge consisted of a 4-span railroad bridge across an Interstate highway. The bridges included 5 simple-span and 5 continuous-beam structures. Additional information on the instrumentation and data collection at the 10 bridges can be found in Gifford et al. (1987).

Figure F.4.1 shows a plot of the data in Table F.4.2 and the spread of the data about the 1:1 diagonal line, which defines the case in which the predicted and measured values are equal. Such a plot provides a visual frame of reference to judge the accuracy of the prediction method, in this case Schmertmann's method. For example, if the data points align closely with the 1:1 diagonal line, then the predictions based on the analytical method being evaluated are close to the measured values and are more accurate compared with

the case in which the data points do not align closely with the 1:1 diagonal line. In the geotechnical literature (e.g., Tan and Duncan 1991), *accuracy* is defined as the mean value of the ratio of the predicted (calculated) to the measured settlements. Table F.4.3 shows the values of accuracy, denoted by  $X$ , where  $X = \delta_p / \delta_M$ , for each footing based on the data in Table F.4.2.

As noted in Step 1 of the calibration process, the value of  $\delta_M$  can be considered to be the resistance and equivalent to the tolerable settlement,  $\delta_T$ . The accuracy,  $X = \delta_p / \delta_M$  (or  $\delta_p / \delta_T$ ), is a random variable that can be modeled by an appropriate probability distribution function (PDF). The data for  $X$  in Table F.4.3 were used to develop a histogram of accuracy ( $X$ ) values as shown in Figure F.4.2.

The arithmetic mean ( $M$ ) and standard deviation (SD) of the data in Table F.4.3 are 1.381 and 1.006, respectively, and are noted in Column 2 of Table F.4.3 and Table F.4.4. The histogram of the data in Column 2 of Table F.4.3 is shown in Figure F.4.2. The histogram does not resemble the classical bell shape that is characteristic of normally distributed data. To evaluate the deviation of the data from a classical normal PDF, the data for the value of accuracy ( $X$ ) in Table F.4.3 were plotted against the standard normal variable,  $z$ , to generate a cumulative distribution function (CDF) as shown in Figure F.4.3 [see Chapter 5 in Allen et al. (2005) for the definition of standard normal variable,  $z$ , and procedures to develop Figure F.4.3]. As noted in Allen et al. (2005), the benefit of plotting the data in this manner on a CDF plot is that normally distributed data plot as a straight line with a slope equal to  $1/SD$ , and the intercept on the horizontal axis corresponding to  $z = 0$  is equal to the mean value  $M$ . As can be seen in Figure F.4.3, the data points based on Table F.4.3 do not plot on the straight line, which confirms the observation made based on the histogram in Figure F.4.2.

By using procedures described in Allen et al. (2005), a lognormal distribution is used to evaluate the nonnormal data. As seen in Figure F.4.3, the lognormal distribution fits the data better than the normal distribution. The lognormal distribution, which is valid between values of 0 and  $+\infty$ , is used in Figure F.4.3 because (a) immediate settlement cannot have negative values, and (b) lognormal PDFs have been used in the past for nonnormal distributions during calibration of the strength limit state for geotechnical as well as structural features in the *AASHTO LRFD* framework (2012). For service limit state, a PDF with an upper bound and lower bound (e.g., beta distribution) instead of open tail(s) (e.g., normal or lognormal distribution) may be more appropriate since the conditions represented by an open tail PDF are not physically possible when one considers foundation deformations. As noted, the lognormal PDF is used here simply to be consistent with the PDFs that have been used in the LRFD calibration processes to date.

Table F.4.1. Study Bridge Data

Element Designation	$q$ (ksf)	$N_f$ (blows/ft)	$N_c$ (blows/ft)	$\gamma$ (kcf)	Water Level (ft)	B (ft)	L (ft)	D (ft)	$q_c$ (kg/cm <sup>2</sup> )	H (ft)	$\bar{\sigma}_{vo}$ max
S1	3.20	23 to 36	44	0.120	12	17.0	63.7	F	NA	117	2(F)
S2	2.67	60	58	0.120	12	17.0	63.7	F	NA	117	2(F)
S3	2.32	32 to 44	43	0.120	11.5	15.25	52.5	F	NA	35	2(F)
S4	2.44	18 to 24	19	0.120	9	16.75	52.5	4	NA	42	3
S5	1.88	12 to 13	12	0.120	4	12.50	41.0	5	NA	40	3
S6	1.70	18 to 20	34	0.120	31	11.0	74.6	F	28,61,90,125	155	1(F)
S7	2.34	22	22	0.115	12	18.5	79.0	5	NA	130	1
S8	2.10	18 to 19	18	0.120	6	21.0	21.0	5	NA	150	1
S9	1.50	18 to 19	18	0.120	6	21.0	30.4	5	NA	150	1
S10	2.34	16 to 17	20	0.115	12	16.0	26.8	5	90,70,88	153	1
S11	2.48	18 to 22	22	0.115	12	16.0	18.5	5	74	155	1
S12	1.48	13 to 14	15	0.115	12	21.0	33.0	5	NA	120	1
S13	1.60	23 to 28	25	0.115	12	21.0	30.0	5	NA	120	1
S14	3.30	21	21	0.120	28	8.1	42.9	F	165	197	2(F)
S15	3.43	8	8	0.120	26.5	8.1	42.9	F	53	>150	2(F)
S16	2.40	34 to 37	42	0.120	10	16.75	76.9	6	NA	52	2
S17	2.34	21 to 27	24	0.125	8	15.25	76.1	6.5	NA	51	2
S18	1.88	37 to 53	55	0.120	2	15.25	61.7	9	NA	10	2
S19	1.79	25 to 34	39	0.120	2	15.25	67.3	9	NA	10	2
S20	2.14	19 to 22	24	0.113, 0.115	44	28.0	28.0	0	62,131	>2B	2
S21	3.01	25 to 26	23	0.115	0	20.0	100.8	22	NA	>2B	3
S22	3.25	26 to 31	38	0.115	1	20.0	100.8	5	NA	>2B	3
S23	3.51	33 to 40	39	0.115, 0.120	17	21.75	44.4	F	NA	41	2(F)
S24	3.37	37 to 38	49	0.115	13	16.0	44.7	0	114,183	48	2

Notes:

 $q$  = footing bearing pressure (average) $N_f$  = field standard penetration test  $N$ -value (range of  $N$ -values is due to different depths of influence for different settlement calculation methods) $N_c$  = corrected  $N$ -value (corrected for overburden per Peck and Bazaraa 1969) $\gamma$  = soil total unit weight (assumed) (kips per cubic foot)

Water Level = depth of water table (below footing bearing elevation)

B = footing width

L = footing length

D = depth of footing embedment below ground surface; (F) indicates footing is on new fill

 $q_c$  = static cone penetration test cone resistance (multiple values indicate that profile was subdivided into layers with corresponding  $q_c$  values)H = depth below footing to (relatively) incompressible stratum ( $H > 2B$  indicates an incompressible stratum is located below the depth of influence) $\bar{\sigma}_{vo}$  max = soil stress history: 1 = preloaded; 2 = normally loaded; 3 = partially preloaded

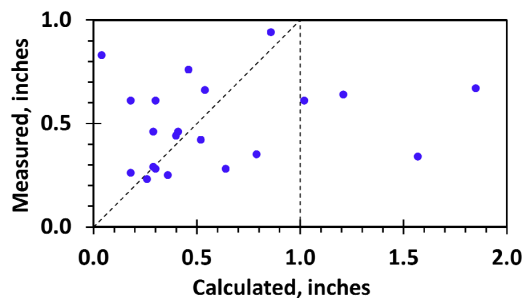
NA = not available

Source: Gifford et al. (1987).

**Table F.4.2. Data for Measured and Calculated Settlements**

Footing Designation	Settlement (in.)	
	Measured ( $\delta_M$ )	Calculated ( $\delta_P$ )
S1	0.35	0.79
S2	0.67	1.85
S3	0.94	0.86
S4	0.76	0.46
S5	0.61	0.30
S6	0.42	0.52
S7	0.61	0.18
S8	0.28	0.30
S9	0.26	0.18
S10	0.29	0.29
S11	0.25	0.36
S14	0.46	0.41
S15	0.34	1.57
S16	0.23	0.26
S17	0.44	0.40
S20	0.64	1.21
S21	0.46	0.29
S22	0.66	0.54
S23	0.61	1.02
S24	0.28	0.64

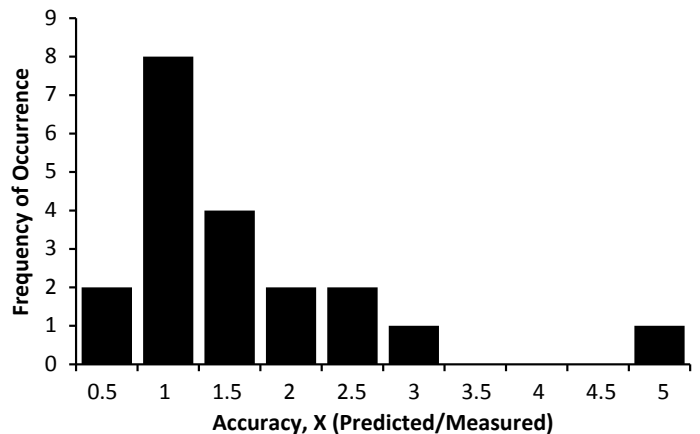
Note: Gifford et al. (1987), the source for the table, notes that data for Footings S12, S13, and S18 were not included because construction problems at those sites resulted in disturbance of the subgrade soils and short term settlement was increased. Data for Footing S19 appear to be anomalous and have been excluded from this table and from Figure F.4.1.



**Figure F.4.1. Comparison of measured and calculated settlements based on service load data in Table F.4.2 for Schmertmann’s method.**

**Table F.4.3. Values and Statistics of Accuracy ( $X = \delta_P/\delta_M$ ) and Natural Log of X Values [ $\ln(X)$ ] Based on Data Shown in Table F.4.2**

Footing Designation	X	$\ln(X)$
S1	2.257	0.814
S2	2.761	1.016
S3	0.915	-0.089
S4	0.605	-0.502
S5	0.492	-0.710
S6	1.238	0.214
S7	0.295	-1.221
S8	1.071	0.069
S9	0.692	-0.368
S10	1.000	0.000
S11	1.440	0.365
S14	0.891	-0.115
S15	4.618	1.530
S16	1.130	0.123
S17	0.909	-0.095
S20	1.891	0.637
S21	0.630	-0.461
S22	0.818	-0.201
S23	1.672	0.514
S24	2.286	0.827
Mean	1.381	0.1173
Standard deviation	1.006	0.6479
Coefficient of variation	0.728	



**Figure F.4.2. Histogram for accuracy (X) of Schmertmann et al. (1978) method.**



**Table F.4.4. Statistics for Accuracy Based on Normal and Lognormal Distributions**

Statistic	Normal	Lognormal	Lognormal
	Arithmetic	Correlated	Arithmetic
Mean	$M = 1.381$	$M_{LNC} = 0.1100$	$M_{LNA} = 0.1173$
Standard deviation	$SD = 1.006$	$SD_{LNC} = 0.6525$	$SD_{LNA} = 0.6479$
Coefficient of variation	$CV = 0.728$		

Notes:

1. The correlated mean ( $M_{LNC}$ ) and standard deviation ( $SD_{LNC}$ ) values for lognormal distribution were calculated from the normal (arithmetic) mean ( $M$ ) and standard deviation ( $SD$ ) values of 1.381 and 1.006, respectively, by using the following equations based on idealized normal and lognormal PDFs:

$$M_{LNC} = LN(M) - 0.50(SD_{LNC})^2$$

$$SD_{LNC} = [LN\{(SD/M)^2 + 1\}]^{0.5}$$

2. The arithmetic mean ( $M_{LNA}$ ) and standard deviation ( $SD_{LNA}$ ) values of 0.1173 and 0.6479, respectively, were calculated for the lognormal distribution directly from the  $\ln(X)$  values shown in Column 3 of Table F.4.3.

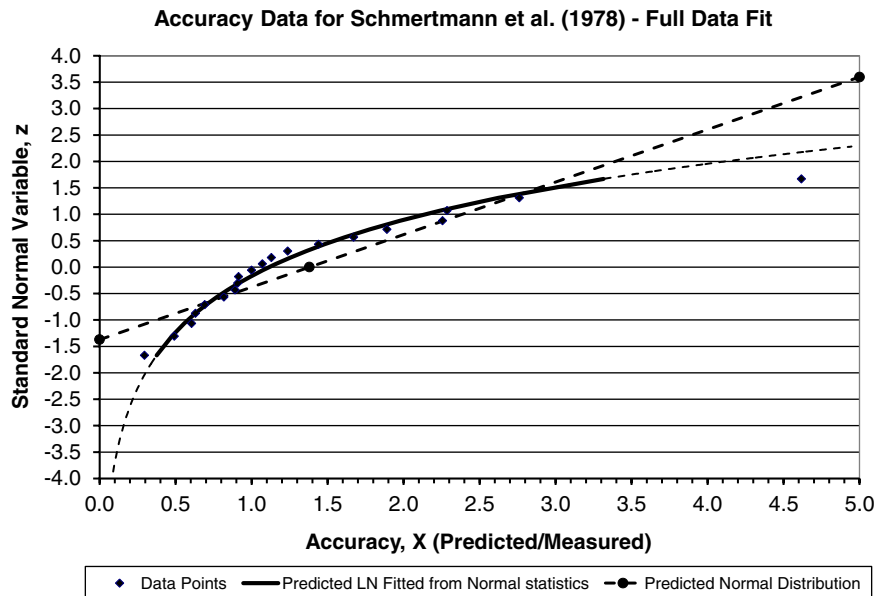
Guidance for the selection of an appropriate PDF and development of the distribution parameters shown in Table F.4.4 is provided in Nowak and Collins (2000) and other similar books that deal with the subject of probabilistic methods.

Table F.4.4 presents the values of the mean and standard deviation based on the normal (straight line) and lognormal (curved line) PDFs shown in Figure F.4.3. Correlated and

arithmetic values of the mean and standard deviation for the lognormal distribution are shown in Table F.4.4. The correlated and the arithmetic values of mean ( $M_{LNC}$  and  $M_{LNA}$ ) and standard deviation ( $SD_{LNC}$  and  $SD_{LNA}$ ) for lognormal distributions are similar but not equal. This is because the correlated values ( $M_{LNC}$  and  $SD_{LNC}$ ) are based on derivations for an idealized lognormal distribution and not a sample distribution from actual data which may not necessarily fit an idealized lognormal distribution. In contrast, the arithmetic values ( $M_{LNA}$  and  $SD_{LNA}$ ) are obtained by taking the arithmetic mean and standard deviation directly from the  $\ln(X)$  value of each data point noted in Column 3 of Table F.4.3.

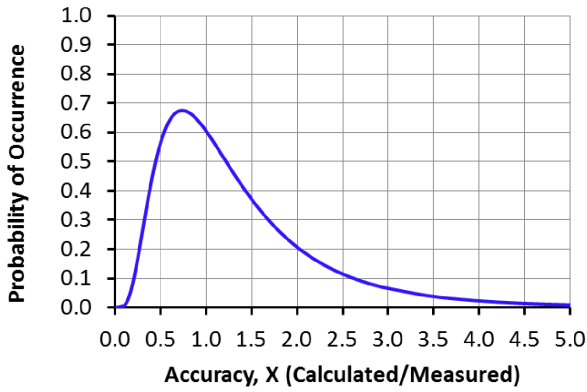
It is important to recognize the use of appropriate values of mean and standard deviation based on the syntax for a lognormal distribution function used by a particular computational program. For example, if one is using the @RISK program by Palisade Corporation, then the RISKLOGNORM function in that program is based on arithmetic values ( $M$  and  $SD$ ) of the normal distribution. In contrast, the Microsoft Excel LOGNORMDIST (or LOGNORM.DIST) function uses the arithmetic mean ( $M_{LNA}$ ) and standard deviation ( $SD_{LNA}$ ) values of  $\ln(X)$ . Use of improper values of mean and standard deviation can lead to drastically different results. This issue is of critical importance since the presented process is based on use of Microsoft Excel as mentioned earlier.

Figure F.4.4 and Figure F.4.5, respectively, show the PDF and CDF based on use of the LOGNORM.DIST function in the 2010 version of Microsoft Excel with  $M_{LNA} = 0.1173$  and  $SD_{LNA} = 0.6479$ .



**Figure F.4.3. Standard normal variable,  $z$ , as a function of the accuracy ( $X$ ) of Schmertmann et al. (1978) method.**

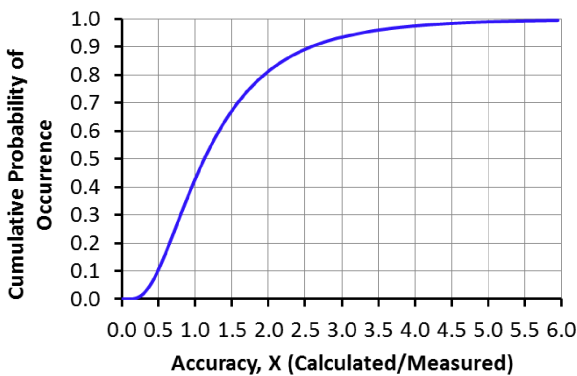




**Figure F.4.4. Probability distribution function for accuracy (X) of Schmertmann et al. (1978) method.**

**F.4.3 Step 3: Select the Target Reliability Index,  $\beta_T$**

For strength limit states, reliability index values in the range of 3.09 to 3.54 are used. Ultimate or strength limit states pertain to structural safety and the loss of load-carrying capacity. In contrast, service limit states are user-defined limiting conditions that affect the function of the structure under expected service conditions. Violation of service limit states occurs at loads much smaller than those for strength limit states. Since there is no danger of collapse if a service limit state is violated, a smaller value of target reliability index may be used for service limit states. In the case of settlement, the structural load effect is manifested in terms of increased moments and potential cracking. The load effect due to the settlement relative to the load effect due to dead and live loads would generally be small because in the



**Figure F.4.5. Cumulative distribution function (CDF) for accuracy (X) of Schmertmann et al. (1978) method.**

Service I limit state the load factor  $\gamma_{SE}$ , which represents the uncertainty in estimated settlement, is only one of the many load factors. Furthermore, the primary moments due to the dead and live loads are much larger than the additional (secondary) moments due to settlement. Based on a consideration of reversible and irreversible service limit states for bridge superstructures, a target reliability index,  $\beta_T$ , in the range of 0.50 to 1.00 for calibration of load factor  $\gamma_{SE}$  for foundation deformation in the Service I limit state is recommended. For demonstration purposes, a value of  $\beta_T = 0.50$  is used in the included example. Using the procedure demonstrated here, the end user can develop the appropriate values of  $\gamma_{SE}$  for other values of  $\beta_T$ . Additional discussion on the meaning and use of  $\gamma_{SE}$  is presented in Chapter 6.

**F.4.4 Step 4: Compute the Probability of Exceedance,  $P_e$ , of Predicted Value for  $\beta_T$**

The reliability index,  $\beta$ , can be expressed in terms of probability of exceedance,  $P_e$ , of a predicted value by using the following formula in Microsoft Excel (Equation F.4.2).

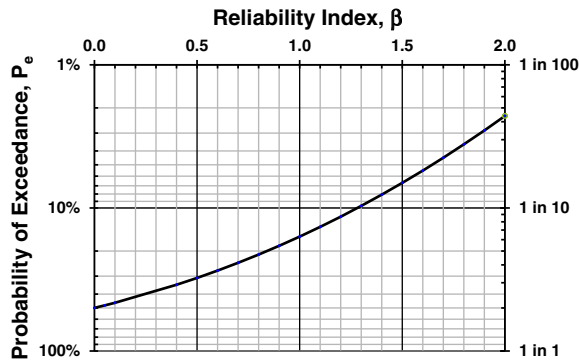
$$\beta = \text{NORMSINV}(1 - P_e) \tag{F.4.2}$$

Table F.4.5 and Figure F.4.6 were generated by using Equation F.4.2. In Table F.4.5, linear interpolation may be used as an approximation for values intermediate to those shown.

**Table F.4.5. Reliability Index,  $\beta$ , and Corresponding Values of Probability of Exceedance,  $P_e$ , Based on Normally Distributed Data**

$\beta$	$P_e$ (%)	$\beta$	$P_e$ (%)	$\beta$	$P_e$ (%)	$\beta$	$P_e$ (%)
2.00	2.28	1.50	6.68	1.00	15.87	0.50	30.85
1.95	2.56	1.45	7.35	0.95	17.11	0.45	32.64
1.90	2.87	1.40	8.08	0.90	18.41	0.40	34.46
1.85	3.22	1.35	8.85	0.85	19.77	0.35	36.32
1.80	3.59	1.30	9.68	0.80	21.19	0.30	38.21
1.75	4.01	1.25	10.56	0.75	22.66	0.25	40.13
1.70	4.46	1.20	11.51	0.70	24.20	0.20	42.07
1.65	4.95	1.15	12.51	0.65	25.78	0.15	44.04
1.60	5.48	1.10	13.57	0.60	27.43	0.10	46.02
1.55	6.06	1.05	14.69	0.55	29.12	0.05	48.01
						0.00	50.00

Note: Probability of Success,  $P_s = 1 - P_e$ .



**Figure F.4.6. Relationship between  $\beta$  and  $P_e$  for case of single load and single resistance.**

Based on either Equation F.4.2 or Table F.4.5, a value of  $P_e \approx 0.3085$  or 30.85% is obtained for  $\beta = 0.50$ .

#### F.4.5 Step 5: Compute the Load Factor, $\gamma_{SE}$ , due to Foundation Deformations

The load factor,  $\gamma_{SE}$ , is a function of the probability of exceedance,  $P_e$ , of the foundation deformation under consideration, which in this example is the immediate settlement of spread footings calculated by using the analytical method of Schmertmann et al. (1978). Equation F.4.3 is the formula in Microsoft Excel for determining a value of accuracy,  $X$ , in terms of  $P_e$ , the arithmetic mean ( $M_{LNA}$ ), and the standard deviation ( $SD_{LNA}$ ) of the lognormal distribution function as computed in Step 2. The value of  $X$  represents the probability of the accuracy value ( $\delta_p/\delta_T$ ) being less than a specified value.

$$P_e = \text{LOGNORMDIST}(X, M_{LNA}, SD_{LNA}) \quad (\text{F.4.3})$$

From Table F.4.4, for the Schmertmann method,  $M_{LNA} = 0.1173$  and  $SD_{LNA} = 0.6479$ . The goal is to determine the value of  $X$  that gives  $P_e = 0.3085$ . Thus, for this example, the expression for  $P_e$  can be written as follows:

$$P_e = \text{LOGNORMDIST}(X, 0.1173, 0.6479) = 0.3085 \text{ or } 30.85\%$$

Using Goal Seek in Microsoft Excel,  $X (= \delta_p/\delta_T) \approx 0.813$ . [Note that in the 2010 version of Microsoft Excel, another function LOGNORM.DIST is also available that can be used. In this case, the same result ( $X \approx 0.813$ ) is obtained by using the following syntax and the Goal Seek function to determine  $X$  ("TRUE" indicates the use of cumulative distribution function):  $P_e = \text{LOGNORM.DIST}(X, 0.1173, 0.6479, \text{TRUE}) = 0.3085$ .]

In the context of the AASHTO LRFD framework, the load factor,  $\gamma_{SE}$ , is the reciprocal of  $X$ . Thus, for immediate settlement of spread footings based on the method of Schmertmann et al. (1978),  $\gamma_{SE} = 1/0.813 \approx 1.23$ .

As per the AASHTO LRFD framework, the load factor is rounded up to the nearest 0.05. Thus, use  $\gamma_{SE} = 1.25$ .

#### F.4.6 Summary

The presented information describes the process for developing the load factor  $\gamma_{SE}$  which incorporates the uncertainty in the model that is used for predicting foundation deformations and its effect on the bridge superstructure. The key to successful calibration is the development and maintenance of a quality database of deformation measurements on foundations for transportation bridge structures. Using the process described, an owner can develop the load factor of  $\gamma_{SE}$  for any foundation type (e.g., spread footing, driven piles, drilled shafts), for any mode of deformation (e.g., vertical, lateral, rotation) and for any appropriate analytical method based on local geologic conditions—as long as the owner has established a quality database of measurements of foundation deformations in the local geologic conditions. Finally, care must be taken to use appropriate load types in the calibration process. For example, as per Article 10.6.2.3 of AASHTO (2012), for immediate settlements both permanent and transient loads are used, while for long-term settlements only the permanent loads are used since transient loads are not there long enough to affect the long-term settlements. The consideration of load types will be based on the type of the foundation and the foundation deformation being evaluated in the calibration process.

#### References for F.4

- AASHTO LRFD Bridge Design Specifications, 6th ed. 2012. American Association of State Highway and Transportation Officials, Washington, D.C.
- Allen, T., A. Nowak, and R. Bathurst. 2005. *Transportation Research Circular E-C079: Calibration to Determine Load and Resistance Factors for Geotechnical and Structural Design*. Transportation Research Board of the National Academies, Washington, D.C. <http://onlinepubs.trb.org/onlinepubs/circulars/ec079.pdf>.
- Gifford, D., S. Kraemer, J. Wheeler, and A. McKown. 1987. *Spread Footings for Highway Bridges*. FHWA/RD-86-185. Haley and Aldrich, FHWA, Cambridge, Mass.
- Nowak, A. S., and K. C. Collins. 2000. *Reliability of Structures*. University of Michigan, Ann Arbor, and McGraw-Hill, New York.
- Nowak, A., and K. Collins. 2013. *Reliability of Structures*. McGraw-Hill, New York.
- Peck, R., and A. Bazaraa. 1969. Discussion of Settlement of Spread Footings on Sand. *ASCE Journal of the Soil Mechanics and Foundations Division*, Vol. 95, No. 3, pp. 900–916.
- Schmertmann, J., P. Brown, and J. Hartman. 1978. Improved Strain Influence Factor Diagrams. *ASCE Journal of the Geotechnical Engineering Division*, Vol. 104, No. 8, pp. 1131–1135.
- Tan, C., and J. Duncan. 1991. Settlement of Footings on Sands—Accuracy and Reliability. *Proceedings of the Geotechnical Engineering Congress 1991, ASCE Geotechnical Special Publication No. 27*, Vol. 1, pp. 446–455.

## F.5 Concrete Girder Database

This section includes descriptions of the concrete bridges selected from the NCHRP Project 12-78 database and used for various studies reported here (Mlynarski et al. 2011, in References, p. 266). Other bridges could be substituted.

### Strand Legend

Legend:

- ✕ No strand at this position at the current section location
- ✕ No strand at this position at the current location but a strand is harped to this position
- A strand occupies this position at the current section location
- The strand is debonded at the current section location
- The strand is debonded between the current section and the mid-span
- The harped position of a harped strand
- The mid-span position of a harped strand
- The mid-span position of one strand and the harped position of another strand
- Mild steel

NA = not available

na = not applicable (no harped strands were used)

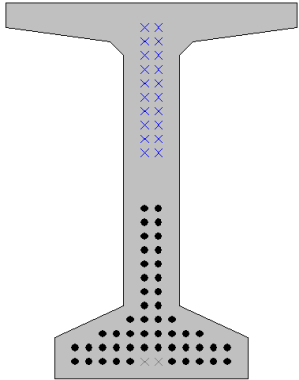
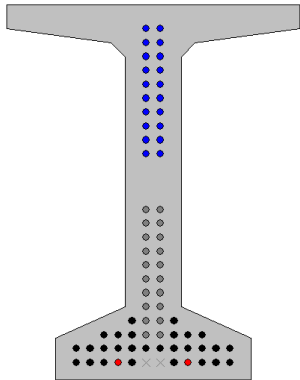
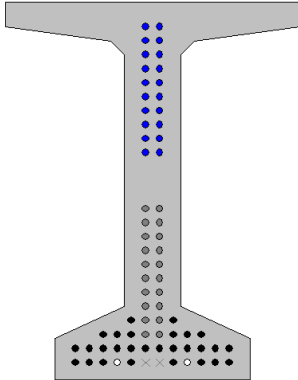
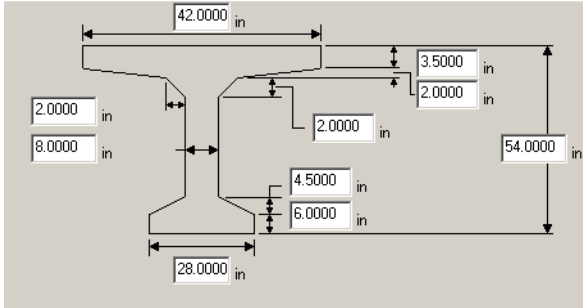
### Tendon Types

LR = Low Relaxation

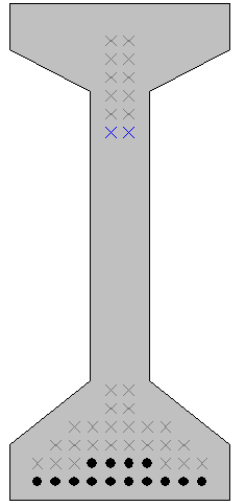
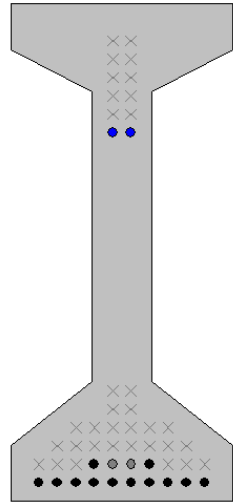
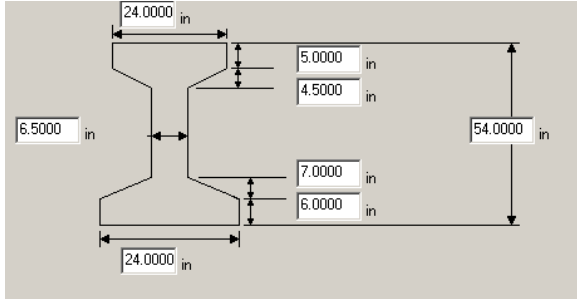
SR = Stress Relieved

# Prestressed Concrete I-Beams

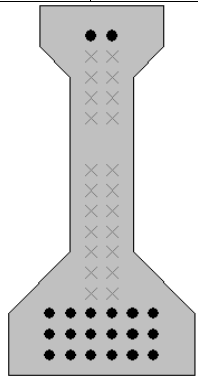
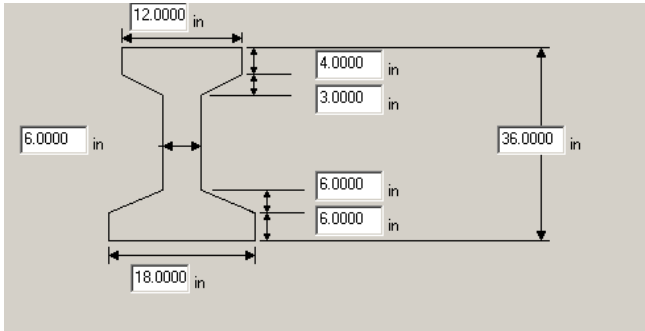
## Bridge 18067

Bridge #	Virtis BID #	Span Length (ft)	t <sub>slab</sub> (in.)	Girder Spacing (ft)	Overhang Width (ft)	# of Girders	Skew (deg)	Materials			Dist. to Extreme Strands (in.)		Harp Point (ft)	Beam Section	
								P/S Tendons	f <sub>c</sub> ' (ksi)	f <sub>c</sub> ' <sub>1</sub> (ksi)	f <sub>c</sub> ' <sub>deck</sub> (ksi)	Bottom			Top
18067	562	131'-0 1/4"	6	5'-3 1/2"	3'-0 1/2"	17	112.5	50-0.6" Gr. 270 LR	7.5	6.5	3.0	2.5	3.5	44.51	AL BT-54 Mod
									<p>Strand Spacing: Horizontal: 2" Vertical: 2"</p> <p># of Strands: 50 Number of Harped Strands: 20 Center of gravity (CG) from bottom at Midspan: 8.9" CG from Bottom at Support: 20.0" Debonded Strands: 2 Debonded Length: 60 inches CG from Bottom at 60": 18.78"</p> 						
Strand Layout at Midspan			Strand Layout at 60" from Support			Strand Layout at Support			Cross-Section						

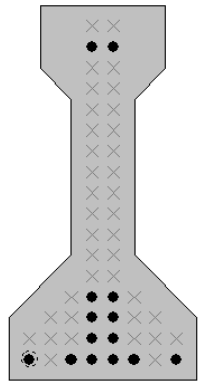
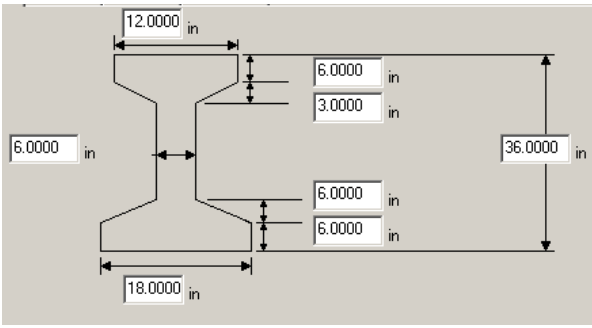
Bridge 8891

Bridge #	Virtis BID #	Span Length (ft)	t <sub>slab</sub> (in.)	Girder Spacing (ft)	Overhang Width (ft)	# of Girders	Skew (deg)	Materials			Dist. to Extreme Strands (in.)		Harp Point (ft)	Beam Section	
								P/S Tendons	f' <sub>c</sub> (ksi)	f' <sub>c1</sub> (ksi)	f' <sub>c deck</sub> (ksi)	Bottom			Top
8891	571	47'-2"	8.5	1 @ 7'-10, 12 @ 10'-8"	3'-4"	14	90	14-0.5" Gr. 270 LR	6.0	5.0	4.0	2.0	14.0	19.33	Beam Type 6
		 <p>Strand Layout at Midspan</p>		 <p>Strand Layout at Support</p>		<p>Strand Spacing: Horizontal: 2" Vertical: 2"</p> <p># of Strands: 14 Number of Harped Strands: 2 CG from bottom at Midspan: 2.57" CG from Bottom at Support: 7.71"</p>  <p>Cross-Section</p>									

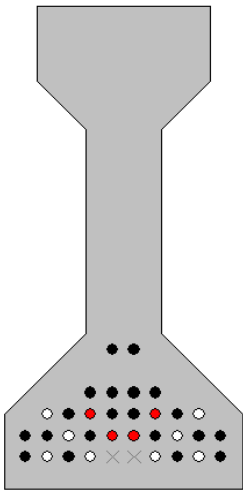
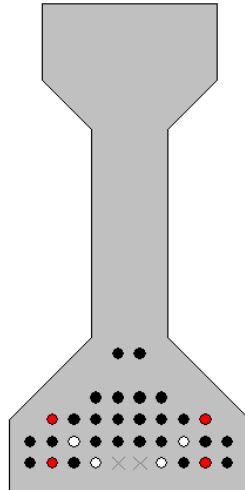
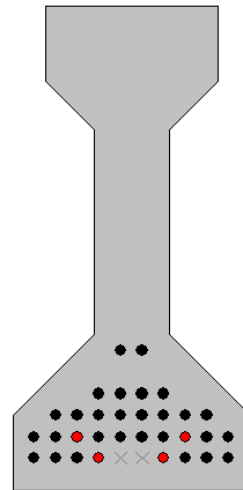
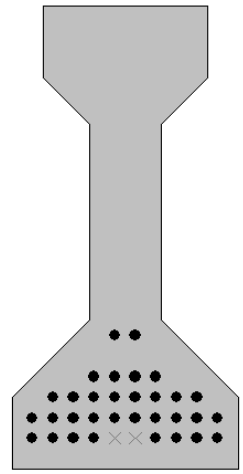
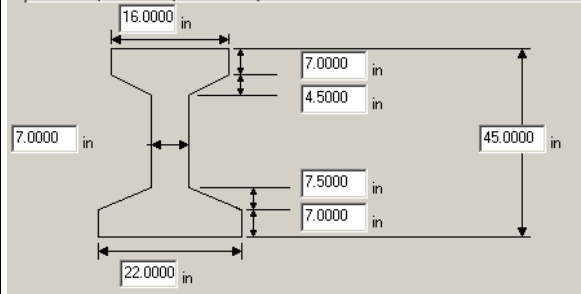
Bridge 8832

Bridge #	Virtis BID #	Span Length (ft)	t <sub>slab</sub> (in.)	Girder Spacing (ft)	Overhang Width (ft)	# of Girders	Skew (deg)	Materials			Dist. to Extreme Strands (in.)		Harp Point (ft)	Beam Section	
								P/S Tendons	f' <sub>c</sub> (ksi)	f' <sub>c1</sub> (ksi)	f' <sub>c deck</sub> (ksi)	Bottom			Top
8832	570	43'-3½"	8.5	10	2'-4"	16	87.5	20-0.5" Gr. 270 LR	8.0	6.0	4.0	2.0	3.0	na	36" I-Beam
		 <p>Strand Layout at Midspan</p>		<p>Strand Spacing: Horizontal: 2" Vertical: 2"</p> <p># of Strands: 20 Number of Harped Strands: 0 CG from bottom at Midspan: 6.90"</p> <p>Cross-Section</p>		 <p>Cross-Section</p>									

Bridge 12603

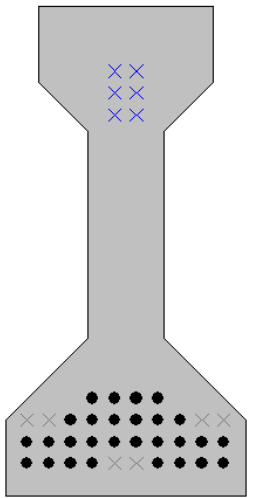
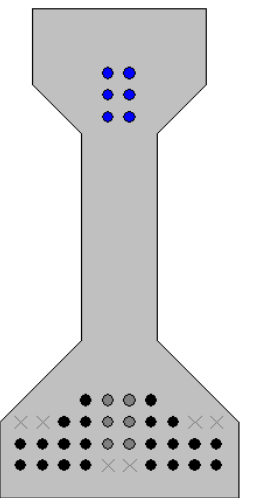
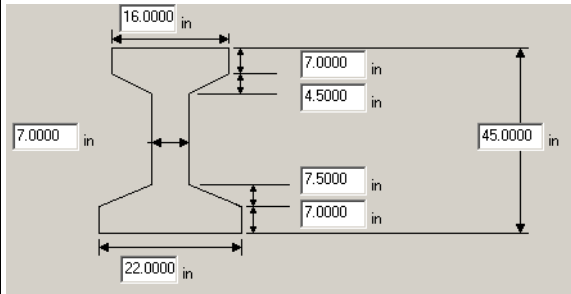
Bridge #	Virtis BID #	Span Length (ft)	t <sub>slab</sub> (in.)	Girder Spacing (ft)	Overhang Width (ft)	# of Girders	Skew (deg)	Materials			Dist. to Extreme Strands (in.)		Harp Point (ft)	Beam Section	
								P/S Tendons	f' <sub>c</sub> (ksi)	f' <sub>t</sub> (ksi)	f' <sub>c,deck</sub> (ksi)	Bottom			Top
12603	572	37'-8¾"	7.87 5	11'-5¾"	3'-6½"	4	90	14-0.6" Gr. 270 LR	7.25	5.5	4.0	2.0	4.0	na	AASHTO Type II
 <p>Strand Spacing: Horizontal: 2" Vertical: 2"</p> <p># of Strands: 14 Number of Harped Strands: 0 CG from bottom at Midspan: 8.00"</p>						<p>Strand Layout at Midspan</p> <p>Cross-Section</p> <p>Cross-Section</p>									

Bridge 10740

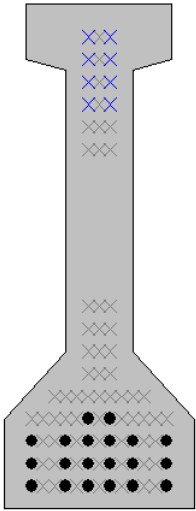
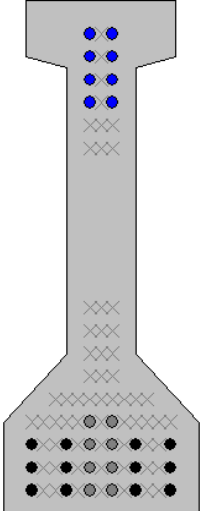
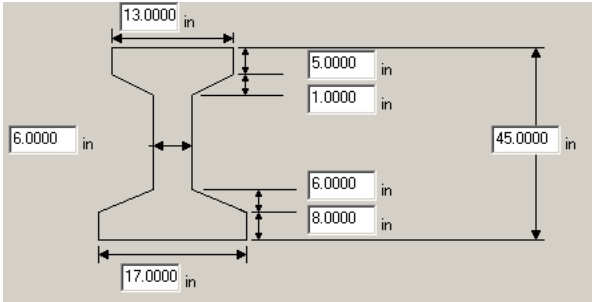
Bridge #	Virtis BID #	Span Length (ft)	t <sub>slab</sub> (in.)	Girder Spacing (ft)	Overhang Width (ft)	# of Girders	Skew (deg)	Materials			Dist. to Extreme Strands (in.)		Harp Point (ft)	Beam Section					
								P/S Tendons	f' <sub>c</sub> (ksi)	f' <sub>t</sub> (ksi)	f' <sub>c,deck</sub> (ksi)	Bottom			Top				
10740	575	78'-6½"	6.25	7	3'-10½"	6	90	32-0.5" Gr. 270 LR	6.0	5.4	3.0	3.0	na	AASHTO Type III					
																<p>Strand Spacing: Horizontal: 2" Vertical: 2" (4" to top pair of strands)</p> <p># of Strands: 32 Number of Harped Strands: 0 CG from bottom at 48": 6.60" CG from bottom at 120": 6.50" CG from bottom at 168": 6.29" CG from bottom at Midspan: 6.00"</p> 			
<p>@ 48" from left support</p>				<p>@ 120" from left support</p>				<p>@ 168" from left support</p>				<p>Strand Layout at Midspan</p> <p>Cross-Section</p>							



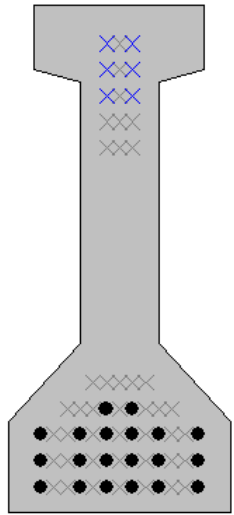
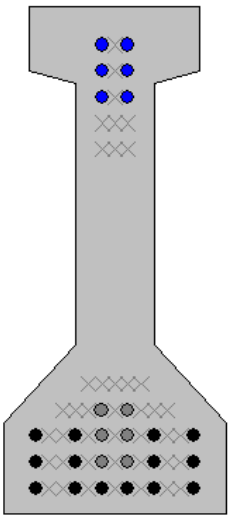
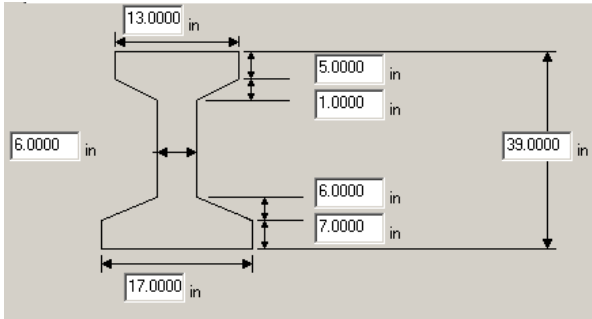
Bridge 10269

Bridge #	Virtis BID #	Span Length (ft)	t <sub>slab</sub> (in.)	Girder Spacing (ft)	Overhang Width (ft)	# of Girders	Skew (deg)	Materials			Dist. to Extreme Strands (in.)		Harp Point (ft)	Beam Section	
								P/S Tendons	f <sub>c</sub> ' (ksi)	f <sub>c</sub> l (ksi)	f <sub>c</sub> ' <sub>deck</sub> (ksi)	Bottom			Top
10269	0576	78'-0"	6.25	6'-8"	3'-4 1/2"	7	90	28-0.5" Gr. 270 LR	6.0	5.0	3.3	3.0	6.0	28.75	AASHTO Type III
						<p>Strand Spacing: Horizontal: 2" Vertical: 2"</p> <p># of Strands: 28 Number of Harped Strands: 6 CG from bottom at Midspan: 5.43" CG from Bottom at Support: 11.86"</p> 									
Strand Layout at Midspan			Strand Layout at Support			Cross-Section									

Bridge 5624

Bridge #	Virtis BID #	Span Length (ft)	t <sub>slab</sub> (in.)	Girder Spacing (ft)	Overhang Width (ft)	# of Girders	Skew (deg)	Materials			Dist. to Extreme Strands (in.)		Harp Point (ft)	Beam Section	
								P/S Tendons	f <sub>c</sub> ' (ksi)	f <sub>c1</sub> ' (ksi)	f <sub>c deck</sub> ' (ksi)	Bottom			Top
5624	0588	59'-4 $\frac{1}{2}$ "	9	7'-3"	2'-10"	21	109.9	20-0.5" Gr. 270 LR	6.0	4.5	4.0	2.0	3.0	24.15	Beam Type 4
						<p>Strand Spacing: Horizontal: 1" Vertical: 2"</p> <p># of Strands: 20 Number of Harped Strands: 8 CG from bottom at Midspan: 4.40" CG from Bottom at Support: 18.00"</p> 									
		Strand Layout at Midspan		Strand Layout at Support		Cross-Section									

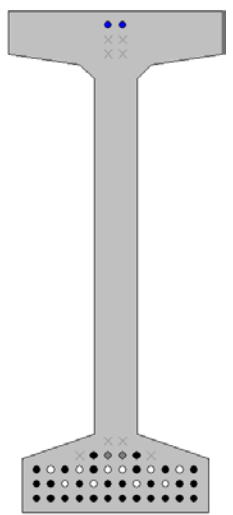
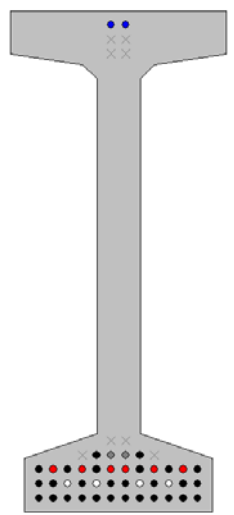
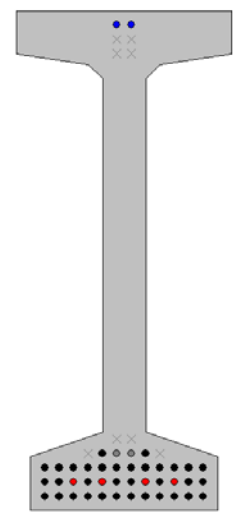
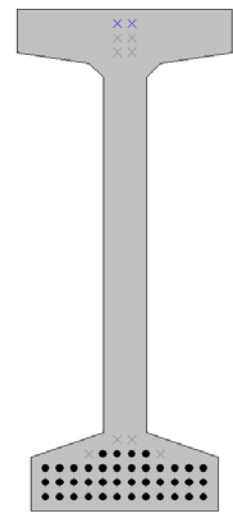
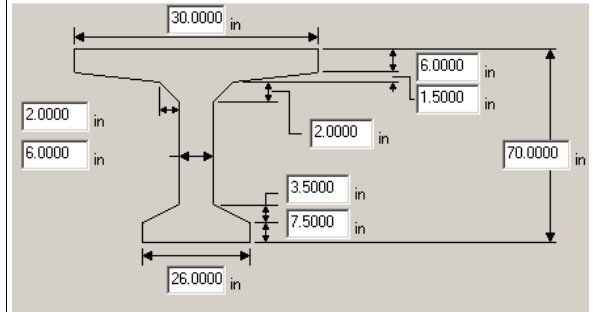
Bridge 5794

Bridge #	Virtis BID #	Span Length (ft)	t <sub>slab</sub> (in.)	Girder Spacing (ft)	Overhang Width (ft)	# of Girders	Skew (deg)	Materials				Dist. to Extreme Strands (in.)		Harp Point (ft)	Beam Section
								P/S Tendons	f <sub>c</sub> ' (ksi)	f <sub>c1</sub> ' (ksi)	f <sub>c deck</sub> ' (ksi)	Bottom	Top		
5794	0589	72'-0"	8.5	5'-10"	2'-9"	6	100.0	20-0.6" Gr. 270 LR	9.0	7.0	4.0	2.0	3.0	29.13	Beam Type 3
						<p>Strand Spacing: Horizontal: 1" Vertical: 2"</p> <p># of Strands: 20 Number of Harped Strands: 6 CG from bottom at Midspan: 4.40" CG from Bottom at Support: 12.80"</p> 									
<b>Strand Layout at Midspan</b>			<b>Strand Layout at Support</b>			<b>Cross-Section</b>									

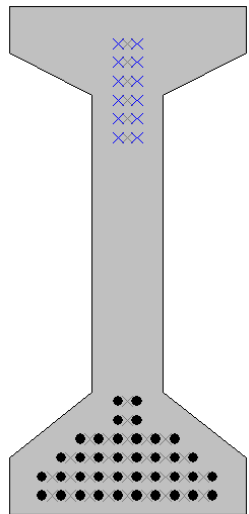
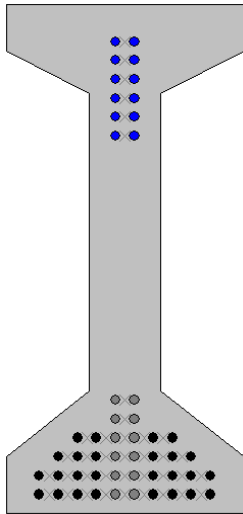
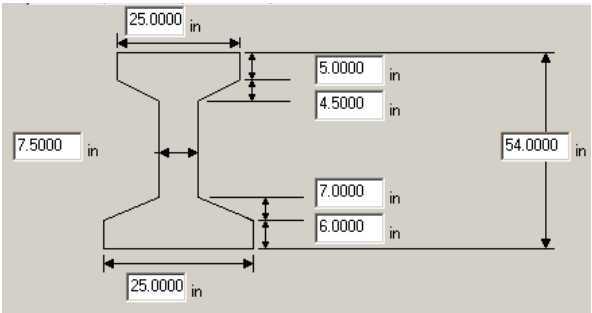
Bridge 9378

Bridge #	Virtis BID #	Span Length (ft)	t <sub>slab</sub> (in.)	Girder Spacing (ft)	Overhang Width (ft)	# of Girders	Skew (deg)	Materials			Dist. to Extreme Strands (in.)		Harp Point (ft)	Beam Section	
								P/S Tendons	f <sub>c</sub> ' (ksi)	f <sub>c</sub> ' <sub>1</sub> (ksi)	f <sub>c</sub> ' <sub>deck</sub> (ksi)	Bottom			Top
9378	0598	101'-10"	9	10'-5"	2'-7½"	5	90	40-0.5" Gr. 270 LR	6.0	5.1	4.0	2.0	2.0	41.17	Wisconsin 70"

				<p>Strand Spacing: Horizontal: 2" Vertical: 2"</p> <p># of Strands: 40 Number of Harped Strands: 2 CG from bottom at Left Support": 8.13" CG from bottom at 78": 7.50" CG from bottom at 318": 5.63" CG from bottom at Midspan: 4.40"</p>	
@ left support	@ 78" from left support	@ 318" from left support	Strand Layout at Midspan	Cross-Section	

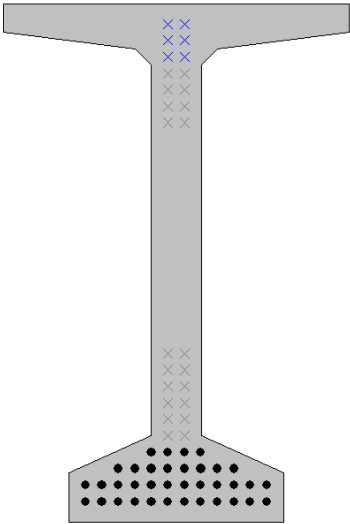
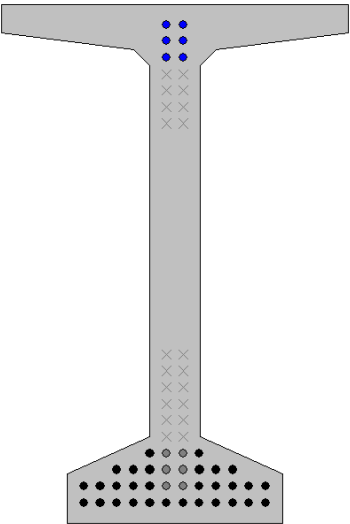
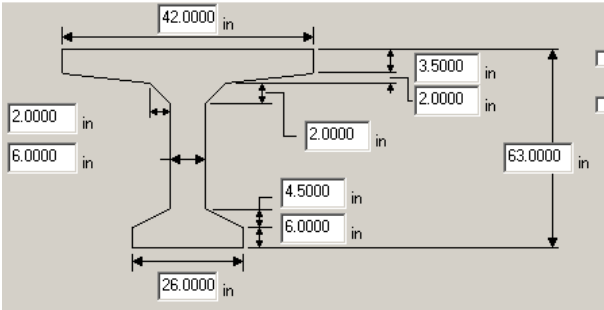
Bridge 5884

Bridge #	Virtis BID #	Span Length (ft)	t <sub>slab</sub> (in.)	Girder Spacing (ft)	Overhang Width (ft)	# of Girders	Skew (deg)	Materials				Dist. to Extreme Strands (in.)		Harp Point (ft)	Beam Section
								P/S Tendons	f <sub>c</sub> ' (ksi)	f <sub>c</sub> ' <sub>1</sub> (ksi)	f <sub>c</sub> ' <sub>deck</sub> (ksi)	Bottom	Top		
5884	0602	90'-0"	8.5	8'-2"	3'-1"	4	110.0	38-0.5" Gr. 270 LR	7.0	5.0	4.0	2.0	4.0	27.28	Beam Type 6
						<p>Strand Spacing: Horizontal: 1" Vertical: 2"</p> <p># of Strands: 38 Number of Harped Strands: 12 CG from Bottom at Midspan: 5.26" CG from Bottom at Support: 17.26"</p> 									
		Strand Layout at Midspan		Strand Layout at Support		Cross-Section									

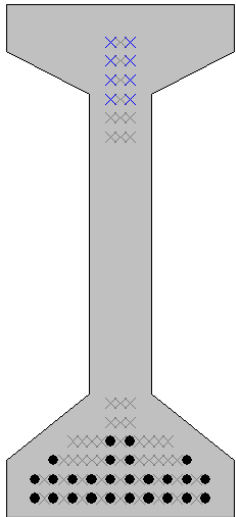
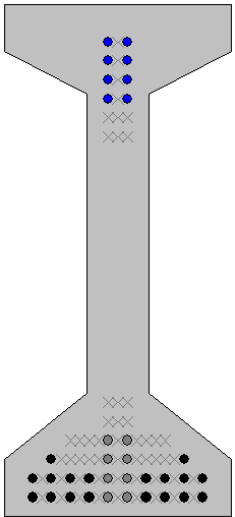
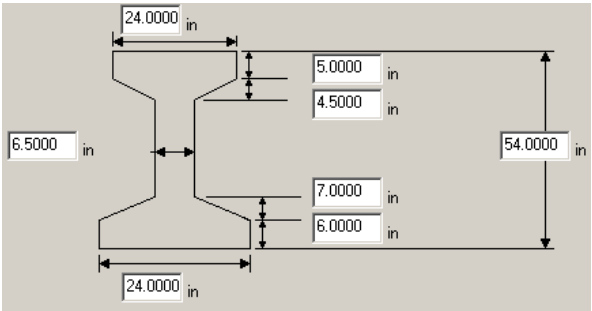
Bridge 8885

Bridge #	Virtis BID #	Span Length (ft)	t <sub>slab</sub> (in.)	Girder Spacing (ft)	Overhang Width (ft)	# of Girders	Skew (deg)	Materials			Dist. to Extreme Strands (in.)		Harp Point (ft)	Beam Section	
								P/S Tendons	f <sub>c</sub> ' (ksi)	f <sub>c</sub> ' <sub>1</sub> (ksi)	f <sub>c</sub> ' <sub>deck</sub> (ksi)	Bottom			Top
8885	0603	90'-0"	8.5	10'-7"	3'-5½"	4	105.8	36-0.5" Gr. 270 LR	7.0	5.5	4.0	2.5	2.5	36.00	BT-63

 <p style="text-align: center;">Strand Layout at Midspan</p>	 <p style="text-align: center;">Strand Layout at Support</p>	<p>Strand Spacing: Horizontal: 2" Vertical: 2"</p> <p># of Strands: 36 Number of Harped Strands: 6 CG from Bottom at Midspan: 4.72" CG from Bottom at Support: 13.39"</p>  <p style="text-align: center;">Cross-Section</p>
--	---	---

Bridge 8957

Bridge #	Virtis BID #	Span Length (ft)	t <sub>slab</sub> (in.)	Girder Spacing (ft)	Overhang Width (ft)	# of Girders	Skew (deg)	Materials			Dist. to Extreme Strands (in.)		Harp Point (ft)	Beam Section Beam Type 6	
								P/S Tendons	f' <sub>c</sub> (ksi)	f' <sub>c1</sub> (ksi)	f' <sub>c deck</sub> (ksi)	Bottom			Top
8957	0604	98'-0"	8.5	8'-8"	3'-0"	5	90.0	26-0.6" Gr. 270 LR	8.0	6.4	4.0	2.0	4.0	39.67	
						<p>Strand Spacing: Horizontal: 1" Vertical: 2"</p> <p># of Strands: 26 Number of Harped Strands: 8 CG from Bottom at Midspan: 3.85" CG from Bottom at Support: 16.77"</p> 									
		Strand Layout at Midspan		Strand Layout at Support		Cross-Section									



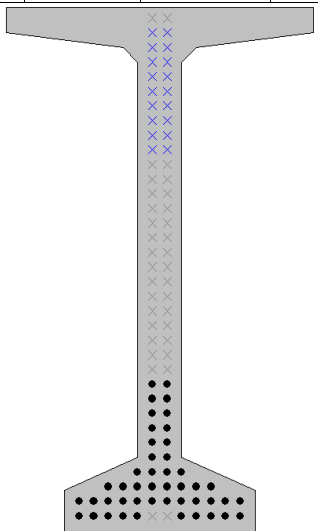
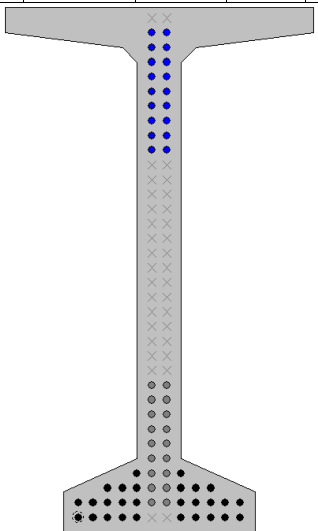
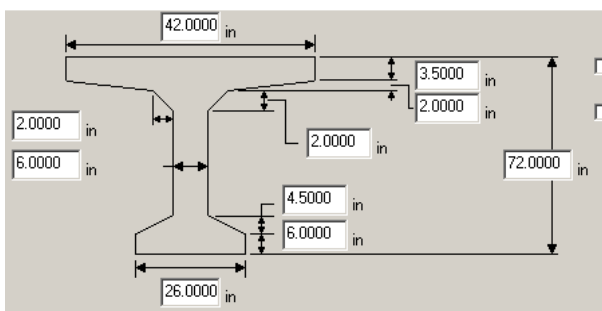
Bridge 12596

Bridge #	Virtis BID #	Span Length (ft)	t <sub>slab</sub> (in.)	Girder Spacing (ft)	Overhang Width (ft)	# of Girders	Skew (deg)	Materials				Dist. to Extreme Strands (in.)		Harp Point (ft)	Beam Section
								P/S Tendons	f <sub>c</sub> ' (ksi)	f <sub>e</sub> i' (ksi)	f <sub>c</sub> ' deck (ksi)	Bottom	Top		
12596	0610	96'-9 3/4"	7.875	11'-1 1/8"	4'-0 7/16"	4	90	50-0.6" Gr. 270 LR	10.2	7.1	4.0	2.0	2.0	na	AASHTO Type IV
										Strand Spacing: Horizontal: 2" Vertical: 2"  # of Strands: 50 Number of Harped Strands: 0 CG from bottom at Left Support to 102.36": 12.55" CG from bottom at 133.86": 12.09" CG from bottom at 157.48": 11.67" CG from bottom at Midspan: 11.36"					
										<b>Cross-Section</b>					

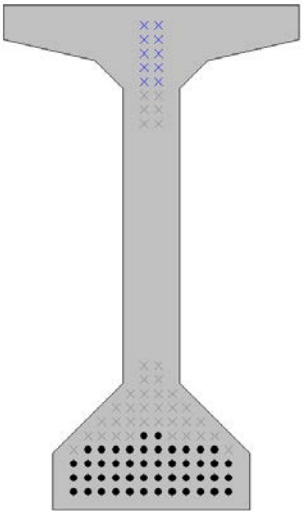
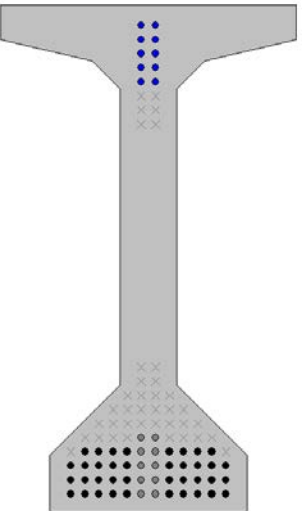
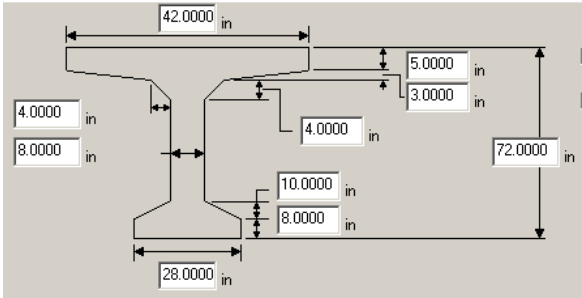
Bridge 10803

Bridge #	Virtis BID #	Span Length (ft)	t <sub>slab</sub> (in.)	Girder Spacing (ft)	Overhang Width (ft)	# of Girders	Skew (deg)	Materials			Dist. to Extreme Strands (in.)		Harp Point (ft)	Beam Section	
								P/S Tendons	f' <sub>c</sub> (ksi)	f' <sub>ci</sub> (ksi)	f' <sub>c deck</sub> (ksi)	Bottom			Top
10803	0611	138'-3"	6.25	6'-0"	3'-4½"	7	90.0	46-0.5" Gr. 270 LR	7.0	6.0	4.0	2.5	3.5	54.75	BT-72

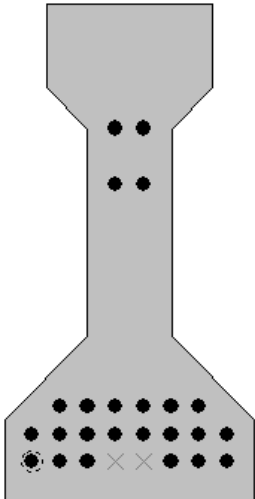
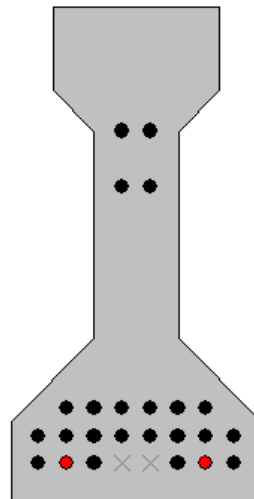
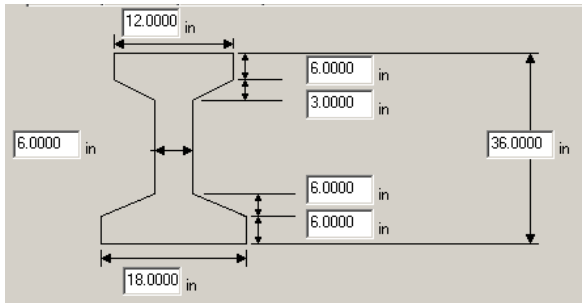
  

		<p>Strand Spacing: Horizontal: 2" Vertical: 2"</p> <p># of Strands: 46 Number of Harped Strands: 18 CG from Bottom at Midspan: 7.63" CG from Bottom at Support: 26.41"</p> 
Strand Layout at Midspan	Strand Layout at Support	Cross-Section

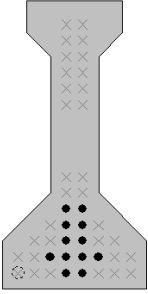
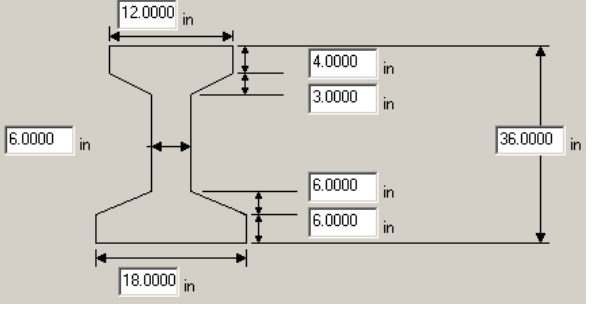
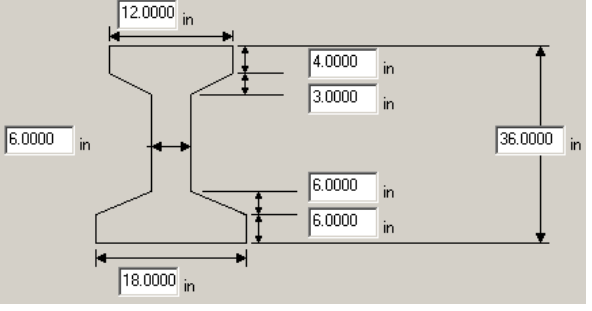
Bridge 8890

Bridge #	Virtis BID #	Span Length (ft)	t <sub>slab</sub> (in.)	Girder Spacing (ft)	Overhang Width (ft)	# of Girders	Skew (deg)	Materials			Dist. to Extreme Strands (in.)		Harp Point (ft)	Beam Section	
								P/S Tendons	f <sub>c</sub> ' (ksi)	f <sub>c</sub> ' <sub>i</sub> (ksi)	f <sub>c</sub> ' <sub>deck</sub> (ksi)	Bottom			Top
8890	0613	143'-6"	8.5	8'-0"	2'-9"	14	92.8	48-0.6" Gr. 270 LR	8.0	6.0	4.0	2.5	3	57.90	AASHTO Type VI
						<p>Strand Spacing: Horizontal: 2" Vertical: 2"</p> <p># of Strands: 48 Number of Harped Strands: 10 CG from Bottom at Midspan: 5.58" CG from Bottom at Support: 17.77"</p> 									
		Strand Layout at Midspan		Strand Layout at Support		Cross-Section									

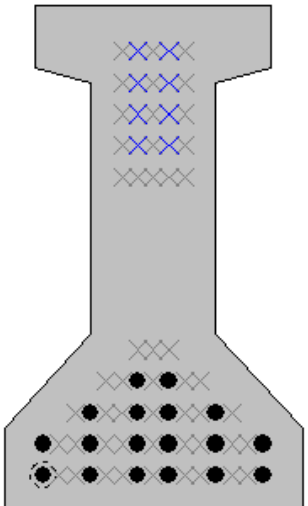
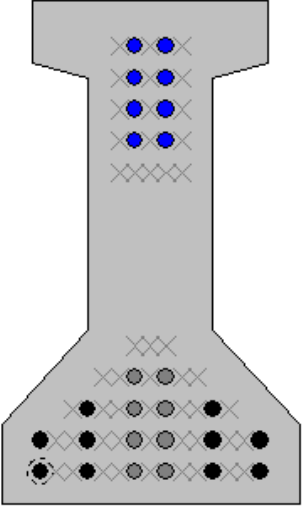
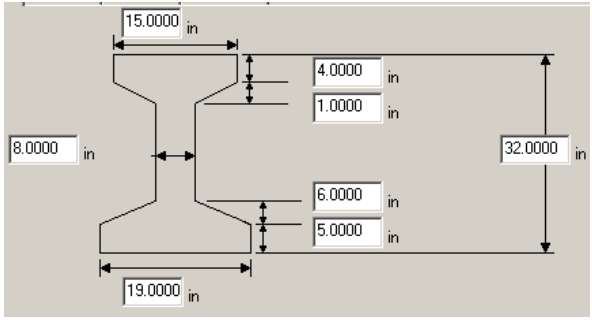
Bridge 10755

Bridge #	Virtis BID #	Span Length (ft)	t <sub>slab</sub> (in.)	Girder Spacing (ft)	Overhang Width (ft)	# of Girders	Skew (deg)	Materials			Dist. to Extreme Strands (in.)		Harp Point (ft)	Beam Section	
								P/S Tendons	f <sub>c</sub> ' (ksi)	f <sub>c</sub> ' <sub>i</sub> (ksi)	f <sub>c</sub> ' <sub>deck</sub> (ksi)	Bottom			Top
10755	0411	52'-6"	6.25	7'-0"	3'-10½"	6	90.0	24-0.5" Gr. 270 SR	6.0	5.0	3.0	3.0	9.0	na	AASHTO Type II
						<p>Strand Spacing: Horizontal: 2" Vertical: 2"</p> <p># of Strands: 24 Number of Harped Strands: 0 CG from Bottom at Midspan: 8.33" CG from Bottom at 60": 8.82"</p> 									
		Strand Layout at Midspan		@ 60" from left support		Cross-Section									

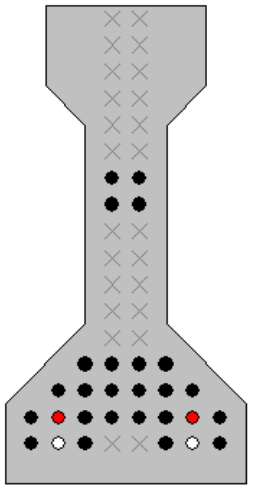
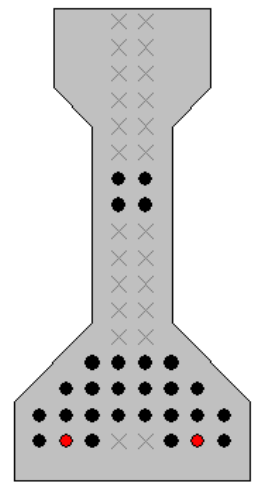
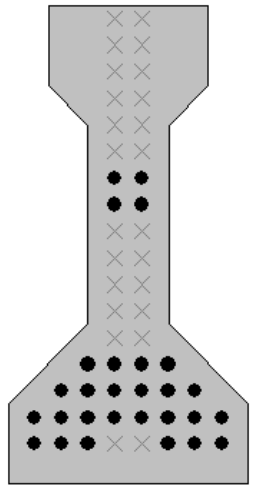
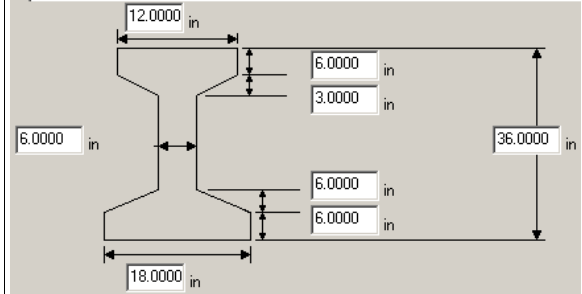
Bridge 3107

Bridge #	Virtis BID #	Span Length (ft)	t <sub>slab</sub> (in.)	Girder Spacing (ft)	Overhang Width (ft)	# of Girders	Skew (deg)	Materials			Dist. to Extreme Strands (in.)		Harp Point (ft)	Beam Section	
								P/S Tendons	f' <sub>c</sub> (ksi)	f' <sub>c1</sub> (ksi)	f' <sub>c deck</sub> (ksi)	Bottom			Top
3107	0416	49'-6½"	7.6875	5'-9¼"	2'-9 7/16"	6	90.0	12-0.5" Gr. 270 LR	6.1	5.1	3.5	2		na	I-Beam
 <p>Strand Spacing: Horizontal: 2" Vertical: 2"</p> <p># of Strands: 12 Number of Harped Strands: 0 CG from bottom at Midspan: 5.67"</p>															
Strand Layout at Midspan				Cross-Section				Cross-Section							

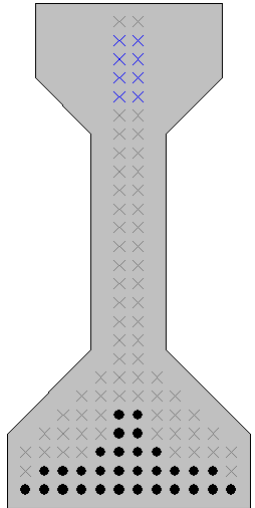
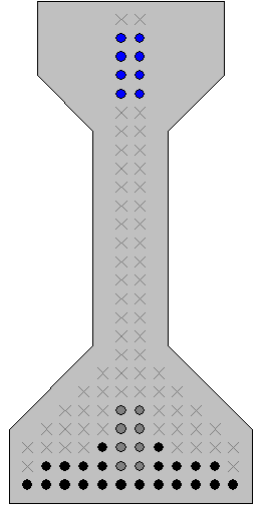
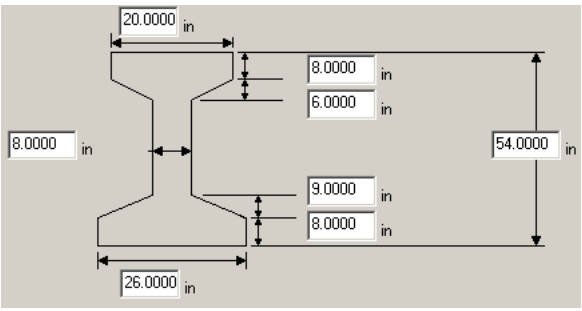
Bridge 4827

Bridge #	Virtis BID #	Span Length (ft)	t <sub>slab</sub> (in.)	Girder Spacing (ft)	Overhang Width (ft)	# of Girders	Skew (deg)	Materials			Dist. to Extreme Strands (in.)		Harp Point (ft)	Beam Section	
								P/S Tendons	f' <sub>c</sub> (ksi)	f' <sub>c1</sub> (ksi)	f' <sub>c deck</sub> (ksi)	Bottom			Top
4827	0418	50'-7"	8.5	7'-2"	3'-0"	5	125.0	18-0.5" Gr. 270 LR	6.0	4.5	4.0	2	3	20.54	Beam Type 2
								<p>Strand Spacing: Horizontal: 1" Vertical: 2"</p> <p># of Strands: 18 Number of Harped Strands: 8 CG from Bottom at Midspan: 4.22" CG from bottom at Left Support: 13.56"</p> 							
Strand Layout at Midspan				Strand Layout at Left Support				Cross-Section							

Bridge 10599

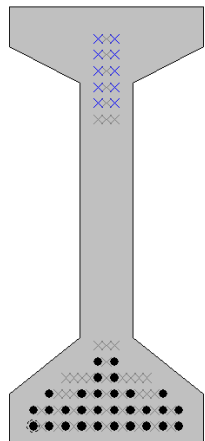
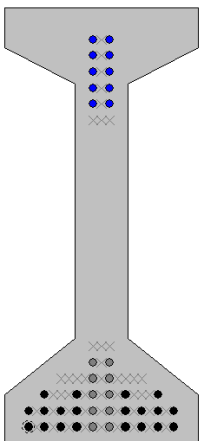
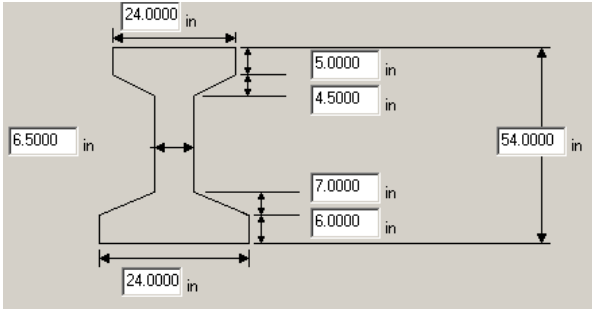
Bridge #	Virtis BID #	Span Length (ft)	t <sub>slab</sub> (in.)	Girder Spacing (ft)	Overhang Width (ft)	# of Girders	Skew (deg)	Materials			Dist. to Extreme Strands (in.)		Harp Point (ft)	Beam Section	
								P/S Tendons	f' <sub>c</sub> (ksi)	f' <sub>c1</sub> (ksi)	f' <sub>c deck</sub> (ksi)	Bottom			Top
10599	0476	62'-10"	8.0	6'-9"	3'-3"	4	90	28-0.5" Gr. 270 LR	7.0	6.5	4.0	3.0	13.0	na	AASHTO Type II
												<p>Strand Spacing: Horizontal: 2" Vertical: 2"</p> <p># of Strands: 28 Number of Harped Strands: 0 CG from bottom at 66.75": 8.67" CG from bottom at 138.75": 8.38" CG from bottom at Midspan: 8.0"</p> 			
			<p>@ 66.75" from left support</p>			<p>@ 138.75" from left support</p>			<p>Strand Layout at Midspan</p>			<p>Cross-Section</p>			

Bridge 12589

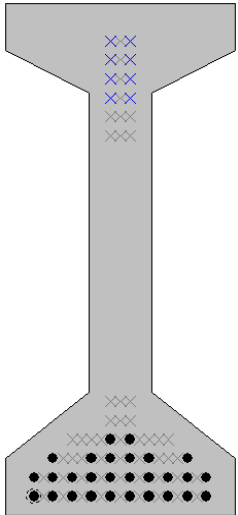
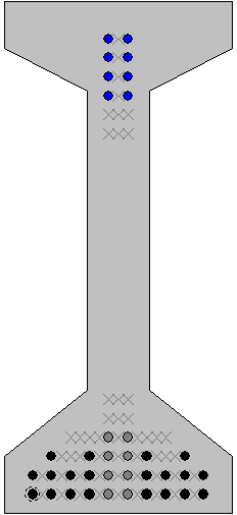
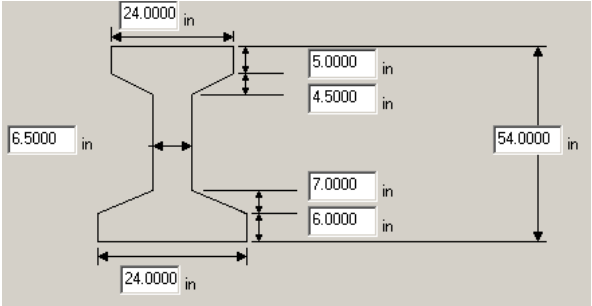
Bridge #	Virtis BID #	Span Length (ft)	t <sub>slab</sub> (in.)	Girder Spacing (ft)	Overhang Width (ft)	# of Girders	Skew (deg)	Materials			Dist. to Extreme Strands (in.)		Harp Point (ft)	Beam Section	
								P/S Tendons	f <sub>c</sub> ' (ksi)	f <sub>c1</sub> ' (ksi)	f <sub>c,deck</sub> ' (ksi)	Bottom			Top
12589	0478	73'-2 1/2"	9.0	8'-9"	3'-0"	5	90	30-0.5" Gr. 270 LR	6.0	4.8	4.0	2.0	4.0	29.58	AASHTO Type IV
								<p>Strand Spacing: Horizontal: 2" Vertical: 2"</p> <p># of Strands: 30 Number of Harped Strands: 8 CG from bottom at Midspan: 4.13" CG from bottom at Left Support: 14.80"</p> 							
				Strand Layout at Midspan		Strand Layout at Left Support		Cross-Section							



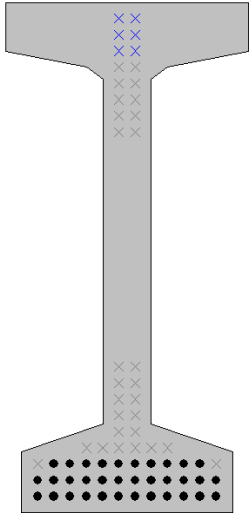
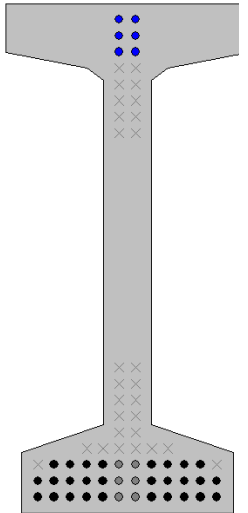
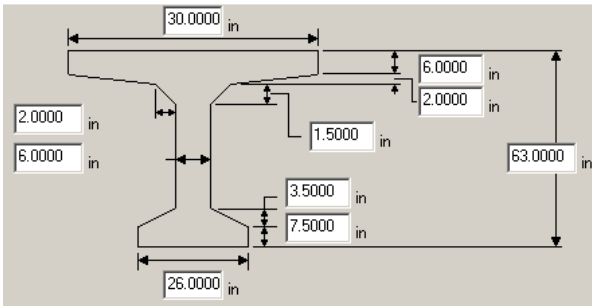
Bridge 5840

Bridge #	Virtis BID #	Span Length (ft)	t <sub>slab</sub> (in.)	Girder Spacing (ft)	Overhang Width (ft)	# of Girders	Skew (deg)	Materials			Dist. to Extreme Strands (in.)		Harp Point (ft)	Beam Section Beam Type 6	
								P/S Tendons	f' <sub>c</sub> (ksi)	f' <sub>cl</sub> (ksi)	f' <sub>c,deck</sub> (ksi)	Bottom			Top
5840	0489	85'-0"	8.5	9'-0"	3'-4"	5	70.0	30-0.5" Gr. 270 LR	7.5	5.25	4.0	2.0	4.0	34.47	
						<p>Strand Spacing: Horizontal: 1" Vertical: 2"</p> <p># of Strands: 30 Number of Harped Strands: 10 CG from bottom at Midspan: 4.40" CG from bottom at Left Support: 17.73"</p> 									
		Strand Layout at Midspan		Strand Layout at Left Support		Cross-Section									

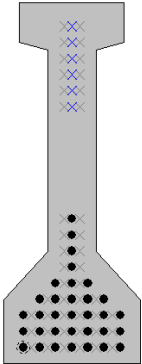
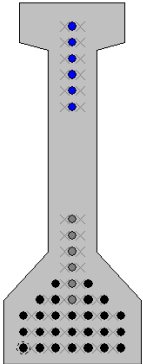
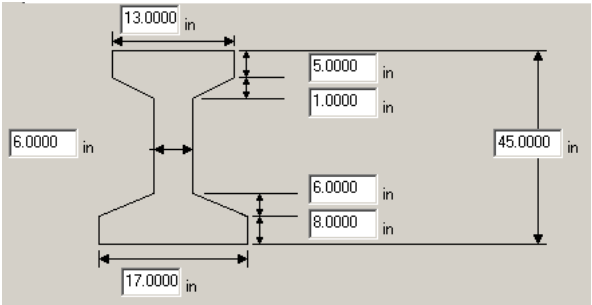
Bridge 8330

Bridge #	Virtis BID #	Span Length (ft)	t <sub>slab</sub> (in.)	Girder Spacing (ft)	Overhang Width (ft)	# of Girders	Skew (deg)	Materials			Dist. to Extreme Strands (in.)		Harp Point (ft)	Beam Section Beam Type 6	
								P/S Tendons	f' <sub>c</sub> (ksi)	f' <sub>c1</sub> (ksi)	f' <sub>c,deck</sub> (ksi)	Bottom			Top
8330	0491	76'-4 1/2"	8.5	8'-8"	3'-0"	5	75.5	28-0.5" Gr. 270 LR	6.0	4.5	4.0	2	4	31.14	
						<p>Strand Spacing: Horizontal: 1" Vertical: 2"</p> <p># of Strands: 28 Number of Harped Strands: 8 CG from bottom at Midspan: 4.00" CG from bottom at Left Support: 16.00"</p> 									
		Strand Layout at Midspan		Strand Layout at Left Support		Cross-Section									

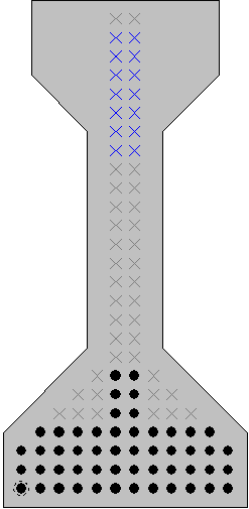
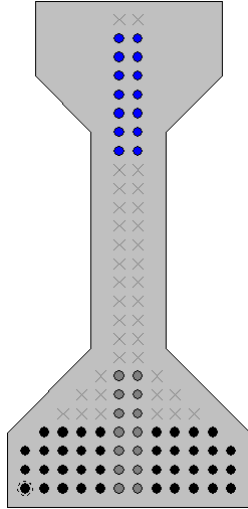
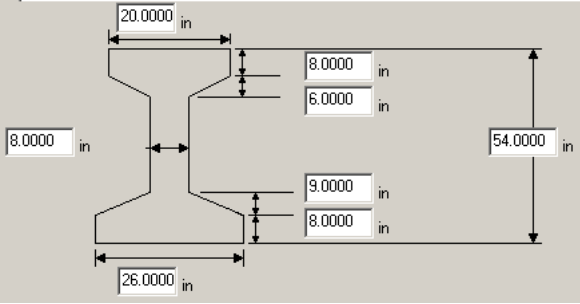
Bridge 82

Bridge #	Virtis BID #	Span Length (ft)	$t_{slab}$ (in.)	Girder Spacing (ft)	Overhang Width (ft)	# of Girders	Skew (deg)	Materials			Dist. to Extreme Strands (in.)		Harp Point (ft)	Beam Section	
								P/S Tendons	$f'_c$ (ksi)	$f'_t$ (ksi)	$f'_{c,deck}$ (ksi)	Bottom			Top
82	0498	82'-9"	8.75	10'-4"	3'-6"	4	105.0	34-0.5" Gr. 270 LR	5.0	4.8	4.5	2.0	2.0	33.38	MN Type 63
						<p>Strand Spacing: Horizontal: 2" Vertical: 2"</p> <p># of Strands: 34 Number of Harped Strands: 6 CG from bottom at Midspan: 3.88" CG from bottom at Left Support: 13.59"</p> 									
		Strand Layout at Midspan		Strand Layout at Left Support		Cross-Section									

Bridge 4794

Bridge #	Virtis BID #	Span Length (ft)	t <sub>slab</sub> (in.)	Girder Spacing (ft)	Overhang Width (ft)	# of Girders	Skew (deg)	Materials			Dist. to Extreme Strands (in.)		Harp Point (ft)	Beam Section	
								P/S Tendons	f' <sub>c</sub> (ksi)	f' <sub>c1</sub> (ksi)	f' <sub>c,deck</sub> (ksi)	Bottom			Top
4794	0497	66'-8"	8.5	3@7'-4", 7@9'-4"	3'-7"	11	90	33-0.5" Gr. 270 LR	10.0	7.0	6.0	2	3	27.92	Beam Type 4
										<p>Strand Spacing: Horizontal: 1" Vertical: 2"</p> <p># of Strands: 33 Number of Harped Strands: 6 CG from bottom at Midspan: 6.48" CG from bottom at Left Support: 10.85"</p> 					
				Strand Layout at Midspan			Strand Layout at Left Support			Cross-Section					

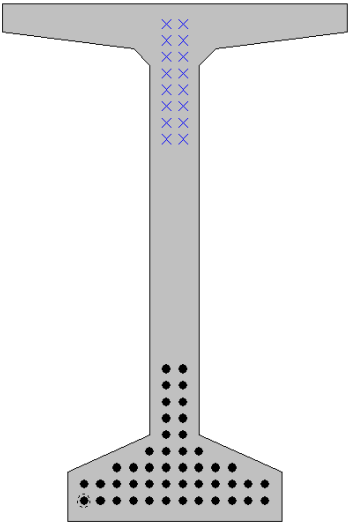
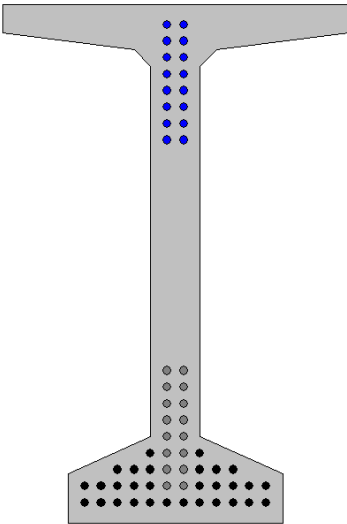
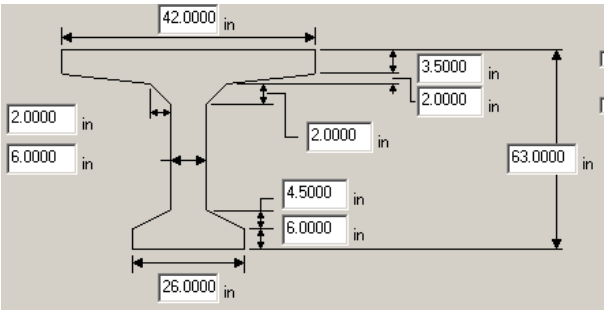
Bridge 12610

Bridge #	Virtis BID #	Span Length (ft)	t <sub>slab</sub> (in.)	Girder Spacing (ft)	Overhang Width (ft)	# of Girders	Skew (deg)	Materials			Dist. to Extreme Strands (in.)		Harp Point (ft)	Beam Section	
								P/S Tendons	f' <sub>c</sub> (ksi)	f' <sub>c1</sub> (ksi)	f' <sub>c,deck</sub> (ksi)	Bottom			Top
12610	0539	108'-6 3/4"	8.0	8@7'-1 1/2", 4@6'-11"	3'-2 1/2" (L) 3'-0 1/2" (R)	13	90.0	52-0.5" Gr. 270 LR	7.0	5.4	4.0	2.0	4.0	44.85	AASHTO Type IV
						<p>Strand Spacing: Horizontal: 2" Vertical: 2"</p> <p># of Strands: 52 Number of Harped Strands: 14 CG from bottom at Midspan: 5.69" CG from bottom at Left Support: 15.38"</p> 									
		Strand Layout at Midspan		Strand Layout at Left Support		Cross-Section									

Bridge 11938

Bridge #	Virtis BID #	Span Length (ft)	t <sub>slab</sub> (in.)	Girder Spacing (ft)	Overhang Width (ft)	# of Girders	Skew (deg)	Materials			Dist. to Extreme Strands (in.)		Harp Point (ft)	Beam Section	
								P/S Tendons	f' <sub>c</sub> (ksi)	f' <sub>c1</sub> (ksi)	f' <sub>c deck</sub> (ksi)	Bottom			Top
11938	0545	116'-6¼"	7	7' - 3 ¾"	3'-9"	8	117.9	46-0.5" Gr. 270 LR	7.0	6.0	3.0	2.5	2.5	47.64	BT-63

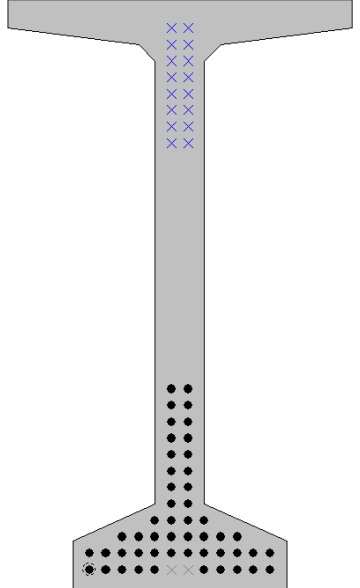
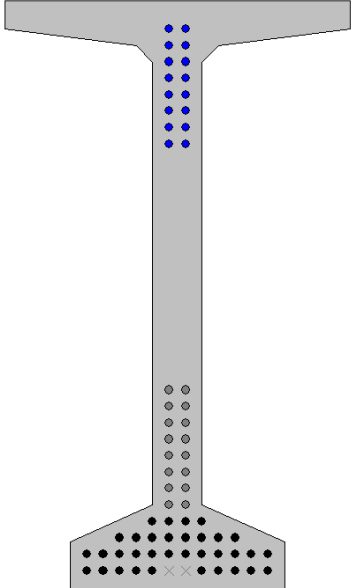
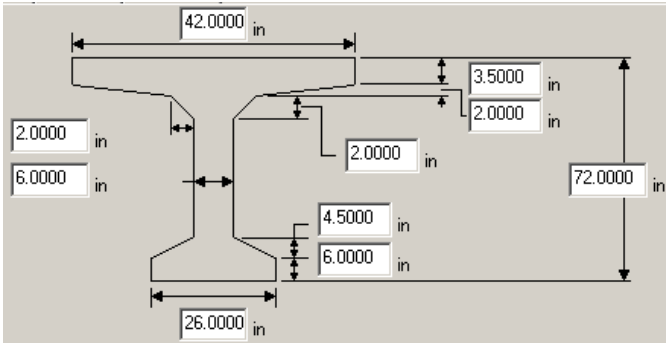
  

		<p>Strand Spacing: Horizontal: 2" Vertical: 2"</p> <p># of Strands: 46 Number of Harped Strands: 16 CG from bottom at Midspan: 6.85" CG from bottom at Left Support: 21.46"</p> 
Strand Layout at Midspan	Strand Layout at Left Support	Cross-Section

Bridge 11030

Bridge #	Virtis BID #	Span Length (ft)	t <sub>slab</sub> (in.)	Girder Spacing (ft)	Overhang Width (ft)	# of Girders	Skew (deg)	Materials			Dist. to Extreme Strands (in.)		Harp Point (ft)	Beam Section	
								P/S Tendons	f' <sub>c</sub> (ksi)	f' <sub>c1</sub> (ksi)	f' <sub>c,deck</sub> (ksi)	Bottom			Top
11030	0551	136'-0"	6.25	6'-4 1/2"	3'-10 1/2"	9	90.0	50-0.5" Gr. 270 LR	7.0	6.0	3.0	2.5	3.5	48.75	BT-72

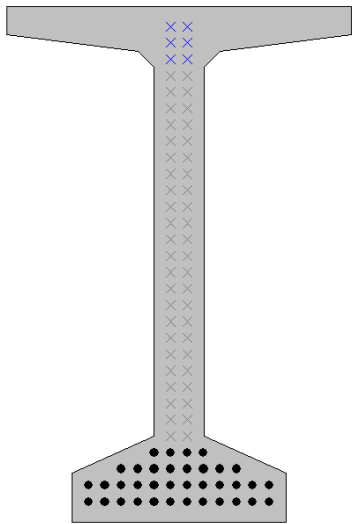
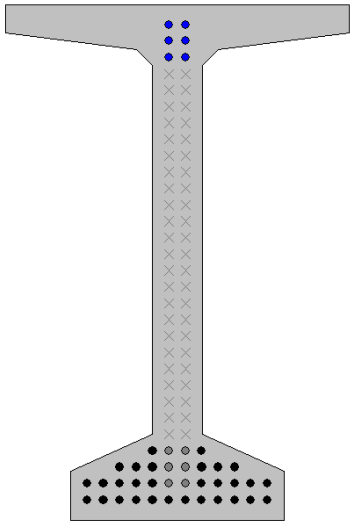
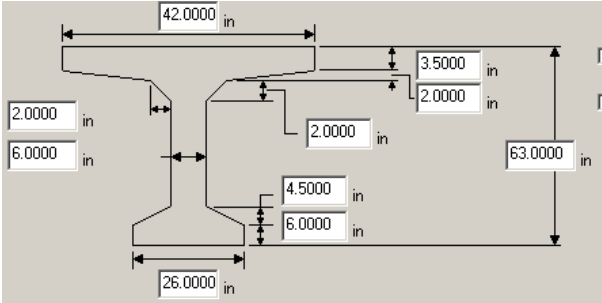
		<p>Strand Spacing: Horizontal: 2" Vertical: 2"</p> <p># of Strands: 50 Number of Harped Strands: 16 CG from bottom at Midspan: 8.90" CG from bottom at Left Support: 22.98"</p> 
Strand Layout at Midspan	Strand Layout at Left Support	Cross-Section



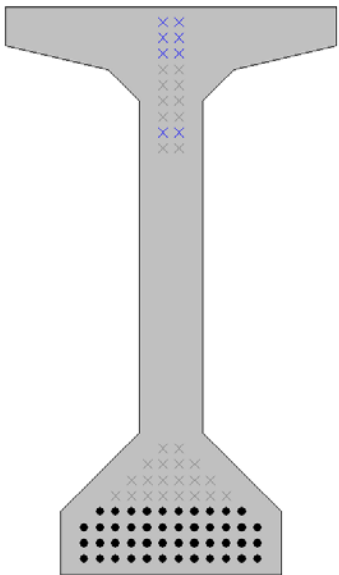
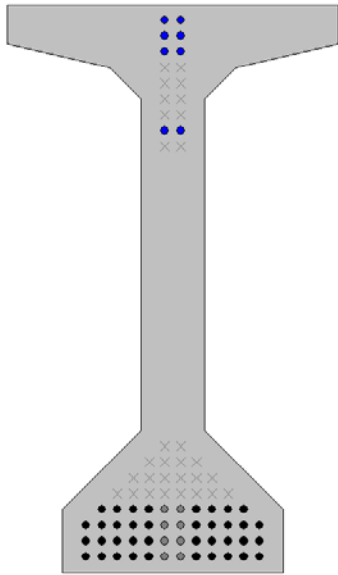
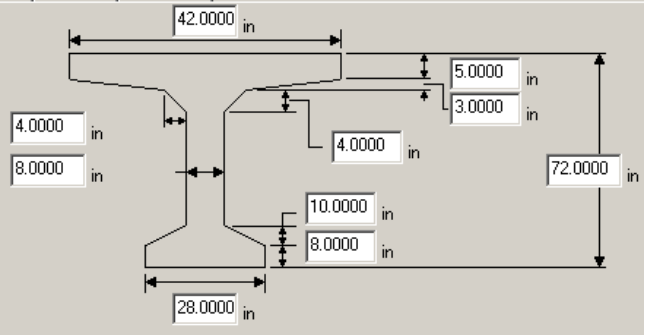
Bridge 8889

Bridge #	Virtis BID #	Span Length (ft)	t <sub>slab</sub> (in.)	Girder Spacing (ft)	Overhang Width (ft)	# of Girders	Skew (deg)	Materials			Dist. to Extreme Strands (in.)		Harp Point (ft)	Beam Section	
								P/S Tendons	f <sub>c</sub> ' (ksi)	f <sub>c</sub> i (ksi)	f <sub>c</sub> deck (ksi)	Bottom			Top
8889	0549	90'-10¼"	8.5	10'-7"	3'-7" (L) 4'-1" (R)	4	70.6	36-0.5" Gr. 270 LR	7.0	5.5	4.0	2.5	2.5	36.74	BT-63

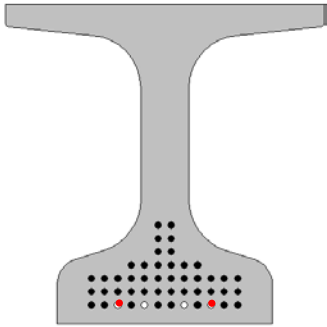
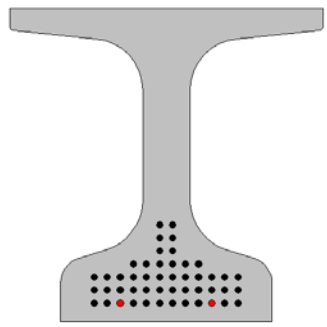
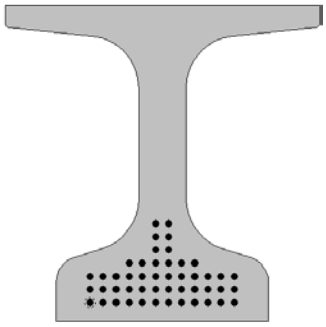
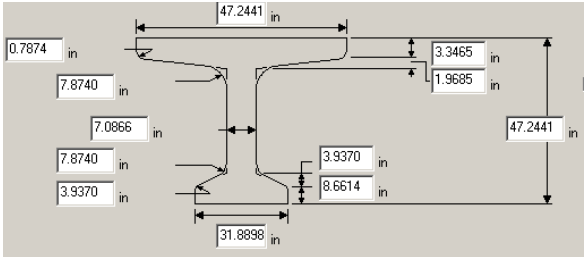
  

		<p>Strand Spacing: Horizontal: 2" Vertical: 2"</p> <p># of Strands: 36 Number of Harped Strands: 6 CG from bottom at Midspan: 4.72" CG from bottom at Left Support: 13.39"</p> 
Strand Layout at Midspan	Strand Layout at Left Support	Cross-Section

Bridge 8783

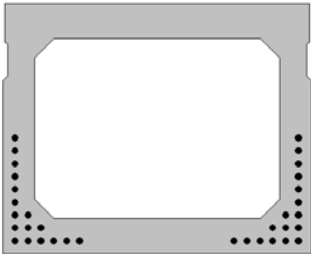
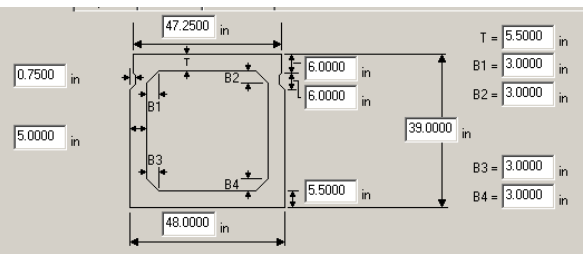
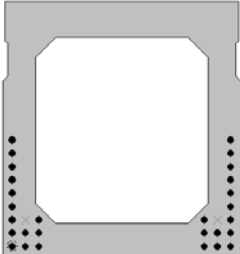
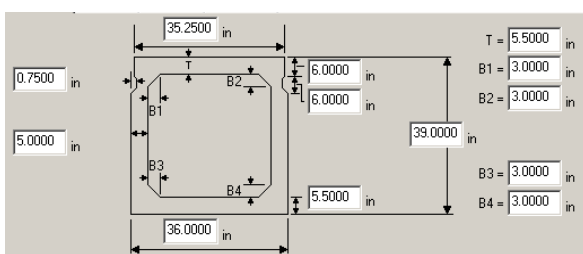
Bridge #	Virtis BID #	Span Length (ft)	t <sub>slab</sub> (in.)	Girder Spacing (ft)	Overhang Width (ft)	# of Girders	Skew (deg)	Materials			Dist. to Extreme Strands (in.)		Harp Point (ft)	Beam Section	
								P/S Tendons	f' <sub>c</sub> (ksi)	f' <sub>e1</sub> (ksi)	f' <sub>c deck</sub> (ksi)	Bottom			Top
8783	0553	141'-1¾"	8.5	7'-9"	3'-1"	8	96.9	46-0.6" Gr. 270 LR	8.0	6.0	4.0	2.0	2.0	57.78	AASHTO Type VI
						<p>Strand Spacing: Horizontal: 2" Vertical: 2"</p> <p># of Strands: 46 Number of Harped Strands: 8 CG from bottom at Midspan: 4.87" CG from bottom at Left Support: 15.30"</p> 									
		Strand Layout at Midspan		Strand Layout at Left Support		Cross-Section									

Bridge 15620

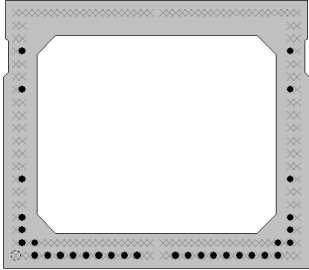
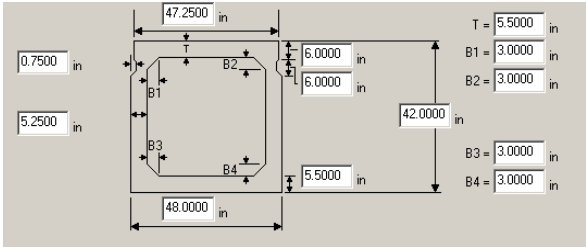
Bridge #	Virtis BID #	Span Length (ft)	t <sub>slab</sub> (in.)	Girder Spacing (ft)	Overhang Width (ft)	# of Girders	Skew (deg)	Materials			Dist. to Extreme Strands (in.)		Harp Point (ft)	Beam Section		
								P/S Tendons	f' <sub>c</sub> (ksi)	f' <sub>c</sub> (ksi)	f' <sub>c deck</sub> (ksi)	Bottom			Top	
15620	0561	119'-9 3/4"	9.4375	5'-4 1/8"	3'-3 3/8"	11	90	48-0.6" Gr. 270 LR	10.0	8.0	3.0	2.7559		na	Bulb Tee	
								Strand Spacing: Horizontal: 1.9685" Vertical: 1.9685"								
								# of Strands: 48 Number of Harped Strands: 0 CG from bottom at 51.57": 6.51" CG from bottom at 75.20": 6.35" CG from bottom at Midspan: 6.20"								
																
			<p>@ 51.57" from Left Support</p>			<p>@ 75.20" from Left Support</p>			<p>Strand Layout at Midspan</p>			<p>Cross-Section</p>				

### Adjacent Precast Box Girders

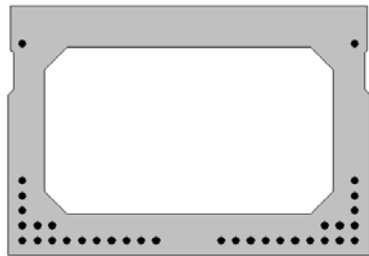
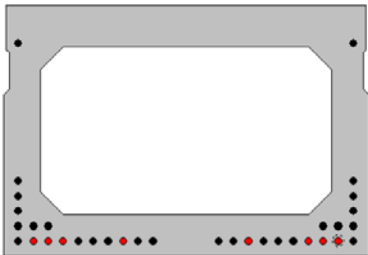
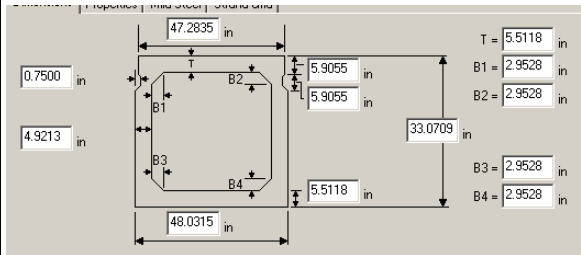
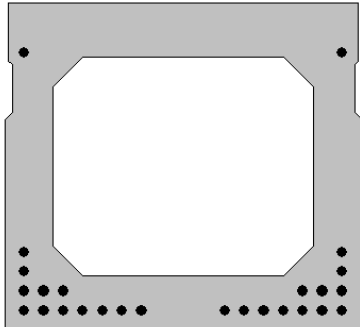
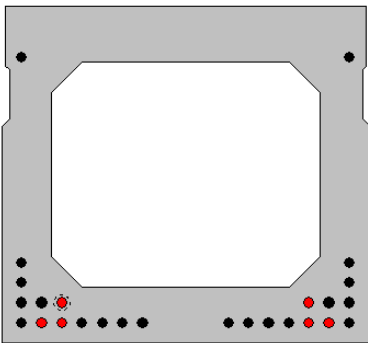
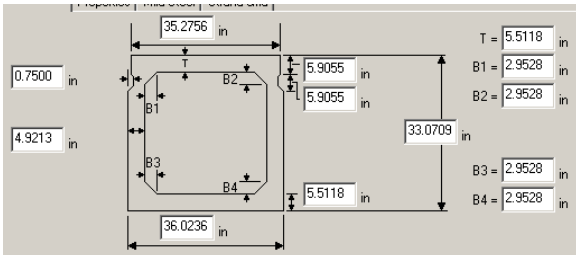
#### Bridge 12807

Bridge #	Virtis BID #	Span Length (ft)	t <sub>slab</sub> (in.)	Girder Spacing (ft)	Overhang Width (ft)	# of Girders	Skew (deg)	Materials				Dist. to Extreme Strands (in.)		Harp Point (ft)	Beam Section
								P/S Tendons	f <sub>c</sub> ' (ksi)	f <sub>c</sub> ' <sub>i</sub> (ksi)	f <sub>c</sub> ' <sub>deck</sub> (ksi)	Bottom	Top		
12807	0780	84'-0 1/4"	6.0	3 @ 4'-0 1/2", 1 @ 3'-6 1/2", 2 @ 3'-0 1/2", 1 @ 3'-6 1/2", 3 @ 4'-0 1/2"	2'-4 1/2"	11	48.0	34-0.5" Gr. 270 SR	6.0	4.8	3.0	2.0	na	BIII-48	
								28-0.5" Gr. 270 SR				2.0			BIII-36
					Strand Spacing: Horizontal: 2" Vertical: 2"  # of Strands: 34 CG from bottom at Midspan: 6.71"										
<b>Strand Layout at Midspan</b>					<b>Cross-Section - BIII-48</b>					<b>Cross-Section - BIII-48</b>					
					Strand Spacing: Horizontal: 2" Vertical: 2"  # of Strands: 28 CG from bottom at Midspan: 7.71"										
<b>Strand Layout at Midspan</b>					<b>Cross-Section - BIII-36</b>					<b>Cross-Section - BIII-36</b>					

Bridge 13788

Bridge #	Virtis BID #	Span Length (ft)	t <sub>slab</sub> (in.)	Girder Spacing (ft)	Overhang Width (ft)	# of Girders	Skew (deg)	Materials			Dist. to Extreme Strands (in.)		Harp Point (ft)	Beam Section	
								P/S Tendons	f <sub>c</sub> ' (ksi)	f <sub>c</sub> l (ksi)	f <sub>c</sub> ' <sub>deck</sub> (ksi)	Bottom			Top
13788	0781	83'-0"	6.0	4'-0½"	2'-5"	9	56.8	32-0.5" Gr. 270 SR	6.0	4.8	3.0	2.0		na	BIV-48
					<p>Strand Spacing: Horizontal: 1" Vertical: 2"</p> <p># of Strands: 32 CG from bottom at Midspan: 7.25"</p>										
<b>Strand Layout at Midspan</b>					<b>Strand Layout at Left Support</b>					<b>Cross-Section</b>					

Bridge 15238

Bridge #	Virtis BID #	Span Length (ft)	t <sub>slab</sub> (in.)	Girder Spacing (ft)	Overhang Width (ft)	# of Girders	Skew (deg)	Materials			Dist. to Extreme Strands (in.)		Harp Point (ft)	Beam Section	
								P/S Tendons	f <sub>c</sub> ' (ksi)	f <sub>c</sub> ' <sub>i</sub> (ksi)	f <sub>c</sub> ' <sub>deck</sub> (ksi)	Bottom			Top
15238	0782	73'-9 <sup>5</sup> / <sub>8</sub> "	5.875	1 @ 3'-6 <sup>3</sup> / <sub>8</sub> " 9 @ 4'-0 <sup>3</sup> / <sub>8</sub> " 1 @ 3'-6 <sup>3</sup> / <sub>8</sub> "	1'-11 15/16"	12	90.0	34-0.5" Gr. 270 SR	6.5	5.2	3.0	1.9685	5.118	na	BII-48
								26-0.5" Gr. 270 SR				1.9685	5.118	na	BII-36
								Strand Spacing: Horizontal: 1.9685" Vertical: 1.9685"							
								# of Strands: 34 CG from bottom at 94.49": 5.78" CG from bottom at Midspan: 4.89"							
															
Strand Layout at Midspan				@94.49" from Left Support				Cross-Section- BII-48							
								Strand Spacing: Horizontal: 1.9685" Vertical: 1.9685"							
								# of Strands: 26 CG from bottom at 94.49": 5.94" CG from bottom at Midspan: 5.18"							
															
Strand Layout at Midspan				Cross-Section- BII-36				Cross-Section- BII-36							

Bridge 9314

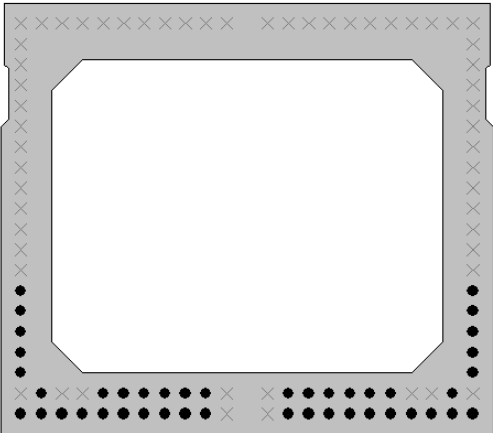
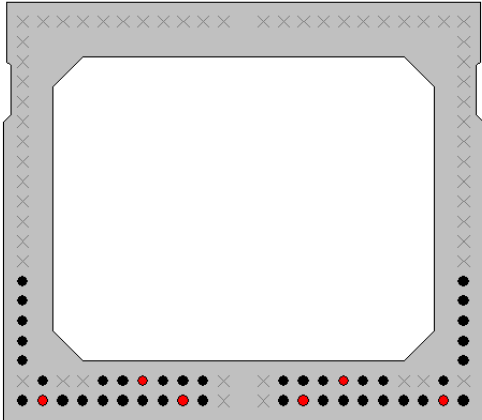
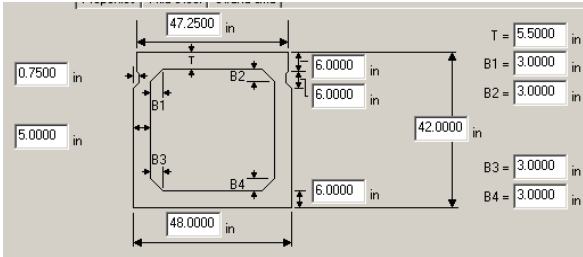
Bridge #	Virtis BID #	Span Length (ft)	t <sub>slab</sub> (in.)	Girder Spacing (ft)	Overhang Width (ft)	# of Girders	Skew (deg)	Materials			Dist. to Extreme Strands (in.)		Harp Point (ft)	Beam Section
								P/S Tendons	f <sub>c</sub> ' (ksi)	f <sub>c1</sub> ' (ksi)	f <sub>c</sub> ' <sub>deck</sub> (ksi)	Bottom		
9314	0783	83'-8"	6.0	3'-1½"	1'-6"	16	90.0	22-0.6" Gr. 270 LR	5.2	5.0	4.0	2	na	27x36 Box Beam
												Strand Spacing: Horizontal: 2" Vertical: 2" # of Strands: 22 CG from bottom at Left Support to 96" : 3.14" CG from bottom at 156" : 2.89" CG from bottom at 240" : 3.00" CG from bottom at Midspan: 3.27"		
												@ left support to 96" from left support      @ 156" from left support      @ 240" from left support      Strand Layout at Midspan      Cross-Section (Interior)		
												Strand Spacing: Horizontal: 2" Vertical: 2" # of Strands: 22 CG from bottom at Left Support to 96": 3.14" CG from bottom at 156": 2.89" CG from bottom at 240": 3.00" CG from bottom at Midspan: 3.27"		
												@ left support to 96" from left support      @ 156" from left support      @ 240" from left support      Strand Layout at Midspan      Cross-Section (Exterior)		



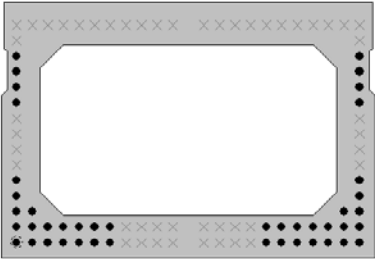
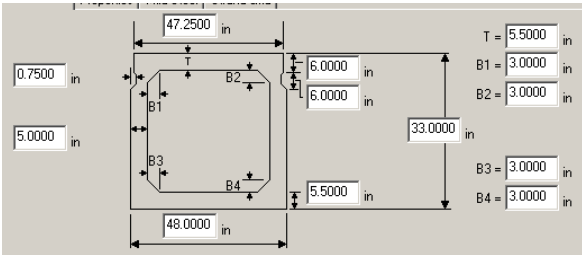
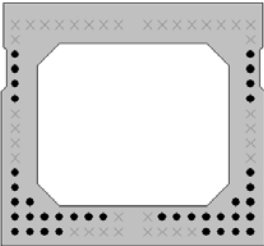
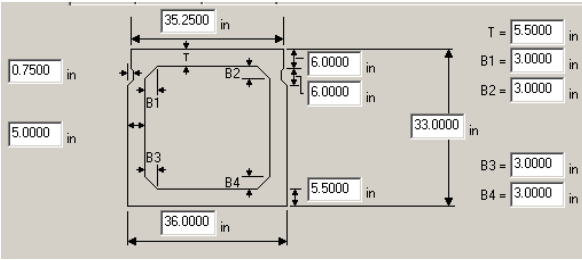
Bridge 17075

Bridge #	Virtis BID #	Span Length (ft)	t <sub>slab</sub> (in.)	Girder Spacing (ft)	Overhang Width (ft)	# of Girders	Skew (deg)	Materials			Dist. to Extreme Strands (in.)		Harp Point (ft)	Beam Section	
								P/S Tendons	f <sub>c</sub> ' (ksi)	f <sub>c1</sub> ' (ksi)	f <sub>c,deck</sub> ' (ksi)	Bottom			Top
17075	0785	107'-0"	6.0	4'-0"	2'-7½"	10	90	44-0.5" Gr. 270 SR	6.0	4.8	3.3	2.0		na	BIV-48

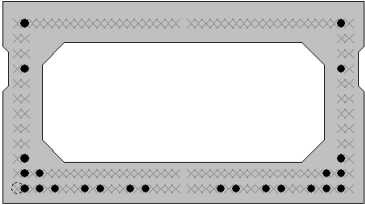
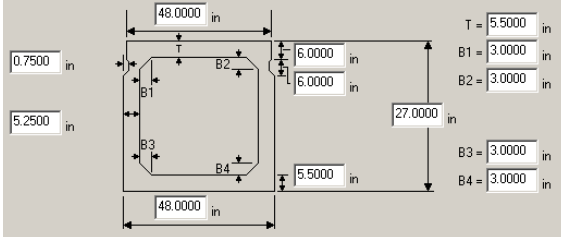
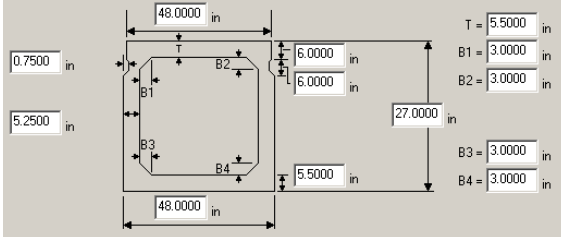
  

		<p>Strand Spacing: Horizontal: 2" Vertical: 2"</p> <p># of Strands: 44 CG from bottom at left support to 138": 4.74" CG from bottom at Midspan: 4.45"</p> 
Strand Layout at Midspan	Strand Layout at Left Support to 138"	Cross-Section


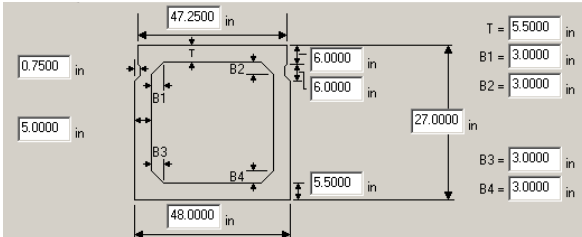
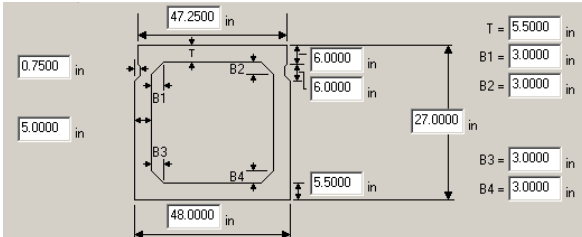
Bridge 17175

Bridge #	Virtis BID #	Span Length (ft)	t <sub>slab</sub> (in.)	Girder Spacing (ft)	Overhang Width (ft)	# of Girders	Skew (deg)	Materials			Dist. to Extreme Strands (in.)		Harp Point (ft)	Beam Section	
								P/S Tendons	f <sub>c</sub> ' (ksi)	f <sub>c</sub> i (ksi)	f <sub>c</sub> deck (ksi)	Bottom			Top
17175	0786	88'-9"	6.0	1@4'-0", 1@3'-6", 2@3'-0", 1@3'-6", 1@4'-0"	2'-6"	7	90.0	44-0.5" Gr. 270 SR	6.0	4.8	3.0	2.0	7.0	na	BII-48
								38-0.5" Gr. 270 SR				2	7.0	na	BII-36
								<p>Strand Spacing: Horizontal: 2" Vertical: 2"</p> <p># of Strands: 44 CG from bottom at Midspan: 7.45"</p>							
				<b>Strand Layout at Midspan – 4' Box</b>				<b>Cross-Section – BII 48</b>				<b>Cross-Section – BII 48</b>			
								<p>Strand Spacing: Horizontal: 2" Vertical: 2"</p> <p># of Strands: 38 CG from bottom at Midspan: 8.32"</p>							
				<b>Strand Layout at Midspan -3' Interior Box</b>				<b>Cross-Section – BII-36</b>				<b>Cross-Section – BII-36</b>			

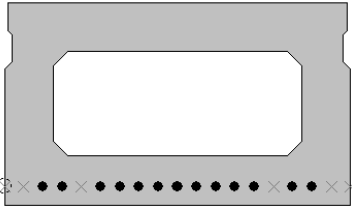
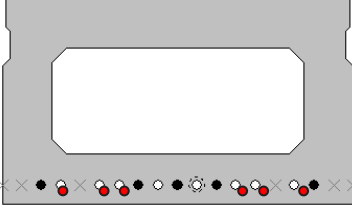
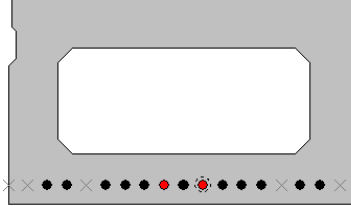
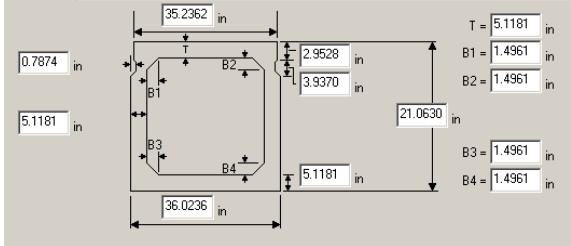
Bridge 13805

Bridge #	Virtis BID #	Span Length (ft)	t <sub>slab</sub> (in.)	Girder Spacing (ft)	Overhang Width (ft)	# of Girders	Skew (deg)	Materials				Dist. to Extreme Strands (in.)		Harp Point (ft)	Beam Section
								P/S Tendons	f <sub>c</sub> ' (ksi)	f <sub>c1</sub> ' (ksi)	f <sub>c deck</sub> ' (ksi)	Bottom	Top		
13805	0681	52'-6"	3.5	4'-0 11/16"	2'-0" (L), 1'-11 3/16" (R)	7	75	24-0.5" Gr. 270 SR	5.0	4.0	3.0	2.0	3.0	na	BI-48
 <p>Strand Spacing: Horizontal: 1" Vertical: 2"</p> <p># of Strands: 24 CG from bottom at Midspan: 5.83"</p>															
Strand Layout at Midspan					Cross-Section					Cross-Section					

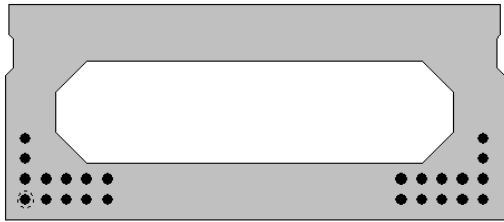
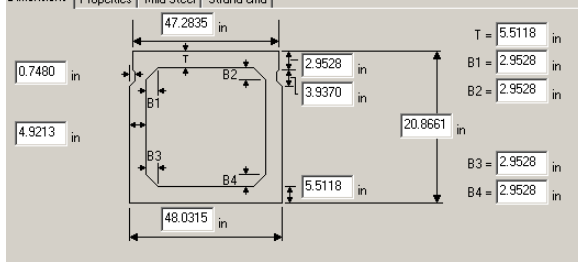
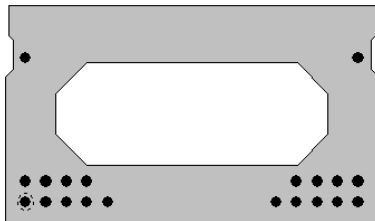
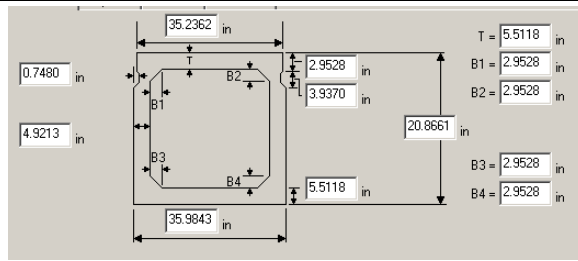
Bridge 14246

Bridge #	Virtis BID #	Span Length (ft)	t <sub>slab</sub> (in.)	Girder Spacing (ft)	Overhang Width (ft)	# of Girders	Skew (deg)	Materials				Dist. to Extreme Strands (in.)		Harp Point (ft)	Beam Section
								P/S Tendons	f <sub>c</sub> ' (ksi)	f <sub>c1</sub> ' (ksi)	f <sub>c deck</sub> ' (ksi)	Bottom	Top		
14246	0684	52'-0"	6.0	4'-0 1/2"	2'-4 1/4"	8	90.0	24-0.5" Gr. 270 SR	5.0	4.0	3.0	2.0	3.0	na	BI-48
 <p>Strand Spacing: Horizontal: 2" Vertical: 2"</p> <p># of Strands: 24 CG from bottom at Midspan: 7.50"</p>															
Strand Layout at Midspan					Cross-Section					Cross-Section					

Bridge 9180

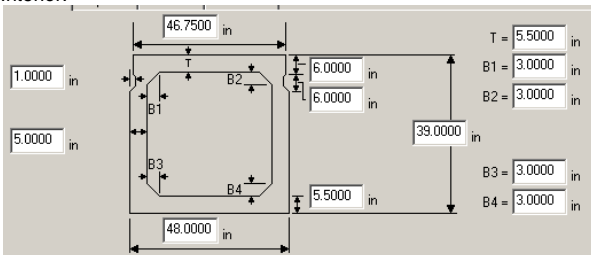
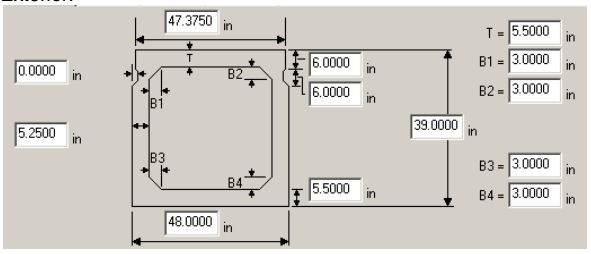
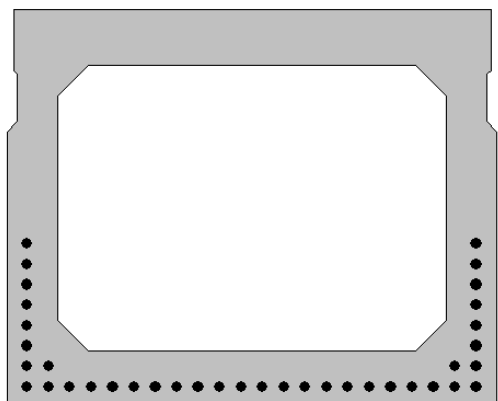
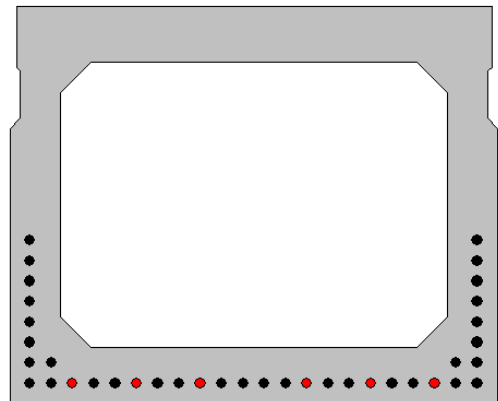
Bridge #	Virtis BID #	Span Length (ft)	$t_{slab}$ (in.)	Girder Spacing (ft)	Overhang Width (ft)	# of Girders	Skew (deg)	Materials			Dist. to Extreme Strands (in.)		Harp Point (ft)	Beam Section	
								P/S Tendons	$f'_c$ (ksi)	$f'_{c1}$ (ksi)	$f'_{c\ deck}$ (ksi)	Bottom			Top
9180	0690	44'-8 $\frac{3}{8}$ "	5.875	3'-1 1/2"	1'-6"	27	78.6	13-0.6" Gr. 270 LR	5.0	4.0	4.0	1.9685	na	MDOT 535x915	
												<p>Strand Spacing: Horizontal: 2"</p> <p># of Strands: 13 CG from bottom at left support: 1.97" CG from bottom at 98.425": 1.97" CG from bottom at Midspan: 1.97"</p> 			
			Strand Layout at Midspan			Strand layout at 59.055"			Strand layout at 98.425"			Cross-Section			

Bridge 17042

Bridge #	Virtis BID #	Span Length (ft)	t <sub>slab</sub> (in.)	Girder Spacing (ft)	Overhang Width (ft)	# of Girders	Skew (deg)	Materials			Dist. to Extreme Strands (in.)		Harp Point (ft)	Beam Section	
								P/S Tendons	f <sub>c</sub> ' (ksi)	f <sub>c1</sub> ' (ksi)	f <sub>c,deck</sub> ' (ksi)	Bottom			Top
17042	0693	50'-0 3/4"	5.875	1@4'-0", 4@3'-6", 1@4'-0"	2'-5 7/16"	7	57.0	24-0.5" Gr. 270 SR	6.0	4.8	3.0	1.9685	na	4' Box	
								20-0.5" Gr. 270 SR				1.9685	5.118	na	3' Box
								<p>Strand Spacing: Horizontal: 1.9685" Vertical: 1.9685"</p> <p># of Strands: 24 CG from bottom at Midspan: 3.61"</p>							
<b>Strand Layout at Midspan – 4' Box</b>				<b>Cross-Section – 4' Box</b>				<b>Cross-Section – 4' Box</b>							
								<p>Strand Spacing: Horizontal: 1.9685" Vertical: 1.9685"</p> <p># of Strands: 20 CG from bottom at Midspan: 4.13"</p>							
<b>Strand Layout at Midspan -3' Interior Box</b>				<b>Cross-Section – 3' Box</b>				<b>Cross-Section – 3' Box</b>							

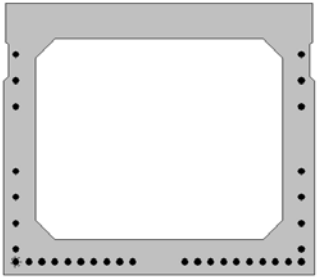
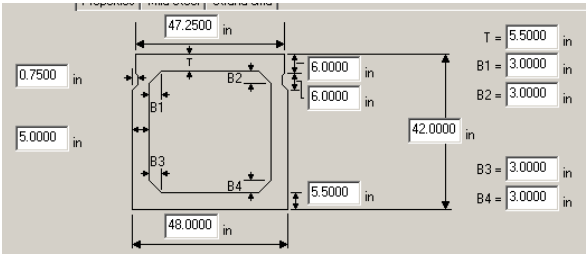


Bridge 16799

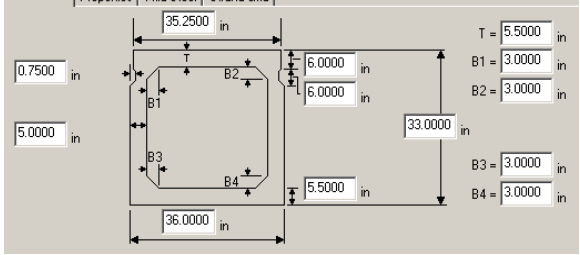
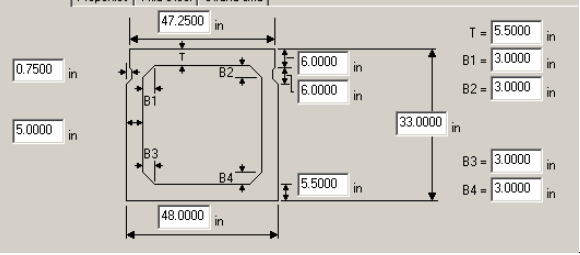
Bridge #	Virtis BID #	Span Length (ft)	t <sub>slab</sub> (in.)	Girder Spacing (ft)	Overhang Width (ft)	# of Girders	Skew (deg)	Materials			Dist. to Extreme Strands (in.)		Harp Point (ft)	Beam Section	
								P/S Tendons	f <sub>c</sub> ' (ksi)	f <sub>c1</sub> ' (ksi)	f <sub>c'</sub> deck (ksi)	Bottom			Top
16799	0737	84'-0"	0.0	4'-0"	2'-1 1/2"	5	90.0	38-0.5" Gr. 270 LR	5.0	4.0	3.3	2.0	na		
								Strand Spacing: Horizontal: 2.0952" Vertical: 2"  # of Strands: 38 CG from bottom at left support: 5.63" CG from bottom at Midspan: 5.05"  Interior:  Exterior: 							
												Cross-Section			



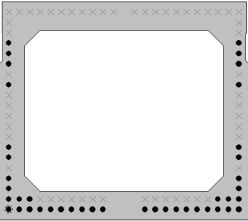
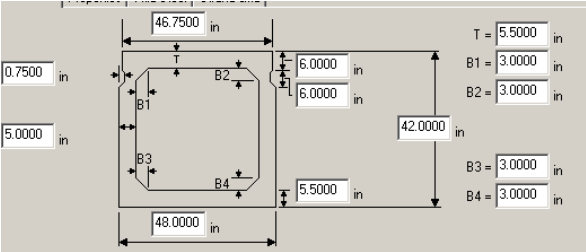
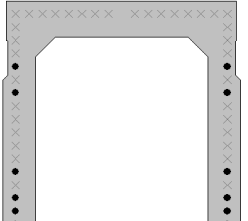
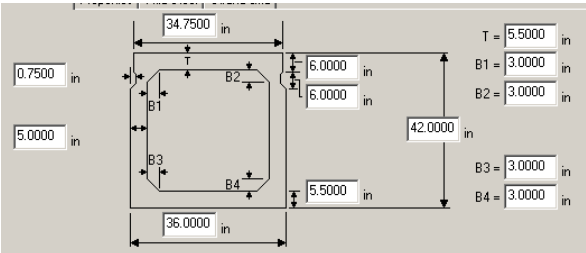
Bridge 14987

Bridge #	Virtis BID #	Span Length (ft)	t <sub>slab</sub> (in.)	Girder Spacing (ft)	Overhang Width (ft)	# of Girders	Skew (deg)	Materials			Dist. to Extreme Strands (in.)		Harp Point (ft)	Beam Section	
								P/S Tendons	f <sub>c</sub> ' (ksi)	f <sub>c</sub> i (ksi)	f <sub>c</sub> ' deck (ksi)	Bottom			Top
14987	0738	73'-0"	6.0	3 @ 4'-0¾" 1 @ 4'-7¼"	2'-3" (L) 2'-6" (R)	5	99.7	34-0.5" Gr. 270 SR	5.0	4.0	3.3	2.0	8	na	BIV-48
 <p style="text-align: center;"><b>Strand Layout at Midspan</b></p>					<p>Strand Spacing: Horizontal: 2" Vertical: 2", 4"</p> <p># of Strands: 34 CG from bottom at Midspan: 8.82"</p> <p style="text-align: center;"><b>Cross-Section</b></p>					 <p style="text-align: center;"><b>Cross-Section</b></p>					

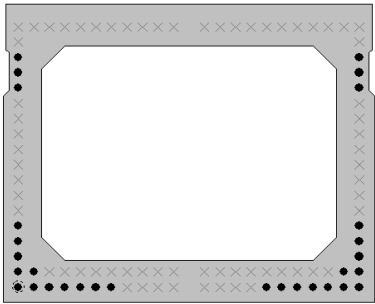
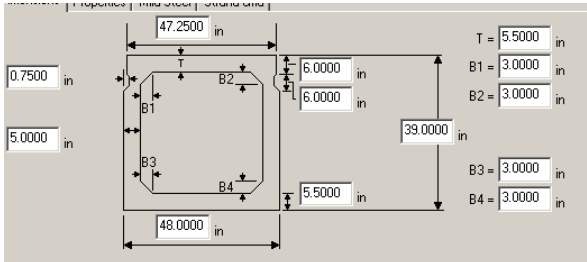
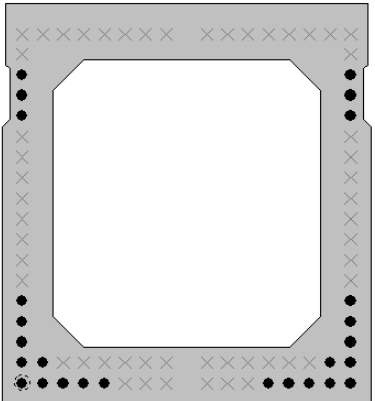
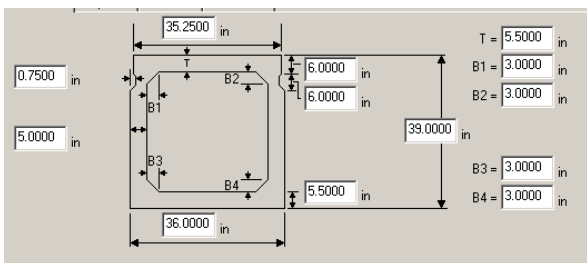
Bridge 12809

Bridge #	Virtis BID #	Span Length (ft)	t <sub>slab</sub> (in.)	Girder Spacing (ft)	Overhang Width (ft)	# of Girders	Skew (deg)	Materials			Dist. to Extreme Strands (in.)		Harp Point (ft)	Beam Section
								P/S Tendons	f <sub>c</sub> ' (ksi)	f <sub>c</sub> i' (ksi)	f <sub>c</sub> 'deck (ksi)	Bottom		
12809	0739	82'-0"	6.0	3@4'-0 ½", 1@3'-6	2'-4 ¾"	11	90.0	28-0.5" Gr. 270 SR	5.0	4.0	3.0	2.0	na	BII-36
				36-0.5" Gr. 270 SR				2.0				na	BII-48	
								<p>Strand Spacing: Horizontal: 2" Vertical: 2" # of Strands: 28 CG from bottom at 72": 3.33" CG from bottom at 120": 3.17" CG from bottom at Midspan: 3.14"</p> 						
Strand Layout at 72" from Left Support		Strand Layout at 120" from Left Support		Strand Layout at Midspan- BII-36		Cross-Section – BII-36								
								<p>Strand Spacing: Horizontal: 2" Vertical: 2", 8" # of Strands: 36 CG from bottom at 72": 3.38" CG from bottom at 144": 3.33" CG from bottom at Midspan: 3.33"</p> 						
Strand Layout at 72" from Left Support		Strand Layout at 144" from Left Support		Strand Layout at Midspan - BII-48		Cross-Section – BII-48								

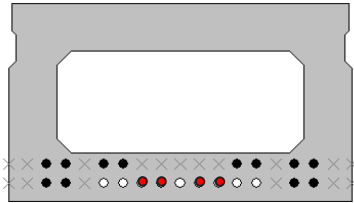
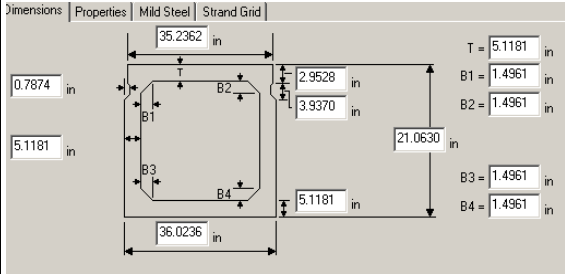
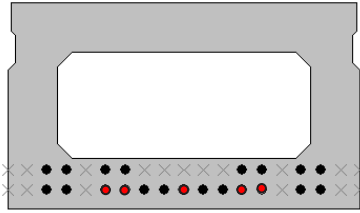
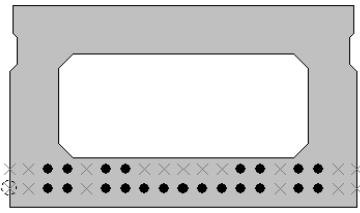
Bridge 12952

Bridge #	Virtis BID #	Span Length (ft)	t <sub>slab</sub> (in.)	Girder Spacing (ft)	Overhang Width (ft)	# of Girders	Skew (deg)	Materials			Dist. to Extreme Strands (in.)		Harp Point (ft)	Beam Section	
								P/S Tendons	f <sub>c</sub> ' (ksi)	f <sub>c1</sub> ' (ksi)	f <sub>c,deck</sub> ' (ksi)	Bottom			Top
12952	0741	79'-11 1/2"	8.25	1 @ 4'-0 1/2", 10 @ 3'-6 1/2", 1 @ 4'-0 1/2"	2'-4"	13	59.8	42-0.5" Gr. 270 LR	6.0	4.8	3.0	2.0	2.0	na	BIV-48
								30-0.5" Gr. 270 LR				2.0	2.0	na	BIV-36
					<p>Strand Spacing: Horizontal: 2" Vertical: 2"</p> <p># of Strands: 42 CG from bottom at Midspan: 9.24"</p>										
<b>Strand Layout at Midspan – BIV-48</b>					<b>Cross-Section – BIV-48</b>			<b>Cross-Section – BIV-48</b>							
					<p>Strand Spacing: Horizontal: 2" Vertical: 2"</p> <p># of Strands: 30 CG from bottom at Midspan: 8.67"</p>										
<b>Strand Layout at Midspan – BIV-36</b>					<b>Cross-Section – BIV-36</b>			<b>Cross-Section – BIV-36</b>							

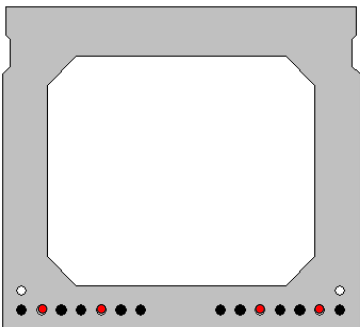
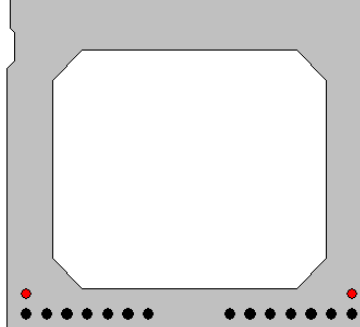
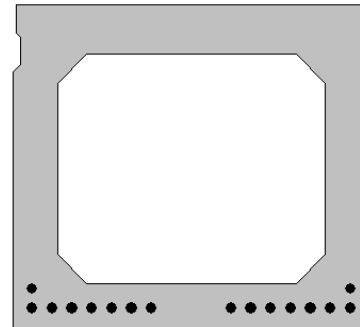
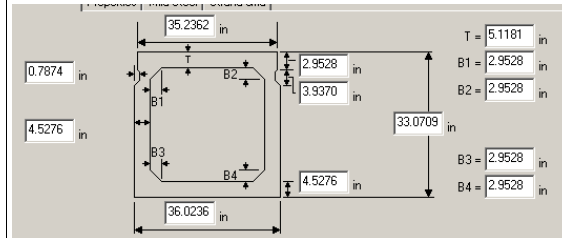
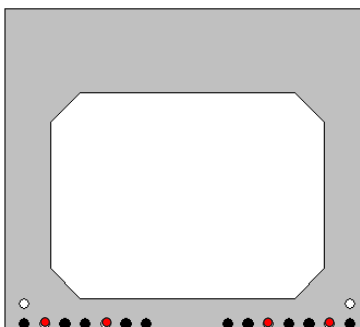
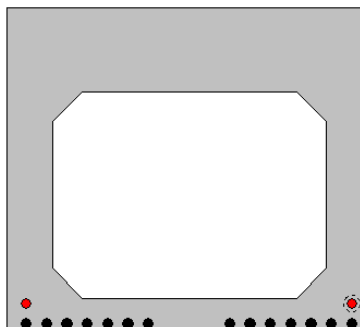
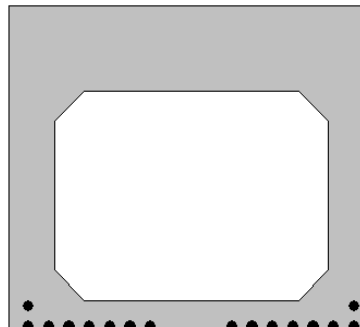
Bridge 17143

Bridge #	Virtis BID #	Span Length (ft)	t <sub>slab</sub> (in.)	Girder Spacing (ft)	Overhang Width (ft)	# of Girders	Skew (deg)	Materials				Dist. to Extreme Strands (in.)		Harp Point (ft)	Beam Section
								P/S Tendons	f' <sub>c</sub> (ksi)	f' <sub>cl</sub> (ksi)	f' <sub>c deck</sub> (ksi)	Bottom	Top		
17143	0742	70'-0"	6.0	1 @ 4'-0", 2 @ 3'-6", 1 @ 4'-0"	2'-6"	5	90	30-0.5" Gr. 270 SR	5.0	4.0	3.0	2.0	7.0	na	BIII-48
								26-0.5" Gr. 270 SR				2.0	7.0	na	BIII-36
				 <p>Strand Spacing: Horizontal: 2" Vertical: 2"</p> <p># of Strands: 30 CG from bottom at Midspan: 9.07"</p>				 <p><b>Cross-Section – BIII-48</b></p>							
<b>Strand Layout at Midspan – 4' Box</b>				<b>Cross-Section – BIII-48</b>				<b>Cross-Section – BIII-48</b>							
				 <p>Strand Spacing: Horizontal: 2" Vertical: 2"</p> <p># of Strands: 26 CG from bottom at Midspan: 10.15"</p>				 <p><b>Cross-Section – BIII-36</b></p>							
<b>Strand Layout at Midspan</b>				<b>Cross-Section – BIII-36</b>				<b>Cross-Section – BIII-36</b>							

Bridge 9181

Bridge #	Virtis BID #	Span Length (ft)	t <sub>slab</sub> (in.)	Girder Spacing (ft)	Overhang Width (ft)	# of Girders	Skew (deg)	Materials			Dist. to Extreme Strands (in.)		Harp Point (ft)	Beam Section	
								P/S Tendons	f <sub>c</sub> ' (ksi)	f <sub>c</sub> ' <sub>i</sub> (ksi)	f <sub>c</sub> ' <sub>deck</sub> (ksi)	Bottom			Top
9181	0743	60'-4 $\frac{3}{8}$ "	5.875	3'-1 $\frac{5}{8}$ "	1'-7 $\frac{1}{8}$ "	15	90.0	21-0.5" Gr. 270 LR	6.5	5.0	4.0	1.9685	na	MDOT 535x915	
															<p>Strand Spacing: Horizontal: 2" Vertical: 2.0079"</p> <p># of Strands: 21 CG from bottom at 36.02": 3.31" CG from bottom at 72.05": 2.97" CG from bottom at Midspan: 2.73"</p> 
															
															
												<p><b>@ 36.02" from left support</b>      <b>@ 72.05" from left support</b>      <b>Strand Layout at Midspan</b>      <b>Cross-Section</b></p>			

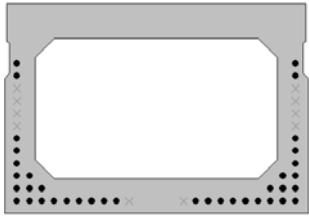
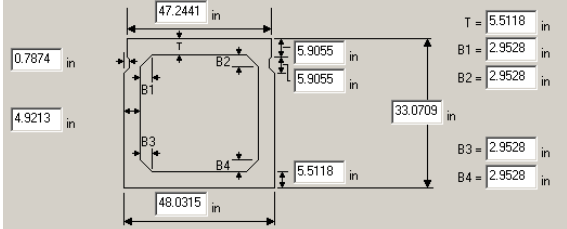
Bridge 9071

Bridge #	Virtis BID #	Span Length (ft)	t <sub>slab</sub> (in.)	Girder Spacing (ft)	Overhang Width (ft)	# of Girders	Skew (deg)	Materials			Dist. to Extreme Strands (in.)		Harp Point (ft)	Beam Section	
								P/S Tendons	f' <sub>c</sub> (ksi)	f' <sub>c1</sub> (ksi)	f' <sub>c deck</sub> (ksi)	Bottom			Top
9071	0745	83'-7 <sup>5</sup> / <sub>8</sub> "	5.875	3'-1 <sup>1</sup> / <sub>8</sub> "	1'-6 <sup>1</sup> / <sub>8</sub> "	15	120.0	16-0.6" Gr. 270 LR	5.0	3.5	4.0	2.0		na	MDOT 840x915
									Strand Spacing: Horizontal: 2" Vertical: 2"  # of Strands: 16 CG from bottom at 157.5": 2.00" CG from bottom at 248": 2.00" CG from bottom at Midspan: 2.25"						
															
@ 157.5" from left support			@ 248.0" from left support			Strand Layout at Midspan			Cross-Section						
									Strand Spacing: Horizontal: 2" Vertical: 2"  # of Strands: 16 CG from bottom at 157.5": 2.00" CG from bottom at 248": 2.25" CG from bottom at Midspan: 2.25"						
@ 157.5" from left support			@ 248.0" from left support			Strand Layout at Midspan			Cross-Section						

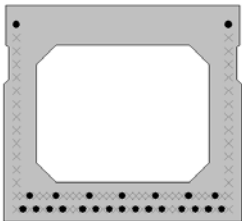
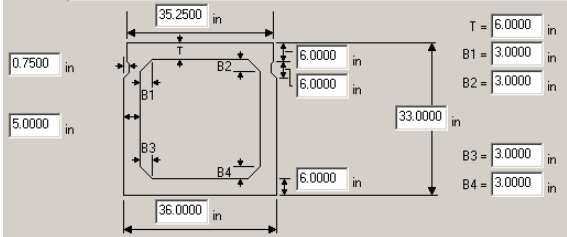
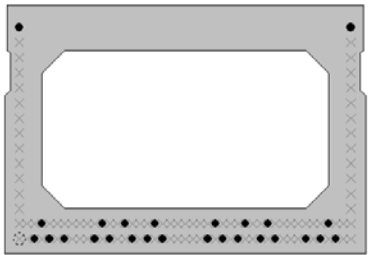
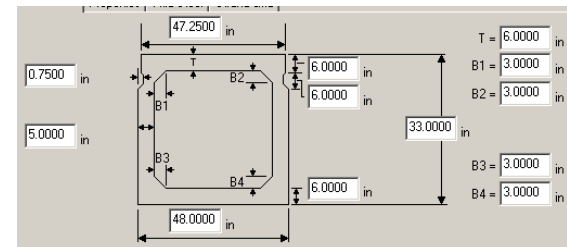
Bridge 9167

Bridge #	Virtis BID #	Span Length (ft)	t <sub>slab</sub> (in.)	Girder Spacing (ft)	Overhang Width (ft)	# of Girders	Skew (deg)	Materials				Dist. to Extreme Strands (in.)		Harp Point (ft)	Beam Section
								P/S Tendons	f' <sub>c</sub> (ksi)	f' <sub>c1</sub> (ksi)	f' <sub>c deck</sub> (ksi)	Bottom	Top		
9167	0746	75'-6¾"	5.875	4'-1½"	2'-1½"	12	120.0	22-0.6" Gr. 270 LR	5.0	4.0	4.0	1.9685		na	MDOT 685x1220
												Strand Spacing: Horizontal: 1.9685" Vertical: 2.0079"  # of Strands: 22 CG from bottom at 63.0": 3.10" CG from bottom at 118.125": 3.20" CG from bottom at 185.04": 3.07" CG from bottom at Midspan: 2.97"			
												<b>Cross-Section - Interior</b>			
												Strand Spacing: Horizontal: 1.9685" Vertical: 2.0079"  # of Strands: 22 CG from bottom at 63.0": 3.10" CG from bottom at 118.11": 3.20" CG from bottom at 185.04": 3.07" CG from bottom at Midspan: 2.97"			
												<b>Cross-Section - Exterior</b>			

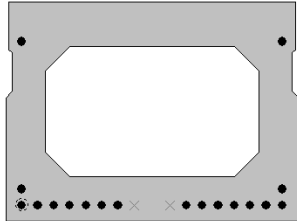
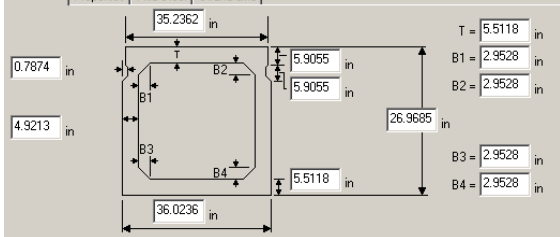

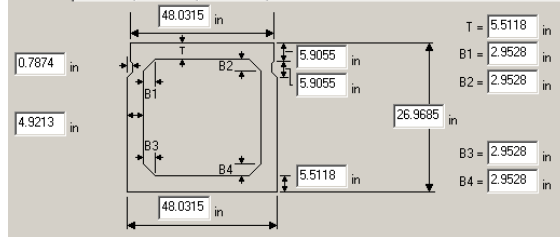


Bridge #	Virtis BID #	Span Length (ft)	t <sub>slab</sub> (in.)	Girder Spacing (ft)	Overhang Width (ft)	# of Girders	Skew (deg)	Materials				Dist. to Extreme Strands (in.)		Harp Point (ft)	Beam Section
								P/S Tendons	f' <sub>c</sub> (ksi)	f' <sub>ci</sub> (ksi)	f' <sub>c deck</sub> (ksi)	Bottom	Top		
17008	0747	82'-6 1/8"	6.25	4'-0"	2'-6"	8	115.0	38-0.5" Gr. 270 SR	7.0	5.6	3.0	1.9685		na	AASHTO BII-1220
				 <p>Strand Spacing: Horizontal: 1.9685" Vertical: 1.9685"</p> <p># of Strands: 38 CG from bottom at Midspan: 6.11"</p>											
Strand Layout at Midspan				Cross-Section				Cross-Section							

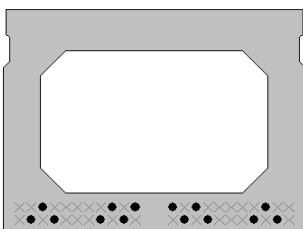
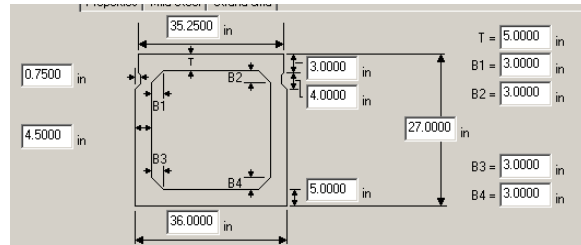
Bridge 5125

Bridge #	Virtis BID #	Span Length (ft)	t <sub>slab</sub> (in.)	Girder Spacing (ft)	Overhang Width (ft)	# of Girders	Skew (deg)	Materials				Dist. to Extreme Strands (in.)		Harp Point (ft)	Beam Section
								P/S Tendons	f' <sub>c</sub> (ksi)	f' <sub>ci</sub> (ksi)	f' <sub>c deck</sub> (ksi)	Bottom	Top		
5125	0748	66'-0"	5.5	1 @ 3'-6", 7 @ 4'-0", 1 @ 3'-6", 2 @ 3'-0", 1 @ 3'-6", 7 @ 4'-0", 1 @ 3'-6"	1-6"	22	108.0	24-0.5" Gr. 270 LR	6.0	4.5	4.0	2.0	3.0	na	36"x33" Box Girder
				26-0.5" Gr. 270 LR				2.0				3.0	48"x33" Box Girder		
				 <p>Strand Spacing: Horizontal: 1" Vertical: 2"</p> <p># of Strands: 24 CG from bottom at Midspan: 4.92"</p>											
Strand Layout at Midspan				Cross-Section				Cross-Section – 36"x33" Box Girder							
				 <p>Strand Spacing: Horizontal: 1" Vertical: 2"</p> <p># of Strands: 26 CG from bottom at Midspan: 4.77"</p>											
Strand Layout at Midspan				Cross-Section				Cross-Section – 48"x33" Box Girder							

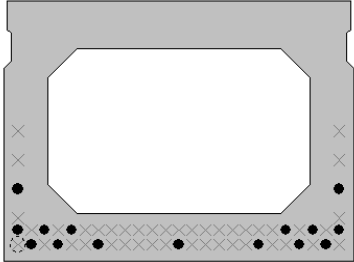
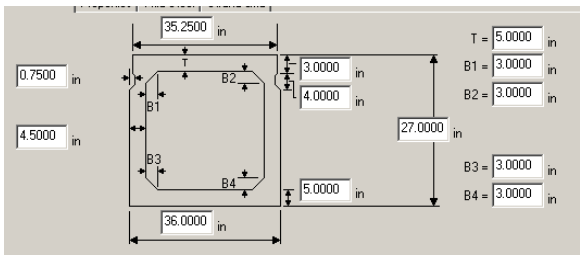
Bridge 13118

Bridge #	Virtis BID #	Span Length (ft)	t <sub>slab</sub> (in.)	Girder Spacing (ft)	Overhang Width (ft)	# of Girders	Skew (deg)	Materials			Dist. to Extreme Strands (in.)		Harp Point (ft)	Beam Section	
								P/S Tendons	f <sub>c</sub> ' (ksi)	f <sub>c1</sub> ' (ksi)	f <sub>c,deck</sub> ' (ksi)	Bottom			Top
13118	0749	69'-2 3/4"	5.875	1 @ 3'-7 3/16", 2 @ 3'-1 3/16", 1 @ 3'-7 1/4", 2 @ 4'-1 3/16", 1 @ 3'-7 1/4", 2 @ 3'-1 3/16", 1 @ 3'-7 3/16"	2'-3 15/16"	11	60.0	18-0.6" Gr. 270 LR	10.2	8.0	3.0	1.9685	4.9213	na	AASHTO BI-915
								19-0.6" Gr. 270 LR				1.9685	4.9213	na	AASHTO BI-1220
						Strand Spacing: Horizontal: 1.9685" Vertical: 1.9685"  # of Strands: 18 CG from bottom at Midspan: 4.42"									
				<b>Strand Layout at Midspan</b>		<b>Cross-Section</b>			<b>Cross-Section – AASHTO BI-915</b>						
						Strand Spacing: Horizontal: 1.9685" Vertical: 1.9685"  # of Strands: 19 CG from bottom at Midspan: 4.08"									
				<b>Strand Layout at Midspan</b>		<b>Cross-Section</b>			<b>Cross-Section – AASHTO BI-1220</b>						

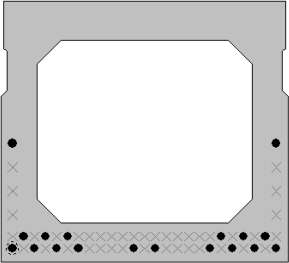
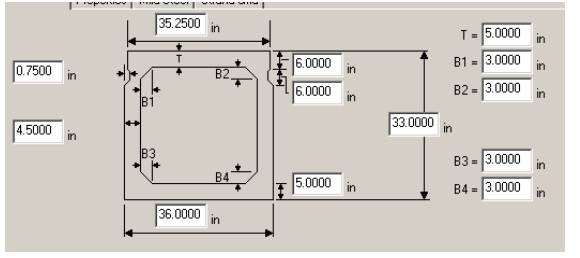
Bridge 5911

Bridge #	Virtis BID #	Span Length (ft)	t <sub>slab</sub> (in.)	Girder Spacing (ft)	Overhang Width (ft)	# of Girders	Skew (deg)	Materials			Dist. to Extreme Strands (in.)		Harp Point (ft)	Beam Section	
								P/S Tendons	f <sub>c</sub> ' (ksi)	f <sub>c1</sub> ' (ksi)	f <sub>c,deck</sub> ' (ksi)	Bottom			Top
5911	0750	59'-5"	5.5	3'-0"	1'-6"	50	125	14-0.5" Gr. 270 LR	5.0	4.0	4.0	1.75		na	27x36 Box
						Strand Spacing: Horizontal: 1.375" Vertical: 1.5"  # of Strands: 14 CG from bottom at Midspan: 2.39"									
				<b>Strand Layout at Midspan</b>		<b>Cross-Section</b>			<b>Cross-Section – 27x36 Box</b>						

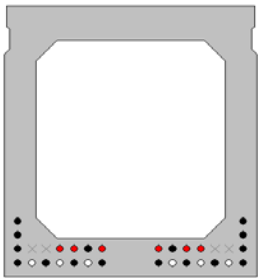
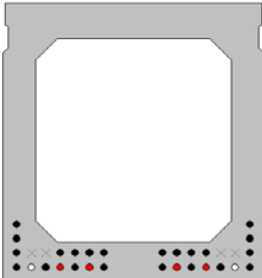
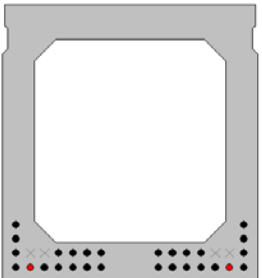
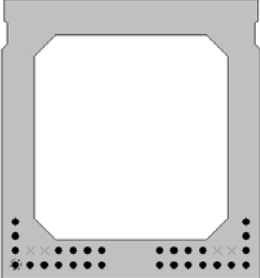
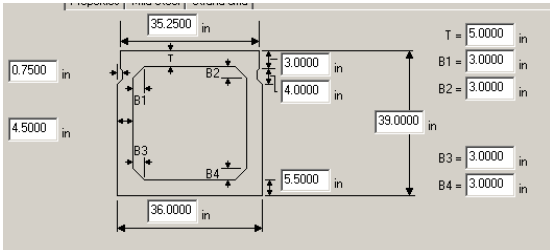
Bridge 3805

Bridge #	Virtis BID #	Span Length (ft)	t <sub>slab</sub> (in.)	Girder Spacing (ft)	Overhang Width (ft)	# of Girders	Skew (deg)	Materials			Dist. to Extreme Strands (in.)		Harp Point (ft)	Beam Section	
								P/S Tendons	f <sub>c</sub> ' (ksi)	f <sub>c</sub> ' <sub>i</sub> (ksi)	f <sub>c</sub> ' <sub>deck</sub> (ksi)	Bottom			Top
3805	0751	59'-0½"	0.0	3'-0"	1'-6"	14	90.0	15-0.5" Gr. 270 LR	5.0	4.0	3.5	1.75	na	27"x36" IDOT Beam	
								<p>Strand Spacing: Horizontal: 1.375", 3" Vertical: 1.5", 1.25", 3"</p> <p># of Strands: 15 CG from bottom at Midspan: 3.12"</p>							
Strand Layout at Midspan				Cross-Section				Cross-Section – 27"x36" IDOT Beam							

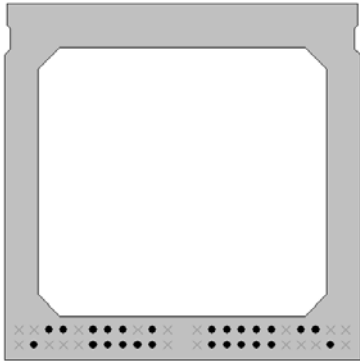
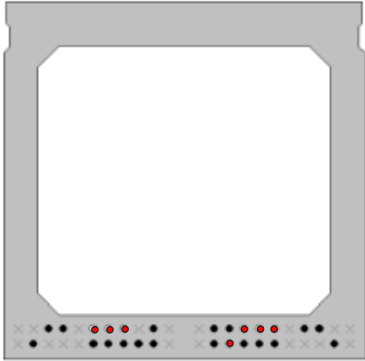
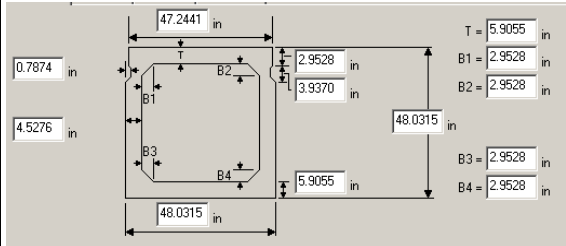
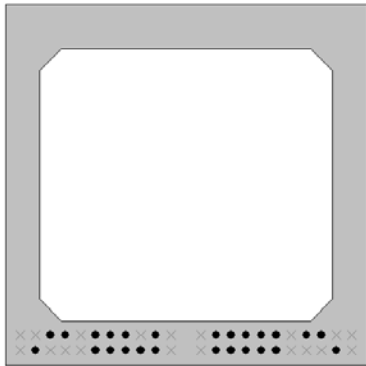
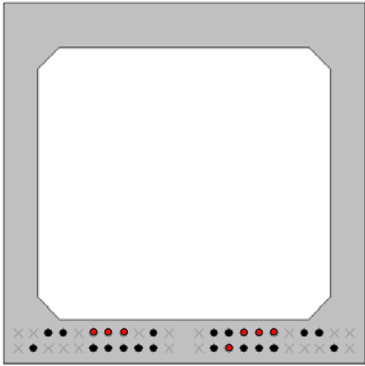
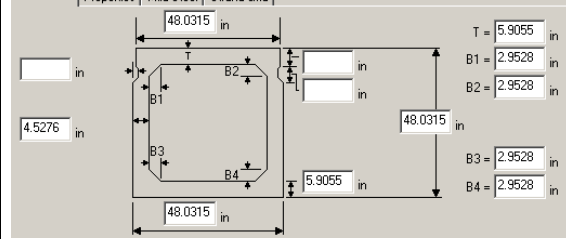
Bridge 3819

Bridge #	Virtis BID #	Span Length (ft)	t <sub>slab</sub> (in.)	Girder Spacing (ft)	Overhang Width (ft)	# of Girders	Skew (deg)	Materials			Dist. to Extreme Strands (in.)		Harp Point (ft)	Beam Section	
								P/S Tendons	f <sub>c</sub> ' (ksi)	f <sub>c</sub> ' <sub>i</sub> (ksi)	f <sub>c</sub> ' <sub>deck</sub> (ksi)	Bottom			Top
3819	0752	74'-10½"	0.0	3'-0"	1'-6"	11	128.8	18-0.5" Gr. 270 LR	5.0	4.0	3.5	1.75	na	33"x36" Box Beam	
								<p>Strand Spacing: Horizontal: 1.375", 3" Vertical: 1.5", 2.75", 3"</p> <p># of Strands: 18 CG from bottom at Midspan: 3.72"</p>							
Strand Layout at Midspan				Cross-Section				Cross-Section							

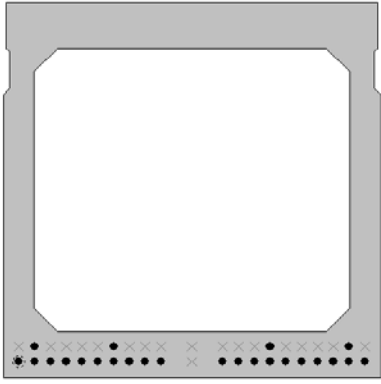
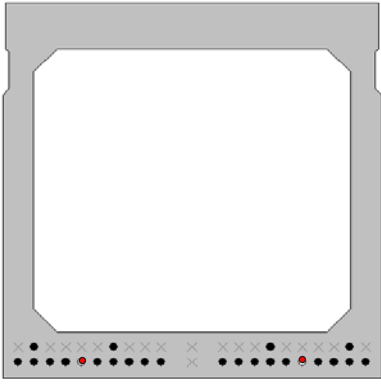
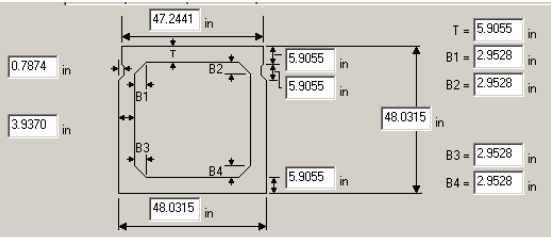
Bridge 9240

Bridge #	Virtis BID #	Span Length (ft)	t <sub>slab</sub> (in.)	Girder Spacing (ft)	Overhang Width (ft)	# of Girders	Skew (deg)	Materials			Dist. to Extreme Strands (in.)		Harp Point (ft)	Beam Section								
								P/S Tendons	f <sub>c</sub> ' (ksi)	f <sub>c</sub> l (ksi)	f <sub>c</sub> deck (ksi)	Bottom			Top							
9240	0763	97'-11"	6.0	3'-1 1/2"	1'-6"	25	90.0	28-0.5" Gr. 270 LR	5.5	3.6	4.0	2.0	na	33"x36" MDOT Beam								
																			<p>Strand Spacing: Horizontal: 2" Vertical: 2"</p> <p># of Strands: 28 CG from bottom at Left Support to 132": 3.75" CG from bottom at 252": 3.82" CG from bottom at 312": 3.54" CG from bottom at Midspan: 3.43"</p> 			
			<p>@ left support to 132" from left support</p>				<p>@ 252" from left support</p>				<p>@ 312" from left support</p>				<p>Strand Layout at Midspan</p>				<p>Cross-Section</p>			

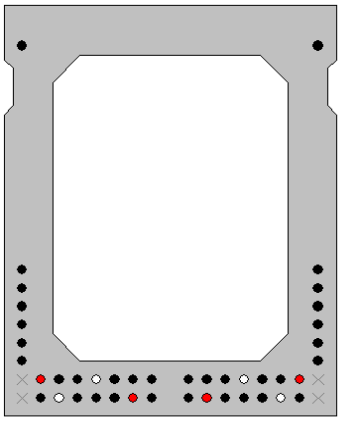
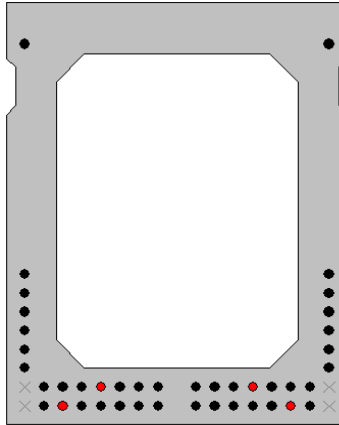
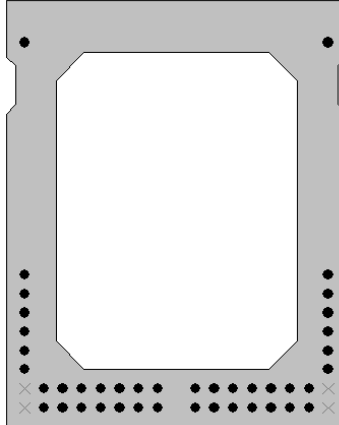
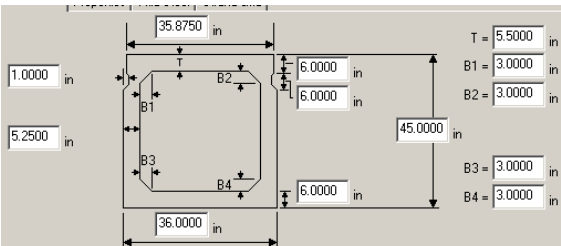
Bridge 9103

Bridge #	Virtis BID #	Span Length (ft)	t <sub>slab</sub> (in.)	Girder Spacing (ft)	Overhang Width (ft)	# of Girders	Skew (deg)	Materials			Dist. to Extreme Strands (in.)		Harp Point (ft)	Beam Section	
								P/S Tendons	f <sub>c</sub> ' (ksi)	f <sub>c</sub> l (ksi)	f <sub>c</sub> 'deck (ksi)	Bottom			Top
9103	0764	111'-2 <sup>5</sup> / <sub>8</sub> "	5.875	4'-1 <sup>5</sup> / <sub>8</sub> "	2'-1 1/2"	16	100.8	25-0.6" Gr. 270 LR	5.0	3.5	4.0	2.0		na	MDOT 1220x1220
										<p>Strand Spacing: Horizontal: 2" Vertical: 2"</p> <p># of Strands: 25 CG from bottom at left support: 2.78" CG from bottom at Midspan: 3.04"</p> 					
				<p style="text-align: center;"><b>Strand Layout at Midspan</b></p>				<p style="text-align: center;"><b>Strand layout at Support to 157.48"</b></p>		<p style="text-align: center;"><b>Cross-Section - Interior</b></p>					
										<p>Strand Spacing: Horizontal: 2" Vertical: 2"</p> <p># of Strands: 25 CG from bottom at left support: 2.78" CG from bottom at Midspan: 3.04"</p> 					
				<p style="text-align: center;"><b>Strand Layout at Midspan</b></p>				<p style="text-align: center;"><b>Strand layout at Support to 157.5"</b></p>		<p style="text-align: center;"><b>Cross-Section - Exterior</b></p>					

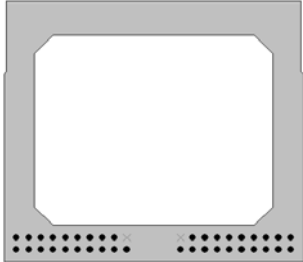
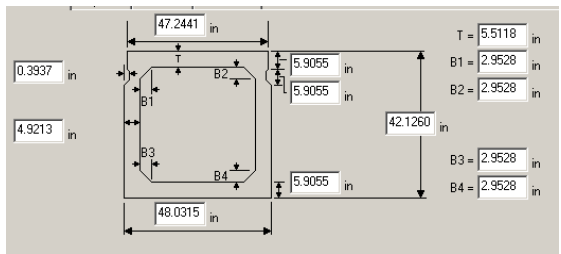
### Bridge 9228

Bridge #	Virtis BID #	Span Length (ft)	t <sub>slab</sub> (in.)	Girder Spacing (ft)	Overhang Width (ft)	# of Girders	Skew (deg)	Materials				Dist. to Extreme Strands (in.)		Harp Point (ft)	Beam Section
								P/S Tendons	f <sub>c'</sub> (ksi)	f <sub>c'l</sub> (ksi)	f <sub>c'deck</sub> (ksi)	Bottom	Top		
9228	0765	110'-5¼"	5.875	4'-2 13/16"	2'-1 ½"	11	72.2	24-0.6" Gr. 270 LR	6.1	4.6	4.0	1.9685		na	MDOT 1220x1220
												<p>Strand Spacing: Horizontal: 2.0079" Vertical: 1.9685"</p> <p># of Strands: 24 CG from bottom at left support: 2.33" CG from bottom at Midspan: 2.30"</p> 			
				Strand Layout at Midspan				Strand layout at Support to 19.685"				Cross-Section			

### Bridge 14070

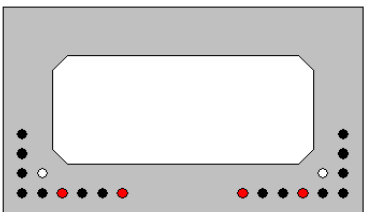
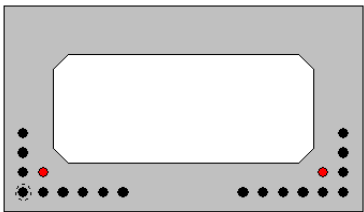
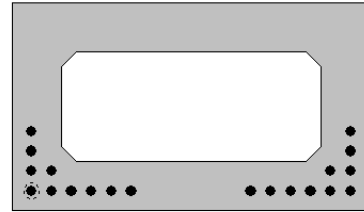
Bridge #	Virtis BID #	Span Length (ft)	t <sub>slab</sub> (in.)	Girder Spacing (ft)	Overhang Width (ft)	# of Girders	Skew (deg)	Materials				Dist. to Extreme Strands (in.)		Harp Point (ft)	Beam Section				
								P/S Tendons	f <sub>c'</sub> (ksi)	f <sub>c'l</sub> (ksi)	f <sub>c'deck</sub> (ksi)	Bottom	Top						
14070	0766	115'-0"	0.0	3'-1 3/16"	1'-6"	11	60.0	42-0.5" Gr. 270 LR	7.5	5.5		2.0	4.5	na	36"x45" Beam				
																<p>Strand Spacing: Horizontal: 2" Vertical: 2"</p> <p># of Strands: 42 CG from bottom at 36": 8.03" CG from bottom at 72": 7.50" CG from bottom at Midspan: 7.07"</p> 			
				@ 36" from left support				@ 72" from left support				Strand Layout at Midspan				Cross-Section			

Bridge 16538

Bridge #	Virtis BID #	Span Length (ft)	t <sub>slab</sub> (in.)	Girder Spacing (ft)	Overhang Width (ft)	# of Girders	Skew (deg)	Materials			Dist. to Extreme Strands (in.)		Harp Point (ft)	Beam Section
								P/S Tendons	f' <sub>c</sub> (ksi)	f' <sub>c1</sub> (ksi)	f' <sub>c,deck</sub> (ksi)	Bottom		
16538	0767	101'-8½"	5.875	4'-0¾"	2'-4"	9	90.0	38-0.5" Gr. 270 LR	7.25	5.1	3.0	1.9685	na	AASHTO BIV-48 mod
				Strand Spacing: Horizontal: 1.9685" Vertical: 1.9685"  # of Strands: 38 CG from bottom at Midspan: 2.90"										
								<b>Cross-Section</b>						

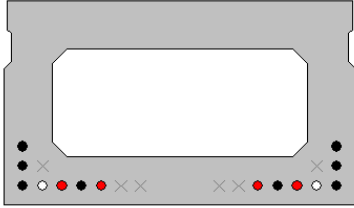


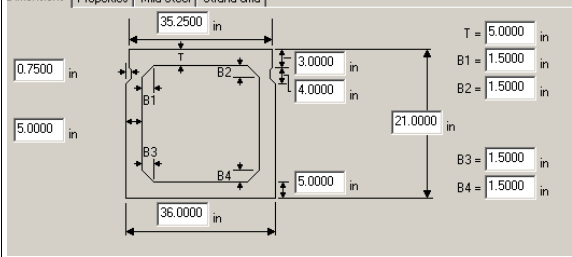
Spread Precast Box Girders

Bridge 9310

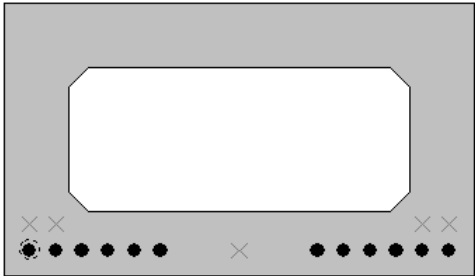
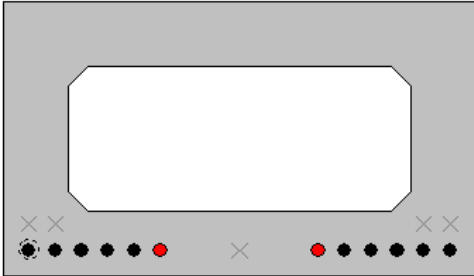
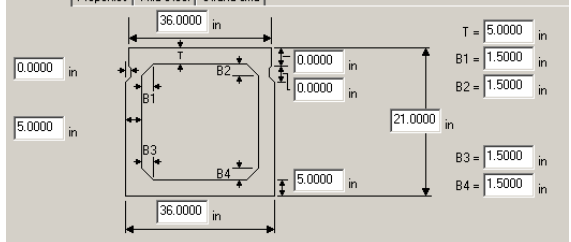
Bridge #	Virtis BID #	Span Length (ft)	t <sub>slab</sub> (in.)	Girder Spacing (ft)	Overhang Width (ft)	# of Girders	Skew (deg)	Materials			Dist. to Extreme Strands (in.)		Harp Point (ft)	Beam Section	
								P/S Tendons	f' <sub>c</sub> (ksi)	f' <sub>c1</sub> (ksi)	f' <sub>c,deck</sub> (ksi)	Bottom			Top
9310	0774	51'-11½"	9.0	5'-11½"	2'-2¼"	12	90.0	20-0.6" Gr. 270 LR	6.0	5.5	4.0	2.0	na	21x36 Box Beam	
												Strand Spacing: Horizontal: 2" Vertical: 2"  # of Strands: 20 CG from bottom at 118.1": 3.71" CG from bottom at 196.85": 3.33" CG from bottom at Midspan: 3.40"			
												<b>Cross-Section</b>			



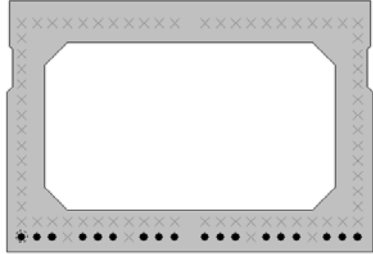
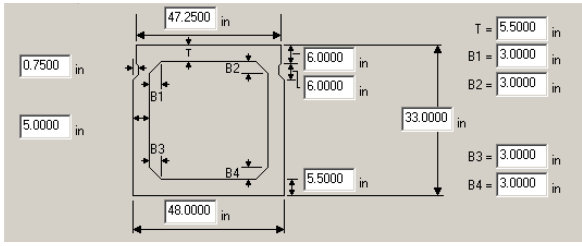
Bridge 9384

Bridge #	Virtis BID #	Span Length (ft)	t <sub>slab</sub> (in.)	Girder Spacing (ft)	Overhang Width (ft)	# of Girders	Skew (deg)	Materials			Dist. to Extreme Strands (in.)		Harp Point (ft)	Beam Section
								P/S Tendons	f' <sub>c</sub> (ksi)	f' <sub>c1</sub> (ksi)	f' <sub>c deck</sub> (ksi)	Bottom		
9384	0622	44'-1½"	9.0	6'-7¼"	3'-3⅜"	10	89.4	14-0.6" Gr. 270 LR	6.1	4.6	4.0	2	na	21x36 Box Beam
									<p>Strand Spacing: Horizontal: 2" Vertical: 2"</p> <p># of Strands: 14 CG from bottom at 59.0": 3.50" CG from bottom at 86.6": 3.00" CG from bottom at Midspan: 2.86"</p> 					
			@ 59.0" from left support		@ 86.6" from left support		Strand Layout at Midspan		Cross-Section					

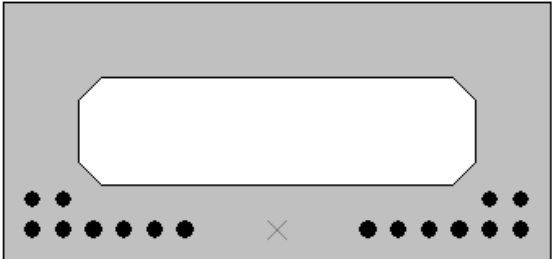
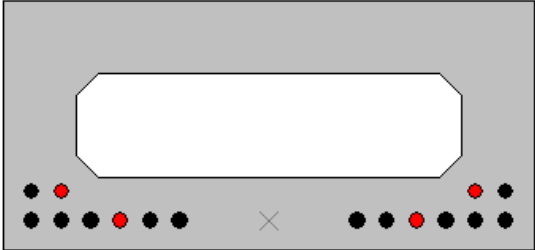
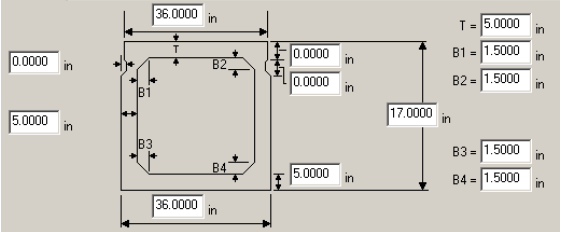
Bridge 9380

Bridge #	Virtis BID #	Span Length (ft)	t <sub>slab</sub> (in.)	Girder Spacing (ft)	Overhang Width (ft)	# of Girders	Skew (deg)	Materials			Dist. to Extreme Strands (in.)		Harp Point (ft)	Beam Section
								P/S Tendons	f' <sub>c</sub> (ksi)	f' <sub>c1</sub> (ksi)	f' <sub>c deck</sub> (ksi)	Bottom		
9380	0629	32'-1"	9.0	9'-1 3/16"	2'-6'	10	85.6	12-0.5" Gr. 270 LR	5.0	3.0	4.0	2.0	na	21x36 Box Beam
							<p>Strand Spacing: Horizontal: 2" Vertical: 2"</p> <p># of Strands: 12 CG from bottom at left support: 2.00" CG from bottom at Midspan: 2.00"</p> 							
			Strand Layout at Midspan		Strand layout at Support to 36.0"		Cross-Section							

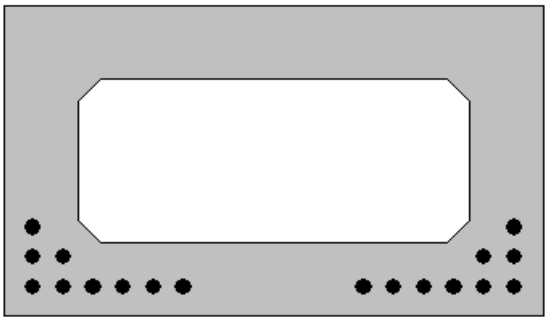
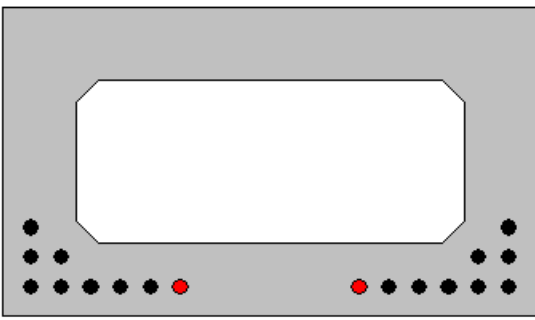
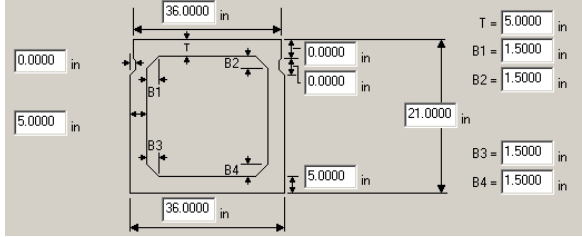
Bridge 17338

Bridge #	Virtis BID #	Span Length (ft)	t <sub>slab</sub> (in.)	Girder Spacing (ft)	Overhang Width (ft)	# of Girders	Skew (deg)	Materials			Dist. to Extreme Strands (in.)		Harp Point (ft)	Beam Section
								P/S Tendons	f <sub>c</sub> ' (ksi)	f <sub>c</sub> ' <sub>i</sub> (ksi)	f <sub>c</sub> ' <sub>deck</sub> (ksi)	Bottom		
17338	0675	49'-0"	8.5	8'-0"	4'-0"	4	135	18-0.5" Gr. 270 SR	5.0	4.0	3.0	2.0	na	AASHTO BII-48
 <p>Strand Spacing: Horizontal: 2" Vertical: 2"</p> <p># of Strands: 18 CG from bottom at Midspan: 2.00"</p>					<p><b>Cross-Section</b></p>					 <p><b>Cross-Section</b></p>				

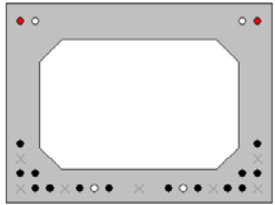
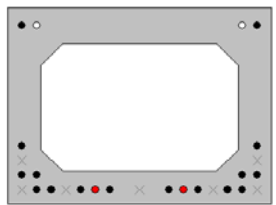
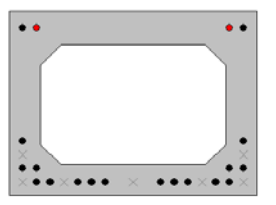
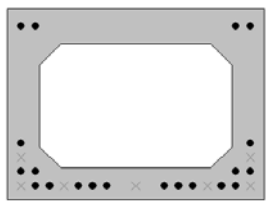
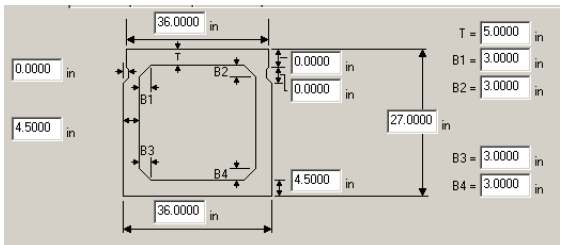
Bridge 9282

Bridge #	Virtis BID #	Span Length (ft)	t <sub>slab</sub> (in.)	Girder Spacing (ft)	Overhang Width (ft)	# of Girders	Skew (deg)	Materials			Dist. to Extreme Strands (in.)		Harp Point (ft)	Beam Section
								P/S Tendons	f <sub>c</sub> ' (ksi)	f <sub>c</sub> ' <sub>i</sub> (ksi)	f <sub>c</sub> ' <sub>deck</sub> (ksi)	Bottom		
9282	0679	36'-3 3/8"	9.0	7'-10"	3'-0" (L), 4'-0" (R)	12	67.3	16-0.5" Gr. 270 LR	5.0	4.0	4.0	2	na	17"x36" Box Beam
										<p>Strand Spacing: Horizontal: 2" Vertical: 2"</p> <p># of Strands: 16 CG from bottom at left support to 120": 2.33" CG from bottom at Midspan: 2.50"</p>  <p><b>Cross-Section</b></p>				

Bridge 9192

Bridge #	Virtis BID #	Span Length (ft)	t <sub>slab</sub> (in.)	Girder Spacing (ft)	Overhang Width (ft)	# of Girders	Skew (deg)	Materials			Dist. to Extreme Strands (in.)		Harp Point (ft)	Beam Section
								P/S Tendons	f <sub>c</sub> ' (ksi)	f <sub>c</sub> ' <sub>l</sub> (ksi)	f <sub>c</sub> ' <sub>deck</sub> (ksi)	Bottom		
9192	0686	38'-8"	9.0	3@6'-6 11/16" 5@9'-10"	3'-9 1/2"	9	80	18-0.5" Gr. 270 LR	5.5	4.4	4.0	2.0	na	21"x36" Box Beam
										<p>Strand Spacing: Horizontal: 2" Vertical: 2"</p> <p># of Strands: 18 CG from bottom at Support to 24": 3.00" CG from bottom at Midspan: 2.89"</p> 				
				Strand Layout at Midspan		Strand Layout at Support to 24"		Cross-Section – 21"x36" Box Beam						

Bridge 9286

Bridge #	Virtis BID #	Span Length (ft)	t <sub>slab</sub> (in.)	Girder Spacing (ft)	Overhang Width (ft)	# of Girders	Skew (deg)	Materials			Dist. to Extreme Strands (in.)		Harp Point (ft)	Beam Section		
								P/S Tendons	f <sub>c</sub> ' (ksi)	f <sub>c</sub> ' <sub>l</sub> (ksi)	f <sub>c</sub> ' <sub>deck</sub> (ksi)	Bottom			Top	
9286	0695	50'-8"	9.0	8'-0 1/2"	3'-2 1/8"	6	90	20-0.6" Gr. 270 LR	6.0	5.0	4.0	2.0	2.5	na	27"x36" Box Beam	
												<p>Strand Spacing: Horizontal: 2" Vertical: 2"</p> <p># of Strands: 20 CG from bottom at 0.5" from LS: 3.43" CG from bottom at 48" from LS: 6.06" CG from bottom at 140" from LS: 5.61" CG from bottom at Midspan: 7.50"</p> 				
				@ 0.5" from left support		@ 48" from left support		@ 140.0" from left support		Strand Layout at Midspan		Cross-Section				

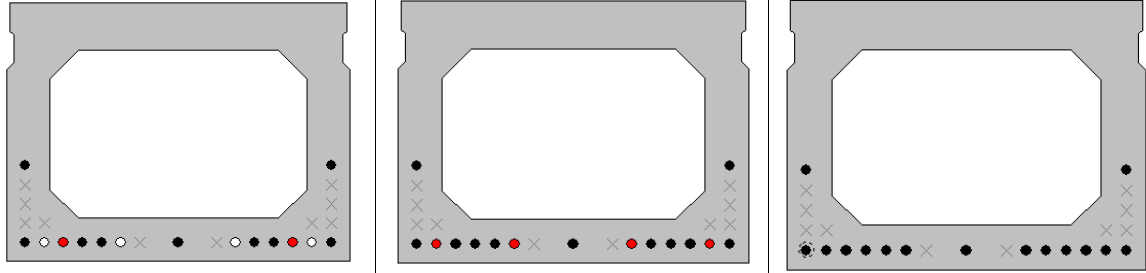
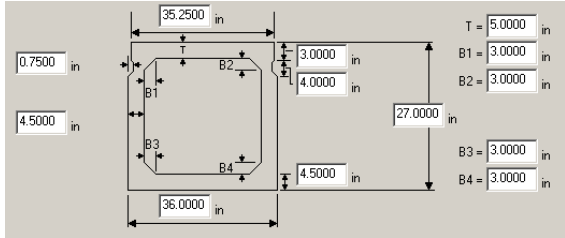
Bridge 9368

Bridge #	Virtis BID #	Span Length (ft)	t <sub>slab</sub> (in.)	Girder Spacing (ft)	Overhang Width (ft)	# of Girders	Skew (deg)	Materials				Dist. to Extreme Strands (in.)		Harp Point (ft)	Beam Section							
								P/S Tendons	f' <sub>c</sub> (ksi)	f' <sub>c1</sub> (ksi)	f' <sub>c deck</sub> (ksi)	Bottom	Top									
9368	0707	71'-3"	9.0	7'-4 1/2"	2'-11 1/2"	5	97.4	30-0.5" Gr. 270 LR	6.3	4.9	4.0	2.0		na	33"x36" Box Beam							
											<p>Strand Spacing: Horizontal: 2" Vertical: 2"</p> <p># of Strands: 30 CG from bottom at 63" from LS: 3.75" CG from bottom at 102" from LS: 3.64" CG from bottom at 147" from LS: 3.38" CG from bottom at Midspan: 3.20"</p>											
			<p>@ 63" from left support</p>				<p>@ 102" from left support</p>				<p>@ 147.0" from left support</p>				<p>Strand Layout at Midspan</p>				<p>Cross-Section</p>			

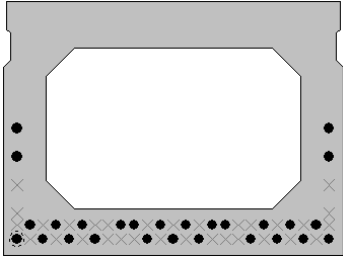
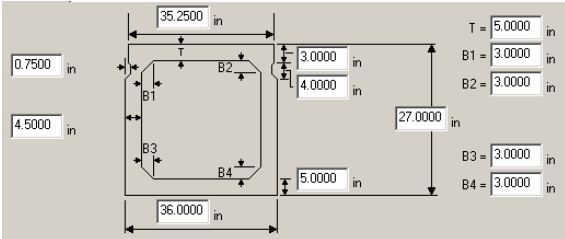
Bridge 9328

Bridge #	Virtis BID #	Span Length (ft)	t <sub>slab</sub> (in.)	Girder Spacing (ft)	Overhang Width (ft)	# of Girders	Skew (deg)	Materials				Dist. to Extreme Strands (in.)		Harp Point (ft)	Beam Section			
								P/S Tendons	f' <sub>c</sub> (ksi)	f' <sub>c1</sub> (ksi)	f' <sub>c deck</sub> (ksi)	Bottom	Top					
9328	0740	57'-3 1/4"	9.0	6'-11"	3'-3 3/8"	6	90.0	26-0.5" Gr. 270 LR	6.5	5.3	4.0	2		na	27x36 Box Beam			
											<p>Strand Spacing: Horizontal: 2" Vertical: 2"</p> <p># of Strands: 26 CG from bottom at 36.0": 3.20" CG from bottom at 114.0": 3.33" CG from bottom at Midspan: 3.38"</p>							
			<p>@ 36.0" from left support</p>				<p>@ 114.0" from left support</p>				<p>Strand Layout at Midspan</p>				<p>Cross-Section</p>			

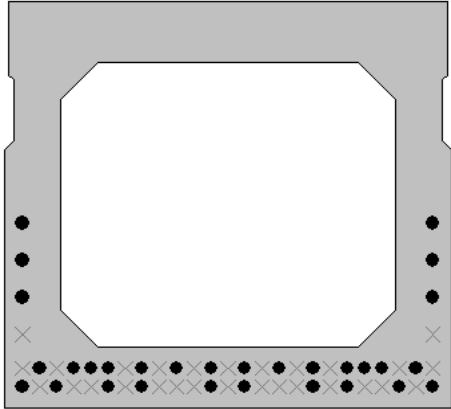
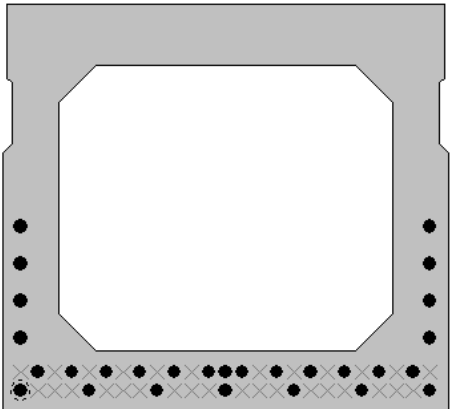
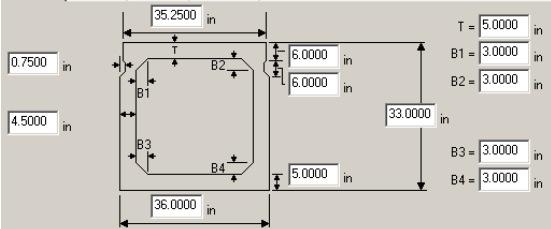
Bridge 9376

Bridge #	Virtis BID #	Span Length (ft)	t <sub>slab</sub> (in.)	Girder Spacing (ft)	Overhang Width (ft)	# of Girders	Skew (deg)	Materials			Dist. to Extreme Strands (in.)		Harp Point (ft)	Beam Section	
								P/S Tendons	f' <sub>c</sub> (ksi)	f' <sub>c1</sub> (ksi)	f' <sub>c deck</sub> (ksi)	Bottom			Top
9376	0744	53'-4¼"	9.0	7'-4¾"	3'-5 5/16"	12	90.0	15-0.6" Gr. 270 LR	7.0	6.2	4.0	2		na	27x36 Box Beam
								<p>Strand Spacing: Horizontal: 2" Vertical: 2"</p> <p># of Strands: 15 CG from bottom at 72.0": 3.78" CG from bottom at 108.0": 3.45" CG from bottom at Midspan: 3.07"</p> 							
				@ 72.0" from left support	@ 108.0" from left support	Strand Layout at Midspan		Cross-Section							

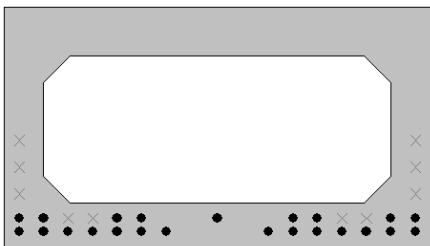
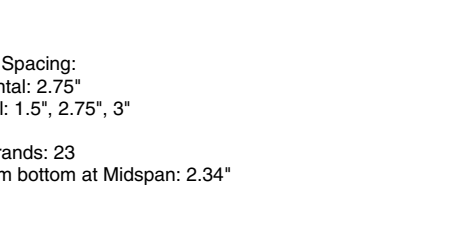
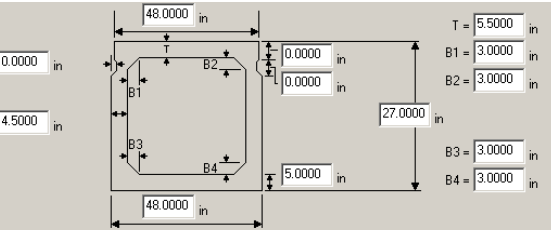
Bridge 3577

Bridge #	Virtis BID #	Span Length (ft)	t <sub>slab</sub> (in.)	Girder Spacing (ft)	Overhang Width (ft)	# of Girders	Skew (deg)	Materials			Dist. to Extreme Strands (in.)		Harp Point (ft)	Beam Section	
								P/S Tendons	f' <sub>c</sub> (ksi)	f' <sub>c1</sub> (ksi)	f' <sub>c deck</sub> (ksi)	Bottom			Top
3577	0222003	38'-7"	7.5	6'-8¾"	4'-0 7/16"	4	101.3	27-0.4375" Gr. 248 SR	5.0	4.0	3.5	1.75		na	27"x36" IDOT Beam
								<p>Strand Spacing: Horizontal: 1.375", 3" Vertical: 1.5", 1.25", 3"</p> <p># of Strands: 27 CG from bottom at Midspan: 3.94"</p>							
				Strand Layout at Midspan				Cross-Section				Cross-Section			

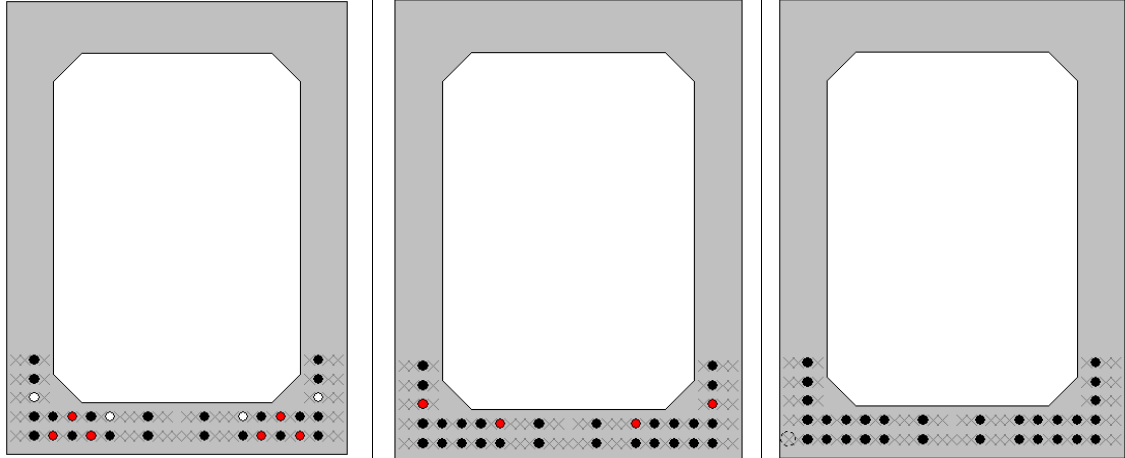
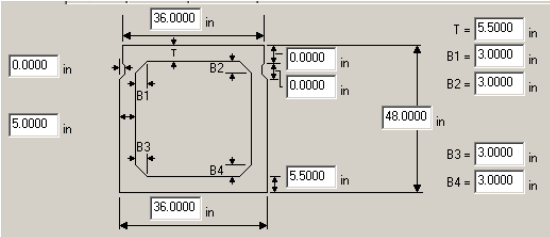
Bridge 3754

Bridge #	Virtis BID #	Span Length (ft)	t <sub>slab</sub> (in.)	Girder Spacing (ft)	Overhang Width (ft)	# of Girders	Skew (deg)	Materials			Dist. to Extreme Strands (in.)		Harp Point (ft)	Beam Section
								P/S Tendons	f <sub>c</sub> ' (ksi)	f <sub>c</sub> ' <sub>l</sub> (ksi)	f <sub>c</sub> ' <sub>deck</sub> (ksi)	Bottom		
3754	0980015	53'-7¼"	7.0	1 @ 6'-6", 7 @ 6' 2 9/16", 2 @ 6'-0"	1'-6"	11	151.7	30 (or 28) -0.4375" Gr. 248 SR	5.0	4.0	3.5	1.75	na	33x36 IDOT Beam
						<p>Strand Spacing: Horizontal: 1.375", 3" Vertical: 1.5", 2.75", 3"</p> <p>All girders except far left and two far right: # of Strands: 30 CG from bottom at Midspan: 4.50"</p> <p>Far left and two far right girders: # of Strands: 28 CG from bottom at Midspan: 4.95"</p> 								
Strand Layout at Midspan			Cross-Section											

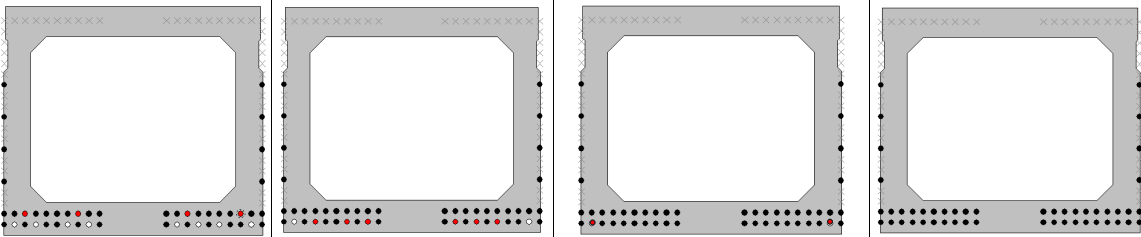
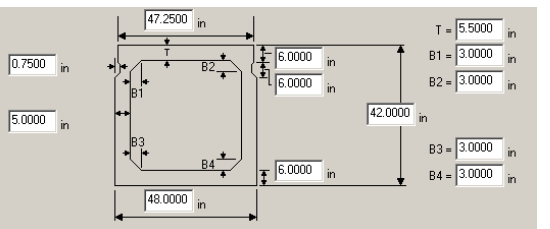
Bridge 8875

Bridge #	Virtis BID #	Span Length (ft)	t <sub>slab</sub> (in.)	Girder Spacing (ft)	Overhang Width (ft)	# of Girders	Skew (deg)	Materials			Dist. to Extreme Strands (in.)		Harp Point (ft)	Beam Section
								P/S Tendons	f <sub>c</sub> ' (ksi)	f <sub>c</sub> ' <sub>l</sub> (ksi)	f <sub>c</sub> ' <sub>deck</sub> (ksi)	Bottom		
8875	A8029	38'-0"	8.5	11'-3"	3'-1½"	12	96.4	23-0.5" Gr. 270 LR	8.0	5.0	4.0	1.75	na	27x48 Box Beam
						<p>Strand Spacing: Horizontal: 2.75" Vertical: 1.5", 2.75", 3"</p> <p># of Strands: 23 CG from bottom at Midspan: 2.34"</p> 								
Strand Layout at Midspan			Cross-Section			Cross-Section								

Bridge 12870

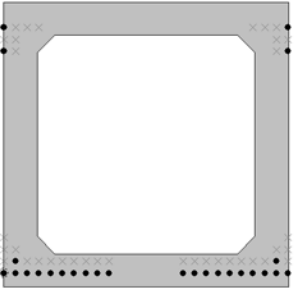
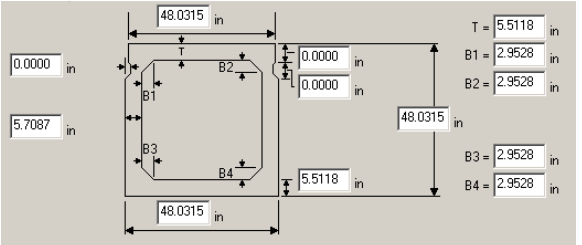
Bridge #	Virtis BID #	Span Length (ft)	t <sub>slab</sub> (in.)	Girder Spacing (ft)	Overhang Width (ft)	# of Girders	Skew (deg)	Materials			Dist. to Extreme Strands (in.)		Harp Point (ft)	Beam Section
								P/S Tendons	f' <sub>c</sub> (ksi)	f' <sub>c1</sub> (ksi)	f' <sub>c,deck</sub> (ksi)	Bottom		
12870	2219470	77'-6"	8.5	6'-6"	2'-0"	5	105.0	30-0.5" Gr. 270 SR	6.0	4.8	3.0	2.0	na	36x48 Box Beam
									<p>Strand Spacing: Horizontal: 1" Vertical: 2"</p> <p># of Strands: 30 CG from bottom at 120.0": 4.20" CG from bottom at 144.0": 3.85" CG from bottom at Midspan: 4.00"</p> 					
			@ 120.0" from left support	@ 144.0" from left support	Strand Layout at Midspan			Cross-Section						

Bridge 14969


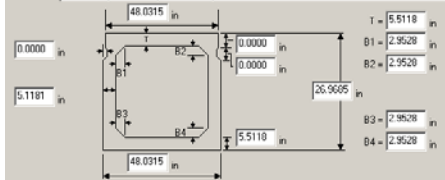
Bridge #	Virtis BID #	Span Length (ft)	t <sub>slab</sub> (in.)	Girder Spacing (ft)	Overhang Width (ft)	# of Girders	Skew (deg)	Materials			Dist. to Extreme Strands (in.)		Harp Point (ft)	Beam Section
								P/S Tendons	f' <sub>c</sub> (ksi)	f' <sub>c1</sub> (ksi)	f' <sub>c,deck</sub> (ksi)	Bottom		
14969	1023430	78'-8 $\frac{1}{2}$ "	9.4375	7'-10 $\frac{1}{4}$ "	4'-5 5/16" (L), 4'-11 3/16" (R)	7	90.0	48-0.5" Gr. 270 LR	6.5	4.5	3.0	1.9685	na	AASHTO BIV-48
									<p>Strand Spacing: Horizontal: 1.9685" Vertical: 1.9685"</p> <p># of Strands: 48 CG from bottom at 98.4" from LS: 6.69" CG from bottom at 141.75" from LS: 6.30" CG from bottom at 216.5" from LS: 5.73" CG from bottom at Midspan: 5.58"</p> 					
			@ 98.4" from left support	@ 141.75" from left support	@ 216.5" from left support	Strand Layout at Midspan			Cross-Section					



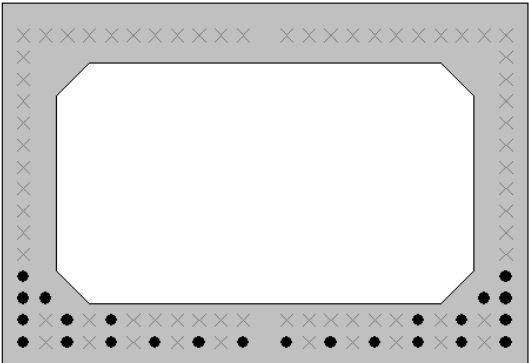
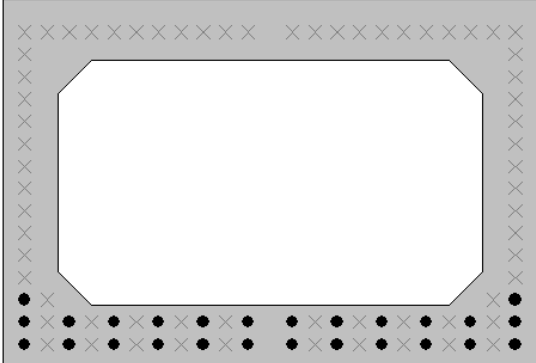
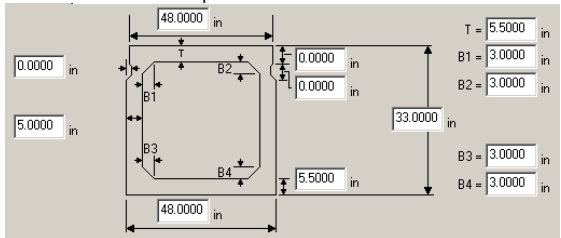
Bridge 16293

Bridge #	Virtis BID #	Span Length (ft)	t <sub>slab</sub> (in.)	Girder Spacing (ft)	Overhang Width (ft)	# of Girders	Skew (deg)	Materials				Dist. to Extreme Strands (in.)		Harp Point (ft)	Beam Section
								P/S Tendons	f <sub>c</sub> ' (ksi)	f <sub>c</sub> l (ksi)	f <sub>c</sub> deck (ksi)	Bottom	Top		
16293	BID_2751	57'-3¼"	9.4375	8'-10 5/16"	4'-1 5/8"	7	96.0	26-0.6" Gr. 270 LR	10.2	7.1	3.0	2.2441	4.252	na	1220x1220 Box Beam
								Strand Spacing: Horizontal: 1.9685" Vertical: 2"  # of Strands: 26 CG from bottom at Midspan: 8.48"							
Strand Layout at Midspan				Cross-Section				Cross-Section							

Bridge 16366

Bridge #	Virtis BID #	Span Length (ft)	t <sub>slab</sub> (in.)	Girder Spacing (ft)	Overhang Width (ft)	# of Girders	Skew (deg)	Materials				Dist. to Extreme Strands (in.)		Harp Point (ft)	Beam Section
								P/S Tendons	f <sub>c</sub> ' (ksi)	f <sub>c</sub> l (ksi)	f <sub>c</sub> deck (ksi)	Bottom	Top		
16366	2223270	60'-4 5/8"	9.4375	6'-7"	4'-0 1/16"	6	102.4	38-0.5" Gr. 270 LR	7.5	6.0	3.0	1.9685		na	Based on AASHTO BI-48
								Strand Spacing: Horizontal: 1.9685" Vertical: 1.9685", 3.937", 1.9685", 5.9055", 1.9685"  # of Strands: 38 CG from bottom at Midspan: 5.39"							
Strand Layout at Midspan				Cross-Section				Cross-Section							

Bridge 17240

Bridge #	Virtis BID #	Span Length (ft)	t <sub>elab</sub> (in.)	Girder Spacing (ft)	Overhang Width (ft)	# of Girders	Skew (deg)	Materials			Dist. to Extreme Strands (in.)		Harp Point (ft)	Beam Section
								P/S Tendons	f <sub>c</sub> ' (ksi)	f <sub>c1</sub> ' (ksi)	f <sub>c,deck</sub> ' (ksi)	Bottom		
17240	3300870	51'-6"	8.5	8'-0"	4'-0"	4	90.0	24 (or 26)-0.5" Gr. 270 SR	6.0	4.8	3.0	2.0	na	AASHTO BII-48
									<p>Strand Spacing: Horizontal: 2.0" Vertical: 2.0"</p> <p>Interior: # of Strands: 24 CG from bottom at Midspan: 3.67"</p> <p>Exterior: # of Strands: 26 CG from bottom at Midspan: 3.23"</p> 					
			Strand Layout at Midspan – Interior Girder			Strand Layout at Midspan – Exterior Girder			Cross-Section					

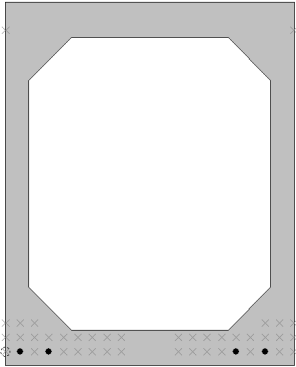
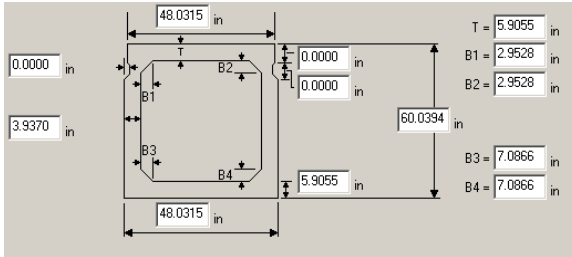
Bridge 9090

Bridge #	Virtis BID #	Span Length (ft)	t <sub>slab</sub> (in.)	Girder Spacing (ft)	Overhang Width (ft)	# of Girders	Skew (deg)	Materials			Dist. to Extreme Strands (in.)		Harp Point (ft)	Beam Section
								P/S Tendons	f <sub>c</sub> <sup>+</sup> (ksi)	f <sub>c1</sub> <sup>+</sup> (ksi)	f <sub>c,deck</sub> <sup>+</sup> (ksi)	Bottom		
9090	13113081000S053	66'-0½"	9.0	7'-1"	3'-5"	9	68.6	20-0.6" Gr. 270 LR	5.3	5.3				MDOT 33" Box Beam (Int)
									5.6	5.6	4.0	2.0	na	MDOT 33" Box Beam (Ext)
								<p>Strand Spacing: Horizontal: 2" Vertical: 2"</p> <p># of Strands: 20</p> <p>Interior: CG from bottom at 60.0" from LS: 3.14" CG from bottom at 84.0" from LS: 3.25" CG from bottom at 174.0" from LS: 3.11" CG from bottom at Midspan: 3.00"</p> <p>Exterior: CG from bottom at 54.0" from LS: 3.14" CG from bottom at 78.0" from LS: 3.25" CG from bottom at 114.0" from LS: 3.11" CG from bottom at Midspan: 3.00"</p>						
@ 60.0" from left support		@ 84.0" from left support		@ 174.0" from left support		Strand Layout at Midspan		Cross-Section						

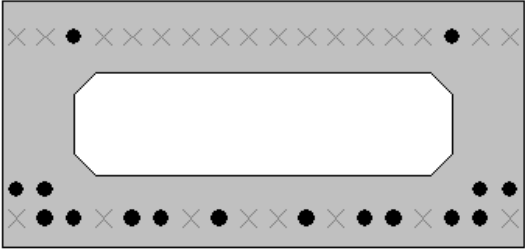
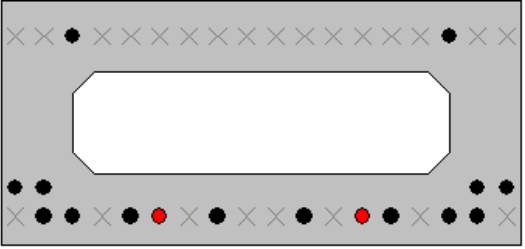
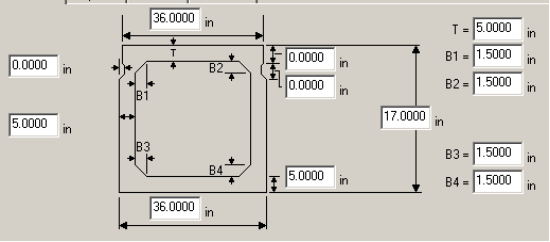
Bridge 9091

Bridge #	Virtis BID #	Span Length (ft)	t <sub>slab</sub> (in.)	Girder Spacing (ft)	Overhang Width (ft)	# of Girders	Skew (deg)	Materials			Dist. to Extreme Strands (in.)		Harp Point (ft)	Beam Section
								P/S Tendons	f <sub>c</sub> <sup>i</sup> (ksi)	f <sub>c1</sub> <sup>i</sup> (ksi)	f <sub>c</sub> <sup>d</sup> (ksi)	Bottom		
9091	13113081000S054	66'-2½"	9.0	7'-1"	3'-5"	9	68.3	20-0.6" Gr. 270 LR	5.3	5.3	4.0	2.0	na	MDOT 33" Box Beam (Int.) MDOT 33" Box Beam (Ext.)
											Strand Spacing: Horizontal: 2" Vertical: 2"  # of Strands: 20  Interior: CG from bottom at 60.0" from LS: 3.14" CG from bottom at 84.0" from LS: 3.25" CG from bottom at 174.0" from LS: 3.11" CG from bottom at Midspan: 3.00"  Exterior: CG from bottom at 54.0" from LS: 3.14" CG from bottom at 78.0" from LS: 3.25" CG from bottom at 132.0" from LS: 3.11" CG from bottom at Midspan: 3.00"			
		@ 60.0" from left support		@ 84.0" from left support		@ 174.0" from left support		Strand Layout at Midspan		Cross-Section				


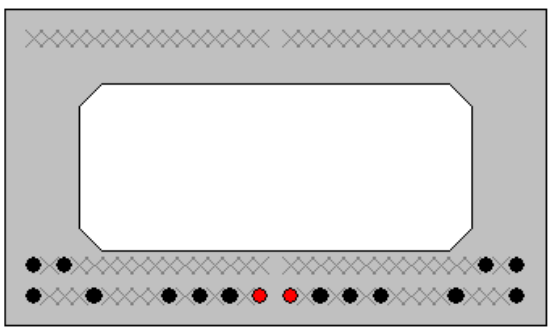
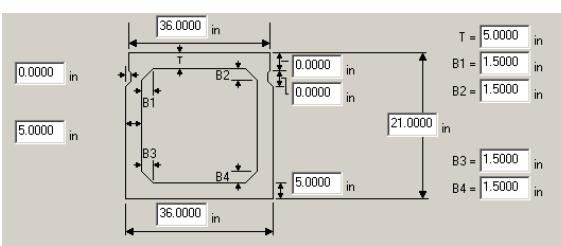
Bridge 9128

Bridge #	Virtis BID #	Span Length (ft)	t <sub>slab</sub> (in.)	Girder Spacing (ft)	Overhang Width (ft)	# of Girders	Skew (deg)	Materials			Dist. to Extreme Strands (in.)		Harp Point (ft)	Beam Section	
								P/S Tendons	f' <sub>c</sub> (ksi)	f' <sub>c1</sub> (ksi)	f' <sub>c deck</sub> (ksi)	Bottom			Top
9128	29129011000S140	33'-8 <sup>3</sup> / <sub>8</sub> "	9.0625	7'-5 <sup>1</sup> / <sub>8</sub> "	3'-1 <sup>1</sup> / <sub>4</sub> "	8	90.0	4-0.6" Gr. 270 LR	6.0	4.5	4.0	2.28	na	1525 Box Beam	
								<p>Strand Spacing: Horizontal: 2.402" Vertical: 2.402"</p> <p># of Strands: 4 CG from bottom at Midspan: 2.28"</p>							
<b>Strand Layout at Midspan</b>				<b>Cross-Section</b>				<b>Cross-Section</b>							

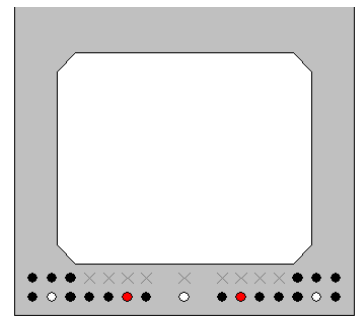
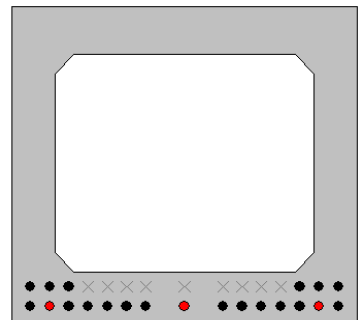
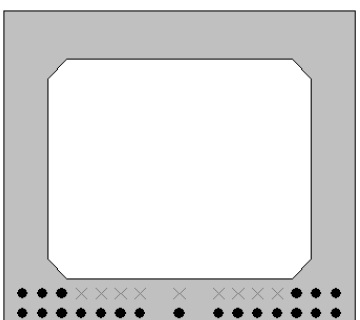
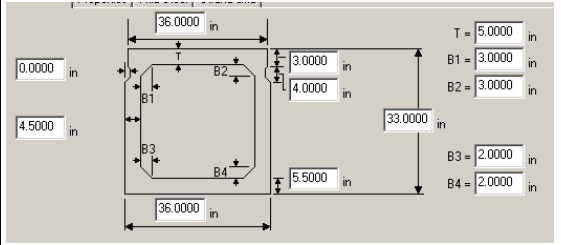
Bridge 9217

Bridge #	Virtis BID #	Span Length (ft)	t <sub>slab</sub> (in.)	Girder Spacing (ft)	Overhang Width (ft)	# of Girders	Skew (deg)	Materials			Dist. to Extreme Strands (in.)		Harp Point (ft)	Beam Section				
								P/S Tendons	f <sub>c</sub> <sup>i</sup> (ksi)	f <sub>c1</sub> <sup>i</sup> (ksi)	f <sub>c deck</sub> <sup>i</sup> (ksi)	Bottom			Top			
9217	45145071000B010	42'-3½"	9.25	3@6'-2 ½", 7@5'-8 ⅝"	3'-3"	11	90.0	16-0.6" Gr. 270 LR	5.8	5.3	4.0	2.0	2.5	na	17" Box Beam (A)			
									5.6	5.2					17" Box Beam (B and C)			
									5.2	5.1					17" Box Beam (D)			
									5.0	4.9					17" Box Beam (E thru K)			
									5.9	5.3					17" Box Beam (L)			
											<p>Strand Spacing: Horizontal: 2" Vertical: 2"</p> <p>Beams: (A) is far left girder, (L) is far right girder</p> <p># of Strands: 16 Girders: A and L CG from bottom at Midspan: 4.06"</p> <p>Girders: B, C, D CG from bottom at Support to 54": 4.36" CG from bottom at Midspan: 4.06"</p> <p>Girders: E thru K CG from bottom at Support to 96": 4.36" CG from bottom at Midspan: 4.06"</p>							
																		
Strand Layout at Midspan (All girders)											Strand Layout at Support to 96" (E thru K), 54" (B thru D)				Cross-Section			

Bridge 9219

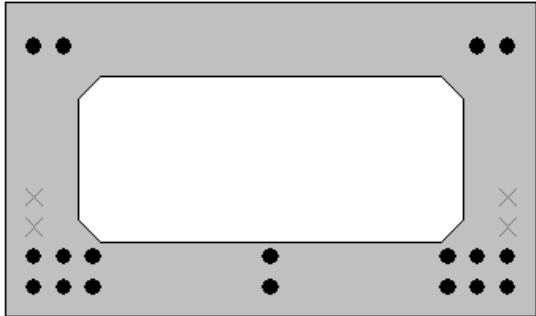
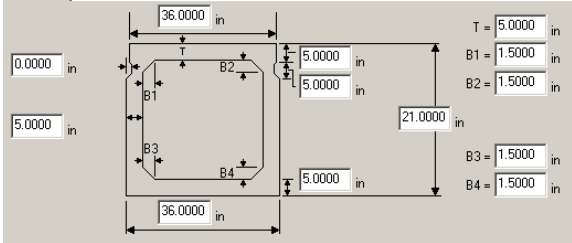
Bridge #	Virtis BID #	Span Length (ft)	t <sub>slab</sub> (in.)	Girder Spacing (ft)	Overhang Width (ft)	# of Girders	Skew (deg)	Materials				Dist. to Extreme Strands (in.)		Harp Point (ft)	Beam Section	
								P/S Tendons	f' <sub>c</sub> (ksi)	f' <sub>c1</sub> (ksi)	f' <sub>c deck</sub> (ksi)	Bottom	Top			
9219	16116032000B030	53'-2"	9.0	5'-3"	2'-7½"	9	90.0	16-0.6" Gr. 270 LR	5.7	5.6	4.0	2.0		na	MDOT 21" Box Beam	
								<p>Strand Spacing: Horizontal: 1" Vertical: 2"</p> <p># of Strands: 16 CG from bottom at Support to 72": 2.57" CG from bottom at Midspan: 2.50"</p> 								
		Strand Layout at Midspan			Strand Layout at Support to 72"			Cross-Section								

Bridge 9243

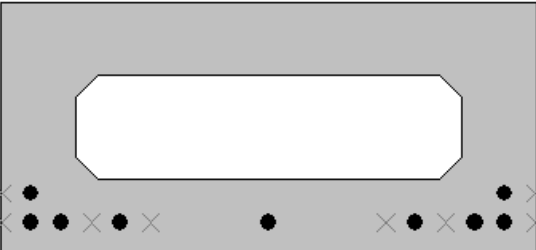
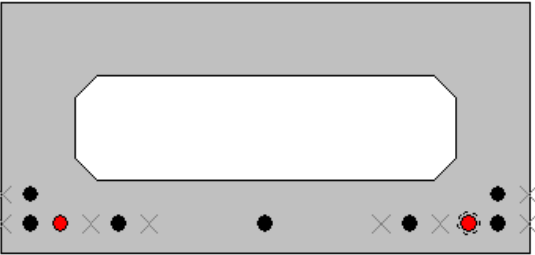
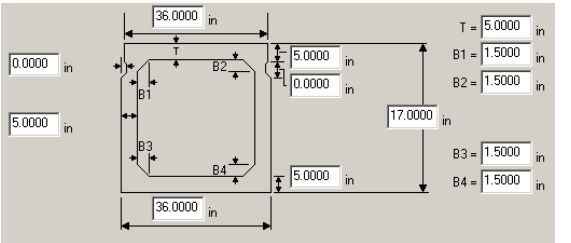
Bridge #	Virtis BID #	Span Length (ft)	t <sub>slab</sub> (in.)	Girder Spacing (ft)	Overhang Width (ft)	# of Girders	Skew (deg)	Materials				Dist. to Extreme Strands (in.)		Harp Point (ft)	Beam Section	
								P/S Tendons	f' <sub>c</sub> (ksi)	f' <sub>c1</sub> (ksi)	f' <sub>c deck</sub> (ksi)	Bottom	Top			
9243	82182041000S020	73'-4"	9.0	6'-2"	2'-3¾"	13	90.0	21-0.6" Gr. 270 LR	7.0	6.0	4.0	2.0		na	33"x36" Box Beam	
											<p>Strand Spacing: Horizontal: 2" Vertical: 2"</p> <p># of Strands: 21 CG from bottom at 24.0": 2.75" CG from bottom at 48.0": 2.67" CG from bottom at Midspan: 2.57"</p> 					
		@ 24.0" from left support			@ 48.0" from left support			Strand Layout at Midspan			Cross-Section					



Bridge 9248

Bridge #	Virtis BID #	Span Length (ft)	t <sub>slab</sub> (in.)	Girder Spacing (ft)	Overhang Width (ft)	# of Girders	Skew (deg)	Materials			Dist. to Extreme Strands (in.)		Harp Point (ft)	Beam Section	
								P/S Tendons	f <sub>c</sub> ' (ksi)	f <sub>c</sub> l' (ksi)	f <sub>c</sub> 'deck (ksi)	Bottom			Top
9248	02102041000B020	37'-9"	9.0	8'-0"	3'-2½"	6	90.0	18-0.6" Gr. 270 LR	6.0	5.0	4.0	2.0	3.0	na	21" Box Beam
				<p>Strand Spacing: Horizontal: 2.0", Vertical: 2.0", 10.0"</p> <p># of Strands: 18 CG from bottom at Midspan: 6.33"</p>											
Strand Layout at Midspan				Cross-Section				Cross-Section							

Bridge 9284

Bridge #	Virtis BID #	Span Length (ft)	t <sub>slab</sub> (in.)	Girder Spacing (ft)	Overhang Width (ft)	# of Girders	Skew (deg)	Materials			Dist. to Extreme Strands (in.)		Harp Point (ft)	Beam Section	
								P/S Tendons	f <sub>c</sub> ' (ksi)	f <sub>c</sub> l' (ksi)	f <sub>c</sub> 'deck (ksi)	Bottom			Top
9284	33133082000B030	31'-6¾"	9.0625	6'-7⅞"	2'-5½"	10	90.0	9-0.6" Gr. 270 LR	5.0	3.0	4.0	2.0		na	17"x36" Box Beam
								<p>Strand Spacing: Horizontal: 2" Vertical: 2"</p> <p># of Strands: 9 CG from bottom at Support to 78.74": 2.57" CG from bottom at Midspan: 2.44"</p>							
Strand Layout at Midspan				Strand Layout at Support to 78.74"				Cross-Section							

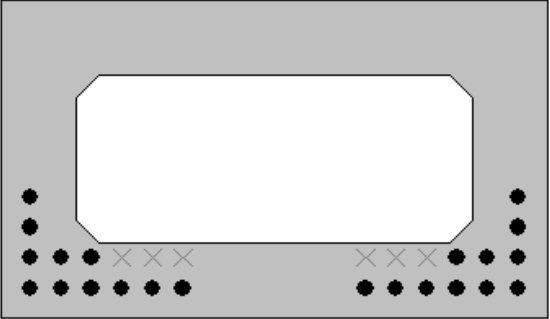
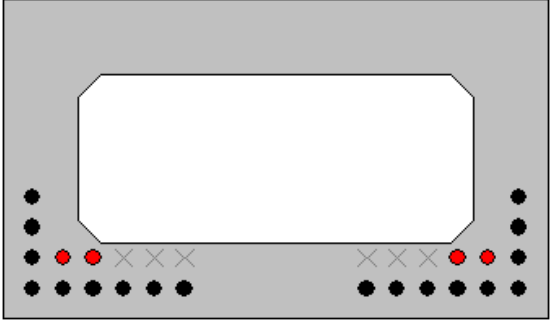
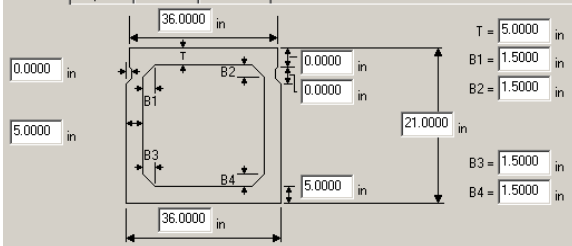
Bridge 9289

Bridge #	Virtis BID #	Span Length (ft)	t <sub>slab</sub> (in.)	Girder Spacing (ft)	Overhang Width (ft)	# of Girders	Skew (deg)	Materials			Dist. to Extreme Strands (in.)		Harp Point (ft)	Beam Section	
								P/S Tendons	f' <sub>c</sub> (ksi)	f' <sub>c1</sub> (ksi)	f' <sub>c,deck</sub> (ksi)	Bottom			Top
9289	45145012000B010	63'-7 $\frac{1}{2}$ "	9.0625	6'-4"	3'-1 3/16"	7	45.0	22-0.6" Gr. 270 LR	5.0	4.0	4.0	2.0	3.0	na	27"x36" Box Beam
												Strand Spacing: Horizontal: 2" Vertical: 2"  # of Strands: 22 CG from bottom at 62.99": 2.33" CG from bottom at 86.61": 2.29" CG from bottom at 141.73": 2.50" CG from bottom at 173.91": 3.11" CG from bottom at Midspan: 6.90"			
												@ 62.99" from left support    @ 86.61" from left support    @ 141.73" from left support    @ 173.91" from left support    Strand Layout at Midspan			
												<b>Cross-Section</b>			

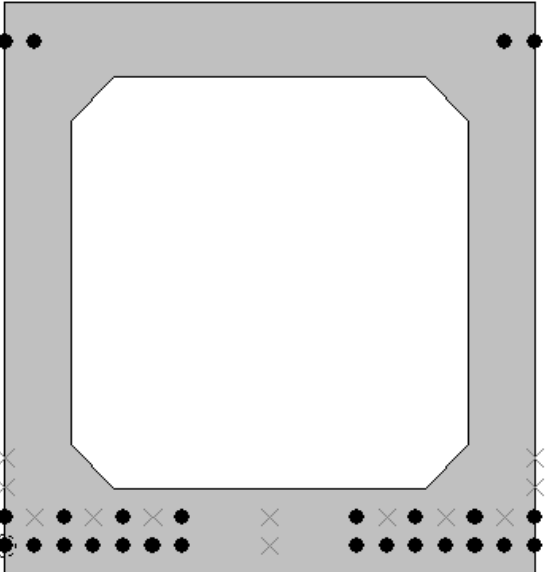
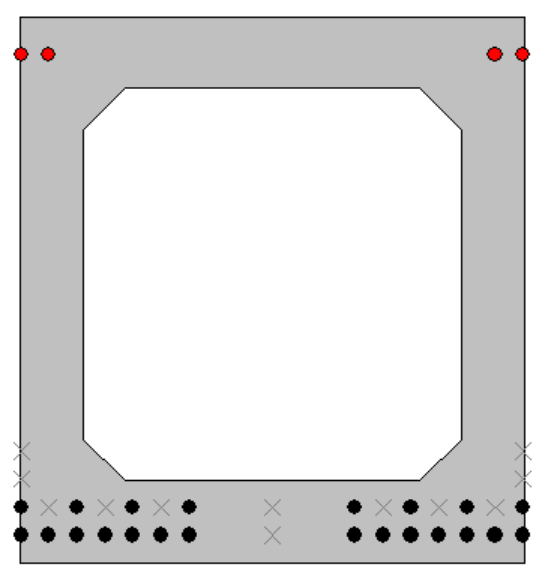
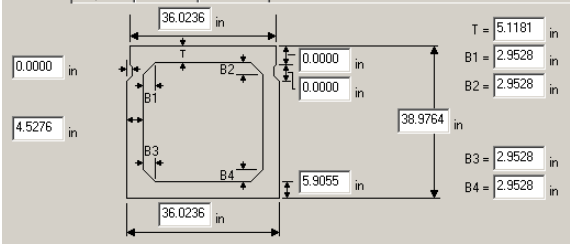
Bridge 9324

Bridge #	Virtis BID #	Span Length (ft)	t <sub>slab</sub> (in.)	Girder Spacing (ft)	Overhang Width (ft)	# of Girders	Skew (deg)	Materials			Dist. to Extreme Strands (in.)		Harp Point (ft)	Beam Section
								P/S Tendons	f' <sub>c</sub> (ksi)	f' <sub>c1</sub> (ksi)	f' <sub>c,deck</sub> (ksi)	Bottom		
9324	14114041000B010	42'-4"	9.0	10'-6"	2'-7 $\frac{1}{2}$ "	5	90.0	20-0.5" Gr. 270 LR	5.5	4.4	4.0	2.0	na	27"x36" Box Beam
												Strand Spacing: Horizontal: 2" Vertical: 2"  # of Strands: 20 CG from bottom at Support to 66.0": 3.50" CG from bottom at Midspan: 3.40"		
												Strand Layout at Midspan    Strand Layout at Support to 66.0"		
												<b>Cross-Section</b>		

Bridge 9349

Bridge #	Virtis BID #	Span Length (ft)	t <sub>slab</sub> (in.)	Girder Spacing (ft)	Overhang Width (ft)	# of Girders	Skew (deg)	Materials			Dist. to Extreme Strands (in.)		Harp Point (ft)	Beam Section
								P/S Tendons	f' <sub>c</sub> (ksi)	f' <sub>c1</sub> (ksi)	f' <sub>c deck</sub> (ksi)	Bottom		
9349	72172041000B010	48'-8"	9.0	7'-0"	3'-6"	6	90.0	22-0.5" Gr. 270 LR	6.0	4.9	4.0	2.0	na	21"x36" Box Beam
 <p>Strand Layout at Midspan</p>					 <p>Strand Layout at Support to 66.0"</p>					<p>Strand Spacing: Horizontal: 2" Vertical: 2"</p> <p># of Strands: 22 CG from bottom at Support to 66.0": 3.33" CG from bottom at Midspan: 3.45"</p>  <p>Cross-Section</p>				

Bridge 9355

Bridge #	Virtis BID #	Span Length (ft)	t <sub>slab</sub> (in.)	Girder Spacing (ft)	Overhang Width (ft)	# of Girders	Skew (deg)	Materials			Dist. to Extreme Strands (in.)		Harp Point (ft)	Beam Section	
								P/S Tendons	f' <sub>c</sub> (ksi)	f' <sub>c1</sub> (ksi)	f' <sub>c deck</sub> (ksi)	Bottom			Top
9355	38138111000R021	75'-2 1/2"	9.0625	7'-11"	3'-6"	6	109.6	26-0.6" Gr. 270 LR	7.0	6.2	4.0	2.0	2.75	na	39"x36" Box Beam
 <p>Strand Layout at Midspan</p>					 <p>Strand Layout at Support to 225.60"</p>					<p>Strand Spacing: Horizontal: 2" Vertical: 2"</p> <p># of Strands: 26 CG from bottom at Support to 225.60": 2.73" CG from bottom at Midspan: 7.88"</p>  <p>Cross-Section</p>					

Bridge 9356

Bridge #	Virtis BID #	Span Length (ft)	t <sub>slab</sub> (in.)	Girder Spacing (ft)	Overhang Width (ft)	# of Girders	Skew (deg)	Materials				Dist. to Extreme Strands (in.)		Harp Point (ft)	Beam Section
								P/S Tendons	f <sub>c</sub> ' (ksi)	f <sub>c</sub> ' <sub>i</sub> (ksi)	f <sub>c</sub> ' <sub>deck</sub> (ksi)	Bottom	Top		
9356	38138111000R022	75'-2 3/4"	9.062	7'-11"	3'-6"	6	109.6	26-0.6" Gr. 270 LR	7.0	6.2	4.0	2.0	2.75	na	39"x36" Box Beam

		<p>Strand Spacing: Horizontal: 2" Vertical: 2"</p> <p># of Strands: 26 CG from bottom at Support to 213.04": 2.73" CG from bottom at Midspan: 7.88"</p>
Strand Layout at Midspan	Strand Layout at Support to 213.04"	Cross-Section

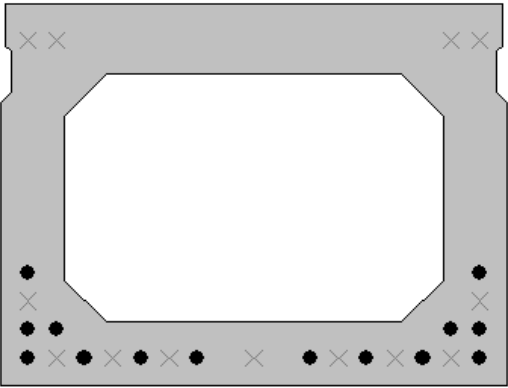
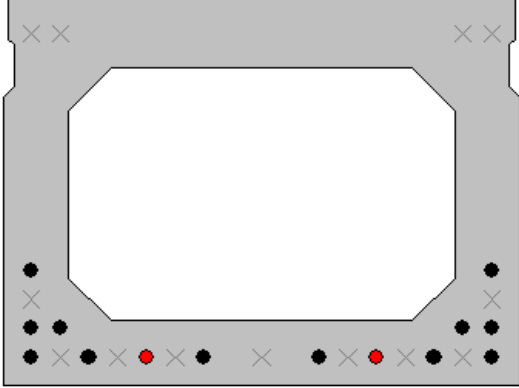
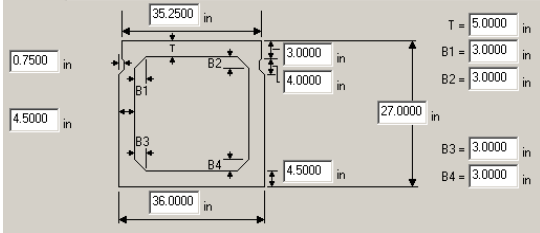
Bridge 9361

Bridge #	Virtis BID #	Span Length (ft)	t <sub>slab</sub> (in.)	Girder Spacing (ft)	Overhang Width (ft)	# of Girders	Skew (deg)	Materials			Dist. to Extreme Strands (in.)		Harp Point (ft)	Beam Section
								P/S Tendons	f <sub>c</sub> ' (ksi)	f <sub>c1</sub> ' (ksi)	f <sub>c</sub> ' deck (ksi)	Bottom		
9361	47147065000R033	65'-9½"	9.0	6'-0"	2'-7½"	11	137.2	30-0.5" Gr. 270 LR	6.5	5.5	4.0	2.0	na	27"x36" Box Beam
								Strand Spacing: Horizontal: 2" Vertical: 2"  # of Strands: 30 CG from bottom at 18.0" from LS: 3.82" CG from bottom at 79.2" from LS: 3.54" CG from bottom at 150.0" from LS: 3.43" CG from bottom at Midspan: 3.47"						
								@ 18.0" from left support    @ 79.2" from left support    @ 150.0" from left support    Strand Layout at Midspan			Cross-Section			

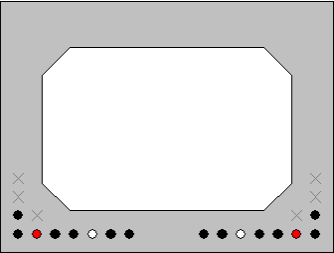
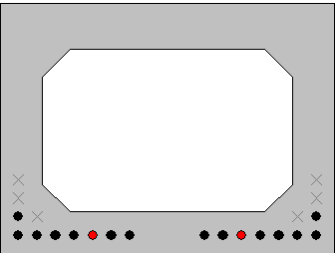
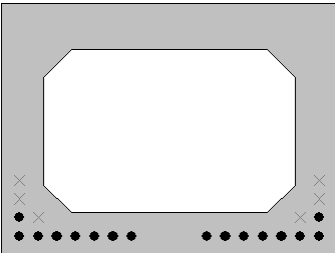
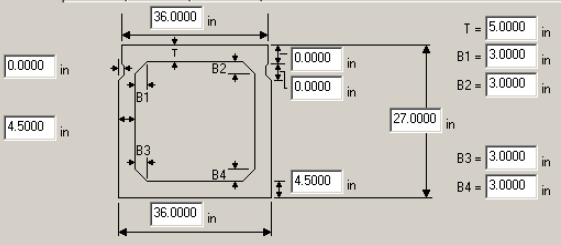
Bridge 9369

Bridge #	Virtis BID #	Span Length (ft)	t <sub>slab</sub> (in.)	Girder Spacing (ft)	Overhang Width (ft)	# of Girders	Skew (deg)	Materials			Dist. to Extreme Strands (in.)		Harp Point (ft)	Beam Section
								P/S Tendons	f <sub>c</sub> ' (ksi)	f <sub>c1</sub> ' (ksi)	f <sub>c</sub> ' deck (ksi)	Bottom		
9369	11111015000R033	51'-3¾"	9.0	6'-6"	3'-4½"	10	115.7	14-0.6" Gr. 270 LR	5.4	4.5	4.0	2.0	na	27"x36" Box Beam
								Strand Spacing: Horizontal: 2" Vertical: 2"  # of Strands: 14 CG from bottom at Support to 48.0": 3.67" CG from bottom at Midspan: 3.43"						
								Strand Layout at Midspan    Strand Layout at Support to 48.0"			Cross-Section			


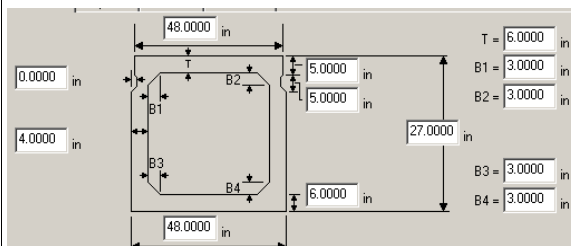
Bridge 9370

Bridge #	Virtis BID #	Span Length (ft)	t <sub>slab</sub> (in.)	Girder Spacing (ft)	Overhang Width (ft)	# of Girders	Skew (deg)	Materials				Dist. to Extreme Strands (in.)		Harp Point (ft)	Beam Section
								P/S Tendons	f <sub>c</sub> ' (ksi)	f <sub>c1</sub> ' (ksi)	f <sub>c deck</sub> ' (ksi)	Bottom	Top		
9370	11111015000R034	51'-3 <sup>7</sup> / <sub>8</sub> "	9.0	6'-5"	3'-4"	12	115.7	14-0.6" Gr. 270 LR	5.2	4.4	4.0	2.0		na	27"x36" Box Beam
								<p>Strand Spacing: Horizontal: 2" Vertical: 2"</p> <p># of Strands: 14 CG from bottom at Support to 54.0": 3.67" CG from bottom at Midspan: 3.43"</p> 							
				Strand Layout at Midspan				Strand Layout at Support to 54.0"				Cross-Section			

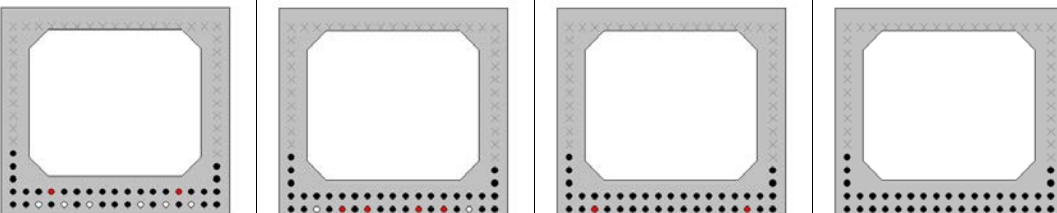
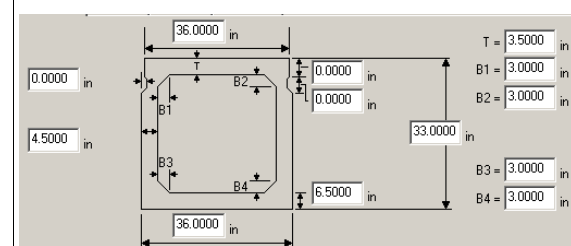
Bridge 9383

Bridge #	Virtis BID #	Span Length (ft)	t <sub>slab</sub> (in.)	Girder Spacing (ft)	Overhang Width (ft)	# of Girders	Skew (deg)	Materials				Dist. to Extreme Strands (in.)		Harp Point (ft)	Beam Section
								P/S Tendons	f <sub>c</sub> ' (ksi)	f <sub>c1</sub> ' (ksi)	f <sub>c deck</sub> ' (ksi)	Bottom	Top		
9383	71171073000B010	46'-9 <sup>3</sup> / <sub>4</sub> "	9.0	10'-7"	2'-6"	5	45.0	16-0.6" Gr. 270 LR	6.0	5.0	4.0	2.0		na	27"x36" Box Beam
										<p>Strand Spacing: Horizontal: 2" Vertical: 2"</p> <p># of Strands: 16 CG from bottom at 24.0": 2.33" CG from bottom at 72.0": 2.29" CG from bottom at Midspan: 2.25"</p> 					
				@ 24.0" from left support		@ 72.0" from left support		Strand Layout at Midspan		Cross-Section					

Bridge 9394

Bridge #	Virtis BID #	Span Length (ft)	t <sub>slab</sub> (in.)	Girder Spacing (ft)	Overhang Width (ft)	# of Girders	Skew (deg)	Materials			Dist. to Extreme Strands (in.)		Harp Point (ft)	Beam Section
								P/S Tendons	f <sub>c</sub> ' (ksi)	f <sub>c1</sub> ' (ksi)	f <sub>c</sub> ' <sub>deck</sub> (ksi)	Bottom		
9394	25125031000S010	66'-10 <sup>5</sup> / <sub>8</sub> "	9.0	7'-6"	4'-1 <sup>1</sup> / <sub>2</sub> "	11	59.8	34-0.5" Gr. 270 LR	6.0	5.0	4.0	2	na	27"x48" Box Beam
							<p>Strand Spacing: Horizontal: 2" Vertical: 2"</p> <p># of Strands: 34 CG from bottom at 54.0": 2.75" CG from bottom at 96.0": 3.00" CG from bottom at Midspan: 3.12"</p>							
			@ 54.0" from left support	@ 96.0" from left support	Strand Layout at Midspan			Cross-Section						

Bridge 1150

Bridge #	Virtis BID #	Span Length (ft)	t <sub>slab</sub> (in.)	Girder Spacing (ft)	Overhang Width (ft)	# of Girders	Skew (deg)	Materials			Dist. to Extreme Strands (in.)		Harp Point (ft)	Beam Section	
								P/S Tendons	f <sub>c</sub> ' (ksi)	f <sub>c1</sub> ' (ksi)	f <sub>c</sub> ' <sub>deck</sub> (ksi)	Bottom			Top
1150	550A0490001	70'-7"	8.25	8'-6"	3'-8"	3	118.0	39-0.5" Gr. 270 LR	6.5	6.0	3.0	2.0	na	33"x36" Box Beam	
							<p>Strand Spacing: Horizontal: 2" Vertical: 2"</p> <p># of Strands: 39 CG from bottom at 36.0" from LS: 3.87" CG from bottom at 72.0" from LS: 3.88" CG from bottom at 108.0" from LS: 3.68" CG from bottom at Midspan: 3.59"</p>								
			@ 36.0" from left support	@ 72.0" from left support	@ 108.0" from left support	Strand Layout at Midspan			Cross-Section						



## F.6 Steel Girder Database

This section includes descriptions of the steel bridges selected from the NCHRP Project 12-78 database and used for various studies reported here (Mlynarski et al. 2011). Other bridges could be substituted.

Bridge #	Span Length (ft)	$f_{slab}$ (in.)	Girder Spacing (ft)	# of Girders	Overhang Width (ft)	Skew (deg)	Materials			Cross-Frame Spacing (ft)	Girder Description
							$f_{yw}$ (ksi)	$f_{yr}$ (ksi)	$f'_{c \text{ deck}}$ (ksi)		
0032	31.00	6.75	7.21	6	1.06	125.0	33	33	3.0	<i>Fascia</i> 1 @ 19.00 1 @ 12.00 <i>Interior</i> 1 @ 13.95 1 @ 5.05 1 @ 12.00	<u>Rolled Beam</u> W27X91
0053	38.00	5.50	4.75	8	0.63	90.0	30	30	2.5	None	<u>Rolled Beam</u> <i>Fascia</i> B28, 28X10X85 <i>Interior</i> CB213, 21X13X112
0058	25.80	11.00	1 @ 8.25 4 @ 8.00 1 @ 8.25 1 @ 2.68 1 @ 7.71	9	0.56 at G1 0.58 at G9	60.0	33	33	3.3	None	<u>Rolled Beam</u> W21X83
0075	32.00	10.00	3.91	11	0.03	66.0	30	30	2.5	None	<u>Rolled Beam</u> S20X75F
0076	40.09	7.00	6.00	4	1.67	115.0	30	30	2.5	<i>G1</i> 1 @ 16.69 1 @ 16.00 1 @ 7.40 <i>G2</i> 1 @ 13.90 1 @ 16.00 1 @ 10.19	<u>Rolled Beam</u> <i>G1</i> 24WF74 <i>G2</i> 24WF80
0078	51.92	8.00	4.13	7	0.83 at G1 1.08 at G7	80.0	33	33	2.5	None	<u>Rolled Beam</u> CB30X180
0146	34.67	7.25	8.75	7	2.08	102.0	33	33	3.3	2 @ 17.33	<u>Rolled Beam</u> 33WF(B33), 33X11.5X130

(continued on next page)

(continued)

Bridge #	Span Length (ft)	t <sub>slab</sub> (in.)	Girder Spacing (ft)	# of Girders	Overhang Width (ft)	Skew (deg)	Materials			Cross-Frame Spacing (ft)	Girder Description
							f <sub>yw</sub> (ksi)	f <sub>yr</sub> (ksi)	f' <sub>c deck</sub> (ksi)		
0151	39.79	7.00	6	4	3.33	130.0	36	36	4.0	G1 1 @ 22.41 1 @ 17.38 G2 1 @ 17.38 1 @ 5.03 1 @ 17.38	<u>Rolled Beam</u> G1 W24X68 G2 W24X76
0179	47.50	9.50	9.75	5	1.27	75.0	36	36	3.0	G1 1 @ 23.50 1 @ 24.00 G2 1 @ 23.50 1 @ 2.61 1 @ 21.39	<u>Rolled Beam</u> 0 ft. to 6.89 ft. W30X99 W30X99 6.89 ft. to 8 1/2X9/16 Bott 23.75 ft. Cover PI (Symm.)
0199	43.50	5.88	1 @ 1.60 10 @ 2.00 1 @ 1.60	13	0.37	90.0	36	36	3.0	2 @ 21.75	<u>Rolled Beam</u> W24X94
0208	48.75	8.50	5.00	7	2.00 at G1 1.25 at G7	90.0	30	30	3.3	2 @ 24.38	<u>Rolled Beam</u> W28X145
0224	38.60	1.31	1 @ 1.58 10 @ 2.00 1 @ 1.58	13	0.34	90.0	36	36	2.4	2 @ 19.30	<u>Rolled Beam</u> W21X63
0256	79.45	6.50	8.00	4	4.00	45.0	33	33	3.0	G1 1 @ 9.87 2 @ 19.75 1 @ 13.17 1 @ 16.91 G2 1 @ 16.46 2 @ 19.75 1 @ 13.17 1 @ 10.32 G3 1 @ 9.87 1 @ 13.17 2 @ 19.75 1 @ 16.91 G4 1 @ 16.46 1 @ 13.17 2 @ 19.75 1 @ 10.32	<u>Built-up I-Shape</u> 0 ft. to 10.22 ft. L4X7X3/4 Top and Bott Angles 47X3/8 Web  10.22 ft. to 20.22 ft. L4X7X3/4 Top and Bott Angles 16X1/2 Top and Bott Cover Pls 47X3/8 Web  20.22 ft. to 39.72 ft. L4X7X3/4 Top and Bott Angles 16X15/16 Top and Bott Cover Pls 47X3/8 Web (Symm.)

(continued on next page)

(continued)

Bridge #	Span Length (ft)	$f_{slab}$ (in.)	Girder Spacing (ft)	# of Girders	Overhang Width (ft)	Skew (deg)	Materials			Cross-Frame Spacing (ft)	Girder Description
							$f_{yw}$ (ksi)	$f_{yr}$ (ksi)	$f'_c$ deck (ksi)		
0260	85.00	8.50	9.50	4	3.75 at G1 3.92 at G4	40.0	50	50	3.3	G1 1 @ 2.35 2 @ 23.17 1 @ 19.33 1 @ 16.98 G2 1 @ 13.68 2 @ 23.17 1 @ 19.33 1 @ 5.65 G3 1 @ 5.65 1 @ 19.34 2 @ 23.17 1 @ 13.67 G4 1 @ 16.98 1 @ 19.33 2 @ 23.17 1 @ 2.35	<u>Welded I-Shape</u> 0 ft. to 25.00 ft. 13X5/8 Top Flg 17X3/4 Bott Flg 52X1/2 Web  25 ft. to 42.50 ft. 13X5/8 Top Flg (Symm.) 17X1 Bott Flg 52X1/2 Web
0267	63.00	6.00	3.50	11	1.38	52.9	36	36	3.0	G1 4 @ 15.75 G2 2 @ 15.75 1 @ 13.00 1 @ 2.75 1 @ 13.00 1 @ 2.75 1 @ 13.00 G10 1 @ 15.75 1 @ 2.75 1 @ 13.00 1 @ 2.75 1 @ 13.00 1 @ 2.75 1 @ 13.00 G11 1 @ 18.50 2 @ 15.75 1 @ 13.00	<u>Welded I-Shape</u> G1/G2/G10/G11 15x1 1/8 Top Flg 15X1 1/8 Bott Flg 19 3/4X5/8 Web

(continued on next page)

(continued)

Bridge #	Span Length (ft)	$f_{slab}$ (in.)	Girder Spacing (ft)	# of Girders	Overhang Width (ft)	Skew (deg)	Materials			Cross-Frame Spacing (ft)	Girder Description
							$f_{yw}$ (ksi)	$f_{yr}$ (ksi)	$f'_c$ deck (ksi)		
0268	82.00	7.25	8.52	7	1.60	65.9	36	36	3.3	G1 1 @ 2.54 3 @ 18.00 1 @ 25.46 G2 1 @ 6.36 3 @ 18.00 1 @ 21.64 G3 1 @ 10.18 3 @ 18.00 1 @ 17.82 G4 1 @ 14.00 3 @ 18.00 1 @ 14.00 G5 1 @ 17.81 3 @ 18.00 1 @ 10.19 G6 1 @ 21.63 3 @ 18.00 1 @ 6.37 G7 1 @ 25.44 3 @ 18.00 1 @ 2.56	<u>Welded I-Shape</u> G1/G7 0 ft. to 20.00 ft. 12X3/4 Top Flg 14X3/4 Bott Flg 54X3/8 Web 20.00 ft. to 41.00 ft. 12X3/4 Top Flg 14X1 1/4 Bott Flg (Symm.) 54X3/8 Web <u>G2/G3/G4/G5/G6</u> 0 ft. to 16.00 ft. 12X3/4 Top Flg 14X3/4 Bott Flg 54X3/8 Web 16.00 ft. to 41.00 ft. 12X3/4 Top Flg 14X1 1/2 Bott Flg (Symm.) 54X3/8 Web
0272	75.00	8.50	9.00	5	3.00	125.0	50	50	3.0	G1 1 @ 15.00 1 @ 12.60 2 @ 22.50 1 @ 2.40 G2 1 @ 8.75 1 @ 12.55 2 @ 22.50 1 @ 8.70	<u>Welded I-Shape</u> 0 ft. to 16.00 ft. 12X1/2 Top Flg 16X3/4 Bott Flg 38X7/16 Web 16.00 ft. to 26.50 ft. 12X1/2 Top Flg 16X1 1/4 Bott Flg 38X7/16 Web 26.50 ft. to 37.50 ft. 12X5/8 Top Flg 16X1 1/4 Bott Flg (Symm.) 38X7/16 Web

(continued on next page)

(continued)

Bridge #	Span Length (ft)	$f_{slab}$ (in.)	Girder Spacing (ft)	# of Girders	Overhang Width (ft)	Skew (deg)	Materials			Cross-Frame Spacing (ft)	Girder Description
							$f_{yw}$ (ksi)	$f_{yr}$ (ksi)	$f'_c$ deck (ksi)		
0273	68.00	8.75	10.33	4	3.83	60.0	36	36 (Top) 50 (Bott)	4.5	<i>Fascia</i> 1 @ 19.04 1 @ 23.96 1 @ 25.00 <i>Interior</i> 1 @ 19.04 1 @ 5.97 1 @ 18.00 1 @ 5.97 1 @ 19.03	<u>Welded I-Shape</u> 12X3/4 Top Flg 15X1 1/4 Bott Flg 42X3/8 Web
0277	80.00	8.50	10.50	4	2.08 at G12.11 at G4	90.0	50	50	3.0	G1 11 @ 6.67 1 @ 6.63 G2 2 @ 6.67 1 @ 6.66 1 @ 0.01 2 @ 6.67 1 @ 6.66 1 @ 0.02 2 @ 6.67 1 @ 6.64 1 @ 0.03 2 @ 6.67 1 @ 6.62 G3/G4 4 @ 20.00	<u>Welded I-Shape</u> 0 ft. to 14.50 ft.    10X1/2 Top Flg 14X3/4 Bott Flg 50X3/8 Web 14.50 ft. to 21.50 ft.            10X1/2 Top Flg 14X1 1/2 Bott Flg 50X3/8 Web 21.50 ft. to 40.00 ft.            10X7/8 Top Flg 14X1 1/2 Bott Flg (Symm.)            50X3/8 Web
0283	58.48	6.00	6.00	4	2.17	65.0	33	33	3.0	G1 1 @ 13.26 2 @ 14.58 1 @ 16.06 G2 1 @ 13.26 1 @ 2.80 1 @ 11.78 1 @ 2.80 1 @ 11.78 1 @ 2.80 1 @ 13.26	<u>Rolled Beam</u> G1/G2 30WF108
0304	55.67	7.00	7.92	5	2.33	58.0	33	33	3.5	1 @ 13.56 1 @ 4.95 1 @ 13.68 1 @ 4.95 1 @ 18.53	<u>Rolled Beam</u> 36WF(CB362), 36X16.5X230

(continued on next page)

(continued)

Bridge #	Span Length (ft)	$f_{slab}$ (in.)	Girder Spacing (ft)	# of Girders	Overhang Width (ft)	Skew (deg)	Materials			Cross-Frame Spacing (ft)	Girder Description
							$f_{yw}$ (ksi)	$f_{yr}$ (ksi)	$f'_c$ deck (ksi)		
0314	84.00	8.50	7.75	9	3.08 at G1 2.42 at G9	90.0	32 (G1– G5)36 (G6–G9)	32 (G1– G5)36(G6– G9)	4.0	1 @ 16.76 3 @ 16.83 1 @ 16.75	<u>Rolled Beam</u> G1/G5 0 ft. to 13.00 ft. 36WF(B36a), 36X16.5X300  13.00 ft. to 41.00 ft. (Symm.) 36WF(B36a), 36X16.5X300 15X1 1/2 Bott Cover PI  G2/G3/G4 0 ft. to 13.00 ft. 36WF(CB362), 36X16.5X230  13.00 ft. to 41.00 ft. (Symm.) 36WF(CB362), 36X16.5X230 15X1 1/4 Bott Cover PI  G6/G7/G8/G9 36WF(CB362), 36X16.5X230 14 1/2X1 1/8 Bott Cover PI
0317	84.31	7.50	4.60	6	2.34 at G1 2.16 at G6	133.5	33	33	3.0	G1 3 @ 21.08 1 @ 21.07 G3 1 @ 16.72 1 @ 4.36 1 @ 16.72 1 @ 4.36 1 @ 16.72 1 @ 4.36 1 @ 21.07 G6 1 @ 16.72 2 @ 21.08 1 @ 25.43	<u>Rolled Beam</u> G1/G3/G6 0 ft. to 15.53 ft. W36X182  15.53 ft. to 42.18 ft. (Symm.) W36X182 11X1 Bott Cover PI
0329	75.75	6.50	7.08	6	2.55	90.0	36	36	3.0	4 @ 18.94	<u>Rolled Beam</u> 0 ft. to 13.25 ft. W36X160  13.25 ft. to 37.88 ft. (Symm.) W36X160 11X3/4 Bott Cover PI

(continued on next page)

(continued)

Bridge #	Span Length (ft)	$f_{slab}$ (in.)	Girder Spacing (ft)	# of Girders	Overhang Width (ft)	Skew (deg)	Materials			Cross-Frame Spacing (ft)	Girder Description
							$f_{yw}$ (ksi)	$f_{yt}$ (ksi)	$f'_c$ deck (ksi)		
0332	71.58	6.00	1 @ 4.52 1 @ 4.50 1 @ 4.52 1 @ 4.54	5	0.96 at G1 1.08 at G2	90.0	36	36	3.0	1 @ 1.17 1 @ 13.66 3 @ 13.75 1 @ 14.00 1 @ 1.50	<u>Rolled Beam</u> W36X160
0337	78.45	9.44	5.49	11	2.54	130.7	50	50	3.0	G1 1 @ 16.35 1 @ 6.56 2 @ 20.01 1 @ 15.52 G2 1 @ 11.62 1 @ 6.56 2 @ 20.01 1 @ 20.25 G3 1 @ 13.46 3 @ 20.01 1 @ 4.96	<u>Rolled Beam</u> G1/G2/G3 W690X323
0345	100.00	8.00	9.50	5	3.00	90.0	50	46/50 (Top)46 (Bott)	3.0	G1/G2 4 @ 25.00	<u>Welded I-Shape</u> G1/G2 0 ft. to 22.75 ft. 12X3/4 Top Flg (50 ksi) 22X1 Bott Flg 44X3/8 Web  22.75 ft. to 25.75 ft. 12X3/4 Top Flg (50 ksi) 22X1 1/2 Bott Flg 44X3/8 Web  25.75 ft. to 74.75 ft. 12X1 1/2 Top Flg (46 ksi) 22X1 1/2 Bott Flg 44X3/8 Web  74.75 ft. to 77.75 ft. 12X3/4 Top Flg (50 ksi) 22X1 1/2 Bott Flg 44X3/8 Web  77.75 ft. to 100.00 ft. 12X3/4 Top Flg (50 ksi) 22X1 Bott Flg 44X3/8 Web

(continued on next page)



(continued)

Bridge #	Span Length (ft)	$f_{slab}$ (in.)	Girder Spacing (ft)	# of Girders	Overhang Width (ft)	Skew (deg)	Materials			Cross-Frame Spacing (ft)	Girder Description
							$f_{yw}$ (ksi)	$f_{yr}$ (ksi)	$f'_c$ deck (ksi)		
0347	109.58	6.50	7.00	6	2.79	90.0	36	36	3.3	G1/G2 5 @ 21.92	<u>Welded I-Shape</u> G1/G2 0 ft. to 21.92 ft. 16X1 1/4 Top Flg 18X1 1/8 Bott Flg 44X1/2 Web  21.9 ft. to 54.79 ft. (Symm.) 16X1 1/4 Top Flg 18X1 7/8 Bott Flg 44X1/2 Web
0348	109.00	7.50	7.67	8	3.50 at G1 3.38 at G8	56.0	36	36	3.5	G11/G15 1 @ 18.16 1 @ 5.18 1 @ 17.32 1 @ 5.18 1 @ 17.32 1 @ 5.18 1 @ 17.32 1 @ 5.18 1 @ 17.32 1 @ 5.18 1 @ 18.16	<u>Welded I-Shape</u> G11/G15 0 ft. to 28.00 ft. 14X3/4 Top Flg 16X1 1/2 Bott Flg 54X1/2 Web  28.00 ft. to 54.50 ft. (Symm.) 14X1 1/4 Top Flg 16X2 Bott Flg 54X1/2 Web
0349	115.00	8.75	10.33	4	3.83	90.0	50	36	4.5	5 @ 23.00	<u>Welded I-Shape</u> 0 ft. to 45.00 ft. 14X1 Top Flg 18X1 1/2 Bott Flg 48X3/8 to 70X3/8 Web (Varies)  45.00 ft. to 57.50 ft. (Symm.) 14X1 Top Flg 18X1 1/2 Bott Flg 70X3/8 Web
0356	99.48	9.00	5.36	12	1.21 at G1 1.19 at G12	50.5	33	32	4.0	G1 1 @ 14.26 3 @ 23.78 1 @ 12.72 1 @ 1.16 G2 1 @ 18.66 3 @ 23.78 1 @ 8.30 1 @ 1.16 G3 1 @ 23.08 3 @ 23.78 1 @ 3.90 1 @ 1.16	<u>Built-up I-Shape</u> G1 0 ft. to 24.74 ft. L3.10X6.33X1 Top Angles L4X6X5/8 Bott Angles 14X3/8 Bott Cover PI 53 1/4X3/8 Web  24.74 ft. to 49.74 ft. (Symm.) L3.10X6.33X1 Top Angles L4X6X5/8 Bott Angles 14X3/4 Bott Cover PI 53 1/4X3/8 Web

(continued on next page)

(continued)

Bridge #	Span Length (ft)	$f_{slab}$ (in.)	Girder Spacing (ft)	# of Girders	Overhang Width (ft)	Skew (deg)	Materials			Cross-Frame Spacing (ft)	Girder Description	
							$f_{yw}$ (ksi)	$f_{yr}$ (ksi)	$f'_c$ deck (ksi)			
0356 (cont.)											G2 0 ft. to 23.24 ft.	L3.10X6.33X1 Top Angles L4X6X5/8 Bott Angles 14X1/2 Bott Cover PI 53 1/4X3/8 Web
											23.24 ft. to 49.74 ft. (Symm.)	L3.10X6.33X1 Top Angles L4X6X5/8 Bott Angles 14X1 Bott Cover PI 53 1/4X3/8 Web
											G3 0 ft. to 22.74 ft.	L3.10X6.33X1 Top Angles L4X6X5/8 Bott Angles 14X1/2 Bott Cover PI 53 1/4X3/8 Web
											22.74 ft. to 49.74 ft. (Symm.)	L3.10X6.33X1 Top Angles L4X6X5/8 Bott Angles 14X1 Bott Cover PI 53 1/4X3/8 Web

(continued on next page)

(continued)

Bridge #	Span Length (ft)	$f_{slab}$ (in.)	Girder Spacing (ft)	# of Girders	Overhang Width (ft)	Skew (deg)	Materials			Cross-Frame Spacing (ft)	Girder Description
							$f_{yw}$ (ksi)	$f_{yr}$ (ksi)	$f'_c$ deck (ksi)		
0357	110.00	10.00	6.00	5	1.50	90.0	36	36	3.0	G1/G212 @ 18.33	<u>Built-up I-Shape</u> G1/G2 0 ft. to 15.50 ft. L4.60X6.27X1.14 Top Angles L6X6X3/4 Bott Angles 58 1/2X1/2 Web  15.50 ft. to 22.50 ft. L4.60X6.27X1.14 Top Angles L6X6X3/4 Bott Angles 14X7/16 Bott Cover PI 58 1/2X1/2 Web  22.50 ft. to 29.00 ft. L4.60X6.27X1.14 Top Angles L6X6X3/4 Bott Angles 14X7/8 Bott Cover PI 58 1/2X1/2 Web  29.00 ft. to 55.00 ft. L4.60X6.27X1.14 (Symm.)                  Top Angles L6X6X3/4 Bott Angles 14X1 5/16 Bott Cover PI 58 1/2X1/2 Web

(continued on next page)

(continued)

Bridge #	Span Length (ft)	$f_{slab}$ (in.)	Girder Spacing (ft)	# of Girders	Overhang Width (ft)	Skew (deg)	Materials			Cross-Frame Spacing (ft)	Girder Description
							$f_{yw}$ (ksi)	$f_{yr}$ (ksi)	$f'_c$ deck (ksi)		
0358	90.00	9.00	7.04	10	2.13 at G1 3.00 at G10	128.5	33	33	3.0	G1/G2 4 @ 22.50 G10 1 @ 16.60 2 @ 22.50 1 @ 28.40	<u>Rolled Beam</u> G1 0 ft. to 0.40 ft. 36WF(CB362), 36X16.5X230  0.40 ft. to 90.00 ft. 36WF(CB362), 36X16.5X230 18X1 Bott Cover PI  G2 0 ft. to 10.00 ft. 36WF(CB362), 36X16.5X230 10.00 ft. to 45.00 ft. 36WF(CB362), 36X16.5X230 (Symm.) 18X1 1/2 Bott Cover PI  G10 0 ft. to 11.00 ft. 36WF(CB362), 36X16.5X230 11.00 ft. to 45.00 ft. 36WF(CB362), 36X16.5X230 (Symm.) 18X1 1/4 Bott Cover PI
0359	115.00	7.50	8.50	6	2.60	144.9	33	33	3.0	G1 1 @ 0.43 1 @ 15.05 1 @ 24.21 1 @ 24.07 2 @ 24.08 1 @ 2.65 1 @ 0.43 G2 1 @ 0.43 1 @ 2.93 1 @ 12.12 1 @ 12.09 1 @ 0.08 1 @ 24.00 1 @ 0.21 1 @ 23.87 1 @ 0.21 1 @ 23.87 1 @ 0.21 1 @ 11.97 1 @ 2.58 1 @ 0.43	<u>Rolled Beam</u> G1/G6 0 ft. to 1.00 ft. 21X1 1/8 Top Flg 21X1 13/16 Bott Flg 56X0.319 Web  1.00 ft. to 25.17 ft. 21X1 1/8 Top Flg 21X1 13/16 Bott Flg 56X3/8 Web  25.17 ft. to 57.50 ft. 21X1 9/16 Top Flg 21X2 3/8 Bott Flg (Symm.) 56X3/8 Web  G2/G3/G4 0 ft. to 25.17 ft. 21x15/16 Top Flg 21X1 3/4 Bott Flg 56X3/8 Web  25.17 ft. to 57.50 ft. 21X1 3/8 Bott Flg 21X2 5/16 Top Flg (Symm.) 56X3/8 Web

(continued on next page)

(continued)

Bridge #	Span Length (ft)	$f_{slab}$ (in.)	Girder Spacing (ft)	# of Girders	Overhang Width (ft)	Skew (deg)	Materials			Cross-Frame Spacing (ft)	Girder Description
							$f_{yw}$ (ksi)	$f_{yr}$ (ksi)	$f'_c$ deck (ksi)		
0359 (cont.)										G3 1 @ 0.43 1 @ 0.04 1 @ 2.89 1 @ 12.12 1 @ 0.05 1 @ 24.16 1 @ 0.05 1 @ 24.03 1 @ 0.05 1 @ 24.03 1 @ 0.05 1 @ 11.98 1 @ 12.05 1 @ 2.64 1 @ 0.43 G4 1 @ 0.47 1 @ 2.89 1 @ 12.12 1 @ 12.09 1 @ 0.08 1 @ 24.00 1 @ 0.08 1 @ 24.00 1 @ 0.08 1 @ 24.00 1 @ 0.08 1 @ 12.16 1 @ 2.52 1 @ 0.43 G5 1 @ 0.47 1 @ 2.89 1 @ 12.12 1 @ 0.05 1 @ 24.03 1 @ 0.05 1 @ 24.03 1 @ 0.05 1 @ 24.03 1 @ 0.05 1 @ 12.16 1 @ 11.87 1 @ 2.78 1 @ 0.42	G5 0 ft. to 25.17 ft. 21x15/16 Top Flg 21X1 3/4 Bott Flg 56X3/8 Web 25.17 ft. to 57.50 ft. (Symm.) 21X15/16 Bott Flg 21X2 5/16 Top Flg 56X3/8 Web

(continued on next page)

(continued)

Bridge #	Span Length (ft)	$f_{slab}$ (in.)	Girder Spacing (ft)	# of Girders	Overhang Width (ft)	Skew (deg)	Materials			Cross-Frame Spacing (ft)	Girder Description
							$f_{yw}$ (ksi)	$f_{yt}$ (ksi)	$f'_c$ deck (ksi)		
0359 (cont.)										G6 1 @ 0.47 1 @ 2.89 4 @ 24.08 1 @ 14.90 1 @ 0.43	
0366	100.00	9.50	6.83	12	2.42	90.0	50	50	4.0	G1/G4/G5/G6 5 @ 20.00 G2/G3/G7/ G8/ G9/G10 10 @ 10.00 G11/G12 20 @ 5.00	<u>Rolled Beam</u> 0 ft. to 15.00 ft. W36X230 15.00 ft. to 50.00 ft. W36X230 (Symm.) 15X1 1/2 Bott Cover Pl
0367	138.58	8.00	8.45	7	4.25	121.7	50	50	4.0	<i>Fascia</i> 1 @ 19.75 1 @ 20.00 4 @ 22.50 1 @ 8.83 <i>Interior</i> 1 @ 14.55 1 @ 20.00 4 @ 22.50 1 @ 14.04	<u>Welded I-Shape</u> 0 ft. to 34.42 ft. 13X1 Top Flg 13X1 Bott Flg 71X1/2 Web 34.42 ft. to 93.92 ft. 13X1 Top Flg 13X1 1/2 Bott Flg 71X1/2 Web 93.92 ft. to 138.58 ft. 13X1 Top Flg 13X1 Bott Flg 71X1/2 Web
0368	178.20	9.00	8.33	7	2.33 at G1 1.37 at G7	84.2	50	50	4.0	1 @ 3.00 1 @ 19.26 6 @ 22.28 1 @ 19.26 1 @ 3.00	<u>Welded I-Shape</u> 0 ft. to 28.10 ft. 18x1 1/4 Top Flg 18X1 1/4 Bott Flg 72X5/8 Web 28.10 ft. to 89.10 ft. 18x1 3/4 Top Flg 24X1 7/8 Bott Flg (Symm.) 72X1/2 Web
0369	136.85	9.00	7.25	7	2.00	91.1	50	50	4.0	1 @ 3.59 1 @ 19.23 4 @ 22.81 1 @ 20.79 1 @ 2.00	<u>Welded I-Shape</u> 0 ft. to 28.00 ft. 14X3/4 Top Flg 16X1 3/8 Bott Flg 54X1/2 Web 28.00 ft. to 68.43 ft. 14X1 1/8 Top Flg (Symm.) 16X1 3/4 Bott Flg 54X1/2 Web

(continued on next page)

(continued)

Bridge #	Span Length (ft)	$f_{slab}$ (in.)	Girder Spacing (ft)	# of Girders	Overhang Width (ft)	Skew (deg)	Materials			Cross-Frame Spacing (ft)	Girder Description
							$f_{yw}$ (ksi)	$f_{yr}$ (ksi)	$f'_c$ deck (ksi)		
0370	153.61	6.50	5 @ 7.252 @ 6.38	8	2.50 at G1 2.46 at G8	22.5	36	36	3.0	G1 1 @ 3.00 5 @ 25.00 1 @ 25.61 G2 1 @ 3.95 1 @ 16.72 1 @ 8.28 1 @ 16.72 1 @ 8.28 1 @ 16.72 1 @ 8.28 1 @ 16.72 1 @ 8.28 1 @ 16.72 1 @ 8.28 1 @ 16.72 1 @ 7.94 G5 1 @ 0.83 1 @ 17.36 1 @ 7.64 1 @ 17.36 1 @ 7.64 1 @ 17.36 1 @ 7.64 1 @ 17.36 1 @ 7.64 1 @ 17.36 1 @ 10.42 G6 1 @ 0.98 1 @ 17.36 1 @ 7.64 1 @ 17.36 1 @ 7.64 1 @ 17.36 1 @ 7.64 1 @ 17.36 1 @ 7.64 1 @ 17.36 1 @ 10.27	<u>Welded I-Shape</u> G1 0 ft. 19.25 ft. 20X1 Top Flg 22X1 Bott Flg 60X3/8 Web 19.25 ft. to 20X2 1/4 Top Flg 76.81 ft. 22X2 1/4 Bott Flg (Symm.) 60X3/8 Web G2 0 ft. 20.50 ft. 20X1 Top Flg 22X1 Bott Flg 60X3/8 Web 20.50 ft. to 20X2 1/4 Top Flg 76.81 ft. 22X2 1/4 Bott Flg (Symm.) 60X3/8 Web G5 0 ft. 20.50 ft. 20X1 Top Flg 22X1 Bott Flg 60X3/8 Web 20.50 ft. to 20X2 Top Flg 76.81 ft. 22X2 Bott Flg (Symm.) 60X3/8 Web G6 0 ft. 21.50 ft. 20X1 Top Flg 22X1 Bott Flg 60X3/8 Web 21.50 ft. to 20X2 Top Flg 76.81 ft. 22X2 Bott Flg (Symm.) 60X3/8 Web <u>Welded I-Shape</u> G7 0 ft. 20.00 ft. 20X1 Top Flg 22X1 Bott Flg 60X3/8 Web 20.00 ft. to 20X1 3/4 Top Flg 76.81 ft. 22X2 1/8 Bott Flg (Symm.) 60X3/8 Web G8 0 ft. 20.00 ft. 20X1 Top Flg 22X1 Bott Flg 60X3/8 Web

(continued on next page)



(continued)

Bridge #	Span Length (ft)	$f_{slab}$ (in.)	Girder Spacing (ft)	# of Girders	Overhang Width (ft)	Skew (deg)	Materials			Cross-Frame Spacing (ft)	Girder Description
							$f_{yw}$ (ksi)	$f_{yt}$ (ksi)	$f'_c$ deck (ksi)		
0370 (cont.)										G7 1 @ 1.11 1 @ 15.25 1 @ 9.75 1 @ 15.25 1 @ 9.75 1 @ 15.25 1 @ 9.75 1 @ 15.25 1 @ 9.75 1 @ 15.25 1 @ 9.75 1 @ 15.25 1 @ 9.75 1 @ 15.25 1 @ 12.25 G8 1 @ 16.50 5 @ 25.00 1 @ 12.11	20.00 ft. to 76.81 ft. (Symm.) 20X1 3/4 Top Flg 22X2 1/8 Bott Flg 60X3/8 Web
0371	120.00	9.00	7.40	10	2.98 at G1 3.00 at G10	90.0	50	50	4.0	G1/G6/G10 1 @ 2.50 5 @ 23.50	<u>Welded I-Shape</u> G1/G6/G10 0 ft. to 21.00 ft. 12X1 1/8 Top Flg 16X1 1/4 Bott Flg 42X1/2 Web  21.00 ft. to 60.00 ft. (Symm.) 12X1 1/8 Top Flg 16X2 1/2 Bott Flg 42X1/2 Web
0372	163.38	7.00	8.50	4	3.08	45.0	33	33	3.0	G2 1 @ 10.92 1 @ 8.50 1 @ 16.50 1 @ 8.50 1 @ 16.50 1 @ 8.50 1 @ 16.50 1 @ 8.50 1 @ 16.50 1 @ 8.50 1 @ 16.50 1 @ 8.50 1 @ 18.96	<u>Welded I-Shape</u> G2 0 ft. to 21.67 ft. 12X13/16 Top Flg 20X1 3/8 Bott Flg 84X1/2 Web  21.67 ft. to 46.67 ft. 20X1 3/4 Top Flg 20X2 3/4 Bott Flg 84X1/2 Web  46.67 ft. to 84.00 ft. 20X2 Top Flg 20X3 Bott Flg 84X1/2 Web  84.00 ft. to 141.71 ft. 20X1 3/4 Top Flg 20X2 3/4 Bott Flg 84X1/2 Web  141.71 ft. to 163.38 ft. 20X13/16 Top Flg 20X1 3/8 Bott Flg 84X1/2 Web

(continued on next page)

(continued)

Bridge #	Span Length (ft)	$f_{slab}$ (in.)	Girder Spacing (ft)	# of Girders	Overhang Width (ft)	Skew (deg)	Materials			Cross-Frame Spacing (ft)	Girder Description
							$f_{yw}$ (ksi)	$f_{yr}$ (ksi)	$f'_c$ deck (ksi)		
0373	146.92	9.00	6.50	8	2.25	120.0	50	50	4.0	G1 1 @ 10.95 7 @ 18.91 1 @ 3.60 G2 1 @ 7.20 7 @ 18.91 1 @ 7.35	<u>Welded I-Shape</u> 15X1 Top Flg 21X1 5/8 Bott Flg 59X5/8 Web
0374	150.75	8.00	7.50	5	1.44	56.5	36	36	3.0	G1 1 @ 1.75 1 @ 3.82 1 @ 21.50 4 @ 25.00 1 @ 23.68	<u>Welded I-Shape</u> G1 0 ft. to 25.00 ft. 22X15/16 Top Flg 22X27/32 Bott Flg 78X0.48 Web 25.00 ft. to 41.00 ft. 22X15/16 Top Flg 22X1.74 Bott Flg 78X0.48 Web 41.00 ft. to 109.75 ft. 22X1 3/16 Top Flg 22X1.74 Bott Flg 78X0.48 Web 109.75 ft. to 150.75 ft. 22X15/16 Top Flg 22X27/32 Bott Flg 78X0.48 Web
0375	172.50	7.50	9.08	7	1.75	81.7	50	46 (Top)46/42 (Bott)	3.0	G2 1 @ 23.00 1 @ 1.32 1 @ 23.68 1 @ 1.32 1 @ 23.68 1 @ 1.32 1 @ 23.68 1 @ 1.32 1 @ 23.68 1 @ 1.32 1 @ 23.68 1 @ 1.32 1 @ 23.68 1 @ 1.32 1 @ 23.18	<u>Welded I-Shape</u> G2 0 ft. to 30.25 ft. 22X1 Top Flg 24X1 Bott Flg (46 ksi) 76X9/16 Web 30.25 ft. to 48.25 ft. 22X1 Top Flg 24X1 7/8 Bott Flg (42 ksi) 76X9/16 Web 48.25 ft. to 86.25 ft. 22X1 3/8 Top Flg 24X1 7/8 Bott Flg (42 ksi) (Symm.) 76X9/16 Web

(continued on next page)



(continued)

Bridge #	Span Length (ft)	$f_{slab}$ (in.)	Girder Spacing (ft)	# of Girders	Overhang Width (ft)	Skew (deg)	Materials			Cross-Frame Spacing (ft)	Girder Description
							$f_{yw}$ (ksi)	$f_{yr}$ (ksi)	$f'_c$ deck (ksi)		
0377	169.83	7.00	9.50	5	2.00	31.5	50	50	3.0	G2 1 @ 4.38 1 @ 16.13 4 @ 25.00 1 @ 16.13 1 @ 0.31 1 @ 15.83 1 @ 0.61 1 @ 16.44 G3 1 @ 3.76 2 @ 16.13 4 @ 25.00 2 @ 16.13 1 @ 1.55	<u>Welded I-Shape</u> G2/G3 0 ft. to 30.00 ft. 24X1 Top Flg 24X1 Bott Flg 78X9/16 to 73X9/16 Web (Varies) 30.00 ft. to 49.00 ft. 24X1 Top Flg 24X2 Bott Flg 73X9/16 Web 49.00 ft. to 84.92 ft. 24X1 7/16 Top Flg 24X2 Bott Flg (Symm.) 73X9/16 Web
0378	140.30	8.50	1 @ 8.004 @ 6.855 @ 8.25	11	2.42 at G1 2.04 at G11	76.5	50	45/50 (Top)42/46 (Bott)	3.3	G8 1 @ 24.41 4 @ 26.00 1 @ 11.89 G10 1 @ 28.37 4 @ 26.00 1 @ 7.93 G11 1 @ 30.35 4 @ 26.00 1 @ 5.95	<u>Welded I-Shape</u> G8 0 ft. to 28.65 ft. 18X3/4 Top Flg (50 ksi) 17X7/8 Bott Flg (45 ksi) 86X5/8 Web 28.65 ft. to 45.65 ft. 18X3/4 Top Flg (50 ksi) 17X1 3/4 Bott Flg (42 ksi) 86X5/8 Web 45.65 ft. to 70.15 ft. 18X7/8 Top Flg (45 ksi) 17X1 3/4 Bott Flg (42 ksi) 86X5/8 Web (Symm.) G10 0 ft. to 29.15 ft. 18X3/4 Top Flg (50 ksi) 16X3/4 Bott Flg (50 ksi) 86X5/8 Web 29.15 ft. to 70.15 ft. 18X3/4 Top Flg (50 ksi) 16X1 1/2 Bott Flg (45 ksi) 86X5/8 Web (Symm.)

(continued on next page)

(continued)

Bridge #	Span Length (ft)	$f_{slab}$ (in.)	Girder Spacing (ft)	# of Girders	Overhang Width (ft)	Skew (deg)	Materials			Cross-Frame Spacing (ft)	Girder Description
							$f_{yw}$ (ksi)	$f_{yt}$ (ksi)	$f'_c$ deck (ksi)		
0378 (cont.)											<p><i>G11</i></p> <p>0 ft. to 35.65 ft. 18X3/4 Top Flg (50 ksi) 18X3/4 Bott Flg (50 ksi) 86X5/8 Web</p> <p>35.65 ft. to 70.15 ft. (Symm.) 18X3/4 Top Flg (50 ksi) 18X1 1/4 Bott Flg (45 ksi) 86X5/8 Web</p>
0379	212.00	9.50	10.25	12	2.21	66.5	70	70	5.0	<p>1 @ 22.00 8 @ 21.00 1 @ 22.00</p>	<p><u>Welded I-Shape</u></p> <p>0 ft. to 1.25 ft. 21X1 1/2 Top Flg 16X1 3/4 Bott Flg 84X3/4 Web</p> <p>1.25 ft. to 48.00 ft. 21X1 1/2 Top Flg 27X1 3/4 Bott Flg 84X3/4 Web</p> <p>48.00 ft. to 106.00 ft. (Symm.) 21X2 1/8 Top Flg 27X2 3/8 Bott Flg 84X3/4 Web</p>
0380	126.00	8.50	9.75	6	2.96	90.0	50	50	4.0	<p><i>G1/G2</i> 6 @ 21.00</p>	<p><u>Welded I-Shape</u></p> <p><i>G1/G2</i></p> <p>0 ft. to 37.80 ft. 16X1 Top Flg 20X1 5/8 Bott Flg 60X9/16 Web</p> <p>37.80 ft. to 61.00 ft. (Symm.) 18X1 5/8 Top Flg 24X2 Bott Flg 60X9/16 Web</p>

(continued on next page)

(continued)

Bridge #	Span Length (ft)	$f_{slab}$ (in.)	Girder Spacing (ft)	# of Girders	Overhang Width (ft)	Skew (deg)	Materials			Cross-Frame Spacing (ft)	Girder Description
							$f_{yw}$ (ksi)	$f_{yr}$ (ksi)	$f'_c$ deck (ksi)		
0381	204.00	8.50	9.67	6	3.42	95.0	50	50	4.0	G1 9 @ 22.67 G2 1 @ 21.82 1 @ 0.85 1 @ 21.82 1 @ 0.85 1 @ 21.82 1 @ 0.85 1 @ 21.82 1 @ 0.85 1 @ 21.82 1 @ 0.85 1 @ 21.82 1 @ 0.85 1 @ 21.82 1 @ 0.84 1 @ 21.82 1 @ 0.84 1 @ 22.66	Welded I-Shape G1/G2 0 ft. to 62.00 ft.    18X1 3/4 Top Flg 21X2 3/4 Bott Flg 78X5/8 Web  62.00 ft. to 102.00 ft. (Symm.)                25X1 3/4 Top Flg 25X2 3/4 Bott Flg 78X5/8 Web

## F.7 Steel Fatigue Database

**Table F.7.1. Fatigue Test Data**

Units	Load Type	Detail	ID Number	Stress Range	Cycles	Result	Min. Stress	Max. Stress	Yield Stress
Imp.	Const.	40	0NC1CRA131	16	393000	crack	-6	10	36
Imp.	Const.	40	0NC1CWA132	16	393000	crack	-6	10	36
Imp.	Const.	40	0NC1CWA133	16	337000	crack	-6	10	36
Imp.	Const.	40	0NC1CRA141	20	192000	crack	-6	14	36
Imp.	Const.	40	0NC1CWA142	20	168000	crack	-6	14	36
Imp.	Const.	40	0NC1CWA143	20	288000	crack	-6	14	36
Imp.	Const.	40	0NC1CRA144	20	176000	crack	-6	14	36
Imp.	Const.	40	0NC1CRA151	24	114000	crack	-6	18	36
Imp.	Const.	40	0NC1CWA152	24	94000	crack	-6	18	36
Imp.	Const.	40	0NC1CWA153	24	85000	crack	-6	18	36
Imp.	Const.	40	0NC1CRA221	12	798000	crack	2	14	36
Imp.	Const.	40	0NC1CWA222	12	655000	crack	2	14	36
Imp.	Const.	40	0NC1CWA223	12	724000	crack	2	14	36
Imp.	Const.	40	0NC1CRA231	16	277000	crack	2	18	36
Imp.	Const.	40	0NC1CWA232	16	317000	crack	2	18	36
Imp.	Const.	40	0NC1CWA233	16	329000	crack	2	18	36
Imp.	Const.	40	0NC1CRA234	16	325000	crack	2	18	36
Imp.	Const.	40	0NC1CRA241	20	198000	crack	2	18	36
Imp.	Const.	40	0NC1CWA242	20	159000	crack	2	18	36
Imp.	Const.	40	0NC1CWA243	20	148000	crack	2	18	36
Imp.	Const.	40	0NC1CRA311	8	2227000	crack	10	18	36
Imp.	Const.	40	0NC1CWA312	8	2693000	crack	10	18	36
Imp.	Const.	40	0NC1CWA313	8	2453000	crack	10	18	36
Imp.	Const.	40	0NC1CRA321	12	676000	crack	10	22	36
Imp.	Const.	40	0NC1CWA322	12	778000	crack	10	22	36
Imp.	Const.	40	0NC1CWA323	12	658000	crack	10	22	36
Imp.	Const.	40	0NC1CRA324	12	739000	crack	10	22	36
Imp.	Const.	40	0NC1CRA331	16	301000	crack	10	26	36
Imp.	Const.	40	0NC1CWA332	16	344000	crack	10	26	36
Imp.	Const.	40	0NC1CWA333	16	297000	crack	10	26	36
Imp.	Const.	40	0NC1CRA341	20	108000	crack	10	30	36
Imp.	Const.	40	0NC1CWA342	20	180000	crack	10	30	36
Imp.	Const.	40	0NC1CWA343	20	172000	crack	10	30	36
Imp.	Const.	40	0NC1CRA344	20	166000	crack	10	30	36
Imp.	Const.	40	0NC1CRB131	16	418000	crack	-6	10	50
Imp.	Const.	40	0NC1CWB132	16	356000	crack	-6	10	50

(continued on next page)



Table F.7.1. Fatigue Test Data (continued)

Units	Load Type	Detail	ID Number	Stress Range	Cycles	Result	Min. Stress	Max. Stress	Yield Stress
Imp.	Const.	40	0NC1CWB133	16	290000	crack	-6	10	50
Imp.	Const.	40	0NC1CRB141	20	187000	crack	-6	14	50
Imp.	Const.	40	0NC1CWB142	20	154000	crack	-6	14	50
Imp.	Const.	40	0NC1CBW143	20	171000	crack	-6	14	50
Imp.	Const.	40	0NC1CRB144	20	231000	crack	-6	14	50
Imp.	Const.	40	0NC1CRB151	24	108000	crack	-6	18	50
Imp.	Const.	40	0NC1CRB221	12	842000	crack	2	14	50
Imp.	Const.	40	0NC1CWB222	12	667000	crack	2	14	50
Imp.	Const.	40	0NC1CWB223	12	709000	crack	2	14	50
Imp.	Const.	40	0NC1CRB231	16	366000	crack	2	18	50
Imp.	Const.	40	0NC1CWB232	16	264000	crack	2	18	50
Imp.	Const.	40	0NC1CWB233	16	318000	crack	2	18	50
Imp.	Const.	40	0NC1CRB234	16	369000	crack	2	18	50
Imp.	Const.	40	0NC1CRB241	20	177000	crack	2	22	50
Imp.	Const.	40	0NC1CWB242	20	172000	crack	2	22	50
Imp.	Const.	40	0NC1CWB243	20	149000	crack	2	22	50
Imp.	Const.	40	0NC1CWB251	24	83100	crack	2	26	50
Imp.	Const.	40	0NC1CWB301	6	6317000	crack	10	16	50
Imp.	Const.	40	0NC1CRB311	8	2443000	crack	10	18	50
Imp.	Const.	40	0NC1CWB312	8	1977000	crack	10	18	50
Imp.	Const.	40	0NC1CWC313	8	2278000	crack	10	18	50
Imp.	Const.	40	0NC1CRB321	12	702000	crack	10	22	50
Imp.	Const.	40	0NC1CWB322	12	757000	crack	10	22	50
Imp.	Const.	40	0NC1CWB323	12	747000	crack	10	22	50
Imp.	Const.	40	0NC1CRB324	12	658000	crack	10	22	50
Imp.	Const.	40	0NC1CRB331	16	273000	crack	10	26	50
Imp.	Const.	40	0NC1CWB332	16	314000	crack	10	26	50
Imp.	Const.	40	0NC1CWB333	16	295000	crack	10	26	50
Imp.	Const.	40	0NC1CRB341	20	178000	crack	10	30	50
Imp.	Const.	40	0NC1CWB342	20	204000	crack	10	30	50
Imp.	Const.	40	0NC1CWB343	20	160000	crack	10	30	50
Imp.	Const.	40	0NC1CRB344	20	200000	crack	10	30	50
Imp.	Const.	40	0NC1CRC131	16	395000	crack	-6	10	100
Imp.	Const.	40	0NC1CWC132	16	483000	crack	-6	10	100
Imp.	Const.	40	0NC1CWC133	16	547000	crack	-6	10	100
Imp.	Const.	40	0NC1CRC141	20	243000	crack	-6	14	100
Imp.	Const.	40	0NC1CWC142	20	295000	crack	-6	14	100
Imp.	Const.	40	0NC1CWC143	20	254000	crack	-6	14	100
Imp.	Const.	40	0NC1CRC144	20	282000	crack	-6	14	100

(continued on next page)

Table F.7.1. Fatigue Test Data (continued)

Units	Load Type	Detail	ID Number	Stress Range	Cycles	Result	Min. Stress	Max. Stress	Yield Stress
Imp.	Const.	40	0NC1CRC151	24	157000	crack	-6	18	100
Imp.	Const.	40	0NC1CWC152	24	137000	crack	-6	18	100
Imp.	Const.	40	0NC1CWC153	24	171000	crack	-6	18	100
Imp.	Const.	40	0NC1CRC221	12	844000	crack	2	14	100
Imp.	Const.	40	0NC1CWC222	12	848000	crack	2	14	100
Imp.	Const.	40	0NC1CWC223	12	1311000	crack	2	14	100
Imp.	Const.	40	0NC1CRC231	16	429000	crack	2	18	100
Imp.	Const.	40	0NC1CWC232	16	382000	crack	2	18	100
Imp.	Const.	40	0NC1CWC233	16	498000	crack	2	18	100
Imp.	Const.	40	0NC1CRC234	16	378000	crack	2	18	100
Imp.	Const.	40	0NC1CRC241	20	192000	crack	2	22	100
Imp.	Const.	40	0NC1CWC242	20	243000	crack	2	22	100
Imp.	Const.	40	0NC1CWC243	20	260000	crack	2	22	100
Imp.	Const.	40	0NC1CWC251	24	154000	crack	2	26	100
Imp.	Const.	40	0NC1CRC311	8	1989000	crack	10	18	100
Imp.	Const.	40	0NC1CWC312	8	5699000	crack	10	18	100
Imp.	Const.	40	0NC1CWC313	8	3409000	crack	10	18	100
Imp.	Const.	40	0NC1CRC321	12	822000	crack	10	22	100
Imp.	Const.	40	0NC1CWC322	12	1005000	crack	10	22	100
Imp.	Const.	40	0NC1CWC323	12	1220000	crack	10	22	100
Imp.	Const.	40	0NC1CRC324	12	755000	crack	10	22	100
Imp.	Const.	40	0NC1CRC331	16	325000	crack	10	26	100
Imp.	Const.	40	0NC1CWC332	16	378000	crack	10	26	100
Imp.	Const.	40	0NC1CWC333	16	441000	crack	10	26	100
Imp.	Const.	40	0NC1CRC341	20	196000	crack	10	30	100
Imp.	Const.	40	0NC1CWC342	20	245000	crack	10	30	100
Imp.	Const.	40	0NC1CWC343	20	220000	crack	10	30	100
Imp.	Const.	40	0NC1CRC344	20	174000	crack	10	30	100
Imp.	Const.	30	0NC1CRA131	16	555000	crack	-6	10	36
Imp.	Const.	30	0NC1CWA132	16	553000	crack	-6	10	36
Imp.	Const.	30	0NC1CWA133	16	484000	crack	-6	10	36
Imp.	Const.	30	0NC1CRA141	20	192000	crack	-6	14	36
Imp.	Const.	30	0NC1CWA142	20	228000	crack	-6	14	36
Imp.	Const.	30	0NC1CWA143	20	288000	crack	-6	14	36
Imp.	Const.	30	0NC1CRA144	20	243000	crack	-6	14	36
Imp.	Const.	30	0NC1CRA151	24	114000	crack	-6	18	36
Imp.	Const.	30	0NC1CWA152	24	135000	crack	-6	18	36
Imp.	Const.	30	0NC1CWA153	24	209000	crack	-6	18	36
Imp.	Const.	30	0NC1CRA221	12	1074000	crack	2	14	36

(continued on next page)

Table F.7.1. Fatigue Test Data (continued)

Units	Load Type	Detail	ID Number	Stress Range	Cycles	Result	Min. Stress	Max. Stress	Yield Stress
Imp.	Const.	30	0NC1CWA222	12	1272000	crack	2	14	36
Imp.	Const.	30	0NC1CWA223	12	1392000	crack	2	14	36
Imp.	Const.	30	0NC1CRA231	16	364000	crack	2	18	36
Imp.	Const.	30	0NC1CWA232	16	566000	crack	2	18	36
Imp.	Const.	30	0NC1CWA233	16	648000	crack	2	18	36
Imp.	Const.	30	0NC1CRA234	16	546000	crack	2	18	36
Imp.	Const.	30	0NC1CRA241	20	248000	crack	2	22	36
Imp.	Const.	30	0NC1CWA242	20	246000	crack	2	22	36
Imp.	Const.	30	0NC1CWA243	20	310000	crack	2	22	36
Imp.	Const.	30	0NC1CRA311	8	2227000	crack	10	18	36
Imp.	Const.	30	0NC1CWA312	8	2693000	crack	10	18	36
Imp.	Const.	30	0NC1CWA313	8	3428000	crack	10	18	36
Imp.	Const.	30	0NC1CRA321	12	845000	crack	10	22	36
Imp.	Const.	30	0NC1CWA322	12	945000	crack	10	22	36
Imp.	Const.	30	0NC1CWA323	12	1039000	crack	10	22	36
Imp.	Const.	30	0NC1CRA324	12	812000	crack	10	22	36
Imp.	Const.	30	0NC1CRA331	16	379000	crack	10	26	36
Imp.	Const.	30	0NC1CWA332	16	441000	crack	10	26	36
Imp.	Const.	30	0NC1CWA333	16	410000	crack	10	26	36
Imp.	Const.	30	0NC1CRA341	20	108000	crack	10	30	36
Imp.	Const.	30	0NC1CWA342	20	207000	crack	10	30	36
Imp.	Const.	30	0NC1CWA343	20	196000	crack	10	30	36
Imp.	Const.	30	0NC1CRA344	20	193000	crack	10	30	36
Imp.	Const.	30	0NC1CRB131	16	660000	crack	-6	10	50
Imp.	Const.	30	0NC1CWB132	16	568000	crack	-6	10	50
Imp.	Const.	30	0NC1CWB133	16	530000	crack	-6	10	50
Imp.	Const.	30	0NC*CRB141	20	187000	crack	-6	14	50
Imp.	Const.	30	0NC1CWB142	20	318000	crack	-6	14	50
Imp.	Const.	30	0NC1CWB143	20	320000	crack	-6	14	50
Imp.	Const.	30	0NC1CRB144	20	317000	crack	-6	14	50
Imp.	Const.	30	0NC1CRB151	24	151000	crack	-6	18	50
Imp.	Const.	30	0NC1CRB221	12	1005000	crack	2	14	50
Imp.	Const.	30	0NC*CWB222	12	667000	crack	2	14	50
Imp.	Const.	30	0NC1CWB223	12	1151000	crack	2	14	50
Imp.	Const.	30	0NC1CRB231	16	366000	crack	2	18	50
Imp.	Const.	30	0NC1CWB232	16	475000	crack	2	18	50
Imp.	Const.	30	0NC1CWB234	16	424000	crack	2	18	50
Imp.	Const.	30	0NC1CRB241	20	257000	crack	2	22	50
Imp.	Const.	30	0NC1CWB242	20	249000	crack	2	22	50

(continued on next page)

Table F.7.1. Fatigue Test Data (continued)

Units	Load Type	Detail	ID Number	Stress Range	Cycles	Result	Min. Stress	Max. Stress	Yield Stress
Imp.	Const.	30	0NC1CWB243	20	258000	crack	2	22	50
Imp.	Const.	30	0NC1CWB251	24	114000	crack	2	26	50
Imp.	Const.	30	0NC1CWB301	6	5488000	crack	10	16	50
Imp.	Const.	30	0NC1CRB311	8	2714000	crack	10	18	50
Imp.	Const.	30	0NC1CWB312	8	3132000	crack	10	18	50
Imp.	Const.	30	0NC1CWB313	8	2920000	crack	10	18	50
Imp.	Const.	30	0NC1CRB321	12	966000	crack	10	22	50
Imp.	Const.	30	0NC1CWB322	12	1086000	crack	10	22	50
Imp.	Const.	30	0NC1CWB323	12	994000	crack	10	22	50
Imp.	Const.	30	0NC1CRB324	12	931000	crack	10	22	50
Imp.	Const.	30	0NC1CRB331	16	446000	crack	10	26	50
Imp.	Const.	30	0NC1CWB332	16	459000	crack	10	26	50
Imp.	Const.	30	0NC1CWB333	16	451000	crack	10	26	50
Imp.	Const.	30	0NC1CRB341	20	229000	crack	10	30	50
Imp.	Const.	30	0NC1CWB342	20	266000	crack	10	30	50
Imp.	Const.	30	0NC1CWB343	20	218000	crack	10	30	50
Imp.	Const.	30	0NC1CRB344	20	200000	crack	10	30	50
Imp.	Const.	30	0NC1CRC131	16	515000	crack	-6	10	100
Imp.	Const.	30	0NC1CWC132	16	1228000	crack	-6	10	100
Imp.	Const.	30	0NC1CWC133	16	855000	crack	-6	10	100
Imp.	Const.	30	0NC1CRC141	20	341000	crack	-6	14	100
Imp.	Const.	30	0NC1CWC142	20	429000	crack	-6	14	100
Imp.	Const.	30	0NC1CWC143	20	446000	crack	-6	14	100
Imp.	Const.	30	0NC1CRC144	20	282000	crack	-6	14	100
Imp.	Const.	30	0NC1CRC151	24	157000	crack	-6	18	100
Imp.	Const.	30	0NC1CWC152	24	214000	crack	-6	18	100
Imp.	Const.	30	0NC1CWC153	24	285000	crack	-6	18	100
Imp.	Const.	30	0NC1CRC221	12	1031000	crack	2	14	100
Imp.	Const.	30	0NC1CWC222	12	848000	crack	2	14	100
Imp.	Const.	30	0NC1CWC223	12	1311000	crack	2	14	100
Imp.	Const.	30	0NC1CRC231	16	429000	crack	2	18	100
Imp.	Const.	30	0NC1CWC232	16	542000	crack	2	18	100
Imp.	Const.	30	0NC1CWC233	16	599000	crack	2	18	100
Imp.	Const.	30	0NC1CRC234	16	493000	crack	2	18	100
Imp.	Const.	30	0NC1CRC241	20	192000	crack	2	22	100
Imp.	Const.	30	0NC1CWC242	20	340000	crack	2	22	100
Imp.	Const.	30	0NC1CWC243	20	260000	crack	2	22	100
Imp.	Const.	30	0NC1CWC251	24	193000	crack	2	26	100
Imp.	Const.	30	0NC1CRC311	8	1989000	crack	10	18	100

(continued on next page)

Table F.7.1. Fatigue Test Data (continued)

Units	Load Type	Detail	ID Number	Stress Range	Cycles	Result	Min. Stress	Max. Stress	Yield Stress
Imp.	Const.	30	0NC1CWC312	8	2916000	crack	10	18	100
Imp.	Const.	30	0NC1CWC313	8	3409000	crack	10	18	100
Imp.	Const.	30	0NC1CRC321	12	822000	crack	10	22	100
Imp.	Const.	30	0NC1CWC322	12	1005000	crack	10	22	100
Imp.	Const.	30	0NC1CWC323	12	1220000	crack	10	22	100
Imp.	Const.	30	0NC1CRC324	12	755000	crack	10	22	100
Imp.	Const.	30	0NC1CRC331	16	413000	crack	10	26	100
Imp.	Const.	30	0NC1CWC332	16	590000	crack	10	26	100
Imp.	Const.	30	0NC1CWC333	16	578000	crack	10	26	100
Imp.	Const.	30	0NC1CRC341	20	239000	crack	10	30	100
Imp.	Const.	30	0NC1CWC342	20	374000	crack	10	30	100
Imp.	Const.	30	0NC1CWC343	20	296000	crack	10	30	100
Imp.	Const.	30	0NC1CRC344	20	207000	crack	10	30	100
Imp.	Const.	40	0NC1CMA131	16	427000	crack	-6	10	36
Imp.	Const.	40	0NC1CMA132	16	412000	crack	-6	10	36
Imp.	Const.	40	0NC1CMA133	16	593000	crack	-6	10	36
Imp.	Const.	40	0NC1CMA141	20	150000	crack	-6	14	36
Imp.	Const.	40	0NC1CMA142	20	190000	crack	-6	14	36
Imp.	Const.	40	0NC1CMA143	20	218000	crack	-6	14	36
Imp.	Const.	40	0NC1CMA151	24	112000	crack	-6	18	36
Imp.	Const.	40	0NC1CMA152	24	80800	crack	-6	18	36
Imp.	Const.	40	0NC1CMA153	24	101000	crack	-6	18	36
Imp.	Const.	40	0NC1CMA221	12	904000	crack	2	14	36
Imp.	Const.	40	0NC1CMA222	12	1034000	crack	2	14	36
Imp.	Const.	40	0NC1CMA223	12	755000	crack	2	14	36
Imp.	Const.	40	0NC1CMA231	16	374000	crack	2	18	36
Imp.	Const.	40	0NC1CMA232	16	346000	crack	2	18	36
Imp.	Const.	40	0NC1CMA233	16	481000	crack	2	18	36
Imp.	Const.	40	0NC1CMA241	20	166000	crack	2	22	36
Imp.	Const.	40	0NC1CMA242	20	186000	crack	2	22	36
Imp.	Const.	40	0NC1CMA243	20	188000	crack	2	22	36
Imp.	Const.	40	0NC1CMA251	24	84500	crack	2	26	36
Imp.	Const.	40	0NC1CMA301	6	8946000	crack	10	16	36
Imp.	Const.	40	0NC1CMA311	8	3211000	crack	10	18	36
Imp.	Const.	40	0NC1CMA312	8	4979000	crack	10	18	36
Imp.	Const.	40	0NC1CMA313	8	4798000	crack	10	18	36
Imp.	Const.	40	0NC1CMA321	12	779000	crack	10	22	36
Imp.	Const.	40	0NC1CMA322	12	632000	crack	10	22	36
Imp.	Const.	40	0NC1CMA323	12	919000	crack	10	22	36

(continued on next page)

Table F.7.1. Fatigue Test Data (continued)

Units	Load Type	Detail	ID Number	Stress Range	Cycles	Result	Min. Stress	Max. Stress	Yield Stress
Imp.	Const.	40	0NC1CMA331	16	423000	crack	10	26	36
Imp.	Const.	40	0NC1CMA332	16	503000	crack	10	26	36
Imp.	Const.	40	0NC1CMA333	16	371000	crack	10	26	36
Imp.	Const.	40	0NC1CMA341	20	190000	crack	10	30	36
Imp.	Const.	40	0NC1CTA131	16	320000	crack	-6	10	36
Imp.	Const.	40	0NC1CTA132	16	392000	crack	-6	10	36
Imp.	Const.	40	0NC1CTA133	16	266000	crack	-6	10	36
Imp.	Const.	40	0NC1CTA141	20	160000	crack	-6	14	36
Imp.	Const.	40	0NC1CTA142	20	121000	crack	-6	14	36
Imp.	Const.	40	0NC1CTA143	20	123000	crack	-6	14	36
Imp.	Const.	40	0NC1CTA151	24	80700	crack	-6	18	36
Imp.	Const.	40	0NC1CTA152	24	105000	crack	-6	18	36
Imp.	Const.	40	0NC1CTA153	24	83300	crack	-6	18	36
Imp.	Const.	40	0NC1CTA221	12	949000	crack	2	14	36
Imp.	Const.	40	0NC1CTA222	12	951000	crack	2	14	36
Imp.	Const.	40	0NC1CTA223	12	977000	crack	2	14	36
Imp.	Const.	40	0NC1CTA231	16	343000	crack	2	18	36
Imp.	Const.	40	0NC1CTA232	16	358000	crack	2	18	36
Imp.	Const.	40	0NC1CTA233	16	473000	crack	2	18	36
Imp.	Const.	40	0NC1CTA241	20	172000	crack	2	22	36
Imp.	Const.	40	0NC1CTA242	20	167000	crack	2	22	36
Imp.	Const.	40	0NC1CTA243	20	226000	crack	2	22	36
Imp.	Const.	40	0NC1CTA311	8	3729000	crack	10	18	36
Imp.	Const.	40	0NC1CTA312	8	3679000	crack	10	18	36
Imp.	Const.	40	0NC1CTA313	8	3218000	crack	10	18	36
Imp.	Const.	40	0NC1CTA321	12	1011000	crack	10	22	36
Imp.	Const.	40	0NC1CTA322	12	856000	crack	10	22	36
Imp.	Const.	40	0NC1CTA323	12	1186000	crack	10	22	36
Imp.	Const.	40	0NC1CTA331	16	334000	crack	10	26	36
Imp.	Const.	40	0NC1CTA332	16	598000	crack	10	26	36
Imp.	Const.	40	0NC1CTA333	16	433000	crack	10	26	36
Imp.	Const.	40	0NC1CTA341	20	185000	crack	10	30	36
Imp.	Const.	40	0NC1CTA342	20	141000	crack	10	30	36
Imp.	Const.	40	0NC1CTA343	20	274000	crack	10	30	36
Imp.	Const.	60	0NC1CBA131	16	353000	crack	-6	10	36
Imp.	Const.	60	0NC1CBA132	16	276000	crack	-6	10	36
Imp.	Const.	60	0NC1CBA133	16	291000	crack	-6	10	36
Imp.	Const.	60	0NC1CBA141	20	186000	crack	-6	14	36
Imp.	Const.	60	0NC1CBA142	20	158000	crack	-6	14	36

(continued on next page)

Table F.7.1. Fatigue Test Data (continued)

Units	Load Type	Detail	ID Number	Stress Range	Cycles	Result	Min. Stress	Max. Stress	Yield Stress
Imp.	Const.	60	0NC1CBA143	20	204000	crack	-6	14	36
Imp.	Const.	60	0NC1CBA151	24	89300	crack	-6	18	36
Imp.	Const.	60	0NC1CBA152	24	97000	crack	-6	18	36
Imp.	Const.	60	0NC1CBA153	24	70500	crack	-6	18	36
Imp.	Const.	60	0NC1CBA221	12	1769000	crack	2	14	36
Imp.	Const.	60	0NC1CBA222	12	1139000	crack	2	14	36
Imp.	Const.	60	0NC1CBA223	12	1109000	crack	2	14	36
Imp.	Const.	60	0NC1CBA231	16	500000	crack	2	18	36
Imp.	Const.	60	0NC1CBA232	16	444000	crack	2	18	36
Imp.	Const.	60	0NC1CBA233	16	410000	crack	2	18	36
Imp.	Const.	60	0NC1CBA241	20	208000	crack	2	22	36
Imp.	Const.	60	0NC1CBA242	20	176000	crack	2	22	36
Imp.	Const.	60	0NC1CBA243	20	155000	crack	2	22	36
Imp.	Const.	60	0NC1CBA311	8	3589000	crack	10	18	36
Imp.	Const.	60	0NC1CBA312	8	3461000	crack	10	18	36
Imp.	Const.	60	0NC1CBA313	8	4707000	crack	10	18	36
Imp.	Const.	60	0NC1CBA321	12	1113000	crack	10	22	36
Imp.	Const.	60	0NC1CBA322	12	879000	crack	10	22	36
Imp.	Const.	60	0NC1CBA323	12	908000	crack	10	22	36
Imp.	Const.	60	0NC1CBA331	16	278000	crack	10	26	36
Imp.	Const.	60	0NC1CBA332	16	473000	crack	10	26	36
Imp.	Const.	60	0NC1CBA333	16	523000	crack	10	26	36
Imp.	Const.	60	0NC1CBA341	20	120000	crack	10	30	36
Imp.	Const.	60	0NC1CBA342	20	148000	crack	10	30	36
Imp.	Const.	60	0NC1CBA343	20	234000	crack	10	30	36
Imp.	Const.	50	0NC1CBA131	16	308000	crack	-6	10	36
Imp.	Const.	50	0NC1CBA132	16	157000	crack	-6	10	36
Imp.	Const.	50	0NC1CBA133	16	199000	crack	-6	10	36
Imp.	Const.	50	0NC1CBA141	20	186000	crack	-6	14	36
Imp.	Const.	50	0NC1CBA142	20	158000	crack	-6	14	36
Imp.	Const.	50	0NC1CBA143	20	122000	crack	-6	14	36
Imp.	Const.	50	0NC1CBA151	24	77000	crack	-6	18	36
Imp.	Const.	50	0NC1CBA152	24	47500	crack	-6	18	36
Imp.	Const.	50	0NC1CBA153	24	53600	crack	-6	18	36
Imp.	Const.	50	0NC1CBA221	12	558000	crack	2	14	36
Imp.	Const.	50	0NC1CBA222	12	433000	crack	2	14	36
Imp.	Const.	50	0NC1CBA223	12	441000	crack	2	14	36
Imp.	Const.	50	0NC1CBA231	16	232000	crack	2	18	36
Imp.	Const.	50	0NC1CBA232	16	179000	crack	2	18	36

(continued on next page)



Table F.7.1. Fatigue Test Data (continued)

Units	Load Type	Detail	ID Number	Stress Range	Cycles	Result	Min. Stress	Max. Stress	Yield Stress
Imp.	Const.	50	0NC1CBA233	16	198000	crack	2	18	36
Imp.	Const.	50	0NC1CBA241	20	99700	crack	2	22	36
Imp.	Const.	50	0NC1CBA242	20	103000	crack	2	22	36
Imp.	Const.	50	0NC1CBA243	20	142000	crack	2	22	36
Imp.	Const.	50	0NC1CBA311	8	1534000	crack	10	18	36
Imp.	Const.	50	0NC1CBA312	8	1212000	crack	10	18	36
Imp.	Const.	50	0NC1CBA313	8	1374000	crack	10	18	36
Imp.	Const.	50	0NC1CBA321	12	386000	crack	10	22	36
Imp.	Const.	50	0NC1CBA322	12	313000	crack	10	22	36
Imp.	Const.	50	0NC1CBA323	12	551000	crack	10	22	36
Imp.	Const.	50	0NC1CBA331	16	150000	crack	10	26	36
Imp.	Const.	50	0NC1CBA332	16	209000	crack	10	26	36
Imp.	Const.	50	0NC1CBA333	16	221000	crack	10	26	36
Imp.	Const.	50	0NC1CBA341	20	68700	crack	10	30	36
Imp.	Const.	50	0NC1CBA342	20	101000	crack	10	30	36
Imp.	Const.	50	0NC1CBA343	20	136000	crack	10	30	36
Imp.	Const.	27	0NC1PWA131	30	677000	crack	-10	20	36
Imp.	Const.	26	0NC1PWA132	30	506000	crack	-10	20	36
Imp.	Const.	25	0NC1PWA141	36	413000	crack	-10	26	36
Imp.	Const.	20	0NC1PWA142	36	432000	crack	-10	26	36
Imp.	Const.	27	0NC1PWA151	42	113000	crack	-10	32	36
Imp.	Const.	27	0NC1PWA152	42	258000	crack	-10	32	36
Imp.	Const.	20	0NC1PWA221	24	1577000	crack	2	26	36
Imp.	Const.	20	0NC1PWA222	24	1910000	crack	2	26	36
Imp.	Const.	20	0NC1PWA231	30	705000	crack	2	32	36
Imp.	Const.	25	0NC1PWA232	30	832000	crack	2	32	36
Imp.	Const.	20	0NC1PWA241	36	389000	crack	2	38	36
Imp.	Const.	20	0NC1PWA242	36	546000	crack	2	38	36
Imp.	Const.	20	0NC1PWA311	18	10200000	runout	14	32	36
Imp.	Const.	25	0NC1PWA312	18	9654000	crack	14	32	36
Imp.	Const.	20	0NC1PWA321	24	1490000	crack	14	38	36
Imp.	Const.	20	0NC1PWA322	24	2021000	crack	14	38	36
Imp.	Const.	20	0NC1PWB131	30	855000	crack	-10	20	50
Imp.	Const.	20	0NC1PWB132	30	998000	crack	-10	20	50
Imp.	Const.	20	0NC1PWB141	36	505000	crack	-10	26	50
Imp.	Const.	25	0NC1PWB142	36	514000	crack	-10	26	50
Imp.	Const.	26	0NC1PWB151	42	149000	crack	-10	32	50
Imp.	Const.	20	0NC1PWB152	42	317000	crack	-10	32	50
Imp.	Const.	26	0NC1PWB221	24	1292000	crack	2	26	50

(continued on next page)

Table F.7.1. Fatigue Test Data (continued)

Units	Load Type	Detail	ID Number	Stress Range	Cycles	Result	Min. Stress	Max. Stress	Yield Stress
Imp.	Const.	25	0NC1PWB222	24	1593000	crack	2	26	50
Imp.	Const.	20	0NC1PWB231	30	742000	crack	2	32	50
Imp.	Const.	20	0NC1PWB232	30	1129000	crack	2	32	50
Imp.	Const.	20	0NC1PWB241	36	481000	crack	2	38	50
Imp.	Const.	20	0NC1PWB242	36	382000	crack	2	38	50
Imp.	Const.	25	0NC1PWB311	18	3080000	crack	14	32	50
Imp.	Const.	20	0NC1PWB312	18	4465000	crack	14	32	50
Imp.	Const.	25	0NC1PWB321	24	1523000	crack	14	38	50
Imp.	Const.	20	0NC1PWB322	24	2054000	crack	14	38	50
Imp.	Const.	20	0NC1PWB331	30	563000	crack	14	44	50
Imp.	Const.	25	0NC1PWB332	30	847000	crack	14	44	50
Imp.	Const.	26	0NC1PWB341	36	192000	crack	14	50	50
Imp.	Const.	25	0NC1PWB342	36	719000	crack	14	50	50
Imp.	Const.	27	0NC1PWC131	30	783000	crack	-10	20	100
Imp.	Const.	27	0NC1PWC132	30	858000	crack	-10	20	100
Imp.	Const.	20	0NC1PWC141	36	486000	crack	-10	26	100
Imp.	Const.	21	0NC1PWC142	36	561000	crack	-10	26	100
Imp.	Const.	21	0NC1PWC151	42	389000	crack	-10	32	100
Imp.	Const.	25	0NC1PWC152	42	397000	crack	-10	32	100
Imp.	Const.	20	0NC1PWC221	24	2228000	crack	2	26	100
Imp.	Const.	20	0NC1PWC222	24	1526000	crack	2	26	100
Imp.	Const.	20	0NC1PWC231	30	693000	crack	2	32	100
Imp.	Const.	20	0NC1PWC232	30	685000	crack	2	32	100
Imp.	Const.	20	0NC1PWC241	36	357000	crack	2	38	100
Imp.	Const.	25	0NC1PWC242	36	452000	crack	2	38	100
Imp.	Const.	20	0NC1PWC311	18	2368000	crack	14	32	100
Imp.	Const.	20	0NC1PWC312	18	2137000	crack	14	32	100
Imp.	Const.	20	0NC1PWC321	24	1319000	crack	14	38	100
Imp.	Const.	20	0NC1PWC322	24	1466000	crack	14	38	100
Imp.	Const.	20	0NC1PWC331	30	670000	crack	14	44	100
Imp.	Const.	20	0NC1PWC332	30	1020000	crack	14	44	100
Imp.	Const.	25	0NC1PWC341	36	319000	crack	14	50	100
Imp.	Const.	25	0NC1PWC342	36	534000	crack	14	50	100
Imp.	Const.	15	0NC1PRA131	30	1505000	crack	-10	20	36
Imp.	Const.	10	0NC1PRA132	30	4910000	runout	-10	20	36
Imp.	Const.	15	0NC1PRA141	36	1290000	crack	-10	26	36
Imp.	Const.	15	0NC1PRA142	36	1343000	crack	-10	26	36
Imp.	Const.	15	0NC1PRA151	42	623000	crack	-10	32	36
Imp.	Const.	10	0NC1PRA152	42	1070000	crack	-10	32	36

(continued on next page)

Table F.7.1. Fatigue Test Data (continued)

Units	Load Type	Detail	ID Number	Stress Range	Cycles	Result	Min. Stress	Max. Stress	Yield Stress
Imp.	Const.	10	0NC1PRA231	30	12200000	runout	2	32	36
Imp.	Const.	10	0NC1PRA232	30	10500000	runout	2	32	36
Imp.	Const.	10	0NC1PRA241	36	855000	crack	2	38	36
Imp.	Const.	10	0NC1PRA242	36	998000	crack	2	38	36
Imp.	Const.	15	0NC1PRB141	36	1207000	crack	-10	26	50
Imp.	Const.	15	0NC1PRB142	36	826000	crack	-10	26	50
Imp.	Const.	15	0NC1PRB151	42	1001000	crack	-10	32	50
Imp.	Const.	10	0NC1PRB152	42	1820000	crack	-10	32	50
Imp.	Const.	10	0NC1PRB231	30	2677000	crack	2	32	50
Imp.	Const.	10	0NC1PRB241	36	1519000	crack	2	38	50
Imp.	Const.	15	0NC1PRB242	36	978000	crack	2	38	50
Imp.	Const.	10	0NC1PRB251	42	592000	crack	2	44	50
Imp.	Const.	10	0NC1PRB252	42	692000	crack	2	44	50
Imp.	Const.	15	0NC1PRB331	30	2401000	crack	14	44	50
Imp.	Const.	15	0NC1PRB341	36	5850000	crack	14	50	50
Imp.	Const.	15	0NC1PRB342	36	846000	crack	14	50	50
Imp.	Const.	20	0NC1FSA221	15.8	5808000	crack	1.7	-1	36
Imp.	Const.	20	0NC1FSA211	17.5	6953000	crack	1.9	-1	36
Imp.	Const.	20	0NC1FSA212	13.5	6117000	crack	1.5	-1	36
Imp.	Const.	20	0NC1FSA212	17.8	7754000	crack	2	-1	36
Imp.	Const.	20	0NC1FSA213	18	6413000	crack	2	-1	36
Imp.	Const.	20	0NC1FSA213	13.3	9105000	crack	1.5	-1	36
Imp.	Const.	20	0NC1FSA311	18	10500000	runout	14	-1	36
Imp.	Const.	20	0NC1FSA312	18	12200000	runout	14	-1	36
Imp.	Const.	20	0NC1FSA313	18	11400000	runout	14	-1	36
Imp.	Const.	20	0NC1FSA121	22.7	2908000	crack	-9.5	-1	36
Imp.	Const.	21	0NC1FSA121	18.4	3687000	crack	7.7	-1	36
Imp.	Const.	21	0NC1FSA122	23.7	3508000	crack	9.9	-1	36
Imp.	Const.	21	0NC1FSA123	21.8	1945000	crack	9.1	-1	36
Imp.	Const.	21	0NC1FSA123	23.3	2897000	crack	9.7	-1	36
Imp.	Const.	20	0NC1FSA221	23.7	2255000	crack	2	-1	36
Imp.	Const.	21	0NC1FSA221	20.6	2255000	crack	-1.8	-1	36
Imp.	Const.	20	0NC1FSA223	25.7	1575000	crack	2.1	-1	36
Imp.	Const.	20	0NC1FSA223	23.5	2257000	crack	2	-1	36
Imp.	Const.	20	0NC1FSA322	24.3	2539000	crack	14.2	-1	36
Imp.	Const.	20	0NC1FSA323	22.2	4769000	crack	12.9	-1	36
Imp.	Const.	20	0NC1FSA131	27.3	2227000	crack	-9.1	-1	36
Imp.	Const.	20	0NC1FSA132	28.9	1217000	crack	-9.6	-1	36
Imp.	Const.	20	0NC1FSA132	29.2	1516000	crack	-9.7	-1	36

(continued on next page)

Table F.7.1. Fatigue Test Data (continued)

Units	Load Type	Detail	ID Number	Stress Range	Cycles	Result	Min. Stress	Max. Stress	Yield Stress
Imp.	Const.	20	0NC1FSA133	27.5	965000	crack	-9.2	-1	36
Imp.	Const.	20	0NC1FSA133	28.7	1135000	crack	-9.6	-1	36
Imp.	Const.	20	0NC1FSA231	29.6	1205000	crack	2	-1	36
Imp.	Const.	20	0NC1FSA232	30.7	782000	crack	2	-1	36
Imp.	Const.	20	0NC1FSA232	29.6	782000	crack	2	-1	36
Imp.	Const.	21	0NC1FSA141	34	883000	crack	9.4	-1	36
Imp.	Const.	20	0NC1FSA141	34.5	1185000	crack	-9.6	-1	36
Imp.	Const.	20	0NC1FSA142	35.3	1160000	crack	-9.8	-1	36
Imp.	Const.	20	0NC1FSA143	31	914000	crack	-8.6	-1	36
Imp.	Const.	20	0NC1FSA143	31	914000	crack	-8.6	-1	36
Imp.	Const.	20	0NC1FSA241	30.8	334000	crack	1.7	-1	36
Imp.	Const.	20	0NC1FSA241	26.6	749000	crack	1.5	-1	36
Imp.	Const.	20	0NC1FSA243	35.3	691000	crack	1.9	-1	36
Imp.	Const.	20	0NC1FSB312	13	10550000	crack	10.2	-1	50
Imp.	Const.	20	0NC1FSB221	22.6	1859000	crack	1.9	-1	50
Imp.	Const.	20	0NC1FSB222	24	1917000	crack	2	-1	50
Imp.	Const.	20	0NC1FSB223	24.1	1035000	crack	2	-1	50
Imp.	Const.	20	0NC1FSB321	22.3	2289000	crack	13.1	-1	50
Imp.	Const.	20	0NC1FSB322	20.3	2520000	crack	11.8	-1	50
Imp.	Const.	20	0NC1FSB322	24	10500000	runout	14	-1	50
Imp.	Const.	21	0NC1FSB132	29.2	1491000	crack	9.8	-1	50
Imp.	Const.	21	0NC1FSB133	24.5	1201000	crack	8.2	-1	50
Imp.	Const.	20	0NC1FSB133	27.9	1523000	crack	-9.3	-1	50
Imp.	Const.	20	0NC1FSB231	29	970000	crack	1.9	-1	50
Imp.	Const.	20	0NC1FSB232	30	949000	crack	2	-1	50
Imp.	Const.	20	0NC1FSB232	27.5	1498000	crack	1.8	-1	50
Imp.	Const.	20	0NC1FSB233	27.9	1091000	crack	1.9	-1	50
Imp.	Const.	20	0NC1FSB233	28.6	1375000	crack	1.9	-1	50
Imp.	Const.	20	0NC1FSB331	30.6	560000	crack	14.3	-1	50
Imp.	Const.	20	0NC1FSB332	28.1	818000	crack	13.1	-1	50
Imp.	Const.	20	0NC1FSB332	30.8	1414000	crack	14.4	-1	50
Imp.	Const.	21	0NC1FSB141	36	425000	crack	10	-1	50
Imp.	Const.	20	0NC1FSB142	34.2	776000	crack	-9.5	-1	50
Imp.	Const.	21	0NC1FSB143	35.5	636000	crack	9.9	-1	50
Imp.	Const.	20	0NC1FSB143	33.2	961000	crack	-9.2	-1	50
Imp.	Const.	20	0NC1FSB241	36.4	821000	crack	2	-1	50
Imp.	Const.	20	0NC1FSB242	35	288000	crack	1.9	-1	50
Imp.	Const.	20	0NC1FSB243	35.4	775000	crack	2	-1	50
Imp.	Const.	20	0NC1FSB341	35.8	543000	crack	14	-1	50

(continued on next page)

Table F.7.1. Fatigue Test Data (continued)

Units	Load Type	Detail	ID Number	Stress Range	Cycles	Result	Min. Stress	Max. Stress	Yield Stress
Imp.	Const.	20	0NC1FSB341	35	989000	crack	13.6	-1	50
Imp.	Const.	20	0NC1FSB342	30.8	471000	crack	12	-1	50
Imp.	Const.	20	0NC1FSB343	34.3	511000	crack	7.9	-1	50
Imp.	Const.	20	0NC1FSC311	12.5	3704000	crack	9.7	-1	100
Imp.	Const.	20	0NC1FSC311	17.6	9807000	crack	13.7	-1	100
Imp.	Const.	20	0NC1FSC313	17.4	2807000	crack	13.5	-1	100
Imp.	Const.	20	0NC1FSC221	22.8	2021000	crack	1.9	-1	100
Imp.	Const.	20	0NC1FSC222	24.7	2479000	crack	2	-1	100
Imp.	Const.	20	0NC1FSC223	23.1	1302000	crack	1.9	-1	100
Imp.	Const.	20	0NC1FSC223	15	5706000	crack	1.2	-1	100
Imp.	Const.	20	0NC1FSC321	24.2	1031000	crack	14.2	-1	100
Imp.	Const.	20	0NC1FSC323	24	1102000	crack	14	-1	100
Imp.	Const.	21	0NC1FSC131	27.5	1259000	crack	9.2	-1	100
Imp.	Const.	21	0NC1FSC132	30	1263000	crack	10	-1	100
Imp.	Const.	21	0NC1FSC132	21.7	1592000	crack	7.2	-1	100
Imp.	Const.	20	0NC1FSC133	29.2	887000	crack	-9.7	-1	100
Imp.	Const.	20	0NC1FSC231	29.2	658000	crack	1.9	-1	100
Imp.	Const.	20	0NC1FSC232	23.8	1211000	crack	1.6	-1	100
Imp.	Const.	20	0NC1FSC233	27.9	1112000	crack	1.9	-1	100
Imp.	Const.	20	0NC1FSC333	29.2	1184000	crack	13.6	-1	100
Imp.	Const.	21	0NC1FSC141	35	562000	crack	9.7	-1	100
Imp.	Const.	21	0NC1FSC142	34.3	483000	crack	9.5	-1	100
Imp.	Const.	20	0NC1FSC241	33	341000	crack	1.8	-1	100
Imp.	Const.	20	0NC1FSC241	36.4	562000	crack	2	-1	100
Imp.	Const.	20	0NC1FSC242	34.4	403000	crack	1.9	-1	100
Imp.	Const.	20	0NC1FSC242	29.1	403000	crack	1.6	-1	100
Imp.	Const.	20	0NC1FSC341	36	334000	crack	14	-1	100
Imp.	Const.	20	0NC1FSC343	35.9	1001000	crack	12.3	-1	100
Imp.	Const.	80	0NC1FSA122	22.6	3778000	crack	-9.4	-1	36
Imp.	Const.	80	0NC1FSA222	24	10300000	runout	2	-1	36
Imp.	Const.	70	0NC1FSA222	24	10300000	runout	2	-1	36
Imp.	Const.	80	0NC1FSA321	24	1834000	crack	14	-1	36
Imp.	Const.	80	0NC1FSA322	24	10900000	runout	14	-1	36
Imp.	Const.	70	0NC1FSA322	24	10900000	runout	14	-1	36
Imp.	Const.	70	0NC1FSA323	24.3	3137000	crack	14.2	-1	36
Imp.	Const.	80	0NC1FSA131	28	989000	crack	-9.3	-1	36
Imp.	Const.	80	0NC1FSA231	30	3910000	runout	2	-1	36
Imp.	Const.	70	0NC1FSA231	30	3910000	runout	2	-1	36
Imp.	Const.	70	0NC1FSA233	30.3	803000	crack	2	-1	36

(continued on next page)

Table F.7.1. Fatigue Test Data (continued)

Units	Load Type	Detail	ID Number	Stress Range	Cycles	Result	Min. Stress	Max. Stress	Yield Stress
Imp.	Const.	80	0NC1FSA233	29.2	1743000	crack	1.9	-1	36
Imp.	Const.	80	0NC1FSA142	36	734000	crack	-10	-1	36
Imp.	Const.	70	0NC1FSA241	34.2	749000	crack	1.9	-1	36
Imp.	Const.	80	0NC1FSA242	36	456000	crack	2	-1	36
Imp.	Const.	70	0NC1FSA242	35.3	1039000	crack	2	-1	36
Imp.	Const.	80	0NC1FSA243	36	427000	crack	2	-1	36
Imp.	Const.	80	0NC1FSB313	18	3068000	crack	14	-1	50
Imp.	Const.	80	0NC1FSB221	22.3	2627000	crack	1.8	-1	50
Imp.	Const.	80	0NC1FSB222	24	1592000	crack	2	-1	50
Imp.	Const.	80	0NC1FSB223	24	828000	crack	2	-1	50
Imp.	Const.	80	0NC1FSB321	24	1239000	crack	14	-1	50
Imp.	Const.	80	0NC1FSB323	24	1366000	crack	14	-1	50
Imp.	Const.	70	0NC1FSB323	24.3	3056000	crack	14.2	-1	50
Imp.	Const.	70	0NC1FSB131	29.9	1147000	crack	-9.9	-1	50
Imp.	Const.	80	0NC1FSB131	28	1288000	crack	-9.3	-1	50
Imp.	Const.	70	0NC1FSB132	29.6	1321000	crack	-9.9	-1	50
Imp.	Const.	80	0NC1FSB231	25.8	422000	crack	1.7	-1	50
Imp.	Const.	80	0NC1FSB331	30	514000	crack	14	-1	50
Imp.	Const.	80	0NC1FSB333	30	521000	crack	14.4	-1	50
Imp.	Const.	70	0NC1FSB333	30	1354000	crack	14.4	-1	50
Imp.	Const.	80	0NC1FSB141	36	839000	crack	-10	-1	50
Imp.	Const.	80	0NC1FSB142	36	733000	crack	-10	-1	50
Imp.	Const.	80	0NC1FSB241	35.7	505000	crack	2	-1	50
Imp.	Const.	80	0NC1FSB242	36	288000	crack	2	-1	50
Imp.	Const.	80	0NC1FSB243	36	299000	crack	2	-1	50
Imp.	Const.	80	0NC1FSB342	36	333000	crack	14	-1	50
Imp.	Const.	80	0NC1FSB343	36	325000	crack	14	-1	50
Imp.	Const.	80	0NC1FSC312	18.9	835000	crack	14.8	-1	100
Imp.	Const.	70	0NC1FSC312	18.4	9840000	runout	14	-1	100
Imp.	Const.	70	0NC1FSC313	18	12200000	runout	14	-1	100
Imp.	Const.	80	0NC1FSC313	18	12200000	runout	14	-1	100
Imp.	Const.	80	0NC1FSC221	24	1500000	crack	2	-1	100
Imp.	Const.	80	0NC1FSC222	22.2	1170000	crack	1.9	-1	100
Imp.	Const.	80	0NC1FSC321	24	657000	crack	14	-1	100
Imp.	Const.	80	0NC1FSC322	24	658000	crack	14	-1	100
Imp.	Const.	70	0NC1FSC322	24	800000	crack	14	-1	100
Imp.	Const.	80	0NC1FSC323	24	566000	crack	14	-1	100
Imp.	Const.	70	0NC1FSC131	29.6	1259000	crack	-9.8	-1	100
Imp.	Const.	80	0NC1FSC132	26	1592000	crack	-8.7	-1	100

(continued on next page)

Table F.7.1. Fatigue Test Data (continued)

Units	Load Type	Detail	ID Number	Stress Range	Cycles	Result	Min. Stress	Max. Stress	Yield Stress
Imp.	Const.	80	0NC1FSC133	30	1239000	crack	-10	-1	100
Imp.	Const.	80	0NC1FSC231	29.6	759000	crack	2	-1	100
Imp.	Const.	80	0NC1FSC232	30	953000	crack	2	-1	100
Imp.	Const.	80	0NC1FSC233	30	532000	crack	2	-1	100
Imp.	Const.	80	0NC1FSC331	29.8	406000	crack	13.9	-1	100
Imp.	Const.	70	0NC1FSC331	30.3	907000	crack	14.2	-1	100
Imp.	Const.	80	0NC1FSC332	27.8	764000	crack	13	-1	100
Imp.	Const.	70	0NC1FSC332	30.8	1310000	crack	14.4	-1	100
Imp.	Const.	80	0NC1FSC333	28.8	511000	crack	13.4	-1	100
Imp.	Const.	80	0NC1FSC141	35.1	700000	crack	-9.7	-1	100
Imp.	Const.	80	0NC1FSC142	36	483000	crack	-10	-1	100
Imp.	Const.	70	0NC1FSC143	35.8	463000	crack	-10	-1	100
Imp.	Const.	80	0NC1FSC143	34.9	811000	crack	-9.7	-1	100
Imp.	Const.	80	0NC1FSC243	36	333000	crack	2	-1	100
Imp.	Const.	70	0NC1FSC243	36	731000	crack	2	-1	100
Imp.	Const.	70	0NC1FSC341	29.6	274000	crack	11.6	-1	100
Imp.	Const.	80	0NC1FSC342	35.5	335000	crack	13.8	-1	100
Imp.	Const.	70	0NC1FSC342	35.5	619000	crack	13.8	-1	100
Imp.	Const.	80	0NC1FSC343	32.5	343000	crack	14	-1	100
Imp.	Const.	17	0NC1PRB141	36	4799000	crack	-10	-1	50
Imp.	Const.	11	0NC1PRB142	36	4456000	crack	-10	-1	50
Imp.	Const.	15	0NC1PRB151	42	1670000	crack	-10	-1	50
Imp.	Const.	15	0NC1PRB151	42	1670000	crack	-10	-1	50
Imp.	Const.	10	0NC1PRB231	30	10800000	runout	2	-1	50
Imp.	Const.	10	0NC1PRB241	36	1857000	crack	2	-1	50
Imp.	Const.	10	0NC1PRB251	42	845000	crack	2	-1	50
Imp.	Const.	10	0NC1PRB331	30	6382000	crack	14	-1	50
Imp.	Const.	10	0NC1PRB341	36	7866000	crack	14	-1	50
Imp.	Const.	90	0NC2SCB211	13.7	2893000	crack	1.5	-1	50
Imp.	Const.	90	0NC2SCB212	13.7	9740000	runout	1.5	-1	50
Imp.	Const.	90	0NC2SCB213	13.7	7040000	runout	1.5	-1	50
Imp.	Const.	90	0NC2SCB311	13.7	13100000	runout	10.6	-1	50
Imp.	Const.	90	0NC2SCB312	13.7	3197000	crack	10.6	-1	50
Imp.	Const.	90	0NC2SCB221	18.2	2907000	crack	1.5	-1	50
Imp.	Const.	90	0NC2SCB222	18.2	3165000	crack	1.5	-1	50
Imp.	Const.	90	0NC2SCB223	18.2	2320000	runout	1.5	-1	50
Imp.	Const.	90	0NC2SCB321	18.2	1830000	runout	10.6	-1	50
Imp.	Const.	90	0NC2SCB322	18.2	1481000	crack	10.6	-1	50
Imp.	Const.	90	0NC2SCB131	22.8	1119000	crack	-7.6	-1	50

(continued on next page)



Table F.7.1. Fatigue Test Data (continued)

Units	Load Type	Detail	ID Number	Stress Range	Cycles	Result	Min. Stress	Max. Stress	Yield Stress
Imp.	Const.	90	0NC2SCB132	22.8	1210000	crack	-7.6	-1	50
Imp.	Const.	90	0NC2SCB231	22.8	774000	crack	1.5	-1	50
Imp.	Const.	90	0NC2SCB232	22.8	860000	crack	1.5	-1	50
Imp.	Const.	90	0NC2SCB233	22.8	1030000	runout	1.5	-1	50
Imp.	Const.	90	0NC2SCB331	22.8	1150000	crack	10.6	-1	50
Imp.	Const.	90	0NC2SCB332	22.8	819000	crack	10.6	-1	50
Imp.	Const.	90	0NC2SCB141	27.4	867000	crack	-7.6	-1	50
Imp.	Const.	90	0NC2SCB142	27.4	574000	crack	-7.6	-1	50
Imp.	Const.	90	0NC2SCB241	27.4	521000	crack	1.5	-1	50
Imp.	Const.	90	0NC2SCB242	27.4	676000	crack	1.5	-1	50
Imp.	Const.	90	0NC2SCB243	27.4	669000	crack	1.5	-1	50
Imp.	Const.	90	0NC2SAB111	17.6	4770000	crack	4.4	-1	50
Imp.	Const.	90	0NC2SAB112	17.6	3190000	crack	4.4	-1	50
Imp.	Const.	90	0NC2SAB113	17.6	3425000	crack	4.4	-1	50
Imp.	Const.	90	0NC2SAB114	17.6	6227000	crack	4.4	-1	50
Imp.	Const.	90	0NC2SAB221	23.8	883000	crack	6.9	-1	50
Imp.	Const.	90	0NC2SAB222	23.8	1017000	crack	6.9	-1	50
Imp.	Const.	90	0NC2SAB223	23.8	1161000	crack	6.9	-1	50
Imp.	Const.	90	0NC2SAB224	23.8	1064000	crack	6.9	-1	50
Imp.	Const.	90	0NC2SGB211	15.4	4433000	crack	1.7	-1	50
Imp.	Const.	90	0NC2SGC212	15.4	3016000	crack	1.7	-1	100
Imp.	Const.	90	0NC2SGB311	15.4	4869000	crack	12	-1	50
Imp.	Const.	90	0NC2SGB312	15.4	2293000	crack	12	-1	50
Imp.	Const.	90	0NC2SGB221	20.5	1939000	crack	1.7	-1	50
Imp.	Const.	90	0NC2SGC222	20.5	838000	crack	1.7	-1	100
Imp.	Const.	90	0NC2SGB321	20.5	769000	crack	12	-1	50
Imp.	Const.	90	0NC2SGB322	20.5	1210000	crack	12	-1	50
Imp.	Const.	90	0NC2SGB323	20.5	774000	crack	12	-1	50
Imp.	Const.	90	0NC2SGB231	25.7	643000	crack	1.7	-1	50
Imp.	Const.	90	0NC2SGC232	25.7	452000	crack	1.7	-1	100
Imp.	Const.	90	0NC2SGB331	25.7	413000	crack	12	-1	50
Imp.	Const.	90	0NC2SGB332	25.7	500000	crack	12	-1	50
Imp.	Const.	90	0NC2SGC333	25.7	401000	crack	12	-1	100
Imp.	Const.	90	0NC2SBB221	20.5	1264000	crack	1.7	-1	50
Imp.	Const.	90	0NC2SBB222	20.5	1409000	crack	1.7	-1	50
Imp.	Const.	90	0NC2SBB321	20.5	1388000	crack	1.7	-1	50
Imp.	Const.	90	0NC2SBB322	20.5	1401000	crack	1.7	-1	50
Imp.	Const.	90	0NC2SBB231	25.7	1037000	crack	1.7	-1	50
Imp.	Const.	90	0NC2SBB232	25.7	561000	crack	1.7	-1	50

(continued on next page)

Table F.7.1. Fatigue Test Data (continued)

Units	Load Type	Detail	ID Number	Stress Range	Cycles	Result	Min. Stress	Max. Stress	Yield Stress
Imp.	Const.	90	0NC2SBB331	25.7	577000	crack	1.7	-1	50
Imp.	Const.	90	0NC2SBB332	25.7	555000	crack	1.7	-1	50
Imp.	Const.	90	0NC2SGB211	13.7	4430000	runout	1.5	-1	50
Imp.	Const.	90	0NC2SGC212	13.7	1790000	crack	1.5	-1	100
Imp.	Const.	90	0NC2SGC212	13.7	1790000	crack	1.5	-1	100
Imp.	Const.	90	0NC2SGB311	13.7	5230000	runout	10.7	-1	50
Imp.	Const.	90	0NC2SGB312	13.7	2204000	crack	10.7	-1	50
Imp.	Const.	90	0NC2SGB312	13.7	2012000	crack	10.7	-1	50
Imp.	Const.	90	0NC2SGB221	18.3	1165000	crack	1.5	-1	50
Imp.	Const.	90	0NC2SGC222	18.3	838000	crack	1.5	-1	100
Imp.	Const.	90	0NC2SGC222	18.3	838000	crack	1.5	-1	100
Imp.	Const.	90	0NC2SGB321	18.3	1063000	crack	10.7	-1	50
Imp.	Const.	90	0NC2SGB322	18.3	1553000	crack	10.7	-1	50
Imp.	Const.	90	0NC2SGB323	18.3	1131000	crack	10.7	-1	50
Imp.	Const.	90	0NC2SGB231	22.9	552000	crack	1.5	-1	50
Imp.	Const.	90	0NC2SGC232	22.9	452000	crack	1.5	-1	100
Imp.	Const.	90	0NC2SGC232	22.9	452000	crack	1.5	-1	100
Imp.	Const.	90	0NC2SGB332	22.9	786000	crack	10.7	-1	50
Imp.	Const.	90	0NC2SGB332	22.9	481000	crack	10.7	-1	50
Imp.	Const.	90	0NC2SGC333	22.9	537000	crack	10.7	-1	100
Imp.	Const.	90	0NC2SBB221	18.3	1264000	crack	1.5	-1	50
Imp.	Const.	90	0NC2SBB222	18.3	1234000	crack	1.5	-1	50
Imp.	Const.	90	0NC2SBB321	18.3	1388000	crack	1.5	-1	50
Imp.	Const.	90	0NC2SBB321	18.3	1388000	crack	1.5	-1	50
Imp.	Const.	90	0NC2SBB322	18.3	1329000	crack	1.5	-1	50
Imp.	Const.	90	0NC2SBB322	18.3	1401000	crack	1.5	-1	50
Imp.	Const.	90	0NC2SBB231	22.9	718000	crack	1.5	-1	50
Imp.	Const.	90	0NC2SBB231	22.9	718000	crack	1.5	-1	50
Imp.	Const.	90	0NC2SBB232	22.9	533000	crack	1.5	-1	50
Imp.	Const.	90	0NC2SBB232	22.9	533000	crack	1.5	-1	50
Imp.	Const.	90	0NC2SBB331	22.9	684000	crack	1.5	-1	50
Imp.	Const.	90	0NC2SBB331	22.9	684000	crack	1.5	-1	50
Imp.	Const.	90	0NC2SBB332	22.9	499000	crack	1.5	-1	50
Imp.	Const.	90	0NC2SBB332	22.9	725000	crack	1.5	-1	50
Imp.	Const.	100	0NC2SCB211	14.4	2616000	crack	1.6	-1	50
Imp.	Const.	100	0NC2SCB212	14.4	3787000	crack	1.6	-1	50
Imp.	Const.	100	0NC2SCB213	14.4	4512000	crack	1.6	-1	50
Imp.	Const.	100	0NC2SCB311	14.4	4741000	crack	11.2	-1	50
Imp.	Const.	100	0NC2SCB312	14.4	3197000	crack	11.2	-1	50

(continued on next page)

Table F.7.1. Fatigue Test Data (continued)

Units	Load Type	Detail	ID Number	Stress Range	Cycles	Result	Min. Stress	Max. Stress	Yield Stress
Imp.	Const.	100	0NC2SCB221	19.2	1691000	crack	1.6	-1	50
Imp.	Const.	100	0NC2SCB222	19.2	1329000	crack	1.6	-1	50
Imp.	Const.	100	0NC2SCB223	19.2	807000	crack	1.6	-1	50
Imp.	Const.	100	0NC2SCB321	19.2	1438000	crack	11.2	-1	50
Imp.	Const.	100	0NC2SCB322	19.2	1092000	crack	11.2	-1	50
Imp.	Const.	100	0NC2SCB131	23.9	584000	crack	-8	-1	50
Imp.	Const.	100	0NC2SCB132	23.9	579000	crack	-8	-1	50
Imp.	Const.	100	0NC2SCB231	23.9	492000	crack	1.6	-1	50
Imp.	Const.	100	0NC2SCB232	23.9	527000	crack	1.6	-1	50
Imp.	Const.	100	0NC2SCB233	23.9	421000	crack	1.6	-1	50
Imp.	Const.	100	0NC2SCB331	23.9	322000	crack	11.2	-1	50
Imp.	Const.	100	0NC2SCB332	23.9	428000	crack	11.2	-1	50
Imp.	Const.	100	0NC2SCB141	28.7	355000	crack	-8	-1	50
Imp.	Const.	100	0NC2SCB142	28.7	302000	crack	-8	-1	50
Imp.	Const.	100	0NC2SCB241	28.7	214000	crack	1.6	-1	50
Imp.	Const.	100	0NC2SCB242	28.7	361000	crack	1.6	-1	50
Imp.	Const.	100	0NC2SCB243	28.7	495000	crack	1.6	-1	50
Imp.	Const.	100	0NC2SGB211	13.8	6620000	runout	1.5	-1	50
Imp.	Const.	100	0NC2SGC212	13.8	3850000	runout	1.5	-1	100
Imp.	Const.	100	0NC2SGB311	13.8	6060000	runout	10.7	-1	50
Imp.	Const.	100	0NC2SGB312	13.8	2012000	crack	10.7	-1	50
Imp.	Const.	100	0NC2SGB221	18.4	1742000	crack	1.5	-1	50
Imp.	Const.	100	0NC2SGC222	18.4	1366000	crack	1.5	-1	100
Imp.	Const.	100	0NC2SGB321	18.4	1316000	crack	10.7	-1	50
Imp.	Const.	100	0NC2SGB322	18.4	1553000	crack	10.7	-1	50
Imp.	Const.	100	0NC2SGB323	18.4	1261000	crack	10.7	-1	50
Imp.	Const.	100	0NC2SGB231	22.9	676000	crack	1.5	-1	50
Imp.	Const.	100	0NC2SGC232	22.9	737000	crack	1.5	-1	100
Imp.	Const.	100	0NC2SGB331	22.9	786000	crack	10.7	-1	50
Imp.	Const.	100	0NC2SGB332	22.9	700000	crack	10.7	-1	50
Imp.	Const.	100	0NC2SGC333	22.9	627000	crack	10.7	-1	100
Imp.	Const.	100	0NC2SGC333	22.9	627000	crack	10.7	-1	100
Imp.	Const.	100	0NC2SBB221	18.4	1264000	crack	1.5	-1	50
Imp.	Const.	100	0NC2SBB222	18.4	1641000	crack	1.5	-1	50
Imp.	Const.	100	0NC2SBB321	18.4	1206000	crack	1.5	-1	50
Imp.	Const.	100	0NC2SBB322	18.4	1329000	crack	1.5	-1	50
Imp.	Const.	100	0NC2SBB231	22.9	1037000	crack	1.5	-1	50
Imp.	Const.	100	0NC2SBB232	22.9	561000	crack	1.5	-1	50
Imp.	Const.	100	0NC2SBB331	22.9	804000	crack	1.5	-1	50

(continued on next page)

Table F.7.1. Fatigue Test Data (continued)

Units	Load Type	Detail	ID Number	Stress Range	Cycles	Result	Min. Stress	Max. Stress	Yield Stress
Imp.	Const.	100	0NC2SBB332	22.9	950000	crack	1.5	-1	50
Imp.	Const.	130	0NC2AQB221	12	10800000	runout	2	-1	50
Imp.	Const.	130	0NC2AQB321	12	15600000	runout	2	-1	50
Imp.	Const.	130	0NC2AQB131	16	3095000	crack	-6	-1	50
Imp.	Const.	130	0NC2AQB131	16	3619000	crack	-6	-1	50
Imp.	Const.	130	0NC2AQB231	16	3113000	crack	2	-1	50
Imp.	Const.	130	0NC2AQB331	16	3703000	crack	10	-1	50
Imp.	Const.	130	0NC2AQB141	20	1096000	crack	-6	-1	50
Imp.	Const.	130	0NC2AQB141	20	1096000	crack	-6	-1	50
Imp.	Const.	130	0NC2AQB241	20	1616000	crack	2	-1	50
Imp.	Const.	130	0NC2AQB241	20	1861000	crack	2	-1	50
Imp.	Const.	130	0NC2AQB341	20	1593000	crack	10	-1	50
Imp.	Const.	130	0NC2AQB341	20	1821000	crack	10	-1	50
Imp.	Const.	130	0NC2AQB161	28	353000	crack	-6	-1	50
Imp.	Const.	130	0NC2AQB161	28	440000	crack	-6	-1	50
Imp.	Const.	130	0NC2AQB261	28	506000	crack	2	-1	50
Imp.	Const.	130	0NC2AQB261	28	521000	crack	2	-1	50
Imp.	Const.	130	0NC2A2B221	12	3812000	crack	2	-1	50
Imp.	Const.	130	0NC2A2B221	12	3911000	crack	2	-1	50
Imp.	Const.	130	0NC2A2B321	12	2881000	crack	10	-1	50
Imp.	Const.	130	0NC2A2B321	12	4368000	crack	10	-1	50
Imp.	Const.	130	0NC2A2B231	16	1121000	crack	2	-1	50
Imp.	Const.	130	0NC2A2B231	16	1258000	crack	2	-1	50
Imp.	Const.	130	0NC2A2B331	16	1168000	crack	10	-1	50
Imp.	Const.	130	0NC2A2B331	16	1476000	crack	10	-1	50
Imp.	Const.	130	0NC2A2B241	20	658000	crack	2	-1	50
Imp.	Const.	130	0NC2A2B241	20	685000	crack	2	-1	50
Imp.	Const.	130	0NC2A2B341	20	543000	crack	10	-1	50
Imp.	Const.	130	0NC2A2B341	20	627000	crack	10	-1	50
Imp.	Const.	130	0NC2A2B261	28	242000	crack	2	-1	50
Imp.	Const.	130	0NC2A2B261	28	250000	crack	2	-1	50
Imp.	Const.	130	0NC2A8B211	8	6111000	crack	2	-1	50
Imp.	Const.	130	0NC2A8B211	8	6317000	crack	2	-1	50
Imp.	Const.	130	0NC2A8B311	8	2866000	crack	10	-1	50
Imp.	Const.	130	0NC2A8B311	8	7004000	crack	10	-1	50
Imp.	Const.	130	0NC2A8B221	8.9	2960000	crack	1.5	-1	50
Imp.	Const.	130	0NC2A8B221	8.9	3681000	crack	1.5	-1	50
Imp.	Const.	130	0NC2A8B221	12	808000	crack	2	-1	50
Imp.	Const.	130	0NC2A8B321	12	1147000	crack	10	-1	50

(continued on next page)

Table F.7.1. Fatigue Test Data (continued)

Units	Load Type	Detail	ID Number	Stress Range	Cycles	Result	Min. Stress	Max. Stress	Yield Stress
Imp.	Const.	130	0NC2A8B321	12	1225000	crack	10	-1	50
Imp.	Const.	130	0NC2A8B131	16	595000	crack	-6	-1	50
Imp.	Const.	130	0NC2A8B131	16	714000	crack	-6	-1	50
Imp.	Const.	130	0NC2A8B231	16	491000	crack	2	-1	50
Imp.	Const.	130	0NC2A8B231	16	885000	crack	2	-1	50
Imp.	Const.	130	0NC2A8B331	16	518000	crack	10	-1	50
Imp.	Const.	130	0NC2A8B331	16	714000	crack	10	-1	50
Imp.	Const.	130	0NC2A8B141	20	279000	crack	-6	-1	50
Imp.	Const.	130	0NC2A8B141	20	279000	crack	-6	-1	50
Imp.	Const.	130	0NC2A8B241	20	192000	crack	2	-1	50
Imp.	Const.	130	0NC2A8B241	20	213000	crack	2	-1	50
Imp.	Const.	130	0NC2A8B341	14.9	786000	crack	7.4	-1	50
Imp.	Const.	130	0NC2A8B341	14.9	855000	crack	7.4	-1	50
Imp.	Const.	130	0NC2A8B341	20	175000	crack	10	-1	50
Imp.	Const.	130	0NC2A8B341	20	190000	crack	10	-1	50
Imp.	Const.	130	0NC2A8B151	24	165000	crack	-6	-1	50
Imp.	Const.	130	0NC2A8B151	24	165000	crack	-6	-1	50
Imp.	Const.	130	0NC2A8B251	24	167000	crack	2	-1	50
Imp.	Const.	135	0NC2A4B211	8	6023000	crack	2	-1	50
Imp.	Const.	135	0NC2A4B212	8	5621000	crack	2	-1	50
Imp.	Const.	135	0NC2A4B311	5.9	13600000	runout	7.4	-1	50
Imp.	Const.	135	0NC2A4B312	8	9057000	crack	10	-1	50
Imp.	Const.	135	0NC2A4B221	12	2439000	crack	2	-1	50
Imp.	Const.	135	0NC2A4B222	8.9	4844000	crack	1.5	-1	50
Imp.	Const.	135	0NC2A4B321	12	1208000	crack	10	-1	50
Imp.	Const.	135	0NC2A4B322	12	2154000	crack	10	-1	50
Imp.	Const.	135	0NC2A4B131	16	850000	crack	-6	-1	50
Imp.	Const.	135	0NC2A4B132	16	931000	crack	-6	-1	50
Imp.	Const.	135	0NC2A4B231	16	785000	crack	2	-1	50
Imp.	Const.	135	0NC2A4B232	16	760000	crack	2	-1	50
Imp.	Const.	135	0NC2A4B331	16	732000	crack	10	-1	50
Imp.	Const.	135	0NC2A4B332	11.9	2205000	crack	7.4	-1	50
Imp.	Const.	135	0NC2A4B141	20	589000	crack	-6	-1	50
Imp.	Const.	135	0NC2A4B142	20	491000	crack	-6	-1	50
Imp.	Const.	135	0NC2A4B241	20	593000	crack	2	-1	50
Imp.	Const.	135	0NC2A4B242	20	486000	crack	2	-1	50
Imp.	Const.	135	0NC2A4B341	20	526000	crack	10	-1	50
Imp.	Const.	135	0NC2A4B342	20	440000	crack	10	-1	50
Imp.	Const.	135	0NC1A4B161	28	181000	crack	-6	-1	50

(continued on next page)

Table F.7.1. Fatigue Test Data (continued)

Units	Load Type	Detail	ID Number	Stress Range	Cycles	Result	Min. Stress	Max. Stress	Yield Stress
Imp.	Const.	135	0NC2A4B162	28	161000	crack	-6	-1	50
Imp.	Const.	135	0NC2A4B261	28	175000	crack	2	-1	50
Imp.	Const.	135	0NC2A4B262	28	227000	crack	2	-1	50
Imp.	Const.	135	0NC2A4B221	12	1858000	crack	2	-1	50
Imp.	Const.	130	0NC2A4B222	8.9	7177000	crack	1.5	-1	50
Imp.	Const.	130	0NC2A4B222	12	1124000	crack	2	-1	50
Imp.	Const.	130	0NC2A4B321	12	1509000	crack	10	-1	50
Imp.	Const.	130	0NC2A4B322	12	1743000	crack	10	-1	50
Imp.	Const.	130	0NC2A4B131	16	793000	crack	-6	-1	50
Imp.	Const.	130	0NC2A4B132	16	801000	crack	-6	-1	50
Imp.	Const.	130	0NC2A4B231	16	819000	crack	2	-1	50
Imp.	Const.	130	0NC2A4B232	16	652000	crack	2	-1	50
Imp.	Const.	130	0NC2A4B331	16	882000	crack	10	-1	50
Imp.	Const.	130	0NC2A4B332	11.9	2205000	crack	7.4	-1	50
Imp.	Const.	130	0NC2A4B332	16	499000	crack	10	-1	50
Imp.	Const.	130	0NC1A4B332	16	536000	crack	10	-1	50
Imp.	Const.	130	0NC1A4B141	20	310000	crack	-6	-1	50
Imp.	Const.	130	0NC1A4B142	20	378000	crack	-6	-1	50
Imp.	Const.	130	0NC2A4B241	20	305000	crack	2	-1	50
Imp.	Const.	130	0NC2A4B242	20	400000	crack	2	-1	50
Imp.	Const.	130	0NC2A4B341	20	401000	crack	10	-1	50
Imp.	Const.	130	0NC2A4B342	20	368000	crack	10	-1	50
Imp.	Const.	130	0NC2A4B161	28	116000	crack	-6	-1	50
Imp.	Const.	130	0NC2A4B162	28	123000	crack	-6	-1	50
Imp.	Const.	130	0NC2A4B161	28	101000	crack	2	-1	50
Imp.	Const.	130	0NC2A4B262	28	143000	crack	2	-1	50
Imp.	Const.	11	0NC2PRC041	36	3113000	crack	-22	-1	100
Imp.	Const.	10	0NC2PRC061	45	759000	crack	-22	-1	100
Imp.	Const.	10	0NC2PRC241	34.3	10000000	runout	1.9	-1	100
Imp.	Const.	10	0NC2PRC242	34.3	10000000	runout	1.9	-1	100
Imp.	Const.	10	0NC2PRC261	45.7	702000	crack	1.9	-1	100
Imp.	Const.	16	0NC2PRC262	45	338000	crack	2	-1	100
Imp.	Const.	10	0NC2PRC342	34.3	10000000	runout	13.3	-1	100
Imp.	Const.	15	0NC2PRC441	34.3	5194000	crack	24.8	-1	100
Imp.	Const.	17	0NC2PRC042	36	1983000	crack	-22	-1	100
Imp.	Const.	18	0NC2PRC062	45	1789000	crack	-22	-1	100
Imp.	Const.	17	0NC2PRC081	54	247000	crack	-22	-1	100
Imp.	Const.	17	0NC2PRC083	54	1067000	crack	-22	-1	100
Imp.	Const.	15	0NC2PRC082	54	1164000	crack	-22	-1	100

(continued on next page)

Table F.7.1. Fatigue Test Data (continued)

Units	Load Type	Detail	ID Number	Stress Range	Cycles	Result	Min. Stress	Max. Stress	Yield Stress
Imp.	Const.	10	0NC2PRC243	36	1000000	runout	2	-1	100
Imp.	Const.	18	0NC2PRC244	36	3090000	crack	2	-1	100
Imp.	Const.	15	0NC2PRC263	45	2284000	crack	2	-1	100
Imp.	Const.	15	0NC2PRC264	45	1242000	crack	2	-1	100
Imp.	Const.	15	0NC2PRC281	54	440000	crack	2	-1	100
Imp.	Const.	18	0NC2PRC282	54	238000	crack	2	-1	100
Imp.	Const.	18	0NC2PRC283	54	645000	crack	2	-1	100
Imp.	Const.	15	0NC2PRC343	36	2396000	crack	14	-1	100
Imp.	Const.	10	0NC2PRC344	36	1000000	runout	14	-1	100
Imp.	Const.	16	0NC2PRC381	54	211000	crack	14	-1	100
Imp.	Const.	15	0NC2PRC382	51.4	615000	crack	13.3	-1	100
Imp.	Const.	15	0NC2PRC383	54	1196000	crack	14	-1	100
Imp.	Const.	16	0NC2PRC442	20.5	2846000	crack	26	-1	100
Imp.	Const.	10	0NC2PRC461	45	558000	crack	26	-1	100
Imp.	Const.	10	0NC2PRC462	42.8	2717000	crack	24.8	-1	100
Imp.	Const.	20	0NC2SGB211	18	4433000	crack	2	-1	50
Imp.	Const.	20	0NC2SGC212	18	2194000	crack	2	-1	100
Imp.	Const.	20	0NC2SGB311	18	3230000	crack	14	-1	50
Imp.	Const.	20	0NC2SGB312	18	2012000	crack	14	-1	50
Imp.	Const.	20	0NC2SGB221	24	1046000	crack	2	-1	50
Imp.	Const.	20	0NC2SGC222	24	838000	crack	2	-1	100
Imp.	Const.	20	0NC2SGB321	24	1063000	crack	14	-1	50
Imp.	Const.	20	0NC2SGB322	24	1052000	crack	14	-1	50
Imp.	Const.	20	0NC2SGB323	24	1131000	crack	14	-1	50
Imp.	Const.	20	0NC2SGB231	30	520000	crack	2	-1	50
Imp.	Const.	20	0NC2SGC232	30	452000	crack	2	-1	100
Imp.	Const.	20	0NC2SGB331	30	746000	crack	14	-1	50
Imp.	Const.	20	0NC2SGB332	30	539000	crack	14	-1	50
Imp.	Const.	20	0NC2SGC333	30	627000	crack	14	-1	100
Imp.	Const.	20	0NC2SBB221	24	1197000	crack	2	-1	50
Imp.	Const.	20	0NC2SBB222	24	1061000	crack	2	-1	50
Imp.	Const.	20	0NC2SBB321	24	1388000	crack	2	-1	50
Imp.	Const.	20	0NC2SBB322	24	1401000	crack	2	-1	50
Imp.	Const.	20	0NC2SBB231	30	718000	crack	2	-1	50
Imp.	Const.	20	0NC2SBB232	30	533000	crack	2	-1	50
Imp.	Const.	20	0NC2SBB331	30	684000	crack	2	-1	50
Imp.	Const.	20	0NC2SBB332	30	725000	crack	2	-1	50
Imp.	Const.	17	0NC2PRC083	54	1067000	crack	-22	-1	100
Imp.	Const.	40	1NC3010002	8	950000	crack	-1	-1	50

(continued on next page)



Table F.7.1. Fatigue Test Data (continued)

Units	Load Type	Detail	ID Number	Stress Range	Cycles	Result	Min. Stress	Max. Stress	Yield Stress
Imp.	Const.	40	1NC3010003	8	1090000	crack	-1	-1	100
Imp.	Const.	40	1NC3010004	8	1400000	crack	-1	-1	36
Imp.	Const.	40	1NC3010005	8	1450000	crack	-1	-1	36
Imp.	Const.	40	1NC3010006	8	1530000	crack	-1	-1	36
Imp.	Const.	40	1NC3010007	8	1550000	crack	-1	-1	50
Imp.	Const.	40	1NC3010008	8	1650000	crack	-1	-1	50
Imp.	Const.	40	1NC3010009	8	1770000	crack	-1	-1	100
Imp.	Const.	40	1NC3010010	8	2010000	crack	-1	-1	50
Imp.	Const.	40	1NC3010011	8	2150000	crack	-1	-1	50
Imp.	Const.	40	1NC3010012	8	2060000	crack	-1	-1	50
Imp.	Const.	40	1NC3010013	8	2100000	crack	-1	-1	36
Imp.	Const.	40	1NC3010014	6	2120000	crack	-1	-1	36
Imp.	Const.	40	1NC3010015	8	2360000	crack	-1	-1	50
Imp.	Const.	40	1NC3010016	8	2580000	crack	-1	-1	50
Imp.	Const.	40	1NC3010017	8	2970000	crack	-1	-1	36
Imp.	Const.	40	1NC3010018	8	3880000	crack	-1	-1	50
Imp.	Const.	40	1NC3010019	6	3490000	crack	-1	-1	50
Imp.	Const.	40	1NC3010020	6	5070000	crack	-1	-1	36
Imp.	Const.	40	1NC3010021	6	7650000	crack	-1	-1	50
Imp.	Const.	40	1NC3010022	6	9480000	crack	-1	-1	50
Imp.	Const.	40	1NC3010023	6	11300000	crack	-1	-1	50
Imp.	Const.	40	1NC3010024	4	12600000	crack	-1	-1	50
Imp.	Const.	40	1NC3010025	6	21500000	runout	-1	-1	50
Imp.	Const.	40	1NC3010026	6	23800000	runout	-1	-1	36
Imp.	Const.	40	1NC3010027	6	27200000	runout	-1	-1	50
Imp.	Const.	40	1NC3010028	4	32500000	crack	-1	-1	36
Imp.	Const.	40	1NC3010029	4	41700000	runout	-1	-1	50
Imp.	Const.	40	1NC3010030	4	48100000	runout	-1	-1	50
Imp.	Const.	40	1NC3010031	4	48500000	runout	-1	-1	50
Imp.	Const.	40	1NC3010032	4	58000000	runout	-1	-1	36
Imp.	Const.	40	1NC3010033	4	58500000	runout	-1	-1	36
Imp.	Const.	40	1NC3010034	4	66300000	runout	-1	-1	36
Imp.	Const.	230	1NC4A10101	21	160000	crack	-1	-1	36
Imp.	Const.	230	1NC4A10102	21	170000	crack	-1	-1	36
Imp.	Const.	230	1NC4A10103	15	850000	crack	-1	-1	36
Imp.	Const.	230	1NC4A10104	15	920000	crack	-1	-1	36
Imp.	Const.	230	1NC4A10105	12	930000	crack	-1	-1	36
Imp.	Const.	230	1NC4A10106	12	1060000	crack	-1	-1	36
Imp.	Const.	230	1NC4A10107	9	4900000	crack	-1	-1	36

(continued on next page)

Table F.7.1. Fatigue Test Data (continued)

Units	Load Type	Detail	ID Number	Stress Range	Cycles	Result	Min. Stress	Max. Stress	Yield Stress
Imp.	Const.	230	1NC4A10108	9	9480000	runout	-1	-1	36
Imp.	Const.	230	1NC4A10201	12	1240000	crack	-1	-1	36
Imp.	Const.	230	1NC4A10202	12	1970000	crack	-1	-1	36
Imp.	Const.	230	1NC4A10203	12	2190000	crack	-1	-1	36
Imp.	Const.	230	1NC4A10204	12	2440000	crack	-1	-1	36
Imp.	Const.	230	1NC4A20101	15	490000	crack	-1	-1	36
Imp.	Const.	230	1NC4A20102	15	530000	crack	-1	-1	36
Imp.	Const.	230	1NC4A20103	12	1150000	crack	-1	-1	36
Imp.	Const.	230	1NC4A20104	12	1280000	crack	-1	-1	36
Imp.	Const.	230	1NC4A20105	9	1430000	crack	-1	-1	36
Imp.	Const.	230	1NC4A20106	9	1510000	crack	-1	-1	36
Imp.	Const.	230	1NC4A20107	12	2040000	crack	-1	-1	36
Imp.	Const.	230	1NC4A20108	12	2060000	crack	-1	-1	36
Imp.	Const.	230	1NC4A20109	9	3550000	crack	-1	-1	36
Imp.	Const.	230	1NC4A20110	9	4020000	runout	-1	-1	36
Imp.	Const.	230	1NC4A20111	6	12000000	runout	-1	-1	36
Imp.	Const.	230	1NC4A20112	6	13000000	runout	-1	-1	36
Imp.	Const.	120	1NC4A30101	15	400000	crack	-1	-1	36
Imp.	Const.	120	1NC4A30102	15	620000	crack	-1	-1	36
Imp.	Const.	120	1NC4A30103	15	700000	crack	-1	-1	36
Imp.	Const.	120	1NC4A30104	15	740000	crack	-1	-1	36
Imp.	Const.	120	1NC4A30105	9	1380000	crack	-1	-1	36
Imp.	Const.	120	1NC4A30106	9	1800000	crack	-1	-1	36
Imp.	Const.	120	1NC4A30107	12	1870000	crack	-1	-1	36
Imp.	Const.	120	1NC4A30108	12	2230000	runout	-1	-1	36
Imp.	Const.	120	1NC4A30109	6	8670000	crack	-1	-1	36
Imp.	Const.	120	1NC4A30110	6	9480000	runout	-1	-1	36
Imp.	Const.	120	1NC4A30111	6	13500000	runout	-1	-1	36
Imp.	Const.	251	1NC4A50101	21	160000	crack	-1	-1	36
Imp.	Const.	251	1NC4A50102	12	970000	runout	-1	-1	36
Imp.	Const.	251	1NC4A50103	15	1160000	runout	-1	-1	36
Imp.	Const.	251	1NC4A50104	12	1610000	runout	-1	-1	36
Imp.	Const.	251	1NC4A50105	12	1870000	runout	-1	-1	36
Imp.	Const.	251	1NC4A50106	10	9710000	runout	-1	-1	36
Imp.	Const.	256	1NC4A50201	15	860000	runout	-1	-1	36
Imp.	Const.	256	1NC4A50202	15	1390000	runout	-1	-1	36
Imp.	Const.	256	1NC4A50203	12.2	2380000	runout	-1	-1	36
Imp.	Const.	256	1NC4A50204	12.2	3510000	runout	-1	-1	36
Imp.	Const.	256	1NC4A50205	9	4020000	runout	-1	-1	36

(continued on next page)

Table F.7.1. Fatigue Test Data (continued)

Units	Load Type	Detail	ID Number	Stress Range	Cycles	Result	Min. Stress	Max. Stress	Yield Stress
Imp.	Const.	256	1NC4A50206	9	7310000	runout	-1	-1	36
Imp.	Const.	256	1NC4A50207	6	18200000	runout	-1	-1	36
Imp.	Const.	256	1NC4A50301	15	760000	crack	-1	-1	36
Imp.	Const.	256	1NC4A50302	12.2	2000000	runout	-1	-1	36
Imp.	Const.	256	1NC4A50303	10	2680000	runout	-1	-1	36
Imp.	Const.	256	1NC4A50304	6	9280000	runout	-1	-1	36
Imp.	Const.	256	1NC4A50305	6	13100000	runout	-1	-1	36
Imp.	Const.	120	1NC4A60301	5.7	4330000	crack	-1	-1	36
Imp.	Const.	120	1NC4A60201	11.4	780000	crack	-1	-1	36
Imp.	Const.	120	1NC4A60401	8.8	1770000	crack	-1	-1	36
Imp.	Const.	120	1NC4A60402	11.4	1430000	crack	-1	-1	36
Imp.	Const.	121	1NC4A70901	11.4	1500000	crack	-1	-1	36
Imp.	Const.	125	1NC4A80901	11.4	1080000	crack	-1	-1	36
Imp.	Const.	120	1NC4A61801	6.2	4940000	crack	-1	-1	36
Imp.	Const.	120	1NC4A61802	8.1	4960000	crack	-1	-1	36
Imp.	Const.	121	1NC4A71001	8.6	960000	crack	-1	-1	36
Imp.	Const.	121	1NC4A71002	6.6	980000	crack	-1	-1	36
Imp.	Const.	125	1NC4A81301	11.7	910000	crack	-1	-1	36
Imp.	Const.	125	1NC4A81101	14.3	350000	crack	-1	-1	36
Imp.	Const.	125	1NC4A81601	10.4	500000	crack	-1	-1	36
Imp.	Const.	125	1NC4A81602	13.5	520000	crack	-1	-1	36
Imp.	Const.	120	1NC4A60601	9.3	680000	crack	-1	-1	36
Imp.	Const.	120	1NC4A60602	9.3	940000	crack	-1	-1	36
Imp.	Const.	121	1NC4A70701	5.1	3300000	crack	-1	-1	36
Imp.	Const.	121	1NC4A70702	7	3500000	crack	-1	-1	36
Imp.	Const.	121	1NC4A70801	6.8	1170000	crack	-1	-1	36
Imp.	Const.	121	1NC4A70802	9.3	1170000	crack	-1	-1	36
Imp.	Const.	121	1NC4A70803	9.3	1060000	crack	-1	-1	36
Imp.	Const.	125	1NC4A80801	6.8	1190000	crack	-1	-1	36
Imp.	Const.	125	1NC4A80801	9.3	1060000	crack	-1	-1	36
Imp.	Const.	125	1NC4A81201	7.3	970000	crack	-1	-1	36
Imp.	Const.	125	1NC4A81201	10	550000	crack	-1	-1	36
Imp.	Const.	125	1NC4A81501	11.6	140000	crack	-1	-1	36
Imp.	Const.	125	1NC4A81701	5.1	8630000	crack	-1	-1	36
Imp.	Const.	334	1NC4A50101	14	340000	crack	-1	-1	36
Imp.	Const.	334	1NC4A50102	12.2	350000	crack	-1	-1	36
Imp.	Const.	334	1NC4A50103	12.2	420000	crack	-1	-1	36
Imp.	Const.	334	1NC4A50104	12.2	560000	crack	-1	-1	36
Imp.	Const.	334	1NC4A50105	10.6	1220000	crack	-1	-1	36

(continued on next page)

Table F.7.1. Fatigue Test Data (continued)

Units	Load Type	Detail	ID Number	Stress Range	Cycles	Result	Min. Stress	Max. Stress	Yield Stress
Imp.	Const.	334	1NC4A50106	5	350000	crack	-1	-1	36
Imp.	Const.	334	1NC4A50201	12.8	70000	crack	-1	-1	36
Imp.	Var.	120	1NC600A1WW	3.6	22900000	crack	-2	-1	50
Imp.	Var.	120	1NC600A1MW	3.6	17800000	crack	-2	-1	50
Imp.	Var.	120	1NC600A1EW	3.6	17800000	crack	-2	-1	50
Imp.	Var.	120	1NC600A1EE	3.6	15500000	crack	-2	-1	50
Imp.	Var.	120	1NC600A2WE	4.2	19000000	crack	-2	-1	50
Imp.	Var.	120	1NC600A2EE	4.2	16500000	crack	-2	-1	50
Imp.	Var.	120	1NC600B1WW	2.2	71000000	crack	-2	-1	50
Imp.	Var.	120	1NC600B1EE	2.2	70000000	crack	-2	-1	50
Imp.	Var.	120	1NC600B2WW	2.6	40500000	crack	-2	-1	50
Imp.	Var.	120	1NC600B2WE	2.6	31200000	crack	-2	-1	50
Imp.	Var.	120	1NC600B2MW	2.6	31200000	crack	-2	-1	50
Imp.	Var.	120	1NC600B2ME	2.6	35700000	crack	-2	-1	50
Imp.	Var.	120	1NC600B2EW	2.6	28100000	crack	-2	-1	50
Imp.	Var.	120	1NC600C1WW	2.6	13600000	crack	-2	-1	50
Imp.	Var.	120	1NC600C1WW	3.5	13600000	crack	-1	-1	50
Imp.	Var.	120	1NC600C1WE	3.5	11900000	crack	-1	-1	50
Imp.	Var.	120	1NC600C1MW	3.5	9100000	crack	-1	-1	50
Imp.	Var.	120	1NC600C1EW	3.5	13000000	crack	-1	-1	50
Imp.	Var.	120	1NC600C1EE	3.5	16800000	crack	-1	-1	50
Imp.	Var.	120	1NC600C2WW	4	16100000	crack	-1	-1	50
Imp.	Var.	120	1NC600C2WE	4	15700000	crack	-1	-1	50
Imp.	Var.	120	1NC600C2MW	4	13000000	crack	-1	-1	50
Imp.	Var.	120	1NC600C2EW	4	13600000	crack	-1	-1	50
Imp.	Var.	120	1NC600C2EE	4	10700000	crack	-1	-1	50
Imp.	Var.	120	1NC600D1WW	2.9	103600000	crack	-1	-1	50
Imp.	Var.	120	1NC600D1WE	2.9	116200000	crack	-1	-1	50
Imp.	Var.	120	1NC600D1MW	2.9	112200000	crack	-1	-1	50
Imp.	Var.	120	1NC600D1ME	2.9	112200000	crack	-1	-1	50
Imp.	Var.	120	1NC600D1EE	2.9	103600000	crack	-1	-1	50
Imp.	Var.	120	1NC600D1EW	2.9	127000000	crack	-1	-1	50
Imp.	Var.	120	1NC600D2WW	2.9	110000000	crack	-1	-1	50
Imp.	Var.	120	1NC600D2WE	2.9	110000000	crack	-1	-1	50
Imp.	Var.	120	1NC600D2MW	2.9	110000000	crack	-1	-1	50
Imp.	Var.	120	1NC600D2ME	2.9	110000000	crack	-1	-1	50
Imp.	Var.	120	1NC600D2EW	2.9	110000000	crack	-1	-1	50
Imp.	Var.	120	1NC600D2EE	2.9	110000000	crack	-1	-1	50
Imp.	Var.	40	1NC600A101	3.4	25900000	crack	-2	-1	50

(continued on next page)

Table F.7.1. Fatigue Test Data (continued)

Units	Load Type	Detail	ID Number	Stress Range	Cycles	Result	Min. Stress	Max. Stress	Yield Stress
Imp.	Var.	40	1NC600A201	3.6	17500000	crack	-2	-1	50
Imp.	Var.	40	1NC600B101	2.1	200000000	crack	-2	-1	50
Imp.	Var.	40	1NC600B201	2.2	120000000	crack	-2	-1	50
Imp.	Var.	40	1NC600C101	3.7	7250000	crack	-2	-1	50
Imp.	Var.	40	1NC600C201	3.9	10700000	crack	-2	-1	50
Imp.	Var.	40	1NC600D101	2.8	150000000	crack	-2	-1	50
Imp.	Var.	40	1NC600D201	2.8	130000000	crack	-2	-1	50
Imp.	Var.	30	1NC600A102	3.4	30600000	crack	-2	-1	50
Imp.	Var.	30	1NC600A202	3.6	19500000	crack	-2	-1	50
Imp.	Var.	30	1NC600B102	2.1	200000000	crack	-2	-1	50
Imp.	Var.	30	1NC600B202	2.2	150000000	crack	-2	-1	50
Imp.	Var.	30	1NC600C102	3.7	7250000	crack	-2	-1	50
Imp.	Var.	30	1NC600C202	3.9	44000000	crack	-2	-1	50
Imp.	Var.	30	1NC600D102	2.8	140000000	crack	-2	-1	50
Imp.	Var.	30	1NC600D202	2.8	130000000	crack	-2	-1	50
S.I.	Const.	150	1JPN01N022	408	211000	crack	20	-1	600
S.I.	Const.	150	1JPN01N008	343	474000	crack	20	-1	600
S.I.	Const.	150	1JPN01N007	300	2000000	runout	20	-1	600
S.I.	Const.	150	1JPN01N018	313	848000	crack	20	-1	600
S.I.	Const.	150	1JPN01N017	305	1490000	crack	20	-1	600
S.I.	Const.	150	1JPN01N009	352	1610000	runout	20	-1	600
S.I.	Const.	150	1JPN01N014	450	154000	crack	20	-1	600
S.I.	Const.	150	1JPN01N006	287	2040000	runout	20	-1	600
S.I.	Const.	150	1JPN01N010	349	565000	crack	20	-1	600
S.I.	Const.	150	1JPN01S014	303	878000	crack	20	-1	600
S.I.	Const.	150	1JPN01S085	300	2340000	crack	20	-1	600
S.I.	Const.	150	1JPN01S087	349	924000	crack	20	-1	600
S.I.	Const.	150	1JPN01S100	351	506000	crack	20	-1	600
S.I.	Const.	150	1JPN01SA33	300	819000	crack	20	-1	600
S.I.	Const.	150	1JPN01M005	302	290000	crack	20	-1	600
S.I.	Const.	150	1JPN01M036	300	555000	crack	20	-1	600
S.I.	Const.	150	1JPN01M043	301	392000	crack	20	-1	600
S.I.	Const.	150	1JPN01M068	254	1900000	crack	20	-1	600
S.I.	Const.	150	1JPN01M069	254	1050000	crack	20	-1	600
S.I.	Const.	150	1JPN01M0A1	249	2290000	crack	20	-1	600
S.I.	Const.	150	1JPN01M0A2	300	1050000	crack	20	-1	600
S.I.	Const.	150	1JPN01M0B5	250	1490000	crack	20	-1	600
S.I.	Const.	150	1JPN01M096	305	172000	crack	20	-1	600
S.I.	Const.	150	1JPN01M0B4	281	233000	crack	20	-1	600

(continued on next page)

Table F.7.1. Fatigue Test Data (continued)

Units	Load Type	Detail	ID Number	Stress Range	Cycles	Result	Min. Stress	Max. Stress	Yield Stress
S.I.	Const.	150	1JPN01M0B7	243	537000	crack	20	-1	600
S.I.	Const.	150	1JPN01M0B8	280	268000	crack	20	-1	600
S.I.	Const.	150	1JPN01MC18	284	332000	crack	20	-1	600
S.I.	Const.	150	1JPN01M0C5	236	696000	crack	20	-1	600
S.I.	Const.	150	1JPN01LB18	300	348000	crack	20	-1	600
S.I.	Const.	150	1JPN01LB19	301	258000	crack	20	-1	600
S.I.	Const.	150	1JPN01LB20	301	236000	crack	20	-1	600
S.I.	Const.	150	1JPN01L0C7	250	456000	crack	20	-1	600
S.I.	Const.	150	1JPN01L0C9	249	567000	crack	20	-1	600
S.I.	Const.	150	1JPN01LC21	251	530000	crack	20	-1	600
S.I.	Const.	150	1JPN01LC22	200	1210000	crack	20	-1	600
S.I.	Const.	150	1JPN01LC23	200	1690000	crack	20	-1	600
S.I.	Const.	150	1JPN01LB14	182	687000	crack	20	-1	600
S.I.	Const.	150	1JPN01LB17	210	548000	crack	20	-1	600
S.I.	Const.	150	1JPN01LC11	184	1110000	crack	20	-1	600
S.I.	Const.	150	1JPN01LC12	234	470000	crack	20	-1	600
S.I.	Const.	150	1JPN01LC15	183	901000	crack	20	-1	600
S.I.	Const.	150	1JPN01LC20	286	205000	crack	20	-1	600
S.I.	Const.	150	1JPN01L0B6	181	1180000	crack	20	-1	600
S.I.	Const.	150	1JPN01LB11	231	408000	crack	20	-1	600
S.I.	Const.	150	1JPN01LC13	230	602000	crack	20	-1	600
S.I.	Const.	150	1JPN01LC19	278	273000	crack	20	-1	600
S.I.	Const.	150	1JPN01SBA1	140	2200000	crack	20	-1	600
S.I.	Const.	150	1JPN01SBA2	120	4800000	runout	20	-1	600
S.I.	Const.	150	1JPN01SBA3	181	922000	crack	20	-1	600
S.I.	Const.	150	1JPN01SBA4	219	378000	crack	20	-1	600
S.I.	Const.	150	1JPN01SBA5	250	284000	crack	20	-1	600
S.I.	Const.	150	1JPN01SBA6	302	141000	crack	20	-1	600
S.I.	Const.	150	1JPN01SBB1	300	266000	crack	20	-1	600
S.I.	Const.	150	1JPN01SBB2	200	2390000	crack	20	-1	600
S.I.	Const.	150	1JPN01SBC1	299	417000	crack	20	-1	600
S.I.	Const.	150	1JPN01SBC2	250	2920000	crack	20	-1	600
S.I.	Const.	150	1JPN01N023	482	124000	crack	20	-1	600
S.I.	Const.	150	1JPN01N024	426	151000	crack	20	-1	600
S.I.	Const.	150	1JPN01N025	381	187000	crack	20	-1	600
S.I.	Const.	150	1JPN01N037	338	281000	crack	20	-1	600
S.I.	Const.	150	1JPN01N038	308	1110000	crack	20	-1	600
S.I.	Const.	150	1JPN01N039	282	2300000	runout	20	-1	600
S.I.	Const.	160	1JPN1100S1	196	370000	crack	-98	-1	580

(continued on next page)

Table F.7.1. Fatigue Test Data (continued)

Units	Load Type	Detail	ID Number	Stress Range	Cycles	Result	Min. Stress	Max. Stress	Yield Stress
S.I.	Const.	160	1JPN1100S2	196	495000	crack	-131	-2	580
S.I.	Const.	160	1JPN1100S3	196	700000	crack	-164	-5	580
S.I.	Const.	160	1JPN1100S4	196	321000	crack	0	0	580
S.I.	Const.	160	1JPN1100S5	127	3480000	crack	-64	-1	580
S.I.	Const.	160	1JPN1100S6	147	1028000	crack	-74	-1	580
S.I.	Const.	160	1JPN1100S7	147	1792000	crack	-98	-2	580
S.I.	Const.	160	1JPN1100S8	147	1414000	crack	1	0	580
S.I.	Const.	160	1JPN1100S9	147	4700000	runout	-123	-5	580
S.I.	Const.	150	1JPN0200T1	247	1762000	crack	10	-1	800
S.I.	Const.	150	1JPN0200T2	245	1249000	crack	10	-1	800
S.I.	Const.	150	1JPN0200T3	267	527000	crack	10	-1	800
S.I.	Const.	150	1JPN0200T4	220	555000	crack	10	-1	800
S.I.	Const.	150	1JPN0200T5	222	1224000	crack	10	-1	800
S.I.	Const.	150	1JPN0200T7	197	2567000	crack	10	-1	800
S.I.	Const.	150	1JPN0200T8	216	1708000	crack	10	-1	800
S.I.	Const.	150	1JPN0200T9	267	400000	crack	10	-1	800
S.I.	Const.	150	1JPN020T10	199	1243000	crack	10	-1	800
S.I.	Const.	170	1JPN05AB01	135	1200000	crack	-1	-1	800
S.I.	Const.	170	1JPN05AB02	135	1200000	crack	-1	-1	800
S.I.	Const.	170	1JPN05AB03	135	2150000	crack	-1	-1	800
S.I.	Const.	170	1JPN05AB04	125	1200000	crack	-1	-1	800
S.I.	Const.	170	1JPN05AB05	125	1620000	crack	-1	-1	800
S.I.	Const.	170	1JPN05AB06	125	1700000	crack	-1	-1	800
S.I.	Const.	170	1JPN5DEF01	150	1100000	crack	-1	-1	580
S.I.	Const.	170	1JPN5DEF02	150	1210000	crack	-1	-1	580
S.I.	Const.	170	1JPN5DEF03	150	1480000	crack	-1	-1	580
S.I.	Const.	170	1JPN5DEF04	150	1520000	crack	-1	-1	580
S.I.	Const.	170	1JPN5DEF05	150	1600000	crack	-1	-1	580
S.I.	Const.	170	1JPN5DEF06	150	2050000	crack	-1	-1	580
S.I.	Const.	170	1JPN5DEF07	115	1050000	crack	-1	-1	580
S.I.	Const.	170	1JPN5DEF08	115	1680000	crack	-1	-1	580
S.I.	Const.	170	1JPN5DEF09	115	1730000	crack	-1	-1	580
S.I.	Const.	170	1JPN5DEF10	115	1900000	crack	-1	-1	580
S.I.	Const.	170	1JPN5DEF11	115	2050000	crack	-1	-1	580
S.I.	Const.	170	1JPN5DEF12	115	2150000	crack	-1	-1	580
S.I.	Const.	170	1JPN5DEF13	115	2400000	crack	-1	-1	580
S.I.	Const.	170	1JPN5DEF14	115	2750000	crack	-1	-1	580
S.I.	Const.	170	1JPN05G001	115	2150000	crack	-1	-1	800
S.I.	Const.	170	1JPN05G002	115	2350000	crack	-1	-1	800

(continued on next page)



Table F.7.1. Fatigue Test Data (continued)

Units	Load Type	Detail	ID Number	Stress Range	Cycles	Result	Min. Stress	Max. Stress	Yield Stress
S.I.	Const.	150	1JPN09SB01	395	180000	crack	10	1	800
S.I.	Const.	150	1JPN09SB02	395	310000	crack	10	1	800
S.I.	Const.	150	1JPN09SB03	300	375000	crack	10	1	800
S.I.	Const.	150	1JPN09SB04	300	570000	crack	10	1	800
S.I.	Const.	150	1JPN09SB05	290	620000	crack	10	1	800
S.I.	Const.	150	1JPN09SB06	250	1200000	crack	10	1	800
S.I.	Const.	150	1JPN09SB07	250	2100000	runout	10	1	800
S.I.	Const.	150	1JPN09SB08	230	2150000	crack	10	1	800
S.I.	Const.	150	1JPN09SB09	290	500000	crack	10	0	800
S.I.	Const.	150	1JPN09SB10	290	520000	crack	10	0	800
S.I.	Const.	150	1JPN09SB11	290	765000	crack	10	0	800
S.I.	Const.	150	1JPN09SB12	230	760000	crack	10	0	800
S.I.	Const.	150	1JPN09SB13	230	1120000	crack	10	0	800
S.I.	Const.	150	1JPN09SB14	190	1600000	crack	10	0	800
S.I.	Const.	160	1JPN05JS01	200	470000	crack	300	0.6	800
S.I.	Const.	160	1JPN05JS02	132	4000000	runout	198	0.6	800
S.I.	Const.	160	1JPN05JS03	310	183000	crack	0	0	800
S.I.	Const.	160	1JPN05JS04	217	445000	crack	0	0	800
S.I.	Const.	160	1JPN05JS05	148	1150000	crack	0	0	800
S.I.	Const.	160	1JPN05JS06	140	1300000	crack	0	0	800
S.I.	Const.	160	1JPN05JS07	135	1600000	crack	0	0	800
S.I.	Const.	160	1JPN05JS08	140	1820000	crack	0	0	800
S.I.	Const.	160	1JPN05JS09	135	3200000	runout	0	0	800
S.I.	Const.	160	1JPN05JS10	140	4000000	crack	0	0	800
S.I.	Const.	160	1JPN05JS11	390	112000	crack	-195	-1	800
S.I.	Const.	160	1JPN05JS12	280	394000	crack	-140	-1	800
S.I.	Const.	160	1JPN05JS13	200	385000	crack	0	0	800
S.I.	Const.	160	1JPN05JS14	135	3150000	crack	0	0	800
S.I.	Const.	160	1JPN05JS15	145	3150000	crack	0	0	800
S.I.	Const.	170	1JPN05BA01	156	890000	crack	0	0	800
S.I.	Const.	170	1JPN05BA02	133	1310000	crack	0	0	800
S.I.	Const.	170	1JPN05BA03	155	2780000	crack	0	0	800
S.I.	Const.	150	1JPN05JS16	270	400000	crack	0	0	800
S.I.	Const.	150	1JPN05JS17	270	530000	crack	0	0	800
S.I.	Const.	150	1JPN05JS18	222	555000	crack	0	0	800
S.I.	Const.	150	1JPN05JS19	248	1270000	crack	0	0	800
S.I.	Const.	150	1JPN05JS20	223	1250000	crack	0	0	800
S.I.	Const.	150	1JPN05JS21	200	1270000	crack	0	0	800
S.I.	Const.	150	1JPN05JS22	250	1800000	crack	0	0	800

(continued on next page)

Table F.7.1. Fatigue Test Data (continued)

Units	Load Type	Detail	ID Number	Stress Range	Cycles	Result	Min. Stress	Max. Stress	Yield Stress
S.I.	Const.	150	1JPN05JS23	220	1750000	crack	0	0	800
S.I.	Const.	150	1JPN05JS24	200	2600000	crack	0	0	800
S.I.	Const.	170	1JPN05BB01	174	1200000	crack	0	0	800
S.I.	Const.	170	1JPN05BB02	148	1990000	crack	0	0	800
S.I.	Const.	170	1JPN05BB03	127	3000000	runout	0	0	800
S.I.	Const.	170	1JPN05BE01	219	1010000	crack	0	0	800
S.I.	Const.	170	1JPN05BE02	192	1280000	crack	0	0	800
S.I.	Const.	170	1JPN05BE03	163	2190000	crack	0	0	800
S.I.	Const.	171	1JPN05BD01	228	1040000	crack	0	0	800
S.I.	Const.	171	1JPN05BD02	198	1080000	crack	0	0	800
S.I.	Const.	171	1JPN05BD03	168	1940000	crack	0	0	800
S.I.	Const.	172	1JPN05BF01	202	807000	crack	0	0	800
S.I.	Const.	172	1JPN05BF02	198	740000	crack	0	0	800
S.I.	Const.	172	1JPN05BF03	198	1350000	crack	0	0	800
S.I.	Const.	172	1JPN05BF04	168	3150000	crack	0	0	800
S.I.	Const.	170	1JPN05BG01	175	1190000	crack	-1	-1	500
S.I.	Const.	170	1JPN05BG02	182	3000000	runout	-1	-1	500
S.I.	Const.	170	1JPN05BG02	217	1240000	crack	-1	-1	500
S.I.	Const.	170	1JPN05BG03	221	1570000	crack	-1	-1	500
S.I.	Const.	150	1JPN100201	392	405000	crack	10	-1	800
S.I.	Const.	150	1JPN100202	343	842000	crack	10	-1	800
S.I.	Const.	150	1JPN100203	324	1010000	crack	10	-1	800
S.I.	Const.	150	1JPN100204	284	2000000	runout	10	-1	800
S.I.	Const.	150	1JPN100205	343	540000	crack	10	-1	800
S.I.	Const.	150	1JPN100206	275	860000	crack	10	-1	800
S.I.	Const.	150	1JPN100207	294	960000	crack	10	-1	800
S.I.	Const.	150	1JPN100208	255	1100000	crack	10	-1	800
S.I.	Const.	150	1JPN100301	333	305000	crack	10	-1	500
S.I.	Const.	150	1JPN100302	314	510000	crack	10	-1	500
S.I.	Const.	150	1JPN100303	294	870000	crack	10	-1	500
S.I.	Const.	150	1JPN100304	265	1100000	crack	10	-1	500
S.I.	Const.	150	1JPN100305	255	1400000	crack	10	-1	500
S.I.	Const.	150	1JPN100306	353	210000	crack	10	-1	500
S.I.	Const.	150	1JPN100307	294	590000	crack	10	-1	500
S.I.	Const.	150	1JPN100308	275	620000	crack	10	-1	500
S.I.	Const.	150	1JPN100309	265	1020000	crack	10	-1	500
S.I.	Const.	150	1JPN100401	343	290000	crack	10	-1	800
S.I.	Const.	150	1JPN100402	265	700000	crack	10	-1	800
S.I.	Const.	150	1JPN100403	314	1200000	crack	10	-1	800

(continued on next page)

Table F.7.1. Fatigue Test Data (continued)

Units	Load Type	Detail	ID Number	Stress Range	Cycles	Result	Min. Stress	Max. Stress	Yield Stress
S.I.	Const.	150	1JPN100404	294	1400000	crack	10	-1	800
S.I.	Const.	150	1JPN100405	245	1550000	crack	10	-1	800
S.I.	Const.	150	1JPN100406	294	430000	crack	10	-1	800
S.I.	Const.	150	1JPN100407	245	1050000	crack	10	-1	800
S.I.	Const.	150	1JPN100408	265	1200000	crack	10	-1	800
S.I.	Const.	150	1JPN100409	226	3000000	crack	10	-1	800
S.I.	Const.	150	1JPN100410	294	350000	crack	10	-1	800
S.I.	Const.	150	1JPN100411	235	610000	crack	10	-1	800
S.I.	Const.	150	1JPN100412	255	750000	crack	10	-1	800
S.I.	Const.	150	1JPN100413	235	840000	crack	10	-1	800
S.I.	Const.	150	1JPN100414	216	1500000	crack	10	-1	800
S.I.	Const.	150	1JPN100501	343	250000	crack	10	-1	500
S.I.	Const.	150	1JPN100502	294	480000	crack	10	-1	500
S.I.	Const.	150	1JPN100503	324	660000	crack	10	-1	500
S.I.	Const.	150	1JPN100504	255	1100000	crack	10	-1	500
S.I.	Const.	150	1JPN100505	343	95000	crack	10	-1	500
S.I.	Const.	150	1JPN100506	324	180000	crack	10	-1	500
S.I.	Const.	150	1JPN100507	294	770000	crack	10	-1	500
S.I.	Const.	150	1JPN100508	265	780000	crack	10	-1	500
S.I.	Const.	150	1JPN100509	265	2000000	runout	10	-1	500
S.I.	Const.	150	1JPN100510	314	260000	crack	10	-1	500
S.I.	Const.	150	1JPN100511	294	270000	crack	10	-1	500
S.I.	Const.	150	1JPN100512	255	300000	crack	10	-1	500
S.I.	Const.	150	1JPN100513	216	870000	crack	10	-1	500
S.I.	Const.	150	1JPN100514	206	2000000	runout	10	-1	500
S.I.	Const.	151	1JPN100601	373	81000	crack	10	-1	800
S.I.	Const.	151	1JPN100602	412	120000	crack	10	-1	800
S.I.	Const.	151	1JPN100603	412	360000	crack	10	-1	800
S.I.	Const.	151	1JPN100604	451	670000	crack	10	-1	800
S.I.	Const.	151	1JPN100605	343	720000	crack	10	-1	800
S.I.	Const.	151	1JPN100606	373	1300000	crack	10	-1	800
S.I.	Const.	151	1JPN100607	314	1600000	crack	10	-1	800
S.I.	Const.	151	1JPN100701	363	310000	crack	10	-1	500
S.I.	Const.	151	1JPN100702	333	330000	crack	10	-1	500
S.I.	Const.	151	1JPN100703	343	660000	crack	10	-1	500
S.I.	Const.	151	1JPN100704	324	180000	crack	10	-1	500
S.I.	Const.	150	1JPN12T102	449	128000	crack	10	0	800
S.I.	Const.	150	1JPN12T103	198	2022000	crack	10	0	800
S.I.	Const.	150	1JPN12T104	303	288000	crack	10	0	800

(continued on next page)

Table F.7.1. Fatigue Test Data (continued)

Units	Load Type	Detail	ID Number	Stress Range	Cycles	Result	Min. Stress	Max. Stress	Yield Stress
S.I.	Const.	150	1JPN12T105	191	696000	crack	10	0	800
S.I.	Const.	150	1JPN12T106	413	690000	crack	10	0	800
S.I.	Const.	150	1JPN12T107	209	1503000	crack	10	0	800
S.I.	Const.	150	1JPN12T108	216	799000	crack	10	0	800
S.I.	Const.	150	1JPN12T109	222	930000	crack	10	0	800
S.I.	Const.	150	1JPN12T201	191	1468000	crack	10	0	800
S.I.	Const.	150	1JPN12T202	212	663000	crack	10	0	800
S.I.	Const.	150	1JPN12T203	304	161000	crack	10	0	800
S.I.	Const.	150	1JPN12T204	279	212000	crack	10	0	800
S.I.	Const.	150	1JPN12T301	174	1781000	crack	10	0	800
S.I.	Const.	150	1JPN12T302	194	2535000	crack	10	0	800
S.I.	Const.	150	1JPN12T303	270	535000	crack	10	0	800
S.I.	Const.	150	1JPN12T304	352	242000	crack	10	0	800
S.I.	Const.	150	1JPN12T401	215	1356000	crack	10	0	800
S.I.	Const.	150	1JPN12T402	278	643000	crack	10	0	800
S.I.	Const.	150	1JPN12T403	349	292000	crack	10	0	800
S.I.	Const.	160	1JPN130P01	245	172000	crack	27	-1	370
S.I.	Const.	160	1JPN130P02	245	216000	crack	27	-1	370
S.I.	Const.	160	1JPN130P03	245	307000	crack	27	-1	370
S.I.	Const.	160	1JPN130P04	177	565000	crack	27	-1	370
S.I.	Const.	160	1JPN130P05	177	821000	crack	27	-1	370
S.I.	Const.	160	1JPN130P06	177	741000	crack	27	-1	370
S.I.	Const.	160	1JPN130P07	147	2117000	crack	27	-1	370
S.I.	Const.	160	1JPN130P08	127	10000000	runout	27	-1	370
S.I.	Const.	160	1JPN130P09	127	5340000	runout	27	-1	370
S.I.	Const.	160	1JPN130W01	245	242000	crack	27	-1	370
S.I.	Const.	160	1JPN130W02	245	217000	crack	27	-1	370
S.I.	Const.	160	1JPN130W03	245	274000	crack	27	-1	370
S.I.	Const.	160	1JPN130W04	177	774000	crack	27	-1	370
S.I.	Const.	160	1JPN130W05	177	432000	crack	27	-1	370
S.I.	Const.	160	1JPN130W06	177	822000	crack	27	-1	370
S.I.	Const.	160	1JPN130W07	147	2160000	crack	27	-1	370
S.I.	Const.	160	1JPN130W08	147	1820000	crack	27	-1	370
S.I.	Const.	160	1JPN130W09	147	5030000	runout	27	-1	370
S.I.	Const.	160	1JPN130W10	147	5340000	runout	27	-1	370
S.I.	Const.	160	1JPN130N01	245	268000	crack	27	-1	370
S.I.	Const.	160	1JPN130N02	245	170000	crack	27	-1	370
S.I.	Const.	160	1JPN130N03	245	219000	crack	27	-1	370
S.I.	Const.	160	1JPN130N04	177	660000	crack	27	-1	370

(continued on next page)

Table F.7.1. Fatigue Test Data (continued)

Units	Load Type	Detail	ID Number	Stress Range	Cycles	Result	Min. Stress	Max. Stress	Yield Stress
S.I.	Const.	160	1JPN130N05	177	826000	crack	27	-1	370
S.I.	Const.	160	1JPN130N06	177	608000	crack	27	-1	370
S.I.	Const.	160	1JPN130N07	147	5480000	runout	27	-1	370
S.I.	Const.	160	1JPN130N08	147	1170000	crack	27	-1	370
S.I.	Const.	160	1JPN130N09	147	1720000	crack	27	-1	370
S.I.	Const.	165	1JPN132W01	245	379000	crack	27	-1	370
S.I.	Const.	165	1JPN132W02	245	318000	crack	27	-1	370
S.I.	Const.	165	1JPN132W03	245	267000	crack	27	-1	370
S.I.	Const.	165	1JPN132W04	177	955000	crack	27	-1	370
S.I.	Const.	165	1JPN132W05	177	1869000	crack	27	-1	370
S.I.	Const.	165	1JPN132W06	177	1034000	crack	27	-1	370
S.I.	Const.	165	1JPN132W07	147	3250000	runout	27	-1	370
S.I.	Const.	165	1JPN132W08	147	3030000	runout	27	-1	370
S.I.	Const.	165	1JPN132W09	147	2740000	crack	27	-1	370
S.I.	Const.	165	1JPN132N01	245	379000	crack	27	-1	370
S.I.	Const.	165	1JPN132N02	245	634000	crack	27	-1	370
S.I.	Const.	165	1JPN132N03	245	440000	crack	27	-1	370
S.I.	Const.	165	1JPN132N04	177	631000	crack	27	-1	370
S.I.	Const.	165	1JPN132N05	177	2210000	runout	27	-1	370
S.I.	Const.	165	1JPN132N06	177	720000	crack	27	-1	370
S.I.	Const.	165	1JPN132N07	147	3470000	runout	27	-1	370
S.I.	Const.	165	1JPN132N08	147	1790000	crack	27	-1	370
S.I.	Const.	165	1JPN132N09	147	3620000	runout	27	-1	370
S.I.	Const.	165	1JPN134W01	245	740000	crack	27	-1	370
S.I.	Const.	165	1JPN134W02	245	233000	crack	27	-1	370
S.I.	Const.	165	1JPN134W03	245	578000	crack	27	-1	370
S.I.	Const.	165	1JPN134W04	177	1733000	crack	27	-1	370
S.I.	Const.	165	1JPN134W05	177	4470000	runout	27	-1	370
S.I.	Const.	165	1JPN134W06	177	652000	crack	27	-1	370
S.I.	Const.	165	1JPN134W07	177	1506000	crack	27	-1	370
S.I.	Const.	165	1JPN134W08	147	4750000	runout	27	-1	370
S.I.	Const.	165	1JPN134W09	147	4710000	runout	27	-1	370
S.I.	Const.	165	1JPN134W10	147	3930000	runout	27	-1	370
S.I.	Const.	165	1JPN134N01	245	482000	crack	27	-1	370
S.I.	Const.	165	1JPN134N02	245	368000	crack	27	-1	370
S.I.	Const.	165	1JPN134N03	245	392000	crack	27	-1	370
S.I.	Const.	165	1JPN134N04	177	974000	crack	27	-1	370
S.I.	Const.	165	1JPN134N05	177	1694000	crack	27	-1	370
S.I.	Const.	165	1JPN134N06	177	4750000	runout	27	-1	370

(continued on next page)

Table F.7.1. Fatigue Test Data (continued)

Units	Load Type	Detail	ID Number	Stress Range	Cycles	Result	Min. Stress	Max. Stress	Yield Stress
S.I.	Const.	165	1JPN134N07	177	1386000	crack	27	-1	370
S.I.	Const.	165	1JPN134N08	147	4490000	runout	27	-1	370
S.I.	Const.	165	1JPN134N09	147	4510000	runout	27	-1	370
S.I.	Const.	165	1JPN134N10	147	4680000	runout	27	-1	370
S.I.	Const.	165	1JPN135W01	245	336000	crack	27	-1	370
S.I.	Const.	165	1JPN135W02	245	364000	crack	27	-1	370
S.I.	Const.	165	1JPN135W03	245	274000	crack	27	-1	370
S.I.	Const.	165	1JPN135W04	177	2493000	crack	27	-1	370
S.I.	Const.	165	1JPN135W05	177	5210000	runout	27	-1	370
S.I.	Const.	165	1JPN135W06	177	1387000	crack	27	-1	370
S.I.	Const.	165	1JPN135W07	177	1558000	crack	27	-1	370
S.I.	Const.	165	1JPN135W08	147	2315000	crack	27	-1	370
S.I.	Const.	165	1JPN135W09	147	3940000	runout	27	-1	370
S.I.	Const.	165	1JPN135W10	147	1110000	crack	27	-1	370
S.I.	Const.	200	1JPN130P01	245	123000	crack	27	-1	370
S.I.	Const.	200	1JPN130P02	245	109000	crack	27	-1	370
S.I.	Const.	200	1JPN130P03	245	158000	crack	27	-1	370
S.I.	Const.	200	1JPN130P04	177	359000	crack	27	-1	370
S.I.	Const.	200	1JPN130P05	177	373000	crack	27	-1	370
S.I.	Const.	200	1JPN130P06	177	321000	crack	27	-1	370
S.I.	Const.	200	1JPN130P07	127	1040000	crack	27	-1	370
S.I.	Const.	200	1JPN130P08	127	1005000	crack	27	-1	370
S.I.	Const.	200	1JPN130P09	127	720000	crack	27	-1	370
S.I.	Const.	200	1JPN130P10	127	1310000	crack	27	-1	370
S.I.	Const.	200	1JPN130W01	245	135000	crack	27	-1	370
S.I.	Const.	200	1JPN130W02	245	130000	crack	27	-1	370
S.I.	Const.	200	1JPN130W03	245	154000	crack	27	-1	370
S.I.	Const.	200	1JPN130W04	177	323000	crack	27	-1	370
S.I.	Const.	200	1JPN130W05	177	314000	crack	27	-1	370
S.I.	Const.	200	1JPN130W06	177	372000	crack	27	-1	370
S.I.	Const.	200	1JPN130W07	177	297000	crack	27	-1	370
S.I.	Const.	200	1JPN130W08	127	1322000	crack	27	-1	370
S.I.	Const.	200	1JPN130W09	127	5330000	runout	27	-1	370
S.I.	Const.	200	1JPN130W10	127	1028000	crack	27	-1	370
S.I.	Const.	200	1JPN130W11	127	5340000	runout	27	-1	370
S.I.	Const.	200	1JPN130N01	245	144000	crack	27	-1	370
S.I.	Const.	200	1JPN130N02	245	137000	crack	27	-1	370
S.I.	Const.	200	1JPN130N03	245	151000	crack	27	-1	370
S.I.	Const.	200	1JPN130N04	245	139000	crack	27	-1	370

(continued on next page)

Table F.7.1. Fatigue Test Data (continued)

Units	Load Type	Detail	ID Number	Stress Range	Cycles	Result	Min. Stress	Max. Stress	Yield Stress
S.I.	Const.	200	1JPN130N05	177	422000	crack	27	-1	370
S.I.	Const.	200	1JPN130N06	177	709000	crack	27	-1	370
S.I.	Const.	200	1JPN130N07	177	356000	crack	27	-1	370
S.I.	Const.	200	1JPN130N08	127	958000	crack	27	-1	370
S.I.	Const.	200	1JPN130N09	127	787000	crack	27	-1	370
S.I.	Const.	200	1JPN130N10	127	777000	crack	27	-1	370
S.I.	Const.	205	1JPN132W01	245	195000	crack	27	-1	370
S.I.	Const.	205	1JPN132W02	245	168000	crack	27	-1	370
S.I.	Const.	205	1JPN132W03	245	154000	crack	27	-1	370
S.I.	Const.	205	1JPN132W04	177	360000	crack	27	-1	370
S.I.	Const.	205	1JPN132W05	177	377000	crack	27	-1	370
S.I.	Const.	205	1JPN132W06	177	348000	crack	27	-1	370
S.I.	Const.	205	1JPN132W07	147	2370000	runout	27	-1	370
S.I.	Const.	205	1JPN132W08	147	705000	crack	27	-1	370
S.I.	Const.	205	1JPN132W09	147	1100000	crack	27	-1	370
S.I.	Const.	205	1JPN132W10	127	2990000	runout	27	-1	370
S.I.	Const.	205	1JPN132W11	127	1179000	crack	27	-1	370
S.I.	Const.	205	1JPN132W12	127	1056000	crack	27	-1	370
S.I.	Const.	205	1JPN134W01	245	177000	crack	27	-1	370
S.I.	Const.	205	1JPN134W02	245	166000	crack	27	-1	370
S.I.	Const.	205	1JPN134W03	245	213000	crack	27	-1	370
S.I.	Const.	205	1JPN134W04	177	668000	crack	27	-1	370
S.I.	Const.	205	1JPN134W05	177	327000	crack	27	-1	370
S.I.	Const.	205	1JPN134W06	177	357000	crack	27	-1	370
S.I.	Const.	205	1JPN134W07	147	662000	crack	27	-1	370
S.I.	Const.	205	1JPN134W08	147	915000	crack	27	-1	370
S.I.	Const.	205	1JPN134W09	147	4470000	runout	27	-1	370
S.I.	Const.	205	1JPN134W10	127	1624000	crack	27	-1	370
S.I.	Const.	205	1JPN134N01	245	150000	crack	27	-1	370
S.I.	Const.	205	1JPN134N02	245	248000	crack	27	-1	370
S.I.	Const.	205	1JPN134N03	245	130000	crack	27	-1	370
S.I.	Const.	205	1JPN134N04	177	415000	crack	27	-1	370
S.I.	Const.	205	1JPN134N05	177	532000	crack	27	-1	370
S.I.	Const.	205	1JPN134N06	177	631000	crack	27	-1	370
S.I.	Const.	205	1JPN134N07	127	1086000	crack	27	-1	370
S.I.	Const.	205	1JPN134N08	127	968000	crack	27	-1	370
S.I.	Const.	205	1JPN134N09	127	623000	crack	27	-1	370
S.I.	Const.	26	1ORE11156	188	2940000	crack	9	-1	331
S.I.	Const.	20	1ORE11157	154	774000	runout	7	-1	331

(continued on next page)

Table F.7.1. Fatigue Test Data (continued)

Units	Load Type	Detail	ID Number	Stress Range	Cycles	Result	Min. Stress	Max. Stress	Yield Stress
S.I.	Const.	26	1ORE11155S	166	666000	crack	6	-1	331
S.I.	Const.	26	1ORE11157S	158	1153000	crack	6	-1	331
S.I.	Const.	140	1ORE11155	185	747000	crack	9	-1	331
S.I.	Const.	140	1ORE11157	173	774000	crack	8	-1	331
S.I.	Const.	145	1ORE1156S	179	503000	crack	8	-1	331
S.I.	Const.	145	1ORE11157S	181	1150000	runout	8	-1	331
S.I.	Const.	170	1ORE212321	166	818000	crack	-1	-1	331
S.I.	Const.	170	1ORE212322	166	481000	crack	-1	-1	331
S.I.	Const.	170	1ORE212323	161	797000	crack	-1	-1	331
S.I.	Const.	170	1ORE212324	157	921000	crack	-1	-1	331
S.I.	Const.	170	1ORE212325	166	494000	crack	-1	-1	331
S.I.	Const.	170	1ORE212326	162	766000	crack	-1	-1	331
S.I.	Const.	20	1ORE312571	154	1142000	crack	-1	-1	331
S.I.	Const.	20	1ORE312571	154	1530000	crack	-1	-1	331
S.I.	Const.	20	1ORE312571	154	1640000	crack	-1	-1	331
S.I.	Var.	20	1ORE312572	155	5200000	crack	-1	-1	331
S.I.	Var.	25	1ORE312573	178	4118000	crack	-1	-1	331
S.I.	Var.	20	1ORE312574	93	10500000	runout	-1	-1	331
S.I.	Var.	140	1ORE312574	178	10450000	crack	-1	-1	331
S.I.	Const.	132	1ORE50A201	156	1633000	crack	-1	-1	331
S.I.	Const.	132	1ORE50A301	154	656000	crack	-1	-1	331
S.I.	Const.	132	1ORE50A401	155	585000	crack	-1	-1	331
S.I.	Const.	132	1ORE50B101	134	618000	crack	-1	-1	331
S.I.	Const.	132	1ORE50B201	135	873000	crack	-1	-1	331
S.I.	Const.	132	1ORE50B301	133	1558000	crack	-1	-1	331
S.I.	Const.	190	1ORE60R101	103	3121000	crack	10	-1	331
S.I.	Const.	190	1ORE60R102	118	1702000	crack	10	-1	331
S.I.	Const.	190	1ORE60R103	118	1593000	crack	10	-1	331
S.I.	Const.	190	1ORE60R104	118	1818000	crack	10	-1	331
S.I.	Const.	190	1ORE60R105	118	1921000	crack	10	-1	331
S.I.	Const.	190	1ORE60R106	118	1402000	crack	10	-1	331
S.I.	Var.	100	1ORE80A601	55.9	24300000	crack	-1	-1	331
S.I.	Var.	100	1ORE80A602	55.9	27620000	crack	-1	-1	331
S.I.	Var.	140	1ORE712811	74.7	38500000	runout	-1	-1	331
S.I.	Var.	140	1ORE712812	74.7	19100000	runout	-1	-1	331
S.I.	Var.	140	1ORE712813	74.7	18200000	runout	-1	-1	331
S.I.	Var.	20	1ORE712811	65.6	38500000	runout	-1	-1	331
S.I.	Var.	21	1ORE712811	65.6	20750000	crack	-1	-1	331
S.I.	Var.	20	1ORE712812	65.6	19100000	runout	-1	-1	331

(continued on next page)



Table F.7.1. Fatigue Test Data (continued)

Units	Load Type	Detail	ID Number	Stress Range	Cycles	Result	Min. Stress	Max. Stress	Yield Stress
S.I.	Var.	20	1ORE712813	65.6	18200000	runout	-1	-1	331
S.I.	Var.	132	1ORE712811	36.5	12770000	crack	-1	-1	331
S.I.	Var.	132	1ORE712812	43.3	2335000	crack	-1	-1	331
S.I.	Var.	132	1ORE712813	45.6	2345000	crack	-1	-1	331
S.I.	Var.	132	1ORE712812	69	6367000	crack	-1	-1	331
S.I.	Const.	27	10RE11156	160	2833000	crack	-5	-1	331
S.I.	Const.	20	10RE11156S	160	503000	runout	5	-1	331
S.I.	Const.	170	10RE212324	175	921000	runout	-1	-1	331
S.I.	Const.	160	1ENG014301	200	145000	crack	0	-1	262
S.I.	Const.	160	1ENG014302	140	470000	crack	0	-1	262
S.I.	Const.	160	1ENG014303	100	10000000	runout	0	-1	262
S.I.	Const.	160	1ENG015001	220	100000	crack	0	-1	727
S.I.	Const.	160	1ENG015002	200	170000	crack	0	-1	727
S.I.	Const.	160	1ENG015003	192	290000	crack	0	-1	727
S.I.	Const.	160	1ENG015004	180	245000	crack	0	-1	727
S.I.	Const.	160	1ENG015005	140	545000	crack	0	-1	727
S.I.	Const.	160	1ENG015006	140	660000	crack	0	-1	727
S.I.	Const.	160	1ENG015007	132	470000	crack	0	-1	727
S.I.	Const.	160	1ENG015008	112	1330000	crack	0	-1	727
S.I.	Const.	160	1ENG015009	100	1500000	crack	0	-1	727
S.I.	Const.	160	1ENG015010	100	2550000	crack	0	-1	727
S.I.	Const.	160	1ENG015011	90	10500000	runout	0	-1	727
S.I.	Const.	160	1ENG015012	80	12500000	runout	0	-1	727
S.I.	Const.	160	1ENG015013	260	100000	crack	-130	-1	727
S.I.	Const.	160	1ENG015014	220	122000	crack	-110	-1	727
S.I.	Const.	160	1ENG015015	180	170000	crack	-90	-1	727
S.I.	Const.	160	1ENG015016	150	510000	crack	-75	-1	727
S.I.	Const.	160	1ENG015017	120	735000	crack	-60	-1	727
S.I.	Const.	160	1ENG015018	200	100000	crack	200	-1	727
S.I.	Const.	160	1ENG015019	160	325000	crack	160	-1	727
S.I.	Const.	160	1ENG015020	126	678000	crack	126	-1	727
S.I.	Const.	160	1ENG015021	116	543000	crack	116	-1	727
S.I.	Const.	160	1ENG015022	100	1250000	crack	100	-1	727
S.I.	Const.	160	1ENG015023	85	5100000	crack	85	-1	727
S.I.	Const.	160	1ENG015024	70	12000000	runout	70	-1	727
S.I.	Const.	200	1ENG01F301	220	120000	crack	0	-1	392
S.I.	Const.	200	1ENG01F302	200	123000	crack	0	-1	392
S.I.	Const.	200	1ENG01F303	180	245000	crack	0	-1	392
S.I.	Const.	200	1ENG01F304	180	290000	crack	0	-1	392

(continued on next page)

Table F.7.1. Fatigue Test Data (continued)

Units	Load Type	Detail	ID Number	Stress Range	Cycles	Result	Min. Stress	Max. Stress	Yield Stress
S.I.	Const.	200	1ENG01F305	150	340000	crack	0	-1	392
S.I.	Const.	200	1ENG01F306	130	735000	crack	0	-1	392
S.I.	Const.	200	1ENG01F307	120	455000	crack	0	-1	392
S.I.	Const.	200	1ENG01F309	100	1150000	crack	0	-1	392
S.I.	Const.	200	1ENG01F310	90	1720000	crack	0	-1	392
S.I.	Const.	200	1ENG01F311	80	2300000	crack	0	-1	392
S.I.	Const.	200	1ENG01F312	70	7800000	runout	0	-1	392
S.I.	Const.	256	1GDR010301	220	226000	crack	-1	-1	-1
S.I.	Const.	256	1GDR010302	220	400000	crack	-1	-1	-1
S.I.	Const.	256	1GDR010303	175	354000	crack	-1	-1	-1
S.I.	Const.	256	1GDR010304	175	376000	crack	-1	-1	-1
S.I.	Const.	256	1GDR010305	175	410000	crack	-1	-1	-1
S.I.	Const.	256	1GDR010306	175	673000	crack	-1	-1	-1
S.I.	Const.	256	1GDR010307	175	707000	crack	-1	-1	-1
S.I.	Const.	256	1GDR010308	145	683000	crack	-1	-1	-1
S.I.	Const.	256	1GDR010309	135	539000	crack	-1	-1	-1
S.I.	Const.	256	1GDR010310	135	1280000	crack	-1	-1	-1
S.I.	Const.	256	1GDR010311	135	2180000	crack	-1	-1	-1
S.I.	Const.	256	1GDR010312	135	4100000	runout	-1	-1	-1
S.I.	Const.	256	1GDR010313	110	771000	crack	-1	-1	-1
S.I.	Const.	256	1GDR010314	110	1560000	crack	-1	-1	-1
S.I.	Const.	256	1GDR010315	110	4640000	runout	-1	-1	-1
S.I.	Const.	256	1GDR010316	80	4530000	runout	-1	-1	-1
S.I.	Const.	256	1GDR010317	80	4750000	runout	-1	-1	-1
S.I.	Const.	256	1GDR010318	145	336000	crack	-1	0.5	-1
S.I.	Const.	256	1GDR010319	145	420000	crack	-1	0.5	-1
S.I.	Const.	251	1GDR010320	125	500000	crack	-1	0.5	-1
S.I.	Const.	256	1GDR010321	125	862000	crack	-1	0.5	-1
S.I.	Const.	256	1GDR010322	105	1540000	crack	-1	0.5	-1
S.I.	Const.	256	1GDR010323	105	1770000	crack	-1	0.5	-1
S.I.	Const.	256	1GDR010324	105	2260000	crack	-1	0.5	-1
S.I.	Const.	256	1GDR010325	105	2790000	crack	-1	0.5	-1
S.I.	Const.	256	1GDR010326	105	3280000	runout	-1	0.5	-1
S.I.	Const.	256	1GDR010327	105	5000000	runout	-1	0.5	-1
S.I.	Const.	256	1GDR010328	95	880000	crack	-1	0.5	-1
S.I.	Const.	256	1GDR010328	95	1130000	crack	-1	0.5	-1
S.I.	Const.	256	1GDR010329	95	1560000	crack	-1	0.5	-1
S.I.	Const.	256	1GDR010330	95	1720000	crack	-1	0.5	-1
S.I.	Const.	256	1GDR010331	95	3230000	crack	-1	0.5	-1

(continued on next page)

Table F.7.1. Fatigue Test Data (continued)

Units	Load Type	Detail	ID Number	Stress Range	Cycles	Result	Min. Stress	Max. Stress	Yield Stress
S.I.	Const.	256	1GDR010332	95	3900000	runout	-1	0.5	-1
S.I.	Const.	256	1GDR010333	85	4530000	runout	-1	0.5	-1
S.I.	Const.	251	1GDR010401	175	98000	crack	-1	-1	-1
S.I.	Const.	251	1GDR010402	175	118000	crack	-1	-1	-1
S.I.	Const.	251	1GDR010403	135	226000	crack	-1	-1	-1
S.I.	Const.	251	1GDR010404	135	259000	crack	-1	-1	-1
S.I.	Const.	251	1GDR010405	90	654000	crack	-1	-1	-1
S.I.	Const.	251	1GDR010406	90	905000	crack	-1	-1	-1
S.I.	Const.	251	1GDR010407	61	1490000	crack	-1	-1	-1
S.I.	Const.	251	1GDR010408	61	2340000	crack	-1	-1	-1
S.I.	Const.	251	1GDR010409	125	202000	crack	-1	0.5	-1
S.I.	Const.	251	1GDR010410	125	223000	crack	-1	0.5	-1
S.I.	Const.	251	1GDR010411	125	228000	crack	-1	0.5	-1
S.I.	Const.	251	1GDR010412	125	246000	crack	-1	0.5	-1
S.I.	Const.	251	1GDR010413	105	308000	crack	-1	0.5	-1
S.I.	Const.	251	1GDR010414	105	449000	crack	-1	0.5	-1
S.I.	Const.	251	1GDR010415	83	368000	crack	-1	0.5	-1
S.I.	Const.	251	1GDR010416	83	548000	crack	-1	0.5	-1
S.I.	Const.	251	1GDR010417	83	722000	crack	-1	0.5	-1
S.I.	Const.	251	1GDR010418	83	798000	crack	-1	0.5	-1
S.I.	Const.	251	1GDR010419	73	1150000	crack	-1	0.5	-1
S.I.	Const.	251	1GDR010420	63	1130000	crack	-1	0.5	-1
S.I.	Const.	251	1GDR010421	63	1920000	crack	-1	0.5	-1
S.I.	Const.	251	1GDR010422	63	2000000	crack	-1	0.5	-1
S.I.	Const.	251	1GDR010423	63	2170000	crack	-1	0.5	-1
S.I.	Const.	40	1GDR010501	220	226000	crack	-1	-1	-1
S.I.	Const.	40	1GDR010502	220	269000	crack	-1	-1	-1
S.I.	Const.	40	1GDR010503	175	256000	crack	-1	-1	-1
S.I.	Const.	40	1GDR010504	175	453000	crack	-1	-1	-1
S.I.	Const.	40	1GDR010505	133	453000	crack	-1	-1	-1
S.I.	Const.	40	1GDR010506	133	633000	crack	-1	-1	-1
S.I.	Const.	40	1GDR010507	133	906000	crack	-1	-1	-1
S.I.	Const.	40	1GDR010508	95	2210000	crack	-1	-1	-1
S.I.	Const.	40	1GDR010509	90	2000000	runout	-1	-1	-1
S.I.	Const.	40	1GDR010510	90	3010000	crack	-1	-1	-1
S.I.	Const.	40	1GDR010511	83	4150000	crack	-1	-1	-1
S.I.	Const.	40	1GDR010512	145	410000	crack	-1	0.5	-1
S.I.	Const.	40	1GDR010513	145	442000	crack	-1	0.5	-1
S.I.	Const.	40	1GDR010514	145	500000	crack	-1	0.5	-1

(continued on next page)

Table F.7.1. Fatigue Test Data (continued)

Units	Load Type	Detail	ID Number	Stress Range	Cycles	Result	Min. Stress	Max. Stress	Yield Stress
S.I.	Const.	40	1GDR010515	145	640000	crack	-1	0.5	-1
S.I.	Const.	40	1GDR010516	125	464000	crack	-1	0.5	-1
S.I.	Const.	40	1GDR010517	125	725000	crack	-1	0.5	-1
S.I.	Const.	40	1GDR010518	125	780000	crack	-1	0.5	-1
S.I.	Const.	40	1GDR010519	125	884000	crack	-1	0.5	-1
S.I.	Const.	40	1GDR010520	105	1220000	crack	-1	0.5	-1
S.I.	Const.	40	1GDR010521	105	1720000	crack	-1	0.5	-1
S.I.	Const.	40	1GDR010522	105	1950000	crack	-1	0.5	-1
S.I.	Const.	40	1GDR010523	105	2150000	crack	-1	0.5	-1
S.I.	Const.	40	1GDR010524	95	1400000	crack	-1	0.5	-1
S.I.	Const.	40	1GDR010525	80	2630000	crack	-1	0.5	-1
S.I.	Const.	40	1GDR010601	180	119000	crack	-1	-1	-1
S.I.	Const.	40	1GDR010602	180	190000	crack	-1	-1	-1
S.I.	Const.	40	1GDR010603	135	170000	crack	-1	-1	-1
S.I.	Const.	40	1GDR010604	135	220000	crack	-1	-1	-1
S.I.	Const.	40	1GDR010605	135	303000	crack	-1	-1	-1
S.I.	Const.	40	1GDR010606	90	669000	crack	-1	-1	-1
S.I.	Const.	40	1GDR010607	90	1480000	crack	-1	-1	-1
S.I.	Const.	40	1GDR010608	60	2130000	runout	-1	-1	-1
S.I.	Const.	40	1GDR010609	60	2780000	runout	-1	-1	-1
S.I.	Const.	40	1GDR010610	145	252000	crack	-1	0.5	-1
S.I.	Const.	40	1GDR010611	145	322000	crack	-1	0.5	-1
S.I.	Const.	40	1GDR010612	135	322000	crack	-1	0.5	-1
S.I.	Const.	40	1GDR010613	125	464000	crack	-1	0.5	-1
S.I.	Const.	40	1GDR010614	125	578000	crack	-1	0.5	-1
S.I.	Const.	40	1GDR010615	105	637000	crack	-1	0.5	-1
S.I.	Const.	40	1GDR010616	105	699000	crack	-1	0.5	-1
S.I.	Const.	40	1GDR010617	105	720000	crack	-1	0.5	-1
S.I.	Const.	40	1GDR010618	105	875000	crack	-1	0.5	-1
S.I.	Const.	40	1GDR010619	90	885000	crack	-1	0.5	-1
S.I.	Const.	40	1GDR010620	90	941000	crack	-1	0.5	-1
S.I.	Const.	40	1GDR010621	90	1170000	crack	-1	0.5	-1
S.I.	Const.	40	1GDR010622	90	1280000	crack	-1	0.5	-1
S.I.	Const.	40	1GDR010623	72	1310000	crack	-1	0.5	-1
S.I.	Const.	40	1GDR010624	72	2080000	crack	-1	0.5	-1
S.I.	Const.	40	1GDR010625	72	2210000	crack	-1	0.5	-1
S.I.	Const.	40	1GDR010626	72	2850000	crack	-1	0.5	-1
S.I.	Const.	256	1GDR020201	145	802000	crack	-1	0.5	-1
S.I.	Const.	256	1GDR020202	145	882000	crack	-1	0.5	-1

(continued on next page)

Table F.7.1. Fatigue Test Data (continued)

Units	Load Type	Detail	ID Number	Stress Range	Cycles	Result	Min. Stress	Max. Stress	Yield Stress
S.I.	Const.	256	1GDR020203	145	1153000	crack	-1	0.5	-1
S.I.	Const.	256	1GDR020204	145	1480000	runout	-1	0.5	-1
S.I.	Const.	256	1GDR020205	125	777000	crack	-1	0.5	-1
S.I.	Const.	256	1GDR020206	125	854000	crack	-1	0.5	-1
S.I.	Const.	256	1GDR020207	125	1134000	crack	-1	0.5	-1
S.I.	Const.	256	1GDR020208	125	1287000	crack	-1	0.5	-1
S.I.	Const.	256	1GDR020209	105	2033000	crack	-1	0.5	-1
S.I.	Const.	256	1GDR020210	105	3940000	crack	-1	0.5	-1
S.I.	Const.	130	1GDR020301	230	352000	crack	-1	-1	-1
S.I.	Const.	130	1GDR020302	230	450000	crack	-1	-1	-1
S.I.	Const.	130	1GDR020303	260	398000	crack	-1	-1	-1
S.I.	Const.	130	1GDR020304	260	603000	crack	-1	-1	-1
S.I.	Const.	130	1GDR020305	260	759000	crack	-1	-1	-1
S.I.	Const.	130	1GDR020306	160	819000	crack	-1	-1	-1
S.I.	Const.	130	1GDR020307	160	1360000	crack	-1	-1	-1
S.I.	Const.	130	1GDR020308	135	1260000	crack	-1	-1	-1
S.I.	Const.	130	1GDR020309	135	1740000	crack	-1	-1	-1
S.I.	Const.	130	1GDR020310	112	4100000	runout	-1	-1	-1
S.I.	Const.	130	1GDR020311	120	960000	crack	-1	0.5	-1
S.I.	Const.	130	1GDR020312	120	1260000	crack	-1	0.5	-1
S.I.	Const.	130	1GDR020313	120	1360000	crack	-1	0.5	-1
S.I.	Const.	130	1GDR020314	145	1630000	crack	-1	0.5	-1
S.I.	Const.	130	1GDR020315	145	1970000	crack	-1	0.5	-1
S.I.	Const.	130	1GDR020316	145	2050000	crack	-1	0.5	-1
S.I.	Const.	130	1GDR020317	125	3630000	runout	-1	0.5	-1
S.I.	Const.	130	1GDR020318	125	3920000	runout	-1	0.5	-1
S.I.	Const.	130	1GDR020319	125	4370000	runout	-1	0.5	-1
S.I.	Const.	130	1GDR020401	175	110000	crack	-1	-1	-1
S.I.	Const.	130	1GDR020402	135	210000	crack	-1	-1	-1
S.I.	Const.	130	1GDR020403	135	230000	crack	-1	-1	-1
S.I.	Const.	130	1GDR020404	110	570000	crack	-1	-1	-1
S.I.	Const.	130	1GDR020405	90	970000	crack	-1	-1	-1
S.I.	Const.	130	1GDR020406	90	1070000	crack	-1	-1	-1
S.I.	Const.	130	1GDR020407	67	1480000	crack	-1	-1	-1
S.I.	Const.	130	1GDR020408	67	1660000	crack	-1	-1	-1
S.I.	Const.	130	1GDR020409	55	4040000	runout	-1	-1	-1
S.I.	Const.	130	1GDR020410	55	4840000	runout	-1	-1	-1
S.I.	Const.	130	1GDR020411	170	130000	crack	-1	0.5	-1
S.I.	Const.	130	1GDR020412	170	150000	crack	-1	0.5	-1

(continued on next page)

Table F.7.1. Fatigue Test Data (continued)

Units	Load Type	Detail	ID Number	Stress Range	Cycles	Result	Min. Stress	Max. Stress	Yield Stress
S.I.	Const.	130	1GDR020413	145	300000	crack	-1	0.5	-1
S.I.	Const.	130	1GDR020414	145	340000	crack	-1	0.5	-1
S.I.	Const.	130	1GDR020415	125	310000	crack	-1	0.5	-1
S.I.	Const.	130	1GDR020416	125	380000	crack	-1	0.5	-1
S.I.	Const.	130	1GDR020417	90	1170000	crack	-1	0.5	-1
S.I.	Const.	130	1GDR020418	90	1330000	crack	-1	0.5	-1
S.I.	Const.	130	1GDR020419	75	1660000	crack	-1	0.5	-1
S.I.	Const.	130	1GDR020420	75	2130000	crack	-1	0.5	-1
S.I.	Const.	130	1GDR020421	75	2420000	crack	-1	0.5	-1
S.I.	Const.	130	1GDR020422	62	1460000	crack	-1	0.5	-1
S.I.	Const.	130	1GDR020423	62	1560000	crack	-1	0.5	-1
S.I.	Const.	130	1GDR020424	62	1740000	crack	-1	0.5	-1
S.I.	Const.	130	1GDR020425	62	1850000	crack	-1	0.5	-1
S.I.	Const.	130	1GDR020426	62	3020000	crack	-1	0.5	-1
Imp.	Const.	41	0NC1CWA133	16	336700	crack	-10	-1	36
Imp.	Const.	41	0NC1CRA141	20	192200	crack	-14	-1	36
Imp.	Const.	41	0NC1CRA144	20	176100	crack	-14	-1	36
Imp.	Const.	41	0NC1CRA151	24	114400	crack	-18	-1	36
Imp.	Const.	41	0NC1CRB131	16	418100	crack	-10	-1	50
Imp.	Const.	41	0NC1CWB132	16	356300	crack	-10	-1	50
Imp.	Const.	41	0NC1CRB141	20	186600	crack	-14	-1	50
Imp.	Const.	41	0NC1CWB142	20	154200	crack	-14	-1	50
Imp.	Const.	41	0NC1CWB143	20	170500	crack	-14	-1	50
Imp.	Const.	41	0NC1CRB151	24	108200	crack	-18	-1	50
Imp.	Const.	41	0NC1CRC131	16	394700	crack	-10	-1	100
Imp.	Const.	41	0NC1CWC132	16	482800	crack	-10	-1	100
Imp.	Const.	41	0NC1CRC141	20	242700	crack	-14	-1	100
Imp.	Const.	41	0NC1CWC142	20	295000	crack	-14	-1	100
Imp.	Const.	41	0NC1CWC143	20	254300	crack	-14	-1	100
Imp.	Const.	41	0NC1CRC151	24	156600	crack	-18	-1	100
Imp.	Const.	41	0NC1CWC152	24	137400	crack	-18	-1	100
Imp.	Const.	41	0NC1CWC153	24	170700	crack	-18	-1	100
Imp.	Const.	41	0NC1CRC231	16	428500	crack	-18	-1	100
Imp.	Const.	41	0NC1CWC242	20	242800	crack	-22	-1	100
Imp.	Const.	41	0NC1CWC251	24	154100	crack	-26	-1	100
Imp.	Const.	41	0NC1CRC341	20	196400	crack	-30	-1	100
Imp.	Const.	31	0NC1CRA131	16	555000	crack	-10	-1	36
Imp.	Const.	31	0NC1CRC131	16	514800	crack	-10	-1	100
Imp.	Const.	31	0NC1CWC132	16	1228000	crack	-10	-1	100

(continued on next page)

Table F.7.1. Fatigue Test Data (continued)

Units	Load Type	Detail	ID Number	Stress Range	Cycles	Result	Min. Stress	Max. Stress	Yield Stress
Imp.	Const.	31	0NC1CRC141	16	341300	crack	-10	-1	100
Imp.	Const.	31	0NC1CWC143	20	445900	crack	-14	-1	100
Imp.	Const.	31	0NC1CRC144	20	282300	crack	-14	-1	100
Imp.	Const.	31	0NC1CWC251	24	192500	crack	-26	-1	100
Imp.	Const.	41	0NC1CTA141	20	160300	crack	-14	-1	36
Imp.	Const.	41	0NC1CTA243	20	226400	crack	-22	-1	36
Imp.	Const.	61	0NC1CBA132	16	275700	crack	-10	-1	36
Imp.	Const.	61	0NC1CBA143	20	204000	crack	-14	-1	36
Imp.	Const.	51	0NC1CBA131	16	308200	crack	-10	-1	36
Imp.	Const.	51	0NC1CBA132	16	156700	crack	-10	-1	36
Imp.	Const.	51	0NC1CBA133	16	198600	crack	-10	-1	36
Imp.	Const.	51	0NC1CBA141	20	186300	crack	-14	-1	36
Imp.	Const.	51	0NC1CBA142	20	158200	crack	-14	-1	36
Imp.	Const.	51	0NC1CBA143	20	122400	crack	-14	-1	36
Imp.	Const.	51	0NC1CBA151	24	77400	crack	-18	-1	36
Imp.	Const.	51	0NC1CBA152	24	47500	crack	-18	-1	36
Imp.	Const.	51	0NC1CBA243	20	142200	crack	-22	-1	36
S.I.	Const.	220	1MAR01F111	104	3517000	crack	3	107	345
S.I.	Const.	220	1MAR01F112	104	2065000	crack	3	107	345
S.I.	Const.	220	1MAR01F113	104	10000000	runout	3	107	345
S.I.	Const.	220	1MAR01F114	104	2046000	crack	3	107	345
S.I.	Const.	220	1MAR01F115	104	2178000	crack	3	107	345
S.I.	Const.	220	1MAR01F211	145	1209000	crack	3	148	345
S.I.	Const.	220	1MAR01F212	145	706000	crack	3	148	345
S.I.	Const.	220	1MAR01F213	145	1075000	crack	3	148	345
S.I.	Const.	220	1MAR01F214	145	1523000	crack	3	148	345
S.I.	Const.	220	1MAR01F215	145	967000	crack	3	148	345
S.I.	Const.	220	1MAR01F311	207	410000	crack	3	210	345
S.I.	Const.	220	1MAR01F312	207	292000	crack	3	210	345
S.I.	Const.	220	1MAR01F313	207	260000	crack	3	210	345
S.I.	Const.	220	1MAR01F314	207	289000	crack	3	210	345
S.I.	Const.	220	1MAR01F315	207	255000	crack	3	210	345
S.I.	Const.	220	1MAR01F411	290	86000	crack	3	293	345
S.I.	Const.	220	1MAR01F412	290	102000	crack	3	293	345
S.I.	Const.	220	1MAR01F413	290	79000	crack	3	293	345
S.I.	Const.	220	1MAR01F414	290	120000	crack	3	193	345
S.I.	Const.	220	1MAR01F415	290	111000	crack	3	293	345
S.I.	Const.	225	1MAR01F121	104	4476000	crack	3	107	345
S.I.	Const.	225	1MAR01F122	104	3502000	crack	3	107	345

(continued on next page)

Table F.7.1. Fatigue Test Data (continued)

Units	Load Type	Detail	ID Number	Stress Range	Cycles	Result	Min. Stress	Max. Stress	Yield Stress
S.I.	Const.	225	1MAR01F123	104	2922000	crack	3	107	345
S.I.	Const.	225	1MAR01F124	104	3498000	crack	3	107	345
S.I.	Const.	225	1MAR01F125	104	3159000	crack	3	107	345
S.I.	Const.	225	1MAR01F221	145	959000	crack	3	148	345
S.I.	Const.	225	1MAR01F222	145	805000	crack	3	148	345
S.I.	Const.	225	1MAR01F223	145	668000	crack	3	148	345
S.I.	Const.	225	1MAR01F224	145	832000	crack	3	148	345
S.I.	Const.	225	1MAR01F225	145	879000	crack	3	148	345
S.I.	Const.	225	1MAR01F321	207	294000	crack	3	210	345
S.I.	Const.	225	1MAR01F322	207	398000	crack	3	210	345
S.I.	Const.	225	1MAR01F323	207	269000	crack	3	210	345
S.I.	Const.	225	1MAR01F324	207	327000	crack	3	210	345
S.I.	Const.	225	1MAR01F325	207	366000	crack	3	210	345
S.I.	Const.	225	1MAR01F131	104	5754000	crack	3	107	345
S.I.	Const.	225	1MAR01F132	104	1830000	crack	3	107	345
S.I.	Const.	225	1MAR01F133	104	3442000	crack	3	107	345
S.I.	Const.	225	1MAR01F134	104	1598000	crack	3	107	345
S.I.	Const.	225	1MAR01F231	145	891000	crack	3	148	345
S.I.	Const.	225	1MAR01F231	145	1184000	crack	3	148	345
S.I.	Const.	225	1MAR01F233	145	1062000	crack	3	148	345
S.I.	Const.	225	1MAR01F234	145	1569000	crack	3	148	345
S.I.	Const.	225	1MAR01F141	104	3273000	crack	3	107	345
S.I.	Const.	225	1MAR01F142	104	4189000	crack	3	107	345
S.I.	Const.	225	1MAR01F143	104	2288000	crack	3	107	345
S.I.	Const.	225	1MAR01F144	104	2415000	crack	3	107	345
S.I.	Const.	225	1MAR01F145	104	1477000	crack	3	107	345
S.I.	Const.	225	1MAR01F241	145	891000	crack	3	148	345
S.I.	Const.	225	1MAR01F242	145	862000	crack	3	148	345
S.I.	Const.	225	1MAR01F243	145	1024000	crack	3	148	345
S.I.	Const.	225	1MAR01F244	145	890000	crack	3	148	345
S.I.	Const.	225	1MAR01F245	145	1019000	crack	3	148	345
S.I.	Const.	225	1MAR01F341	207	319000	crack	3	210	345
S.I.	Const.	225	1MAR01F342	207	272000	crack	3	210	345
S.I.	Const.	225	1MAR01F343	207	264000	crack	3	210	345
S.I.	Const.	225	1MAR01F344	207	202000	crack	3	210	345
S.I.	Const.	225	1MAR01F345	207	281000	crack	3	210	345
S.I.	Const.	225	1MAR01F441	290	95000	crack	3	293	345
S.I.	Const.	225	1MAR01F442	290	82000	crack	3	293	345
S.I.	Const.	225	1MAR01F443	290	126000	crack	3	293	345

(continued on next page)



Table F.7.1. Fatigue Test Data (continued)

Units	Load Type	Detail	ID Number	Stress Range	Cycles	Result	Min. Stress	Max. Stress	Yield Stress
S.I.	Const.	225	1MAR01F444	290	96000	crack	3	293	345
S.I.	Const.	225	1MAR01F445	290	84000	crack	3	293	345
S.I.	Const.	225	1MAR01F151	104	5570000	crack	3	107	345
S.I.	Const.	225	1MAR01F152	104	1636000	crack	3	107	345
S.I.	Const.	225	1MAR01F153	104	2750000	crack	3	107	345
S.I.	Const.	225	1MAR01F154	104	1970000	crack	3	107	345
S.I.	Const.	225	1MAR01F251	145	1187000	crack	3	148	345
S.I.	Const.	225	1MAR01F252	145	1003000	crack	3	148	345
S.I.	Const.	225	1MAR01F253	145	909000	crack	3	148	345
S.I.	Const.	225	1MAR01F254	145	824000	crack	3	148	345
Imp.	Const.	251	1USA01BA00	9	3370000	crack	10.8	0.55	36
Imp.	Const.	251	1USA01B4A0	9	3277000	crack	10.8	0.55	36
Imp.	Const.	251	1USA01B6A0	9	2823000	crack	10	0.53	50
Imp.	Const.	251	1USA01B200	8.7	2024000	crack	17.3	0.67	100
Imp.	Const.	251	1USA01B2A0	8.7	2866000	crack	17.3	0.67	100
Imp.	Const.	130	1USA01B600	8	2955000	crack	16.4	0.67	50
Imp.	Const.	40	1USA01B100	8	1806000	crack	18	0.7	100
Imp.	Const.	40	1USA01B1A0	8	1134000	crack	18	0.7	100
Imp.	Const.	40	1USA01B300	8	2171000	crack	1.8	0.2	36
Imp.	Const.	30	1USA01B3A0	8	1817000	crack	1.8	0.2	36
Imp.	Const.	40	1USA01B500	8	2013000	crack	2.5	0.24	50
Imp.	Const.	40	1USA01B5A0	8	2020000	crack	2.5	0.24	50
Imp.	Const.	260	1USA01B1A0	18	3069000	crack	1.8	0.1	36
Imp.	Const.	260	1USA01B100	18	3312000	crack	1.8	0.1	36
Imp.	Const.	260	1USA01B120	18	3069000	crack	1.8	0.1	50
Imp.	Const.	260	1USA01B8A0	18	4180000	runout	8.7	0.33	100
Imp.	Const.	100	1USA01B9A0	13.6	5440000	crack	7.1	0.34	36
Imp.	Const.	100	1USA01B11A	15.7	1825000	crack	5	0.24	50
Imp.	Const.	90	1USA01B110	15	3064000	crack	4.8	0.24	50
Imp.	Const.	100	1USA01B7A0	15.6	1452000	crack	14.4	0.48	100
Imp.	Const.	100	1USA01B700	13.6	8360000	runout	14.4	0.51	100
Imp.	Const.	40	1USA02CP01	4	98000000	runout	10	-1	50
Imp.	Const.	30	1USA01CP02	4	98500000	runout	10	-1	50
Imp.	Const.	40	1USA02CP03	4	99000000	runout	10	-1	50
Imp.	Const.	30	1USA01CP04	4	99500000	runout	10	-1	50
Imp.	Const.	40	1USA02CP05	4.6	98000000	runout	10	-1	50
Imp.	Const.	30	1USA01CP06	4.6	98500000	runout	10	-1	50
Imp.	Const.	40	1USA02CP07	4.6	99000000	runout	10	-1	50
Imp.	Const.	30	1USA01CP08	4.6	99500000	runout	10	-1	50

(continued on next page)

Table F.7.1. Fatigue Test Data (continued)

Units	Load Type	Detail	ID Number	Stress Range	Cycles	Result	Min. Stress	Max. Stress	Yield Stress
Imp.	Const.	40	1USA02CM09	4.7	34930000	crack	9.3	-1	36
Imp.	Const.	30	1USA01CM10	4.7	37710000	crack	9.3	-1	36
Imp.	Const.	40	1USA02CP11	5	16610000	crack	10	-1	50
Imp.	Const.	30	1USA01CP12	5	32510000	crack	10	-1	50
Imp.	Const.	40	1USA02CP13	5	8451000	crack	10	-1	50
Imp.	Const.	30	1USA01CP14	5	47290000	crack	10	-1	50
Imp.	Const.	40	1USA02CW15	5	89200000	runout	24	-1	50
Imp.	Const.	30	1USA01CW16	5	89400000	runout	24	-1	50
Imp.	Const.	40	1USA02CT17	6	11420000	crack	10	-1	36
Imp.	Const.	30	1USA01CT18	6	12160000	crack	10	-1	36
Imp.	Const.	40	1USA02CW19	6	4327000	crack	10	-1	50
Imp.	Const.	30	1USA01CW20	6	12160000	crack	10	-1	50
Imp.	Const.	40	1USA02CW21	6	99500000	runout	24	-1	50
Imp.	Const.	30	1USA01CW22	6	99000000	runout	24	-1	50
Imp.	Const.	40	1USA02CP23	8	2334000	crack	10	-1	50
Imp.	Const.	30	1USA01CP24	8	5006000	crack	10	-1	50
Imp.	Const.	40	1USA02CP25	8	4235000	crack	10	-1	50
Imp.	Const.	30	1USA01CP26	8	13510000	crack	10	-1	50
S.I.	Const.	240	CDN010001	119	1190000	crack	-1	-1	-1
S.I.	Const.	240	CDN010002	119	1280000	crack	-1	-1	-1
S.I.	Const.	240	CDN010003	119	1970000	crack	-1	-1	-1
S.I.	Const.	240	CDN010004	112	2090000	crack	-1	-1	-1
S.I.	Const.	240	CDN010005	103	2960000	crack	-1	-1	-1
S.I.	Const.	240	CDN010006	103	4090000	crack	-1	-1	-1
S.I.	Const.	240	CDN010007	103	4410000	crack	-1	-1	-1
S.I.	Const.	240	CDN010008	83	7860000	crack	-1	-1	-1
Imp.	Const.	120	1CDN021W01	5	15900000	runout	2.78	-1	36
Imp.	Const.	120	1CDN022W01	10	1442000	crack	2.78	-1	36
Imp.	Const.	120	1CDN022W02	10	1739000	crack	2.78	-1	36
Imp.	Const.	120	1CDN022W03	10	1814000	crack	2.78	-1	36
Imp.	Const.	120	1CDN022W04	10	1830000	crack	2.78	-1	36
Imp.	Const.	120	1CDN023W01	15	350000	crack	2.78	-1	36
Imp.	Const.	120	1CDN023W02	15	357000	crack	2.78	-1	36
Imp.	Const.	120	1CDN023W03	15	365000	crack	2.78	-1	36
Imp.	Const.	120	1CDN024W01	10	1296000	crack	2.64	-1	36
Imp.	Const.	120	1CDN024W02	10	1821000	crack	2.64	-1	36
Imp.	Const.	120	1CDN025W01	17	144000	crack	2.64	-1	36
Imp.	Const.	120	1CDN025W02	17	222000	crack	2.64	-1	36
Imp.	Const.	120	1CDN026W01	13	794000	crack	2.64	-1	36

(continued on next page)

Table F.7.1. Fatigue Test Data (continued)

Units	Load Type	Detail	ID Number	Stress Range	Cycles	Result	Min. Stress	Max. Stress	Yield Stress
Imp.	Const.	120	1CDN026W02	13	798000	crack	2.64	-1	36
Imp.	Const.	120	1CDN026W03	13	804000	crack	2.64	-1	36
Imp.	Const.	232	1CDN021RG1	11	1329000	crack	2.78	-1	36
Imp.	Const.	232	1CDN021RG2	11	2240000	runout	2.78	-1	36
Imp.	Const.	232	1CDN022RG1	13	1337000	crack	2.78	-1	36
Imp.	Const.	232	1CDN022RG2	13	1388000	crack	2.78	-1	36
Imp.	Const.	232	1CDN023RG1	17	432000	crack	2.78	-1	36
Imp.	Const.	232	1CDN023RG2	17	498000	crack	2.78	-1	36
Imp.	Const.	232	1CDN024RG1	10	3741000	crack	2.78	-1	36
Imp.	Const.	232	1CDN024RG2	10	8090000	runout	2.78	-1	36
Imp.	Const.	232	1CDN026RG1	19	506000	crack	2.78	-1	36
Imp.	Const.	232	1CDN026RG2	19	845000	crack	2.78	-1	36
Imp.	Const.	233	1CDN021T01	11	875000	crack	2.78	-1	36
Imp.	Const.	233	1CDN021T02	11	988000	crack	2.78	-1	36
Imp.	Const.	233	1CDN022T01	17	223000	crack	2.78	-1	36
Imp.	Const.	233	1CDN022T02	17	226000	crack	2.78	-1	36
Imp.	Const.	233	1CDN02P101	13	714000	crack	2.78	-1	36
Imp.	Const.	233	1CDN02P102	13	744000	crack	2.78	-1	36
Imp.	Const.	234	1CDN021TG1	11	1163000	crack	2.78	-1	36
Imp.	Const.	234	1CDN021TG2	11	1754000	crack	2.78	-1	36
Imp.	Const.	10	2NC1620001	33.6	734000	crack	1	-1	33
Imp.	Const.	10	2NC1620002	30	1760000	crack	1	-1	33
Imp.	Const.	10	2NC1620003	33.6	3271000	crack	1	-1	33
Imp.	Const.	10	2NC1320001	40.6	1055000	crack	1	-1	33
Imp.	Const.	10	2NC1320002	38.4	1668000	crack	1	-1	33
Imp.	Const.	10	2NC1320003	37.4	3452000	crack	1	-1	33
Imp.	Const.	10	2NC1320004	36.4	5100000	crack	1	-1	33
Imp.	Const.	10	2NC1090001	52.5	77000	crack	1	-1	33
Imp.	Const.	10	2NC1090002	52.5	97000	crack	1	-1	33
Imp.	Const.	10	2NC1090003	52.5	103000	crack	1	-1	33
Imp.	Const.	10	2NC1090004	52.5	165000	crack	1	-1	33
Imp.	Const.	10	2NC1520001	53.8	336000	crack	1	-1.01	0
Imp.	Const.	10	2NC1520002	45.8	3000000	runout	1	-1.01	0
Imp.	Const.	10	2NC1420001	67.7	119000	crack	1	-1.01	0
Imp.	Const.	10	2NC1420002	65.9	196000	crack	1	-1.01	0
Imp.	Const.	10	2NC1420003	56.8	440000	crack	1	-1.01	0
Imp.	Const.	10	2NC1420004	56	483000	crack	1	-1.01	0
Imp.	Const.	10	2NC1420005	55.3	734000	crack	1	-1.01	0
Imp.	Const.	10	2NC1420006	44	758000	crack	1	-1.01	0

(continued on next page)

Table F.7.1. Fatigue Test Data (continued)

Units	Load Type	Detail	ID Number	Stress Range	Cycles	Result	Min. Stress	Max. Stress	Yield Stress
Imp.	Const.	10	2NC1420007	47	1041000	crack	1	-1.01	0
Imp.	Const.	10	2NC1420008	42.2	1345000	crack	1	-1.01	0
Imp.	Const.	10	2NC1420009	40	1883000	crack	1	-1.01	0
Imp.	Const.	10	2NC1420010	36.4	6240000	runout	1	-1.01	0
Imp.	Const.	10	2NC1420011	41.1	6410000	runout	1	-1.01	0
Imp.	Const.	10	2NC1420012	55.3	6770000	runout	1	-1.01	0
Imp.	Const.	10	2NC1420013	36	7340000	runout	1	-1.01	0
Imp.	Const.	100	1USA040103	16.3	1460000	crack	1	-1	36
Imp.	Const.	100	1USA040107	16.4	1465000	crack	1	-1	36
Imp.	Const.	251	1USA03010H	11.5	760000	crack	1	-1	36
Imp.	Const.	251	1USA03010I	11.5	950000	crack	1	-1	36
Imp.	Const.	251	1USA03020E	11	1270000	crack	1	-1	36
Imp.	Const.	251	1USA03020G	10.8	1860000	crack	1	-1	36
Imp.	Const.	251	1USA03030E	10.8	1450000	crack	1	-1	36
Imp.	Const.	251	1USA0303EE	8.7	2070000	crack	1	-1	36
Imp.	Const.	251	1USA03040H	11.8	970000	crack	1	-1	36
Imp.	Const.	251	1USA03040I	11.9	800000	crack	1	-1	36
Imp.	Const.	251	1USA03040J	8.5	1320000	crack	1	-1	36
Imp.	Const.	251	1USA03050O	11	1270000	crack	1	-1	36
Imp.	Const.	251	1USA03050R	11.1	1300000	crack	1	-1	36
Imp.	Const.	251	1USA0305BB	9.6	2140000	crack	1	-1	36
Imp.	Const.	130	1USA030100	10.7	950000	crack	1	-1	36
Imp.	Const.	130	1USA03010S	11.8	1610000	crack	1	-1	36
Imp.	Const.	130	1USA03010Y	11.9	1630000	crack	1	-1	36
Imp.	Const.	130	1USA03030C	13.2	1020000	crack	1	-1	36
Imp.	Const.	130	1USA03030L	13.9	1600000	crack	1	-1	36
Imp.	Const.	130	1USA03040Q	10	1320000	crack	1	-1	36
Imp.	Const.	130	1USA03050K	13.3	2140000	crack	1	-1	36
Imp.	Const.	230	1USA03020T	10.7	1380000	crack	1	-1	36
Imp.	Const.	230	1USA0303II	10.6	1600000	crack	1	-1	36
Imp.	Const.	230	1USA03040S	9.2	1640000	crack	1	-1	36
Imp.	Const.	230	1USA03040T	10.6	1640000	crack	1	-1	36
Imp.	Const.	230	1USA03050U	11.2	2140000	crack	1	-1	36
Imp.	Const.	230	1USA03050W	10.4	2140000	crack	1	-1	36
Imp.	Const.	230	1USA04010C	14.6	460000	crack	1	-1	36
Imp.	Const.	230	1USA0401CC	15.1	770000	crack	1	-1	36
Imp.	Const.	230	1USA04010F	9.5	1077000	crack	1	-1	36
Imp.	Const.	230	1USA0401FF	9.1	1460000	crack	1	-1	36
Imp.	Const.	230	1USA04010G	9.2	1460000	crack	1	-1	36

(continued on next page)

Table F.7.1. Fatigue Test Data (continued)

Units	Load Type	Detail	ID Number	Stress Range	Cycles	Result	Min. Stress	Max. Stress	Yield Stress
Imp.	Const.	230	1USA0401GG	9	1671000	crack	1	-1	36
Imp.	Const.	230	1USA0401HH	9.5	1460000	crack	1	-1	36
Imp.	Const.	230	1USA04010G	8.7	1556000	crack	1	-1	36
Imp.	Const.	230	1USA0401GG	8.7	1761000	crack	1	-1	36
Imp.	Const.	253	1USA03040B	15.3	1640000	crack	1	-1	36
Imp.	Const.	253	1USA03040Z	16.4	1320000	crack	1	-1	36
Imp.	Const.	253	1USA0305DD	15.4	1560000	crack	1	-1	36
Imp.	Const.	253	1USA0305EE	17	930000	crack	1	-1	36
Imp.	Const.	253	1USA0305FF	16.5	2140000	crack	1	-1	36
Imp.	Const.	233	1USA04020H	16.9	853000	crack	1	-1	36
Imp.	Const.	233	1USA0402HH	16.2	1021000	crack	1	-1	36
Imp.	Const.	233	1USA04030I	15.2	1369000	crack	1	-1	36
Imp.	Const.	233	1USA0403II	15.7	1369000	crack	1	-1	36
Imp.	Const.	231	1USA04010I	16.9	701000	crack	1	-1	36
Imp.	Const.	231	1USA0401II	16.3	1077000	crack	1	-1	36
S.I.	Const.	250	1ICOM10501	150	100000	crack	-1	-1	-1
S.I.	Const.	250	1ICOM10502	120	220000	crack	-1	-1	-1
S.I.	Const.	250	1ICOM10503	120	290000	crack	-1	-1	-1
S.I.	Const.	250	1ICOM10504	120	310000	crack	-1	-1	-1
S.I.	Const.	250	1ICOM10505	120	415000	crack	-1	-1	-1
S.I.	Const.	250	1ICOM10506	80	1720000	crack	-1	-1	-1
S.I.	Const.	250	1ICOM10507	60	5010000	crack	-1	-1	-1
S.I.	Const.	250	1ICOM10508	50	7440000	crack	-1	-1	-1
S.I.	Const.	255	1ICOM10601	135	640000	crack	-1	-1	-1
S.I.	Const.	255	1ICOM10602	135	1050000	crack	-1	-1	-1
S.I.	Const.	255	1ICOM10603	130	1300000	crack	-1	-1	-1
S.I.	Const.	255	1ICOM10604	120	710000	crack	-1	-1	-1
S.I.	Const.	255	1ICOM10605	120	760000	crack	-1	-1	-1
S.I.	Const.	255	1ICOM10606	120	1700000	runout	-1	-1	-1
S.I.	Const.	255	1ICOM10607	120	2430000	crack	-1	-1	-1
S.I.	Const.	255	1ICOM10608	120	3610000	crack	-1	-1	-1
S.I.	Const.	255	1ICOM10609	120	4470000	runout	-1	-1	-1
S.I.	Const.	120	1ICOM10701	120	220000	crack	-1	-1	-1
S.I.	Const.	120	1ICOM10702	105	355000	crack	-1	-1	-1
S.I.	Const.	120	1ICOM10703	105	360000	crack	-1	-1	-1
S.I.	Const.	120	1ICOM10704	90	744000	crack	-1	-1	-1
S.I.	Const.	120	1ICOM10705	90	750000	crack	-1	-1	-1
S.I.	Const.	120	1ICOM10706	70	1700000	crack	-1	-1	-1
S.I.	Const.	120	1ICOM10707	70	1750000	crack	-1	-1	-1

(continued on next page)

Table F.7.1. Fatigue Test Data (continued)

Units	Load Type	Detail	ID Number	Stress Range	Cycles	Result	Min. Stress	Max. Stress	Yield Stress
S.I.	Const.	120	1ICOM10708	70	1760000	crack	-1	-1	-1
S.I.	Const.	120	1ICOM10709	125	370000	crack	-1	-1	-1
S.I.	Const.	120	1ICOM10710	125	373000	crack	-1	-1	-1
S.I.	Const.	120	1ICOM10711	125	405000	crack	-1	-1	-1
S.I.	Const.	120	1ICOM10712	125	518000	crack	-1	-1	-1
S.I.	Const.	120	1ICOM10713	85	910000	crack	-1	-1	-1
S.I.	Const.	120	1ICOM10714	85	915000	crack	-1	-1	-1
S.I.	Const.	120	1ICOM10715	85	1160000	crack	-1	-1	-1
S.I.	Const.	120	1ICOM10716	85	1170000	crack	-1	-1	-1
S.I.	Const.	200	1ICOM10301	240	105000	crack	-1	-1	-1
S.I.	Const.	200	1ICOM10302	240	122000	crack	-1	-1	-1
S.I.	Const.	200	1ICOM10303	240	128000	crack	-1	-1	-1
S.I.	Const.	200	1ICOM10304	240	133000	crack	-1	-1	-1
S.I.	Const.	200	1ICOM10305	240	153000	crack	-1	-1	-1
S.I.	Const.	200	1ICOM10206	240	159000	crack	-1	-1	-1
S.I.	Const.	200	1ICOM10307	175	284000	crack	-1	-1	-1
S.I.	Const.	200	1ICOM10308	175	306000	crack	-1	-1	-1
S.I.	Const.	200	1ICOM10309	175	310000	crack	-1	-1	-1
S.I.	Const.	200	1ICOM10310	175	324000	crack	-1	-1	-1
S.I.	Const.	200	1ICOM10311	175	358000	crack	-1	-1	-1
S.I.	Const.	200	1ICOM10312	175	364000	crack	-1	-1	-1
S.I.	Const.	200	1ICOM10313	175	370000	crack	-1	-1	-1
S.I.	Const.	200	1ICOM10314	125	706000	crack	-1	-1	-1
S.I.	Const.	200	1ICOM10315	125	980000	crack	-1	-1	-1
S.I.	Const.	200	1ICOM10316	125	1010000	crack	-1	-1	-1
S.I.	Const.	200	1ICOM10317	125	1020000	crack	-1	-1	-1
S.I.	Const.	200	1ICOM10318	125	1080000	crack	-1	-1	-1
S.I.	Const.	200	1ICOM10319	125	1090000	crack	-1	-1	-1
S.I.	Const.	200	1ICOM10320	125	5000000	runout	-1	-1	-1
S.I.	Const.	200	1ICOM10321	125	5000000	runout	-1	-1	-1
S.I.	Const.	200	1ICOM10322	240	130000	crack	-1	-1	-1
S.I.	Const.	200	1ICOM10323	240	135000	crack	-1	-1	-1
S.I.	Const.	200	1ICOM10324	240	144000	crack	-1	-1	-1
S.I.	Const.	200	1ICOM10325	240	170000	crack	-1	-1	-1
S.I.	Const.	200	1ICOM10326	175	346000	crack	-1	-1	-1
S.I.	Const.	200	1ICOM10327	175	402000	crack	-1	-1	-1
S.I.	Const.	200	1ICOM10328	175	700000	crack	-1	-1	-1
S.I.	Const.	200	1ICOM10329	125	755000	crack	-1	-1	-1
S.I.	Const.	200	1ICOM10330	125	793000	crack	-1	-1	-1

(continued on next page)

Table F.7.1. Fatigue Test Data (continued)

Units	Load Type	Detail	ID Number	Stress Range	Cycles	Result	Min. Stress	Max. Stress	Yield Stress
S.I.	Const.	200	1ICOM10331	125	921000	crack	-1	-1	-1
S.I.	Const.	200	1ICOM10332	150	270000	crack	-1	-1	-1
S.I.	Const.	200	1ICOM10333	150	314000	crack	-1	-1	-1
S.I.	Const.	200	1ICOM10334	150	335000	crack	-1	-1	-1
S.I.	Const.	200	1ICOM10335	150	507000	crack	-1	-1	-1
S.I.	Const.	200	1ICOM10336	80	2490000	crack	-1	-1	-1
S.I.	Const.	200	1ICOM10337	80	5030000	crack	-1	-1	-1
S.I.	Const.	220	1ICOM20201	180	179000	crack	-1	0.1	470
S.I.	Const.	220	1ICOM20202	150	504000	crack	-1	0.1	470
S.I.	Const.	220	1ICOM20203	110	1470000	crack	-1	0.1	470
S.I.	Const.	220	1ICOM20204	80	15800000	crack	-1	0.1	470
S.I.	Const.	200	1ICOM20301	180	164000	crack	-1	0.1	470
S.I.	Const.	130	1ICOM3PSR1	120	1234000	crack	20	140	510
S.I.	Const.	130	1ICOM3PSR2	120	572000	crack	20	140	510
S.I.	Const.	130	1ICOM3PSR2	120	673000	crack	20	140	510
S.I.	Const.	130	1ICOM3PSR3	120	463000	crack	20	140	510
S.I.	Const.	130	1ICOM3PSR4	120	531000	crack	20	140	510
S.I.	Const.	130	1ICOM3PSR4	120	540000	crack	20	140	510
S.I.	Const.	130	1ICOM3PSR4	120	1308000	crack	20	140	510
S.I.	Const.	130	1ICOM3PSR4	120	1350000	crack	20	140	510
S.I.	Const.	130	1ICOM3PSR5	120	451000	crack	20	140	510
S.I.	Const.	130	1ICOM3PSR5	120	455000	crack	20	140	510
S.I.	Const.	130	1ICOM3PSR5	120	773000	crack	20	140	510
S.I.	Const.	130	1ICOM3PSR5	120	780000	crack	20	140	510
S.I.	Const.	130	1ICOM3PRG1	80	2764000	crack	20	100	510
S.I.	Const.	130	1ICOM3PRG2	80	1945000	crack	20	100	510
S.I.	Const.	130	1ICOM3PRG2	80	1960000	crack	20	100	510
S.I.	Const.	130	1ICOM3PRG3	120	617000	crack	20	140	510
S.I.	Const.	130	1ICOM3PRG3	120	620000	crack	20	140	510
S.I.	Const.	130	1ICOM3PRG4	120	612000	crack	20	140	510
S.I.	Const.	130	1ICOM3PRG4	120	618000	crack	20	140	510
S.I.	Const.	130	1ICOM3PRG5	160	261000	crack	20	180	510
S.I.	Const.	130	1ICOM3PRG5	160	268000	crack	20	180	510
S.I.	Const.	130	1ICOM3PRG6	160	271000	crack	20	180	510
S.I.	Const.	130	1ICOM3PRG6	160	275000	crack	20	180	510
S.I.	Const.	251	1ICOM3PRG1	80	1922000	crack	20	100	510
S.I.	Const.	251	1ICOM3PRG1	80	1950000	crack	20	100	510
S.I.	Const.	251	1ICOM3PRG2	80	1810000	crack	20	100	510
S.I.	Const.	251	1ICOM3PRG3	120	514000	crack	20	140	510

(continued on next page)

Table F.7.1. Fatigue Test Data (continued)

Units	Load Type	Detail	ID Number	Stress Range	Cycles	Result	Min. Stress	Max. Stress	Yield Stress
S.I.	Const.	251	1ICOM3PRG4	120	361000	crack	20	140	510
S.I.	Const.	251	1ICOM3PRG5	160	210000	crack	20	180	510
S.I.	Const.	251	1ICOM3PRG6	160	199000	crack	20	180	510
S.I.	Const.	251	1ICOM3PSG1	120	297000	crack	20	140	510
S.I.	Const.	251	1ICOM3PSG1	120	300000	crack	20	140	510
S.I.	Const.	251	1ICOM3PSG2	120	307000	crack	20	140	510
S.I.	Const.	251	1ICOM3PSG2	120	315000	crack	20	140	510
S.I.	Const.	251	1ICOM3PSG3	120	222000	crack	20	140	510
S.I.	Const.	256	1ICOM3PSG1	120	798000	crack	20	140	510
S.I.	Const.	256	1ICOM3PSG2	120	1720000	runout	20	140	510
S.I.	Const.	256	1ICOM3PSG3	120	726000	crack	20	140	510
S.I.	Const.	100	1ICOM3PSR1	120	3050000	runout	20	140	510
S.I.	Const.	100	1ICOM3PSR2	120	2795000	crack	20	140	510
S.I.	Const.	100	1ICOM3PSR3	120	2670000	crack	20	140	510
S.I.	Const.	20	1ICOM3PSR1	120	2355000	crack	20	140	510
S.I.	Const.	20	1ICOM3PLT1	220	469000	crack	20	240	510
S.I.	Const.	20	1ICOM3PLT2	220	713000	crack	20	240	510
S.I.	Const.	20	1ICOM3PLT3	160	1475000	crack	20	180	510
Imp.	Const.	220	1NC5CPS91A	10	25600000	runout	0	0	100
Imp.	Const.	220	1NC5CPS25A	10	9244000	crack	0	0	100
Imp.	Var.	220	1NC5CPS84A	12	3179000	crack	0	0.5	100
Imp.	Var.	220	1NC5CPS116	12	5010000	crack	0	0.5	100
Imp.	Var.	220	1NC5CPS109	12	3855000	crack	0	0.5	100
Imp.	Var.	220	1NC5CPS102	15	2445000	crack	0	1	100
Imp.	Var.	220	1NC5CPS98A	15	2443000	crack	0	1	100
Imp.	Var.	220	1NC5CPS35A	15	2294000	crack	0	1	100
Imp.	Const.	220	1NC5CPS33A	30	276000	crack	0	0	100
Imp.	Const.	220	1NC5CPS115	30	269000	crack	0	0	100
Imp.	Const.	220	1NC5CPS101	30	195000	crack	0	0	100
Imp.	Var.	220	1NC5CPS76A	36	187000	crack	0	0.5	100
Imp.	Var.	220	1NC5CPS34A	36	209000	crack	0	0.5	100
Imp.	Var.	220	1NC5CPS604	36	161000	crack	0	0.5	100
Imp.	Var.	220	1NC5CPS07A	45	167000	crack	0	1	100
Imp.	Var.	220	1NC5CPS43A	45	110000	crack	0	1	100
Imp.	Var.	220	1NC5CPS82A	45	138000	crack	0	1	100
Imp.	Const.	220	1NC5CPS02A	10	4354000	crack	10	0	100
Imp.	Const.	220	1NC5CPS04A	10	5308000	crack	10	0	100
Imp.	Const.	220	1NC5CPS57A	10	3696000	crack	10	0	100
Imp.	Var.	220	1NC5CPS20A	12	5414000	crack	10	0.5	100

(continued on next page)



Table F.7.1. Fatigue Test Data (continued)

Units	Load Type	Detail	ID Number	Stress Range	Cycles	Result	Min. Stress	Max. Stress	Yield Stress
Imp.	Var.	220	1NC5CPS78A	12	2448000	crack	10	0.5	100
Imp.	Var.	220	1NC5CPS14A	12	3396000	crack	10	0.5	100
Imp.	Var.	220	1NC5CPS21A	15	1907000	crack	10	1	100
Imp.	Var.	220	1NC5CPS51A	15	2313000	crack	10	1	100
Imp.	Var.	220	1NC5CPS70A	15	2032000	crack	10	1	100
Imp.	Const.	220	1NC5CPS08A	30	231000	crack	10	0	100
Imp.	Const.	220	1NC5CPS11A	30	283000	crack	10	0	100
Imp.	Const.	220	1NC5CPS29A	30	213000	crack	10	0	100
Imp.	Var.	220	1NC5CPS18A	36	171000	crack	10	0.5	100
Imp.	Var.	220	1NC5CPS37A	36	204000	crack	10	0.5	100
Imp.	Var.	220	1NC5CPS22A	36	181000	crack	10	0.5	100
Imp.	Var.	220	1NC5CPS06A	45	128000	crack	10	1	100
Imp.	Var.	220	1NC5CPS16A	45	123000	crack	10	1	100
Imp.	Var.	220	1NC5CPS56A	45	119000	crack	10	1	100
Imp.	Const.	220	1NC5CPS114	60	31000	crack	10	0	100
Imp.	Const.	220	1NC5CPS114	60	41000	crack	10	0	100
Imp.	Const.	220	1NC5CPS114	60	35000	crack	10	0	100
Imp.	Const.	220	1NC5CPS93A	10	4210000	crack	40	0	100
Imp.	Const.	220	1NC5CPS69A	10	6190000	crack	40	0	100
Imp.	Const.	220	1NC5CPS69A	10	6760000	crack	40	0	100
Imp.	Var.	220	1NC5CPS73A	12	2036000	crack	40	0.5	100
Imp.	Var.	220	1NC5CPS54A	12	2095000	crack	40	0.5	100
Imp.	Var.	220	1NC5CPS64A	12	3502000	crack	40	0.5	100
Imp.	Const.	220	1NC5CPS80A	30	216000	crack	40	0	100
Imp.	Const.	220	1NC5CPS17A	30	241000	crack	40	0	100
Imp.	Const.	220	1NC5CPS36A	30	248000	crack	40	0	100
Imp.	Var.	220	1NC5CPS30A	36	109000	crack	40	0.5	100
Imp.	Var.	220	1NC5CPS88A	36	152000	crack	40	0.5	100
Imp.	Var.	220	1NC5CPS68A	36	162000	crack	40	0.5	100
Imp.	Var.	220	1NC5CPS42A	45	86000	crack	0	1	100
Imp.	Var.	220	1NC5CPS97A	45	89000	crack	0	1	100
Imp.	Var.	220	1NC5CPS87A	45	155000	crack	0	1	100
Imp.	Var.	220	1NC5CPS23A	45	97000	crack	0	1	100
Imp.	Var.	220	1NC5CPS105	45	100000	crack	0	1	100
Imp.	Var.	220	1NC5CPS107	45	103000	crack	0	1	100
Imp.	Var.	220	1NC5CPS03A	45	99000	crack	0	1	100
Imp.	Var.	220	1NC5CPS67A	45	126000	crack	0	1	100
Imp.	Var.	220	1NC5CPS92A	45	111000	crack	0	1	100
Imp.	Var.	220	1NC5CPS118	45	84000	crack	0	1	100

(continued on next page)

Table F.7.1. Fatigue Test Data (continued)

Units	Load Type	Detail	ID Number	Stress Range	Cycles	Result	Min. Stress	Max. Stress	Yield Stress
Imp.	Var.	220	1NC5CPS106	45	105000	crack	0	1	100
Imp.	Var.	220	1NC5CPS108	45	96000	crack	0	1	100
Imp.	Var.	220	1NC5CPS113	45	92000	crack	0	1	100
Imp.	Var.	220	1NC5CPS50A	45	81000	crack	0	1	100
Imp.	Var.	220	1NC5CPS72A	45	86000	crack	0	1	100
Imp.	Var.	220	1NC5CPS112	45	136000	crack	0	1	100
Imp.	Var.	220	1NC5CPS85A	45	102000	crack	0	1	100
Imp.	Var.	220	1NC5CPS63A	45	110000	crack	0	1	100
Imp.	Var.	220	1NC5CPS111	45	109000	crack	0	1	100
Imp.	Var.	220	1NC5CPS61A	45	107000	crack	0	1	100
Imp.	Var.	220	1NC5CPS47A	45	102000	crack	0	1	100
Imp.	Var.	220	1NC5CPS32A	45	116000	crack	0	1	100
Imp.	Var.	220	1NC5CPS48A	45	81000	crack	0	1	100
Imp.	Var.	220	1NC5CPS38A	45	108000	crack	0	1	100
Imp.	Const.	220	1NC5CPS24A	30	262000	crack	0	0	100
Imp.	Const.	220	1NC5CPS120	30	213000	crack	0	0	100
Imp.	Const.	220	1NC5CPS83A	30	336000	crack	0	0	100
Imp.	Const.	220	1NC5CPS09A	30	277000	crack	0	0	100
Imp.	Const.	220	1NC5CPS44A	30	456000	crack	0	0	100
Imp.	Const.	220	1NC5CPS39A	30	298000	crack	0	0	100
Imp.	Const.	220	1NC5CPS90A	30	302000	crack	0	0	100
Imp.	Const.	220	1NC5CPS40A	30	168000	crack	0	0	100
Imp.	Const.	220	1NC5CPS95A	30	213000	crack	0	0	100
Imp.	Var.	40	1NC5WBC141	4.5	21660000	crack	15	1	100
Imp.	Var.	40	1NC5WBC141	4.5	21940000	crack	15	1	100
Imp.	Var.	40	1NC5WBC141	4.5	16990000	crack	15	1	100
Imp.	Var.	40	1NC5WBC141	3	103700000	crack	10	1	100
Imp.	Var.	40	1NC5WBC141	3	104000000	runout	10	1	100
Imp.	Var.	40	1NC5WBC141	3	60220000	crack	10	1	100
Imp.	Const.	40	1NC5WBC148	10	1128000	crack	10	0	100
Imp.	Const.	40	1NC5WBC148	10	1335000	crack	10	0	100
Imp.	Const.	40	1NC5WBC148	10	1370000	crack	10	0	100
Imp.	Var.	40	1NC5WBC149	12	1431000	crack	10	0.5	100
Imp.	Var.	40	1NC5WBC149	12	1004000	crack	10	0.5	100
Imp.	Var.	40	1NC5WBC149	12	1120000	crack	10	0.5	100
Imp.	Var.	40	1NC5WBC141	15	555000	crack	10	1	100
Imp.	Var.	40	1NC5WBC141	15	336000	crack	10	1	100
Imp.	Var.	40	1NC5WBC141	15	555000	crack	10	1	100
Imp.	Const.	40	1NC5WBC148	20	248000	crack	10	0	100

(continued on next page)

Table F.7.1. Fatigue Test Data (continued)

Units	Load Type	Detail	ID Number	Stress Range	Cycles	Result	Min. Stress	Max. Stress	Yield Stress
Imp.	Const.	40	1NC5WBC148	20	189000	crack	10	0	100
Imp.	Const.	40	1NC5WBC148	20	257000	crack	10	0	100
Imp.	Var.	40	1NC5WBC149	24	133000	crack	10	0.5	100
Imp.	Var.	40	1NC5WBC149	24	171000	crack	10	0.5	100
Imp.	Var.	40	1NC5WBC149	24	205000	crack	10	0.5	100
Imp.	Var.	40	1NC5WBC147	30	186000	crack	10	1	100
Imp.	Var.	40	1NC5WBC147	30	73000	crack	10	1	100
Imp.	Var.	40	1NC5WBC147	30	80000	crack	10	1	100
Imp.	Const.	40	1NC5WBC148	30	88000	crack	10	0	100
Imp.	Const.	40	1NC5WBC148	30	77000	crack	10	0	100
Imp.	Const.	40	1NC5WBC148	30	70000	crack	10	0	100
Imp.	Var.	40	1NC5WBC147	36	87000	crack	10	0.5	100
Imp.	Var.	40	1NC5WBC147	36	81000	crack	10	0.5	100
Imp.	Var.	40	1NC5WBC147	36	63000	crack	10	0.5	100
Imp.	Const.	40	1NC5WBC149	10	948000	crack	0	0	100
Imp.	Const.	40	1NC5WBC149	10	1820000	crack	0	0	100
Imp.	Const.	40	1NC5WBC149	10	1606000	crack	0	0	100
Imp.	Var.	40	1NC5WBC141	15	832000	crack	0	1	100
Imp.	Var.	40	1NC5WBC141	15	729000	crack	0	1	100
Imp.	Var.	40	1NC5WBC141	15	654000	crack	0	1	100
Imp.	Const.	30	1NC5WBC147	10	2020000	crack	0	0	100
Imp.	Const.	30	1NC5WBC147	10	2122000	crack	0	0	100
Imp.	Const.	30	1NC5WBC147	10	1491000	crack	0	0	100
Imp.	Var.	30	1NC5WBC147	15	1079000	crack	0	1	100
Imp.	Var.	30	1NC5WBC147	15	856000	crack	0	1	100
Imp.	Var.	30	1NC5WBC147	15	867000	crack	0	1	100
Imp.	Const.	20	1NC5WBP141	20	3377000	crack	0	0	100
Imp.	Const.	20	1NC5WBP141	20	3432000	crack	0	0	100
Imp.	Const.	20	1NC5WBP141	20	3829000	crack	0	0	100
Imp.	Var.	20	1NC5WBP141	24	1542000	crack	0	0.5	100
Imp.	Var.	20	1NC5WBP141	24	878000	crack	0	0.5	100
Imp.	Var.	20	1NC5WBP141	24	1341000	crack	0	0.5	100
Imp.	Var.	20	1NC5WBP140	30	8060000	crack	0	1	100
Imp.	Var.	20	1NC5WBP140	30	486000	crack	0	1	100
Imp.	Var.	20	1NC5WBP140	30	606000	crack	0	1	100
Imp.	Const.	20	1NC5WBP141	30	384000	crack	0	0	100
Imp.	Const.	20	1NC5WBP141	30	885000	crack	0	0	100
Imp.	Const.	20	1NC5WBP141	30	570000	crack	0	0	100
Imp.	Var.	20	1NC5WBP140	36	472000	crack	0	0.5	100

(continued on next page)

Table F.7.1. Fatigue Test Data (continued)

Units	Load Type	Detail	ID Number	Stress Range	Cycles	Result	Min. Stress	Max. Stress	Yield Stress
Imp.	Var.	20	1NC5WBP140	36	598000	crack	0	0.5	100
Imp.	Var.	20	1NC5WBP140	36	5072000	crack	0	0.5	100
Imp.	Var.	20	1NC5WBP140	45	335000	crack	0	1	100
Imp.	Var.	20	1NC5WBP140	45	298000	crack	0	1	100
Imp.	Var.	20	1NC5WBP140	45	342000	crack	0	1	100
Imp.	Const.	20	1NC5WBP142	40	433000	crack	0	0	100
Imp.	Const.	20	1NC5WBP142	40	299000	crack	0	0	100
Imp.	Const.	20	1NC5WBC142	40	300000	crack	0	0	100
Imp.	Var.	20	1NC5WBP141	48	260000	crack	0	0.5	100
Imp.	Var.	20	1NC5WBP141	48	306000	crack	0	0.5	100
Imp.	Var.	20	1NC5WBP141	48	299000	crack	0	0.5	100
Imp.	Var.	20	1NC5WBP142	15	6383000	crack	0	1	100
Imp.	Var.	20	1NC5WBP142	15	5724000	crack	0	1	100
Imp.	Var.	20	1NC5WBP142	15	10090000	crack	0	1	100
Imp.	Const.	40	1NC5WBC361	10	1122000	crack	0	0	36
Imp.	Const.	40	1NC5WBC361	10	1386000	crack	0	0	36
Imp.	Const.	40	1NC5WBC361	10	2644000	crack	0	0	36
Imp.	Var.	40	1NC5WBC362	10.95	886000	crack	0	0.25	36
Imp.	Var.	40	1NC5WBC362	10.95	905000	crack	0	0.25	36
Imp.	Var.	40	1NC5WBC362	10.95	728000	crack	0	0.25	36
Imp.	Var.	40	1NC5WBC363	12	634000	crack	0	0.5	36
Imp.	Var.	40	1NC5WBC363	12	570000	crack	0	0.5	36
Imp.	Var.	40	1NC5WBC363	12	640000	crack	0	0.5	36
Imp.	Const.	40	1NC5WBC362	20	156000	crack	0	0	36
Imp.	Const.	40	1NC5WBC362	20	151000	crack	0	0	36
Imp.	Const.	40	1NC5WBC362	20	150000	crack	0	0	36
Imp.	Var.	40	1NC5WBC363	21.9	127000	crack	0	0.25	36
Imp.	Var.	40	1NC5WBC363	21.9	141000	crack	0	0.25	36
Imp.	Var.	40	1NC5WBC363	21.9	120000	crack	0	0.25	36
Imp.	Var.	40	1NC5WBC364	24	72000	crack	0	0.5	36
Imp.	Var.	40	1NC5WBC364	24	141000	crack	0	0.5	36
Imp.	Var.	40	1NC5WBC364	24	100000	crack	0	0.5	36
Imp.	Const.	40	1NC5WBC363	40	16000	crack	0	0	36
Imp.	Const.	40	1NC5WBC363	40	17000	crack	0	0	36
Imp.	Const.	40	1NC5WBC363	40	15000	crack	0	0	36
Imp.	Var.	40	1NC5WBC364	6	9453000	crack	0	0.5	36
Imp.	Var.	40	1NC5WBC364	6	3924000	crack	0	0.5	36
Imp.	Var.	40	1NC5WBC364	6	5724000	crack	0	0.5	36
Imp.	Const.	40	1NC5WBC362	10	1088000	crack	10	0	36

(continued on next page)

Table F.7.1. Fatigue Test Data (continued)

Units	Load Type	Detail	ID Number	Stress Range	Cycles	Result	Min. Stress	Max. Stress	Yield Stress
Imp.	Const.	40	1NC5WBC362	10	1000000	crack	10	0	36
Imp.	Const.	40	1NC5WBC362	10	846000	crack	10	0	36
Imp.	Var.	40	1NC5WBC364	12	580000	crack	10	0.5	36
Imp.	Var.	40	1NC5WBC364	12	511000	crack	10	0.5	36
Imp.	Var.	40	1NC5WBC364	12	506000	crack	10	0.5	36
Imp.	Const.	27	1NC5WBP360	20	4700000	crack	-10	0	36
Imp.	Const.	27	1NC5WBP360	20	2978000	crack	-10	0	36
Imp.	Const.	25	1NC5WBP360	20	1346000	crack	-10	0	36
Imp.	Var.	20	1NC5WBP361	21.9	2944000	crack	0	0.25	36
Imp.	Var.	20	1NC5WBP361	21.9	1702000	crack	0	0.25	36
Imp.	Var.	27	1NC5WBP361	21.9	4540000	crack	0	0.25	36
Imp.	Var.	27	1NC5WBP361	24	1469000	crack	-10	0.5	36
Imp.	Var.	20	1NC5WBP361	24	1751000	crack	-10	0.5	36
Imp.	Var.	20	11NC5WBP36	24	1521000	crack	-10	0.5	36
Imp.	Const.	20	1NC5WBP362	30	938000	crack	-10	0	36
Imp.	Const.	27	1NC5WBP362	30	963000	crack	-10	0	36
Imp.	Const.	20	1NC5WBP362	30	1072000	crack	-10	0	36
Imp.	Var.	25	1NC5WBP362	32.85	556000	crack	-10	0.25	36
Imp.	Var.	21	1NC5WBP362	32.85	784000	crack	-10	0.25	36
Imp.	Var.	27	1NC5WBP362	32.85	708000	crack	-10	0.25	36
Imp.	Const.	20	1NC5WBP360	20	4549000	crack	0	0	36
Imp.	Const.	27	1NC5WBP360	20	2371000	crack	0	0	36
Imp.	Const.	20	1NC5WBP360	20	7337000	crack	0	0	36
Imp.	Var.	20	1NC5WBP361	21.9	2148000	crack	0	0.25	36
Imp.	Var.	21	1NC5WBP361	21.9	3940000	crack	0	0.25	36
Imp.	Var.	20	1NC5WBP361	21.9	2139000	crack	0	0.25	36
Imp.	Var.	25	1NC5WBP362	24	1056000	crack	0	0.5	36
Imp.	Var.	20	1NC5WBP362	24	2731000	crack	0	0.5	36
Imp.	Var.	25	1NC5WBP362	24	2024000	crack	0	0.5	36
Imp.	Const.	20	1NC5WBP362	30	953000	crack	0	0	36
Imp.	Const.	25	1NC5WBP362	30	1007000	crack	0	0	36
Imp.	Const.	25	1NC5WBP362	30	1044000	crack	0	0	36
Imp.	Var.	20	1NC5WBP363	29.24	1067000	crack	0	0.25	36
Imp.	Var.	20	1NC5WBP363	29.24	964000	crack	0	0.25	36
Imp.	Const.	25	1NC5WBP363	50	196000	crack	-10	0	36
Imp.	Const.	20	1NC5WBP363	50	125000	crack	-10	0	36
Imp.	Const.	20	1NC5WBP363	50	217000	crack	-10	0	36
Imp.	Var.	120	1NC7000001	2.4	43600000	crack	2	4.1	36
S.I.	Const.	150	1JPN01N022	408	211000	crack	20	-1	600

(continued on next page)

Table F.7.1. Fatigue Test Data (continued)

Units	Load Type	Detail	ID Number	Stress Range	Cycles	Result	Min. Stress	Max. Stress	Yield Stress
S.I.	Const.	150	1JPN01N008	343	474000	crack	20	-1	600
S.I.	Const.	150	1JPN01N007	300	2000000	runout	20	-1	600
S.I.	Const.	150	1JPN01N018	313	848000	crack	20	-1	600
S.I.	Const.	150	1JPN01N017	305	1490000	crack	20	-1	600
S.I.	Const.	150	1JPN01N009	352	1610000	runout	20	-1	600
S.I.	Const.	150	1JPN01N014	450	154000	crack	20	-1	600
S.I.	Const.	150	1JPN01N006	287	2040000	runout	20	-1	600
S.I.	Const.	150	1JPN01N010	349	565000	crack	20	-1	600
S.I.	Const.	150	1JPN01S014	303	878000	crack	20	-1	600
S.I.	Const.	150	1JPN01S085	300	2340000	crack	20	-1	600
S.I.	Const.	150	1JPN01S087	349	924000	crack	20	-1	600
S.I.	Const.	150	1JPN01S100	351	506000	crack	20	-1	600
S.I.	Const.	150	1JPN01SA33	300	819000	crack	20	-1	600
S.I.	Const.	150	1JPN01M005	302	290000	crack	20	-1	600
S.I.	Const.	150	1JPN01M036	300	555000	crack	20	-1	600
S.I.	Const.	150	1JPN01M043	301	392000	crack	20	-1	600
S.I.	Const.	150	1JPN01M068	254	1900000	crack	20	-1	600
S.I.	Const.	150	1JPN01M069	254	1050000	crack	20	-1	600
S.I.	Const.	150	1JPN01M0A1	249	2290000	crack	20	-1	600
S.I.	Const.	150	1JPN01M0A2	300	1050000	crack	20	-1	600
S.I.	Const.	150	1JPN01M0B5	250	1490000	crack	20	-1	600
S.I.	Const.	150	1JPN01M096	305	172000	crack	20	-1	600
S.I.	Const.	150	1JPN01M0B4	281	233000	crack	20	-1	600
S.I.	Const.	150	1JPN01M0B7	243	537000	crack	20	-1	600
S.I.	Const.	150	1JPN01M0B8	280	268000	crack	20	-1	600
S.I.	Const.	150	1JPN01MC18	284	332000	crack	20	-1	600
S.I.	Const.	150	1JPN01M0C5	236	696000	crack	20	-1	600
S.I.	Const.	150	1JPN01LB18	300	348000	crack	20	-1	600
S.I.	Const.	150	1JPN01LB19	301	258000	crack	20	-1	600
S.I.	Const.	150	1JPN01LB20	301	236000	crack	20	-1	600
S.I.	Const.	150	1JPN01LOC7	250	456000	crack	20	-1	600
S.I.	Const.	150	1JPN01LOC9	249	567000	crack	20	-1	600
S.I.	Const.	150	1JPN01LC21	251	530000	crack	20	-1	600
S.I.	Const.	150	1JPN01LC22	200	1210000	crack	20	-1	600
S.I.	Const.	150	1JPN01LC23	200	1690000	crack	20	-1	600
S.I.	Const.	150	1JPN01LB14	182	687000	crack	20	-1	600
S.I.	Const.	150	1JPN01LB17	210	548000	crack	20	-1	600
S.I.	Const.	150	1JPN01LC11	184	1110000	crack	20	-1	600
S.I.	Const.	150	1JPN01LC12	234	470000	crack	20	-1	600

(continued on next page)

Table F.7.1. Fatigue Test Data (continued)

Units	Load Type	Detail	ID Number	Stress Range	Cycles	Result	Min. Stress	Max. Stress	Yield Stress
S.I.	Const.	150	1JPN01LC15	183	901000	crack	20	-1	600
S.I.	Const.	150	1JPN01LC20	286	205000	crack	20	-1	600
S.I.	Const.	150	1JPN01LOB6	181	1180000	crack	20	-1	600
S.I.	Const.	150	1JPN01LB11	231	408000	crack	20	-1	600
S.I.	Const.	150	1JPN01LC13	230	602000	crack	20	-1	600
S.I.	Const.	150	1JPN01LC19	278	273000	crack	20	-1	600
S.I.	Const.	150	1JPN01SBA1	140	2200000	crack	20	-1	600
S.I.	Const.	150	1JPN01SBA2	120	4800000	runout	20	-1	600
S.I.	Const.	150	1JPN01SBA3	181	922000	crack	20	-1	600
S.I.	Const.	150	1JPN01SBA4	219	378000	crack	20	-1	600
S.I.	Const.	150	1JPN01SBA5	250	284000	crack	20	-1	600
S.I.	Const.	150	1JPN01SBA6	302	141000	crack	20	-1	600
S.I.	Const.	150	1JPN01SBB1	300	266000	crack	20	-1	600
S.I.	Const.	150	1JPN01SBB2	200	2390000	crack	20	-1	600
S.I.	Const.	150	1JPN01SBC1	299	417000	crack	20	-1	600
S.I.	Const.	150	1JPN01SBC2	250	2920000	crack	20	-1	600
S.I.	Const.	150	1JPN01N023	482	124000	crack	20	-1	600
S.I.	Const.	150	1JPN01N024	426	151000	crack	20	-1	600
S.I.	Const.	150	1JPN01N025	381	187000	crack	20	-1	600
S.I.	Const.	150	1JPN01N037	338	281000	crack	20	-1	600
S.I.	Const.	150	1JPN01N038	308	1110000	crack	20	-1	600
S.I.	Const.	150	1JPN01N039	282	2300000	runout	20	-1	600
S.I.	Const.	160	1JPN1100S1	196	370000	crack	-98	-1	580
S.I.	Const.	160	1JPN1100S2	196	495000	crack	-131	-2	580
S.I.	Const.	160	1JPN1100S3	196	700000	crack	-164	-5	580
S.I.	Const.	160	1JPN1100S4	196	321000	crack	0	0	580
S.I.	Const.	160	1JPN1100S5	127	3480000	crack	-64	-1	580
S.I.	Const.	160	1JPN1100S6	147	1028000	crack	-74	-1	580
S.I.	Const.	160	1JPN1100S7	147	1792000	crack	-98	-2	580
S.I.	Const.	160	1JPN1100S8	147	1414000	crack	1	0	580
S.I.	Const.	160	1JPN1100S9	147	4700000	runout	-123	-5	580
S.I.	Const.	150	1JPN0200T1	247	1762000	crack	10	-1	800
S.I.	Const.	150	1JPN0200T2	245	1249000	crack	10	-1	800
S.I.	Const.	150	1JPN0200T3	267	527000	crack	10	-1	800
S.I.	Const.	150	1JPN0200T4	220	555000	crack	10	-1	800
S.I.	Const.	150	1JPN0200T5	222	1224000	crack	10	-1	800
S.I.	Const.	150	1JPN0200T7	197	2567000	crack	10	-1	800
S.I.	Const.	150	1JPN0200T8	216	1708000	crack	10	-1	800
S.I.	Const.	150	1JPN0200T9	267	400000	crack	10	-1	800

(continued on next page)

Table F.7.1. Fatigue Test Data (continued)

Units	Load Type	Detail	ID Number	Stress Range	Cycles	Result	Min. Stress	Max. Stress	Yield Stress
S.I.	Const.	150	1JPN020T10	199	1243000	crack	10	-1	800
S.I.	Const.	170	1JPN05AB01	135	1200000	crack	-1	-1	800
S.I.	Const.	170	1JPN05AB02	135	1200000	crack	-1	-1	800
S.I.	Const.	170	1JPN05AB03	135	2150000	crack	-1	-1	800
S.I.	Const.	170	1JPN05AB04	125	1200000	crack	-1	-1	800
S.I.	Const.	170	1JPN05AB05	125	1620000	crack	-1	-1	800
S.I.	Const.	170	1JPN05AB06	125	1700000	crack	-1	-1	800
S.I.	Const.	170	1JPN5DEF01	150	1100000	crack	-1	-1	580
S.I.	Const.	170	1JPN5DEF02	150	1210000	crack	-1	-1	580
S.I.	Const.	170	1JPN5DEF03	150	1480000	crack	-1	-1	580
S.I.	Const.	170	1JPN5DEF04	150	1520000	crack	-1	-1	580
S.I.	Const.	170	1JPN5DEF05	150	1600000	crack	-1	-1	580
S.I.	Const.	170	1JPN5DEF06	150	2050000	crack	-1	-1	580
S.I.	Const.	170	1JPN5DEF07	115	1050000	crack	-1	-1	580
S.I.	Const.	170	1JPN5DEF08	115	1680000	crack	-1	-1	580
S.I.	Const.	170	1JPN5DEF09	115	1730000	crack	-1	-1	580
S.I.	Const.	170	1JPN5DEF10	115	1900000	crack	-1	-1	580
S.I.	Const.	170	1JPN5DEF11	115	2050000	crack	-1	-1	580
S.I.	Const.	170	1JPN5DEF12	115	2150000	crack	-1	-1	580
S.I.	Const.	170	1JPN5DEF13	115	2400000	crack	-1	-1	580
S.I.	Const.	170	1JPN5DEF14	115	2750000	crack	-1	-1	580
S.I.	Const.	170	1JPN05G001	115	2150000	crack	-1	-1	800
S.I.	Const.	170	1JPN05G002	115	2350000	crack	-1	-1	800
S.I.	Const.	160	1JPN05JS01	200	470000	crack	300	0.6	800
S.I.	Const.	160	1JPN05JS02	132	4000000	runout	198	0.6	800
S.I.	Const.	160	1JPN05JS03	310	183000	crack	0	0	800
S.I.	Const.	160	1JPN05JS04	217	445000	crack	0	0	800
S.I.	Const.	160	1JPN05JS05	148	1150000	crack	0	0	800
S.I.	Const.	160	1JPN05JS06	140	1300000	crack	0	0	800
S.I.	Const.	160	1JPN05JS07	135	1600000	crack	0	0	800
S.I.	Const.	160	1JPN05JS08	140	1820000	crack	0	0	800
S.I.	Const.	160	1JPN05JS09	135	3200000	runout	0	0	800
S.I.	Const.	160	1JPN05JS10	140	4000000	crack	0	0	800
S.I.	Const.	160	1JPN05JS11	390	112000	crack	-195	-1	800
S.I.	Const.	160	1JPN05JS12	280	394000	crack	-140	-1	800
S.I.	Const.	160	1JPN05JS13	200	385000	crack	0	0	800
S.I.	Const.	160	1JPN05JS14	135	3150000	crack	0	0	800
S.I.	Const.	160	1JPN05JS15	145	3150000	crack	0	0	800
S.I.	Const.	170	1JPN05BA01	156	890000	crack	0	0	800

(continued on next page)



Table F.7.1. Fatigue Test Data (continued)

Units	Load Type	Detail	ID Number	Stress Range	Cycles	Result	Min. Stress	Max. Stress	Yield Stress
S.I.	Const.	170	1JPN05BA02	133	1310000	crack	0	0	800
S.I.	Const.	170	1JPN05BA03	155	2780000	crack	0	0	800
S.I.	Const.	150	1JPN05JS16	270	400000	crack	0	0	800
S.I.	Const.	150	1JPN05JS17	270	530000	crack	0	0	800
S.I.	Const.	150	1JPN05JS18	222	555000	crack	0	0	800
S.I.	Const.	150	1JPN05JS19	248	1270000	crack	0	0	800
S.I.	Const.	150	1JPN05JS20	223	1250000	crack	0	0	800
S.I.	Const.	150	1JPN05JS21	200	1270000	crack	0	0	800
S.I.	Const.	150	1JPN05JS22	250	1800000	crack	0	0	800
S.I.	Const.	150	1JPN05JS23	220	1750000	crack	0	0	800
S.I.	Const.	150	1JPN05JS24	200	2600000	crack	0	0	800
S.I.	Const.	170	1JPN05BB01	174	1200000	crack	0	0	800
S.I.	Const.	170	1JPN05BB02	148	1990000	crack	0	0	800
S.I.	Const.	170	1JPN05BB03	127	3000000	runout	0	0	800
S.I.	Const.	170	1JPN05BE01	219	1010000	crack	0	0	800
S.I.	Const.	170	1JPN05BE02	192	1280000	crack	0	0	800
S.I.	Const.	170	1JPN05BE03	163	2190000	crack	0	0	800
S.I.	Const.	171	1JPN05BD01	228	1040000	crack	0	0	800
S.I.	Const.	171	1JPN05BD02	198	1080000	crack	0	0	800
S.I.	Const.	171	1JPN05BD03	168	1940000	crack	0	0	800
S.I.	Const.	172	1JPN05BF01	202	807000	crack	0	0	800
S.I.	Const.	172	1JPN05BF02	198	740000	crack	0	0	800
S.I.	Const.	172	1JPN05BF03	198	1350000	crack	0	0	800
S.I.	Const.	172	1JPN05BF04	168	3150000	crack	0	0	800
S.I.	Const.	170	1JPN05BG01	175	1190000	crack	-1	-1	500
S.I.	Const.	170	1JPN05BG02	182	3000000	runout	-1	-1	500
S.I.	Const.	170	1JPN05BG02	217	1240000	crack	-1	-1	500
S.I.	Const.	170	1JPN05BG03	221	1570000	crack	-1	-1	500
S.I.	Const.	150	1JPN09SB01	395	180000	crack	10	1	800
S.I.	Const.	150	1JPN09SB02	395	310000	crack	10	1	800
S.I.	Const.	150	1JPN09SB03	300	375000	crack	10	1	800
S.I.	Const.	150	1JPN09SB04	300	570000	crack	10	1	800
S.I.	Const.	150	1JPN09SB05	290	620000	crack	10	1	800
S.I.	Const.	150	1JPN09SB06	250	1200000	crack	10	1	800
S.I.	Const.	150	1JPN09SB07	250	2100000	runout	10	1	800
S.I.	Const.	150	1JPN09SB08	230	2150000	crack	10	1	800
S.I.	Const.	150	1JPN09SB09	290	500000	crack	10	0	800
S.I.	Const.	150	1JPN09SB10	290	520000	crack	10	0	800
S.I.	Const.	150	1JPN09SB11	290	765000	crack	10	0	800

(continued on next page)

Table F.7.1. Fatigue Test Data (continued)

Units	Load Type	Detail	ID Number	Stress Range	Cycles	Result	Min. Stress	Max. Stress	Yield Stress
S.I.	Const.	150	1JPN09SB12	230	760000	crack	10	0	800
S.I.	Const.	150	1JPN09SB13	230	1120000	crack	10	0	800
S.I.	Const.	150	1JPN09SB14	190	1600000	crack	10	0	800
S.I.	Const.	150	1JPN100201	392	405000	crack	10	-1	800
S.I.	Const.	150	1JPN100202	343	842000	crack	10	-1	800
S.I.	Const.	150	1JPN100203	324	1010000	crack	10	-1	800
S.I.	Const.	150	1JPN100204	284	2000000	runout	10	-1	800
S.I.	Const.	150	1JPN100205	343	540000	crack	10	-1	800
S.I.	Const.	150	1JPN100206	275	860000	crack	10	-1	800
S.I.	Const.	150	1JPN100207	294	960000	crack	10	-1	800
S.I.	Const.	150	1JPN100208	255	1100000	crack	10	-1	800
S.I.	Const.	150	1JPN100301	333	305000	crack	10	-1	500
S.I.	Const.	150	1JPN100302	314	510000	crack	10	-1	500
S.I.	Const.	150	1JPN100303	294	870000	crack	10	-1	500
S.I.	Const.	150	1JPN100304	265	1100000	crack	10	-1	500
S.I.	Const.	150	1JPN100305	255	1400000	crack	10	-1	500
S.I.	Const.	150	1JPN100306	353	210000	crack	10	-1	500
S.I.	Const.	150	1JPN100307	294	590000	crack	10	-1	500
S.I.	Const.	150	1JPN100308	275	620000	crack	10	-1	500
S.I.	Const.	150	1JPN100309	265	1020000	crack	10	-1	500
S.I.	Const.	150	1JPN100401	343	290000	crack	10	-1	800
S.I.	Const.	150	1JPN100402	265	700000	crack	10	-1	800
S.I.	Const.	150	1JPN100403	314	1200000	crack	10	-1	800
S.I.	Const.	150	1JPN100404	294	1400000	crack	10	-1	800
S.I.	Const.	150	1JPN100405	245	1550000	crack	10	-1	800
S.I.	Const.	150	1JPN100406	294	430000	crack	10	-1	800
S.I.	Const.	150	1JPN100407	245	1050000	crack	10	-1	800
S.I.	Const.	150	1JPN100408	265	1200000	crack	10	-1	800
S.I.	Const.	150	1JPN100409	226	3000000	crack	10	-1	800
S.I.	Const.	150	1JPN100410	294	350000	crack	10	-1	800
S.I.	Const.	150	1JPN100411	235	610000	crack	10	-1	800
S.I.	Const.	150	1JPN100412	255	750000	crack	10	-1	800
S.I.	Const.	150	1JPN100413	235	840000	crack	10	-1	800
S.I.	Const.	150	1JPN100414	216	1500000	crack	10	-1	800
S.I.	Const.	150	1JPN100501	343	250000	crack	10	-1	500
S.I.	Const.	150	1JPN100502	294	480000	crack	10	-1	500
S.I.	Const.	150	1JPN100503	324	660000	crack	10	-1	500
S.I.	Const.	150	1JPN100504	255	1100000	crack	10	-1	500
S.I.	Const.	150	1JPN100505	343	95000	crack	10	-1	500

(continued on next page)

Table F.7.1. Fatigue Test Data (continued)

Units	Load Type	Detail	ID Number	Stress Range	Cycles	Result	Min. Stress	Max. Stress	Yield Stress
S.I.	Const.	150	1JPN100506	324	180000	crack	10	-1	500
S.I.	Const.	150	1JPN100507	294	770000	crack	10	-1	500
S.I.	Const.	150	1JPN100508	265	780000	crack	10	-1	500
S.I.	Const.	150	1JPN100509	265	2000000	runout	10	-1	500
S.I.	Const.	150	1JPN100510	314	260000	crack	10	-1	500
S.I.	Const.	150	1JPN100511	294	270000	crack	10	-1	500
S.I.	Const.	150	1JPN100512	255	300000	crack	10	-1	500
S.I.	Const.	150	1JPN100513	216	870000	crack	10	-1	500
S.I.	Const.	150	1JPN100514	206	2000000	runout	10	-1	500
S.I.	Const.	151	1JPN100601	373	81000	crack	10	-1	800
S.I.	Const.	151	1JPN100602	412	120000	crack	10	-1	800
S.I.	Const.	151	1JPN100603	412	360000	crack	10	-1	800
S.I.	Const.	151	1JPN100604	451	670000	crack	10	-1	800
S.I.	Const.	151	1JPN100605	343	720000	crack	10	-1	800
S.I.	Const.	151	1JPN100606	373	1300000	crack	10	-1	800
S.I.	Const.	151	1JPN100607	314	1600000	crack	10	-1	800
S.I.	Const.	151	1JPN100701	363	310000	crack	10	-1	500
S.I.	Const.	151	1JPN100702	333	330000	crack	10	-1	500
S.I.	Const.	151	1JPN100703	343	660000	crack	10	-1	500
S.I.	Const.	151	1JPN100704	324	180000	crack	10	-1	500
S.I.	Const.	150	1JPN12T102	449	128000	crack	10	0	800
S.I.	Const.	150	1JPN12T103	198	2022000	crack	10	0	800
S.I.	Const.	150	1JPN12T104	303	288000	crack	10	0	800
S.I.	Const.	150	1JPN12T105	191	696000	crack	10	0	800
S.I.	Const.	150	1JPN12T106	413	690000	crack	10	0	800
S.I.	Const.	150	1JPN12T107	209	1503000	crack	10	0	800
S.I.	Const.	150	1JPN12T108	216	799000	crack	10	0	800
S.I.	Const.	150	1JPN12T109	222	930000	crack	10	0	800
S.I.	Const.	150	1JPN12T201	191	1468000	crack	10	0	800
S.I.	Const.	150	1JPN12T202	212	663000	crack	10	0	800
S.I.	Const.	150	1JPN12T203	304	161000	crack	10	0	800
S.I.	Const.	150	1JPN12T204	279	212000	crack	10	0	800
S.I.	Const.	150	1JPN12T301	174	1781000	crack	10	0	800
S.I.	Const.	150	1JPN12T302	194	2535000	crack	10	0	800
S.I.	Const.	150	1JPN12T303	270	535000	crack	10	0	800
S.I.	Const.	150	1JPN12T304	352	242000	crack	10	0	800
S.I.	Const.	150	1JPN12T401	215	1356000	crack	10	0	800
S.I.	Const.	150	1JPN12T402	278	643000	crack	10	0	800
S.I.	Const.	150	1JPN12T403	349	292000	crack	10	0	800

(continued on next page)

Table F.7.1. Fatigue Test Data (continued)

Units	Load Type	Detail	ID Number	Stress Range	Cycles	Result	Min. Stress	Max. Stress	Yield Stress
S.I.	Const.	160	1JPN130P01	245	172000	crack	27	-1	370
S.I.	Const.	160	1JPN130P02	245	216000	crack	27	-1	370
S.I.	Const.	160	1JPN130P03	245	307000	crack	27	-1	370
S.I.	Const.	160	1JPN130P04	177	565000	crack	27	-1	370
S.I.	Const.	160	1JPN130P05	177	821000	crack	27	-1	370
S.I.	Const.	160	1JPN130P06	177	741000	crack	27	-1	370
S.I.	Const.	160	1JPN130P07	147	2117000	crack	27	-1	370
S.I.	Const.	160	1JPN130P08	127	10000000	runout	27	-1	370
S.I.	Const.	160	1JPN130P09	127	5340000	runout	27	-1	370
S.I.	Const.	160	1JPN130W01	245	242000	crack	27	-1	370
S.I.	Const.	160	1JPN130W02	245	217000	crack	27	-1	370
S.I.	Const.	160	1JPN130W03	245	274000	crack	27	-1	370
S.I.	Const.	160	1JPN130W04	177	774000	crack	27	-1	370
S.I.	Const.	160	1JPN130W05	177	432000	crack	27	-1	370
S.I.	Const.	160	1JPN130W06	177	822000	crack	27	-1	370
S.I.	Const.	160	1JPN130W07	147	2160000	crack	27	-1	370
S.I.	Const.	160	1JPN130W08	147	1820000	crack	27	-1	370
S.I.	Const.	160	1JPN130W09	147	5030000	runout	27	-1	370
S.I.	Const.	160	1JPN130W10	147	5340000	runout	27	-1	370
S.I.	Const.	160	1JPN130N01	245	268000	crack	27	-1	370
S.I.	Const.	160	1JPN130N02	245	170000	crack	27	-1	370
S.I.	Const.	160	1JPN130N03	245	219000	crack	27	-1	370
S.I.	Const.	160	1JPN130N04	177	660000	crack	27	-1	370
S.I.	Const.	160	1JPN130N05	177	826000	crack	27	-1	370
S.I.	Const.	160	1JPN130N06	177	608000	crack	27	-1	370
S.I.	Const.	160	1JPN130N07	147	5480000	runout	27	-1	370
S.I.	Const.	160	1JPN130N08	147	1170000	crack	27	-1	370
S.I.	Const.	160	1JPN130N09	147	1720000	crack	27	-1	370
S.I.	Const.	165	1JPN132W01	245	379000	crack	27	-1	370
S.I.	Const.	165	1JPN132W02	245	318000	crack	27	-1	370
S.I.	Const.	165	1JPN132W03	245	267000	crack	27	-1	370
S.I.	Const.	165	1JPN132W04	177	955000	crack	27	-1	370
S.I.	Const.	165	1JPN132W05	177	1869000	crack	27	-1	370
S.I.	Const.	165	1JPN132W06	177	1034000	crack	27	-1	370
S.I.	Const.	165	1JPN132W07	147	3250000	runout	27	-1	370
S.I.	Const.	165	1JPN132W08	147	3030000	runout	27	-1	370
S.I.	Const.	165	1JPN132W09	147	2740000	crack	27	-1	370
S.I.	Const.	165	1JPN132N01	245	379000	crack	27	-1	370
S.I.	Const.	165	1JPN132N02	245	634000	crack	27	-1	370

(continued on next page)

Table F.7.1. Fatigue Test Data (continued)

Units	Load Type	Detail	ID Number	Stress Range	Cycles	Result	Min. Stress	Max. Stress	Yield Stress
S.I.	Const.	165	1JPN132N03	245	440000	crack	27	-1	370
S.I.	Const.	165	1JPN132N04	177	631000	crack	27	-1	370
S.I.	Const.	165	1JPN132N05	177	2210000	runout	27	-1	370
S.I.	Const.	165	1JPN132N06	177	720000	crack	27	-1	370
S.I.	Const.	165	1JPN132N07	147	3470000	runout	27	-1	370
S.I.	Const.	165	1JPN132N08	147	1790000	crack	27	-1	370
S.I.	Const.	165	1JPN132N09	147	3620000	runout	27	-1	370
S.I.	Const.	165	1JPN134W01	245	740000	crack	27	-1	370
S.I.	Const.	165	1JPN134W02	245	233000	crack	27	-1	370
S.I.	Const.	165	1JPN134W03	245	578000	crack	27	-1	370
S.I.	Const.	165	1JPN134W04	177	1733000	crack	27	-1	370
S.I.	Const.	165	1JPN134W05	177	4470000	runout	27	-1	370
S.I.	Const.	165	1JPN134W06	177	652000	crack	27	-1	370
S.I.	Const.	165	1JPN134W07	177	1506000	crack	27	-1	370
S.I.	Const.	165	1JPN134W08	147	4750000	runout	27	-1	370
S.I.	Const.	165	1JPN134W09	147	4710000	runout	27	-1	370
S.I.	Const.	165	1JPN134W10	147	3930000	runout	27	-1	370
S.I.	Const.	165	1JPN134N01	245	482000	crack	27	-1	370
S.I.	Const.	165	1JPN134N02	245	368000	crack	27	-1	370
S.I.	Const.	165	1JPN134N03	245	392000	crack	27	-1	370
S.I.	Const.	165	1JPN134N04	177	974000	crack	27	-1	370
S.I.	Const.	165	1JPN134N05	177	1694000	crack	27	-1	370
S.I.	Const.	165	1JPN134N06	177	4750000	runout	27	-1	370
S.I.	Const.	165	1JPN134N07	177	1386000	crack	27	-1	370
S.I.	Const.	165	1JPN134N08	147	4490000	runout	27	-1	370
S.I.	Const.	165	1JPN134N09	147	4510000	runout	27	-1	370
S.I.	Const.	165	1JPN134N10	147	4680000	runout	27	-1	370
S.I.	Const.	165	1JPN135W01	245	336000	crack	27	-1	370
S.I.	Const.	165	1JPN135W02	245	364000	crack	27	-1	370
S.I.	Const.	165	1JPN135W03	245	274000	crack	27	-1	370
S.I.	Const.	165	1JPN135W04	177	2493000	crack	27	-1	370
S.I.	Const.	165	1JPN135W05	177	5210000	runout	27	-1	370
S.I.	Const.	165	1JPN135W06	177	1387000	crack	27	-1	370
S.I.	Const.	165	1JPN135W07	177	1558000	crack	27	-1	370
S.I.	Const.	165	1JPN135W08	147	2315000	crack	27	-1	370
S.I.	Const.	165	1JPN135W09	147	3940000	runout	27	-1	370
S.I.	Const.	165	1JPN135W10	147	1110000	crack	27	-1	370
S.I.	Const.	200	1JPN130P01	245	123000	crack	27	-1	370
S.I.	Const.	200	1JPN130P02	245	109000	crack	27	-1	370

(continued on next page)

Table F.7.1. Fatigue Test Data (continued)

Units	Load Type	Detail	ID Number	Stress Range	Cycles	Result	Min. Stress	Max. Stress	Yield Stress
S.I.	Const.	200	1JPN130P03	245	158000	crack	27	-1	370
S.I.	Const.	200	1JPN130P04	177	359000	crack	27	-1	370
S.I.	Const.	200	1JPN130P05	177	373000	crack	27	-1	370
S.I.	Const.	200	1JPN130P06	177	321000	crack	27	-1	370
S.I.	Const.	200	1JPN130P07	127	1040000	crack	27	-1	370
S.I.	Const.	200	1JPN130P08	127	1005000	crack	27	-1	370
S.I.	Const.	200	1JPN130P09	127	720000	crack	27	-1	370
S.I.	Const.	200	1JPN130P10	127	1310000	crack	27	-1	370
S.I.	Const.	200	1JPN130W01	245	135000	crack	27	-1	370
S.I.	Const.	200	1JPN130W02	245	130000	crack	27	-1	370
S.I.	Const.	200	1JPN130W03	245	154000	crack	27	-1	370
S.I.	Const.	200	1JPN130W04	177	323000	crack	27	-1	370
S.I.	Const.	200	1JPN130W05	177	314000	crack	27	-1	370
S.I.	Const.	200	1JPN130W06	177	372000	crack	27	-1	370
S.I.	Const.	200	1JPN130W07	177	297000	crack	27	-1	370
S.I.	Const.	200	1JPN130W08	127	1322000	crack	27	-1	370
S.I.	Const.	200	1JPN130W09	127	5330000	runout	27	-1	370
S.I.	Const.	200	1JPN130W10	127	1028000	crack	27	-1	370
S.I.	Const.	200	1JPN130W11	127	5340000	runout	27	-1	370
S.I.	Const.	200	1JPN130N01	245	144000	crack	27	-1	370
S.I.	Const.	200	1JPN130N02	245	137000	crack	27	-1	370
S.I.	Const.	200	1JPN130N03	245	151000	crack	27	-1	370
S.I.	Const.	200	1JPN130N04	245	139000	crack	27	-1	370
S.I.	Const.	200	1JPN130N05	177	422000	crack	27	-1	370
S.I.	Const.	200	1JPN130N06	177	709000	crack	27	-1	370
S.I.	Const.	200	1JPN130N07	177	356000	crack	27	-1	370
S.I.	Const.	200	1JPN130N08	127	958000	crack	27	-1	370
S.I.	Const.	200	1JPN130N09	127	787000	crack	27	-1	370
S.I.	Const.	200	1JPN130N10	127	777000	crack	27	-1	370
S.I.	Const.	205	1JPN132W01	245	195000	crack	27	-1	370
S.I.	Const.	205	1JPN132W02	245	168000	crack	27	-1	370
S.I.	Const.	205	1JPN132W03	245	154000	crack	27	-1	370
S.I.	Const.	205	1JPN132W04	177	360000	crack	27	-1	370
S.I.	Const.	205	1JPN132W05	177	377000	crack	27	-1	370
S.I.	Const.	205	1JPN132W06	177	348000	crack	27	-1	370
S.I.	Const.	205	1JPN132W07	147	2370000	runout	27	-1	370
S.I.	Const.	205	1JPN132W08	147	705000	crack	27	-1	370
S.I.	Const.	205	1JPN132W09	147	1100000	crack	27	-1	370
S.I.	Const.	205	1JPN132W10	127	2990000	runout	27	-1	370

(continued on next page)

Table F.7.1. Fatigue Test Data (continued)

Units	Load Type	Detail	ID Number	Stress Range	Cycles	Result	Min. Stress	Max. Stress	Yield Stress
S.I.	Const.	205	1JPN132W11	127	1179000	crack	27	-1	370
S.I.	Const.	205	1JPN132W12	127	1056000	crack	27	-1	370
S.I.	Const.	205	1JPN134W01	245	177000	crack	27	-1	370
S.I.	Const.	205	1JPN134W02	245	166000	crack	27	-1	370
S.I.	Const.	205	1JPN134W03	245	213000	crack	27	-1	370
S.I.	Const.	205	1JPN134W04	177	668000	crack	27	-1	370
S.I.	Const.	205	1JPN134W05	177	327000	crack	27	-1	370
S.I.	Const.	205	1JPN134W06	177	357000	crack	27	-1	370
S.I.	Const.	205	1JPN134W07	147	662000	crack	27	-1	370
S.I.	Const.	205	1JPN134W08	147	915000	crack	27	-1	370
S.I.	Const.	205	1JPN134W09	147	4470000	runout	27	-1	370
S.I.	Const.	205	1JPN134W10	127	1624000	crack	27	-1	370
S.I.	Const.	205	1JPN134N01	245	150000	crack	27	-1	370
S.I.	Const.	205	1JPN134N02	245	248000	crack	27	-1	370
S.I.	Const.	205	1JPN134N03	245	130000	crack	27	-1	370
S.I.	Const.	205	1JPN134N04	177	415000	crack	27	-1	370
S.I.	Const.	205	1JPN134N05	177	532000	crack	27	-1	370
S.I.	Const.	205	1JPN134N06	177	631000	crack	27	-1	370
S.I.	Const.	205	1JPN134N07	127	1086000	crack	27	-1	370
S.I.	Const.	205	1JPN134N08	127	968000	crack	27	-1	370
S.I.	Const.	205	1JPN134N09	127	623000	crack	27	-1	370
Imp.	Var.	30	1NC8004W01	4.09	34700000	crack	4.17	7.88	36
Imp.	Var.	30	1NC8004W01	4.09	35000000	runout	4.17	7.88	36
Imp.	Var.	30	1NC8004W17	4.09	35000000	runout	4.17	7.88	36
Imp.	Var.	30	1NC8004W17	4.09	35000000	runout	4.17	7.88	36
Imp.	Var.	30	1NC8004E01	4.09	34700000	crack	4.17	7.88	36
Imp.	Var.	30	1NC8004E01	4.09	35000000	runout	4.17	7.88	36
Imp.	Var.	30	1NC8004E17	4.09	35000000	runout	4.17	7.88	36
Imp.	Var.	30	1NC8004E17	4.09	32000000	crack	4.17	7.88	36
Imp.	Var.	30	1NC8002N01	3.25	86900000	crack	4.17	12.5	36
Imp.	Var.	30	1NC8002N01	3.25	120000000	runout	4.17	12.5	36
Imp.	Var.	30	1NC8002N17	3.25	120000000	runout	4.17	12.5	36
Imp.	Var.	30	1NC8002N17	3.25	120000000	runout	4.17	12.5	36
Imp.	Var.	30	1NC8002S01	3.25	120000000	runout	4.17	12.5	36
Imp.	Var.	30	1NC8002S01	3.25	87200000	crack	4.17	12.5	36
Imp.	Var.	30	1NC8002S17	3.25	120000000	runout	4.17	12.5	36
Imp.	Var.	30	1NC8002S17	3.25	120000000	runout	4.17	12.5	36
Imp.	Var.	40	1NC8003E01	1.87	109000000	runout	2.22	5.92	36
Imp.	Var.	40	1NC8003E01	1.87	109000000	runout	2.22	5.92	36

(continued on next page)

Table F.7.1. Fatigue Test Data (continued)

Units	Load Type	Detail	ID Number	Stress Range	Cycles	Result	Min. Stress	Max. Stress	Yield Stress
Imp.	Var.	40	1NC8003E17	1.87	109000000	runout	2.22	5.92	36
Imp.	Var.	40	1NC8003E17	1.87	109000000	runout	2.22	5.92	36
Imp.	Var.	40	1NC8003W01	1.99	104000000	runout	2.65	7.09	36
Imp.	Var.	40	1NC8003W01	1.99	104000000	runout	2.65	7.09	36
Imp.	Var.	40	1NC8003W17	1.99	104000000	runout	2.65	7.09	36
Imp.	Var.	40	1NC8003W17	1.99	104000000	crack	2.65	7.09	36
Imp.	Var.	40	1NC8001N01	2.07	107000000	runout	2.47	6.62	36
Imp.	Var.	40	1NC8001N01	2.07	107000000	runout	2.47	6.62	36
Imp.	Var.	40	1NC8001N17	2.07	107000000	runout	2.47	6.62	36
Imp.	Var.	40	1NC8001N17	2.07	107000000	runout	2.47	6.62	36
Imp.	Var.	40	1NC8001S01	2.07	107000000	runout	2.47	6.62	36
Imp.	Var.	40	1NC8001S01	2.07	107000000	runout	2.47	6.62	36
Imp.	Var.	40	1NC8001S17	2.07	107000000	runout	2.47	6.62	36
Imp.	Var.	40	1NC8001S17	2.07	107000000	runout	2.47	6.62	36
Imp.	Const.	90	1NC8003E08	6.29	109000000	crack	7.5	20	36
Imp.	Const.	90	1NC8002N08	7.02	89470000	crack	9	27	36
Imp.	Const.	90	1NC8103E08	12.5	5010000	crack	7.5	20	36
Imp.	Const.	90	1NC8102N08	16	110000	crack	9	27	36
Imp.	Const.	90	1NC8003E09	6.29	109000000	crack	7.5	20	36
Imp.	Const.	90	1NC8103E09	12.5	5010000	crack	7.5	20	36
Imp.	Const.	90	1NC8003E10	6.29	112000000	runout	7.5	20	36
Imp.	Const.	90	1NC8001N08	7.12	107000000	runout	8.3	22.3	36
Imp.	Const.	90	1NC8001N09	7.12	107000000	runout	8.3	22.3	36
Imp.	Const.	90	1NC8001N10	7.12	107000000	runout	8.3	22.3	36
Imp.	Const.	90	1NC8001S08	7.12	107000000	runout	8.3	22.3	36
Imp.	Const.	90	1NC8001S09	7.12	107000000	runout	8.3	22.3	36
Imp.	Const.	90	1NC8001S10	7.12	107000000	runout	8.3	22.3	36
Imp.	Const.	90	1NC8002S08	7.02	125000000	runout	9	27	36
Imp.	Const.	90	1NC8002S09	5.66	125000000	runout	7.26	21.77	36
Imp.	Const.	90	1NC8002S10	7.02	125000000	runout	9	27	36
Imp.	Const.	90	1NC8002N09	5.66	125000000	runout	7.26	21.77	36
Imp.	Const.	90	1NC8002N10	7.02	120000000	crack	9	27	36
Imp.	Const.	90	1NC8003W08	6.7	104000000	runout	9	24	36
Imp.	Const.	90	1NC8003W09	6.7	104000000	runout	9	24	36
Imp.	Const.	90	1NC8003W10	6.7	104000000	runout	9	24	36
Imp.	Const.	90	1NC8004W08	8.83	34700000	runout	9	25	36
Imp.	Const.	90	1NC8004W09	8.83	34700000	runout	9	25	36
Imp.	Const.	90	1NC8004W10	8.83	34700000	runout	9	25	36
Imp.	Const.	90	1NC8004E08	8.83	34700000	runout	9	25	36

(continued on next page)



Table F.7.1. Fatigue Test Data (continued)

Units	Load Type	Detail	ID Number	Stress Range	Cycles	Result	Min. Stress	Max. Stress	Yield Stress
Imp.	Const.	90	1NC8004E09	8.83	34700000	runout	9	25	36
Imp.	Const.	90	1NC8004E10	8.83	34700000	runout	9	25	36
S.I.	Var.	90	00RE80A601	55.9	24290000	crack	9	1	311
S.I.	Var.	90	00RE80A602	55.9	27620000	crack	2	1	311
Imp.	Var.	120	1NC8001N02	1.36	107000000	runout	1.61	4.32	36
Imp.	Var.	120	1NC8001N03	1.74	107000000	runout	2.07	5.54	36
Imp.	Var.	120	1NC8001N04	1.76	107000000	runout	2.09	5.61	36
Imp.	Var.	120	1NC8001N05	2.08	107000000	runout	2.45	6.59	36
Imp.	Var.	120	1NC8001N06	2.15	107000000	runout	2.56	6.85	36
Imp.	Var.	120	1NC8001N07	2.42	107000000	runout	2.88	7.71	36
Imp.	Var.	120	1NC8001N11	2.42	107000000	runout	2.88	7.71	36
Imp.	Var.	120	1NC8001N12	2.15	107000000	runout	2.56	6.85	36
Imp.	Var.	120	1NC8001N13	2.08	107000000	runout	2.45	6.59	36
Imp.	Var.	120	1NC8001N14	1.76	107000000	runout	2.09	5.61	36
Imp.	Var.	120	1NC8001N15	1.74	107000000	runout	2.07	5.54	36
Imp.	Var.	120	1NC8001N16	1.36	107000000	runout	1.61	4.32	36
Imp.	Var.	120	1NC8001S02	1.36	107000000	runout	1.61	4.32	36
Imp.	Var.	120	1NC8001S03	1.74	107200000	crack	2.07	5.54	36
Imp.	Var.	120	1NC8001S04	1.76	107000000	runout	2.09	5.61	36
Imp.	Var.	120	1NC8001S05	2.08	107000000	runout	2.45	6.59	36
Imp.	Var.	120	1NC8001S06	2.15	86000000	crack	2.56	6.85	36
Imp.	Var.	120	1NC8001S07	2.42	107000000	runout	2.88	7.71	36
Imp.	Var.	120	1NC8001S11	2.42	43600000	crack	2.88	7.71	36
Imp.	Var.	120	1NC8001S12	2.15	107000000	runout	2.56	6.85	36
Imp.	Var.	120	1NC8001S13	2.08	107000000	runout	2.45	6.59	36
Imp.	Var.	120	1NC8001S14	1.76	107000000	runout	2.09	5.61	36
Imp.	Var.	120	1NC8001S15	1.74	107000000	runout	2.07	5.54	36
Imp.	Var.	120	1NC8001S16	1.36	107000000	runout	1.61	4.32	36
Imp.	Var.	120	1NC8002S02	1.36	120000000	crack	1.74	5.23	36
Imp.	Var.	120	1NC8002S03	1.74	120000000	crack	2.23	6.69	36
Imp.	Var.	120	1NC8002S04	1.76	120000000	crack	2.26	6.77	36
Imp.	Var.	120	1NC8002S05	2.08	120000000	crack	2.67	8	36
Imp.	Var.	120	1NC8002S06	2.15	120000000	runout	2.76	8.27	36
Imp.	Var.	120	1NC8002S07	2.42	69500000	crack	3.1	9.31	36
Imp.	Var.	120	1NC8002S11	2.42	120000000	crack	3.1	9.31	36
Imp.	Var.	120	1NC8002S12	2.15	120000000	runout	2.76	8.27	36
Imp.	Var.	120	1NC8002S13	2.08	99600000	crack	2.67	8	36
Imp.	Var.	120	1NC8002S14	1.76	120000000	runout	2.26	6.77	36
Imp.	Var.	120	1NC8002S15	1.74	120000000	runout	2.23	6.69	36

(continued on next page)

Table F.7.1. Fatigue Test Data (continued)

Units	Load Type	Detail	ID Number	Stress Range	Cycles	Result	Min. Stress	Max. Stress	Yield Stress
Imp.	Var.	120	1NC8002S16	1.36	120000000	runout	1.74	5.23	36
Imp.	Var.	120	1NC8002N02	1.36	94300000	crack	1.74	5.23	36
Imp.	Var.	120	1NC8002N03	1.74	120000000	runout	2.23	6.69	36
Imp.	Var.	120	1NC8002N04	1.76	120000000	runout	2.26	6.77	36
Imp.	Var.	120	1NC8002N05	2.08	120000000	crack	2.67	8	36
Imp.	Var.	120	1NC8002N06	2.15	120000000	crack	2.76	8.27	36
Imp.	Var.	120	1NC8002N07	2.42	120000000	crack	3.1	9.31	36
Imp.	Var.	120	1NC8002N11	2.42	71900000	crack	3.1	9.31	36
Imp.	Var.	120	1NC8002N12	2.15	120000000	crack	2.76	8.27	36
Imp.	Var.	120	1NC8002N13	2.08	120000000	crack	2.67	8	36
Imp.	Var.	120	1NC8002N14	1.76	120000000	runout	2.26	6.77	36
Imp.	Var.	120	1NC8002N15	1.74	120000000	runout	2.23	6.69	36
Imp.	Var.	120	1NC8002N16	1.36	120000000	runout	1.74	5.23	36
Imp.	Var.	120	1NC8003W02	1.29	104000000	runout	1.75	4.65	36
Imp.	Var.	120	1NC8003W03	1.66	104000000	runout	2.23	5.94	36
Imp.	Var.	120	1NC8003W04	1.69	104000000	runout	2.26	6.03	36
Imp.	Var.	120	1NC8003W05	1.98	104000000	runout	2.65	7.08	36
Imp.	Var.	120	1NC8003W06	2.05	104000000	runout	2.74	7.33	36
Imp.	Var.	120	1NC8003W07	2.31	37800000	crack	3.11	8.29	36
Imp.	Var.	120	1NC8003W11	2.31	104000000	runout	3.11	8.29	36
Imp.	Var.	120	1NC8003W12	2.05	67200000	crack	2.74	7.33	36
Imp.	Var.	120	1NC8003W13	1.98	104000000	runout	2.65	7.08	36
Imp.	Var.	120	1NC8003W14	1.69	104000000	runout	2.26	6.03	36
Imp.	Var.	120	1NC8003W15	1.66	104000000	runout	2.23	5.94	36
Imp.	Var.	120	1NC8003W16	1.29	104000000	runout	1.75	3.65	36
Imp.	Var.	120	1NC8003E02	1.22	109000000	runout	1.45	3.87	36
Imp.	Var.	120	1NC8003E03	1.55	109000000	runout	1.85	4.94	36
Imp.	Var.	120	1NC8003E04	1.59	109000000	runout	1.88	5.02	36
Imp.	Var.	120	1NC8003E05	1.86	109000000	runout	2.22	5.92	36
Imp.	Var.	120	1NC8003E06	1.92	109000000	runout	2.3	6.13	36
Imp.	Var.	120	1NC8003E07	1.93	104000000	crack	2.59	6.91	36
Imp.	Var.	120	1NC8003E11	2.17	109000000	crack	2.59	6.91	36
Imp.	Var.	120	1NC8003E12	1.92	109000000	crack	2.3	6.13	36
Imp.	Var.	120	1NC8003E13	1.86	109000000	runout	2.22	5.92	36
Imp.	Var.	120	1NC8003E14	1.59	109000000	runout	1.88	5.02	36
Imp.	Var.	120	1NC8003E15	1.55	109000000	runout	1.85	4.94	36
Imp.	Var.	120	1NC8003E16	1.22	109000000	runout	1.45	3.87	36
Imp.	Var.	120	1NC8004W02	1.71	34700000	runout	1.74	3.29	36
Imp.	Var.	120	1NC8004W03	2.18	34700000	runout	2.23	4.21	36

(continued on next page)

Table F.7.1. Fatigue Test Data (continued)

Units	Load Type	Detail	ID Number	Stress Range	Cycles	Result	Min. Stress	Max. Stress	Yield Stress
Imp.	Var.	120	1NC8004W04	2.22	34700000	runout	2.26	4.27	36
Imp.	Var.	120	1NC8004W05	2.61	34700000	runout	2.67	5.04	36
Imp.	Var.	120	1NC8004W06	2.7	34700000	runout	2.76	5.21	36
Imp.	Var.	120	1NC8004W07	3.05	34700000	runout	3.12	8.65	36
Imp.	Var.	120	1NC8004W11	3.05	22600000	crack	3.12	8.65	36
Imp.	Var.	120	1NC8004W12	2.7	33000000	crack	2.76	5.21	36
Imp.	Var.	120	1NC8004W13	2.61	18600000	crack	2.67	5.04	36
Imp.	Var.	120	1NC8004W14	2.22	33000000	crack	2.26	4.27	36
Imp.	Var.	120	1NC8004W15	2.18	34700000	runout	2.23	4.21	36
Imp.	Var.	120	1NC8004W16	1.71	34700000	runout	1.74	3.29	36
Imp.	Var.	120	1NC8004E02	1.71	34700000	runout	1.74	3.29	36
Imp.	Var.	120	1NC8004E03	2.18	34700000	runout	2.23	4.21	36
Imp.	Var.	120	1NC8004E04	2.22	34700000	runout	2.26	4.27	36
Imp.	Var.	120	1NC8004E05	2.61	34700000	crack	2.67	5.04	36
Imp.	Var.	120	1NC8004E06	2.7	32000000	crack	2.76	5.21	36
Imp.	Var.	120	1NC8004E07	3.05	34700000	runout	3.12	8.65	36
Imp.	Var.	120	1NC8004E11	3.05	34700000	runout	3.12	8.65	36
Imp.	Var.	120	1NC8004E12	2.7	34700000	runout	2.76	5.21	36
Imp.	Var.	120	1NC8004E13	2.61	34700000	crack	2.67	5.04	36
Imp.	Var.	120	1NC8004E14	2.22	34700000	runout	2.26	4.27	36
Imp.	Var.	120	1NC8004E15	2.18	34700000	runout	2.23	4.21	36
Imp.	Var.	120	1NC8004E16	1.71	17400000	crack	1.74	3.29	36
S.I.	Const.	100	3CHIS104.0	146	3900000	crack			390
S.I.	Const.	100	3CHIS203.0	172	4300000	crack			390
S.I.	Const.	100	3CHIS204.0	161	1330000	crack			390
S.I.	Const.	100	3CHIS205.0	181	875000	crack			390
S.I.	Const.	100	3CHIS206.0	146	1938000	crack			390
S.I.	Const.	50	3ICOM001.0	180	170300	crack			355
S.I.	Const.	50	3ICOM002.0	180	203000	crack			355
S.I.	Const.	50	3ICOM003.0	180	200400	crack			355
S.I.	Const.	50	3ICOM004.0	180	220300	crack			355
S.I.	Const.	50	3ICOM005.0	180	159300	crack			355
S.I.	Const.	50	3ICOM006.0	180	155400	crack			355
S.I.	Const.	50	3ICOM007.0	100	1454500	crack			355
S.I.	Const.	50	3ICOM008.0	100	1364700	crack			355
S.I.	Const.	50	3ICOM009.0	100	1390100	crack			355
S.I.	Const.	50	3ICOM010.0	100	1001200	crack			355
S.I.	Const.	50	3ICOM011.0	100	956200	crack			355
S.I.	Const.	50	3ICOM012.0	100	1273200	crack			355

(continued on next page)

Table F.7.1. Fatigue Test Data (continued)

Units	Load Type	Detail	ID Number	Stress Range	Cycles	Result	Min. Stress	Max. Stress	Yield Stress
S.I.	Const.	100	3BELG011.0	95	1650000	crack			355
S.I.	Const.	100	3BELG012.0	100	1900000	crack			355
S.I.	Const.	100	3BELG013.0	92	1750000	crack			355
S.I.	Const.	100	3BELG014.0	130	425000	crack			355
S.I.	Const.	100	3BELG015.0	160	407000	crack			355
S.I.	Const.	100	3BELG021.0	160	528000	crack			355
S.I.	Const.	100	3BELG022.0	206	697000	crack			355
S.I.	Const.	100	3BELG023.0	125	716000	crack			355
S.I.	Const.	100	3BELG024.0	130	484000	crack			355
S.I.	Const.	100	3BELG031.0	109	2217000	runout			355
S.I.	Const.	100	3BELG032.0	131	660000	crack			355
S.I.	Const.	100	3BELG033.0	120	1050000	crack			355
S.I.	Const.	100	3BELG012.1	103	2060000	runout			355
S.I.	Const.	100	3BELG015.1	126	650000	crack			355
S.I.	Var.	90	3TFHD009.1	45.2	9262000	crack			
S.I.	Var.	90	3TFHD009.2	40.3	13765700	crack			
S.I.	Var.	90	3TFHD009.3	45.2	10400700	crack			
S.I.	Var.	90	3TFHD009.4	40.3	12185400	crack			
S.I.	Var.	90	3TFHD009.5	45.2	10217900	crack			
S.I.	Var.	90	3TFHD009.6	40.3	17105200	crack			
S.I.	Var.	90	3TFHD007.1	56.7	11737900	crack			
S.I.	Var.	90	3TFHD007.2	63.6	4637600	crack			
S.I.	Var.	90	3TFHD007.3	56.7	4486950	crack			
S.I.	Var.	90	3TFHD007.4	63.6	4407900	crack			
S.I.	Var.	90	3TFHD007.5	56.7	7733800	crack			
S.I.	Var.	90	3TFHD007.6	63.6	6120000	crack			
S.I.	Var.	90	3TFHC001.0	63.2	21400000	runout			
S.I.	Var.	90	3TFHC002.0	80	4500000	runout			
S.I.	Var.	90	3TFHC012.1	70.7	7900000	crack			
S.I.	Var.	90	3TFHC012.2	70.7	7850000	crack			
S.I.	Var.	90	3TFHC012.3	70.7	6019000	crack			
S.I.	Var.	90	3TFHC012.4	70.7	6300000	crack			
S.I.	Var.	90	3TFHC012.5	70.7	6200000	crack			
S.I.	Var.	90	3TFHC012.6	70.7	5650000	crack			
S.I.	Var.	90	3TFHC011.1	70.7	7654000	crack			
S.I.	Var.	90	3TFHC011.2	70.7	8600000	crack			
S.I.	Var.	90	3TFHC011.3	70.7	7300000	crack			
S.I.	Var.	90	3TFHC011.4	70.7	10400000	crack			
S.I.	Var.	90	3TFHC011.5	70.7	10850000	crack			

(continued on next page)

Table F.7.1. Fatigue Test Data (continued)

Units	Load Type	Detail	ID Number	Stress Range	Cycles	Result	Min. Stress	Max. Stress	Yield Stress
S.I.	Var.	90	3TFHC011.6	70.7	12130000	runout			
S.I.	Var.	90	3TFHD008.1	37.1	18737000	crack			
S.I.	Var.	90	3TFHD008.2	37.1	24962000	crack			
S.I.	Var.	90	3TFHD008.3	37.1	25406000	crack			
S.I.	Var.	90	3TFHD008.4	37.1	42000000	runout			
S.I.	Var.	90	3TFHC006.1	54.1	20100000	crack			
S.I.	Var.	90	3TFHC006.2	54.1	78000000	runout			
Imp.	Const.	140	1DTRG001	20	12634300	crack			550
Imp.	Const.	140	1DTRG002	24	775600	crack			550
Imp.	Const.	140	1DTRG003	30	572000	crack			550
Imp.	Const.	140	1DTRG004	60	66500	crack			550
Imp.	Const.	140	1DTRG005	90	14500	crack			550
Imp.	Const.	140	1DTRG006	140	1010	crack			550
Imp.	Const.	140	1DTRG007	20	2903700	crack			550
Imp.	Const.	140	1DTRG008	24	3732900	crack			550
Imp.	Const.	140	1DTRG009	30	779500	crack			550
Imp.	Const.	140	1DTRG010	60	61900	crack			550
Imp.	Const.	140	1DTRG011	90	14800	crack			550
Imp.	Const.	140	1DTRG012	140	2020	crack			550
Imp.	Const.	140	1DTRG013	20	26195300	runout			550
Imp.	Const.	140	1DTRG014	24	1118600	crack			550
Imp.	Const.	140	1DTRG015	30	515000	crack			550
Imp.	Const.	140	1DTRG016	60	70600	crack			550
Imp.	Const.	140	1DTRG017	90	16300	crack			550
Imp.	Const.	140	1DTRG018	140	2680	crack			550
Imp.	Const.	130	1DTRAC06	33.2	152950	crack			550
Imp.	Const.	130	1DTRAC14	26	392300	crack			550
Imp.	Const.	130	1DTRAC09	22.2	703170	crack			550
Imp.	Const.	130	1DTRAC13	18.1	1438000	crack			550
Imp.	Const.	130	1DTRAC05	15.6	4453420	crack			550
Imp.	Const.	130	1DTRAC11	13.9	25467460	runout			550
Imp.	Const.	130	1DTRAC10	12.2	2502800	crack			550
Imp.	Const.	130	1DTRAC07	12.2	22962600	runout			550
Imp.	Const.	130	1DTRAC01	11.3	50804500	runout			550
Imp.	Const.	130	2DTRAC15	33.3	58410	crack			550
Imp.	Const.	130	2DTRAC21	33.3	103010	crack			550
Imp.	Const.	130	2DTRAC20	26.1	339910	crack			550
Imp.	Const.	130	2DTRAC19	18.2	927040	crack			550
Imp.	Const.	130	2DTRAC22	15.7	981270	crack			550

(continued on next page)

**Table F.7.1. Fatigue Test Data (continued)**

Units	Load Type	Detail	ID Number	Stress Range	Cycles	Result	Min. Stress	Max. Stress	Yield Stress
Imp.	Const.	130	2DTRAC17	14	2030830	crack			550
Imp.	Const.	130	2DTRAC18	12.2	4039940	crack			550
Imp.	Const.	130	2DTRAC16	11.3	28899840	crack			550
Imp.	Const.	130	2DTRAC23	9.5	50545730	runout			550

Sources: Keating and Fisher 1986; P. B. Keating, personal communication requesting to locate and use the fatigue test database, 2012.

## Reference for F.7

Keating, P. B., and J. W. Fisher. 1986. *NCHRP Report 286: Evaluation of Fatigue Tests and Design Criteria on Welded Details*. TRB, National Research Council, Washington, D.C.

## F.8 Concrete Fatigue Database

**Table F.8.1. Fatigue Data for Plain Concrete in Compression**

S <sub>max</sub> /f' <sub>c</sub>	S <sub>min</sub> (ksi)	S <sub>r</sub> (ksi)	N	Reference No.	Notes
0.75	0.6	3.9	17000	1	Group 2A; e=0in
0.75	0.6	3.9	24000	1	Group 2A; e=0in
0.75	0.6	3.9	36000	1	Group 2A; e=0in
0.75	0.6	3.9	39000	1	Group 2A; e=0in
0.75	0.6	3.9	40000	1	Group 2A; e=0in
0.75	0.6	3.9	47000	1	Group 2A; e=0in
0.75	0.6	3.9	53000	1	Group 2A; e=0in
0.75	0.6	3.9	59000	1	Group 2A; e=0in
0.75	0.6	3.9	65000	1	Group 2A; e=0in
0.75	0.6	3.9	70000	1	Group 2A; e=0in
0.725	0.6	3.75	39000	1	Group 2A; e=0in
0.725	0.6	3.75	60000	1	Group 2A; e=0in
0.725	0.6	3.75	107000	1	Group 2A; e=0in
0.725	0.6	3.75	110000	1	Group 2A; e=0in
0.725	0.6	3.75	130000	1	Group 2A; e=0in
0.725	0.6	3.75	136000	1	Group 2A; e=0in
0.725	0.6	3.75	192000	1	Group 2A; e=0in
0.725	0.6	3.75	275000	1	Group 2A; e=0in
0.7	0.6	3.6	55000	1	Group 2A; e=0in
0.7	0.6	3.6	106000	1	Group 2A; e=0in
0.7	0.6	3.6	135000	1	Group 2A; e=0in
0.7	0.6	3.6	152000	1	Group 2A; e=0in
0.7	0.6	3.6	155000	1	Group 2A; e=0in
0.7	0.6	3.6	206000	1	Group 2A; e=0in

(continued on next page)

**Table F.8.1. Fatigue Data for Plain Concrete in Compression  
(continued)**

<b>S<sub>max</sub>/f'<sub>c</sub></b>	<b>S<sub>min</sub> (ksi)</b>	<b>S<sub>r</sub> (ksi)</b>	<b>N</b>	<b>Reference No.</b>	<b>Notes</b>
0.7	0.6	3.6	269000	1	Group 2A; e=0in
0.7	0.6	3.6	313000	1	Group 2A; e=0in
0.7	0.6	3.6	320000	1	Group 2A; e=0in
0.7	0.6	3.6	356000	1	Group 2A; e=0in
0.7	0.6	3.6	429000	1	Group 2A; e=0in
0.7	0.6	3.6	492000	1	Group 2A; e=0in
0.675	0.6	3.45	159000	1	Group 2A; e=0in
0.675	0.6	3.45	256000	1	Group 2A; e=0in
0.675	0.6	3.45	270000	1	Group 2A; e=0in
0.675	0.6	3.45	655000	1	Group 2A; e=0in
0.675	0.6	3.45	779000	1	Group 2A; e=0in
0.675	0.6	3.45	970000	1	Group 2A; e=0in
0.675	0.6	3.45	1048000	1	Group 2A; e=0in
0.675	0.6	3.45	1051000	1	Group 2A; e=0in
0.675	0.6	3.45	1318000	1	Group 2A; e=0in
0.675	0.6	3.45	1661000	1	Group 2A; e=0in
0.675	0.6	3.45	2000000	1	Group 2A; e=0in
0.675	0.6	3.45	2000000	1	Group 2A; e=0in
0.9	0.6	4.8	28000	1	Group 2B; e=1in
0.9	0.6	4.8	31000	1	Group 2B; e=1in
0.9	0.6	4.8	35000	1	Group 2B; e=1in
0.9	0.6	4.8	45000	1	Group 2B; e=1in
0.9	0.6	4.8	46000	1	Group 2B; e=1in
0.9	0.6	4.8	58000	1	Group 2B; e=1in
0.9	0.6	4.8	61000	1	Group 2B; e=1in
0.9	0.6	4.8	129000	1	Group 2B; e=1in
0.875	0.6	4.65	81000	1	Group 2B; e=1in
0.875	0.6	4.65	120000	1	Group 2B; e=1in
0.875	0.6	4.65	131000	1	Group 2B; e=1in
0.875	0.6	4.65	141000	1	Group 2B; e=1in
0.875	0.6	4.65	156000	1	Group 2B; e=1in
0.875	0.6	4.65	180000	1	Group 2B; e=1in
0.875	0.6	4.65	190000	1	Group 2B; e=1in
0.875	0.6	4.65	226000	1	Group 2B; e=1in
0.875	0.6	4.65	242000	1	Group 2B; e=1in
0.875	0.6	4.65	317000	1	Group 2B; e=1in
0.875	0.6	4.65	351000	1	Group 2B; e=1in
0.875	0.6	4.65	527000	1	Group 2B; e=1in

(continued on next page)

**Table F.8.1. Fatigue Data for Plain Concrete in Compression  
(continued)**

<b>S<sub>max</sub>/f'<sub>c</sub></b>	<b>S<sub>min</sub> (ksi)</b>	<b>S<sub>r</sub> (ksi)</b>	<b>N</b>	<b>Reference No.</b>	<b>Notes</b>
0.85	0.6	4.5	305000	1	Group 2B; e=1in
0.85	0.6	4.5	684000	1	Group 2B; e=1in
0.85	0.6	4.5	730000	1	Group 2B; e=1in
0.85	0.6	4.5	859000	1	Group 2B; e=1in
0.85	0.6	4.5	860000	1	Group 2B; e=1in
0.85	0.6	4.5	1045000	1	Group 2B; e=1in
0.85	0.6	4.5	2105000	1	Group 2B; e=1in
0.85	0.6	4.5	2751000	1	Group 2B; e=1in
0.85	0.6	4.5	2000000	1	Group 2B; e=1in
0.85	0.6	4.5	16000	1	Group 2C; e=1/3in
0.85	0.6	4.5	26000	1	Group 2C; e=1/3in
0.85	0.6	4.5	35000	1	Group 2C; e=1/3in
0.85	0.6	4.5	37000	1	Group 2C; e=1/3in
0.85	0.6	4.5	46000	1	Group 2C; e=1/3in
0.85	0.6	4.5	65000	1	Group 2C; e=1/3in
0.8	0.6	4.2	108000	1	Group 2C; e=1/3in
0.8	0.6	4.2	206000	1	Group 2C; e=1/3in
0.8	0.6	4.2	224000	1	Group 2C; e=1/3in
0.8	0.6	4.2	249000	1	Group 2C; e=1/3in
0.8	0.6	4.2	270000	1	Group 2C; e=1/3in
0.8	0.6	4.2	364000	1	Group 2C; e=1/3in
0.8	0.6	4.2	542000	1	Group 2C; e=1/3in
0.8	0.6	4.2	2000000	1	Group 2C; e=1/3in
0.775	0.6	4.05	464000	1	Group 2C; e=1/3in
0.775	0.6	4.05	888000	1	Group 2C; e=1/3in
0.775	0.6	4.05	941000	1	Group 2C; e=1/3in
0.775	0.6	4.05	1198000	1	Group 2C; e=1/3in
0.775	0.6	4.05	2000000	1	Group 2C; e=1/3in



**Table F.8.2. Concrete Fatigue Data for Reinforced Concrete**

f_min	S <sub>r</sub>	N	Reference No.	Notes/Specimen No.
5.0	39.0	216,400	2	
5.0	39.0	288,100	2	
5.0	39.0	315,600	2	
5.0	34.0	356,800	2	
15.0	34.0	406,600	2	
15.0	34.0	441,000	2	
5.0	34.0	506,100	2	
5.0	34.0	515,300	2	
5.0	29.0	626,000	2	
15.0	34.0	645,300	2	
15.0	29.0	746,000	2	
5.0	29.0	864,500	2	
5.0	29.0	920,200	2	
15.0	29.0	971,900	2	
15.0	29.0	1,232,300	2	
15.0	26.0	2,214,500	2	
15.0	24.0	3,187,500	2	
15.0	25.0	3,496,500	2	
15.0	24.0	3,702,400	2	
15.0	24.0	8,164,000	2	
4.31	39.42	6,250,000	3	Bar A-A15
24.8	22.2	5,200,000	3	Bar A-A15
4.31	34.27	3,782,000	3	Bar A-A15
12.85	31.62	3,375,000	3	Bar A-A15
4.31	38.56	3,142,800	3	Bar A-A15
4.32	38.66	2,934,000	3	Bar A-A15
12.89	34.11	2,342,000	3	Bar A-A15
4.31	42.69	2,037,000	3	Bar A-A15
12.85	36.18	1,598,000	3	Bar A-A15
4.31	39.39	1,316,000	3	Bar A-A15
4.31	38.64	1,060,000	3	Bar A-A15
12.87	35.06	964,000	3	Bar A-A15
4.31	40.2	881,000	3	Bar A-A15
4.32	41.81	750,000	3	Bar A-A15
12.87	35.06	555,000	3	Bar A-A15
4.32	40.21	526,000	3	Bar A-A15
4.31	42.69	450,000	3	Bar A-A15
12.85	34.01	435,000	3	Bar A-A15

(continued on next page)

**Table F.8.2. Concrete Fatigue Data for Reinforced Concrete (continued)**

f_min	S <sub>r</sub>	N	Reference No.	Notes/Specimen No.
4.31	42.69	431,000	3	Bar A-A15
4.32	40.22	359,000	3	Bar A-A15
4.32	41.81	281,000	3	Bar A-A15
4.31	42.59	245,500	3	Bar A-A15
4.31	41.75	224,300	3	Bar A-A15
4.31	42.69	183,000	3	Bar A-A15
18.99	44.31	89,200	3	Bar A-A15
5.95	62.75	92,200	3	Bar A-A15
5.93	53.96	113,500	3	Bar A-A15
18.97	47.24	169,500	3	Bar A-A15
5.93	47.61	286,000	3	Bar A-A15
5.93	44.46	317,800	3	Bar A-A15
19.11	42.42	389,200	3	Bar A-A15
19.11	44.6	406,300	3	Bar A-A15
5.95	40.8	432,400	3	Bar A-A440
19.06	37.91	432,600	3	Bar A-A440
19.13	41.23	456,100	3	Bar A-A440
5.93	47.61	505,600	3	Bar A-A440
19.05	37.89	526,800	3	Bar A-A440
5.92	41.46	561,700	3	Bar A-A440
5.94	41.41	590,000	3	Bar A-A440
5.94	38.18	914,700	3	Bar A-A440
18.99	33.44	990,000	3	Bar A-A440
5.95	36.07	1,073,000	3	Bar A-A440
5.94	36.6	1,123,000	3	Bar A-A440
19.04	36.09	1,160,000	3	Bar A-A440
19.02	37.84	1,193,000	3	Bar A-A440
5.93	38.17	1,285,000	3	Bar A-A440
5.92	41.45	1,315,600	3	Bar A-A440
19.07	36.16	1,475,750	3	Bar A-A440
5.94	36.06	1,589,000	3	Bar A-A440
5.94	38.44	2,330,000	3	Bar A-A440
5.92	35.93	2,772,300	3	Bar A-A440
18.98	31.45	2,867,000	3	Bar A-A440
5.95	29.75	3,097,000	3	Bar A-A440
19.03	34.69	3,705,200	3	Bar A-A440
5.93	35.99	3,766,000	3	Bar A-A440
5.96	29.78	4,405,000	3	Bar A-A440

(continued on next page)

**Table F.8.2. Concrete Fatigue Data for Reinforced Concrete (continued)**

f_min	S <sub>r</sub>	N	Reference No.	Notes/Specimen No.
18.98	28.28	4,514,000	3	Bar A-A440
8.94	67.1	75,000	3	Bar A-A431
8.94	67.1	101,000	3	Bar A-A431
27.14	58.48	135,000	3	Bar A-A431
26.94	58.04	137,100	3	Bar A-A431
27	48.95	152,000	3	Bar A-A431
8.99	60.72	201,100	3	Bar A-A431
27	48.95	215,000	3	Bar A-A431
26.95	49.09	216,000	3	Bar A-A431
8.94	54.7	225,100	3	Bar A-A431
9	55.03	253,000	3	Bar A-A431
26.9	49.44	301,000	3	Bar A-A431
8.94	45.61	307,600	3	Bar A-A431
26.76	49.18	474,100	3	Bar A-A431
9	45.91	512,000	3	Bar A-A431
27.12	37.18	642,300	3	Bar A-A431
27.15	40.92	702,500	3	Bar A-A431
8.36	40.85	714,200	3	Bar A-A431
26.94	40.61	1,006,000	3	Bar A-A431
26.96	37.06	1,044,000	3	Bar A-A431
8.99	40.53	1,048,000	3	Bar A-A431
26.93	40.59	1,075,000	3	Bar A-A431
26.97	37.07	1,456,000	3	Bar A-A431
26.91	36.99	1,560,000	3	Bar A-A431
8.93	40.26	2,250,000	3	Bar A-A431
8.93	40.23	4,160,000	3	Bar A-A431
27	31.56	6,654,000	3	Bar A-A431
4.85	45.68	127,500	3	Bar B-A15
14.42	38.12	259,000	3	Bar B-A15
4.83	43.09	290,000	3	Bar B-A15
4.85	36	352,000	3	Bar B-A15
14.44	35.81	372,000	3	Bar B-A15
4.83	40.69	411,000	3	Bar B-A15
14.5	33.57	477,200	3	Bar B-A15
4.84	36	504,500	3	Bar B-A15
4.84	43.4	538,200	3	Bar B-A15
14.42	33.38	568,000	3	Bar B-A15
14.46	32.3	646,000	3	Bar B-A15

(continued on next page)

**Table F.8.2. Concrete Fatigue Data for Reinforced Concrete (continued)**

f_min	S <sub>r</sub>	N	Reference No.	Notes/Specimen No.
4.84	40.77	661,300	3	Bar B-A15
4.85	36.13	665,000	3	Bar B-A15
4.85	34.73	887,000	3	Bar B-A15
14.44	32.25	890,400	3	Bar B-A15
14.5	31.19	1,157,300	3	Bar B-A15
14.47	29.93	1,478,000	3	Bar B-A15
14.43	31.11	1,664,200	3	Bar B-A15
4.84	34.67	1,900,000	3	Bar B-A15
4.83	33.6	3,012,800	3	Bar B-A15
14.44	29.87	4,819,500	3	Bar B-A15
14.46	28.71	5,350,000	3	Bar B-A15
8.11	38.38	91,500	3	Bar B-A431
8.13	62.66	102,000	3	Bar B-A431
8.13	57.69	110,000	3	Bar B-A431
24.33	52.23	120,200	3	Bar B-A431
8.13	52.55	174,000	3	Bar B-A431
24.39	48.37	188,000	3	Bar B-A431
24.41	44.45	255,300	3	Bar B-A431
8.13	48.37	266,000	3	Bar B-A431
24.26	40.22	313,000	3	Bar B-A431
8.13	44.39	428,000	3	Bar B-A431
24.26	36.08	541,000	3	Bar B-A431
24.38	36.28	604,200	3	Bar B-A431
8.12	40.42	651,000	3	Bar B-A431
24.41	32.14	979,000	3	Bar B-A431
8.13	36.49	1,630,000	3	Bar B-A431
8.11	36.4	1,697,000	3	Bar B-A431
24.2	31.87	3,150,000	3	Bar B-A431
24.39	30.33	4,270,000	3	Bar B-A431
9.32	51.35	134,200	3	Bar C-A431
28.04	46.53	158,000	3	Bar C-A431
9.35	46.73	225,000	3	Bar C-A431
9.31	41.78	257,000	3	Bar C-A431
31.89	38.04	311,000	3	Bar C-A431
9.32	41.81	415,500	3	Bar C-A431
9.32	37.26	428,000	3	Bar C-A431
9.31	41.78	430,000	3	Bar C-A431
9.34	37.36	430,000	3	Bar C-A431

(continued on next page)

**Table F.8.2. Concrete Fatigue Data for Reinforced Concrete (continued)**

<b>f_min</b>	<b>S<sub>r</sub></b>	<b>N</b>	<b>Reference No.</b>	<b>Notes/Specimen No.</b>
9.32	37.26	431,000	3	Bar C-A431
28.05	35.61	462,400	3	Bar C-A431
28.02	35.57	477,700	3	Bar C-A431
31.9	31.5	499,300	3	Bar C-A431
9.28	35.16	503,300	3	Bar C-A431
27.94	30.32	648,400	3	Bar C-A431
27.85	27.86	1,056,000	3	Bar C-A431
9.28	33.15	1,072,000	3	Bar C-A431
9.35	31.81	1,250,000	3	Bar C-A431
28.05	26.06	2,037,000	3	Bar C-A431
9.34	29.82	2,631,000	3	Bar C-A431
5	39	216,400	3	Bar D-A15
5	39	288,000	3	Bar D-A15
5	39	315,600	3	Bar D-A15
5	34	356,800	3	Bar D-A15
15	34	365,200	3	Bar D-A15
15	34	406,600	3	Bar D-A15
5	34	435,000	3	Bar D-A15
15	34	441,000	3	Bar D-A15
5	34	506,100	3	Bar D-A15
5	34	510,000	3	Bar D-A15
5	34	515,300	3	Bar D-A15
5	29	626,600	3	Bar D-A15
15	34	645,300	3	Bar D-A15
15	29	673,000	3	Bar D-A15
15	29	746,000	3	Bar D-A15
5	29	864,500	3	Bar D-A15
15	29	888,400	3	Bar D-A15
5	29	920,200	3	Bar D-A15
15	29	971,000	3	Bar D-A15
15	29	1,030,000	3	Bar D-A15
5	34	1,120,000	3	Bar D-A15
15	29	1,232,000	3	Bar D-A15
15	26	2,214,500	3	Bar D-A15
15	24	3,187,500	3	Bar D-A15
15	25	3,496,500	3	Bar D-A15
15	24	3,702,400	3	Bar D-A15
15	24	8,164,000	3	Bar D-A15

(continued on next page)

**Table F.8.2. Concrete Fatigue Data for Reinforced Concrete (continued)**

<b>f<sub>min</sub></b>	<b>S<sub>r</sub></b>	<b>N</b>	<b>Reference No.</b>	<b>Notes/Specimen No.</b>
4.6	39.7	88,900	4	44CH
4.6	39.7	129,200	4	44CV
4.7	35.5	219,800	4	40CH
4.7	35.5	334,200	4	40CV
4.7	33.5	364,000	4	38CV
4.7	31.6	507,000	4	36CH
4.7	29.5	517,000	4	34CH
4.7	29.5	575,000	4	34CH
4.7	31.5	627,300	4	36CV
4.7	29.5	903,000	4	34CV
4.7	27.5	1,434,000	4	32CH
4.7	27.5	1,941,900	4	32CV
4.7	25.5	2,819,800	4	30CH
4.7	25.5	2,984,600	4	30CV
4.8	23.4	5,237,000	4	28CV
4.7	24.5	5,731,000	4	29CV
4.8	23.4	6,266,500	4	28CH
23.7	51.1	160,000	5	F75-5
22.1	49.4	248,000	5	F75-3
17.1	37.9	350,000	5	F50-7
19.3	47.3	401,000	5	F75-1
15.2	41.2	429,000	5	F60-1
21.3	40.6	604,000	5	F75-4
12.5	34.1	610,000	5	F50-1
13.6	37.8	624,000	5	F50-5
12.3	39.7	672,000	5	F60-3
15	32.4	787,000	5	F40-4
14	33.5	893,000	5	F50-3
13.5	31.9	1,063,000	5	F40-3
14.1	30.7	1,316,000	5	F50-6
16.4	28.6	1,348,000	5	F40-1
12.4	29.6	1,488,000	5	F40-2
21.5	40	1,781,000	5	F75-2
16.1	32.1	1,877,000	5	F60-2
16.4	31.9	3,004,000	5	F60-4
13.9	26.1	3,272,000	5	F50-4
12.3	27.7	3,623,000	5	F50-2

## References for F.8

1. Ople, F. S., and C. L. Hulsbos. 1966. Probable Fatigue Life of Plain Concrete with Stress Gradient. *Journal Proceedings, American Concrete Institute*, Vol. 63, No. (1), pp. 59–82.
2. Fisher, J. W., and I. M. Viest. 1961. *Special Report 66: Fatigue Tests of Bridge Materials of the AASHTO Road Test*. HRB, National Research Council, Washington, D.C., pp. 132–147.
3. Pfister, J. F., and E. Hognestad. 1964. High-Strength Bars As Concrete Reinforcement, Part 6: Fatigue Tests. *Journal of the Portland Cement Association Research and Development Laboratories*, Vol. 6, No. 1, pp. 65–84.
4. Hanson, J. M., K. T. Burton, and E. Hognestad. 1968. Fatigue Tests of Reinforcing Bars: Effect of Deformation Pattern. *Journal of the Portland Cement Association Research and Development Laboratories*, Vol. 10, No. 3, pp. 2–13.
5. Lash, S. 1969. Can High-Strength Reinforcement Be Used in Highway Bridges? In *First International Symposium on Concrete Bridge Design*, SP-23, American Concrete Institute, Detroit, Mich., pp. 283–299.

## **TRB OVERSIGHT COMMITTEE FOR THE STRATEGIC HIGHWAY RESEARCH PROGRAM 2\***

CHAIR: **Kirk T. Steudle**, *Director, Michigan Department of Transportation*

### **MEMBERS**

**H. Norman Abramson**, *Executive Vice President (retired), Southwest Research Institute*  
**Alan C. Clark**, *MPO Director, Houston–Galveston Area Council*  
**Frank L. Danchetz**, *Vice President, ARCADIS-US, Inc. (deceased January 2015)*  
**Malcolm Dougherty**, *Director, California Department of Transportation*  
**Stanley Gee**, *Executive Deputy Commissioner, New York State Department of Transportation*  
**Mary L. Klein**, *President and CEO, NatureServe*  
**Michael P. Lewis**, *Director, Rhode Island Department of Transportation*  
**John R. Njord**, *Executive Director (retired), Utah Department of Transportation*  
**Charles F. Potts**, *Chief Executive Officer, Heritage Construction and Materials*  
**Ananth K. Prasad**, *Secretary, Florida Department of Transportation*  
**Gerald M. Ross**, *Chief Engineer (retired), Georgia Department of Transportation*  
**George E. Schoener**, *Executive Director, I-95 Corridor Coalition*  
**Kumares C. Sinha**, *Olson Distinguished Professor of Civil Engineering, Purdue University*  
**Paul Trombino III**, *Director, Iowa Department of Transportation*

### **EX OFFICIO MEMBERS**

**Victor M. Mendez**, *Administrator, Federal Highway Administration*  
**David L. Strickland**, *Administrator, National Highway Transportation Safety Administration*  
**Frederick “Bud” Wright**, *Executive Director, American Association of State Highway and Transportation Officials*

### **LIAISONS**

**Ken Jacoby**, *Communications and Outreach Team Director, Office of Corporate Research, Technology, and Innovation Management, Federal Highway Administration*  
**Tony Kane**, *Director, Engineering and Technical Services, American Association of State Highway and Transportation Officials*  
**Jeffrey F. Paniati**, *Executive Director, Federal Highway Administration*  
**John Pearson**, *Program Director, Council of Deputy Ministers Responsible for Transportation and Highway Safety, Canada*  
**Michael F. Trentacoste**, *Associate Administrator, Research, Development, and Technology, Federal Highway Administration*

\*Membership as of January 2015.

## **RENEWAL TECHNICAL COORDINATING COMMITTEE\***

CHAIR: **Daniel D’Angelo**, *Recovery Acting Manager, Director and Deputy Chief Engineer, Office of Design, New York State Department of Transportation*

### **MEMBERS**

**Rachel Arulraj**, *President, InfoInnovation*  
**Michael E. Ayers**, *Consultant, Technology Services, American Concrete Pavement Association*  
**Thomas E. Baker**, *State Materials Engineer, Washington State Department of Transportation*  
**John E. Breen**, *Al-Rashid Chair in Civil Engineering Emeritus, University of Texas at Austin*  
**Steven D. DeWitt**, *Chief Engineer (retired), North Carolina Turnpike Authority*  
**Tom W. Donovan**, *Senior Right of Way Agent (retired), California Department of Transportation*  
**Alan D. Fisher**, *Manager, Construction Structures Group, Cianbro Corporation*  
**Michael Hemmingsen**, *Davison Transportation Service Center Manager (retired), Michigan Department of Transportation*  
**Bruce Johnson**, *State Bridge Engineer, Oregon Department of Transportation, Bridge Engineering Section*  
**Leonnice Kavanagh**, *PhD Candidate, Seasonal Lecturer, Civil Engineering Department, University of Manitoba*  
**Cathy Nelson**, *Technical Services Manager/Chief Engineer (retired), Oregon Department of Transportation*  
**John J. Robinson, Jr.**, *Assistant Chief Counsel, Pennsylvania Department of Transportation, Governor’s Office of General Counsel*  
**Ted M. Scott II**, *Director, Engineering, American Trucking Associations, Inc.*  
**Gary D. Taylor**, *Professional Engineer*  
**Gary C. Whited**, *Program Manager, Construction and Materials Support Center, University of Wisconsin–Madison*

### **AASHTO LIAISON**

**James T. McDonnell**, *Program Director for Engineering, American Association of State Highway and Transportation Officials*

### **FHWA LIAISONS**

**Steve Gaj**, *Leader, System Management and Monitoring Team, Office of Asset Management, Federal Highway Administration*  
**Cheryl Allen Richter**, *Assistant Director, Pavement Research and Development, Office of Infrastructure Research and Development, Federal Highway Administration*  
**J. B. “Butch” Wlaschin**, *Director, Office of Asset Management, Federal Highway Administration*

### **CANADA LIAISON**

**Lance Vigfusson**, *Assistant Deputy Minister of Engineering & Operations, Manitoba Infrastructure and Transportation*

\*Membership as of July 2014.



## Related SHRP 2 Research

Geotechnical Solutions for Soil Improvement, Rapid Embankment Construction, and Stabilization of the Pavement Working Platform (R02)

Innovative Bridge Designs for Rapid Renewal (R04)

Nondestructive Testing to Identify Concrete Bridge Deck Deterioration (R06A)

Mapping Voids, Debonding, Delaminations, Moisture, and Other Defects Behind or Within Tunnel Linings (R06G)

Bridges for Service Life Beyond 100 Years: Innovative Systems, Subsystems, and Components (R19A)